ISSN 1007-9327 (print)
ISSN 2219-2840 (online)

World Journal of *Gastroenterology*

World J Gastroenterol 2015 April 14; 21(14): 4103-4426

Published by Baishideng Publishing Group Inc

World Journal of Gastroenterology

A peer-reviewed, online, open-access journal of gastroenterology and hepatology

Editorial Board

2014-2017

The *World Journal of Gastroenterology* Editorial Board consists of 1378 members, representing a team of worldwide experts in gastroenterology and hepatology. They are from 68 countries, including Algeria (2), Argentina (7), Australia (31), Austria (9), Belgium (11), Brazil (20), Brunei Darussalam (1), Bulgaria (2), Cambodia (1), Canada (26), Chile (4), China (163), Croatia (2), Cuba (1), Czech (6), Denmark (2), Egypt (9), Estonia (2), Finland (6), France (20), Germany (58), Greece (31), Guatemala (1), Hungary (15), Iceland (1), India (33), Indonesia (2), Iran (10), Ireland (9), Israel (18), Italy (195), Japan (151), Jordan (1), Kuwait (1), Lebanon (7), Lithuania (1), Malaysia (1), Mexico (11), Morocco (1), Netherlands (5), New Zealand (4), Nigeria (3), Norway (6), Pakistan (6), Poland (12), Portugal (8), Puerto Rico (1), Qatar (1), Romania (10), Russia (3), Saudi Arabia (2), Singapore (7), Slovenia (2), South Africa (1), South Korea (69), Spain (51), Sri Lanka (1), Sudan (1), Sweden (12), Switzerland (5), Thailand (7), Trinidad and Tobago (1), Tunisia (2), Turkey (55), United Kingdom (49), United States (180), Venezuela (1), and Vietnam (1).

Alfred King Lam, *Gold Coast*
Ian C Lawrance, *PerthFremantle*
Barbara Anne Leggett, *Brisbane*
Daniel A Lemberg, *Sydney*
Rupert W Leong, *Sydney*
Finlay A Macrae, *Victoria*
Vance Matthews, *Melbourne*
David L Morris, *Sydney*
Reme Mountifield, *Bedford Park*
Hans J Netter, *Melbourne*
Nam Q Nguyen, *Adelaide*
Liang Qiao, *Westmead*
Rajvinder Singh, *Adelaide*
Ross Cyril Smith, *StLeonards*
Kevin J Spring, *Sydney*
Debbie Trinder, *Fremantle*
Daniel R van Langenberg, *Box Hill*
David Ian Watson, *Adelaide*
Desmond Yip, *Garran*
Li Zhang, *Sydney*

Austria

Felix Aigner, *Innsbruck*
Gabriela A Berlakovich, *Vienna*
Herwig R Cerwenka, *Graz*
Peter Ferenci, *Wien*
Alfred Gangl, *Vienna*
Kurt Lenz, *Linz*
Markus Peck-Radosavljevic, *Vienna*
Markus Raderer, *Vienna*
Stefan Riss, *Vienna*

Belgium

Michael George Adler, *Brussels*
Benedicte Y De Winter, *Antwerp*
Mark De Ridder, *Jette*
Olivier Detry, *Liege*
Denis Dufrane Dufrane, *Brussels*
Sven M Francque, *Edegem*
Nikos Kotzampassakis, *Liège*
Geert KMM Robaeys, *Genk*
Xavier Sagaert, *Leuven*
Peter Starkel, *Brussels*
Eddie Wisse, *Keerbergen*

Brazil

SMP Balzan, *Santa Cruz do Sul*
JLF Caboclo, *Sao jose do rio preto*
Fábio Guilherme Campos, *Sao Paulo*
Claudia RL Cardoso, *Rio de Janeiro*
Roberto J Carvalho-Filho, *Sao Paulo*
Carla Daltro, *Salvador*
José Sebastiao dos Santos, *Ribeirao Preto*
Eduardo LR Mello, *Rio de Janeiro*
Sthela Maria Murad-Regadas, *Fortaleza*
Claudia PMS Oliveira, *Sao Paulo*
Júlio C Pereira-Lima, *Porto Alegre*
Marcos V Perini, *Sao Paulo*
Vietla Satyanarayana Rao, *Fortaleza*
Raquel Rocha, *Salvador*
AC Simoes e Silva, *Belo Horizonte*
Mauricio F Silva, *Porto Alefre*
Aytan Miranda Sipahi, *Sao Paulo*
Rosa Leonôra Salerno Soares, *Niterói*
Cristiane Valle Tovo, *Porto Alegre*
Eduardo Garcia Vilela, *Belo Horizonte*

Brunei Darussalam

Vui Heng Chong, *Bandar Seri Begawan*

Bulgaria

Tanya Kirilova Kadiyska, *Sofia*
Mihaela Petrova, *Sofia*

Cambodia

Francois Rouet, *Phnom Penh*

Canada

Brian Bressler, *Vancouver*
Frank J Burczynski, *Winnipeg*
Wangxue Chen, *Ottawa*
Francesco Crea, *Vancouver*
Mirko Diksic, *Montreal*
Jane A Foster, *Hamilton*
Hugh J Freeman, *Vancouver*
Shahrokh M Ghobadloo, *Ottawa*
Yuewen Gong, *Winnipeg*
Philip H Gordon, *Quebec*
Rakesh Kumar, *Edmonton*
Wolfgang A Kunze, *Hamilton*
Patrick Labonte, *Laval*
Zhikang Peng, *Winnipeg*
Jayadev Raju, *Ottawa*
Maitreyi Raman, *Calgary*
Giada Sebastiani, *Montreal*
Maida J Sewitch, *Montreal*
Eldon A Shaffer, *Alberta*
Christopher W Teshima, *Edmonton*
Jean Sévigny, *Québec*
Pingchang Yang, *Hamilton*
Pingchang Yang, *Hamilton*
Eric M Yoshida, *Vancouver*
Bin Zheng, *Edmonton*

Chile

Marcelo A Beltran, *La Serena*
Flavio Nervi, *Santiago*
Adolfo Parra-Blanco, *Santiago*
Alejandro Soza, *Santiago*

China

Zhao-Xiang Bian, *Hong Kong*
San-Jun Cai, *Shanghai*
Guang-Wen Cao, *Shanghai*
Long Chen, *Nanjing*
Ru-Fu Chen, *Guangzhou*
George G Chen, *Hong Kong*
Li-Bo Chen, *Wuhan*
Jia-Xu Chen, *Beijing*
Hong-Song Chen, *Beijing*
Lin Chen, *Beijing*
Yang-Chao Chen, *Hong Kong*
Zhen Chen, *Shanghai*
Ying-Sheng Cheng, *Shanghai*
Kent-Man Chu, *Hong Kong*
Zhi-Jun Dai, *Xi'an*
Jing-Yu Deng, *Tianjin*
Yi-Qi Du, *Shanghai*
Zhi Du, *Tianjin*
Hani El-Nezami, *Hong Kong*
Bao-Ying Fei, *Hangzhou*
Chang-Ming Gao, *Nanjing*
Jian-Ping Gong, *Chongqing*
Zuo-Jiong Gong, *Wuhan*
Jing-Shan Gong, *Shenzhen*
Guo-Li Gu, *Beijing*
Yong-Song Guan, *Chengdu*
Mao-Lin Guo, *Luoyang*
Jun-Ming Guo, *Ningbo*
Yan-Mei Guo, *Shanghai*
Xiao-Zhong Guo, *Shenyang*
Guo-Hong Han, *Xi'an*
Ming-Liang He, *Hong Kong*
Peng Hou, *Xi'an*
Zhao-Hui Huang, *Wuxi*
Feng Ji, *Hangzhou*
Simon Law, *Hong Kong*
Yu-Yuan Li, *Guangzhou*
Meng-Sen Li, *Haikou*
Shu-De Li, *Shanghai*
Zong-Fang Li, *Xi'an*
Qing-Quan Li, *Shanghai*
Kang Li, *Lasa*
Han Liang, *Tianjin*
Xing'e Liu, *Hangzhou*
Zheng-Wen Liu, *Xi'an*
Xiao-Fang Liu, *Yantai*
Bin Liu, *Tianjin*
Quan-Da Liu, *Beijing*
Hai-Feng Liu, *Beijing*
Fei Liu, *Shanghai*
Ai-Guo Lu, *Shanghai*
He-Sheng Luo, *Wuhan*
Xiao-Peng Ma, *Shanghai*
Yong Meng, *Shantou*
Ke-Jun Nan, *Xi'an*
Siew Chien Ng, *Hong Kong*
Simon SM Ng, *Hong Kong*
Zhao-Shan Niu, *Qingdao*
Bo-Rong Pan, *Xi'an*
Di Qu, *Shanghai*
Rui-Hua Shi, *Nanjing*
Bao-Min Shi, *Shanghai*
Xiao-Dong Sun, *Hangzhou*
Si-Yu Sun, *Shenyang*
Guang-Hong Tan, *Haikou*
Wen-Fu Tang, *Chengdu*
Anthony YB Teoh, *Hong Kong*
Wei-Dong Tong, *Chongqing*
Eric Tse, *Hong Kong*
Hong Tu, *Shanghai*
Rong Tu, *Haikou*
Jian-She Wang, *Shanghai*
Kai Wang, *Jinan*
Xiao-Ping Wang, *Xianyang*
Dao-Rong Wang, *Yangzhou*
De-Sheng Wang, *Xi'an*
Chun-You Wang, *Wuhan*
Ge Wang, *Chongqing*

Xi-Shan Wang, *Harbin*
Wei-hong Wang, *Beijing*
Zhen-Ning Wang, *Shenyang*
Wai Man Raymond Wong, *Hong Kong*
Chun-Ming Wong, *Hong Kong*
Jian Wu, *Shanghai*
Sheng-Li Wu, *Xi'an*
Wu-Jun Wu, *Xi'an*
Qing Xia, *Chengdu*
Yan Xin, *Shenyang*
Dong-Ping Xu, *Beijing*
Jian-Min Xu, *Shanghai*
Wei Xu, *Changchun*
Ming Yan, *Jinan*
Xin-Min Yan, *Kunming*
Yi-Qun Yan, *Shanghai*
Feng Yang, *Shanghai*
Yong-Ping Yang, *Beijing*
He-Rui Yao, *Guangzhou*
Thomas Yau, *Hong Kong*
Winnie Yeo, *Hong Kong*
Jing You, *Kunming*
Jian-Qing Yu, *Wuhan*
Ying-Yan Yu, *Shanghai*
Wei-Zheng Zeng, *Chengdu*
Zong-Ming Zhang, *Beijing*
Dian-Liang Zhang, *Qingdao*
Ya-Ping Zhang, *Shijiazhuang*
You-Cheng Zhang, *Lanzhou*
Jian-Zhong Zhang, *Beijing*
Ji-Yuan Zhang, *Beijing*
Hai-Tao Zhao, *Beijing*
Jian Zhao, *Shanghai*
Jian-Hong Zhong, *Nanning*
Ying-Qiang Zhong, *Guangzhou*
Ping-Hong Zhou, *Shanghai*
Yan-Ming Zhou, *Xiamen*
Tong Zhou, *Nanchong*
Li-Ming Zhou, *Chengdu*
Guo-Xiong Zhou, *Nantong*
Feng-Shang Zhu, *Shanghai*
Jiang-Fan Zhu, *Shanghai*
Zhao-Hui Zhu, *Beijing*

Croatia

Tajana Filipec Kanizaj, *Zagreb*
Mario Tadic, *Zagreb*

Cuba

Damian Casadesus, *Havana*

Czech

Jan Bures, *Hradec Kralove*
Marcela Kopacova, *Hradec Kralove*
Otto Kucera, *Hradec Kralove*
Marek Minarik, *Prague*
Pavel Soucek, *Prague*
Miroslav Zavoral, *Prague*

Denmark

Vibeke Andersen, *Odense*
E Michael Danielsen, *Copenhagen*

Egypt

Mohamed MM Abdel-Latif, *Assiut*
Hussein Atta, *Cairo*
Ashraf Elbahrawy, *Cairo*
Mortada Hassan El-Shabrawi, *Cairo*
Mona El Said El-Raziky, *Cairo*
Elrashdy M Redwan, *New Borg Alrab*
Zeinab Nabil Ahmed Said, *Cairo*
Ragaa HM Salama, *Assiut*
Maha Maher Shehata, *Mansoura*

Estonia

Margus Lember, *Tartu*
Tamara Vorobjova, *Tartu*

Finland

Marko Kalliomäki, *Turku*
Thomas Kietzmann, *Oulu*
Kaija-Leena Kolho, *Helsinki*
Eija Korkeila, *Turku*
Heikki Makisalo, *Helsinki*
Tanja Pessi, *Tampere*

France

Armando Abergel Clermont, *Ferrand*
Elie K Chouillard, *Polssy*
Pierre Cordelier, *Toulouse*
Pascal P Crenn, *Garches*
Catherine Daniel, *Lille*
Fanny Daniel, *Paris*
Cedric Dray, *Toulouse*
Benoit Foligne, *Lille*
Jean-Noel Freund, *Strasbourg*
Hervé Guillou, *Toulouse*
Nathalie Janel, *Paris*
Majid Khatib, *Bordeaux*
Jacques Marescaux, *Strasbourg*
Jean-Claude Marie, *Paris*
Driffa Moussata, *Pierre Benite*
Hang Nguyen, *Clermont-Ferrand*
Hugo Perazzo, *Paris*
Alain L Servin, *Chatenay-Malabry*
Chang Xian Zhang, *Lyon*

Germany

Stavros A Antoniou, *Monchengladbach*
Erwin Biecker, *Siegburg*
Hubert E Blum, *Freiburg*
Thomas Bock, *Berlin*
Katja Breitkopf-Heinlein, *Mannheim*
Elke Cario, *Essen*
Güralp Onur Ceyhan, *Munich*
Angel Cid-Arregui, *Heidelberg*
Michael Clemens Roggendorf, *München*
Christoph F Dietrich, *Bad Mergentheim*
Valentin Fuhrmann, *Hamburg*
Nikolaus Gassler, *Aachen*
Andreas Geier, *Wuerzburg*
Markus Gerhard, *Munich*
Anton Gillessen, *Muenster*
Thorsten Oliver Goetze, *Offenbach*
Daniel Nils Gotthardt, *Heidelberg*
Robert Grützmann, *Dresden*
Thilo Hackert, *Heidelberg*
Joerg Haier, *Muenster*
Claus Hellerbrand, *Regensburg*
Harald Peter Hoensch, *Darmstadt*
Jens Hoeppner, *Freiburg*
Richard Hummel, *Muenster*
Jakob Robert Izbicki, *Hamburg*
Gernot Maximilian Kaiser, *Essen*
Matthias Kapischke, *Hamburg*
Michael Keese, *Frankfurt*
Andrej Khandoga, *Munich*
Jorg Kleeff, *Munich*
Alfred Koenigsrainer, *Tuebingen*
Peter Christopher Konturek, *Saalfeld*
Michael Linnebacher, *Rostock*
Stefan Maier, *Kaufbeuren*
Oliver Mann, *Hamburg*
Marc E Martignoni, *Munic*
Thomas Minor, *Bonn*
Oliver Moeschler, *Osnabrueck*
Jonas Mudter, *Eutin*
Sebastian Mueller, *Heidelberg*
Matthias Ocker, *Berlin*
Andreas Ommer, *Essen*
Albrecht Piiper, *Frankfurt*
Esther Raskopf, *Bonn*
Christoph Reichel, *Bad Brückenau*
Elke Roeb, *Giessen*
Udo Rolle, *Frankfurt*
Karl-Herbert Schafer, *Zweibrücken*
Peter Schemmer, *Heidelberg*
Andreas G Schreyer, *Regensburg*
Manuel A Silva, *Penzberg*
Georgios C Sotiropoulos, *Essen*
Ulrike S Stein, *Berlin*
Dirk Uhlmann, *Leipzig*
Michael Weiss, *Halle*
Hong-Lei Weng, *Mannheim*
Karsten Wursthorn, *Hamburg*

Greece

Alexandra Alexopoulou, *Athens*
Nikolaos Antonakopoulos, *Athens*
Stelios F Assimakopoulos, *Patras*
Grigoris Chatzimavroudis, *Thessaloniki*
Evangelos Cholongitas, *Thessaloniki*
Gregory Christodoulidis, *Larisa*
George N Dalekos, *Larissa*
Urania Georgopoulou, *Athens*
Eleni Gigi, *Thessaloniki*
Stavros Gourgiotis, *Athens*
Leontios J Hadjileontiadis, *Thessaloniki*
Thomas Hyphantis, *Ioannina*
Ioannis Kanellos, *Thessaloniki*
Stylianos Karatapanis, *Rhodes*
Michael Koutsilieris, *Athens*
Spiros D Ladas, *Athens*
Theodoros K Liakakos, *Athens*
Emanuel K Manesis, *Athens*
Spilios Manolakopoulos, *Athens*
Gerassimos John Mantzaris, *Athens*
Athanasios D Marinis, *Piraeus*

Nikolaos Ioannis Nikiteas, *Athens*
Konstantinos X Papamichael, *Athens*
George Sgourakis, *Athens*
Konstantinos C Thomopoulos, *Patras*
Konstantinos Triantafyllou, *Athens*
Christos Triantos, *Patras*
Georgios Zacharakis, *Athens*
Petros Zezos, *Alexandroupolis*
Demosthenes E Ziogas, *Ioannina*

Guatemala

Carlos Maria Parellada, *Guatemala*

Hungary

Mihaly Boros, *Szeged*
Tamás Decsi, *Pécs*
Gyula Farkas, *Szeged*
Andrea Furka, *Debrecen*
Y vette Mandi, *Szeged*
Peter L Lakatos, *Budapest*
Pal Miheller, *Budapest*
Tamás Molnar, *Szeged*
Attila Olah, *Gyor*
Maria Papp, *Debrecen*
Zoltan Rakonczay, *Szeged*
Ferenc Sipos, *Budapest*
Miklós Tanyi, *Debrecen*
Tibor Wittmann, *Szeged*

Iceland

Tryggvi Bjorn Stefánsson, *Reykjavík*

India

Brij B Agarwal, *New Delhi*
Deepak N Amarapurkar, *Mumbai*
Shams ul Bari, *Srinagar*
Sriparna Basu, *Varanasi*
Runu Chakravarty, *Kolkata*
Devendra C Desai, *Mumbai*
Nutan D Desai, *Mumbai*
Suneela Sunil Dhaneshwar, *Pune*
Radha K Dhiman, *Chandigarh*
Pankaj Garg, *Mohali*
Uday C Ghoshal, *Lucknow*
Kalpesh Jani, *Vadodara*
Premashis Kar, *New Delhi*
Jyotdeep Kaur, *Chandigarh*
Rakesh Kochhar, *Chandigarh*
Pradyumna K Mishra, *Mumbai*
Asish K Mukhopadhyay, *Kolkata*
Imtiyaz Murtaza, *Srinagar*
P Nagarajan, *New Delhi*
Samiran Nundy, *Delhi*
Gopal Pande, *Hyderabad*
Benjamin Perakath, *Vellore*
Arun Prasad, *New Delhi*
D Nageshwar Reddy, *Hyderabad*
Lekha Saha, *Chandigarh*
Sundeep Singh Saluja, *New Delhi*
Mahesh Prakash Sharma, *New Delhi*
Sadiq Saleem Sikora, *Bangalore*
Sarman Singh, *New Delhi*
Rajeev Sinha, *Jhansi*
Rupjyoti Talukdar, *Hyderabad*
Rakesh Kumar Tandon, *New Delhi*
Narayanan Thirumoorthy, *Coimbatore*

Indonesia

David Handojo Muljono, *Jakarta*
Andi Utama, *Jakarta*

Iran

Arezoo Aghakhani, *Tehran*
Seyed Mohsen Dehghani, *Shiraz*
Ahad Eshraghian, *Shiraz*
Hossein Khedmat, *Tehran*
Sadegh Massarrat, *Tehran*
Marjan Mohammadi, *Tehran*
Roja Rahimi, *Tehran*
Farzaneh Sabahi, *Tehran*
Majid Sadeghizadeh, *Tehran*
Farideh Siavoshi, *Tehran*

Ireland

Gary Alan Bass, *Dublin*
David J Brayden, *Dublin*
Ronan A Cahill, *Dublin*
Glen A Doherty, *Dublin*
Liam J Fanning, *Cork*
Barry Philip McMahon, *Dublin*
RossMcManus, *Dublin*
Dervla O'Malley, *Cork*
Sinead M Smith, *Dublin*

Israel

Dan Carter, *Ramat Gan*
Jorge-Shmuel Delgado, *Metar*
Eli Magen, *Ashdod*
Nitsan Maharshak, *Tel Aviv*
Shaul Mordechai, *Beer Sheva*
Menachem Moshkowitz, *Tel Aviv*
William Bahij Nseir, *Nazareth*
Shimon Reif, *Jerusalem*
Ram Reifen, *Rehovot*
Ariella Bar-Gil Shitrit, *Jerusalem*
Noam Shussman, *Jerusalem*
Igor Sukhotnik, *Haifa*
Nir Wasserberg, *Petach Tiqwa*
Jacob Yahav, *Rehovot*
Doron Levi Zamir, *Gedera*
Shira Zelber-Sagi, *Haifa*
Romy Zemel, *Petach-Tikva*

Italy

Ludovico Abenavoli, *Catanzaro*
Luigi Elio Adinolfi, *Naples*
Carlo Virginio Agostoni, *Milan*
Anna Alisi, *Rome*
Piero Luigi Almasio, *Palermo*
Donato Francesco Altomare, *Bari*
Amedeo Amedei, *Florence*
Pietro Andreone, *Bologna*
Imerio Angriman, *Padova*
Vito Annese, *Florence*
Paolo Aurello, *Rome*
Salavtore Auricchio, *Naples*
Gian Luca Baiocchi, *Brescia*
Gianpaolo Balzano, *Milan*
Antonio Basoli, *Rome*
Gabrio Bassotti, *San Sisto*
Mauro Bernardi, *Bologna*
Alberto Biondi, *Rome*
Ennio Biscaldi, *Genova*
Massimo Bolognesi, *Padua*
Luigi Bonavina, *Milano*
Aldo Bove, *Chieti*
Raffaele Bruno, *Pavia*
Luigi Brusciano, *Napoli*
Giuseppe Cabibbo, *Palermo*
Carlo Calabrese, *Bologna*
Daniele Calistri, *Meldola*
Vincenza Calvaruso, *Palermo*
Lorenzo Camellini, *Reggio Emilia*
Marco Candela, *Bologna*
Raffaele Capasso, *Naples*
Lucia Carulli, *Modena*
Renato David Caviglia, *Rome*
Luigina Cellini, *Chieti*
Giuseppe Chiarioni, *Verona*
Claudio Chiesa, *Rome*
Michele Cicala, *Roma*
Rachele Ciccocioppo, *Pavia*
Sandro Contini, *Parma*
Gaetano Corso, *Foggia*
Renato Costi, *Parma*
Alessandro Cucchetti, *Bologna*
Rosario Cuomo, *Napoli*
Giuseppe Currò, *Messina*
Paola De Nardi, *Milano*
Giovanni D De Palma, *Naples*
Raffaele De Palma, *Napoli*
Giuseppina De Petro, *Brescia*
Valli De Re, *Aviano*
Paolo De Simone, *Pisa*
Giuliana Decorti, *Trieste*
Emanuele Miraglia del Giudice, *Napoli*
Isidoro Di Carlo, *Catania*
Matteo Nicola Dario Di Minno, *Naples*
Massimo Donadelli, *Verona*
Mirko D'Onofrio, *Verona*
Maria Pina Dore, *Sassari*
Luca Elli, *Milano*
Massimiliano Fabozzi, *Aosta*
Massimo Falconi, *Ancona*
Ezio Falletto, *Turin*
Silvia Fargion, *Milan*
Matteo Fassan, *Verona*
Gianfranco Delle Fave, *Roma*
Alessandro Federico, *Naples*
Francesco Feo, *Sassari*
Davide Festi, *Bologna*
Natale Figura, *Siena*
Vincenzo Formica, *Rome*
Mirella Fraquelli, *Milan*
Marzio Frazzoni, *Modena*
Walter Fries, *Messina*
Gennaro Galizia, *Naples*
Andrea Galli, *Florence*
Matteo Garcovich, *Rome*
Eugenio Gaudio, *Rome*
Paola Ghiorzo, *Genoa*
Edoardo G Giannini, *Genova*

Luca Gianotti, *Monza*
Maria Cecilia Giron, *Padova*
Alberto Grassi, *Rimini*
Gabriele Grassi, *Trieste*
Francesco Greco, *Bergamo*
Luigi Greco, *Naples*
Antonio Grieco, *Rome*
Fabio Grizzi, *Rozzano*
Laurino Grossi, *Pescara*
Simone Guglielmetti, *Milan*
Tiberiu Hershcovici, *Jerusalem*
Calogero Iacono, *Verona*
Enzo Ierardi, *Bari*
Amedeo Indriolo, *Bergamo*
Raffaele Iorio, *Naples*
Paola Iovino, *Salerno*
Angelo A Izzo, *Naples*
Loreta Kondili, *Rome*
Filippo La Torre, *Rome*
Giuseppe La Torre, *Rome*
Giovanni Latella, *L'Aquila*
Salvatore Leonardi, *Catania*
Massimo Libra, *Catania*
Anna Licata, *Palermo*
C armela Loguercio, *Naples*
Amedeo Lonardo, *Modena*
Carmelo Luigiano, *Catania*
Francesco Luzza, *Catanzaro*
Giovanni Maconi, *Milano*
Antonio Macrì, *Messina*
Mariano Malaguarnera, *Catania*
Francesco Manguso, *Napoli*
Tommaso Maria Manzia, *Rome*
Daniele Marrelli, *Siena*
Gabriele Masselli, *Rome*
Sara Massironi, *Milan*
Giuseppe Mazzarella, *Avellino*
Michele Milella, *Rome*
Giovanni Milito, *Rome*
Antonella d'Arminio Monforte, *Milan*
Fabrizio Montecucco, *Genoa*
Giovanni Monteleone, *Rome*
Mario Morino, *Torino*
Vincenzo La Mura, *Milan*
Gerardo Nardone, *Naples*
Riccardo Nascimbeni, *Brescia*
Gabriella Nesi, *Florence*
Giuseppe Nigri, *Rome*
Erica Novo, *Turin*
Veronica Ojetti, *Rome*
Michele Orditura, *Naples*
Fabio Pace, *Seriate*
Lucia Pacifico, *Rome*
Omero Alessandro Paoluzi, *Rome*
Valerio Pazienza, *San Giovanni Rotondo*
Rinaldo Pellicano, *Turin*
Adriano M Pellicelli, *Rome*
Nadia Peparini, *Ciampino*
Mario Pescatori, *Rome*
Antonio Picardi, *Rome*
Alberto Pilotto, *Padova*
Alberto Piperno, *Monza*
Anna Chiara Piscaglia, *Rome*
Maurizio Pompili, *Rome*
Francesca Romana Ponziani, *Rome*
Cosimo Prantera, *Rome*
Girolamo Ranieri, *Bari*
Carlo Ratto, *Tome*
Barbara Renga, *Perugia*
Alessandro Repici, *Rozzano*
Maria Elena Riccioni, *Rome*
Lucia Ricci-Vitiani, *Rome*
Luciana Rigoli, *Messina*
Mario Rizzetto, *Torino*
Ballarin Roberto, *Modena*
Roberto G Romanelli, *Florence*
Claudio Romano, *Messina*
Luca Roncucci, *Modena*
Cesare Ruffolo, *Treviso*
L ucia Sacchetti, *Napoli*
Rodolfo Sacco, *Pisa*
Lapo Sali, *Florence*
Romina Salpini, *Rome*
Giulio Aniello, *Santoro Treviso*
Armando Santoro, *Rozzano*
Edoardo Savarino, *Padua*
Marco Senzolo, *Padua*
Annalucia Serafino, *Rome*
Giuseppe S Sica, *Rome*
Pierpaolo Sileri, *Rome*
Cosimo Sperti, *Padua*
Vincenzo Stanghellini, *Bologna*
Cristina Stasi, *Florence*
Gabriele Stocco, *Trieste*
Roberto Tarquini, *Florence*
Mario Testini, *Bari*
Guido Torzilli, *Milan*
Guido Alberto Massimo, *Tiberio Brescia*
Giuseppe Toffoli, *Aviano*
Alberto Tommasini, *Trieste*
Francesco Tonelli, *Florence*
Cesare Tosetti Porretta, *Terme*
Lucio Trevisani, *Cona*
Guglielmo M Trovato, *Catania*
Mariapia Vairetti, *Pavia*
Luca Vittorio Valenti, *Milano*
Mariateresa T Ventura, *Bari*
Giuseppe Verlato, *Verona*
Alessandro Vitale, *Padova*
Marco Vivarelli, *Ancona*
Giovanni Li Volti, *Catania*
Giuseppe Zanotti, *Padua*
Vincenzo Zara, *Lecce*
Gianguglielmo Zehender, *Milan*
Anna Linda Zignego, *Florence*
Rocco Antonio Zoccali, *Messina*
Angelo Zullo, *Rome*

Japan

Yasushi Adachi, *Sapporo*
Takafumi Ando, *Nagoya*
Masahiro Arai, *Tokyo*
Makoto Arai, *Chiba*
Takaaki Arigami, *Kagoshima*
Itaru Endo,*Yokohama*
Munechika Enjoji, *Fukuoka*
Shunji Fujimori, *Tokyo*
Yasuhiro Fujino, *Akashi*
Toshiyoshi Fujiwara, *Okayama*
Yosuke Fukunaga, *Tokyo*
Toshio Fukusato, *Tokyo*
Takahisa Furuta, *Hamamatsu*
Osamu Handa, *Kyoto*
Naoki Hashimoto, *Osaka*
Yoichi Hiasa, *Toon*
Masatsugu Hiraki, *Saga*
Satoshi Hirano, *Sapporo*
Keiji Hirata, *Fukuoka*
Toru Hiyama, *Higashihiroshima*
Akira Hokama, *Nishihara*
Shu Hoteya, *Tokyo*
Masao Ichinose, *Wakayama*
Tatsuya Ide, *Kurume*
Masahiro Iizuka, *Akita*
Toshiro Iizuka, *Tokyo*
Kenichi Ikejima, *Tokyo*
Tetsuya Ikemoto, *Tokushima*
Hiroyuki Imaeda, *Saitama*
Atsushi Imagawa, *Kan-onji*
Hiroo Imazu, *Tokyo*
Shuji Isaji, *Tsu*
Toru Ishikawa, *Niigata*
Toshiyuki Ishiwata, *Tokyo*
Soichi Itaba, *Kitakyushu*
Yoshiaki Iwasaki, *Okayama*
Tatehiro Kagawa, *Isehara*
Satoru Kakizaki, *Maebashi*
Naomi Kakushima, *Shizuoka*
Terumi Kamisawa, *Tokyo*
Akihide Kamiya, *Isehara*
Osamu Kanauchi, *Tokyo*
Tatsuo Kanda, *Chiba*
Shin Kariya, *Okayama*
Shigeyuki Kawa, *Matsumoto*
Takumi Kawaguchi, *Kurume*
Takashi Kawai, *Tokyo*
Soo Ryang Kim, *Kobe*
Shinsuke Kiriyama, *Gunma*
Tsuneo Kitamura, *Urayasu*
Masayuki Kitano, *Osakasayama*
Hirotoshi Kobayashi, *Tokyo*
Hironori Koga, *Kurume*
Takashi Kojima, *Sapporo*
Satoshi Kokura, *Kyoto*
Shuhei Komatsu, *Kyoto*
Tadashi Kondo, *Tokyo*
Yasuteru Kondo, *Sendai*
Yasuhiro Kuramitsu, *Yamaguchi*
Yukinori Kurokawa, *Osaka*
Shin Maeda, *Yokohama*
Koutarou Maeda, *Toyoake*
Hitoshi Maruyama, *Chiba*
Atsushi Masamune, *Sendai*
Hiroyuki Matsubayashi, *Suntogun*
Akihisa Matsuda, *Inzai*
Hirofumi Matsui, *Tsukuba*
Akira Matsumori, *Kyoto*
Yoichi Matsuo, *Nagoya*
Y Matsuzaki, *Ami*
Toshihiro Mitaka, *Sapporo*
Kouichi Miura, *Akita*
Shinichi Miyagawa, *Matumoto*
Eiji Miyoshi, *Suita*
Toru Mizuguchi, *Sapporo*
Nobumasa Mizuno, *Nagoya*
Zenichi Morise, *Nagoya*
Tomohiko Moriyama, *Fukuoka*
Kunihiko Murase, *Tusima*
Michihiro Mutoh, *Tsukiji*
Akihito Nagahara, *Tokyo*
Hikaru Nagahara, *Tokyo*
Hidenari Nagai, *Tokyo*
Koichi Nagata, *Shimotsuke-shi*

Masaki Nagaya, *Kawasaki*
Hisato Nakajima, *Nishi-Shinbashi*
Toshifusa Nakajima, *Tokyo*
Hiroshi Nakano, *Kawasaki*
Hiroshi Nakase, *Kyoto*
Toshiyuki Nakayama, *Nagasaki*
Takahiro Nakazawa, *Nagoya*
Shoji Natsugoe, *Kagoshima City*
Tsutomu Nishida, *Suita*
Shuji Nomoto, *Naogya*
Sachiyo Nomura, *Tokyo*
Takeshi Ogura, *Takatsukishi*
Nobuhiro Ohkohchi, *Tsukuba*
Toshifumi Ohkusa, *Kashiwa*
Hirohide Ohnishi, *Akita*
Teruo Okano, *Tokyo*
Satoshi Osawa, *Hamamatsu*
Motoyuki Otsuka, *Tokyo*
Michitaka Ozaki, *Sapporo*
Satoru Saito, *Yokohama*
Chouhei Sakakura, *Kyoto*
Naoaki Sakata, *Sendai*
Ken Sato, *Maebashi*
Toshiro Sato, *Tokyo*
Tomoyuki Shibata, *Toyoake*
H Shimada, *Tokyo*
Tomohiko Shimatani, *Kure*
Yukihiro Shimizu, *Nanto*
Tadashi Shimoyama, *Hirosaki*
Masayuki Sho, *Nara*
Ikuo Shoji, *Kobe*
Atsushi Sofuni, *Tokyo*
Takeshi Suda, *Niigata*
M Sugimoto, *Hamamatsu*
Ken Sugimoto, *Hamamatsu*
Haruhiko Sugimura, *Hamamatsu*
Shoichiro Sumi, *Kyoto*
Hidekazu Suzuki, *Tokyo*
Masahiro Tajika, *Nagoya*
Hitoshi Takagi, *Takasaki*
Toru Takahashi, *Niigata*
Yoshihisa Takahashi, *Tokyo*
Shinsuke Takeno, *Fukuoka*
Akihiro Tamori, *Osaka*
Kyosuke Tanaka, *Tsu*
Shinji Tanaka, *Hiroshima*
Atsushi Tanaka, *Tokyo*
Yasuhito Tanaka, *Nagoya*
Shinji Tanaka, *Tokyo*
Minoru Tomizawa, *Yotsukaido City*
Kyoko Tsukiyama-Kohara, *Kagoshima*
Takuya Watanabe, *Niigata*
Kazuhiro Watanabe, *Sendai*
Satoshi Yamagiwa, *Niigata*
Takayuki Yamamoto, *Yokkaichi*
Hiroshi Yamamoto, *Otsu*
Kosho Yamanouchi, *Nagasaki*
Ichiro Yasuda, *Gifu*
Yutaka Yata, *Maebashi-city*
Shin-ichi Yokota, *Sapporo*
Norimasa Yoshida, *Kyoto*
Hiroshi Yoshida, *Tama-City*
Hitoshi Yoshiji, *Kashihara*
Kazuhiko Yoshimatsu, *Tokyo*
Kentaro Yoshioka, *Toyoake*
Nobuhiro Zaima, *Nara*

Jordan
Khaled Ali Jadallah, *Irbid*

Kuwait
Islam Khan, *Kuwait*

Lebanon
Bassam N Abboud, *Beirut*
Kassem A Barada, *Beirut*
Marwan Ghosn, *Beirut*
Iyad A Issa, *Beirut*
Fadi H Mourad, *Beirut*
AIa Sharara, *Beirut*
Rita Slim, *Beirut*

Lithuania
Antanas Mickevicius, *Kaunas*

Malaysia
Huck Joo Tan, *Petaling Jaya*

Mexico
Richard A Awad, *Mexico City*
Carlos R Camara-Lemarroy, *Monterrey*
Norberto C Chavez-Tapia, *Mexico City*
Wolfgang Gaertner, *Mexico City*
Diego Garcia-Compean, *Monterrey*
Arturo Panduro, *Guadalajara*
OT Teramoto-Matsubara, *Mexico City*
Felix Tellez-Avila, *Mexico City*
Omar Vergara-Fernandez, *Mexico City*
Saúl Villa-Trevino, *Cuidad de México*

Morocco
Samir Ahboucha, *Khouribga*

Netherlands
Robert J de Knegt, *Rotterdam*
Tom Johannes Gerardus Gevers, *Nijmegen*
Menno Hoekstra, *Leiden*
BW Marcel Spanier, *Arnhem*
Karel van Erpecum, *Utrecht*

New Zealand
Leo K Cheng, *Auckland*
Andrew Stewart Day, *Christchurch*
Jonathan Barnes Koea, *Auckland*
Max Petrov, *Auckland*

Nigeria
Olufunmilayo Adenike Lesi, *Lagos*
Jesse Abiodun Otegbayo, *Ibadan*
Stella Ifeanyi Smith, *Lagos*

Norway
Trond Berg, *Oslo*
Trond Arnulf Buanes, *Krokkleiva*
Thomas de Lange, *Rud*
Magdy El-Salhy, *Stord*
Rasmus Goll, *Tromso*
Dag Arne Lihaug Hoff, *Aalesund*

Pakistan
Zaigham Abbas, *Karachi*
Usman A Ashfaq, *Faisalabad*
Muhammad Adnan Bawany, *Hyderabad*
Muhammad Idrees, *Lahore*
Saeed Sadiq Hamid, *Karachi*
Yasir Waheed, *Islamabad*

Poland
Thomas Brzozowski, *Cracow*
Magdalena Chmiela, *Lodz*
Krzysztof Jonderko, *Sosnowiec*
Anna Kasicka-Jonderko, *Sosnowiec*
Michal Kukla, *Katowice*
Tomasz Hubert Mach, *Krakow*
Agata Mulak, *Wroclaw*
Danuta Owczarek, *Kraków*
Piotr Socha, *Warsaw*
Piotr Stalke, *Gdansk*
Julian Teodor Swierczynski, *Gdansk*
Anna M Zawilak-Pawlik, *Wroclaw*

Portugal
Marie Isabelle Cremers, *Setubal*
Ceu Figueiredo, *Porto*
Ana Isabel Lopes, *LIsbon*
M Paula Macedo, *Lisboa*
Ricardo Marcos, *Porto*
Rui T Marinho, *Lisboa*
Guida Portela-Gomes, *Estoril*
Filipa F Vale, *Lisbon*

Puerto Rico
Caroline B Appleyard, *Ponce*

Qatar
Abdulbari Bener, *Doha*

Romania
Mihai Ciocirlan, *Bucharest*
Dan LucianDumitrascu, *Cluj-Napoca*
Carmen Fierbinteanu-Braticevici, *Bucharest*
Romeo G Mihaila, *Sibiu*
Lucian Negreanu, *Bucharest*
Adrian Saftoiu, *Craiova*
Andrada Seicean, *Cluj-Napoca*
Ioan Sporea, *Timisoara*
Letiția Adela Maria Streba, *Craiova*
Anca Trifan, *Iasi*

Russia

Victor Pasechnikov, *Stavropol*
Vasiliy Ivanovich Reshetnyak, *Moscow*
Vitaly Skoropad, *Obninsk*

Saudi Arabia

Abdul-Wahed N Meshikhes, *Dammam*
M Ezzedien Rabie, *Khamis Mushait*

Singapore

Brian KP Goh, *Singapore*
Richie Soong, *Singapore*
Ker-Kan Tan, *Singapore*
Kok-Yang Tan, *Singapore*
Yee-Joo Tan, *Singapore*
Mark Wong, *Singapore*
Hong Ping Xia, *Singapore*

Slovenia

Matjaz Homan, *Ljubljana*
Martina Perse, *Ljubljana*

South Korea

Sang Hoon Ahn, *Seoul*
Seung Hyuk Baik, *Seoul*
Soon Koo Baik, *Wonju*
Soo-Cheon Chae, *Iksan*
Byung-Ho Choe, *Daegu*
Suck Chei Choi, *Iksan*
Hoon Jai Chun, *Seoul*
Yeun-Jun Chung, *Seoul*
Young-Hwa Chung, *Seoul*
Ki-Baik Hahm, *Seongnam*
Sang Young Han, *Busan*
Seok Joo Han, *Seoul*
Seung-Heon Hong, *Iksan*
Jin-Hyeok Hwang, *Seoungnam*
Jeong Won Jang, *Seoul*
Jin-Young Jang, *Seoul*
Dae-Won Jun, *Seoul*
Young Do Jung, *Kwangju*
Gyeong Hoon Kang, *Seoul*
Sung-Bum Kang, *Seoul*
Koo Jeong Kang, *Daegu*
Ki Mun Kang, *Jinju*
Chang Moo Kang, *Seodaemun-gu*
Gwang Ha Kim, *Busan*
Sang Soo Kim, *Goyang-si*
Jin Cheon Kim, *Seoul*
Tae Il Kim, *Seoul*
Jin Hong Kim, *Suwon*
Kyung Mo Kim, *Seoul*
Kyongmin Kim, *Suwon*
Hyung-Ho Kim, *Seongnam*
Seoung Hoon Kim, *Goyang*
Sang Il Kim, *Seoul*
Hyun-Soo Kim, *Wonju*
Jung Mogg Kim, *Seoul*
Dong Yi Kim, *Gwangju*
Kyun-Hwan Kim, *Seoul*
Jong-Han Kim, *Ansan*
Sang Wun Kim, *Seoul*
Ja-Lok Ku, *Seoul*
Kyu Taek Lee, *Seoul*
Hae-Wan Lee, *Chuncheon*
Inchul Lee, *Seoul*
Jung Eun Lee, *Seoul*
Sang Chul Lee, *Daejeon*
Song Woo Lee, *Ansan-si*
Hyuk-Joon Lee, *Seoul*
Seong-Wook Lee, *Yongin*
Kil Yeon Lee, *Seoul*
Jong-Inn Lee, *Seoul*
Kyung A Lee, *Seoul*
Jong-Baeck Lim, *Seoul*
Eun-Yi Moon, *Seoul*
SH Noh, *Seoul*
Seung Woon Paik, *Seoul*
Won Sang Park, *Seoul*
Sung-Joo Park, *Iksan*
Kyung Sik Park, *Daegu*
Se Hoon Park, *Seoul*
Yoonkyung Park, *Gwangju*
Seung-Wan Ryu, *Daegu*
Il Han Song, *Cheonan*
Myeong Jun Song, *Daejeon*
Yun Kyoung Yim, *Daejeon*
Dae-Yeul Yu *Daejeon*

Spain

Mariam Aguas, *Valencia*
Raul J Andrade, *Málaga*
Antonio Arroyo, *Elche*
Josep M Bordas, *Barcelona*
Lisardo Boscá, *Madrid*
Ricardo Robles Campos, *Murcia*
Jordi Camps, *Reus*
Carlos Cervera *Barcelona*
Alfonso Clemente, *Granada*
Pilar Codoner-Franch, *Valencia*
Fernando J Corrales, *Pamplona*
Fermin Sánchez de Medina, *Granada*
Alberto Herreros de Tejada, *Majadahonda*
Enrique de-Madaria, *Alicante*
JE Dominguez-Munoz, *Santiago de Compostela*
Vicente Felipo, *Valencia*
CM Fernandez-Rodriguez, *Madrid*
Carmen Frontela-Saseta, *Murcia*
Julio Galvez, *Granada*
Maria Teresa García, *Vigo*
MI Garcia-Fernandez, *Málaga*
Emilio Gonzalez-Reimers, *La Laguna*
Marcel Jimenez, *Bellaterra*
Angel Lanas, *Zaragoza*
Juan Ramón Larrubia, *Guadalajara*
Antonio Lopez-Sanroman, *Madrid*
Vicente Lorenzo-Zuniga, *Badalona*
Alfredo J Lucendo, *Tomelloso*
Vicenta Soledad Martinez-Zorzano, *Vigo*
José Manuel Martin-Villa, *Madrid*
Julio Mayol, *Madrid*
Manuel Morales-Ruiz, *Barcelona*
Alfredo Moreno-Egea, *Murcia*
Albert Pares, *Barcelona*
Maria Pellise, *Barcelona*
José Perea, *Madrid*
Miguel Angel Plaza, *Zaragoza*
María J Pozo, *Cáceres*
Enrique Quintero, *La Laguna*
Jose M Ramia, *Madrid*
Francisco Rodriguez-Frias, *Barcelona*
Silvia Ruiz-Gaspa, *Barcelona*
Xavier Serra-Aracil, *Barcelona*
Vincent Soriano, *Madrid*
Javier Suarez, *Pamplona*
Carlos Taxonera, *Madrid*
M Isabel Torres, *Jaén*
Manuel Vazquez-Carrera, *Barcelona*
Benito Velayos, *Valladolid*
Silvia Vidal, *Barcelona*

Sri Lanka

Arjuna Priyadarsin De Silva, *Colombo*

Sudan

Ishag Adam, *Khartoum*

Sweden

Roland G Andersson, *Lund*
Bergthor Björnsson, *Linkoping*
Johan Christopher Bohr, *Örebro*
Mauro D'Amato, *Stockholm*
Thomas Franzen, *Norrkoping*
Evangelos Kalaitzakis, *Lund*
Riadh Sadik, *Gothenburg*
Per Anders Sandstrom, *Linkoping*
Ervin Toth, *Malmö*
Konstantinos Tsimogiannis, *Vasteras*
Apostolos V Tsolakis, *Uppsala*

Switzerland

Gieri Cathomas, *Liestal*
Jean Louis Frossard, *Geneve*
Christian Toso, *Geneva*
Stephan Robert Vavricka, *Zurich*
Dominique Velin, *Lausanne*

Thailand

Thawatchai Akaraviputh, *Bangkok*
P Yoysungnoen Chintana, *Pathumthani*
Veerapol Kukongviriyapan, *Muang*
Vijittra Leardkamolkarn, *Bangkok*
Varut Lohsiriwat, *Bangkok*
Somchai Pinlaor, *Khaon Kaen*
D Wattanasirichaigoon, *Bangkok*

Trinidad and Tobago

B Shivananda Nayak, *Mount Hope*

Tunisia

Ibtissem Ghedira, *Sousse*
Lilia Zouiten-Mekki, *Tunis*

Turkey

Inci Alican, *Istanbul*

Mustafa Altindis, *Sakarya*
Mutay Aslan, *Antalya*
Oktar Asoglu, *Istanbul*
Yasemin Hatice Balaban, *Istanbul*
Metin Basaranoglu, *Ankara*
Yusuf Bayraktar, *Ankara*
Süleyman Bayram, *Adiyaman*
Ahmet Bilici, *Istanbul*
Ahmet Sedat Boyacioglu, *Ankara*
Züleyha Akkan Cetinkaya, *Kocaeli*
Cavit Col, *Bolu*
Yasar Colak, *Istanbul*
Cagatay Erden Daphan, *Kirikkale*
Mehmet Demir, *Hatay*
Ahmet Merih Dobrucali, *Istanbul*
Gülsüm Ozlem Elpek, *Antalya*
Ayse Basak Engin, *Ankara*
Eren Ersoy, *Ankara*
Osman Ersoy, *Ankara*
Yusuf Ziya Erzin, *Istanbul*
Mukaddes Esrefoglu, *Istanbul*
Levent Filik, *Ankara*
Ozgur Harmanci, *Ankara*
Koray Hekimoglu, *Ankara*
Abdurrahman Kadayifci, *Gaziantep*
Cem Kalayci, *Istanbul*
Selin Kapan, *Istanbul*
Huseyin Kayadibi, *Adana*
Sabahattin Kaymakoglu, *Istanbul*
Metin Kement, *Istanbul*
Mevlut Kurt, *Bolu*
Resat Ozaras, *Istanbul*
Elvan Ozbek, *Adapazari*
Cengiz Ozcan, *Mersin*
Hasan Ozen, *Ankara*
Halil Ozguc, *Bursa*
Mehmet Ozturk, *Izmir*
Orhan V Ozkan, *Sakarya*
Semra Paydas, *Adana*
Ozlem Durmaz Suoglu, *Istanbul*
Ilker Tasci, *Ankara*
Müge Tecder-ünal, *Ankara*
Mesut Tez, *Ankara*
Serdar Topaloglu, *Trabzon*
Murat Toruner, *Ankara*
Gokhan Tumgor, *Adana*
Oguz Uskudar, *Adana*
Mehmet Yalniz, *Elazig*
Mehmet Yaman, *Elazig*
Veli Yazisiz, *Antalya*
Yusuf Yilmaz, *Istanbul*
Ozlem Yilmaz, *Izmir*
Oya Yucel, *Istanbul*
Ilhami Yuksel, *Ankara*

United Kingdom

Nadeem Ahmad Afzal, *Southampton*
Navneet K Ahluwalia, *Stockport*
Yeng S Ang, *Lancashire*
Ramesh P Arasaradnam, *Coventry*
Ian Leonard Phillip Beales, *Norwich*
John Beynon, *Swansea*
Barbara Braden, *Oxford*
Simon Bramhall, *Birmingham*
Geoffrey Burnstock, *London*
Ian Chau, *Sutton*
Thean Soon Chew, *London*
Helen G Coleman, *Belfast*
Anil Dhawan, *London*
Sunil Dolwani, *Cardiff*
Piers Gatenby, *London*
Anil T George, *London*
Pasquale Giordano, *London*
Paul Henderson, *Edinburgh*
Georgina Louise Hold, *Aberdeen*
Stefan Hubscher, *Birmingham*
Robin D Hughes, *London*
Nusrat Husain, *Manchester*
Matt W Johnson, *Luton*
Konrad Koss, *Macclesfield*
Anastasios Koulaouzidis, *Edinburgh*
Simon Lal, *Salford*
John S Leeds, *Aberdeen*
JK K Limdi, *Manchester*
Hongxiang Liu, *Cambridge*
Michael Joseph McGarvey, *London*
Michael Anthony Mendall, *London*
Alexander H Mirnezami, *Southampton*
J Bernadette Moore, *Guildford*
Claudio Nicoletti, *Norwich*
Savvas Papagrigoriadis, *London*
Sylvia LF Pender, *Southampton*
David Mark Pritchard, *Liverpool*
James A Ross, *Edinburgh*
Kamran Rostami, *Worcester*
Xiong Z Ruan, *London*
Dina Tiniakos, *Newcastle upon Tyne*
Frank I Tovey, *London*
Dhiraj Tripathi, *Birmingham*
Vamsi R Velchuru, *Great Yarmouth*
Nicholas T Ventham, *Edinburgh*
Diego Vergani, *London*
Jack Westwood Winter, *Glasgow*
Terence Wong, *London*
Ling Yang, *Oxford*

United States

Daniel E Abbott, *Cincinnati*
Ghassan K Abou-Alfa, *New York*
Julian Abrams, *New York*
David William Adelson, *Los Angeles*
Jonathan Steven Alexander, *Shreveport*
Tauseef Ali, *Oklahoma City*
Mohamed R Ali, *Sacramento*
Rajagopal N Aravalli, *Minneapolis*
Hassan Ashktorab, *Washington*
Shashi Bala, *Worcester*
Charles F Barish, *Raleigh*
P Patrick Basu, *New York*
Robert L Bell, *Berkeley Heights*
David Bentrem, *Chicago*
Henry J Binder, *New Haven*
Joshua Bleier, *Philadelphia*
Wojciech Blonski, *Johnson City*
Kenneth Boorom, *Corvallis*
Brian Boulay, *Chicago*
Carla W Brady, *Durham*
Kyle E Brown, *Iowa City*
Adeel A Butt, *Pittsburgh*
Weibiao Cao, *Providence*
Andrea Castillo, *Cheney*
Fernando J Castro, *Weston*
Adam S Cheifetz, *Boston*
Xiaoxin Luke Chen, *Durham*
Ramsey Cheung, *Palo Alto*
Parimal Chowdhury, *Little Rock*
Edward John Ciaccio, *New York*
Dahn L Clemens, *Omaha*
Yingzi Cong, *Galveston*
Laura Iris Cosen-Binker, *Boston*
Joseph John Cullen, *Lowa*
Mark J Czaja, *Bronx*
Mariana D Dabeva, *Bronx*
Christopher James Damman, *Seattle*
Isabelle G De Plaen, *Chicago*
Punita Dhawan, *Nashville*
Hui Dong, *La Jolla*
Wael El-Rifai, *Nashville*
Sukru H Emre, *New Haven*
Paul Feuerstadt, *Hamden*
Josef E Fischer, *Boston*
Laurie N Fishman, *Boston*
Joseph Che Forbi, *Atlanta*
Temitope Foster, *Atlanta*
Amy E Foxx-Orenstein, *Scottsdale*
Daniel E Freedberg, *New York*
Shai Friedland, *Palo Alto*
Virgilio George, *Indianapolis*
Ajay Goel, *Dallas*
Oliver Grundmann, *Gainesville*
Stefano Guandalini, *Chicago*
Chakshu Gupta, *St. Joseph*
Grigoriy E Gurvits, *New York*
Xiaonan Han, *Cincinnati*
Mohamed Hassan, *Jackson*
Martin Hauer-Jensen, *Little Rock*
Koichi Hayano, *Boston*
Yingli Hee, *Atlanta*
Samuel B Ho, *San Diego*
Jason Ken Hou, *Houston*
Lifang Hou, *Chicago*
K-Qin Hu, *Orange*
Jamal A Ibdah, *Columbia*
Robert Thomas Jensen, *Bethesda*
Huanguang "Charlie" Jia, *Gainesville*
Rome Jutabha, *Los Angeles*
Andreas M Kaiser, *Los Angeles*
Avinash Kambadakone, *Boston*
David Edward Kaplan, *Philadelphia*
Randeep Kashyap, *Rochester*
Rashmi Kaul, *Tulsa*
Ali Keshavarzian, *Chicago*
Amir Maqbul Khan, *Marshall*
Nabeel Hasan Khan, *New Orleans*
Sahil Khanna, *Rochester*
Kusum K Kharbanda, *Omaha*
Hyun Sik Kim, *Pittsburgh*
Joseph Kim, *Duarte*
Jae S Kim, *Gainesville*
Miran Kim, *Providence*
Timothy R Koch, *Washington*
Burton I Korelitz, *New York*
Betsy Kren, *Minneapolis*
Shiu-Ming Kuo, *Buffalo*
Michelle Lai, *Boston*
Andreas Larentzakis, *Boston*
Edward Wolfgang Lee, *Los Angeles*
Daniel A Leffler, *Boston*
Michael Leitman, *New York*

World Journal of Gastroenterology

Contents

Weekly Volume 21 Number 14 April 14, 2015

Contents

World Journal of Gastroenterology
Volume 21 Number 14 April 14, 2015

LETTERS TO THE EDITOR

World Journal of Gastroenterology
Volume 21 Number 14 April 14, 2015

Contents

NAME OF JOURNAL
World Journal of Gastroenterology

ISSN
ISSN 1007-9327 (print)
ISSN 2219-2840 (online)

LAUNCH DATE
October 1, 1995

FREQUENCY
Weekly

EDITORIAL OFFICE
Jin-Lei Wang, Director
Xiu-Xia Song, Vice Director
World Journal of Gastroenterology
Room 903, Building D, Ocean International Center,
No. 62 Dongsihuan Zhonglu, Chaoyang District,
Beijing 100025, China
Telephone: +86-10-59080039
Fax: +86-10-85381893
E-mail: editorialoffice@wjgnet.com
Help Desk: http://www.wjgnet.com/esps/helpdesk.aspx
http://www.wjgnet.com

PUBLISHER
Baishideng Publishing Group Inc
8226 Regency Drive,
Pleasanton, CA 94588, USA
Telephone: +1-925-223-8242
Fax: +1-925-223-8243
E-mail: bpgoffice@wjgnet.com
Help Desk: http://www.wjgnet.com/esps/helpdesk.aspx
http://www.wjgnet.com

PUBLICATION DATE
April 14, 2015

INSTRUCTIONS TO AUTHORS
Full instructions are available online at http://www.wjgnet.com/1007-9327/g_info_20100315215714.htm

ONLINE SUBMISSION
http://www.wjgnet.com/esps/

World Journal of Gastroenterology

Submit a Manuscript: http://www.wjgnet.com/esps/
Help Desk: http://www.wjgnet.com/esps/helpdesk.aspx
DOI: 10.3748/wjg.v21.i14.4103

World J Gastroenterol 2015 April 14; 21(14): 4103-4110
ISSN 1007-9327 (print) ISSN 2219-2840 (online)

EDITORIAL

Nonalcoholic fatty liver disease, metabolic risk factors, and hepatocellular carcinoma: An open question

Letiția Adela Maria Streba, Cristin Constantin Vere, Ion Rogoveanu, Costin Teodor Streba

Letiția Adela Maria Streba, Internal Medicine, Medical Semiology, University of Medicine and Pharmacy of Craiova, 200639 Craiova, Romania
Cristin Constantin Vere, Ion Rogoveanu, Costin Teodor Streba, Research Center of Gastroenterology and Hepatology of Craiova, University of Medicine and Pharmacy of Craiova, 200639 Craiova, Romania
Cristin Constantin Vere, Ion Rogoveanu, Internal Medicine, Gastroenterology, University of Medicine and Pharmacy of Craiova, 200639 Craiova, Romania
Author contributions: Streba LAM, Vere CC, and Rogoveanu I contributed equally to this manuscript and share first authorship; Streba LAM and Vere CC wrote this paper; Rogoveanu I and Streba CT performed the literature search and critically revised the text.
Supported by Grant from European Social Found, Human Resources Development Operational Programme 2007-2013, No. POSDRU/159/1.5/133377.
Conflict-of-interest: The authors have no conflicts of interest to disclose.

Correspondence to: Costin Teodor Streba, MD, PhD, MSc, Research Center of Gastroenterology and Hepatology of Craiova, University of Medicine and Pharmacyof Craiova, 1 Mai 66, 200639 Craiova, Romania. costinstreba@gmail.com
Telephone: +40-722-389906
Fax: +40-351-401376
Received: November 29, 2014
Peer-review started: November 29, 2014
First decision: December 26, 2014
Revised: January 17, 2015
Accepted: February 13, 2015
Article in press: February 13, 2015
Published online: April 14, 2015

Abstract

Non-alcoholic liver disease (NAFLD) defines liver abnormalities ranging from simple steatosis to nonalcoholic steatohepatitis with or without cirrhosis development, occurring in the absence of significant alcohol consumption, use of teratogenic medication, or hereditary disorders. The association between NAFLD and metabolic syndrome is well documented and widely recognized. Obesity, type 2 diabetes mellitus (T2DM), and dyslipidemia are the most common metabolic risk factors associated with NAFLD. Among the components of metabolic syndrome, current evidence strongly indicates obesity and diabetes as hepatocellular carcinoma (HCC) risk factors. There is also growing evidence that suggests an increased risk of HCC in NAFLD patients, even surpassing other etiologies in some high-income countries. Epidemiologic data demonstrate a parallel rise in prevalence of obesity, diabetes, NAFLD, and HCC. As obesity and its related diseases have steadily afflicted larger populations, HCC incidence is expected to increase in the future. Pathophysiologic mechanisms that underlie NAFLD development and subsequent progression to nonalcoholic steatohepatitis and cirrhosis (insulin resistance and hyperinsulinemia, oxidative stress, hepatic stellate cell activation, cytokine/adipocytokine signaling pathways, and genetic and environmental factors) appear to play a significant role in the development of NAFLD-related HCC. However, a comprehensive view of molecular mechanisms linking obesity, T2DM, and NAFLD-related HCC, as well as the exact sequence of molecular events, is still not understood in its entirety. Good-quality data are still necessary, and efforts should continue towards better understanding the underlying carcinogenic mechanisms of NAFLD-related HCC. In this paper, we aimed to centralize the most important links supporting these relationships, focusing on obesity, T2DM, and NAFLD-

related HCC, as well as point out the major gaps in knowledge regarding the underlying molecular mechanisms behind them.

Key words: Diabetes mellitus; Hepatocellular carcinoma; Metabolic syndrome; Non-alcoholic fatty liver disease; Obesity

Core tip: Nonalcoholic liver disease (NAFLD) comprises both simple steatosis or nonalcoholic fatty liver and nonalcoholic steatohepatitis, with or without cirrhosis. Recent data demonstrate a strong association between most features of metabolic syndrome and NAFLD. Hepatocellular carcinoma (HCC) is the most common primary malignancy of the liver, for which current epidemiologic data show an increased incidence in NAFLD patients. Basic research has identified pathways linking obesity, type 2 diabetes, systemic inflammation, NAFLD/nonalcoholic steatohepatitis, and HCC. However, more data are necessary in order to effectively establish these relationships, and perhaps pave the way for possible cures to prevent HCC in certain populations.

Streba LAM, Vere CC, Rogoveanu I, Streba CT. Nonalcoholic fatty liver disease, metabolic risk factors, and hepatocellular carcinoma: An open question. *World J Gastroenterol* 2015; 21(14): 4103-4110 Available from: URL: http://www.wjgnet.com/1007-9327/full/v21/i14/4103.htm DOI: http://dx.doi.org/10.3748/wjg.v21.i14.4103

INTRODUCTION

Nonalcoholic liver disease (NAFLD) defines liver abnormalities ranging from simple steatosis or nonalcoholic fatty liver to nonalcoholic steatohepatitis (NASH) with or without cirrhosis development. The current definition of NAFLD does not require secondary hepatic fat accumulation, such as significant alcohol consumption, use of steatogenic medication, or hereditary disorders[1-3]. Several studies have independently demonstrated a strong association between NAFLD and each feature of metabolic syndrome (MetS)[4-7]. Currently, all guidelines agree that NAFLD is strictly associated with metabolic risk factors[3], especially obesity, type 2 diabetes mellitus (T2DM), and dyslipidemia[2]. Although it has been suggested that NAFLD is a MetS hepatic feature[5,8,9], a study based on data analysis from 3846 subjects of the United States third National Health and Nutrition Examination Survey found that NAFLD is not an independent component or manifestation of MetS, but rather a condition strongly associated with MetS features[10].

Although being overweight and obese are preventable and modifiable conditions, their prevalence has increased globally in recent decades[11]. These conditions, as well as their related diseases such as T2DM, coronary heart disease, stroke, some cancer types, NAFLD, and osteoarthritis, have a large economic impact on the health care system[12-14]. There is numerous evidence that obesity is a risk factor for digestive cancers such as esophageal[15], colorectal[16-18], bile duct[13], pancreatic[12,19], and liver[12,18,20,21] cancer.

Primary liver cancer is a major contributor to global cancer incidence and mortality[22]. Worldwide, liver cancer is the fifth most common cancer and the second most frequent cause of cancer death in men, while in women it is the seventh most commonly diagnosed cancer and the sixth leading cause of cancer death[23]. Major risk factors for hepatocellular carcinoma (HCC), the most common histologic type of primary liver cancer, include hepatitis B virus (HBV) and hepatitis C virus (HCV) chronic infections, alcoholic liver disease, and NAFLD[24].

Several population-based studies conducted in various geographic areas have recorded a significantly increased incidence of HCC in patients with diabetes and obesity[12,18,20,21,25]. There is also growing evidence that suggests an increased risk of HCC in NAFLD patients[26-28]. Under these circumstances, NAFLD-related HCC incidence is expected to increase in the future.

Considering that obesity is preventable, and other metabolic features (*i.e.*, diabetes mellitus and dyslipidemia) can be "controlled", a question arises: "Can NAFLD, and consequently NAFLD-related HCC, be prevented in some way?" According to a perhaps overly simplistic interpretation, due to a present lack of a comprehensive view of multiple pathways involved in NAFLD-related HCC pathogenesis, the answer might be "Yes".

METABOLIC RISK FACTORS, NAFLD, AND HCC

Epidemiologic evidence

There is growing evidence that overweight and obesity, defined by the body mass index (BMI)[11], and MetS have reached a pandemic dimension. According to the World Health Organization, more than 1.4 billion adults (35% of adults) worldwide were overweight (BMI $\geqslant$ 25-29.9 kg/m^2), and of these, 500 million (13% of adults) were obese (BMI $\geqslant$ 30 kg/m^2), in 2008[29]. If overweight and obesity rates continue at their current pace, it is estimated that 3.3 billion adults (57.8% of adults) will become overweight or obese by 2030[30]. On the other hand, overweight and obesity are leading risks for overall mortality, accounting for approximately 3.4 million adult deaths each year. Additionally, they are responsible for 44% of the diabetes burden, 23% of the ischemic heart disease burden, and between 7%

and 41% of certain cancer burdens[11].

Although BMI is the most commonly reported index in epidemiologic studies, body fat topography, and especially truncal or central obesity, appear to be more important in pathophysiologic mechanisms that link obesity and cancer. Central obesity, measured by waist circumference or the waist-to-hip or waist-to-height ratios, is the key feature of most MetS definitions, and has also been known to be directly correlated with insulin resistance[31-33].

There is a strong evidence for the association between obesity and T2DM. According to results of a study that analyzed the United States third National Health and Nutrition Examination Survey 1999-2006 data, the prevalences of overweight and obesity among United States adults with diabetes were 80.3% and 49.1%, respectively[34]. Overweight and obesity are responsible for about 80% of cases of T2DM in most European countries[35]. The same parallel between obesity and T2DM rates was not observed in Asian populations, where the risk to develop diabetes begins even at a lower BMI. Despite lower rates of overweight and obesity than the United States or Europe, many Asian countries have similar or higher rates of T2DM. Higher prevalence of central obesity without necessarily developing generalized obesity in Asian populations may explain the increased T2DM predisposition among normal-weight individuals[36].

Current evidence strongly indicates that obesity and diabetes are HCC risk factors[37-40]. A meta-analysis of 11 cohort studies from Europe, the United States, and Asia showed that summary relative risks (SRRs) with 95%CI of HCC were 1.17 (95%CI: 1.02-1.34) for overweight and 1.89 (95%CI: 1.51-2.36) for obese individuals, compared with normal-weight individuals[41]. Similarly, a meta-analysis of 26 prospective observational studies including 25337 HCC cases reported that excess body weight (SRR = 1.48, 95%CI: 1.31-1.67) and obesity (SRR = 1.83, 95%CI: 1.59-2.11) are associated with an increased risk of HCC in both males and females[42]. The positive associations observed in that study were independent of geographic location, alcohol consumption, and history of diabetes or HBV and/or HCV infections. An evaluation based on a systematic review of nine cohort studies in a Japanese population indicates a relative risk of 1.74 (95%CI: 1.33-2.28) for overweight/obese individuals compared with normal/low-weight individuals[43].

The association between general obesity and the risk of HCC has been studied more than the relationship between central obesity and HCC risk. According to the results of a recent multicenter prospective European cohort study, central obesity promotes a high risk for HCC, as waist-to-height ratio showed the strongest association with HCC, independent of general body weight[44].

Epidemiologic studies estimate that diabetes is associated with a 2-4-fold greater risk of HCC compared with nondiabetics, independently of other major HCC risk factors[39]. In a large longitudinal study (173643 patients with diabetes and 650620 patients without) with a follow-up of 10-15 years, NAFLD incidence was significantly higher among patients with diabetes (incidence rate 18.13 *vs* 9.55 per 10000 person-years, respectively, $P < 0.0001$). Similarly, a significantly higher incidence of HCC among patients with diabetes was obtained (incidence rate: 2.39 *vs* 0.87 per 10000 person-years, respectively, $P < 0.0001$)[45]. A systematic review and meta-analysis of 26 studies (13 case-control and 13 cohort) published in 2006 by El-Serag *et al*[46] revealed a 2.5-fold greater risk of HCC among patients with diabetes compared with nondiabetic controls. This significant association was independent of alcohol use or viral hepatitis in studies that examined these factors. Another systematic review and meta-analysis, published in 2012 by Wang *et al*[47], showed slightly lower SRRs. Based on 25 cohort studies, this meta-analysis revealed that individuals with diabetes have a 2.0-fold increased risk of HCC, compared with nondiabetics (SRR = 2.01, 95%CI: 1.61-2.51).

Epidemiologic data demonstrate that both obesity and T2DM increases the HCC risk. NAFLD, which is present in up to 90% of all obese persons and up to 70% of T2DM patients[24], appears to play a key role in HCC development. In a large United States healthcare database study between 2002 and 2008, NAFLD was the most common underlying HCC risk factor (59%), followed by diabetes (36%) and HCV infection (22%)[48]. Similar results were obtained in a study performed in Germany, which identified NAFLD as the most common etiology for HCC, exceeding HBV and HCV chronic infection, as well as alcoholic liver disease[49]. These results could be explained by effective measures to reduce HCV infection incidence, the major source of HCC in the United States and other developed countries, together with increasing NAFLD prevalence in these geographic areas[50].

The majority of patients with NAFLD have fatty livers, and their liver-related death rate is significantly lower, while approximately 20% of NAFLD cases have NASH that may progress to cirrhosis (20%-45%), a well-recognized HCC risk factor[51,52]. On the other hand, most cases of HCC (80%-90%) occur in liver cirrhosis of various etiologies[24], and NAFLD seems to be no exception[22]. HCC development in cirrhotic NAFLD is well documented. Results of a recent meta-analysis showed an increased HCC risk for cohorts with NASH and cirrhosis (cumulative incidence between 2.4% over 7 years to 12.8% over 3 years)[28]. However, the HCC risk in NASH cohorts was substantially lower than in HCV-related cirrhosis cohorts according to this study. Recent epidemiologic evidence also suggests an association between noncirrhotic NAFLD and HCC risk[53-58]. Yet, several gaps were identified in current understanding of the epidemiologic evidence that support the occurrence of HCC in noncirrhotic and cirrhotic NAFLD: there were few large cohorts with

long-term follow-up, most studies were underpowered to perform multivariate analysis[28], few studies on ethnicity-dependent differences[59], and few studies to assess the quality of epidemiologic evidence.

In summary, epidemiologic data demonstrate a parallel increase in the prevalences of obesity, T2DM, and NAFLD-related HCC. Cumulatively, the epidemiologic evidence suggests an association between the main components of MetS (obesity and T2DM) together with NAFLD, and an increased HCC risk, which is better documented in NASH-cirrhosis cohorts.

Animal models

Findings from animal models are necessary for a better understanding of the complex inter-relationships between NAFLD, metabolic risk factors and HCC. Using a novel mouse model of NASH-HCC on a diabetic background *via* a combination of streptozotocin and high-fat diet (the STAM model), Fujii *et al*[60] demonstrated the inter-relationships between NAFLD/NASH, T2DM, and HCC development. This study provided strong evidence that NASH-related fibrosis is an essential histologic process for HCC development in diabetic populations.

In a recent study, Dowman *et al*[61] evaluated the liver-related consequences of long-term diet-induced obesity in a murine model of NASH, using the American Lifestyle-Induced Obesity Syndrome (ALIOS) based on high-fat/fructose diet and sedentary lifestyle. This study indicates that, in the absence of toxins or genetic variation, ALIOS mice developed NASH, stem cell mediated-regeneration, and HCC. Park *et al*[62] demonstrated in an experimental mouse model the key role of dietary or genetic obesity in HCC development, as well as the pathophysiologic mechanisms linking obesity, inflammation, and HCC.

Pathophysiologic link

Although there is a great amount of progress in understanding the carcinogenesis, the exact mechanism of HCC development in NAFLD has not yet been fully elucidated. However, several lines of evidence demonstrate a strong association between chronic inflammation and cancer, including HCC[63].

Dysregulation of both hormonal axes and cytokines pathways during obesity, diabetes, and NAFLD promotes a vicious cycle between metabolic and immune responses, inducing a chronic active inflammatory state that may lead to hepatocarcinogenesis. Thus, pathophysiologic mechanisms that underlay nonalcoholic fatty liver development and subsequent progression to NASH and cirrhosis (insulin resistance and hyperinsulinemia, oxidative stress, hepatic stellate cells activation, cytokine/adipocytokine signaling pathways, genetic and environmental factors)[64] have also been shown to promote the development of NAFLD-related HCC[38,40,55,57,65].

Insulin resistance and subsequent compensatory hyperinsulinemia have been shown to have a key role in the pathogenesis of NAFLD-related HCC[66]. The insulin-like growth factor (IGF) axis, closely linked to insulin resistance and hyperinsulinemia, plays an important role in HCC pathogenesis[67], particularly in NAFLD-related HCC[68].

The IGF axis includes three ligands (insulin, IGF-1, and IGF-2), three receptors (insulin receptor, IGF-1R, and IGF-2R), substrates [insulin receptor substrate (IRS) and Shc proteins], and ligand binding proteins[69,70]. Insulin resistance and hyperinsulinemia have been shown to upregulate IGFs and IRS-1 production[71], thus contributing to HCC pathogenesis[66]. IGF-1 is produced by several tissues such as liver, bone, muscle, and brain[70]. However, the liver is the main source of circulating IGF-1 during the postnatal period. IGF-1 synthesized in the liver acts as an endocrine growth factor, while IGF-1 synthesized by other tissues acts locally, in a paracrine and/or autocrine manner[72]. Yet, during hepatocarcinogenesis, IGF-1 secretion by adjacent hepatocytes may lead to paracrine stimulation of HCC and more aggressive tumor behavior[68].

IGF-1 can act on various receptors, but has a higher affinity for IGF-1R[70]. IGF-1R, a tyrosine kinase receptor, is overexpressed *in vitro* and in animal models of HCC, and is also involved in the degeneration of preneoplastic lesions[40]. However, insulin receptors and IGF-1R share almost the same signaling pathway[70]. Binding of insulin and IGF-1 to insulin receptors and IGF-1R, respectively, promotes liver carcinomatosis and tumor development by stimulating cell proliferation and inhibiting apoptosis. IGF-1 also promotes angiogenesis through increased vascular endothelial growth factor production[58,73,74].

IGF-2 is highly expressed in fetal liver, but its level decreases after birth. However, IGF-2 expression is increased in viral hepatitis and cirrhosis, as well as in HCC[69]. During hepatocarcinogenesis, IGF-2 has multiple protumorigenic functions such as inhibiting apoptosis, promoting cellular proliferation, and activating angiogenesis[74].

Another key component of the IGF axis and hepatocarcinogenesis is IRS-1, the main substrate of IGF-IR activation. IRS-1 is overexpressed in HCC and is also shown to be involved in cytokine signaling pathways[75].

Oxidative stress and cytokine/adipocytokine pathways are two other important links in NAFLD-related HCC pathogenesis. The development and progression of NAFLD is also associated with oxidative stress and release of reactive oxygen species (ROS), which likely contribute to the development of HCC[38]. Existence of preneoplastic changes such as increased hepatocyte proliferation and decreased apoptosis have been documented in the steatotic liver of *ob/ob* mice, before fibrosis or cirrhosis occurs. Because hepatic mitochondrial production of ROS is significantly

increased in *ob/ob* mice, it has been suggested that oxidative stress is one of the mechanisms driving hepatocyte proliferation in nonalcoholic fatty livers[76].

Increased oxidative stress induced by hepatic mitochondrial, peroxisomal, and microsomal ROS[77,78] results in apoptosis, necrosis, inflammation, hepatic stellate cell activation and fibrogenesis, proinflammatory cytokine expression, and cell proliferation[26,79]. Direct effects of ROS, generally attributed to high concentrations at the damage site, include DNA alteration that leads to genomic instability and mutations in proto-oncogenes and tumor suppressor genes, thus fostering neoplastic transformation[80]. An eloquent example is the product of lipid peroxidation, trans-4-hydroxy-2-nonenal, which has been shown to be responsible for mutations of the *p53* tumor suppressor gene, the most frequent abnormality identified in human tumors, including HCC[81]. In addition, ROS can stimulate signal transduction pathways and lead to activation of key transcription factors such as nuclear respiratory factor (Nrf) and nuclear factor (NF)-κB. Nrf1-deficient hepatocytes in an animal model showed increased susceptibility to oxidative stress and damage, resulting in NAFLD and HCC[82]. Inhibition of NF-κB in mouse livers induces NASH and HCC by sensitizing hepatocytes to spontaneous apoptosis[38]. In the setting of hyperinsulinemia, ROS plays an important role in the activation of c-Jun amino-terminal kinase 1 (JNK1). JNK1 appears to be the most important kinase that is upregulated in NAFLD-related HCC[83]. On the other hand, ROS trigger the release of proinflammatory cytokines, which in turn enhance ROS production and cellular injury[84].

The role of proinflammatory cytokines including tumor necrosis factor (TNF)-α, interleukin (IL)-6, leptin, and resistin, as well as the role of decreased amounts of adiponectin in NAFLD development and progression, is well documented[4,5,85-87]. TNF-α activates pro-oncogenic pathways, including JNK, NF-κB, mammalian target of rapamycin, and the extracellular signal-regulated kinases, thus enhancing the production of IL-6[40,87]. IL-6 intracellular signaling involves a complex network of various pathways, including phosphoinositide 3-kinase/protein kinase B, mitogen activated protein kinase, and signal transducer and activator of transcription 3, which lead to cell proliferation, protection from apoptosis, and increased metastatic potential[88]. Adiponectin has been shown to have hepatic cytoprotective properties, improving both hepatic and peripheral insulin sensitivity, and preventing steatosis, inflammation, necrosis, and fibrosis[64]. Animal model studies have shown that hypoadiponectinemia is involved in HCC development[89].

Genetic and environmental factors, as well as the interaction between them, may be responsible for both the individual susceptibility and the clinical course of NAFLD. Recent studies emphasize the role of specific genetic variation in NAFLD susceptibility and NAFLD-related hepatocarcinogenesis. To date, several genetic variants that contribute to NAFLD susceptibility and its progression were identified by genome-wide association studies. Additionally, genetic risk factors for NAFLD were evaluated and validated in large multicenter studies[90,91]. In 2008, two genome-wide association studies independently identified several single nucleotide polymorphisms that are associated with increased hepatic fat content[92] and elevated plasma liver enzyme levels[93]. Romeo *et al*[92] identified a non-synonymous coding single nucleotide polymorphism (rs738409 C/G) that results in an isoleucine to methionine substitution at residue 148 (I148M) in human patatin-like phospholipase domain-containing 3 (*PNPLA3*), which is strongly associated with increased hepatic fat levels. This study also demonstrated that variation in *PNPLA3* contributes to inter-individual differences in hepatic fat content and NAFLD susceptibility. Moreover, it has been shown that the *PNPLA3* I148M polymorphism favors NAFLD progression and liver fibrosis[94], is associated with an increased risk of HCC in severely obese individuals[95], and confers an increased risk of NAFLD-related HCC[96].

In summary, the interplay, interaction and overlapping of all pathogenic pathways creates a vicious circle that leads to NAFLD-related HCC development.

CONCLUSION

Although significant progress has been made in NAFLD-related HCC, many issues remain to be resolved. A unified and comprehensive view of multiple pathways involved in NAFLD-related HCC pathogenesis is currently lacking.

Uncovering the intricate molecular pathways facilitating HCC development will pave the way for developing molecular therapeutic agents aimed at the receptors and specific signaling agents involved. Additionally, preventing obesity, diabetes, MeTs, and NAFLD through efficient measures might lead to a decreased rate of NAFLD-related HCC.

REFERENCES

1 **Angulo P**. Nonalcoholic fatty liver disease. *N Engl J Med* 2002; **346**: 1221-1231 [PMID: 11961152 DOI: 10.1056/NEJMra011775]

2 **Chalasani N**, Younossi Z, Lavine JE, Diehl AM, Brunt EM, Cusi K, Charlton M, Sanyal AJ. The diagnosis and management of non-alcoholic fatty liver disease: practice Guideline by the American Association for the Study of Liver Diseases, American College of Gastroenterology, and the American Gastroenterological Association. *Hepatology* 2012; **55**: 2005-2023 [PMID: 22488764 DOI: 10.1002/hep.25762]

3 **Nascimbeni F**, Pais R, Bellentani S, Day CP, Ratziu V, Loria P, Lonardo A. From NAFLD in clinical practice to answers from guidelines. *J Hepatol* 2013; **59**: 859-871 [PMID: 23751754 DOI: 10.1016/j.jhep.2013.05.044]

4 **Marchesini G**, Brizi M, Morselli-Labate AM, Bianchi G, Bugianesi E, McCullough AJ, Forlani G, Melchionda N. Association of nonalcoholic fatty liver disease with insulin resistance. *Am J Med*

1999; **107**: 450-455 [PMID: 10569299]
5 **Marchesini G**, Brizi M, Bianchi G, Tomassetti S, Bugianesi E, Lenzi M, McCullough AJ, Natale S, Forlani G, Melchionda N. Nonalcoholic fatty liver disease: a feature of the metabolic syndrome. *Diabetes* 2001; **50**: 1844-1850 [PMID: 11473047 DOI: 10.2337/diabetes.50.8.1844]
6 **Hsiao PJ**, Kuo KK, Shin SJ, Yang YH, Lin WY, Yang JF, Chiu CC, Chuang WL, Tsai TR, Yu ML. Significant correlations between severe fatty liver and risk factors for metabolic syndrome. *J Gastroenterol Hepatol* 2007; **22**: 2118-2123 [PMID: 18031368 DOI: 10.1111/j.1440-1746.2006.04698.x]
7 **Jimba S**, Nakagami T, Takahashi M, Wakamatsu T, Hirota Y, Iwamoto Y, Wasada T. Prevalence of non-alcoholic fatty liver disease and its association with impaired glucose metabolism in Japanese adults. *Diabet Med* 2005; **22**: 1141-1145 [PMID: 16108839 DOI: 10.1111/j.1464-5491.2005.01582.x]
8 **Tarantino G**, Saldalamacchia G, Conca P, Arena A. Non-alcoholic fatty liver disease: further expression of the metabolic syndrome. *J Gastroenterol Hepatol* 2007; **22**: 293-303 [PMID: 17295757 DOI: 10.1111/j.1440-1746.2007.04824.x]
9 **Tarantino G**, Finelli C. What about non-alcoholic fatty liver disease as a new criterion to define metabolic syndrome? *World J Gastroenterol* 2013; **19**: 3375-3384 [PMID: 23801829 DOI: 10.3748/wjg.v19.i22.3375]
10 **Smits MM**, Ioannou GN, Boyko EJ, Utzschneider KM. Non-alcoholic fatty liver disease as an independent manifestation of the metabolic syndrome: results of a US national survey in three ethnic groups. *J Gastroenterol Hepatol* 2013; **28**: 664-670 [PMID: 23286209 DOI: 10.1111/jgh.12106]
11 World Health Organisation (WHO): Overweight and Obesity Factsheet. Available from: URL: http://www.who.int/mediacentre/factsheets/fs311/en/
12 **Haslam DW**, James WP. Obesity. *Lancet* 2005; **366**: 1197-1209 [PMID: 16198769 DOI: 10.1016/s0140-6736(05)67483-1]
13 **Parsi MA**. Obesity and cholangiocarcinoma. *World J Gastroenterol* 2013; **19**: 457-462 [PMID: 23382624 DOI: 10.3748/wjg.v19.i4.457]
14 **Polednak AP**. Estimating the number of U.S. incident cancers attributable to obesity and the impact on temporal trends in incidence rates for obesity-related cancers. *Cancer Detect Prev* 2008; **32**: 190-199 [PMID: 18790577 DOI: 10.1016/j.cdp.2008.08.004]
15 **Murray L**, Romero Y. Role of obesity in Barrett's esophagus and cancer. *Surg Oncol Clin N Am* 2009; **18**: 439-452 [PMID: 19500735 DOI: 10.1016/j.soc.2009.03.010]
16 **Frezza EE**, Wachtel MS, Chiriva-Internati M. Influence of obesity on the risk of developing colon cancer. *Gut* 2006; **55**: 285-291 [PMID: 16239255 DOI: 10.1136/gut.2005.073163]
17 **Larsson SC**, Wolk A. Obesity and colon and rectal cancer risk: a meta-analysis of prospective studies. *Am J Clin Nutr* 2007; **86**: 556-565 [PMID: 17823417]
18 **Renehan AG**, Tyson M, Egger M, Heller RF, Zwahlen M. Body-mass index and incidence of cancer: a systematic review and meta-analysis of prospective observational studies. *Lancet* 2008; **371**: 569-578 [PMID: 18280327 DOI: 10.1016/s0140-6736(08)60269-x]
19 **Zyromski NJ**, White PB. Pancreatic cancer in obesity: epidemiology, clinical observations, and basic mechanisms. *Anticancer Agents Med Chem* 2011; **11**: 470-478 [PMID: 21492072 DOI: 10.2174/1871520117956774 45]
20 **Nair S**, Mason A, Eason J, Loss G, Perrillo RP. Is obesity an independent risk factor for hepatocellular carcinoma in cirrhosis? *Hepatology* 2002; **36**: 150-155 [PMID: 12085359 DOI: 10.1053/jhep.2002.33713]
21 **Sun B**, Karin M. Obesity, inflammation, and liver cancer. *J Hepatol* 2012; **56**: 704-713 [PMID: 22120206 DOI: 10.1016/j.jhep.2011.09.020]
22 **McGlynn KA**, London WT. The global epidemiology of hepatocellular carcinoma: present and future. *Clin Liver Dis* 2011; **15**: 223-43, vii-x [PMID: 21689610 DOI: 10.1016/j.cld.2011.03.006]
23 **Jemal A**, Bray F, Center MM, Ferlay J, Ward E, Forman D. Global cancer statistics. *CA Cancer J Clin* 2011; **61**: 69-90 [PMID: 21296855 DOI: 10.3322/caac.20107]
24 **El-Serag HB**. Hepatocellular carcinoma. *N Engl J Med* 2011; **365**: 1118-1127 [PMID: 21992124 DOI: 10.1056/nejmra1001683]
25 **Koh WP**, Wang R, Jin A, Yu MC, Yuan JM. Diabetes mellitus and risk of hepatocellular carcinoma: findings from the Singapore Chinese Health Study. *Br J Cancer* 2013; **108**: 1182-1188 [PMID: 23370206 DOI: 10.1038/bjc.2013.25]
26 **Bugianesi E**, Leone N, Vanni E, Marchesini G, Brunello F, Carucci P, Musso A, De Paolis P, Capussotti L, Salizzoni M, Rizzetto M. Expanding the natural history of nonalcoholic steatohepatitis: from cryptogenic cirrhosis to hepatocellular carcinoma. *Gastroenterology* 2002; **123**: 134-140 [PMID: 12105842 DOI: 10.1053/gast.2002.34168]
27 **Marchesini G**, Forlani G, Bugianesi E. Is liver disease a threat to patients with metabolic disorders? *Ann Med* 2005; **37**: 333-346 [PMID: 16179269 DOI: 10.1080/07853890510011445]
28 **White DL**, Kanwal F, El-Serag HB. Association between nonalcoholic fatty liver disease and risk for hepatocellular cancer, based on systematic review. *Clin Gastroenterol Hepatol* 2012; **10**: 1342-1359.e2 [PMID: 23041539 DOI: 10.1016/j.cgh.2012.10.001]
29 World Health Organisation (WHO): Global Database on Body Mass Index. Available from: URL: http://apps.who.int/bmi/index.jsp?introPage=intro_3.html&
30 **Kelly T**, Yang W, Chen CS, Reynolds K, He J. Global burden of obesity in 2005 and projections to 2030. *Int J Obes* (Lond) 2008; **32**: 1431-1437 [PMID: 18607383 DOI: 10.1038/ijo.2008.102]
31 **Alberti KG**, Zimmet PZ. Definition, diagnosis and classification of diabetes mellitus and its complications. Part 1: diagnosis and classification of diabetes mellitus provisional report of a WHO consultation. *Diabet Med* 1998; **15**: 539-553 [PMID: 9686693 DOI: 10.1002/(SICI)1096-9136(199807)15]
32 **Expert Panel on Detection, Evaluation, and Treatment of High Blood Cholesterol in Adults**. Executive Summary of The Third Report of The National Cholesterol Education Program (NCEP) Expert Panel on Detection, Evaluation, And Treatment of High Blood Cholesterol In Adults (Adult Treatment Panel III). *JAMA* 2001; **285**: 2486-2497 [PMID: 11368702 DOI: 10.1001/jama.285.19.2486]
33 **Alberti KG**, Zimmet P, Shaw J; IDF Epidemiology Task Force Consensus Group. The metabolic syndrome--a new worldwide definition. *Lancet* 2005; **366**: 1059-1062 [PMID: 16182882 DOI: 10.1016/s0140-6736(05)67402-8]
34 **Nguyen NT**, Nguyen XM, Lane J, Wang P. Relationship between obesity and diabetes in a US adult population: findings from the National Health and Nutrition Examination Survey, 1999-2006. *Obes Surg* 2011; **21**: 351-355 [PMID: 21128002 DOI: 10.1007/s11695-010-0335-4]
35 **Tsigos C**, Hainer V, Basdevant A, Finer N, Mathus-Vliegen E, Micic D, Maislos M, Roman G, Schutz Y, Toplak H, Yumuk V, Zahorska-Markiewicz B. Criteria for EASO-collaborating centres for obesity management. *Obes Facts* 2011; **4**: 329-333 [PMID: 21921658 DOI: 10.1159/000331236]
36 **Hu FB**. Globalization of diabetes: the role of diet, lifestyle, and genes. *Diabetes Care* 2011; **34**: 1249-1257 [PMID: 21617109 DOI: 10.2337/dc11-0442]
37 **Yang WS**, Va P, Bray F, Gao S, Gao J, Li HL, Xiang YB. The role of pre-existing diabetes mellitus on hepatocellular carcinoma occurrence and prognosis: a meta-analysis of prospective cohort studies. *PLoS One* 2011; **6**: e27326 [PMID: 22205924 DOI: 10.1371/journal.pone.0027326]
38 **Starley BQ**, Calcagno CJ, Harrison SA. Nonalcoholic fatty liver disease and hepatocellular carcinoma: a weighty connection. *Hepatology* 2010; **51**: 1820-1832 [PMID: 20432259 DOI: 10.1002/hep.23594]
39 **Hung CH**, Wang JH, Hu TH, Chen CH, Chang KC, Yen YH, Kuo YH, Tsai MC, Lu SN, Lee CM. Insulin resistance is associated with hepatocellular carcinoma in chronic hepatitis C infection. *World J Gastroenterol* 2010; **16**: 2265-2271 [PMID: 20458764 DOI: 10.3748/wjg.v16.i18.2265]
40 **Scalera A**, Tarantino G. Could metabolic syndrome lead to

hepatocarcinoma via non-alcoholic fatty liver disease? *World J Gastroenterol* 2014; **20**: 9217-9228 [PMID: 25071314 DOI: 10.3748/wjg.v20.i28.9217]

41 **Larsson SC**, Wolk A. Overweight, obesity and risk of liver cancer: a meta-analysis of cohort studies. *Br J Cancer* 2007; **97**: 1005-1008 [PMID: 17700568 DOI: 10.1002/ijc.23176]

42 **Chen Y**, Wang X, Wang J, Yan Z, Luo J. Excess body weight and the risk of primary liver cancer: an updated meta-analysis of prospective studies. *Eur J Cancer* 2012; **48**: 2137-2145 [PMID: 22446023 DOI: 10.1016/j.ejca.2012.02.063]

43 **Tanaka K**, Tsuji I, Tamakoshi A, Matsuo K, Ito H, Wakai K, Nagata C, Mizoue T, Sasazuki S, Inoue M, Tsugane S. Obesity and liver cancer risk: an evaluation based on a systematic review of epidemiologic evidence among the Japanese population. *Jpn J Clin Oncol* 2012; **42**: 212-221 [PMID: 22241822 DOI: 10.1093/jjco/hyr198]

44 **Schlesinger S**, Aleksandrova K, Pischon T, Fedirko V, Jenab M, Trepo E, Boffetta P, Dahm CC, Overvad K, Tjønneland A, Halkjær J, Fagherazzi G, Boutron-Ruault MC, Carbonnel F, Kaaks R, Lukanova A, Boeing H, Trichopoulou A, Bamia C, Lagiou P, Palli D, Grioni S, Panico S, Tumino R, Vineis P, Bueno-de-Mesquita HB, van den Berg S, Peeters PH, Braaten T, Weiderpass E, Quirós JR, Travier N, Sánchez MJ, Navarro C, Barricarte A, Dorronsoro M, Lindkvist B, Regner S, Werner M, Sund M, Khaw KT, Wareham N, Travis RC, Norat T, Wark PA, Riboli E, Nöthlings U. Abdominal obesity, weight gain during adulthood and risk of liver and biliary tract cancer in a European cohort. *Int J Cancer* 2013; **132**: 645-657 [PMID: 22618881 DOI: 10.1002/ijc.27645]

45 **El-Serag HB**, Tran T, Everhart JE. Diabetes increases the risk of chronic liver disease and hepatocellular carcinoma. *Gastroenterology* 2004; **126**: 460-468 [PMID: 14762783 DOI: 10.1053/j.gastro.2003.10.065]

46 **El-Serag HB**, Hampel H, Javadi F. The association between diabetes and hepatocellular carcinoma: a systematic review of epidemiologic evidence. *Clin Gastroenterol Hepatol* 2006; **4**: 369-380 [PMID: 16527702 DOI: 10.1016/j.cgh.2005.12.007]

47 **Wang P**, Kang D, Cao W, Wang Y, Liu Z. Diabetes mellitus and risk of hepatocellular carcinoma: a systematic review and meta-analysis. *Diabetes Metab Res Rev* 2012; **28**: 109-122 [PMID: 21898753 DOI: 10.1002/dmrr.1291]

48 **Sanyal A**, Poklepovic A, Moyneur E, Barghout V. Population-based risk factors and resource utilization for HCC: US perspective. *Curr Med Res Opin* 2010; **26**: 2183-2191 [PMID: 20666689 DOI: 10.1185/03007995.2010.506375]

49 **Ertle J**, Dechêne A, Sowa JP, Penndorf V, Herzer K, Kaiser G, Schlaak JF, Gerken G, Syn WK, Canbay A. Non-alcoholic fatty liver disease progresses to hepatocellular carcinoma in the absence of apparent cirrhosis. *Int J Cancer* 2011; **128**: 2436-2443 [PMID: 21128245 DOI: 10.1002/ijc.25797]

50 **Baffy G**, Brunt EM, Caldwell SH. Hepatocellular carcinoma in non-alcoholic fatty liver disease: an emerging menace. *J Hepatol* 2012; **56**: 1384-1391 [PMID: 22326465 DOI: 10.1016/j.jhep.2011.10.027]

51 **Dam-Larsen S**, Franzmann M, Andersen IB, Christoffersen P, Jensen LB, Sørensen TI, Becker U, Bendtsen F. Long term prognosis of fatty liver: risk of chronic liver disease and death. *Gut* 2004; **53**: 750-755 [PMID: 15082596 DOI: 10.1136/gut.2003.019984]

52 **Dixon JB**, Bhathal PS, O'Brien PE. Nonalcoholic fatty liver disease: predictors of nonalcoholic steatohepatitis and liver fibrosis in the severely obese. *Gastroenterology* 2001; **121**: 91-100 [PMID: 11438497 DOI: 10.1053/gast.2001.25540]

53 **Guzman G**, Brunt EM, Petrovic LM, Chejfec G, Layden TJ, Cotler SJ. Does nonalcoholic fatty liver disease predispose patients to hepatocellular carcinoma in the absence of cirrhosis? *Arch Pathol Lab Med* 2008; **132**: 1761-1766 [PMID: 18976012 DOI: 10.1043/1543-2165-132.11.1761]

54 **Kawada N**, Imanaka K, Kawaguchi T, Tamai C, Ishihara R, Matsunaga T, Gotoh K, Yamada T, Tomita Y. Hepatocellular carcinoma arising from non-cirrhotic nonalcoholic steatohepatitis. *J Gastroenterol* 2009; **44**: 1190-1194 [PMID: 19672551 DOI: 10.1007/s00535-009-0112-0]

55 **Rahman RN**, Ibdah JA. Nonalcoholic fatty liver disease without cirrhosis is an emergent and independent risk factor of hepatocellular carcinoma: A population based study. *Hepatology* 2012; **56**: 241A

56 **Alexander J**, Torbenson M, Wu TT, Yeh MM. Non-alcoholic fatty liver disease contributes to hepatocarcinogenesis in non-cirrhotic liver: a clinical and pathological study. *J Gastroenterol Hepatol* 2013; **28**: 848-854 [PMID: 23302015 DOI: 10.1111/jgh.12116]

57 **Dongiovanni P**, Romeo S, Valenti L. Hepatocellular carcinoma in nonalcoholic fatty liver: role of environmental and genetic factors. *World J Gastroenterol* 2014; **20**: 12945-12955 [PMID: 25278690 DOI: 10.3748/wjg.v20.i36.12945]

58 **Torres DM**, Harrison SA. Nonalcoholic steatohepatitis and noncirrhotic hepatocellular carcinoma: fertile soil. *Semin Liver Dis* 2012; **32**: 30-38 [PMID: 22418886 DOI: 10.1055/s-0032-1306424]

59 **Wong RJ**, Ahmed A. Obesity and non-alcoholic fatty liver disease: Disparate associations among Asian populations. *World J Hepatol* 2014; **6**: 263-273 [PMID: 24868320 DOI: 10.4254/wjh.v6.i5.263]

60 **Fujii M**, Shibazaki Y, Wakamatsu K, Honda Y, Kawauchi Y, Suzuki K, Arumugam S, Watanabe K, Ichida T, Asakura H, Yoneyama H. A murine model for non-alcoholic steatohepatitis showing evidence of association between diabetes and hepatocellular carcinoma. *Med Mol Morphol* 2013; **46**: 141-152 [PMID: 23430399 DOI: 10.1007/s00795-013-0016-1]

61 **Dowman JK**, Hopkins LJ, Reynolds GM, Nikolaou N, Armstrong MJ, Shaw JC, Houlihan DD, Lalor PF, Tomlinson JW, Hübscher SG, Newsome PN. Development of hepatocellular carcinoma in a murine model of nonalcoholic steatohepatitis induced by use of a high-fat/fructose diet and sedentary lifestyle. *Am J Pathol* 2014; **184**: 1550-1561 [PMID: 24650559 DOI: 10.1016/j.ajpath.2014.01.034]

62 **Park EJ**, Lee JH, Yu GY, He G, Ali SR, Holzer RG, Osterreicher CH, Takahashi H, Karin M. Dietary and genetic obesity promote liver inflammation and tumorigenesis by enhancing IL-6 and TNF expression. *Cell* 2010; **140**: 197-208 [PMID: 20141834 DOI: 10.1016/j.cell.2009.12.052]

63 **Grivennikov SI**, Greten FR, Karin M. Immunity, inflammation, and cancer. *Cell* 2010; **140**: 883-899 [PMID: 20303878 DOI: 10.1016/j.cell.2010.01.025]

64 **Streba LA**, Cârstea D, Mitruț P, Vere CC, Dragomir N, Streba CT. Nonalcoholic fatty liver disease and metabolic syndrome: a concise review. *Rom J Morphol Embryol* 2008; **49**: 13-20 [PMID: 18273497]

65 **Stickel F**, Hellerbrand C. Non-alcoholic fatty liver disease as a risk factor for hepatocellular carcinoma: mechanisms and implications. *Gut* 2010; **59**: 1303-1307 [PMID: 20650925 DOI: 10.1136/gut.2009.199661]

66 **Siddique A**, Kowdley KV. Insulin resistance and other metabolic risk factors in the pathogenesis of hepatocellular carcinoma. *Clin Liver Dis* 2011; **15**: 281-96, vii-x [PMID: 21689613 DOI: 10.1016/j.cld.2011.03.007]

67 **Scharf JG**, Braulke T. The role of the IGF axis in hepatocarcinogenesis. *Horm Metab Res* 2003; **35**: 685-693 [PMID: 14710347 DOI: 10.1055/s-2004-814151]

68 **Chun YS**, Huang M, Rink L, Von Mehren M. Expression levels of insulin-like growth factors and receptors in hepatocellular carcinoma: a retrospective study. *World J Surg Oncol* 2014; **12**: 231 [PMID: 25052889 DOI: 10.1186/1477-7819-12-231]

69 **Wu J**, Zhu AX. Targeting insulin-like growth factor axis in hepatocellular carcinoma. *J Hematol Oncol* 2011; **4**: 30 [PMID: 21729319 DOI: 10.1186/1756-8722-4-8730]

70 **Enguita-Germán M**, Fortes P. Targeting the insulin-like growth factor pathway in hepatocellular carcinoma. *World J Hepatol* 2014; **6**: 716-737 [PMID: 25349643 DOI: 10.4254/wjh.v6.i10.716]

71 **Page JM**, Harrison SA. NASH and HCC. *Clin Liver Dis* 2009; **13**: 631-647 [PMID: 19818310 DOI: 10.1016/j.cld.2009.07.007]

72 **Ohlsson C**, Mohan S, Sjögren K, Tivesten A, Isgaard J, Isaksson O, Jansson JO, Svensson J. The role of liver-derived insulin-like

growth factor-I. *Endocr Rev* 2009; **30**: 494-535 [PMID: 19589948 DOI: 10.1210/er.2009-0010]
73 **Kaaks R**, Lukanova A. Energy balance and cancer: the role of insulin and insulin-like growth factor-I. *Proc Nutr Soc* 2001; **60**: 91-106 [PMID: 11310428 DOI: 10.1079/pns200070]
74 **Breuhahn K**, Longerich T, Schirmacher P. Dysregulation of growth factor signaling in human hepatocellular carcinoma. *Oncogene* 2006; **25**: 3787-3800 [PMID: 16799620 DOI: 10.1038/sj.onc.1209556]
75 **Tanaka S**, Mohr L, Schmidt EV, Sugimachi K, Wands JR. Biological effects of human insulin receptor substrate-1 overexpression in hepatocytes. *Hepatology* 1997; **26**: 598-604 [PMID: 9303488 DOI: 10.1002/hep.510260310]
76 **Yang S**, Lin HZ, Hwang J, Chacko VP, Diehl AM. Hepatic hyperplasia in noncirrhotic fatty livers: is obesity-related hepatic steatosis a premalignant condition? *Cancer Res* 2001; **61**: 5016-5023 [PMID: 11431335 DOI: 10.1016/s0016-5085(08)80527-6]
77 **Day CP**. Pathogenesis of steatohepatitis. *Best Pract Res Clin Gastroenterol* 2002; **16**: 663-678 [PMID: 12406438]
78 **Seki S**, Kitada T, Yamada T, Sakaguchi H, Nakatani K, Wakasa K. In situ detection of lipid peroxidation and oxidative DNA damage in non-alcoholic fatty liver diseases. *J Hepatol* 2002; **37**: 56-62 [PMID: 12076862 DOI: 10.1016/s0168-8278(02)00073-9]
79 **Browning JD**, Horton JD. Molecular mediators of hepatic steatosis and liver injury. *J Clin Invest* 2004; **114**: 147-152 [PMID: 15254578 DOI: 10.1172/JCI200422422]
80 **Reuter S**, Gupta SC, Chaturvedi MM, Aggarwal BB. Oxidative stress, inflammation, and cancer: how are they linked? *Free Radic Biol Med* 2010; **49**: 1603-1616 [PMID: 20840865 DOI: 10.1016/j.freeradbiomed.2010.09.006]
81 **Hu W**, Feng Z, Eveleigh J, Iyer G, Pan J, Amin S, Chung FL, Tang MS. The major lipid peroxidation product, trans-4-hydroxy-2-nonenal, preferentially forms DNA adducts at codon 249 of human p53 gene, a unique mutational hotspot in hepatocellular carcinoma. *Carcinogenesis* 2002; **23**: 1781-1789 [PMID: 12419825 DOI: 10.1093/carcin/23.11.1781]
82 **Xu Z**, Chen L, Leung L, Yen TS, Lee C, Chan JY. Liver-specific inactivation of the Nrf1 gene in adult mouse leads to nonalcoholic steatohepatitis and hepatic neoplasia. *Proc Natl Acad Sci USA* 2005; **102**: 4120-4125 [PMID: 15738389 DOI: 10.1073/pnas.0500660102]
83 **Maeda S**. NF-κB, JNK, and TLR Signaling Pathways in Hepatocarcinogenesis. *Gastroenterol Res Pract* 2010; **2010**: 367694 [PMID: 21151655 DOI: 10.1155/2010/367694]
84 **Savini I**, Catani MV, Evangelista D, Gasperi V, Avigliano L. Obesity-associated oxidative stress: strategies finalized to improve redox state. *Int J Mol Sci* 2013; **14**: 10497-10538 [PMID: 23698776 DOI: 10.3390/ijms140510497]
85 **Hui JM**, Hodge A, Farrell GC, Kench JG, Kriketos A, George J. Beyond insulin resistance in NASH: TNF-alpha or adiponectin? *Hepatology* 2004; **40**: 46-54 [PMID: 15239085]
86 **Masaki T**, Chiba S, Tatsukawa H, Yasuda T, Noguchi H, Seike M, Yoshimatsu H. Adiponectin protects LPS-induced liver injury through modulation of TNF-alpha in KK-Ay obese mice. *Hepatology* 2004; **40**: 177-184 [PMID: 15239101 DOI: 10.1002/hep.20282]
87 **Shimizu M**, Tanaka T, Moriwaki H. Obesity and hepatocellular carcinoma: targeting obesity-related inflammation for chemoprevention of liver carcinogenesis. *Semin Immunopathol* 2013; **35**: 191-202 [PMID: 22945457 DOI: 10.1007/s00281-012-0336-6]
88 **Johnson C**, Han Y, Hughart N, McCarra J, Alpini G, Meng F. Interleukin-6 and its receptor, key players in hepatobiliary inflammation and cancer. *Transl Gastrointest Cancer* 2012; **1**: 58-70 [PMID: 22724089]
89 **Fukushima J**, Kamada Y, Matsumoto H, Yoshida Y, Ezaki H, Takemura T, Saji Y, Igura T, Tsutsui S, Kihara S, Funahashi T, Shimomura I, Tamura S, Kiso S, Hayashi N. Adiponectin prevents progression of steatohepatitis in mice by regulating oxidative stress and Kupffer cell phenotype polarization. *Hepatol Res* 2009; **39**: 724-738 [PMID: 19473437 DOI: 10.1111/j.1872-034X.2009.00509.x]
90 **Anstee QM**, Daly AK, Day CP. Genetics of alcoholic and nonalcoholic fatty liver disease. *Semin Liver Dis* 2011; **31**: 128-146 [PMID: 21538280 DOI: 10.1055/s-0031-1276643]
91 **Dongiovanni P**, Anstee QM, Valenti L. Genetic predisposition in NAFLD and NASH: impact on severity of liver disease and response to treatment. *Curr Pharm Des* 2013; **19**: 5219-5238 [PMID: 23394097 DOI: 10.2174/1381612811319990381]
92 **Romeo S**, Kozlitina J, Xing C, Pertsemlidis A, Cox D, Pennacchio LA, Boerwinkle E, Cohen JC, Hobbs HH. Genetic variation in PNPLA3 confers susceptibility to nonalcoholic fatty liver disease. *Nat Genet* 2008; **40**: 1461-1465 [PMID: 18820647 DOI: 10.1038/ng.257]
93 **Yuan X**, Waterworth D, Perry JR, Lim N, Song K, Chambers JC, Zhang W, Vollenweider P, Stirnadel H, Johnson T, Bergmann S, Beckmann ND, Li Y, Ferrucci L, Melzer D, Hernandez D, Singleton A, Scott J, Elliott P, Waeber G, Cardon L, Frayling TM, Kooner JS, Mooser V. Population-based genome-wide association studies reveal six loci influencing plasma levels of liver enzymes. *Am J Hum Genet* 2008; **83**: 520-528 [PMID: 18940312 DOI: 10.1016/j.ajhg.2008.09.012]
94 **Valenti L**, Al-Serri A, Daly AK, Galmozzi E, Rametta R, Dongiovanni P, Nobili V, Mozzi E, Roviaro G, Vanni E, Bugianesi E, Maggioni M, Fracanzani AL, Fargion S, Day CP. Homozygosity for the patatin-like phospholipase-3/adiponutrin I148M polymorphism influences liver fibrosis in patients with nonalcoholic fatty liver disease. *Hepatology* 2010; **51**: 1209-1217 [PMID: 20373368 DOI: 10.1002/hep.23622]
95 **Burza MA**, Pirazzi C, Maglio C, Sjöholm K, Mancina RM, Svensson PA, Jacobson P, Adiels M, Baroni MG, Borén J, Ginanni Corradini S, Montalcini T, Sjöström L, Carlsson LM, Romeo S. PNPLA3 I148M (rs738409) genetic variant is associated with hepatocellular carcinoma in obese individuals. *Dig Liver Dis* 2012; **44**: 1037-1041 [PMID: 22704398 DOI: 10.1016/j.dld.2012.05.006]
96 **Liu YL**, Patman GL, Leathart JB, Piguet AC, Burt AD, Dufour JF, Day CP, Daly AK, Reeves HL, Anstee QM. Carriage of the PNPLA3 rs738409 C >G polymorphism confers an increased risk of non-alcoholic fatty liver disease associated hepatocellular carcinoma. *J Hepatol* 2014; **61**: 75-81 [PMID: 24607626 DOI: 10.1016/j.jhep.2014.02.030]

P- Reviewer: Aygun F, Divanovic S, Toshikuni N **S- Editor**: Qi Y
L- Editor: AmEditor **E- Editor**: Ma S

World Journal of Gastroenterology

Submit a Manuscript: http://www.wjgnet.com/esps/
Help Desk: http://www.wjgnet.com/esps/helpdesk.aspx
DOI: 10.3748/wjg.v21.i14.4111

World J Gastroenterol 2015 April 14; 21(14): 4111-4120
ISSN 1007-9327 (print) ISSN 2219-2840 (online)

REVIEW

Point-of-care testing in the diagnosis of gastrointestinal cancers: Current technology and future directions

Jeremy R Huddy, Melody Z Ni, Sheraz R Markar, George B Hanna

Jeremy R Huddy, Melody Z Ni, Sheraz R Markar, George B Hanna, Department of Surgery and Cancer, Imperial College London, St Mary's Hospital, South Wharf Road, W2 1NY London, United Kingdom

Author contributions: Hanna GB conceptualized the paper; Huddy JR conducted the literature search; all authors were involved in the manuscript development and its revision; all authors read and approved the final manuscript.

Supported by NIHR Diagnostic Evidence Co-operative London at Imperial College Healthcare NHS Trust is funded by the National Institute for Health Research.

Conflict-of-interest: The authors declare no conflicts-of-interest.

Correspondence to: George B Hanna, PhD, FRCS, Professor, Head, Department of Surgery and Cancer, Imperial College London, St Mary's Hospital, Academic Surgical Unit, 10th Floor, QEQM Building, South Wharf Road, W2 1NY London, United Kingdom. g.hanna@imperial.ac.uk
Telephone: +44-207-8862124
Fax: +44-207-8866309

Received: December 17, 2014
Peer-review started: December 18, 2014
First decision: January 8, 2015
Revised: January 20, 2015
Accepted: February 13, 2015
Article in press: February 13, 2015
Published online: April 14, 2015

Abstract

Point-of-care (POC) tests enable rapid results and are well established in medical practice. Recent advances in analytical techniques have led to a new generation of POC devices that will alter gastrointestinal diagnostic pathways. This review aims to identify current and new technologies for the POC diagnosis of gastrointestinal cancer. A structured search of the Embase and Medline databases was performed. Papers reporting diagnostic tests for gastrointestinal cancer available as a POC device or containing a description of feasibility for POC application were included. Studies recovered were heterogeneous and therefore results are presented as a narrative review. Six diagnostic methods were identified (fecal occult blood, fecal proteins, volatile organic compounds, pyruvate kinase isoenzyme type M2, tumour markers and DNA analysis). Fecal occult blood testing has a reported sensitivity of 66%-85% and specificity greater than 95%. The others are at a range of development and clinical application. POC devices have a proven role in the diagnosis of gastrointestinal cancer. Barriers to their implementation exist and the transition from experimental to clinical medicine is currently slow. New technologies demonstrate potential to provide accurate POC tests and an ability to diagnose gastrointestinal cancer at an early stage with improved clinical outcome and survival.

Key words: Colorectal cancer; Cancer-diagnosis; Gastric cancer; Esophageal cancer; Diagnostic tests

Core tip: Point-of-care tests are well established. They facilitate real time clinical decision-making and can be cost-effective, reduce in-patient hospital stay and increase patient satisfaction. Faecal Occult Blood has been used internationally since 1993 in screening for colorectal cancer. Six technologies for current or potential point-of-care diagnosis of gastro-intestinal cancer were identified from the literature (faecal occult blood, faecal proteins, volatile organic compounds, pyruvate kinase isoenzyme type M2, tumour markers and DNA analysis). Currently, three have commercially available point-of-care devices. New technologies demonstrate potential to provide accuracy and an

ability to diagnose gastrointestinal cancer earlier leading to improved clinical outcome and survival.

Huddy JR, Ni MZ, Markar SR, Hanna GB. Point-of-care testing in the diagnosis of gastrointestinal cancers: Current technology and future directions. *World J Gastroenterol* 2015; 21(14): 4111-4120 Available from: URL: http://www.wjgnet.com/1007-9327/full/v21/i14/4111.htm DOI: http://dx.doi.org/10.3748/wjg.v21.i14.4111

INTRODUCTION

Point-of-care (POC) testing enables near patient or bedside tests that provide instant or rapid results to facilitate real time clinical decision making within established patient care pathways. POC tests are well established in some areas of medical practice including monitoring of blood glucose levels, anti-coagulation and in pregnancy. They bring potential advantages by decreasing the time to diagnosis and institution of treatment, whilst eliminating requirements for specialist clinical and laboratory staff to perform and analyse tests. This stream-lined approach to diagnostic medicine has further advantages including improved cost-effectiveness[1,2], reduced in-patient hospital stay and increased patient satisfaction[3]. Furthermore recent advances in analytical techniques such as microfluidics[4], metabolomics[5] and nanotechnology[6] has led to the development of POC testing with improved sensitivity and specificity for the diagnosis, monitoring and response to treatment in common disease processes including cancer.

The three most common sites for gastrointestinal cancer are colorectal, stomach and esophagus which together account for more than 56400 new cases of cancer each year in the United Kingdom[7] and early detection is paramount to improving outcomes. This is demonstrated by direct comparison between institutions in the East and the West that have shown a better long-term survival following surgical resection of gastric cancer in Eastern centres[8-11], where early detection and treatment of esophago-gastric cancers is achieved through the utilization of endoscopic screening programmes.

The current established diagnostic pathway for gastrointestinal cancers follows an index of clinical suspicion based upon presenting symptoms and clinical assessment in primary care leading to referral to secondary care, supported by two-week referral guidelines, and followed by specialist multidisciplinary investigation with endoscopy, histological diagnosis and radiology. This current diagnostic model may be subject to several points of potential failure, with the most important being the initial primary care assessment and index of suspicion which is highly assessor dependent and subject to bias. Therefore, these pathways often have a low sensitivity and result in large numbers of negative endoscopies representing significant financial waste along with patient discomfort and potentially harm.

POC techniques are already utilised in primary care for screening patients in gastrointestinal cancer for example fecal occult blood in colorectal carcinoma, and advances in technology and translational medicine suggest that POC tests may in the future be able to diagnose gastrointestinal cancers at the patient's bedside, in the outpatient clinic or even by the patient self-testing at home. Ideally, new diagnostic tests should demonstrate diagnostic accuracy similar to or better than current reference tests, although it is conceivable that a poorer accuracy may be accepted as a tradeoff for the convenience of POC devices or a lower risk of associated complications. New tests must also be usable and cost-efficient in comparison to current standard tests.

POC technologies have the potential to dramatically alter established patient care pathways, as results can be immediately available in primary care or the home, resulting in a faster application of appropriate treatment or referral for further investigation. This needs evaluation to ascertain whether current treatment algorithms based on evidence generated from reference testing practices will still apply and how this will affect patient's quality of life. For example patients self-diagnosing themselves with a new diagnosis of suspected cancer in their own home would leave them feeling unsupported, without access to information or counseling and may have a detrimental effect on their state of mind, compliance with further treatment and potential outcome from disease.

The aim of this present review is to identify and critically evaluate the current use of POC tests in the diagnosis and assessment of gastrointestinal cancer and consider the techniques and technology that demonstrate potential for the POC devices of the future.

RESEARCH

An initial review of the literature was performed. Electronic searches of EMBASE and MEDLINE databases were searched from 1946 to October 2013. The search strategy consisted of keywords and MeSH headings designed to identify articles related to POC tests and gastrointestinal cancers and these were then combined with the Boolean operators AND and OR. The full search strategy used is described in Table 1.

Titles and abstracts were then reviewed to ensure relevance by meeting inclusion criteria. Papers describing a diagnostic test for gastrointestinal cancer that was achievable at the POC were included. Papers reporting diagnostic tests not yet commercially available as a POC device, but containing an explanation of feasibility for POC application were also included.

Table 1 Full search strategy used is described

MEDLINE search strategy
1. [(point of care or near patient or poc or rapid or bedside) adj3 (test* or analys* or immunoassay* or technique* or assay* or diagnos* or technology* or system?)].mp
2. Point-of-Care Systems/
3. 1 or 2
4. exp Gastrointestinal Neoplasms/
5. [(oesohag* or esophag* or gast* or stomach* or duoden* or ile* or jeun* or caec* or append* or cec* or colo* or rect* or anal or anus or intestin*) adj2 (cancer? or carcinoma? or malignancy or malignant or neoplasm?)].mp
6. 4 or 5
7. 3 and 6

EMBASE search strategy
1. [(point of care or point-of-care or near patient or poc or rapid or bedside) adj3 (test* or analys* or immunoassay* or technique* or assay* or diagnos* or technology* or system?)].mp
2. "point of care testing"/
3. 1 or 2
4. [(oesohag* or esophag* or gast* or stomach* or duoden* or ile* or jeun* or caec* or append* or cec* or colo* or rect* or anal or anus or intestin*) adj2 (cancer? or carcinoma? or malignancy or malignant or neoplasm?)].mp
5. digestive system cancer/or exp esophagus cancer/or exp intestine cancer/or exp stomach cancer/
6. 4 or 5
7. 3 and 6

Table 2 Described methods of testing for gastrointestinal cancer and accuracy of commercially available tests based on recent evidence (point-of-care)

Technology	Commercial available POC device	POC sensitivity	POC specificity	Level of evidence	Papers retrieved in primary search (*n*)
Occult blood	Yes	79%[25]	94%[25]	1	10[20,22,34,66-72]
Fecal proteins	Yes	83%[33] (calprotectin)	84%[33] (calprotectin)	2	3[34,73,74]
Volatile organic compounds	No				0
Pyruvate kinase isoenzyme type M2	Yes	80.3%[48]	95.2%[48]	1	1[72]
Tumour markers	No				6[47,49,68,75-77]
DNA mutation analysis	No				4[56,76,78,79]
Multitarget stool DNA test	No				0

POC: Point-of-care.

Animal studies were included but papers not published in English were excluded during the initial review. Full texts of eligible papers were then reviewed.

This initial search was undertaken to identify POC devices and their underlying technologies. The studies recovered from the search were heterogeneous and therefore results are presented as a narrative review. Secondary literature searches were performed within MEDLINE that were specific to identified technologies to ensure the full scope of current literature was evaluated and diagnostic tests that were recovered in these secondary searches were also included in the review.

RESULTS

The initial search highlighted 1014 articles after duplications were removed. 414 articles recovered in the initial search were related to POC testing for *Helicobacter pylori* but these did not meet inclusion criteria and were excluded. From the review of titles and abstracts 20 were retrieved for further evaluation. Four further papers were excluded on review of the full manuscripts as they did not relate to POC technologies. Five POC methods were identified with a current or potential role in the diagnosis of gastrointestinal cancer and one further technology (volatile organic compounds) was also included as it was identified in the supplementary detailed technology-specific searches. These are summarized in Table 2.

The results are described individually with an overview of their development, role in patient care pathway and where possible validity.

Fecal occult blood

The most widely accepted POC test for gastrointestinal cancer is fecal occult blood (FOB) sampling. Whilst occult blood detection was first described in 1864, it was not until 1967 that the hypothesis was suggested for its role in the early detection of colorectal cancer with the first described guaiac based assays[12]. In 1993 the Minnesota Colon Cancer Control Study demonstrated that an annual screening programme of 50-80 years old using guaiac based FOB kits and colonoscopy in patients testing positive decreased the 13 years cumulative mortality from colorectal

cancer by 33%[13]. Since this landmark study national colorectal cancer screening programs have been widely adopted in countries across the world[14] including the United Kingdom[15].

Whilst colorectal cancer screening programs have demonstrable benefit in reducing disease specific mortality[16-19], guaiac based tests do have inherent limitations that translate into a reduced sensitivity and specificity. These include a lack of specificity for human blood and therefore false positive results can be caused by meat, vegetable and fruit products containing peroxidase[20] as well as upper gastrointestinal sources of bleeding, especially when provoked by aspirin or non-steroidal anti-inflammatory drugs. Specificity can be improved to some extent by dietary and medication restrictions prior to test sampling and sensitivity by the rehydration of slides[13], although this is at the expense of specificity. A further disadvantage of guaiac based tests is the relatively low sensitivity (16%-31%)[21] for advanced adenomas.

To address the above limitations, newer immunochemical FOB tests have been developed that are specific for human FOB and exclude upper GI occult blood as globin is metabolised by gastric enzymes. Although more expensive, they achieve better sensitivity, with comparable specificity[22] and compliance is better due to the more amenable sampling procedure with fewer consecutive stool samples required for testing[23,24]. Accuracy of FOB test devices can be titrated accordingly to threshold levels, hydration state of slides and device or combination used, but pooled analysis suggests a sensitivity of approximately 79% and specificity of 94% with immunochemical tests[25]. Currently the FOB test represents the most widely applied POC test in the setting of gastrointestinal cancer. However, as described there are concerns regarding diagnostic accuracy associated with its application that have in more recent years suggested flexible sigmoidoscopy may represent an alternative screening investigation in asymptomatic individuals[26].

Fecal proteins

Several proteins including lactoferrin, lysozyme and albumin have been investigated as potential fecal markers of organic bowel pathology but with the exception of calprotectin they have shown little promise in view of their poor diagnostic accuracy[27].

Calprotectin is a protein derived predominantly from neutrophils and has been shown to be increased in inflammation and malignant processes within the large bowel[28]. It has been suggested that calprotectin can offer greater accuracy than FOB in the diagnosis of organic colorectal disease, as calprotectin is present continuously within the gut lumen as a result of leucocyte recruitment to tumour tissue and does not rely on intermittent bleeding[29]. However, calprotectin has a low specificity as it does not differentiate between inflammatory and cancer and therefore is unsuitable for screening in colorectal cancer[30-32]. A recent review reported a mean sensitivity of 83% and a specificity of 84%[33] for all organic bowel disease. POC test kits for calprotectin and FOB have been compared[34] and strategies for combination testing using FOB and calprotectin[35] have been proposed to increase accuracy but this has not been adopted into screening programmes at the present time.

Overall, it is diagnostic accuracy and specificity that prevents the widespread use of POC calprotectin testing in diagnosing gastrointestinal cancer. Although, its use as a combination approach with FOB to provide more accurate fecal screening or the ability to screen for all organic bowel disease including inflammatory conditions may permit continued commercial viability, further evidence is required to define the nature of this role.

Volatile organic compounds

Metabolomics is a fast growing area of medical research and represents an area of particular promising growth towards the development of POC diagnostic technology. Volatile organic compounds (VOC), resulting from the chemical output of metabolic processes within the body, can be measured in-vitro through exhaled air, sweat, urine and faeces with modern laboratory techniques. Selected ion flow tube mass spectrometry is one method that allows real time quantification of multiple VOCs in human breath without sample modification and therefore represents huge potential as a medium to allow non-invasive POC testing[36]. Preliminary work at our institution in VOC profiling for esophago-gastric cancer has led to the discovery of four VOCs (hexanoic acid, phenol, methyl phenol, and ethyl phenol) that are statistically different in the exhaled breath of patients with esophago-gastric cancer when compared to controls and gave an accuracy of 0.91 based on the integrated area under receiver operating characteristic curve[5]. Similar VOC profiling patterns in esophago-gastric cancer patients have been achieved for urine[37] and gastric contents[38].

Similar studies in colorectal cancer have demonstrated a different VOC pattern in the exhaled breath of colorectal cancer patients when compared to controls with a sensitivity of 86% and a specificity of 83%[39]. However technology utilised for this analysis was gas-chromatography mass spectrometry (GC-MS), which does not permit real-time on-line analysis.

As well as mass spectrometry techniques, nanosensors based on gold nanoparticles have also been shown to be effective at differentiating between VOC profiles in colorectal[40] and gastric[41] cancer. VOCs in colorectal cancer from breath and fecal samples have even been distinguished from controls with impressive sensitivity and specificity by canine scent detection without confounders for benign disease

or inflammation[42].

Advances in metabolomics has allowed identification of individual VOC profiling of diseases such as tuberculosis and cancer, giving each in effect a recognizable and quantifiable signature[43,44]. This is an area for future investigation before VOC profiling becomes widely applied in cancer diagnostics, however the results of these preliminary studies do suggest that VOC analysis has tremendous potential as a non-invasive POC test for a wide variety of important diseases including cancer. Whilst VOC profiles can be quantified in association with certain disease states, the mechanism of VOC production in these disease states is poorly understood. This is clearly an area for further investigation before the widespread application of this technology in POC testing.

Pyruvate kinase isoenzyme type M2

Pyruvate kinase isoenzyme type M2 (M2-PK) has been proposed as a biomarker of many cancers, including gastric, esophageal and colorectal. Different isoenzymes of pyruvate kinase are expressed depending on the metabolic functions of tissues and during rapidly dividing cells such as seen in tumour formation tissue specific isoenzymes are replaced with M2-PK in the dimeric form[45]. Therefore, M2-PK has been investigated as a potential diagnostic marker for various cancers particularly colorectal[46,47]. POC test devices are now commercially viable for stool analysis of fecal M2-PK with sampling requiring only one stool sample. Like calprotectin, these assays do not rely on tumours bleeding and have improved specificity by excluding other bowel sources of bleeding such as haemorrhoids and fissures. A recent pooled analysis demonstrated M2-PK detection by either ELISA or the POC lateral flow rapid test as having a sensitivity of about 80% for colorectal cancer and 44% for an adenoma greater than 1 cm[48]. This concluded that M2-PK should be used routinely for colorectal cancer screening, however this assertion has two limitations. Firstly, this justification of this was based on a combined analysis of the laboratory ELISA methods as well as the POC device and secondly as noted in regards calprotectin assay devices, the studies included are small in size and underpowered, and even when combined with pooled analysis the 12 studies together included just 704 cancer samples between them. Therefore larger studies with significant power are required to give weight to these proposals before this technology can be implemented on a wider scale.

Tumour markers

Modern techniques such as dielectrophoresis[49], microfluidics and nanotechnology have allowed multiple complex laboratory processes to be scaled down and automated leading to the development of so-called "lab on a chip" devices. Circulating tumour cells are cells released by certain tumour types into the bloodstream but occur in small quantities making detection technically difficult[50], Dielectrophoresis has been demonstrated in the laboratory to be able to quantify these cells using an electrical field to separate circulating tumour cells from blood cells by way of their different charge characteristics. Experimental dielectrophoresis within a microfluidic chip has been studied for stool sample analysis of circulating tumour cells in a laboratory setting. HTC 116 cells were isolated from a mixture of human embryonic kidney 293 (HEK 293) and *E. coli* cells demonstrating its feasibility[51] but so far this has not been translated into a test appropriate for clinical use. Whilst, these advances have definite potential for POC devices to assay circulating tumour cells in vitro and therefore provide diagnostic tools, current methodologies still require the pre-treatment of samples and the technology is not yet fulfilled for POC testing.

Further down the design pathway and therefore closer to implementation are POC devices for common tumour markers. Gold nanoparticle microfluidic chips for tumour markers such as carcinogenic embryonic antigen (CEA) where feasibility studies for POC have been reported[52]. Whilst this test has been demonstrated, CEA does not currently serve a role in the screening or diagnosis of colorectal cancer[53] and this could therefore impact on its role in POC as the test is unlikely to be utilized or affect the patient diagnostic pathway. CEA is used for follow up of patients and to prompt further investigation, in most cases in an outpatient setting and therefore the benefit of rapid assay is negated unless justification can be demonstrated by improved cost-effectiveness, accuracy or patient experience.

DNA analysis

It is well established that mutations in the DNA of oncogenes and tumor suppressor genes are involved in the process of carcinogenesis. Specific genetic mutations have been attributed to several cancers and identification of these with DNA sequencing can play a role in stratifying risk, predicting response to treatment and in early diagnosis. Feasibility reports of POC devices for DNA mutation analysis are now present in the literature[54] and stool DNA testing has shown promising results[31,55,56]. DNA mutations associated with colorectal cancer include Kirsten-ras (K-ras) (seen in 40% of colorectal cancer patients and 60% of adenomas greater than 1cm)[57,58], adenomatous polyposis coli (APC), deleted in colorectal cancer (DCC) and tumor protein 53 (p53) and associated mutations can predict carcinogenesis or be indicative of specific events such as the activation of adenoma to carcinoma.

More recently, DNA methylation biomarkers including *SEPT9* (ColoVantage®) and *vimentin* (ColoSure™) have been investigated for their potential in colorectal cancer diagnosis[59]. DNA methylation

occurs early in carcinogenesis and therefore biomarkers for these epigenetic events may permit the diagnosis of cancer earlier.

Combining biomarker assays for DNA mutation and DNA methylation can improve accuracy and has been the focus of novel test development. The United States Food and Drug Administration has recently approved Cologuard (Exact Sciences Corporation, Madison, WI, United States), a multitarget stool DNA test in screening for colorectal cancer. Cologuard combines molecular assays for aberrantly methylated *BMP3* and *NDRG4* promoter regions, mutant *KRAS* and *β-actin* (a reference gene for human DNA quantity) with an immunochemical assay for human hemoglobin (as used in immunochemical FOB testing)[60]. A large study of asymptomatic patients[61] using this multitarget approach demonstrated a significantly better sensitivity for cancer than immunochemical FOB testing alone (92.3% *vs* 73.8%, $P = 0.002$) but this was at the expense of specificity. Whilst non-invasive the test is not currently available as a POC device with amplification and detection undertaken in a laboratory using Quantitative Allele-specific Real-time Target and Signal Amplification (QuARTS™) technology.

Technology for DNA based biomarkers is progressing. Microfluidics have led to lab on a chip technology that has the potential for DNA sequencing in a POC device. Kitano *at al* describe a point of care device able to perform extraction, purification, DNA amplification, mutation detection and interpretation in an automated analyser taking 70 min. Furthermore, Toumazou *et al*[62] have since used pH-sensing complementary metal-oxide semiconductor technology to develop their platform that has reduced genotyping to 30 min on a chip the size of a finger-nail.

Whilst at present the cost of these technologies is high[63], the scaling and portability of DNA sequencing devices with multitarget approaches to detect the genetic and epigenetic events that arise from cancer presents exciting promise for highly sophisticated and accurate POC tests for the future. However, this technology remains in its infancy and will require significant investment in research development before translation into viable clinical POC tests for cancer.

DISCUSSION

POC devices have a proven role in the diagnosis and assessment of gastrointestinal cancer. There are also exciting new technologies at various stages of development showing significant promise for the future. FOB testing is well established and validated in multiple commercially available POC devices. Along with *Helicobacter pylori* testing these devices have consistently demonstrated that POC devices are acceptable to patients and clinicians, economically viable and can play a role in the clinical care pathway of gastrointestinal disease. However, the gold standard for diagnosis of gastrointestinal disease and specifically cancer remains endoscopy with histological diagnosis, despite being invasive, expensive and carrying the associated risks of bleeding and perforation.

Whilst screening programmes have been designed and investigated worldwide, the accuracy of POC devices remains its drawback. To some extent this can be seen as a tradeoff for its non-invasive nature but current vogues in colorectal cancer screening are shifting away from POC tests towards flexible sigmoidoscopy[26,64]. Furthermore esophago-gastro-duodenoscopy remains the choice of test for surveillance of pre-malignant conditions including Barrett's esophagus and diagnosis of upper gastro-intestinal cancers. This is understandable given that in the current care pathway histological confirmation is critical in the appropriate diagnosis, staging and allocation of treatment for gastrointestinal cancers. However, POC can still have a hugely valuable role if developed with robust methodology and validation to assign risk of gastrointestinal cancer. This will allow more appropriate allocation of diagnostic endoscopy, which may in turn lead to a reduction in negative endoscopies and a more cost-effective diagnostic pathway.

With more modern techniques such as VOC biomarkers, circulating tumour cells and DNA analysis which have the potential of providing the clinician with accurate POC tests the landscape for the diagnosis of gastrointestinal cancer has the potential to change rapidly, completely re-defining the patient care pathways as they currently exist. Changes in patient diagnostic and treatment algorithms resulting from the institution of POC tests must be carefully introduced with particular attention paid to the psychological and economic effects of these changes.

Even tests that are well established take a great deal of time to make the transition from the laboratory to clinical usage. Hold ups occur at multiple levels as seen in FOB sampling that was first described over a century before its role in colorectal cancer was discovered and a further 26 years passed before there was sufficient evidence to justify its use in screening programmes. With the potential advantages of POC devices barriers to their implementation need to be identified and overcome. Hold-ups in implementation can occur at multiple levels and industry, clinicians, researchers, policy makers and patients all have a role.

The POC diagnostic industry is expanding rapidly with an estimated 35% share of the in vitro diagnostic market within the United States and was valued at $15.1 billion in 2011[65]. This is forecast to grow and similar trends can be seen across the developed and developing world. The potential for commercial gain by novel POC diagnostic tests especially in prevalent diseases such as gastrointestinal cancer is apparent and therefore there should exist a clear motive to industry to pursue evidence generation in evaluating these products further but when assessing the literature this is not seen.

One reason for this apparent void of evidence

generation maybe that further studies are in fact being performed but results are not being published in the literature as there exists a publication bias against negative results, particularly with diagnostic test studies, compounded by the restricted access to intellectual property regarding design process and evaluation within industry. The prevalence of unknown reporting in this respect is difficult to determine and it is understandable that industry may want to protect their investment potential with emerging commercial devices.

Whilst a detailed description of design methodology is outside the scope of this review it is worth considering the route a new technology takes from proof of concept to a commercially available device, as this will highlight various barriers to their implementation. A design process is undertaken, usually within industry, which incorporates the validity of the testing methods into a device that is usable by the appropriate population, meets safety and regulatory standards and demonstrates a sustainable business model to justify this initial financial outlay. Usability is particularly important with POC devices as the user may have minimal or no training and all involved steps including sample collection, analysis and interpretation of result interface must be tested with the appropriate population as each may be the subject of heterogeneity that can adversely affect the overall quality and accuracy of results gained.

Effective design is a time consuming and expensive process that increases exponentially with complexity, this is especially true of medical devices with the inherent hazards of poor design. Device evaluation has the potential to benefit greatly if a culture of coordinated and complimentary evidence generation from both industry and clinical academia can be achieved, with a shared aim to drive concepts along this pathway so that the benefits of new technologies can be realised.

Once launched, POC tests challenge established patient diagnostic pathways. Current pathways are based on best evidence, almost universally developed with reference testing methods and it is vital that evidence based clinical practice remains valid with the introduction of new POC test devices. This will depend both on the accuracy of new tests but also their impact on patient care pathways.

Modeling techniques can be used to evaluate these changes in more detail and demonstrate cost-effectiveness. This ensures that the analysis is based not just on a test-by-test comparison basis but a full evaluation of pathways and outcomes associated with implementing new devices. This evidence is vital for large healthcare organisations such as the National Health Service.

Finally, patient and public involvement is required to implement POC testing strategies and the benefits offered should be enough to achieve this, providing safety is not compromised. POC technologies tend to be non-or minimally-invasive and provide rapid results and therefore studies repeatedly demonstrate better adherence to treatment, patient satisfaction and quality of life, especially at home where new devices can be integrated with wireless or mobile technology to completely alter the way healthcare is delivered.

CONCLUSION

There exists a wide range of technologies described as POC relating to gastrointestinal cancer. Whilst some are in routine clinical use, others remain described only in theory and ex-vitro experiments. There is a broad scope of exciting promise for the future and the potential benefits that they can bring but we can see from experience that barriers to their implementation exist and their transition from experimental to clinical medicine is slow. Further work needs to address these obstacles to provide better efficiency in evidence generation so that current POC proposals do not follow the example of FOB in taking over a century to translate from discovery to clinical use. With the creation of the National Institute for Health Research Diagnostic Evaluation Cooperatives this paucity of evidence aims to be addressed and this standardized pathway of stream-lined, efficient development and validation of POC devices will be the focus of future investigation.

ACKNOWLEDGMENTS

The authors would like to thank Tim Reeves and Jacqueline Cousins for their assistance in designing the literature search strategy.

REFERENCES

1 **Huang W**, Gaydos CA, Barnes MR, Jett-Goheen M, Blake DR. Comparative effectiveness of a rapid point-of-care test for detection of Chlamydia trachomatis among women in a clinical setting. *Sex Transm Infect* 2013; **89**: 108-114 [PMID: 22984085 DOI: 10.1136/sextrans-2011-050355]

2 **Mahieu L**, Marien A, De Dooy J, Mahieu M, Mahieu H, Van Hoof V. Implementation of a multi-parameter Point-of-Care-blood test analyzer reduces central laboratory testing and need for blood transfusions in very low birth weight infants. *Clin Chim Acta* 2012; **413**: 325-330 [PMID: 22056692 DOI: 10.1016/j.cca.2011.10.027]

3 **Al-Ansary L**, Farmer A, Hirst J, Roberts N, Glasziou P, Perera R, Price CP. Point-of-care testing for Hb A1c in the management of diabetes: a systematic review and metaanalysis. *Clin Chem* 2011; **57**: 568-576 [PMID: 21368238 DOI: 10.1373/clinchem.2010.157586]

4 **Zhang Z**, Nagrath S. Microfluidics and cancer: are we there yet? *Biomed Microdevices* 2013; **15**: 595-609 [PMID: 23358873 DOI: 10.1007/s10544-012-9734-8]

5 **Kumar S**, Huang J, Abbassi-Ghadi N, Španěl P, Smith D, Hanna GB. Selected ion flow tube mass spectrometry analysis of exhaled breath for volatile organic compound profiling of esophago-gastric cancer. *Anal Chem* 2013; **85**: 6121-6128 [PMID: 23659180 DOI: 10.1021/ac4010309]

6 **Chi X**, Huang D, Zhao Z, Zhou Z, Yin Z, Gao J. Nanoprobes for in vitro diagnostics of cancer and infectious diseases. *Biomaterials* 2012; **33**: 189-206 [PMID: 21959007 DOI: 10.1016/j.biomaterials.2011.09.032]

7 **UK CR**. Cancer incidence for common cancers. Available from: URL: http://www.cancerresearchuk.org/cancer-info/cancerstats/incidence/commoncancers/#Top

8 **Bollschweiler E**, Boettcher K, Hoelscher AH, Sasako M, Kinoshita T, Maruyama K, Siewert JR. Is the prognosis for Japanese and German patients with gastric cancer really different? *Cancer* 1993; **71**: 2918-2925 [PMID: 8490819]

9 **Noguchi Y**, Yoshikawa T, Tsuburaya A, Motohashi H, Karpeh MS, Brennan MF. Is gastric carcinoma different between Japan and the United States? *Cancer* 2000; **89**: 2237-2246 [PMID: 11147594]

10 **Strong VE**, Song KY, Park CH, Jacks LM, Gonen M, Shah M, Coit DG, Brennan MF. Comparison of gastric cancer survival following R0 resection in the United States and Korea using an internationally validated nomogram. *Ann Surg* 2010; **251**: 640-646 [PMID: 20224369 DOI: 10.1097/SLA.0b013e3181d3d29b]

11 **Markar SR**, Karthikesalingam A, Jackson D, Hanna GB. Long-term survival after gastrectomy for cancer in randomized, controlled oncological trials: comparison between West and East. *Ann Surg Oncol* 2013; **20**: 2328-2338 [PMID: 23340695 DOI: 10.1245/s10434-012-2862-9]

12 **Simon JB**. Occult blood screening for colorectal carcinoma: a critical review. *Gastroenterology* 1985; **88**: 820-837 [PMID: 3917961]

13 **Mandel JS**, Bond JH, Church TR, Snover DC, Bradley GM, Schuman LM, Ederer F. Reducing mortality from colorectal cancer by screening for fecal occult blood. Minnesota Colon Cancer Control Study. *N Engl J Med* 1993; **328**: 1365-1371 [PMID: 8474513 DOI: 10.1056/NEJM199305133281901]

14 **Benson VS**, Patnick J, Davies AK, Nadel MR, Smith RA, Atkin WS. Colorectal cancer screening: a comparison of 35 initiatives in 17 countries. *Int J Cancer* 2008; **122**: 1357-1367 [PMID: 18033685 DOI: 10.1002/ijc.23273]

15 **Logan RF**, Patnick J, Nickerson C, Coleman L, Rutter MD, von Wagner C. Outcomes of the Bowel Cancer Screening Programme (BCSP) in England after the first 1 million tests. *Gut* 2012; **61**: 1439-1446 [PMID: 22156981 DOI: 10.1136/gutjnl-2011-300843]

16 **Hardcastle JD**, Chamberlain JO, Robinson MH, Moss SM, Amar SS, Balfour TW, James PD, Mangham CM. Randomised controlled trial of faecal-occult-blood screening for colorectal cancer. *Lancet* 1996; **348**: 1472-1477 [PMID: 8942775 DOI: 10.1016/S0140-6736(96)03386-7]

17 **Kronborg O**, Fenger C, Olsen J, Jørgensen OD, Søndergaard O. Randomised study of screening for colorectal cancer with faecal-occult-blood test. *Lancet* 1996; **348**: 1467-1471 [PMID: 8942774 DOI: 10.1016/S0140-6736(96)03430-7]

18 **Lindholm E**, Brevinge H, Haglind E. Survival benefit in a randomized clinical trial of faecal occult blood screening for colorectal cancer. *Br J Surg* 2008; **95**: 1029-1036 [PMID: 18563785 DOI: 10.1002/bjs.6136]

19 **Mandel JS**, Church TR, Ederer F, Bond JH. Colorectal cancer mortality: effectiveness of biennial screening for fecal occult blood. *J Natl Cancer Inst* 1999; **91**: 434-437 [PMID: 10070942 DOI: 10.1093/jnci/91.5.434]

20 **Hoepffner N**, Shastri YM, Hanisch E, Rösch W, Mössner J, Caspary WF, Stein J. Comparative evaluation of a new bedside faecal occult blood test in a prospective multicentre study. *Aliment Pharmacol Ther* 2006; **23**: 145-154 [PMID: 16393292 DOI: 10.1111/j.1365-2036.2006.02702.x]

21 **Whitlock EP**, Lin JS, Liles E, Beil TL, Fu R. Screening for colorectal cancer: a targeted, updated systematic review for the U.S. Preventive Services Task Force. *Ann Intern Med* 2008; **149**: 638-658 [PMID: 18838718 DOI: 10.7326/0003-4819-149-9-200811040-00245]

22 **Trojan J**, Povse N, Schröder O, Stein J. A new immunological test strip device for the rapid, qualitative detection of faecal occult blood. *Z Gastroenterol* 2002; **40**: 921-924 [PMID: 12436369]

23 **van Rossum LG**, van Rijn AF, Laheij RJ, van Oijen MG, Fockens P, van Krieken HH, Verbeek AL, Jansen JB, Dekker E. Random comparison of guaiac and immunochemical fecal occult blood tests for colorectal cancer in a screening population. *Gastroenterology* 2008; **135**: 82-90 [PMID: 18482589]

24 **Hol L**, van Leerdam ME, van Ballegooijen M, van Vuuren AJ, van Dekken H, Reijerink JC, van der Togt AC, Habbema JD, Kuipers EJ. Screening for colorectal cancer: randomised trial comparing guaiac-based and immunochemical faecal occult blood testing and flexible sigmoidoscopy. *Gut* 2010; **59**: 62-68 [PMID: 19671542 DOI: 10.1136/gut.2009.177089]

25 **Lee JK**, Liles EG, Bent S, Levin TR, Corley DA. Accuracy of fecal immunochemical tests for colorectal cancer: systematic review and meta-analysis. *Ann Intern Med* 2014; **160**: 171 [PMID: 24658694]

26 **Holme Ø**, Bretthauer M, Fretheim A, Odgaard-Jensen J, Hoff G. Flexible sigmoidoscopy versus faecal occult blood testing for colorectal cancer screening in asymptomatic individuals. *Cochrane Database Syst Rev* 2013; **9**: CD009259 [PMID: 24085634 DOI: 10.1002/14651858.CD009259.pub2]

27 **Ahlquist DA**, Shuber AP. Stool screening for colorectal cancer: evolution from occult blood to molecular markers. *Clin Chim Acta* 2002; **315**: 157-168 [PMID: 11728417 DOI: 10.1016/S0009-8981(01)00712-4]

28 **Røseth AG**, Kristinsson J, Fagerhol MK, Schjønsby H, Aadland E, Nygaard K, Roald B. Faecal calprotectin: a novel test for the diagnosis of colorectal cancer? *Scand J Gastroenterol* 1993; **28**: 1073-1076 [PMID: 8303210]

29 **Røseth AG**, Fagerhol MK, Aadland E, Schjønsby H. Assessment of the neutrophil dominating protein calprotectin in feces. A methodologic study. *Scand J Gastroenterol* 1992; **27**: 793-798 [PMID: 1411288]

30 **Kristinsson J**, Røseth A, Fagerhol MK, Aadland E, Schjønsby H, Børmer OP, Raknerud N, Nygaard K. Fecal calprotectin concentration in patients with colorectal carcinoma. *Dis Colon Rectum* 1998; **41**: 316-321 [PMID: 9514426]

31 **Limburg PJ**, Devens ME, Harrington JJ, Diehl NN, Mahoney DW, Ahlquist DA. Prospective evaluation of fecal calprotectin as a screening biomarker for colorectal neoplasia. *Am J Gastroenterol* 2003; **98**: 2299-2305 [PMID: 14572583 DOI: 10.1111/j.1572-0241.2003.07630.x]

32 **von Roon AC**, Karamountzos L, Purkayastha S, Reese GE, Darzi AW, Teare JP, Paraskeva P, Tekkis PP. Diagnostic precision of fecal calprotectin for inflammatory bowel disease and colorectal malignancy. *Am J Gastroenterol* 2007; **102**: 803-813 [PMID: 17324124 DOI: 10.1111/j.1572-0241.2007.01126.x]

33 **Gisbert JP**, McNicholl AG. Questions and answers on the role of faecal calprotectin as a biological marker in inflammatory bowel disease. *Dig Liver Dis* 2009; **41**: 56-66 [PMID: 18602356 DOI: 10.1016/j.dld.2008.05.008]

34 **Kok L**, Elias SG, Witteman BJ, Goedhard JG, Muris JW, Moons KG, de Wit NJ. Diagnostic accuracy of point-of-care fecal calprotectin and immunochemical occult blood tests for diagnosis of organic bowel disease in primary care: the Cost-Effectiveness of a Decision Rule for Abdominal Complaints in Primary Care (CEDAR) study. *Clin Chem* 2012; **58**: 989-998 [PMID: 22407858 DOI: 10.1373/clinchem.2011.177980]

35 **Mikhaĭlova EI**, Pimanov SI, Voropaev EV. [Fecal oncomarkers in the diagnostics of colorectal cancer]. *Klin Med* (Mosk) 2007; **85**: 62-67 [PMID: 18318171]

36 **Smith D**, Spanel P. Selected ion flow tube mass spectrometry (SIFT-MS) for on-line trace gas analysis. *Mass Spectrom Rev* 2005; **24**: 661-700 [PMID: 15495143 DOI: 10.1002/mas.20033]

37 **Huang J**, Kumar S, Abbassi-Ghadi N, Spaněl P, Smith D, Hanna GB. Selected ion flow tube mass spectrometry analysis of volatile metabolites in urine headspace for the profiling of gastro-esophageal cancer. *Anal Chem* 2013; **85**: 3409-3416 [PMID: 23421902 DOI: 10.1021/ac4000656]

38 **Kumar S**, Huang J, Cushnir JR, Španěl P, Smith D, Hanna GB. Selected ion flow tube-MS analysis of headspace vapor from gastric content for the diagnosis of gastro-esophageal cancer. *Anal Chem* 2012; **84**: 9550-9557 [PMID: 23035898 DOI: 10.1021/ac302409a]

39 **Altomare DF**, Di Lena M, Porcelli F, Trizio L, Travaglio E, Tutino

M, Dragonieri S, Memeo V, de Gennaro G. Exhaled volatile organic compounds identify patients with colorectal cancer. *Br J Surg* 2013; **100**: 144-150 [PMID: 23212621 DOI: 10.1002/bjs.8942]

40 **Peng G**, Hakim M, Broza YY, Billan S, Abdah-Bortnyak R, Kuten A, Tisch U, Haick H. Detection of lung, breast, colorectal, and prostate cancers from exhaled breath using a single array of nanosensors. *Br J Cancer* 2010; **103**: 542-551 [PMID: 20648015 DOI: 10.1038/sj.bjc.6605810]

41 **Xu ZQ**, Broza YY, Ionsecu R, Tisch U, Ding L, Liu H, Song Q, Pan YY, Xiong FX, Gu KS, Sun GP, Chen ZD, Leja M, Haick H. A nanomaterial-based breath test for distinguishing gastric cancer from benign gastric conditions. *Br J Cancer* 2013; **108**: 941-950 [PMID: 23462808 DOI: 10.1038/bjc.2013.44]

42 **Sonoda H**, Kohnoe S, Yamazato T, Satoh Y, Morizono G, Shikata K, Morita M, Watanabe A, Morita M, Kakeji Y, Inoue F, Maehara Y. Colorectal cancer screening with odour material by canine scent detection. *Gut* 2011; **60**: 814-819 [PMID: 21282130 DOI: 10.1136/gut.2010.218305]

43 **McNerney R**, Mallard K, Okolo PI, Turner C. Production of volatile organic compounds by mycobacteria. *FEMS Microbiol Lett* 2012; **328**: 150-156 [PMID: 22224870 DOI: 10.1111/j.1574-6968.2011.02493.x]

44 **Davis VW**, Bathe OF, Schiller DE, Slupsky CM, Sawyer MB. Metabolomics and surgical oncology: Potential role for small molecule biomarkers. *J Surg Oncol* 2011; **103**: 451-459 [PMID: 21400531 DOI: 10.1002/jso.21831]

45 **Mazurek S**. Pyruvate kinase type M2: a key regulator of the metabolic budget system in tumor cells. *Int J Biochem Cell Biol* 2011; **43**: 969-980 [PMID: 20156581 DOI: 10.1016/j.biocel.2010.02.005]

46 **Hardt PD**, Mazurek S, Toepler M, Schlierbach P, Bretzel RG, Eigenbrodt E, Kloer HU. Faecal tumour M2 pyruvate kinase: a new, sensitive screening tool for colorectal cancer. *Br J Cancer* 2004; **91**: 980-984 [PMID: 15266315 DOI: 10.1038/sj.bjc.6602033]

47 **Sherwood RA**. Faecal markers of gastrointestinal inflammation. *J Clin Pathol* 2012; **65**: 981-985 [DOI: 10.1136/jclinpath-2012-200901]

48 **Tonus C**, Sellinger M, Koss K, Neupert G. Faecal pyruvate kinase isoenzyme type M2 for colorectal cancer screening: a meta-analysis. *World J Gastroenterol* 2012; **18**: 4004-4011 [PMID: 22912551 DOI: 10.3748/wjg.v18.i30.4004]

49 **Demircan Y**, Özgür E, Külah H. Dielectrophoresis: applications and future outlook in point of care. *Electrophoresis* 2013; **34**: 1008-1027 [PMID: 23348714 DOI: 10.1002/elps.201200446]

50 **Harouaka R**, Kang Z, Zheng SY, Cao L. Circulating tumor cells: advances in isolation and analysis, and challenges for clinical applications. *Pharmacol Ther* 2014; **141**: 209-221 [PMID: 24134902 DOI: 10.1016/j.pharmthera.2013.10.004]

51 **Yang F**, Yang X, Jiang H, Bulkhaults P, Wood P, Hrushesky W, Wang G. Dielectrophoretic separation of colorectal cancer cells. *Biomicrofluidics* 2010; **4**: 13204 [PMID: 20644667 DOI: 10.1063/1.3279786]

52 **Yan J**, Pan D, Zhu C, Wang L, Song S, Fan C. A gold nanoparticle-based microfluidic protein chip for tumor markers. *J Nanosci Nanotechnol* 2009; **9**: 1194-1197 [PMID: 19441486]

53 **Duffy MJ**, van Dalen A, Haglund C, Hansson L, Klapdor R, Lamerz R, Nilsson O, Sturgeon C, Topolcan O. Clinical utility of biochemical markers in colorectal cancer: European Group on Tumour Markers (EGTM) guidelines. *Eur J Cancer* 2003; **39**: 718-727 [PMID: 12651195]

54 **Kitano S**, Myers J, Nakamura J, Yamane A, Yamashita M, Nakayama M, Tsukahara Y, Ushida H, Liu W, Ratain MJ, Amano M. A novel fully automated molecular diagnostic system (AMDS) for colorectal cancer mutation detection. *PLoS One* 2013; **8**: e62989 [PMID: 23671647 DOI: 10.1371/journal.pone.0062989]

55 **Ahlquist DA**, Zou H, Domanico M, Mahoney DW, Yab TC, Taylor WR, Butz ML, Thibodeau SN, Rabeneck L, Paszat LF, Kinzler KW, Vogelstein B, Bjerregaard NC, Laurberg S, Sørensen HT, Berger BM, Lidgard GP. Next-generation stool DNA test accurately detects colorectal cancer and large adenomas. *Gastroenterology* 2012; **142**: 248-56; quiz e25-6 [PMID: 22062357 DOI: 10.1053/j.gastro.2011.10.031]

56 **Ahlquist DA**, Sargent DJ, Loprinzi CL, Levin TR, Rex DK, Ahnen DJ, Knigge K, Lance MP, Burgart LJ, Hamilton SR, Allison JE, Lawson MJ, Devens ME, Harrington JJ, Hillman SL. Stool DNA and occult blood testing for screen detection of colorectal neoplasia. *Ann Intern Med* 2008; **149**: 441-50, W81 [PMID: 18838724]

57 **Saif MW**, Shah M. K-ras mutations in colorectal cancer: a practice changing discovery. *Clin Adv Hematol Oncol* 2009; **7**: 45-53, 64 [PMID: 19274041]

58 **Duffy MJ**. Can molecular markers now be used for early diagnosis of malignancy? *Clin Chem* 1995; **41**: 1410-1413 [PMID: 7586509]

59 **Gyparaki MT**, Basdra EK, Papavassiliou AG. DNA methylation biomarkers as diagnostic and prognostic tools in colorectal cancer. *J Mol Med* (Berl) 2013; **91**: 1249-1256 [PMID: 24057814]

60 A stool DNA test (Cologuard) for colorectal cancer screening. *Med Lett Drugs Ther* 2014; **56**: 100-101 [PMID: 25296259]

61 **Imperiale TF**, Ransohoff DF, Itzkowitz SH, Levin TR, Lavin P, Lidgard GP, Ahlquist DA, Berger BM. Multitarget stool DNA testing for colorectal-cancer screening. *N Engl J Med* 2014; **370**: 1287-1297 [PMID: 24645800 DOI: 10.1056/NEJMoa1311194]

62 **Toumazou C**, Shepherd LM, Reed SC, Chen GI, Patel A, Garner DM, Wang CJ, Ou CP, Amin-Desai K, Athanasiou P, Bai H, Brizido IM, Caldwell B, Coomber-Alford D, Georgiou P, Jordan KS, Joyce JC, La Mura M, Morley D, Sathyavruthan S, Temelso S, Thomas RE, Zhang L. Simultaneous DNA amplification and detection using a pH-sensing semiconductor system. *Nat Methods* 2013; **10**: 641-646 [PMID: 23749303 DOI: 10.1038/nmeth.2520]

63 **Loitsch SM**, Shastri Y, Stein J. Stool test for colorectal cancer screening--it's time to move! *Clin Lab* 2008; **54**: 473-484 [PMID: 19216253]

64 **Atkin WS**, Edwards R, Kralj-Hans I, Wooldrage K, Hart AR, Northover JM, Parkin DM, Wardle J, Duffy SW, Cuzick J. Once-only flexible sigmoidoscopy screening in prevention of colorectal cancer: a multicentre randomised controlled trial. *Lancet* 2010; **375**: 1624-1633 [PMID: 20430429 DOI: 10.1016/S0140-6736(10)60551-X]

65 Point of Care Diagnostics Market (POC) Analysis and 5 Year Forecast in New Research Report at ReportsnReports.com. Available from: URL: http://www.prweb.com/releases/point-of-care-diagnostics/poc-analysis/prweb10768012.htm

66 **Leodolter A**, Zielinski, Vieth M, Labenz J. Comparison of different immunological fobts for colorectal cancer screening: Wide range of sensitivity between different rapid tests. *Gastroenterology* 2010; **138**: S159 [DOI: 10.1016/S0016-5085(10)60727-5]

67 **Sanford KW**, McPherson RA. Fecal occult blood testing. *Clin Lab Med* 2009; **29**: 523-541 [PMID: 19840685]

68 **Agius A**, Azzopardi LM, Serracino Inglott A. Faecal occult blood testing in community pharmacy. *Int Pharm Pract* 2012; **20**: 61-62 [DOI: 10.1111/j.2042-7174.2012.00235.x]

69 **Kim HJ**, Kim HS, Lee JI, Lee SC, Lee IK, Cho HM, Han KJ, Oh ST. Clinical significance of fecal occult blood and fecal CEA dual rapid test kit for the detection of colorectal cancer. *Ann Oncol* 2010; **21**: i21 [DOI: 10.1093/annonc/mdq005]

70 **Shastri YM**, Loitsch S, Nowak R, Povse N, Stein J. Prospective comparative evaluation of an office-based rapid immunological test with a Guaiac-based fecal occult blood test for colorectal cancer screening in general population with average-risk. *Clin Lab* 2008; **54**: 385-387 [PMID: 19097496]

71 **Ottó S**, Czalbert JH, Papp I, Eckhardt S. Early detection of colorectal cancer. Preliminary report on the prospective value of a combined screening method for occult rectal bleeding. *Oncology* 1990; **47**: 209-214 [PMID: 2342763]

72 **Shastri YM**, Loitsch S, Hoepffner N, Povse N, Hanisch E, Rösch W, Mössner J, Stein JM. Comparison of an established simple office-based immunological FOBT with fecal tumor pyruvate kinase type M2 (M2-PK) for colorectal cancer screening: prospective

multicenter study. *Am J Gastroenterol* 2008; **103**: 1496-1504 [PMID: 18510609]
73 **Damms A**, Bischoff SC. Validation and clinical significance of a new calprotectin rapid test for the diagnosis of gastrointestinal diseases. *Int J Colorectal Dis* 2008; **23**: 985-992 [PMID: 18629518 DOI: 10.1007/s00384-008-0506-0]
74 **Sakai T**, Yamamoto K, Yokota H, Hakozaki-Usui K, Hino F, Kato I. Rapid, simple enzymatic assay of free L-fucose in serum and urine, and its use as a marker for cancer, cirrhosis, and gastric ulcers. *Clin Chem* 1990; **36**: 474-476 [PMID: 2311216]
75 **Ferté C**, André F, Soria JC. Molecular circuits of solid tumors: prognostic and predictive tools for bedside use. *Nat Rev Clin Oncol* 2010; **7**: 367-380 [PMID: 20551944 DOI: 10.1038/nrclinonc.2010.84]
76 **Danila DC**, Pantel K, Fleisher M, Scher HI. Circulating tumors cells as biomarkers: progress toward biomarker qualification. *Cancer J* 2011; **17**: 438-450 [PMID: 22157288 DOI: 10.1097/PPO.0b013e31823e69ac]
77 **Medley CD**, Smith JE, Tang Z, Wu Y, Bamrungsap S, Tan W. Gold nanoparticle-based colorimetric assay for the direct detection of cancerous cells. *Anal Chem* 2008; **80**: 1067-1072 [PMID: 18198894 DOI: 10.1021/ac702037y]
78 **Lopez-Crapez E**, Livache T, Marchand J, Grenier J. K-ras mutation detection by hybridization to a polypyrrole DNA chip. *Clin Chem* 2001; **47**: 186-194 [PMID: 11159765]
79 **Wen Y**, Pei H, Shen Y, Xi J, Lin M, Lu N, Shen X, Li J, Fan C. DNA Nanostructure-based Interfacial engineering for PCR-free ultrasensitive electrochemical analysis of microRNA. *Sci Rep* 2012; **2**: 867 [PMID: 23162691 DOI: 10.1038/srep00867]

P- Reviewer: Tsuchida A, Wang ZH **S- Editor**: Qi Y **L- Editor**: A
E- Editor: Ma S

World Journal of Gastroenterology

Submit a Manuscript: http://www.wjgnet.com/esps/
Help Desk: http://www.wjgnet.com/esps/helpdesk.aspx
DOI: 10.3748/wjg.v21.i14.4121

World J Gastroenterol 2015 April 14; 21(14): 4121-4125
ISSN 1007-9327 (print) ISSN 2219-2840 (online)

MINIREVIEWS

Optimum chemotherapy for the management of advanced biliary tract cancer

Marwan Ghosn, Hampig Raphael Kourie, Elie El Rassy, Ralph Chebib, Fadi El Karak, Colette Hanna, Dolly Nasr

Marwan Ghosn, Hampig Raphael Kourie, Elie El Rassy, Ralph Chebib, Fadi El Karak, Colette Hanna, Dolly Nasr, Department of Oncology, Faculty of Medicine, Saint Joseph University, Beirut 2038 3054, Lebanon

Author contributions: Ghosn M initiated the review; Ghosn M, Kourie HR, El Rassy E performed the review, analyzed the data and wrote first draft; Ghosn M, Kourie HR, El Rassy E, Chebib R, El Karak F, Hanna C and Nasr D reviewed and commented on the paper and provided final approval.

Conflict-of-interest: To the best of our knowledge, no conflict of interest exists.

Correspondence to: Marwan Ghosn, MD, Department of Oncology, Faculty of Medicine, Saint Joseph University, Monot St, Beirut, PO Box 166830, Beirut 2038 3054, Lebanon. mghosn.hdf@usj.edu.lb
Telephone: +961-1-3226842
Fax: +961-1-1613397

Received: November 30, 2014
Peer-review started: November 30, 2014
First decision: December 26, 2014
Revised: January 13, 2015
Accepted: February 13, 2015
Article in press: February 13, 2015
Published online: April 14, 2015

Abstract

Biliary tract cancers (BTCs) are highly fatal malignancies, which are often diagnosed at an advanced stage and have relatively poor prognosis. The treatment of patients with advanced BTC is systemic, based on chemotherapy or best supportive care, depending on their performance status. Despite clinical trials studying many chemotherapeutic regimens and targeted therapies for the treatment of BTC, the standard of care for advanced BTC remains the combination of gemcitabine with cisplatin. Many new molecules targeting proliferation and survival pathways, the immune response and angiogenesis are currently undergoing phase Ⅰ and Ⅱ trials for the treatment of advanced BTC with promising results.

Key words: Biliary tract cancer; Chemotherapy; Updates; Treatment modalities; Novel therapies

Core tip: This paper is a recent study outlining the most recent updates on the treatment of advanced biliary tract cancers. After a brief review of the different treatments used for advanced biliary tract cancers, current treatment options, novel therapies and future approaches are discussed.

Ghosn M, Kourie HR, El Rassy E, Chebib R, El Karak F, Hanna C, Nasr D. Optimum chemotherapy for the management of advanced biliary tract cancer. *World J Gastroenterol* 2015; 21(14): 4121-4125 Available from: URL: http://www.wjgnet.com/1007-9327/full/v21/i14/4121.htm DOI: http://dx.doi.org/10.3748/wjg.v21.i14.4121

INTRODUCTION

Biliary tract cancers (BTCs) are orphan, heterogeneous and highly fatal malignancies that represent less than 1% of all cancers including gallbladder cancer (GBC), cholangiocarcinoma (CC) and cancers of the ampulla of Vater (CAV). CAV are excluded from this review because of their different characteristics and better prognosis.

Of the two other BTCs, GBC is two times more frequent than CC, and between the two known CC subtypes, the extra-hepatic subtype is more common than intra-hepatic CC (15%). Moreover, the incidence of intra-hepatic CC is increasing in different countries (United States, United Kingdom and Australia), but its cause has not yet been elucidated[1].

These cancers are often diagnosed at an advanced stage defined as unresectable disease (metastatic or locally advanced) due to their nonspecific symptomatology, and they are associated with relatively poor prognosis. Five-year survival rates are 5%-10% for GBC and 10%-40% for CC[2].

Given its rarity and diversity, few clinical trials have studied optimum treatment for BTC. Historically, there has been no standard treatment for neither advanced (defined as stage ⅣA) nor metastatic BTC (defined as stage ⅣB). Treatments for these cancers have been extrapolated from treatment regimens for metastatic pancreatic cancer. However, as of 2010, many new trials have been designed to achieve optimum chemotherapeutic treatment for advanced BTC.

EVOLUTION OF TREATMENT MODALITIES

BTC studies between 1985 and 2006 have enrolled small numbers of patients (5-65 patients) but were limited by heterogeneity. Only three studies were randomized, including two phase Ⅱ trials[3,4] and one phase Ⅲ trial[5].

In 2007, Eckel *et al*[6] attempted to pioneer a chemotherapy standard of care for BTC. This group published a pooled analysis of 104 clinical trials that regrouped greater than 2800 patients and evaluated different treatment modalities. This pooled analysis suggested that the combination of gemcitabine and cisplatin or oxaliplatin is the most active regimen. Therefore, this modality was considered a provisional standard regimen for BTC until a new evidence-based standard was defined.

The first large randomized study (81 patients) was an Indian monocentric series that exclusively included GBC. This study compared the best supportive care (BSC) to 5-FU and folinic acid (FUFA) and modified gemcitabine and oxaliplatin. The results demonstrated improved overall survival (OS) and progression-free survival (PFS) with GEMOX compared with BSC and FUFA in unresectable GBC[7].

The British United Kingdom ABC-02 trial is the largest published trial designed for BTC. This study enrolled 410 patients and compared gemcitabine with its combination with cisplatin. The latter was associated with a significant survival advantage without adverse substantial toxicity. Thus, this regimen was considered an appropriate treatment option for patients with advanced BTC[8]. Another Japanese trial confirmed this conclusion. This study also showed that GBC has a poorer prognosis compared with non-GBC with a median OS of 9.1 mo for GBC and 13 mo for non-GBC[9]. A recent meta-analysis of these two studies recommended the combination of gemcitabine and cisplatin as a standard of care for the first-line treatment of advanced BTC for patients with good PS[10].

A Japanese phase Ⅱ trial associating S1 with gemcitabine demonstrated a better response rate compared with gemcitabine alone, but the superiority of this combination therapy was not completely clear[11].

With the era of targeted therapies, many strategies have been considered for BCT treatment. Single-agent or combined targeted therapies and chemotherapy combinations were the available options. The most frequent mutations targeted in these cancers include those in EGFR, Her2, KRAS and BRAF.

Since 2006, multiple phase Ⅱ trials have studied single-agent or combined targeted therapies. Studied have included erlotinib[12], bortezomib[13], lapatinib[14], everolimus[15], sorafenib[16,17], selumetinib[18], and sunitinib[19] and the combinations erlotinib and bevacizumab[20] and sorafenib and erlotinib[21]. All of the corresponding trials were negative (Table 1).

The association between targeted therapy and chemotherapy was also evaluated. Many clinical trials have evaluated the combination of a targeted therapeutic agent with the standard of care, which is gemcitabine plus cisplatin or oxaliplatin. The combination of gemcitabine and oxaliplatin with bevacizumab revealed a response rate (RR) of 40%, PFS of 7.0 mo and OS of 12.7 mo[22].

Adding an anti-EGFR drug (cetuximab, erlotinib and panitumumab) to gemcitabine and oxaliplatin was studied in several phase Ⅱ and Ⅲ trials. A phase Ⅱ study of 30 patients testing the association between gemcitabine, oxaliplatin and cetuximab in

Table 1 Single-agent targeted therapies in phase Ⅱ trials for advanced biliary tract cancer

Ref.	Line	*N*	Target	Treatment	RR (%)	PFS	OS
Philip *et al*[12] 2006	1-2	42	EGFR	Erlotinib	8	2.6	7.5
Costello *et al*[13] 2009	1-3	20	Proteasome	Bortezomib	0	1.5	9.5
Ramanathan *et al*[14] 2009	1-2	17	EGFR, HER2	Lapatinib	0	1.8	5.2
Buzzoni *et al*[15] 2010	2	18	mTOR	Everolimus	6	NA	NA
Bengala *et al*[16] 2010	1-5	46	VEGF, BRAF	Sorafenib	2	2.3	4.4
El Khoueiry *et al*[17] 2011	1	31	VEGF, BRAF	Sorafenib	0	3.0	9.0
Bekaii-Saab *et al*[18] 2011	1-2	28	MEK1-2	Selumetinib	12	3.7	9.8
Yi *et al*[19] 2012	2	56	VEGF	Sunitinib	8.9	1.7	NA

N: Number of participants; NA: Not available; OS: Overall survival; PFS: Progression-free survival; RR: Response rate.

advanced or metastatic BTC showed an objective RR of 63%[23]. These results were confirmed in a French-German phase Ⅱ randomized trial (BINGO) that evaluated the addition of cetuximab to the combination of gemcitabine and oxaliplatin. The RR overcame the 60% barrier in the first four months after adding cetuximab. The PFS and OS were not significantly different between the two concerned arms[24]. A randomized phase Ⅲ trial studied the addition of erlotinib to gemcitabine and oxaliplatin; the PFS increase observed with erlotinib was not statistically significant, and the OS was the same for the two groups. In subgroup analyses, the PFS was only significantly increased in the CC group. In a phase Ⅱ marker-driven trial of panitumumab and GEMOX followed by capecitabine for seven days for KRAS wild-type BTC, the results met the efficacy criteria for future testing in a randomized trial with a RR of 33%, PFS of 8.3 mo and OS of 10 mo[25]. All of the studies evaluating the addition of anti-EGFR to GEMOX in BTC failed to approve this combination as a standard of care.

The association between gemcitabine, the most effective chemotherapy for BTC, and MEK inhibitors, which showed an acceptable response, could be considered a perfect combination if it were not for their antagonist effects. A recent study revealed this combination as highly schedule-dependent with better results when these two drugs are used sequentially rather than simultaneously[26].

CURRENT TREATMENT OPTIONS

Despite evaluating many chemotherapeutic regimens and targeted therapies for the treatment of BTC, the standard of care for advanced BTC remains the combination of gemcitabine with cisplatin[8]. A regimen of gemcitabine and 5-FU is an acceptable option under some circumstances[27]. In the particular case of Klatskin tumors, aggressive surgery may be performed in a curative perspective. Effective, liver and portal vein resections are recommended for selected patients with advanced Klatskin tumors[28]. In general, the BSC is possible for patients with poor PS. OS with the standard of care is less than one year. Therefore, enrolling patients in clinical trials is recommended.

NOVEL THERAPIES AND APPROACHES

Many new concepts for treating advanced BTC are being evaluated, including angiogenesis inhibition, targeting tyrosine kinase signaling cascade components, manipulating the stromal reaction, the immune response, oncofetal signaling and epigenetic modifications[27].

Immunotherapy and vaccination

Immunotherapy in cancer has moved forward during the last few years, and several regimens have been approved as a standard of care for different cancers *e.g.,* ipilimumab for melanoma.

BTC has been reported to express a variety of tumor-associated antigens, such as Wilms' tumor gene 1 and mucin 1, which could be potential targets for immunotherapies[29-31]. Several clinical trials for immunotherapies targeting these molecules have been recently reported with promising results[32,33].

Inhibition of angiogenesis

After the failure of many trials evaluating anti-angiogenic drugs for the management of BTC, axitinib (AG-013736), an oral specific VEGFR TKI, shows potential therapeutic utility for vascular endothelial growth factor-expressing CCs[34].

Targeting signaling pathways

IFG1R, MEK, PI3K, AKT, and mTOR are the most frequent signaling pathway targets evaluated for the treatment of advanced BTC.

A phase Ⅰ study evaluating a MEK inhibitor (MEK162) showed an acceptable safety profile and desirable pharmacokinetics properties at 60 mg BID, and RECIST responses were observed in patients with BTC[35].

Everolimus (RAD001) exhibits multiple effects mediated by the inhibition of mTOR and may serve as a promising agent for the treatment of CC[36].

CONCLUSION

Despite numerous trials evaluating the chemotherapeutic regimens and targeted therapies for BTC, the combination of gemcitabine and cisplatin remains the gold standard for the treatment of BTC. At this time, OS is less than one year, and enrolling patients in clinical trials is also recommended. New strategies should be adopted for the management of BTC. As the molecular biology and genetic origin of this cancer improves and becomes completely elucidated, perhaps personalized therapy will achieve better outcomes. Subsequently, individualized treatments may be established according to molecular profiles and epigenetics with targeted and immunotherapies.

REFERENCES

1 **Rajagopalan V**, Daines WP, Grossbard ML, Kozuch P. Gallbladder and biliary tract carcinoma: A comprehensive update, Part 1. *Oncology* (Williston Park) 2004; **18**: 889-896 [PMID: 15255172]

2 **de Groen PC**, Gores GJ, LaRusso NF, Gunderson LL, Nagorney DM. Biliary tract cancers. *N Engl J Med* 1999; **341**: 1368-1378 [PMID: 10536130 DOI: 10.1056/NEJM199910283411807]

3 **Kornek GV**, Schuell B, Laengle F, Gruenberger T, Penz M, Karall K, Depisch D, Lang F, Scheithauer W. Mitomycin C in combination with capecitabine or biweekly high-dose gemcitabine in patients with advanced biliary tract cancer: a randomised phase II trial. *Ann Oncol* 2004; **15**: 478-483 [PMID: 14998852]

4 **Ducreux M**, Van Cutsem E, Van Laethem JL, Gress TM, Jeziorski K, Rougier P, Wagener T, Anak O, Baron B, Nordlinger B. A randomised phase II trial of weekly high-dose 5-fluorouracil with and without folinic acid and cisplatin in patients with advanced biliary tract carcinoma: results of the 40955 EORTC trial. *Eur*

J Cancer 2005; **41**: 398-403 [PMID: 15691639 DOI: 10.1016/j.ejca.2004.10.026]

5 **Rao S**, Cunningham D, Hawkins RE, Hill ME, Smith D, Daniel F, Ross PJ, Oates J, Norman AR. Phase III study of 5FU, etoposide and leucovorin (FELV) compared to epirubicin, cisplatin and 5FU (ECF) in previously untreated patients with advanced biliary cancer. *Br J Cancer* 2005; **92**: 1650-1654 [PMID: 15856037 DOI: 10.1038/sj.bjc.6602576]

6 **Eckel F**, Schmid RM. Chemotherapy in advanced biliary tract carcinoma: a pooled analysis of clinical trials. *Br J Cancer* 2007; **96**: 896-902 [PMID: 17325704 DOI: 10.1038/sj.bjc.6603648]

7 **Sharma A**, Dwary AD, Mohanti BK, Deo SV, Pal S, Sreenivas V, Raina V, Shukla NK, Thulkar S, Garg P, Chaudhary SP. Best supportive care compared with chemotherapy for unresectable gall bladder cancer: a randomized controlled study. *J Clin Oncol* 2010; **28**: 4581-4586 [PMID: 20855823 DOI: 10.1200/JCO.2010.29.3605]

8 **Valle J**, Wasan H, Palmer DH, Cunningham D, Anthoney A, Maraveyas A, Madhusudan S, Iveson T, Hughes S, Pereira SP, Roughton M, Bridgewater J. Cisplatin plus gemcitabine versus gemcitabine for biliary tract cancer. *N Engl J Med* 2010; **362**: 1273-1281 [PMID: 20375404 DOI: 10.1056/NEJMoa0908721]

9 **Okusaka T**, Nakachi K, Fukutomi A, Mizuno N, Ohkawa S, Funakoshi A, Nagino M, Kondo S, Nagaoka S, Funai J, Koshiji M, Nambu Y, Furuse J, Miyazaki M, Nimura Y. Gemcitabine alone or in combination with cisplatin in patients with biliary tract cancer: a comparative multicentre study in Japan. *Br J Cancer* 2010; **103**: 469-474 [PMID: 20628385 DOI: 10.1038/sj.bjc.6605779]

10 **Valle JW**, Furuse J, Jitlal M, Beare S, Mizuno N, Wasan H, Bridgewater J, Okusaka T. Cisplatin and gemcitabine for advanced biliary tract cancer: a meta-analysis of two randomised trials. *Ann Oncol* 2014; **25**: 391-398 [PMID: 24351397 DOI: 10.1093/annonc/mdt540]

11 **Sasaki T**, Isayama H, Nakai Y, Ito Y, Yasuda I, Toda N, Kogure H, Hanada K, Maguchi H, Sasahira N, Kamada H, Mukai T, Okabe Y, Hasebe O, Maetani I, Koike K. A randomized phase II study of gemcitabine and S-1 combination therapy versus gemcitabine monotherapy for advanced biliary tract cancer. *Cancer Chemother Pharmacol* 2013; **71**: 973-979 [PMID: 23355041 DOI: 10.1007/s00280-013-2090-4]

12 **Philip PA**, Mahoney MR, Allmer C, Thomas J, Pitot HC, Kim G, Donehower RC, Fitch T, Picus J, Erlichman C. Phase II study of erlotinib in patients with advanced biliary cancer. *J Clin Oncol* 2006; **24**: 3069-3074 [PMID: 16809731 DOI: 10.1200/JCO.2005.05.3579]

13 **Costello MR**, Meropol NJ, Denlinger CS, Engstrom PF, Wright JJ, Li T, Mclaughlin S, Beard M, Cimildoro R, Cohen SJ. A phase II trial of the proteasome inhibitor bortezomib in patients with recurrent or metastatic adenocarcinoma of the bile duct or gallbladder (NCI #6135). *J Clin Oncol* 2009; **27** suppl: e15605

14 **Ramanathan RK**, Belani CP, Singh DA, Tanaka M, Lenz HJ, Yen Y, Kindler HL, Iqbal S, Longmate J, Mack PC, Lurje G, Gandour-Edwards R, Dancey J, Gandara DR. A phase II study of lapatinib in patients with advanced biliary tree and hepatocellular cancer. *Cancer Chemother Pharmacol* 2009; **64**: 777-783 [PMID: 19169683 DOI: 10.1007/s00280-009-0927-7]

15 **Buzzoni R**, Pusceddu S, Platania M, Barone G, Valente M, Di Guardo L, Bajetta E. Efficacy and safety of RAD001 in advanced biliary tract cancer (BTC) patients (pts) progressing after first-line chemotherapy: A phase II study. *ASCO Meet Abstr* 2010; **28** (15_suppl): e14500

16 **Bengala C**, Bertolini F, Malavasi N, Boni C, Aitini E, Dealis C, Zironi S, Depenni R, Fontana A, Del Giovane C, Luppi G, Conte P. Sorafenib in patients with advanced biliary tract carcinoma: a phase II trial. *Br J Cancer* 2010; **102**: 68-72 [PMID: 19935794 DOI: 10.1038/sj.bjc.6605458]

17 **El-Khoueiry AB**, Rankin CJ, Ben-Josef E, Lenz HJ, Gold PJ, Hamilton RD, Govindarajan R, Eng C, Blanke CD. SWOG 0514: a phase II study of sorafenib in patients with unresectable or metastatic gallbladder carcinoma and cholangiocarcinoma. *Invest New Drugs* 2012; **30**: 1646-1651 [PMID: 21748296 DOI: 10.1007/s10637-011-9719-0]

18 **Bekaii-Saab T**, Phelps MA, Li X, Saji M, Goff L, Kauh JS, O'Neil BH, Balsom S, Balint C, Liersemann R, Vasko VV, Bloomston M, Marsh W, Doyle LA, Ellison G, Grever M, Ringel MD, Villalona-Calero MA. Multi-institutional phase II study of selumetinib in patients with metastatic biliary cancers. *J Clin Oncol* 2011; **29**: 2357-2363 [PMID: 21519026 DOI: 10.1200/JCO.2010.33.9473]

19 **Yi JH**, Thongprasert S, Lee J, Doval DC, Park SH, Park JO, Park YS, Kang WK, Lim HY. A phase II study of sunitinib as a second-line treatment in advanced biliary tract carcinoma: a multicentre, multinational study. *Eur J Cancer* 2012; **48**: 196-201 [PMID: 22176869 DOI: 10.1016/j.ejca.2011.11.017]

20 **Lubner SJ**, Mahoney MR, Kolesar JL, Loconte NK, Kim GP, Pitot HC, Philip PA, Picus J, Yong WP, Horvath L, Van Hazel G, Erlichman CE, Holen KD. Report of a multicenter phase II trial testing a combination of biweekly bevacizumab and daily erlotinib in patients with unresectable biliary cancer: a phase II Consortium study. *J Clin Oncol* 2010; **28**: 3491-3497 [PMID: 20530271 DOI: 10.1200/JCO.2010.28.4075]

21 **El-Khoueiry AB**, Rankin C, Siegel AB, Iqbal S, Gong IY, Micetich KC, Kayaleh OR, Lenz HJ, Blanke CD. S0941: a phase 2 SWOG study of sorafenib and erlotinib in patients with advanced gallbladder carcinoma or cholangiocarcinoma. *Br J Cancer* 2014; **110**: 882-887 [PMID: 24423918 DOI: 10.1038/bjc.2013.801]

22 **Zhu AX**, Meyerhardt JA, Blaszkowsky LS, Kambadakone AR, Muzikansky A, Zheng H, Clark JW, Abrams TA, Chan JA, Enzinger PC, Bhargava P, Kwak EL, Allen JN, Jain SR, Stuart K, Horgan K, Sheehan S, Fuchs CS, Ryan DP, Sahani DV. Efficacy and safety of gemcitabine, oxaliplatin, and bevacizumab in advanced biliary-tract cancers and correlation of changes in 18-fluorodeoxyglucose PET with clinical outcome: a phase 2 study. *Lancet Oncol* 2010; **11**: 48-54 [PMID: 19932054 DOI: 10.1016/S1470-2045(09)70333-X]

23 **Gruenberger B**, Schueller J, Heubrandtner U, Wrba F, Tamandl D, Kaczirek K, Roka R, Freimann-Pircher S, Gruenberger T. Cetuximab, gemcitabine, and oxaliplatin in patients with unresectable advanced or metastatic biliary tract cancer: a phase 2 study. *Lancet Oncol* 2010; **11**: 1142-1148 [PMID: 21071270 DOI: 10.1016/S1470-2045(10)70247-3]

24 **Malka D**, Cervera P, Heurteau-Foulon S, Wendum D, Trarbach T, De La Fouchardiere C, Boucher E, Fartoux L, Faivre S, Pignon JP, Rosmorduc O, Greten F. Gemcitabine and oxaliplatin (GEMOX) alone or with cetuximab in first-line treatment of advanced biliary cancers (ABC): Exploratory analyses according to tumor KRAS/BRAF mutations and EGFR expression in a randomized phase II trial (BINGO). *ASCO Meet Abstr* 2013; **31** (15_suppl): 4127

25 **Jensen LH**, Lindebjerg J, Ploen J, Hansen TF, Jakobsen A. Phase II marker-driven trial of panitumumab and chemotherapy in KRAS wild-type biliary tract cancer. *Ann Oncol* 2012; **23**: 2341-2346 [PMID: 22367707 DOI: 10.1093/annonc/mds008]

26 **Xu J**, Knox JJ, Ibrahimov E, Chen E, Serra S, Tsao M, Cao P, Vines D, Green DE, Metran-Nascente C, McNamara MG, Hedley DW. Sequence dependence of MEK inhibitor AZD6244 combined with gemcitabine for the treatment of biliary cancer. *Clin Cancer Res* 2013; **19**: 118-127 [PMID: 23091117 DOI: 10.1158/1078-0432.CCR-12-2557]

27 **Hezel AF**, Zhu AX. Systemic therapy for biliary tract cancers. *Oncologist* 2008; **13**: 415-423 [PMID: 18448556 DOI: 10.1634/theoncologist.2007-0252]

28 **Nimura Y**, Hayakawa N, Kamiya J, Maeda S, Kondo S, Yasui A, Shionoya. Combined portal vein and liver resection for carcinoma of the biliary tract. *British J Surg* 1991; **78**: 727-731 [DOI: 10.1002/bjs.1800780629]

29 **Nakatsuka S**, Oji Y, Horiuchi T, Kanda T, Kitagawa M, Takeuchi T, Kawano K, Kuwae Y, Yamauchi A, Okumura M, Kitamura Y, Oka Y, Kawase I, Sugiyama H, Aozasa K. Immunohistochemical detection of WT1 protein in a variety of cancer cells. *Mod Pathol* 2006; **19**: 804-814 [PMID: 16547468 DOI: 10.1038/modpathol.3800588]

30 **Higashi M**, Yonezawa S, Ho JJ, Tanaka S, Irimura T, Kim YS, Sato E. Expression of MUC1 and MUC2 mucin antigens in intrahepatic bile duct tumors: its relationship with a new morphological classification of cholangiocarcinoma. *Hepatology* 1999; **30**: 1347-1355 [PMID: 10573510 DOI: 10.1002/hep.510300609]

31 **Mall AS**, Tyler MG, Ho SB, Krige JE, Kahn D, Spearman W, Myer L, Govender D. The expression of MUC mucin in cholangiocarcinoma. *Pathol Res Pract* 2010; **206**: 805-809 [PMID: 20947262 DOI: 10.1016/j.prp.2010.08.004]

32 **Kaida M**, Morita-Hoshi Y, Soeda A, Wakeda T, Yamaki Y, Kojima Y, Ueno H, Kondo S, Morizane C, Ikeda M, Okusaka T, Takaue Y, Heike Y. Phase 1 trial of Wilms tumor 1 (WT1) peptide vaccine and gemcitabine combination therapy in patients with advanced pancreatic or biliary tract cancer. *J Immunother* 2011; **34**: 92-99 [PMID: 21150717 DOI: 10.1097/CJI.0b013e3181fb65b9]

33 **Shimizu K**, Kotera Y, Aruga A, Takeshita N, Takasaki K, Yamamoto M. Clinical utilization of postoperative dendritic cell vaccine plus activated T-cell transfer in patients with intrahepatic cholangiocarcinoma. *J Hepatobiliary Pancreat Sci* 2012; **19**: 171-178 [PMID: 21874278 DOI: 10.1007/s00534-011-0437-y]

34 **Takahashi H**, Ojima H, Shimizu H, Furuse J, Furukawa H, Shibata T. Axitinib (AG-013736), an oral specific VEGFR TKI, shows potential therapeutic utility against cholangiocarcinoma. *Jpn J Clin Oncol* 2014; **44**: 570-578 [PMID: 24755544 DOI: 10.1093/jjco/hyu045]

35 **Finn RS**, Javle MM, Tan BR, Weekes CD, Bendell JC, Patnaik A, Naaz Khan G, Laheru D, Anderson L, Christy-Bittel JL, Barrett E, Guthrie G, Litwiler K, Bekaii-Saab T. A phase I study of MEK inhibitor MEK162 (ARRY-438162) in patients with biliary tract cancer. *J Clin Oncol* 2012; **30** suppl 4: abstr 220

36 **Moolthiya P**, Tohtong R, Keeratichamroen S, Leelawat K. Role of mTOR inhibitor in cholangiocarcinoma cell progression. *Oncol Lett* 2014; **7**: 854-860 [PMID: 24527093 DOI: 10.3892/ol.2014.1799]

P- Reviewer: Kaiser GM **S- Editor**: Qi Y **L- Editor**: A
E- Editor: Zhang DN

World Journal of Gastroenterology

Submit a Manuscript: http://www.wjgnet.com/esps/
Help Desk: http://www.wjgnet.com/esps/helpdesk.aspx
DOI: 10.3748/wjg.v21.i14.4126

World J Gastroenterol 2015 April 14; 21(14): 4126-4135
ISSN 1007-9327 (print) ISSN 2219-2840 (online)

ORIGINAL ARTICLE

Basic Study

Thalidomide ameliorates portal hypertension *via* nitric oxide synthase independent reduced systolic blood pressure

Nicholas G Theodorakis, Yining N Wang, Vyacheslav A Korshunov, Mary A Maluccio, Nicholas J Skill

Nicholas G Theodorakis, Mary A Maluccio, Nicholas J Skill, Division of Transplant Surgery, Department of Surgery, School of Medicine, Indiana University, Indianapolis, IN 46202, United States
Yining N Wang, Vyacheslav A Korshunov, School of Medicine, University of Rochester, Rochester, NY 14611, United States
Author contributions: Theodorakis NG, Wang YN, Korshunov VA and Skill NJ performed the research; Skill NJ and Theodorakis NG designed the research; Skill NJ and Maluccio MA wrote the paper.
Supported by The Departments of Surgery at the University of Rochester and Indiana University.

Correspondence to: Nicholas J Skill, PhD, Assistant Professor, Division of Transplant Surgery, Department of Surgery, School of Medicine, Indiana University, C519, 980 West Walnut Street (R3), Indianapolis, IN 46202, United States. nskill@iupui.edu
Telephone: +1-317-2744532
Fax: +1-317-2748046
Received: June 12, 2014
Peer-review started: June 12, 2014
First decision: July 9, 2014
Revised: July 30, 2014
Accepted: October 15, 2014
Article in press: October 15, 2014
Published online: April 14, 2015

Abstract

AIM: Portal hypertension is a common complication of liver cirrhosis and significantly increases mortality and morbidity. Previous reports have suggested that the compound thalidomide attenuates portal hypertension (PHT). However, the mechanism for this action is not fully elucidated. One hypothesis is that thalidomide destabilizes tumor necrosis factor α (TNFα) mRNA and therefore diminishes TNFα induction of nitric oxide synthase (NOS) and the production of nitric oxide (NO). To examine this hypothesis, we utilized the murine partial portal vein ligation (PVL) PHT model in combination with endothelial or inducible NOS isoform gene knockout mice.

METHODS: Wild type, inducible nitric oxide synthase (iNOS)$^{-/-}$ and endothelial nitric oxide synthase (eNOS)$^{-/-}$ mice received either PVL or sham surgery and were given either thalidomide or vehicle. Serum nitrate (total nitrate, NOx) was measured daily for 7 d as a surrogate of NO synthesis. Serum TNFα level was quantified by enzyme-linked immunosorbent assay. TNFα mRNA was quantified in liver and aorta tissue by reverse transcription-polymerase chain reaction. PHT was determined by recording splenic pulp pressure (SPP) and abdominal aortic flow after 0-7 d. Response to thalidomide was determined by measurement of SPP and mean arterial pressure (MAP).

RESULTS: SPP, abdominal aortic flow (Qao) and plasma NOx were increased in wild type and iNOS$^{-/-}$ PVL mice when compared to sham operated control mice. In contrast, SPP, Qao and plasma NOx were not increased in eNOS$^{-/-}$ PVL mice when compared to sham controls. Serum TNFα level in both sham and PVL mice was below the detection limit of the commercial ELISA used. Therefore, the effect of thalidomide on serum TNFα levels was undetermined in wild type, eNOS$^{-/-}$ or iNOS$^{-/-}$ mice. Thalidomide acutely increased plasma NOx in wild type and eNOS$^{-/-}$ mice but not iNOS$^{-/-}$ mice. Moreover, thalidomide temporarily (0-90 min) decreased mean arterial pressure, SPP and Qao in wild type, eNOS$^{-/-}$ and iNOS$^{-/-}$ PVL mice, after which time levels returned to the respective baseline.

CONCLUSION: Thalidomide does not reduce portal

pressure in the murine PVL model by modulation of NO biosynthesis. Rather, thalidomide reduces PHT by decreasing MAP by an undetermined mechanism.

Key words: Portal hypertension; Thalidomide; Nitric oxide; Knockout mice; Endothelial nitric oxide synthase; Inducible nitric oxide synthase; Tumor necrosis factor alpha

Core tip: The research innovation detailed in this manuscript is the use of nitric oxide synthase (NOS) isoform specific gene deleted mice to better understand the underlying mechanisms for the development of portal hypertension (PHT). PHT is a significant complication of liver disease and increases morbidity and mortality. Our study examined the hypothesis that the compound thalidomide reduces PHT by decreasing the biosynthesis of nitric oxide (NO) *via* destabilizing tumor necrosis factor alpha mRNA levels. We demonstrate that thalidomide induces NO *via* increased inducible nitric oxide synthase isoform of NOS; however, thalidomide reduction in PHT was NOS isoform independent.

Theodorakis NG, Wang YN, Korshunov VA, Maluccio MA, Skill NJ. Thalidomide ameliorates portal hypertension *via* nitric oxide synthase independent reduced systolic blood pressure. *World J Gastroenterol* 2015; 21(14): 4126-4135 Available from: URL: http://www.wjgnet.com/1007-9327/full/v21/i14/4126.htm DOI: http://dx.doi.org/10.3748/wjg.v21.i14.4126

INTRODUCTION

Portal hypertension (PHT) is a complication typically associated with underlying liver disease whereby portal pressure exceeds 10 mmHg[1]. In general, PHT is predominantly a sequela of alcoholic, non-alcoholic steatohepatitis or viral cirrhosis[2] and is augmented by the formation of a systemic hyper-dynamic circulation manifesting as a generalized reduced vascular resistance, *via* vasodilation, promoting systemic and mesenteric hyperemia[3,4]. Increased hepatic resistance in combination with hyperemia promotes redirection of portal venous flow from the liver towards, *inter alia,* mesenteric and azygous venous beds to form esophageal and ectopic varices[5]. Generally, esophagogastric varices have the greatest capacity for hemorrhage amongst varices and in combination with liver failure significantly increase mortality and morbidity[6].

Previous studies have detailed the importance of nitric oxide synthase (NOS) enzymes in the development of PHT. In particular, the NOS isoform endothelial NOS (eNOS) is thought to be important to PHT by regulating biosynthesis of the potent vasodilator nitric oxide (NO)[7-9]. Decreased hepatic eNOS results in hepatic sinusoid constriction and increased hepatic resistance to portal venous flow[10]. In contrast, increased extra-hepatic vascular eNOS promotes vasodilation and the development of hyper-dynamic circulation by increasing blood flow to the liver[11,12]. Moreover, functional eNOS is also found in circulating micro-particles (< 1 μm) shed from endothelial and blood cells. Studies show that micro-particles are increased in patients with endothelial dysfunction but eNOS expression is decreased[13]. Consequently, the precise mechanism/role for eNOS in PHT is not clear. We do know that eNOS activation is multifaceted and includes protein kinase B AKT, GTPase-activating protein, sarcoma proto-oncogene and G protein-coupled receptor-2 kinase activity culminating with eNOS phosphorylation and translocation to the cell membrane[8,14-16].

In addition, the cytokine tumor necrosis factor-alpha (TNF-α) is thought to be important in the pathogenesis of PHT by increasing eNOS activity and NO production[17,18]. Therefore, inhibition of TNFα has the potential to ameliorate portal pressure and reduce mortality and morbidity associated with PHT. Previous studies have shown that the compound thalidomide destabilizes TNFα mRNA[19] and prevents the development of PHT in portal vein ligated (PVL) animals[20,21]. However, the precise mechanism by which thalidomide abrogates PHT is not fully understood. In human studies, thalidomide reduces hepatic venous pressure gradient without reducing systemic hemodynamic parameters[22]. This suggests that: (1) TNFα is not associated with PHT associated hyper-dynamic circulation; and (2) thalidomide reduces PHT independent of TNFα and NO.

To examine the mechanistic connection between thalidomide, TNFα and NO on PHT, we utilized the murine, non-inflammatory, pre-hepatic PVL model of PHT and commercially available iNOS and eNOS gene knockout mice and examined changes to TNFα and PHT in response to thalidomide. We have previously shown that in the PVL model of PHT, eNOS is the dominant NOS isoform and in its absence PHT does not develop[9]. We anticipated that in PVL mice, TNFα would be increased and that thalidomide would reduce this increase and associated PHT but there would be no response to thalidomide in eNOS$^{-/-}$ mice. In contrast to this expectation, we found that TNFα levels were below detectable limits of the enzyme-linked immunosorbent assay (ELISA) used and that thalidomide caused: (1) an iNOS dependent increase in circulating NOx levels; and (2) thalidomide reduction of portal pressure was NOS isoform independent and was commensurate with a NOS independent drop in systolic blood pressure. Because TNFα levels in mice were below detectable levels, we were unable to determine response to thalidomide administration. Liver and thoracic aorta tissue TNFα mRNA expression levels were detectable and levels were not significantly

changed in response to PVL surgery but were increased following thalidomide administration. This information demonstrates that thalidomide improves portal hemodynamics independent of NO and is linked to a reduction in mean arterial blood pressure.

MATERIALS AND METHODS

Unless otherwise stated, all chemicals were purchased from Sigma, MO. The partial portal vein ligation pre-hepatic PHT model was used. All studies were approved by the University of Rochester committee for animal research and adhered to AAALC and federal guidelines for the humane care and treatment of animals. Mice were maintained in sterilized isolette cages on a 12-h light/dark cycle and were allowed access to food and water ad libitum. Mice [C57B/6J, C57BL/6J-NOS2^{tm1Unc} (iNOS$^{-/-}$)[23] and C57BL/6J-NOS3^{tm1Unc} (eNOS$^{-/-}$)[24] (Jackson Labs, MA)] were anesthetized using halothane inhalation. A midline laparotomy was performed and the portal vein was exposed. A blunt-ended 27-gauge needle was placed alongside the portal vein and a 4-0 silk suture was tied around the vein and needle, after which the needle was withdrawn, producing a standardized stenosis. In sham animals, the procedure consisted of dissection and visual inspection of the portal vein without ligature. The abdomen was closed and the animals were allowed to recover under a heat lamp. For thalidomide studies, (25-100 mg/kg per day) thalidomide (α-N-phthalyllutamic-acid-imine) or dimethyl sulfoxide (DMSO) vehicle was given 16 h prior and 4 h following PVL or sham and every 24 h thereafter.

Physiological measurements

Physiological measurements were performed as previously described[9]. At the indicated times post sham-operation or PVL, animals were anesthetized (halothane) and subjected to laparotomy to allow physiological measurements to be taken. Splenic pulp pressure (SPP) was measured as an index of portal venous pressure. To measure SPP, a cannula made from a 25-gauge needle connected to a saline-filled manometer was inserted into the spleen pulp. Abdominal aortic flow was measured by placing an ultrasonic Doppler flow probe (Transonic #11RB) around the abdominal aorta between the diaphragm and celiac artery. Flow rates were obtained with a Transonic T206 Blood Flow Meter (Transonic Instruments, Ithaca, NY). Aortic blood flows were standardized per gram of body weight.

Systolic blood pressure and heart rate were determined by non-invasive tail cuff plethysmography using the Visitech BP-2000 Blood Pressure Analysis system as per manufacturer's instructions (Visitech systems, Apex, NC). Baseline values were obtained for 4 d to train the mice (n = 8) in the measurement of blood pressure and heart rate. On the fifth day, mice were given 50 mg/kg thalidomide and the blood pressure and heart rate was calculated for 10 min every 20 min.

Plasma TNFα and NOx levels

Blood was collected by cardiac puncture, injected into heparinized tubes and centrifuged. Plasma TNFα was measured by sandwich ELISA in accordance with manufacturer's instructions (#MTA00B, RD systems, Minneapolis, MN). TNFα was measured 0, 1, 3, 6, 12, 16, 20 and 24 h and 2, 3, 4, 5, 6 and 7 d following PVL operation. Plasma NOx was determined using the Griess reaction[25] using a commercially available kit (#NB98, Oxford Biomedical, Rochester Hills, MI).

***In vitro* cell culture:** RAW264 mouse macrophage cells (#TIB-71 ATCC, Manassas, VI) were cultured in the presence or absence of LPA and/or 25-100 μg/mL thalidomide for 0-24 h.

Gene expression: TNFα, eNOS and iNOS mRNA from liver, aorta or RAW264 cells were determined by reverse transcription-polymerase chain reaction (RT-PCR) using gene-specific primers (200 ng) and 1 μg cDNA: eNOS: 5'GTGTGAAGGCAACCATTCTG 3'ACTCATCCATG CACAGGACC, INOS: 5'GGCTTCACGGGTCAGAGCCA 3'TGCCCATTGC TGGGACAGTC TNFα 5'CTGTAGCC-CACGTCGTAGC 3'TTGAGATCCATGCCGTTG 3 (cycle = 1 min each of 94 oc, 60 oc and 74 oc × 35). Primers were purchased from Life Technologies, Grand Island, NY.

Statistical analysis

The data shown are mean ± SE, with 3-7 animals per experimental group. Statistical significance was estimated using ANOVA statistical analysis (SPSS, IBM).

RESULTS

TNF-α and NOx levels following PVL or thalidomide administration: plasma TNFα and NOx levels were determined following sham or PVL ligation and after thalidomide injection. TNFα levels were below the detectable levels of the assay. Consequently, no increase was detected following PVL and no decrease following thalidomide injection. Injection of 1 mg/kg LPS increased serum TNFα from undetectable levels to 192 pg/mL. Plasma NOx was increased significantly following PVL in wild type mice, peaking at 2 d post PVL surgery (Figure 1A). This PVL induced NOx at 2 d post-surgery was eNOS specific. NOx was not increased in eNOS$^{-/-}$ mice following PVL but was increased in iNOS$^{-/-}$ mice (Figure 1B). Thalidomide induction of NOx was iNOS specific. Serum NOx was not increased in iNOS$^{-/-}$ mice following thalidomide injection but was increased in eNOS$^{-/-}$ mice (Figure 1C). Thalidomide increased iNOS mRNA levels in aorta and liver tissue samples (75% and 162% respectively at 100 mg/kg). No change in eNOS expression was

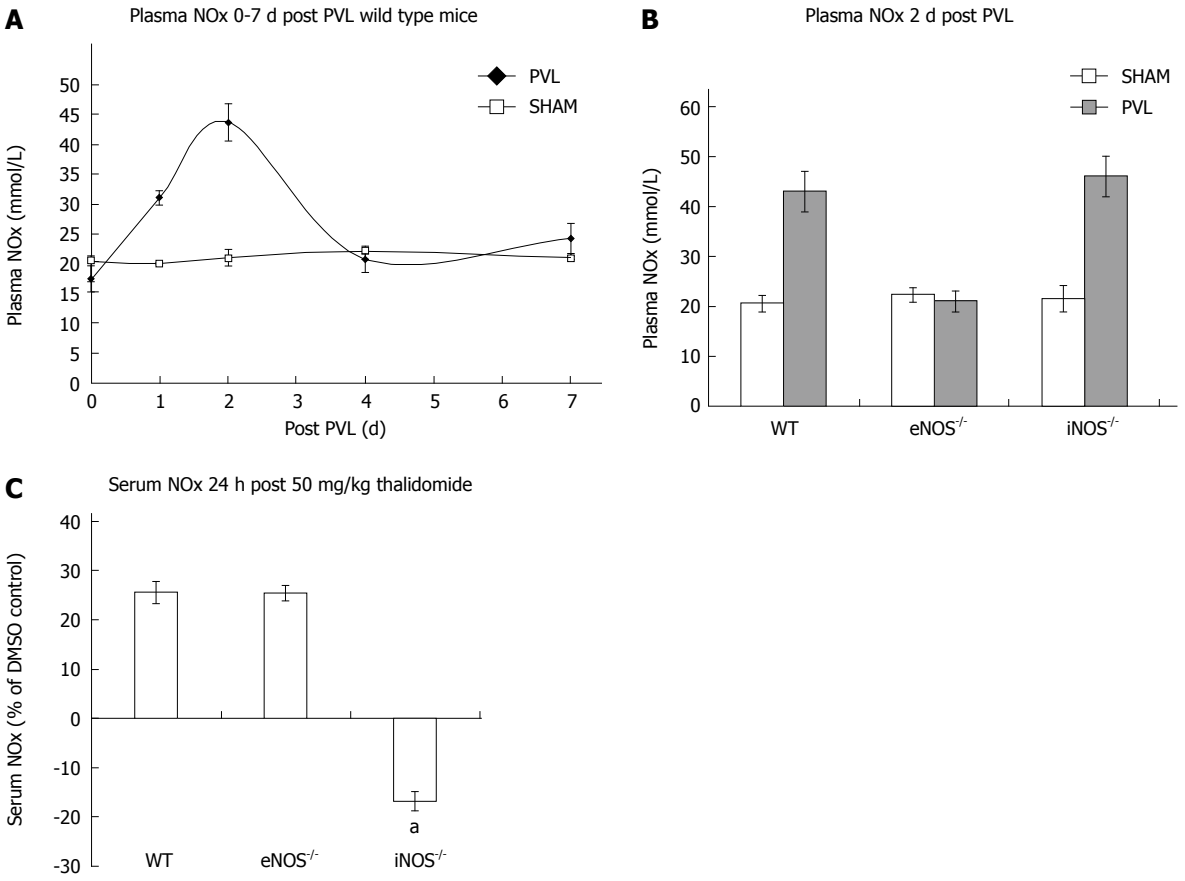

Figure 1 Portal vein ligation and thalidomide increases nitric oxide *via* endothelial and inducible nitric oxide synthase respectively. Plasma total nitrate (NOx) was measured daily for 7 d in wild type (WT), endothelial nitric oxide synthase (eNOS)$^{-/-}$ and inducible nitric oxide synthase (iNOS)$^{-/-}$ mice following portal vein ligation (PVL) or sham surgery. A: Plasma NOx increased following PVL in wild type mice but not following sham surgery. Levels increased to a maximum 2 d after PVL, after which NOx returned to pre-surgical baseline; B: Plasma NOx increased 2 d following PVL in iNOS$^{-/-}$ but not eNOS mice. In eNOS$^{-/-}$ mice NO was not increased following PVL; C: Unadulterated 8 wk WT, eNOS$^{-/-}$ and iNOS$^{-/-}$ mice were given 50 mg/kg thalidomide or vehicle. Blood was collected by cardiac puncture and plasma was assayed for NOx. Plasma NOx was significantly increased by the administration of thalidomide in WT and eNOS$^{-/-}$ mice but was reduced in iNOS$^{-/-}$ mice. $^{a}P < 0.05$ *vs* other groups.

Table 1 Splenic pulp pressure and abdominal aortic flow 7 d post portal vein ligation or sham

	Splenic pulp pressure (cmH_2O)	Abdominal aortic flow (mL/min per gram)
Wild type sham	6.9 ± 0.4	0.17 ± 0.02
Wild type 7 d PVL	25.4 ± 3.1[a]	0.27 ± 0.04[a]
eNOS$^{-/-}$ sham	6.9 ± 0.3	0.15 ± 0.01
eNOS$^{-/-}$ 7 d PVL	7 ± 0.5	0.15 ± 0.01
iNOS$^{-/-}$ 7 d sham	6.7 ± 1	0.16 ± 0.01
iNOS$^{-/-}$ 7 d PVL	21.1 ± 0.4[c]	0.23 ± 0.06[c]

$^{a}P < 0.05$ *vs* wild type sham *t*-test; $^{c}P < 0.05$ *vs* iNOS$^{-/-}$ 7d sham *t*-test; mean ± SE (n = 4-7). iNOS: Inducible nitric oxide synthase.

observed.

Hepatic and arterial TNFα, eNOS and iNOS expression following thalidomide administration: thalidomide is reported to destabilize TNFα mRNA[19]. In immortalized macrophage cells (RAW263.3), we found that thalidomide reduced TNFα mRNA in unstimulated and LPS stimulated cells (81.7% and 78.6% respectively). In contrast, thalidomide did not reduce LPS stimulated iNOS mRNA induction. The effect of thalidomide *in vivo* was determined by quantification of hepatic and arterial tissue TNFα, eNOS and iNOS expression ± thalidomide by RT-PCR. TNFα mRNA was increased by 62% in thoracic aorta tissues and 34% in the liver tissues. In a similar manner, hepatic iNOS was increased 70% and 49% respectively. No change in eNOS mRNA was observed.

Effects of thalidomide on mean blood pressure, heart rate and portal hemodynamics following PVL: in vehicle treated mice, splenic pulp pressure and abdominal aortic flow were increased significantly 7 d following PVL (Table 1). Treatment of mice with 50 mg/kg thalidomide resulted in a temporary (90 min) reduction in elevated splenic pressure and mean systolic blood pressure (58% and 70% reduction respectively) (Figure 2A and B). Thalidomide induced reduction was maximal 30-60 min following injection and after which time splenic pulp pressure and mean arterial pressure recovered to an elevated level by 90 min. No significant change in heart rate was observed following thalidomide administration in PVL or sham mouse groups.

Role of NOS isoforms on thalidomide: to determine

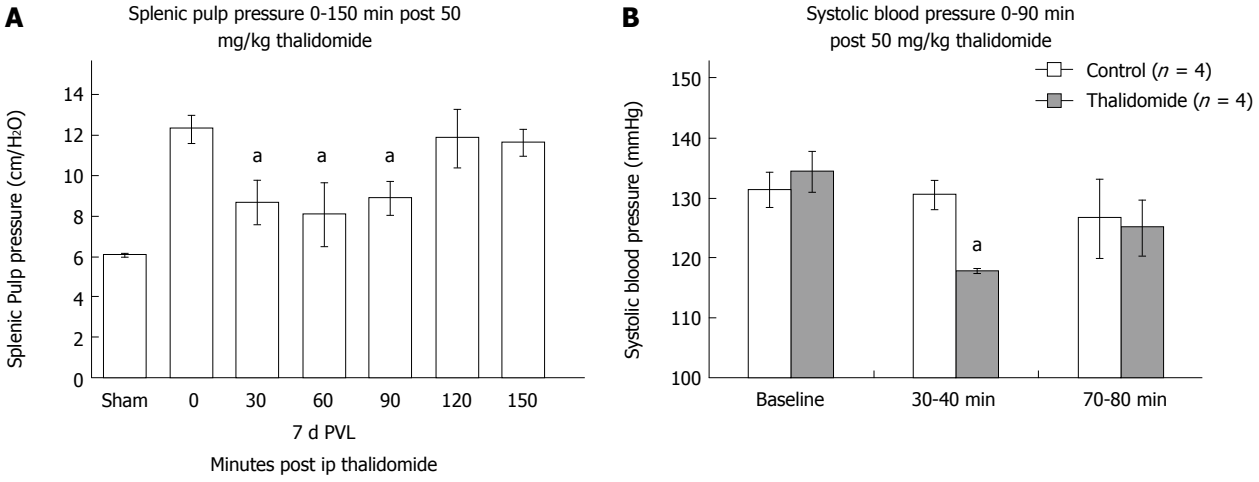

Figure 2 Thalidomide temporarily ameliorates splenic pulp pressure and mean systolic blood pressure in 7 d portal vein ligation mice. A: 7 d wild type sham and portal vein ligation (PVL) mice were treated with 50 mg/kg thalidomide *ip* and splenic pulp pressure was measured 0-150 min following administration. Splenic pulp pressure was rapidly and temporarily decreased by thalidomide; after 2 h pressure returned back to pre-thalidomide levels; B: Systolic blood pressure was also measured in 7 d PVL wild type mice following the administration of 50 mg/kg thalidomide or vehicle control. In a similar manner to splenic pulp pressure the systolic blood pressure was temporarily decreased by thalidomide. $^{a}P < 0.05$ *vs* control group.

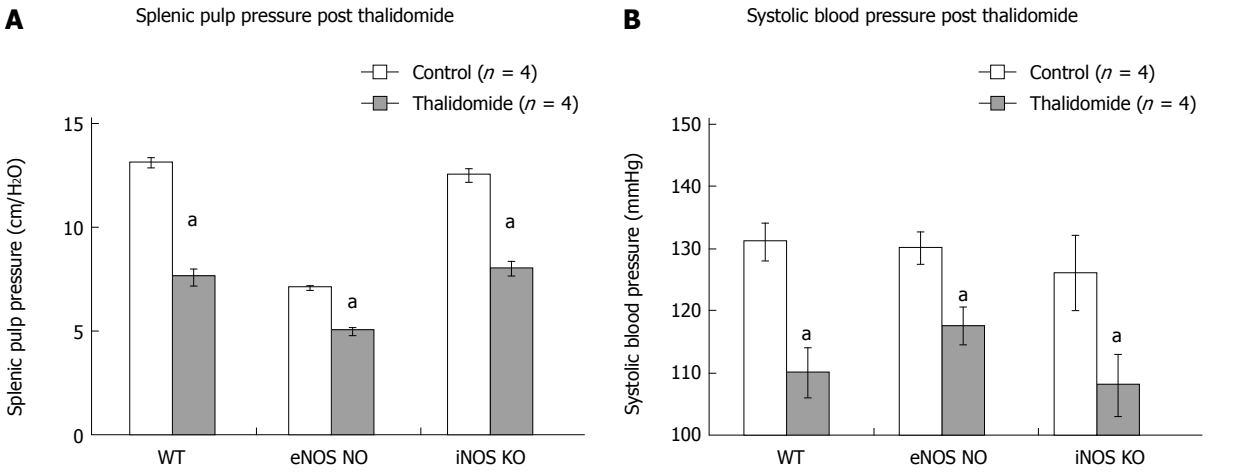

Figure 3 Thalidomide reduction of splenic pulp pressure and systolic blood pressure is endothelial and inducible nitric oxide synthase independent. 7 d portal vein ligation wild type, endothelial nitric oxide synthase (eNOS)$^{-/-}$ and inducible nitric oxide synthase (iNOS)$^{-/-}$ mice were treated with 50 mg/kg thalidomide or dimethyl sulfoxide vehicle control *ip*. Splenic pulp pressure (A) and systolic blood pressure (B) were measure 60 min after administration. Thalidomide reduced splenic pulp pressure and systolic pulp pressure in wild type, eNOS$^{-/-}$ and iNOS$^{-/-}$ mice ($n = 4$ mice per group, $^{a}P < 0.05$ *vs* control group).

the role of NOS isoforms on the transient hemodynamic response to thalidomide, wild type, eNOS$^{-/-}$ and iNOS$^{-/-}$ 7 d PVL mice were treated with 50 mg/kg thalidomide and hemodynamic measurements were performed 30 min thereafter. Portal pressure and systolic blood pressure were significantly reduced in all mice groups (Figure 3). Reduction in hemodynamics in response to thalidomide was NOS isoform independent.

TNFα aortic and hepatic expression post PVL: to evaluate the role of TNFα in the PVL model, levels were determined by RT-PCR in aorta and liver tissue samples 0-4 d following PVL. TNFα was generally unchanged in response to PVL in both liver and aorta samples. However, there was a transient reduction in TNFα expression 3 h post PVL within aortic tissues but this reduction was not significantly significant ($P = 0.1$) (Figure 4). Whole tissues were used and so differentiation between muscle, nervous, connective and epithelial tissue was not investigated.

DISCUSSION

In 1998, the US Food and Drug Administration approved the use of thalidomide for the treatment of leprosy and multiple myeloma. Additional research has investigated the benefit of thalidomide in animal models of Alzheimer's[26], pancreatitis[27], colitis[28] and PHT[20].

The purpose of this manuscript is not to advocate the use of thalidomide for the treatment of PHT. That claim is beyond the scope of our experimental studies and we leave that analysis for others. Using the PVL murine model of pre-hepatic PHT in eNOS$^{-/-}$ and INOS$^{-/-}$ deficient animals, this study investigates thalidomide abrogation of PHT *via* mediating activation of NO

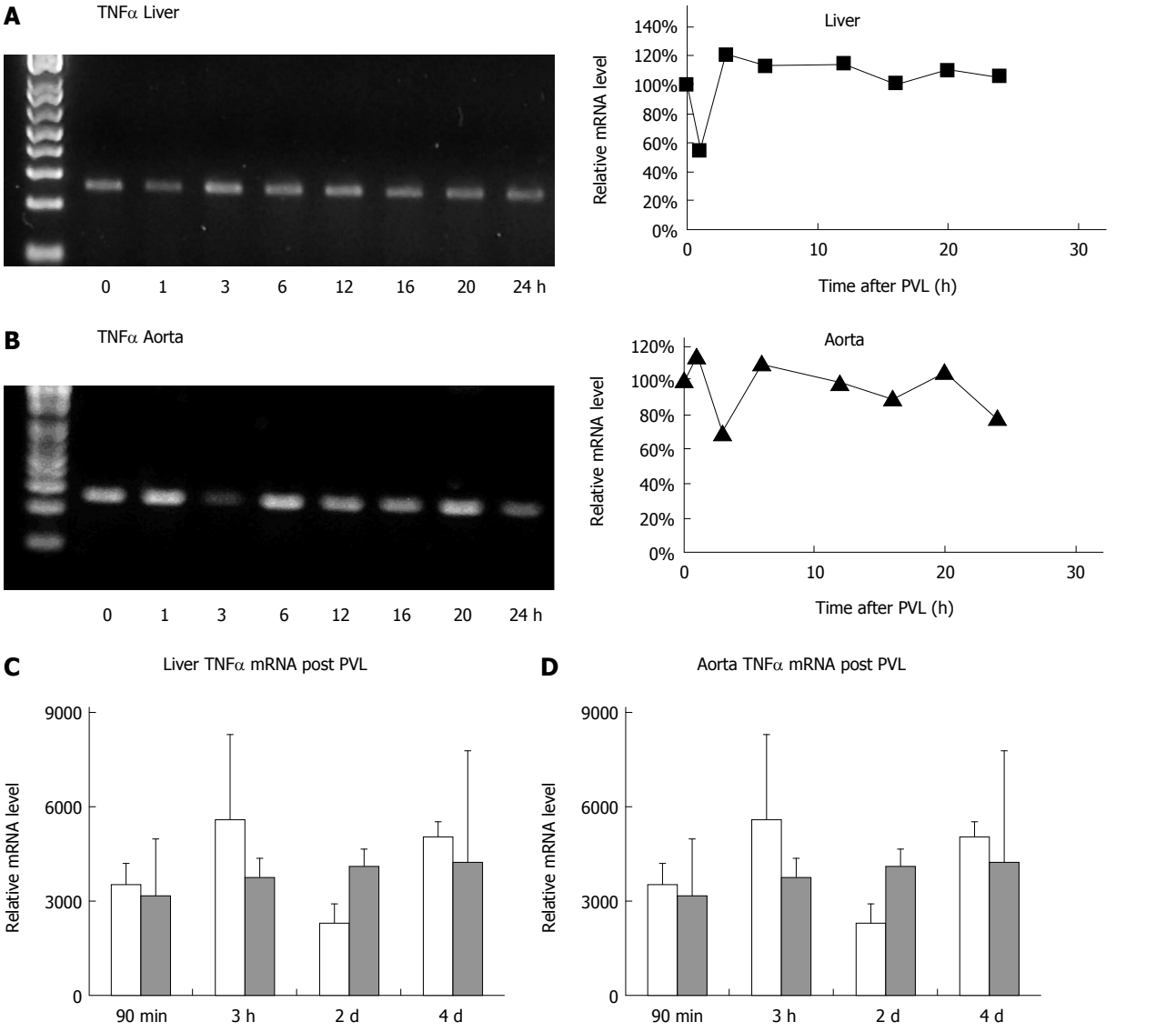

Figure 4 Portal vein ligation does not increase hepatic or aortic tumor necrosis factor alpha mRNA expression. Pre-hepatic portal hypertension was induced in wild type mice by partial ligation of the portal vein. 0-24 h post ligation livers (A) and thoracic aortas (B) were harvested and quantified for tumor necrosis factor (TNF) mRNA by reverse transcription-polymerase chain reaction. TNFα was not changed within livers and aorta following portal vein ligation (PVL). Figures are representative of three experiments. Hepatic (C) and aortic (D) TNFα expression was unchanged 0-4 d post PVL. Line graphs represent mean ± SE. *n* = 5 mice.

production. Our data shows that thalidomide increases NO production, *via* induction of iNOS, but this increase is not important to thalidomide transient reduction of PHT. Moreover, given that TNFα expression in liver and aorta tissues was unchanged in response to PVL, the murine PVL model is not suitable to study the role of TNFα in PHT. However, the demonstration that thalidomide temporarily reduces mean systemic blood pressure by an NO independent mechanism illustrates that thalidomide may be beneficial to prevent variceal formation and hemorrhage, a common problem associated with PHT, especially in patients that are non-responsive to current β-blocker therapy to reduce systemic blood pressure[29].

The scientific consensus is that the vasodilator NO plays a major role in the development and sustained vasculopathy of PHT[4]. However, the mechanisms controlling NO biosynthesis in the context of PHT are not clearly defined. Previous investigations using animal models of PHT and human studies suggest a role for TNF-α in vasodilatation by promoting increased NO production[30] by arguing that TNF-α induction of NOS isoforms (eNOS, and/or iNOS) promotes the development of a hyper-dynamic circulation and vascular hypo-responsiveness to vasoconstrictors associated with this pathological dysfunction[31]. Therefore, inhibition of TNFα is a potential mechanism in which to reduce PHT. Previous studies have shown that the compound thalidomide reduces TNFα[8,32]. The purpose of this manuscript was to investigate the hypothesis that TNFα modulates PHT *via* nitric oxide synthase enzyme[33]. We found that thalidomide, rather than reduce NO levels, increased circulating plasma NOx levels *via* iNOS. Moreover, although

thalidomide does reduce TNFα mRNA levels in mouse macrophage cells (RAW286.3), thalidomide increased TNFα and iNOS mRNA expression in murine liver and thoracic aorta tissues, suggesting that *in vivo* thalidomide increases TNFα and iNOS levels. It is not unexpected that thalidomide would modulate TNFα and iNOS similarly as co-regulation of TNFα and iNOS in response to stimuli is well described[34,35], as is the interaction between TNFα expression and iNOS expression[36,37]. Moreover, TNFα neutralizing antibodies are known to reduce iNOS expression[38-40].

Despite detecting an increase in TNFα expression, we were unable to detect circulating TNFα in sham or PVL mice irrespective of thalidomide administration using a highly specific commercially available ELISA, arguing against a role for TNFα in PVL models of PHT. However, studies by others have detected TNFα in rodent models of PVL using biological cell based assays[20]. The fact that TNFα neutralizing antibodies reduce NO and portal pressure in PVL rats suggests that TNFα is important in the PVL model *via* modulation of NOS[30]. Although TNFα levels were undetectable, the effects of thalidomide on NOS isoforms can be determined by measuring circulating NO levels, hemodynamic changes and TNFα mRNA levels.

In rat PHT models, thalidomide administration demonstrated a significant correlation between TNFα plasma levels and mean arterial pressure among PVL animals[20]. Thalidomide has been noted to have many possible vascular effects, including anti-angiogenesis[41], disruption of mRNA transcription causing attenuation of the nuclear factor kappa B mediated gene expression[42], increase of the production of free radicals to elicit oxidative stress[43] and directly through systemic circulatory and/or direct cardiac effects[44]. Consequently, a therapeutic role for thalidomide in patients with cirrhosis has been proposed[22]. We found that thalidomide reduced PHT *via* a significant reduction in mean arterial pressure (MAP) that was NOS isoform independent and irrelevant to circulating NO levels. MAP is approximately determined from measurements of the systolic pressure and the diastolic pressure over a cardiac cycle and is determined by the cardiac output (CO), systemic vascular resistance (SVR) and central venous pressure [MAP = (CO - SVR) + CVR]. Cardiac output is related to both heart rate and stroke volume (SV). Both thalidomide and TNFα have been linked to vascular regulation.

Thalidomide has been shown to improve CO by increasing the left ventricular ejection fraction[44,45] and causes an imbalance between vasodilators (NO) and vasoconstrictors (endothelin-1) that impacts SVR[46]. Our data suggests that modulation of NO is linked to iNOS. Studies by others have reported that thalidomide does not change endothelin-1 levels in human endothelial cells[47]. While the vascular response to thalidomide was not the original focus of this study, we did observe that heart rate was not affected by thalidomide. This suggests changes in SVR, CVR or SV. TNFα has been shown to directly increase cardiac index and mean arterial pressure, systemic vascular resistance index, temperature, and heart rate[48,49]. However, because there appears to be no discernable increase in TNFα within the PVL murine model of PHT, other models are required to fully understand the connections amongst TNFα, thalidomide and PHT.

In conclusion, although previous reports demonstrate the importance of TNFα in the development of PHT, TNFα does not appear to be important in the murine PVL model. This correlates with our previous study demonstrating that gene deletion of TNFα receptors does not ameliorate PHT in mice following PVL[50]. Consequently, the PVL model of PHT is not conducive to the study of TNFα in PHT. Despite this lack of TNFα involvement, thalidomide treatment demonstrated a temporary reduction in PHT *via* a NOS isoform independent mechanism, indicating a non-TNFα and non-NO mechanism for thalidomide in PHT. While this observation is interesting because thalidomide may be beneficial for the treatment of PHT associated variceal formation and bleeding, the use of thalidomide is cautioned since thalidomide is associated with thromboembolic events that would exacerbate PHT and enhance liver damage[51]. However, use of thalidomide analogs may demonstrate therapeutic benefit without vascular complications[52]. Further investigation is required to better understand the mechanism by which thalidomide reduces portal pressure with the anticipation that advances can be translated to clinical practice and improve outcomes for patients with liver disease and a high risk of developing PHT. We do not suggest by what mechanism thalidomide reduces mean arterial blood pressure because thalidomide is linked to many biological mechanisms, including vascular endothelial growth factor and thromboxane, both of which have been linked to PHT[53-55]. Moreover, thalidomide is known to modulate PHT *via* cannabinoid receptor-2 (CB2) expression and studies show that targeting CB2 receptor agonists ameliorate PHT in bile duct ligated rats and that thalidomide increases CB2 receptor expression and reduces cannabinoid receptor-1 expression[56,57].

ACKNOWLEDGMENTS

The authors would like to thank Dr. James Sitzmann and Dr. Brad Berk, University of Rochester School of Medicine, for fostering the completion of this work.

COMMENTS

Background

Portal hypertension is an elevation in the portal venous pressure and increases mortality and morbidity in patients. The compound thalidomide has been shown to reduce portal hypertension. However, the mechanism of this response is unclear and the use of thalidomide is controversial. Previous studies have demonstrated that thalidomide reduces biosynthesis of the potent vasodilator nitric oxide (NO) by destabilizing tumor necrosis factor alpha mRNA. The

purpose of this study was to test this hypothesis using mice that have targeted gene deletions affecting NO biosynthesis.

Research frontiers

There is a need to find alternative treatment paradigms for treating portal hypertension, including diagnosis, measurement and treatment. Thalidomide has been shown to reduce portal pressure and thalidomide derivatives are being explored. The hot spot is to better understand how these compounds work in order to facilitate translation in to the clinic.

Innovations and breakthroughs

The innovation of this research is the utilization of gene deleted mice and the microsurgery. In combination, this provides a cleaner understanding of the role of individual genes within disease pathology. The portal vein ligation model avoids the inflammatory and cytokine milieu associated with the carbon tetrachloride or bile duct ligation models of portal hypertension.

Applications

This study confirms that thalidomide does reduce portal hypertension but that this response is transient and last about 1 h. Moreover, the reduction is not linked to NO biosynthesis but *via* a nitric oxide synthase (NOS) independent reduction in mean systolic pressure. These results support the use of thalidomide or its derivatives and will direct further studies to investigate alternative targets other than NO.

Terminology

Portal hypertension is driven by two main pathologies and both are related to NO. Reduced hepatic NO biosynthesis causes sinusoidal constriction that increases resistance to portal flow and increases portal pressure. In contrast, NO is increased within the systemic vasculature, resulting in increased cardiac output and increased portal venous flow that increase portal pressure.

Peer-review

The authors examined the hypothesis that thalidomide diminishes tumor necrosis factor alpha induction of NOS and the production of NO. They concluded that the transitory reduction in portal pressure was associated with an inducible NOS dependent increase in NO and a NOS isoform independent reduction in blood pressure.

REFERENCES

1 **Nusrat S**, Khan MS, Fazili J, Madhoun MF. Cirrhosis and its complications: evidence based treatment. *World J Gastroenterol* 2014; **20**: 5442-5460 [PMID: 24833875 DOI: 10.3748/wjg.v20.i18.5442]

2 **Sanyal AJ**, Bosch J, Blei A, Arroyo V. Portal hypertension and its complications. *Gastroenterology* 2008; **134**: 1715-1728 [PMID: 18471549 DOI: 10.1053/j.gastro.2008.03.007]

3 **Vorobioff J**, Bredfeldt JE, Groszmann RJ. Hyperdynamic circulation in portal-hypertensive rat model: a primary factor for maintenance of chronic portal hypertension. *Am J Physiol* 1983; **244**: G52-G57 [PMID: 6849394]

4 **Hu LS**, George J, Wang JH. Current concepts on the role of nitric oxide in portal hypertension. *World J Gastroenterol* 2013; **19**: 1707-1717 [PMID: 23555159 DOI: 10.3748/wjg.v19.i11.1707]

5 **Al-Busafi SA**, McNabb-Baltar J, Farag A, Hilzenrat N. Clinical manifestations of portal hypertension. *Int J Hepatol* 2012; **2012**: 203794 [PMID: 23024865 DOI: 10.1155/2012/203794]

6 **Sato M**, Tateishi R, Yasunaga H, Horiguchi H, Yoshida H, Fushimi K, Koike K. Variceal hemorrhage: Analysis of 9987 cases from a Japanese nationwide database. *Hepatol Res* 2015; **45**: 288-293 [PMID: 24827451 DOI: 10.1111/hepr.12357]

7 **Heinemann A**, Wachter CH, Holzer P, Fickert P, Stauber RE. Nitric oxide-dependent and -independent vascular hyporeactivity in mesenteric arteries of portal hypertensive rats. *Br J Pharmacol* 1997; **121**: 1031-1037 [PMID: 9222564 DOI: 10.1038/sj.bjp.0701220]

8 **Liu S**, Rockey DC. Cicletanine stimulates eNOS phosphorylation and NO production via Akt and MAP kinase/Erk signaling in sinusoidal endothelial cells. *Am J Physiol Gastrointest Liver Physiol* 2013; **305**: G163-G171 [PMID: 23639812 DOI: 10.1152/ajpgi.00003.2013]

9 **Theodorakis NG**, Wang YN, Skill NJ, Metz MA, Cahill PA, Redmond EM, Sitzmann JV. The role of nitric oxide synthase isoforms in extrahepatic portal hypertension: studies in gene-knockout mice. *Gastroenterology* 2003; **124**: 1500-1508 [PMID: 12730888]

10 **Rockey DC**, Chung JJ. Reduced nitric oxide production by endothelial cells in cirrhotic rat liver: endothelial dysfunction in portal hypertension. *Gastroenterology* 1998; **114**: 344-351 [PMID: 9453496]

11 **Cahill PA**, Redmond EM, Hodges R, Zhang S, Sitzmann JV. Increased endothelial nitric oxide synthase activity in the hyperemic vessels of portal hypertensive rats. *J Hepatol* 1996; **25**: 370-378 [PMID: 8895017]

12 **Wiest R**, Shah V, Sessa WC, Groszmann RJ. NO overproduction by eNOS precedes hyperdynamic splanchnic circulation in portal hypertensive rats. *Am J Physiol* 1999; **276**: G1043-G1051 [PMID: 10198349]

13 **Horn P**, Cortese-Krott MM, Amabile N, Hundsdörfer C, Kröncke KD, Kelm M, Heiss C. Circulating microparticles carry a functional endothelial nitric oxide synthase that is decreased in patients with endothelial dysfunction. *J Am Heart Assoc* 2013; **2**: e003764 [PMID: 23525410 DOI: 10.1161/JAHA.112.003764]

14 **Liu S**, Premont RT, Kontos CD, Zhu S, Rockey DC. A crucial role for GRK2 in regulation of endothelial cell nitric oxide synthase function in portal hypertension. *Nat Med* 2005; **11**: 952-958 [PMID: 16142243 DOI: 10.1038/nm1289]

15 **Liu S**, Premont RT, Rockey DC. G-protein-coupled receptor kinase interactor-1 (GIT1) is a new endothelial nitric-oxide synthase (eNOS) interactor with functional effects on vascular homeostasis. *J Biol Chem* 2012; **287**: 12309-12320 [PMID: 22294688 DOI: 10.1074/jbc.M111.320465]

16 **Liu S**, Premont RT, Rockey DC. Endothelial nitric-oxide synthase (eNOS) is activated through G-protein-coupled receptor kinase-interacting protein 1 (GIT1) tyrosine phosphorylation and Src protein. *J Biol Chem* 2014; **289**: 18163-18174 [PMID: 24764294 DOI: 10.1074/jbc.M113.521203]

17 **Kaviani A**, Ohta M, Itani R, Sander F, Tarnawski AS, Sarfeh IJ. Tumor necrosis factor-alpha regulates inducible nitric oxide synthase gene expression in the portal hypertensive gastric mucosa of the rat. *J Gastrointest Surg* 1997; **1**: 371-376 [PMID: 9834372]

18 **Paz Y**, Frolkis I, Pevni D, Shapira I, Yuhas Y, Iaina A, Wollman Y, Chernichovski T, Nesher N, Locker C, Mohr R, Uretzky G. Effect of tumor necrosis factor-alpha on endothelial and inducible nitric oxide synthase messenger ribonucleic acid expression and nitric oxide synthesis in ischemic and nonischemic isolated rat heart. *J Am Coll Cardiol* 2003; **42**: 1299-1305 [PMID: 14522499]

19 **Moreira AL**, Sampaio EP, Zmuidzinas A, Frindt P, Smith KA, Kaplan G. Thalidomide exerts its inhibitory action on tumor necrosis factor alpha by enhancing mRNA degradation. *J Exp Med* 1993; **177**: 1675-1680 [PMID: 8496685]

20 **Lopez-Talavera JC**, Cadelina G, Olchowski J, Merrill W, Groszmann RJ. Thalidomide inhibits tumor necrosis factor alpha, decreases nitric oxide synthesis, and ameliorates the hyperdynamic circulatory syndrome in portal-hypertensive rats. *Hepatology* 1996; **23**: 1616-1621 [PMID: 8675185 DOI: 10.1002/hep.510230644]

21 **Soupison T**, Yang S, Bernard C, Moreau R, Kirstetter P, D' Almeida M, Cailmail S, Tedgui A, Lebrec D. Acute haemodynamic responses and inhibition of tumour necrosis factor-alpha by pentoxifylline in rats with cirrhosis. *Clin Sci* (Lond) 1996; **91**: 29-33 [PMID: 8774257]

22 **Austin AS**, Mahida YR, Clarke D, Ryder SD, Freeman JG. A pilot study to investigate the use of oxpentifylline (pentoxifylline) and thalidomide in portal hypertension secondary to alcoholic cirrhosis. *Aliment Pharmacol Ther* 2004; **19**: 79-88 [PMID: 14687169]

23 **Laubach VE**, Shesely EG, Smithies O, Sherman PA. Mice lacking inducible nitric oxide synthase are not resistant to lipopolysaccharide-induced death. *Proc Natl Acad Sci USA* 1995; **92**: 10688-10692 [PMID: 7479866]

24 **Shesely EG**, Maeda N, Kim HS, Desai KM, Krege JH, Laubach VE, Sherman PA, Sessa WC, Smithies O. Elevated blood pressures in mice lacking endothelial nitric oxide synthase. *Proc Natl Acad*

Sci USA 1996; **93**: 13176-13181 [PMID: 8917564]
25 **Golikov PP**, Nikolaeva NIu. [Analysis of nitrites/nitrates (NOx) in serum]. *Biomed Khim* 2004; **50**: 79-85 [PMID: 15108630]
26 **Alkam T**, Nitta A, Mizoguchi H, Saito K, Seshima M, Itoh A, Yamada K, Nabeshima T. Restraining tumor necrosis factor-alpha by thalidomide prevents the amyloid beta-induced impairment of recognition memory in mice. *Behav Brain Res* 2008; **189**: 100-106 [PMID: 18325608 DOI: 10.1016/j.bbr.2007.12.014]
27 **Malleo G**, Mazzon E, Genovese T, Di Paola R, Muià C, Crisafulli C, Siriwardena AK, Cuzzocrea S. Effects of thalidomide in a mouse model of cerulein-induced acute pancreatitis. *Shock* 2008; **29**: 89-97 [PMID: 18246603]
28 **Mazzon E**, Muià C, Di Paola R, Genovese T, De Sarro A, Cuzzocrea S. Thalidomide treatment reduces colon injury induced by experimental colitis. *Shock* 2005; **23**: 556-564 [PMID: 15897810]
29 **Bellot P**, García-Pagán JC, Abraldes JG, Bosch J. Primary prophylaxis of esophageal variceal bleeding in cirrhosis. *Gastroenterol Clin Biol* 2008; **32**: 532-540 [PMID: 18456445 DOI: 10.1016/j.gcb.2008.03.012]
30 **Wang JJ**, Gao GW, Gao RZ, Liu CA, Ding X, Yao ZX. Effects of tumor necrosis factor, endothelin and nitric oxide on hyperdynamic circulation of rats with acute and chronic portal hypertension. *World J Gastroenterol* 2004; **10**: 689-693 [PMID: 14991939]
31 **Cahill PA**, Redmond EM, Sitzmann JV. Endothelial dysfunction in cirrhosis and portal hypertension. *Pharmacol Ther* 2001; **89**: 273-293 [PMID: 11516480]
32 **Enomoto N**, Takei Y, Hirose M, Kitamura T, Ikejima K, Sato N. Protective effect of thalidomide on endotoxin-induced liver injury. *Alcohol Clin Exp Res* 2003; **27**: 2S-6S [PMID: 12960498 DOI: 10.1097/01.ALC.0000078606.59842.01]
33 **Park E**, Levis WR, Greig N, Jung E, Schuller-Levis G. Effect of thalidomide on nitric oxide production in lipopolysaccharide-activated RAW 264.7 cells. *J Drugs Dermatol* 2010; **9**: 330-333 [PMID: 20514789]
34 **Hijikawa T**, Kaibori M, Uchida Y, Yamada M, Matsui K, Ozaki T, Kamiyama Y, Nishizawa M, Okumura T. Insulin-like growth factor 1 prevents liver injury through the inhibition of TNF-alpha and iNOS induction in D-galactosamine and LPS-treated rats. *Shock* 2008; **29**: 740-747 [PMID: 18004231 DOI: 10.1097/shk.0b013e31815d0780]
35 **Marchi P**, Paiotti AP, Artigiani Neto R, Oshima CT, Ribeiro DA. Concentrated grape juice (G8000™) reduces immunoexpression of iNOS, TNF-alpha, COX-2 and DNA damage on 2,4,6-trinitrobenzene sulfonic acid-induced-colitis. *Environ Toxicol Pharmacol* 2014; **37**: 819-827 [PMID: 24637249 DOI: 10.1016/j.etap.2014.02.006]
36 **Aires RD**, Capettini LS, Silva JF, Rodrigues-Machado Mda G, Pinho V, Teixeira MM, Cortes SF, Lemos VS. Paraquat poisoning induces TNF-α-dependent iNOS/NO mediated hyporesponsiveness of the aorta to vasoconstrictors in rats. *PLoS One* 2013; **8**: e73562 [PMID: 24039983 DOI: 10.1371/journal.pone.0073562]
37 **Zheng Z**, Li Z, Chen S, Pan J, Ma X. Tetramethylpyrazine attenuates TNF-α-induced iNOS expression in human endothelial cells: Involvement of Syk-mediated activation of PI3K-IKK-IκB signaling pathways. *Exp Cell Res* 2013; **319**: 2145-2151 [PMID: 23726836 DOI: 10.1016/j.yexcr.2013.05.018]
38 **Medeiros R**, Prediger RD, Passos GF, Pandolfo P, Duarte FS, Franco JL, Dafre AL, Di Giunta G, Figueiredo CP, Takahashi RN, Campos MM, Calixto JB. Connecting TNF-alpha signaling pathways to iNOS expression in a mouse model of Alzheimer's disease: relevance for the behavioral and synaptic deficits induced by amyloid beta protein. *J Neurosci* 2007; **27**: 5394-5404 [PMID: 17507561 DOI: 10.1523/JNEUROSCI.5047-06.2007]
39 **Lee SK**, Huang H, Lee SW, Kim KH, Kim KK, Kim HM, Lee ZH, Kim HH. Involvement of iNOS-dependent NO production in the stimulation of osteoclast survival by TNF-alpha. *Exp Cell Res* 2004; **298**: 359-368 [PMID: 15265685 DOI: 10.1016/j.yexcr.2004.04.039]
40 **Saud B**, Nandi J, Ong G, Finocchiaro S, Levine RA. Inhibition of TNF-alpha improves indomethacin-induced enteropathy in rats by modulating iNOS expression. *Dig Dis Sci* 2005; **50**: 1677-1683 [PMID: 16133968 DOI: 10.1007/s10620-005-2914-0]
41 **Reichen J**. Portal hypertension: cytokines and endothelins. *Hepatogastroenterology* 1999; **46** Suppl 2: 1434-1436 [PMID: 10431705]
42 **Lv P**, Luo HS, Zhou XP, Xiao YJ, Paul SC, Si XM, Zhou YH. Reversal effect of thalidomide on established hepatic cirrhosis in rats via inhibition of nuclear factor-kappaB/inhibitor of nuclear factor-kappaB pathway. *Arch Med Res* 2007; **38**: 15-27 [PMID: 17174718 DOI: 10.1016/j.arcmed.2006.09.006]
43 **Hyakkoku K**, Nakajima Y, Izuta H, Shimazawa M, Yamamoto T, Shibata N, Hara H. Thalidomide protects against ischemic neuronal damage induced by focal cerebral ischemia in mice. *Neuroscience* 2009; **159**: 760-769 [PMID: 19166916 DOI: 10.1016/j.neuroscience.2008.12.043]
44 **Aukrust P**, Yndestad A, Damås JK, Ueland T, Øie E, Gullestad L. Potential mechanisms of benefit with thalidomide in chronic heart failure. *Am J Cardiovasc Drugs* 2007; **7**: 127-134 [PMID: 17503883]
45 **Gullestad L**, Semb AG, Holt E, Skårdal R, Ueland T, Yndestad A, Frøland SS, Aukrust P. Effect of thalidomide in patients with chronic heart failure. *Am Heart J* 2002; **144**: 847-850 [PMID: 12422154]
46 **Lafaras C**, Mandala E, Verrou E, Platogiannis D, Barbetakis N, Bischiniotis T, Zervas K. Non-thromboembolic pulmonary hypertension in multiple myeloma, after thalidomide treatment: a pilot study. *Ann Oncol* 2008; **19**: 1765-1769 [PMID: 18480066 DOI: 10.1093/annonc/mdn287]
47 **Zhang SZ**, Li MT, He JG, Zeng XF. [Effects of three immunosuppressive agents and simvastatin on cell-proliferation and endothelin secretion of human endothelial cells]. *Zhonghua Neike Zazhi* 2008; **47**: 495-498 [PMID: 19040069]
48 **Mitaka C**, Hirata Y, Ichikawa K, Yokoyama K, Emori T, Kanno K, Amaha K. Effects of TNF-alpha on hemodynamic changes and circulating endothelium-derived vasoactive factors in dogs. *Am J Physiol* 1994; **267**: H1530-H1536 [PMID: 7943398]
49 **Osiovich H**, Goldberg RN, Suguihara C, Adams JA, Martinez O, Kuo G, Feuer WI, Offenbacher S, Bancalari E. Cardiopulmonary effects of tumor necrosis factor-alpha in the piglet: influence of cyclooxygenase inhibition. *Biol Neonate* 1995; **68**: 342-353 [PMID: 8835089]
50 **Theodorakis NG**, Wang YN, Wu J, Maluccio MA, Skill NJ. Tumor necrosis factor alpha signaling in the development of experimental murine pre-hepatic portal hypertension. *Int J Physiol Pathophysiol Pharmacol* 2010; **2**: 104-110 [PMID: 21383890]
51 **Cavo M**, Zamagni E, Cellini C, Tosi P, Cangini D, Cini M, Valdrè L, Palareti G, Masini L, Tura S, Baccarani M. Deep-vein thrombosis in patients with multiple myeloma receiving first-line thalidomide-dexamethasone therapy. *Blood* 2002; **100**: 2272-2273 [PMID: 12229885]
52 **Niwayama S**, Loh C, Turk BE, Liu JO, Miyachi H, Hashimoto Y. Enhanced potency of perfluorinated thalidomide derivatives for inhibition of LPS-induced tumor necrosis factor-alpha production is associated with a change of mechanism of action. *Bioorg Med Chem Lett* 1998; **8**: 1071-1076 [PMID: 9871710]
53 **Chang CC**, Wang SS, Huang HC, Lee FY, Lin HC, Lee JY, Chen YC, Lee SD. Chronic thalidomide administration enhances vascular responsiveness to vasopressin in portal-systemic collaterals of bile duct-ligated rats. *J Chin Med Assoc* 2009; **72**: 234-242 [PMID: 19467946 DOI: 10.1016/S1726-4901(09)70063-2]
54 **Yang YY**, Huang YT, Lin HC, Lee FY, Lee KC, Chau GY, Loong CC, Lai CR, Lee SD. Thalidomide decreases intrahepatic resistance in cirrhotic rats. *Biochem Biophys Res Commun* 2009; **380**: 666-672 [PMID: 19285019 DOI: 10.1016/j.bbrc.2009.01.160]
55 **Moreau R**. VEGF-induced angiogenesis drives collateral circulation in portal hypertension. *J Hepatol* 2005; **43**: 6-8 [PMID: 15893843 DOI: 10.1016/j.jhep.2005.04.002]
56 **Huang HC**, Wang SS, Hsin IF, Chang CC, Lee FY, Lin HC, Chuang CL, Lee JY, Hsieh HG, Lee SD. Cannabinoid receptor 2

agonist ameliorates mesenteric angiogenesis and portosystemic collaterals in cirrhotic rats. *Hepatology* 2012; **56**: 248-258 [PMID: 22290687 DOI: 10.1002/hep.25625]

57 **Yang YY**, Lee KC, Huang YT, Lee FY, Chau GY, Loong CC, Lin HC, Lee SD. Inhibition of hepatic tumour necrosis factor-alpha attenuates the anandamide-induced vasoconstrictive response in cirrhotic rat livers. *Liver Int* 2009; **29**: 678-685 [PMID: 19413671 DOI: 10.1111/j.1478-3231.2009.01983.x]

P- Reviewer: Farias AQ, Sharma V **S- Editor**: Gou SX
L- Editor: Roemmele A **E- Editor**: Liu XM

World Journal of Gastroenterology

Submit a Manuscript: http://www.wjgnet.com/esps/
Help Desk: http://www.wjgnet.com/esps/helpdesk.aspx
DOI: 10.3748/wjg.v21.i14.4136

World J Gastroenterol 2015 April 14; 21(14): 4136-4149
ISSN 1007-9327 (print) ISSN 2219-2840 (online)

ORIGINAL ARTICLE

Basic Study

Candidate colorectal cancer predisposing gene variants in Chinese early-onset and familial cases

Jun-Xiao Zhang, Lei Fu, Richarda M de Voer, Marc-Manuel Hahn, Peng Jin, Chen-Xi Lv, Eugène TP Verwiel, Marjolijn JL Ligtenberg, Nicoline Hoogerbrugge, Roland P Kuiper, Jian-Qiu Sheng, Ad Geurts van Kessel

Jun-Xiao Zhang, Richarda M de Voer, Marc-Manuel Hahn, Eugène TP Verwiel, Marjolijn JL Ligtenberg, Nicoline Hoogerbrugge, Roland P Kuiper, Ad Geurts van Kessel, Department of Human Genetics, Radboud University Medical Center, Radboud Institute for Molecular Life Sciences, 6500 HB Nijmegen, The Netherlands
Lei Fu, Peng Jin, Chen-Xi Lv, Jian-Qiu Sheng, Department of Gastroenterology, General Hospital of Beijing Military Region, Beijing 100700, China
Lei Fu, Third Military Medical University, Chongqing 400038, China
Marjolijn JL Ligtenberg, Department of Human Genetics and Department of Pathology, Radboud University Medical Center, 6500 HB Nijmegen, The Netherlands
Author contributions: Zhang JX, Fu L contributed equally to this paper; Zhang JX analyzed the data and performed the experiments; Fu L prepared the samples for exome sequencing, provided clinical information and performed validation experiments; de Voer RM, Hahn MM and Verwiel ET participated in the data analysis; Jin P participated in the sample collection; Lv CX performed the experiment for screening the control cohort; Ligtenberg MJ and Hoogerbrugge N participated in the design of the study; Kuiper RP, Sheng JQ and Geurts van Kessel A conceived and coordinated the study; Sheng JQ, de Voer RM, Kuiper RP and Geurts van Kessel A wrote the manuscript, which was approved by all co-authors.
Supported by research grants from the Dutch Cancer Society (KWF, KUN-4335), the Netherlands Organization for Scientific Research (NWO, 91710358), the Royal Dutch Academy of Sciences (KNAW), National Natural Science Foundation of China (NSFC, 81272194 and 81072041), and a scholarship from the China Scholarship Council (CSC) to Zhang JX.

Correspondence to: Jian-Qiu Sheng, Professor, Department of Gastroenterology, General Hospital of Beijing Military Region, 5 Nanmenchang, Dongcheng, Beijing 100700, China. jianqiu@263.net
Telephone: +86-10-66721299
Fax: +86-10-66721299
Received: June 12, 2014
Peer-review started: June 13, 2014
First decision: July 21, 2014
Revised: October 17, 2014
Accepted: December 1, 2014
Article in press: December 1, 2014
Published online: April 14, 2015

Abstract

AIM: To investigate whether whole-exome sequencing may serve as an efficient method to identify known or novel colorectal cancer (CRC) predisposing genes in early-onset or familial CRC cases.

METHODS: We performed whole-exome sequencing in 23 Chinese patients from 21 families with non-polyposis CRC diagnosed at ⩽ 40 years of age, or from multiple affected CRC families with at least 1 first-degree relative diagnosed with CRC at ⩽ 55 years of age. Genomic DNA from blood was enriched for exome sequences using the SureSelect Human All Exon Kit, version 2 (Agilent Technologies) and sequencing was performed on an Illumina HiSeq 2000 platform. Data were processed through an analytical pipeline to search for rare germline variants in known or novel CRC predisposing genes.

RESULTS: In total, 32 germline variants in 23 genes were identified and confirmed by Sanger sequencing. In 6 of the 21 families (29%), we identified 7 mutations in 3 known CRC predisposing genes including *MLH1* (5 patients), *MSH2* (1 patient), and *MUTYH* (biallelic, 1 patient), five of which were reported as pathogenic. In

the remaining 15 families, we identified 20 rare and novel potentially deleterious variants in 19 genes, six of which were truncating mutations. One previously unreported variant identified in a conserved region of EIF2AK4 (p.Glu738_Asp739insArgArg) was found to represent a local Chinese variant, which was significantly enriched in our early-onset CRC patient cohort compared to a control cohort of 100 healthy Chinese individuals scored negative by colonoscopy (33.3% *vs* 7%, $P < 0.001$).

CONCLUSION: Whole-exome sequencing of early-onset or familial CRC cases serves as an efficient method to identify known and potential pathogenic variants in established and novel candidate CRC predisposing genes.

Key words: Colorectal cancer; Cancer predisposition; Early-onset; Germline variants; Exome sequencing

Core tip: Mendelian colorectal cancer (CRC) predisposition syndromes underlie about 5% of all CRCs, and are caused by germline mutations in a limited set of genes. The overall heritability of CRC, however, is estimated to be approximately 30% and as yet many families at risk remain unexplained. This research identifies seven mutations of known CRC predisposing genes (*MLH1*, *MSH2* and *MUTYH*) in 6 of the 21 families (29%), five of which were previously reported as pathogenic. One unreported variant EIF2AK4 (p.Glu738_Asp739insArgArg) located at conserved region was found to represent a local Chinese variant and significantly enriched in our early-onset CRC patient cohort.

Zhang JX, Fu L, de Voer RM, Hahn MM, Jin P, Lv CX, Verwiel ET, Ligtenberg MJ, Hoogerbrugge N, Kuiper RP, Sheng JQ, Geurts van Kessel A. Candidate colorectal cancer predisposing gene variants in Chinese early-onset and familial cases. *World J Gastroenterol* 2015; 21(14): 4136-4149 Available from: URL: http://www.wjgnet.com/1007-9327/full/v21/i14/4136.htm DOI: http://dx.doi.org/10.3748/wjg.v21.i14.4136

INTRODUCTION

Colorectal cancer (CRC; MIM 114500) is the third most common cancer worldwide and the fourth leading cause of cancer-related death, with over one million new cases diagnosed and approximately 600000 deaths each year[1]. In China, it is the third most common cancer and the fifth leading cause of death from cancer. Moreover, the incidence of CRC in China has been increasing in recent years[2]. Genetic factors are estimated to account for the development of approximately 30% of all CRC cases[3]. However, Mendelian colorectal cancer predisposition syndromes, such as Lynch syndrome (LS), familial adenomatous polyposis (FAP), MUTYH-associated polyposis (MAP), juvenile polyposis syndrome (JPS) and polymerase proofreading-associated polyposis (PPAP), account for only approximately 5%-10% of all CRC cases and are associated with high-penetrance germline mutations in various mismatch repair (MMR) genes or the *APC*, *MUTYH*, *SMAD4*, *BMPR1A*, *POLE* and *POLD1* genes, respectively[4,5]. The remaining approximately 20%-25% of the cases are thought to be due to moderate- to low-penetrance variants, most of which remain to be identified.

CRC patients with a family history of CRC or an early age at diagnosis are especially suggestive of a hereditary contribution and may be used in genetic association studies to increase the likelihood of identifying susceptibility variants[6-10]. Whereas CRC families with multiple affected individuals may be employed to search for high penetrance genetic susceptibility variants using linkage-based approaches, moderate- to low-penetrance variants cannot be identified through linkage-based studies in large families. In more recent years, multiple low-penetrance genetic loci associated with CRC susceptibility have been identified by genome-wide association studies (GWAS)[11,12]. However, not all results from linkage studies turned out to be consistent, and GWAS are not ideal for the identification of rare variants. Recent advances in next-generation sequencing (NGS) technologies, in particular whole-exome sequencing, have provided efficient means to identify germline variants in individuals with familial or inherited cancer syndromes[5,13-15]. We hypothesized that the majority of the yet unidentified CRC predisposing variants can be identified using whole-exome sequencing when applied to a strictly selected cohort of CRC patients and families. Several cellular signaling pathways appear to be involved in the development of CRC, including the WNT, DNA repair, BMP/TGF-β, apoptosis, MMIF/GIF, and PI3K/AKT pathways[16]. In addition, "sleeping beauty" transposon tagging has recently been employed as an effective forward genetic screening tool for the discovery of novel cancer initiating genes in the mouse intestinal tract, resulting in the identification of hundreds of novel candidate cancer driver genes[17-19].

In this study, we aimed to identify rare and novel germline variants in known and novel candidate CRC predisposing genes by performing whole-exome sequencing of germline DNA of 23 Chinese patients from 21 families diagnosed with non-polyposis CRC at a young age. We initially focused on genes that, based on genetic and functional data, are likely to play a role in CRC development, and on candidate genes that have been identified through GWAS studies.

MATERIALS AND METHODS

Recruitment of patient and control cohorts

Twenty-three patients from 21 families included in this study were recruited through the Department of

Gastroenterology of the General Hospital of Beijing Military Region, Beijing, China. All patients were diagnosed with CRC without polyposis at ⩽ 40 years of age[20] or from multiple affected CRC families with at least one first-degree relative diagnosed with CRC at ⩽ 55 years of age. Additionally, 100 colonoscopy test-negative, unrelated controls with Chinese Han ancestry without inflammatory bowel disease or any family history of CRC were collected from a subject pool who participated in health check-up programs, including colonoscopy, at the department of Gastroenterology of the General Hospital of Beijing Military Region, Beijing, China. This study was approved by the Institutional Review Board of the General Hospital of Beijing Military Region (No. 2014-035), and all patients have provided written informed consent.

Whole-exome sequencing

Genomic DNA was extracted from peripheral blood cells using a QIAamp DNA Kit (QIAGEN, Hilden, Germany) according to the protocol provided by the manufacturer and whole-exome sequencing was performed at the Beijing Genome Institute (BGI, Shenzhen, China) according to manufacturer's guidelines. Briefly, genomic DNA was fragmented and enriched for exome sequences using the SureSelect Human All Exon Kit, version 2 (Agilent Technologies, Santa Clara, CA, United States) and sequencing was performed at a minimal average coverage of 50 × on an Illumina HiSeq 2000 platform (Illumina, Inc., San Diego, CA).

Bioinformatics analyses

After removing sequence adaptors and low-quality reads, Burrows-Wheeler Aligner (BWA)[21] was used to align the reads to the NCBI human reference genome (hg19). Single nucleotide variants (SNVs) were called using SOAPsnp[22] and small insertion/deletions (indels) were detected using the SAMtools software package[23]. All variants were annotated using an in-house annotation pipeline, as described previously[24]. High-confidence variants (total ⩾ 10 reads, ⩾ 5 variant reads and ⩾ 20% variant reads) were subsequently prioritized for variants that were non-synonymous and not found in our in-house database (1302 in-house analyzed exomes, mostly from European ancestry). In addition, dbSNPv138, the National Heart, Lung, and Blood Institute (NHLBI) Exome Sequencing Project database (ESP, 6503 exomes, http://evs.gs.washington.edu/EVS/), and 700 control exome data sets from Chinese subjects with Han ancestry (Juan Tian and Zhimin Feng, BGI, personal communication) were used to exclude recurrent variants with a minor allele frequency (MAF) > 0.001.

Functional impact of variant analyses

Non-synonymous variants that result in alterations in protein function, including protein truncation, splice site defects and missense mutations at highly conserved (phyloP ⩾ 3.0) nucleotide positions, were included in our analyses. Alamut v.2.0 software (Interactive Biosoftware) and integrated mutation prediction software (align GVDV, SIFT and PolyPhen-2)[25-27] packages were used for analyses of the identified variants. The prediction of splicing effects was evaluated based on five different algorithms (SpliceSiteFinder, MaxEntScan, NNSPLICE, GeneSplicer, Human Splicing Finder) through the bioinformatics tools of the Alamut v.2.0 software. The online tool "Project HOPE"[28] (http://www.cmbi.ru.nl/hope/) was used for revealing the structural consequences of missense mutations.

Candidate gene selection

We initially selected germline variants in CRC predisposing genes known to be associated with hereditary CRC syndromes and searched for evidence of pathogenicity in relevant databases, *i.e.*, InSiGHT (http://www.insight-group.org/), LOVD (https://atlas.cmm.ki.se/LOVDv.2.0/) and the Mismatch Repair Genes Variant Database (http://www.med.mun.ca/mmrvariants/).

Next to the identification of variants in known CRC predisposing genes, we searched for potential pathogenic variants in novel candidate genes using the remaining exome data of our CRC patient cohort. For the selection of these variants, we focused on genes that meet the following criteria: (1) genes exhibiting recurrent variants; (2) 582 known cancer genes, including somatically mutated cancer genes (Cancer Gene Census, http://www.sanger.ac.uk/genetics/CGP/Census/)[29,30], cancer predisposing genes of which rare germline variants are known to confer a highly or moderately increased risk of cancer and for which at least 5% of individuals with the relevant variants develop cancer[31], and genes that are included in the Radboud university medical center hereditary cancer gene list[32]; (3) 286 genes that have been identified as candidate CRC driver genes by the "sleeping beauty" transposon tagging system in mice[18,19]; (4) 588 genes included in the following KEGG pathways: WNT signaling pathway (hsa04310), TGF-β signaling pathway (hsa04350), base excision repair (BER, hsa03410), nucleotide excision repair (NER, hsa03420), mismatch repair (MMR, hsa03430), non-homologous end-joining (NHEJ, hsa03450), Fanconi anemia pathway (hsa03460) and pathways involved in cancer (hsa05200); and (5) 268 genes likely to play a role in CRC susceptibility identified by GWAS studies[11,12,33,34] and included in the NHGRI GWAS Catalog (http://www.genome.gov/gwastudies/)[35].

Variant validation by Sanger sequencing

Identified germline variants were validated by Sanger sequencing after PCR amplification. The PCR primers were designed *in silico* using the Primer3 software package[36]. PCR reactions were performed on a Dual

Table 1 Clinical characteristics and family histories of 23 early-onset and familial colorectal cancer patients

Patient ID	Gender	Patient's history	Family history
43-1A	Female	RC at 37 yr	Brother RC at 53 yr
43-2A	Male	RC at 53 yr	Sister RC at 37 yr
49-4A	Male	CC at 30 yr	Brother CC at 43 yr; sister CC at 23 yr
49-5A	Female	CC at 23 yr	Brother CC at 43 yr; brother CC at 30 yr
50-11A	Male	CC at 34 yr and relapse at 36	Father CRC at 35 yr and death at 52 yr; brother CC at 34 yr and death at 36 yr
54-2A	Female	RC at 44 yr	Sister CRC; Brother CC at 76 yr and death
66-1-1A	Female	CC at 47 yr	Sister CC at 51 yr
71A	Female	RC at 57 yr	Sister RC at 53 yr
77-1A	Female	CRC at 38 yr	Father EC at 64 yr and death; uncle CRC at 68 yr and death
102-1A	Male	RC at 25 yr	
103-1A	Male	CC at 53 yr	Brother CC at 36 yr and death at 48 yr; mother IO at 63 yr and death
106-2A	Male	JC at 34 yr, CC at 39 yr, KC at 44 yr and PC at 45 yr	Father EC and death; mother RC at 42 yr and death; Sister CP
108-1A	Male	RC at 33 yr	
110-1A	Male	CC at 36 yr	
116-1A	Female	CC at 31 yr and HC at 57 yr	Brother intussusception and death at 40 yr; Brother CC at 50 yr, RC and SMT at 58 yr; brother IC at 50 yr, CC at 53 yr and RC at 61 yr; sister GC at 56 yr
120-1A	Female	RC at 36 yr	
142-1A	Male	RC at 34 yr	
149-1A	Male	CRC at 31 yr	Father EC and death, mother GC at 56 yr
154-1A	Female	CRC at 40 yr	Father HC, RC and death at 57 yr
156-1A	Female	CRC at 54 yr	Sister CP at 54 yr; sister CP; mother CC at 48 yr; grandfather EC and death.
164-1A	Male	CC at 30 yr	Uncle colonitls at 42 yr
165-1A	Male	CRC at 43 yr	Sister RC at 31 yr and death; grandmother RC at 65 yr and death.
180-1	Male	CRC at 40 yr	Sister CP at 46 yr

CRC: Colorectal cancer; CC: Colon cancer; RC: Rectal cancer; IC: Ileocecus carcinoma; IO: Intestinal obstruction; JC: Jejunum cancer; KC: Kidney cancer; PC: Pulmonary carcinoma; CP: Colonic polyps; HC: Hepatic carcinoma; GC: Gastric cancer; EC: Esophageal cancer; SMT: Splenic metastatic tumors.

96-Well GeneAmp PCR System 9700 (Applied Biosystems) using standard protocols (primer sequences available upon request). Mutation analyses were performed using the Vector NTI software package (Invitrogen, Paisley, United Kingdom).

RESULTS

Patient cohort characteristics

In order to identify known and potential pathogenic variants in established and novel candidate CRC predisposing genes, we performed whole-exome sequencing on germline DNA of 23 CRC patients from 21 families with non-polyposis CRC diagnosed at ⩽ 40 years of age (n = 16), or from multiple affected CRC families with at least one first-degree relative diagnosed with CRC at ⩽ 55 years of age (n = 7). The mean age at diagnosis was 38.6 years, and 43% (n = 10) of the patients were female (Table 1).

Exome sequencing performance

Overall, we generated a mean of 68 M raw reads per sample, of which 77.6% to 89.5% were aligned to the human reference genome (hg19; Table 2). The mean coverage of the exome for the 23 samples was 58.5 × (range: 53.0-64.7×). On average, 87.03% of the reads was covered at least 10 times and 76.35% of the reads was covered at least 20 times.

We identified on average 46437 SNVs (range: 44353-48114) and 1678 indels (range: 1630-1719) per exome. Over 95.3% of these substitutions and 73.1% of indels represented known variants listed in private and public databases (Figure 1). A prioritization scheme was applied to identify candidate variants (Table 3). Initial quality filtering (total ⩾ 10 reads, ⩾ 5 variant reads and ⩾ 20% variant reads) resulted in the identification of 13819 genetic variants in coding regions or canonical splice sites, including 9833 non-synonymous changes. A total of 4432 variants that result in alterations in protein function, including 172 nonsense variants, 188 frame shift variants, 943 canonical splice site variants, 237 in-frame deletions, 191 in-frame insertions and 2701 missense variants with high conservation scores (phyloP ⩾ 3.0), were identified. Subsequently, we excluded known variants present in our in-house database and variants with MAF scores > 0.001 in dbSNPv138, reducing the number of variants to 2883. Subsequently, we prioritized variants in known CRC predisposing genes and in genes likely to play a role in CRC development, and excluded variants with MAF scores > 0.1 in the ESP database or in the 700 control exomes from Chinese subjects with Han ancestry, thereby reducing the number of candidate variants to 61. Of these 61, 39 (32 different variants in 23 genes) were validated by Sanger sequencing (Figure 2).

Identification of germline variants in known CRC predisposing genes

A total of seven CRC patients from six families (30%) were identified with germline variants in known CRC

Table 2 Alignment and coverage statistics for 23 early-onset and familial colorectal cancer patients

Sample ID	Total reads	Total mapped	Reads mapped to genome	Covered ⩾ 4×	Covered ⩾10×	Covered ⩾ 20×	Average target coverage
43-1A	62997602	52130593	45528212	93.30%	85.80%	74.30%	55.88×
43-2A	57099664	50367772	43924906	93.60%	86.40%	75.00%	54.94×
49-4A	67025248	51978393	45418701	93.30%	85.70%	74.10%	55.30×
49-5A	60632336	51598017	45450431	92.60%	85.00%	73.40%	55.49×
50-11A	68991044	58507454	51033221	94.00%	87.20%	76.80%	60.71×
54-2A	68459832	57860336	50820626	93.40%	86.50%	76.10%	61.71×
66-1-1A	69759994	58838035	51472112	94.10%	87.60%	77.50%	61.82×
71A	68055130	58181783	51012277	94.00%	87.60%	77.70%	61.50×
77-1A	65956248	56894265	49817369	93.80%	87.30%	77.10%	61.06×
102-1A	64702600	57086284	49672873	94.40%	87.90%	77.70%	59.92×
103-1A	66004146	55109962	48218769	93.80%	86.90%	76.40%	59.28×
106-2A	61956558	54367359	47567033	93.80%	86.80%	76.00%	57.97×
108-1A	64764180	56469665	49473520	94.00%	87.20%	76.50%	57.52×
110-1A	68883264	56962439	49975545	94.10%	87.30%	76.90%	59.31×
116-1A	68975484	60681318	53305706	93.70%	86.70%	75.60%	55.86×
120-1A	64307066	56593051	49900259	94.20%	87.30%	75.90%	53.02×
142-1A	72999930	65321752	57822754	94.70%	87.60%	76.20%	53.19×
149-1A	69636008	59789305	52641740	93.90%	87.20%	76.90%	61.19×
154-1A	80632788	63934448	56196297	94.40%	88.30%	78.90%	64.69×
156-1A	94340904	82125696	73199086	94.20%	87.10%	76.10%	56.48×
164-1A	67813680	58837471	51779826	93.60%	86.50%	75.80%	58.83×
165-1A	68657326	59845292	52561646	94.30%	87.80%	77.70%	60.99×
180-1	65727112	57908057	50742938	94.40%	87.90%	77.50%	59.01×
Average	68190354	58321250	51197211	93.90%	87.03%	76.35%	58.51×

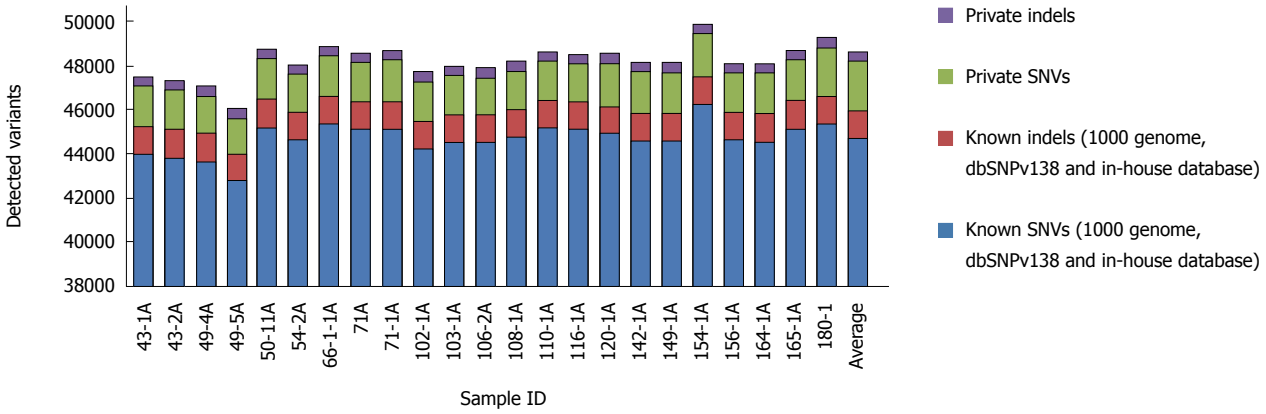

Figure 1 Variant statistics (marked in colors) for 23 early-onset colorectal cancer patient samples. The numbers of detected variants are listed on the left hand side and the patient samples ID on the bottom. The different colors represent different types of variants, *i.e.*, purple represents "private indels", green represents "private SNVs", red and blue represent known indels and known SNVs listed in the 1000 genome, dbSNPv138 and in-house databases, respectively. SNV: Single nucleotide variant.

predisposing genes. Of these, five variants (in four patients) were reported as being pathogenic in public databases, three of which were located in *MLH1*[37] (Table 4), including a canonical splice site mutation (c.453+1G>T) in patient 106-2A (colon cancer at age of 39), a canonical splice site mutation (c.208-1G>A) in patient 116-1A (colon cancer at age of 31), and a missense mutation (c.677G>A, p.Arg226Gln) in patient 43-1A (rectal cancer at age of 37). This latter mutation has been reported to result in a complete skipping of exon 8 at the mRNA level[38]. The brother of patient 43-1A was also subjected to exome sequencing (patient 43-2A, rectal cancer at age of 53), but the *MLH1* mutation c.677G>A was not encountered in this patient, and subsequent Sanger sequencing confirmed this finding. Compound heterozygous MUTYH mutations (p.Gln267* and p.Gly286Glu) were found in patient 180-1 (CRC at age of 40). The sister of patient 180-1 (colonic polyps at age of 46) also carried both MUTYH mutations (p.Gln267* and p.Gly286Glu). Both mutations have been reported to be causative for MUTYH-associated polyposis (MAP)[39,40].

Three mismatch repair gene mutations, observed in three unrelated patients, were not previously reported in public databases. A novel splice site mutation in *MSH2* (c.793-2A>T) was identified in patient 50-11A (colon cancer at age of 34). This canonical splice site is inactivated and a splice site seven nucleotides

Table 3 Prioritization scheme for exome data analysis of all 23 patients

Type of prioritization filter	Remaining variants (*n*)
All variants	1106642
Coding region and canonical splice site variants after quality filtering (total ⩾ 10 reads, ⩾ 5 variant reads and ⩾ 20% variant reads)	13819
Non-synonymous variants, canonical splice site variants	9833
Variants that result in alterations in protein function (protein truncation, splice site defects and missense mutations at highly conserved (phyloP ⩾ 3.0) nucleotide positions.	4432[1]
Not in in-house database and MAF ⩽ 0.001 in dbSNPv138	2883
Variants in known CRC predisposing genes and genes likely to play a role in CRC development (MAF ⩽ 0.001 in ESP and 700 control Chinese exome data sets)	61
Variants/genes validated by Sanger sequencing	39 (32 different variants in 23 genes)

[1]Including 172 nonsense variants, 188 frame shift variants, 943 canonical splice site variants, 237 in-frame deletions, 191 in-frame insertions and 2701 missense variants with highly conserved (phyloP ⩾ 3.0); In-house database: 1302 in-house analyzed exomes, mostly from European ancestry. MAF: Minor allele frequency; ESP: Exome Sequencing Project database (6503 exomes, http://evs.gs.washington.edu/EVS/); 700 control Chinese exome data sets: Chinese subjects with Han ancestry (Juan Tian and Zhi-Min Feng, BGI, personal communication).

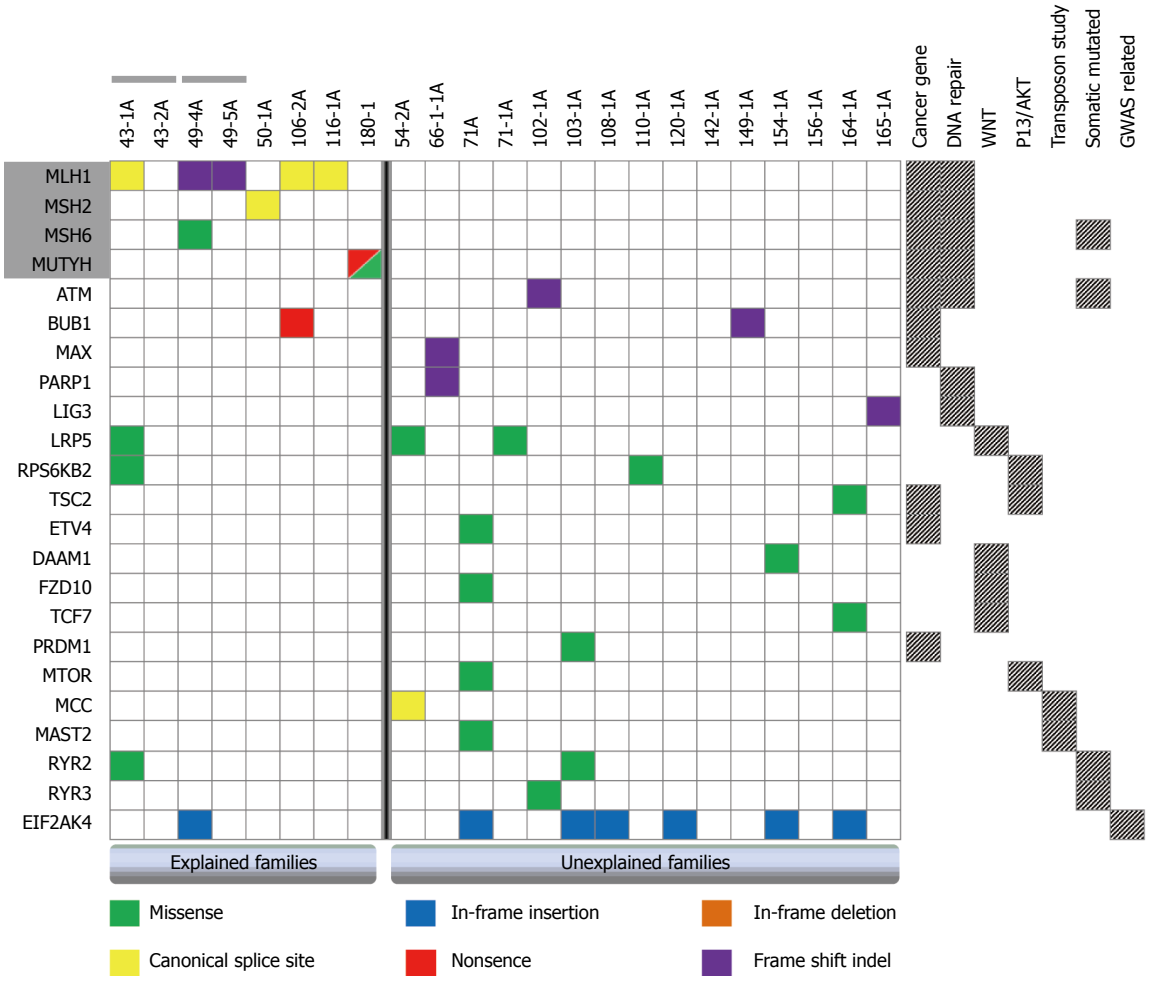

Figure 2 Germline variants identified in known colorectal cancer predisposing genes and genes likely to play a role in colorectal cancer development. The genes are listed on the left hand side and the patient samples on top. Patient samples from the same families are marked (bars). Known colorectal cancer (CRC) predisposing genes are marked by shading (left). The shades at the right hand side of the figure indicate functional (groups of) genes considered to play a role in CRC development. The different variant types are indicated in colors (right). The red-triangle/green-triangle square in sample 180-1 indicates the presence of one *MUTYH* nonsense and one *MUTYH* missense mutation.

Table 4 Identification of germline mutations in known colorectal cancer predisposing genes

Sample ID	Gene name	Gene ID	Genomic change	cDNA change	Protein change	Pathogenicity
43-1A	*MLH1*	NM_000249	g.chr3:37053590G>A	c.677G>A[1]	p.Arg226Gln[a]	Yes[38,44]
106-2A	*MLH1*	NM_000249	chr3:g.37048555G>T	c.453+1G>T	SSM	Yes[42]
116-1A	*MLH1*	NM_000249	g.chr3:37042445G>A	c.208-1G>A	SSM	Yes[43]
180-1	*MUTYH*	NM_001128425	g.chr1:45797972G>A	c.799C>T	p.Gln267*	Yes[39]
180-1	*MUTYH*	NM_001128425	g.chr1:45797914C>T	c.857G>A	p.Gly286Glu	Yes[40]
49-4A	*MLH1*	NM_000249	g.chr3:37067252_37067253insT	c.1163_1164insT	p.Arg389Profs*6	NR
49-5A	*MLH1*	NM_000249	g.chr3:37067252_37067253insT	c.1163_1164insT	p.Arg389Profs*6	NR
49-4A	*MSH6*	NM_000179	g.chr2:48027422C>G	c.2300C>G	p.Thr767Ser	NR
50-11A	*MSH2*	NM_000251	g.chr2:47641406A>T	c.793-2A>T	SSM	NR

[1]This substitution results in a complete loss of exon 8 of *MLH1* by RNA analysis[38]. NR: Not reported; SSM: Splice site mutation.

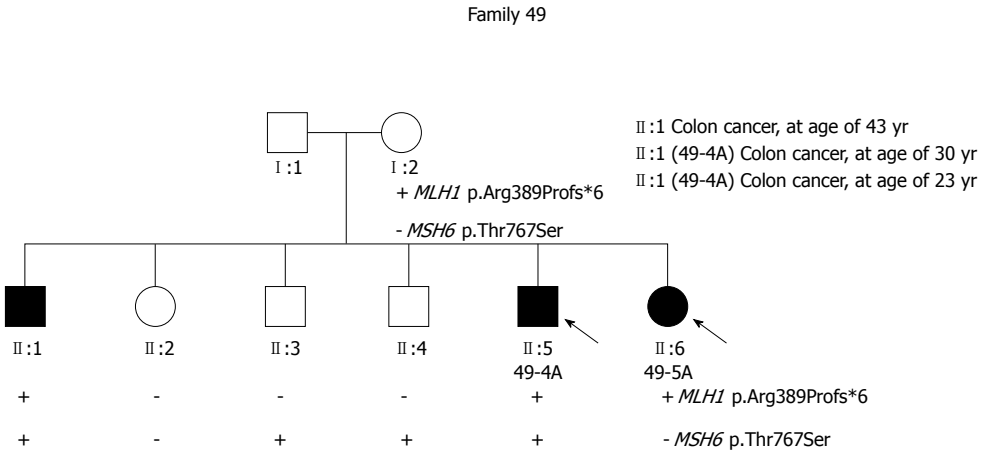

Figure 3 Pedigree and segregation analysis in family members of index patients for *MLH1* and *MSH6* mutations. Index patients are indicated by arrows. Both index patients Ⅱ:5 (sample 49-4A) and Ⅱ:6 (sample 49-5A) carried *MLH1* frame shift mutation (c.1163_1164insT, p.Arg389Profs*6) and Ⅱ:5 also carried *MSH6* missense mutation (c.2300C>G, p.Thr767Ser). Two brothers Ⅱ:1 (colon cancer at age of 43) and Ⅱ:3 (no cancer) carried both mutations. A sister (Ⅱ:2, no cancer) carried neither the *MLH1* nor the *MSH6* mutation. A third brother (Ⅱ:4) carried the *MSH6* mutation, but not the *MLH1* mutation. And the mother of index patients carried *MLH1* mutation, but not the *MSH6* mutation. Both did not develop cancer.

downstream is used according to Alamut prediction. Both a frame shift mutation in MLH1 (p.Arg389Profs*6) and a missense variant in MSH6 (p.Thr767Ser) were found in patient 49-4A (colon cancer at age of 30). The MLH1 mutation p.Arg389Profs*6 was also found in his sister, patient 49-5A (colon cancer at age of 23), whereas this sister was found to be negative for the MSH6 variant p.Thr767Ser. Segregation analysis of four siblings and the mother in this family (Figure 3) showed that the brothers of index patient 49-4A, *i.e.*, family members Ⅱ:1 (colon cancer at age of 43 years) and Ⅱ:3 (no cancer), carried both mutations. The MLH1 p.Arg389Profs*6 mutation-positive, MSH6 wild-type mother I:2 and the MLH1 wild-type, MSH6 p.Thr767Ser variant-positive brother Ⅱ:4 both did not develop cancer. We, therefore, conclude that the MLH1 frame shift mutation (p.Arg389Profs*6) acts as the main contributor to the development of CRC in this family.

Rare germline variants of novel candidate CRC predisposing genes

After extrusion of variants in known CRC predisposing genes, a set of 24 rare candidate germline variants remained (Table 5). Of these, seven represent truncating mutations (five frame-shift indels, one nonsense and one canonical splice site). In addition, one in-frame insertion and 16 highly conserved non-synonymous missense variants are present in this set. For these latter variants, SIFT and Polyphen2 algorithms were used to estimate their functional effects on the respective encoded proteins. In all cases, both SIFT and Polyphen2 predicted the variants to be functionally impaired or possibly/probably functionally impaired (Table 6). Four rare or novel variants were found in cancer predisposing genes that are not directly linked to an increased CRC risk, including ATM p.Lys468Glufs*18 in patient 102-1A (rectal cancer at age of 25 years), MAX p.Leu61Serfs*15 in patient 66-1-1A (colon cancer at age of 47 years), TSC2 p.Asp1734Asn in patient 164-1A (colon cancer at age of 30 years) and ETV4 p.Glu331Lys in patient 71A (rectal cancer at age of 57 years). ATM and MAX are involved in DNA repair pathways, and TSC2 plays a role in the PI3K/AKT pathway. These pathways are also active in CRC. Interestingly, in patient 66-1-1A we also observed a potentially deleterious variant in PARP1

Table 5 Characteristics of 24 variants identified in 19 novel genes likely to play a role in colorectal cancer development

Sample ID	Gene name	Gene/pathway involved	cDNA change	Protein change	rs ID in dbSNP138	MAF (700 Chinese exomes)	MAF (NHLBI ESP)	MAF (1000 genome)
102-1A	*ATM*	Cancer gene, DNArep	c.1402_1403del	p.Lys468Glufs*18	NR	NR	NR	NR
66-1-1A	*PARP1*	DNArep	c.758dup	p.Lys254Glufs*6	NR	NR	0.000077	NR
66-1-1A	*MAX*	Cancer gene	c.181del	p.Leu61Serfs*15	NR	NR	NR	NR
106-2A	*BUB1*	Cancer gene	c.46C>T	p.Gln16*	NR	NR	NR	NR
149-1A	*BUB1*	Cancer gene	c.2844del	p.Gln949Argfs*3	NR	NR	NR	NR
165-1A	*LIG3*	DNArep	c.218del	p.Phe73Serfs*41	NR	NR	NR	NR
54-2A	*MCC*	Transposon studies	c.1355+1_1355+2ins14	SMM	NR	NR	NR	NR
49-4A	*EIF2AK4*	GWAS related	c.2214_2215insCGACGA	p.Glu738_Asp739insArgArg	NR	NR	NR	NR
71A	*EIF2AK4*	GWAS related	c.2214_2215insCGACGA	p.Glu738_Asp739insArgArg	NR	NR	NR	NR
103-1A	*EIF2AK4*	GWAS related	c.2214_2215insCGACGA	p.Glu738_Asp739insArgArg	NR	NR	NR	NR
108-1A	*EIF2AK4*	GWAS related	c.2214_2215insCGACGA	p.Glu738_Asp739insArgArg	NR	NR	NR	NR
120-1A	*EIF2AK4*	GWAS related	c.2214_2215insCGACGA	p.Glu738_Asp739insArgArg	NR	NR	NR	NR
154-1A	*EIF2AK4*	GWAS related	c.2214_2215insCGACGA	p.Glu738_Asp739insArgArg	NR	NR	NR	NR
164-1A	*EIF2AK4*	GWAS related	c.2214_2215insCGACGA	p.Glu738_Asp739insArgArg	NR	NR	NR	NR
77-1A	*LRP5*	WNT	c.2156A>G	p.Tyr719Cys	NR	NR	NR	NR
43-1A	*LRP5*	WNT	c.3536G>A	p.Arg1179His	NR	NR	0.000077	NR
54-2A	*LRP5*	WNT	c.3919C>T	p.Arg1307Trp	NR	NR	0.000077	NR
110-1A	*RPS6KB2*	PI3K/AKT	c.331A>G	p.Lys111Glu	NR	0.00075	NR	NR
43-1A	*RPS6KB2*	PI3K/AKT	c.683C>A	p.Thr228Asn	rs183360785	NR	NR	0.001
43-1A	*RYR2*	Somatic mutation gene	c.2701G>A	p.Gly901Ser	NR	NR	NR	NR
103-1A	*RYR2*	Somatic mutation gene	c.6457A>G	p.Lys2153Glu	NR	NR	NR	NR
102-1A	*RYR3*	Somatic mutation gene	c.13507G>A	p.Val4503Met	NR	NR	NR	NR
71A	*ETV4*	Cancer gene	c.991G>A	p.Glu331Lys	NR	NR	NR	NR
103-1A	*PRDM1*	Cancer gene	c.1499A>G	p.Gln500Arg	rs201512476	NR	NR	0.001
164-1A	*TSC2*	Cancer gene, PI3K/AKT	c.5200G>A	p.Asp1734Asn	NR	NR	NR	NR
71A	*MTOR*	PI3K/AKT	c.5857G>T	p.Val1953Leu	NR	0.000714	NR	NR
154-1A	*DAAM1*	WNT	c.667G>A	p.Val223Met	NR	NR	NR	NR
71A	*FZD10*	WNT	c.1341C>G	p.Phe447Leu	NR	NR	NR	NR
164-1A	*TCF7*	WNT	c.572G>T	p.Arg191Met	NR	NR	NR	NR
71A	*MAST2*	Transposon studies	c.3482A>G	p.Asn1161Ser	NR	NR	0.000077	NR

MAF: Minor allele frequency; NR: Not reported; DNArep: DNA repair pathway; WNT: WNT signaling pathway; SSM: Splice site mutation.

(p.Lys254Glufs*6), another gene involved in DNA repair.

Genes recurrently affected by potentially deleterious variants

Despite the limited size of our cohort, the recurrent detection of rare potentially deleterious variants is another way to select candidates from the list of rare variants. Four genes were found to be recurrently affected by different rare variants, and two of them (*BUB1* and *LRP5*) were encountered in patients that also carried pathogenic *MLH1* mutations (patients 106-2A and 43-1A, respectively; Figure 2). In total, two truncating BUB1 variants were found (p.Gln16* and p.Gln949Argfs*3). As reported previously, these BUB1 variants may be associated with an increased risk for aneuploidy and, in patient 106-2A, this may have contributed to somatic loss of the wild-type MLH1 allele in the tumor[15]. The other recurrently affected genes were *LRP5*, *RPS6KB2* and *RYR2*. LRP5 may be of particular interest since it is a component of the WNT-FZD-LRP5-LRP6 complex that triggers β-catenin signaling through the induction of aggregation of receptor-ligand complexes into ribosome-sized signalsomes. We identified three highly conserved *LRP5* missense variants in three unrelated patients (Figure 2). Two of these, p.Tyr719Cys and p.Arg1179His, were found to be located in the conserved low-density lipoprotein (LDLR) class B repeat region. To investigate the functional consequences of these three mutations on the LRP5 protein structure, the online tool "Project HOPE" was used. By doing so, we found that variant p.Tyr719Cys gives rise to a mutant residue that is smaller and more hydrophobic than the wild-type residue, which may lead to loss of protein-protein interactions and hydrogen bonds and/or disturb correct protein folding. Through variant p.Arg1179His, a positively charged residue is replaced by a neutral and smaller residue, which again may lead to loss of interactions with other molecules or residues. Through variant p.Arg1307Trp, a positively charged residue is replaced by a neutral, larger and more hydrophobic residue, which may lead to loss of interactions with other molecules or residues, loss of hydrogen bonds and/or disturbance of correct protein folding giving rise to collisions with other molecules or residues.

We also identified a recurrent insertion in EIF2AK4 (p.Glu738_Asp739insArgArg) in seven (33.3%) unrelated patients, which was absent in local in-house and public databases. EIF2AK4 is located in a region previously found to be associated with CRC susceptibility in GWAS studies[11,35]. Since this variant could be common in the Han Chinese population, we screened a cohort of 100

Table 6 *In silico* functional prediction of 16 missense variants

Sample ID	Gene name	Gene/ pathway involved	cDNA change	Protein change	Domain	PhyloP score	Grantham score	Align GVGD	SIFT score	SIFT prediction	Polyphen2 score	Polyphen2 prediction
77-1A	*LRP5*	WNT	c.2156A>G	p.Tyr719Cys	LDLR class B repeat	4.751	194	C65	0.000	D	0.999	PrD
43-1A	*LRP5*	WNT	c.3536G>A	p.Arg1179His	LDLR class B repeat	3.712	29	C25	0.000	D	0.953	PrD
54-2A	*LRP5*	WNT	c.3919C>T	p.Arg1307Trp	LDLR class A repeat	3.172	101	C35	0.000	D	0.948	PrD
110-1A	*RPS6KB2*	PI3K/ AKT	c.331A>G	p.Lys111Glu	Protein kinase, catalytic domain	4.639	56	C55	0.000	D	0.535	PoD
43-1A	*RPS6KB2*	PI3K/ AKT	c.683C>A	p.Thr228Asn	Protein kinase, catalytic domain	5.062	65	C55	0.001	D	0.994	PrD
43-1A	*RYR2*	Somatic mutation gene	c.2701G>A	p.Gly901Ser	Ryanodine receptor	6.081	56	C55	0.010	D	1.000	PrD
103-1A	*RYR2*	Somatic mutation gene	c.6457A>G	p.Lys2153Glu	Intracellular calcium-release channel	5.067	56	C0	0.020	D	0.615	PoD
102-1A	*RYR3*	Somatic mutation gene	c.13507G>A	p.Val4503Met	Ryanodine Receptor TM 4-6	6.012	21	C15	0.000	D	1.000	PrD
71A	*ETV4*	Cancer gene	c.991G>A	p.Glu331Lys	PEA3-type ETS-domain transcrip-tion factor, N-terminal	6.424	56	C55	0.001	D	0.862	PoD
103-1A	*PRDM1*	Cancer gene	c.1499A>G	p.Gln500Arg	Zinc finger, C2H2	4.875	43	C0	0.050	D	0.570	PoD
164-1A	*TSC2*	Cancer gene, PI3K/ AKT	c.5200G>A	p.Asp1734Asn	Rap/ran-GAP	5.538	23	C0	0.000	D	0.998	PrD
71A	*MTOR*	PI3K/ AKT	c.5857G>T	p.Val1953Leu	PIK-related kinase	5.634	32	C0	0.001	D	0.827	PoD
154-1A	*DAAM1*	WNT	c.667G>A	p.Val223Met	Diaphanous GTPase-binding	6.347	21	C0	0.000	D	0.998	PrD
71A	*FZD10*	WNT	c.1341C>G	p.Phe447Leu	Frizzled protein	4.229	22	C15	0.000	D	0.984	PrD
164-1A	*TCF7*	WNT	c.572G>T	p.Arg191Met	High mobil-ity group, HMG1/ HMG2	4.202	91	C65	0.000	D	0.999	PrD
71A	*MAST2*	Trans-poson studies	c.3482A>G	p.Asn1161Ser	PDZ/ DHR/ GLGF	4.854	46	C0	0.000	D	0.999	PrD

D: Damaging; PoD: Possibly damaging; PrD: Probably damaging.

colonoscopy test-negative, unrelated local Han Chinese individuals using Sanger sequencing. We found that 7 (7%) of them carried this variant, revealing a significant enrichment in the early-onset/familial CRC cohort as compared to the ethnicity matched control cohort (χ^2 test, $P = 0.000604$).

DISCUSSION

In order to identify rare and novel germline variants that may predispose to CRC, we applied whole-exome sequencing to 23 Chinese patients from 21 families with non-polyposis CRC diagnosed at $\leqslant$ 40 years of age or from multiple affected CRC families with at least one first-degree relative diagnosed with CRC at $\leqslant$ 55 years of age. Initially we selected variants in genes that are known to be associated with hereditary CRC syndromes, and we assessed their pathogenicity as reported in public databases such as InSiGHT, LOVD and the Mismatch Repair Genes Variant database. Among

the 23 patients included, we identified seven patients (from six families; approximately 30%) with variants in known CRC predisposing genes. This percentage is lower than that previously reported by Tanskanen *et al*[41], (42%, 16/38) in a cohort of early-onset CRC patients (< 40 years) using exome sequencing. In a study by Tanskanen *et al*[41], of 38 patients, four were clinically diagnosed with gastrointestinal polyposis (three FAP and one JPS), and 12 were identified with germline MMR mutations and enriched in patients with MSI tumors (86%, 12/14). This discrepancy may be due to the fact that our cohort is a non-polyposis cohort and also includes patients from multiple affected CRC families with at least one first-degree relative diagnosed with CRC at ⩽ 55 years of age. In our cohort, six patients were identified with variants in the high-penetrance genes *MLH1*, *MSH2* and *MSH6* underlying Lynch syndrome. In addition, we identified biallelic *MUTYH* mutations, underlying MAP, in one index patient (patient 180-1, CRC at age of 40) and the sister of the patient (colonic polyps at age of 46). Of the eight variants that we identified in known high-penetrance CRC predisposing genes, *MLH1* c.453+1G>T, *MLH1* c.208-1G>A, *MLH1* c.677G>A, MUTYH p.Gln267* and MUTYH p.Gly286Glu were reported as being pathogenic in public databases[39,40,42-44]. In addition, we identified novel rare variants of which two, MLH1 p.Arg389Profs*6 and *MSH2* c.793-2A>T, are most likely pathogenic based on both familial segregation and *in silico* prediction analyses.

In our search for novel germline predisposing variants, we focused on known cancer-associated genes, CRC pathway-associated genes, mouse CRC susceptibility genes identified by transposon ('sleeping beauty') tagging, GWAS-associated genes and genes with reported somatic mutations that are considered likely to be involved in CRC predisposition and/or development. Using these criteria, we identified a total of 19 novel candidate CRC susceptibility genes carrying rare, likely deleterious, variants.

One ATM truncating variant (p.Lys468Glufs*18) identified in patient 102-1A (rectal cancer at age of 25) may be particularly relevant. *ATM* is a gene encoding a protein that belongs to the PI3/PI4-kinase family[45]. The ATM protein represents an important cell cycle checkpoint kinase that is required for a cell's response to DNA damage and for ensuring genomic integrity[46]. Diseases associated with ATM mutations include ataxia telangiectasia (AT), an autosomal recessive disorder[47]. Because of its role in maintaining genomic integrity, ATM may, when mutated, increase the risk for tumor development[48]. Indeed, germline mutations in *ATM* have been shown to increase the risk of breast cancer development through the (de)regulation of BRCA1[49]. In addition, loss of heterozygosity at the *ATM* locus has been found in CRC[50]. Taken together, it appears plausible to assume that germline *ATM* mutations may increase the risk for CRC development. However, considering the high frequency of truncating mutation in ESP database and in-house database, it is crucial for targeted screening of *ATM* in a large early-onset and/or familial CRC cohort. Another interesting candidate is the truncating MAX variant (p.Leu61Serfs*15) identified in patient 66-1-1A. The protein encoded by the *MAX* gene represents the most conserved dimerization component of the MYC-MAX-MXD1 network of basic helix-loop-helix leucine zipper (bHLHZ) transcription factors that regulate cellular proliferation, differentiation and apoptosis[51,52]. It has been shown that the MAX protein interacts with MSH2[53], and that mutant MAX is able to alter the growth and morphology of CRC cells through inactivation of c-MYC[32]. Mutations in the MAX gene have been reported to be associated with the occurrence of hereditary pheochromocytomas and paragangliomas[54]. Interestingly, an additional truncating variant in PARP1 (p.Lys254Glufs*6) was identified in this patient (66-1-1A). PARP1 is activated in response to DNA damage and plays an important role in DNA repair processes, apoptosis and cell cycle control[55]. Since MAX and PARP1 are both involved in DNA repair, and since it has been shown that PARP1 is essential for c-MYC-induced transactivation and retardation of the G2-M transition in cancer cells[56], the combination of these two variants may have a synergistic effect. Therefore, we anticipate that both truncating variants most likely play a role in CRC development in this family.

Other interesting candidate genes recurrently affected by potentially deleterious variants include *BUB1*, *LRP5* and *EIF2AK4*. Two truncating variants in BUB1 (p.Gln16* and p.Gln949Argfs*3) were found to be present in patient 106-2A and patient 149-1A, respectively. The BUB1 protein is an integral component of the spindle assembly checkpoint (SAC), and we have previously shown that germline variants in the corresponding gene may serve as risk factors for CRC[15]. Patient 106-2A was found to carry both BUB1 p.Gln16* and *MLH1* c.453+1G>T variants. We suggest that BUB1 may have contributed to loss of the wild-type *MLH1* allele in this patient[15]. Obviously, this latter scenario requires validation in larger CRC cohorts.

Three missense LRP5 variants (p.Tyr719Cys, p.Arg1179His and p.Arg1307Trp), found in three CRC cases, were predicted to be deleterious. LRP5 p.Tyr719Cys and LRP5 p.Arg1307Trp were observed in patient 54-2A and patient 77-1A, respectively. In both cases no other putative pathogenic germline variants were detected. Variant LRP5 p.Arg1179His was found in patient 43-1A, who also carried a pathogenic *MLH1* c.677G>A splice site mutation. The LRP5 protein is a component of the WNT-FZD-LRP5-LRP6 complex and, as such, represents an important partner in the WNT signal transduction pathway[57]. Variants LRP5 p.Tyr719Cys and p.Arg1179His are both located in the conserved low-density lipoprotein receptor (LDLR) class B repeat region of LRP5, which is the binding region of Dickkopf-1, a developmental protein antagonist of the canonical WNT-β-catenin pathway[58].

Further assessment of both LRP5 variants using the "Project HOPE" tool indicated that these variants may also result in loss of interactions with other proteins or residues. It has previously been shown that truncated LRP5 proteins are frequently expressed in breast tumors of different developmental stages[59] and that these proteins are strongly implicated in the deregulation of the WNT-β-catenin signaling pathway in hyperparathyroid tumors[60].

One EIF2AK4 variant (p.Glu738_Asp739insArgArg) was recurrently found in seven (33.3%) unrelated patients within our cohort. After comparison of our cohort to an ethnicity matched control cohort, this variant was found to be significantly enriched (P = 0.000604). We, therefore, conclude that also this latter gene may be considered a candidate CRC predisposing gene.

A major challenge of using whole-exome sequencing is the identification of predisposing pathogenic variants within the vast background of non-pathogenic variants. Targeted screening of those genes and variants in replicate large early-onset and/or familial CRC cohorts will be instrumental in gaining more robust evidence for pathogenicity. Our current results, however, already vividly illustrate that whole-exome sequencing in carefully selected cases at risk for hereditary cancer may serve as an attractive approach to identify rare and novel variants in known and novel candidate CRC predisposing genes.

ACKNOWLEDGMENTS

We appreciate Dr. Ying Han, Dr. Hai-Hong Wang, Dr. Xin Wang, Dr. Ai-Qin Li, Dr. Xiao-Wei Wang and Dr. Hui Su from Department of Gastroenterology, General Hospital of Beijing Military Region, Beijing, China for their kindly help in sample collection and we thank the patients and families for participating and their cooperation in this study.

COMMENTS

Background

Mendelian colorectal cancer (CRC) predisposition syndromes underlie about 5% of all CRC cases, and are caused by germline mutations in a limited set of genes. The current selection of causative genes to be screened in high-risk families is based on several phenotypic characteristics, including polyposis (*e.g., APC* and *MUTYH*) and microsatellite instability (*MLH1, MSH2, MSH6* and *PMS2*). The overall heritability of CRC, however, is estimated to be approximately 30%. Excluding hereditary forms, there is an important fraction of CRC cases that present familial aggregation for the disease with an unknown germline genetic cause.

Research frontiers

CRC patients with a family history of CRC or an early age at diagnosis are especially suggestive of a hereditary contribution and may be used in genetic association studies to increase the likelihood of identifying susceptibility variants. Whereas CRC families with multiple affected individuals may be employed to search for high penetrance genetic susceptibility variants using linkage-based approaches, moderate- to low-penetrance variants cannot be identified through linkage-based studies in large families. In more recent years, multiple low-penetrance genetic loci associated with CRC susceptibility have been identified by genome-wide association studies (GWAS). However, not all results from linkage studies turned out to be consistent, and GWAS are not ideal for the identification of rare variants. Recently, advances in next-generation sequencing technologies, in particular whole-exome sequencing, have provided efficient means to identify germline variants in individuals with familial or inherited cancer syndromes.

Innovations and breakthroughs

A major challenge of using whole-exome sequencing is the identification of predisposing pathogenic variants within the vast background of non-pathogenic variants. In this study, we performed whole-exome sequencing in a strictly selected cohort of CRC patients and families that are very young CRC patients (diagnosed at ⩽ 40 years of age) or familial CRC cases. And data were processed through a tailored analytical pipeline to search for rare germline variants in known or novel CRC predisposing genes.

Applications

The study show that whole-exome sequencing of early-onset or familial CRC cases serves as an efficient method to identify known and potential pathogenic variants in established and novel candidate CRC predisposing genes. The findings also provide insight into the role of these variants in CRC development. Targeted screening of those genes and variants in replicate large early-onset and/or familial CRC cohorts will be instrumental in gaining more robust evidence for pathogenicity.

Terminology

"Early-onset" CRC: CRC is traditionally thought to be a disease of older patients with most being diagnosed after the age of 50 years; however, a significant proportion of young patients present with this disease. Early age of onset is a central characteristic of hereditary predisposition to cancer. Familiar aggregation of tumors and hereditary cases are constantly more frequent under the age of 40 years.

Peer-review

This study investigated the efficiency of whole-exome sequencing in identifying known or novel CRC predisposing genes in early-onset or familial CRC cases. This is a well written paper that has been performed stringently. Although the number of included patients is very low, the authors present very interesting results with a straight forward conclusion.

REFERENCES

1 **Jemal A**, Bray F, Center MM, Ferlay J, Ward E, Forman D. Global cancer statistics. *CA Cancer J Clin* 2011; **61**: 69-90 [PMID: 21296855 DOI: 10.3322/caac.20107]

2 **Chen W**, Zheng R, Zhang S, Zhao P, Li G, Wu L, He J. Report of incidence and mortality in China cancer registries, 2009. *Chin J Cancer Res* 2013; **25**: 10-21 [PMID: 23372337 DOI: 10.3978/j.issn.1000-9604.2012.12.04]

3 **Lichtenstein P**, Holm NV, Verkasalo PK, Iliadou A, Kaprio J, Koskenvuo M, Pukkala E, Skytthe A, Hemminki K. Environmental and heritable factors in the causation of cancer--analyses of cohorts of twins from Sweden, Denmark, and Finland. *N Engl J Med* 2000; **343**: 78-85 [PMID: 10891514 DOI: 10.1056/NEJM200007133430201]

4 **de la Chapelle A**. Genetic predisposition to colorectal cancer. *Nat Rev Cancer* 2004; **4**: 769-780 [PMID: 15510158 DOI: 10.1038/nrc1453]

5 **Palles C**, Cazier JB, Howarth KM, Domingo E, Jones AM, Broderick P, Kemp Z, Spain SL, Guarino E, Salguero I, Sherborne A, Chubb D, Carvajal-Carmona LG, Ma Y, Kaur K, Dobbins S, Barclay E, Gorman M, Martin L, Kovac MB, Humphray S, Lucassen A, Holmes CC, Bentley D, Donnelly P, Taylor J, Petridis C, Roylance R, Sawyer EJ, Kerr DJ, Clark S, Grimes J, Kearsey SE, Thomas HJ, McVean G, Houlston RS, Tomlinson I. Germline mutations affecting the proofreading domains of POLE and POLD1 predispose to colorectal adenomas and carcinomas. *Nat Genet* 2013; **45**: 136-144 [PMID: 23263490 DOI: 10.1038/ng.2503]

6 **Lynch HT**, Smyrk T. Hereditary nonpolyposis colorectal cancer (Lynch syndrome). An updated review. *Cancer* 1996; **78**: 1149-1167 [PMID: 8826936]

7 **Schoen RE**. Families at risk for colorectal cancer: risk assessment and genetic testing. *J Clin Gastroenterol* 2000; **31**: 114-120 [PMID: 10993425]

8 **Gryfe R**, Kim H, Hsieh ET, Aronson MD, Holowaty EJ, Bull

SB, Redston M, Gallinger S. Tumor microsatellite instability and clinical outcome in young patients with colorectal cancer. *N Engl J Med* 2000; **342**: 69-77 [PMID: 10631274 DOI: 10.1056/NEJM200001133420201]

9 **Giráldez MD**, Balaguer F, Bujanda L, Cuatrecasas M, Muñoz J, Alonso-Espinaco V, Larzabal M, Petit A, Gonzalo V, Ocaña T, Moreira L, Enríquez-Navascués JM, Boland CR, Goel A, Castells A, Castellví-Bel S. MSH6 and MUTYH deficiency is a frequent event in early-onset colorectal cancer. *Clin Cancer Res* 2010; **16**: 5402-5413 [PMID: 20924129 DOI: 10.1158/1078-0432.CCR-10-1491]

10 **Chang DT**, Pai RK, Rybicki LA, Dimaio MA, Limaye M, Jayachandran P, Koong AC, Kunz PA, Fisher GA, Ford JM, Welton M, Shelton A, Ma L, Arber DA, Pai RK. Clinicopathologic and molecular features of sporadic early-onset colorectal adenocarcinoma: an adenocarcinoma with frequent signet ring cell differentiation, rectal and sigmoid involvement, and adverse morphologic features. *Mod Pathol* 2012; **25**: 1128-1139 [PMID: 22481281 DOI: 10.1038/modpathol.2012.61]

11 **Tenesa A**, Dunlop MG. New insights into the aetiology of colorectal cancer from genome-wide association studies. *Nat Rev Genet* 2009; **10**: 353-358 [PMID: 19434079 DOI: 10.1038/nrg2574]

12 **Houlston RS**, Cheadle J, Dobbins SE, Tenesa A, Jones AM, Howarth K, Spain SL, Broderick P, Domingo E, Farrington S, Prendergast JG, Pittman AM, Theodoratou E, Smith CG, Olver B, Walther A, Barnetson RA, Churchman M, Jaeger EE, Penegar S, Barclay E, Martin L, Gorman M, Mager R, Johnstone E, Midgley R, Niittymäki I, Tuupanen S, Colley J, Idziaszczyk S, Thomas HJ, Lucassen AM, Evans DG, Maher ER, Maughan T, Dimas A, Dermitzakis E, Cazier JB, Aaltonen LA, Pharoah P, Kerr DJ, Carvajal-Carmona LG, Campbell H, Dunlop MG, Tomlinson IP. Meta-analysis of three genome-wide association studies identifies susceptibility loci for colorectal cancer at 1q41, 3q26.2, 12q13.13 and 20q13.33. *Nat Genet* 2010; **42**: 973-977 [PMID: 20972440 DOI: 10.1038/ng.670]

13 **Jones S**, Hruban RH, Kamiyama M, Borges M, Zhang X, Parsons DW, Lin JC, Palmisano E, Brune K, Jaffee EM, Iacobuzio-Donahue CA, Maitra A, Parmigiani G, Kern SE, Velculescu VE, Kinzler KW, Vogelstein B, Eshleman JR, Goggins M, Klein AP. Exomic sequencing identifies PALB2 as a pancreatic cancer susceptibility gene. *Science* 2009; **324**: 217 [PMID: 19264984 DOI: 10.1126/science.1171202]

14 **Comino-Méndez I**, Gracia-Aznárez FJ, Schiavi F, Landa I, Leandro-García LJ, Letón R, Honrado E, Ramos-Medina R, Caronia D, Pita G, Gómez-Graña A, de Cubas AA, Inglada-Pérez L, Maliszewska A, Taschin E, Bobisse S, Pica G, Loli P, Hernández-Lavado R, Díaz JA, Gómez-Morales M, González-Neira A, Roncador G, Rodríguez-Antona C, Benítez J, Mannelli M, Opocher G, Robledo M, Cascón A. Exome sequencing identifies MAX mutations as a cause of hereditary pheochromocytoma. *Nat Genet* 2011; **43**: 663-667 [PMID: 21685915 DOI: 10.1038/ng.861]

15 **de Voer RM**, Geurts van Kessel A, Weren RD, Ligtenberg MJ, Smeets D, Fu L, Vreede L, Kamping EJ, Verwiel ET, Hahn MM, Ariaans M, Spruijt L, van Essen T, Houge G, Schackert HK, Sheng JQ, Venselaar H, van Ravenswaaij-Arts CM, van Krieken JH, Hoogerbrugge N, Kuiper RP. Germline mutations in the spindle assembly checkpoint genes BUB1 and BUB3 are risk factors for colorectal cancer. *Gastroenterology* 2013; **145**: 544-547 [PMID: 23747338 DOI: 10.1053/j.gastro.2013.06.001]

16 **Wood LD**, Parsons DW, Jones S, Lin J, Sjöblom T, Leary RJ, Shen D, Boca SM, Barber T, Ptak J, Silliman N, Szabo S, Dezso Z, Ustyanksky V, Nikolskaya T, Nikolsky Y, Karchin R, Wilson PA, Kaminker JS, Zhang Z, Croshaw R, Willis J, Dawson D, Shipitsin M, Willson JK, Sukumar S, Polyak K, Park BH, Pethiyagoda CL, Pant PV, Ballinger DG, Sparks AB, Hartigan J, Smith DR, Suh E, Papadopoulos N, Buckhaults P, Markowitz SD, Parmigiani G, Kinzler KW, Velculescu VE, Vogelstein B. The genomic landscapes of human breast and colorectal cancers. *Science* 2007; **318**: 1108-1113 [PMID: 17932254 DOI: 10.1126/science.1145720]

17 **Starr TK**, Largaespada DA. Cancer gene discovery using the Sleeping Beauty transposon. *Cell Cycle* 2005; **4**: 1744-1748 [PMID: 16294016]

18 **Starr TK**, Allaei R, Silverstein KA, Staggs RA, Sarver AL, Bergemann TL, Gupta M, O'Sullivan MG, Matise I, Dupuy AJ, Collier LS, Powers S, Oberg AL, Asmann YW, Thibodeau SN, Tessarollo L, Copeland NG, Jenkins NA, Cormier RT, Largaespada DA. A transposon-based genetic screen in mice identifies genes altered in colorectal cancer. *Science* 2009; **323**: 1747-1750 [PMID: 19251594 DOI: 10.1126/science.1163040]

19 **March HN**, Rust AG, Wright NA, ten Hoeve J, de Ridder J, Eldridge M, van der Weyden L, Berns A, Gadiot J, Uren A, Kemp R, Arends MJ, Wessels LF, Winton DJ, Adams DJ. Insertional mutagenesis identifies multiple networks of cooperating genes driving intestinal tumorigenesis. *Nat Genet* 2011; **43**: 1202-1209 [PMID: 22057237 DOI: 10.1038/ng.990]

20 **Domati F**, Maffei S, Kaleci S, Di Gregorio C, Pedroni M, Roncucci L, Benatti P, Magnani G, Marcheselli L, Bonetti LR, Mariani F, Alberti AM, Rossi V, Ponz de Leon M. Incidence, clinical features and possible etiology of early onset (≤40 years) colorectal neoplasms. *Intern Emerg Med* 2014; **9**: 623-631 [PMID: 23929387 DOI: 10.1007/s11739-013-0981-3]

21 **Li H**, Durbin R. Fast and accurate short read alignment with Burrows-Wheeler transform. *Bioinformatics* 2009; **25**: 1754-1760 [PMID: 19451168 DOI: 10.1093/bioinformatics/btp324]

22 **Li R**, Li Y, Kristiansen K, Wang J. SOAP: short oligonucleotide alignment program. *Bioinformatics* 2008; **24**: 713-714 [PMID: 18227114 DOI: 10.1093/bioinformatics/btn025]

23 **Li H**, Handsaker B, Wysoker A, Fennell T, Ruan J, Homer N, Marth G, Abecasis G, Durbin R. The Sequence Alignment/Map format and SAMtools. *Bioinformatics* 2009; **25**: 2078-2079 [PMID: 19505943 DOI: 10.1093/bioinformatics/btp352]

24 **Vissers LE**, de Ligt J, Gilissen C, Janssen I, Steehouwer M, de Vries P, van Lier B, Arts P, Wieskamp N, del Rosario M, van Bon BW, Hoischen A, de Vries BB, Brunner HG, Veltman JA. A de novo paradigm for mental retardation. *Nat Genet* 2010; **42**: 1109-1112 [PMID: 21076407 DOI: 10.1038/ng.712]

25 **Tavtigian SV**, Deffenbaugh AM, Yin L, Judkins T, Scholl T, Samollow PB, de Silva D, Zharkikh A, Thomas A. Comprehensive statistical study of 452 BRCA1 missense substitutions with classification of eight recurrent substitutions as neutral. *J Med Genet* 2006; **43**: 295-305 [PMID: 16014699 DOI: 10.1136/jmg.2005.033878]

26 **Kumar P**, Henikoff S, Ng PC. Predicting the effects of coding non-synonymous variants on protein function using the SIFT algorithm. *Nat Protoc* 2009; **4**: 1073-1081 [PMID: 19561590 DOI: 10.1038/nprot.2009.86]

27 **Adzhubei IA**, Schmidt S, Peshkin L, Ramensky VE, Gerasimova A, Bork P, Kondrashov AS, Sunyaev SR. A method and server for predicting damaging missense mutations. *Nat Methods* 2010; **7**: 248-249 [PMID: 20354512 DOI: 10.1038/nmeth0410-248]

28 **Venselaar H**, Te Beek TA, Kuipers RK, Hekkelman ML, Vriend G. Protein structure analysis of mutations causing inheritable diseases. An e-Science approach with life scientist friendly interfaces. *BMC Bioinformatics* 2010; **11**: 548 [PMID: 21059217 DOI: 10.1186/1471-2105-11-548]

29 **Cancer Genome Atlas Network**. Comprehensive molecular characterization of human colon and rectal cancer. *Nature* 2012; **487**: 330-337 [PMID: 22810696 DOI: 10.1038/nature11252]

30 **Futreal PA**, Coin L, Marshall M, Down T, Hubbard T, Wooster R, Rahman N, Stratton MR. A census of human cancer genes. *Nat Rev Cancer* 2004; **4**: 177-183 [PMID: 14993899 DOI: 10.1038/nrc1299]

31 **Rahman N**. Realizing the promise of cancer predisposition genes. *Nature* 2014; **505**: 302-308 [PMID: 24429628 DOI: 10.1038/nature12981]

32 **Neveling K**, Feenstra I, Gilissen C, Hoefsloot LH, Kamsteeg EJ, Mensenkamp AR, Rodenburg RJ, Yntema HG, Spruijt L, Vermeer S, Rinne T, van Gassen KL, Bodmer D, Lugtenberg D, de Reuver R, Buijsman W, Derks RC, Wieskamp N, van den Heuvel B, Ligtenberg MJ, Kremer H, Koolen DA, van de Warrenburg BP,

Cremers FP, Marcelis CL, Smeitink JA, Wortmann SB, van Zelst-Stams WA, Veltman JA, Brunner HG, Scheffer H, Nelen MR. A post-hoc comparison of the utility of sanger sequencing and exome sequencing for the diagnosis of heterogeneous diseases. *Hum Mutat* 2013; **34**: 1721-1726 [PMID: 24123792 DOI: 10.1002/humu.22450]

33 **Tomlinson IP**, Carvajal-Carmona LG, Dobbins SE, Tenesa A, Jones AM, Howarth K, Palles C, Broderick P, Jaeger EE, Farrington S, Lewis A, Prendergast JG, Pittman AM, Theodoratou E, Olver B, Walker M, Penegar S, Barclay E, Whiffin N, Martin L, Ballereau S, Lloyd A, Gorman M, Lubbe S, Howie B, Marchini J, Ruiz-Ponte C, Fernandez-Rozadilla C, Castells A, Carracedo A, Castellvi-Bel S, Duggan D, Conti D, Cazier JB, Campbell H, Sieber O, Lipton L, Gibbs P, Martin NG, Montgomery GW, Young J, Baird PN, Gallinger S, Newcomb P, Hopper J, Jenkins MA, Aaltonen LA, Kerr DJ, Cheadle J, Pharoah P, Casey G, Houlston RS, Dunlop MG. Multiple common susceptibility variants near BMP pathway loci GREM1, BMP4, and BMP2 explain part of the missing heritability of colorectal cancer. *PLoS Genet* 2011; **7**: e1002105 [PMID: 21655089 DOI: 10.1371/journal.pgen.1002105]

34 **Smith CG**, Naven M, Harris R, Colley J, West H, Li N, Liu Y, Adams R, Maughan TS, Nichols L, Kaplan R, Wagner MJ, McLeod HL, Cheadle JP. Exome resequencing identifies potential tumor-suppressor genes that predispose to colorectal cancer. *Hum Mutat* 2013; **34**: 1026-1034 [PMID: 23585368 DOI: 10.1002/humu.22333]

35 **Hindorff LA**, Sethupathy P, Junkins HA, Ramos EM, Mehta JP, Collins FS, Manolio TA. Potential etiologic and functional implications of genome-wide association loci for human diseases and traits. *Proc Natl Acad Sci USA* 2009; **106**: 9362-9367 [PMID: 19474294 DOI: 10.1073/pnas.0903103106]

36 **Untergasser A**, Cutcutache I, Koressaar T, Ye J, Faircloth BC, Remm M, Rozen SG. Primer3--new capabilities and interfaces. *Nucleic Acids Res* 2012; **40**: e115 [PMID: 22730293 DOI: 10.1093/nar/gks596]

37 **Thompson BA**, Spurdle AB, Plazzer JP, Greenblatt MS, Akagi K, Al-Mulla F, Bapat B, Bernstein I, Capellá G, den Dunnen JT, du Sart D, Fabre A, Farrell MP, Farrington SM, Frayling IM, Frebourg T, Goldgar DE, Heinen CD, Holinski-Feder E, Kohonen-Corish M, Robinson KL, Leung SY, Martins A, Moller P, Morak M, Nystrom M, Peltomaki P, Pineda M, Qi M, Ramesar R, Rasmussen LJ, Royer-Pokora B, Scott RJ, Sijmons R, Tavtigian SV, Tops CM, Weber T, Wijnen J, Woods MO, Macrae F, Genuardi M. Application of a 5-tiered scheme for standardized classification of 2,360 unique mismatch repair gene variants in the InSiGHT locus-specific database. *Nat Genet* 2014; **46**: 107-115 [PMID: 24362816 DOI: 10.1038/ng.2854]

38 **Pagenstecher C**, Wehner M, Friedl W, Rahner N, Aretz S, Friedrichs N, Sengteller M, Henn W, Buettner R, Propping P, Mangold E. Aberrant splicing in MLH1 and MSH2 due to exonic and intronic variants. *Hum Genet* 2006; **119**: 9-22 [PMID: 16341550 DOI: 10.1007/s00439-005-0107-8]

39 **Kim DW**, Kim IJ, Kang HC, Jang SG, Kim K, Yoon HJ, Ahn SA, Han SY, Hong SH, Hwang JA, Sohn DK, Jeong SY, Choi HS, Hong CW, Lim SB, Park JG. Germline mutations of the MYH gene in Korean patients with multiple colorectal adenomas. *Int J Colorectal Dis* 2007; **22**: 1173-1178 [PMID: 17703316 DOI: 10.1007/s00384-007-0289-8]

40 **Yanaru-Fujisawa R**, Matsumoto T, Ushijima Y, Esaki M, Hirahashi M, Gushima M, Yao T, Nakabeppu Y, Iida M. Genomic and functional analyses of MUTYH in Japanese patients with adenomatous polyposis. *Clin Genet* 2008; **73**: 545-553 [PMID: 18422726 DOI: 10.1111/j.1399-0004.2008.00998.x]

41 **Tanskanen T**, Gylfe AE, Katainen R, Taipale M, Renkonen-Sinisalo L, Mecklin JP, Järvinen H, Tuupanen S, Kilpivaara O, Vahteristo P, Aaltonen LA. Exome sequencing in diagnostic evaluation of colorectal cancer predisposition in young patients. *Scand J Gastroenterol* 2013; **48**: 672-678 [PMID: 23544471 DOI: 10.3109/00365521.2013.783102]

42 **Sheng JQ**, Fu L, Sun ZQ, Huang JS, Han M, Mu H, Zhang H, Zhang YZ, Zhang MZ, Li AQ, Wu ZT, Han Y, Li SR. Mismatch repair gene mutations in Chinese HNPCC patients. *Cytogenet Genome Res* 2008; **122**: 22-27 [PMID: 18931482]

43 **Goldberg Y**, Porat RM, Kedar I, Shochat C, Sagi M, Eilat A, Mendelson S, Hamburger T, Nissan A, Hubert A, Kadouri L, Pikarski E, Lerer I, Abeliovich D, Bercovich D, Peretz T. Mutation spectrum in HNPCC in the Israeli population. *Fam Cancer* 2008; **7**: 309-317 [PMID: 18389388 DOI: 10.1007/s10689-008-9191-y]

44 **Arnold S**, Buchanan DD, Barker M, Jaskowski L, Walsh MD, Birney G, Woods MO, Hopper JL, Jenkins MA, Brown MA, Tavtigian SV, Goldgar DE, Young JP, Spurdle AB. Classifying MLH1 and MSH2 variants using bioinformatic prediction, splicing assays, segregation, and tumor characteristics. *Hum Mutat* 2009; **30**: 757-770 [PMID: 19267393 DOI: 10.1002/humu.20936]

45 **Savitsky K**, Sfez S, Tagle DA, Ziv Y, Sartiel A, Collins FS, Shiloh Y, Rotman G. The complete sequence of the coding region of the ATM gene reveals similarity to cell cycle regulators in different species. *Hum Mol Genet* 1995; **4**: 2025-2032 [PMID: 8589678]

46 **Abraham RT**. Cell cycle checkpoint signaling through the ATM and ATR kinases. *Genes Dev* 2001; **15**: 2177-2196 [PMID: 11544175 DOI: 10.1101/gad.914401]

47 **McKinnon PJ**. ATM and the molecular pathogenesis of ataxia telangiectasia. *Annu Rev Pathol* 2012; **7**: 303-321 [PMID: 22035194 DOI: 10.1146/annurev-pathol-011811-132509]

48 **Pusapati RV**, Rounbehler RJ, Hong S, Powers JT, Yan M, Kiguchi K, McArthur MJ, Wong PK, Johnson DG. ATM promotes apoptosis and suppresses tumorigenesis in response to Myc. *Proc Natl Acad Sci USA* 2006; **103**: 1446-1451 [PMID: 16432227 DOI: 10.1073/pnas.0507367103]

49 **Broeks A**, Urbanus JH, Floore AN, Dahler EC, Klijn JG, Rutgers EJ, Devilee P, Russell NS, van Leeuwen FE, van 't Veer LJ. ATM-heterozygous germline mutations contribute to breast cancer-susceptibility. *Am J Hum Genet* 2000; **66**: 494-500 [PMID: 10677309]

50 **Uhrhammer N**, Bay J, Pernin D, Rio P, Grancho M, Kwiatkowski F, Gosse-Brun S, Daver A, Bignon Y. Loss of heterozygosity at the ATM locus in colorectal carcinoma. *Oncol Rep* 1999; **6**: 655-658 [PMID: 10203610]

51 **Blackwood EM**, Eisenman RN. Max: a helix-loop-helix zipper protein that forms a sequence-specific DNA-binding complex with Myc. *Science* 1991; **251**: 1211-1217 [PMID: 2006410]

52 **Blackwood EM**, Lüscher B, Eisenman RN. Myc and Max associate in vivo. *Genes Dev* 1992; **6**: 71-80 [PMID: 1730411]

53 **Mac Partlin M**, Homer E, Robinson H, McCormick CJ, Crouch DH, Durant ST, Matheson EC, Hall AG, Gillespie DA, Brown R. Interactions of the DNA mismatch repair proteins MLH1 and MSH2 with c-MYC and MAX. *Oncogene* 2003; **22**: 819-825 [PMID: 12584560 DOI: 10.1038/sj.onc.1206252]

54 **Burnichon N**, Cascón A, Schiavi F, Morales NP, Comino-Méndez I, Abermil N, Inglada-Pérez L, de Cubas AA, Amar L, Barontini M, de Quirós SB, Bertherat J, Bignon YJ, Blok MJ, Bobisse S, Borrego S, Castellano M, Chanson P, Chiara MD, Corssmit EP, Giacchè M, de Krijger RR, Ercolino T, Girerd X, Gómez-García EB, Gómez-Graña A, Guilhem I, Hes FJ, Honrado E, Korpershoek E, Lenders JW, Letón R, Mensenkamp AR, Merlo A, Mori L, Murat A, Pierre P, Plouin PF, Prodanov T, Quesada-Charneco M, Qin N, Rapizzi E, Raymond V, Reisch N, Roncador G, Ruiz-Ferrer M, Schillo F, Stegmann AP, Suarez C, Taschin E, Timmers HJ, Tops CM, Urioste M, Beuschlein F, Pacak K, Mannelli M, Dahia PL, Opocher G, Eisenhofer G, Gimenez-Roqueplo AP, Robledo M. MAX mutations cause hereditary and sporadic pheochromocytoma and paraganglioma. *Clin Cancer Res* 2012; **18**: 2828-2837 [PMID: 22452945 DOI: 10.1158/1078-0432.CCR-12-0160]

55 **Schreiber V**, Dantzer F, Ame JC, de Murcia G. Poly(ADP-ribose): novel functions for an old molecule. *Nat Rev Mol Cell Biol* 2006; **7**: 517-528 [PMID: 16829982 DOI: 10.1038/nrm1963]

56 **Pyndiah S**, Tanida S, Ahmed KM, Cassimere EK, Choe C, Sakamuro D. c-MYC suppresses BIN1 to release poly(ADP-ribose) polymerase 1: a mechanism by which cancer cells acquire cisplatin resistance. *Sci Signal* 2011; **4**: ra19 [PMID: 21447800

DOI: 10.1126/scisignal.2001556]
57 **MacDonald BT**, He X. Frizzled and LRP5/6 receptors for Wnt/β-catenin signaling. *Cold Spring Harb Perspect Biol* 2012; **4**: [PMID: 23209147 DOI: 10.1101/cshperspect.a007880]
58 **Zorn AM**. Wnt signalling: antagonistic Dickkopfs. *Curr Biol* 2001; **11**: R592-R595 [PMID: 11516963]
59 **Björklund P**, Svedlund J, Olsson AK, Akerström G, Westin G. The internally truncated LRP5 receptor presents a therapeutic target in breast cancer. *PLoS One* 2009; **4**: e4243 [PMID: 19158955 DOI: 10.1371/journal.pone.0004243]
60 **Björklund P**, Akerström G, Westin G. An LRP5 receptor with internal deletion in hyperparathyroid tumors with implications for deregulated WNT/beta-catenin signaling. *PLoS Med* 2007; **4**: e328 [PMID: 18044981 DOI: 10.1371/journal.pmed.0040328]

P- Reviewer: Krieg A **S- Editor**: Gou SX
L- Editor: Wang TQ **E- Editor**: Liu XM

World Journal of Gastroenterology

Submit a Manuscript: http://www.wjgnet.com/esps/
Help Desk: http://www.wjgnet.com/esps/helpdesk.aspx
DOI: 10.3748/wjg.v21.i14.4150

World J Gastroenterol 2015 April 14; 21(14): 4150-4158
ISSN 1007-9327 (print) ISSN 2219-2840 (online)

ORIGINAL ARTICLE

Basic Study

Changes in the colon microbiota and intestinal cytokine gene expression following minimal intestinal surgery

Susan Lapthorne, Julie E Bines, Fiona Fouhy, Nicole L Dellios, Guineva Wilson, Sarah L Thomas, Michelle Scurr, Catherine Stanton, Paul D Cotter, Prue M Pereira-Fantini

Susan Lapthorne, Nicole L Dellios, Sarah L Thomas, Michelle Scurr, Prue M Pereira-Fantini, Intestinal Failure and Clinical Nutrition group, Murdoch Childrens Research Institute, Royal Children's Hospital, Parkville, Victoria 3052, Australia
Julie E Bines, Intestinal Failure and Clinical Nutrition group, Murdoch Childrens Research Institute, Parkville, Victoria 3052, Australia
Julie E Bines, Department of Paediatrics, the University of Melbourne, Parkville, Victoria 3052, Australia
Julie E Bines, Department of Gastroenterology and Clinical Nutrition, Royal Children's Hospital, Parkville, Victoria 3052, Australia
Fiona Fouhy, Teagasc Food Research Centre, Moorepark, Fermoy, Cork, Ireland
Fiona Fouhy, Department of Microbiology, University College Cork, Cork, Ireland
Guineva Wilson, Intestinal Failure and Clinical Nutrition group, Murdoch Childrens Research Institute, Parkville, Victoria 3052, Australia
Guineva Wilson, Department of Surgery, Monash Medical Centre, Clayton, Victoria 3052, Australia
Catherine Stanton, Paul D Cotter, Teagasc Food Research Centre, Moorepark, Fermoy, Cork, Ireland
Catherine Stanton, Paul D Cotter, Alimentary Pharmabiotic Centre, University College Cork, Cork, Ireland
Author contributions: Lapthorne S, Bines J and Pereira-Fantini P designed the research, performed the research, analyzed the data and wrote the paper; Fouhy F, Dellios NL, Wilson G, Thomas SL and Scurr M, performed the research; Stanton C and Cotter PD contributed new reagents/analytic tools and analyzed the data.
Supported by Victorian Government's Operational Infrastructure Support program; The PC lab is supported in part by grants from Science Foundation Ireland in the form of a center grant (Alimentary Pharmabiotic Centre; No. SFI/12/RC/2273 and No. 12/RC/2273 and a PI grand to PCR No.11/PI/1137; FF is in receipt of an Irish Research Council EMBARK scholarship and is a Teagasc Walsk Fellow.

Correspondence to: Prue M Pereira-Fantini, PhD, Head of Laboratory Research, Intestinal Failure and Clinical Nutrition group, Murdoch Childrens Research Institute, Royal Children's Hospital, Flemington Road, Parkville Victoria 3052, Australia. prue.pereira@mcri.edu.au
Telephone: +61-3-83416452
Fax: +61-3-93481391
Received: May 28, 2014
Peer-review started: May 28, 2014
First decision: July 21, 2014
Revised: August 6, 2014
Accepted: October 21, 2014
Article in press: October 21, 2014
Published online: April 14, 2015

Abstract

AIM: To investigate the impact of minor abdominal surgery on the caecal microbial population and on markers of gut inflammation.

METHODS: Four week old piglets were randomly allocated to a no-surgery "control" group (n = 6) or a "transection surgery" group (n = 5). During the transection surgery procedure, a conventional midline incision of the lower abdominal wall was made and the small intestine was transected at a site 225 cm proximal to the ileocaecal valve, a 2 cm segment was removed and the intestine was re-anastomosed. Piglets received a polymeric infant formula diet throughout the study period and were sacrificed at two weeks post-surgery. Clinical outcomes including weight, stool consistency and presence of stool fat globules were monitored. High throughput DNA sequencing of colonic content was used to detect surgery-related

disturbances in microbial composition at phylum, family and genus level. Diversity and richness estimates were calculated for the control and minor surgery groups. As disturbances in the gut microbial community are linked to inflammation we compared the gene expression of key inflammatory cytokines (TNF, IL1B, IL18, IL12, IL8, IL6 and IL10) in ileum, terminal ileum and colon mucosal extracts obtained from control and abdominal surgery groups at two weeks post-surgery.

RESULTS: Changes in the relative abundance of bacterial species at family and genus level were confined to bacterial members of the *Proteobacteria* and *Bacteroidetes* phyla. Family level compositional shifts included a reduction in the relative abundance of *Enterobacteriaceae* (22.95 ± 5.27 *vs* 2.07 ± 0.72, $P < 0.01$), *Bacteroidaceae* (2.54 ± 0.56 *vs* 0.86 ± 0.43, $P < 0.05$) and *Rhodospirillaceae* (0.40 ± 0.14 *vs* 0.00 ± 0.00, $P < 0.05$) following transection surgery. Similarly, at the genus level, changes associated with transection surgery were restricted to members of the *Proteobacteria* and *Bacteroidetes* phyla and included decreased relative abundance of *Enterobacteriaceae* (29.20 ± 6.74 *vs* 2.88 ± 1.08, $P < 0.01$), *Alistipes* (4.82 ± 1.73 *vs* 0.18 ± 0.13, $P < 0.05$) and *Thalassospira* (0.53 ± 0.19 *vs* 0.00 ± 0.00, $P < 0.05$). Surgery-associated microbial dysbiosis was accompanied by increased gene expression of markers of inflammation. Within the ileum IL6 expression was decreased (4.46 ± 1.60 *vs* 0.24 ± 0.06, $P < 0.05$) following transection surgery. In the terminal ileum, gene expression of TNF was decreased (1.51 ± 0.13 *vs* 0.80 ± 0.16, $P < 0.01$) and IL18 (1.21 ± 0.18 *vs* 2.13 ± 0.24, $P < 0.01$), IL12 (1.04 ± 0.16 *vs* 1.82 ± 0.32, $P < 0.05$) and IL10 (1.04 ± 0.06 *vs* 1.43 ± 0.09, $P < 0.01$) gene expression increased following transection surgery. Within the colon, IL12 (0.72 ± 0.13 *vs* 1.78 ± 0.28, $P < 0.01$) and IL10 (0.98 ± 0.02 *vs* 1.95 ± 0.14, $P < 0.01$) gene expression were increased following transection surgery.

CONCLUSION: This study suggests that minor abdominal surgery in infants, results in long-term alteration of the colonic microbial composition and persistent gastrointestinal inflammation.

Key words: Surgery; Intestinal; Microbiota; Dysbiosis; Inflammation; Surgery; Bacteria; Infant; Pediatric; Transection

Core tip: Early colonization of the infant gut is increasingly recognized as impacting on health due to the influence of resident microbes on nutritional, immunological and physiological functions. However, medical and surgical interventions required during infancy, including abdominal surgery, have the potential to modify the microbiome. Using 454-pyrosequencing technology we have described microbial dysbiosis within the *Proteobacteria* and *Bacteriodetes* phylum and increased gut inflammatory cytokines following transection surgery in a juvenile pig model. This is the first study examining minor surgery-associated changes in the gut microbiome and inflammation and provides new insights into potential long-term consequences of abdominal surgery in infancy.

Lapthorne S, Bines JE, Fouhy F, Dellios NL, Wilson G, Thomas SL, Scurr M, Stanton C, Cotter PD, Pereira-Fantini PM. Changes in the colon microbiota and intestinal cytokine gene expression following minimal intestinal surgery. *World J Gastroenterol* 2015; 21(14): 4150-4158 Available from: URL: http://www.wjgnet.com/1007-9327/full/v21/i14/4150.htm DOI: http://dx.doi.org/10.3748/wjg.v21.i14.4150

INTRODUCTION

The gut microbiota is essential to human health, yet the acquisition of this microbial community during infancy remains poorly understood. At birth, humans are essentially free of bacteria, with colonization of the gastrointestinal tract beginning during the birthing process as the newborn is exposed to maternal and environmental microbes[1]. The infant microbiota is marked by heterogeneity and instability until approximately 2-4 years of age[2,3], when it becomes more stable, resembling an adult microbiota[4]. The development of the microbiota is known to be strongly influenced by early extrinsic factors including mode of infant delivery[5], type of feeding[6,7] and antibiotic therapy[8-10]. Acute intestinal conditions including intestinal obstruction, perforation and intussusception may necessitate exploratory abdominal surgery and/or surgical intervention during the neonatal or infant period; however the impact of abdominal surgery on the microbiota has not previously been studied.

Colonization of the newborn intestine plays a key role in the development and fine-tuning of intestinal immune responses[11], and disruption of the gut microbiota has been linked to an increasing number of immune-related diseases, including inflammatory bowel disease, necrotizing enterocolitis (NEC), eczema, allergies and asthma[12]. Given the previously demonstrated impact of early life bacterial dysbiosis on future adult health, characterization of the impact of laparotomy in infancy on the development of the microbiome and inflammation is clinically relevant. The neonatal piglet surgical model is an excellent alternative model for the study of human gastrointestinal disease due to physiological[13,14], bacteriological[15] and immunological[16,17] similarities between pigs and humans. In addition, the accelerated ageing rate of pigs when compared with humans allows us to study the equivalent human timeframe of infancy to early childhood within a two week study period.

The primary aim of the present study was to use

454-pyrosequencing technology to assess the impact of minor abdominal surgery on the colonic microbiota in a juvenile pig model of intestinal transection surgery. Our secondary aim was to perform a multi-site assessment of molecular alterations in key gut inflammatory markers to assess if surgery-related microbial dysbiosis was associated with intestinal inflammation at two weeks following surgery.

MATERIALS AND METHODS

Animals

This study was approved by the Animal Ethics Committee of the Murdoch Childrens Research Institute. Weaned female three-week-old piglets (Landrace/Large White cross; Aussie Pride Pork) were transported to the University of Melbourne Centre for Animal Biotechnology and acclimatized prior to surgery. Piglets were fed a polymeric infant formula diet (Karicare De-Lact, Nutricia) supplemented to meet the daily requirements for piglets as described previously[18-23]. The diets were isocaloric and isonitrogenous among the groups and were administered on a per kilogram basis. Water was given twice daily. Piglets were housed separately throughout the study to allow accurate daily monitoring of food and water intake and collection of stool (analysed for consistency, presence of fat globules and presence of fatty acid crystals). Piglet weight was measured weekly before feeding.

Experimental design

Four week old piglets were randomly allocated to a no-surgery "control" group (n = 6) or a "transection" surgery group (n = 5). During the surgery procedure, a conventional midline incision of the lower abdominal wall was made and the small intestine was transected at a site 225 cm proximal to the ileocaecal valve, a 2 cm segment was removed and the intestine was re-anastomosed. The removal of 2 cm of intestine was equivalent to a mean of 0.11% of the initial intestinal length. Both groups received intramuscular amoxicillin (70 mg/kg; CSL Limited) 24 h pre-surgery, and for three days post-surgery in line with current clinical practice. In addition, both groups received oral rehydration salts (Sanofi-Aventis Australia) for three days post-surgery or equivalent date, with water and the polymeric infant formula diet re-introduced from the third day post-operation.

Sample collection

Animals in the transection group were sacrificed two weeks post-surgery and at an age-matched time in the control group. Ileum tissue was collected 8 cm distal to the anastomosis in the transection group and 217 cm proximal to the ileocaecal valve in the control group. Terminal ileum tissue was collected 7 cm proximal to the ileocaecal valve and colon tissue was collected 3 cm distal to the caecum in both groups. Samples from each site were snap frozen in liquid nitrogen. Colonic content was collected from the proximal colon.

High-throughput sequencing

The 16S rRNA amplicons from colonic content were generated using a previously outlined approach[24]. Amplicons were generated using one forward primer and a combination of four reverse primers as described previously[24]. Each primer contained a distinct multiple identifier (MID) allowing pooling of the amplicons and subsequent separation of the results for analysis. Duplicate PCR products were pooled and cleaned using Agencourt AMPure kit (Beckman Coulter, A63880). Quantification was completed using Quant-iT Picogreen quantification kit (Invitrogen, P7589) and the Nanodrop 3300 (Thermo Scientific). The V4 region of the 16S rRNA was sequenced at the Teagasc 454-Sequencing facility on a Genome Sequencer FLX platform (Roche Diagnostics Ltd.).

Bioinformatic analysis

Raw sequencing reads were quality trimmed using the RDP Pyrosequencing Pipeline applying the following criteria (1) exact matches to primer sequences and barcode tags; (2) no ambiguous bases (Ns); and (3) read-lengths no shorter than 150 base pairs. Trimmed FASTA sequences were then BLASTED[25] against the SILVA (v100) database for 16S reads[26]. Phylum, family and genus counts were extracted from MEGAN using a bit score cut-off of 86[26]. Clustering into operational taxonomical units (OTUs), alignments, chimera-checking and alpha diversities were implemented using the Qiime suite of tools. The relative abundance was determined for individual pigs as the number of reads for each species as a proportion of the total number of reads for that pig at the relevant level of phylum, family or genus.

Real-time reverse transcription PCR

The muscle layer was stripped from the ileum, terminal ileum and colon tissue leaving the mucosa, which comprised the epithelium and the lamina propria. Total RNA was extracted from 100 mg of intestinal mucosa using TRIzol (Invitrogen). Complementary DNA (cDNA) was synthesized with the Transcriptor First Strand cDNA Synthesis Kit (Roche Applied Science). PCR primers were designed against pig gene sequences using Roche Universal ProbeLibrary Assay Design Centre (Roche Applied Science). Primer sequences and probe combinations are listed in Table 1. PCR reactions were performed in triplicate on the LightCycler 480. The $2^{-\Delta\Delta Ct}$ method[27] was used to calculate relative changes in gene expression in the surgical group relative to the non-surgical control group, using RPL32 as a housekeeping gene.

Statistical analysis

Sequencing analysis was completed using Minitab

Table 1 List of primer sequences and Universal ProbeLibrary combinations used in this study

Primer	Sequence 5′ to 3′	UPL Probe
RPL32 Forward	AACTGGCCATCAGGGTCAC	#64
RPL32 Reverse	CACAACTGGAACTCCTGTCTATTC	
TNF Forward	TTGTCGCTACATCGCTGAAC	#32
TNF Reverse	CCAGTAGGGCGGTTACAGAC	
IL1β Forward	CCAATTCAGGGACCCTACC	#19
IL1β Reverse	CATGGCTGCTTCAGAAACCT	
IL18 Forward	ACTTTACTTTGTAGCTGAAAACGATG	#85
IL18 Reverse	TTTAGGTTCAAGCTTGCCAAA	
IL12 Forward	GAGGGTGAGTGAGTGCCTTG	#62
IL12 Reverse	ACTCCGCCTAGGTTCGACTT	
IL8 Forward	TTCTTCTTTATCCCCAAACTGG	#41
IL8 Reverse	CCACATGTCCTCAAGGTAGGA	
IL6 Forward	TGAACTCCCTCTCCACAAGC	#7
IL6 Reverse	GGCAGTAGCCATCACCAGA	
IL10 Forward	TCCAGTTTTACCTGGAAGACG	#8
IL10 Reverse	CCTTGATATCCTCCCCATCA	

Release 15.1.1.0 (Minitab Inc 2007). Parametric unpaired *t*-test was employed to identify significant differences in the percentage of assignable reads at phylum, family and genus levels between non-surgery control and transaction surgery groups. (GraphPad Prism Software 6.0). Parametric unpaired *t*-tests were also employed to test for statistical significance in the relative gene expression of inflammation markers between non-surgery control and transaction surgery groups. Statistical significance for all testing was accepted at $P < 0.05$.

RESULTS

Weight gain throughout the time course studied was comparable between the no-surgery control and transection surgery groups and both groups consumed equivalent energy per kilogram per day. There was no evidence of diarrhea or steatorrhea in any piglets in the transaction group and they were considered to be clinically well.

Microbial composition is significantly altered following transaction surgery

High throughput DNA sequencing was used to detect disturbances in microbial composition following transection surgery. Diversity and richness estimates were calculated for the control and transection surgery groups. The Chao 1 calculation is an estimator of phylotype richness in a dataset and the Shannon index of diversity reflects both the richness and the community evenness (*i.e.*, proportional phylotype abundance)[28]. The overall alpha diversity of the colonic microbiota was unchanged following surgery as calculated by either the Chao 1 richness estimate (905 + 41 *vs* 892 ± 123) or the Shannon's index for diversity (6.9 ± 0.2 *vs* 6.5 ± 0.6), and there was no difference in the number of observed species.

16S rRNA sequence data obtained from colonic content samples was analyzed to determine if transection surgery was associated with changes in the proportion of assignable reads at the phylum, family or genus level when compared with no surgery controls. There was no difference in composition at a phylum level between the control group and the transection group. Changes were observed however, at family and genus level (Tables 2 and 3). Changes in the relative abundance of bacterial species at family and genus level were confined to members of the *Proteobacteria* and *Bacteroidetes* phyla, with no difference in the relative abundance at family or genus level of species belonging to the *Firmicute, Actinobacteria, Fusobacteria* or *Spirochaetes* phylum.

As can be seen in Table 2, family level compositional shifts included a 10-fold reduction in the relative abundance of *Enterobacteriacceae* and a 3-fold reduction in the relative abundance of *Bacteriodaceae* following transection surgery. The proportion of *Bifidobacteriaceae* was reduced 10-fold in surgical samples (0.40 ± 0.16 *vs* 0.04 ± 0.03, $P = 0.0712$) and although *Rhodospirillaceae* was present in 5/6 control samples, *Rhodospirillaceae* was not detected amongst any of the surgical samples (0.40 ± 0.14 *vs* 0.00 ± 0.00, $P = 0.0370$). Similarly at the genus level, changes associated with transection surgery were restricted to members of the *Proteobacteria* and *Bacteroidetes* phyla (Table 3). Specifically transection surgery resulted in a 10-fold decrease in the relative abundance of members of the *Enterobacteriaceae,* a 27-fold decrease in the relative abundance of *Alistipes* and a two-fold decrease in the relative abundance of *Bacteroides.* The relative abundance of *Thalassospira* (0.53 ± 0.19 *vs* 0.00 ± 0.00, $P = 0.0379$) and *Bifidobacterium* (0.51 ± 0.21 *vs* 0.06 ± 0.04, $P = 0.0838$) was also decreased (though not significantly) following surgery. *Thalassospira* was detected in all control samples but was undetectable in the surgical samples.

A tissue-specific pattern of inflammation occurs following transaction surgery

Disturbances of the gut microbial community are closely linked to inflammation[29], therefore given the detected bacterial dysbiosis in the transection surgery model we next examined changes in the mucosal gene expression of key inflammatory cytokines within the ileum, terminal ileum and colon (Figure 1). Within the ileum, a decrease in interleukin 6 (*IL6*) gene expression followed surgery ($P = 0.0383$; Figure 1A). In the terminal ileum, gene expression of the pro-inflammatory cytokine tumor necrosis factor (*TNF*) was decreased ($P = 0.0072$), and interleukin 18 (*IL18*) and interleukin 12 (*IL12*) gene expression was increased following surgery when compared with controls ($P = 0.0123$ and $P = 0.0430$ respectively; Figure 1B). Gene expression of the anti-inflammatory cytokine interleukin 10 (IL10) was increased in terminal ileum

Table 2 Relative abundance of bacterial species at the family level in colonic content samples obtained from no-surgery control animals (n = 6) or animals who have undergone a transaction surgery (n = 5)

Phylum level	Family level	Control (Rel. Abundance)	Transection (Rel. Abundance)	*P* value
Proteobacteria	Enterobacteriaceae	22.95 + 5.27	2.07 + 0.72[a]	0.0104
	Desulfovibrionaceae	2.89 + 1.26	2.95 + 1.16	0.9716
	Moraxellaceae	0.69 + 0.55	8.81 + 8.72	0.4501
	Pseudoalteromonadaceae	0.55 + 0.43	1.42 + 1.42	0.5844
	Vibrionaceae	0.52 + 0.37	6.03 + 5.91	0.4038
Bacteriodetes	Rikenallaceae	6.00 + 1.87	3.70 + 1.31	0.3416
	Porphyromonadaceae	2.33 + 0.76	4.50 + 1.78	0.3080
	Prevotellaceae	2.76 + 0.39	8.05 + 2.60	0.1105
	Bacteroidaceae	2.54 + 0.56	0.86 + 0.43[a]	0.0432
Firmicutes	Ruminococcaceae	19.97 + 2.01	15.26 + 4.71	0.3962
	Veillonellaceae	14.19 + 4.12	22.40 + 7.73	0.3834
	Lachnospiraceae	7.63 + 2.31	6.19 + 2.00	0.6475
	Peptostreptococcaceae	3.19 + 1.06	1.52 + 1.08	0.2991
	Erysipeolotrichales Incertae Sedis	1.78 + 0.61	1.03 + 0.53	0.3809
	Clostridiaceae	1.45 + 0.35	0.73 + 0.36	0.1843
	Lactobacillaceae	1.09 + 0.45	1.58 + 0.83	0.6197
	Streptococcaceae	0.13 + 0.06	1.56 + 1.54	0.4056
Actinobacteria	Micrococcinea	0.07 + 0.07	1.54 + 1.54	0.3926
Fusobacteria	Fusobacteriaceae	0.98 + 0.44	3.85 + 3.09	0.4079
Spirochaetes	Spirochaetaceae	1.83 + 1.15	0.09 + 0.08	0.1898
Other		6.49 + 1.09	5.84 + 1.41	0.7245

Data are expressed as mean + SEM (%). [a]$P < 0.05$ *vs* control. Bacterial species whose relative abundance was < 1% in both the control and transaction surgery group are compiled within the "other" category. Significant changes in bacteria whose relative abundance was < 1% are detailed within the text.

Table 3 Relative abundance of bacterial species at the genus level in colonic content samples obtained from no-surgery control animals (n = 6) or animals who have undergone a transaction surgery (n = 5)

Phylum	Genus level	Control (Rel. Abundance)	Transection (Rel. Abundance)	*P* value
Proteobacteria	Members of the Enterobacteriaceae	29.20 + 6.74	2.88 + 1.08[a]	0.0108
	Desulfovibrio	2.08 + 0.68	2.74 + 0.78	0.5389
	Bilophila	1.48 + 0.81	1.13 + 0.95	0.7847
	Psychrobacter	0.90 + 0.72	9.13 + 9.01	0.4136
	Vibrio	0.62 + 0.46	5.89 + 5.70	0.4105
	Pseudoalteromonas	0.15 + 0.12	1.47 + 1.47	0.4192
Bacteriodetes	Alistipes	4.82 + 1.73	0.18 + 0.13[a]	0.0441
	Prevotella	3.61 + 0.59	11.11 + 3.68	0.1110
	Bacteroides	3.25 + 0.71	1.24 + 0.63	0.0625
	Parabacteroides	2.88 + 0.65	5.59 + 2.41	0.3313
	Lachnospitaceae Incertae sedis	2.50 + 1.02	1.10 + 0.47	0.2548
Firmicutes	Megasphaera	9.71 + 3.87	14.18 + 4.01	0.4434
	Phascolartobacterium	4.07 + 1.00	6.90 + 1.89	0.2330
	Rumminococcaceae Incertae sedis	2.94 + 0.71	1.78 + 0.47	0.2106
	peptostreptococcaceae incertae sedis	2.79 + 1.23	1.80 + 1.49	0.6208
	Subdoligranulum	2.49 + 0.99	1.28 + 0.57	0.3264
	Acidaminococcus	2.40 + 0.71	3.53 + 1.82	0.5866
	Erysipelotrichales incertae sedis	2.28 + 0.77	1.48 + 0.78	0.4859
	Lactobacillus	1.96 + 0.74	2.15 + 1.16	0.8958
	Clostridium	1.86 + 0.45	1.05 + 0.52	0.2732
	Anaerotruncus	2.23 + 0.71	0.97 + 0.31	0.1501
	Oribacterium	0.63 + 0.25	1.88 + 0.88	0.2341
	Lactococcus	0.06 + 0.06	1.60 + 1.58	0.3860
	Mitsuokella	0.05 + 0.05	1.90 + 1.82	0.3664
Actinobacteria	Micrococcaceae	0.07 + 0.07	1.38 + 1.38	0.3959
Fusobacteria	Fusobacterium	1.27 + 0.60	5.43 + 4.39	0.3986
Spirochaetes	Treponema	2.29 + 1.44	0.13 + 0.11	0.1951
Uncult. Clone	EU774397	1.43 + 0.73	0.05 + 0.05	0.1178
	AF371921	1.43 + 0.47	2.18 + 0.99	0.5217
	AF371920	0.24 + 0.14	1.11 + 0.79	0.3315
Other		8.05 + 0.69	6.66 + 1.21	0.3549

Data are expressed as mean + SEM (%). [a]$P < 0.05$ *vs* control. Bacterial species whose relative abundance was < 1% in both the control and transaction surgery group are compiled within the "other" category. Significant changes in bacteria whose relative abundance was < 1% are detailed within the text.

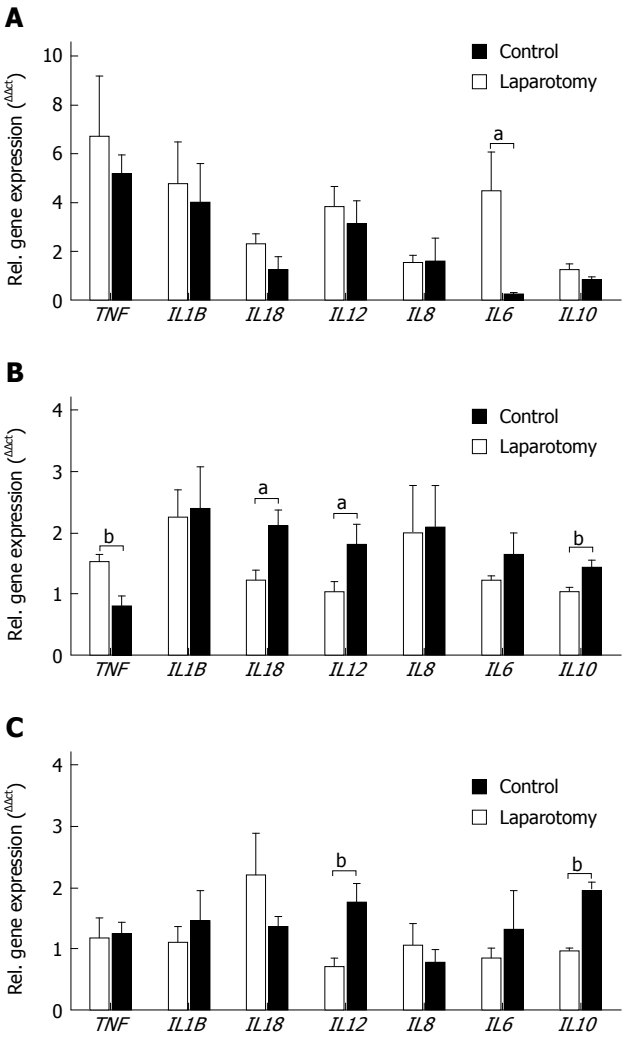

Figure 1 Relative gene expression of pro- and anti-inflammatory cytokines in (A) ileum, (B) terminal ileum and (C) colon from no-surgery control and transection surgery groups. Mean ± SEM. $^{a}P < 0.05$, $^{b}P < 0.01$ *vs* control.

samples from the surgery group when compared with controls ($P = 0.0054$). Similar to the terminal ileum *IL12* and *IL10* gene expression was increased within the colon following surgery ($P = 0.0055$ and $P = 0.0001$ respectively; Figure 1C).

DISCUSSION

Immediately after birth, the newborn gut environment is colonized by facultative anaerobic bacteria such as *Enterobacteriaceae* and *Streptococcaceae*[11]. These bacteria gradually consume the oxygen in the intestine and produce new metabolites, preparing the intestinal environment for the establishment of a strict anaerobic population dominated by *Bifidobacterium, Clostridium* and *Bacteroides* sp., genera that may contribute to neonatal gut maturation[11]. However, medical and surgical interventions required during infancy, including abdominal surgery, have the potential to modify the microbiome. As, microbial colonization of the infant gut plays a key role in the development and fine-tuning of the intestinal immune responses[11], it is essential to detail the effect of minor abdominal surgery performed during the infant period, on the major microbial community and associated inflammation.

Our current study details alterations in the colonic microbial community in response to abdominal surgery. We chose to focus on the colonic microbiota as (1) the colonic microbial community represents the largest, and most widely studied microbial community in both health and disease states; and (2) any alterations to the colonic microbial community are likely to influence the immune response *via* interactions with the gut-associated lymphoid tissue. In the current study, whilst there was no observed effect on the overall richness or diversity of the colonic microbiota, there were alterations in specific bacterial genera that are likely to be of clinical relevance. Similarly, studies of irritable bowel syndrome also describe significant associations between quantitative differences in specific bacterial components of the gut microbiome and disease symptoms[30,31] in the face of unchanged overall microbial diversity. In particular, we observed alterations only within the *Proteobacteria* and *Bacteriodetes* phylum and report reductions in the relative abundance of family level members *Enterobacteriacceae, Rhodaspirillaceae* and *Bacteroidaceae* and genus level reductions in the relative abundance of *Enterobacteriaceae, Thalassospira, Alistipes* and *Bacteroides* following transection surgery.

The reduction in the relative abundance of *Bacteroides* sp. is of particular clinical relevance as, in early life, the intestinal microbiota of healthy infants displays a large abundance of *Bacteriodes* sp.[32]. *Bacteroides* sp. play a fundamental role in host metabolic processes[33] and prevents the colonisation of the gut by potential pathogens[34]. Depletions in *Bacteroides* species are observed in children with inflammatory conditions including IgE mediated food allergy[35] and inflammatory bowel disease[36]. Furthermore, *Bacteroides* is postulated to play a crucial role in the development of gastrointestinal-associated lymphoid tissues and in the modulation of T-helper Th1/Th2/T-regulatory balance[37]. Therefore reduction in relative abundance of *Bacteroides* in the gut following intestinal transaction surgery may, at least in-part, explain the observed increase in *IL12* and *IL18* gene expression within the terminal ileum. IL12 and IL18 form a link between innate resistance and adaptive immunity and may be produced by a wide range of immune cells in response to bacteria and bacterial products[38].

Interestingly, we observed markers of an active gut inflammatory response at two weeks post-surgery that was not limited to the area within the immediate proximity of the intestinal transection and re-anastomosis. Specifically, we observed increased gene expression of *IL12* and *IL10* in both terminal ileum and colon, and increased IL18 and decreased TNF gene

expression in terminal ileum. Whilst it is not possible to ascertain the underlying mechanism responsible for the wide-spread increase in inflammatory mediators observed in our juvenile pig model, we postulate surgery-related alterations in the small intestine microbiota may influence inflammatory marker expression within the ileum and terminal ileum. Alternatively, surgery-related factors including bowel handling could have contributed to the inflammatory response observed. However, bowel handling has been reported to induce TNF, IL6 and IL1B production[39,40], cytokines that remained unchanged or were decreased in this study (Figure 1).

Early colonization of the infant gut is increasingly recognized as impacting on health due to the influence of resident microbes on nutritional, immunological and physiological functions. However, medical and surgical interventions required during infancy, including abdominal surgery, have the potential to modify the microbiome, sometimes permanently. We have described microbial dysbiosis within the *Proteobacteria* and *Bacteriodetes* phylum and increased gut inflammatory cytokines following surgery in a juvenile pig model. This is the first study examining changes in the gut microbiome and in gut inflammation that occur following transaction surgery in infancy and provides new insights into potential long-term consequences of abdominal surgery in infancy.

ACKNOWLEDGMENTS

The authors acknowledge Professors Gerald Fitzgerald and Paul Ross for their continued support and thank Magdy Sourial, Shane Osterfield and Dr Andrew French for expert technical assistance with the animals, Dr Jean-Pierre Scheerlinck and The University of Melbourne Centre for Animal Biotechnology for the use of their facilities, and Drs Orla O'Sullivan and Eva Rosberg-Cody for assistance with high-throughput DNA sequencing.

COMMENTS

Background

Early colonization of the infant gut is increasingly recognized as impacting on health due to the influence of resident microbes on nutritional, immunological and physiological functions. However, medical and surgical interventions required during infancy, including abdominal surgery, have the potential to modify the microbiome. This is the first study examining minor surgery-associated changes in the gut microbiome and inflammation and provides new insights into potential long-term consequences of abdominal surgery in infancy.

Research frontiers

Colonization of the newborn intestine plays a key role in the development and fine-tuning of intestinal immune responses, and disruption of the gut microbiota has been linked to an increasing number of immune-related diseases, including inflammatory bowel disease, necrotizing enterocolitis, eczema, allergies and asthma. The current research hotspot is to characterize intervention-related alterations in microbial communities and assess the impact of these changes on future clinical outcome.

Innovations and breakthroughs

This is the first study to apply 454-pyrosequencing technology to assess the impact of minor abdominal surgery on the colonic microbial population using a juvenile pig model of intestinal transaction surgery. The authors observed reduced abundance of family and genus level members of the *Proteobacteria* and *Bacteriodetes* phylum, concurrent with unresolved gastrointestinal inflammation within the ileum, terminal ileum and colon. Importantly, this study provides new insights into potential long-term consequences of abdominal surgery in infancy.

Applications

Whilst for the majority of intestinal surgeries, the benefits of the operative procedure far outweigh the potential risks of altering the gut microbiota and increasing the level of inflammatory cytokines, this study suggests that a straight-forward and uncomplicated laparotomy with minimal bowel resection and re-anastomosis may have secondary unforeseen circumstances that may have a long-term impact on the health of pediatric patients.

Terminology

The term colonic microbiota is the name given to the microbe population living within the caecum.

Peer-review

This is the first study examining minor surgery-associated changes in the gut microbiome and inflammation and provides new insights into potential long-term consequences of abdominal surgery in infancy. This is a well-conducted and well written study. The experiments are described in detail, the results are shown nicely and the figures are impressive.

REFERENCES

1 **Tapiainen T**, Ylitalo S, Eerola E, Uhari M. Dynamics of gut colonization and source of intestinal flora in healthy newborn infants. *APMIS* 2006; **114**: 812-817 [PMID: 17078863]
2 **Koenig JE**, Spor A, Scalfone N, Fricker AD, Stombaugh J, Knight R, Angenent LT, Ley RE. Succession of microbial consortia in the developing infant gut microbiome. *Proc Natl Acad Sci U S A* 2011; **108** Suppl 1: 4578-4585 [PMID: 20668239 DOI: 10.1073/pnas.1000081107]
3 **Palmer C**, Bik EM, DiGiulio DB, Relman DA, Brown PO. Development of the human infant intestinal microbiota. *PLoS Biol* 2007; **5**: e177 [PMID: 17594176]
4 **Mackie RI**, Sghir A, Gaskins HR. Developmental microbial ecology of the neonatal gastrointestinal tract. *Am J Clin Nutr* 1999; **69**: 1035S-1045S [PMID: 10232646]
5 **Penders J**, Thijs C, Vink C, Stelma FF, Snijders B, Kummeling I, van den Brandt PA, Stobberingh EE. Factors influencing the composition of the intestinal microbiota in early infancy. *Pediatrics* 2006; **118**: 511-521 [PMID: 16882802]
6 **Jacquot A**, Neveu D, Aujoulat F, Mercier G, Marchandin H, Jumas-Bilak E, Picaud JC. Dynamics and clinical evolution of bacterial gut microflora in extremely premature patients. *J Pediatr* 2011; **158**: 390-396 [PMID: 20961563 DOI: 10.1016/j.jpeds.2010.09.007]
7 **Penders J**, Vink C, Driessen C, London N, Thijs C, Stobberingh EE. Quantification of Bifidobacterium spp., Escherichia coli and Clostridium difficile in faecal samples of breast-fed and formula-fed infants by real-time PCR. *FEMS Microbiol Lett* 2005; **243**: 141-147 [PMID: 15668012]
8 **Kalenić S**, Francetić I, Polak J, Zele-Starcević L, Bencić Z. Impact of ampicillin and cefuroxime on bacterial colonization and infection in patients on a neonatal intensive care unit. *J Hosp Infect* 1993; **23**: 35-41 [PMID: 8095946]
9 **Dethlefsen L**, Relman DA. Incomplete recovery and individualized responses of the human distal gut microbiota to repeated antibiotic perturbation. *Proc Natl Acad Sci USA* 2011; **108** Suppl 1: 4554-4561 [PMID: 20847294 DOI: 10.1073/pnas.1000087107]
10 **Tanaka S**, Kobayashi T, Songjinda P, Tateyama A, Tsubouchi M, Kiyohara C, Shirakawa T, Sonomoto K, Nakayama J. Influence of antibiotic exposure in the early postnatal period on the development of intestinal microbiota. *FEMS Immunol Med Microbiol* 2009; **56**: 80-87 [PMID: 19385995 DOI: 10.1111/j.1574-695X.2009.00553.x]
11 **Marques TM**, Wall R, Ross RP, Fitzgerald GF, Ryan CA, Stanton

C. Programming infant gut microbiota: influence of dietary and environmental factors. *Curr Opin Biotechnol* 2010; **21**: 149-156 [PMID: 20434324 DOI: 10.1016/j.copbio.2010.03.020]

12 **Young VB**. The intestinal microbiota in health and disease. *Curr Opin Gastroenterol* 2012; **28**: 63-69 [PMID: 22080827 DOI: 10.1097/MOG.0b013e32834d61e9]

13 **Moughan PJ**, Birtles MJ, Cranwell PD, Smith WC, Pedraza M. The piglet as a model animal for studying aspects of digestion and absorption in milk-fed human infants. *World Rev Nutr Diet* 1992; **67**: 40-113 [PMID: 1557912]

14 **Miller ER**, Ullrey DE. The pig as a model for human nutrition. *Annu Rev Nutr* 1987; **7**: 361-382 [PMID: 3300739 DOI: 10.1146/annurev.nu.07.070187.002045]

15 **Buzoianu SG**, Walsh MC, Rea MC, O'Sullivan O, Cotter PD, Ross RP, Gardiner GE, Lawlor PG. High-throughput sequence-based analysis of the intestinal microbiota of weanling pigs fed genetically modified MON810 maize expressing Bacillus thuringiensis Cry1Ab (Bt maize) for 31 days. *Appl Environ Microbiol* 2012; **78**: 4217-4224 [PMID: 22467509 DOI: 10.1128/AEM.00307-12]

16 **Butler JE**, Weber P, Sinkora M, Baker D, Schoenherr A, Mayer B, Francis D. Antibody repertoire development in fetal and neonatal piglets. VIII. Colonization is required for newborn piglets to make serum antibodies to T-dependent and type 2 T-independent antigens. *J Immunol* 2002; **169**: 6822-6830 [PMID: 12471114]

17 **Scharek L**, Guth J, Reiter K, Weyrauch KD, Taras D, Schwerk P, Schierack P, Schmidt MF, Wieler LH, Tedin K. Influence of a probiotic Enterococcus faecium strain on development of the immune system of sows and piglets. *Vet Immunol Immunopathol* 2005; **105**: 151-161 [PMID: 15797484]

18 **Lapthorne S**, Pereira-Fantini PM, Fouhy F, Wilson G, Thomas SL, Dellios NL, Scurr M, O'Sullivan O, Ross RP, Stanton C, Fitzgerald GF, Cotter PD, Bines JE. Gut microbial diversity is reduced and is associated with colonic inflammation in a piglet model of short bowel syndrome. *Gut Microbes* 2013; **4**: 212-221 [PMID: 23549027 DOI: 10.4161/gmic.24372]

19 **Pereira-Fantini PM**, Thomas SL, Wilson G, Taylor RG, Sourial M, Bines JE. Short- and long-term effects of small bowel resection: a unique histological study in a piglet model of short bowel syndrome. *Histochem Cell Biol* 2011; **135**: 195-202 [PMID: 21249379 DOI: 10.1007/s00418-011-0778-2]

20 **Healey KL**, Bines JE, Thomas SL, Wilson G, Taylor RG, Sourial M, Pereira-Fantini PM. Morphological and functional changes in the colon after massive small bowel resection. *J Pediatr Surg* 2010; **45**: 1581-1590 [PMID: 20713204 DOI: 10.1016/j.jpedsurg.2010.02.040]

21 **Stephens AN**, Pereira-Fantini PM, Wilson G, Taylor RG, Rainczuk A, Meehan KL, Sourial M, Fuller PJ, Stanton PG, Robertson DM, Bines JE. Proteomic analysis of the intestinal adaptation response reveals altered expression of fatty acid binding proteins following massive small bowel resection. *J Proteome Res* 2010; **9**: 1437-1449 [PMID: 19943703 DOI: 10.1021/pr900976f]

22 **Pereira-Fantini PM**, Thomas SL, Taylor RG, Nagy E, Sourial M, Fuller PJ, Bines JE. Colostrum supplementation restores insulin-like growth factor -1 levels and alters muscle morphology following massive small bowel resection. *JPEN J Parenter Enteral Nutr* 2008; **32**: 266-275 [PMID: 18443138 DOI: 10.1177/0148607108316197]

23 **Pereira-Fantini PM**, Nagy ES, Thomas SL, Taylor RG, Sourial M, Paris MC, Holst JJ, Fuller PJ, Bines JE. GLP-2 administration results in increased proliferation but paradoxically an adverse outcome in a juvenile piglet model of short bowel syndrome. *J Pediatr Gastroenterol Nutr* 2008; **46**: 20-28 [PMID: 18162829 DOI: 10.1097/01.mpg.0000304449.46434.06]

24 **Murphy EF**, Cotter PD, Healy S, Marques TM, O'Sullivan O, Fouhy F, Clarke SF, O'Toole PW, Quigley EM, Stanton C, Ross PR, O'Doherty RM, Shanahan F. Composition and energy harvesting capacity of the gut microbiota: relationship to diet, obesity and time in mouse models. *Gut* 2010; **59**: 1635-1642 [PMID: 20926643 DOI: 10.1136/gut.2010.215665]

25 **Altschul SF**, Madden TL, Schäffer AA, Zhang J, Zhang Z, Miller W, Lipman DJ. Gapped BLAST and PSI-BLAST: a new generation of protein database search programs. *Nucleic Acids Res* 1997; **25**: 3389-3402 [PMID: 9254694 DOI: 10.1093/nar/25.17.3389]

26 **Pruesse E**, Quast C, Knittel K, Fuchs BM, Ludwig W, Peplies J, Glöckner FO. SILVA: a comprehensive online resource for quality checked and aligned ribosomal RNA sequence data compatible with ARB. *Nucleic Acids Res* 2007; **35**: 7188-7196 [PMID: 17947321 DOI: 10.1093/nar/gkm864]

27 **Livak KJ**, Schmittgen TD. Analysis of relative gene expression data using real-time quantitative PCR and the 2(-Delta Delta C(T)) Method. *Methods* 2001; **25**: 402-408 [PMID: 11846609]

28 **Fouhy F**, Guinane CM, Hussey S, Wall R, Ryan CA, Dempsey EM, Murphy B, Ross RP, Fitzgerald GF, Stanton C, Cotter PD. High-throughput sequencing reveals the incomplete, short-term recovery of infant gut microbiota following parenteral antibiotic treatment with ampicillin and gentamicin. *Antimicrob Agents Chemother* 2012; **56**: 5811-5820 [PMID: 22948872 DOI: 10.1128/AAC.00789-12]

29 **Candela M**, Turroni S, Biagi E, Carbonero F, Rampelli S, Fiorentini C, Brigidi P. Inflammation and colorectal cancer, when microbiota-host mutualism breaks. *World J Gastroenterol* 2014; **20**: 908-922 [PMID: 24574765 DOI: 10.3748/wjg.v20.i4.908]

30 **Saulnier DM**, Riehle K, Mistretta TA, Diaz MA, Mandal D, Raza S, Weidler EM, Qin X, Coarfa C, Milosavljevic A, Petrosino JF, Highlander S, Gibbs R, Lynch SV, Shulman RJ, Versalovic J. Gastrointestinal microbiome signatures of pediatric patients with irritable bowel syndrome. *Gastroenterology* 2011; **141**: 1782-1791 [PMID: 21741921 DOI: 10.1053/j.gastro.2011.06.072]

31 **Jeffery IB**, O'Toole PW, Öhman L, Claesson MJ, Deane J, Quigley EM, Simrén M. An irritable bowel syndrome subtype defined by species-specific alterations in faecal microbiota. *Gut* 2012; **61**: 997-1006 [PMID: 22180058 DOI: 10.1136/gutjnl-2011-301501]

32 **Adlerberth I**, Wold AE. Establishment of the gut microbiota in Western infants. *Acta Paediatr* 2009; **98**: 229-238 [PMID: 19143664 DOI: 10.1111/j.1651-2227.2008.01060.x]

33 **Marcobal A**, Barboza M, Sonnenburg ED, Pudlo N, Martens EC, Desai P, Lebrilla CB, Weimer BC, Mills DA, German JB, Sonnenburg JL. Bacteroides in the infant gut consume milk oligosaccharides via mucus-utilization pathways. *Cell Host Microbe* 2011; **10**: 507-514 [PMID: 22036470 DOI: 10.1016/j.chom.2011.10.007]

34 **Yamamoto-Osaki T**, Kamiya S, Sawamura S, Kai M, Ozawa A. Growth inhibition of Clostridium difficile by intestinal flora of infant faeces in continuous flow culture. *J Med Microbiol* 1994; **40**: 179-187 [PMID: 8114067]

35 **Ling Z**, Li Z, Liu X, Cheng Y, Luo Y, Tong X, Yuan L, Wang Y, Sun J, Li L, Xiang C. Altered fecal microbiota composition associated with food allergy in infants. *Appl Environ Microbiol* 2014; **80**: 2546-2554 [PMID: 24532064 DOI: 10.1128/AEM.00003-14]

36 **Aomatsu T**, Imaeda H, Fujimoto T, Takahashi K, Yoden A, Tamai H, Fujiyama Y, Andoh A. Terminal restriction fragment length polymorphism analysis of the gut microbiota profiles of pediatric patients with inflammatory bowel disease. *Digestion* 2012; **86**: 129-135 [PMID: 22846404 DOI: 10.1159/000339777]

37 **Rodriguez B**, Prioult G, Hacini-Rachinel F, Moine D, Bruttin A, Ngom-Bru C, Labellie C, Nicolis I, Berger B, Mercenier A, Butel MJ, Waligora-Dupriet AJ. Infant gut microbiota is protective against cow's milk allergy in mice despite immature ileal T-cell response. *FEMS Microbiol Ecol* 2012; **79**: 192-202 [PMID: 22029421 DOI: 10.1111/j.1574-6941.2011.01207.x]

38 **Trinchieri G**. Interleukin-12 and the regulation of innate resistance and adaptive immunity. *Nat Rev Immunol* 2003; **3**: 133-146 [PMID: 12563297 DOI: 10.1038/nri1001]

39 **Wehner S**, Schwarz NT, Hundsdoerfer R, Hierholzer C, Tweardy DJ, Billiar TR, Bauer AJ, Kalff JC. Induction of IL-6 within the rodent intestinal muscularis after intestinal surgical stress.

Surgery 2005; **137**: 436-446 [PMID: 15800492 DOI: 10.1016/j.surg.2004.11.003]

40 **Kalff JC**, Schraut WH, Simmons RL, Bauer AJ. Surgical manipulation of the gut elicits an intestinal muscularis inflammatory response resulting in postsurgical ileus. *Ann Surg* 1998; **228**: 652-663 [PMID: 9833803]

P- Reviewer: Triantafyllou K, Zhu X **S- Editor**: Qi Y **L- Editor**: A
E- Editor: Liu XM

World Journal of Gastroenterology

Submit a Manuscript: http://www.wjgnet.com/esps/
Help Desk: http://www.wjgnet.com/esps/helpdesk.aspx
DOI: 10.3748/wjg.v21.i14.4159

World J Gastroenterol 2015 April 14; 21(14): 4159-4168
ISSN 1007-9327 (print) ISSN 2219-2840 (online)

ORIGINAL ARTICLE

Basic Study

Effects of Institut Georges Lopez-1 and Celsior preservation solutions on liver graft injury

Donia Tabka, Mohamed Bejaoui, James Javellaud, Joan Roselló-Catafau, Jean-Michel Achard, Hassen Ben Abdennebi

Donia Tabka, Hassen Ben Abdennebi, Unité de recherche "Biologie et anthropologie moléculaire appliquées au développement et à la santé" (UR12ES11), University of Monastir, Faculty of Pharmacy, Monastir 5000, Tunisia
Mohamed Bejaoui, Joan Roselló-Catafau, Experimental Hepatic Ischemia-Reperfusion Unit, Institut d'Investigacions Biomèdiques de Barcelona-Consejo Superior de Investigaciones Cientificas, 08036 Barcelona, Spain
James Javellaud, Jean-Michel Achard, INSERM, Unité Mixte de Recherche S-850, 8000 Limoges, France
Author contributions: Tabka D and Bejaoui M performed the animal experiments, interpreted the data and wrote the article; Javellaud J did the teaching work and participated in the surgery required for the rat hepatic artery rings model; Roselló-Catafau J contributed to the critical revision of the article; Achard JM and Abdennebi HB designed the study and wrote the article; all the authors have read and approved the final manuscript.
Supported by Tunisian Ministry of Higher Education and Scientific Research, No.UR12ES11.
Institutional animal care and use committee: All procedures involving animals were reviewed and approved by the Institutional Animal Care and Use Committee of the Comité Regional D'Ethique pour L'Expérimentation Animale du Limousin (No.33).
Conflict-of-interest: There is no conflict of interest with any financial organization regarding the material discussed in the manuscript.
Data sharing: Technical appendix, statistical code and dataset are available from the corresponding author at (hbenabdennebi@yahoo.fr); all participants gave informed consent for data sharing.

Correspondence to: Hassen Ben Abdennebi, Professor, Department of Physiology, Unité de Recherche "Biologie et anthropologie moléculaire appliquées au développement et à la santé" (UR12ES11), University of Monastir, Faculty of Pharmacy, Rue Avicenne, Monastir 5000, Tunisia. hbenabdennebi@yahoo.fr
Telephone: +216-73-461000
Received: November 6, 2014
Peer-review started: November 9, 2014
First decision: December 11, 2014
Revised: December 30, 2014
Accepted: January 30, 2015
Article in press: January 30, 2015
Published online: April 14, 2015

Abstract

AIM: To compare Institut Georges Lopez (IGL-1) and Celsior preservation solutions for hepatic endothelium relaxation and liver cold ischemia reperfusion injury (IRI).

METHODS: Two experimental models were used. In the first one, acetylcholine-induced endothelium-dependent relaxation (EDR) was measured in isolated ring preparations of rat hepatic arteries preserved or not in IGL-1 or Celsior solutions (24 h at 4 ℃). To determine nitric oxide (NO) and cyclooxygenase EDR, hepatic arteries were incubated with L-NG-nitroarginine methyl ester (L-NAME), an inhibitor of endothelium nitric oxide synthase (eNOS), or with L-NAME plus indomethacin, an inhibitor of cyclooxygenase. In the second experiment, rat livers were cold-stored in IGL-1 or Celsior solutions for 24 h at 4 ℃ and then perfused "*ex vivo*" for 2 h at 37 ℃. Liver injury was assessed by transaminase measurements, liver function by bile production and bromosulfophthalein clearance, oxidative stress by malondialdehyde levels and catalase activity and alterations in cell signaling pathways by pAkt, pAMPK, eNOS and MAPKs proteins level.

RESULTS: After cold storage for 24 h with either Celsior or IGL-1, EDR was only slightly altered. In

freshly isolated arteries, EDR was exclusively mediated by NO. However, cold-stored arteries showed NO- and COX-dependent relaxation. The decrease in NO-dependent relaxation after cold storage was significantly more marked with Celsior. The second study indicated that IGL-1 solution obtained better liver preservation and protection against IRI than Celsior. Liver injury was reduced, function was improved and there was less oxidative stress. IGL-1 solution activated Akt and AMPK, which was concomitant with increased eNOS expression and nitrite/nitrate levels. Furthermore, MAPKs kinases were regulated in livers preserved with IGL-1 solution since reductions in p-p38, p-ERK and p-JNK protein levels were observed.

CONCLUSION: IGL-1 solution preserved NO-dependent relaxation better than Celsior storage solution and enhanced liver graft preservation.

Key words: Organ preservation solutions; Institut Georges Lopez solution; Celsior; Reperfusion injury; Endothelium-dependent relaxing factors; Nitric oxide

Core tip: Vascular endothelium dysfunction plays an important role in various pathophysiological conditions. Protection of the vascular endothelium is a critical factor in organ preservation. This evaluation of the endothelium-dependent relaxation of rat hepatic artery after preservation in Celsior and Institut Georges Lopez (IGL-1) solutions provides the first head-to-head comparison of these two storage solutions. Our results show that cold storage of the hepatic artery with IGL-1 preserves nitric oxide-dependent endothelium-mediated relaxation better than cold storage with Celsior solution. In addition, we provide evidence that IGL-1 is more efficient than Celsior for liver preservation using an isolated perfused rat liver model.

Tabka D, Bejaoui M, Javellaud J, Roselló-Catafau J, Achard JM, Abdennebi HB. Effects of Institut Georges Lopez-1 and Celsior preservation solutions on liver graft injury. *World J Gastroenterol* 2015; 21(14): 4159-4168 Available from: URL: http://www.wjgnet.com/1007-9327/full/v21/i14/4159.htm DOI: http://dx.doi.org/10.3748/wjg.v21.i14.4159

INTRODUCTION

During transplantation, all organs are exposed to ischemia reperfusion injury (IRI). These lesions are related to hypothermia and hypoxia during *ex vivo* preservation of the graft and to the rewarming associated with reoxygenation during reperfusion[1-3]. Throughout preservation, tissues are exposed to cold and deprived of oxygen and nutrients, leading to the accumulation of metabolic waste. At the cellular level, the main biochemical changes of cold ischemia are ATP depletion, inhibition of oxidative metabolism, alteration of ionic homeostasis and increased acidosis due to anaerobic glycolysis[4]. These biochemical changes result in the establishment of a number of processes that will be amplified during the reperfusion phase.

Providing optimal organ preservation remains an important way to ensure the quality of the transplanted organ. The University of Wisconsin (UW) solution is the standard liquid for the procurement of abdominal organs and their static cold storage[4-6]. Celsior preservation solution, originally used for cardioplegia[7-9], has demonstrated its safety and effectiveness for cold preservation of the lungs[10], liver[11], kidneys[12] and pancreas[13,14] in different clinical studies and is now widely used in European countries. It is a colloid-free extracellular-type solution containing high molecular weight impermeants (lactobionic acid and mannitol), free radical scavengers (reduced glutathione) and an energy precursor (glutamic acid). Histidine is added in order to buffer intracellular acidosis and contributes to preventing calcium overload. Studies suggest that the benefits of this solution are due to its low viscosity, which results in better flushing of the biliary tree and of the hepatic vasculature during graft procurement[11,15].

Institut Georges Lopez-1 (IGL-1) preservation solution was designed following the same specifications as the UW solution; however, it is characterized by the inversion of K+ and Na+ concentrations and the replacement of hydroxyethyl starch by a high molecular weight polyethylene glycol of 35 kDa (PEG35)[16]. It has demonstrated its effectiveness for cold preservation of kidney[17], intestine[18], liver[19] and pancreas[20] in experimental and clinical settings. The benefits of IGL-1 are due, in part, to its capacity to increase nitric oxide (NO) levels, thus protecting the liver against IRI and mitigating the alterations to hepatic microcirculation[21]. In an experimental model of rat liver transplantation, it was recently observed that IGL-1 reduced endoplasmic reticulum stress and apoptosis[22]. Therefore, the use of IGL-1 solution may offer certain advantages for attenuating injury associated with liver transplantation.

Although several comparative studies of preservation solutions have evaluated the benefits and disadvantages of each solution in animal experimental models and randomized controlled trials[6,12,23], no direct head-to-head comparison of IGL-I and Celsior has been reported to date.

The purpose of this study was therefore to compare the protective effects of Celsior and IGL-1 solutions against IRI and to study their effects on endothelium-dependent relaxation (EDR).

MATERIALS AND METHODS

Animal care and use statement

Male Sprague-Dawley rats weighing 250-300 g were

Table 1 Composition of Institut Georges Lopez-1 and Celsior preservation solutions

Components	IGL-1	Celsior
K^+ (mmol/L)	25	15
Na^+ (mmol/L)	125	100
Mg^{2+} (mmol/L)	5	13
Ca^{2+} (mmol/L)	-	0.25
Cl^- (mmol/L)	-	40
SO_4^{2-} (mmol/L)	5	-
Diphosphate (mmol/L)	25	-
Histidine (mmol/L)	-	30
Raffinose (mmol/L)	30	-
Lactobionic acid (mmol/L)	100	80
Mannitol (mmol/L)	-	60
Polyethylene glycol-35 (g/L)	1	-
Reduced glutathione (mmol/L)	3	3
Allopurinol (mmol/L)	1	-
Adenosine (mmol/L)	5	-
Glutamic acid (mmol/L)	-	20
pH (room T°)	7.3 ± 0.1	7.3 ± 0.1

IGL-1: Institut Georges Lopez-1.

used. They were acclimatized to laboratory conditions (23 ℃, 12 h/12 h light/dark, 50% humidity, ad libitum access to food and water) for 2 wk prior to experimentation. All experiments were in accordance with guidelines for the ethical care of experimental animals of the European Community and were approved by the Regional Ethics Committee for Animal Experimentation of Limousin (CREEAL) (authorization No. 33). Two studies were conducted with different experimental models: hepatic artery rings in the first and isolated perfused rat liver (IPRL) in the second.

Effect of Celsior and IGL-1 cold storage solutions on endothelium relaxation

The tissue preparation procedure was performed as previously reported[24]. Briefly, rats were anesthetized with isoflurane inhalation and then underwent laparotomy. The hepatic artery was exposed and cleaned of adhering fat and connective tissues. After sacrificing the rat, the hepatic artery was cut and stored in Celsior (n = 11) or IGL-1 (n = 11) storage solutions at 4 ℃ for 24 h (composition in Table 1) and then suspended in the organ bath. Hepatic artery rings from the control group (n = 12) were suspended immediately in the organ bath without cold storage.

Vasomotor responses were assessed as previously described[24]. The hepatic arteries were cut in rings of 2-3 mm in length and were then maintained between two stainless steel wires (100 μm) connected to an isometric force transducer (Powerlab, AD Instruments). The rings were placed in an organ bath (9 mL, 37 ℃) filled with gassed (95% O_2 - 5% CO_2) Krebs Bicarbonate Buffer (KBB, pH 7.4) (VWR, France). Tissues were stretched to their optimum tension of 0.75 g and equilibrated and then washed with fresh KBB at 20 min intervals for 60 min. Care was taken to avoid rubbing the endothelial surface of the vessels with the intact endothelium.

To determine EDR, hepatic artery rings were maximally pre-contracted with phenylephrine (Phe 10^{-6} mol/L, Sigma) before cumulative application of acetylcholine (ACh 10^{-9} to 3 × 10^{-6} mol/L, Sigma). Relaxation activity was evaluated as the effective concentration of ACh producing 50% relaxation of pre-contracted rings (EC_{50}).

To study the respective contribution of endothelial nitric oxide synthase (eNOS) and cyclooxygenase (COX) to vessel relaxation, ACh-induced relaxation curves were constructed with artery rings pretreated either with L-NG-nitroarginine methyl ester (L-NAME 10^{-4} mol/L, Sigma), an inhibitor of eNOS, or with the combination of L-NAME and indomethacin (10^{-4} mol/L, Sigma), a cyclooxygenase inhibitor.

Effect of Celsior and IGL-1 cold storage solutions on liver preservation

The rats were anesthetized with intraperitoneal administration of urethane (1.5 g/kg). The surgical procedure was performed as previously reported[21]. Briefly, after laparotomy, a catheter was inserted into the common bile duct for bile collection and the aorta, vena cava and portal vein were dissected. Organs were washed out with Celsior (n = 6) or IGL-1 (n = 6) storage solution and then excised and trimmed of adhering tissue. Livers were stored in a small container with 50 mL of either solution for 24 h at 4 ℃. Livers of the control group (n = 6) were flushed with Ringer's lactate and immediately perfused *ex vivo* without cold ischemic storage.

Before *ex vivo* reperfusion, all the livers were exposed to 20 min ischemia at room temperature (in order to simulate the rewarming period during surgical implantation *in vivo*) and then flushed with 10 mL of Ringer's lactate solution. Effluent liquid was sampled for measurement of cumulative transaminases after prolonged ischemia. Livers were then connected *via* the portal vein to a recirculating perfusion system for 120 min at 37 ℃. The reperfusion liquid (140 mL) was KBB enriched with 5% albumin (Sigma). The buffer was continuously gassed with a 95% O_2 and 5% CO_2 gas mixture and subsequently passed through a heat exchanger (37 ℃) and bubble trap prior to entering the liver. At the end of the normothermic reperfusion, the effluent fluid and tissue specimens were collected for examination.

Transaminase assay

The extent of hepatic injury after cold preservation and reperfusion periods was assessed in terms of activities of alanine aminotransferase (ALT) and aspartate aminotransferase (AST) in perfusate. Enzyme activities were determined at 340 nm with an UV-visible spectrometer using a commercialized kit (bioMérieux, France).

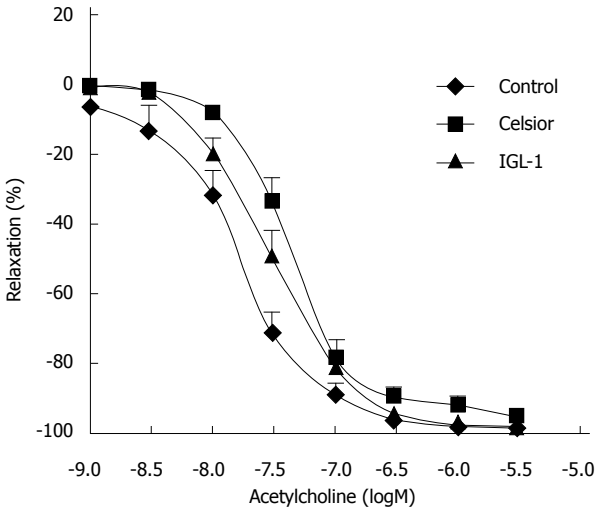

	Control	IGL-1	Celsior
Emax (%)	98.1 ± 0.6	98.0 ± 0.7	95.0 ± 2.4
EC_{50} (M)	$(1.8 \pm 0.2) \times 10^{-8}$	$(4.2 \pm 0.9) \times 10^{-8}$	$(4.8 \pm 0.7) \times 10^{-8a}$

Figure 1 Concentration-response curve for acetylcholine in rat hepatic arterial rings pre-contracted with phenylephrine: maximal effect (Emax) and EC_{50} values. Control (n = 12): hepatic artery rings were reoxygenated in the organ bath without cold storage. IGL-1 (n = 11): hepatic artery rings were reoxygenated in the organ bath after cold preservation in IGL-1 solution. Celsior (n = 11): hepatic artery rings were reoxygenated in the organ bath after cold preservation in Celsior solution. Values are means ± SD. $^{a}P < 0.05$ *vs* Control. IGL-1: Institut Georges Lopez-1.

Hepatic clearance

Hepatic clearance was performed as previously reported[21]. Briefly, 1 mg of bromosulfophthalein (BSP, Sigma) was added to the perfusate after 30 min of normothermic perfusion. BSP clearance in bile was measured at 580 nm and expressed as percentage of perfusate content.

Bile flow

Bile production was monitored during reperfusion *via* cannulation of the bile duct and collection of bile. Bile output was reported as μL/g of liver.

Malondialdehyde assay

Lipid peroxidation was used as an indirect indicator of the oxidative injury induced by reactive oxygen species. It was assessed by determination of malondialdehyde (MDA) with the thiobarbiturate reaction.

Catalase activity assay

Catalase activity was measured by the amount of hydrogen peroxide split by catalase in 5, 10, 15, 20, 25 and 30 s at 25 ℃. The reaction was started by addition of the liver supernatant and assayed at 240 nm using a UV-visible spectrometer.

Determination of nitrate and nitrite

Nitrate and nitrite levels in the liver tissue were determined by the Greiss reaction using a colorimetric assay kit (Cayman Chemical, United States).

Western blotting analysis

Frozen tissue was homogenized as previously described[25]. Equal amounts of protein were suspended in Laemmli buffer and loaded on SDS-PAGE gel, then transferred to PVDF membranes. Membranes were immunoblotted using the following antibodies: eNOS (Transduction Laboratories, Lexington, KY, United States), β-actin (Sigma Chemical, St. Louis, MO, United States), total and phosphorylated protein kinase B (AKT), mitogen-activated protein kinase (MAPK) p38, extracellular signal-regulated kinases (ERK) and c-Jun N-terminal kinase (JNK), total and phosphorylated AMP activated protein kinase (AMPK) (Cell Signaling, Beverly, MA, United States). Proteins were visualized on X-ray film *via* chemiluminescence (Bio-Rad Laboratories, Hercules, CA, United States) and quantified by scanning densitometry.

Statistical analysis

Results were expressed as mean ± SEM and were evaluated by one-way ANOVA followed by the Newman-Keuls test for multiple comparisons (Graph Pad Prism software version 4 for Windows). Statistical significance was defined as a $P < 0.05$.

RESULTS

Effect of Celsior and IGL-1 cold storage solutions on endothelium relaxation

EDR of hepatic artery rings stored in Celsior and IGL-1 liquids was compared with that of freshly isolated arteries (Figure 1). No statistical differences between the experimental groups were found for ACh relaxation (Emax). However, the curves of both cold-stored groups were shifted to the right with regard to the control group and the relaxation activity was significantly decreased in the Celsior group [$EC_{50} = (4.8 \pm 0.7) \times 10^{-8}$ *vs* $(1.8 \pm 0.2) \times 10^{-8}$ for control and Celsior groups respectively, $P < 0.05$].

The artery rings were incubated with L-NAME in order to evaluate the role of eNOS pathway in vessel relaxation after cold storage. As shown in Figure 2A, EDR was almost completely inhibited in the control group after incubation with L-NAME, evidencing that, in freshly isolated hepatic arteries, the endothelium-dependent relaxation was virtually exclusively NO-dependent. A small relaxation was still observed in the IGL-1 group, with no significant difference compared to controls. However, hepatic artery rings preserved in Celsior solution showed greater relaxation than in the other groups ($P < 0.05$). Moreover, the incubation of cold-stored hepatic arteries in the presence of both L-NAME and indomethacin (Figure 2B) completely abolished the relaxation induced by ACh.

Effect of Celsior and IGL-1 cold storage solutions on liver preservation

The livers preserved in the IGL-1 released significantly lower levels of AST and ALT than those preserved in

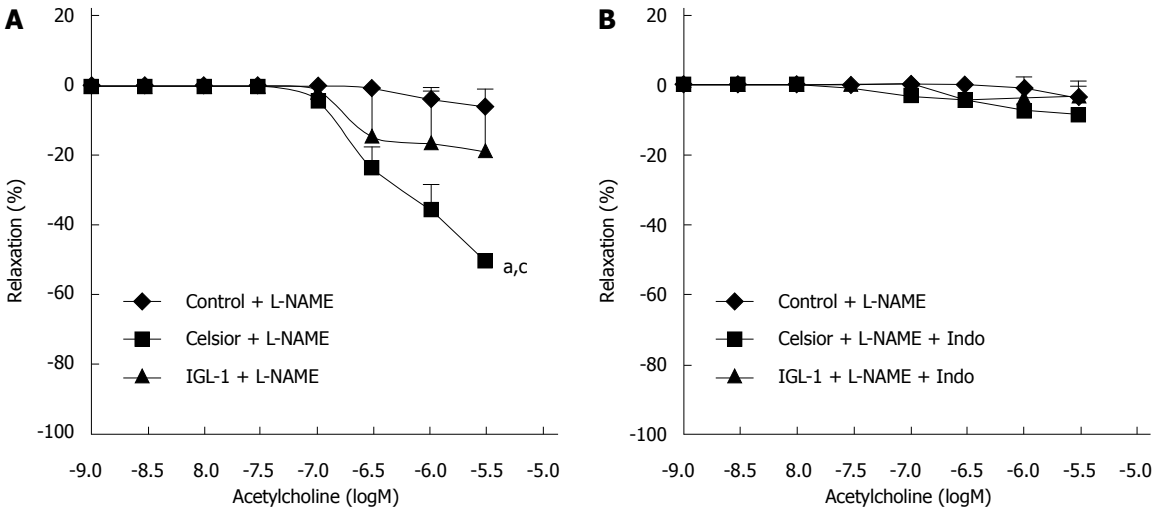

Figure 2 Concentration-response curves for acetylcholine in rat hepatic arterial rings precontracted with phenylephrine in presence of L-NAME (A) and after pretreatment with L-NAME + indomethacin (B). Control (*n* = 12): hepatic artery rings were reoxygenated in the organ bath without cold storage and pretreated with L-NAME. IGL-1 (*n* = 11): hepatic artery rings were reoxygenated in the organ bath after cold preservation in IGL-1 solution and pretreatment. Celsior (*n* = 11): hepatic artery rings were reoxygenated in the organ bath after cold preservation in Celsior solution and pretreatment. [a]*P* < 0.05 *vs* Control + L-NAME, [c]*P* < 0.05 *vs* IGL-1 + L-NAME. IGL-1: Institut Georges Lopez-1.

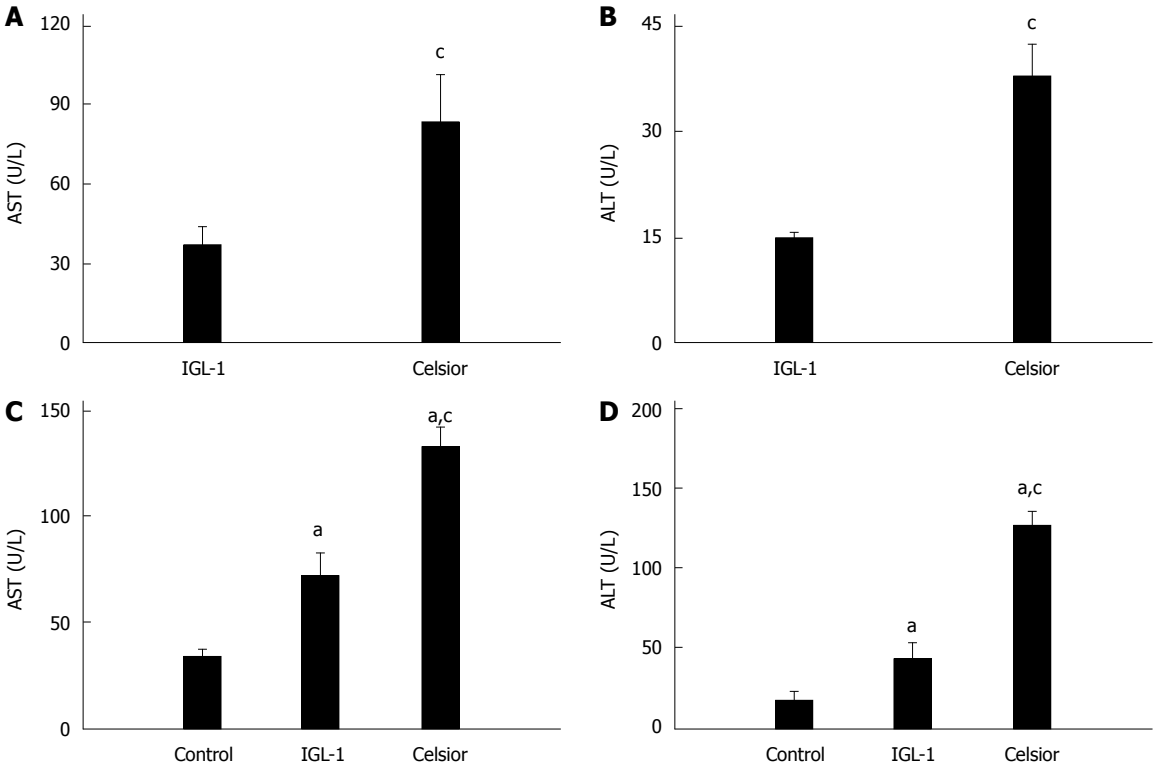

Figure 3 Alanine aminotransferase and aspartate aminotransferase activities in flushing effluent after 24 h of ischemic cold preservation (A, B) and after 2 h of normothermic reperfusion (C, D). Control (*n* = 6): livers were flushed and perfused *ex vivo* without cold storage. IGL-1 (*n* = 6): livers were preserved in IGL-1 solution at 4 ℃ for 24 h. Celsior (*n* = 6): livers were preserved in Celsior solution at 4 ℃ for 24 h. [a]*P* < 0.05 *vs* Control, [c]*P* < 0.05 *vs* IGL-1. IGL-1: Institut Georges Lopez-1.

the Celsior solution after 24 h of cold ischemia (Figure 3A and B) and after 2 h of normothermic reperfusion (Figure 3C and D). Liver function was assessed by the measurement of bile production and BSP clearance. As indicated in Figure 4A and B, both bile flow and BSP clearance were significantly higher in the IGL-1 group than in the Celsior group.

In order to evaluate the effect of preservation solutions on oxidative stress, we measured MDA levels (Figure 4C) and catalase activity (Figure 4D). We found a significant reduction in MDA in liver preserved in IGL-1 solution when compared to Celsior.

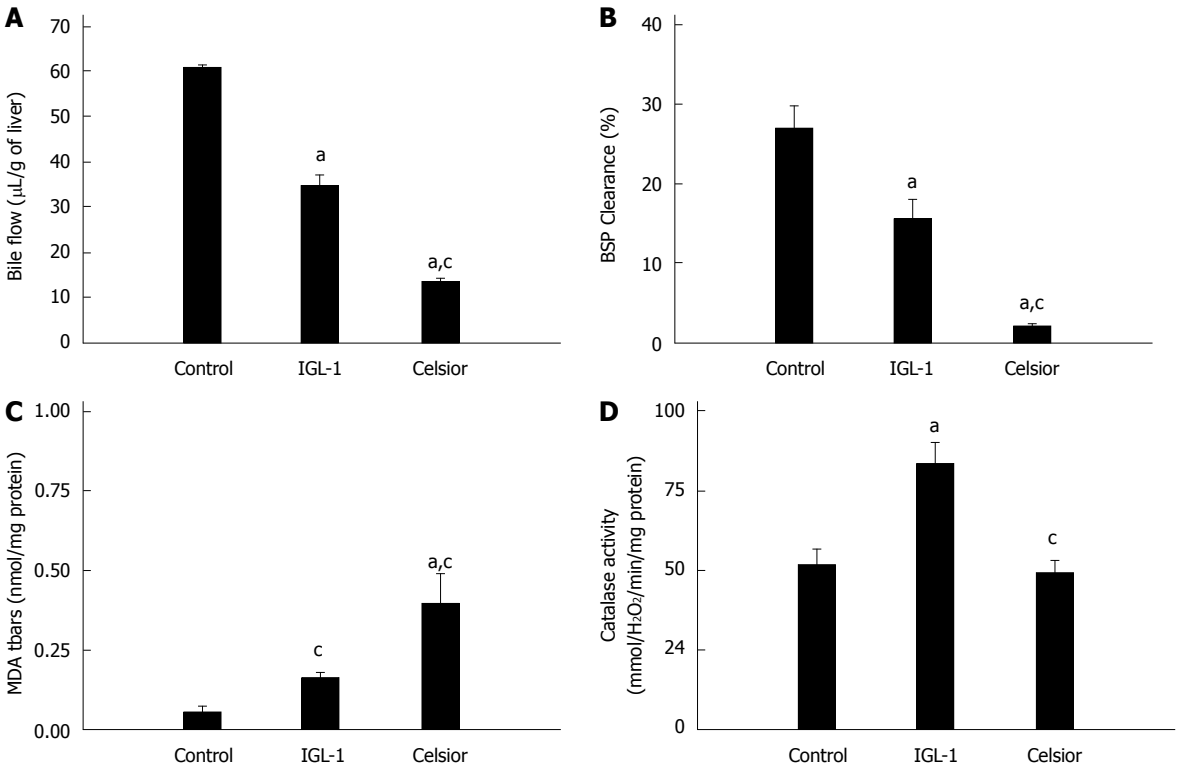

Figure 4 Liver function expressed as bile flow (A) and bromosulfophthalein clearance (B) and oxidative stress expressed as hepatic malondialdehyde concentration (C) and catalase activity (D) after 2 h of normothermic reperfusion. Control (n = 6): livers were flushed and perfused *ex vivo* without cold storage. IGL-1 (n = 6): livers were preserved in IGL-1 solution at 4 ℃ for 24 h. Celsior (n = 6): livers were preserved in Celsior solution at 4 ℃ for 24 h. $^{a}P < 0.05$ *vs* Control, $^{c}P < 0.05$ *vs* IGL-1. IGL-1: Institut Georges Lopez-1.

Livers preserved in IGL-1 solution also showed higher catalase activity after normothermic perfusion than those preserved in Celsior solution.

The role of NO after cold storage was evaluated by the phosphorylation status of AMPK (Figure 5A) and AKT (Figure 5B) and their target protein eNOS (Figure 5C) after cold preservation and reperfusion. The use of IGL-1 solution significantly increased the phosphorylation of AMPK and AKT. This was concomitant with eNOS activation and increased NO production, as evidenced by the higher concentrations of nitrites and nitrates in tissues (Figure 5D).

We also examined whether the MAPKs kinase signaling pathway was activated after liver cold preservation and reperfusion. As shown in Figure 6, we found that the levels of phosphorylated JNK, ERK and p38 MAPK were significantly higher in the Celsior group than in the control and IGL-1 groups. No statistical differences were observed between IGL-1 and control groups.

DISCUSSION

Vascular endothelium dysfunction plays an important role in various pathophysiological conditions. Protection of the vascular endothelium is a critical factor in organ preservation[26-28]. In the present study, we aimed to evaluate the EDR of rat hepatic artery after preservation in Celsior and IGL-1 solutions. The EDR mechanism is based on three effectors: NO, prostanoids derived from COX and EDHF, whose exact nature has not been fully elucidated[29]. Current data show that the endothelium is significantly damaged in stored tissues. Jeng *et al*[30] showed that cold preservation of human hepatic artery in UW solution, even for a short period, attenuated the EDR and maintained the hypoxia-induced contraction, suggesting an increased risk of vasospasm and thrombosis. A more recent study comparing eight preservation solutions, not including IGL-1, evidenced altered endothelial structure and function after exposure to a combination of warm and cold ischemia[31]. Our results indicate that, after cold storage for 24 h with either Celsior or IGL-1, EDR was only slightly altered. Emax was not affected and the concentration-response curves of cold-stored hepatic arterial segments with both preservation solutions were shifted only slightly to the right. The small increase in the EC_{50} was only significant for Celsior preservation in comparison with the freshly isolated control arteries. Interestingly, the analysis of the effect of NO and COX inhibition revealed substantial differences. Whereas in freshly isolated arteries EDR was virtually abolished after incubation with L-NAME, indicating that the relaxation was exclusively NO-dependent, cold-stored arteries were still relaxed following NO inhibition. This remaining relaxation was completely blunted with indomethacin pre-incubation, suggesting that cold storage was responsible for the decrease in NO-

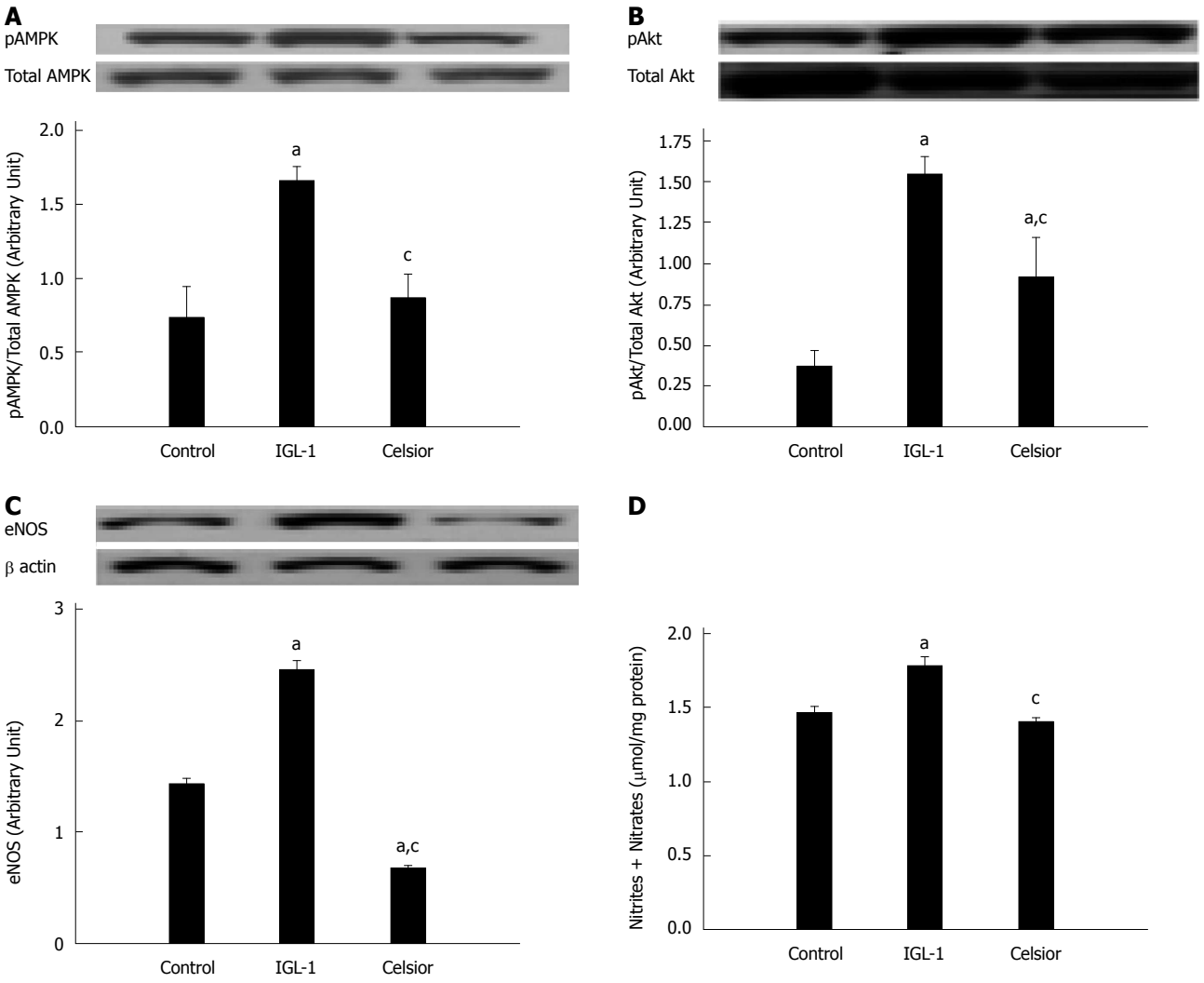

Figure 5 Phosphorylated AMP activated protein kinase (A) and AKT levels (B) and endothelial nitric oxide synthase protein (C) levels and nitrate and nitrite contents (D) in liver tissues after 2 h of warm reperfusion. The upper panels show one representative blot of three independent experiments and the lower panels show densitometric evaluation of the protein blot. Control (n = 6): livers were flushed and perfused *ex vivo* without cold storage. IGL-1 (n = 6): livers were preserved in IGL-1 solution at 4 ℃ for 24 h. Celsior (n = 6): livers were preserved in Celsior solution at 4 ℃ for 24 h. $^{a}P < 0.05$ *vs* Control, $^{c}P < 0.05$ *vs* IGL-1. IGL-1: Institut Georges Lopez-1.

dependent relaxation and for the recruitment of a compensatory induction of COX-dependent relaxation. The molecular mechanisms involved in the reciprocal regulation of COX and NOS enzymes are complex and still not fully understood[32]. It has been reported that the increased production of the vasodilating prostaglandin I_2 (PGI_2) by COX is caused by the NOS inhibitor L-NAME, indicating that low concentrations of NO are necessary to induce the production of prostacyclin. Gambone *et al*[33] have proposed that this interaction between PGI_2 and NO may represent a compensatory mechanism allowing an increase in one of these agents when the concentration of the other one decreases. Our data emphasize reduced NO production rather than elevated prostacyclin production in hepatic arteries undergoing 24 h of cold storage. This compensatory mechanism likely explains why the final result of acetylcholine stimulation relaxation (Emax) is similar in freshly isolated and cold-stored hepatic artery rings.

As regards the comparison of the two preservation solutions, our most salient finding is that, whereas the prostacyclin-mediated relaxation accounted for 50% of the maximal relaxation in arteries stored with Celsior, it accounted for significantly less (20%) after storage with IGL-1. In other words, 50% of NO-dependent relaxation was lost after storage with Celsior, whereas 80% of the NO-dependent relaxation of hepatic arteries was preserved after storage with IGL-1.

The future success of liver transplantation will depend on achieving marked improvements in graft quality and preservation techniques[6,34]. Static cold storage is the most commonly applied method for liver grafts. Preservation solutions play a crucial role in maintaining graft viability and in improving outcomes after transplantation[35]. In the second part of this study, we compared the effects of Celsior and IGL-1 solutions on liver cold preservation and demonstrated

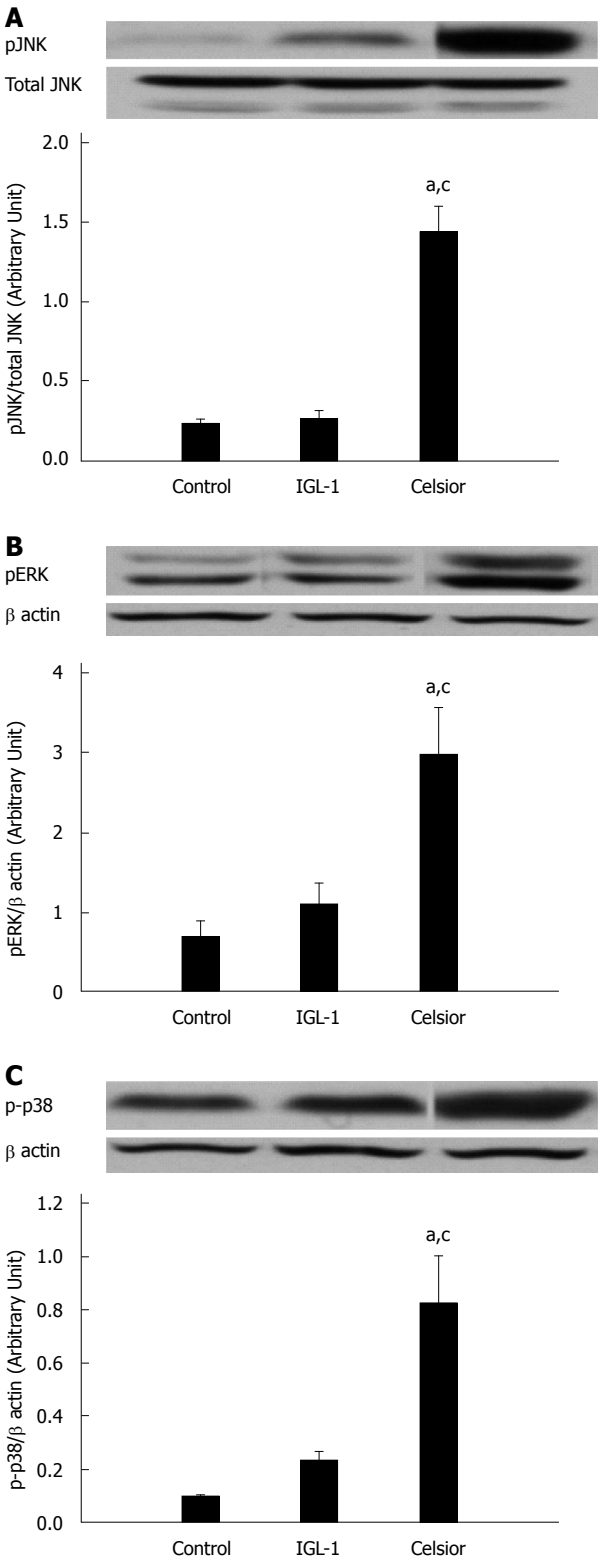

Figure 6 Phosphorylated c-Jun N-terminal kinase protein (A), ERK protein (B) and p38 protein (C) levels after two hours of normothermic reperfusion. The upper panels show one representative blot of three independent experiments and the lower panels show densitometric evaluation of the protein blot. Control (n = 6): livers were flushed and perfused *ex vivo* without cold storage. IGL-1 (n = 6): livers were preserved in IGL-1 solution at 4 ℃ for 24 h. Celsior (n = 6): livers were preserved in Celsior solution at 4 ℃ for 24 h. $^{a}P < 0.05$ *vs* Control, $^{c}P < 0.05$ *vs* IGL-1. IGL-1: Institut Georges Lopez-1.

that IGL-1 solution was more efficient in preventing cold IRI. This effective protection was concomitant with the prevention of oxidative stress and the subsequent improvement in the hepatic function, reflected by bile production and BSP clearance.

It is well known that sinusoidal endothelial cells cannot tolerate prolonged cold ischemia[27]. Endothelial dysfunction is commonly associated with a decrease in eNOS-derived NO bioavailability, leading to the initiation of liver reperfusion injury[36]. It is now agreed that eNOS activation protects against cold ischemia by the subsequent release of NO[28]. One intracellular route that mediates the activation of eNOS in ischemic liver is the Akt-eNOS pathway[37,38]. Moreover, AMPK, an enzyme that senses the cellular energy balance and regulates downstream signaling pathways, has been shown to activate eNOS and increase NO release in rat liver after cold preservation[39]. AMPK activation is known to limit endothelial dysfunction after cold preservation and protect against IRI[40,41]. Our results show a significant increase in Akt and AMPK phosphorylation, concomitant with improvements in eNOS and nitrite and nitrate levels in livers stored in IGL-1 solution when compared to Celsior solution. This may demonstrate the ability of IGL-1 solution to prevent endothelial dysfunction through the activation of eNOS by both AMPK and AKT.

The renewed interest in organ preservation has resulted in the recognition of new mechanisms involved in graft cytoprotection and viability. In the last part of this study, we investigated the repercussion of cold preservation of livers with Celsior and IGL-1 solutions on MAPKs. The MAPK superfamily represents a group of proteins (pP38, pJNK and pERK) that are known to be important mediators of cold ischemia-related events. It has been reported that MAPKs are activated after cold preservation and contribute to liver apoptosis and necrosis[42,43]. The use of IGL-1 seems to minimize the harmful effects of cold storage, as shown by the lower levels of phosphorylated p38, JNK and ERK when compared to Celsior group.

In conclusion, this study shows that cold storage of hepatic artery with IGL-1 preserves NO-dependent endothelium-mediated relaxation better than storage with Celsior. In addition, we provide evidence that IGL-1 is more efficient than Celsior for liver preservation.

COMMENTS

Background

Organ preservation solutions maintain graft viability until the transplantation of the organ. Providing optimal organ preservation remains an important way to ensure the quality of the transplanted organ.

Research frontiers

Celsior preservation solution, which was originally used for cardioplegia, has proved its safety and effectiveness for cold preservation of the lungs, liver,

kidneys and pancreas in different clinical studies and is now widely used in European countries. Institut Georges Lopez (IGL-1) preservation solution has proved its effectiveness for cold preservation of kidney, intestine, liver and pancreas in clinical settings. Its benefits are due, in part, to its capacity to increase the levels of nitric oxide (NO), thus protecting the liver against I/R injury and mitigating the alterations to hepatic microcirculation. Vascular endothelium dysfunction plays an important role in various pathophysiological conditions. Protection of the vascular endothelium is a critical factor in organ preservation. In this study, the authors demonstrate that IGL-1 solution preserved NO-dependent relaxation better than Celsior storage solution and enhanced liver graft preservation.

Innovations and breakthroughs

Several comparative studies of preservation solutions have aimed to evaluate the benefits and disadvantages of each of these solutions on animal experiments models and randomized controlled trials. This is the first study to provide a head-to-head comparison between IGL-1 and Celsior. This study demonstrates that IGL-1 solution is more effective for preserving endothelium function after cold preservation.

Applications

This study highlights the importance of the storage solution in the preservation of endothelium function and graft quality. Moreover, it may help researchers to develop more effective preservation solutions and may guide clinicians' choice of solution when risk factors are present.

Peer-review

This is a nice paper providing new insights into mechanisms of action of IGL-1 and Celsior preservation solutions in liver cold ischemia reperfusion injury. The authors have shown that a decrease in NO dependent relaxation after cold storage was less pronounced with IGl-1 solution and that IGL-1 offered better protection against IRI in comparison to Celsior.

REFERENCES

1 **Henry SD**, Nachber E, Tulipan J, Stone J, Bae C, Reznik L, Kato T, Samstein B, Emond JC, Guarrera JV. Hypothermic machine preservation reduces molecular markers of ischemia/reperfusion injury in human liver transplantation. *Am J Transplant* 2012; **12**: 2477-2486 [PMID: 22594953 DOI: 10.1111/j.1600-6143.2012.04086.x]

2 **Zaouali MA**, Boncompagni E, Reiter RJ, Bejaoui M, Freitas I, Pantazi E, Folch-Puy E, Abdennebi HB, Garcia-Gil FA, Roselló-Catafau J. AMPK involvement in endoplasmic reticulum stress and autophagy modulation after fatty liver graft preservation: a role for melatonin and trimetazidine cocktail. *J Pineal Res* 2013; **55**: 65-78 [PMID: 23551302 DOI: 10.1111/jpi.12051]

3 **Brunner SM**, Junger H, Ruemmele P, Schnitzbauer AA, Doenecke A, Kirchner GI, Farkas SA, Loss M, Scherer MN, Schlitt HJ, Fichtner-Feigl S. Bile duct damage after cold storage of deceased donor livers predicts biliary complications after liver transplantation. *J Hepatol* 2013; **58**: 1133-1139 [PMID: 23321317 DOI: 10.1016/j.jhep.2012.12.022]

4 **Belzer FO**, Southard JH. Principles of solid-organ preservation by cold storage. *Transplantation* 1988; **45**: 673-676 [PMID: 3282347]

5 **O'Callaghan JM**, Knight SR, Morgan RD, Morris PJ. Preservation solutions for static cold storage of kidney allografts: a systematic review and meta-analysis. *Am J Transplant* 2012; **12**: 896-906 [PMID: 22221739 DOI: 10.1111/j.1600-6143.2011.03908.x]

6 **Parsons RF**, Guarrera JV. Preservation solutions for static cold storage of abdominal allografts: which is best? *Curr Opin Organ Transplant* 2014; **19**: 100-107 [PMID: 24553501 DOI: 10.1097/MOT.0000000000000063]

7 **Menasché P**, Termignon JL, Pradier F, Grousset C, Mouas C, Alberici G, Weiss M, Piwnica A, Bloch G. Experimental evaluation of Celsior, a new heart preservation solution. *Eur J Cardiothorac Surg* 1994; **8**: 207-213 [PMID: 8031565]

8 **Karam G**, Compagnon P, Hourmant M, Despins P, Duveau D, Noury D, Boudjema K. A single solution for multiple organ procurement and preservation. *Transpl Int* 2005; **18**: 657-663 [PMID: 15910289 DOI: 10.1111/j.1432-2277.2005.00083.x]

9 **George TJ**, Arnaoutakis GJ, Baumgartner WA, Shah AS, Conte JV. Organ storage with University of Wisconsin solution is associated with improved outcomes after orthotopic heart transplantation. *J Heart Lung Transplant* 2011; **30**: 1033-1043 [PMID: 21683620 DOI: 10.1016/j.healun.2011.05.005]

10 **De Santo LS**, Romano G, Amarelli C, Della Corte A, Onorati F, Torella M, De Feo M, Nappi GA, Cotrufo M. Pilot study on prevention of lung injury during surgery for type A acute aortic dissection: no evident improvements with celsior flushing through the pulmonary artery. *Int J Artif Organs* 2003; **26**: 1032-1038 [PMID: 14708832]

11 **Boudjema K**, Grandadam S, Compagnon P, Salamé E, Wolf P, Ducerf C, Le Treut P, Soubrane O, Cherqui D, Mouchel C, Renault A, Bellissant E. Efficacy and safety of Celsior preservation fluid in liver transplantation: one-year follow up of a prospective, multicenter, non-randomized study. *Clin Transplant* 2012; **26**: 199-207 [PMID: 21517997 DOI: 10.1111/j.1399-0012.2011.01447.x]

12 **Tillou X**, Collon S, Surga N, Jaureguy M, Viart L, Mazouz H, Gigante M. Comparison of UW and Celsior: long-term results in kidney transplantation. *Ann Transplant* 2013; **18**: 146-152 [PMID: 23792514 DOI: 10.12659/AOT.883862]

13 **Uhlmann D**, Armann B, Ludwig S, Escher E, Pietsch UC, Tannapfel A, Teupser D, Hauss J, Witzigmann H. Comparison of Celsior and UW solution in experimental pancreas preservation. *J Surg Res* 2002; **105**: 173-180 [PMID: 12121704]

14 **Boggi U**, Vistoli F, Del Chiaro M, Signori S, Croce C, Pietrabissa A, Berchiolli R, Marchetti P, Del Prato S, Mosca F. Pancreas preservation with University of Wisconsin and Celsior solutions: a single-center, prospective, randomized pilot study. *Transplantation* 2004; **77**: 1186-1190 [PMID: 15114082]

15 **van As AB**, Lotz Z, Tyler M, Kahn D. Impact of Celsior solution on hepatocellular, reperfusion and endothelial cell injury after liver transplantation. *Dig Liver Dis* 2001; **33**: 181-186 [PMID: 11346148]

16 **Ben Abdennebi H**, Steghens JP, Hadj-Aïssa A, Barbieux A, Ramella-Virieux S, Gharib C, Boillot O. A preservation solution with polyethylene glycol and calcium: a possible multiorgan liquid. *Transpl Int* 2002; **15**: 348-354 [PMID: 12122511 DOI: 10.1007/s00147-002-0427-8]

17 **Codas R**, Petruzzo P, Morelon E, Lefrançois N, Danjou F, Berthillot C, Contu P, Espa M, Martin X, Badet L. IGL-1 solution in kidney transplantation: first multi-center study. *Clin Transplant* 2009; **23**: 337-342 [PMID: 19210685 DOI: 10.1111/j.1399-0012.2009.00959.x]

18 **Yandza T**, Tauc M, Canioni D, Rogel-Gaillard C, Bernard G, Bernard A, Gugenheim J. Effect of polyethylene glycol in pig intestinal allotransplantation without immunosuppression. *J Surg Res* 2012; **176**: 621-628 [PMID: 22137987 DOI: 10.1016/j.jss.2011.10.012]

19 **Dondéro F**, Paugam-Burtz C, Danjou F, Stocco J, Durand F, Belghiti J. A randomized study comparing IGL-1 to the University of Wisconsin preservation solution in liver transplantation. *Ann Transplant* 2010; **15**: 7-14 [PMID: 21183870]

20 **Niclauss N**, Wojtusciszyn A, Morel P, Demuylder-Mischler S, Brault C, Parnaud G, Ris F, Bosco D, Badet L, Benhamou PY, Berney T. Comparative impact on islet isolation and transplant outcome of the preservation solutions Institut Georges Lopez-1, University of Wisconsin, and Celsior. *Transplantation* 2012; **93**: 703-708 [PMID: 22343333 DOI: 10.1097/TP.0b013e3182476cc8]

21 **Ben Mosbah I**, Roselló-Catafau J, Franco-Gou R, Abdennebi HB, Saidane D, Ramella-Virieux S, Boillot O, Peralta C. Preservation of steatotic livers in IGL-1 solution. *Liver Transpl* 2006; **12**: 1215-1223 [PMID: 16724331 DOI: 10.1002/lt.20788]

22 **Mosbah IB**, Zaouali MA, Martel C, Bjaoui M, Abdennebi HB, Hotter G, Brenner C, Roselló-Catafau J. IGL-1 solution reduces endoplasmic reticulum stress and apoptosis in rat liver transplantation. *Cell Death Dis* 2012; **3**: e279 [PMID: 22402603 DOI: 10.1038/cddis.2012.12]

23 **Lema Zuluaga GL**, Serna Agudelo RE, Zuleta Tobón JJ. Preservation solutions for liver transplantation in adults: celsior versus custodiol: a systematic review and meta-analysis with an indirect

comparison of randomized trials. *Transplant Proc* 2013; **45**: 25-32 [PMID: 23267794 DOI: 10.1016/j.transproceed.2012.02.031]
24 **Nasser M**, Clere N, Botelle L, Javellaud J, Oudart N, Faure S, Achard JM. Opposite effects of angiotensins receptors type 2 and type 4 on streptozotocin induced diabetes vascular alterations in mice. *Cardiovasc Diabetol* 2014; **13**: 40 [PMID: 24511993 DOI: 10.1186/1475-2840-13-40]
25 **Bejaoui M**, Zaouali MA, Folch-Puy E, Pantazi E, Bardag-Gorce F, Carbonell T, Oliva J, Rimola A, Abdennebi HB, Roselló-Catafau J. Bortezomib enhances fatty liver preservation in Institut George Lopez-1 solution through adenosine monophosphate activated protein kinase and Akt/mTOR pathways. *J Pharm Pharmacol* 2014; **66**: 62-72 [PMID: 24127984 DOI: 10.1111/jphp.12154]
26 **Janssen H**, Janssen PH, Broelsch CE. Value of energy substrates in HTK and UW to protect human liver endothelial cells against ischemia and reperfusion injury. *Eur Surg Res* 2004; **36**: 26-32 [PMID: 14730220 DOI: 10.1159/000075071]
27 **Stolz DB**, Ross MA, Ikeda A, Tomiyama K, Kaizu T, Geller DA, Murase N. Sinusoidal endothelial cell repopulation following ischemia/reperfusion injury in rat liver transplantation. *Hepatology* 2007; **46**: 1464-1475 [PMID: 17929236 DOI: 10.1002/hep.21887]
28 **Russo L**, Gracia-Sancho J, García-Calderó H, Marrone G, García-Pagán JC, García-Cardeña G, Bosch J. Addition of simvastatin to cold storage solution prevents endothelial dysfunction in explanted rat livers. *Hepatology* 2012; **55**: 921-930 [PMID: 22031447 DOI: 10.1002/hep.24755]
29 **Knes JM**, Hansen TN, Gilligan B, Woo H, Mangino M, Haworth RA, Southard JH. Loss of endothelium-dependent relaxation in abdominal aorta preserved in a co-storage system. *Transpl Int* 2005; **17**: 699-706 [PMID: 15551051 DOI: 10.1007/s00147-004-0788-2]
30 **Jeng LB**, Lin PJ, Yao PC, Chen MF, Tsai KT, Chang CH. Impaired endothelium-dependent relaxation of human hepatic arteries after preservation with the University of Wisconsin solution. *Arch Surg* 1997; **132**: 7-12 [PMID: 9006546]
31 **Wilson CH**, Stansby G, Haswell M, Cunningham AC, Talbot D. Evaluation of eight preservation solutions for endothelial in situ preservation. *Transplantation* 2004; **78**: 1008-1013 [PMID: 15480166]
32 **Cuzzocrea S**, Salvemini D. Molecular mechanisms involved in the reciprocal regulation of cyclooxygenase and nitric oxide synthase enzymes. *Kidney Int* 2007; **71**: 290-297 [PMID: 17200681 DOI: 10.1038/sj.ki.5002058]
33 **Gambone LM**, Murray PA, Flavahan NA. Synergistic interaction between endothelium-derived NO and prostacyclin in pulmonary artery: potential role for K+ATP channels. *Br J Pharmacol* 1997; **121**: 271-279 [PMID: 9154337 DOI: 10.1038/sj.bjp.0701082]
34 **Akhtar MZ**, Henderson T, Sutherland A, Vogel T, Friend PJ. Novel approaches to preventing ischemia-reperfusion injury during liver transplantation. *Transplant Proc* 2013; **45**: 2083-2092 [PMID: 23953517 DOI: 10.1016/j.transproceed.2013.04.004]
35 **Ploeg RJ**, van Bockel JH, Langendijk PT, Groenewegen M, van der Woude FJ, Persijn GG, Thorogood J, Hermans J. Effect of preservation solution on results of cadaveric kidney transplantation. The European Multicentre Study Group. *Lancet* 1992; **340**: 129-137 [PMID: 1352564]
36 **Peralta C**, Jiménez-Castro MB, Gracia-Sancho J. Hepatic ischemia and reperfusion injury: effects on the liver sinusoidal milieu. *J Hepatol* 2013; **59**: 1094-1106 [PMID: 23811302 DOI: 10.1016/j.jhep.2013.06.017]
37 **Zaouali MA**, Padrissa-Altés S, Ben Mosbah I, Ben Abdennebi H, Boillot O, Rimola A, Saidane-Mosbahi D, Roselló-Catafau J. Insulin like growth factor-1 increases fatty liver preservation in IGL-1 solution. *World J Gastroenterol* 2010; **16**: 5693-5700 [PMID: 21128318]
38 **Grossini E**, Pollesello P, Bellofatto K, Sigaudo L, Farruggio S, Origlia V, Mombello C, Mary DA, Valente G, Vacca G. Protective effects elicited by levosimendan against liver ischemia/reperfusion injury in anesthetized rats. *Liver Transpl* 2014; **20**: 361-375 [PMID: 24273004 DOI: 10.1002/lt.23799]
39 **Ben Mosbah I**, Roselló-Catafau J, Alfany-Fernandez I, Rimola A, Parellada PP, Mitjavila MT, Lojek A, Ben Abdennebi H, Boillot O, Rodés J, Peralta C. Addition of carvedilol to University Wisconsin solution improves rat steatotic and nonsteatotic liver preservation. *Liver Transpl* 2010; **16**: 163-171 [PMID: 20104484 DOI: 10.1002/lt.21968]
40 **Bouma HR**, Ketelaar ME, Yard BA, Ploeg RJ, Henning RH. AMP-activated protein kinase as a target for preconditioning in transplantation medicine. *Transplantation* 2010; **90**: 353-358 [PMID: 20571465 DOI: 10.1097/TP.0b013e3181e7a3aa]
41 **Padrissa-Altés S**, Zaouali MA, Bartrons R, Roselló-Catafau J. Ubiquitin-proteasome system inhibitors and AMPK regulation in hepatic cold ischaemia and reperfusion injury: possible mechanisms. *Clin Sci* (Lond) 2012; **123**: 93-98 [PMID: 22455352 DOI: 10.1042/CS20110093]
42 **Amersi F**, Shen XD, Anselmo D, Melinek J, Iyer S, Southard DJ, Katori M, Volk HD, Busuttil RW, Buelow R, Kupiec-Weglinski JW. Ex vivo exposure to carbon monoxide prevents hepatic ischemia/reperfusion injury through p38 MAP kinase pathway. *Hepatology* 2002; **35**: 815-823 [PMID: 11915027 DOI: 10.1053/jhep.2002.32467]
43 **Kaizu T**, Ikeda A, Nakao A, Tsung A, Toyokawa H, Ueki S, Geller DA, Murase N. Protection of transplant-induced hepatic ischemia/reperfusion injury with carbon monoxide via MEK/ERK1/2 pathway downregulation. *Am J Physiol Gastrointest Liver Physiol* 2008; **294**: G236-G244 [PMID: 18006605 DOI: 10.1152/ajpgi.00144.2007]

P- Reviewer: Rydzewski A **S- Editor**: Qi Y **L- Editor**: Roemmele A
E- Editor: Ma S

World Journal of Gastroenterology

Submit a Manuscript: http://www.wjgnet.com/esps/
Help Desk: http://www.wjgnet.com/esps/helpdesk.aspx
DOI: 10.3748/wjg.v21.i14.4169

World J Gastroenterol 2015 April 14; 21(14): 4169-4177
ISSN 1007-9327 (print) ISSN 2219-2840 (online)

ORIGINAL ARTICLE

Basic Study

Increase in apoptosis by combination of metformin with silibinin in human colorectal cancer cells

Cheng-Chia Tsai, Tang-Wei Chuang, Li-Jen Chen, Ho-Shan Niu, Kun-Ming Chung, Juei-Tang Cheng, Kao-Chang Lin

Cheng-Chia Tsai, Department of Surgery, Mackay Memorial Hospital, Taipei City 10401, Taiwan
Cheng-Chia Tsai, Graduate Institute of Disease Prevention and Control, College of Medicine, Taipei Medical University, Taipei City 10361, Taiwan
Tang-Wei Chuang, Division of Hepatogastroenterology, Department of Internal Medicine, Chi Mei Medical Center, Liouying 73654, Taiwan
Li-Jen Chen, Institute of Basic Medical Science, College of Medicine, National Cheng Kung University, Tainan City 70101, Taiwan
Ho-Shan Niu, Department of Nursing, Tzu Chi College of Technology, Hualien City 97005, Taiwan
Kun-Ming Chung, Division of Gastroenterology, Department of Internal Medicine, Chi-Mei Medical Center, Yong Kang, Tainan City 71003, Taiwan
Juei-Tang Cheng, Institute of Medical Sciences, Chang Jung Christian University, Gueiren, Tainan City 71101, Taiwan
Kao-Chang Lin, Department of Neurology, Chi Mei Medical Center, Yong Kang, Tainan City 71003, Taiwan
Kao-Chang Lin, Department of Medical Research, Chi Mei Medical Center, Yong Kang, Tainan City 71003, Taiwan
Kao-Chang Lin, Institute of Biotechnology, Southern Taiwan University, Yong Kang, Tainan City 71004, Taiwan
Author contributions: Chuang TW, Tsai CC and Lin KC designed the research; Chen LJ and Niu HS performed the research; Chung KM and Tsai CC analyzed the data; Chen LJ and Cheng JT wrote the paper; Tsai CC and Chuang TW contributed equally to this work.
Supported by A grant from the Chi Mei Medical Center in Taiwan (partly), No. CMFHR10302.

Correspondence to: Juei-Tang Cheng, PhD, FCP, Professor, Institute of Medical Sciences, Chang Jung Christian University, Geuiren, Tainan City 71101, Taiwan. jtcheng@mail.cjcu.edu.tw
Telephone: +886-6-331-8516
Fax: +886-6-2386548
Received: July 3, 2014
Peer-review started: July 3, 2014
First decision: July 21, 2014
Revised: October 25, 2014
Accepted: December 22, 2014
Article in press: December 22, 2014
Published online: April 14, 2015

Abstract

AIM: To investigate the effect of metformin on silibinin-induced apoptosis in human colorectal cancer (COLO 205) cells.

METHODS: MTT assays were performed to quantify cell viability. Western blot assays were applied to identify the expression of signaling proteins.

RESULTS: The combined treatment of COLO 205 cells with metformin and silibinin decreased cell survival at a dose insufficient to influence the non-malignant cells [Human colonic epithelial cells (HCoEpiC)]. Silibinin and metformin increased phosphatase and tensin homolog and 5′-adenosine monophosphate-activated protein kinase expression in COLO 205 cells and inhibited the phosphorylation of mammol/Lalian target of rapamycin. This combined treatment resulted in an increase in the expression of activated caspase 3 and apoptosis inducing factor, indicating apoptosis.

CONCLUSION: The combined treatment of human colorectal cancer cells with silibinin and metformin may induce apoptosis at a dose that does not affect HCoEpiC. This finding reveals a potential therapeutic strategy for the treatment of colorectal cancer.

Key words: Silibinin; Metformin; COLO 205; Mammol/Lalian target of rapamycin; Apoptosis; Colorectal cancer

Core tip: Silibinin is known to provide protection against hepatotoxic stress. Silibinin has also been shown to have high efficacy against cancer cells through increased expression of the phosphatase and tensin homolog; Metformin, a well-known antidiabetic agent, has recently been reported to inhibit cancer by increasing adenosine monophosphate-activated protein kinase expression. We investigated the effect of metformin on silibinin-induced apoptosis in human colorectal cancer cells. The combined treatment of human colorectal cancer cells with silibinin and metformin may induce apoptosis at a dose that does not affect human colonic epithelial cells. This finding reveals a potential therapeutic strategy for the treatment of colorectal cancer.

Tsai CC, Chuang TW, Chen LJ, Niu HS, Chung KM, Cheng JT, Lin KC. Increase in apoptosis by combination of metformin with silibinin in human colorectal cancer cells. *World J Gastroenterol* 2015; 21(14): 4169-4177 Available from: URL: http://www.wjgnet.com/1007-9327/full/v21/i14/4169.htm DOI: http://dx.doi.org/10.3748/wjg.v21.i14.4169

INTRODUCTION

Colorectal cancer is one of the leading causes of cancer associated deaths globally[1]. The high mortality of patients with colorectal cancer is mainly attributed to its metastasis to distant organs[2]. The application of traditional radiotherapy and chemotherapy treatments is limited due to their high toxicity and damaging side effects. Therefore, the development of alternative treatments is a viable strategy that may help lower the side effects from the treatment of colorectal cancer. Interventions using nontoxic phytochemicals, which are aimed at multiple targets, have been shown to reduce carcinogenesis and overall cancer risk[3]. Numerous studies have reported strong anticancer properties of both dietary and non-dietary phytochemicals against multiple cancers, including colorectal cancer[4]. Thus, phytochemicals have received increased attention due to their potential uses in cancer therapy, and many phytochemicals have been investigated in various phases of clinical trials[5].

Milk thistle (*Silybum marianum*) has been widely utilized in the United States and Europe as a popular dietary supplement for treating liver diseases[6]. Silibinin, a polyphenolic flavonoid, is the major active compound in milk thistle[7]. Milk thistle is known to be safe and effective without side effects when administered to protect the liver against chemical or alcohol-related injury[8]. The inhibitory action of silibinin has been demonstrated in multiple cancer cell lines, including lung[9], liver[10], skin[11], colon[12] and prostate[13] cancer cells.

Metformin is an antidiabetic agent widely used to treat diabetic patients. Its action is mainly mediated by the activation of 5'-adenosine monophosphate (AMP)-activated protein kinase (AMPK), which inhibits hepatic gluconeogenesis and enhances glucose uptake in skeletal muscle[14]. In addition, metformin has been reported to reduce cell proliferation in several human tumors, including breast cancer[15], pancreatic cancer[16] and gastric cancer[17]. Metformin also inhibited the growth of tumors in xenograft mouse models of breast cancer[18], prostate cancer[19], ovarian cancer[20] and melanoma[21]. The administration of metformin to diabetic patients was associated with lower rates of cancer incidence and mortality[22]. Colorectal cancer patients with diabetes who were treated with metformin as part of their diabetic therapy exhibited a greater overall survival rate[23].

Metformin might inhibit mammol/Lalian target of rapamycin (mTOR) through regulation at multiple sites. The low energy charge in metformin-treated cancer cells activates AMPK, which can inhibit cell growth and proliferation. AMPK activates the tumor suppressor gene, resulting in inhibition of mTOR and an increase in apoptosis[24]. Silibinin was shown to be associated with increased phosphatase and tensin homolog (PTEN) activity and decreased phosphorylated protein kinase B (p-Akt) production, indicating a role for the PTEN/Akt pathway in the apoptosis of cancer cells[25].

Both metformin and silibinin exhibit anticancer activities. Thus, we administered silibinin and metformin in combination to investigate the anticancer efficacy of the combination therapy in human colorectal cancer cell line (COLO 205). In the present study, we determined an effective dose for this combination of two agents that was not nontoxic to non-malignant cells.

MATERIALS AND METHODS

Materials

Antibodies against activated caspase 3 and apoptosis inducing factor (AIF) were purchased from Millipore (Millipore, Bedford, MA, United States). Antibodies against the PTEN, signal transducer and p-Akt, phosphorylated-AMPK (p-AMPK), phosphorylated mammol/Lalian target of rapamycin (p-mTOR) and β-actin (actin) were purchased from Abcam (Cambridge, MA, United States). Metformin and silibinin were purchased form Sigma-Aldrich (St Louis, MO, United States).

Cell culture

The human colorectal cancer cell line (COLO 205) was purchased from the Culture Collection and Research Center of the Food Industry Institute (Hsin-Chiu City, Taiwan). Human colonic epithelial cells (HCoEpiC) were purchased from ScienCell (CA, United States). COLO 205 cells were cultured in RPMI-1640 supplemented with 10% heat-inactivated fetal bovine serum (FBS; GIBCO). HCoEpiC were cultured in Colonic Epithelial

Cell Medium (CoEpiCM, Cat. No. 2951) purchased from ScienCell (CA, United States). The cells were maintained at 37 ℃ in a humidified atmosphere of 5% CO_2. When cells reached approximately 60% confluence, the medium was replaced with serum-free cell medium containing various concentrations of silibinin (0, 50, 100, 150 or 200 μmol/L)[10] and metformin (0, 5, 10, 15 or 20 mmol/L) and the cells were cultured for 24 h as previously described[21]. The cells were trypsinized with 0.25% trypsin and 0.2 g/L EDTA and harvested for further studies.

Analysis of synergy by combination index

The Loewe additivity model[26] was used as a second method of analyzing the interaction between silibinin and metformin. The interaction between the compounds is reported as the combination index (CI) in the following equation: $CI = (d1/D_{\times,1}) + (d2/D_{\times,2})$.

In the equation, d1 and d2 represent the concentrations of the compounds in combination required to achieve × effect. $D_{\times,1}$ and $D_{\times,2}$ represent the concentrations of the same compounds individually that would quantitatively achieve the same × effect. A CI < 1.0 indicates that the combination is synergistic, and a CI > 1.0 indicates an antagonistic interaction. The combination indexes for this study were determined by using concentrations corresponding to the ED_{50} of the dose response curves for silibinin, metformin and silibinin + metformin.

Apo-Glo assay

Apoptotic response was quantified by the detection of DNA histone complexes released from the nucleus to the cytosol of cells using the Apo-Glo Assay (Promega, WI, United States). The assay was performed to assess viability and caspase 3/7 activation within a single assay well. Briefly, 10^4 cells were seeded on 96-well plates in triplicate and treated with different combinations of varying concentrations of metformin and silibinin for 24 h. Each well contained a final volume of 0.2 mL of culture medium. Viability reagent was added to each well and mixed with culture medium using orbital shaking (500 rpm for 30 s), and the cells were incubated with the viability reagent for 1 h at 37 ℃. Fluorescence was measured at two wavelengths: 400 nm/505 nm. Following the addition of caspase-Glo 3/7 (100 μL), we mixed the samples using orbital shaking (500 rpm for 30 s). After incubation for 30 min at room temperature, luminescence was measured using a microplate reader to assess apoptosis while the fluorescence was measured at 380Ex/510Em.

Western blot analysis

Protein was extracted from tissue homogenates and cell lysates using ice-cold radio-immol/Luno-precipitation assay (RIPA) buffer supplemented with phosphatase and protease inhibitors (50 mmol/L sodium vanadate, 0.5 mmol/L phenylmethylsulphonyl fluoride, 2 mg/mL aprotinin, and 0.5 mg/mL leupeptin). The protein concentrations were determined using a Bio-Rad protein assay (Bio-Rad Laboratories, Inc., Hercules, CA, United States). Total protein samples (30 μg) were separated by SDS/polyacrylamide gel electrophoresis (10% acrylamide gel) using the Bio-Rad Mini-Protein Ⅱ system. The proteins were transferred to polyvinylidene difluoride membranes (PerkinElmer, Waltham, MA, United States) using a Bio-Rad Trans-Blot system. After the transfer, the membrane was blocked with 5% non-fat milk in Tris-buffered saline containing 0.1% Tween 20 (TBS-T) and then incubated for two hours. The membrane was then washed in TBS-T and hybridized with primary antibodies, which were diluted to a suitable concentration in TBS-T, for 16 h. Specific antibodies for activated caspase 3, AIF, PTEN, p-Akt, p-AMPK and p-mTOR (1:1000 dilution) were used. Additionally, the membranes were incubated with a goat polyclonal antibody specific for β-actin (Actin) (1:10000 dilution) to serve as an internal control. Incubation with secondary antibodies and detection of the antigen-antibody complex were performed using an ECL kit (Amersham Biosciences, United Kingdom). After comparing with the marker to determine specificity, the immol/Lunoblots of β-actin (43 kDa), activated caspase 3 (17 kDa), AIF (57 kDa), PTEN (42 kDa), p-Akt (60 kDa), p-AMPK (62 kDa) and p-mTOR (289 kDa) were quantified with a laser densitometer (Avegene Life Science, Taipei, Taiwan).

Statistical analysis

The data are expressed as the mean ± SEM for the indicated number (*n*) of samples in each group. Repeated measures analysis of variance (ANOVA) was used to analyze gene and protein expression level changes and other parameters. Differences resulting in a *P*-value of 0.05 or less were considered to be significant.

RESULTS

Silibinin and metformin inhibit cell viability synergistically

Figure 1A shows the survival rate of COLO 205 cells and HCoEpiC treated with a combination of silibinin and metformin at various concentrations for 24 h. Both silibinin and metformin at their highest dose, in combination or individually, exerted an inhibitory effect on the survival of COLO 205 cells. However, individual treatment with silibinin or metformin at their highest respective dose exerted a toxic effect on HCoEpiC, and the rate of cell death was even greater following the combination treatment. Furthermore, combined treatment with 100 μmol/L silibinin and 10 mmol/L metformin was more effective than treatment with 50 μmol/L silibinin and 5 mmol/L metformin without altering the survival of HCoEpiC. Figure 1B shows

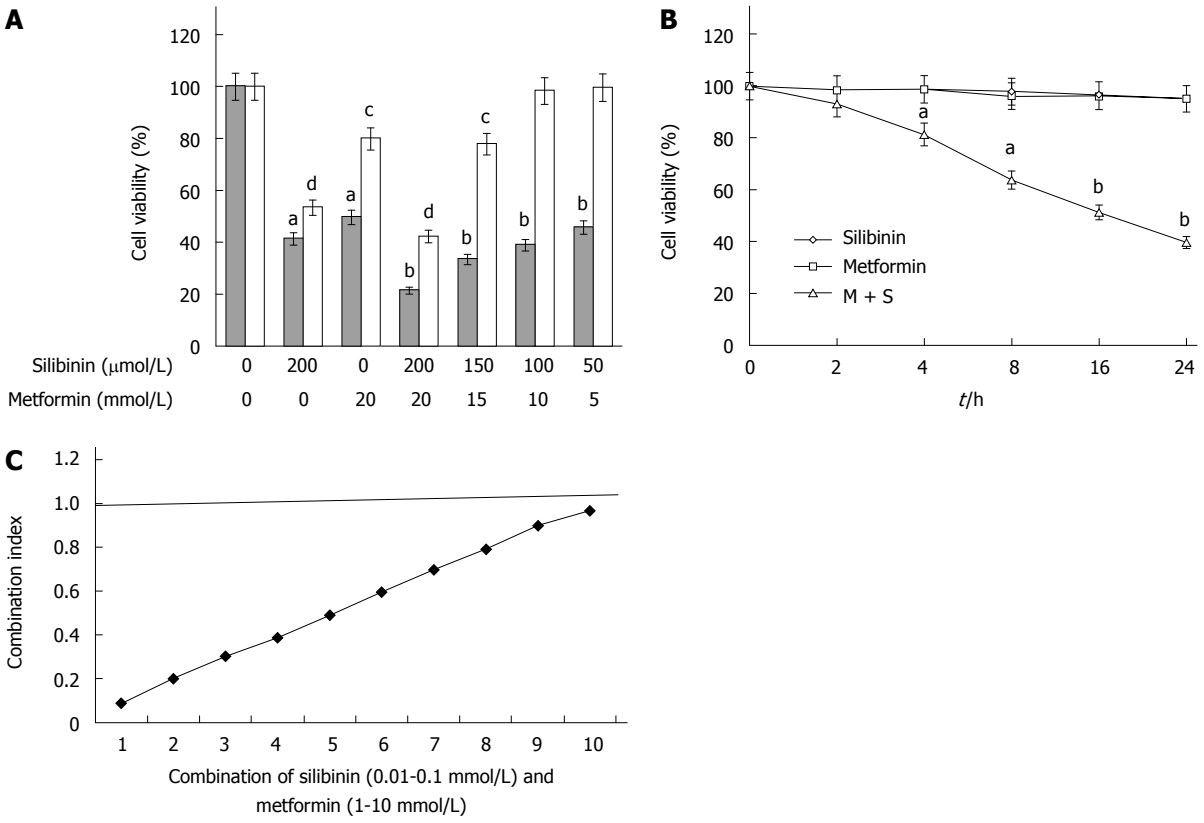

Figure 1 Treatment with silibinin and metformin in combination or alone reduces the viability of COLO 205 cells. Reduced cell viability was observed following 24-h incubation with silibinin (0-200 μmol/L) and metformin (0-20 mmol/L) in combination or alone. The gray bars depict the results from COLO 205 cells, and the open bars correspond to the results from human colonic epithelial cells (HCoEpiC) (A). The time course (0-24 h) (B) and combination index (C) are shown in COLO 205 cells treated with silibinin (100 μmol/L) and metformin (10 mmol/L) in combination (M + S) or alone. The data are expressed as mean ± SE (n = 6 for each group). $^{a}P < 0.01$ and $^{b}P < 0.001$ *vs* Control COLO 205 cells; $^{c}P < 0.05$ and $^{d}P < 0.01$ *vs* Control HCoEpiC. M + S: Metformin and silibinin.

the survival curves of COLO 205 cells treated with silibinin (100 μmol/L) and metformin (10 mmol/L) in combination or individually at different exposure times. The survival curves shifted to the left after a longer exposure to the combined treatment, while the individual treatments did not affect the survival of COLO 205. The synergistic effect of silibinin + metformin on COLO 205 cells was further confirmed using an alternative approach of calculating the CI. The combination of silibinin at concentrations below 100 μmol/L + metformin at concentrations below 10 mmol/L metformin had a CI < 1, indicating synergy between the two compounds (Figure 1C). Thus, in the following experiments, we used 100 μmol/L silibinin with 10 mmol/L metformin in combination to compare the effects of this combination treatment with the individual treatments on COLO 205 cells after 24-h incubation.

Combined metformin and silibinin treatment inhibits Akt phosphorylation by enhancing PTEN expression

The effects of combined metformin and silibinin (M + S) treatment on the expression of PTEN were examined by Western blot. As shown in Figure 2, expression of phosphorylated AKT decreased while expression of PTEN increased in COLO 205 cells after silibinin treatment or M + S treatment for 24 h.

M + S treatment enhances AMPK phosphorylation

The effects of M + S treatment on the phosphorylation of AMPK were examined by Western blot. As shown in Figure 3A, expression of phosphorylated AMPK increased in COLO 205 cells after treatment with metformin or M + S for 24 h. Additionally, treatment with metformin or M + S inhibited the phosphorylation of mTOR in COLO 205 cells (Figure 3B).

M + S treatment induces COLO 205 cell apoptosis

We measured COLO 205 cell apoptosis using an Apo-Tox Glo assay. As shown in Figure 4A, the combination treatment with 100 μmol/L silibinin and 10 mmol/L metformin induced cytotoxicity and apoptosis in COLO 205 cells, however, this effect was not seen when cells were treated with silibinin or metformin alone. The levels of activated caspase 3 and AIF were determined by Western blot, as described previously[27], to assess the apoptosis. M + S treatment increased the levels of activated caspase 3 and AIF in COLO 205 cells, whereas treatment with silibinin or metformin alone did not produce the same effects (Figure 4B and C). Thus, (M + S)-induced inhibition is primarily mediated by the

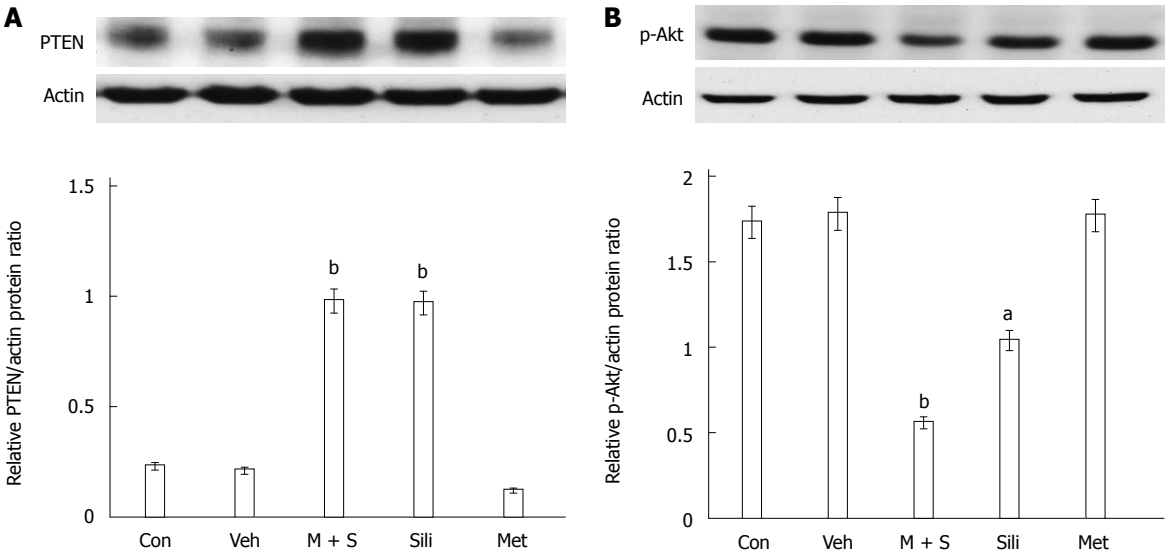

Figure 2 Combined metformin and silibinin treatment inhibits protein kinase B phosphorylation by enhancing phosphatase and tensin homolog expression. Proteins isolated from COLO 205 cells were probed using an antibody against phosphatase and tensin homolog (PTEN) (A) or phosphorylated protein kinase B (p-Akt) (B). The data are expressed as mean ± SE (n = 6 for each group). [a]P < 0.01 and [b]P < 0.001 *vs* Control. Con: Control; Veh: Vehicle; Sili: Silibinin; Met: Metformin; M + S: Metformin and silibinin.

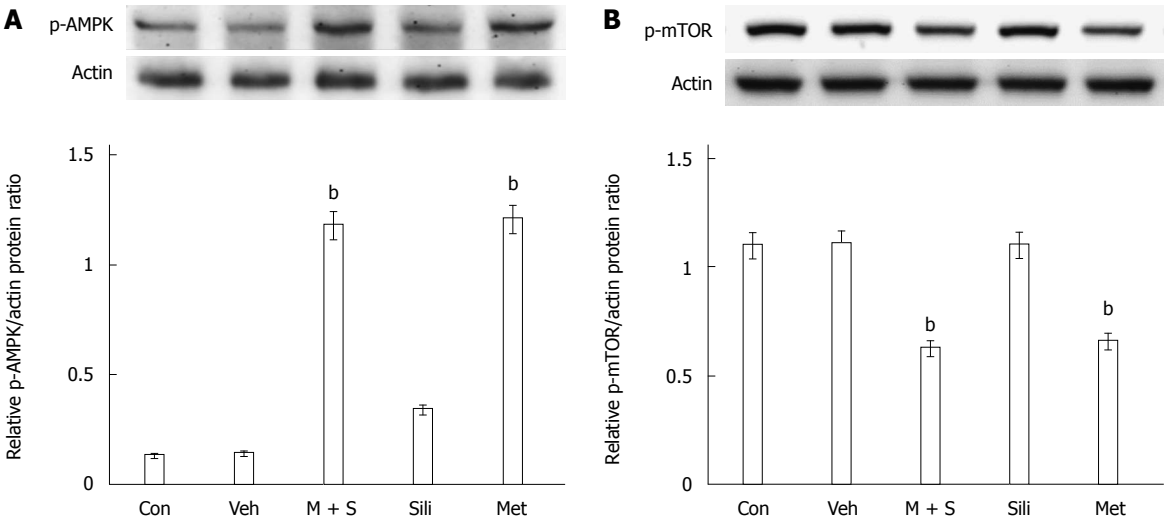

Figure 3 Combined metformin and silibinin treatment enhances AMP-activated protein kinase phosphorylation. COLO 205 cells were treated with silibinin and metformin in combination or alone. The protein samples were then probed using an antibody against phosphorylated AMP-activated protein kinase (p-AMPK) (A) or phosphorylated mammol/Lalian target of rapamycin (p-mTOR) (B). The data are expressed as mean ± SE (n = 6 for each group). [b]P < 0.001 *vs* Control. Con: Control; Veh: Vehicle; Sili: silibinin; Met: Metformin; M + S: Metformin and silibinin.

induction of apoptosis in cancer cells.

DISCUSSION

In the present study, we found that the co-treatment of human colorectal cancer cell line (COLO 205 cells) with silibinin (100 μmol/L) and metformin (10 mmol/L) directly inhibits cell survival. In addition, the combination of silibinin (100 μmol/L) and metformin (10 mmol/L) at the doses that effectively inhibited COLO 205 cell survival did not affect normal HCoEpiC. There was considerable specificity in the inhibition of cancer cells using this combination therapy. Moreover, silibinin alone or in combination with metformin increased the level of PTEN expression in COLO 205 cells, resulting in a significant reduction in phosphorylated Akt (at Ser^{473}). Moreover, metformin alone or in combination with silibinin increased the phosphorylation of AMPK and inhibited the phosphorylation of mTOR in COLO 205 cells. Furthermore, results of the Apo-Glo assay indicated that treatment of COLO 205 cells with 100 μmol/L silibinin and 10 mmol/Lol/Lol/L metformin in combination induced apoptosis, while this effect was not seen when cells were treated with silibinin or metformin alone. Finally, the combined treatment of cells with silibinin and metformin increased caspase 3 activation and AIF expression, both of which are widely used as indicators of apoptosis[27]. Therefore, our results suggest

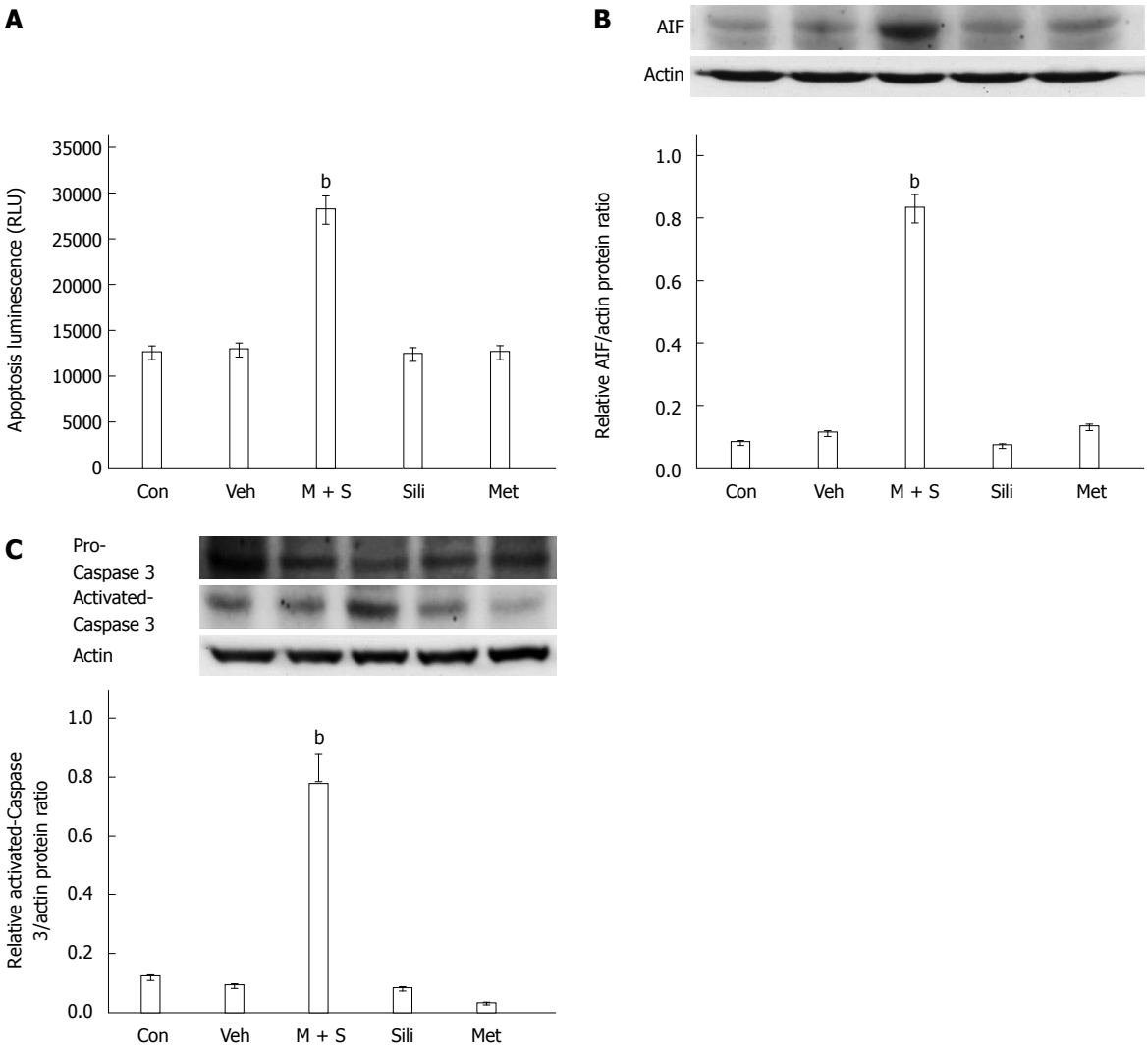

Figure 4 Combined metformin and silibinin treatment induces COLO 205 cell apoptosis. COLO 205 cells were treated with silibinin and metformin in combination or alone. Apo-Glo assay showing apoptosis of COLO 205 cells treated with silibinin (100 μmol/L) and metformin (10 mmol/Lol/L) in combination (M + S) or alone (A); The protein samples were probed using an antibody against AIF (B) or activated caspase 3 (C). All data are expressed as mean ± SE (n = 6 for each group). $^{b}P < 0.001$ *vs* Control. Con: Control; Veh: Vehicle; Sili: silibinin; Met: Metformin; M + S: Metformin and silibinin.

that the combination of silibinin and metformin more effectively induced apoptosis compared to treatment with silibinin or metformin alone in COLO 205 cells and at a dose that was nontoxic to normal cells.

Previous studies have identified the major roles of PTEN/Akt signaling in carcinogenesis and cancer progression[28]. PTEN is an upstream factor that inhibits p-Akt, and silibinin may increase PTEN expression to inhibit cell growth[10,27,29]. The PTEN/PI3K/Akt pathway is associated with silibinin-induced inhibition of growth in human hepatic cellular carcinoma (HCC) cells[25]. Many cellular events are associated with silibinin-induced apoptosis. Silibinin could cause the loss of mitochondrial membrane potential, resulting in an increased release of cytochrome c or Bax from mitochondria, as well as the decrease in expression of Mcl-1 protein, indicating that silibinin-induced apoptosis is mediated through caspase-dependent and/or caspase-independent mechanisms[30]. Additionally, our previous reports show that the silibinin-induced increase in PTEN expression and the resulting decrease in p-Akt expression are associated with decreased survival rate and enhanced apoptosis in FaDu oral cancer cells[29] and c33-A cervical cancer cells[27]. In this study, we found that silibinin alone or in combination with metformin increased PTEN expression, resulting in decreased p-Akt in COLO 205 cells, consistent with our previous reports.

Suppression of growth in human colorectal carcinoma (SW480) cells by silibinin at a concentration of 200 μmol/L has been reported[31], indicating that silibinin exerts anticancer effects at a dose of 200 μmol/L. In this study, we are the first to report that co-treatment with silibinin (100 μmol/L) and metformin (10 mmol/L) more effectively induced apoptosis than treatment with silibinin 100 μmol/L alone. Moreover, this combination treatment did not affect normal HCoEpiC. Thus, there was considerable specificity in the inhibition of cancer cells using this combination therapy.

Metformin has widely been used to treat patients

with type 2 diabetes[23]. Interestingly, the concept that this compound may be a promising anti-cancer agent was first developed in the early 1970s[32]. Later on, two population-based studies provided preliminary evidence that metformin may reduce cancer risk and improve prognosis in type 2 diabetic patients[33]. Metformin inhibits cancer cells by activation of AMPK and S6 kinase and suppression of mTOR[34]. Moreover, significant down-regulation of the anti-apoptotic proteins Bcl-2 and Bcl-xL and up-regulation of the pro-apoptotic protein Bax were observed in malignant cells following metformin treatment[35]. In this study, we found that metformin alone or in combination with silibinin increased the expression of p-AMPK and inhibited the phosphorylation of mTOR, consistent with previous reports[36].

Cell apoptosis is activated in response to both intrinsic and extrinsic pathways. Drug therapies that induce apoptosis cause DNA damage-induced, p53-regulated release of cytochrome c from mitochondria. Cytochrome c then binds to apoptosis-activating factor-1 (Apaf-1), resulting in activation of caspase 9, which is followed by the activation of effector caspases including caspase 3. Following ligation, death receptors signal cell death by inducing a death-inducing signaling complex composed of the cytoplasmic adapter protein FADD (Fas-associated death domain) and caspase 8. Activated caspase 8 can activate caspase 3 both directly and indirectly by truncation of Bid[37]. Metformin[38] and silibinin[39] have been shown to induce cancer cell apoptosis through both the intrinsic and extrinsic pathways. In this study, we observed that the combination of silibinin and metformin increased caspase 3 activation or AIF expression.

Metformin at 20 mmol/L has previously been shown to be effective against breast cancer[40], melanoma[21] and gastric cancer[17]. The concentration of metformin administered to type 2 diabetic patients is approximately 30-60 μmol/L[41]. Thus, the doses of metformin that were shown to be effective against cancer cells are approximately 300-600 fold (approximately 20 mmol/L) greater than the dose routinely administered for diabetic disorders. In this study, we applied a low dose of metformin (10 mmol/L) in combination with silibinin (100 μmol/L) in order to more effectively induce apoptosis than the administration of 10 mmol/L metformin alone. Furthermore, this combination treatment did not affect normal HCoEpiC.

Similarly elevated levels of PTEN expression were observed in both the cells co-treated with metformin and silibinin and those incubated with silibinin (100 μmol/L) alone. Additionally, the increase in AMPK and decrease in mTOR phosphorylation were also the same between combination treatment and metformin (10 mmol/L) alone. In this study, we provide evidence demonstrating that combined treatment with low doses of silibinin and metformin can produce anti-cancer effects on COLO 205 cells similar to the effects of higher doses of each drug. There were no toxic effects observed on HCoEpiC with this co-treatment. We also observed a synergistic effect at the molecular level mainly for the phosphorylation of AKT. The interaction of AMPK and the PTEN/Akt pathway has yet to be elucidated. This could be a new target for our studies in the future.

Recent evidence suggests that the combination of treatment with dietary supplements and other compounds may help to alleviate toxic side effects, enhance quality of life and prolong the lifespan of patients[42]. In the present study, we are the first to examine the effects of co-treatment with low doses of metformin and silibinin on cancer cells. This combination treatment effectively induced apoptosis of COLO 205 cells, but did not affect normal HCoEpiC. Thus, this combinatory therapy may be helpful for the treatment of colorectal cancer due to not only its effectiveness, but also the reduction in toxic side effects with this treatment.

In conclusion, in the present study, the combination treatment of COLO 205 cells with silibinin and metformin synergistically enhanced the inhibition of cell survival through increased PTEN expression and AMPK phosphorylation, resulting in the induction of caspase 3 and AIF. These results suggest a novel therapeutic strategy for colorectal cancer that induces few toxic side effects on COLO 205 cells.

ACKNOWLEDGMENTS

We thank Yan YL and Liao PR for their assistance with research.

COMMENTS

Background

Silibinin is the major active compound in milk thistle and is known to display high efficacy against cancer cells through increasing the expression of phosphatase and tensin homolog (PTEN) and for hepatic protection. Metformin, a well-known antidiabetic agent, has recently been reported to inhibit cancer by increasing AMP-activated protein kinase (AMPK) expression. Recent evidence suggests that combined treatment with dietary supplements and other compounds may help to alleviate toxic side effects, enhance quality of life and prolong the lifespan of patients. However, the effect from combination of silibinin with metformin is still unknown.

Research frontiers

Silibinin is known to display high efficacy against cancer cells in addition to hepatic protection. Metformin, as the well-known antidiabetic agent, has recently been mentioned to produce cancer inhibition. The current research hotspot is to demonstrate that the combined treatment with silibinin and metformin may synergistically enhance the inhibition of COLO 205 cell survival *via* increased PTEN expression and AMPK phosphorylation, resulting in the induction of caspase 3 and AIF.

Innovations and breakthroughs

Metformin at 20 mmol/L has previously been found to be effective against breast cancer, melanoma and gastric cancer. In fact, the doses of metformin that were effective against cancer cells appear to be approximately 300-600 fold (about 20 mmol/L) greater than that which is administered for diabetic disorders. In this study, authors applied a low dose of metformin (10 mmol/L) in combination with silibinin (100 μmol/L) to produce the same result of apoptosis in colon cancer cells.

Applications

In the present study, combined treatment with silibinin and metformin

synergistically enhanced the inhibition of COLO 205 cell survival *via* increased PTEN expression and AMPK phosphorylation, resulting in the induction of apoptosis. The obtained findings suggest a novel therapeutic strategy for colorectal cancer with less side toxic effects.

Terminology

Colorectal cancer is one of the leading causes of global cancer associated deaths. The high mortality of patients with colorectal cancer is mainly attributed to the metastasis. Combined treatment with silibinin and metformin may induce apoptosis of human colorectal cancer cells at a dose that does not affect nonmalignant colon epithelial cells. This finding reveals a potential therapeutic strategy of colorectal cancer.

Peer-review

This paper assessed the efficacy of combined United Statesge of silibinin, which is a phytochemical, and metformin, which is an oral antidiabetic drug in the biguanide class. Authors successfully showed the synergistic effects of the two compounds regarding the apoptosis induction in COLO 205, a human colorectal cancer cell line. They also investigated the molecular basis for the synergism by studying activation of Akt/PTEN and AMPK. This paper is well written, showing a possibility towards a novel therapeutic regimen for the treatment of colorectal cancer.

REFERENCES

1 **Siegel R**, Ma J, Zou Z, Jemal A. Cancer statistics, 2014. *CA Cancer J Clin* 2014; **64**: 9-29 [PMID: 24399786 DOI: 10.3322/caac.21208]

2 **Ottaiano A**, Franco R, Aiello Talamanca A, Liguori G, Tatangelo F, Delrio P, Nasti G, Barletta E, Facchini G, Daniele B, Di Blasi A, Napolitano M, Ieranò C, Calemma R, Leonardi E, Albino V, De Angelis V, Falanga M, Boccia V, Capuozzo M, Parisi V, Botti G, Castello G, Vincenzo Iaffaioli R, Scala S. Overexpression of both CXC chemokine receptor 4 and vascular endothelial growth factor proteins predicts early distant relapse in stage II-III colorectal cancer patients. *Clin Cancer Res* 2006; **12**: 2795-2803 [PMID: 16675573 DOI: 10.1158/1078-0432.CCR-05-2142]

3 **Naithani R**, Huma LC, Moriarty RM, McCormick DL, Mehta RG. Comprehensive review of cancer chemopreventive agents evaluated in experimental carcinogenesis models and clinical trials. *Curr Med Chem* 2008; **15**: 1044-1071 [PMID: 18473802 DOI: 10.2174/092986708784221403]

4 **Wu H**, Dai Q, Shrubsole MJ, Ness RM, Schlundt D, Smalley WE, Chen H, Li M, Shyr Y, Zheng W. Fruit and vegetable intakes are associated with lower risk of colorectal adenomas. *J Nutr* 2009; **139**: 340-344 [PMID: 19091801 DOI: 10.3945/jn.108.098889]

5 **Kaur M**, Velmurugan B, Tyagi A, Deep G, Katiyar S, Agarwal C, Agarwal R. Silibinin suppresses growth and induces apoptotic death of human colorectal carcinoma LoVo cells in culture and tumor xenograft. *Mol Cancer Ther* 2009; **8**: 2366-2374 [PMID: 19638451 DOI: 10.1158/1535-7163.MCT-09-0304]

6 **Kroll DJ**, Shaw HS, Oberlies NH. Milk thistle nomenclature: why it matters in cancer research and pharmacokinetic studies. *Integr Cancer Ther* 2007; **6**: 110-119 [PMID: 17548790]

7 **Gazák R**, Walterová D, Kren V. Silybin and silymarin--new and emerging applications in medicine. *Curr Med Chem* 2007; **14**: 315-338 [PMID: 17305535 DOI: 10.2174/092986707779941159]

8 **Hackett ES**, Twedt DC, Gustafson DL. Milk thistle and its derivative compounds: a review of opportunities for treatment of liver disease. *J Vet Intern Med* 2013; **27**: 10-16 [PMID: 23140176 DOI: 10.1111/jvim.12002]

9 **Chu SC**, Chiou HL, Chen PN, Yang SF, Hsieh YS. Silibinin inhibits the invasion of human lung cancer cells via decreased productions of urokinase-plasminogen activator and matrix metalloproteinase-2. *Mol Carcinog* 2004; **40**: 143-149 [PMID: 15224346 DOI: 10.1002/mc.20018]

10 **Cui W**, Gu F, Hu KQ. Effects and mechanisms of silibinin on human hepatocellular carcinoma xenografts in nude mice. *World J Gastroenterol* 2009; **15**: 1943-1950 [PMID: 19399925 DOI: 10.3748/wjg.15.1943]

11 **Mohan S**, Dhanalakshmi S, Mallikarjuna GU, Singh RP, Agarwal R. Silibinin modulates UVB-induced apoptosis via mitochondrial proteins, caspases activation, and mitogen-activated protein kinase signaling in human epidermoid carcinoma A431 cells. *Biochem Biophys Res Commun* 2004; **320**: 183-189 [PMID: 15207719 DOI: 10.1016/j.bbrc.2004.05.153]

12 **Yang SH**, Lin JK, Chen WS, Chiu JH. Anti-angiogenic effect of silymarin on colon cancer LoVo cell line. *J Surg Res* 2003; **113**: 133-138 [PMID: 12943822 DOI: 10.1016/S0022-4804(03)00229-4]

13 **Singh RP**, Dhanalakshmi S, Tyagi AK, Chan DC, Agarwal C, Agarwal R. Dietary feeding of silibinin inhibits advance human prostate carcinoma growth in athymic nude mice and increases plasma insulin-like growth factor-binding protein-3 levels. *Cancer Res* 2002; **62**: 3063-3069 [PMID: 12036915]

14 **Zhou G**, Myers R, Li Y, Chen Y, Shen X, Fenyk-Melody J, Wu M, Ventre J, Doebber T, Fujii N, Musi N, Hirshman MF, Goodyear LJ, Moller DE. Role of AMP-activated protein kinase in mechanism of metformin action. *J Clin Invest* 2001; **108**: 1167-1174 [PMID: 11602624 DOI: 10.1172/JCI13505]

15 **Lee H**, Park HJ, Park CS, Oh ET, Choi BH, Williams B, Lee CK, Song CW. Response of breast cancer cells and cancer stem cells to metformin and hyperthermia alone or combined. *PLoS One* 2014; **9**: e87979 [PMID: 24505341 DOI: 10.1371/journal.pone.0087979]

16 **Bao B**, Wang Z, Ali S, Ahmad A, Azmi AS, Sarkar SH, Banerjee S, Kong D, Li Y, Thakur S, Sarkar FH. Metformin inhibits cell proliferation, migration and invasion by attenuating CSC function mediated by deregulating miRNAs in pancreatic cancer cells. *Cancer Prev Res* (Phila) 2012; **5**: 355-364 [PMID: 22086681 DOI: 10.1158/1940-6207.CAPR-11-0299]

17 **Kato K**, Gong J, Iwama H, Kitanaka A, Tani J, Miyoshi H, Nomura K, Mimura S, Kobayashi M, Aritomo Y, Kobara H, Mori H, Himoto T, Okano K, Suzuki Y, Murao K, Masaki T. The antidiabetic drug metformin inhibits gastric cancer cell proliferation in vitro and in vivo. *Mol Cancer Ther* 2012; **11**: 549-560 [PMID: 22222629 DOI: 10.1158/1535-7163.MCT-11-0594]

18 **Anisimov VN**, Berstein LM, Egormin PA, Piskunova TS, Popovich IG, Zabezhinski MA, Kovalenko IG, Poroshina TE, Semenchenko AV, Provinciali M, Re F, Franceschi C. Effect of metformin on life span and on the development of spontaneous mammary tumors in HER-2/neu transgenic mice. *Exp Gerontol* 2005; **40**: 685-693 [PMID: 16125352 DOI: 10.1016/j.exger.2005.07.007]

19 **Ben Sahra I**, Laurent K, Loubat A, Giorgetti-Peraldi S, Colosetti P, Auberger P, Tanti JF, Le Marchand-Brustel Y, Bost F. The antidiabetic drug metformin exerts an antitumoral effect in vitro and in vivo through a decrease of cyclin D1 level. *Oncogene* 2008; **27**: 3576-3586 [PMID: 18212742 DOI: 10.1038/sj.onc.1211024]

20 **Rattan R**, Graham RP, Maguire JL, Giri S, Shridhar V. Metformin suppresses ovarian cancer growth and metastasis with enhancement of cisplatin cytotoxicity in vivo. *Neoplasia* 2011; **13**: 483-491 [PMID: 21532889]

21 **Janjetovic K**, Harhaji-Trajkovic L, Misirkic-Marjanovic M, Vucicevic L, Stevanovic D, Zogovic N, Sumarac-Dumanovic M, Micic D, Trajkovic V. In vitro and in vivo anti-melanoma action of metformin. *Eur J Pharmacol* 2011; **668**: 373-382 [PMID: 21806981 DOI: 10.1016/j.ejphar.2011.07.004]

22 **Noto H**, Goto A, Tsujimoto T, Noda M. Cancer risk in diabetic patients treated with metformin: a systematic review and meta-analysis. *PLoS One* 2012; **7**: e33411 [PMID: 22448244 DOI: 10.1371/journal.pone.0033411]

23 **Smiechowski B**, Azoulay L, Yin H, Pollak MN, Suissa S. The use of metformin and colorectal cancer incidence in patients with type II diabetes mellitus. *Cancer Epidemiol Biomarkers Prev* 2013; **22**: 1877-1883 [PMID: 23966577 DOI: 10.1158/1055-9965.EPI-13-0196]

24 **Pernicova I**, Korbonits M. Metformin--mode of action and clinical implications for diabetes and cancer. *Nat Rev Endocrinol* 2014; **10**: 143-156 [PMID: 24393785 DOI: 10.1038/nrendo.2013.256]

25 **Lah JJ**, Cui W, Hu KQ. Effects and mechanisms of silibinin on human hepatoma cell lines. *World J Gastroenterol* 2007; **13**: 5299-5305 [PMID: 17879397 DOI: 10.3748/wjg.v13.i40.5299]

26 **Lee JJ**, Kong M, Ayers GD, Lotan R. Interaction index and

different methods for determining drug interaction in combination therapy. *J Biopharm Stat* 2007; **17**: 461-480 [PMID: 17479394 DOI: 10.1080/10543400701199593]
27 **Yu HC**, Chen LJ, Cheng KC, Li YX, Yeh CH, Cheng JT. Silymarin inhibits cervical cancer cell through an increase of phosphatase and tensin homolog. *Phytother Res* 2012; **26**: 709-715 [PMID: 22016029 DOI: 10.1002/ptr.3618]
28 **Sansal I**, Sellers WR. The biology and clinical relevance of the PTEN tumor suppressor pathway. *J Clin Oncol* 2004; **22**: 2954-2963 [PMID: 15254063 DOI: 10.1200/JCO.2004.02.141]
29 **Su CH**, Chen LJ, Liao JF, Cheng JT. Increase of phosphatase and tensin homolog by silymarin to inhibit human pharynx squamous cancer. *J Med Food* 2013; **16**: 778-784 [PMID: 23909904 DOI: 10.1089/jmf.2012.2534]
30 **Singh RP**, Dhanalakshmi S, Agarwal C, Agarwal R. Silibinin strongly inhibits growth and survival of human endothelial cells via cell cycle arrest and downregulation of survivin, Akt and NF-kappaB: implications for angioprevention and antiangiogenic therapy. *Oncogene* 2005; **24**: 1188-1202 [PMID: 15558015 DOI: 10.1038/sj.onc.1208276]
31 **Kaur M**, Velmurugan B, Tyagi A, Agarwal C, Singh RP, Agarwal R. Silibinin suppresses growth of human colorectal carcinoma SW480 cells in culture and xenograft through down-regulation of beta-catenin-dependent signaling. *Neoplasia* 2010; **12**: 415-424 [PMID: 20454513]
32 **Dilman VM**. Age-associated elevation of hypothalamic, threshold to feedback control, and its role in development, ageine, and disease. *Lancet* 1971; **1**: 1211-1219 [PMID: 4103080]
33 **Berstein LM**, Boyarkina MP, Teslenko SY. Familial diabetes is associated with reduced risk of cancer in diabetic patients: a possible role for metformin. *Med Oncol* 2012; **29**: 1308-1313 [PMID: 21298495 DOI: 10.1007/s12032-011-9840-0]
34 **Yasmeen A**, Beauchamp MC, Piura E, Segal E, Pollak M, Gotlieb WH. Induction of apoptosis by metformin in epithelial ovarian cancer: involvement of the Bcl-2 family proteins. *Gynecol Oncol* 2011; **121**: 492-498 [PMID: 21388661 DOI: 10.1016/j.ygyno.2011.02.021]
35 **Ma J**, Guo Y, Chen S, Zhong C, Xue Y, Zhang Y, Lai X, Wei Y, Yu S, Zhang J, Liu W. Metformin enhances tamoxifen-mediated tumor growth inhibition in ER-positive breast carcinoma. *BMC Cancer* 2014; **14**: 172 [PMID: 24612549 DOI: 10.1186/1471-2407-14-172]
36 **Kusmic C**, L'abbate A, Sambuceti G, Drummond G, Barsanti C, Matteucci M, Cao J, Piccolomini F, Cheng J, Abraham NG. Improved myocardial perfusion in chronic diabetic mice by the up-regulation of pLKB1 and AMPK signaling. *J Cell Biochem* 2010; **109**: 1033-1044 [PMID: 20108250 DOI: 10.1002/jcb.22486]
37 **Oudejans JJ**, Muris JJ, Meijer CJ. Inhibition of caspase 9 and not caspase 8 mediated apoptosis may determine clinical response to chemotherapy in primary nodal diffuse large B-cell lymphomas. *Cell Cycle* 2005; **4**: 526-528 [PMID: 15876872]
38 **Wang LW**, Li ZS, Zou DW, Jin ZD, Gao J, Xu GM. Metformin induces apoptosis of pancreatic cancer cells. *World J Gastroenterol* 2008; **14**: 7192-7198 [PMID: 19084933 DOI: 10.3748/wjg.14.7192]
39 **Kauntz H**, Bousserouel S, Gossé F, Raul F. Silibinin triggers apoptotic signaling pathways and autophagic survival response in human colon adenocarcinoma cells and their derived metastatic cells. *Apoptosis* 2011; **16**: 1042-1053 [PMID: 21779837 DOI: 10.1007/s10495-011-0631-z]
40 **Zakikhani M**, Dowling R, Fantus IG, Sonenberg N, Pollak M. Metformin is an AMP kinase-dependent growth inhibitor for breast cancer cells. *Cancer Res* 2006; **66**: 10269-10273 [PMID: 17062558 DOI: 10.1158/0008-5472.CAN-06-1500]
41 **Martin-Castillo B**, Vazquez-Martin A, Oliveras-Ferraros C, Menendez JA. Metformin and cancer: doses, mechanisms and the dandelion and hormetic phenomena. *Cell Cycle* 2010; **9**: 1057-1064 [PMID: 20305377 DOI: 10.4161/cc.9.6.10994]
42 **Yang CH**, Craise LM. Development of human epithelial cell systems for radiation risk assessment. *Adv Space Res* 1994; **14**: 115-120 [PMID: 11538024 DOI: 10.1016/0273-1177(94)90459-6]

P- Reviewer: Greenberger JS, Hsu LS, Kumiko S
S- Editor: Yu J **L- Editor**: Wang TQ **E- Editor**: Liu XM

World Journal of Gastroenterology

Submit a Manuscript: http://www.wjgnet.com/esps/
Help Desk: http://www.wjgnet.com/esps/helpdesk.aspx
DOI: 10.3748/wjg.v21.i14.4178

World J Gastroenterol 2015 April 14; 21(14): 4178-4183
ISSN 1007-9327 (print) ISSN 2219-2840 (online)

ORIGINAL ARTICLE

Basic Study

Anti-*Helicobacter pylori* activities of *Chenopodium ambrosioides* L. *in vitro* and *in vivo*

Hui Ye, Yu Liu, Ning Li, Jing Yu, Hong Cheng, Jiang Li, Xue-Zhi Zhang

Hui Ye, Ning Li, Jing Yu, Xue-Zhi Zhang, Department of Integrated Traditional Chinese Medicine, Peking University First Hospital, Beijing 100034, China
Yu Liu, Department of Traditional Chinese Medicine,Peking University International Hospital, Beijing 102206, China
Hong Cheng, Jiang Li, Department of Gastroenterology, Peking University First Hospital, Beijing 100034, China
Author contributions: Ye H and Liu Y contributed equally to this work; Ye H performed the *in vivo* experiments, analyzed the data and wrote the manuscript; Liu Y conducted *in vitro* experiments and data analysis; Li N and Yu J participated in animal feeding and *in vivo* sample collection; Cheng H and Li J directed the histologic observations; Zhang XZ reviewed and approved the article for publication; all of the authors read and approved the final version of the manuscript.
Supported by National Natural Science Foundation Project of China, No. 81072952.
Ethics approval: The study was reviewed and approved by the Peking University First Hospital Institutional Review Board.
Institutional animal care and use committee: All procedures involving animals were reviewed and approved by the Institutional Animal Care and Use Committee of the Peking University First Hospital (IACUC protocol number: J201150).
Conflict-of-interest: We declare that we have no competing financial or personal relationships with other people or organizations that can inappropriately influence our work.
Data sharing: Technical appendix, statistical code, and dataset available from the corresponding author at zhang.xuezhi@263.net. Participants gave informed consent for data sharing.

Correspondence to: Xue-Zhi Zhang, Professor, Department of Integrated Traditional Chinese Medicine, Peking University First Hospital, 8th Xishiku Street, Xicheng District, Beijing 100034, China. zhang.xuezhi@263.net
Telephone: +86-10-83572634
Fax: +86-10-83572931

Received: October 30, 2014
Peer-review started: October 31, 2014
First decision: November 14, 2014
Revised: December 9, 2014
Accepted: January 16, 2015
Article in press: January 16, 2015
Published online: April 14, 2015

Abstract

AIM: To investigate the bactericidal effects of *Chenopodium ambrosioides* L. (CAL) against *Helicobacter pylori* (*H. pylori*) both *in vitro* and *in vivo*.

METHODS: For *in vitro* experiments, the inhibitory activity of CAL was tested using an agar dilution method; *H. pylori* strain NCTC11637 was incubated on Columbia blood agar plates containing serial concentrations of CAL. The minimal inhibitory concentration (MIC) was determined by the absence of *H. pylori* colonies on the agar plate. Time-kill curves were used to evaluate bactericidal activity; the average number of colonies was calculated at 0, 2, 8 and 24 h after liquid incubation with concentrations of CAL at 0.5, 1, and 2 × MIC. For *in vivo* experiments, *H. pylori*-infected mice were randomly divided into CAL, triple therapy (lansoprazole, metronidazole, and clarithromycin), blank control, or *H. pylori* control groups. The eradication ratios were determined by positive findings from rapid urease tests (RUTs) and by histopathology.

RESULTS: *In vitro*, the MIC of CAL against *H. pylori* was 16 mg/L. The time-kill curves showed a stable and persistent decreasing tendency with increasing CAL concentration, and the intensity of the bactericidal effect was proportional to dose; the 1 and 2 × MIC completely inhibited the growth of *H. pylori* at 24 h. *In vivo*, the eradication ratios in the CAL group were

60% (6/10) by RUT and 50% (5/10) by histopathology. Ratios in the triple therapy group were both 70% (7/10), and there was no difference between the CAL and triple therapy groups. Histopathologic evaluation revealed massive bacterial colonization on the surface of gastric mucosa and slight infiltration of mononuclear cells after inoculation with *H. pylori*, but no obvious inflammation or other pathologic changes in gastric mucosa of mice from CAL and triple therapy groups.

CONCLUSION: CAL demonstrates effective bactericidal activity against *H. pylori* both *in vitro* and *in vivo*.

Key words: *Helicobacter pylori*; Bactericidal activity; *Chenopodium ambrosioides* L.; Phytotherapy

Core tip: The *Helicobacter pylori* (*H. pylori*) eradication rate of triple therapy has been markedly decreased due to increasing bacterial antibiotic resistance. Natural Chinese medicines, such as *Chenopodium ambrosioides* L. (a Chinese herb derived from Jinhua Weikang Capsule utilized for gastritis and peptic ulcers), represent complementary and collaborative therapies. This report demonstrates that *C. ambrosioides* has *in vitro* and *in vivo* bactericidal effects against *H. pylori*, and may be a good candidate for the treatment of *H. pylori* infection.

Ye H, Liu Y, Li N, Yu J, Cheng H, Li J, Zhang XZ. Anti-*Helicobacter pylori* activities of *Chenopodium ambrosioides* L. *in vitro* and *in vivo*. *World J Gastroenterol* 2015; 21(14): 4178-4183 Available from: URL: http://www.wjgnet.com/1007-9327/full/v21/i14/4178.htm DOI: http://dx.doi.org/10.3748/wjg.v21.i14.4178

INTRODUCTION

Helicobacter pylori (*H. pylori*) is the etiologic agent associated with many gastrointestinal diseases, such as chronic gastritis, peptic ulcers, gastric carcinoma, and mucosa-associated lymphoid tissue lymphoma. The eradication of *H. pylori* has thus been utilized as the primary treatment strategy of these diseases for three decades. In the past, standard triple therapy consisting of a proton pump inhibitor and two broad-spectrum antibiotics (usually amoxicillin, clarithromycin or metronidazole) was able to achieve eradication rates > 90%[1]. However, recent studies have demonstrated that the eradication rates of triple therapy have declined below 80%[2-5]. Among the factors causing this decline, antibiotic resistance (particularly clarithromycin and metronidazole resistance) is the primary cause. In China, the eradication rate decreased from 88.9% in 1996[6] to 73.5% in 2012[7], while the prevalence of antibiotic resistance to clarithromycin and metronidazole increased to 65.4% and 78.8%[8], 21.5% and 95.4%[9], and 20.7% and 42.2%[10], respectively, in various regions. Hence, alternative strategies, including sequential, concomitant, and bismuth-based quadruple therapies, have been proposed to counteract increasing antibiotic resistance rates. The updated Chinese guidance for *H. pylori* infection has recommended 10-14 d of bismuth-based quadruple therapy as the initial treatment[11]. However, the additional drugs and prolonged duration result in poorer compliance, severer adverse reactions, and higher costs for sufferers.

The Chinese guidance also describes the application of natural medicine as a complementary and collaborative therapy. The anti-*H. pylori* effects of dozens of herbs and formulas have been investigated, but the findings are limited by varying drug quality and sources, as well as the numerous and complicated components of formulas. Thus, a drug utilized clinically with simple ingredients, reliable and stable quality, and traceable sources of raw materials is an ideal choice. Jinghua Weikang Capsule (JWC) is a popular Chinese patent drug that consists of two ingredients, *Chenopodium ambrosioides* L. (CAL) and *Adina pilulifera* (AP). Our previous works demonstrated the inhibitory, bactericidal, and synergistic effects (with clarithromycin and metronidazole) of CAL against *H. pylori* strain 26695 and antibiotic-resistant strains isolated from patients suffering from *H. pylori*-associated gastric ulcers[12-14]. In addition, multicenter, randomized, controlled clinical trials demonstrated that *H. pylori* eradication of JWC-containing therapy was superior to standard triple therapy and equal to bismuth-based quadruple therapy[15,16]. These results indicate the synergistic effect of the drug, of which CAL is the major effective ingredient, with antibiotics. However, it is not known if CAL alone is capable of eradicating *H. pylori in vivo*. The intragastric environment differs dramatically from agar plates, thus the drug effect might be conflicting. This study investigated the bactericidal activities of CAL against *H. pylori in vivo* and *in vitro* to confirm the consistency effects in different environments.

MATERIALS AND METHODS

H. pylori strains and experimental animals

H. pylori strains (NCTC11637 and Sydney strain 1) were kindly provided by the Department of Gastroenterology of Peking University First Hospital and preserved in brain heart infusion broth (No. 783396; OXOID of Thermo Fisher Scientific, Waltham, MA, United States) at -80 ℃.

Forty-four specific-pathogen-free (SPF) male Kunming mice (18-22 g) were purchased from Viral River Laboratories (Beijing, China; Certification No. SCXK 2012-0001). All the animals were housed in an SPF environment and had free access to sterile neutral water and standard mouse feed. The experimental

procedures in this study were approved by the Experimental Animal Ethics Committee of Peking University First Hospital (Certification No. J201150).

Drugs and reagents

The volatile oil of CAL (No. 20110311; Tianjin Tasly Pharmaceutical Co., Ltd., Tianjin, China) was diluted in DMSO (Sinopharm Chemical Regent Co., Ltd., Shanghai, China). Lansoprazole (No. 20130205), metronidazole (No. 20120228), and clarithromycin (No. 20120704; Dalian Meilun Biology Technology Co., Ltd., Dalian, China) were used as the triple therapy control in animal experiments. Columbia blood agar plates with 5% sheep's blood (No. 20130205; bioMérieux Industry Ltd., France), Columbia agar (No. 848706), Brucella broth (No. 8170491), fetal calf serum (No. NTMO133) and brain heart infusion broth (OXOID) were prepared for *H. pylori* liquid culture and collection.

Culture and collection of H. pylori

Frozen stocks of *H. pylori* were recovered at room temperature, inoculated on the Columbia blood agar base, and incubated under a microaerobic environment (15% CO_2, 5% O_2, 80% N_2) at 37 ℃ with over 90% humidity for 48-72 h. The bacterial colonies were collected and prepared in Brucella broth with fetal calf serum for *in vitro* bactericidal tests, or in brain heart infusion broth for oral gavage of animals.

Inhibitory and bactericidal activities test

The inhibitory activity of CAL against the growth of *H. pylori* was assessed using an agar dilution method. Briefly, serial dilutions (1:2) of CAL were added to the Columbia blood agar for final concentrations starting from 512 mg/L down to 1 mg/L. The non-drug agar and DMSO agar served as negative controls. Agar plates were inoculated with *H. pylori* [NCTC11637; 3 × 10^8 colony forming units (CFU)/mL] and cultured for 72 h. The minimal inhibitory concentration (MIC) was defined as the minimal concentration of CAL required for complete inhibition of *H. pylori* growth.

Bactericidal activity was evaluated using time-kill curves with 0.5, 1.0 and 2.0 × MIC CAL, and blank and DMSO controls. *H. pylori* (NCTC11637; 0.1 mL at 1 × 10^6 CFU/mL) was added to 90 mm plates with the calculated concentrations of CAL or DMSO and Brucella broth containing fetal calf serum (final volume 10 mL) and cultured with gentle shaking at 37 ℃ in a microaerobic environment. At 0, 4, 8 and 24 h, 0.5 mL of liquid was removed, serially diluted, and plated on Columbia blood agar plates (n = 2 per group). The colonies were counted and averaged after 72 h incubation.

In vivo inoculation

Mice (n = 44) were randomly divided into four groups: blank control, *H. pylori* control, CAL, and triple therapy group. Except for the blank controls, all animals received a single intraperitoneal injection of cyclophosphamide (200 mg/kg), followed by a total of five gastric intubations (every other day) with 0.4 mL of *H. pylori* (Sydney strain 1; 12 × 10^8 CFU/mL). Animals were fasted 24 h before and 2 h after each inoculation. Two weeks after the last inoculation, one mouse was randomly selected from each group and sacrificed to test the bacterial colonization by rapid urease test (RUT) and hematoxylin and eosin (HE) staining of gastric tissue. Giemsa staining was performed to detect *H. pylori* colonization when HE results were unclear.

Drug administration

Drug doses used in *in vivo* experiments are equivalent to clinical administrations. The CAL group was treated with 49.32 mg/kg daily for 4 wk. The triple therapy group was treated daily with a suspension of lansoprazole (12.33 mg/kg), metronidazole (164.40 mg/kg), and clarithromycin (205.54 mg/kg) for 1 wk. The *H. pylori* group was given the same volume of sterile water, and the blank control group was free of any gavage. All drugs were suspended in sterile water and administrated by gastric intubation.

Determination of H. pylori colonization and gastric inflammation

Four weeks after inoculation, animals were deprived of feed but allowed free access to water for 24 h and then sacrificed. Stomachs were collected at the time of sacrifice, opened at the side of the greater curvature, and washed with 4 ℃ PBS. Half of the antral section was isolated for RUT determination at room temperature within 24 h to observe the change to pink color as positive. The second half of the antral section and partial gastric body tissue were fixed in formaldehyde for histopathology. Fixed tissues were embedded in paraffin, sectioned, and stained with HE or Giemsa to determine inflammation and degree of *H. pylori* colonization. Eradication success was determined by negative findings from both RUT and histopathology.

The degrees of *H. pylori* colonization and inflammation were scored by a pathologist blind to treatment groups using the visual analogue scale of the updated Sydney System[17]. *H. pylori* colonization was graded as: 0, no bacteria detected; +, occasional or several bacterial colonies distributed within 1/3 of the specimen length; ++, consecutive but thin bacterial colonization in the mucosal surface between 1/3 and 2/3 specimen length; +++, piles of bacterial colonies along the length of the specimen. Mononuclear infiltration in the gastric mucosa was graded as: 0, < 5 mononuclear cells in each high power field; +, few mononuclear cells restricted to superficial layer within 1/3 of the mucosa; ++, moderate mononuclear infiltration within 2/3 of the mucosa; +++, intensive

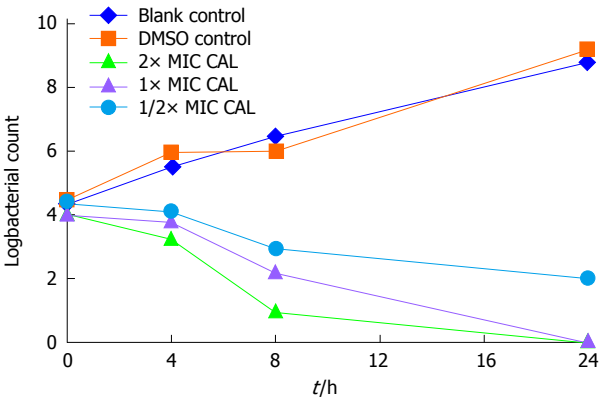

Figure 1 Time-kill curves of *Chenopodium ambrosioides* L. at different concentrations. MIC: Minimal inhibitory concentration; CAL: *Chenopodium ambrosioides* L.

mononuclear infiltration throughout the mucosa.

Statistical analysis

Eradication rates were compared among groups by a Fisher's exact test using SPSS 20.0 software (IBM Corp., Armonk, NY, United States). $P < 0.05$ was considered as statistically significant.

RESULTS

In vitro

Results of the *in vitro* inhibitory activity test indicated that there was no visible growth of bacterial colonies after 72 h incubation on the plate containing 16 mg/L CAL, thus defined as the MIC of CAL. Construction of the time-kill curve reveals continual growth of *H. pylori* colonies in blank and DMSO control groups, but marked inhibition in a dose-dependent manner with CAL (Figure 1). No *H. pylori* colonies could be detected at 24 h in the 1 and 2 × MIC CAL groups.

In vivo

H. pylori eradication rates, as determined by RUT and histopathology, are presented in Table 1. There was no significant difference between CAL and the triple therapy groups ($P = 0.650$). *H. pylori* colonization and inflammation scores are presented in Table 2. Images of HE staining are shown in Figure 2.

Table 1 Negative rapid urease test and histopathology results

Group	RUT (*n*)	Histopathology (*n*)	Eradication ratio
Blank control	10	10	-
Helicobacter pylori	0	0	0/10
Chenopodium ambrosioides L.	6	5	5/10[1]
Triple therapy	7	7	7/10

[1]The P value is 0.650, *vs* triple therapy. $n = 10$/group. RUT: Rapid urease test.

Table 2 *Helicobacter pylori* colonization and gastric inflammation scores

Group	*H. pylori* colonization				Gastric inflammation			
	0	+	++	+++	0	+	++	+++
Blank control	10	0	0	0	10	0	0	0
H. pylori	4	5	1	0	7	3	0	0
CAL	5	5	0	0	8	2	0	0
Triple therapy	7	3	0	0	10	0	0	0

$n = 10$/group. CAL: *Chenopodium ambrosioides* L.; *H. pylori*: *Helicobacter pylori*.

DISCUSSION

In China, the prevalence of *H. pylori* infection is 56.22%[18], which is higher than the global level. Bismuth-based quadruple therapy has become the preferred therapeutic regimen for *H. pylori* eradication because of increasing antibiotic resistance. However, adverse effects and poor compliance necessitate the development of alternative therapies. Traditional Chinese herbs can promote relief of symptoms as well as producing anti-*H. pylori* activities. However, the active ingredient is not always obvious, and the *in vitro* efficacy does not always correlate with eradication in animal models[19].

JWC has been utilized for gastritis and peptic ulcers, with effects of regulating qi, dissipating cold, clearing heat, and resolving stasis according to Chinese medicine theory. Our previous work indicated that CAL was the active ingredient in JWC[12], which was confirmed by the *in vitro* experiments in the present study. To eliminate possible effects of Tween-80 used in the previous study, we utilized DMSO, which showed no effect on *H. pylori* growth. The MIC of 16 mg/L was sufficient to completely eliminate *H. pylori* after 24 h. The *in vivo* experiments demonstrate the clinical potential of CAL for *H. pylori* eradication, with efficacy equivalent to the triple therapy.

Despite the promising results, the eradication with CAL was not ideal, possibly be due to the acidic environment of the mucous layer of stomach, or an insufficient dose converted from clinical usage. Furthermore, the conspicuous and classic mucosal inflammation was not observed in this study, which might be ascribed to the short infection period and the application of cyclophosphamide. The conclusion that the effect of CAL rivals triple therapy should be made prudently due to the small sample size. Furthermore, the mice may have had other bacterial species present, as *H. hepaticus* has been detected in 19.2%-29.5% of SPF mice in China[20,21]. In order to eliminate the interference of other *Helicobacter* spp., a PCR test should be added in future studies.

In our previous random clinical trial, the therapy containing JWC, a proton pump inhibitor, amoxicillin, and clarithromycin achieved a higher eradication ratio than triple therapy[15]. CAL is a complex compound, for

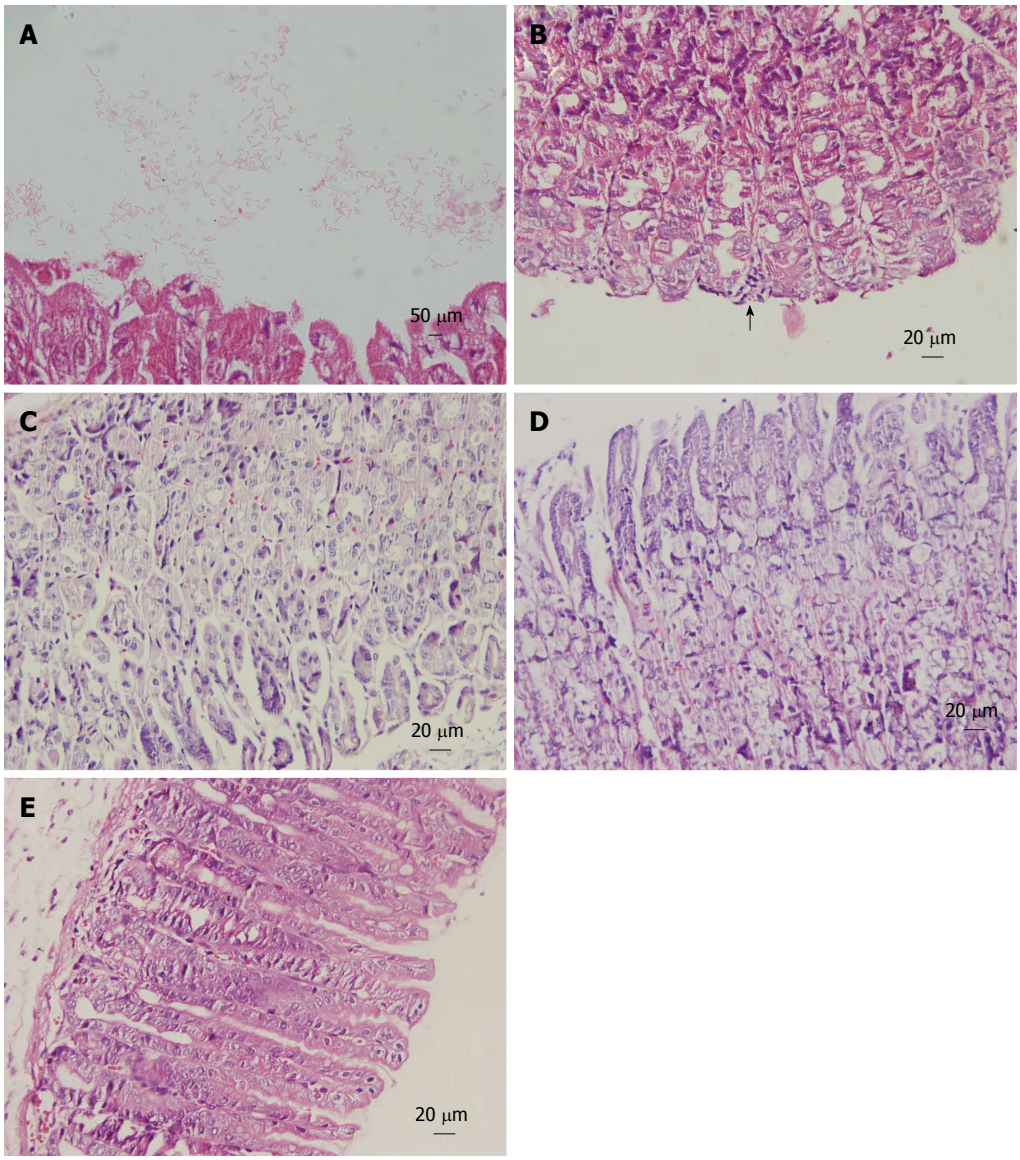

Figure 2 Histopathology of gastric mucosa. Hematoxylin and eosin staining of gastric mucosa from mice inoculated with *Helicobacter pylori*. A: *Helicobacter pylori* (*H. pylori*) colonization on the surface of gastric mucosa (magnification × 100); B: Mononuclear cell infiltrates (arrow; magnification × 40); C: Uninfected mice exhibit a normal gastric mucosa (magnification × 40); D: Treatment with *Chenopodium ambrosioides* L. for 4 wk revealed no obvious inflammation (magnification × 40); E: Treatment with lansoprazole, metronidazole and clarithromycin for 1 wk showed no pathologic changes (magnification × 40).

which the effective composition remains undiscovered. Hence, further research to identify the active ingredients would be helpful to evaluate and improve the intensity of the effect. Nevertheless, this study confirms the *in vitro* and *in vivo* anti-*H. pylori* effects of CAL, providing experimental support for future human trials.

ACKNOWLEDGMENTS

We would like to thank Institute of Clinical Pharmacology Peking University for kindly providing facilities.

COMMENTS

Background

Helicobacter pylori (*H. pylori*) infects more than half of the human population, causing a global public health issue associated with gastritis, peptic ulcer, gastric carcinoma, mucosa-associated lymphoid tissue lymphoma, and other diseases. Successful eradication of bacteria is the effective approach to cure related diseases or to improve prognosis. Antibiotic resistance has become the leading cause of treatment failure, thus new regimens or medicines are required.

Research frontiers

Alternative and complementary treatment approaches including phytomedicine have been focused on eradicating *H. pylori* or enhancing the bactericidal effect of antibiotics. Various basic and clinical studies have been performed to explore the anti-*H. pylori* effect of herbs and patent medicines, and some of these traditional therapies have enormous potential. Testing the bactericidal activity or the synergistic effect with antibiotics *in vitro* and *in vivo* will provide additional evidence.

Innovations and breakthroughs

This study demonstrates the *in vitro* and *in vivo* anti-*H. pylori* effect of *Chenopodium ambrosioides* L. (CAL), derived from the Chinese patent medicine, Jinghua Weikang Capsule. The *in vivo* bactericidal activity was reported for the first time. The effect on *H. pylori* eradication was equivalent to

that of a triple therapy.

Applications

Chenopodium ambrosioides L. has been utilized for gastritis and peptic ulcers under the guidance of traditional Chinese theory. The authors' research provides experimental evidence for further clinical study of this compound, and the possible application for treating *H. pylori* infection.

Terminology

The agar dilution method provides the minimal inhibitory concentration of an antimicrobial agent. The time-kill curve method indicates the bactericidal effect of a testing agent.

Peer-review

This study investigated *in vitro* and *in vivo* the bactericidal activities against *H. pylori* strains using a Chinese patent drug containing the volatile oil of CAL. Currently, there is interest in alternative treatments for *H. pylori* infection due to the high resistance to antibiotics used as the gold standard.

REFERENCES

1 **Malfertheiner P**, Megraud F, O'Morain CA, Atherton J, Axon AT, Bazzoli F, Gensini GF, Gisbert JP, Graham DY, Rokkas T, El-Omar EM, Kuipers EJ. Management of Helicobacter pylori infection--the Maastricht IV/ Florence Consensus Report. *Gut* 2012; **61**: 646-664 [PMID: 22491499 DOI: 10.1136/gutjnl-2012-302084]

2 **Qua CS**, Manikam J, Goh KL. Efficacy of 1-week proton pump inhibitor triple therapy as first-line Helicobacter pylori eradication regime in Asian patients: is it still effective 10 years on? *J Dig Dis* 2010; **11**: 244-248 [PMID: 20649738 DOI: 10.1111/j.1751-2980.2010.00445.x]

3 **Sasaki M**, Ogasawara N, Utsumi K, Kawamura N, Kamiya T, Kataoka H, Tanida S, Mizoshita T, Kasugai K, Joh T. Changes in 12-Year First-Line Eradication Rate of Helicobacter pylori Based on Triple Therapy with Proton Pump Inhibitor, Amoxicillin and Clarithromycin. *J Clin Biochem Nutr* 2010; **47**: 53-58 [PMID: 20664731 DOI: 10.3164/jcbn.10-10]

4 **Sokwala A**, Shah MV, Devani S, Yonga G. Helicobacter pylori eradication: A randomised comparative trial of 7-day versus 14-day triple therapy. *S Afr Med J* 2012; **102**: 368-371 [PMID: 22668909]

5 **Zhou L**, Zhang J, Chen M, Hou X, Li Z, Song Z, He L, Lin S. A comparative study of sequential therapy and standard triple therapy for Helicobacter pylori infection: a randomized multicenter trial. *Am J Gastroenterol* 2014; **109**: 535-541 [PMID: 24642580 DOI: 10.1038/ajg.2014.26]

6 **Zhou L**, Sung JJ, Lin S, Jin Z, Ding S, Huang X, Xia Z, Guo H, Liu J, Chao W. A five-year follow-up study on the pathological changes of gastric mucosa after H. pylori eradication. *Chin Med J* (Engl) 2003; **116**: 11-14 [PMID: 12667379]

7 **Xue Y**, Feng H, Zhou LY, Yang XL, Lin SR, Wang YC. Analysis of related factors of H.pylori eradication therapy efficiency. *Zhongguo Shiyong Neike Zazhi* 2012; **32**: 693-695

8 **Gao W**, Cheng H, Hu F, Li J, Wang L, Yang G, Xu L, Zheng X. The evolution of Helicobacter pylori antibiotics resistance over 10 years in Beijing, China. *Helicobacter* 2010; **15**: 460-466 [PMID: 21083752 DOI: 10.1111/j.1523-5378.2010.00788.x]

9 **Su P**, Li Y, Li H, Zhang J, Lin L, Wang Q, Guo F, Ji Z, Mao J, Tang W, Shi Z, Shao W, Mao J, Zhu X, Zhang X, Tong Y, Tu H, Jiang M, Wang Z, Jin F, Yang N, Zhang J. Antibiotic resistance of Helicobacter pylori isolated in the Southeast Coastal Region of China. *Helicobacter* 2013; **18**: 274-279 [PMID: 23418857 DOI: 10.1111/hel.12046]

10 **Sun QJ**, Liang X, Zheng Q, Gu WQ, Liu WZ, Xiao SD, Lu H. Resistance of Helicobacter pylori to antibiotics from 2000 to 2009 in Shanghai. *World J Gastroenterol* 2010; **16**: 5118-5121 [PMID: 20976850]

11 **Liu WZ**, Xie Y, Cheng H, Lu NH, Hu FL, Zhang WD, Zhou LY, Chen Y, Zeng ZR, Wang CW, Xiao SD, Pan GZ, Hu PJ. Fourth Chinese National Consensus Report on the management of Helicobacter pylori infection. *J Dig Dis* 2013; **14**: 211-221 [PMID: 23302262 DOI: 10.1111/1751-2980.12034]

12 **Huang XT**, Zhang XZ, Li N, Cheng H. In vitro activity of Jinghuaweikang capsules against clinical isolates of antibiotic-resistant Helicobacter pylori. *Zhongguo Zhongxiyi Jiehe Xiaohua Zazhi* 2010; **18**: 290-293

13 **Liu W**, Zhang XZ, Li N, Li J. Bactericidal action of chenopodium ambrosioides combined with clarithromycin and metronidazole for Helicobacter pylori. *Zhongguo Zhongxiyi Jiehe Xiaohua Zazhi* 2011; **19**: 281-284

14 **Liu W**, Liu Y, Zhang XZ, Li N, Cheng H. In vitro bactericidal activity of Jinghua Weikang Capsule and its individual herb Chenopodium ambrosioides L. against antibiotic-resistant Helicobacter pylori. *Chin J Integr Med* 2013; **19**: 54-57 [PMID: 23275015 DOI: 10.1007/s11655-012-1248-y]

15 **Hu FL**, Cheng H, Zhang XZ, An HJ, Sheng JQ, Lü NH, Xie Y, Chen ZS, Xu JM, Hu NZ, Zheng PY, Zhang L, Zhang LX, Zhang SS, Tao L, Zhang ZY, Cui MH, Yang GB, Wang BM, Jiang K, Yang Q, Gao HJ. [Jinghuaweikang capsules combined with triple therapy in the treatment of Helicobacter pylori associated gastritis and duodenal ulcer and analysis of antibiotic resistance: a multicenter, randomized, controlled, clinical study]. *Zhonghua Yixue Zazhi* 2012; **92**: 679-684 [PMID: 22781295]

16 **Wang TT**, Zhang YM, Zhang XZ, Cheng H, Hu FL, Han HX, Chen XW, Li JX, Lai YL, Liu Y. [Jinghuaweikang gelatin pearls plus proton pump inhibitor-based triple regimen in the treatment of chronic atrophic gastritis with Helicobacter pylori infection: a multicenter, randomized, controlled clinical study]. *Zhonghua Yixue Zazhi* 2013; **93**: 3491-3495 [PMID: 24521887 DOI: 10.3969/j.issn.1671-038X.2013.11.008]

17 **Dixon MF**, Genta RM, Yardley JH, Correa P. Classification and grading of gastritis. The updated Sydney System. International Workshop on the Histopathology of Gastritis, Houston 1994. *Am J Surg Pathol* 1996; **20**: 1161-1181 [PMID: 8827022]

18 **The Team of Collaboration of Helicobacter pylori research in China**. Prevalence of Helicobacter pylori infection in China. *Xiandai Xiaohua and Jieru Zhenliao* 2010; **15**: 265-270 [DOI: 10.3969/j.issn.1672-2159.2010.05.001]

19 **Vale FF**, Oleastro M. Overview of the phytomedicine approaches against Helicobacter pylori. *World J Gastroenterol* 2014; **20**: 5594-5609 [PMID: 24914319 DOI: 10.3748/wjg.v20.i19.5594]

20 **Ding C**, Feng J, Xie JY, Gao C, Hu JH. An Epidemiological Survey of Helicobacter spp. in Laboratory Mice and Rats in the Area around Shanghai by Two Detection Methods. *Zhongguo Bijiao Yixue Zazhi* 2011; **21**: 66-69, 78 [DOI: 10.3969/j.issn.1671.7856.2011.012.016]

21 **Ji SW**, Wang S, Wang JB, Zhang YG. Investigation of Helicobacter hepaticus infection in various species of mice in China. *Zhonghua Xiaohua Zazhi* 2010; **30**: 597-601 [DOI: 10.3760/cma.j.issn.0254-1432.2010.09.006]

P- Reviewer: Chmiela M, Servin AL **S- Editor**: Ma YJ
L- Editor: O'Neill M **E- Editor**: Ma S

World Journal of Gastroenterology

Submit a Manuscript: http://www.wjgnet.com/esps/
Help Desk: http://www.wjgnet.com/esps/helpdesk.aspx
DOI: 10.3748/wjg.v21.i14.4184

World J Gastroenterol 2015 April 14; 21(14): 4184-4194
ISSN 1007-9327 (print) ISSN 2219-2840 (online)

ORIGINAL ARTICLE

Basic Study

Early activated hepatic stellate cell-derived molecules reverse acute hepatic injury

Wen-Ju Chang, Lu-Jun Song, Tuo Yi, Kun-Tang Shen, Hong-Shan Wang, Xiao-Dong Gao, Min Li, Jian-Min Xu, Wei-Xin Niu, Xin-Yu Qin

Wen-Ju Chang, Lu-Jun Song, Tuo Yi, Kun-Tang Shen, Hong-Shan Wang, Xiao-Dong Gao, Min Li, Jian-Min Xu, Wei-Xin Niu, Xin-Yu Qin, Department of General Surgery, Zhongshan Hospital, Institute of General Surgery, Fudan University, Shanghai 200032, China

Author contributions: Chang WJ and Qin XY designed the research; Chang WJ, Song LJ, and Yi T performed the research; Shen KT, Wang HS, Gao XD, and Li M contributed new reagents or analytic tools; Xu JM and Niu WX analyzed the data; Chang WJ and Yi T wrote the paper; Chang WJ, Song LJ, and Yi T contributed equally to this work.

Supported by Doctoral Fund of the Ministry of Education, No. 20130071110041; Young Investigator Funding of Zhongshan Hospital, No. 2014ZSQN37.

Ethics approval: The study was reviewed and approved by the Zhongshan Hospital Review Board.

Institutional animal care and use committee: All procedures involving animals were reviewed and approved by the Institutional Animal Care and Use Committee of the Zhongshan Hospital, Fudan University (IACUC protocol number: Y2013-0019).

Conflict-of-interest: The authors have no conflict of interest related to the manuscript.

Data sharing: No additional data are available.

Correspondence to: Xin-Yu Qin, MD, Department of General Surgery, Zhongshan Hospital, Institute of General Surgery, Fudan University, No. 220 Handan Road, Shanghai 200032, China. qin.xinyu@zs-hospital.sh.cn
Telephone: +86-21-64041990
Fax: +86-21-64037224

Received: September 26, 2014
Peer-review started: September 29, 2014
First decision: October 29, 2014
Revised: December 16, 2014
Accepted: January 16, 2015
Article in press: January 16, 2015
Published online: April 14, 2015

Abstract

AIM: To test whether hepatic stellate cells (HSCs) at different activation stages play different roles in acetaminophen (APAP)-induced acute liver injury (ALI).

METHODS: HSCs were isolated from mouse liver and cultured *in vitro*. Morphological changes of initiation HSCs [HSCs (5d)] and perpetuation HSCs [HSCs (p3)] were observed by immunofluorescence and transmission electron microscopy. The protective effects of HSC-derived molecules, cell lysates and HSC-conditioned medium (HSC-CM) were tested *in vivo* by survival and histopathological analyses. Liver injury was determined by measuring aminotransferase levels in the serum and by histologic examination of tissue sections under a light microscope. Additionally, to determine the molecular mediators of the observed protective effects of initiation HSCs, we examined HSC-CM using a high-density protein array.

RESULTS: HSCs (5d) and HSCs (p3) had different morphological and phenotypic traits. HSCs (5d) presented a star-shaped appearance with expressing α-SMA at non-uniform levels between cells. However, HSCs (p3) evolved into myofibroblast-like cells without lipid droplets and expressed a uniform and higher level of α-SMA. HSC-CM (5d), but not HSC-CM (p3), provided a significant survival benefit and showed a dramatic reduction of hepatocellular necrosis and panlobular leukocyte infiltrates in mice exposed to APAP. However, this protective effect was abrogated at higher cell masses, indicating a therapeutic window of effectiveness. Furthermore, the protein array screen

revealed that HSC-CM (5d) was composed of many chemokines and growth factors that correlated with inflammatory inhibition and therapeutic activity. When compared with HSC-CM (p3), higher levels of monocyte chemoattractant protein-1, macrophage inflammatory protein-1γ, hepatocyte growth factor, interleukin-10, and matrix metalloproteinase-2, but lower levels of stem cell factor and Fas-Ligand were observed in HSC-CM (5d).

CONCLUSION: These data indicated that initiation HSCs and perpetuation HSCs were different in morphology and protein expression, and provided the first experimental evidence of the potential medical value of initiation HSC-derived molecules in the treatment of ALI.

Key words: Hepatic stellate cells; Acute liver injury; Initiation and perpetuation

Core tip: In this study, we isolated hepatic stellate cells (HSCs) from mice by *in situ* perfusion of the liver and created primary and secondary cultures in plastic tissue culture dishes. Then, we observed different morphologies and phenotypes between initiation HSCs and perpetuation HSCs and described the first use of molecules secreted from HSCs in acetaminophen-induced acute liver injury. Initiation HSC-derived molecules showed hepatocyte-protective effects. Our findings provide novel insight into the mechanisms of HSCs in liver injury therapy. Whether the potential value of initiation HSC-derived molecular therapy is derived from the effect of a single cytokine or a combination of cytokines should be explored in future.

Chang WJ, Song LJ, Yi T, Shen KT, Wang HS, Gao XD, Li M, Xu JM, Niu WX, Qin XY. Early activated hepatic stellate cell-derived molecules reverse acute hepatic injury. *World J Gastroenterol* 2015; 21(14): 4184-4194 Available from: URL: http://www.wjgnet.com/1007-9327/full/v21/i14/4184.htm DOI: http://dx.doi.org/10.3748/wjg.v21.i14.4184

INTRODUCTION

Hepatic stellate cells (HSCs), first described by Kupffer in 1876, have emerged in the past 30 years as remarkably versatile mesenchymal cells[1]. Previous studies have explored the importance of HSCs in liver fibrosis, because HSC activation into myofibroblasts is thought to be the major step in hepatic fibrogenesis associated with liver injury[2]. Beyond this well-known characteristic, however, many newly discovered activities have led to a greater understanding of this fascinating cell type and the complexity of cellular homeostasis in the liver[3].

The hepatocyte protecting effects of HSCs in acute liver injury (ALI) has ignited growing interest[4]. We previously performed loss-of-function studies by depleting activated HSCs with gliotoxin in acetaminophen (APAP)-induced ALI in mice[5]. We demonstrated that severe liver damage and decreased survival rate were correlated with depletion of activated HSCs. These data provided clear evidence that activated HSCs are involved in both hepatocyte death and proliferation of hepatocytes and hepatic progenitor cells (HPCs) in APAP-induced ALI.

Quiescent HSCs, characterized by retinoid droplets in the cytoplasm, are present in the space of Disse in close contact with hepatocytes and sinusoidal endothelial cells. When HSCs are activated, they lose retinoid, move from the space of Disse to sites of damage (where the activated HSCs differentiate into myofibroblasts), and secrete extracellular matrix and growth factors that are involved in liver regeneration[6]. Because of the close anatomic relationship between HSCs and epithelial cells (hepatocytes and HPCs), HSCs are part of the stem cell niche and directly contact epithelial cells to participate in the early phase of hepatocyte regeneration[7]. However, it is unclear whether the products of activated HSCs are required to attenuate acute hepatocyte injury. In addition, in the process of differentiation from quiescent HSCs to fully activated HSCs (myofibroblasts), the cells change in morphology and phenotype, but it is not known whether those different stages of cells have different effects on protecting hepatocytes from acute injury. To the best of our knowledge, no previous studies have tried to answer that question.

In this study, we isolated HSCs from mice by *in situ* perfusion of the liver and created primary and secondary cultures in plastic tissue culture dishes. Then, the differences in morphology and phenotypic features were observed between activated HSCs at early stage and later stage. Furthermore, we investigated whether molecules produced by activated HSCs would protect hepatocytes in APAP-induced ALI, and analyzed the difference in the HSC secretome between the early and late stages by a protein array screen.

MATERIALS AND METHODS

Animals

Male C57BL/6J mice (6-8-wk-old, weighing 20 ± 2 g) were purchased from the Shanghai Laboratory Animal Center, Chinese Academy of Sciences. All of the animals were maintained in the animal facility of Zhongshan Hospital, Fudan University. The mice were kept on a 12-h light/dark cycle with access to mouse chow and water *ad libitum*. All surgery was performed under a mixture anesthesia of ketamine (80 mg/kg, Hengrui Medicine, Lianyungang, China) and xylazine (30 mg/kg, Sigma-Aldrich, St. Louis, MO,

United States) given intraperitoneally, and all efforts were made to minimize suffering. The experimental protocol was approved by the Animal Care and Use Committee of Fudan University. All animals were handled in accordance with the Guide for the Care and Use of Laboratory Animals published by the National Institutes of Health.

Isolation and cultivation of HSCs

HSCs were isolated from mouse livers as we described before[8]. Briefly, C57BL/6J mice livers were perfused in situ, and the HSCs were isolated by an optimized density gradient centrifugation technique. HSCs were seeded in high-glucose Dulbecco's Modified Eagle Medium (DMEM, Gibco, New York, United States) containing 10% fetal bovine serum (FBS, Sigma-Aldrich, Poole, United Kingdom). The cells were incubated at 37 ℃ in a humidified atmosphere with 5% carbon dioxide. The primary HSCs cultured for 5 d were defined as HSCs (5d), and after being passaged three generations, HSCs were defined as HSCs (P3).

Preparation and delivery of cells, cell lysates and conditioned medium

Cellular lysates were prepared by sonication (VWR Scientific, West Chester, PA). The dose of cells administered was 2×10^6 per subject. Conditioned medium was prepared by collecting serum-free medium (high-glucose DMEM without FBS; supplemented with 0.05% bovine serum albumin (BSA) to prevent protein aggregation) after 24-h culture of different cell masses. The majority of experiments were performed with the optimal cell mass of 2×10^6 cells. Supernatants were centrifuged and filtered to eliminate potential cell bodies. The medium was then concentrated approximately 25-fold using ultrafiltration units (Amicon Ultra-PL 3, Millipore, Bedford, MA, United States) with a 3 kDa molecular weight cut-off. Finally, the collected medium, containing paracrine molecules (HSC-CM), was stored at -80 ℃ until use.

Immunofluorescence

HSCs (5d) and HSCs (P3) grown in 35-mm tissue culture plates were fixed with ice-cold 2% methanol for 10 min at 4 ℃. After blocking with 5% BSA (Sigma Aldrich, St. Louis, MO, United States) in PBS, cells were incubated with mouse monoclonal anti-α-SMA IgG (Abcam, Cambridge, MA; 1:100) or rabbit anti-desmin (Abcam, Cambridge, MA; 1:100) for 2 h at room temperature, followed by development with donkey anti-mouse Alexa Fluor 488 (Invitrogen, Carlsbad, California, United States; 1:500) or donkey anti-rabbit Alexa Fluor 594 (Invitrogen, Carlsbad, California, United States; 1:500) for 30 min at room temperature, respectively. All plates were examined under an Axiovert 200 (Carl-Zeiss, Jena, Germany) using a computer-assisted image analysis program (AxioVision Ver. 4.0; Carl-Zeiss).

Transmission electron microscopy

HSCs (5d) and HSCs (P3) were harvested by trypsinization and centrifugation for 10 min at 1000 *g* at room temperature. Cells were fixed in 2.5% glutaraldehyde for 1 h at 4 ℃ and postfixed with 1% osmic acid for 30 min. Cells were then stained with lead-uranium, and the ultrastructural organization was observed with a transmission electron microscope (JEM-1200EX, Japan).

APAP administration

All animals were fasted overnight before APAP treatment (Sigma-Aldrich, St. Louis, MO, United States). ALI was induced by intraperitoneal injection of APAP in phosphate-buffered saline (PBS, Gibco, New York, United States) at a dose of 750 mg/kg. Blood samples were obtained at 12, 24, 36, and 48 h after injection by retro-orbital puncture for analysis of liver enzyme levels. Mice were sacrificed 24 h after injection by cervical dislocation under a mixture anesthesia of ketamine and xylazine, and liver tissues were harvested and fixed with 4% paraformaldehyde (Sigma-Aldrich, St. Louis, MO, United States) for histological analysis.

Administration of paracrine molecules

To assess the protective effect of paracrine molecules (HSC-CM) on ALI, after one dose of APAP treatment, all animals were randomly divided into three groups: an HSC-CM (5d) group, an HSC-CM (P3) group and a control group. Two hours after APAP injection, the HSC-CM (5d) group and HSC-CM (P3) group were treated with one dose of paracrine molecules of HSCs (5d) (0.20 mL, about 2×10^6 HSCs) and paracrine molecules of HSCs (P3) (0.20 mL, about 2×10^6 HSCs), respectively, *via* tail vein injection. Control animals received the same volume of blank conditioned medium (0.2 mL, high-glucose DMEM). Four animals per group were sacrificed 24 h later to collect liver tissue, and 13 animals per group were used for survival analysis. Blood samples were collected 12, 24, 36, and 48 h after treatment by retro-orbital puncture for analysis of liver enzyme release levels. The survival analysis was set for 7 d and animal survival was monitored every 12 h. On 7 d after administration of paracrine molecules, the end-point for the survival experiment was reached and the survival rate was analyzed, and all survival mice were sacrificed by cervical dislocation under a mixture anesthesia of ketamine and xylazine.

Assessment of liver injury

Liver injury was determined by measuring aminotransferase levels in the serum and by histologic examination of tissue sections under a light microscope. Serum samples were stored at -80 ℃ until use. Alanine aminotransferase (ALT) and aspartate aminotransferase (AST) were measured using Infinity

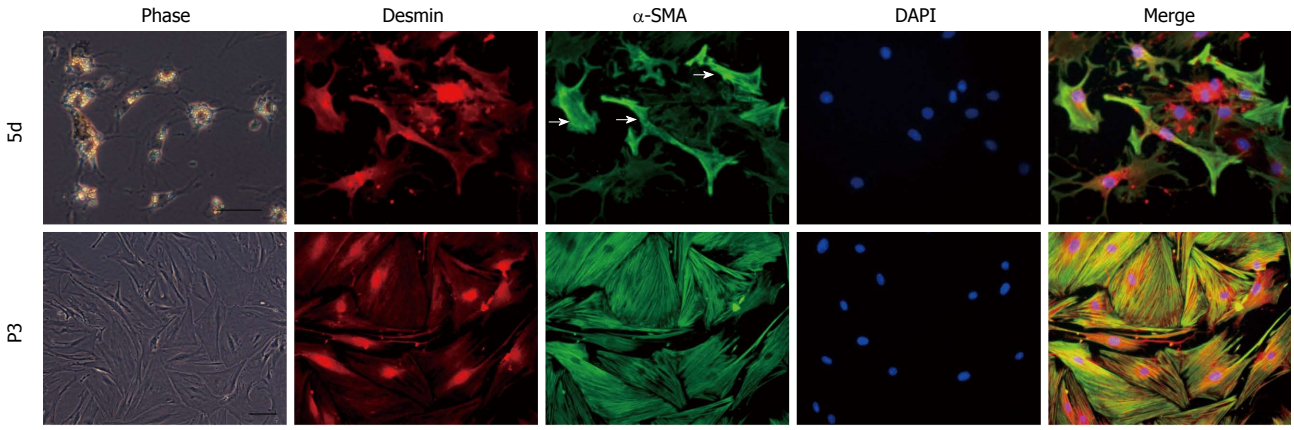

Figure 1 Morphological features and α-SMA expression of cultured hepatic stellate cells during the activation process. Primary hepatic stellate cells (HSCs) were maintained on uncoated plastic dishes. HSCs presented a star-shaped appearance with fewer and smaller lipid droplets in the cytoplasm after primary culture for five days, and began to express α-SMA at non-uniform levels between cells. Subcultured HSCs evolved into myofibroblast-like cells without lipid droplets in the cytoplasm and expressed a uniform and higher level of α-SMA. Red: desmin; green: α-SMA; blue: nucleus (DAPI). Merged images are also shown. White arrows point to HSCs expressing high level of α-SMA. Bar = 100 μm.

ALT reagent and Infinity AST reagent, respectively (Thermo Electron, Louisville, CO, United States) according to the manufacturer's instructions. Liver tissues were fixed with 4% paraformaldehyde in PBS for 18 h and then embedded in paraffin. Sections of 5 μm thickness were cut and stained with hematoxylin and eosin (HE; Sigma-Aldrich, St. Louis, MO, United States). HE-stained liver sections were examined, and necrosis was graded using a previously described system[9].

Protein array of HSC supernatants

For HSC-CM, HSCs were cultured in serum-free DMEM supplemented with 0.05% BSA. Supernatants were prepared by collecting serum-free medium after 24 h culture of approximately 2 × 10^6 HSCs (5d) or HSCs (P3). The media were then concentrated approximately 25-fold using ultrafiltration units (Millipore, Bedford, MA, United States) with a 3 kDa molecular weight cut-off. Finally, the collected medium, containing paracrine molecules (HSC-CM), was stored at -80 ℃ until use. These were analyzed for a panel of specified proteins using an antibody array (RayBio Mouse Cytokine Antibody Array c2000, RayBiotech Inc., Norcross, GA) as specified by the vendor.

Statistical analysis

The quantitative results are expressed as the mean ± SD. For multi-group comparison, one-way analysis of variance was applied. Comparisons between groups were performed using the non-parametric Mann-Whitney *U*-test, or one-way analysis of variance. The Kruskal-Wallis rank-sum test was applied when the samples were not normally distributed. Kaplan-Meier analysis was used for survival analysis. A *P*-value less than 0.05 were considered statistically significant. The statistical methods of this study were reviewed by Department of Biostatistics of Fudan University.

RESULTS

HSC morphology and phenotype changes in the activation process

The isolated HSCs were cultured on uncoated plastic tissue culture plates and observed under a phase contrast microscope. After primary culture for 24 h, HSCs were quiescent, had a spherical shape and displayed a clear nuclear region surrounded by retinoid droplets in the cytoplasm. These cells expressed desmin and were negative for a-smooth muscle actin (α-SMA, data not shown). HSCs presented a star-shaped appearance with fewer and smaller lipid droplets in the cytoplasm after primary culture for five days, (Figure 1) and began to express α-SMA at non-uniform levels between cells (because the activation stage varied between cells) (Figure 1). These cells were at the early stage of activation and defined as "initiation" HSCs. During this activation period, HSCs developed the star-shaped pseudopodium branches with gradually fewer lipid droplets in the cytoplasm. Subcultured HSCs evolved into myofibroblast-like cells without lipid droplets (Figure 1) and expressed a uniform and higher level of α-SMA (Figure 1). These cells were persistently activated and defined as "perpetuation" HSCs.

At the ultrastructural level, primary cultured HSCs contained a small amount of rough endoplasmic reticulum and a few mitochondria, without microfilaments in the cytoplasm (Figure 2A). HSCs (5d) were characterized with increased rough endoplasmic reticulum, Golgi apparatus and microfilaments (Figure 2B). HSCs (P3) exhibited marked hypertrophy of rough endoplasmic reticulum and Golgi apparatus. They also had extensive microfilaments (Figure 2C), suggesting that perpetuation HSCs exhibited active synthesis and secretion function.

In summary, initiation HSCs and perpetuation

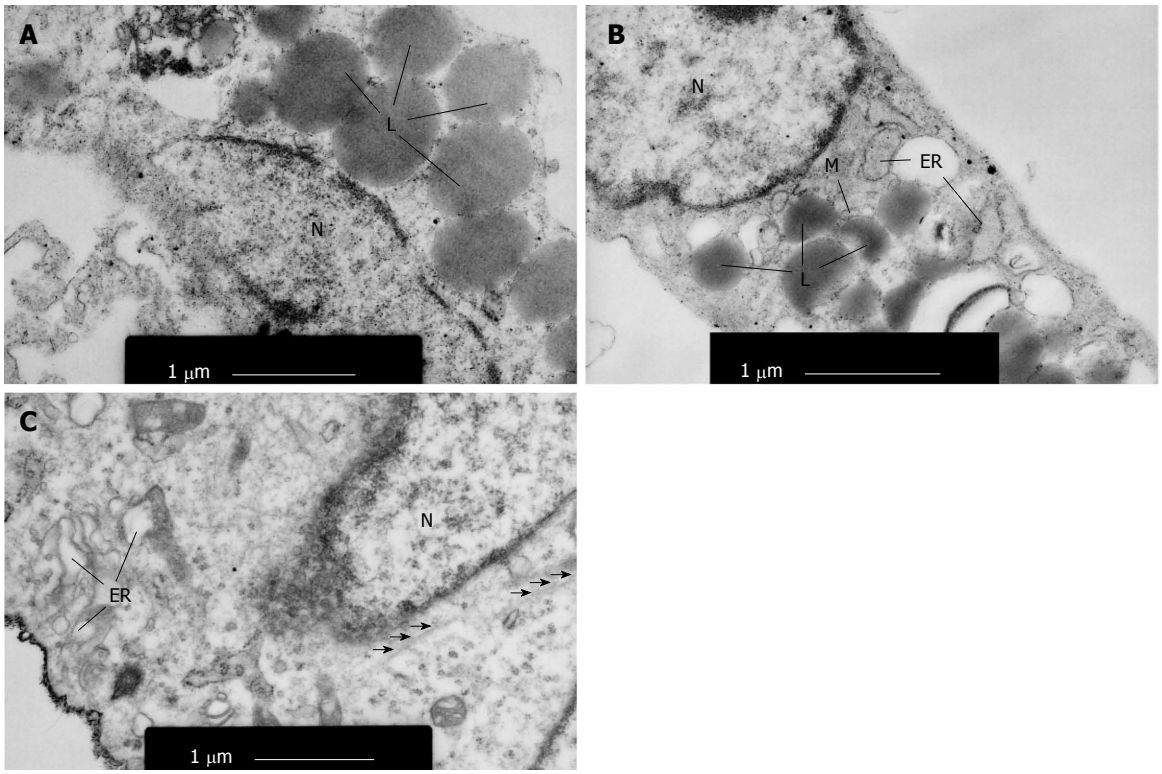

Figure 2 Ultrastructure of hepatic stellate cells observed under a transmission electron microscope. A: HSCs contained lipid droplets (L) around the nucleus (N) after primarily cultured for 24 h; B: Primary HSCs were characterized by decreased lipid droplets and a moderate amount of rough endoplasmic reticulum (ER) and mitochondria (M) when cultured for 5 d; C: HSCs (P3) exhibited marked hypertrophy of rough endoplasmic reticulum and microfilaments, but no lipid droplets. Black arrows point to microfilaments. HSC: Hepatic stellate cell.

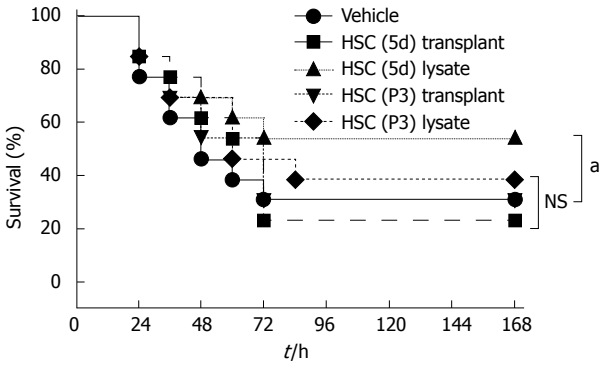

Figure 3 Infusion of hepatic stellate cell lysate provides a trend toward increased survival in acetaminophen-induced acute liver injury. All animals were fasted overnight before acetaminophen (APAP) treatment. Mice administered APAP were treated by intravenous injection of hepatic stellate cells (HSCs) or HSC lysates from the same cell mass (0.2 mL, about 2 × 10^6 cells). Control mice received vehicle (0.2 mL, high-glucose DMEM). Kaplan-Meier survival analysis of APAP-administered mice treated with cell transplants or lysates is performed. Time points of interventions are stated above survival plots. The results are cumulative data of two independent experiments (n = 13 per group) using different batches of HSCs. The number of death mice during survival analysis in each group: 9 in vehicle, 10 in HSC (5d) transplant, 6 in HSC (5d) lysate, 9 in HSC (P3) transplant, and 8 in HSC (P3) lysate. P-values were determined by the Kaplan-Meier analysis. $^aP < 0.05$ *vs* control. NS: Not significant.

HSCs had different morphological and phenotypic traits, which indicated that the synthesis and secretion functions of HSCs changed during the activation process. We speculated that HSCs of these two stages of activation might play different roles in liver regeneration after ALI. Therefore, we assessed the therapeutic effects of HSCs in APAP-induced ALI in mice.

HSC (5d)-derived components reverse APAP-induced ALI

We previously established a mouse model of APAP-induced ALI[9]. Liver enzyme levels measured in the peripheral blood provide a good estimate of ongoing liver damage. In this study, serum ALT and AST started to rise 6 h after APAP treatment, rose rapidly 12 h later, and peaked at 24 h (data not shown).

To reverse the APAP-induced ALI, we first assessed various HSC treatment modalities: cell transplantation, delivery of cellular lysates, and delivery of conditioned medium to assess the most efficacious therapy. Animals were treated 2 h after ALI induction by tail vein injections of wholes cells or cell lysates. No significant survival benefit was observed after the intravenous transplantation of HSCs (5d) or HSCs (P3), which was most likely due to poor engraftment and entrapment in the alveolar capillary (Figure 3). In contrast, treatment with cellular lysates of HSCs (5d), derived from the same cell mass as used for transplantation, resulted in an increased survival trend compared to other four groups ($P < 0.05$).

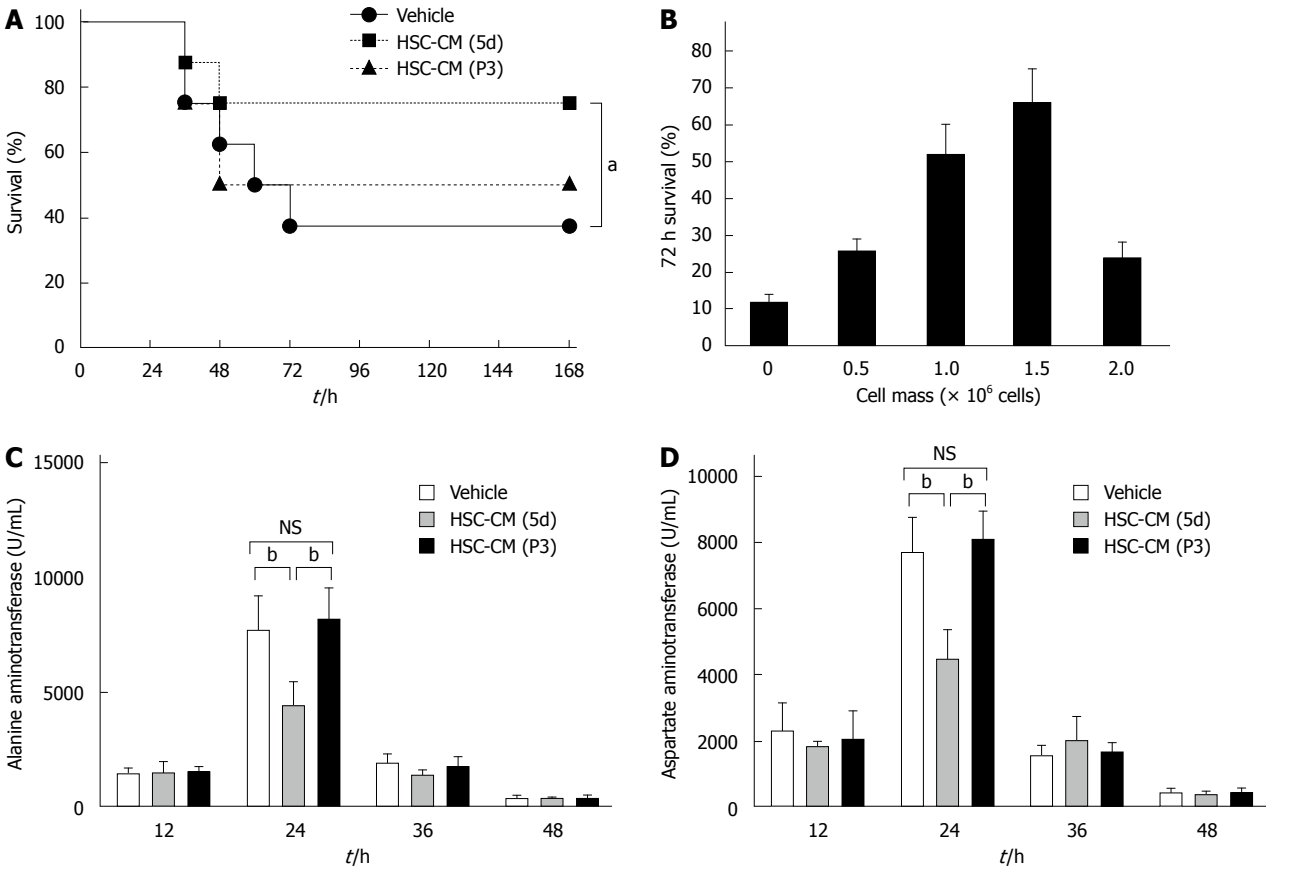

Figure 4 Hepatic stellate cell-CM (5d) provides a survival benefit in acute liver injury mice and reverses acute liver injury in a cell mass-dependent manner. A: Kaplan-Meier survival analysis of acetaminophen (APAP)-administered mice treated with concentrated hepatic stellate cell (HSC)-CM (0.2 mL, conditioned medium of 2 × 10^6 cells HSCs). Control mice received vehicle (0.2 mL, high-glucose DMEM). The results for both panels are cumulative data of two independent experiments (n = 13 per group). The number of death mice during survival analysis in each group: 9 in vehicle, 3 in HSC (5d), and 7 in HSC (P3). P-values were determined by the Kaplan-Meier analysis, $^aP < 0.05$ *vs* control; B: Dose-response graph of animal survival 72 h after acute liver injury (ALI) induction as a function of the mass of HSCs (5d) from which HSC-CM was derived; alanine aminotransferase (C), aspartate aminotransferase levels (D) in peripheral blood samples collected at 12, 24, 36, and 48 h after the systemic treatment. $^bP < 0.01$ *vs* control. NS: No significant.

HSC-CM (5d) provides hepatoprotection and survival benefit

We then determined if the efficacy observed with lysates could be reproduced by using the secreted molecules from HSCs. A longitudinal analysis using HSC-CM (5d) from the same cell mass (*i.e.,* 2 × 10^6 HSCs) revealed a distinct survival benefit compared to vehicle ($P < 0.05$) and HSC-CM (P3) ($P < 0.05$). There was no significant difference between the HSC-CM (P3) and vehicle groups in survival rate (Figure 4A). In addition, we monitored 72 h survival of ALI-induced mice as a function of the mass of HSCs (5d) from which the medium was conditioned (Figure 4B). Interestingly, the effect of HSC (5d) concentrate was abrogated at higher cell masses, indicating a therapeutic window of effectiveness. However, the HSC-CM (P3) could not improve mouse survival in all cell masses (data not show).

Based on these results, we assessed the protective effects of the molecules secreted from HSCs (5d). Animals were treated 2 h after ALI induction by injection of HSC-CM (5d) into the systemic circulation. HSC-CM (P3) and blank-CM (vehicle) served as controls. Serum was obtained every 12 h and analyzed for hepatocyte release. Liver enzyme levels in serum provide a good estimate of ongoing liver damage. The peak in liver damage was observed at 24 h after CM treatment in each group. However, ALT was decreased by 42% ($P < 0.01$) and 45% ($P < 0.01$), respectively, in HSC-CM (5d)-treated mice compared with HSC-CM (P3) and vehicle mice, and AST was decreased by 42% ($P < 0.01$) and 46% ($P < 0.01$), respectively (Figure 4C and D). Overall, these results show that the molecules secreted from initiation HSCs were associated with less severe liver damage and higher survival rate.

HSC-CM therapy inhibits hepatocellular necrosis and panlobular inflammation

Microscopic evaluation of HE-stained liver tissue from HSC-CM (P3) and vehicle mice revealed profound hepatocellular necrosis and panlobular mononuclear leukocyte infiltration with cytoplasmic vacuolization and severe distortion of tissue architecture (Figure 5A and C). HSC-CM (5d)-treated mice showed no signs of disseminated inflammation, although minor

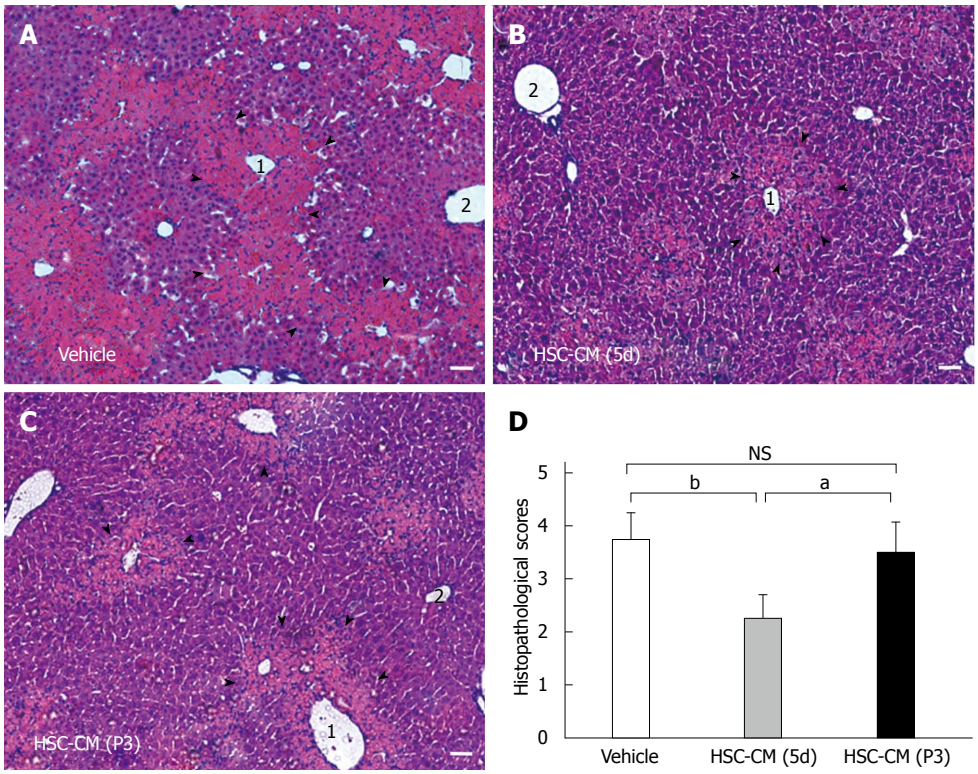

Figure 5 Hepatic stellate cell-CM (5d) treatment improves hepatocellular necrosis and immune cell infiltration in APAP-injured liver tissue. All animals were fasted overnight before APAP treatment. Acute liver injury (ALI) mice were sacrificed 24 h after systemic vehicle or hepatic stellate cell (HSC)-CM treatment. Liver samples were subjected to histological analysis after HE staining. Microscopic low-power fields of liver tissue are shown after vehicle (A), HSC-CM (5d) (B) and HSC-CM (P3) (C) treatment. Necrotic area is indicated by arrowheads. 1: centrilobular vein, 2: portal vein. Bar = 100 μm. Scores were determined by semi-quantitative histological examination (D). Data are the mean ± SE of the mean of 10 random high-power fields per animal. $^{a}P < 0.05$, $^{b}P < 0.01$ *vs* control. Bar = 100 μm. NS: Not significant.

pericentrilobular vein infiltration and hepatocellular death were observed (Figure 5B). Semi-quantitative histological examination of liver tissue confirmed the differences between the three groups (Figure 5D). The average score in the HSC-CM (5d) group was 2.25 ± 0.45, compared with 3.51 ± 0.57 in the HSC-CM (P3) group ($P < 0.05$) and 3.75 ± 0.51 in the vehicle group ($P < 0.01$). There was no difference between HSC-CM (P3) and vehicle. These results demonstrate that the molecules secreted from initiation HSCs correlated with less severe hepatocellular necrosis.

HSC-CM (5d) is composed of many chemokines and growth factors that correlate with inflammatory inhibition and therapeutic activity

To determine the molecular mediators of the observed protective effects of initiation HSCs, we examined HSC-CM using a high-density protein array. HSC-CM contained 69 of the 144 assayed proteins (Figure 6A), which included a broad spectrum of molecules involved in immunomodulation and liver regeneration. Cluster analysis revealed that a large proportion of HSC-CM (5d) was composed of chemokines (36.29%) and growth factors (21.03%) (Figure 6B), many of which were expressed at high relative levels. There was no significant difference between HSC-CM (5d) and HSC-CM (P3) in the constituent ratios of proteins. Only 7 of the 69 proteins had a constituent ratio difference of more than 2-fold between the HSC-CM (5d) and the HSC-CM (P3) group: monocyte chemoattractant protein-1 (MCP-1), macrophage inflammatory protein-1γ (MIP-1γ), hepatocyte growth factor (HGF), interleukin-10 (IL-10), matrix metalloproteinase-2 (MMP-2), stem cell factor (SCF) and Fas-Ligand. HSC-CM (5d) contained significantly more MCP-1, MIP-1γ, HGF, IL-10 and MMP-2, which might correlate with the greater inflammatory inhibition and therapeutic activity of HSC-CM (5d) in ALI.

DISCUSSION

It is becoming increasingly clear that HSCs have a profound impact on the proliferation, differentiation, and morphogenesis of other hepatic cell types during liver development and regeneration. Inhibiting activated HSCs using gliotoxin[5] and L-cysteine[10] prevents normal regenerative responses of both hepatocytes and oval cells in APAP- and 2AAF/PH-induced ALI, respectively. In this study, we observed that initiation HSCs were different from perpetuation HSCs in morphology, phenotype and molecule secretion. Initiation HSC-derived molecules protected hepatocytes against death and increased the survival rate of mice subjected to APAP-induced ALI. The

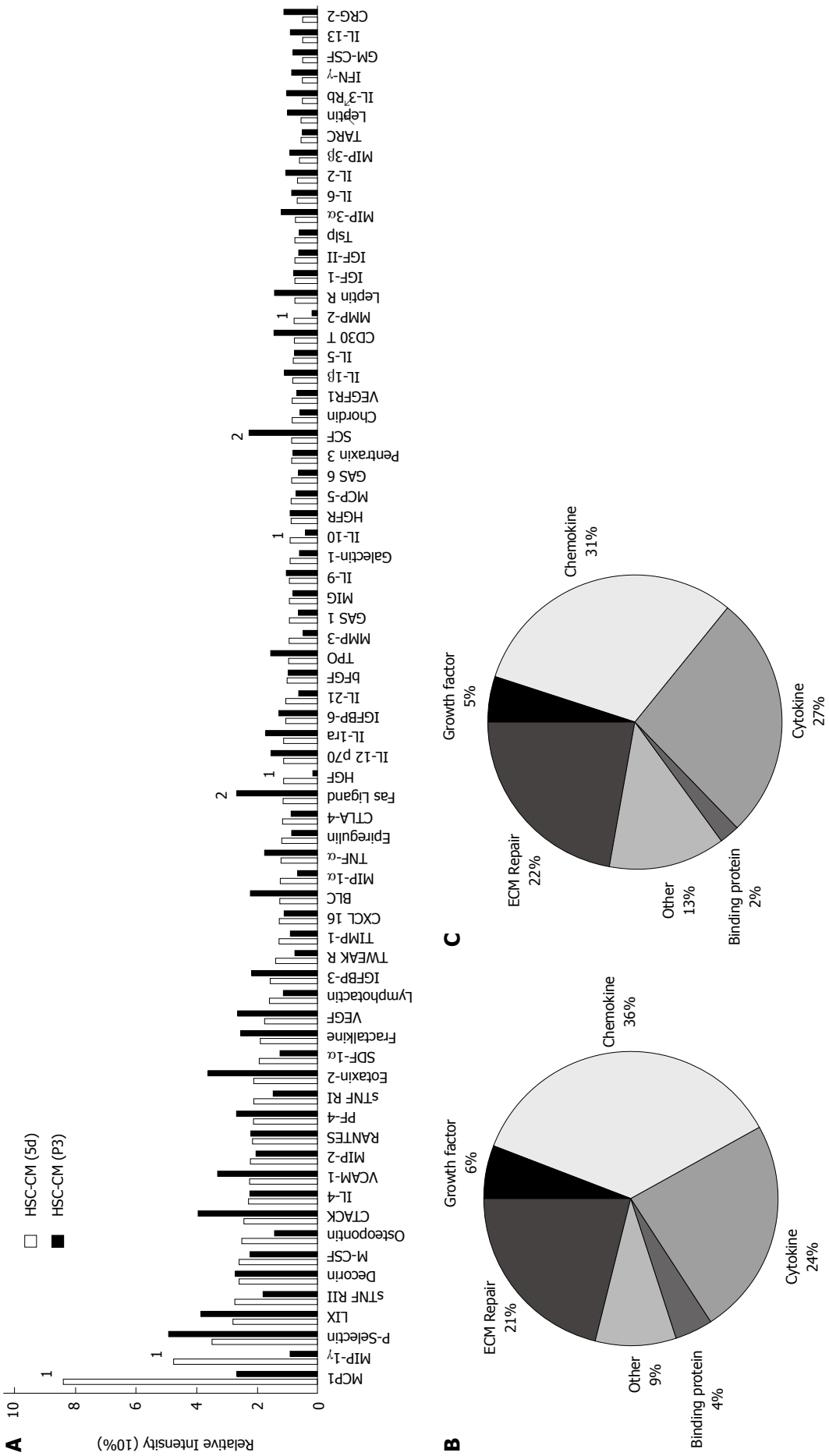

Figure 6 Differences between hepatic stellate cell-CM (5d) and hepatic stellate cell-CM (P3) in cytokine composition. Serum-free hepatic stellate cell (HSC)-CM was analyzed using an antibody array for 144 specified proteins. A: Densitometry of spotted antibody array results. Data are presented as spot intensity relative to the negative control and normalized to the positive control. [1]Molecules whose concentrations in HSC-CM (5d) were more than twice as high as in HSC-CM (P3); [2]molecules whose concentrations in HSC-CM (P3) were more than twice as high as in HSC-CM (5d). Pie chart showing cluster analysis of HSC (5d) secreted proteins (B) and HSC (P3) secreted proteins (C) based on reported function.

efficacy of initiation HSC-CM was a function of the cell mass from which the medium was conditioned, suggesting important pharmacological aspects of this treatment. These results are significant because we identified differences between initiation HSCs and perpetuation HSCs and provide clear evidence that delivery of HSC secretions has the potential to dramatically reduce cell death in the acutely injured liver.

The use of transgenic models has yielded information on how abnormal function of HSCs translates into regenerative defects. Foxf1$^{+/-}$ mice subjected to CCl_4 injury show decreased HSC activation and more severe hepatocyte necrosis during the regenerative period[11]. These results suggest that the defect in HSC activation consecutive to haploinsufficiency of Foxf1 results in impaired regeneration. However, following CCl4 injury, Col-1a1$^{r/r}$ mice show persistent activation of HSCs and fail to regenerate properly[12]. In the context of progressive fibrosis, this inhibition of hepatocyte proliferation may represent a significant mechanism preventing the restoration of effective hepatocellular function. These two examples suggest that deficient as well as uncontrolled HSC activation impairs liver regeneration. Thus, a finely tuned HSC response may be an important factor to ensure adequate regeneration[13]. Based on the data, we speculate that perpetuation HSCs mainly take part in the process of liver fibrosis, but initiation HSCs are involved in hepatocyte protection.

In normal circumstances, the liver hardly proliferates and was therefore classified as a stable organ. After liver injury, however, proliferation of the main epithelial compartments (hepatocytes and cholangiocytes), followed by proliferation of the mesenchymal cells (HSCs and endothelial cells), quickly restores the liver. As the support cell for hepatocytes, HSCs interact in order to control the hepatocytes, and these interactions can often be broken down into one of two major mechanistic categories: physical contact and diffusible factors[14]. It has been showed that HSC-clusters frequently contained α-SMA expressing HSCs and were in close association with hepatocytes, indicating the possibility that activation of HSCs and HSC-hepatocyte interaction were related events during regeneration[7]. However, whether diffusible factors from HSCs have a protective effect on hepatocytes is not clear. In this study, we firstly showed that early activated HSC-derived molecules could reverse ALI. Evarts *et al*[15] used the HSC cell line to verify that naproxen stimulated VEGF and HGF expression was of particular relevance in improving survival of transplanted hepatocytes. Naproxen and celecoxib increased desmin expression in HSCs after hepatocytes transplantation. This desmin-positive phenotype of HSCs was similar to previous cell transplantation studies, where desmin was expressed without α-SMA, presumably because this stimulus was transient and nonfibrogenic.

Following liver injury, HSCs undergo "activation", which consists of two major phases: initiation and perpetuation, followed by resolution of fibrosis if injury subsides[4]. In this study, regarding the morphological and phenotypic differences, initiation HSCs were spherical and expressed little α-SMA, while perpetuation HSCs were myofibroblast-like and expressed a uniform and higher level of α-SMA. Thus, we hypothesized that perpetuation HSCs exhibited active synthesis and secretion. Previous studies have shown that secretion of IL-10 and HGF was gradually reduced with the activation of HSCs, and these factors are confirmed to have a protective effect on hepatocytes in *in vitro* studies[15,16].

To determine the molecular mediators of the observed protective effects of initiation HSCs, we further used proteomic analysis to reveal a broad spectrum of molecules that are involved in immunomodulation and hepatocyte protection. Compared to perpetuation HSC-CM, initiation HSC-CM included higher levels of MCP-1, MIP-1γ, HGF, IL-10 and MMP-2, but less SCF and Fas-Ligand. MCP-1 (CCL2) is a C-C chemokine that attracts monocytes and memory T cells specifically during an inflammatory response *via* its specific receptor, CCR2[17]. MCP-1 is upregulated in a variety of diseases that are characterized by mononuclear cell infiltration[18]. Deficiency of MCP-1 protects mice against alcoholic liver injury[19], but there is also evidence that MCP-1 protects against hepatic injury by directly inhibiting NKT cell IL-4 production in T cell-mediated hepatitis[20]. MIP-1γ also belongs to a C-C chemokine family containing MIP-1α, MIP-1β, and MIP-1γ, which are produced by monocytes and other types of leukocytes. By binding to chemokine receptor 1 (CCR1), a specific receptor on neutrophils, MIP-1γ acts as a chemoattractant that induces the chemotaxis of $CD4^+$ T cells, $CD8^+$ T cells, and monocytes[21]. In this study, we detected high levels of MCP-1 and MIP-1γ in HSC-CM (5d) but observed relatively less monocyte infiltration in hepatic tissue of the HSC (5d) group, indicating that MCP-1 and MIP-1γ might not only affect monocyte trafficking. Further study is needed to determine the specific roles of MCP-1 and MIP-1γ in ALI. IL-10 is an anti-inflammatory pleiotropic cytokine that is secreted by monocytes, macrophages, and other leukocytes upon stimulation. Endogenous IL-10 protects hepatocytes by suppressing the ability of effector cells (*e.g.,* Kupffer cells) to release multiple cytokines, including TNF-α and chemokines, thereby inhibiting cytokine-dependent hepatocyte injury[22]. We speculate that the anti-inflammation effects observed in this study are a comprehensive regulatory process achieved by MCP-1, MIP-1γ and IL-10. HGF is regarded as one of the most potent stimulants for hepatocyte regeneration. All biological effects of HGF are mediated by a single tyrosine kinase receptor, c-Met[23]. Gene-knockout studies have shown that both HGF and c-Met are absolutely required for liver development. HGF/c-Met signaling stimulates hepatocyte growth through

paracrine and autocrine mechanisms, and these can initiate liver regeneration[24]. Matrix metalloproteinases (MMPs) and tissue inhibitors of metalloproteinases (TIMPs) maintain hepatic ECM stability by regulating its formation and degradation[25]. Activated HSCs are responsible for the majority of ECM protein deposition in liver fibrosis[26]. A recent study reported the role of MMP-2 in reducing hepatic injury and enhancing liver regeneration[27]. MMP-2 promotes pericellular collagen deposition, creating a microenvironment supporting the growth of regenerative hepatocytes. In contrast, perpetuation HSC-CM contained more Fas-ligand and SCF than initiation HSC-CM. Fas promotes hepatocyte apoptosis and hepatic fibrogenesis[28]. SCF regulates the differentiation of CD34-positive stem cells and modulates the synthesis of more specific cell types[29]. SCF also plays an important role in liver-remodeling processes. SCF combined with GM-CSF affects cellular differentiation and proliferation in various types of cells besides hepatobiliary epithelial cells[30]. However, our data show that SCF may not protect hepatocytes from ALI. Thus, initiation HSCs attenuate acute hepatocyte injury, while perpetuation HSCs may take part in hepatic fibrosis. The specific mechanisms of action of these molecules may be pluralistic, and whether the molecules could promote liver regeneration after ALI merits further study.

In conclusion, we observed different morphologies and phenotypes between initiation HSCs and perpetuation HSCs, and provide the first experimental evidence of the potential medical value of initiation HSC-derived molecules in the treatment of ALI. Our findings provide novel insight into the mechanisms of HSCs in liver injury therapy. Whether the potential value of initiation HSC-derived molecular therapy is derived from the effect of a single cytokine or a combination of cytokines should be explored in future studies.

COMMENTS

Background

Hepatic stellate cells (HSCs) play a role in hepatic regeneration. The authors have previously demonstrated that activated HSCs are involved in the proliferation of hepatocytes in acetaminophen (APAP)-induced acute liver injury (ALI). The goal was to determine if HSCs at different activation stages had different effects on APAP-induced ALI.

Research frontiers

Some studies directly supported the involvement of hepatocyte stellate cells (HSCs) in liver regeneration. Activated HSCs have been implicated in assisting liver regeneration by producing angiogenic factors as well as factors that modulate endothelial cell and hepatocyte proliferation and by remodeling the extracellular matrix. Inhibiting activated HSCs using gliotoxin and *L*-cysteine prevents normal regenerative responses of both hepatocytes and oval cells in APAP- and 2AAF/PH-induced ALI, respectively. In addition, Foxf1$^{+/-}$ mice subjected to CCl_4 injury show decreased HSC activation and more severe hepatocyte necrosis during the regenerative period. Notably, the mechanisms by which activated HSCs help mediate liver regeneration in experimental animals and human patients remain to be determined and the relative importance of different subtypes of hepatic stellate cells/myofibroblasts is still not clear in liver injury.

Innovations and breakthroughs

In this study, the authors observed different morphologies and phenotypes between initiation HSCs and perpetuation HSCs and described the first use of molecules secreted from HSCs in APAP-induced ALI. Initiation HSC-derived molecules showed hepatocyte-protective effects. This findings provide novel insight into the mechanisms of HSCs in liver injury therapy.

Applications

In conclusion, the current study shows that systemic HSC-CM (5d) therapy has profoundly improved survival in mice undergoing APAP-induced ALI. This work validates that conditioned medium of early activated HSCs induces an integrated response to liver injury and creates potential new avenues for the treatment.

Terminology

HSCs, first described by Kupffer in 1876, have emerged in the past 30 years as remarkably versatile mesenchymal cells. Previous studies have explored the importance of HSCs in liver fibrosis because HSC activation into myofibroblasts is thought to be the major pathway in hepatic fibrogenesis associated with liver injury. Beyond this well-known characteristic, however, many newly discovered activities have led to a greater understanding of this fascinating cell type and the complexity of cellular homeostasis in the liver.

Peer-review

This work by Chang *et al* describes the protective effect of conditioned medium from early activated HSCs on hepatocytes in injured liver from APAP injury. The work is novel and not described before. The findings point towards an *in vivo* protective component of HSCs during early activation.

REFERENCES

1 **Lysy PA**, Campard D, Smets F, Najimi M, Sokal EM. Stem cells for liver tissue repair: current knowledge and perspectives. *World J Gastroenterol* 2008; **14**: 864-875 [PMID: 18240343 DOI: 10.3748/wjg.14.864]

2 **Zhou WC**, Zhang QB, Qiao L. Pathogenesis of liver cirrhosis. *World J Gastroenterol* 2014; **20**: 7312-7324 [PMID: 24966602 DOI: 10.3748/wjg.v20.i23.7312]

3 **Yin C**, Evason KJ, Asahina K, Stainier DY. Hepatic stellate cells in liver development, regeneration, and cancer. *J Clin Invest* 2013; **123**: 1902-1910 [PMID: 23635788 DOI: 10.1172/JCI66369]

4 **Friedman SL**. Hepatic stellate cells: protean, multifunctional, and enigmatic cells of the liver. *Physiol Rev* 2008; **88**: 125-172 [PMID: 18195085 DOI: 10.1152/physrev.00013.2007]

5 **Shen K**, Chang W, Gao X, Wang H, Niu W, Song L, Qin X. Depletion of activated hepatic stellate cell correlates with severe liver damage and abnormal liver regeneration in acetaminophen-induced liver injury. *Acta Biochim Biophys Sin* (Shanghai) 2011; **43**: 307-315 [PMID: 21335335 DOI: 10.1093/abbs/gmr005]

6 **Roskams T**. Different types of liver progenitor cells and their niches. *J Hepatol* 2006; **45**: 1-4 [PMID: 16723168 DOI: 10.1016/j.jhep.2006.05.002]

7 **Mabuchi A**, Mullaney I, Sheard PW, Hessian PA, Mallard BL, Tawadrous MN, Zimmermann A, Senoo H, Wheatley AM. Role of hepatic stellate cell/hepatocyte interaction and activation of hepatic stellate cells in the early phase of liver regeneration in the rat. *J Hepatol* 2004; **40**: 910-916 [PMID: 15158330 DOI: 10.1016/j.jhep.2004.02.005]

8 **Chang W**, Yang M, Song L, Shen K, Wang H, Gao X, Li M, Niu W, Qin X. Isolation and culture of hepatic stellate cells from mouse liver. *Acta Biochim Biophys Sin* (Shanghai) 2014; **46**: 291-298 [PMID: 24389643 DOI: 10.1093/abbs/gmt143]

9 **Liu ZX**, Han D, Gunawan B, Kaplowitz N. Neutrophil depletion protects against murine acetaminophen hepatotoxicity. *Hepatology* 2006; **43**: 1220-1230 [PMID: 16729305 DOI: 10.1002/hep.21175]

10 **Pintilie DG**, Shupe TD, Oh SH, Salganik SV, Darwiche H, Petersen BE. Hepatic stellate cells' involvement in progenitor-mediated liver regeneration. *Lab Invest* 2010; **90**: 1199-1208 [PMID: 20440274 DOI: 10.1038/labinvest.2010.88]

11 **Kalinichenko VV**, Bhattacharyya D, Zhou Y, Gusarova GA, Kim W, Shin B, Costa RH. Foxf1 +/- mice exhibit defective stellate cell activation and abnormal liver regeneration following CCl4 injury. *Hepatology* 2003; **37**: 107-117 [PMID: 12500195 DOI: 10.1053/jhep.2003.50005]

12 **Issa R**, Zhou X, Trim N, Millward-Sadler H, Krane S, Benyon C, Iredale J. Mutation in collagen-1 that confers resistance to the action of collagenase results in failure of recovery from CCl4-induced liver fibrosis, persistence of activated hepatic stellate cells, and diminished hepatocyte regeneration. *FASEB J* 2003; **17**: 47-49 [PMID: 12475903 DOI: 10.1096/fj.02-0494fje]

13 **Balabaud C**, Bioulac-Sage P, Desmoulière A. The role of hepatic stellate cells in liver regeneration. *J Hepatol* 2004; **40**: 1023-1026 [PMID: 15158345 DOI: 10.1016/j.jhep.2004.04.003]

14 **Walker MR**, Patel KK, Stappenbeck TS. The stem cell niche. *J Pathol* 2009; **217**: 169-180 [PMID: 19089901 DOI: 10.1002/path.2474]

15 **Evarts RP**, Hu Z, Fujio K, Marsden ER, Thorgeirsson SS. Activation of hepatic stem cell compartment in the rat: role of transforming growth factor alpha, hepatocyte growth factor, and acidic fibroblast growth factor in early proliferation. *Cell Growth Differ* 1993; **4**: 555-561 [PMID: 7691152]

16 **Wang SC**, Ohata M, Schrum L, Rippe RA, Tsukamoto H. Expression of interleukin-10 by in vitro and in vivo activated hepatic stellate cells. *J Biol Chem* 1998; **273**: 302-308 [PMID: 9417080 DOI: 10.1074/jbc.273.1.302]

17 **Johnston B**, Burns AR, Suematsu M, Issekutz TB, Woodman RC, Kubes P. Chronic inflammation upregulates chemokine receptors and induces neutrophil migration to monocyte chemoattractant protein-1. *J Clin Invest* 1999; **103**: 1269-1276 [PMID: 10225970 DOI: 10.1172/JCI5208]

18 **Daly C**, Rollins BJ. Monocyte chemoattractant protein-1 (CCL2) in inflammatory disease and adaptive immunity: therapeutic opportunities and controversies. *Microcirculation* 2003; **10**: 247-257 [PMID: 12851642 DOI: 10.1038/sj.mn.7800190]

19 **Mandrekar P**, Ambade A, Lim A, Szabo G, Catalano D. An essential role for monocyte chemoattractant protein-1 in alcoholic liver injury: regulation of proinflammatory cytokines and hepatic steatosis in mice. *Hepatology* 2011; **54**: 2185-2197 [PMID: 21826694 DOI: 10.1002/hep.24599]

20 **Ajuebor MN**, Hogaboam CM, Le T, Swain MG. C-C chemokine ligand 2/monocyte chemoattractant protein-1 directly inhibits NKT cell IL-4 production and is hepatoprotective in T cell-mediated hepatitis in the mouse. *J Immunol* 2003; **170**: 5252-5259 [PMID: 12734374]

21 **Shen PC**, Wu CL, Jou IM, Lee CH, Juan HY, Lee PJ, Chen SH, Hsieh JL. T helper cells promote disease progression of osteoarthritis by inducing macrophage inflammatory protein-1γ. *Osteoarthritis Cartilage* 2011; **19**: 728-736 [PMID: 21376128 DOI: 10.1016/j.joca.2011.02.014]

22 **Dinant S**, Veteläinen RL, Florquin S, van Vliet AK, van Gulik TM. IL-10 attenuates hepatic I/R injury and promotes hepatocyte proliferation. *J Surg Res* 2007; **141**: 176-182 [PMID: 17543989 DOI: 10.1016/j.jss.2006.09.018]

23 **Uehara Y**, Minowa O, Mori C, Shiota K, Kuno J, Noda T, Kitamura N. Placental defect and embryonic lethality in mice lacking hepatocyte growth factor/scatter factor. *Nature* 1995; **373**: 702-705 [PMID: 7854453 DOI: 10.1038/373702a0]

24 **Ishikawa T**, Factor VM, Marquardt JU, Raggi C, Seo D, Kitade M, Conner EA, Thorgeirsson SS. Hepatocyte growth factor/c-met signaling is required for stem-cell-mediated liver regeneration in mice. *Hepatology* 2012; **55**: 1215-1226 [PMID: 22095660 DOI: 10.1002/hep.24796]

25 **Zhou X**, Hovell CJ, Pawley S, Hutchings MI, Arthur MJ, Iredale JP, Benyon RC. Expression of matrix metalloproteinase-2 and -14 persists during early resolution of experimental liver fibrosis and might contribute to fibrolysis. *Liver Int* 2004; **24**: 492-501 [PMID: 15482348 DOI: 10.1111/j.1478-3231.2004.0946.x]

26 **Salguero Palacios R**, Roderfeld M, Hemmann S, Rath T, Atanasova S, Tschuschner A, Gressner OA, Weiskirchen R, Graf J, Roeb E. Activation of hepatic stellate cells is associated with cytokine expression in thioacetamide-induced hepatic fibrosis in mice. *Lab Invest* 2008; **88**: 1192-1203 [PMID: 18794850 DOI: 10.1038/labinvest.2008.91]

27 **Padrissa-Altés S**, Zaouali MA, Franco-Gou R, Bartrons R, Boillot O, Rimola A, Arroyo V, Rodés J, Peralta C, Roselló-Catafau J. Matrix metalloproteinase 2 in reduced-size liver transplantation: beyond the matrix. *Am J Transplant* 2010; **10**: 1167-1177 [PMID: 20353474 DOI: 10.1111/j.1600-6143.2010.03092.x]

28 **Rutherford A**, Chung RT. Acute liver failure: mechanisms of hepatocyte injury and regeneration. *Semin Liver Dis* 2008; **28**: 167-174 [PMID: 18452116 DOI: 10.1055/s-2008-1073116]

29 **Akel S**, Petrow-Sadowski C, Laughlin MJ, Ruscetti FW. Neutralization of autocrine transforming growth factor-beta in human cord blood CD34(+)CD38(-)Lin(-) cells promotes stem-cell-factor-mediated erythropoietin-independent early erythroid progenitor development and reduces terminal differentiation. *Stem Cells* 2003; **21**: 557-567 [PMID: 12968110 DOI: 10.1634/stemcells.21-5-557]

30 **Pick M**, Azzola L, Mossman A, Stanley EG, Elefanty AG. Differentiation of human embryonic stem cells in serum-free medium reveals distinct roles for bone morphogenetic protein 4, vascular endothelial growth factor, stem cell factor, and fibroblast growth factor 2 in hematopoiesis. *Stem Cells* 2007; **25**: 2206-2214 [PMID: 17556598 DOI: 10.1634/stemcells.2006-0713]

P- Reviewer: Cappon A, Chao JCJ, Guo JS, Pan Q, Ramani K, Wu TJ, Xiao EH, Yu HP

S- Editor: Qi Y **L- Editor**: Wang TQ **E- Editor**: Ma S

World Journal of Gastroenterology

Submit a Manuscript: http://www.wjgnet.com/esps/
Help Desk: http://www.wjgnet.com/esps/helpdesk.aspx
DOI: 10.3748/wjg.v21.i14.4195

World J Gastroenterol 2015 April 14; 21(14): 4195-4209
ISSN 1007-9327 (print) ISSN 2219-2840 (online)

ORIGINAL ARTICLE

Basic Study

Hydrogen-rich water protects against acetaminophen-induced hepatotoxicity in mice

Jing-Yao Zhang, Si-Dong Song, Qing Pang, Rui-Yao Zhang, Yong Wan, Da-Wei Yuan, Qi-Fei Wu, Chang Liu

Jing-Yao Zhang, Si-Dong Song, Qing Pang, Rui-Yao Zhang, Yong Wan, Chang Liu, Department of Hepatobiliary Surgery, The First Affiliated Hospital of Xi'an Jiaotong University, Xi'an 710061, Shaanxi Province, China
Da-Wei Yuan, Department of Surgical Oncology, The First Affiliated Hospital of Xi'an Jiaotong University, Xi'an 710061, Shaanxi Province, China
Qi-Fei Wu, Department of Thoracic Surgery, The First Affiliated Hospital of Xi'an Jiaotong University, Xi'an 710061, Shaanxi Province, China
Author contributions: Zhang JY and Song SD participated in the research design and in the writing of the paper, they contributed equally to the work; Pang Q participated in the research design; Zhang RY participated in the writing of the paper and in the literature searches; Wan Y participated in the research design and paper revisions; Yuan DW participated in the literature searches; Wu QF participated in the research design; Liu C provided substantial advice in designing the study and assisting in the division of labor.
Ethics approval: The study was reviewed and approved by The First Affiliated Hospital of Xi'an Jiaotong University College of Medicine Institutional Review Board.
Institutional animal care and use committee: All procedures involving animals were reviewed and approved by the Institutional Animal Care and Use Committee of The First Affiliated Hospital of Xi'an Jiaotong University College (IACUC protocol number: XITULAC2014-207).
Conflict-of-interest: Authors declare no competing financial interests.
Data sharing: Technical appendix, statistical code, and dataset available from the corresponding author at liuchangdoctor@163.com. Participants gave informed consent for data sharing.

Correspondence to: Chang Liu, MD, PhD, Department of Hepatobiliary Surgery, The First Affiliated Hospital of Xi'an Jiaotong University, No. 277 Yanta West Road, Xi'an 710061, Shaanxi Province, China. liuchangdoctor@163.com
Telephone: +86-29-82653900
Fax: +86-29-82654642
Received: October 17, 2014
Peer-review started: October 18, 2014
First decision: December 2, 2014
Revised: December 17, 2014
Accepted: February 12, 2015
Article in press: February 13, 2015
Published online: April 14, 2015

Abstract

AIM: To investigate the hepatoprotective effects and mechanisms of hydrogen-rich water (HRW) in acetaminophen (APAP)-induced liver injury in mice.

METHODS: Male mice were randomly divided into the following four groups: normal saline (NS) control group, mice received equivalent volumes of NS intraperitoneally (ip); HRW control group, mice were given HRW (same volume as the NS group); APAP + NS group, mice received NS ip for 3 d (5 mL/kg body weight, twice a day at 8 am and 5 pm) after APAP injection; APAP + HRW group, mice received HRW for 3 d (same as NS treatment) after APAP challenge. In the first experiment, mice were injected ip with a lethal dose of 750 mg/kg APAP to determine the 5-d survival rates. In the second experiment, mice were injected ip with a sub-lethal dose of 500 mg/kg. Blood and liver samples were collected at 24, 48, and 72 h after APAP injection to determine the degree of liver injury.

RESULTS: Treatment with HRW resulted in a significant increase in the 5-d survival rate compared with the APAP + NS treatment group (60% *vs* 26.67%, $P < 0.05$). HRW could significantly decrease the serum alanine aminotransferase level (24 h: 4442 ± 714.3 U/L *vs* 6909 ± 304.8 U/L, $P < 0.01$; 48 h: 3782 ± 557.5 U/L *vs* 5111 ± 404 U/L, $P < 0.01$; and

3255 ± 337.4 U/L *vs* 3814 ± 250.2 U/L, $P < 0.05$, respectively) and aspartate aminotransferase level (24 h: 4683 ± 443.4 U/L *vs* 5307 ± 408.4 U/L, $P < 0.05$; 48 h: 3392 ± 377.6 U/L *vs* 4458 ± 423.6 U/L, $P < 0.01$; and 3354 ± 399.4 U/L *vs* 3778 ± 358 U/L, respectively) compared with the APAP treatment group. The alkaline phosphatase, total bilirubin and lactate dehydrogenase levels had the same result. Seventy-two hours after APAP administration, liver samples were collected for pathological examination and serum was collected to detect the cytokine levels. The liver index (5.16% ± 0.26% *vs* 5.88% ± 0.073%, $P < 0.05$) and percentage of liver necrosis area (27.73% ± 0.58% *vs* 36.87% ± 0.49%, $P < 0.01$) were significantly lower in the HRW-treated animals. The malonyldialdehyde (MDA) contents were significantly reduced in the HRW pretreatment group, but they were increased in the APAP-treated group (10.44 ± 1.339 nmol/mg protein *vs* 16.70 ± 1.646 nmol/mg protein, $P < 0.05$). A decrease in superoxide dismutase (SOD) activity in the APAP treatment group and an increase of SOD in the HRW treatment group were also detected (9.74 ± 0.46 U/mg protein *vs* 12.1 ± 0.67 U/mg protein, $P < 0.05$). Furthermore, HRW could significantly increase the glutathione (GSH) contents (878.7 ± 76.73 mg/g protein *vs* 499.2 ± 48.87 mg/g protein) compared with the APAP treatment group. Meanwhile, HRW could reduce the inflammation level (serum TNF-α: 399.3 ± 45.50 pg/L *vs* 542.8 ± 22.38 pg/L, $P < 0.05$; and serum IL-6: 1056 ± 77.01 pg/L *vs* 1565 ± 42.11 pg/L, $P < 0.01$, respectively). In addition, HRW could inhibit 4-HNE, nitrotyrosine formation, JNK phosphorylation, connexin 32 and cytochrome P4502E expression. Simultaneously, HRW could facilitate hepatocyte mitosis to promote liver regeneration.

CONCLUSION: HRW has significant therapeutic potential in APAP-induced hepatotoxicity by inhibiting oxidative stress and inflammation and promoting liver regeneration.

Key words: Hydrogen; Liver regeneration; Reactive oxygen species; Acetaminophen; Connexin 32

Core tip: Acetaminophen (APAP)-induced liver injury is a devastating and fatal disease. Hydrogen is a newly-developed antioxidant that has an obvious effect of selectively reducing the strongest oxidants, such as hydroxyl radicals and peroxynitrite. We launched a research study to evaluate the protective role of hydrogen-rich water on APAP-induced hepatotoxicity in mice. We found that hydrogen-rich water treatment was effective in counteracting APAP-induced hepatic damage, oxidative stress and cellular necrosis. It could also promote hepatocyte proliferation and inhibit the expression of connexin 32, cytochrome P4502E and JNK phosphorylation after APAP administration. These results provide a potential therapy for APAP-induced liver injury.

Zhang JY, Song SD, Pang Q, Zhang RY, Wan Y, Yuan DW, Wu QF, Liu C. Hydrogen-rich water protects against acetaminophen-induced hepatotoxicity in mice. *World J Gastroenterol* 2015; 21(14): 4195-4209 Available from: URL: http://www.wjgnet.com/1007-9327/full/v21/i14/4195.htm DOI: http://dx.doi.org/10.3748/wjg.v21.i14.4195

INTRODUCTION

Acetaminophen (N-acetyl-p-aminophenol, APAP) is a widely used analgesic and antipyretic drug in the clinic. APAP is believed to be safe within therapeutic doses, but overdose causes centrilobular hepatic necrosis that leads to acute liver failure (ALF)[1]. Surveys have shown that APAP poisoning accounts for approximately one-half of ALF in the US today, which costs as much as $87 million dollars to treat annually[2].

The severity of APAP-induced liver injury has been the focus of many research studies, and a variety of mechanisms of toxicity both in animals and humans have been elucidated[3,4]. According to pharmacological research, overdoses of APAP can promote the generation of the toxic metabolite N-acetyl-p-benzoquinone imine (NAPQI), which is immediately conjugated with glutathione (GSH) to form the nontoxic metabolite cysteine[5,6]. However, when the GSH is exhausted, NAPQI turns to covalently bind with other proteins to form the protein adducts that directly lead to cell death[7]. Some studies have reported that oxidative stress plays an important role in APAP hepatotoxicity[8]. Both the intracellular (mitochondria) and extracellular (inflammatory cells) sources of reactive oxygen species (ROS) contribute to liver injury[9-11]. Many antioxidant agents have been studied in experimental and clinical studies to reduce or prevent APAP-induced hepatotoxicity. Meanwhile, there is some evidence that APAP administration leads to an increase in the pro-inflammatory cytokines, and treatment of APAP-intoxicated mice with either anti-tumor necrosis factor (TNF)-α or anti-interleukin (IL)-1β can prevent hepatotoxicity[12]. Some proteins or enzymes, such as cytochrome P4502E (CYP2E1), inducible nitric oxide synthase (i-NOS) and c-Jun-NH_2-terminal protein kinase (JNK), play important roles in the pathological process of APAP-liver injury[6,13-16].

More recently, the role of gap junctions, which represent an elegant mechanism for direct communication between neighboring cells, has been studied in drug-induced hepatic injury[17]. In liver, connexin 32 (Cx32), the predominant gap junction protein expressed in the liver, has been demonstrated to aggravate drug-induced hepatic injury by enabling direct intercellular communication between coupled cells and the amplification of liver inflammation[18].

Patel *et al*[19] found that mice deficient in Cx32 were protected against thioacetamide (TAA)-induced liver damage. Inhibition of Cx32 by a pharmaceutical strategy can also decrease the TAA or APAP toxicity[19].

Molecular hydrogen, the lightest and most abundant chemical element in nature, has therapeutic efficacy in many diseases through its efficient anti-oxidant, anti-inflammatory, anti-apoptotic, and anti-allergy effects[20,21]. Although the protective effects of hydrogen on liver diseases including ischemia reperfusion injury, concanavalin-A-induced hepatitis, schistosomiasis-associated liver injury, and nonalcoholic steatohepatitis[22-24] have been confirmed, the effect of hydrogen on APAP-induced liver injury has not been studied. Hydrogen-rich water (HRW) is an effective, convenient way to deliver molecular hydrogen, which has the same effectiveness as inhalation of hydrogen gas and is more suitable for application. Therefore, the main aim of our study was to assess the protective role and potential mechanisms of HRW in APAP-induced hepatic injury in mice.

MATERIALS AND METHODS

Experimental animals and preparation of HRW

This study was conducted using male C57Bl/6 mice (4-5 wk old, 21-26 g) (Animal Feeding Center of Xi'an Jiaotong University Medical School). The animals were acclimatized to laboratory conditions (23 ℃, 12 h/12 h light/dark, 50% humidity, and *ad libitum* access to food and water) for one week prior to experimentation. All mice were housed (5 per cage) in clear, pathogen-free polycarbonate cages in the animal care facility, and they were fed a standard animal diet and water *ad libitum* under controlled temperature conditions with 12-h light-dark cycles. They were cared for in accordance with the Ethical Committee, Xi'an Jiaotong University Health Science Center. The study was reviewed and approved by the Xi'an Jiaotong University Health Science Center Institutional Review Board. All procedures involving animals were reviewed and approved by the Institutional Animal Care and Use Committee of the Xi'an Jiaotong University Health Science Center (IACUC protocol number: NO.XJTULAC2014-207). The animal protocol was designed to minimize pain and discomfort to the animals. All animals were euthanized by isoflurane gas for tissue collection. The HRW was produced by Naturally Plus Japan International Co, Ltd, and was stored under atmospheric pressure at 4 ℃ in an aluminum bag with no dead volume. Gas chromatography was used to confirm the content of hydrogen by the method described by Ohsawa *et al*[20] (hydrogen concentration of the HRW used in this study: 0.83-0.91 mmol/L).

Study design

Mice in the present study were divided into the following three groups: (1) normal saline (NS) control group, mice received equivalent volumes of NS intraperitoneally (ip); (2) hydrogen-rich water control group, mice received HRW (same volume as NS); (3) APAP + NS group, mice received NS ip (5 mL/kg body weight, twice per day at 8 am and 5 pm) after APAP injection; and (4) APAP + HRW group, mice received HRW (same volume as NS treatment) after APAP challenge.

In the first experiment, mice (NS control and HRW control groups, n = 5; APAP + NS and APAP + HRW groups, n = 15) were randomly divided as described above and received a lethal dose of 750 mg/kg APAP, administered ip, at 8 am on the first day, and they were monitored for mortality over the next 5 d.

In the second experiment, acute liver injury (ALI) was induced by a sub-lethal dose of 500 mg/kg APAP administered ip at 8 am on the first day. Mice were treated ip with NS or HRW (5 mL/kg, twice a day at 8 am and 5 pm) for 3 d after APAP challenge. Six mice per group were used in this study. Blood samples were collected from all groups by cutting the tail at 24 and 48 h after APAP administration. Mice were sacrificed at 72 h after APAP administration and blood samples were collected from the eyeballs. The serum was separated by centrifugation at 4 ℃, 3000× g for 15 min. The liver was removed immediately from each mouse and kept at -80 ℃ until further analysis.

Measurement of liver function

The serum alanine aminotransferase (ALT), aspartate aminotransferase (AST), total bilirubin and alkaline phosphatase (ALP) activities were determined by an automated procedure in the Department of Inspection, The First Affiliated Hospital of Xi'an Jiaotong University.

Cytokine measurement in murine serum

The levels of serum TNF-α and IL-6 were measured with commercial ELISA kits according to the instructions of the manufacturer (Dakewe, Shenzhen, China).

Measurement of hepatic oxidative stress

The liver tissue was homogenized, and the tissue myeloperoxidase (MPO), malonaldehyde (MDA), superoxide dismutase (SOD), catalase (CAT), glutathione (GSH), glutathione peroxidase (GSH-Px) activities were measured using the activity assay kits from NanJing JianCheng Bioengineering Institute; the methods were previously described[25].

Histological study

Samples from the liver were fixed in 10% formalin solution and embedded in paraffin. Serial sections of 5-μm thickness were obtained and stained with hematoxylin eosin (HE) to evaluate the morphology. Two researchers examined the results in a blinded fashion. For electron microscopy examination, liver tissues were prefixed immediately after harvesting

with 1.5% glutaraldehyde and 0.8% paraformaldehyde (0.1 mol/L cacodylate buffer) at room temperature, and they were postfixed in an aqueous solution of 1% OsO_4 and 1.5% $K_4(FeCN)_6$. Then, the specimens were embedded into Epon by routine procedures. Ultrathin sections (50 nm) were contrasted with lead citrate and uranyl acetate and studied with a CM100 transmission electron microscope.

Immunohistochemistry

Immunohistochemistry (IHC) analysis were performed with 4HNE, nitrotyrosine, bromodeoxyuridine (BrdU), Ki-67, PCNA and Cx32 antibodies (Beijing Biosynthesis Biotechnology Co., Ltd) using previously described methods[26]. Mice given BrdU (0.5 mg/mL) in their drinking water 4 d before APAP administration were analyzed by immunohistochemistry for liver nuclear-labeling indices.

RNA isolation and quantitative reverse transcription-polymerase chain reaction analysis

Total RNA was isolated from liver samples using the RNAfast200 kit (Fastagen Biotech, Shanghai, China). Reverse transcription was performed using the PrimeScript RT reagent kit (TaKaRa Biotechnology, Dalian, China). The mRNA expression was assayed in triplicate and normalized to the 18S mRNA expression. The relative levels were calculated using the Comparative-Ct Method (ΔΔCt method). The primers used in the study are: TNF-α: (Forward 5′-AAGCCTGTAGCCCACGTCGTA-3′ and Reverse 5′-AGGTACAACCCATCGGCTGG-3′); IL-6: (Forward 5′-TCCATCCAGTTGCCTTCTTG-3′ and Reverse 5′-TTCCACGATTTCCCAGAGAAC-3′); Cx32: (Forward 5′-TGAGGCAGGATGAACTGGACAGGT-3′ and Reverse 5′-CACGAAGCAGTCCACTGT-3′); 18S: (Forward 5′-AAACGGCTACCACATCCAAG-3′ and Reverse 5′-CCTCCAATGGATCCTCGTTA -3′).

Western blot analysis

The anti-cyclin D1, PCNA, JNK, phospho-JNK, CYP2E1, and β-actin monoclonal antibodies were purchased from Beijing Biosynthesis Biotechnology CO., Ltd. The protein concentration was determined by the BCA method. Western blot analysis was performed as previously described[27].

Statistical analysis

The survival and mortality rates are expressed as percentages and analyzed using the Kaplan-Meier method. The measurement data are expressed as the mean ± SD. Differences between the experimental and control groups were assessed by either the analysis of variance (ANOVA) or t test, as applicable, using SPSS 18.0 (SPSS, 165 Inc.). A *P* value of less than 0.05 was considered to be statistically significant.

The statistical methods of this study were reviewed by Dr. Kai Xu from Department of Epidemiology, MD Anderson Cancer Center, University of Texas, United States; and Professor Ya-Feng Dong from University of Kansas School of Medicine, United States.

RESULTS

HRW decreased liver injury in APAP-challenged mice and improved the survival rate

The administration of 500 mg/kg APAP caused a severe illness in the mice, which was characterized by weakness and loss of body weight. After a lethal dose of APAP administration (750 mg/kg), NS treatment resulted in a 73.3% mortality rate in a 5-d observation period, while HRW could improve the 5-d survival rate to 60% (Figure 1A). Three days after a sub-lethal APAP challenge (500 mg/kg), mice were sacrificed with cervical dislocation. Necrosis, dropsy and petechiae could be observed in the liver tissue, which could be obviously mitigated by HRW treatment (Figure 1B-D). HE results also showed that HRW could alleviate the centrilobular necrosis, fatty infiltration and lymphocyte infiltration (Figure 1D). Meanwhile, the liver function detected by the serum ALT, AST, bilirubin, ALP and lactate dehydrogenase (LDH) activities was measured at 24, 48, and 72 h after APAP challenge. Compared with APAP + HRW mice, APAP + NS mice showed a significant increase in the serum ALT, bilirubin, AST, ALP and LDH levels (Figure 1E).

HRW inhibited oxidative stress, inflammation and peroxynitrite formation in the liver

Oxidative stress and inflammation could be induced by APAP administration, which played an initial, augmented role in the development of APAP hepatotoxicity. Three days after 500 mg/kg APAP administration, liver samples were removed to assess the oxidative stress in mice. The oxidative stress parameters, including MDA and MPO, in the liver were significantly increased in the APAP + NS group compared with the HRW-treatment group. The protective indicator, SOD, significantly increased with the use of HRW. HRW could also reverse the depletion of GSH and increase the GSH-Px caused by APAP (Figure 2A). Peroxynitrite (NT) formation and 4-HNE expression were also inhibited by HRW treatment (Figure 2B and C). Meanwhile, we also tested the effect of HRW on inflammatory cytokines in the blood and liver tissues 3 d after APAP challenge. The levels of IL-1β and TNF-α in the peripheral blood were markedly increased in the APAP + NS group compared with the normal control and APAP + HRW groups. Meanwhile, HRW could decrease the *IL-1β* and *TNF-α* mRNA levels in the liver (Figure 3).

HRW protected the endoplasmic reticulum and mitochondria in the liver

Three days after APAP administration, mice were sacrificed and the liver tissue was obtained to assess

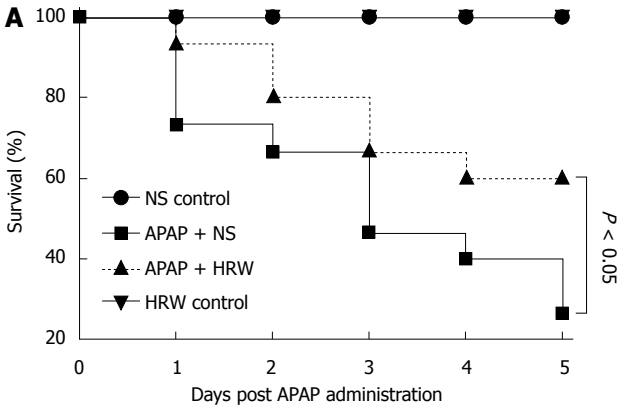
A
Survival (%)
100
80
60
40
20
0
1
2
3
4
5
Days post APAP administration
NS control
APAP + NS
APAP + HRW
HRW control
P < 0.05

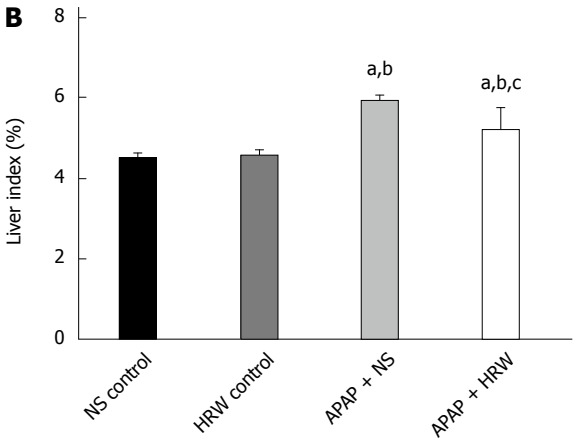
B
Liver index (%)
8
6
4
2
0
a,b
a,b,c
NS control
HRW control
APAP + NS
APAP + HRW

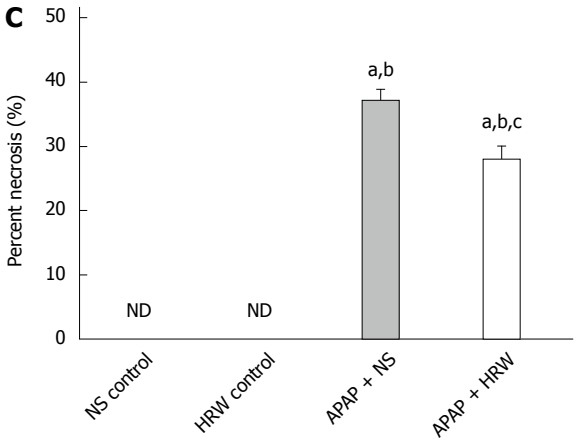
C
Percent necrosis (%)
50
40
30
20
10
0
ND
ND
a,b
a,b,c
NS control
HRW control
APAP + NS
APAP + HRW

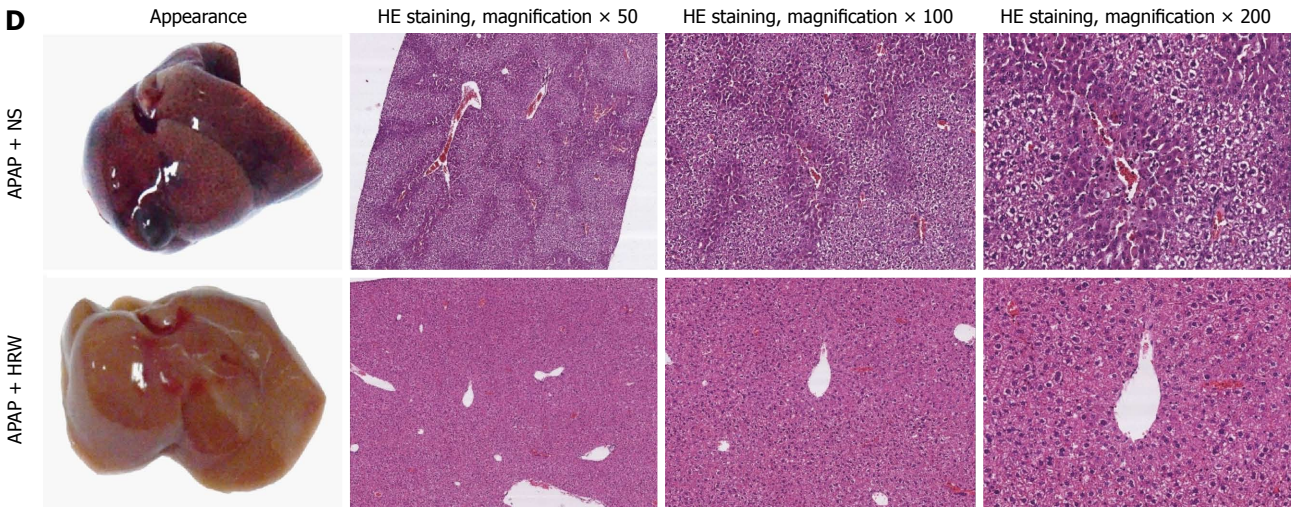
D
Appearance
HE staining, magnification × 50
HE staining, magnification × 100
HE staining, magnification × 200
APAP + NS
APAP + HRW

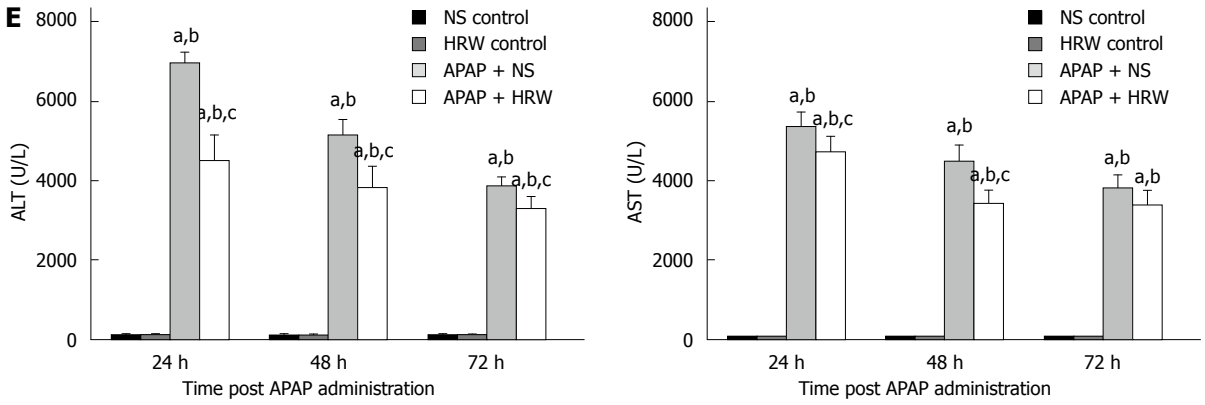
E
ALT (U/L)
AST (U/L)
8000
6000
4000
2000
0
a,b
a,b,c
24 h
48 h
72 h
Time post APAP administration
NS control
HRW control
APAP + NS
APAP + HRW

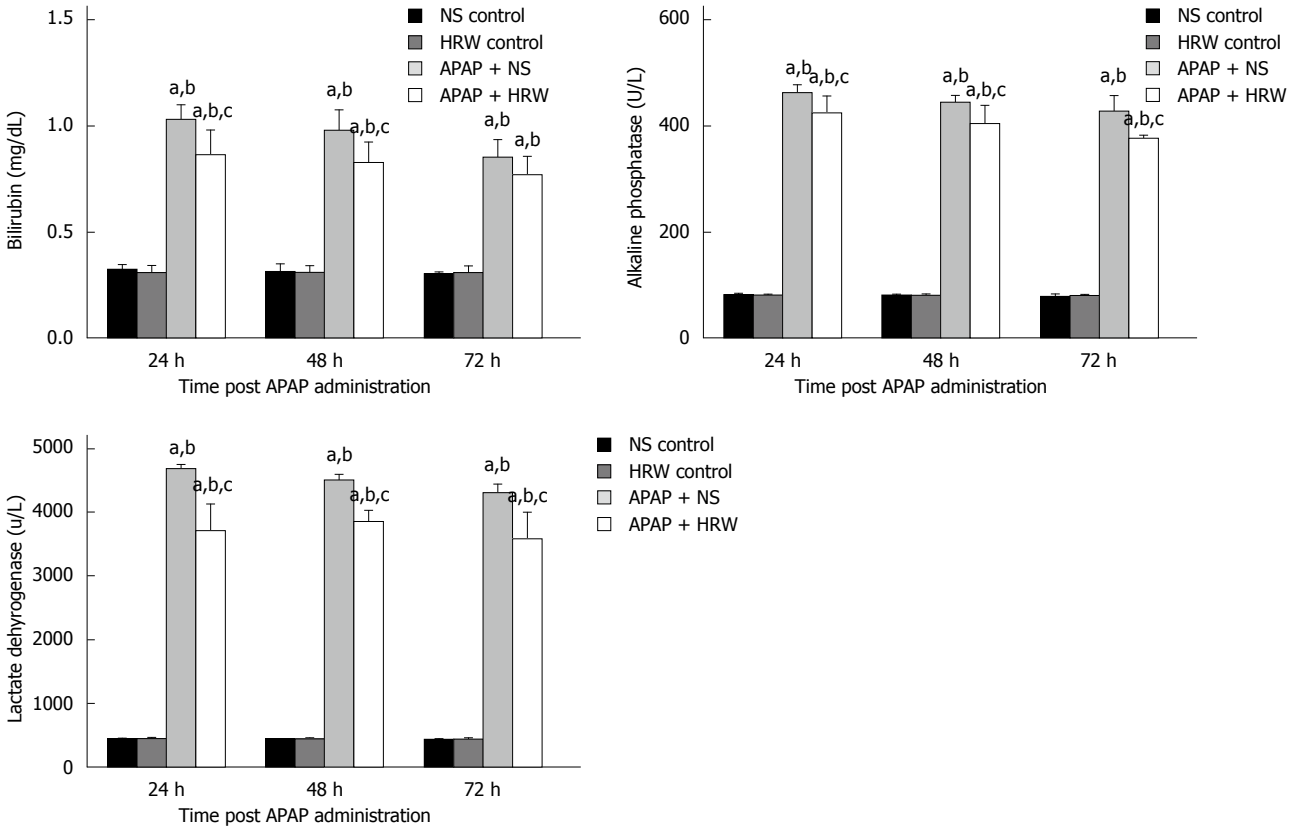

Figure 1 Hydrogen-rich water leads to an obvious enhancement in the survival and decrease in the liver injury after acetaminophen challenge. A: Kaplan-Meier survival curve for mice in three groups in 5 d after a single, lethal dose of 750 mg/kg acetaminophen (APAP) [normal saline (NS) control or hydrogen-rich water (HRW) control groups, n = 5; APAP + NS or APAP + HRW groups, n = 15]; B: Liver tissues were harvested 3 d after a sub-lethal dose of 500 mg/kg APAP. The liver index was used to evaluate the liver injury and it was decreased by HRW administration (n = 6, mean ± SD, $^{a}P < 0.05$ *vs* NS control group, $^{b}P < 0.05$ *vs* HRW control group, and $^{c}P < 0.05$ *vs* APAP + NS group; C: Percent necrosis of mice in different groups (n = 6, mean ± SD, $^{a}P < 0.05$ *vs* NS control group, $^{b}P < 0.05$ *vs* HRW control group, and $^{c}P < 0.05$, *vs* APAP + NS group); D: The representative appearance of livers and HE staining of murine liver sections. Decreased liver hemorrhaging, necrosis, and acute inflammation were observed in the HRW treated mice; E: After a sub-lethal dose of 500 mg/kg APAP administration, blood samples were harvested by tail cutting at 24 and 48 h and eyeball removal at 72 h. Serum was separated by centrifugation from blood to evaluate the liver function. Total bilirubin, alkaline phosphatase (ALP) and lactate dehydrogenase (LDH) at 24, 48 and 72 h were reduced with HRW treatment (n = 6, mean ± SD, $^{a}P < 0.05$ *vs* NS control group; $^{b}P < 0.05$ *vs* HRW control group; and $^{c}P < 0.05$ *vs* APAP + NS group). ALT: Alanine aminotransferase; AST: Aspartate aminotransferase.

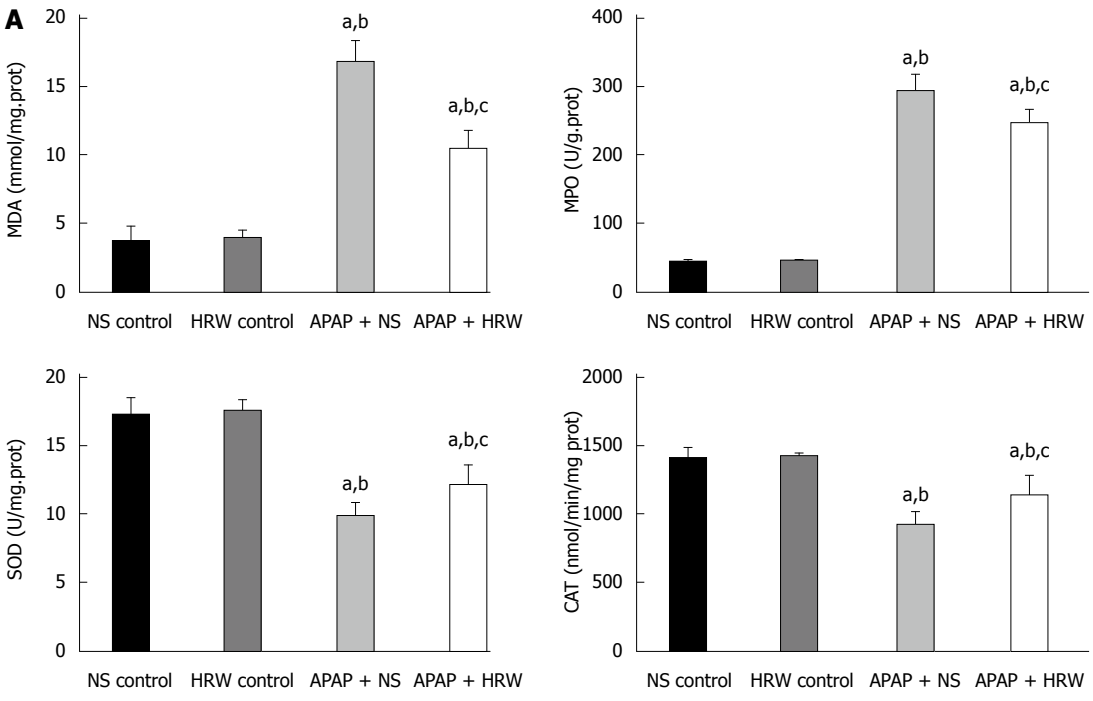

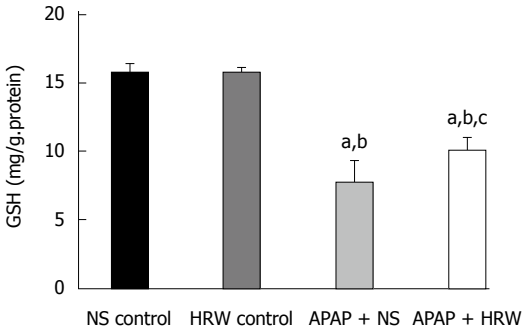
GSH (mg/g.protein)
20
15
10
5
0
a,b
a,b,c
NS control
HRW control
APAP + NS
APAP + HRW

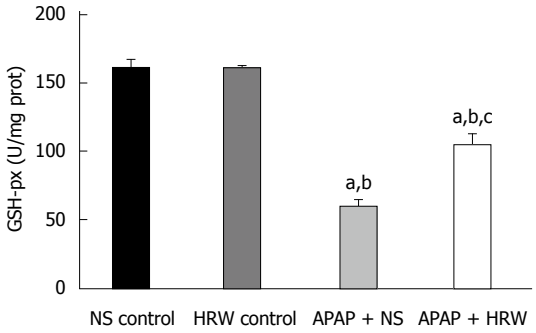
GSH-px (U/mg prot)
200
150
100
50
0
a,b
a,b,c
NS control
HRW control
APAP + NS
APAP + HRW

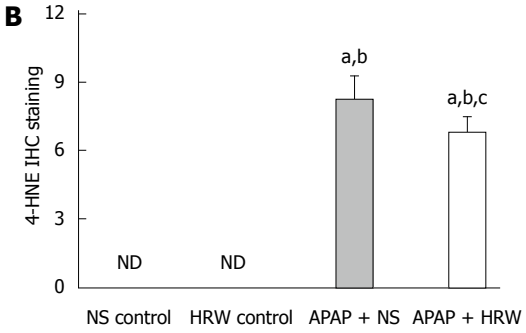
B
4-HNE IHC staining
12
9
6
3
0
ND
ND
a,b
a,b,c
NS control
HRW control
APAP + NS
APAP + HRW

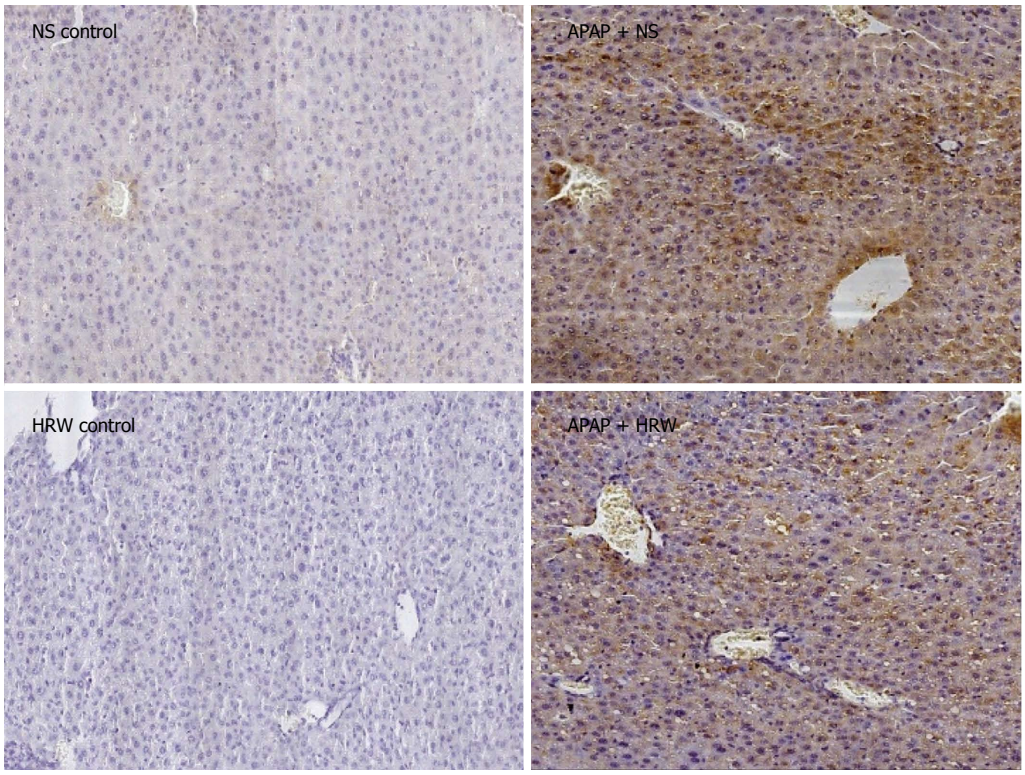
NS control
APAP + NS
HRW control
APAP + HRW

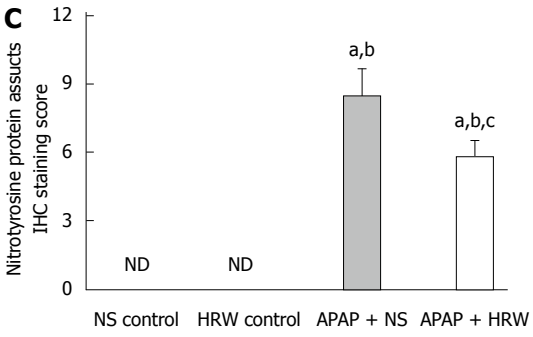
C
Nitrotyrosine protein assucts IHC staining score
12
9
6
3
0
ND
ND
a,b
a,b,c
NS control
HRW control
APAP + NS
APAP + HRW

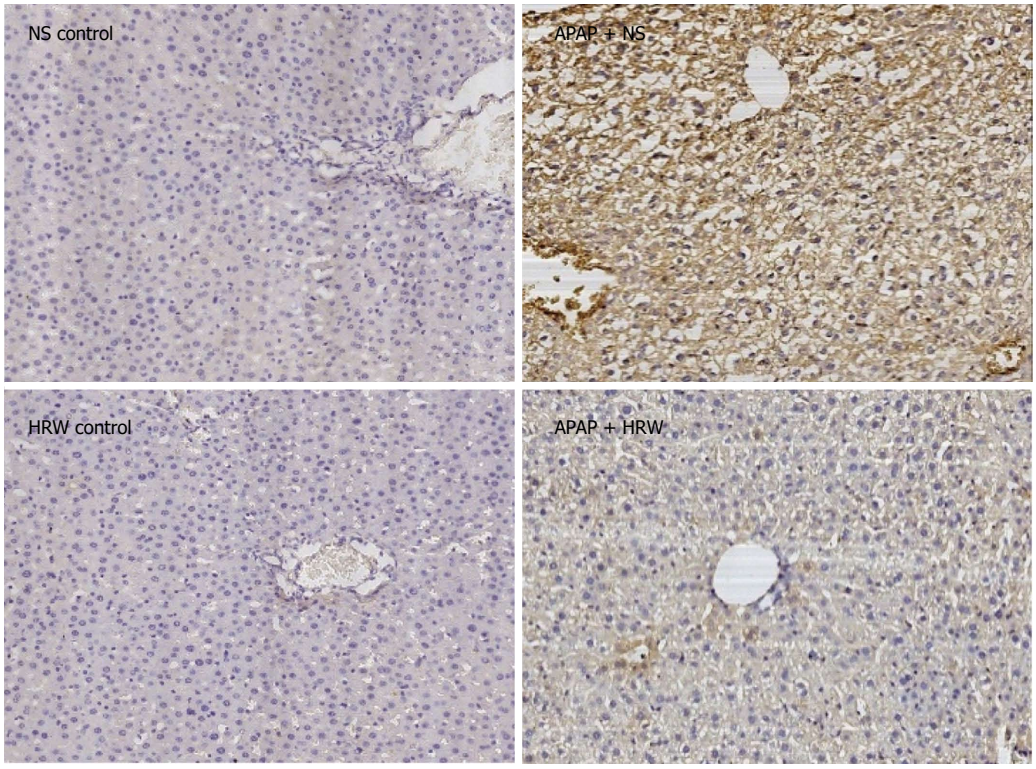

Figure 2 Hydrogen-rich water decreases the oxidative stress and nitrotyrosine formation in the liver after acetaminophen administration. Three days after a sub-lethal dose of 500 mg/kg acetaminophen (APAP) challenge, blood samples and liver tissues were harvested to evaluate the oxidative stress, inflammation and nitrotyrosine formation. A: Hydrogen-rich water (HRW) protected against APAP-induced elevated malonyldialdehyde (MDA) and myeloperoxidase (MPO) levels, decreased superoxide dismutase (SOD), catalase (CAT), glutathione (GSH) and glutathione peroxidase (GSH-px) activities; B: HRW inhibited the expression of 4-HNE in the liver; C: HRW inhibited the nitrotyrosine (NT) protein adduct formation in the liver (n = 6, mean ± SD, $^{a}P < 0.05$ *vs* NS control group; $^{b}P < 0.05$ *vs* HRW control group; and $^{c}P < 0.05$ *vs* APAP + NS group).

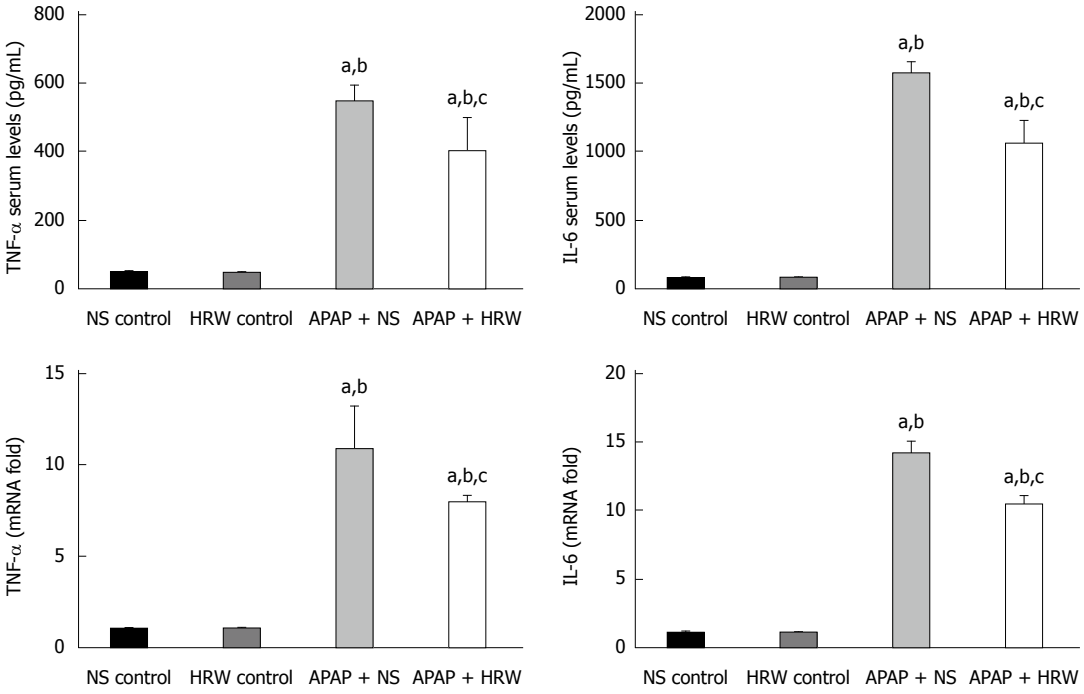

Figure 3 Hydrogen-rich water decreases the inflammation in the liver after acetaminophen administration. Hydrogen-rich water (HRW) reduced the serum TNF-α and IL-6 concentrations and decreased the transcriptional levels of TNF-α and IL-6 in the liver (n = 6, mean ± SD, $^{a}P < 0.05$ *vs* NS control group; $^{b}P < 0.05$ *vs* HRW control group; and $^{c}P < 0.05$ *vs* APAP + NS group). NS: Normal saline.

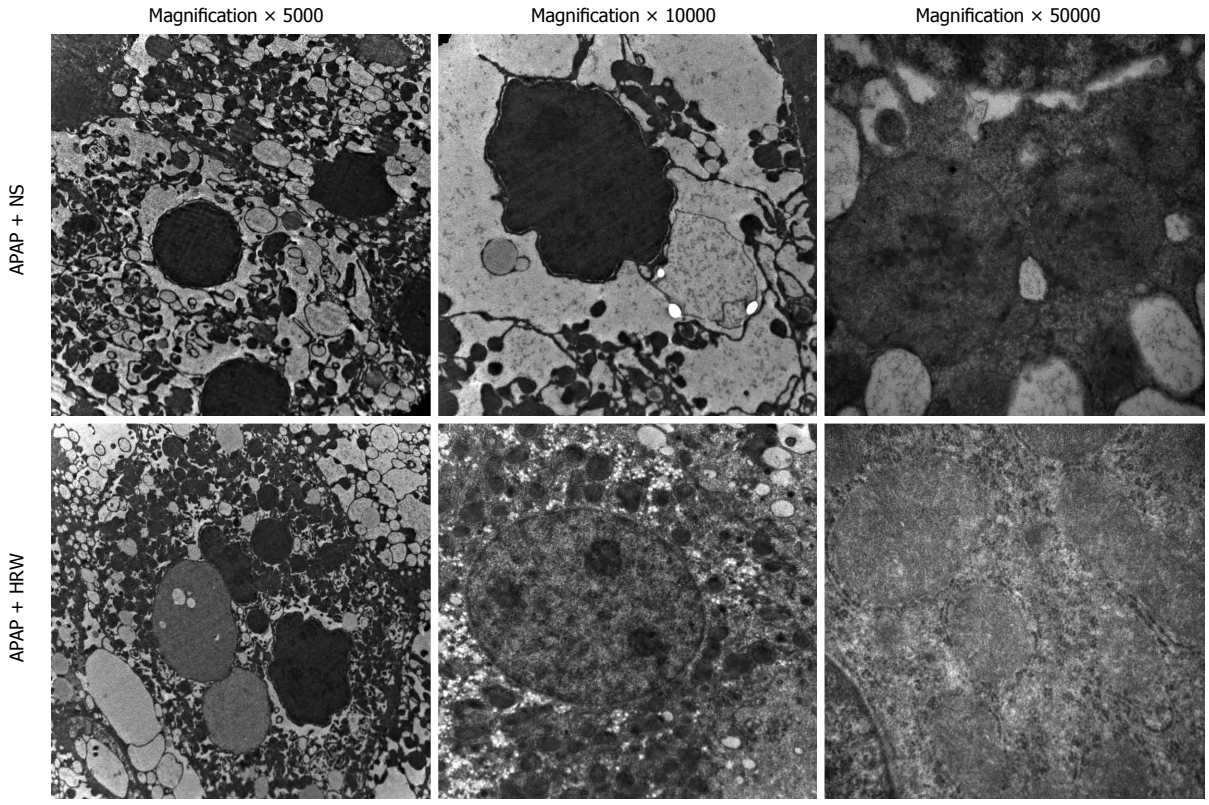

Figure 4 Hydrogen-rich water protects the integrity and stability of organelles after acetaminophen challenge. Representative electron microscopy of endoplasmic reticulum distension, hyperplasia and dissolution as well as hepatocyte megamitochondria in the acetaminophen (APAP) challenged mice. Hydrogen-rich water (HRW) treatment can alleviate the damage to a relatively normal level. NS: Normal saline.

the hepatic subcellular structure injury. Electron microscopy revealed that APAP induced endoplasmic reticulum distension, hyperplasia and breakdown. It could also induce megamitochondria, mitochondria pyknosis, distension and flocculent degeneration. These injuries could be alleviated by different degrees of HRW treatment (Figure 4).

HRW promoted hepatocyte proliferation in vivo after APAP challenge

Hepatocyte proliferation was a key step in recovery from liver injury. Therefore, we hypothesized that HRW might also increase hepatocyte proliferation after APAP overdose. To test this hypothesis, mice were killed at 72 h after APAP administration, and livers were harvested to determine the BrdU, Ki67 and PCNA staining. The tissue from the APAP-challenged mice displayed a small increase in the number of positive staining hepatocytes, which were confined to the centrilobular areas, but HRW significantly enhanced the BrdU, Ki67 and PCNA staining compared with NS-treated APAP-challenged mice (Figure 5A). The induction of cyclin D1 is the most reliable marker for cell cycle (G1 phase) progression in hepatocytes. Western blot was performed using whole-cell extracts prepared from liver tissue to assess the expression of cyclin D1 and PCNA in mice subjected to ALI or the control procedure. As observed in Figure 5B, the cyclin D1 and PCNA expression in the control group was minimal. In contrast, cyclin D1 and PCNA expression was clearly observed in HRW-treated animals at 72 h after APAP administration (Figure 5B).

HRW inhibited Cx32 expression to alleviate liver injury

Three days after APAP administration, mice were sacrificed, the liver tissue was obtained and immunohistochemical analysis was performed to ascertain the localization and expression of Cx32 in liver tissue. Mice treated with APAP displayed significant immunoreactivity for Cx32 around the central veins in the liver. In contrast, the group of mice treated with HRW had lower Cx32 transcription and protein levels (Figure 6A-C).

HRW inhibited APAP-induced phosphorylation of JNK and activation of CYP2E1

JNK activation is mediated by oxidative stress and plays pathogenic roles in a diverse array of cellular programs, including cell differentiation, movement, proliferation and death. Three days after APAP administration, mice were sacrificed and the livers were collected to investigate the mechanism for APAP-induced necrotic hepatocyte death; we studied the JNK activation involved in the signal transduction in the hepatic tissues. Western blot analyses showed a significant enhancement in the expression of phospho-

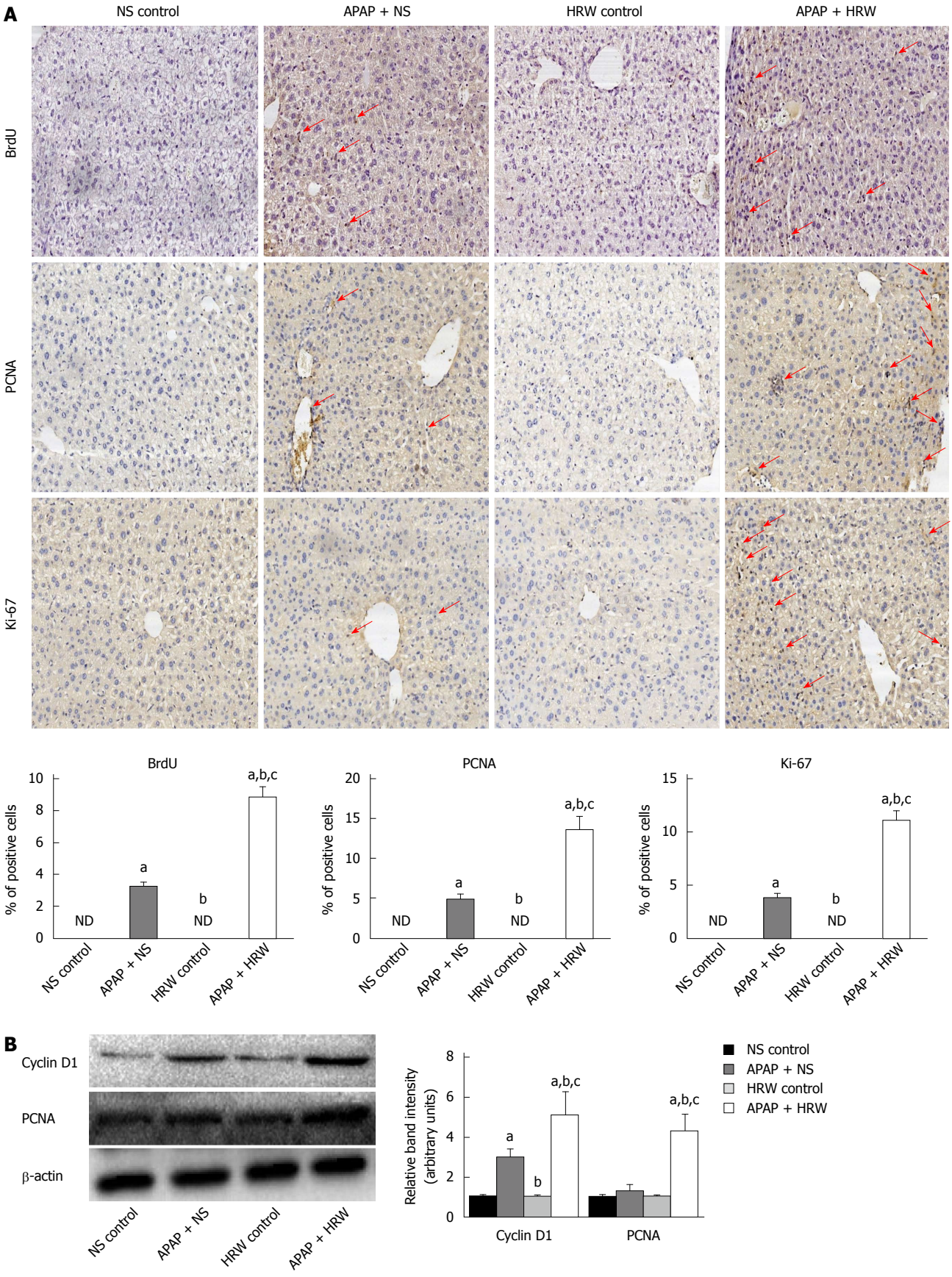

Figure 5 Hydrogen-rich water facilitates hepatocyte proliferation after acetaminophen challenge. A: Representative immunohistochemistry staining of BrdU, Ki67 and PCNA in the saline plus acetaminophen (APAP) as well as hydrogen-rich water (HRW) plus APAP treatment mice. The quantification of hepatocyte proliferation was assessed by calculating the positive cells observed by microscopy (magnification × 200); B: Western blot analysis for the protein content of cyclin D1 and PCNA proteins in response to APAP and HRW treatment in the liver. β-actin was used as an internal control (n = 6, mean ± SD, $^{a}P < 0.05$ *vs* NS control group, $^{b}P < 0.05$ *vs* APAP+NS group, and $^{c}P < 0.05$ *vs* HRW control group). NS: Normal saline.

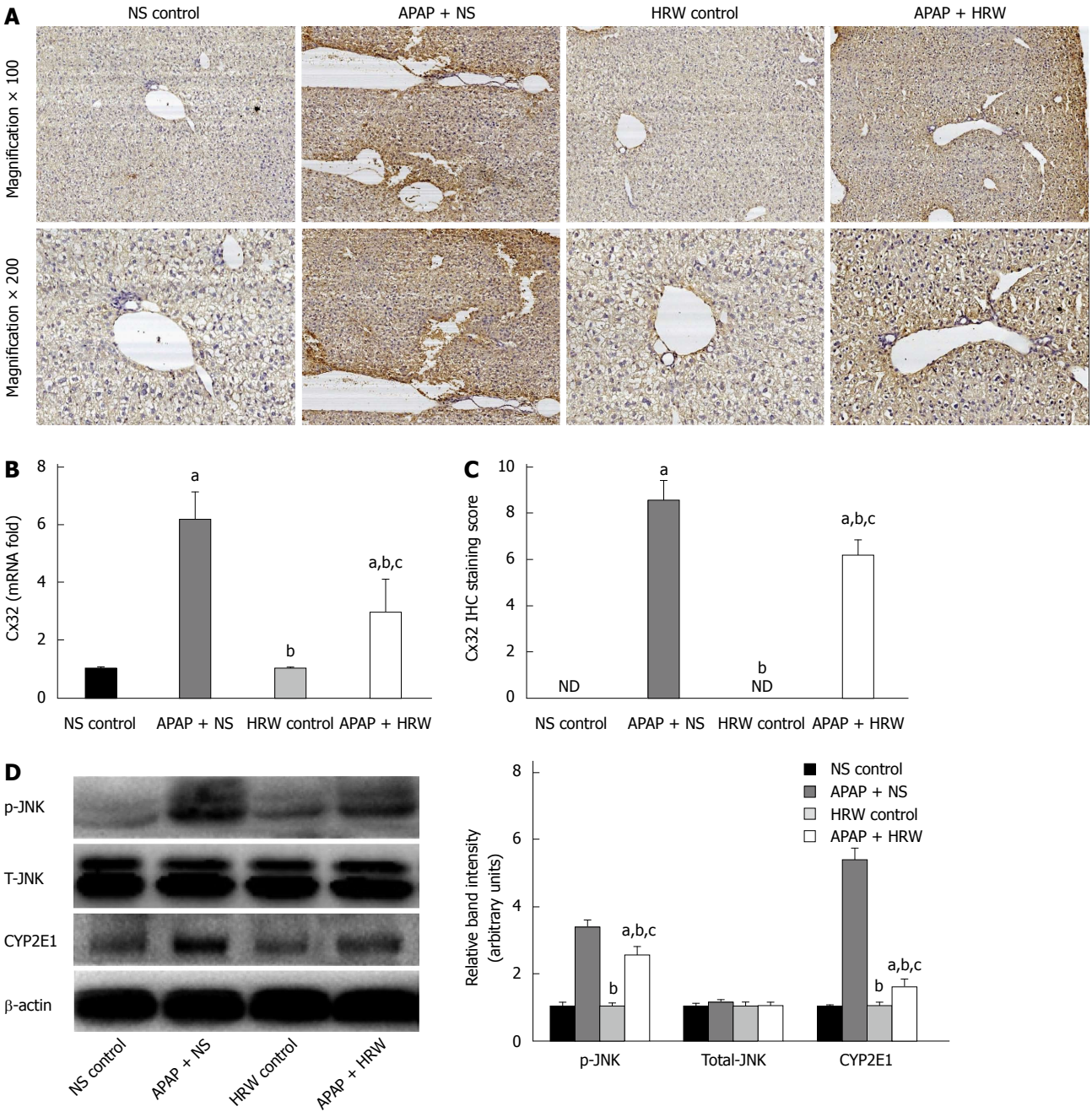

Figure 6 Hydrogen-rich water inhibited connexin 32 expression in the liver tissue. A: Representative photographs of connexin 32 (Cx32) expression in the liver. The acetaminophen (APAP)-challenged mice had more Cx32 immunopositive staining, as indicated by the brown color, while treatment with hydrogen-rich water (HRW) can significantly reduce Cx32 immunostaining; B: The Cx32 IHC staining score indicated that hydrogen therapy could significantly lower the staining score and reduce its activation and expression; C: The relative Cx32 mRNA levels in the three groups; D: Western blot analysis for the protein content of JNK and cytochrome P4502E (CYP2E1) proteins in response to APAP and HRW treatment in the liver. β-actin was used as an internal control (n = 6, mean ± SD, $^{a}P < 0.05$ *vs* NS control group; $^{b}P < 0.05$ *vs* APAP + NS group, and $^{c}P < 0.05$ *vs* HRW control group). NS: Normal saline.

JNK after APAP challenge, which could be reduced by the administration of HRW. No significant changes were found in the expression of total JNK. Furthermore, we investigated the effect of APAP on the CYP2E1 protein level and the result showed that the CYP2E1 protein level was much higher in the APAP + NS group compared with the APAP + HRW group (Figure 6D).

DISCUSSION

Progress has been achieved in the research of hydrogen therapy in diseases such as metabolism disorders, cancer, tissue ischemia reperfusion injury and more. Hydrogen has antioxidant, anti-inflammatory, anti-apoptotic and other protective effects, and it selectively

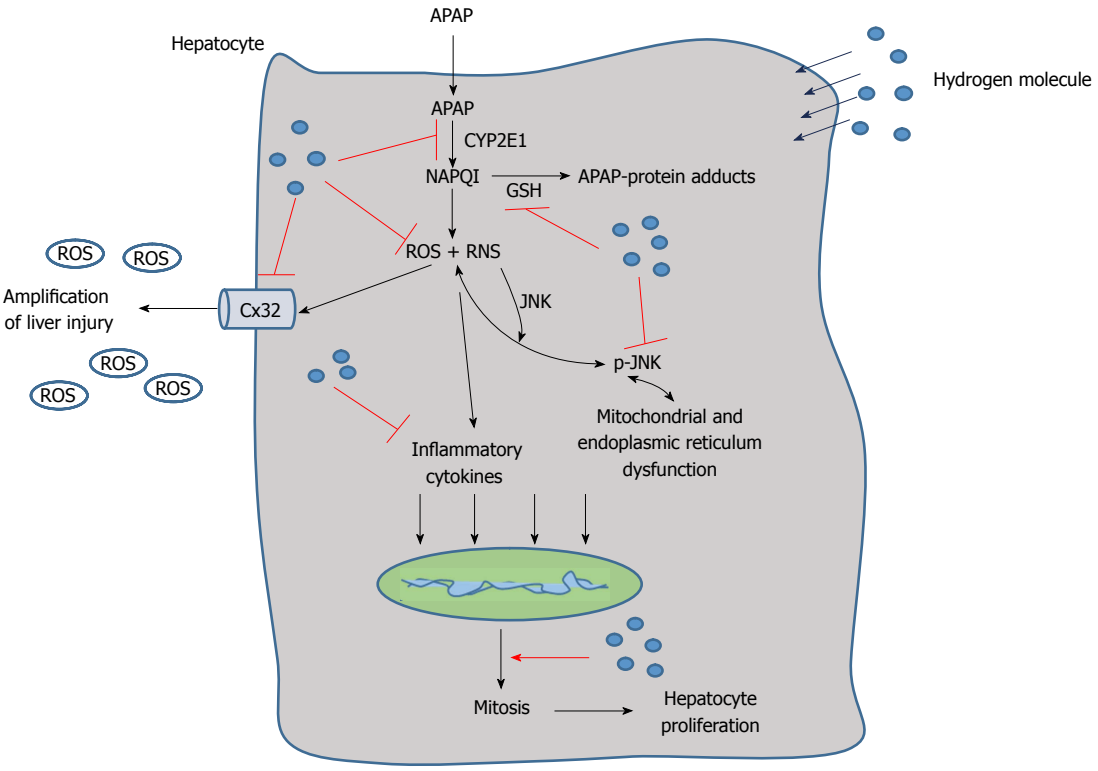

Figure 7 Schematic representation of the proposed effect of the hydrogen molecule in acetaminophen-induced hepatic injury. After acetaminophen (APAP) administration into the hepatocytes, APAP is first metabolized through the cytochrome P4502E (CYP2E1) and generates N-acetyl-p-benzoquinone imine (NAPQI), which binds with glutathione (GSH) and increases reactive oxygen species (ROS) and RNS formation as well as the level of inflammatory cytokines. It can also cause JNK phosphorylation that damages the mitochondria and endoplasmic reticulum. Meanwhile, connexin 32 (Cx32) can be induced with oxidative stress, which can promote the amplification of liver injury. The hepatic self-repair function is also activated after APAP administration, which can promote the cell mitosis to facilitate liver regeneration. In the present study, we found that hydrogen can reduce APAP hepatotoxicity by inhibiting APAP metabolism, ROS and RNS formation, Cx32 expression and promote hepatocyte proliferation.

quenches detrimental ROS, such as hydroxyl radicals and peroxynitrite, but it does not have an effect on physiological ROS, such as superoxide anion radical, hydrogen peroxide, and nitric oxide[20]. Because of its advantageous distribution characteristics, hydrogen can penetrate biomembranes and diffuse into the cytosol, mitochondria, and nucleus, successfully targeting organelles[28]. In this study, we found that hydrogen could reduce APAP-related liver injury by reducing hepatic necrosis, improving survival, reducing oxidative stress and inflammatory reaction in the liver, facilitating liver regeneration, protecting the integrity and stability of the hepatocyte organelles and inhibiting the expression of Cx32, CYP2E1 and phospho-JNK (Figure 7).

APAP is a widely used, safe, effective analgesic when used within therapeutic doses. However, long-term and overdose use of APAP can induce severe hepatotoxicity and nephrotoxicity in both animals and humans[29]. The transport function and membrane permeability are impaired by APAP-induced hepatocyte injury, leading to leakage of enzymes from these cells. Therefore, the marked elevated levels of serum transaminases, bilirubin, ALP and LDH activities could be used to detect severe damage to hepatic tissue membranes during APAP-induced hepatotoxicity. However, treatment with HRW effectively reduced these alterations and improved the 5-d survival, demonstrating its hepatoprotective effects. The histopathological analysis of liver sections indicated moderate centrilobular necrosis, fatty infiltration and lymphocytic infiltration in the HRW + APAP treated mice with respect to the NS + APAP treated mice.

CYP2E1 is the major catalyst involved in the metabolism of drugs, and APAP is mainly metabolized by CYP2E1 to form an electrophilic metabolite, NAPQI, which is primarily inactivated by conjugation with GSH and posterior binding with other proteins to form protein adducts[30,31]. The accumulation of the intermediate metabolites and depletion of GSH are key mechanisms of APAP-hepatotoxicity that directly cause liver damage[6]. To detect whether the protective effects of HRW on the liver are associated with the inhibition of CYP2E1, we investigated the expression of CYP2E1 protein levels in different groups. The results suggest that HRW could obviously reduce APAP-induced CYP2E1 expression, which reduces NAPQI formation associated with APAP hepatotoxicity and effectively protects the liver against that pathophysiology.

A number of pieces of evidence implicate the roles of ROS and inflammation in the development of APAP-

induced liver injury. For instance, excess depletion of GSH beyond a critical level leads to oxidative stress and exacerbates the hepatotoxicity. The masses of the metabolites produced by APAP are also found to generate ROS in biological systems[32,33]. Therefore, we measured the intracellular ROS production, inflammatory cytokines levels, GSH contents, lipid peroxidation, activities of the antioxidant enzymes and oxidation products (SOD, CAT, MDA, and 4-HNE) in hepatic tissues. APAP intoxication significantly increased the intracellular ROS production, inflammation levels and lipid peroxidation as well as decreased the GSH content. APAP intoxication also decreased the activities of the antioxidant enzymes SOD and CAT. However, the effect of HRW compared to the APAP + NS treatment, which was consistent with previous studies, indicates that hydrogen has a powerful anti-inflammatory and antioxidant effect. ROS are not only the direct damaging factors to the liver, they are also important signaling molecules which can activate JNK[34]. JNK activation is a pivotal regulator of mitochondrial permeabilization and plays a key role in the development of APAP-induced hepatotoxicity[35]. ROS may activate JNK through the oxidation of kinase inhibitors, which can inhibit JNK or upstream ASK1[36]. It can also lead to the redox inactivation of JNK phosphatase, which sustains JNK activation[37]. To check whether HRW could inhibit APAP-induced JNK phosphorylation, we tested the JNK phosphorylation by Western blot analysis. The results of our study showed that HRW could greatly attenuate the expression of phospho-JNK in the liver tissue to alleviate liver injury. It is also well established that APAP overdose induces peroxynitrite formation, as indicated by the appearance of nitrotyrosine protein adducts in centrilobular hepatocytes. Also, we found that hydrogen could inhibit the APAP-induced peroxynitrite formation, which might partly explain its protective mechanism.

To determine the deeper mechanism of the protective effect of HRW against APAP-induced hepatotoxicity, we focused on the effect of hydrogen on the hepatocyte proliferation, maintaining the stability of subcellular fraction and Cx32 expression. Liver regeneration is a compensatory process after a toxic insult, which guarantees the replacement of necrotic cells and full recovery of organ function[38]. The exposure of hepatocytes to growth factor leads to the expression of cell cycle proteins. Cyclin D1 is the most reliable marker for cell cycle (G1 phase) progression in hepatocytes. Once hepatocytes express cyclin D1, they have passed the G1 restriction point and are committed to DNA replication[39]. Notably, in the current investigation, we found that HRW could promote BrdU, ki-67 and PCNA expression in the APAP-challenged liver, and these are the iconic markers for liver regeneration. Meanwhile, the Western blot data showed that HRW markedly increased the level of cyclin D1 in the APAP-challenged liver tissue. These changes in cyclin D1 expression were associated with decreased serum ALT/AST levels and improvement of liver regeneration in HRW-treated mice that received APAP, suggesting that HRW facilitates the activation of cyclin D1-mediated regeneration pathways.

The endoplasmic reticulum (ER) is the major cellular site of protein folding and modification. ER stress occurs when the level of APAP-induced protein adducts entering the ER exceeds its folding capacity[40,41]. Meanwhile, APAP metabolites not only damage the structural integrity of mitochondria, resulting in membrane fracture and electronic leak, they also lead to dysfunction of the respiratory chain and energy generation[42]. Mitochondrial dysfunction is believed to be the propagating event of APAP toxicity, resulting in loss of ATP production, mitochondrial swelling, generation of ROS, formation of the mitochondrial permeability transition pore and the release of mitochondrial contents, all of which ultimately result in hepatic necrosis[30,43]. In this study, treatment with HRW could protect the integrity and function of the ER and mitochondria.

Gap junctions are plasma membrane spatial microdomains constituted by assemblies of channel proteins called connexins, which provide direct intercellular communication pathways, allowing cell-to-cell rapid exchange of ions and metabolites[44]. Cx32 is the major gap junction protein in the liver, and previous studies have shown that interfering with Cx32 greatly reduces liver damage due to several toxic agents, including carbon tetrachloride, D-galactosamine, TAA and APAP[19,45]. In this study, we found that the expression of Cx32 was obviously elevated in the APAP-challenged mice and HRW + APAP administration could significantly reduce the expression compared with the APAP + NS treated group.

In conclusion, the results of the present study demonstrate that HRW has a prophylactic as well as a therapeutic role in preventing APAP-induced hepatotoxicity, most likely due to its unique cytoprotective properties such as antioxidant and anti-inflammation activities. Most importantly, HRW can maintain the stability of the cellular structure, promote hepatocyte regeneration and inhibit the expression of the Cx32 gap junction, JNK phosphorylation and CYP2E1 after APAP challenge. All of these findings indicate that HRW can be a potential therapy for preventing liver injury caused by APAP overdose.

ACKNOWLEDGMENTS

We thank UNIVA Guangzhou Trading Co., Ltd for their assistance in providing hydrogen-rich water.

COMMENTS

Background

Acetaminophen (N-acetyl-p-aminophenol, APAP) is a widely used analgesic

and antipyretic drug in the clinic. APAP is believed to be safe within therapeutic doses, but overdose usage causes a centrilobular hepatic necrosis that leads to acute liver failure. Overdoses of APAP can promote the generation of the toxic metabolite N-acetyl-quinoneimine (NAPQI), which is immediately conjugated with glutathione (GSH) to form the nontoxic metabolites cysteine. However, when the GSH is exhausted, NAPQI covalently binds with other proteins to form protein adducts, directly leading to cell death.

Research frontiers

Hydrogen therapy is a new medical approach that has recently become increasingly appreciated. Hydrogen has anti-oxidant, anti-inflammatory, anti-apoptotic, anti-allergy, and anti-cancer effects. Several methods invented to deliver hydrogen, including inhalation, drinking hydrogen-rich water (HRW) and injection with hydrogen-saturated saline, are valid and reliable. In the area of prevention of APAP-induced liver injury, a research hotspot is to search for more effective and convenient methods that more people will accept. Meanwhile, the mechanism of a new medicine is another hotspot.

Innovations and breakthroughs

The authors investigated the effects of HRW on APAP-induced liver injury in mice. The present study concluded that HRW can significantly prevent the APAP-induced acute hepatotoxicity by enhancing the hepatic antioxidant activity, reducing inflammation, protecting the hepatic subcellular structure, promoting liver regeneration, and inhibiting CX32, CYP2E1 and phospho-JNK activation.

Applications

Hydrogen therapy might be safe and effective for preventing liver injury derived from APAP application.

Terminology

Hydrogen is the lightest gas in nature, but it has anti-oxidant and anti-inflammatory effects. It has been proven effective in treating many diseases. HRW is produced by pressurizing the hydrogen gas into the water by a specific device under high pressure.

Peer-review

The manuscript is well-written and interesting because it investigates the hepatoprotective effects and mechanisms of HRW in APAP-induced liver injury in mice. The authors first generated a murine model of APAP-induced liver injury; then, HRW was administered intraperitoneally for 3 d to explore whether HRW has a hepatoprotective effect. They then go on to detect the change in the liver injury index and several cytokines. Meanwhile, they found that HRW promoted hepatocyte proliferation and liver regeneration after APAP administration, indicating that HRW is expected to be a potent hepatoprotective agent in the future and the hepatoprotective effect of HRW is worth studying.

REFERENCES

1 **Larson AM**. Acetaminophen hepatotoxicity. *Clin Liver Dis* 2007; **11**: 525-48, vi [PMID: 17723918 DOI: 10.1016/j.cld.2007.06.006]

2 **Larson AM**, Polson J, Fontana RJ, Davern TJ, Lalani E, Hynan LS, Reisch JS, Schiødt FV, Ostapowicz G, Shakil AO, Lee WM. Acetaminophen-induced acute liver failure: results of a United States multicenter, prospective study. *Hepatology* 2005; **42**: 1364-1372 [PMID: 16317692 DOI: 10.1002/hep.20948]

3 **Jaeschke H**, Bajt ML. Intracellular signaling mechanisms of acetaminophen-induced liver cell death. *Toxicol Sci* 2006; **89**: 31-41 [PMID: 16177235 DOI: 10.1093/toxsci/kfi336]

4 **McGill MR**, Sharpe MR, Williams CD, Taha M, Curry SC, Jaeschke H. The mechanism underlying acetaminophen-induced hepatotoxicity in humans and mice involves mitochondrial damage and nuclear DNA fragmentation. *J Clin Invest* 2012; **122**: 1574-1583 [PMID: 22378043 DOI: 10.1172/JCI59755]

5 **Dahlin DC**, Miwa GT, Lu AY, Nelson SD. N-acetyl-p-benzoquinone imine: a cytochrome P-450-mediated oxidation product of acetaminophen. *Proc Natl Acad Sci USA* 1984; **81**: 1327-1331 [PMID: 6424115 DOI: 10.1073/pnas.81.5.1327]

6 **Hinson JA**, Roberts DW, James LP. Mechanisms of acetaminophen-induced liver necrosis. *Handb Exp Pharmacol* 2010; (**196**): 369-405 [PMID: 20020268 DOI: 10.1007/978-3-642-00663-0_12]

7 **Muldrew KL**, James LP, Coop L, McCullough SS, Hendrickson HP, Hinson JA, Mayeux PR. Determination of acetaminophen-protein adducts in mouse liver and serum and human serum after hepatotoxic doses of acetaminophen using high-performance liquid chromatography with electrochemical detection. *Drug Metab Dispos* 2002; **30**: 446-451 [PMID: 11901099 DOI: 10.1124/dmd.30.4.446]

8 **Jaeschke H**, McGill MR, Ramachandran A. Oxidant stress, mitochondria, and cell death mechanisms in drug-induced liver injury: lessons learned from acetaminophen hepatotoxicity. *Drug Metab Rev* 2012; **44**: 88-106 [PMID: 22229890 DOI: 10.3109/03602532.2011.602688]

9 **Agarwal R**, MacMillan-Crow LA, Rafferty TM, Saba H, Roberts DW, Fifer EK, James LP, Hinson JA. Acetaminophen-induced hepatotoxicity in mice occurs with inhibition of activity and nitration of mitochondrial manganese superoxide dismutase. *J Pharmacol Exp Ther* 2011; **337**: 110-116 [PMID: 21205919 DOI: 10.1124/jpet.110.176321]

10 **Cover C**, Liu J, Farhood A, Malle E, Waalkes MP, Bajt ML, Jaeschke H. Pathophysiological role of the acute inflammatory response during acetaminophen hepatotoxicity. *Toxicol Appl Pharmacol* 2006; **216**: 98-107 [PMID: 16781746 DOI: 10.1016/j.taap.2006.04.010]

11 **Bajt ML**, Ramachandran A, Yan HM, Lebofsky M, Farhood A, Lemasters JJ, Jaeschke H. Apoptosis-inducing factor modulates mitochondrial oxidant stress in acetaminophen hepatotoxicity. *Toxicol Sci* 2011; **122**: 598-605 [PMID: 21572097 DOI: 10.1093/toxsci/kfr116]

12 **Blazka ME**, Wilmer JL, Holladay SD, Wilson RE, Luster MI. Role of proinflammatory cytokines in acetaminophen hepatotoxicity. *Toxicol Appl Pharmacol* 1995; **133**: 43-52 [PMID: 7597709 DOI: 10.1006/taap.1995.1125]

13 **James LP**, McCullough SS, Knight TR, Jaeschke H, Hinson JA. Acetaminophen toxicity in mice lacking NADPH oxidase activity: role of peroxynitrite formation and mitochondrial oxidant stress. *Free Radic Res* 2003; **37**: 1289-1297 [PMID: 14753753 DOI: 10.1080/10715760310001617776]

14 **Das J**, Ghosh J, Manna P, Sil PC. Acetaminophen induced acute liver failure via oxidative stress and JNK activation: protective role of taurine by the suppression of cytochrome P450 2E1. *Free Radic Res* 2010; **44**: 340-355 [PMID: 20166895 DOI: 10.3109/10715760903513017]

15 **Hinson JA**, Bucci TJ, Irwin LK, Michael SL, Mayeux PR. Effect of inhibitors of nitric oxide synthase on acetaminophen-induced hepatotoxicity in mice. *Nitric Oxide* 2002; **6**: 160-167 [PMID: 11890740 DOI: 10.1006/niox.2001.0404]

16 **Bae MA**, Pie JE, Song BJ. Acetaminophen induces apoptosis of C6 glioma cells by activating the c-Jun NH(2)-terminal protein kinase-related cell death pathway. *Mol Pharmacol* 2001; **60**: 847-856 [PMID: 11562448]

17 **Segretain D**, Falk MM. Regulation of connexin biosynthesis, assembly, gap junction formation, and removal. *Biochim Biophys Acta* 2004; **1662**: 3-21 [PMID: 15033576 DOI: 10.1016/j.bbamem.2004.01.007]

18 **Patel SJ**, King KR, Casali M, Yarmush ML. DNA-triggered innate immune responses are propagated by gap junction communication. *Proc Natl Acad Sci USA* 2009; **106**: 12867-12872 [PMID: 19617563 DOI: 10.1073/pnas.0809292106]

19 **Patel SJ**, Milwid JM, King KR, Bohr S, Iracheta-Velle A, Li M, Vitalo A, Parekkadan B, Jindal R, Yarmush ML. Gap junction inhibition prevents drug-induced liver toxicity and fulminant hepatic failure. *Nat Biotechnol* 2012; **30**: 179-183 [PMID: 22252509 DOI: 10.1038/nbt.2089]

20 **Ohsawa I**, Ishikawa M, Takahashi K, Watanabe M, Nishimaki K, Yamagata K, Katsura K, Katayama Y, Asoh S, Ohta S. Hydrogen acts as a therapeutic antioxidant by selectively reducing cytotoxic oxygen radicals. *Nat Med* 2007; **13**: 688-694 [PMID: 17486089 DOI: 10.1038/nm1577]

21 **Zhang JY**, Liu C, Zhou L, Qu K, Wang R, Tai MH, Lei Lei JC, Wu QF, Wang ZX. A review of hydrogen as a new medical therapy. *Hepatogastroenterology* 2012; **59**: 1026-1032 [PMID: 22328284 DOI: 10.5754/hge11883]

22 **Sun H**, Chen L, Zhou W, Hu L, Li L, Tu Q, Chang Y, Liu Q, Sun X, Wu M, Wang H. The protective role of hydrogen-rich saline in experimental liver injury in mice. *J Hepatol* 2011; **54**: 471-480 [PMID: 21145612 DOI: 10.1016/j.jhep.2010.08.011]

23 **Kawai D**, Takaki A, Nakatsuka A, Wada J, Tamaki N, Yasunaka T, Koike K, Tsuzaki R, Matsumoto K, Miyake Y, Shiraha H, Morita M, Makino H, Yamamoto K. Hydrogen-rich water prevents progression of nonalcoholic steatohepatitis and accompanying hepatocarcinogenesis in mice. *Hepatology* 2012; **56**: 912-921 [PMID: 22505328 DOI: 10.1002/hep.25782]

24 **Ohta S**. Molecular hydrogen as a preventive and therapeutic medical gas: initiation, development and potential of hydrogen medicine. *Pharmacol Ther* 2014; **144**: 1-11 [PMID: 24769081 DOI: 10.1016/j.pharmthera.2014.04.006]

25 **Zhang J**, Wu Q, Song S, Wan Y, Zhang R, Tai M, Liu C. Effect of hydrogen-rich water on acute peritonitis of rat models. *Int Immunopharmacol* 2014; **21**: 94-101 [PMID: 24793096 DOI: 10.1016/j.intimp.2014.04.011]

26 **Zhang JY**, Wu QF, Wan Y, Song SD, Xu J, Xu XS, Chang HL, Tai MH, Dong YF, Liu C. Protective role of hydrogen-rich water on aspirin-induced gastric mucosal damage in rats. *World J Gastroenterol* 2014; **20**: 1614-1622 [PMID: 24587639 DOI: 10.3748/wjg.v20.i6.1614]

27 **Qu K**, Xu X, Liu C, Wu Q, Wei J, Meng F, Zhou L, Wang Z, Lei L, Liu P. Negative regulation of transcription factor FoxM1 by p53 enhances oxaliplatin-induced senescence in hepatocellular carcinoma. *Cancer Lett* 2013; **331**: 105-114 [PMID: 23262037 DOI: 10.1016/j.canlet.2012.12.008]

28 **James AM**, Cochemé HM, Murphy MP. Mitochondria-targeted redox probes as tools in the study of oxidative damage and ageing. *Mech Ageing Dev* 2005; **126**: 982-986 [PMID: 15923020 DOI: 10.1016/j.mad.2005.03.026]

29 **Lee WM**, Ostapowicz G. Acetaminophen: pathology and clinical presentation of hepatotoxicity. *Drug induced liver disease* 2007; 389-405

30 **Kon K**, Kim JS, Jaeschke H, Lemasters JJ. Mitochondrial permeability transition in acetaminophen-induced necrosis and apoptosis of cultured mouse hepatocytes. *Hepatology* 2004; **40**: 1170-1179 [PMID: 15486922 DOI: 10.1002/hep.20437]

31 **Lee SS**, Buters JT, Pineau T, Fernandez-Salguero P, Gonzalez FJ. Role of CYP2E1 in the hepatotoxicity of acetaminophen. *J Biol Chem* 1996; **271**: 12063-12067 [PMID: 8662637 DOI: 10.1074/jbc.271.20.12063]

32 **Yan HM**, Ramachandran A, Bajt ML, Lemasters JJ, Jaeschke H. The oxygen tension modulates acetaminophen-induced mitochondrial oxidant stress and cell injury in cultured hepatocytes. *Toxicol Sci* 2010; **117**: 515-523 [PMID: 20616211 DOI: 10.1093/toxsci/kfq208]

33 **Park BK**, Laverty H, Srivastava A, Antoine DJ, Naisbitt D, Williams DP. Drug bioactivation and protein adduct formation in the pathogenesis of drug-induced toxicity. *Chem Biol Interact* 2011; **192**: 30-36 [PMID: 20846520 DOI: 10.1016/j.cbi.2010.09.011]

34 **Hanawa N**, Shinohara M, Saberi B, Gaarde WA, Han D, Kaplowitz N. Role of JNK translocation to mitochondria leading to inhibition of mitochondria bioenergetics in acetaminophen-induced liver injury. *J Biol Chem* 2008; **283**: 13565-13577 [PMID: 18337250 DOI: 10.1074/jbc.M708916200]

35 **Latchoumycandane C**, Goh CW, Ong MM, Boelsterli UA. Mitochondrial protection by the JNK inhibitor leflunomide rescues mice from acetaminophen-induced liver injury. *Hepatology* 2007; **45**: 412-421 [PMID: 17366662 DOI: 10.1002/hep.21475]

36 **Saitoh M**, Nishitoh H, Fujii M, Takeda K, Tobiume K, Sawada Y, Kawabata M, Miyazono K, Ichijo H. Mammalian thioredoxin is a direct inhibitor of apoptosis signal-regulating kinase (ASK) 1. *EMBO J* 1998; **17**: 2596-2606 [PMID: 9564042 DOI: 10.1093/emboj/17.9.2596]

37 **Shen HM**, Liu ZG. JNK signaling pathway is a key modulator in cell death mediated by reactive oxygen and nitrogen species. *Free Radic Biol Med* 2006; **40**: 928-939 [PMID: 16540388 DOI: 10.1016/j.freeradbiomed.2005.10.056]

38 **Fausto N**, Campbell JS, Riehle KJ. Liver regeneration. *Hepatology* 2006; **43**: S45-S53 [PMID: 16447274 DOI: 10.1002/hep.20969]

39 **Yang R**, Zhang S, Cotoia A, Oksala N, Zhu S, Tenhunen J. High mobility group B1 impairs hepatocyte regeneration in acetaminophen hepatotoxicity. *BMC Gastroenterol* 2012; **12**: 45 [PMID: 22569100 DOI: 10.1186/1471-230X-12-45]

40 **Ron D**, Walter P. Signal integration in the endoplasmic reticulum unfolded protein response. *Nat Rev Mol Cell Biol* 2007; **8**: 519-529 [PMID: 17565364 DOI: 10.1038/nrm2199]

41 **Uzi D**, Barda L, Scaiewicz V, Mills M, Mueller T, Gonzalez-Rodriguez A, Valverde AM, Iwawaki T, Nahmias Y, Xavier R, Chung RT, Tirosh B, Shibolet O. CHOP is a critical regulator of acetaminophen-induced hepatotoxicity. *J Hepatol* 2013; **59**: 495-503 [PMID: 23665281 DOI: 10.1016/j.jhep.2013.04.024]

42 **Burke AS**, MacMillan-Crow LA, Hinson JA. Reactive nitrogen species in acetaminophen-induced mitochondrial damage and toxicity in mouse hepatocytes. *Chem Res Toxicol* 2010; **23**: 1286-1292 [PMID: 20578685 DOI: 10.1021/tx1001755]

43 **Cover C**, Mansouri A, Knight TR, Bajt ML, Lemasters JJ, Pessayre D, Jaeschke H. Peroxynitrite-induced mitochondrial and endonuclease-mediated nuclear DNA damage in acetaminophen hepatotoxicity. *J Pharmacol Exp Ther* 2005; **315**: 879-887 [PMID: 16081675 DOI: 10.1124/jpet.105.088898]

44 **Maurel M**, Rosenbaum J. Closing the gap on drug-induced liver injury. *Hepatology* 2012; **56**: 781-783 [PMID: 22833250 DOI: 10.1002/hep.25779]

45 **Asamoto M**, Hokaiwado N, Murasaki T, Shirai T. Connexin 32 dominant-negative mutant transgenic rats are resistant to hepatic damage by chemicals. *Hepatology* 2004; **40**: 205-210 [PMID: 15239104 DOI: 10.1002/hep.20256]

P- Reviewer: Kucera O, Xu CS **S- Editor**: Yu J **L- Editor**: Logan S **E- Editor**: Ma S

World Journal of Gastroenterology

Submit a Manuscript: http://www.wjgnet.com/esps/
Help Desk: http://www.wjgnet.com/esps/helpdesk.aspx
DOI: 10.3748/wjg.v21.i14.4210

World J Gastroenterol 2015 April 14; 21(14): 4210-4215
ISSN 1007-9327 (print) ISSN 2219-2840 (online)

ORIGINAL ARTICLE

Basic Study

Multiphoton microscopy for tumor regression grading after neoadjuvant treatment for colorectal carcinoma

Lian-Huang Li, Zhi-Fen Chen, Xing-Fu Wang, Shuang-Mu Zhuo, Hong-Sheng Li, Wei-Zhong Jiang, Guo-Xian Guan, Jian-Xin Chen

Lian-Huang Li, Shuang-Mu Zhuo, Hong-Sheng Li, Jian-Xin Chen, Institute of Laser and Optoelectronics Technology, Fujian Provincial Key Laboratory for Photonics Technology, Key Laboratory of Optoelectronic Science and Technology for Medicine of Ministry of Education, Fujian Normal University, Fuzhou 350007, Fujian Province, China
Zhi-Fen Chen, Wei-Zhong Jiang, Guo-Xian Guan, Department of Colorectal Surgery, Fujian Medical University Union Hospital, Fuzhou 350001, Fujian Province, China
Xing-Fu Wang, Department of Pathology, the First Affiliated Hospital of Fujian Medical University, Fuzhou 350001, Fujian Province, China
Jian-Xin Chen, College of Photonic and Electronic Engineering, Fujian Normal University, Fuzhou 350007, Fujian Province, China
Author contributions: Li LH, Chen ZF and Wang XF contributed equally to this work; Li LH and Chen JX were responsible for study conception and design; Li LH and Li HS obtained the data; Chen ZF, Wang XF, Zhuo SM, Jiang WZ and Guan GX provided technical support; all authors contributed to analysis and interpretation of data, wrote, reviewed and approved the final manuscript.
Supported by Program for Changjiang Scholars and Innovative Research Team in University, No. IRT1115; the National Natural Science Foundation of China, No. 81271620; the Natural Science Foundation for Distinguished Young Scholars of Fujian Province, No. 2014J06016; the Youth Scientific Research Foundation of Fujian Provincial Department of Health (2013-2-36); and National Clinical Key Specialty Construction Project (General Surgery).
Ethics approval: This study was reviewed and approved by the Fujian Medical University Union Hospital Institutional Review Board.
Informed consent: All study participants provided informed written consent prior to study enrollment.
Conflict-of-interest: The authors declare that they have no conflict of interest.
Data sharing: No additional data are available.

Correspondence to: Jian-Xin Chen, PhD, Professor, College of Photonic and Electronic Engineering, Fujian Normal University, No. 8 Shangsan Road, Cangshan District, Fuzhou 350007, Fujian Province, China. chenjianxin@fjnu.edu.cn
Telephone: +86-591-22686078
Fax: +86-591-83465373
Received: November 4, 2014
Peer-review started: November 5, 2014
First decision: November 26, 2014
Revised: January 10, 2015
Accepted: January 21, 2015
Article in press: January 21, 2015
Published online: April 14, 2015

Abstract

AIM: To evaluate the feasibility of using multiphoton microscopy (MPM) to assess a tumor regression grading (TRG) system.

METHODS: Fresh specimens from seven patients with colorectal carcinoma undergoing neoadjuvant radiochemotherapy at the Fujian Medical University Union Hospital were obtained immediately after proctectomy. Specimens were serially sectioned (10 μm thickness) and used for MPM or stained with hematoxylin and eosin for comparison. Sections were imaged by MPM using 810 nm excitation, and images were collected in two wavelength channels corresponding to second-harmonic generation (SHG) and two-photon excited fluorescence (TPEF) signals. The ratio of these signal intensities was used to distinguish fibrosis from normal mucosal and serosal tissues.

RESULTS: TRG of specimens assessed by MPM

were in complete agreement with histologic grading performed by a consulting pathologist. SHG and TPEF images clearly revealed collagen fibers and fragmented elastic fibers in the muscularis propria specimens following neoadjuvant radiochemotherapy. Additionally, blood vessel hyperplasia was observed as thickening and fibrosis of the intima and media, which was accompanied by minimal inflammatory cell infiltration. Furthermore, the SHG/TPEF ratio in stromal fibrosis (4.15 ± 0.58) was significantly higher than those in the normal submucosal (2.31 ± 0.52) and serosal (1.47 ± 0.10) tissues (P < 0.001 for both). Analysis of emission spectra from cancerous tumor cells revealed two peaks corresponding to nicotinamide adenine dinucleotide hydrogen and flavin adenine dinucleotide signals; the ratio of these values was 1.19 ± 0.02, which is close to a normal metabolic state.

CONCLUSION: MPM can be used to perform real-time diagnosis of tumor response after neoadjuvant treatment, and can be applied to evaluate TRG.

Key words: Multiphoton microscopy; Neoadjuvant treatment; Second-harmonic generation; Tumor regression grading; Two-photon excited fluorescence

Core tip: This study evaluated the feasibility of using multiphoton microscopy for the assessment of a tumor regression grading system. Multiphoton microscopy allows diagnostic features of colorectal carcinoma treated with neoadjuvant therapy to be visualized. Quantitative image analyses can be used to distinguish fibrotic tissue from normal submucosal and serosal tissues. This is the first study demonstrating the application of multiphoton microscopy for tumor regression grading.

Li LH, Chen ZF, Wang XF, Zhuo SM, Li HS, Jiang WZ, Guan GX, Chen JX. Multiphoton microscopy for tumor regression grading after neoadjuvant treatment for colorectal carcinoma. *World J Gastroenterol* 2015; 21(14): 4210-4215 Available from: URL: http://www.wjgnet.com/1007-9327/full/v21/i14/4210.htm DOI: http://dx.doi.org/10.3748/wjg.v21.i14.4210

INTRODUCTION

For patients with locally advanced gastrointestinal cancer, neoadjuvant therapy followed by surgery or perioperative treatment provides a survival benefit over surgery alone, particularly for patients with complete or subtotal tumor regression[1-5]. As such, assessment of therapeutic response and evaluation of residual disease are very important. The response to therapy can be evaluated histologically *via* a tumor regression grading (TRG) system, which has been shown to correlate with survival[6,7]. The TRG system aims to categorize the extent of regressive changes with consideration of the percentage of the tumor that is residual and the degree of therapy-induced fibrosis[7-10]. This system provides valuable prognostic information, and may serve as a morphologic indicator for neoadjuvant treatment and surgery[11,12].

Histopathologic evaluation of resected specimens can be subject to crush artifacts and sampling error, and involves time-consuming pathologic procedures[13,14]. In contrast, multiphoton microscopy (MPM), which relies on the nonlinear optical processes of second-harmonic generation (SHG) and two-photon excited fluorescence (TPEF), provides high resolution visualization of cell morphology and tissue architecture without the use of exogenous contrast agents[15,16]. The value of this method for use in the TRG system has not been examined. Therefore, the purpose of this study was to evaluate the accuracy and feasibility of MPM for optical diagnoses with the TRG system.

MATERIALS AND METHODS

Specimen preparation

Fresh specimens were obtained immediately after proctectomy from seven patients with colorectal carcinoma undergoing neoadjuvant radiochemotherapy at the Fujian Medical University Union Hospital. Normal tissue specimens were also obtained 6 cm away from the cancer margin. This investigation was approved by the Institutional Review Board of the Fujian Medical University Union Hospital. Written informed consent was obtained before study participation from patients.

Specimens were sectioned (10 μm thickness) and five serial slices were selected. The middle section was stained with hematoxylin and eosin (HE) for histologic comparison and imaged under a standard bright-field light microscope (Eclipse Ci-L; Nikon Corp., Tokyo, Japan) with a CCD (DS-Fi2; Nikon). The remaining four sections were used for MPM imaging.

MPM

MPM was performed using an LSM 510 META imaging system (Carl Zeiss AG, Jena, Germany) equipped with a femtosecond Ti:sapphire laser (110 fs, 76 MHz, Mira 900-F; Coherent Inc., Santa Clara, CA, United States) mode-locked at a wavelength of 810 nm as described previously[17,18]. A Plan-Apochromat oil immersion objective (× 63, numerical aperture = 1.4) was used for image acquisition to collect the backscattered intrinsic SHG and TPEF signals. SHG signals were collected in one channel with a wavelength range of 387-419 nm, and TPEF signals were collected in another channel with a wavelength range of 430-698 nm.

Histopathologic evaluation

TRG from MPM was performed by two independent

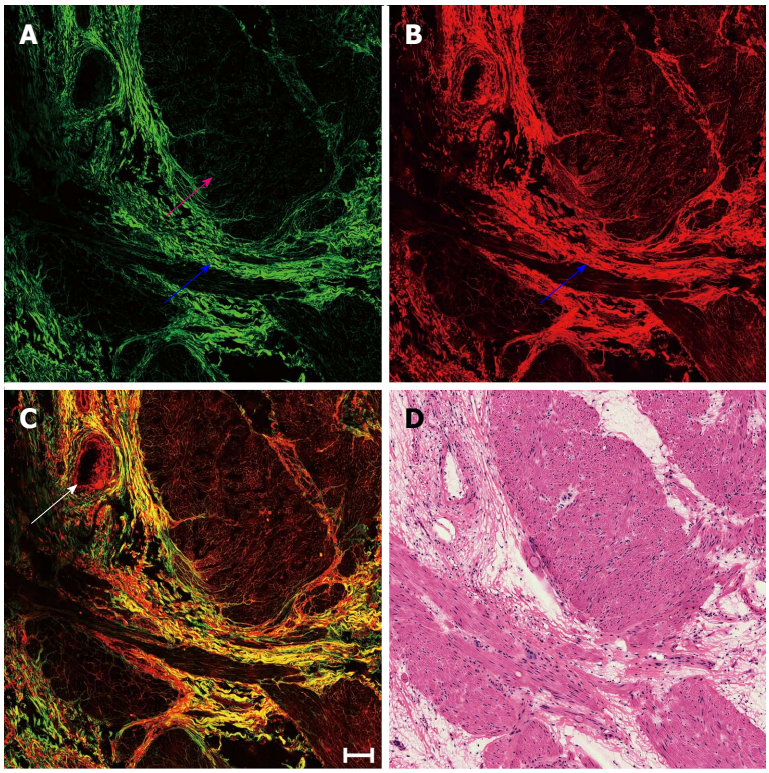

Figure 1 Representative multiphoton microscopy images from a muscularis propria specimen, color-coded green represents the second-harmonic generation signal and color-coded red corresponds to the two-photon excited fluorescence signal. After neoadjuvant radiochemotherapy, predominant fibrosis changes can be seen with minimal inflammatory cells replacing tumor cells. A: Multiphoton microscopy of second-harmonic generation from collagen; B: Two-photon excited fluorescence of collagen, elastin, inflammatory cells, and blood vessels; C: Overlay image (scale bar: 100 μm); D: Hematoxylin and eosin staining of an adjacent section (magnification × 40). The tumor underwent complete regression and was replaced by fibrous tissues (blue arrows). Blood vessel hyperplasia is denoted with a white arrow. Muscular tissue is denoted with a pink arrow.

Table 1 Tumor regression grading scores as determined by histology and microscopy

Patient	Sex	Age (yr)	Cancer classification	TRG score	
				HE	MPM
1	Male	44	Adenocarcinoma	TRG-1	TRG-1
2	Male	38	Adenocarcinoma	TRG-2	TRG-2
3	Female	67	Adenocarcinoma	TRG-2	TRG-2
4	Female	59	Adenocarcinoma	TRG-1	TRG-1
5	Male	59	Adenocarcinoma	TRG-2	TRG-2
6	Male	57	Adenocarcinoma	TRG-3	TRG-3
7	Male	47	Adenocarcinoma	TRG-2	TRG-2

HE: Hematoxylin and eosin staining; TRG: Tumor regression grading; MPM: Multiphoton microscopy.

investigators who were blinded to the results. Tumor regression was classified into five histologic grades according to vital tumor tissue at the ratio of fibrosis[8]: TRG-1: fibrosis without detectable tumor tissue (complete regression); TRG-2: fibrosis with scattered tumor cells; TRG-3: fibrosis and tumor cells with preponderance of fibrosis; TRG-4: fibrosis and tumor cells with preponderance of tumor cells; TRG-5: tumor tissue without regression. TRG scores were confirmed by comparison with corresponding HE-stained sections that were reviewed by a consulting pathologist (Table 1).

Quantification of morphologic features

All quantitative analyses were performed by two individuals experienced in identification of TPEF/SHG images. Collagen and elastin changes and metabolic status after neoadjuvant radiochemotherapy were quantified as SHG/TPEF and redox ratios.

Statistical analysis

One-way analyses of variance were conducted to compare differences using SPSS, version 15.0 statistical software (SPSS Inc., Chicago, IL, United States). Data are presented as mean ± SD, and a P-value < 0.05 was considered significant.

RESULTS

Stromal fibrosis

Representative MPM images depicting the predominant fibrosis with minimal inflammatory cell infiltration replacing large parts of a previous tumor in the muscularis propria following neoadjuvant radiochemotherapy are shown in Figure 1. The smooth muscle was divided due to prior cancer invasion, and the tumor underwent complete regression and was replaced by fibrous tissue mainly composed of collagen fibers, which simultaneously generated SHG (blue

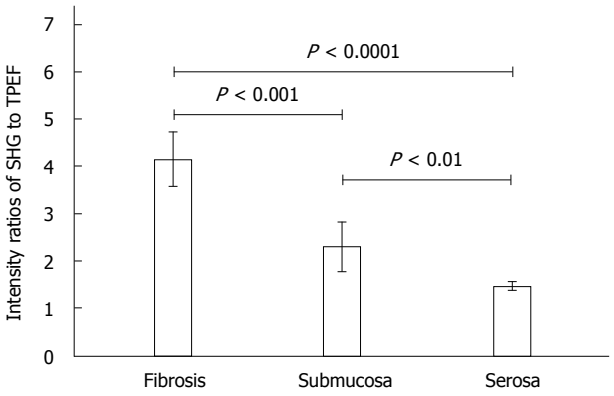

Figure 2 Ratios of second-harmonic generation and two-photon excited fluorescence intensity. Error bars indicate the standard deviation. SHG: Second-harmonic generation; TPEF: Two-photon excited fluorescence.

arrow in Figure 1A) and TPEF (blue arrow in Figure 1B) signals. Additionally, blood vessel hyperplasia was observed as thickening and fibrosis of the intima and media accompanied by minimal inflammatory cell infiltration (white arrow in Figure 1C).

Although fibrosis can easily be differentiated from muscular tissues (pink arrow in Figure 1A) by strong SHG signals, the submucosa and serosa also contain connective tissue comprised of collagen. Therefore, the ratio of SHG to TPEF intensity was calculated to distinguish fibrosis from normal submucosal and serosal tissues, as well as to quantitatively describe the change in fibrous tissue. SHG/TPEF ratio in stromal fibrosis was significantly higher than those in the submucosa and serosa ($P < 0.001$ for both) (Figure 2).

Residual tumors

Representative MPM images depicting remaining malignant glands dispersed within the muscularis propria with minimal inflammatory cell infiltration are shown in Figure 3. Tumor cells in post-treatment rectal carcinoma may show marked changes and these altered tumor cells may become more solid (blue arrows in Figure 3C) or still have a glandular growth pattern (white arrow in Figure 3C). The elastic fibers became fragmented (pink arrows in Figure 3B), while there was an increase in collagen fibers because of stromal fibrosis (Figure 3A).

To further characterize the residual tumors, an image-guide spectral analysis method was used to obtain emission spectra of the cancerous cells, revealing two peaks at 470 and 530 nm (red arrows in Figure 4). These peaks were used to calculate the redox ratio of nicotinamide adenine dinucleotide hydrogen (NADH) to flavin adenine dinucleotide (FAD), represented by fluorescence at 470 and 530 nm, respectively[19,20]. The NADH/FAD ratio was 1.19 ± 0.02.

DISCUSSION

A recent meta-analysis found that partial tumor regression is associated with improvement in disease-free survival[21]. Furthermore, TRG can serve as an independent predictor of disease-free and metastases-free survivals[6,11,22]. The prognostic value of this measure may even exceed that of currently used staging systems (*e.g.*, tumor-node-metastasis staging), which are based on characteristics of untreated tumors[12]. The evaluation criteria of the TRG system incorporate the ratio of tumor cells to fibrosis. However, evaluating TRG using current approaches such as computerized tomography, magnetic resonance imaging, and positron emission computed tomography is challenging, as these medical imaging technologies lack sufficient resolution[23].

MPM relies on nonlinear optical processes to achieve high resolution imaging of biologic tissues, and can detect cellular and subcellular tissue microstructures. Compared with its single-photon counterpart, TPEF offers an inherent optical sectioning property and deep penetration, and the nonlinear scattering from non-centrosymmetric structures provides complementary information to visualize endogenous structures in intact tissues. Residual tumor cells are detected by the TPEF signal, and the SHG signal is used to detect fibrotic tissue. The SHG/TPEF ratio can be used to distinguish fibrosis from submucosal and serosal tissues, as well as to quantify the fibrotic change, which has been proposed as a diagnostic indicator for gastrointestinal diseases[24,25].

Neoadjuvant radiochemotherapy can result in significant morphologic changes, including disrupted muscles, tumor regression, and extensive fibrosis[26]. Moreover, tumor cells in post-treatment rectal carcinoma can become more solid or retain a glandular growth pattern similar to untreated colorectal adenocarcinoma[27]. These alterations were readily detected in the specimens evaluated by MPM in this study. Also observed was the division and damage of muscular tissue by invasion of the adenocarcinoma, which can cause destruction or elimination of collagen and elastic fibers[24].

The redox ratio is an indicator of cellular metabolic state[28]. As this is known to be accelerated in cancerous cells, the redox ratio can be used to quantitatively monitor tumor regression[29]. In this work, the redox ratio in specimens was close to the metabolic state of normal cells[20]. This result supports the notion that abnormal cells undergo significant regression after neoadjuvant radiochemotherapy, which can be assessed *via* MPM.

In conclusion, MPM was used to evaluate TRG in colorectal cancer after neoadjuvant treatment. Spectral analyses provided quantitative evaluations of tumor regression and fibrosis, which corresponded to TRG *via* histopathologic investigation. Given the advantages of this method, including the capacity to produce real-time, label-free images that can be acquired in the near-infrared range, MPM may represent a valuable

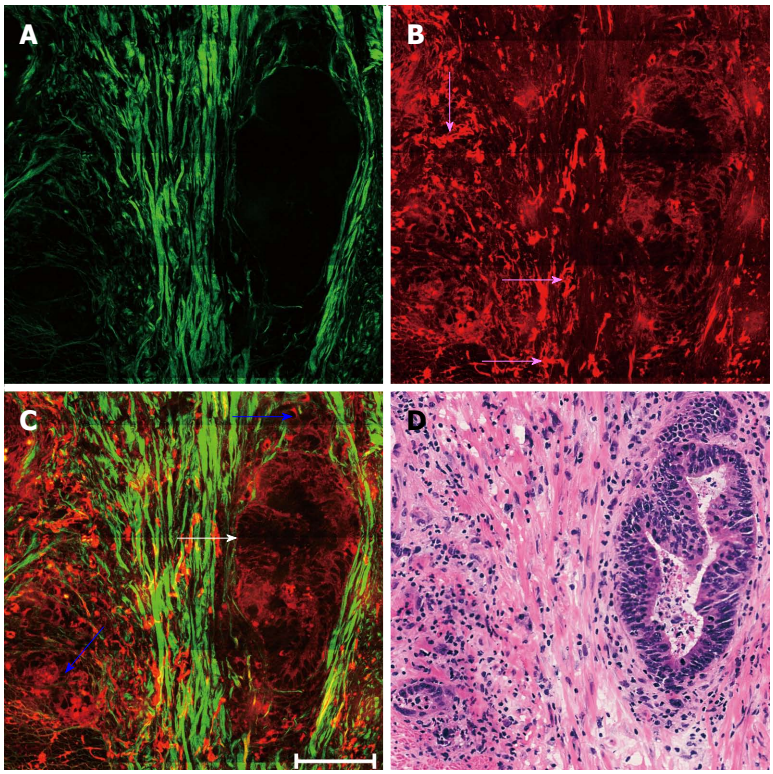

Figure 3 Representative multiphoton microscopy images from a muscularis propria specimen after neoadjuvant radiochemotherapy, color-coded green represents the second-harmonic generation signal and color-coded red corresponds to the two-photon excited fluorescence signal. Remaining malignant glands are dispersed deep within the rectal muscularis propria. A: Multiphoton microscopy of second-harmonic generation from collagen; B: Two-photon excited fluorescence of carcinomatous cells, inflammatory cells, and elastin; C: Overlay image (scale bar: 100 μm); D: Hematoxylin and eosin staining of an adjacent section (magnification × 40). Tumor cells in post-treatment rectal carcinoma show marked changes, and can become more solid (blue arrows) or retain a glandular growth pattern (white arrow). Fragmented elastic fibers are denoted by pink arrows.

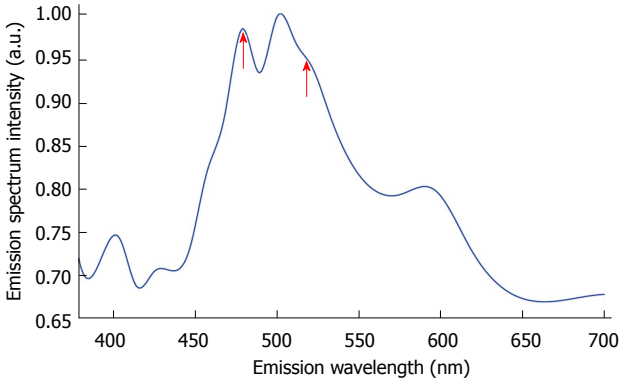

Figure 4 Normalized emission spectrum of residual tumor cells. Excitation wavelength (810 nm) revealed two emission peaks (red arrows).

tool to evaluate TRG after neoadjuvant therapy to treat colorectal carcinoma. This is the first demonstration of the use of MPM to estimate TRG of colorectal carcinoma following neoadjuvant treatment. The results suggest that MPM has a promising future for real-time optical biopsy diagnosis of tumor regression.

COMMENTS

Background

Tumor regression grading (TRG) can provide important prognostic information and should be included in histopathologic reports of colorectal carcinoma after neoadjuvant treatment. However, the resolution of current imaging approaches, such as computerized tomography, magnetic resonance imaging, and positron emission tomography, is insufficient for accurate and easy assessment. The purpose of this study was to evaluate the feasibility of using multiphoton microscopy (MPM) to obtain optical diagnoses for the TRG system.

Research frontiers

The TRG system provides highly valuable prognostic information for evaluating colorectal cancer after neoadjuvant treatment.

Innovations and breakthroughs

This is the first study evaluating the use of MPM for optical diagnosis of tumor regression.

Applications

These results are essential and significant for developing MPM for TRG, and to perform real-time diagnosis of tumor response after neoadjuvant treatment.

Terminology

MPM incorporates nonlinear optical processes to generate second-harmonic generation and two photon excited fluorescence signals.

Peer-review

The article has good characteristics, value, and significance.

REFERENCES

1 **Hwang MR**, Park JW, Park S, Yoon H, Kim DY, Chang HJ, Kim SY, Park SC, Choi HS, Oh JH, Jeong SY. Prognostic impact of circumferential resection margin in rectal cancer treated with preoperative chemoradiotherapy. *Ann Surg Oncol* 2014; **21**: 1345-1351 [PMID: 24468928 DOI: 10.1245/s10434-014-3484-1]

2 **van Hagen P**, Hulshof MC, van Lanschot JJ, Steyerberg EW, van Berge Henegouwen MI, Wijnhoven BP, Richel DJ, Nieuwenhuijzen GA, Hospers GA, Bonenkamp JJ, Cuesta MA, Blaisse RJ, Busch

OR, ten Kate FJ, Creemers GJ, Punt CJ, Plukker JT, Verheul HM, Spillenaar Bilgen EJ, van Dekken H, van der Sangen MJ, Rozema T, Biermann K, Beukema JC, Piet AH, van Rij CM, Reinders JG, Tilanus HW, van der Gaast A. Preoperative chemoradiotherapy for esophageal or junctional cancer. *N Engl J Med* 2012; **366**: 2074-2084 [PMID: 22646630 DOI: 10.1056/NEJMoa1112088]

3 **Martin ST**, Heneghan HM, Winter DC. Systematic review and meta-analysis of outcomes following pathological complete response to neoadjuvant chemoradiotherapy for rectal cancer. *Br J Surg* 2012; **99**: 918-928 [PMID: 22362002 DOI: 10.1002/bjs.8702]

4 **Ychou M**, Boige V, Pignon JP, Conroy T, Bouché O, Lebreton G, Ducourtieux M, Bedenne L, Fabre JM, Saint-Aubert B, Genève J, Lasser P, Rougier P. Perioperative chemotherapy compared with surgery alone for resectable gastroesophageal adenocarcinoma: an FNCLCC and FFCD multicenter phase III trial. *J Clin Oncol* 2011; **29**: 1715-1721 [PMID: 21444866 DOI: 10.1200/JCO.2010.33.0597]

5 **Schrag D**, Weiser MR, Goodman KA, Gonen M, Hollywood E, Cercek A, Reidy-Lagunes DL, Gollub MJ, Shia J, Guillem JG, Temple LK, Paty PB, Saltz LB. Neoadjuvant chemotherapy without routine use of radiation therapy for patients with locally advanced rectal cancer: a pilot trial. *J Clin Oncol* 2014; **32**: 513-518 [PMID: 24419115 DOI: 10.1200/JCO.2013.51.7904]

6 **Abdul-Jalil KI**, Sheehan KM, Kehoe J, Cummins R, O'Grady A, McNamara DA, Deasy J, Breathnach O, Grogan L, O'Neill BD, Faul C, Parker I, Kay EW, Hennessy BT, Gillen P. The prognostic value of tumour regression grade following neoadjuvant chemoradiation therapy for rectal cancer. *Colorectal Dis* 2014; **16**: O16-O25 [PMID: 24119076 DOI: 10.1111/codi.12439]

7 **Rödel C**, Martus P, Papadoupolos T, Füzesi L, Klimpfinger M, Fietkau R, Liersch T, Hohenberger W, Raab R, Sauer R, Wittekind C. Prognostic significance of tumor regression after preoperative chemoradiotherapy for rectal cancer. *J Clin Oncol* 2005; **23**: 8688-8696 [PMID: 16246976 DOI: 10.1200/JCO.2005.02.1329]

8 **Mandard AM**, Dalibard F, Mandard JC, Marnay J, Henry-Amar M, Petiot JF, Roussel A, Jacob JH, Segol P, Samama G. Pathologic assessment of tumor regression after preoperative chemoradiotherapy of esophageal carcinoma. Clinicopathologic correlations. *Cancer* 1994; **73**: 2680-2686 [PMID: 8194005 DOI: 10.1002/1097-0142(19940601)73]

9 **Dworak O**, Keilholz L, Hoffmann A. Pathological features of rectal cancer after preoperative radiochemotherapy. *Int J Colorectal Dis* 1997; **12**: 19-23 [PMID: 9112145 DOI: 10.1007/s003840050072]

10 **Becker K**, Mueller JD, Schulmacher C, Ott K, Fink U, Busch R, Böttcher K, Siewert JR, Höfler H. Histomorphology and grading of regression in gastric carcinoma treated with neoadjuvant chemotherapy. *Cancer* 2003; **98**: 1521-1530 [PMID: 14508841 DOI: 10.1002/cncr.11660]

11 **Bouzourene H**, Bosman FT, Seelentag W, Matter M, Coucke P. Importance of tumor regression assessment in predicting the outcome in patients with locally advanced rectal carcinoma who are treated with preoperative radiotherapy. *Cancer* 2002; **94**: 1121-1130 [PMID: 11920483 DOI: 10.1002/cncr.10327]

12 **Thies S**, Langer R. Tumor regression grading of gastrointestinal carcinomas after neoadjuvant treatment. *Front Oncol* 2013; **3**: 262 [PMID: 24109590 DOI: 10.3389/fonc.2013.00262]

13 **Ying M**, Zhuo S, Chen G, Zhuo C, Lu J, Zhu W, Xie S, Chen J, Yan J. Real-time noninvasive optical diagnosis for colorectal cancer using multiphoton microscopy. *Scanning* 2012; **34**: 181-185 [PMID: 21898461 DOI: 10.1002/sca.20286]

14 **Wu X**, Chen G, Lu J, Zhu W, Qiu J, Chen J, Xie S, Zhuo S, Yan J. Label-free detection of breast masses using multiphoton microscopy. *PLoS One* 2013; **8**: e65933 [PMID: 23755295 DOI: 10.1371/journal.pone.0065933]

15 **Hoover EE**, Squier JA. Advances in multiphoton microscopy technology. *Nat Photonics* 2013; **7**: 93-101 [PMID: 24307915 DOI: 10.1038/nphoton.2012.361]

16 **Campagnola PJ**, Loew LM. Second-harmonic imaging microscopy for visualizing biomolecular arrays in cells, tissues and organisms. *Nat Biotechnol* 2003; **21**: 1356-1360 [PMID: 14595363 DOI: 10.1038/nbt894]

17 **Chen J**, Zhuo S, Chen G, Yan J, Yang H, Liu N, Zheng L, Jiang X, Xie S. Establishing diagnostic features for identifying the mucosa and submucosa of normal and cancerous gastric tissues by multiphoton microscopy. *Gastrointest Endosc* 2011; **73**: 802-807 [PMID: 21457819 DOI: 10.1016/j.gie.2010.12.016]

18 **Chen J**, Xu J, Kang D, Xu M, Zhuo S, Zhu X, Jiang X. Multiphoton microscopic imaging of histological sections without hematoxylin and eosin staining differentiates carcinoma in situ lesion from normal oesophagus. *Appl Phys Lett* 2013; **103**: 183701 [DOI: 10.1063/1.4826322]

19 **Monici M**. Cell and tissue autofluorescence research and diagnostic applications. *Biotechnol Annu Rev* 2005; **11**: 227-256 [PMID: 16216779 DOI: 10.1016/S1387-2656(05)11007-2]

20 **Zhuo S**, Chen J, Luo T, Jiang X, Xie S, Chen R. Two-layered multiphoton microscopic imaging of cervical tissue. *Lasers Med Sci* 2009; **24**: 359-363 [PMID: 18536958 DOI: 10.1007/s10103-008-0570-2]

21 **Lee YC**, Hsieh CC, Chuang JP. Prognostic significance of partial tumor regression after preoperative chemoradiotherapy for rectal cancer: a meta-analysis. *Dis Colon Rectum* 2013; **56**: 1093-1101 [PMID: 23929020 DOI: 10.1097/DCR.0b013e318298e36b]

22 **Rubbia-Brandt L**, Giostra E, Brezault C, Roth AD, Andres A, Audard V, Sartoretti P, Dousset B, Majno PE, Soubrane O, Chaussade S, Mentha G, Terris B. Importance of histological tumor response assessment in predicting the outcome in patients with colorectal liver metastases treated with neo-adjuvant chemotherapy followed by liver surgery. *Ann Oncol* 2007; **18**: 299-304 [PMID: 17060484 DOI: 10.1093/annonc/mdl386]

23 **Weissleder R**, Pittet MJ. Imaging in the era of molecular oncology. *Nature* 2008; **452**: 580-589 [PMID: 18385732 DOI: 10.1038/nature06917]

24 **Liu N**, Chen J, Chen G, Yan J, Zhuo S, Jiang X. Detecting the imaging characteristics of colorectal carcinoma invading the muscularis propria with multiphoton microscopy. *Laser Phys Lett* 2012; **9**: 155-159 [DOI: 10.1002/lapl.201110106]

25 **Vidal Bde C**, Mello ML. Optical anisotropy of collagen fibers of rat calcaneal tendons: An approach to spatially resolved supramolecular organization. *Acta Histochem* 2010; **112**: 53-61 [PMID: 18835013 DOI: 10.1016/j.acthis.2008.07.005]

26 **O'Neil M**, Damjanov I. Histopathology of colorectal cancer after neoadjuvant chemoradiation therapy. *Open Pathol J* 2009; **3**: 91-98 [DOI: 10.2174/1874375700903020091]

27 **Shia J**, Guillem JG, Moore HG, Tickoo SK, Qin J, Ruo L, Suriawinata A, Paty PB, Minsky BD, Weiser MR, Temple LK, Wong WD, Klimstra DS. Patterns of morphologic alteration in residual rectal carcinoma following preoperative chemoradiation and their association with long-term outcome. *Am J Surg Pathol* 2004; **28**: 215-223 [PMID: 15043311 DOI: 10.1097/00000478-200402000-00009]

28 **Skala MC**, Riching KM, Gendron-Fitzpatrick A, Eickhoff J, Eliceiri KW, White JG, Ramanujam N. In vivo multiphoton microscopy of NADH and FAD redox states, fluorescence lifetimes, and cellular morphology in precancerous epithelia. *Proc Natl Acad Sci USA* 2007; **104**: 19494-19499 [PMID: 18042710 DOI: 10.1073/pnas.0708425104]

29 **Tiede LM**, Rocha-Sanchez SM, Hallworth R, Nichols MG, Beisel K. Determination of hair cell metabolic state in isolated cochlear preparations by two-photon microscopy. *J Biomed Opt* 2007; **12**: 021004 [PMID: 17477711 DOI: 10.1117/1.2714777]

P- Reviewer: Gassler N **S- Editor**: Qi Y **L- Editor**: Wang TQ
E- Editor: Ma S

World Journal of Gastroenterology

Submit a Manuscript: http://www.wjgnet.com/esps/
Help Desk: http://www.wjgnet.com/esps/helpdesk.aspx
DOI: 10.3748/wjg.v21.i14.4216

World J Gastroenterol 2015 April 14; 21(14): 4216-4224
ISSN 1007-9327 (print) ISSN 2219-2840 (online)

ORIGINAL ARTICLE

Basic Study

Th22 cell accumulation is associated with colorectal cancer development

Yong-Hong Huang, Yun-Fei Cao, Zhi-Yuan Jiang, Sen Zhang, Feng Gao

Yong-Hong Huang, Yun-Fei Cao, Zhi-Yuan Jiang, Sen Zhang, Feng Gao, Department of Colorectal and Anal Surgery, First Affiliated Hospital of Guangxi Medical University, Nanning 530021, Guangxi Zhuang Autonomous Region, China

Author contributions: Huang YH and Cao YF contributed equally to this work; Gao F designed the research; Zhang S and Cao YF contributed new reagents; Jiang ZY and Huang YH performed research; Cao YF and Huang YH analyzed data; and Huang YH wrote the paper.

Supported by National Natural Science Foundation of China, No. 81260316 and No. 81260335.

Ethics approval: This study was reviewed and approved by the First Affiliated Hospital of Guangxi Medical University Institutional Review Board.

Institutional animal care and use committee: All procedures involving animals were reviewed and approved by the Institutional Animal Care and Use Committee of the First Affiliated Hospital of Guangxi Medical University (IACUC No: 201402068).

Conflict-of-interest: The authors report no conflicts of interest in this work.

Data sharing: The technical appendix, statistical code, and dataset are available from the corresponding author at doctorgao0771@hotmail.com. All participants gave informed consent for data sharing.

Correspondence to: Feng Gao, Professor, Department of Colorectal and Anal Surgery, First Affiliated Hospital of Guangxi Medical University, No. 6 Shuangyong Road, Nanning 530021, Guangxi Zhuang Autonomous Region, China. doctorgao0771@hotmail.com
Telephone: +86-771-5356529
Fax: +86-771-5351442

Received: October 26, 2014
Peer-review started: October 27, 2014
First decision: November 14, 2014
Revised: November 27, 2014
Accepted: January 16, 2015
Article in press: January 16, 2015
Published online: April 14, 2015

Abstract

AIM: To investigate the expression of Th22 cells and related cytokines in colorectal cancer (CRC) tissues, and the probably mechanism.

METHODS: CRC tumor and paratumor tissues were collected to detect the expression levels of Th22 cells and of related cytokines by immunohistochemistry, flow cytometry and real-time quantitative polymerase chain reaction (RT-qPCR). Interleukin (IL)-22 alone or with a STAT3 inhibitor was co-cultured with RKO cells *in vitro* to study the effects of IL-22 on colon cancer cells. IL-22 alone or with a STAT3 inhibitor was injected into a BALB/c nude mouse model with subcutaneously transplanted RKO cells to study the effects of IL-22 on colon cancer growth.

RESULTS: The percentage of Th22 cells in the $CD4^+$ T subset was significantly higher in tumor tissues compared with that in paratumor tissues (1.47% ± 0.083% *vs* 1.23% ± 0.077%, $P < 0.05$) as determined by flow cytometry. RT-qPCR analysis revealed that the mRNA expression levels of IL-22, aryl hydrocarbon receptor, CCL20 and CCL22 were significantly higher in tumor tissues compared with those in paratumor tissues. CCL27 mRNA also displayed a higher expression level in tumor tissues compared with that in paratumor tissues; however, these levels were not significantly different (2.58 ± 0.93 *vs* 2.30 ± 0.78, $P > 0.05$). IL-22 enhanced colon cancer cell proliferation *in vitro* and displayed anti-apoptotic effects; these effects were blocked by adding a STAT3 inhibitor. IL-22 promoted tumor growth in BALB/c nude mice; however, this effect was reversed by adding a STAT3 inhibitor.

CONCLUSION: Th22 cells that accumulate in CRC may be associated with the chemotactic effect of the tumor microenvironment. IL-22 is associated with CRC development, most likely *via* STAT3 activation.

Key words: Th22 cells; Interleukin-22; STAT3; Colorectal cancer; Tumor microenvironment

Core tip: Although the functional characteristics of Th22 cells in inflammatory and autoimmune diseases have been extensively studied, their role in colorectal cancer (CRC) remains unclear. This study demonstrated the differences in the expression of Th22 cells and their related cytokines between colorectal tumor and paratumor tissues and the accumulation of Th22 cells in CRC may be associated with the functions of chemotactic factors that are secreted by the tumor microenvironment. Interleukin-22 was found to be the functional factor of Th22 cells that is associated with CRC development in both *in vitro* and *in vivo* experiments, most likely *via* STAT3 pathway activation.

Huang YH, Cao YF, Jiang ZY, Zhang S, Gao F. Th22 cell accumulation is associated with colorectal cancer development. *World J Gastroenterol* 2015; 21(14): 4216-4224 Available from: URL: http://www.wjgnet.com/1007-9327/full/v21/i14/4216.htm DOI: http://dx.doi.org/10.3748/wjg.v21.i14.4216

INTRODUCTION

Colorectal cancer (CRC) is the third most commonly occurring cancer in males and the second most commonly occurring cancer in females[1]. An increased overall survival rate has been observed in patients with CRC due to the detection of early stage CRC and to the improvement of therapeutic strategies[2]. However, over 1 million people develop CRC every year worldwide, and more than 500000 patients die, particularly those patients with advanced cancer[1,3]. Currently, the incidence rates of CRC are increasing in developing countries, including China[4].

Understanding the molecular pathways involved in CRC will help to improve cancer prevention and treatment[5]. Increasing evidence has shown that the dysregulation of different $CD4^+$ T lymphocyte subpopulations and cytokine networks is involved in the pathogenesis and progression of CRC[6-8]. *In situ* analysis of tumor-infiltrating immune cells may be a valuable prognostic tool in the treatment of CRC and possibly of other malignant tumors[9,10].

Traditionally, $CD4^+$ T helper cells (Th cells) include Th1, Th2, Th7, and regulatory T cells according to their cytokine milieu. Interleukin (IL)-22, which is a member of the IL-10 cytokine family, is regarded as a cytokine produced by Th1 cells and Th17 cells. Recently, two studies have shed new light on the unique features of this cytokine. IL-22-producing CD4+ T cells (Th22 cells), which are a new T helper cell subset, differ from Th1, Th2, or Th17 cells because this population only produces IL-22 and has low or undetectable expression of the Th17 and Th1 transcription factors ROR-γ and T-bet. Th22 cells express the chemokine receptors CCR4, CCR6 and CCR10 in human skin, and the transcription factor aryl hydrocarbon receptor (AHR) is required for IL-22 production[11,12]. The functional characteristics of Th22 cells in inflammatory and autoimmune diseases have been extensively studied[13]. Nevertheless, knowledge regarding the role of Th22 cells in malignant tumor immunity is limited; further research elucidating the pathogenesis of and therapy for carcinoma will be of interest. In the current study, we investigated the expression of Th22 cells and their related cytokines in colorectal tumor and paratumor tissues and determined their effects on colorectal cancer using *in vivo* and *in vitro* experiments.

MATERIALS AND METHODS

Ethics statement

All patients enrolled in this study provided written informed consent. This study protocol conformed to the ethical guidelines of the Declaration of Helsinki (Fortaleza, Brazil, October 2013) and was approved by the ethical committees and institutional Review Board of the First Affiliated Hospital of Guangxi Medical University, PRC.

Research subjects and samples

Fifty patients diagnosed with CRC who received surgical resection at The First Affiliated Hospital of Guangxi Medical University from April 2013 to March 2014 were enrolled in this study. None of the patients had received radiotherapy or chemotherapy before sampling. Individuals with an autoimmune disease, infectious disease, or multiple primary cancers were excluded. The basic data regarding the study population are shown in Table 1. The tumor and paratumor tissues (at least 5 cm away from the tumor site) were collected immediately after surgical resection and stored in liquid nitrogen for polymerase chain reaction (PCR), fixed with 4% paraformaldehyde for immunohistochemistry (IHC) or immediately isolated for flow cytometry.

IHC

Fresh tumor and paratumor tissues were fixed in 4% paraformaldehyde, embedded with paraffin and sectioned at 4-μm thickness. IHC was performed as previously described[14]; the sectioned slides were stained using IL-22 antibody, which was purchased from Bioss Company (Beijing, China).

Table 1 Basic data of the study population

Characteristics	Value
Sex	
Male	33
Female	17
Age (yr), mean (range)	60 (38-81)
Colon	22
Rectum	28
TNM stage	
Stage Ⅰ-Ⅱ	23
Stage Ⅲ-Ⅳ	27

Table 2 Primer sequences for polymerase chain reaction

Gene	Sequence (5′ to 3′)	Product (bp)	Tm (℃)
IL-22	F: GTTCTCCTTCCCCAGTCACCA R: AGCTGCTCCTCCCTGTACCAA	145	60
AHR	F: ACATCACCTACGCCAGTCG R: CGCTTGGAAGGATTTGACTTGA	94	60
CCL20	F: ATCCAAAACAGACTTGGGTGAA R: TCCATTCCAGAAAAGCCACA	89	60
CCL22	F: ATTACGTCCGTTACCGTCTGC R: TCCCTGAAGGTTAGCAACACC	100	60
CCL27	F: TCCTGAGCCCAGACCCTACA R: CGTTGAGCCAGGTGAAGCA	175	60
β-actin	F: TGACGTGGACATCCGCAAAG R: CTGGAAGGTGGACAGCGAGG	205	60

Real-time quantitative PCR

Fresh tumor and paratumor tissue samples for determining cytokine expression were stored at -80 ℃ until analysis. Total RNA was extracted using TRIzol reagent (Invitrogen) according to the manufacturer's instructions. The cDNA was immediately reverse transcribed from the extracted total RNA using the SuperScript Ⅲ First-Strand Synthesis System (Invitrogen). Real-time quantitative PCR (RT-qPCR) was performed using a SYBR Green PCR kit (Roche). Amplification was performed using standard conditions and was normalized to transcripts of the housekeeping gene β-actin. The primer sequences for PCR are shown in Table 2. Relative expression levels of mRNA were calculated using the $2^{-\Delta\Delta Ct}$ method as described by Livak *et al*[15] and adjusted by the level of β-actin mRNA for each sample.

Cell isolation

Tumor and paratumor tissues were washed three times in RPMI 1640 before being cut into small pieces (1 mm tissue samples). Then, the specimens were collected in RPMI 1640 containing 1 mg/mL collagenase Ⅳ, 30 μg/mL DNase I and 0.1 mg/mL hyaluronidase, and then a magnetic stirrer was used for stirring the digestion mixture for 3 h. Next, the dissociated cell suspensions were filtered through 150-μm and 70-μm cell strainers to obtain cell suspensions, which were centrifuged in a discontinuous Percoll gradient (75% and 40%). The cells at the interface were harvested and resuspended at 1 × 10^6 cells/mL in RPMI 1640 containing 10% fetal calf serum. Cell viability was determined by trypan blue exclusion.

Flow cytometry

The cell suspensions were stimulated in culture for 4 h with 50 ng/mL PMA, 1 μg/mL ionomycin and 0.7 μL/mL GolgiStop reagent at 37 ℃ in a CO_2 incubator (5% CO_2 in humidified air). The cultured cell suspensions were stained with surface and intracellular anti-human-specific antibodies, which were conjugated with PE, PE-Cy5 or APC. These human antibodies included anti-CD4, IL-22 and IL-17, which were purchased from BD Biosciences (Franklin Lakes, NJ, United States) or eBioscience (San Diego, CA, United States). Then, the cells were resuspended and analyzed using a FACSCaliburflow cytometer (BD Bioscience). The data were analyzed using FlowJo software (TreeStar, Ashland, OR, United States). Cellular debris was eliminated from the analysis using a gate set at forward and side scatter.

Cell co-culture in vitro

The human colon cancer cell line RKO was purchased from the Type Culture Collection of the Chinese Academy of Sciences, Shanghai, China. Recombinant human IL-22 was purchased from PeproTech Company, United States. STAT3 inhibitor (S3I-201) was purchased from Selleck Chemicals, United States. RKO cells were cultured in complete DMEM medium supplemented with 10% FBS and 1% antibiotic/antimycotic in a humidified incubator at 37 ℃ in an atmosphere of 95% air and 5% CO_2 for 24 h. Then, IL-22 (50 ng/mL) or S3I-201 (50 μmol/L) was added to the experimental medium for co-culture. After 24 h, the RKO cells were trypsinized and then stained with intracellular Ki-67 (BD Bioscience) to detect cell proliferation or stained with Annexin V and 7-amino-actinomycin (7-AAD) (BD Bioscience) to detect apoptosis.

Animal experiments in vivo

BALB/c nude mice (6-8 wk of age) were obtained from Guangxi Medical University Animal Experiment Center, and all animal experiments conformed to the National Guidelines of the Animal Care Committee. Twenty-one BALB/c nude mice were injected subcutaneously with RKO cells; each mouse was injected with 5 × 10^6 cells in 300 μL of saline solution. Tumor growth was monitored every two days. Tumor volume was calculated by the following formula: (major circumference×minor circumference^2)/2. After the tumor volumes reached 60 mm^3, the 21 mice were divided into 3 groups. The IL-22 group was injected intraperitoneally with IL-22 (1 μg/100 μL) and DMSO (100 μL) every other day, the IL-22 + S3I-201 group was injected with IL-22 (1 μg/100 μL) and S3I-201 (100 μg/100 μL), and the control group was injected with saline solution (100 μL) and DMSO (100 μL) simultaneously, each group for a total of 5 times. The

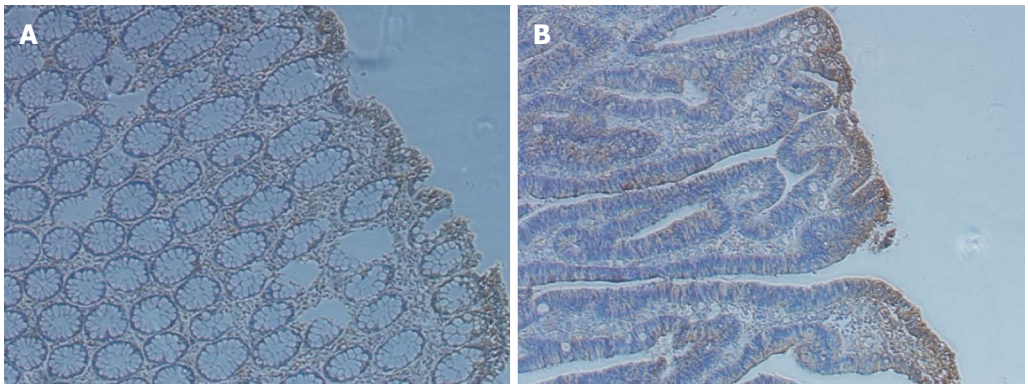

Figure 1 Immunohistochemistry staining of tissues. A: Immunohistochemistry (IHC) staining of normal colon tissues; B: IHC staining of colon cancer tissues.

mice were sacrificed at 48 h after the last intervention.

Statistical analysis

The data are expressed as the mean ± SE. Data comparisons between the different groups were performed using Student's *t*-test, a paired *t*-test or one-way ANOVA. Analysis was completed using GraphPad Prism 5.0 software (GraphPad, San Diego, CA, United States), and *P* values that were less than 0.05 were considered statistically significant.

RESULTS

Th22 cells are enriched in CRC tumor tissues

IL-22 is a functional cytokine that is primarily produced by Th22 cells. By IHC, we observed that IL-22 was present in both tumor and paratumor tissues and was particularly enriched in tumor tissues (Figure 1). To further understand the roles of Th22 cells in the tumor microenvironment in patients with CRC, the proportion of Th22 cells in tumor and paratumor tissue was detected by flow cytometry (Figure 2A). As shown in Figure 2B, the prevalence of Th22 cells in the $CD4^+$ T subset was higher in tumor tissues compared with that in paratumor tissues ($P < 0.05$).

Expression of Th22 cells and related cytokines in the CRC microenvironment

The relative expression levels of IL-22, AHR, CCL20, CCL22 and CCL27 in colorectal tumor and paratumor tissues were measured by RT-qPCR. CCL20, CCL22 and CCL27 are common chemokines that have been identified as attractants of different types of leukocytes to sites of tumors and of inflammation. As shown in Figure 2C, the mRNA expression levels of IL-22, AHR, CCL20 and CCL22 were significantly higher in tumor tissues compared with those in paratumor tissues ($P < 0.05$). CCL27 mRNA also displayed a higher expression level in tumor tissues compared with that in paratumor tissues; however, these levels were not significantly different ($P > 0.05$).

Effects of IL-22 on colon cancer cells in vitro

The effects of IL-22 on colon cancer cells were assessed by co-culturing with RKO cells *in vitro*. As shown in Figure 3A and C, compared with control medium, the proliferation of RKO cells was significantly promoted by IL-22 treatment ($P < 0.05$). This enhanced proliferation was blocked when S3I-201 was added to the RKO cell culture in the presence of IL-22. In contrast, the apoptosis of RKO cells was significantly inhibited by IL-22 treatment ($P < 0.05$) compared with the control medium. The inhibition of STAT3 signaling by S3I-201 completely abrogated this suppression of apoptosis (Figure 3B and 3D).

Effects of IL-22 on colon cancer in vivo

BALB/c nude mice transplanted subcutaneously with RKO cells were used to investigate the effects of IL-22 on colon cancer growth *in vivo*. As shown in Figure 4, the tumor growth of nude mice was significantly promoted ($P < 0.05$) after intraperitoneal injection with IL-22 every other day compared with that of the control mice. However, this promoting effect induced by IL-22 treatment could be completely reversed by S3I-201 treatment.

DISCUSSION

The roles of tumor antigen-specific $CD4^+$ T cells in cancer immunity have been extensively studied in recent years[16,17]. Th22 cells, which are a newly described subset of $CD4^+$ T cells, play important roles in a variety of carcinomas. The percentage of Th22 cells is significantly increased in both the peripheral blood and tumor tissues in patients with gastric cancer; this percentage correlates with gastric cancer progression and can predict poor patient survival[18,19]. The over-expression of Th22 cells is also present in hepatocellular carcinoma[20], pancreatic cancer[21] and malignant pleural effusion[22]. In the current study, we demonstrated that the proportion of Th22 cells was enriched in tumor tissues relative to paratumor

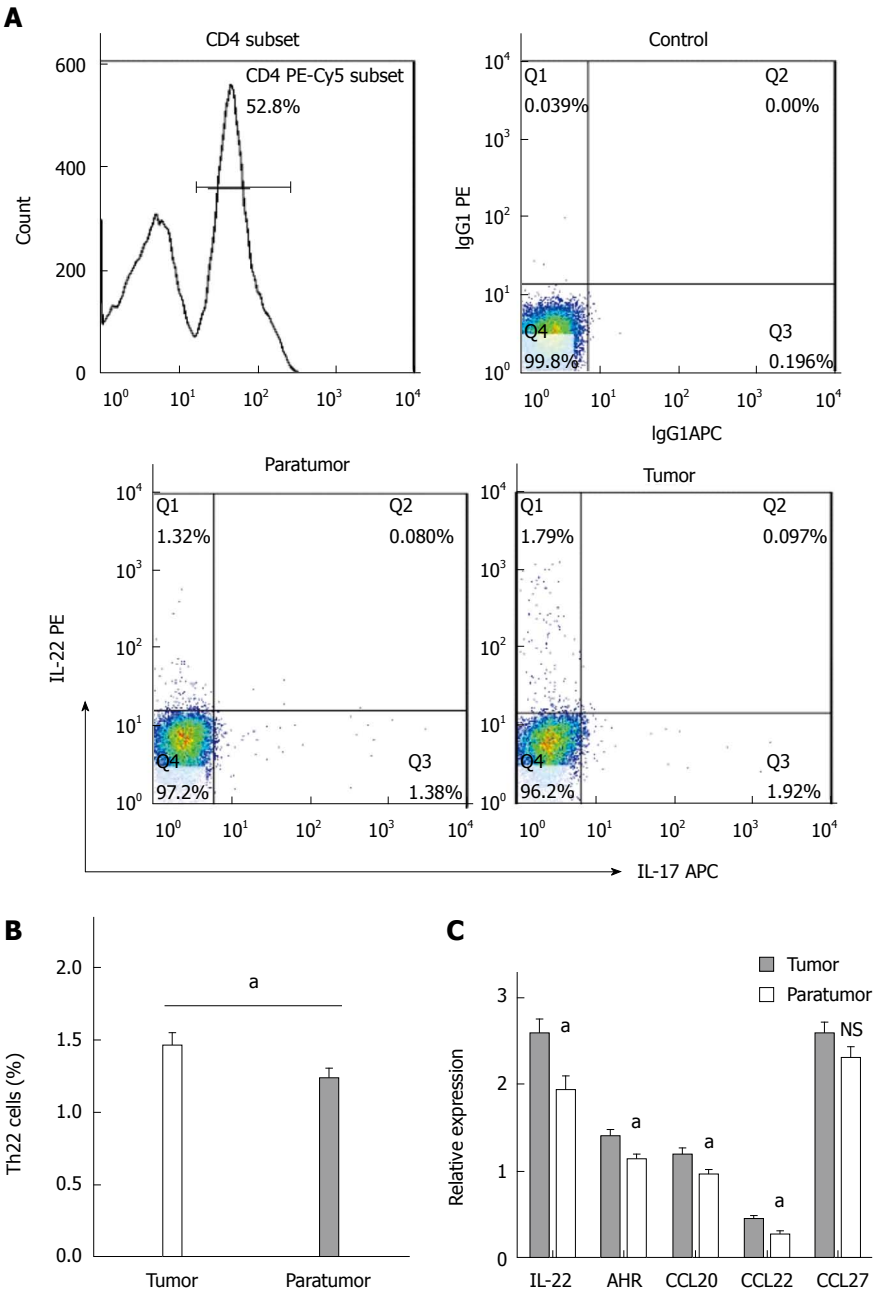

Figure 2 Expression of Th22 cells and related cytokines in colorectal cancer. A: Gated on FSC/SSC and $CD4^+$ subset, the proportion of Th22 cells in the $CD4^+$ subset is presented in quadrant Q1; B: Average proportion of Th22 cells in tumor and paratumor tissues; C: Expression levels of interleukin-22, AHR, CCL20, CCL22 and CCL27 in tumor and paratumor tissues were measured by RT-qPCR. The relative expression levels were normalized to the level of β-actin mRNA for each sample. Each bar represents the mean ± SE (n = 50), $^aP < 0.05$, tumor *vs* paratumor. NS: Not significant.

tissues in patients with CRC. By IHC and RT-qPCR, we observed that the expression level of IL-22 was significantly higher in tumor tissues than in paratumor tissues. AHR is known as the key transcription factor of Th22 cells[11,12]; in the present study, AHR displayed a higher level of expression in tumor tissues compared with that in paratumor tissues. These results are similar to those of aforementioned reports that indicated that the accumulation and differentiation of Th22 cells are induced by the tumor microenvironment.

The phenotypic characteristics of Th22 cells have been described as $CCR4^+CCR6^+CCR10^+$, and the chemotactic factors CCL22, CCL20 and CCL27 are their corresponding ligands[12]. In this study, we observed that the colorectal tumor microenvironment expressed higher levels of CCL22, CCL20 and CCL27 compared with those of the paratumor tissues, suggesting that the accumulation of Th22 cells in tumor tissues may be mediated by the chemotactic cytokines that are secreted by the tumor microenvironment. This result is similar to that of a study of malignant pleural effusion[22].

Many studies have demonstrated the constitutive activation of STAT3 in a wide variety of human car-

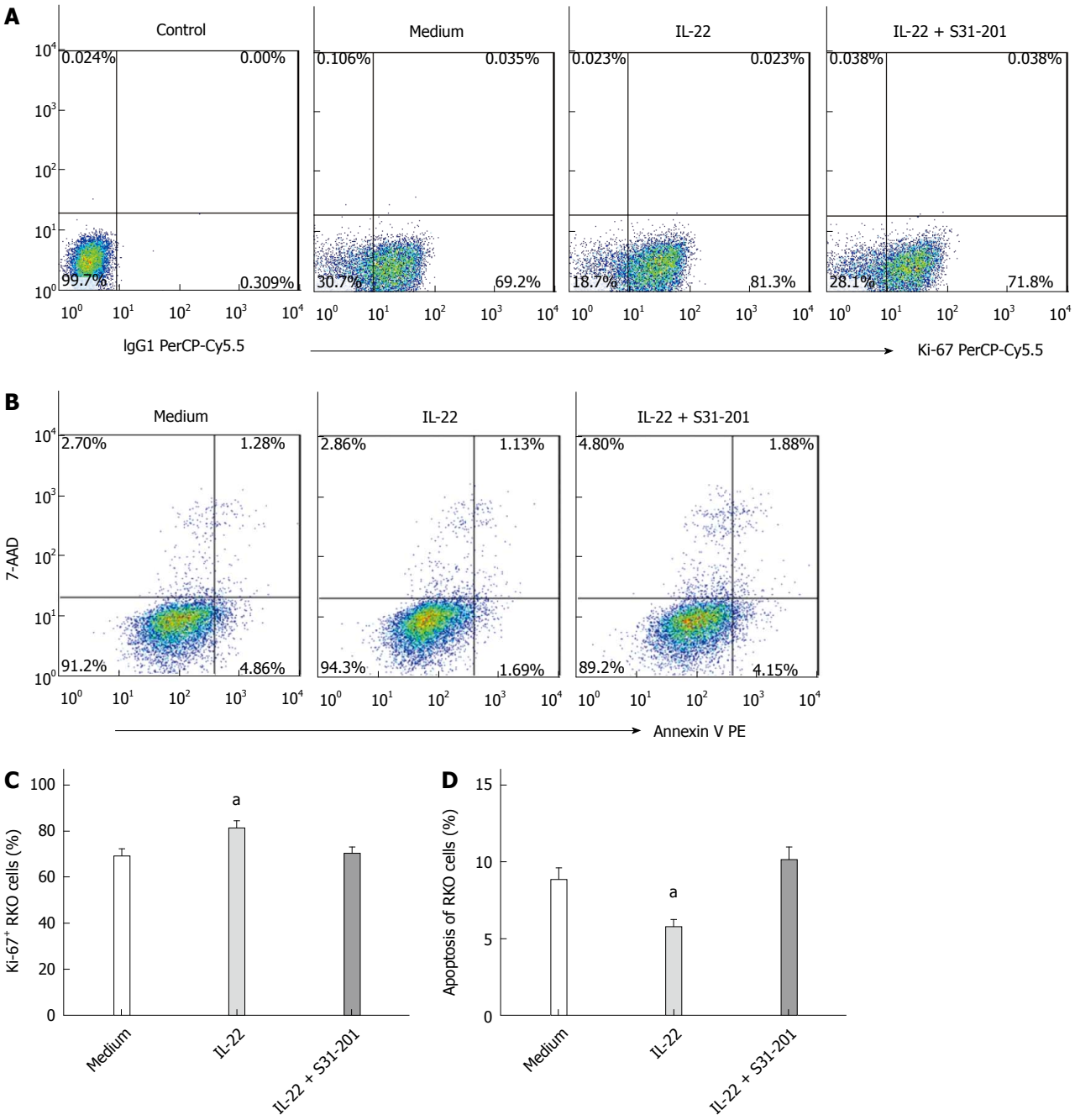

Figure 3 Effects of interleukin-22 on colon cancer cells. A: Flow cytometry to measure colon cancer cell proliferation in the presence of interleukin (IL)-22 or IL-22 + S3I-201; B: Flow cytometry for colon cancer cell apoptosis in the presence of IL-22 or IL-22 + S3I-201; C: Average proportion of proliferating colon cancer cells in the presence of IL-22 or IL-22 + S3I-201; D: Average proportion of apoptotic colon cancer cells in the presence of IL-22 or IL-22 + S3I-201. Each bar represents the mean ± SE (n = 18). $^{a}P < 0.05$ *vs* the control medium.

cinomas, including hematological malignancies and diverse solid tumors[23]. Abundant evidence has suggested that the dysregulation of IL-22 is associated with aberrant STAT3 signaling in liver injury[24], ulcerative colitis[25], oral squamous cell carcinoma[26], and gastric cancer[27]. STAT3 activation in CRC correlates with adverse clinical results[28]. In this study, we co-cultured RKO cells with IL-22 *in vitro* to investigate the effects of IL-22 on colon cancer cells. We observed that IL-22 enhanced RKO cell proliferation and had anti-apoptotic effects; these effects were blocked by adding S3I-201, suggesting that IL-22 exerts its functions in CRC *via* STAT3 signaling. These results are similar to those found in studies of lung cancer cells[22] and of Hct-116 colon cancer cells[29]. Moreover, by activating the STAT3 pathway, IL-22 may act as a novel chemoresistance cytokine that prevents CRC patients from benefiting from FOLFOX chemotherapy[30], and promote CRC invasiveness and stemness[31]. Finally, we verified this effect in a subcutaneous tumor model. We observed that tumor growth in nude mice could be significantly promoted by IL-22 but completely reversed by adding

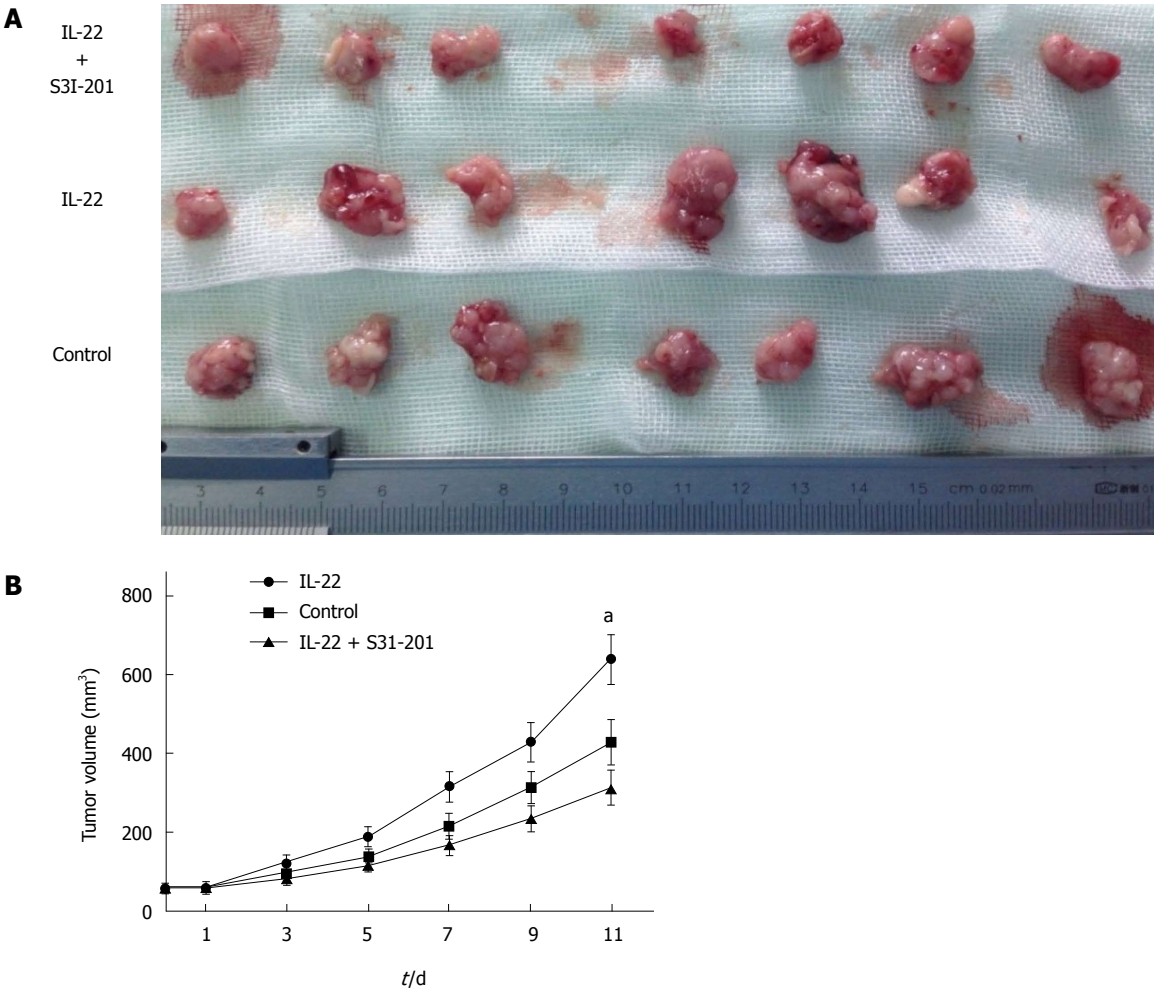

Figure 4 Effects of interleukin-22 on colon cancer *in vivo*. A: Tumor tissues were obtained from BALB/c nude mice; B: Tumor growth curves for interleukin (IL)-22, IL-22 + S3I-201 and control group mice. The tumor volume was calculated as follows: (major circumference × minor circumference^2)/2. Each plot represents the mean ± SE (n = 7). $^aP < 0.05$ *vs* the control.

a STAT3 inhibitor.

In conclusion, we measured the proportion of Th22 cells in the colorectal tumor microenvironment and found that the accumulation of Th22 cells in tumor sites may be related to the functions of chemotactic factors that are secreted by the tumor microenvironment. In addition, IL-22 was associated with CRC development in both *in vitro* and *in vivo* experiments, most likely by activating the STAT3 signaling pathway. The correlation between immunology and malignant tumors has become an important research area[32,33]. Further understanding the regulation and mechanism of Th22 cells in tumor microenvironments may provide new insights into immune therapeutic strategies for patients with CRC.

COMMENTS

Background

Colorectal cancer (CRC) is one of the most commonly occurring cancers worldwide. In recent years, tumor immunology has become a research hotspot, and understanding the molecular pathway involved in CRC will help to improve cancer prevention and treatment. Th22 cells were first introduced in 2009, and the functional characteristics of these cells in inflammatory and autoimmune diseases have been extensively studied. However, knowledge regarding their role in tumor immunity is relatively limited, particularly in CRC.

Research frontiers

Studies have shown that Th22 cells are involved in the progression of many digestive malignant tumors. However, the specific participation mechanism of these cells remains unclear.

Innovations and breakthroughs

The authors analyzed the relation between Th22 cells and the colorectal tumor microenvironment from a new perspective, verified their effects on CRC *via in vivo* and *in vitro* experiments, and attempted to demonstrate the specific signaling pathway by which Th22 cells participate in carcinogenesis.

Applications

The results of this study indicated that Th22 cells might be a prognostic factor and a potential therapeutic target for patients with CRC.

Terminology

Flow cytometry, which is a biophysical technology employed in cell counting, cell sorting and biomarker detection, widely used in basic research, clinical trials and blood cancer diagnosis.

Peer-review

This is a well conducted study on very timely topics. The authors can improve this paper with more thorough literature review in the context of tumor changes

and immunity.

REFERENCES

1 **Jemal A**, Bray F, Center MM, Ferlay J, Ward E, Forman D. Global cancer statistics. *CA Cancer J Clin* 2011; **61**: 69-90 [PMID: 21296855 DOI: 10.3322/caac.20107]

2 **Edwards BK**, Noone AM, Mariotto AB, Simard EP, Boscoe FP, Henley SJ, Jemal A, Cho H, Anderson RN, Kohler BA, Eheman CR, Ward EM. Annual Report to the Nation on the status of cancer, 1975-2010, featuring prevalence of comorbidity and impact on survival among persons with lung, colorectal, breast, or prostate cancer. *Cancer* 2014; **120**: 1290-1314 [PMID: 24343171 DOI: 10.1002/cncr.28509]

3 **Weitz J**, Koch M, Debus J, Höhler T, Galle PR, Büchler MW. Colorectal cancer. *Lancet* 2005; **365**: 153-165 [PMID: 15639298 DOI: 10.1016/S0140-6736(05)17706-X]

4 **Bishehsari F**, Mahdavinia M, Vacca M, Malekzadeh R, Mariani-Costantini R. Epidemiological transition of colorectal cancer in developing countries: environmental factors, molecular pathways, and opportunities for prevention. *World J Gastroenterol* 2014; **20**: 6055-6072 [PMID: 24876728 DOI: 10.3748/wjg.v20.i20.6055]

5 **Colussi D**, Brandi G, Bazzoli F, Ricciardiello L. Molecular pathways involved in colorectal cancer: implications for disease behavior and prevention. *Int J Mol Sci* 2013; **14**: 16365-16385 [PMID: 23965959 DOI: 10.3390/ijms140816365]

6 **Hou N**, Zhang X, Zhao L, Zhao X, Li Z, Song T, Huang C. A novel chronic stress-induced shift in the Th1 to Th2 response promotes colon cancer growth. *Biochem Biophys Res Commun* 2013; **439**: 471-476 [PMID: 24036270 DOI: 10.1016/j.bbrc.2013.08.101]

7 **Hua D**, Sun J, Mao Y, Chen LJ, Wu YY, Zhang XG. B7-H1 expression is associated with expansion of regulatory T cells in colorectal carcinoma. *World J Gastroenterol* 2012; **18**: 971-978 [PMID: 22408358 DOI: 10.3748/wjg.v18.i9.971]

8 **Waldner M**, Schimanski CC, Neurath MF. Colon cancer and the immune system: the role of tumor invading T cells. *World J Gastroenterol* 2006; **12**: 7233-7238 [PMID: 17143936]

9 **Galon J**, Costes A, Sanchez-Cabo F, Kirilovsky A, Mlecnik B, Lagorce-Pagès C, Tosolini M, Camus M, Berger A, Wind P, Zinzindohoué F, Bruneval P, Cugnenc PH, Trajanoski Z, Fridman WH, Pagès F. Type, density, and location of immune cells within human colorectal tumors predict clinical outcome. *Science* 2006; **313**: 1960-1964 [PMID: 17008531 DOI: 10.1126/science.1129139]

10 **Pernot S**, Terme M, Voron T, Colussi O, Marcheteau E, Tartour E, Taieb J. Colorectal cancer and immunity: what we know and perspectives. *World J Gastroenterol* 2014; **20**: 3738-3750 [PMID: 24833840 DOI: 10.3748/wjg.v20.i14.3738]

11 **Duhen T**, Geiger R, Jarrossay D, Lanzavecchia A, Sallusto F. Production of interleukin 22 but not interleukin 17 by a subset of human skin-homing memory T cells. *Nat Immunol* 2009; **10**: 857-863 [PMID: 19578369 DOI: 10.1038/ni.1767]

12 **Trifari S**, Kaplan CD, Tran EH, Crellin NK, Spits H. Identification of a human helper T cell population that has abundant production of interleukin 22 and is distinct from T(H)-17, T(H)1 and T(H)2 cells. *Nat Immunol* 2009; **10**: 864-871 [PMID: 19578368 DOI: 10.1038/ni.1770]

13 **Tian T**, Yu S, Ma D. Th22 and related cytokines in inflammatory and autoimmune diseases. *Expert Opin Ther Targets* 2013; **17**: 113-125 [PMID: 23256771 DOI: 10.1517/14728222.2013.736497]

14 **Li L**, Huang YH, Li Y, Wang FQ, Shang BY, Zhen YS. Antitumor activity of anti-type IV collagenase monoclonal antibody and its lidamycin conjugate against colon carcinoma. *World J Gastroenterol* 2005; **11**: 4478-4483 [PMID: 16052675]

15 **Livak KJ**, Schmittgen TD. Analysis of relative gene expression data using real-time quantitative PCR and the 2(-Delta Delta C(T)) Method. *Methods* 2001; **25**: 402-408 [PMID: 11846609 DOI: 10.1006/meth.2001.1262]

16 **Zhang S**, Li W, Xia Z, Mao Y. CD4 T cell dependent tumor immunity stimulated by dendritic cell based vaccine. *Biochem Biophys Res Commun* 2011; **413**: 294-298 [PMID: 21893031 DOI: 10.1016/j.bbrc.2011.08.089]

17 **Chang WJ**, Du Y, Zhao X, Ma LY, Cao GW. Inflammation-related factors predicting prognosis of gastric cancer. *World J Gastroenterol* 2014; **20**: 4586-4596 [PMID: 24782611 DOI: 10.3748/wjg.v20.i16.4586]

18 **Liu T**, Peng L, Yu P, Zhao Y, Shi Y, Mao X, Chen W, Cheng P, Wang T, Chen N, Zhang J, Liu X, Li N, Guo G, Tong W, Zhuang Y, Zou Q. Increased circulating Th22 and Th17 cells are associated with tumor progression and patient survival in human gastric cancer. *J Clin Immunol* 2012; **32**: 1332-1339 [PMID: 22760549 DOI: 10.1007/s10875-012-9718-8]

19 **Zhuang Y**, Peng LS, Zhao YL, Shi Y, Mao XH, Guo G, Chen W, Liu XF, Zhang JY, Liu T, Luo P, Yu PW, Zou QM. Increased intratumoral IL-22-producing CD4(+) T cells and Th22 cells correlate with gastric cancer progression and predict poor patient survival. *Cancer Immunol Immunother* 2012; **61**: 1965-1975 [PMID: 22527243 DOI: 10.1007/s00262-012-1241-5]

20 **Qin S**, Ma S, Huang X, Lu D, Zhou Y, Jiang H. Th22 cells are associated with hepatocellular carcinoma development and progression. *Chin J Cancer Res* 2014; **26**: 135-141 [PMID: 24826053 DOI: 10.3978/j.issn.1000-9604.2014.02.14]

21 **Xu X**, Tang Y, Guo S, Zhang Y, Tian Y, Ni B, Wang H. Increased intratumoral interleukin 22 levels and frequencies of interleukin 22-producing CD4+ T cells correlate with pancreatic cancer progression. *Pancreas* 2014; **43**: 470-477 [PMID: 24622082 DOI: 10.1097/MPA.0000000000000055]

22 **Ye ZJ**, Zhou Q, Yin W, Yuan ML, Yang WB, Xiang F, Zhang JC, Xin JB, Xiong XZ, Shi HZ. Interleukin 22-producing CD4+ T cells in malignant pleural effusion. *Cancer Lett* 2012; **326**: 23-32 [PMID: 22809567 DOI: 10.1016/j.canlet.2012.07.013]

23 **Siveen KS**, Sikka S, Surana R, Dai X, Zhang J, Kumar AP, Tan BK, Sethi G, Bishayee A. Targeting the STAT3 signaling pathway in cancer: role of synthetic and natural inhibitors. *Biochim Biophys Acta* 2014; **1845**: 136-154 [PMID: 24388873 DOI: 10.1016/j.bbcan.2013.12.005]

24 **Feng D**, Wang Y, Wang H, Weng H, Kong X, Martin-Murphy BV, Li Y, Park O, Dooley S, Ju C, Gao B. Acute and chronic effects of IL-22 on acetaminophen-induced liver injury. *J Immunol* 2014; **193**: 2512-2518 [PMID: 25063867 DOI: 10.4049/jimmunol.1400588]

25 **Yu LZ**, Wang HY, Yang SP, Yuan ZP, Xu FY, Sun C, Shi RH. Expression of interleukin-22/STAT3 signaling pathway in ulcerative colitis and related carcinogenesis. *World J Gastroenterol* 2013; **19**: 2638-2649 [PMID: 23674871 DOI: 10.3748/wjg.v19.i17.2638]

26 **Naher L**, Kiyoshima T, Kobayashi I, Wada H, Nagata K, Fujiwara H, Ookuma YF, Ozeki S, Nakamura S, Sakai H. STAT3 signal transduction through interleukin-22 in oral squamous cell carcinoma. *Int J Oncol* 2012; **41**: 1577-1586 [PMID: 22922995 DOI: 10.3892/ijo.2012.1594]

27 **Fukui H**, Zhang X, Sun C, Hara K, Kikuchi S, Yamasaki T, Kondo T, Tomita T, Oshima T, Watari J, Imura J, Fujimori T, Sasako M, Miwa H. IL-22 produced by cancer-associated fibroblasts promotes gastric cancer cell invasion via STAT3 and ERK signaling. *Br J Cancer* 2014; **111**: 763-771 [PMID: 24937671 DOI: 10.1038/bjc.2014.336]

28 **Morikawa T**, Baba Y, Yamauchi M, Kuchiba A, Nosho K, Shima K, Tanaka N, Huttenhower C, Frank DA, Fuchs CS, Ogino S. STAT3 expression, molecular features, inflammation patterns, and prognosis in a database of 724 colorectal cancers. *Clin Cancer Res* 2011; **17**: 1452-1462 [PMID: 21310826 DOI: 10.1158/1078-0432.CCR-10-2694]

29 **Jiang R**, Wang H, Deng L, Hou J, Shi R, Yao M, Gao Y, Yao A, Wang X, Yu L, Sun B. IL-22 is related to development of human colon cancer by activation of STAT3. *BMC Cancer* 2013; **13**: 59 [PMID: 23379788 DOI: 10.1186/1471-2407-13-59]

30 **Wu T**, Wang Z, Liu Y, Mei Z, Wang G, Liang Z, Cui A, Hu X, Cui L, Yang Y, Liu CY. Interleukin 22 protects colorectal cancer cells from chemotherapy by activating the STAT3 pathway and inducing autocrine expression of interleukin 8. *Clin Immunol* 2014; **154**: 116-126 [PMID: 25063444 DOI: 10.1016/j.clim.2014.07.005]

31 **Kryczek I**, Lin Y, Nagarsheth N, Peng D, Zhao L, Zhao E, Vatan L, Szeliga W, Dou Y, Owens S, Zgodzinski W, Majewski M, Wallner G, Fang J, Huang E, Zou W. IL-22(+)CD4(+) T cells promote colorectal cancer stemness via STAT3 transcription factor activation and induction of the methyltransferase DOT1L. *Immunity* 2014; **40**: 772-784 [PMID: 24816405 DOI: 10.1016/j.immuni.2014.03.010]

32 **Ogino S**, Galon J, Fuchs CS, Dranoff G. Cancer immunology--analysis of host and tumor factors for personalized medicine. *Nat Rev Clin Oncol* 2011; **8**: 711-719 [PMID: 21826083 DOI: 10.1038/nrclinonc.2011.122]

33 **Galon J**, Mlecnik B, Bindea G, Angell HK, Berger A, Lagorce C, Lugli A, Zlobec I, Hartmann A, Bifulco C, Nagtegaal ID, Palmqvist R, Masucci GV, Botti G, Tatangelo F, Delrio P, Maio M, Laghi L, Grizzi F, Asslaber M, D'Arrigo C, Vidal-Vanaclocha F, Zavadova E, Chouchane L, Ohashi PS, Hafezi-Bakhtiari S, Wouters BG, Roehrl M, Nguyen L, Kawakami Y, Hazama S, Okuno K, Ogino S, Gibbs P, Waring P, Sato N, Torigoe T, Itoh K, Patel PS, Shukla SN, Wang Y, Kopetz S, Sinicrope FA, Scripcariu V, Ascierto PA, Marincola FM, Fox BA, Pagès F. Towards the introduction of the 'Immunoscore' in the classification of malignant tumours. *J Pathol* 2014; **232**: 199-209 [PMID: 24122236 DOI: 10.1002/path.4287]

P- Reviewer: Ogino S **S- Editor**: Ma YJ
L- Editor: O'Neill M **E- Editor**: Liu XM

World Journal of Gastroenterology

Submit a Manuscript: http://www.wjgnet.com/esps/
Help Desk: http://www.wjgnet.com/esps/helpdesk.aspx
DOI: 10.3748/wjg.v21.i14.4225

World J Gastroenterol 2015 April 14; 21(14): 4225-4231
ISSN 1007-9327 (print) ISSN 2219-2840 (online)

ORIGINAL ARTICLE

Basic Study

Inhibitory effects of emodin, baicalin, schizandrin and berberine on *hefA* gene: Treatment of *Helicobacter pylori*-induced multidrug resistance

Yan-Qiang Huang, Gan-Rong Huang, Ming-Hui Wu, Hua-Ying Tang, Zan-Song Huang, Xi-Han Zhou, Wen-Qiang Yu, Jian-Wei Su, Xiao-Qiang Mo, Bing-Pu Chen, Li-Juan Zhao, Xiao-Feng Huang, Hong-Yu Wei, Lian-Deng Wei

Yan-Qiang Huang, Gan-Rong Huang, Hua-Ying Tang, Xiao-Qiang Mo, Bing-Pu Chen, Li-Juan Zhao, Xiao-Feng Huang, Hong-Yu Wei, Lian-Deng Wei, Department of Medical Microbiology and Immunology, Youjiang Medical College for Nationalities, Baise 533000, Guangxi Zhuang Autonomous Region, China

Ming-Hui Wu, Zan-Song Huang, Xi-Han Zhou, Wen-Qiang Yu, Jian-Wei Su, Institute of Digestive Disease, Affiliated Hospital of Youjiang Medical University for Nationalities, Baise 533000, Guangxi Zhuang Autonomous Region, China

Author contributions: Huang GR, Wu MH, Tang HY, Huang XF, Wei LD and Wei HY performed the majority of experiments; Zhou XH, Yu WQ, and Su JW provided vital reagents and analytical tools and were also involved in editing the manuscript; Chen BP, Mo XQ, Zhao LJ and Huang ZS co-ordinated and provided the collection of all the human material in addition to providing financial support for this work; Huang YQ designed the study and wrote the manuscript; Huang YQ and Huang GR contributed equally to this work.

Supported by Grants from Guangxi Key Discipline Fund (Pathogenic Microbiology), No. [2013]16; Key Laboratory Fund of Colleges and Universities in Guangxi, No. Gui Jiao Ke Yan [2014]6; National Natural Science Foundation of China, No. 31460023; and Natural Science Foundation of Guangxi, No. 2014GXNSFAA118206.

Ethics approval: The study was reviewed and approved by the Youjiang Medical College Institutional Review Board.

Institutional animal care and use committee: All procedures involving animals were reviewed and approved by the Institutional Animal Care and Use Committee of the Guangxi Zhuang Autonomous Region Science and Technology Agency (IACUC protocol number: SCXK 2012-0003).

Conflict-of-interest: The authors declare no conflicts of interest to disclose.

Data sharing: No additional data are available.

Correspondence to: Yan-Qiang Huang, Associate Professor, Department of Medical Microbiology and Immunology, Youjiang Medical College for Nationalities, No. 98 Countryside Road, Baise 533000, Guangxi Zhuang Autonomous Region, China. hyq77615@163.com
Telephone: +86-776-2853272
Fax: +86-776-2853272

Received: November 2, 2014
Peer-review started: November 2, 2014
First decision: December 2, 2014
Revised: December 22, 2014
Accepted: February 5, 2015
Article in press: February 5, 2015
Published online: April 14, 2015

Abstract

AIM: To investigate the inhibitory effects of emodin, baicalin, *etc*. on the *hefA* gene of multidrug resistance (MDR) in *Helicobacter pylori* (*H. pylori*).

METHODS: The double dilution method was used to screen MDR *H. pylori* strains and determine the minimum inhibitory concentrations (MICs) of emodin, baicalin, schizandrin, berberine, clarithromycin, metronidazole, tetracycline, amoxicillin and levofloxacin against *H. pylori* strains. After the screened MDR stains were treated with emodin, baicalin, schizandrin or berberine at a 1/2 MIC concentration for 48 h, changes in MICs of amoxicillin, tetracycline, levofloxacin, metronidazole and clarithromycin were determined.

MDR strains with reduced MICs of amoxicillin were selected to detect the *hefA* mRNA expression by real-time quantitative PCR.

RESULTS: A total of four MDR *H. pylori* strains were screened. Treatment with emodin, baicalin, schizandrin and berberine significantly decreased the MICs of amoxicillin and tetracycline against some strains, decreased by 1 to 2 times, but did not significantly change the MICs of clarithromycin, levofloxacin, and metronidazole against MDR strains. In the majority of strains with reduced MICs of amoxicillin, *hefA* mRNA expression was decreased; one-way ANOVA (SPSS 12.0) used for comparative analysis, $P < 0.05$.

CONCLUSION: Emodin, baicalin, schizandrin and berberine significantly decreased the MICs of amoxicillin and tetracycline against some *H. pylori* strains, possibly by mechanisms associated with decreasing *hefA* mRNA expression.

Key words: Traditional Chinese medicine; Multidrug resistance; *Helicobacter pylori*; Efflux pump; hefA

Core tip: Clinical signs of *Helicobacter pylori* (*H. pylori*)-induced drug resistance have become more and more prevalent, thus resulting in reduced cure rates. In this study, we used herbal extracts, such as berberine, to inhibit multidrug resistance in *H. pylori*. The results indicated that the minimum inhibitory concentration of amoxicillin and tetracycline was lowered after the intervention; the regulatory mechanism was related to down-regulation of efflux pump *hefA* mRNA expression. This suggests a novel strategy for prophylaxis and treatment of *H. pylori*-induced resistance.

Huang YQ, Huang GR, Wu MH, Tang HY, Huang ZS, Zhou XH, Yu WQ, Su JW, Mo XQ, Chen BP, Zhao LJ, Huang XF, Wei HY, Wei LD. Inhibitory effects of emodin, baicalin, schizandrin and berberine on *hefA* gene: Treatment of *Helicobacter pylori*-induced multidrug resistance. *World J Gastroenterol* 2015; 21(14): 4225-4231 Available from: URL: http://www.wjgnet.com/1007-9327/full/v21/i14/4225.htm DOI: http://dx.doi.org/10.3748/wjg.v21.i14.4225

INTRODUCTION

Helicobacter pylori (*H. pylori*) is the pathogen of multiple digestive system diseases including chronic active gastritis and peptic ulcer, and has been categorized as a class Ⅰ carcinogen by the World Health Organization[1,2]. Globally, the rate of *H. pylori* infection is as high as 50%[3-5], and it is even higher in developing countries. In China, the rate of *H. pylori* infection is 60%-90%[6,7]. Studies have found that 15% of clinical isolates of *H. pylori* develop multiple drug resistance (MDR; resistance to three or more antibiotics)[8-11], and this causes a decline in *H. pylori* eradication rate, posing a serious threat to human health. Therefore, the mechanism of MDR of *H. pylori* has become a hot research topic. Bacterial efflux pumps play an important role in the development of MDR. Liu *et al*[12] found that high expression of the *hefA* gene, which encodes a member of the active efflux system, resulted in the development of MDR in *H. pylori*. Zhang *et al*[13] artificially induced MDR and, for the first time, found that efflux pump inhibitors could partially reverse MDR. Studies have shown that traditional Chinese medicines emodin and baicalin have an obvious inhibitory effect on *H. pylori*[14-17]. The present study investigated the possible inhibitory effect of emodin, baicalin, schizandrin and berberine on MDR of *H. pylori* strains and the relationship between efflux pump *hefA* mRNA expression and reduced minimum inhibitory concentrations (MICs) of antibiotics, with an aim to explore the effect of Chinese herbs on *H. pylori* efflux pumps and to provide a theoretical basis for reversing MDR.

MATERIALS AND METHODS

Materials

H. pylori strains were obtained from the Department of Gastroenterology, Affiliated Hospital of Youjiang Medical University for Nationalities. For isolating *H. pylori* strains, gastric mucosal specimens were collected, ground, inoculated on Columbia blood agar plates containing 5% fresh rabbit blood, and cultured at 37 ℃ under micro-aerobic conditions (850 mL/L N_2, 100 mL/L CO_2, 50 mL/L O_2) in > 98% relative humidity for 3 to 5 d. The isolated strains were confirmed as *H. pylori* by biochemical tests (urease, catalase, oxidase), hematoxylin and eosin staining, and morphological analysis. Antibiotics used in this study included: amoxicillin (Lot No. 10807; Sichuan Pharmaceutical, Inc., China), clarithromycin (Lot No. 111202; Harbin Pharmaceutical Group Sixth Pharm Factory, China), levofloxacin (Lot No. 120120, Xinchang Pharmaceutical Factory of Zhejiang Pharmaceutical Co., LTD., China), tetracycline (Lot No. 20110902, Guangdong Taicheng Pharmaceutical Co., LTD., China), and metronidazole (Lot No.10091544, Zhejiang Jimin Pharmaceutical Co., LTD., China). Emodin (Lot No. 120908; purity, 98%), berberine (Lot No. 120810; purity, 97%), schizandrin (Lot No. 120908; purity, 98%), and baicalin (Lot No. 120908; purity, 90%) were purchased from Shaanxi Angsheng Biological Technology Co., LTD (China). Other reagents or kits used included Trizol reagent kit (Shanghai Invitrogen, China); RevertAid First Strand cDNA Synthesis Kit and DNase Ⅰ (Fermentas); 2 × SYBRGreen quantitative PCR (qPCR) Mix (Beijing Zhuangment Co., LTD, China). PCR primers were designed based on the *H. pylori hefABC* gene

Table 1 Resistance of multidrug resistance strains to the five antibiotics

No.	Levofloxacin	Amoxicillin	Clarithromycin	Tetracycline	Metronidazole
23	R	R	R	R	R
40	R	R	R	R	R
41	S	R	R	R	R
42	R	R	I	R	R

R: Resistant; S: Sensitive; I: Intermediate.

Table 2 Minimum inhibitory concentrations of the four Chinese medicines against multidrug resistance strains (mg/mL)

No.	Emodin	Berberine	Berberine	Schizandrin
23	12.5	50	200	50
40	12.5	100	100	100
41	12.5	100	100	100
42	12.5	25	100	50

sequences deposited in GenBank. Through sequence homology analysis, the primers were selected in the conserved region. 16S rRNA was used as an internal control. The primers were synthesized by Shanghai Sangon Biotech (China).

Screening of MDR strains

The double dilution method was used to determine the MICs of emodin, baicalin, schizandrin, berberine, clarithromycin, metronidazole, tetracycline, amoxicillin and levofloxacin against *H. pylori* strains. According to the Clinical and Laboratory Standards Institute (NCCLS) criteria, *H. pylori* strains that could grow in medium containing three or more of amoxicillin (≥ 4 μg/mL), levofloxacin (≥ 8 μg/mL), clarithromycin (≥ 1 μg/mL), metronidazole (≥ 8 μg/mL), and tetracycline (≥ 4 μg/mL) were identified as MDR strains.

Determination of antibiotic susceptibility of MDR strains before and after treatment with traditional Chinese medicines

Based on the method described previously[18], the MICs of the traditional Chinese medicines against MDR strains were calculated, and the next concentration below MIC was 1/2 MIC. The screened MDR stains were treated with emodin, baicalin, schizandrin or berberine at a 1/2 MIC concentration for 48 h to determine their effect on the MICs of amoxicillin, tetracycline, levofloxacin, metronidazole and clarithromycin. A positive control (10 mg/mL pantoprazole) and a negative control (culture medium) were also run at the same time.

Reverse transcription-PCR for detection of hefA mRNA expression in MDR strains with reduced MICs of amoxicillin

MDR strains with reduced MICs of amoxicillin after treatment with emodin, baicalin, schizandrin and berberine at a 1/2 MIC concentration were screened, and total RNA was prepared with Trizol reagent according to the manufacturer's instructions. Reverse transcription was then performed in a 20-μL system containing 5 μL total RNA, 1 μL random primer p(dN)6 (0.2 μg/μL), 5 μL RNase-free ddH$_2$O, 4.0 μL, 5 × reaction buffer, 2.0 μL dNTP mix (10 mmol/L), 1.0 μL Rnase inhibitor (20 U/μL) and 2.0 μL AMV reverse transcriptase (10 U/μL). The reaction parameters were 37 ℃ for 5 min, 42 ℃ for 60 min, and 70 ℃ for 10 min. PCR was then performed in a 20-μL system containing 10 μL SybrGreen qPCR Master Mix, 1 μL forward primer (10 μmol/L), 1 μL reverse primer (10 μmol/L), 7 μL ddH$_2$0, and 1 μL template (cDNA; 1:6 dilution). Cycling parameters were pre-denaturation at 95 ℃ for 2 min, and 40 cycles of denaturation at 95 ℃ for 10 s and annealing at 60 ℃ for 40 s.

Statistical analysis

Statistical analyses were performed using SPSS12.0. The differences in *hefA* mRNA expression were compared using analysis of variance (ANOVA) and Tukey tests.

RESULTS

Screening of MDR strains

A total of four MDR strains were screened, of which two were resistant to amoxicillin, clarithromycin, levofloxacin, tetracycline, and metronidazole, one was resistant to amoxicillin, clarithromycin, tetracycline, and metronidazole, and one was resistant to amoxicillin, levofloxacin, tetracycline, and metronidazole. These MDR strains are shown in Table 1.

MICs of the four traditional Chinese medicines against MDR strains

The MICs of emodin, baicalin, schizandrin and berberine against MDR strains are shown in Table 2.

Changes in MICs of the determined antibiotics against MDR strains after treatment with the four traditional Chinese medicines

After the four MDR strains were treated with emodin, baicalin, schizandrin and berberine at a 1/2 MIC concentration or pantoprazole, the MICs of amoxicillin and tetracycline against some strains were decreased compared with before treatment or the negative control group. Compared with 10 mg/mL pantoprazole,

Table 3 Minimum inhibitory concentrations of amoxicillin against the four multidrug resistance strains after treatment with the four traditional Chinese medicines (μg/mL)

No.	Emodin	Berberine	Berberine	Schizandrin	Pantoprazole	NC
23	32	16	64	32	32	64
40	16	8	16	16	16	32
41	64	64	21	64	32	64
42	32	16	32	32	32	32

Pantoprazole was used as a positive control, and culture medium was used as a negative control. NC: Negative control.

Table 4 Minimum inhibitory concentrations of tetracycline against the four multidrug resistance strains after treatment with the four traditional Chinese medicines (μg/mL)

No.	Emodin	Berberine	Berberine	Schizandrin	Pantoprazole	NC
23	64	32	64	64	32	64
40	16	16	32	32	32	32
41	32	32	32	64	16	32
42	32	16	32	32	32	32

NC: Negative control.

Table 5 Minimum inhibitory concentrations of metronidazole against the four multidrug resistance strains after treatment with the four traditional Chinese medicines (μg/mL)

No.	Emodin	Berberine	Berberine	Schizandrin	Pantoprazole	NC
23	128	128	128	128	64	128
40	64	64	64	64	32	64
41	64	64	64	64	32	64
42	64	64	64	64	64	64

NC: Negative control.

Table 6 Minimum inhibitory concentrations of clarithromycin against the four multidrug resistance strains after treatment with the four traditional Chinese medicines (μg/mL)

No.	Emodin	Berberine	Berberine	Schizandrin	Pantoprazole	NC
23	64	64	64	64	32	64
40	32	32	32	32	16	32
41	32	32	32	32	16	32
42	32	32	32	32	32	32

NC: Negative control.

the effects of the traditional Chinese medicines were comparable or superior (Tables 3 and 4). However, the MICs of clarithromycin, levofloxacin, and metronidazole against MDR strains showed no significant changes (Tables 5-7).

Expression of hefA mRNA in MDR strains with significantly changed MICs of amoxicillin

Sixteen sub-cultured strains with significantly reduced MICs of amoxicillin after treatment with emodin, baicalin, schizandrin, berberine or pantoprazole (Table 3) were selected and used to detect the *hefA* mRNA expression by reverse transcription-PCR. After No. 23 MDR strain was treated with emodin, schizandrin or berberine, both MICs of amoxicillin and *hefA* mRNA expression were decreased. After No. 40 MDR strain was treated with emodin, baicalin, schizandrin and berberine, both MICs of amoxicillin and hefA mRNA expression were decreased. For No. 41 MDR strain, treatment with baicalin decreased MIC of amoxicillin but increased *hefA* mRNA expression. For No. 42 MDR strain, treatment with berberine decreased MIC of amoxicillin but increased *hefA* mRNA expression, while treatment with pantoprazole did not significantly change MIC of amoxicillin but increased *hefA* mRNA expression. The amplification curves, melting curves, PCR products and quantitative results for the 16 sub-cultured strains are shown in Figures 1-3 and Table 8, respectively.

Table 7 Minimum inhibitory concentrations of levofloxacin against the four multidrug resistance strains after treatment with the four traditional Chinese medicines (μg/mL)

No.	Emodin	Berberine	Berberine	Schizandrin	Pantoprazole	NC
23	64	64	64	64	32	64
40	32	32	32	32	16	32
41	32	32	32	32	16	32
42	64	64	64	64	64	64

NC: Negative control.

Table 8 Real-time PCR quantitative results for *hefA* gene expression in 16 sub-cultured strains with significantly changed minimum inhibitory concentration of amoxicillin

No.	hefA	16S rRNA	ΔCt	ΔΔCt	$2^{-(\Delta\Delta Ct)}$
1	31.0933170	14.457372	16.63595	0	1
2	30.2871494	15.427569	14.85958	-1.77637	3.425620
3	29.8203506	16.133926	13.68642	-2.94952	7.724926
4	30.2641807	16.449774	13.81441	-2.82154	7.069158
5	33.8933296	15.226003	18.66733	2.031382	0.244621
6	32.0969762	15.256840	16.84014	0.204191	0.868025
7	29.9665985	15.307595	14.65900	-1.97694	3.936578
8	31.2955170	14.817378	16.47814	-0.15781	1.115590
9	31.6979313	14.758531	16.93940	0.303455	0.810309
10	30.7486935	14.488201	16.26049	-0.37545	1.297247
11	34.3626747	18.408577	15.95410	-0.68185	1.604193
12	36.2199669	18.414414	17.80555	1.169608	0.444542
13	33.9337616	17.102884	16.83088	0.194932	0.873614
14	31.4263000	14.820235	16.60606	-0.02988	1.020928
15	32.9468956	14.884178	18.06272	1.426772	0.371962
16	31.6464024	15.465043	16.18136	-0.45459	1.370390

DISCUSSION

In recent years, there have been more and more studies on traditional Chinese medicines. As a result, the mechanisms of action of many traditional Chinese medicines have been gradually elucidated. Heat-

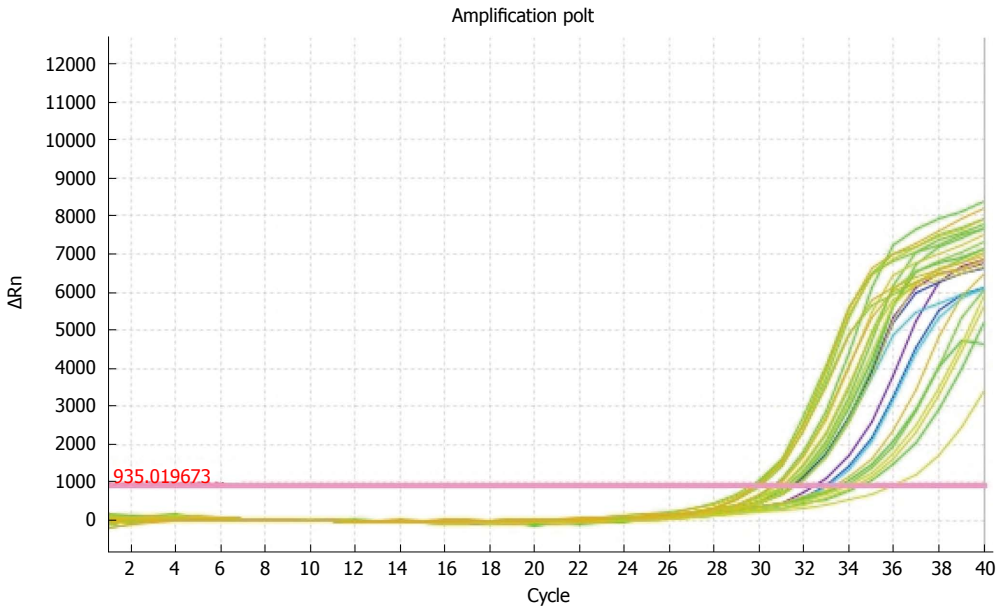

Figure 1 Amplification curves for the *hefA* gene in 16 sub-cultured strains with significantly changed minimum inhibitory concentration of amoxicillin.

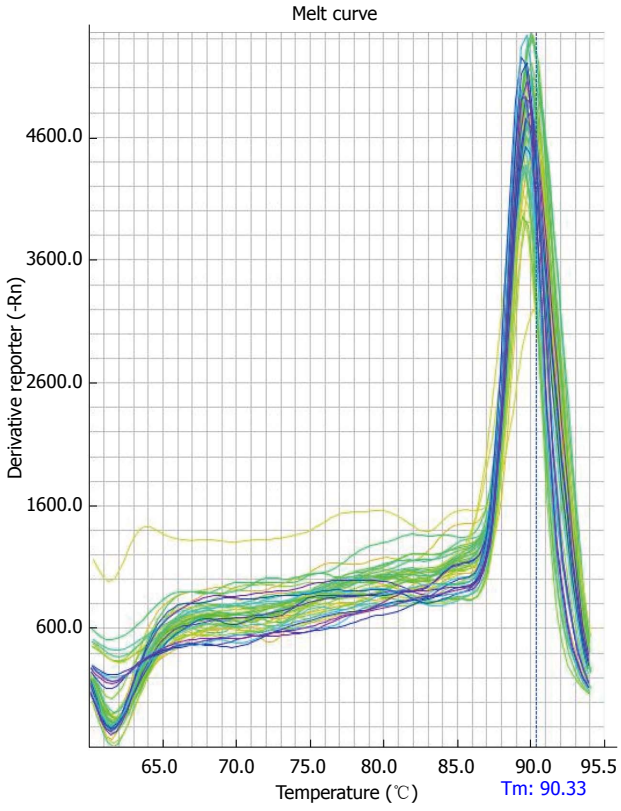

Figure 2 Melting curves for the *hefA* gene in 16 sub-cultured strains with significantly changed minimum inhibitory concentration of amoxicillin.

clearing and detoxicating Chinese medicines have strong antibacterial effects and are therefore called plant antibiotics; these include *Rhizoma coptidis*, *Radix scutellariae*, *Andrographis paniculata*, rhubarb, and *Radix isatidis*[17,19-24]. Baicalin is the main effective ingredient of *Radix scutellariae*, and its bacteriostatic mechanisms include destroying bacterial cell membrane, inhibition of bacterial DNA, RNA and protein biosynthesis, and degradation of endotoxins[25]. Berberine, also called berberine hydrochloride, is the main ingredient of *Rhizoma coptidis*. It exerts bacteriostatic effects probably by inhibiting bacterial growth and respiration, suppressing the oxidation of glucose and sugar metabolic intermediates, especially deoxidization reactions[26]. Rhubarb consists mainly of anthraquinone compounds including emodin, rhein, and chrysophanol. Emodin has purgative, antibacterial, antitumor and hemostatic effects, and its antibacterial effects are associated with inhibiting bacterial nucleic acid biosynthesis and breathing processes, because it can cause bacterial DNA damage and result in the production of small pieces of DNA[27,28]. However, some studies found that the inhibitory effect of emodin on *H. pylori* is related to the inhibition of aromatic amine-N-acetyl transferase activity[29]. Berberine, emodin, schizandrin, and baicalin have inhibitory and killing effects against *H. pylori*, even in drug-resistant strains. Currently, there have been no other reports of the effects of traditional Chinese medicines on MDR and the underlying mechanisms.

The results of the present study, together with our previous findings, showed that berberine, emodin, schizandrin, and baicalin have certain inhibitory and killing effects against MDR *H. pylori* strains. Additionally, emodin, baicalin, schizandrin or berberine at a 1/2 MIC concentration could reduce the MICs of amoxicillin and tetracycline against some MDR strains. Compared with 10 mg/mL pantoprazole, the effects of the traditional Chinese medicines were comparable or superior; however, they could not reduce the MICs of clarithromycin, levofloxacin, and metronidazole against MDR strains. The possible reasons are: (1) different MDR strains may have different drug resistance

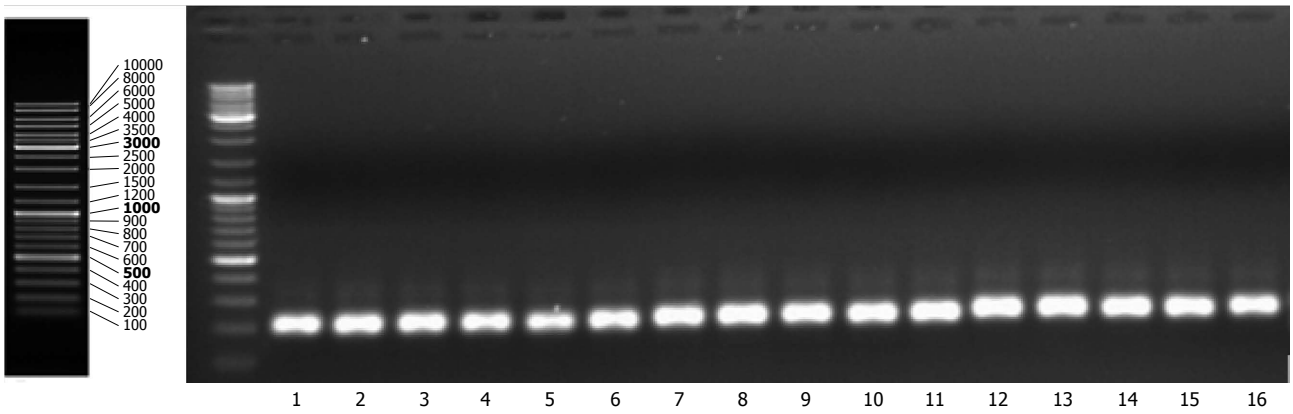

Figure 3 Agarose gel electrophoresis analysis of PCR products for *hefA* in 16 sub-cultured strains with significantly changed minimum inhibitory concentration of amoxicillin.

patterns, thus resulting in different MICs; (2) different traditional Chinese medicine ingredients have different bacteriostatic effects. Berberine has obvious, relatively stable bacteriostatic effects, while the other three medicines have unobvious, unstable antibacterial effects; and (3) bacterial strains came from different sources and had different growth environments, which may also affect MICs.

While exploring the mechanism by which emodin, baicalin, schizandrin, berberine and pantoprazole reduced the MICs of amoxicillin against MDR strains, we found that both MICs of amoxicillin and *hefA* mRNA expression were reduced in No. 23 and No. 40 MDR strains, suggesting that *hefA* mRNA expression may be positively correlated with the effects of emodin, baicalin, schizandrin, berberine and pantoprazole in reducing the MICs of amoxicillin against MDR strains. However, in No. 41 MDR strain, treatment with baicalin decreased the MIC but increased *hefA* mRNA expression; for No. 42 MDR strain, treatment with berberine decreased the MIC but increased *hefA* mRNA expression, and treatment with pantoprazole did not significantly change the MIC but increased *hefA* mRNA expression. On one hand, this may be associated with drug resistance patterns of MDR strains. Both No. 23 and No 40 MDR strains had the same pattern of resistance to levofloxacin, clarithromycin, amoxicillin, tetracycline, and metronidazole, while No. 41 was sensitive to levofloxacin, and No. 42 was moderately sensitive to clarithromycin. On the other hand, the existence of multiple efflux pump gene families may result in the above discrepancy. Since the *hefA* gene is only one member of one of the five efflux pump families, other members of the five efflux pump families may mediate the MIC reduction.

The present study showed that berberine, baicalin, emodin, and schizandrin all have antibacterial activities against MDR, and can reduce the MICs of amoxicillin and tetracycline, possibly *via* mechanisms associated with altering *hefA* gene expression. These findings provide a new idea and new method for solving the problem of increasingly serious MDR. However, it remains to be investigated why these Chinese medicines only reduced the MICs of amoxicillin and tetracycline, and did not alter those of levofloxacin, clarithromycin and metronidazole, and why *hefA* gene expression was not correlated with MIC reduction in some strains.

COMMENTS

Background

There are different mechanisms of *Helicobacter pylori* (*H. pylori*)-induced resistance to various antibiotics, but its multidrug resistance may be closely linked to the activity of efflux pumps. However, there is not yet an accredited method to prevent or reverse multidrug-resistance induced by *H. pylori*. Our research group has found that herbal extracts (especially emodin) have an effective inhibitory effect on *H. pylori*-induced multi-drug resistance, and that they reduced the minimum inhibitory concentration (MIC) of some antibiotics. Thus, the authors further explored the molecular mechanism of emodin lowering of antibiotic MIC by assessing the expression of the efflux pump gene *hefA*.

Research frontiers

The issue of *H. pylori*-induced drug resistance has become one of the current research directions, and seeking to optimally measure its resistance is an urgent scientific project. Chinese herbal medicine has pronounced characteristics, such as anti-inflammatory, immunomodulatory, anti-tumor roles and it lowers side effects. Therefore, developing some substitutes extracted from Chinese herbals would provide new ideas or methods to solve the drug resistance.

Innovations and breakthroughs

A class of fever-reducing and detoxification herbals generally has antibacterial effects, and some herbals, such as berberine, play an inhibitory role against *H. pylori*-induced drug resistance; however, its mechanism remains unclear. This study found that berberine had an effective inhibitory effect on *H. pylori*-induced drug resistance and decreased the MIC of amoxicillin antibiotic, *etc*. The authors also report that the mechanism may be related to reduction of efflux pump *hefA* gene expression.

Applications

This study found that berberine has an effective inhibitory effect on *H. pylori*-induced multi-drug resistance, and lowered the MIC of amoxicillin antibiotic *etc*. The findings suggest new ideas or methods to solve the drug-resistance induced by *H. pylori*, thereby aiming to cure this disease.

Terminology

Minimum inhibitory concentration is the lowest antimicrobial concentration that can inhibit the growth of bacteria; Multidrug resistance is a condition enabling disease-causing microorganisms (bacteria, viruses, fungi or parasites) to resist

distinct antimicrobials.

Peer-review

The present study revealed that berberine *etc.* has an effective inhibitory effect on *H. pylori*-induced multi-drug resistance and lowered the MIC of amoxicillin antibiotic *etc.*; the mechanism may be related to down-regulation of efflux pump *hefA* gene expression. The findings demonstrate that use of berberine has a relatively large practical value, and it would provide the scientific theory for developing effective medication against resistance induced by *H. pylori*.

REFERENCES

1 **Wang H**, Liu J, Dai DF, Guan XW, Ding J, Shao SL. Construction of cagL gene mutant in Helicobacter pylori. *Zhongguo Mianyixue Zazhi* 2012; **28**: 775-778 [DOI: 10.3969/j.issn.1000-484X.2012.09.002]

2 **Gisbert JP**. [Helicobacter pylori-related diseases]. *Gastroenterol Hepatol* 2012; **35** Suppl 1: 12-25 [PMID: 23018004 DOI: 10.1016/S0210-5705(12)70030-4]

3 **Cid TP**, Fernández MC, Benito Martínez S, Jones NL. Pathogenesis of Helicobacter pylori infection. *Helicobacter* 2013; **18** Suppl 1: 12-17 [PMID: 24011239 DOI: 10.1111/hel.12076]

4 **Thirumurthi S**, Graham DY. Helicobacter pylori infection in India from a western perspective. *Indian J Med Res* 2012; **136**: 549-562 [PMID: 23168695]

5 **Vilaichone RK**, Yamaoka Y, Shiota S, Ratanachu-ek T, Tshering L, Uchida T, Fujioka T, Mahachai V. Antibiotics resistance rate of Helicobacter pylori in Bhutan. *World J Gastroenterol* 2013; **19**: 5508-5512 [PMID: 24023494 DOI: 10.3748/wjg.v19.i33.5508]

6 **Malfertheiner P**, Megraud F, O'Morain CA, Atherton J, Axon AT, Bazzoli F, Gensini GF, Gisbert JP, Graham DY, Rokkas T, El-Omar EM, Kuipers EJ. Management of Helicobacter pylori infection--the Maastricht IV/ Florence Consensus Report. *Gut* 2012; **61**: 646-664 [PMID: 22491499 DOI: 10.1136/gutjnl-2012-302084]

7 **Gao HJ**, Sheng HH. Drug resistance related gene detection and Helicobacter pylori eradication. *Zhonghue Yixue Zazhi* 2012; **92**: 657-658

8 **Abdollahi H**, Savari M, Zahedi MJ, Moghadam SD, Hayatbakhsh Abasi M. Detection of A2142C, A2142G, and A2143G Mutations in 23s rRNA Gene Conferring Resistance to Clarithromycin among Helicobacter pylori Isolates in Kerman, Iran. *Iran J Med Sci* 2011; **36**: 104-110 [PMID: 23359224]

9 **Vega AE**, Cortiñas TI, Puig ON, Silva HJ. Molecular characterization and susceptibility testing of Helicobacter pylori strains isolated in western Argentina. *Int J Infect Dis* 2010; **14** Suppl 3: e85-e92 [PMID: 20304694 DOI: 10.1016/j.ijid.2009.11.022]

10 **Kim MS**, Kim N, Kim SE, Jo HJ, Shin CM, Lee SH, Park YS, Hwang JH, Kim JW, Jeong SH, Lee DH, Kim JM, Jung HC. Long-term follow-up Helicobacter pylori reinfection rate and its associated factors in Korea. *Helicobacter* 2013; **18**: 135-142 [PMID: 23066652 DOI: 10.1111/hel.12018]

11 **Wueppenhorst N**, Stueger HP, Kist M, Glocker E. Identification and molecular characterization of triple- and quadruple-resistant Helicobacter pylori clinical isolates in Germany. *J Antimicrob Chemother* 2009; **63**: 648-653 [PMID: 19190100 DOI: 10.1093/jac/dkp003]

12 **Liu ZQ**, Zheng PY. Important role of efflux pump gene hefA in multidrug resistance of Helicobacter pylori. *Shijie Huaren Xiaohu Zazhi* 2008; **14**: 5217-5222

13 **Zhang Z**, Liu ZQ, Zheng PY, Tang FA, Yang PC. Influence of efflux pump inhibitors on the multidrug resistance of Helicobacter pylori. *World J Gastroenterol* 2010; **16**: 1279-1284 [PMID: 20222174 DOI: 10.3748/wjg.v16.i10.1279]

14 **Zou SP**, Lian JG. Jiawei Banxia Xiexin decoction for treatment of chronic atrophic gastritis: analysis of 35 cases. *Dangdai Yixue* 2013; **19**: 155-156

15 **Zhu FY**, Wu JL, Xu S. Scanning electron microscopic observation of effect of Leweiyin on the gastric mucosa of rats with chronic atrophic gastritis. *JTCM* 2012; **18**: 269 -270

16 **Wang WH**, Hu FL. A multicenter study of Chinese patent medicine Wenweishu /Yangweishu in the treatment of Helicobacter pylori positive patients with chronic gastritis and peptic ulcer. *Zhonghua Yixue Zazhi* 2010; **90**: 75-78

17 **Ma F**, Chen Y, Li J, Qing HP, Wang JD, Zhang YL, Long BG, Bai Y. Screening test for anti-Helicobacter pylori activity of traditional Chinese herbal medicines. *World J Gastroenterol* 2010; **16**: 5629-5634 [PMID: 21105198 DOI: 10.3748/wjg.v16.i44.5629]

18 **Wu J**, Hu D, Wang KX. In vitro antibacterial activity of radix scutellariae and baicalin against Helicobacter pylori. *Zhongyaocai* 2008; **31**: 707-710

19 **Lin J**, Huang WW. A systematic review of treating Helicobacter pylori infection with Traditional Chinese Medicine. *World J Gastroenterol* 2009; **15**: 4715-4719 [PMID: 19787835 DOI: 10.3748/wjg.15.4715]

20 **Bu Y**, Lee K, Jung HS, Moon SK. Therapeutic effects of traditional herbal medicine on cerebral ischemia: a perspective of vascular protection. *Chin J Integr Med* 2013; **19**: 804-814 [PMID: 24170629 DOI: 10.1007/s11655-013-1341-2]

21 **Chang CH**, Huang WY, Lai CH, Hsu YM, Yao YH, Chen TY, Wu JY, Peng SF, Lin YH. Development of novel nanoparticles shelled with heparin for berberine delivery to treat Helicobacter pylori. *Acta Biomater* 2011; **7**: 593-603 [PMID: 20813208 DOI: 10.1016/j.actbio.2010.08.028]

22 **Sun YX**. Treatment of 60 cases of chronic atrophic gastritis based on syndrome differentiation. *Hunan Zhongyi Zazhi* 2010; **26**: 71-72

23 **Zhang L**. Relationship between Helicobacter pylori and chronic atrophic gastritis and its prevention and treatment. *Zhongguo Zhongxiyi Jiehe Zazhi* 2008; **12**: 521-523

24 **Huang YQ**, Huang GR, Li XH, Huang XF, Wei LD, Wei HY, Chen YH, Tang HY, Yang S, Qin YC. Effect of traditional Chinese medicine extracts on bio-membrane formation in drug-resistant Helicobacter pylori. *Zhongguo Yiyao Daobao* 2013; **32**: 1407-1409

25 **Wu ZB**. Pharmacological mechanism of heat-clearing effects of baicalin. *Anmo yu Kangfu Yixue* 2011; **2**

26 **Wang JP**, Peng XW. Single Chinese herb for treatment of Helicobacter pylori infection in animal models. *Weichangbingxue He Ganbingxue Zazhi* 2010; **19**: 345-7

27 **Peng RJ**, Peng XW. In vitro antibacterial activity of vitamin C, resveratrol and emodin against Helicobacter pylori. *JTCM* 2011; **3**: 51-52

28 **Hsu SC**, Chung JG. Anticancer potential of emodin. *BioMedicine* 2012; **2**: 108-16 [DOI: 10.1016/j.biomed.2012.03.003]

29 **Huang XM**, Huang H, Ou LM, Li J. In vitro activity of rhubarb against non-spore-forming anaerobes. *Zhongguo Zhongyiyao Xinxi Zazhi* 2001; **8**: 41-42

P- Reviewer: Miller C, Miller JS, Schaffellner S **S- Editor**: Yu J
L- Editor: Logan S **E- Editor**: Ma S

World Journal of Gastroenterology

Submit a Manuscript: http://www.wjgnet.com/esps/
Help Desk: http://www.wjgnet.com/esps/helpdesk.aspx
DOI: 10.3748/wjg.v21.i14.4232

World J Gastroenterol 2015 April 14; 21(14): 4232-4239
ISSN 1007-9327 (print) ISSN 2219-2840 (online)

ORIGINAL ARTICLE

Case Control Study

Interleukin-21 gene polymorphisms and chronic hepatitis B infection in a Chinese population

Jia-Yan Yao, Kang Chao, Min-Rui Li, Yan-Qing Wu, Bi-Hui Zhong

Jia-Yan Yao, Kang Chao, Min-Rui Li, Yan-Qing Wu, Bi-Hui Zhong, Department of Gastroenterology, The First Affiliated Hospital of Sun Yat-Sen University, Guangzhou 510080, Guangdong Province, China

Author contributions: Yao JY wrote the manuscript and performed the data analysis; Yao JY, Li MR and Wu YQ performed the majority of experiments; Chao K and Yao JY designed the research; Zhong BH revised the paper.

Supported by National Natural Science Foundation of China, No. 81170392.

Ethics approval: The study was reviewed and approved by the First Affiliated Hospital of Sun Yat-Sen University Institutional Review Board.

Informed consent: All study participants, or their legal guardian, provided informed written consent prior to study enrollment.

Data sharing: No additional data are available.

Correspondence to: Bi-Hui Zhong, MD, PhD, Division of Gastroenterology, The First Affiliated Hospital of Sun Yat-Sen University, No. 58 Zhongshan Road II, Guangzhou 510080, Guangdong Province, China. sophiazhong@medmail.com.cn
Telephone: +86-20-87755766
Fax: +86-20-87332916

Received: October 30, 2014
Peer-review started: October 31, 2014
First decision: November 26, 2014
Revised: December 19, 2014
Accepted: February 16, 2015
Article in press: February 16, 2015
Published online: April 14, 2015

Abstract

AIM: To investigate the relationship between interleukin-21 (*IL21*) gene polymorphisms and chronic hepatitis B virus (HBV) infection in a Chinese population.

METHODS: In this case-control study, 366 Chinese HBV-infected patients were recruited and divided into hepatocellular carcinoma (HCC; *n* = 94) and non-HCC (*n* = 272) groups at The First Affiliated Hospital of Sun Yat-Sen University, from April 2009 to December 2012. In the non-HCC group, the patients were classified into three clinical subsets, 76 patients had chronic hepatitis B, 101 were HBV carriers and 95 patients had HBV-related cirrhosis. Two hundred eight unrelated healthy controls were also included. Genomic DNA was extracted from peripheral blood. Single nucleotide polymorphisms (SNPs) rs13143866, rs2221903, and rs907715 were subsequently genotyped using the SNaPshot SNP technique.

RESULTS: There were no significant differences in allele and genotype frequencies of SNPs rs13143866, rs2221903, and rs907715 between chronic HBV-infected patients and control subjects. Furthermore, no significant differences were found in the frequencies of all alleles and genotypes between the HCC group and the non-HCC group. However, in the subgroup analysis, *IL21* rs13143866 genotype AA frequency in the HBV carrier group was higher than in controls (OR = 6.280, 95%CI: 1.238-31.854; *P* = 0.019), and the effect of the recessive model (AA *vs* GG + GA, OR = 6.505, 95%CI: 1.289-32.828) was observed in the HBV carrier group. *IL21* rs2221903 genotype TC frequency in the HBV carrier group was higher than in controls (OR = 1.809, 95%CI: 1.043-3.139; *P* = 0.035). In the haplotype analysis, the ATA haplotype (rs13143866, rs2221903, and rs907715) of *IL21* was more frequent in the HCC group than in the non-HCC group (0.165 *vs* 0.104, *P* = 0.044; OR = 1.700, 95%CI: 1.010-2.863).

CONCLUSION: Genotypes rs13143866 AA and rs2221903 TC are risk factors for carrying HBV; ATA haplotype increases the risk of HBV-related HCC onset

in a Chinese population.

Key words: Chinese population; Chronic hepatitis B virus infection; Interleukin-21 gene; rs13143866; rs2221903; rs907715; Single-nucleotide polymorphism

Core tip: This study is the first to investigate the relationship between single nucleotide polymorphism rs13143866 of the interleukin-21 gene and chronic hepatitis B virus (HBV) infection in a Chinese population. We found that genotypes rs13143866 AA and rs2221903 TC were risk factors for carrying HBV, and the ATA haplotype (rs13143866, rs2221903 and rs907715) increased the risk of HBV-related hepatocellular carcinoma.

Yao JY, Chao K, Li MR, Wu YQ, Zhong BH. Interleukin-21 gene polymorphisms and chronic hepatitis B infection in a Chinese population. *World J Gastroenterol* 2015; 21(14): 4232-4239 Available from: URL: http://www.wjgnet.com/1007-9327/full/v21/i14/4232.htm DOI: http://dx.doi.org/10.3748/wjg.v21.i14.4232

INTRODUCTION

Approximately one-third of the world's population has serologic evidence of past or present infection with hepatitis B virus (HBV), and 350-400 million people are chronic HBV surface antigen (HBsAg) carriers. The spectrum of disease and natural history of chronic HBV infection are diverse and variable, ranging from an inactive carrier state to progressive chronic hepatitis B (CHB), which may evolve to cirrhosis and hepatocellular carcinoma (HCC)[1]. An epidemiologic serosurvey of hepatitis B in China showed that the weighted prevalence of HBsAg in the Chinese population aged 1-59 years was 7.2%[2], which indicated that there were approximately 93 million people infected with HBV in China[3].

Interleukin (IL)-21, mainly produced by a range of differentiated $CD4^+$ T-cell subsets, is a relatively recently discovered multifunctional and pleiotropic cytokine[4,5]. It promotes proliferation and accumulation of Ag-specific $CD8^+$ effector T-cells, and increases their survival and cytolytic potential[6]. It also has a significant influence on the regulation of B-cell functions. It promotes the differentiation of antigen-stimulated B cells into memory and antibody-secreting plasma cells, affects IgE production, and induces Ig switch to IgG1 and IgG3 production[7,8]. In addition, it induces the differentiation of naive T cells into Th17 cells, and is involved in the maturation, activation, and survival of natural killer cells[9-11]. Several *in vivo* studies in animal models have shown that IL-21 is essential for controlling chronic viral infections[12-14]. The adaptive immune response is greatly attenuated in chronic HBV infection. It is likely that the absence of $CD4^+$ T-cells prevents the maturation of a functionally effective $CD8^+$ T-cell response, and is the primary reason for viral persistence[15-18]. Recent investigations have shown that serum levels of IL-21 are increased in CHB patients and associated with severe liver inflammation[19]. The levels of IL-21 expression in the liver tissues are significantly associated with increased degrees of inflammation and fibrosis in CHB patients[20]. High serum IL-21 levels after 12 wk of antiviral therapy predict HBeAg seroconversion in CHB[21]. IL-21 enhances HBcAg-specific interferon-γ^+CD8^+ T-cell proliferation, whereas treatment with anti-IL-21 inhibits expansion *in vitro*[22].

Collectively, these findings suggest that IL-21 may play a critical role in HBV infection. However, the precise mechanisms underlying the effects of IL-21 on hepatitis B pathogenesis have not yet been elucidated. Genetic polymorphisms in *IL21* have been explored in genetic susceptibility to chronic HBV-infected diseases. One report finds that *IL21* rs2221903 TC is less frequent in the HBV patients than in the HBV infection resolvers or in controls[23]. In kidney transplant patients with acute rejection, frequencies of TT homozygote genotype and T allele of IL-21-G1472T (rs2055979) polymorphism and CC homozygote genotype and C allele of IL-21-C5250T (rs4833837) polymorphism are higher in the HBV-infected patients than in the HBV-noninfected patients[24]. Accordingly, this study was conducted to confirm the association of *IL21* rs13143866, rs2221903, and rs907715 gene polymorphisms with susceptibility to chronic HBV infection in a Chinese population.

MATERIALS AND METHODS

The study was performed in accordance with the Declaration of Helsinki of the World Medical Association and was approved by The First Affiliated Hospital of Sun Yat-Sen University Institutional Review Board. All patients signed an informed consent form for this investigation.

Subjects

According to the guideline for the prevention and treatment of CHB (2010 version) and the diagnostic criteria (modified during the 10th National Conference on Viral Hepatitis and Hepatopathy 2000, China), 366 independent chronic HBV-infected patients (103 female and 263 male; mean age 48.3 ± 11.8 years) were recruited from The First Affiliated Hospital of Sun Yat-Sen University from April 2009 to December 2012 and were divided into an HCC (n = 94) and non-HCC (n = 272) group. All patients with HCC were confirmed by pathology. The non-HCC group was classified into three clinical subsets, CHB (n = 76), HBV carrier (n =

Table 1 Demographic data for all groups

Groups	Sex (M/F)	*P* value[1]	*P* value[2]	Age (yr)	*P* value[1]	*P* value[2]
HBV infection	263/103	0.672		48.3 ± 11.8	0.657	
HCC	64/30	0.713	0.345	48.8 ± 12.2	0.935	0.589
non-HCC	199/73	0.473		48.1 ± 11.7	0.544	
Carrier	71/24	0.416		47.9 ± 11.3	0.570	
CHB	58/18	0.310		46.5 ± 11.0	0.151	
Cirrhosis	70/31	1.000		49.4 ± 12.6	0.621	
Control	146/62			48.7 ± 11.3		

[1]*vs* control group; [2]between HCC and non-HCC groups. HBV: Hepatitis B virus; HCC: Chronic HBV-infected patients with hepatocellular carcinoma; non-HCC: Chronic HBV-infected patients without hepatocellular carcinoma; Carrier: HBV carriers; CHB: Patients with chronic hepatitis B; Cirrhosis: Patients with HBV-related cirrhosis.

101), and HBV-related cirrhosis (n = 95). None of the 366 chronic HBV-infected patients had received any antiviral therapy, including nucleoside analogues or interferon, before diagnosis. This study also included 208 geographically and ethnically matched unrelated healthy controls (62 female and 146 male; mean age 48.7 ± 11.3 years). Exclusion criteria included the presence of autoimmune diseases and other liver diseases, such as alcoholic liver disease, silt hemorrhagic liver disease, autoimmune liver disease, and intra-and extrahepatic bile duct stones.

Selection and genotyping of single-nucleotide polymorphisms

For selection of the single-nucleotide polymorphisms (SNPs), Haploview software (http://www.broad.mit.edu/mpg/haploview) was used to perform linkage disequilibrium and haplotype block analyses using HapMap phase genotype data for the chromosomal region 4:123,750,234..123,764,662 (CHB database, HapMap release 27). The amplicon of interest was a 14.4 kb region within *IL21* and approximately 3 kb upstream and 3 kb downstream of the gene. Three previously reported SNPs (rs13143866, rs2221903, and rs907715) with minor allele frequency (MAF) ⩾ 0.05 were chosen. Genomic DNA from peripheral blood was extracted using a commercially available kit (Tiangen Biotech, Beijing, China) according to the manufacturer's instructions. SNPs rs13143866, rs2221903, and rs907715 were subsequently genotyped by the SNaPshot SNP technique. Briefly, three segments were amplified using three pairs of forward and reverse primers: 5′-AAGTACCCACTGGACCAACTCA-3′ and 5′-TCTAGCTCTGAACCCAAACACT-3′, 5′-GGACCACATATTGCCAGACAC-3′ and 5′-GACACTGACGCCCATATTGAT-3′, and 5′-CACACTGGCATTGAGATGCTA-3′ and 5′-CCTCTTTTCACTTGGAGCATTC-3′ for rs13143866, rs2221903, and rs907715, respectively. All primers were designed using the Primer3 program (http://frodo.wi.mit.edu/cgi-bin/primer3/primer3_www.cgi). Multiplex PCR was carried out using the SNaPshot Multiplex Kit (Applied Biosystems of Thermo Fisher Scientific, Waltham, MA, United States) according to the manufacturer's instructions. The reaction was performed in a total volume of 20 μL containing 2 μL 10 × PCR buffer (Mg^{2+}-free) (Invitrogen of Thermo Fisher Scientific), 0.8 μL $MgCl_2$ (50 mmol/L; Invitrogen), 0.5 μL dNTP (10 mmol/L; Takara Bio Inc., Shiga, Japan), 0.5 μL Primer Mix, 1 μL DNA, 0.5 μL Platinum Taq (5U; Invitrogen), and 14.2 μL ddH_2O. Cycling conditions were as follows: 95 ℃ for 2 min; 33 cycles of 95 ℃ for 20 s, 56 ℃ for 30 s, and 72 ℃ for 40 s, followed by 72 ℃ for 5 min. PCR products were purified using shrimp alkaline enzyme (Promega Corp., Madison, WI, United States) and exonuclease Ⅰ (EpiCentre, Palmerston North, New Zealand) according to the manufacturer's instructions. Purified PCR products from two panels were mixed and used as a template for extension. Extension was performed in a total volume of 5 μL comprising 2.5 μL of SNaPshot Multiplex reaction mix (Applied Biosystems), 1.5 μL of purified PCR products, 0.7 μL of Probe Mix, and 0.3 μL of GC buffer. Extension was performed under the following conditions: 25 cycles of 96 ℃ for 10 s, 51 ℃ for 5 s, and 60 ℃ for 30 s, and then kept at 4 ℃. Extension products were purified using shrimp alkaline enzyme (Promega) and loaded onto an ABI PRISM 3730 DNA Sequencer (Applied Biosystems) for sequencing.

Statistical analysis

Distributions of the allele and genotype frequencies were calculated by the χ^2 test or Fisher's exact test. ORs and 95%CIs of genotype frequencies were adjusted by logistic regression analysis. All analyses were performed using SPSS 16.0 software (SPSS Inc., Chicago, IL, United States). The Hardy-Weinberg equilibrium test and the haplotype analysis were completed by SHEsis software (http://analysis.bio-x.cn/myAnalysis.php). All two-sided $P < 0.05$ were considered statistically significant.

RESULTS

Demographic data on each group are shown in Table 1. The allele and genotype frequencies of the three SNPs in *IL21* in the HBV-infected patients and control subjects are shown in Table 2. The Hardy-Weinberg equilibrium P value in each group was > 0.01.

Association between IL21 polymorphisms and HBV infection

Although there was no statistically difference, our data showed a tendency that SNP rs2221903 was associated with an increased risk of chronic HBV infection. The frequency of allele C was 13.7% in the chronic HBV infection group and 10.3% in the control group. Furthermore, the effect of the dominant model was observed (Table 2).

Table 2 Comparison of interleukin-21 polymorphisms between chronic hepatitis B virus-infected patients and controls *n* (%)

Polymorphism		HBV infection (*n* = 366)	Control (*n* = 208)	*P* value	OR (95%CI)
rs13143866					
Allele frequency	Allele G	621 (85.5)	363 (87.3)		Reference
	Allele A	111 (14.5)	53 (12.7)	0.259	1.224 (0.861-1.741)
Genotype frequency[1]	GG	266 (72.7)	157 (75.5)		Reference
	GA	89 (24.3)	49 (23.5)	0.734	0.933 (0.625-1.392)
	AA	11 (3.0)	2 (1.0)	0.290[2]	0.308 (0.067-1.408)
	HWE	0.294	0.391		
Recessive model	GG + GA	355 (97.0)	206 (99.0)		Reference
	AA	11 (3.0)	2 (1.0)	0.149[2]	3.195 (0.701-14.493)
Dominant model	GG	266 (72.7)	157 (75.5)		Reference
	AA + GA	100 (27.3)	51 (24.5)	0.463	1.157 (0.783-1.711)
rs2221903					
Allele frequency	Allele T	632 (86.3)	373 (89.7)		Reference
	Allele C	100 (13.7)	43 (10.3)	0.101	1.373 (0.939-2.006)
Genotype frequency[1]	TT	272 (74.3)	167 (80.3)		Reference
	TC	88 (24.1)	39 (18.7)	0.130	1.385 (0.907-2.116)
	CC	6 (1.6)	2 (1.0)	0.262[2]	1.842 (0.367-9.232)
	HWE	0.712	0.868		
Recessive model	TT+TC	360 (98.4)	206 (99.0)		Reference
	CC	6 (1.6)	2 (1.0)	0.717[2]	1.715 (0.342-8.547)
Dominant model	TT	272 (74.3)	167 (80.3)		Reference
	CC + TC	94 (25.7)	41 (19.7)	0.105	1.408 (0.930-2.130)
rs907715					
Allele frequency	Allele G	415 (56.7)	234 (56.2)		Reference
	Allele A	317 (43.3)	182 (43.8)	0.884	0.982 (0.770-1.252)
Genotype frequency[1]	GG	110 (30.0)	70 (33.7)		Reference
	GA	195 (53.3)	94 (45.2)	0.160	1.320 (0.896-1.945)
	AA	61 (16.7)	44 (21.1)	0.155	0.882 (0.540-1.440)
	HWE	0.104	0.238		
Recessive model	GG + GA	305 (83.3)	164 (78.8)		Reference
	AA	61 (16.7)	44 (21.2)	0.181	0.746 (0.484-1.148)
Dominant model	GG	110 (30.1)	70 (33.7)		Reference
	AA + GA	256 (69.9)	138 (66.3)	0.372	1.181 (0.820-1.699)

[1]The *P* values of rs13143866, rs2221903, and rs907715 genotype distribution between chronic HBV-infected patients and controls were 0.237, 0.876, 0.358, respectively; [2]Fisher's exact test. HWE: Hardy-Weinberg equilibrium.

Association between IL21 polymorphisms and HCC

No significant differences were found in the frequencies of all alleles and genotypes (rs13143866, rs2221903, and rs907715) between the HCC group and the non-HCC group (Table 3).

Association between IL21 polymorphisms and HBV infection subgroups

The distribution of genotypes and alleles of *IL21* rs907715 polymorphisms showed no significant difference among HBV carriers, patients with CHB, patients with HBV-related cirrhosis, and healthy controls. However, *IL21* rs13143866 and rs2221903 polymorphisms were differently distributed between the HBV carrier group and controls (Table 4). *IL21* rs13143866 genotype AA frequency in the HBV carrier group was higher than in controls (5.9% *vs* 1.0%, *P* = 0.019), and the effect of the recessive model (AA *vs* GG + GA, *P* = 0.017) was observed in the HBV carrier group. *IL21* rs2221903 genotype TC frequency in the HBV carrier group was higher than in controls (29.7% *vs* 18.7%, *P* = 0.035).

Haplotype analysis

The results showed that the ATA haplotype (rs13143866, rs2221903, and rs907715) was significantly associated with HBV-related HCC and appeared to be a risk haplotype (*P* = 0.044) (Table 5).

DISCUSSION

In this study, we analyzed allele and genotype frequencies at three SNPs of the *IL21* gene in 366 chronic HBV-infected patients and 208 healthy controls in a Chinese population. The intronic SNPs may not be the actual risk mutation, but they are likely to be a surrogate marker for a mutation with functional consequences. The intronic SNPs may be in high linkage disequilibrium with a variant that associates with translation of the mRNA[25]. In other words, they may associate with protein expression. For example, synonymous SNPs have a substantial contribution to human disease risk and other complex traits[26]. Literature reports explored *IL21* rs907715 and rs2221903 and *IL21R* T-83C and rs3093301

Table 3 Interleukin-21 polymorphisms among chronic hepatitis B virus-infected patients with hepatocellular carcinoma, patients without hepatocellular carcinoma, and controls *n* (%)

Polymorphism		HCC (*n* = 94)	non-HCC (*n* = 272)	Control (*n* = 208)	HCC *vs* non-HCC		HCC *vs* Control		non-HCC *vs* Control	
					P value	OR (95%CI)	*P* value	OR (95%CI)	*P* value	OR (95%CI)
rs13143866										
Allele	Allele G	167 (88.8)	454 (83.5)	363 (87.3)		Reference		Reference		Reference
frequency	Allele A	21 (11.2)	90 (16.5)	53 (12.7)	0.078	1.576 (0.949-2.617)	0.586	0.861 (0.503-1.474)	0.102	1.358 (0.941-1.958)
Genotype	GG	74 (78.7)	192 (70.6)	157 (75.5)		Reference		Reference		Reference
frequency[1]	GA	19 (20.2)	70 (25.7)	49 (23.5)	0.231	1.420 (0.800-2.520)	0.522	0.823 (0.453-1.495)	0.470	1.168 (0.766-1.781)
	AA	1 (1.1)	10 (3.7)	2 (1.0)	0.298[2]	3.854 (0.485-30.637)	1.000[2]	1.061 (0.095-11.886)	0.074[1]	4.089 (0.883-18.934)
	HWE	0.857	0.262	0.391						
Recessive	GG + GA	93 (98.9)	262 (96.3)	206 (99.0)		Reference		Reference		Reference
model	AA	1 (1.1)	10 (3.7)	2 (1.0)	0.230[2]	0.282 (0.036-2.231)	1.000[2]	1.108 (0.099-12.367)	0.077[1]	3.931 (0.852-18.139)
Dominant	GG	74 (78.7)	192 (70.6)	157 (75.5)		Reference		Reference		Reference
model	AA + GA	20 (21.3)	80 (29.4)	51 (24.5)	0.129	1.542 (0.882-2.695)	0.539	0.832 (0.463-1.495)	0.234	1.283 (0.852-1.932)
rs2221903										
Allele	Allele T	163 (86.7)	469 (86.2)	373 (89.7)		Reference		Reference		Reference
frequency	Allele C	25 (13.3)	75 (13.8)	43 (10.3)	0.866	1.043 (0.641-1.696)	0.288	1.330 (0.786-2.252)	0.108	1.387 (0.931-2.067)
Genotype	TT	70 (74.5)	202 (74.3)	167 (80.3)		Reference		Reference		Reference
frequency[1]	TC	23 (24.5)	65 (23.9)	39 (18.7)	0.940	0.979 (0.566-1.694)	0.075	1.668 (0.949-2.932)	0.160	1.378 (0.881-2.154)
	CC	1 (1.1)	5 (1.8)	2 (1.0)	0.696[2]	1.733 (0.199-15.087)	1.000[2]	1.193 (0.106-13.369)	0.466[1]	2.067 (0.396-10.790)
	HWE	0.554	0.931	0.868						
Recessive	TT + TC	93 (98.9)	267 (98.2)	206 (99.0)		Reference		Reference		Reference
model	CC	1 (1.1)	5 (1.8)	2 (1.0)	0.696[2]	1.742 (0.201-15.101)	1.000[2]	1.108 (0.099-12.367)	0.479[1]	1.929 (0.700-10.042)
Dominant	TT	70 (74.5)	202 (74.3)	167 (80.3)		Reference		Reference		Reference
model	CC + TC	24 (25.5)	70 (25.7)	41 (19.7)	0.969	0.989 (0.578-1.693)	0.256	1.397 (0.785-2.484)	0.122	1.411 (0.912-2.184)
rs907715										
Allele	Allele G	106 (56.4)	309 (56.8)	234 (56.2)		Reference		Reference		Reference
frequency	Allele A	82 (43.6)	235 (43.2)	182 (43.8)	0.920	0.983 (0.704-1.374)	0.976	0.995 (0.703-1.408)	0.864	0.978 (0.756-1.265)
Genotype	GG	25 (26.6)	85 (31.2)	70 (33.7)		Reference		Reference		Reference
frequency[1]	GA	56 (59.6)	139 (51.1)	94 (45.2)	0.256	0.730 (0.424-1.257)	0.135	0.598 (0.305-1.173)	0.347	1.218 (0.808-1.836)
	AA	13 (13.8)	48 (17.7)	44 (21.1)	0.831	1.086 (0.509-2.317)	0.062	0.827 (0.383-1.785)	0.685	0.898 (0.536-1.507)
	HWE	0.041	0.496	0.238						
Recessive	GG + GA	81 (86.2)	224 (82.4)	164 (78.8)		Reference		Reference		Reference
model	AA	13 (13.8)	48 (17.6)	44 (21.2)	0.393	1.335 (0.688-2.592)	0.135	0.598 (0.305-1.173)	0.334	0.799 (0.506-1.260)
Dominant	GG	25 (26.6)	85 (31.3)	70 (33.7)		Reference		Reference		Reference
model	AA + GA	69 (73.4)	187 (68.7)	138 (66.3)	0.397	0.797 (0.472-1.347)	0.222	1.400 (0.816-2.403)	0.577	1.116 (0.759-1.640)

[1]The *P* values of rs13143866, rs2221903, and rs907715 genotype distribution among hepatocellular carcinoma (HCC) group, non-HCC group, and controls were 0.237, 0.876, and 0.358, respectively; [2]Fisher's exact test. HWE: Hardy-Weinberg equilibrium.

polymorphisms in chronic HBV-infected patients, and *IL17* rs2275913, *IL23R* rs10889677, *IL21* rs4833837, and *IL21* rs2055979 polymorphisms in kidney transplant patients with HBV infection[23,24].

The statistical difference in genotype frequencies in the recessive model (AA *vs* GG + GA) of SNP rs13143866 showed that the A allele, when present in homozygotes, was a risk factor for carrying HBV. Furthermore, *IL21* rs13143866 genotype AA frequency in the HBV carrier group was higher than that in controls. In other studies, rs13143866 was associated with recurrent idiopathic spontaneous miscarriage[27], juvenile idiopathic arthritis[28], and lupus[29]. Thus, rs13143866 is likely a key genetic factor in both autoimmune diseases and chronic HBV-infected diseases.

Previous studies showed a significant association between rs2221903 and systemic lupus erythematosus (SLE) in the Chinese, European-American, and African-American populations[25,29,30]. Although there was no statistical difference, our data showed that this SNP is also associated with an increased risk of chronic HBV infection. The frequency of allele C was 13.7% in the chronic HBV infection group and 10.3% in the control group. In the subgroup analysis, the frequency of the TC genotype in the HBV carrier group was higher than that in controls. However, Li *et al*[24] found the opposite result, where the C frequency in HBV-infected patients was lower than in controls (8.1% *vs* 12.4%, *P* = 0.023, OR = 0.625, 95%CI: 0.415-0.941) and the TC genotype was less frequent in HBV-infected patients than in controls (16.2% *vs* 24.7%, *P* = 0.017, OR = 0.589, 95%CI: 0.381-0.911). Several potential explanations need to be considered. Firstly, the regulatory mechanisms of *IL21* intronic SNPs are still not clear. Secondly, chronic HBV infection is a complex complication related to other genetic and environmental factors[3].

Our data found no significant association between

Table 4 Interleukin-21 polymorphisms among non-hepatocellular carcinoma subgroups and controls *n* (%)

Polymorphism		Carrier	CHB	Cirrhosis	Control	Carrier *vs* control		CHB *vs* control		Cirrhosis *vs* control	
		(*n* = 101)	(*n* = 76)	(*n* = 95)	(*n* = 208)	*P* value	OR (95%CI)	*P* value	OR (95%CI)	*P* value	OR (95%CI)
rs13143866											
Allele frequency	Allele G	170 (84.2)	128 (84.2)	156 (82.1)	363 (87.3)		Reference		Reference		Reference
	Allele A	32 (15.8)	24 (15.8)	34 (17.9)	53 (12.7)	0.294	1.289 (0.802-2.073)	0.348	1.284 (0.761-2.166)	0.095	1.493 (0.933-2.388)
Genotype frequency	GG	75 (74.3)	53 (69.7)	64 (67.4)	157 (75.5)		Reference		Reference		Reference
	GA	20 (19.8)	22 (28.9)	28 (29.5)	49 (23.5)	0.600	0.854 (0.474-1.539)	0.345	1.330 (0.736-2.403)	0.227	1.402 (0.811-2.424)
	AA	6 (5.9)	1 (1.3)	3 (3.1)	2 (1.0)	0.019[1]	6.280 (1.238-31.854)	1.0001	1.481 (0.132-16.666)	0.156[1]	3.680 (0.601-22.544)
	HWE	0.01	0.44	0.977	0.391						
Recessive model	GG + GA	95 (94.1)	75 (98.7)	92 (96.8)	206 (99.0)		Reference		Reference		Reference
	AA	6 (5.9)	1 (1.3)	3 (3.2)	2 (1.0)	0.017[1]	6.505 (1.289-32.828)	1.000[1]	1.373 (0.123-15.367)	0.330[1]	3.359 (0.552-20.441)
Dominant model	GG	75 (74.3)	53 (69.7)	64 (67.4)	157 (75.5)		Reference		Reference		Reference
	AA + GA	26 (25.7)	23 (30.3)	31 (32.6)	51 (24.5)	0.816	1.067 (0.618-1.843)	0.330	1.336 (0.746-2.392)	0.142	1.491 (0.875-2.540)
rs2221903											
Allele frequency	Allele T	172 (85.1)	130 (85.5)	167 (87.9)	373 (89.7)		Reference		Reference		Reference
	Allele C	30 (14.9)	22 (14.5)	23 (12.1)	43 (10.3)	0.105	1.513 (0.918-2.495)	0.172	1.468 (0.846-2.547)	0.517	1.195 (0.697-2.046)
Genotype frequency	TT	71 (70.3)	56 (73.7)	75 (78.9)	167 (80.3)		Reference		Reference		Reference
	TC	30 (29.7)	18 (23.7)	17 (17.9)	39 (18.7)	0.035	1.809 (1.043-3.139)	0.324	1.367 (0.729-2.598)	0.926	0.971 (0.516-1.825)
	CC	0 (0.00)	2 (2.6)	3 (3.2)	2 (1.0)	-[2]		0.575[1]	2.982 (0.410-21.668)	0.330[1]	3.340 (0.547-20.405)
	HWE	0.080	0.705	0.121	0.868						
Recessive model	TT + TC	101 (100.0)	74 (97.4)	92 (96.8)	206 (99.0)		Reference		Reference		Reference
	CC	0 (0.0)	2 (2.6)	3 (3.2)	2 (1.0)	-[2]		0.577[1]	2.784 (0.385-20.120)	0.330[1]	3.359 (0.552-20.441)
Dominant model	TT	71 (70.3)	56 (73.7)	75 (78.9)	167 (80.3)		Reference		Reference		Reference
	CC + TC	30 (29.7)	20 (26.3)	20 (21.1)	41 (19.7)	0.052	1.721 (0.996-2.973)	0.232	1.455 (0.787-2.689)	0.787	1.086 (0.596-1.979)
rs907715											
Allele frequency	Allele G	115 (56.9)	89 (58.6)	105 (55.3)	234 (56.2)		Reference		Reference		Reference
	Allele A	87 (43.8)	63 (41.4)	85 (44.7)	182 (43.8)	0.873	0.973 (0.693-1.366)	0.624	0.910 (0.625-1.326)	0.820	1.041 (0.737-1.470)
Genotype frequency	GG	33 (32.7)	24 (3.16)	28 (29.5)	70 (33.7)		Reference		Reference		Reference
	GA	49 (48.5)	41 (53.9)	49 (51.6)	94 (45.2)	0.715	1.106 (0.645-1.896)	0.425	1.272 (0.704-2.298)	0.352	1.303 (0.746-2.277)
	AA	19 (18.8)	11 (14.5)	18 (18.9)	44 (21.1)	0.800	0.916 (0.465-1.806)	0.443	0.729 (0.325-1.634)	0.950	1.023 (0.507-2.064)
	HWE	0.914	0.331	0.674	0.238						
Recessive model	GG + GA	82 (81.2)	65 (85.5)	77 (81.1)	164 (78.8)		Reference		Reference		Reference
	AA	19 (18.8)	11 (14.5)	18 (18.9)	44 (21.2)	0.632	0.864 (0.474-1.573)	0.210	0.631 (0.307-1.296)	0.659	0.871 (0.473-1.606)
Dominant model	GG	33 (32.7)	24 (31.6)	28 (29.5)	70 (33.7)		Reference		Reference		Reference
	AA + GA	68 (67.3)	52 (68.4)	67 (70.5)	138 (66.3)	0.864	1.045 (0.630-1.733)	0.742	1.099 (0.626-1.929)	0.471	1.214 (0.717-2.055)

[1]Fisher's exact test; [2]χ^2 test cannot be conducted due to cross tabulation of zero. CHB: Chronic hepatitis B; HWE: Hardy-Weinberg equilibrium.

rs907715 and chronic HBV infection, which is consistent with Li *et al*[24]. The association between this SNP and immune disease has been widely investigated, though the findings are controversial. In a Chinese population, rs907715 was associated with Graves' disease[31] rather than SLE[25], and the two studies had a similar sample size. This discrepancy may be attributable to different diseases. Two studies investigated the same disease in an African-American population. Hughes *et al*[21] found that G allele increased the risk of SLE, but Sawalha *et al*[29] drew the opposite conclusion. These findings require further replication in other independent cohorts of chronic HBV-infected patients.

The data regarding ATA haplotype frequency (rs13143866, rs2221903, and rs907715) in HCC patients compared to non-HCC patients showed that this haplotype may be a risk for HBV-related HCC. This result suggests that the haplotype, according to the *IL21* polymorphisms, might be one of the most important genetic factors for susceptibility to HBV-related HCC.

Table 5 Haplotype analysis of polymorphisms

Haplotype[1]	Frequency		χ^2	*P* value	OR	95%CI
	HBV infection	Control				
A-T-A	0.150	0.127	1.117	0.291	1.209	0.850-1.720
G-C-G	0.137	0.103	2.725	0.099	1.376	0.941-2.011
G-T-A	0.283	0.31	0.883	0.347	0.882	0.678-1.147
G-T-G	0.429	0.459	0.959	0.327	0.886	0.695-1.129
	HCC	non-HCC				
A-T-A	0.165	0.104	4.057	0.044	1.700	1.010-2.863
G-C-G	0.138	0.133	0.017	0.900	1.033	0.635-1.681
G-T-A	0.267	0.333	3.226	0.072	0.072	0.503-1.031
G-T-G	0.430	0.423	0.009	0.926	1.016	0.726-1.422

[1]Haplotype of rs13143866 (G/A), rs2221903 (T/C), and rs907715 (G/A). HBV: Hepatitis B virus; HCC: Chronic HBV-infected patients with hepatocellular carcinoma; non-HCC: Chronic HBV-infected patients without hepatocellular carcinoma.

In conclusion, our study demonstrates that genotypes rs13143866 AA and rs2221903 TC are risk factors for carrying HBV, and ATA haplotype increase the risk of HBV-related HCC onset in a Chinese population. However, further studies are needed to determine the associations and functional consequences of these polymorphisms in chronic HBV-infection susceptibility.

COMMENTS

Background

The pathogenesis of chronic hepatitis B virus (HBV) infection is complicated, and the adaptive immune response plays a significant role in the pathophysiologic process. Interleukin (IL)-21 is a relatively recently discovered multifunctional and pleiotropic cytokine. Recently, investigations have shown that the serum level of IL-21 was increased in chronic hepatitis B patients and associated with severe liver inflammation. Genetic polymorphisms in *IL21* have been explored concerning genetic susceptibility to autoimmune and chronic HBV-infected diseases.

Research frontiers

The relationship between single-nucleotide polymorphisms (rs13143866, rs2221903, and rs907715) and autoimmune disease varies in different ethnicities. Therefore, studies performed using the same procedures and methods and enrolling more ethnic groups are required. In addition, further studies are needed to determine the associations and functional consequences of these polymorphisms in chronic HBV-infection susceptibility.

Innovations and breakthroughs

This is the first published study to investigate the relationship between the *IL21* rs13143866 polymorphism and chronic HBV-infection susceptibility.

Applications

Physicians should pay more attention to individuals who have the rs13143866 AA or rs2221903 TC genotype, or ATA haplotype (rs13143866, rs2221903 and rs907715), and provide early intervention before chronic HBV infection develops and leads to hepatocellular carcinoma.

Terminology

Single-nucleotide polymorphisms refer to DNA sequence polymorphisms at the genomic level caused by a single nucleotide mutation. HBV is a DNA virus, which belongs to the hepatotropic DNA virus (*Hepadnairidae*) group, and causes hepatitis B disease.

Peer-review

In this study, authors investigated the relationship between three single-nucleotide polymorphisms in *IL21* and chronic HBV infection in a Chinese population. They found that the rs13143866 A allele increases the risk of HBV infection and ATA haplotype (rs13143866, rs2221903, and rs907715) increases the risk of HBV-related hepatocellular carcinoma.

REFERENCES

1 **European Association For The Study Of The Liver**. EASL clinical practice guidelines: Management of chronic hepatitis B virus infection. *J Hepatol* 2012; **57**: 167-185 [PMID: 22436845 DOI: 10.1016/j.jhep.2012.02.010]

2 **Liang X**, Bi S, Yang W, Wang L, Cui G, Cui F, Zhang Y, Liu J, Gong X, Chen Y, Wang F, Zheng H, Wang F, Guo J, Jia Z, Ma J, Wang H, Luo H, Li L, Jin S, Hadler SC, Wang Y. Epidemiological serosurvey of hepatitis B in China--declining HBV prevalence due to hepatitis B vaccination. *Vaccine* 2009; **27**: 6550-6557 [PMID: 19729084 DOI: 10.1016/j.vaccine.2009.08.048]

3 **Chinese Society of Hepatology and Chinese Society of Infectious Diseases, Chinese Medical Association**. [The guideline of prevention and treatment for chronic hepatitis B (2010 version)]. *Zhonghua Liu Xing Bing Xue Zazhi* 2011; **32**: 405-415 [PMID: 21569677]

4 **Parrish-Novak J**, Dillon SR, Nelson A, Hammond A, Sprecher C, Gross JA, Johnston J, Madden K, Xu W, West J, Schrader S, Burkhead S, Heipel M, Brandt C, Kuijper JL, Kramer J, Conklin D, Presnell SR, Berry J, Shiota F, Bort S, Hambly K, Mudri S, Clegg C, Moore M, Grant FJ, Lofton-Day C, Gilbert T, Rayond F, Ching A, Yao L, Smith D, Webster P, Whitmore T, Maurer M, Kaushansky K, Holly RD, Foster D. Interleukin 21 and its receptor are involved in NK cell expansion and regulation of lymphocyte function. *Nature* 2000; **408**: 57-63 [PMID: 11081504 DOI: 10.1038/35040504]

5 **Spolski R**, Leonard WJ. Interleukin-21: basic biology and implications for cancer and autoimmunity. *Annu Rev Immunol* 2008; **26**: 57-79 [PMID: 17953510 DOI: 10.1146/annurev.immunol.26.021607.090316]

6 **Leonard WJ**, Zeng R, Spolski R. Interleukin 21: a cytokine/cytokine receptor system that has come of age. *J Leukoc Biol* 2008; **84**: 348-356 [PMID: 18467657 DOI: 10.1189/jlb.0308149]

7 **Ettinger R**, Sims GP, Fairhurst AM, Robbins R, da Silva YS, Spolski R, Leonard WJ, Lipsky PE. IL-21 induces differentiation of human naive and memory B cells into antibody-secreting plasma cells. *J Immunol* 2005; **175**: 7867-7879 [PMID: 16339522]

8 **Ettinger R**, Sims GP, Robbins R, Withers D, Fischer RT, Grammer AC, Kuchen S, Lipsky PE. IL-21 and BAFF/BLyS synergize in stimulating plasma cell differentiation from a unique population of human splenic memory B cells. *J Immunol* 2007; **178**: 2872-2882 [PMID: 17312131]

9 **Yang L**, Anderson DE, Baecher-Allan C, Hastings WD, Bettelli E, Oukka M, Kuchroo VK, Hafler DA. IL-21 and TGF-beta are required for differentiation of human T(H)17 cells. *Nature* 2008; **454**: 350-352 [PMID: 18469800 DOI: 10.1038/nature07021]

10 **Korn T**, Bettelli E, Gao W, Awasthi A, Jäger A, Strom TB, Oukka M, Kuchroo VK. IL-21 initiates an alternative pathway to induce proinflammatory T(H)17 cells. *Nature* 2007; **448**: 484-487 [PMID: 17581588 DOI: 10.1038/nature05970]

11 **Zwirner NW**, Domaica CI. Cytokine regulation of natural killer cell effector functions. *Biofactors* 2010; **36**: 274-288 [PMID: 20623510 DOI: 10.1002/biof.107]

12 **Elsaesser H**, Sauer K, Brooks DG. IL-21 is required to control chronic viral infection. *Science* 2009; **324**: 1569-1572 [PMID: 19423777 DOI: 10.1126/science.1174182]

13 **Fröhlich A**, Kisielow J, Schmitz I, Freigang S, Shamshiev AT, Weber J, Marsland BJ, Oxenius A, Kopf M. IL-21R on T cells is critical for sustained functionality and control of chronic viral infection. *Science* 2009; **324**: 1576-1580 [PMID: 19478140 DOI: 10.1126/science.1172815]

14 **Yi JS**, Du M, Zajac AJ. A vital role for interleukin-21 in the control of a chronic viral infection. *Science* 2009; **324**: 1572-1576 [PMID: 19443735 DOI: 10.1126/science.1175194]

15 **Webster GJ**, Reignat S, Brown D, Ogg GS, Jones L, Seneviratne SL, Williams R, Dusheiko G, Bertoletti A. Longitudinal analysis of CD8+ T cells specific for structural and nonstructural hepatitis B virus proteins in patients with chronic hepatitis B: implications for immunotherapy. *J Virol* 2004; **78**: 5707-5719 [PMID: 15140968

DOI: 10.1128/JVI.78.11.5707-5719.2004]
16 **Chang JJ**, Wightman F, Bartholomeusz A, Ayres A, Kent SJ, Sasadeusz J, Lewin SR. Reduced hepatitis B virus (HBV)-specific CD4+ T-cell responses in human immunodeficiency virus type 1-HBV-coinfected individuals receiving HBV-active antiretroviral therapy. *J Virol* 2005; **79**: 3038-3051 [PMID: 15709024 DOI: 10.1128/JVI.79.5.3038-3051.2005]
17 **Boni C**, Fisicaro P, Valdatta C, Amadei B, Di Vincenzo P, Giuberti T, Laccabue D, Zerbini A, Cavalli A, Missale G, Bertoletti A, Ferrari C. Characterization of hepatitis B virus (HBV)-specific T-cell dysfunction in chronic HBV infection. *J Virol* 2007; **81**: 4215-4225 [PMID: 17287266 DOI: 10.1128/JVI.02844-06]
18 **Urbani S**, Boni C, Amadei B, Fisicaro P, Cerioni S, Valli MA, Missale G, Ferrari C. Acute phase HBV-specific T cell responses associated with HBV persistence after HBV/HCV coinfection. *Hepatology* 2005; **41**: 826-831 [PMID: 15726541 DOI: 10.1002/hep.20614]
19 **Hu X**, Ma S, Huang X, Jiang X, Zhu X, Gao H, Xu M, Sun J, Abbott WG, Hou J. Interleukin-21 is upregulated in hepatitis B-related acute-on-chronic liver failure and associated with severity of liver disease. *J Viral Hepat* 2011; **18**: 458-467 [PMID: 21692955 DOI: 10.1111/j.1365-2893.2011.01475.x]
20 **Pan Q**, Yu Y, Tang Z, Xi M, Jiang H, Xun Y, Liu X, Liu H, Hu J, Zang G. Increased levels of IL-21 responses are associated with the severity of liver injury in patients with chronic active hepatitis B. *J Viral Hepat* 2014; **21**: e78-e88 [PMID: 24611989 DOI: 10.1111/jvh.12242]
21 **Hughes T**, Kim-Howard X, Kelly JA, Kaufman KM, Langefeld CD, Ziegler J, Sanchez E, Kimberly RP, Edberg JC, Ramsey-Goldman R, Petri M, Reveille JD, Martín J, Brown EE, Vilá LM, Alarcón GS, James JA, Gilkeson GS, Moser KL, Gaffney PM, Merrill JT, Vyse TJ, Alarcón-Riquelme ME, Nath SK, Harley JB, Sawalha AH. Fine-mapping and transethnic genotyping establish IL2/IL21 genetic association with lupus and localize this genetic effect to IL21. *Arthritis Rheum* 2011; **63**: 1689-1697 [PMID: 21425124 DOI: 10.1002/art.30320]
22 **Li J**, Ren W, Ma W, Zhang J, Shi J, Qin C. Interleukin-21 responses in patients with chronic hepatitis B. *J Interferon Cytokine Res* 2015; **35**: 134-142 [PMID: 25243706]
23 **Hejr S**, Karimi MH, Yaghobi R, Kamali-Sarvestani E, Geramizadeh B, Roozbeh J. Association of IL-17, IL-21, and IL-23R gene polymorphisms with HBV infection in kidney transplant patients. *Viral Immunol* 2013; **26**: 201-206 [PMID: 23656167 DOI: 10.1089/vim.2013.0007]
24 **Li N**, Zhu Q, Li Z, Han Q, Chen J, Lv Y, Wang Y, Zeng X, Chen Y, Yang C, Liu Z. IL21 and IL21R polymorphisms and their interactive effects on serum IL-21 and IgE levels in patients with chronic hepatitis B virus infection. *Hum Immunol* 2013; **74**: 567-573 [PMID: 23354321 DOI: 10.1016/j.humimm.2013.01.005]
25 **Ding L**, Wang S, Chen GM, Leng RX, Pan HF, Ye DQ. A single nucleotide polymorphism of IL-21 gene is associated with systemic lupus erythematosus in a Chinese population. *Inflammation* 2012; **35**: 1781-1785 [PMID: 22752563 DOI: 10.1002/art.3032010.1007/s10753-012-9497-7]
26 **Sauna ZE**, Kimchi-Sarfaty C. Understanding the contribution of synonymous mutations to human disease. *Nat Rev Genet* 2011; **12**: 683-691 [PMID: 21878961 DOI: 10.1038/nrg3051]
27 **Messaoudi S**, Al-Khateeb GM, Dendana M, Sater MS, Jazia KB, Nouira M, Almawi WY, Mahjoub T. Genetic variations in the interleukin-21 gene and the risk of recurrent idiopathic spontaneous miscarriage. *Eur Cytokine Netw* 2011; **22**: 123-126 [PMID: 21768062 DOI: 10.1684/ecn.2011.0287]
28 **Thompson SD**, Sudman M, Ramos PS, Marion MC, Ryan M, Tsoras M, Weiler T, Wagner M, Keddache M, Haas JP, Mueller C, Prahalad S, Bohnsack J, Wise CA, Punaro M, Zhang D, Rosé CD, Comeau ME, Divers J, Glass DN, Langefeld CD. The susceptibility loci juvenile idiopathic arthritis shares with other autoimmune diseases extend to PTPN2, COG6, and ANGPT1. *Arthritis Rheum* 2010; **62**: 3265-3276 [PMID: 20722033 DOI: 10.1002/art.27688]
29 **Sawalha AH**, Kaufman KM, Kelly JA, Adler AJ, Aberle T, Kilpatrick J, Wakeland EK, Li QZ, Wandstrat AE, Karp DR, James JA, Merrill JT, Lipsky P, Harley JB. Genetic association of interleukin-21 polymorphisms with systemic lupus erythematosus. *Ann Rheum Dis* 2008; **67**: 458-461 [PMID: 17720724 DOI: 10.1136/ard.2007.075424]
30 **Ma SW**, Huang X, Li YY, Tang LB, Sun XF, Jiang XT, Zhang YX, Sun J, Liu ZH, Abbott WG, Dong YH, Naoumov NV, Hou JL. High serum IL-21 levels after 12 weeks of antiviral therapy predict HBeAg seroconversion in chronic hepatitis B. *J Hepatol* 2012; **56**: 775-781 [PMID: 22173154 DOI: 10.1016/j.jhep.2011.10.020]
31 **Jia HY**, Zhang ZG, Gu XJ, Guo T, Cui B, Ning G, Zhao YJ. Association between interleukin 21 and Graves' disease. *Genet Mol Res* 2011; **10**: 3338-3346 [PMID: 22057994 DOI: 10.4238/2011.October.31.6]

P- Reviewer: Gao CM, Zouiten-Mekki L **S- Editor**: Ma YJ
L- Editor: AmEditor **E- Editor**: Ma S

World Journal of Gastroenterology

Submit a Manuscript: http://www.wjgnet.com/esps/
Help Desk: http://www.wjgnet.com/esps/helpdesk.aspx
DOI: 10.3748/wjg.v21.i14.4240

World J Gastroenterol 2015 April 14; 21(14): 4240-4247
ISSN 1007-9327 (print) ISSN 2219-2840 (online)

ORIGINAL ARTICLE

Case Control Study

Methyl-methanesulfonate sensitivity 19 expression is associated with metastasis and chemoradiotherapy response in esophageal cancer

Jin-Liang Zhang, Hui-Yun Wang, Qing Yang, Shi-Yong Lin, Guang-Yu Luo, Rong Zhang, Guo-Liang Xu

Jin-Liang Zhang, Qing Yang, Shi-Yong Lin, Guang-Yu Luo, Rong Zhang, Guo-Liang Xu, Department of Endoscopy and Laser, State Key Laboratory of Oncology in South China, Guangdong Esophageal Cancer Institute, National Collaborative Innovation Center for Cancer Medicine, Sun Yat-Sen University Cancer Center, Guangzhou 510060, Guangdong Province, China
Jin-Liang Zhang, Department of Medical Oncology, Longhua New District Central Hospital of Shenzhen, Shenzhen 518110, China
Hui-Yun Wang, State Key Laboratory of Oncology in South China, Guangdong Esophageal Cancer Institute, National Collaborative Innovation Center for Cancer Medicine, Sun Yat-Sen University Cancer Center, Guangzhou 510060, Guangdong Province, China
Author contributions: Zhang JL and Wang HY contributed equally to this work; Xu GL and Wang HY designed the research; Zhang JL and Yang Q performed the experiments; Lin SY, Luo GY and Zhang R collected the specimens; Zhang JL and Wang HY wrote the paper.
Ethics approval: The study was reviewed and approved by the Medical Ethics Committee of Sun Yat-Sen University Cancer Center.
Informed consent: All study participants, or their legal guardian, provided informed written consent prior to study enrollment.
Conflict-of-interest: We declare no competing commercial, personal, political, intellectual, or religious interests in relation to the submitted work.
Data sharing: No additional data are available.

Correspondence to: Guo-Liang Xu, Professor, Department of Endoscopy and Laser, State Key Laboratory of Oncology in South China, Guangdong Esophageal Cancer Institute, National Collaborative Innovation Center for Cancer Medicine, Sun Yat-Sen University Cancer Center, 651 Dongfeng East Road, East Building, Guangzhou 510060, Guangdong Province, China. xugl@sysucc.org.cn
Telephone: +86-20-87343224
Fax: +86-20-87343224
Received: November 4, 2014
Peer-review started: November 5, 2014
First decision: November 26, 2014
Revised: December 20, 2014
Accepted: January 30, 2015
Article in press: January 30, 2015
Published online: April 14, 2015

Abstract

AIM: To investigate the clinical significance of methyl-methanesulfonate sensitivity 19 (MMS19) expression in esophageal squamous cell carcinoma (ESCC).

METHODS: Between June 2008 and May 2013, specimens from 103 patients who underwent endoscopic biopsy for the diagnosis of ESCC at the endoscopy center of Sun Yat-Sen University Cancer Center were collected; 52 matched-normal esophageal squamous epithelium samples were biopsied as controls. MMS19 protein expression was measured by immunohistochemistry. Of the 103 cases of ESCC, 49 received radical surgery following neoadjuvant chemoradiotherapy consisting of concurrent radiation in a total dose of 40 Gy and two cycles of chemotherapy with vinorelbine and cisplatin. Relationships between MMS19 expression, clinicopathologic characteristics and chemoradiotherapy response were analyzed.

RESULTS: The MMS19 protein could be detected in both the cytoplasm and nucleus of most specimens. High cytoplasmic expression of MMS19 was detected in 63.1% of ESCC samples, whereas high nuclear

expression of MMS19 was found in 35.0%. High cytoplasmic MMS19 expression was associated with regional lymph node metastases (OR = 11.3, 95%CI: 2.3-54.7; $P < 0.001$) and distant metastases (OR = 13.1, 95%CI: 1.7-103.0; $P = 0.002$). Furthermore, high cytoplasmic MMS19 expression was associated with a response of ESCC to chemoradiotherapy (OR = 11.5, 95%CI: 3.0-44.5; $P < 0.001$), with a high cytoplasmic MMS19 expression rates in 79.3% and 25.0% of patients from the good chemoradiotherapy response group and poor response group, respectively. Nuclear MMS19 expression did not show any significant association with clinicopathologic characteristics or chemoradiotherapy response in ESCC.

CONCLUSION: The results of our preliminary study suggest that MMS19 may be a potential new predictor of metastasis and chemoradiotherapy response in ESCC.

Key words: Chemoradiotherapy; Esophageal squamous cell carcinoma; Metastases; Methyl-methanesulfonate sensitivity 19; Surgery

Core tip: Methyl-methanesulfonate sensitivity 19 (MMS19) was first identified as a DNA repair protein, and recently as a part of cytoplasmic Fe-S assembly machinery that produce proteins involved in maintenance of genomic stability, such as DNA polymerase, DNA repair proteins, and DNA nuclease/helicase. However, the clinical significance of MMS19 protein expression in esophageal cancer has not been reported. This study shows that MMS19 is abnormally expressed in esophageal cancer, and the elevated cytoplasmic MMS19 expression is associated with lymph node and distant metastases, and response to chemoradiotherapy in esophageal squamous cell carcinoma.

Zhang JL, Wang HY, Yang Q, Lin SY, Luo GY, Zhang R, Xu GL. Methyl-methanesulfonate sensitivity 19 expression is associated with metastasis and chemoradiotherapy response in esophageal cancer. *World J Gastroenterol* 2015; 21(14): 4240-4247 Available from: URL: http://www.wjgnet.com/1007-9327/full/v21/i14/4240.htm DOI: http://dx.doi.org/10.3748/wjg.v21.i14.4240

INTRODUCTION

Esophageal squamous cell carcinoma (ESCC) is one of the most aggressive tumors, ranking fourth among the top ten cancer-related deaths in China[1,2]. In China, the histology of esophageal cancer is mainly ESCC, whereas esophageal adenocarcinoma is rare[3]. Because of the high recurrence and metastasis rates, the five-year survival rate of ESCC treated with surgery alone is poor, only approximately 25%, and in such circumstances, surgery plus radiotherapy and/or chemotherapy is increasingly adopted for locally advanced esophageal cancer[4]. The results from phase Ⅲ randomized trials of chemoradiotherapy (CRT) prior to surgery are encouraging; however, these studies reveal that only patients who are sensitive to CRT will ultimately benefit from the multimodality treatment[5-7]. Thus, the identification of patients who can benefit from CRT is crucial for the success of the combined treatment of CRT followed by surgery. However, there is currently no biomarker that can predict response of ESCC to CRT. Therefore, the discovery of biomarkers that can predict sensitivity of ESCC to CRT is an urgent need in clinical practice.

The methyl-methanesulfonate sensitivity 19 (*MMS19*) gene, also named as *MMS19L* or *hMMS19*, encodes a multifunctional protein involved in DNA metabolism and the maintenance of genomic stability[8]. Nucleotide excision repair (NER) plays a vital role in the development of carcinogen-induced cancers[9,10] and in tumor resistance to chemo- and radiotherapy[11,12]. By interacting with the core transcription factors of NER, MMS19 can affect NER functions[13,14]. In addition, Fe-S proteins are crucial for genomic instability[15], which is a hallmark of cancer[16]. As a part of the cytoplasmic Fe-S assembly machinery, MMS19 facilitates the transfer of the Fe-S cluster to target Fe-S proteins, which include DNA polymerase δ, xeroderma pigmentosum group D, Fanconi anemia pathway component J (also known as BACH1 or BRIP1)[17], DNA2 nuclease/helicase, RNase L inhibitor (also known as ABCE1), and endonuclease three-like glycosylase 2[18]. Thus, MMS19 is suggested to be involved in maintaining genomic stability[17,18].

At present, some studies have reported that single-nucleotide polymorphisms of the *MMS19* gene are associated with the risk of pancreatic cancer[19], chemotherapy toxicity of non-small-cell lung cancer[20], and chemotherapy response of osteosarcoma[21]. These polymorphisms could increase cancer susceptibility by altering conserved amino acids[22] and could affect cancer prognosis by modulating gene expression[23]. However, the cellular expression level of MMS19 protein in cancer and its clinical significance have not been reported. In this study, we investigated the cellular expression level and distribution of *MMS19* in ESCC and the relationships of *MMS19* expression with the clinicopathologic factors and CRT response of ESCC.

MATERIALS AND METHODS

The study was performed in accordance with the Declaration of Helsinki of the World Medical Association and was approved by the Medical Ethics Committee of Sun Yat-Sen University Cancer Center. All patients signed an informed consent form for this investigation.

Patients

Between June 2008 and May 2013, specimens from 103 ESCC patients who underwent endoscopic biopsy for diagnosis at the endoscopy center of Sun Yat-Sen University Cancer Center were collected. As controls, 52 samples of normal esophageal squamous epithelia (NESE) were biopsied from ≥ 5 cm from the primary lesion in the same patients. Patients who received any anticancer treatments before diagnosis were excluded. The biopsied specimens were diagnosed by two pathologists. Tumor staging was performed based on the combined results of physical examination, endoscopic ultrasonography, CT scan of the chest and abdomen, and color ultrasonography scan of the abdomen and neck. The tumors were staged according to AJCC (2002). The patients were aged from 42 to 83 years (median 59 years), including 84 men and 19 women. Two patients were classified as stage Ⅰ, 25 patients as stage Ⅱ, 58 patients as stage Ⅲ and 18 patients as stage Ⅳ. Among the 103 ESCC patients, a cohort of 49 patients with thoracic esophageal carcinoma staged Ⅱb and Ⅲ received neoadjuvant CRT followed by surgery.

Neoadjuvant chemoradiotherapy and surgery

Radiation treatment planning was designed according to CT simulation or three-dimensional conformal radiation therapy. The patients were treated with 6 or 8 MV photons delivered in a total dose of 40 Gy (20 fractions of 2 Gy per fraction in 4 wk) in anteroposterior fields including esophageal tumors and enlarged lymph nodes, with 3-cm proximal and distal margins, and an 0.8-cm radial margin. The patients received two cycles of vinorelbine and cisplatin. Vinorelbine (25 mg/m^2) was administered intravenously on days 1, 8, 22 and 29, and cisplatin (75 mg/m^2) was infused on day 1 and day 22 (or 25 mg/m^2 on days 1-4 and 22-25). Total thoracic esophagectomy through a right thoracotomy with radical mediastinal and abdominal lymph node dissection was performed ≥ 4-6 wk after the completion of CRT.

Evaluation of histopathologic response to preoperative CRT

For evaluation of response to CRT, surgical cancer samples from 49 patients who underwent CRT and surgery were obtained. The histopathologic response to CRT was evaluated by two experienced pathologists according to previously published criteria[24,25]. The percentage of residual viable tumor cells was estimated, and each patient was subsequently allocated to one of the following four groups: complete response group, no residual tumor cells; major response group, < 10% residual tumor cells; partial response group, 10%-50% of residual tumor cells; minor response group, > 50% of residual tumor cells. For the statistical analysis, the patients were divided into two groups according to CRT response: a good response group, consisting of patients with a complete or major response; and a poor response group, including patients with a partial or minor response.

Immunohistochemical staining

Immunohistochemical staining was performed on 4-μm-thick paraffin sections. The sections were deparaffinized in xylene and rehydrated through graded alcohol. Endogenous peroxidase activity was blocked with 0.3% hydrogen peroxide for 10 min. For epitope retrieval, the tissue slides were immersed in EDTA buffer (pH 8.0) and heated for 2.5 min on high power in a microwave oven. After washing, the tissue slides were incubated with an anti-MMS19 antibody (16015-1-AP; Proteintech, Chicago, IL, United States) at a dilution of 1:50 for 50 min at 37 ℃ in a moist chamber. Subsequently, the secondary antibody (K5007, Real Envision/HRP; Dako of Agilent Technologies, Santa Clara, CA, United States) was applied to the tissue section for 30 min at 37 ℃. Finally, 3.3'-diaminobenzidine was used for color development and hematoxylin for counterstaining. Negative control slides in the absence of primary antibody were included for each batch of staining.

Cytoplasmic and nuclear MMS19 staining was evaluated separately. The immunochemistry staining for the MMS19 protein was evaluated under 400× high-power magnification. The positively stained cells in five separate areas of epithelial or intratumoral regions were counted. The quantification of MMS19 expression was performed according to a previous study[26]. The percentage of cells positively stained was scored as follows: 0 ≤ 5%, 1 = 6%-25%; 2 = 26%-50%; 3 = 51%-75%; 4 > 75%. The staining intensity was scored as follows: 0 = no staining, 1 = weak, 2 = moderate, 3 = strong. For each case, the final score for MMS19 immunostaining was calculated by multiplying the percentage score of positive cells with the staining intensity score. Immunostaining was independently evaluated by two experienced pathologists who had no knowledge of the patients' clinicopathologic information. If different scores for the same sample were made by the two pathologists, the sample was revaluated and, if needed, discussed to decide a final score. Then, a composite score scaled as 0, 1, 2, 3, 4, 6, 8, 9, and 12 was obtained. Based on the final score, each case was divided into a high expression group (≥ 6) or a low expression group (< 6).

Statistical analysis

The statistical analyses were performed using SPSS 20.0 software (IBM Corp., Armonk, NY, United States). Data are expressed as mean ± SE. The differences in *MMS19* expression levels between the different groups and the correlations between *MMS19* expression and clinicopathologic characteristics as well as response to CRT were analyzed by the χ^2 test. Spearman's rank correlation (r) was used to determine whether there

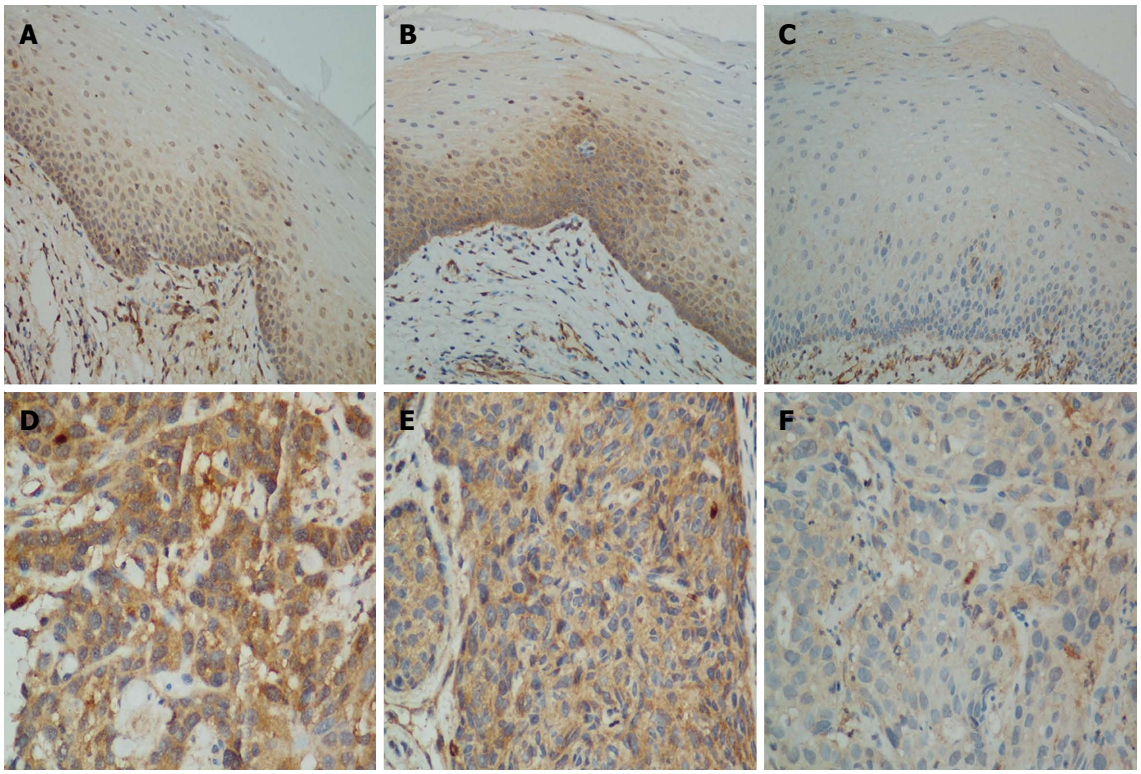

Figure 1 Methyl-methanesulfonate sensitivity 19 immunohistochemistry. Normal esophageal squamous epithelium with A: Strong nuclear but weak cytoplasmic staining; B: Strong cytoplasmic staining in the basal and suprabasal layers, with scattered strong nuclear staining in the normal epithelium area; C: Weak staining in both the cytoplasm and nucleus (Magnification × 200); Esophageal squamous cell carcinoma with D: Strong staining in the cytoplasm and nucleus; E: Strong staining in the cytoplasm and weak staining in the nucleus; F: Weak staining in both the cytoplasm and nucleus (Magnification × 400).

was a positive or negative correlation. Two-tailed $P < 0.05$ was considered statistically significant. The statistical methods of this study were reviewed by Qing Liu from Sun Yat-Sen University Cancer Center.

RESULTS

Different expression levels of MMS19 in biopsied NESE and ESCC tissues

Using immunohistochemistry, the MMS19 protein was detected in both the cytoplasm and nucleus of most endoscopic biopsied specimens (Figure 1), which is consistent with its cellular functions[13,18]. Cytoplasmic MMS19 staining in NESE was mainly found in the basal and suprabasal layers, with a gradually decreased staining from the basal layer to the superficial layer. In contrast, nuclear MMS19 staining in NESE was scattered throughout the entire layer (Figure 1A and B). The intensity of MMS19 staining was typically homogeneous within an ESCC specimen, but varied considerably among different tumors (Figure 1D and E). Figure 1C and F show weak staining in both the cytoplasm and nucleus of NESE and ESCC, respectively.

The mean scores for cytoplasmic MMS19 expression in the high expression group and low expression group were 7.78 ± 0.27 and 2.79 ± 0.21, respectively. Whereas, the mean scores of nuclear MMS19 expression in the high expression group and low expression group were 6.86 ± 0.32 and 2.68 ± 0.14, respectively. High cytoplasmic expression of MMS19 was detected in 63.1% of the ESCC samples, which was significantly higher than the 15.4% in NESE ($P < 0.001$, Table 1). High nuclear expression of MMS19 was found in 35.0% of the ESCC specimens, which was significantly lower than the 69.2% found in NESE ($P < 0.001$, Table 1).

Relationships of MMS19 expression in biopsied ESCC tissues with clinicopathologic features

First, associations of cytoplasmic MMS19 expression with clinicopathologic features were investigated. The results showed that high cytoplasmic MMS19 expression was significantly associated with regional lymph node metastases (LNM) (OR = 11.25, 95%CI: 2.31-54.73; $P < 0.001$) and distant metastases (DM) (OR = 13.10, 95%CI: 1.67-103.00; $P = 0.002$), suggesting that cytoplasmic MMS19 expression might be involved in cancer metastasis. The Spearman correlation coefficients of high cytoplasmic MMS19 expression with LNM and DM were 0.35 and 0.299, respectively, indicating that higher levels of MMS19 expression are positively correlated with ESCC metastasis. There was no significant association of cytoplasmic MMS19 expression with other clinicopathologic features, including histologic grade, invasion depth, patient age, tumor stage, or sex (Table 2). Nuclear MMS19 expression did not show any

Table 1 Methyl-methanesulfonate sensitivity 19 expression *n* (%)

Tissue	Cases (*n*)	Cytoplasmic expression		*P* value	Nuclear expression		*P* value
		High	Low		High	Low	
NESE	52	8 (15.4)	44 (84.6)	< 0.001	36 (69.2)	16 (30.8)	< 0.001
ESCC	103	65 (63.1)	38 (36.9)		36 (35.0)	67 (65.0)	

ESCC: Esophageal squamous cell carcinoma; High: Including composite score of 6, 8, 9 and 12; NESE: Normal esophageal squamous epithelium; Low: Including composite score of 0, 1, 2, 3 and 4.

Table 2 Associations of MMS19 expression with clinicopathologic features of esophageal squamous cell carcinoma

Characteristic	Cases (*n*)	Cytoplasmic MMS19			Nuclear MMS19		
		High	Low	*P* value	High	Low	*P* value
Total	103	65	38		36	67	
Sex							
Male	84	55	29	0.295	32	52	0.159
Female	19	10	9		4	15	
Age (yr)							
< 55	33	18	15	0.216	14	19	0.275
⩾ 55	70	47	23		22	48	
Site							
Upper thoracic	10	7	3	0.686	2	8	0.508
Middle thoracic	47	31	16		16	31	
Lower thoracic	46	27	19		18	28	
Differentiation							
Well	20	13	7	0.785	6	14	0.871
Moderate	52	34	18		19	33	
Poor	31	18	13		11	20	
TNM stage							
Ⅰ + Ⅱ	27	14	13	0.158	8	19	0.500
Ⅲ + Ⅳ	76	51	25		28	48	
Invasion depth							
T1 + T2	25	17	8	0.560	7	18	0.402
T3 + T4	78	48	30		29	49	
LNM							
No	12	2	10	< 0.001	4	8	0.900
Yes	91	63	28		32	59	
DM							
No	85	48	37	0.002	32	53	0.212
Yes	18	17	1		4	14	

DM: Distant metastases; ESCC: Esophageal squamous cell carcinoma; High: Including composite score of 6, 8, 9 and 12; LNM: Lymph node metastases; Low: Including composite score of 0, 1, 2, 3 and 4; MMS19: methyl-methanesulfonate sensitivity 19.

significant association with clinicopathologic parameters (Table 2).

Relationship of MMS19 expression in biopsied specimens with CRT response of resected ESCC

According to the histopathologic response to preoperative CRT, 24 cases showed complete response, 5 cases showed a major response, 9 cases showed a partial response, and 11 cases showed a minor response. Thus the good and poor response groups included 29 and 20 cases, respectively. Then, relationships of MMS19 expression with CRT response of ESCC were investigated. In the good response group, high cytoplasmic expression of MMS19 was observed in 23/29 (79.3%) patients. In contrast, high MMS19 expression was found in only 5/20 (25.0%) patients in the poor response group, and the difference in MMS19 expression between the two groups was statistically significant (OR = 11.5, 95%CI: 2.97-44.51; $P < 0.001$, Table 3). The Spearman correlation coefficient of high cytoplasmic MMS19 expression with a good response was 0.539, suggesting that high cytoplasmic expression of MMS19 is positively correlated with a good response to preoperative CRT. This result suggested that MMS19 might be a potential new biomarker to predict tumor response to preoperative CRT. However, nuclear MMS19 expression was not associated with CRT response, with a rate of high nuclear expression of 31.0% (9/29) in the good response group and 45.0% (9/20) in the poor response group (Table 3).

The relationships of CRT response with clinico-

Table 3 Clinical features of patients receiving neoadjuvant chemoradiotherapy followed by surgery, *n*

Characteristic	Good response (*n* = 29)	Poor response (*n* = 20)	*P* value
Age (yr)			
< 55	11	11	0.238
⩾ 55	18	9	
Sex			
Male	24	15	0.763
Female	5	5	
Tumor size (cm)			
< 5	12	7	0.652
⩾ 5	17	13	
Site			
Upper thoracic	3	2	0.405
Middle thoracic	14	6	
Lower thoracic	12	12	
Differentiation			
Well	5	4	0.936
Moderate	16	10	
Poor	8	6	
TNM stage			
Ⅱb	8	6	0.857
Ⅲ	21	14	
Cytoplasm			
High	23	5	< 0.001
Low	6	15	
Nucleus			
High	9	9	0.319
Low	20	11	

High: Including composite score of 6, 8, 9 and 12; Low: Including composite score of 0, 1, 2, 3 and 4; TNM: Tumor-node-metastasis.

pathologic features were also analyzed. However, there was no relationship between preoperative CRT response and clinicopathologic features, including tumor size, tumor site, differentiation, or Tumor-node-metastasis stage (Table 3). This result indicates that no clinicopathologic features should be used for predicting preoperative CRT response.

DISCUSSION

The results of the present study show, for the first time, that MMS19 expression in ESCC is upregulated in the cytoplasm and downregulated in the nucleus. The abnormal cellular distribution of MMS19 protein suggests that MMS19 is involved in the development and progression of ESCC. Furthermore, we found that MMS19 protein expression is associated with LNM and DM. More importantly, we found that cytoplasmic MMS19 protein expression is associated with the CRT response of ESCC. In clinical management, the therapeutic strategy for ESCC is primarily based on whether metastases exist, which is the most important determinant of patient outcome[27-30]. Furthermore, multimodality treatment only benefits patients who are sensitive to CRT[5-7]. Thus results of this study suggest that MMS19 has the potential to be a new biomarker for predicting metastasis and CRT response in ESCC.

In the present study, we found that the subcellular distribution of high MMS19 expression is changed from the nucleus in NESE to the cytoplasm in ESCC. Although the mechanism for this change in MMS19 expression in ESCC is not yet clear, a similar phenomenon has been reported for the DNA repair genes *Ape1/ref-1* and *JWA*[31,32]. The aberrant subcellular distribution of the MMS19 protein may implicate that the DNA repair function of MMS19 in the nucleus is attenuated. Conversely, as a cytoplasmic Fe-S assembly machinery component in the cytoplasm, MMS19 would promote the synthesis of many Fe-S proteins participating in DNA metabolism in the nucleus. Thus, we hypothesize that, as a consequence, DNA mutations will accumulate in cancer cells due to the impaired DNA repair function, with cell division and proliferation accelerating as a result of the increased DNA metabolism, exerting adaptive pressure on these cells[33-35]. Previous studies have reported that rapidly proliferating esophageal cancer cells are more sensitive to CRT[36,37] and that DNA damage in cancer cells is associated with the sensitivity of cancer to CRT[38,39]. Our finding that ESCC with higher cytoplasmic MMS19 expression is much more sensitive to preoperative CRT is in accord with these studies. Furthermore, ESCC with higher MMS19 expression will accumulate an array of mutations, facilitating cancer metastasis.

Previous studies reported that DNA repair genes are associated with chemo- or radiotherapy response. The low nuclear expressions of *ERCC1* and *XRCC1* are associated with a good chemotherapy response in non-small-cell lung cancer[40-42] and gastric cancer[32], respectively, whereas high nuclear expression is associated with the radio-resistance of laryngeal cancer[43]. Furthermore, high nuclear expression of *RRM1* is significantly associated with a lower disease control rate in non-small-cell lung cancer[44]. However, in the present study, we found that cytoplasmic MMS19 expression, but not nuclear MMS19 expression, is associated with CRT response. In addition to a role in DNA repair, MMS19 in the nucleus is also involved in mitotic segregation[45], histone modification[46], and interaction with regulator of telomere elongation helicase 1[17]. One reason that our study did not reveal an association between nuclear MMS19 and CRT response and metastasis may be that in the situation of abnormally expressed MMS19 in ESCC, the cytoplasmic function, but not the nuclear function of MMS19 plays the dominant role, underlying the development and progression of cancer cells.

In conclusion, the results demonstrate that MMS19 is abnormally expressed in esophageal squamous cell cancer. Elevated cytoplasmic MMS19 expression was associated with regional LNM, DM and a good preoperative chemoradiotherapy response of ESCC. These results provide novel preliminary evidence that MMS19 is involved in a mechanism of cancer development and progression, and has the potential to serve as a tumor biomarker that predicts metastasis

and chemoradiotherapy response in ESCC.

ACKNOWLEDGMENTS

We acknowledge pathologists Jia Fu and Jia-Bin Lu in the department of pathology of Sun Yat-Sen University Cancer Center for their evaluation of the immunohistochemical expression of MMS19.

COMMENTS

Background

Esophageal squamous cell carcinoma (ESCC) is one of the most aggressive, malignant neoplasms. Surgery plus radiotherapy and/or chemotherapy is an effective treatment method for locally advanced esophageal cancer. However, there is no biomarker to predict the response of ESCC to chemoradiotherapy in clinical practice. Methyl-methanesulfonate sensitivity 19 (MMS19) is a multifunctional protein involved in DNA metabolism and genomic stability maintenance. Studies have demonstrated that single-nucleotide polymorphisms of the *MMS19* gene are associated with the risk of pancreatic cancer, chemotherapy toxicity of non-small-cell lung cancer, and chemotherapy response of osteosarcoma. So far, the clinical significance of the expression of MMS19 in ESCC is not clear.

Research frontiers

Fe-S proteins such as DNA glycosylases, primases, DNA helicases, and nuclease are crucial for genomic instability, which is a hallmark of cancer. As a part of the cytoplasmic Fe-S assembly machinery, MMS19 facilitates the transfer of the Fe-S cluster to target Fe-S proteins, such as DNA polymerase, Dna2 nuclease/helicase, RNase L inhibitor, and endonuclease three-like glycosylase 2. However, the roles of the components of this machinery in cancer have rarely been explored.

Innovations and breakthroughs

Previous studies investigated the relationships of single-nucleotide polymorphisms of the *MMS19* gene with cancer. We discovered, for the first time, that MMS19 is abnormally expressed in esophageal squamous cell cancer. Abnormally elevated cytoplasmic MMS19 expression is associated with regional lymph node metastases, distant metastases, and a good preoperative chemoradiotherapy response of ESCC. These results suggest that cytoplasmic Fe-S assembly machinery may play an important role in cancer development and progression, revealing new mechanisms of carcinogenesis and therapeutic targets.

Applications

The study results provide preliminary evidence that MMS19 has the potential to serve as a novel tumor biomarker for predicting metastasis and chemoradiotherapy response in ESCC.

Terminology

Methyl-methanesulfonate is an alkylating agent that can lead to DNA damage.

Peer-review

This is basically an interesting paper assessing a novel prognostic biomarker in ESCC with some potential to open up new lines of research.

REFERENCES

1 **Enzinger PC**, Mayer RJ. Esophageal cancer. *N Engl J Med* 2003; **349**: 2241-2252 [PMID: 14657432 DOI: 10.1056/NEJMra035010]
2 **Liu WL**, Guo XZ, Zhang LJ, Wang JY, Zhang G, Guan S, Chen YM, Kong QL, Xu LH, Li MZ, Song LB, Zeng MS. Prognostic relevance of Bmi-1 expression and autoantibodies in esophageal squamous cell carcinoma. *BMC Cancer* 2010; **10**: 467 [PMID: 20809956 DOI: 10.1186/1471-2407-10-467]
3 **Lin Y**, Totsuka Y, He Y, Kikuchi S, Qiao Y, Ueda J, Wei W, Inoue M, Tanaka H. Epidemiology of esophageal cancer in Japan and China. *J Epidemiol* 2013; **23**: 233-242 [PMID: 23629646 DOI: 10.2188/jea.JE20120162]
4 **Mariette C**, Piessen G, Triboulet JP. Therapeutic strategies in oesophageal carcinoma: role of surgery and other modalities. *Lancet Oncol* 2007; **8**: 545-553 [PMID: 17540306 DOI: 10.1016/S1470-2045(07)70172-9]
5 **Medical Research Council Oesophageal Cancer Working Group**. Surgical resection with or without preoperative chemotherapy in oesophageal cancer: a randomised controlled trial. *Lancet* 2002; **359**: 1727-1733 [PMID: 12049861 DOI: 10.1016/S0140-6736(02)08651-8]
6 **Urba SG**, Orringer MB, Turrisi A, Iannettoni M, Forastiere A, Strawderman M. Randomized trial of preoperative chemoradiation versus surgery alone in patients with locoregional esophageal carcinoma. *J Clin Oncol* 2001; **19**: 305-313 [PMID: 11208820]
7 **Walsh TN**, Noonan N, Hollywood D, Kelly A, Keeling N, Hennessy TP. A comparison of multimodal therapy and surgery for esophageal adenocarcinoma. *N Engl J Med* 1996; **335**: 462-467 [PMID: 8672151 DOI: 10.1056/NEJM199608153350702]
8 **Papatriantafyllou M**. DNA Metabolism: MMS19: CIA agent for DNA-linked affairs. *Nat Rev Mol Cell Biol* 2012; **13**: 538 [PMID: 22828929 DOI: 10.1038/nrm3411]
9 **Cheng L**, Sturgis EM, Eicher SA, Spitz MR, Wei Q. Expression of nucleotide excision repair genes and the risk for squamous cell carcinoma of the head and neck. *Cancer* 2002; **94**: 393-397 [PMID: 11900225 DOI: 10.1002/cncr.10231]
10 **Neumann AS**, Sturgis EM, Wei Q. Nucleotide excision repair as a marker for susceptibility to tobacco-related cancers: a review of molecular epidemiological studies. *Mol Carcinog* 2005; **42**: 65-92 [PMID: 15682379 DOI: 10.1002/mc.20069]
11 **Sarries C**, Haura EB, Roig B, Taron M, Abad A, Scagliotti G, Rosell R. Pharmacogenomic strategies for developing customized chemotherapy in non-small cell lung cancer. *Pharmacogenomics* 2002; **3**: 763-780 [PMID: 12437479 DOI: 10.1200/JCO.2004.08.067]
12 **Xu Z**, Chen ZP, Malapetsa A, Alaoui-Jamali M, Bergeron J, Monks A, Myers TG, Mohr G, Sausville EA, Scudiero DA, Aloyz R, Panasci LC. DNA repair protein levels vis-à-vis anticancer drug resistance in the human tumor cell lines of the National Cancer Institute drug screening program. *Anticancer Drugs* 2002; **13**: 511-519 [PMID: 12045463]
13 **Seroz T**, Winkler GS, Auriol J, Verhage RA, Vermeulen W, Smit B, Brouwer J, Eker AP, Weeda G, Egly JM, Hoeijmakers JH. Cloning of a human homolog of the yeast nucleotide excision repair gene MMS19 and interaction with transcription repair factor TFIIH via the XPB and XPD helicases. *Nucleic Acids Res* 2000; **28**: 4506-4513 [PMID: 11071939 DOI: 10.1093/nar/28.22.4506]
14 **Hatfield MD**, Reis AM, Obeso D, Cook JR, Thompson DM, Rao M, Friedberg EC, Queimado L. Identification of MMS19 domains with distinct functions in NER and transcription. *DNA Repair (Amst)* 2006; **5**: 914-924 [PMID: 16797255 DOI: 10.1016/j.dnarep.2006.05.007]
15 **Wu Y**, Brosh RM. DNA helicase and helicase-nuclease enzymes with a conserved iron-sulfur cluster. *Nucleic Acids Res* 2012; **40**: 4247-4260 [PMID: 22287629 DOI: 10.1093/nar/gks039]
16 **Negrini S**, Gorgoulis VG, Halazonetis TD. Genomic instability--an evolving hallmark of cancer. *Nat Rev Mol Cell Biol* 2010; **11**: 220-228 [PMID: 20177397 DOI: 10.1038/nrm2858]
17 **Gari K**, León Ortiz AM, Borel V, Flynn H, Skehel JM, Boulton SJ. MMS19 links cytoplasmic iron-sulfur cluster assembly to DNA metabolism. *Science* 2012; **337**: 243-245 [PMID: 22678361 DOI: 10.1126/science.1219664]
18 **Stehling O**, Vashisht AA, Mascarenhas J, Jonsson ZO, Sharma T, Netz DJ, Pierik AJ, Wohlschlegel JA, Lill R. MMS19 assembles iron-sulfur proteins required for DNA metabolism and genomic integrity. *Science* 2012; **337**: 195-199 [PMID: 22678362 DOI: 10.1126/science.1219723]
19 **McWilliams RR**, Bamlet WR, de Andrade M, Rider DN, Cunningham JM, Petersen GM. Nucleotide excision repair pathway polymorphisms and pancreatic cancer risk: evidence for role of MMS19L. *Cancer Epidemiol Biomarkers Prev* 2009; **18**: 1295-1302 [PMID: 19318433 DOI: 10.1158/1055-9965.EPI-08-1109]
20 **Zhang L**, Gao G, Li X, Ren S, Li A, Xu J, Zhang J, Zhou C.

Association between single nucleotide polymorphisms (SNPs) and toxicity of advanced non-small-cell lung cancer patients treated with chemotherapy. *PLoS One* 2012; **7**: e48350 [PMID: 23118991 DOI: 10.1371/journal.pone.0048350]
21 **Bai SB**, Chen HX, Bao YX, Luo X, Zhong JJ. Predictive impact of common variations in DNA repair genes on clinical outcome of osteosarcoma. *Asian Pac J Cancer Prev* 2013; **14**: 3677-3680 [PMID: 23886164 DOI: 10.7314/APJCP.2013.14.6.3677]
22 **Zhu Y**, Spitz MR, Amos CI, Lin J, Schabath MB, Wu X. An evolutionary perspective on single-nucleotide polymorphism screening in molecular cancer epidemiology. *Cancer Res* 2004; **64**: 2251-2257 [PMID: 15026370 DOI: 10.1158/00085472.CAN-03-2800]
23 **Vaclavikova R**, Nordgard SH, Alnaes GI, Hubackova M, Kubala E, Kodet R, Mrhalova M, Novotny J, Gut I, Kristensen VN, Soucek P. Single nucleotide polymorphisms in the multidrug resistance gene 1 (ABCB1): effects on its expression and clinicopathological characteristics in breast cancer patients. *Pharmacogenet Genomics* 2008; **18**: 263-273 [PMID: 18300948 DOI: 10.1097/FPC.0b013e3282f60a91]
24 **Becker K**, Mueller JD, Schulmacher C, Ott K, Fink U, Busch R, Böttcher K, Siewert JR, Höfler H. Histomorphology and grading of regression in gastric carcinoma treated with neoadjuvant chemotherapy. *Cancer* 2003; **98**: 1521-1530 [PMID: 14508841 DOI: 10.1002/cncr.11660]
25 **Brücher BL**, Becker K, Lordick F, Fink U, Sarbia M, Stein H, Busch R, Zimmermann F, Molls M, Höfler H, Siewert JR. The clinical impact of histopathologic response assessment by residual tumor cell quantification in esophageal squamous cell carcinomas. *Cancer* 2006; **106**: 2119-2127 [PMID: 16607651 DOI: 10.1002/cncr.21850]
26 **Zhao X**, He Y, Gao J, Fan L, Li Z, Yang G, Chen H. Caveolin-1 expression level in cancer associated fibroblasts predicts outcome in gastric cancer. *PLoS One* 2013; **8**: e59102 [PMID: 23527097 DOI: 10.1371/journal.pone.0059102]
27 **Ando N**, Ozawa S, Kitagawa Y, Shinozawa Y, Kitajima M. Improvement in the results of surgical treatment of advanced squamous esophageal carcinoma during 15 consecutive years. *Ann Surg* 2000; **232**: 225-232 [PMID: 10903602 DOI: 10.1097/00000658-200008000-00013]
28 **Komukai S**, Nishimaki T, Watanabe H, Ajioka Y, Suzuki T, Hatakeyama K. Significance of immunohistochemically demonstrated micrometastases to lymph nodes in esophageal cancer with histologically negative nodes. *Surgery* 2000; **127**: 40-46 [PMID: 10660757 DOI: 10.1067/msy.2000.102754]
29 **Kato H**, Tachimori Y, Watanabe H, Igaki H, Nakanishi Y, Ochiai A. Recurrent esophageal carcinoma after esophagectomy with three-field lymph node dissection. *J Surg Oncol* 1996; **61**: 267-272 [PMID: 8627996]
30 **Matsubara T**, Ueda M, Takahashi T, Nakajima T, Nishi M. Localization of recurrent disease after extended lymph node dissection for carcinoma of the thoracic esophagus. *J Am Coll Surg* 1996; **182**: 340-346 [PMID: 8605557]
31 **Kelley MR**, Cheng L, Foster R, Tritt R, Jiang J, Broshears J, Koch M. Elevated and altered expression of the multifunctional DNA base excision repair and redox enzyme Ape1/ref-1 in prostate cancer. *Clin Cancer Res* 2001; **7**: 824-830 [PMID: 11309329]
32 **Wang S**, Wu X, Chen Y, Zhang J, Ding J, Zhou Y, He S, Tan Y, Qiang F, Bai J, Zeng J, Gong Z, Li A, Li G, Røe OD, Zhou J. Prognostic and predictive role of JWA and XRCC1 expressions in gastric cancer. *Clin Cancer Res* 2012; **18**: 2987-2996 [PMID: 22452940 DOI: 10.1158/1078-0432.CCR-11-2863]
33 **Bayani J**, Selvarajah S, Maire G, Vukovic B, Al-Romaih K, Zielenska M, Squire JA. Genomic mechanisms and measurement of structural and numerical instability in cancer cells. *Semin Cancer Biol* 2007; **17**: 5-18 [PMID: 17126026 DOI: 10.1016/j.semcancer.2006.10.006]
34 **Raptis S**, Bapat B. Genetic instability in human tumors. *EXS* 2006; : 303-320 [PMID: 16383024 DOI: 10.1007/3-7643-7378-4_13]
35 **Hanahan D**, Weinberg RA. Hallmarks of cancer: the next generation. *Cell* 2011; **144**: 646-674 [PMID: 21376230 DOI: 10.1016/j.cell.2011.02.013]
36 **Imdahl A**, Jenkner J, Ihling C, Rückauer K, Farthmann EH. Is MIB-1 proliferation index a predictor for response to neoadjuvant therapy in patients with esophageal cancer? *Am J Surg* 2000; **179**: 514-520 [PMID: 11004343 DOI: 10.1016/S0002-9610(00)00386-X]
37 **Beardsmore DM**, Verbeke CS, Davies CL, Guillou PJ, Clark GW. Apoptotic and proliferative indexes in esophageal cancer: predictors of response to neoadjuvant therapy [corrected]. *J Gastrointest Surg* 2003; **7**: 77-86; discussion 86-87 [PMID: 12559188 DOI: 10.1016/S1091-255X]
38 **Turesson I**, Carlsson J, Brahme A, Glimelius B, Zackrisson B, Stenerlöw B. Biological response to radiation therapy. *Acta Oncol* 2003; **42**: 92-106 [PMID: 12801128 DOI: 10.1080/02841860310004959]
39 **Alexander BM**, Wang XZ, Niemierko A, Weaver DT, Mak RH, Roof KS, Fidias P, Wain J, Choi NC. DNA repair biomarkers predict response to neoadjuvant chemoradiotherapy in esophageal cancer. *Int J Radiat Oncol Biol Phys* 2012; **83**: 164-171 [PMID: 22000749 DOI: 10.1016/j.ijrobp.2011.05.033.]
40 **Hwang IG**, Ahn MJ, Park BB, Ahn YC, Han J, Lee S, Kim J, Shim YM, Ahn JS, Park K. ERCC1 expression as a prognostic marker in N2(+) nonsmall-cell lung cancer patients treated with platinum-based neoadjuvant concurrent chemoradiotherapy. *Cancer* 2008; **113**: 1379-1386 [PMID: 18623378 DOI: 10.1002/cncr.23693]
41 **Olaussen KA**, Dunant A, Fouret P, Brambilla E, André F, Haddad V, Taranchon E, Filipits M, Pirker R, Popper HH, Stahel R, Sabatier L, Pignon JP, Tursz T, Le Chevalier T, Soria JC. DNA repair by ERCC1 in non-small-cell lung cancer and cisplatin-based adjuvant chemotherapy. *N Engl J Med* 2006; **355**: 983-991 [PMID: 16957145 DOI: 10.1056/NEJMoa060570]
42 **Chen S**, Zhang J, Wang R, Luo X, Chen H. The platinum-based treatments for advanced non-small cell lung cancer, is low/negative ERCC1 expression better than high/positive ERCC1 expression? A meta-analysis. *Lung Cancer* 2010; **70**: 63-70 [PMID: 20541281 DOI: 10.1016/j.lungcan.2010.05.010]
43 **Nix P**, Greenman J, Stafford N, Cawkwell L. Expression of XRCC1 and ERCC1 proteins in radioresistant and radiosensitive laryngeal cancer. *Cancer Ther* 2004; **2**: 47-53
44 **Lee JJ**, Maeng CH, Baek SK, Kim GY, Yoo JH, Choi CW, Kim YH, Kwak YT, Kim DH, Lee YK, Kim JB, Kim SY. The immunohistochemical overexpression of ribonucleotide reductase regulatory subunit M1 (RRM1) protein is a predictor of shorter survival to gemcitabine-based chemotherapy in advanced non-small cell lung cancer (NSCLC). *Lung Cancer* 2010; **70**: 205-210 [PMID: 20223551 DOI: 10.1016/j.lungcan.2010.02.005]
45 **Ito S**, Tan LJ, Andoh D, Narita T, Seki M, Hirano Y, Narita K, Kuraoka I, Hiraoka Y, Tanaka K. MMXD, a TFIIH-independent XPD-MMS19 protein complex involved in chromosome segregation. *Mol Cell* 2010; **39**: 632-640 [PMID: 20797633 DOI: 10.1016/j.molcel.2010.07.029]
46 **Li F**, Martienssen R, Cande WZ. Coordination of DNA replication and histone modification by the Rik1-Dos2 complex. *Nature* 2011; **475**: 244-248 [PMID: 21725325 DOI: 10.1038/nature10161]

P- Reviewer: Kim BW, Nilsson M, Shim CS, Yi YX **S- Editor**: Qi Y
L- Editor: AmEditor **E- Editor**: Ma S

World Journal of Gastroenterology

Submit a Manuscript: http://www.wjgnet.com/esps/
Help Desk: http://www.wjgnet.com/esps/helpdesk.aspx
DOI: 10.3748/wjg.v21.i14.4248

World J Gastroenterol 2015 April 14; 21(14): 4248-4254
ISSN 1007-9327 (print) ISSN 2219-2840 (online)

ORIGINAL ARTICLE

Retrospective Study

Is cholecystectomy a reasonable treatment option for simple gallbladder polyps larger than 10 mm?

Hye Yon Park, Se Hoon Oh, Kwang Hyuck Lee, Jong Kyun Lee, Kyu Taek Lee

Hye Yon Park, Se Hoon Oh, Kwang Hyuck Lee, Jong Kyun Lee, Kyu Taek Lee, Division of Gastroenterology, Department of Internal Medicine, Samsung medical center, Sungkyunkwan University School of Medicine, Seoul 135-710, South Korea
Author contributions: Park HY performed research and wrote this paper; Oh SH collected data; Lee KH and Lee JK contributed data analysis; Lee KT designed this study and wrote this paper.

Correspondence to: Kyu Taek Lee, MD, PhD, Professor, Division of Gastroenterology, Department of Internal Medicine, Samsung Medical Center, Sungkyunkwan University School of Medicine, 81 Irwon-ro, Gangnam-gu, Seoul 135-710, South Korea. happymap@skku.edu
Telephone: +82-2-34103406
Fax: +82-2-34106983
Received: July 19, 2014
Peer-review started: July 22, 2014
First decision: August 27, 2014
Revised: September 22, 2014
Accepted: December 1, 2014
Article in press: December 1, 2014
Published online: April 14, 2015

Abstract

AIM: To determine the relevance of the 10-mm size criterion of the generally accepted surgical indication for gallbladder polyps (GBPs).

METHODS: We collected data of patients who were confirmed to have GBPs through cholecystectomy at Samsung Medical Center between January 1997 and December 2012. Among the patients who underwent cholecystectomy for GBP, those with a definite evidence for malignancy such as adjacent organ invasion, metastasis on preoperative imaging studies, polyp larger than 20 mm, absence of preoperative imaging study results, and patients having gallstones were excluded. We retrospectively collected and analyzed information on patient's clinical characteristics, symptoms, ultrasonographic findings, and blood laboratory tests.

RESULTS: A total of 836 patients who had undergone cholecystectomy were retrospectively analyzed. Seven hundred eighty patients (93%) had benign polyps, whereas 56 patients (7%) had malignant polyps. Of the 56 patients with malignancy, 4 patients (7%) had borderline GBP (10-12 mm) and a patient had small GBP (< 10 mm) with T2 stage. We conducted an ROC curve analysis to verify the 10-mm size criteria (AUC = 0.887, SD = 0.21, $P < 0.001$). In the ROC curve for polyp size and malignancy, sensitivity and specificity of the 10-mm size criterion was 98.2% and 19.6%, respectively. The specificity of the 11-mm and 12-mm size criteria was 44.6% and 56%, respectively, whereas the sensitivity of these two size criteria was similar. We defined the GBPs of 10 to 12 mm as a borderline-sized GBP, which were found in 411 patients (49%). In this group, there was a significant difference in age between patients with benign and malignant GBPs (47 years *vs* 60 years, $P < 0.05$).

CONCLUSION: GBPs larger than 13 mm need immediate excision whereas for borderline-sized GBPs detected in young patients, careful medical observation can be a rational decision.

Key words: Gallbladder polyp; Gallbladder cancer; Cholecystectomy; Polyp size; Borderline-sized gallbladder polyp

Core tip: Gallbladder polyp (GBP) is a well-known pre-malignant lesion. The size of GBP, patient's age and presence of symptoms are the risk factors for GB cancer. GBPs of 10 to 12 mm in diameter have lower risk of malignancy compared to that in GBPs larger than 13 mm, which is similar to the risk of malignancy in GBPs smaller than 10 mm. The use of this surgical indication (GBPs larger than 13 mm GBP) can prevent 50% of unnecessary cholecystectomies without the risk of missing malignant GBPs. Our findings suggest that GBPs with a diameter of 10 to 12 mm in patients younger than 45 years of age old can be observed carefully.

Park HY, Oh SH, Lee KH, Lee JK, Lee KT. Is cholecystectomy a reasonable treatment option for simple gallbladder polyps larger than 10 mm? *World J Gastroenterol* 2015; 21(14): 4248-4254 Available from: URL: http://www.wjgnet.com/1007-9327/full/v21/i14/4248.htm DOI: http://dx.doi.org/10.3748/wjg.v21.i14.4248

INTRODUCTION

Polypoid lesions of the gallbladder are becoming an increasingly common incidental finding. It is very important to distinguish between a benign polyp and a malignant polyp because of the poor prognosis of gallbladder (GB) cancer, but the radiologic tools such as abdominal ultrasound (US) and computed tomography (CT) are not sufficient to distinguish between a benign polyp and a malignant polyp[1]. Therefore, many researchers have attempted to identify the factors that can help in preoperative differentiation between a benign polyp and a malignant polyp[2,3].

Although the natural history of gallbladder polyps (GBPs) is not completely understood and most of the available studies are retrospective in nature[4,5], the well-known predictor of malignancy in GBPs is a size greater than 10 mm in diameter[6]. However, when we applied the 10-mm size criterion for performing surgery, many polyps were found to be benign in a clinical setting. Most of the benign polyps had a size of 10 or 11 mm, and the incidence of these polyps is increasing as general medical examination is being universalized. Previous studies have shown that polyp size of more than 10 mm is associated with higher risk of developing malignancy; however so far, none of the studies have tried to differentiate between polyps of more than 10 mm in size for determining the incidence of malignancy.

Therefore, we analyzed the pathologically proven GBPs after cholecystectomy for 16 years at Samsung Medical Center to determine the relevance of the 10-mm size criterion.

MATERIALS AND METHODS

Data source and patient population

We collected data of patients who were confirmed to have GBPs through cholecystectomy at Samsung Medical Center between January 1997 and December 2012. Among the patients who underwent cholecystectomy for GBP, those with a definite evidence for malignancy such as adjacent organ invasion, metastasis on preoperative imaging studies, polyp larger than 20 mm, absence of preoperative imaging study results, and patients having gallstones were excluded. A total of 836 patients were enrolled. Information on age, sex, symptoms, US findings, and blood laboratory tests was reviewed retrospectively.

The patients were categorized as having a benign polyp or a malignant polyp according to their histopathologic results. Benign GBPs were subcategorized as benign tumorous polyps if the pathological finding indicated that the polyps had a potential for malignant transformation, whereas benign non-tumorous polyps were not regarded as precancerous lesions. The benign tumorous polyps included adenomas, lipomas, neurofibromas, leiomyomas, and carcinoid tumors. The benign non-tumorous polyps included cholesterol polyps, inflammatory polyps, fibromas, and adenomyomatosis. Malignant GBPs were defined as GB cancer. This study was approved by the Institutional Review Board of the Samsung Medical Center (SMC 2013-12-063).

Definition of GBPs and imaging study

The following standardized US criteria were used to identify polyps on US: immobile, hyperechoic compared to the surrounding bile, non-shadowing, and attached to the GB wall[7]. US examinations were performed by an experienced certified radiologist by using 3.5-MHz transducers (iU-22, Philips Healthcare, Bothell, Washington; ATL 5000, Philips Healthcare, Acuson 128, Siemens, Mountain View, California). The US examinations were interpreted by board certified radiologists who were trained in abdominal imaging, delineation of the number and size of GBPs.

Statistical analysis

Statistical analysis of the data was performed by utilizing SPSS 11.0 (Chicago, IL, United States). Continuous variables were presented as mean ± SD. Intergroup comparisons were conducted with the χ^2 test. In order to identify the risk factors for gallbladder cancer, the odds ratio was obtained using multiple logistic regression analysis. The area under the curve (AUC) was calculated using the receiver-operating characteristic curve (ROC) to determine the sensitivity and specificity of the 10-mm size criterion for predicting malignant polyps. If the criterion was not considered sufficient, we tried to determine an optimal cut-off point of polyp size to predict malignant polyps. Differences were considered significant

Table 1 Demographic and clinical characteristics of 836 patients *n* (%)

Characteristics	*n* = 836
Female	449 (54)
Age (yr)	47 ± 12.3
Indication for surgery[1]	
Size ⩾ 10 mm	695 (83)
Increased size[2]	184 (22)
Abnormal imaging[3]	59 (7)
Size of the polyp (mm)	11.6 ± 3.5
Number of polyps	
1	460 (55.0)
2	128 (15.3)
⩾ 3	248 (29.6)
BMI (kg/m^2)	26.7 ± 32.1
Total cholesterol (mg/dL)	172.9 ± 33.2
Total bilirubin (mg/dL)	0.8 ± 0.6
ALT (U/L)	32.1 ± 31.3
ALP (U/L)	61.8 ± 25.9
Fasting glucose (mg/dL)	110.3 ± 30.4
CA 19-9 (U/mL)	12.4 ± 38.0
HBsAg positivity	67 (8.0)

[1]Repetition was allowed; [2]If the polyp size was increased during the follow-up period compared to that in the initial imaging study; [3]Gallbladder wall thickness, irregular margin of the polyp, enhancing nodule. GB: Gallbladder; BMI: Body mass index; ALT: Alanine transaminase; ALP: Alkaline phosphatase; CA19-9: Carbohydrate antigen 19-9; HBsAg: Hepatitis B surface antigen.

Table 2 Predictors of gallbladder cancer (multiple logistic regression analysis)

Variables	GB cancer	
	OR (95%CI)	*P* value
Female	0.615 (0.276-1.370)	0.234
Size	1.516 (1.356-1.694)	< 0.001
Number of polyps	0.812 (0.531-1.244)	0.339
Age	1.120 (1.078-1.164)	< 0.001
Symptoms[1]	5.019 (1.649-15.276)	0.005
BMI	1.004 (0.995-1.014)	0.383
Total cholesterol	0.991 (0.980-1.003)	0.139
Total bilirubin	1.534 (0.604-3.894)	0.368
ALT	1.007 (0.999-1.015)	0.079
ALP	1.001 (0.991-1.012)	0.813
Fasting glucose	1.002 (0.991-1.013)	0.771
CA19-9	1.022 (0.005-1.049)	0.116
HBsAg positivity	2.461 (0.587-10.327)	0.218

[1]Right upper quadrant pain, epigastric pain, vague abdominal discomfort, dyspepsia, fatigue, body weight loss. GB: Gallbladder; BMI: Body mass index; ALT: Alanine transaminase; ALP: Alkaline phosphatase; CA19-9: Carbohydrate antigen 19-9; HBsAg: Hepatitis B surface antigen.

when the *P* value was less than 0.05.

RESULTS

Demographic findings and clinical characteristics

Among the 836 patients who underwent cholecystectomy, 780 patients (93%) had benign polyps, and 56 patients (7%) had malignant polyps, which were adenocarcinomas. Benign tumorous polyps were adenomas, and 165 patients (20%) had adenomas. Among all of the polyps, the cholesterol polyp was the most common type, and it was found in 559 patients (67%). The demographic and clinical characteristics of all the 836 patients are listed in Table 1. The mean age of the patients and the mean size of polyps were 47 ± 12.3 years and 11.6 ± 3.5 mm, respectively. The sex ratio was 0.86:1 (male:female = 387:449). Among the 836 patients, 464 patients (55%) had solitary polyps, and 372 patients (45%) had multiple polyps. Indications for surgery were collected while allowing for repetition. The majority (695 patients, 83%) of patients underwent cholecystectomy because they had a polyp of greater than 10 mm; this indicated that the 10-mm size criterion is the most important factor in making a decision regarding surgery in a clinical setting. Fifty-four patients had symptoms; some of the patients had specific symptoms such as right upper quadrant pain or epigastric pain, but the other patients complained of a vague abdominal pain, dyspepsia, fatigue, or loss of body weight.

The patients who had GBPs showed a high BMI and fasting glucose level, but total cholesterol, total bilirubin, ALT, ALP, and CA 19-9 levels were normal. Interestingly, higher proportion of patients with GB polyps showed positivity of hepatitis B surface antigen compared to healthy controls aged from 40 to 49 years in South Korea.

Risk factors for malignant GBPs

The size of GBPs was a significant risk factor for malignant GBPs ($P < 0.001$, OR = 1.516; 95%CI: 1.356-1.694). Old age and presence of symptoms were associated with a higher risk of malignant GBPs ($P < 0.001$, OR = 1.120, 95%CI: 1.078-1.164; $P = 0.005$, OR = 5.019, 95%CI: 1.649-15.276). Number of polyps, ALT, ALP, and fasting glucose levels did not increase the risk of malignancy (Table 2).

Optimal size to predict malignant GBPs

Of 56 patients with malignant pathologic results, only a patient (1.8%) had GBP lesser than 10 mm (intramural, 8 mm). In case of 230 patients with GBP of 10 to 11 mm size, no malignancy was reported. Among 104 patients with GBP of 12 mm, 4 patients (3.8%) have been confirmed to have malignancy. Two of them (50%) were intraepithelial tumors and the other two malignant polyps were intramural tumors.

We calculated the AUC using the ROC curve to test the conventional size criteria for predicting the risk of malignancy (Figure 1, Table 3). When the size cut-off point was set at 10 mm, sensitivity and specificity for predicting malignant polyps was 98.2% and 19.6%, respectively; but when the size cut-off point was set at 11 mm and 12 mm, the sensitivity was the same as that when the size cut-off point was set at 10 mm, but the specificity was increased as the size increased (44.6% and 56.0%, respectively). The sensitivity and the specificity for predicting a polyp of 13 mm was 91.0% and 71.8%, respectively. The sensitivity fell

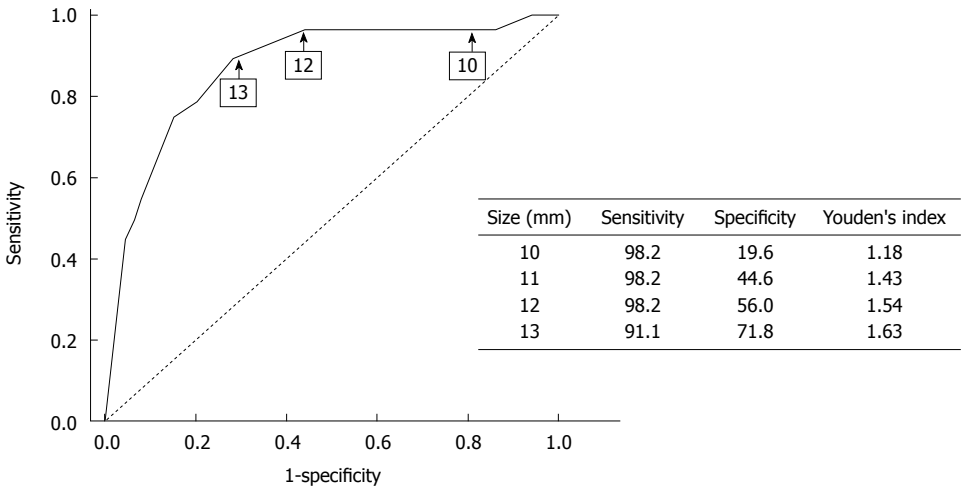

Size (mm)	Sensitivity	Specificity	Youden's index
10	98.2	19.6	1.18
11	98.2	44.6	1.43
12	98.2	56.0	1.54
13	91.1	71.8	1.63

Figure 1 Receiver operating characteristic curves for the size of gallbladder polyp are shown. The area under the curve is 0.887 (95%CI: 0.846-0.927; $P < 0.001$) for the polyp size. The sensitivity and specificity of each size is presented.

Table 3 Receiver operating characteristic curve summary statistics

Size, mm (patients)	Sensitivity	Specificity	Youden's index	ppv	npv
8 (54)	1.000	0.103	1.103	0.074	1.000
9 (87)	0.982	0.144	1.126	0.076	0.991
10 (105)	0.982	0.196	1.178	0.081	0.994
11 (89)	0.982	0.446	1.428	0.113	0.997
12 (127)	0.982	0.560	1.542	0.138	0.998
13 (69)	0.911	0.718	1.629	0.188	0.991
14 (41)	0.804	0.799	1.603	0.223	0.983

Ppv: Positive predictive value; npv: Negative predictive value.

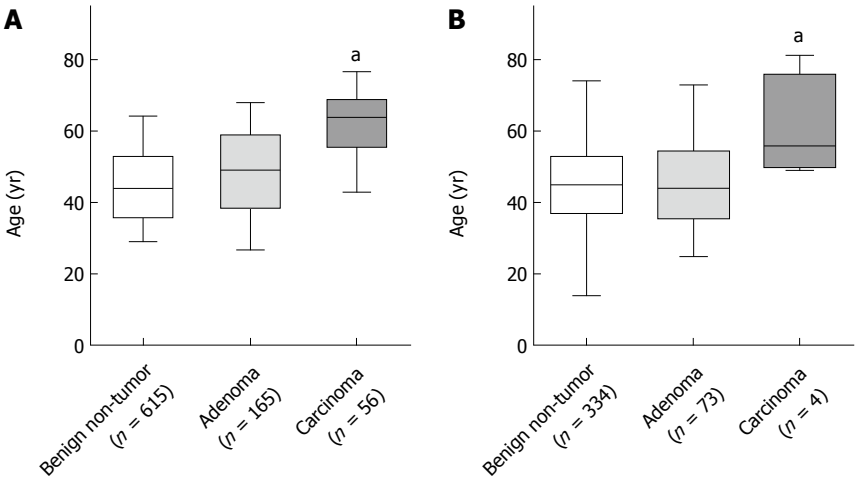

Figure 2 Patient's age was positively correlated with the malignancy risk. A: All of the patients; B: Patients with borderline-sized gallbladder polyps. [a]$P < 0.05$ *vs* benign non-tumor group.

sharply from a size cut-off point of 14 mm. Therefore, after considering the sensitivity and specificity for predicting malignant polyps, 13 mm might be the best cut-off point.

When the size cut-off point was set at 8 mm, the sensitivity was 100%. This result implied that the use of the 10-mm size criterion might lead to unnecessary cholecystectomies, and on the other hand, the 10-mm size criterion might be insufficient to completely exclude malignancy.

Borderline-sized GBPs

We defined GBPs that were more than 10 mm and less than 13 mm in size while maintaining the sensitivity above 90% as "borderline-sized GBPs". Among the 836 cases, there were 411 cases (49%) of borderline-sized

Table 4 Characteristics of patients with malignant borderline-sized gallbladder polyps

Case	Sex/age (yr)	Symptom	Underlying disease	Imaging finding	Operation	TNM stage	Prognosis
1	F/49	Dyspepsia	-	12 mm, polyp	Lap.chole	T2N0M0	63 mo, alive
2	F/52	-	Hypothyroidism	12 mm, enhancing nodule	Lap.chole	T1aN0M0	30 mo, alive
3	F/60	-	-	12 mm, enhancing nodule	Lap.chole	T1aN0M0	24 mo, alive
4	F/81	-	CHF, A fib	12 mm, enhancing sessile nodule	Lap.chole	T2N0M0	13 mo, alive

Lap.chole: Laparoscopic cholecystectomy.

GBPs (Figure 2). In this group, benign non-tumorous polyps accounted for 81% (334 patients) of polyps, which was higher than that in all of the patients. Adenomas were detected in 73 patients. Four patients had malignant polyps, and these patients had polyps measuring 12 mm in size on preoperative imaging studies (Table 4). The patients with borderline GBPs would not have undergone unnecessary surgeries if the criterion for performing surgery was more specific.

To characterize the patients with borderline-sized GBPs, we examined the patient's age, which had a relationship with malignant GBPs on the multivariate analysis (Figure 2). The average age of patients with benign polyps and malignant polyps was 47 years and 60 years, respectively. This difference was statistically significant. Especially all four patients who had malignant polyps were more than 45 years of age.

DISCUSSION

GBPs represent a wide spectrum from pseudo lesions to gall bladder cancer. After Boulton and colleagues reported the strategy for managing GBPs using the risk factors of gallbladder cancer which were identified in previous studies, many reports on the management of GBPs have been published[2]. The risk factors suggested in these studies were symptoms, size greater than 10 mm, age more than 50 years, presence of gallstones etc. The risk factors for malignant polyps in our study were polyp size, patient's age, and presence of symptoms. This result was similar to that in previous reports[8-11].

Polyp size has long been considered to be an important factor[12,13]. Current guidelines recommend cholecystectomy for polyps measuring 10 mm or larger. The use of this strategy may result in a large number of unnecessary cholecystectomies, because the detection rate of relatively small GBPs has been increasing since 2004, which was the year due to the expanded use of abdominal US in South Korea.

In South Korea, the prevalence of GBPs considering this criterion has been increasing steadily since 2004, which was the year in which increased ultrasound surveillance of asymptomatic persons was performed.

Corwin *et al*[7] presented a study in 2011. This study provides further directions for managing incidentally diagnosed polyps in adults. They monitored 346 incidentally detected GBPs, and there were no cases of GB cancer and there were 3 cases of adenomas. In their study, the average size of polyps was 5 mm (range: 1-18 mm), and the proportion of polyps greater than 10mm was only 3.5% (n = 12). This study showed that incidentally discovered polyps were usually small in size and the risk of malignancy was low.

We defined the polyps having a size of 10 to 12 mm as borderline-sized GBPs. These polyps had a low malignant potential, and they were mostly benign non-tumorous polyps. In particular, the polyps were not malignant in any of the patients who had a 10-11 mm sized polyp, thus suggesting that cholecystectomy was an inappropriate management strategy in these patients. The use of this surgical indication (GBPs larger than 13 mm GBP) can prevent 50% of unnecessary cholecystectomies without the risk of missing malignant GBPs.

The role of gallbladder adenoma in the pathogenesis of gallbladder carcinoma is controversial[14]. It is thought that adenoma may play a role in some cases of gallbladder cancer. The adenoma-carcinoma sequence was first suggested by Kozuka *et al*[15], who conducted a study of 1605 resected gallbladder specimens and found 7 adenomas with malignant changes and evidence of adenomatous residue in 15 of 79 (19%) invasive carcinomas[15]. However, the incidence of the combined lesion is low and varies between 0.14% and 1.1% in different series[16-18]. Wistuba *et al*[19] performed molecular studies on tissue from gallbladder adenoma and detected no mutations in the *TP53* gene, a frequent finding in dysplasia, carcinoma in situ, and invasive cancer, which led the researchers to conclude that adenomas are not precursors of invasive gallbladder carcinoma. Similarly, Roa *et al*[20] found no evidence of adenoma residue in their study of completely mapped early carcinomas of the gallbladder. These reports indicate that the adenoma-carcinoma sequence is less important in the gallbladder than in the other organs of the digestive tract[21]. The dysplasia-carcinoma sequence has been considered as the main route of carcinogenesis in the gallbladder[22-24]. We performed this study with more emphasis on GB carcinoma than adenoma. This could be a limitation of our study.

Many studies have demonstrated that malignant GBPs are significantly more common in patients aged more than 50 years[25-27]. Our study confirmed that patient's age was associated with the risk of developing malignant polyps. Besides, there was a significant difference in the mean age of patients with malignant borderline-sized GBPs and those with benign

borderline-sized GBPs. The mean age of patients with malignant polyps was 60 years, whereas that of patients with benign polyps was 47 years, and all of the malignant polyps were detected in patients aged 45 years and older. This finding indicates that there is a low possibility of GB carcinoma in patients having borderline-sized GBPs and who are less than 49 years of age, and there is a high possibility of GB carcinoma in patients having borderline-sized GBPs and who are more than 60 years of age.

GBPs generally do not cause any symptoms[26], although most of the prevalence studies did not assess the symptoms. Terzi *et al*[28] reported that in a series of 74 patients undergoing cholecystectomy for GBPs, 91% of patients had symptoms, most commonly right upper quadrant pain, nausea, dyspepsia, and jaundice. However, about 60% of the patients also had gallstones, and therefore it is unclear whether the polyps were primarily driving the symptoms. The symptoms were related to malignancy in our research, nevertheless, we excluded the patients with gallstones. Kwon *et al*[14] suggested that symptoms may be associated with the size of the polyp rather than the association of gallstone. Therefore, patient's symptoms should be considered as the red flag for malignancy.

Patients with GBPs were classified as over-weight according to BMI and had a high fasting glucose level. The researchers suggested that metabolic syndrome contributes to the formation of cholesterol polyps in the gallbladder[20,29]. However, because of the absence of a similar finding in overt diabetic patients in their study[29] and in other prevalence studies[16,30], the validity of this association is questionable. Also, hepatitis B surface antigen positivity was greater in patients with GBPs compared to the general population. However, in contrast to the findings presented by Lin *et al*[31], hepatitis B surface antigen positivity was not a predictive factor for GB cancer in this study.

Our study indicates that the natural history of borderline-sized GBPs is benign, although most of the borderline-sized GBPs were removed. Hence, it is necessary to redefine the surgical indications for GBPs, which are increasingly being detected on surveillance imaging. Our study is a retrospective study from a single center despite large study subjects. So, prospective multicenter study will be needed to validate our study.

In conclusion, the need for performing immediate surgery for GBPs measuring more than 13 mm in size is undebatable, whereas borderline-sized GBPs, especially in asymptomatic young patients (less than 45 years old), have low risk of malignancy, and therefore, a careful "wait and see" strategy is appropriate. Further studies are needed to define the characteristics of borderline-sized GBPs and to demonstrate the natural history of borderline-sized GBPs.

COMMENTS

Background

Gallbladder polyp (GBP) is a well-known pre-malignant lesion, especially the size of GBP, age and presence of symptoms are risk factors for gallbladder (GB) cancer. The well-known predictor of malignancy in GBPs is a size greater than 10 mm in diameter. However, when we applied the 10-mm size criterion for performing surgery, many polyps were found to be benign in a clinical setting. Most of the benign polyps had a size of 10 or 11 mm, and the incidence of these polyps is increasing as general medical examination is being universalized.

Research frontiers

Some recent studies have shown that incidentally discovered polyps were usually small in size and the risk of malignancy was low.

Innovations and breakthroughs

Previous studies have shown that polyp size of more than 10 mm is associated with higher risk of developing malignancy; however so far, none of the studies have tried to differentiate between polyps of more than 10 mm in size for determining the incidence of malignancy. Therefore, we analyzed the pathologically proven GBPs after cholecystectomy to determine the relevance of the 10-mm size criterion.

Applications

This study aimed to determine the relevance of the 10-mm size criterion of the generally accepted surgical indication for GBPs, and to provide a new surgical indication clues for decrease unnecessary cholecystectomies.

Terminology

GBPs of 10 to 12 mm in diameter (borderline-sized GBPs) have lower risk of malignancy compared to that in GB polyps larger than 13 mm, which is similar to the risk of malignancy in GB polyps smaller than 10 mm. The use of this surgical indication (GBPs larger than 13 mm GBP) can prevent 50% of unnecessary cholecystectomies without the risk of missing malignant GBPs. Also, this study confirmed that patient's age was associated with the risk of developing malignant polyps. This finding indicates that there is a low possibility of GB carcinoma in patients having borderline-sized GBPs and who are less than 49 years of age.

Peer-review

Authors made a retrospective revision of their database regarding gallbladder polyps, in order to find a potential best predictor of malignancies rather than 10 mm size. They concluded that 13 mm size was a better cut-off value to indicate immediately surgery, whereas 11 and 12 mm size polyps, in younger patients could be strictly followed up before undergoing surgery. The paper certainly brings new information on the subject and may represent an interesting option for the readers.

REFERENCES

1 **Konstantinidis IT**, Bajpai S, Kambadakone AR, Tanabe KK, Berger DL, Zheng H, Sahani DV, Lauwers GY, Fernandez-del Castillo C, Warshaw AL, Ferrone CR. Gallbladder lesions identified on ultrasound. Lessons from the last 10 years. *J Gastrointest Surg* 2012; **16**: 549-553 [PMID: 22108768 DOI: 10.1007/s11605-011-1696-2]

2 **Boulton RA**, Adams DH. Gallbladder polyps: when to wait and when to act. *Lancet* 1997; **349**: 817 [PMID: 9121250 DOI: 10.1016/s0140-6736(05)61744-8]

3 **Okamoto M**, Okamoto H, Kitahara F, Kobayashi K, Karikome K, Miura K, Matsumoto Y, Fujino MA. Ultrasonographic evidence of association of polyps and stones with gallbladder cancer. *Am J Gastroenterol* 1999; **94**: 446-450 [PMID: 10022644 DOI: 10.1111/j.1572-0241.1999.875_d.x]

4 **Gurusamy KS**, Abu-Amara M, Farouk M, Davidson BR. Cholecystectomy for gallbladder polyp. *Cochrane Database Syst Rev* 2009; (**1**): CD007052 [PMID: 19160315 DOI: 10.1002/14651858.CD007052.pub2]

5 **Mainprize KS**, Gould SW, Gilbert JM. Surgical management of polypoid lesions of the gallbladder. *Br J Surg* 2000; **87**: 414-417

[PMID: 10759734 DOI: 10.1046/j.1365-2168.2000.01363.x]
6 **Koga A**, Watanabe K, Fukuyama T, Takiguchi S, Nakayama F. Diagnosis and operative indications for polypoid lesions of the gallbladder. *Arch Surg* 1988; **123**: 26-29 [PMID: 3276295]
7 **Corwin MT**, Siewert B, Sheiman RG, Kane RA. Incidentally detected gallbladder polyps: is follow-up necessary?--Long-term clinical and US analysis of 346 patients. *Radiology* 2011; **258**: 277-282 [PMID: 20697115 DOI: 10.1148/radiol.10100273]
8 **Andrén-Sandberg A**. Diagnosis and management of gallbladder polyps. *N Am J Med Sci* 2012; **4**: 203-211 [PMID: 22655278 DOI: 10.4103/1947-2714.95897]
9 **Park JK**, Yoon YB, Kim YT, Ryu JK, Yoon WJ, Lee SH, Yu SJ, Kang HY, Lee JY, Park MJ. Management strategies for gallbladder polyps: is it possible to predict malignant gallbladder polyps? *Gut Liver* 2008; **2**: 88-94 [PMID: 20485616 DOI: 10.5009/gnl.2008.2.2.88]
10 **Park JY**, Hong SP, Kim YJ, Kim HJ, Kim HM, Cho JH, Park SW, Song SY, Chung JB, Bang S. Long-term follow up of gallbladder polyps. *J Gastroenterol Hepatol* 2009; **24**: 219-222 [PMID: 19054258 DOI: 10.1111/j.1440-1746.2008.05689.x]
11 **Shin SR**, Lee JK, Lee KH, Lee KT, Rhee JC, Jang KT, Kim SH, Choi DW. Can the growth rate of a gallbladder polyp predict a neoplastic polyp? *J Clin Gastroenterol* 2009; **43**: 865-868 [PMID: 19398929 DOI: 10.1097/MCG.0b013e31819359aa]
12 **Chattopadhyay D**, Lochan R, Balupuri S, Gopinath BR, Wynne KS. Outcome of gall bladder polypoidal lesions detected by transabdominal ultrasound scanning: a nine year experience. *World J Gastroenterol* 2005; **11**: 2171-2173 [PMID: 15810087]
13 **Lee KF**, Wong J, Li JC, Lai PB. Polypoid lesions of the gallbladder. *Am J Surg* 2004; **188**: 186-190 [PMID: 15249249 DOI: 10.1016/j.amjsurg.2003.11.043]
14 **Kwon W**, Jang JY, Lee SE, Hwang DW, Kim SW. Clinicopathologic features of polypoid lesions of the gallbladder and risk factors of gallbladder cancer. *J Korean Med Sci* 2009; **24**: 481-487 [PMID: 19543513 DOI: 10.3346/jkms.2009.24.3.481]
15 **Kozuka S**, Tsubone N, Yasui A, Hachisuka K. Relation of adenoma to carcinoma in the gallbladder. *Cancer* 1982; **50**: 2226-2234 [PMID: 7127263]
16 **Collett JA**, Allan RB, Chisholm RJ, Wilson IR, Burt MJ, Chapman BA. Gallbladder polyps: prospective study. *J Ultrasound Med* 1998; **17**: 207-211 [PMID: 9544602]
17 **Nakajo S**, Yamamoto M, Tahara E. Morphometrical analysis of gall-bladder adenoma and adenocarcinoma with reference to histogenesis and adenoma-carcinoma sequence. *Virchows Arch A Pathol Anat Histopathol* 1990; **417**: 49-56 [PMID: 2113740]
18 **Roa I**, de Aretxabala X, Morgan R, Molina R, Araya JC, Roa J, Ibacahe G. [Clinicopathological features of gallbladder polyps and adenomas]. *Rev Med Chil* 2004; **132**: 673-679 [PMID: 15332368]
19 **Wistuba II**, Miquel JF, Gazdar AF, Albores-Saavedra J. Gallbladder adenomas have molecular abnormalities different from those present in gallbladder carcinomas. *Hum Pathol* 1999; **30**: 21-25 [PMID: 9923922]
20 **Roa I**, de Aretxabala X, Araya JC, Roa J. Preneoplastic lesions in gallbladder cancer. *J Surg Oncol* 2006; **93**: 615-623 [PMID: 16724345 DOI: 10.1002/jso.20527]
21 **Goldin RD**, Roa JC. Gallbladder cancer: a morphological and molecular update. *Histopathology* 2009; **55**: 218-229 [PMID: 19490172 DOI: 10.1111/j.1365-2559.2008.03192.x]
22 **Ajiki T**, Fujimori T, Onoyama H, Yamamoto M, Kitazawa S, Maeda S, Saitoh Y. K-ras gene mutation in gall bladder carcinomas and dysplasia. *Gut* 1996; **38**: 426-429 [PMID: 8675098]
23 **Roa I**, Araya JC, Villaseca M, De Aretxabala X, Riedemann P, Endoh K, Roa J. Preneoplastic lesions and gallbladder cancer: an estimate of the period required for progression. *Gastroenterology* 1996; **111**: 232-236 [PMID: 8698204]
24 **Yamamoto M**, Nakajo S, Tahara E. Dysplasia of the gallbladder. Its histogenesis and correlation to gallbladder adenocarcinoma. *Pathol Res Pract* 1989; **185**: 454-460 [PMID: 2602218 DOI: 10.1016/s0344-0338(89)80062-7]
25 **Cha BH**, Hwang JH, Lee SH, Kim JE, Cho JY, Kim H, Kim SY. Pre-operative factors that can predict neoplastic polypoid lesions of the gallbladder. *World J Gastroenterol* 2011; **17**: 2216-2222 [PMID: 21633532 DOI: 10.3748/wjg.v17.i17.2216]
26 **Gallahan WC**, Conway JD. Diagnosis and management of gallbladder polyps. *Gastroenterol Clin North Am* 2010; **39**: 359-367, x [PMID: 20478491 DOI: 10.1016/j.gtc.2010.02.001]
27 **Kianmanesh R**, Scaringi S, Castel B, Flamant Y, Msika S. [Precancerous lesions of the gallbladder]. *J Chir* (Paris) 2007; **144**: 278-286 [PMID: 17925730]
28 **Terzi C**, Sökmen S, Seçkin S, Albayrak L, Uğurlu M. Polypoid lesions of the gallbladder: report of 100 cases with special reference to operative indications. *Surgery* 2000; **127**: 622-627 [PMID: 10840356 DOI: 10.1067/msy.2000.105870]
29 **Segawa K**, Arisawa T, Niwa Y, Suzuki T, Tsukamoto Y, Goto H, Hamajima E, Shimodaira M, Ohmiya N. Prevalence of gallbladder polyps among apparently healthy Japanese: ultrasonographic study. *Am J Gastroenterol* 1992; **87**: 630-633 [PMID: 1595653]
30 **Shinchi K**, Kono S, Honjo S, Imanishi K, Hirohata T. Epidemiology of gallbladder polyps: an ultrasonographic study of male self-defense officials in Japan. *Scand J Gastroenterol* 1994; **29**: 7-10 [PMID: 8128179]
31 **Lin WR**, Lin DY, Tai DI, Hsieh SY, Lin CY, Sheen IS, Chiu CT. Prevalence of and risk factors for gallbladder polyps detected by ultrasonography among healthy Chinese: analysis of 34 669 cases. *J Gastroenterol Hepatol* 2008; **23**: 965-969 [PMID: 17725602 DOI: 10.1111/j.1440-1746.2007.05071.x]

P- Reviewer: Li YM, Nagem RG, Tolone S **S- Editor**: Ma YJ
L- Editor: A **E- Editor**: Liu XM

World Journal of Gastroenterology

Submit a Manuscript: http://www.wjgnet.com/esps/
Help Desk: http://www.wjgnet.com/esps/helpdesk.aspx
DOI: 10.3748/wjg.v21.i14.4255

World J Gastroenterol 2015 April 14; 21(14): 4255-4260
ISSN 1007-9327 (print) ISSN 2219-2840 (online)

ORIGINAL ARTICLE

Retrospective Study

Correlation between metastatic lymph node ratio and prognosis in patients with extrahepatic cholangiocarcinoma

Jian-Wei Zhang, Yun-Mian Chu, Zhong-Min Lan, Xiao-Long Tang, Ying-Tai Chen, Cheng-Feng Wang, Xu Che

Jian-Wei Zhang, Yun-Mian Chu, Zhong-Min Lan, Xiao-Long Tang, Ying-Tai Chen, Cheng-Feng Wang, Xu Che, Department of Abdominal Surgery, Cancer Hospital, Chinese Academy of Medical Sciences and Peking Union Medical College, Beijing 100021, China

Author contributions: Zhang JW and Chu YM contributed equally to this work; Che X designed the research; Chu YM, Lan ZM and Tang XL performed the research; Zhang JW contributed new reagents/analytic tools; Chen YT and Wang CF analyzed the data; Chu YM and Lan ZM wrote the paper.

Ethics approval: The study was reviewed and approved by the Cancer Institute and Hospital, Chinese Academy of Medical Sciences and Peking Union Medical College Institutional Review Board.

Informed consent: All study participants or their legal guardian provided informed written consent prior to study enrollment.

Data sharing: No additional data are available.

Correspondence to: Xu Che, MD, Department of Abdominal Surgery, Cancer Hospital, Chinese Academy of Medical Sciences and Peking Union Medical College, No. 17 Panjiayuan Nanli, Chaoyang District, Beijing 100021, China. xu.che@cicams.ac.cn
Telephone: +86-10-87787120
Fax: +86-10-87787120

Received: September 30, 2014
Peer-review started: October 14, 2014
First decision: October 29, 2014
Revised: January 16, 2015
Accepted: February 11, 2015
Article in press: February 11, 2015
Published online: April 14, 2015

Abstract

AIM: To investigate the prognostic value of metastatic lymph node ratio (MLNR) in extrahepatic cholangiocarcinoma (ECC) patients undergoing radical resection.

METHODS: Seventy-eight patients with ECC were enrolled. Associations between various clinicopathologic factors and prognosis were investigated by Kaplan-Meier analyses. The Cox proportional-hazards model was used for multivariate survival analysis.

RESULTS: The overall three- and five-year survival rates were 47.26% and 23.99%, respectively. MLNR of 0, 0-0.2, 0.2-0.5, and > 0.5 corresponded to five-year survival rates of 28.59%, 21.60%, 18.84%, and 10.03%, respectively. Univariate analysis showed that degree of tumor differentiation, lymph node metastasis, MLNR, tumor-node-metastasis (TNM) stage, and margin status were closely associated with postoperative survival in ECC patients ($P < 0.05$). Multivariate analysis showed that MLNR and TNM stage were independent prognostic factors after pancreaticoduodenectomy (HR = 2.13, 95%CI: 1.45-3.11; $P < 0.01$; and HR = 1.97, 95%CI: 1.17-3.31; $P = 0.01$, respectively). The median survival time for MLNR > 0.5, 0.2-0.5, 0-0.2, and 0 was 15 mo, 24 mo, 23 mo, and 35.5 mo, respectively. There were statistical differences in survival time between patients with different MLNR ($\chi^2 = 15.38$; $P < 0.01$).

CONCLUSION: MLNR is an independent prognostic factor for ECC patients after radical resection and is useful for predicting postoperative survival.

Key words: Cholangiocarcinoma; Metastatic lymph node; Prognosis; Surgery

Core tip: This study aims to investigate the prognostic significance of metastatic lymph node ratio in extrahepatic cholangiocarcinoma patients undergoing radical resection. Using univariate and multivariate

analysis, we found that metastatic lymph node ratio was an independent prognostic factor for these patients after radical resection and is useful for predicting postoperative survival.

Zhang JW, Chu YM, Lan ZM, Tang XL, Chen YT, Wang CF, Che X. Correlation between metastatic lymph node ratio and prognosis in patients with extrahepatic cholangiocarcinoma. *World J Gastroenterol* 2015; 21(14): 4255-4260 Available from: URL: http://www.wjgnet.com/1007-9327/full/v21/i14/4255.htm DOI: http://dx.doi.org/10.3748/wjg.v21.i14.4255

INTRODUCTION

Cholangiocarcinoma (CCA) is a malignant tumor that originates from the intra- and extrahepatic biliary epithelium, and it accounts for approximately 3% of all gastrointestinal malignancies[1]. Patients with liver fluke infestation, chronic viral hepatitis, choledochal cysts, and primary sclerosing cholangitis can develop CCA[2]. Intrahepatic CCA arises within the hepatic parenchyma, and most often presents as a mass lesion without major bile duct obstruction or jaundice[3]. Extrahepatic cholangiocarcinoma (ECC) is defined as common bile duct CCA, which accounts for 20%-40% of CCA cases[4]. At present, surgical resection remains the only treatment choice for ECC patients. However, the curative rate of ECC has been low for patients in advanced stages[5]. Even with complete resection of the tumors, most patients are subject to local recurrence or distant metastasis[6]. According to the staging of extrahepatic bile duct cancer, the number of metastatic lymph nodes is a key parameter for tumor staging and prognosis prediction. Lymph node metastasis is a prognostic factor for survival of ECC patients after curative resection[7], and those with peripheral lymph node metastases had notably poorer prognosis.

Metastatic lymph node ratio (MLNR), the ratio of the number of metastatic lymph nodes to the number of lymph nodes removed, is regarded as an important prognostic factor for various tumors[8-14]. However, there are few studies examining the association between MLNR and prognosis in ECC patients. In this study, we analyzed multiple clinicopathologic factors in ECC patients, and investigated the potential association between lymph node metastasis and prognosis. We aimed to find reliable indicators for predicting the prognosis of ECC patients following radical resection.

MATERIALS AND METHODS

Study population

A total of 128 ECC patients were recruited from the Cancer Hospital of Chinese Academy of Medical Sciences between January 1999 and January 2012. The recruited patients needed to meet the following inclusion criteria: (1) complete clinical data available; (2) pathologically confirmed ECC after surgery; (3) neoadjuvant chemoradiotherapy-naïve before surgery; (4) complete follow-up record available (until January 2014); and (5) absence of liver disease or other diseases. All patients received pancreaticoduodenectomy and preoperative assessment, including a detailed history and physical, laboratory, and radiologic examinations. All patients underwent enhanced abdominal CT/magnetic resonance imaging, abdominal ultrasound, and determination of serum tumor markers.

The tumors were classified based on the tumor-node-metastasis (TNM) classification criteria of the American Joint Committee on Cancer (AJCC), 6th edition[15]. The clinicopathologic data analyzed in this study included: age, sex, duration of operation, intraoperative blood loss, tumor differentiation, tumor embolism, perineural invasion, T component of TNM stage, TNM stage, margin status, postoperative adjuvant chemotherapy, total number of dissected lymph nodes, lymph node status, and MLNR.

All patients underwent lymphadenectomy; based on the Japanese Pancreatic Society classification of pancreatic cancer, the extent of lymphadenectomy was defined as follows: around the pancreas and duodenum (stations 13 and 17), inside the hepatoduodenal ligament (station 12), around the stomach (stations 1-6), around the hepatic artery proper (station 8), and around the superior mesenteric artery (station 14).

Data on the total number of lymph nodes dissected and the number of lymph node metastases were obtained from pathologic reports. Patients were divided into four groups according to the MLNR values: patients with negative lymph nodes (MLNR = 0), and patients with positive lymph nodes (0 < MLNR < 0.2, 0.2 < MLNR < 0.5 and 0.5 < MLNR).

Follow-up

Follow-up was performed *via* telephone or mail, and all outpatient records were reviewed. The first follow-up visit was made at 6 mo after surgery. It was then continued every 6-12 mo until March 2014.

Statistical analysis

Statistical analysis was performed using the SAS v 9.2 (SAS Institute Inc., Cary, NC, United States). The life-table method was used to calculate the three- and five-year survivals. The Kaplan-Meier method was used to construct survival curves, which were compared using the log-rank test. Multivariate analysis of prognostic factors was performed using the Cox proportional-hazards model. Survival was calculated from the day of surgery to the time of death (for non-surviving patients) or to the last follow-up (until March 2014 for surviving patients or patients who dropped out). $P < 0.05$ was considered statistically significant.

Table 1 Clinicopathologic factors and prognosis

Clinicopathologic factors	No. of patients	Survival (%)		*P* value[a]
		3-yr	5-yr	
Total cases	78	47.26	23.99	
Age (yr)				0.388
≤ 60	46	57.14	28.57	
> 60	32	45.22	26.65	
Sex				0.748
Male	51	46.92	21.90	
Female	27	48.48	36.36	
Duration of surgery (min)				0.763
≤ 300	41	46.27	27.76	
> 300	37	47.98	18.66	
Intraoperative blood loss (mL)				0.337
≤ 500	47	57.14	28.57	
> 500	31	46.34	26.42	
Differentiation degree				< 0.01
Highly	24	61.32	33.45	
Moderately	44	50.00	28.04	
Poorly	10	23.08	15.38	
Perineural invasion				0.435
Yes	57	38.72	14.75	
No	21	68.38	48.84	
Tumor embolism				0.183
Yes	3	33.33	33.33	
No	75	47.94	25.68	
T stage				0.369
T1	2	100	50	
T2	7	53.07	33.77	
T3	24	46.05	21.98	
T4	45	37.40	18.70	
Total number of lymph node dissected				0.179
≤ 15	30	45.92	26.53	
> 15	48	39.39	26.26	
Lymph node metastasis				0.010
Yes	55	37.74	17.56	
No	23	70.13	28.59	
MLNR				0.002
0	23	70.13	28.59	
0-0.2	12	54.01	21.60	
0.2-0.5	18	48.34	18.84	
> 0.5	25	33.67	10.03	
TNM stage				0.044
Ⅰ	2	54.83	27.95	
Ⅱ	26	41.67	21.03	
Ⅲ	50	35.06	17.53	
Cutting edge				0.043
Negative	75	54.36	25.02	
Positive	3	33.33	10.00	
Postoperative chemotherapy				0.055
Yes	64	54.55	22.02	
No	14	46.80	22.40	

[a]Log-rank test. MLNR: Metastatic lymph node ratio; TNM: Tumor-node-metastasis.

RESULTS

Patient general data

Seventy-eight patients, including 51 men and 27 women, were included in the final analysis. Their average age was 60.2 years, ranging from 42 to 78 years. Two patients were classified as stage Ⅰ, 26 as stage Ⅱ, and 50 as stage Ⅲ. Fifty-five patients were diagnosed with lymph node metastasis. The average number of dissected lymph nodes was 15.4 (range: 10-36). Forty-two patients were lost to follow-up. Eight patients were excluded, among who four were without complete clinical information, two were diagnosed with non-ECC, one had received adjuvant chemotherapy before operation, and one had received interventional chemotherapy before operation.

Table 2 Multivariate analysis for predictive factors of extrahepatic cholangiocarcinoma patient survival

Factors	β	SD	χ^2	*P* value	HR	95%CI
MLNR	0.75	0.19	15.01	< 0.01	2.13	1.45–3.11
TNM stage	0.67	0.26	6.55	0.011	1.97	1.17–3.31

MLNR: Metastatic lymph node ratio; TNM: Tumor-node-metastasis.

Survival rates

The overall three- and five-year survival rates were 47.26% and 23.99%, respectively. There were no statistically significant differences in the survival rates with regard to age, sex, duration of surgery, intraoperative blood loss, perineural invasion, tumor embolism, T stage, number of lymph node dissected, or postoperative chemotherapy. The three- and five-year survival rates of patients with peripheral lymph node metastasis (37.74% and 17.56%, respectively) were lower than those without peripheral lymph node metastasis (70.13% and 28.59%, respectively), and the differences were statistically significant (*P*s < 0.05). Five-year survival rates according to MLNR were: 28.59% (MLNR = 0), 21.60% (MLNR = 0-0.2), 18.84% (MLNR = 0.2-0.5), and 10.03% (MLNR > 0.05).

Associations between clinicopathologic factors and postoperative survival

Univariate analyses showed that degree of tumor differentiation, lymph node metastasis, MLNR, TNM stage, and margin status were significantly correlated with postoperative survival in ECC patients (all $P < 0.05$) (Table 1). Furthermore, the Cox proportional-hazard model for multivariate analysis was used to further investigate these factors, showing that MLNR and TNM stage were independent predictors of survival (Table 2).

Survival curves

To further determine the effects of MLNR and TNM stage on prognosis of patients, survival curves were established. Median survival time for regional lymph node metastases > 0.5, 0.2-0.5, 0-0.2, and 0 were 15 mo, 24 mo, 23 mo, and 35.5 mo, respectively. The log-rank test revealed significant differences in survival time among patients with different MLNR values ($\chi^2 = 15.376$; $P < 0.01$) (Figure 1A). Median survival time for TNM stage Ⅰ, Ⅱ, and Ⅲ were 15.5 mo, 24.0 mo, 23.0 mo, and 35.5 mo, respectively, with significant differences ($\chi^2 = 15.376$; $P < 0.01$) (Figure 1B).

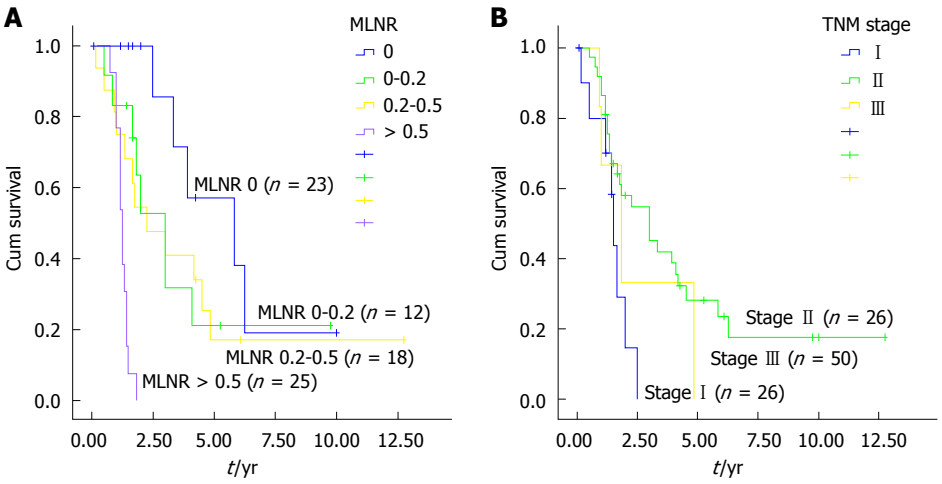

Figure 1 Survival curves of extrahepatic cholangiocarcinoma patients using a Cox model. A: Survival curves of extrahepatic cholangiocarcinoma (ECC) patients with different metastatic lymph node ratio (MLNR) values; B: Survival curves of ECC patients with different tumor-node-metastasis (TNM) stages.

DISCUSSION

Some factors have been found for the prognosis of CCA[16-21]. However, there are few studies on survival outcomes and prognostic factors of ECC patients[22]. The TNM staging system has been widely applied as a simple, convenient, and repeatable method. For ECC patients, the N component, or description of the involvement of regional lymph nodes, is based on the number and location of metastatic lymph nodes retrieved intraoperatively, and is used to predict prognosis. According to the 6th edition of the AJCC Cancer Staging Manual, lymphadenectomy should be considered in patients with more than 15 lymph nodes, which is evaluated as the N component of the TNM stage[23]. All these indicate that the N component may not accurately predict prognosis of ECC patients with fewer than 15 lymph nodes removed. However, the number of lymph nodes removed is often dictated by the knowledge and skill of the surgeon and pathologist. Therefore, MLNR is a more reliable prognostic factor than the number of metastatic lymph nodes[24], and the prognostic value of MLNR is not influenced by the scope of lymph node dissection[25-27].

In the present study, we performed univariate and multivariate analyses to investigate the role of MLNR in prognosis prediction of ECC patients, and found that MLNR is an independent prognostic factor. We also analyzed the prognostic values of other lymph node-related indicators and found that lymph node metastasis, but not the total number of lymph nodes dissected, was closely associated with prognosis. In a retrospective analysis of 93 intrahepatic CCA patients, Tamandl *et al*[28] verified that the total number of lymph nodes dissected was not associated with prognosis. Although no evidence has demonstrated that dissection of more lymph nodes improves the prognosis, extended lymphadenectomy can more accurately identify the status of lymph node metastasis and predict prognosis[29]. As the scope of lymphadenectomy during radical resection of ECC remains controversial, MLNR is particularly important for evaluating the prognosis of ECC patients, which can represent the number and location of metastatic lymph nodes. Furthermore, calculation of MLNR is a simple and highly repeatable method for stratification of outcomes and takes into account not only the number of dissected lymph nodes, but also biologic behavior (*i.e.*, number of positive lymph nodes).

In the present study, MLNR was found to be an independent prognostic indicator of long-term patient survival; a higher MLNR value predicted poorer biologic behavior and prognosis. MLNR can be used in postoperative stratification of ECC patients, *i.e.*, assessment of the appropriateness of further treatment or enrollment in future clinical trials.

In summary, MLNR is an independent prognostic factor for ECC patients who underwent pancreaticoduodenal resection. MLNR can be used as an important tool in postoperative pathologic evaluation to predict prognosis and facilitate stratification for treatment. More cases of ECC should be considered in further studies for verifying the association between MLNR and survival.

COMMENTS

Background

Extrahepatic cholangiocarcinoma (ECC) is a gastrointestinal malignancy with poor prognosis. Surgical resection remains the only treatment choice for ECC. However, the curative rate of ECC has been low for patients diagnosed with advanced stages. There are no effective methods for predicting postoperative survival of patients with ECC.

Research frontiers

Metastatic lymph node ratio (MLNR), the ratio of the number of metastatic lymph nodes to the number of lymph nodes removed, is known as an important prognostic factor for various tumors.

Innovations and breakthroughs

There are few studies examining the association between MLNR and prognosis in ECC patients. The authors firstly investigated the prognostic factors for ECC in a Chinese population. A total of 128 ECC cases were collected from January

1999 to January 2012. Multivariate analysis was performed to investigate the association between clinicopathologic factors and the survival of ECC patients. The Kaplan-Meier method was used to construct survival curves and to investigate the clinicopathologic factors for the survival of ECC patients.

Applications

MLNR is an independent prognostic factor for patients with ECC after radical resection, which may be used as an index for predicting postoperative survival.

Terminology

Cholangiocarcinoma is a malignant tumor that originates from the intra- and extrahepatic biliary epithelium, and accounts for ~3% of all gastrointestinal malignancies. ECC is defined as cholangiocarcinoma of the common bile duct, which accounts for 20-40% of the cases.

Peer-review

It is a good retrospective study in which the authors investigated the prognostic factors for patients with ECC. The results are interesting and suggest that MLNR is an independent prognostic factor for patients with distal cholangiocarcinoma after radical resection and is useful for predicting postoperative survival.

REFERENCES

1 **Shin HR**, Oh JK, Masuyer E, Curado MP, Bouvard V, Fang YY, Wiangnon S, Sripa B, Hong ST. Epidemiology of cholangiocarcinoma: an update focusing on risk factors. *Cancer Sci* 2010; **101**: 579-585 [PMID: 20085587 DOI: 10.1111/j.1349-7006.2009.01458.x]

2 **Braconi C**, Patel T. Cholangiocarcinoma: new insights into disease pathogenesis and biology. *Infect Dis Clin North Am* 2010; **24**: 871-84, vii [PMID: 20937455 DOI: 10.1016/j.idc.2010.07.006]

3 **Bridgewater J**, Galle PR, Khan SA, Llovet JM, Park JW, Patel T, Pawlik TM, Gores GJ. Guidelines for the diagnosis and management of intrahepatic cholangiocarcinoma. *J Hepatol* 2014; **60**: 1268-1289 [PMID: 24681130 DOI: 10.1016/j.jhep.2014.01.021]

4 **Nishimura M**, Naka S, Hanazawa K, Tani T, Fukami M, Okada S, Fujiyama Y. Cholangiocarcinoma in the distal bile duct: a probable etiologic association with choledocholithiasis. *Dig Dis Sci* 2005; **50**: 2153-2158 [PMID: 16240231 DOI: 10.1007/s10620-005-3023-9]

5 **Gwak HK**, Kim WC, Kim HJ, Park JH. Extrahepatic bile duct cancers: surgery alone versus surgery plus postoperative radiation therapy. *Int J Radiat Oncol Biol Phys* 2010; **78**: 194-198 [PMID: 19910130 DOI: 10.1016/j.ijrobp.2009.07.003]

6 **Murakami Y**, Uemura K, Sudo T, Hayashidani Y, Hashimoto Y, Nakamura H, Nakashima A, Sueda T. Adjuvant gemcitabine plus S-1 chemotherapy improves survival after aggressive surgical resection for advanced biliary carcinoma. *Ann Surg* 2009; **250**: 950-956 [PMID: 19953713 DOI: 10.1097/SLA.0b013e3181b0fc8b]

7 **Kim HJ**, Kim CY, Hur YH, Koh YS, Kim JC, Kim HJ, Cho CK. The prognostic factors for survival after curative resection of distal cholangiocarcinoma: perineural invasion and lymphovascular invasion. *Surg Today* 2014; **44**: 1879-1886 [PMID: 24535697 DOI: 10.1007/s00595-014-0846-z]

8 **Berger AC**, Sigurdson ER, LeVoyer T, Hanlon A, Mayer RJ, Macdonald JS, Catalano PJ, Haller DG. Colon cancer survival is associated with decreasing ratio of metastatic to examined lymph nodes. *J Clin Oncol* 2005; **23**: 8706-8712 [PMID: 16314630 DOI: 10.1200/JCO.2005.02.8852]

9 **Nitti D**, Marchet A, Olivieri M, Ambrosi A, Mencarelli R, Belluco C, Lise M. Ratio between metastatic and examined lymph nodes is an independent prognostic factor after D2 resection for gastric cancer: analysis of a large European monoinstitutional experience. *Ann Surg Oncol* 2003; **10**: 1077-1085 [PMID: 14597447 DOI: 10.1245/ASO.2003.03.520]

10 **Riediger H**, Keck T, Wellner U, zur Hausen A, Adam U, Hopt UT, Makowiec F. The lymph node ratio is the strongest prognostic factor after resection of pancreatic cancer. *J Gastrointest Surg* 2009; **13**: 1337-1344 [PMID: 19418101 DOI: 10.1007/s11605-009-0919-2]

11 **Vinh-Hung V**, Verkooijen HM, Fioretta G, Neyroud-Caspar I, Rapiti E, Vlastos G, Deglise C, Usel M, Lutz JM, Bouchardy C. Lymph node ratio as an alternative to pN staging in node-positive breast cancer. *J Clin Oncol* 2009; **27**: 1062-1068 [PMID: 19164210 DOI: 10.1200/JCO.2008.18.6965]

12 **Liu YP**, Ma L, Wang SJ, Chen YN, Wu GX, Han M, Wang XL. Prognostic value of lymph node metastases and lymph node ratio in esophageal squamous cell carcinoma. *Eur J Surg Oncol* 2010; **36**: 155-159 [PMID: 19854606 DOI: 10.1016/j.ejso.2009.09.005]

13 **Falconi M**, Crippa S, Domínguez I, Barugola G, Capelli P, Marcucci S, Beghelli S, Scarpa A, Bassi C, Pederzoli P. Prognostic relevance of lymph node ratio and number of resected nodes after curative resection of ampulla of Vater carcinoma. *Ann Surg Oncol* 2008; **15**: 3178-3186 [PMID: 18712568 DOI: 10.1245/s10434-008-0099-4]

14 **Espín F**, Bianchi A, Llorca S, Feliu J, Palomera E, García O, Remon J, Suñol X. Metastatic lymph node ratio versus number of metastatic lymph nodes as a prognostic factor in gastric cancer. *Eur J Surg Oncol* 2012; **38**: 497-502 [PMID: 22445061 DOI: 10.1016/j.ejso.2012.01.012]

15 **Greene FL**. TNM staging for malignancies of the digestive tract: 2003 changes and beyond. *Semin Surg Oncol* 2003; **21**: 23-29 [PMID: 12923913 DOI: 10.1002/ssu.10018]

16 **Nitta T**, Sato Y, Ren XS, Harada K, Sasaki M, Hirano S, Nakanuma Y. Autophagy may promote carcinoma cell invasion and correlate with poor prognosis in cholangiocarcinoma. *Int J Clin Exp Pathol* 2014; **7**: 4913-4921 [PMID: 25197362]

17 **Wang W**, Zhang J, Zhan X, Lin T, Yang M, Hu J, Han B, Hu S. SOX4 is associated with poor prognosis in cholangiocarcinoma. *Biochem Biophys Res Commun* 2014; **452**: 614-621 [PMID: 25181339 DOI: 10.1016/j.bbrc.2014.08.124]

18 **Park KW**, Jung ES, Kim DG, Yoo YK, Hong TH, Lee IS, Koh YH, Kim JH, Lee MA. ERCC1 Can Be a Prognostic Factor in Hilar Cholangiocarcinoma and Extrahepatic Bile Duct Cancer, But Not in Intrahepatic Cholangiocarcinoma. *Cancer Res Treat* 2013; **45**: 63-69 [PMID: 23613672 DOI: 10.4143/crt.2013.45.1.63]

19 **Cai WK**, Lin JJ, He GH, Wang H, Lu JH, Yang GS. Preoperative serum CA19-9 levels is an independent prognostic factor in patients with resected hilar cholangiocarcinoma. *Int J Clin Exp Pathol* 2014; **7**: 7890-7898 [PMID: 25550829]

20 **Dong ZR**, Zhang C, Cai JB, Zhang PF, Shi GM, Gao DM, Sun HC, Qiu SJ, Zhou J, Ke AW, Fan J. Role of 5-hydroxymethylcytosine level in diagnosis and prognosis prediction of intrahepatic cholangiocarcinoma. *Tumour Biol* 2014; Epub ahead of print [PMID: 25480415 DOI: 10.1007/s13277-014-2900-2]

21 **Tian X**, Wang Q, Li Y, Hu J, Wu L, Ding Q, Zhang C. The expression of S100A4 protein in human intrahepatic cholangiocarcinoma: clinicopathologic significance and prognostic value. *Pathol Oncol Res* 2015; **21**: 195-201 [PMID: 24985031 DOI: 10.1007/s12253-014-9806-6]

22 **Murakami Y**, Uemura K, Sudo T, Hashimoto Y, Kondo N, Nakagawa N, Muto T, Sasaki H, Urabe K, Sueda T. Perineural invasion in extrahepatic cholangiocarcinoma: prognostic impact and treatment strategies. *J Gastrointest Surg* 2013; **17**: 1429-1439 [PMID: 23797881 DOI: 10.1007/s11605-013-2251-0]

23 **Kulig J**, Sierzega M, Kolodziejczyk P, Popiela T. Ratio of metastatic to resected lymph nodes for prediction of survival in patients with inadequately staged gastric cancer. *Br J Surg* 2009; **96**: 910-918 [PMID: 19591164 DOI: 10.1002/bjs.6653]

24 **Yu JX**, Li Y. The staging system of metastatic lymph node ratio in gastric cancer. *Clin Oncol* (R Coll Radiol) 2007; **19**: 269-270 [PMID: 17433973 DOI: 10.1016/j.clon.2007.02.003]

25 **Marchet A**, Mocellin S, Ambrosi A, Morgagni P, Garcea D, Marrelli D, Roviello F, de Manzoni G, Minicozzi A, Natalini G, De Santis F, Baiocchi L, Coniglio A, Nitti D. The ratio between metastatic and examined lymph nodes (N ratio) is an independent prognostic factor in gastric cancer regardless of the type of lymphadenectomy: results from an Italian multicentric study in 1853 patients. *Ann Surg* 2007; **245**: 543-552 [PMID: 17414602 DOI: 10.1097/01.sla.0000250423.43436.e1]

26 **Xu DZ**, Geng QR, Long ZJ, Zhan YQ, Li W, Zhou ZW, Chen YB, Sun XW, Chen G, Liu Q. Positive lymph node ratio is an independent prognostic factor in gastric cancer after d2 resection regardless of the examined number of lymph nodes. *Ann Surg*

Oncol 2009; **16**: 319-326 [PMID: 19050970 DOI: 10.1245/s10434-008-0240-4]

27 **Kim CY**, Yang DH. Adjustment of N stages of gastric cancer by the ratio between the metastatic and examined lymph nodes. *Ann Surg Oncol* 2009; **16**: 1868-1874 [PMID: 19434459 DOI: 10.1245/s10434-009-0430-8]

28 **Tamandl D**, Kaczirek K, Gruenberger B, Koelblinger C, Maresch J, Jakesz R, Gruenberger T. Lymph node ratio after curative surgery for intrahepatic cholangiocarcinoma. *Br J Surg* 2009; **96**: 919-925 [PMID: 19591163 DOI: 10.1002/bjs.6654]

29 **Kawai M**, Tani M, Kobayashi Y, Tsuji T, Tabuse K, Horiuchi T, Oka M, Yamaguchi K, Sakata Y, Shimomura T, Yamaue H. The ratio between metastatic and examined lymph nodes is an independent prognostic factor for patients with resectable middle and distal bile duct carcinoma. *Am J Surg* 2010; **199**: 447-452 [PMID: 19596119 DOI: 10.1016/j.amjsurg.2009.01.019]

P- Reviewer: Andersson RG, Parsi MA, Pinlaor S, Plentz RR, Vegso G
S- Editor: Ma YJ **L- Editor**: AmEditor **E- Editor**: Ma S

World Journal of Gastroenterology

Submit a Manuscript: http://www.wjgnet.com/esps/
Help Desk: http://www.wjgnet.com/esps/helpdesk.aspx
DOI: 10.3748/wjg.v21.i14.4261

World J Gastroenterol 2015 April 14; 21(14): 4261-4267
ISSN 1007-9327 (print) ISSN 2219-2840 (online)

ORIGINAL ARTICLE

Retrospective Study

Biliary tract intraductal papillary mucinous neoplasm: Report of 19 cases

Xing Wang, Yun-Qiang Cai, Yong-Hua Chen, Xu-Bao Liu

Xing Wang, Yun-Qiang Cai, Yong-Hua Chen, Xu-Bao Liu, Department of Hepatopancreatobiliary Surgery, West China Hospital, Sichuan University, Chengdu 610041, Sichuan Province, China

Author contributions: Wang X and Liu XB designed the research; Wang X, Cai YQ, and Chen YH performed the research and analyzed the data; Wang X and Cai YQ wrote the paper; Liu XB proofread and revised the manuscript; all authors approved the version to be published.

Supported by The Research Special Fund for Public Welfare Industry of Health, No. 201202007.

Conflict-of-interest: There is no conflict of interest of the authors.

Data sharing: No additional data are available.

Correspondence to: Xu-Bao Liu, MD, PhD, Department of Hepatopancreatobiliary Surgery, West China Hospital, Sichuan University, No. 37 GuoXue Alley, Chengdu 610041, Sichuan Province, China. shoubulele@gmail.com
Telephone: +86-28-85422477
Fax: +86-28-85422474

Received: September 2, 2014
Peer-review started: September 3, 2014
First decision: November 14, 2014
Revised: November 21, 2014
Accepted: January 8, 2015
Article in press: January 8, 2015
Published online: April 14, 2015

Abstract

AIM: To gain a better understanding of biliary tract intraductal papillary mucinous neoplasm (BT-IPMN).

METHODS: From January 2000 to December 2013, 19 cases of BT-IPMN were retrospectively identified from a total of 343 biliary tract tumors resected in our single institution. Demographic characteristics, clinical data, pathology, surgical strategies, and long-term follow-up were analyzed.

RESULTS: The mean age of the 19 BT-IPMN cases was 53.8 years (range: 25-74 years). The most common symptom was abdominal pain (15/19; 78.9%), followed by jaundice (7/19; 36.8%). Cholangitis was associated with most (16/19; 84.2%) of the BT-IPMN cases. Macroscopically visible mucin was detected in all 19 patients, based on original surgical reports. The most common abnormal preoperative imaging findings for BT-IPMN were bile duct dilation (19/19; 100%) and intraluminal masses (10/19; 52.6%). Thirteen (68.4%) cases involved the intrahepatic bile duct and hilum. We performed left hepatectomy in 11/19 (57.9%), right hepatectomy in 2/19 (10.5%), bile duct resection in 4/19 (21.1%), and pancreatoduodenectomy in 1/19 (5.3%) patients. One (5.3%) patient was biopsied and received a choledochojejunostomy because of multiple tumors involving the right extrahepatic and left intrahepatic bile ducts. Histology showed malignancy in 10/19 (52.6%) patients. The overall median survival was 68 mo. The benign cases showed a non-significant trend towards improved survival compared to malignant cases (68 mo *vs* 48 mo, $P = 0.347$). The patient without tumor resection died of liver failure 22 mo after palliative surgery.

CONCLUSION: BT-IPMN is a rare biliary entity. Complete resection of the tumor is associated with good survival, even in patients with malignant disease.

Key words: Biliary tract; Cystic tumor; Intraductal papillary mucinous neoplasm; Mucinous tumor; Papillary tumor

Core tip: Our study involved a large number of patients with biliary tract intraductal papillary mucinous neoplasm (BT-IPMN) from a large Chinese institution. We summarized the clinical features, radiologic findings, pathology, surgical strategies, and long-term follow-up of these patients to achieve a better understanding of this rare disease. Our findings indicated that BT-IPMN is a rare biliary entity and complete resection of the tumor is associated with good survival, even in patients with malignant disease.

Wang X, Cai YQ, Chen YH, Liu XB. Biliary tract intraductal papillary mucinous neoplasm: Report of 19 cases. *World J Gastroenterol* 2015; 21(14): 4261-4267 Available from: URL: http://www.wjgnet.com/1007-9327/full/v21/i14/4261.htm DOI: http://dx.doi.org/10.3748/wjg.v21.i14.4261

INTRODUCTION

In the past decade, biliary tract intraductal papillary mucinous neoplasm (BT-IPMN) has been increasingly recognized as a unique type of biliary neoplasm, coinciding with widespread acceptance of the nomenclature of pancreatic intraductal papillary mucinous neoplasm (P-IPMN)[1-3]. As the name suggests, BT-IPMN is known to be a biliary counterpart of P-IPMN, but with its own separate identity[4-9]. BT-IPMN is histologically defined as a mucinous and papillary neoplasm, with a clear origin from the biliary epithelium, with solitary or diffuse intraductal growth[1]. It is a rare neoplasm involving the intra- and extrahepatic biliary tract and is characterized by mucin-secreting papillary and/or cystic lesions. BT-IPMN is recognized as a precursor of invasive carcinoma (tubular adenocarcinoma or mucinous carcinoma) and 40%-80% of resected BT-IPMNs contain invasive components[10-12]. BT-IPMN has a more favorable prognosis compared with conventional cholangiocarcinoma[13,14]. The number of reports of BT-IPMN with strict histopathologic criteria is limited. Moreover, most of the data regarding BT-IPMN are from retrospective studies with small samples. There is still controversy about several aspects of BT-IPMN, and the clinicopathologic characteristics, surgical strategies, and prognosis of BT-IPMN are largely unclear[1,2,7].

Our study involved a large number of patients with BT-IPMN from a large Chinese institution. The purpose of this study was to summarize the demographic and clinical features, radiologic findings, pathology, surgical strategies, and long-term follow-up of patients with BT-IPMN for a better understanding of this rare disease.

MATERIALS AND METHODS

Patient selection

From January 2000 to December 2013, 19 patients with BT-IPMN were retrospectively identified in our institution. All diagnoses were established using strict histopathologic criteria for BT-IPMN: a mucinous and papillary neoplasm demonstrating clear origin from the biliary epithelium, with solitary or diffuse intraductal growth[1]. We excluded mucinous cystic neoplasms of the liver (with ovarian or mesenchymal stroma)[15], lesions originating from the periampullary region of the duodenum[16], and lesions without microscopic or macroscopic mucin secretion. All 19 BT-IPMNs were histologically classified into benign (low- or middle-grade dysplasia) and malignant (high-grade dysplasia or invasive carcinoma)[17].

Data collection

Clinical data were obtained from the electronic medical records or external medical reports. Demographic characteristics, clinical presentation, preoperative evaluation, pathology, surgical therapy, postoperative course, and long-term outcomes were included. Postoperative complications (all events recorded within 30 d after surgery) were included in our prospective complication database. Survival was measured from the date of operation to date of death or of last follow-up. We conducted telephone interviews and/or outpatient interview to follow-up these patients. This study was approved by the Ethics Committee of Sichuan University.

Statistical analysis

Survival probability was estimated using the Kaplan-Meier method. Statistical analysis was performed using SPSS version 16.0 (SPSS Inc., Chicago, IL, United States). A $P < 0.05$ was considered statistically significant.

RESULTS

Clinical presentation

Demographic characteristics of the 19 BT-IPMN patients, with a mean age of 53.8 years (range: 25-74 years), are shown in Table 1. The clinical features of these patients are shown in Table 2. Abdominal pain was the most common presenting symptom, and the majority of patients showed acute or chronic cholangitis.

Imaging characteristics

All patients underwent abdominal ultrasonography, and additional imaging examinations were also performed in many patients (Table 3). The bile duct was dilated in all cases, and intraluminal masses were observed in 10/19 (52.6%) cases (Figure 1). Biliary stones were detected in 12/19 (63.2%) patients, primarily located only in the proximal biliary duct (10/12; 83.3%).

Operative strategies and outcomes

The majority (11/19; 57.9%) of patients received

Table 1 Patient demographics (n = 19)

Feature	n (%)
Age (yr)	
⩽ 40	3 (15.8)
40-50	4 (21.1)
50-60	6 (31.6)
⩾ 60	6 (31.6)
Sex	
Male	11 (57.9)
Female	8 (42.1)

Table 2 Clinical features of biliary tract intraductal papillary mucinous neoplasm (n = 19)

Feature	n (%)
Presenting symptoms	
Abdominal pain	15 (78.9)
Jaundice	7 (36.8)
Weight loss	3 (15.8)
None	1 (5.3)
Schistosomiasis[1]	4 (21.1)
Presence of cholangitis	16 (84.2)
Repeated episodes cholangitis	6 (31.6)
Location	
Intrahepatic and hilum	13 (68.4)
Extrahepatic	5 (26.3)
Multifocal	1 (5.3)
Serum chemistry	
Elevated CEA (> 3.4 ng/dL)	5 (26.3)
Elevated CA 19-9 (> 22 U/mL)	8 (42.1)

[1]Detected by postoperative histologic examination. CA: Carbohydrate antigen; CEA: Carcinoembryonic antigen.

a left hepatectomy (Table 4). One patient required pancreaticoduodenectomy for tumor clearance and another received biopsy and choledochojejunostomy for multiple tumors of the extrahepatic and right and left intrahepatic bile ducts. No deaths occurred within 30 d after surgery, though 4/19 (21.1%) patients had postoperative complications. Bile leakage occurred with postoperative pneumonia in a 68-year-old patient who underwent local bile duct excision, resulting in a prolonged (65 d) hospitalization and readmission, which was cured through percutaneous drainage and antibiotics. In addition, three patients had postoperative complications that were cured by conservative therapy. Lymphadenectomy was routinely performed, however, no lymph node metastasis was detected in our series.

Gross appearance

The mean tumor size was 3.5 cm (range: 0.5-12 cm). The gross appearance of BT-IPMN varies with size. Smaller BT-IPMN tumors typically present as an intraluminal mass (Figure 2), though they can appear as cyst-like bile duct dilation. Intraluminal growing intraductal papillary neoplasms (10/19; 52.6%) and visible mucin (19/19; 100%) on the surface of the tumor were typical characteristics of BT-IPMN.

Table 3 Imaging features of biliary tract intraductal papillary mucinous neoplasm (n = 19)

Feature	n (%)
Biliary stones (n = 12)	
Proximal	10 (52.6)
Proximal and distal	2 (10.5)
Cholecystolithiasis	0 (0.0)
Dilated bile duct (n = 19)	
Proximal	6 (31.6)
Proximal and distal	13 (68.4)
Cyst	10 (52.6)
Lesion	10 (52.6)
Liver atrophy	7 (36.8)
Imaging examination	
Ultrasonography	19 (100)
Computed tomography	15 (78.9)
Magnetic resonance imaging	12 (63.2)
Intraoperative choledochoscopy	8 (42.1)
Endoscopic retrograde cholangiography	4 (21.1)

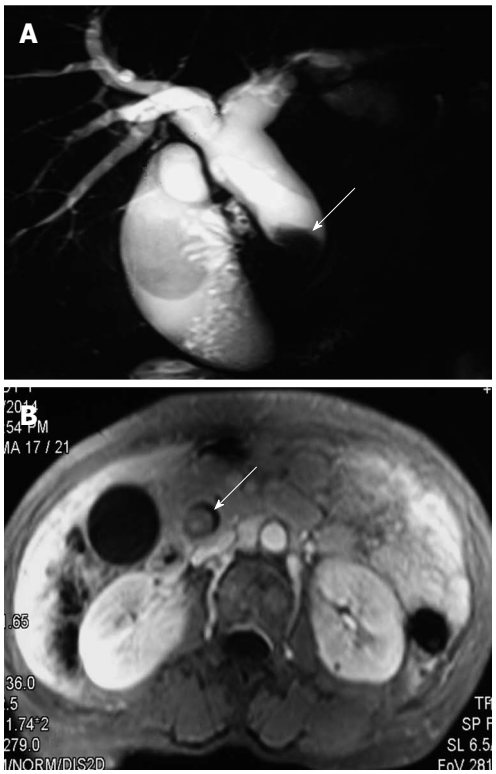

Figure 1 Imaging presentation of biliary tract intraductal papillary mucinous neoplasm. A: Magnetic resonance cholangiography shows dilation of proximal biliary tract and a filling defect in the extrahepatic biliary tract (arrow); B: Magnetic resonance imaging shows an intraluminal polypoid lesion originating from the extrahepatic biliary tract (arrow).

Histopathology

BT-IPMN is known to be classified into four histopathologic subtypes (gastric, intestinal, pancreatobiliary, and oncocytic) based on morphologic appearance and mucin staining properties[15], which are identical to those of P-IPMN. Microscopically, BT-IPMN was mucinous with papillary proliferation of biliary epithelial cells and intraductal growth. Mucin was observed with histopathology (Figure 3) in all 19 patients, and 10/19

Table 4 Operative strategies and outcomes for biliary tract intraductal papillary mucinous neoplasm (*n* = 19)

Feature	*n* (%)
Left hepatectomy (*n* = 11)	
Lobectomy	6 (31.6)
Segmentectomy	5 (26.3)
Right hepatectomy (*n* = 2)	
Segmentectomy	2 (10.5)
Pancreaticoduodenectomy	1 (5.3)
Bile duct excision	4 (21.1)
Biopsy and choledochojejunostomy	1 (5.3)
Complications (*n* = 4)	
Stress ulcer	1 (5.3)
Intra-abdominal abscess	1 (5.3)
Pneumonia and bile leakage	1 (5.3)
Wound infection	1 (5.3)
Pathology	
Benign	9 (47.4)
Malignant	10 (52.6)
Presence of mucin	
Macroscopic visible mucin	19 (100)
Microscopic mucin	19 (100)
Lymph node metastasis	0 (0.0)
Death (*n* = 8)	
Benign	3 (15.8)
Malignant	5 (26.3)

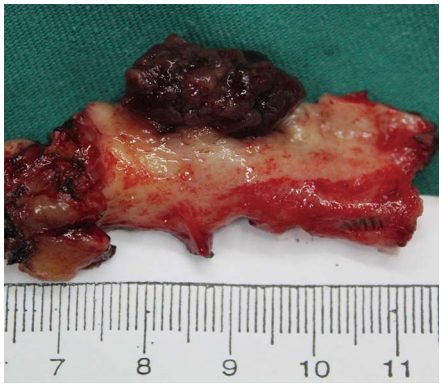

Figure 2 Gross appearance of resected specimen. Biliary tract intraductal papillary mucinous neoplasm appeared as a nodular lesion on the distal common bile duct with massive mucin deposition throughout.

(52.6%) cases were malignant (high-grade cytologic atypia), three of which had invasive components.

Follow-up and survival

All patients underwent imaging examinations every 6-12 mo after surgery, with a median follow-up of 73 mo. Margin-negative resection was achieved in 18/19 (94.7%) patients, and palliative surgery (choledochojejunostomy and biopsy) was performed in one patient with malignant multifocal BT-IPMN.

Overall median survival was 68 mo for the entire cohort; benign cases had a somewhat longer survival compared to malignant cases (68 mo *vs* 48 mo; P = 0.347) (Figure 4). Eight patients with BT-IPMN died; five malignant cases died due to tumors or tumor-related causes, including liver failure in one patient 22 mo after palliative surgery. Death in one benign

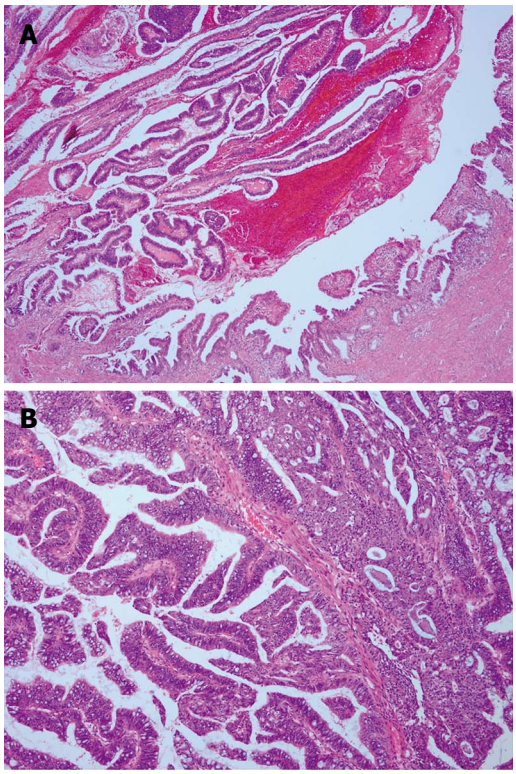

Figure 3 Histopathology of biliary tract intraductal papillary mucinous neoplasm. Hematoxylin and eosin staining of A: Common bile duct biliary tract intraductal papillary mucinous neoplasm, composed of papillary proliferation of atypical biliary epithelial cells (magnification × 40); and B: High-grade cytologic atypia and mucin in the numerous goblet cells (magnification × 100).

BT-IPMN case was due to subsequent small cell lung cancer after 26 mo.

DISCUSSION

Although wide consensus has not yet been reached, BT-IPMN has been increasingly recognized as a unique type of biliary neoplasm and a biliary counterpart of P-IPMN[1,7]. The World Health Organization recognized intraductal papillary neoplasm of the bile duct (IPNB) as a distinct pathological entity in 2010[10]. Ohtsuka *et al*[16] suggested that IPNB with or without macroscopically visible mucin secretion differed in terms of pathologic features. In our study, BT-IPMN was defined as mucinous papillary neoplasm, demonstrating a clear origin from the biliary epithelium[1], and excluded lesions (such as IPNB) without microscopic or macroscopic mucin secretion. To some extent, BT-IPMN is a presumed subtype of IPNB, which has more similarity to P-IPMN than IPNB itself[16].

BT-IPMN shares some radiologic and clinicopathologic features with P-IPMN, but important differences between them may still exist. The frequency of malignancy is higher in patients with BT-IPMN (64%-89%) than in those with P-IPMN (23%-30%)[1,2,7,18]. Consistent with previous studies, the rate of malignant BT-IPMN in our series was > 50%. There are several reasons for the higher rate of malignancy in patients with BT-IPMN. First,

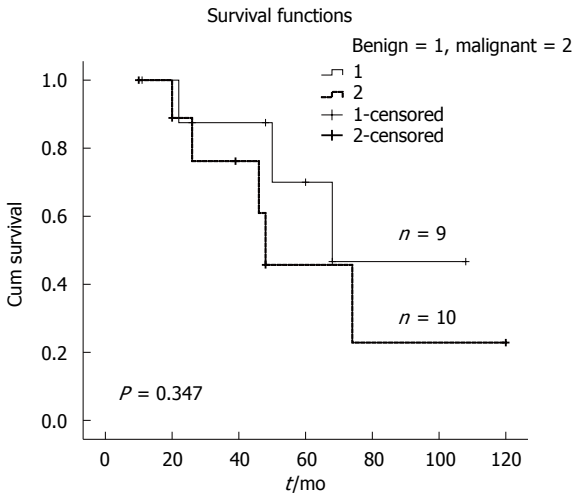

Figure 4 Kaplan-Meier survival curve. Survival curves for patients with benign (n = 9) and malignant (n = 10) biliary tract intraductal papillary mucinous neoplasms.

as several recent reports have suggested, the majority of BT-IPMNs are of an intestinal or pancreatobiliary subtype, resembling those of main-duct-type P-IPMN, which is more aggressive than branch-duct P-IPMN[3,7,19]. Second, the biliary tract and the main pancreatic duct have identical embryologic development from the hepatic diverticulum in the foregut mesoderm[2,7].

In the present study, BT-IPMN mostly presented in patients aged 50-70 years, which is consistent with several other studies[1,3,7,10,20]. Although more male BT-IPMNs patients were found in our study, no difference was found in sex distribution based on previous reports[1,7,10]. The most common presenting symptom was abdominal pain, probably due to biliary stones, cholangitis, or high pressure of biliary tract causing mucin hypersecretion, which are associated with BT-IPMN[10,21]. Intraluminal hypersecretion of mucin from the bile duct may intermittently impede bile flow, leading to repeated episodes of cholangitis. Repeated cholangitis was found in approximately 32% of patients with BT-IPMN in our study, as a typical clinical presentation of BT-IPMN. Nearly 63% of BT-IPMNs were associated with biliary stones; most of which were proximal biliary stones. These findings indicate that the process of inflammatory stimulation may play a role in the development of BT-IPMN. BT-IPMNs were predominantly located in the intrahepatic bile duct and hilum, though the primary site of tumor origin does not affect the progress or prognosis of the disease[10,20,21]. Dilated bile ducts, intraluminal lesions, and/or gross cystic dilatation originating from the biliary tract are the most common abnormal preoperative imaging findings in BT-IPMN. Simultaneous proximal and distal bile duct dilation was found in approximately 68% of patients with BT-IPMN in our study. It has diagnostic significance, as with diffused pancreatic duct dilation for P-IPMN. The large amount of mucin discharged into the duct system leads to diffuse duct dilation.

Surgery is the first choice of treatment for patients with BT-IPMN without distant metastasis[22]. Determination of the optimal surgical strategy depends on the site and extent of the lesions. Intraoperative choledochoscopy and surgical margin frozen sectioning are performed to assess tumor location and extension, including superficial spreading along the biliary epithelium[23]. Hepatectomy should be performed for tumors located in the intrahepatic bile duct, whereas pancreatoduodenectomy and bile duct resection are performed for tumors located in the extrahepatic bile duct. Jarnagin *et al*[24] recommended regional lymphadenectomy for tumors localized in the hilum or distal bile duct. Lymph node metastasis is rare in benign BT-IPMN, and is less common in patients with invasive carcinoma arising from BT-IPMN, compared with conventional cholangiocarcinoma[8]. No patient in our series suffered from lymph node metastases. Portal vein resection is an option for tumors with blood vessel involvement[8]. Theoretically, resection of the entire biliary tract by liver transplantation could be a better option for curative treatment of diffuse BT-IPMN. Palliative surgery was performed in one patient with diffuse BT-IPMN in our study.

Only one patient died 22 mo after palliative surgery, with poorer survival than the overall median survival of 68 mo. Rocha *et al*[10] found that R0 resection was associated with better median survival than R1 resection. The median survival for the benign group in our study appeared better than for malignant cases, though the lack of significance may have been due to the relatively short follow-up period and small sample size. However, the difference may reflect an intrinsic difference in tumor biology. Complete tumor resection is associated with good survival, even in patients with malignant BT-IPMN.

The small number of patients in the present study prevented us from making strong conclusions. Moreover, a major limitation was the retrospective nature of the study. Diagnostic modalities for BT-IPMN, including imaging and pathology, have varied at different times. Nevertheless, due to the scarcity of patients, we are still justified in speculating on the trends that can be observed in this limited set of data. More multicenter prospective studies are necessary to identify the clinical and pathologic characteristics of BT-IPMN.

In conclusion, BT-IPMN is a rare biliary entity. Complete resection of the tumor is associated with good survival, even in patients with malignant BT-IPMN.

COMMENTS

Background

In the past decade, biliary tract intraductal papillary mucinous neoplasm (BT-IPMN) has been increasingly recognized as a unique type of biliary neoplasm, coinciding with widespread acceptance of the nomenclature of pancreatic IPMN. BT-IPMN is a rare neoplasm involving the intra- and extrahepatic biliary tracts and is characterized by mucin-secreting papillary and/or cystic lesions.

However, there is still controversy over several aspects of BT-IPMN.

Research frontiers

BT-IPMN is a rare biliary entity. The number of reports of BT-IPMN with strict histopathologic criteria is limited. Most of the data regarding BT-IPMN are from retrospective studies with small samples. There is still controversy surrounding several aspects of BT-IPMN, and clinicopathologic characteristics, surgical strategies, and prognosis are largely unclear.

Innovations and breakthroughs

This study involved a large number of patients with BT-IPMN from a large Chinese institution. The authors summarized the clinical features, radiologic findings, pathology, surgical strategies, and long-term follow-up of patients with BT-IPMN, and achieved a better understanding of this rare disease. The findings indicate that BT-IPMN is indeed a rare biliary entity and complete resection of the tumor is associated with good survival, even in patients with malignant disease.

Applications

BT-IPMN is a rare biliary entity. Complete resection of the tumor is associated with good survival, even in patients with malignant disease.

Terminology

BT-IPMN is histologically defined as a mucinous and papillary neoplasm demonstrating a clear origin from the biliary epithelium, with solitary or diffuse intraductal growth.

Peer-review

This is a very interesting paper. The data are clearly presented and extensively discussed on the basis of the recent relevant international literature.

REFERENCES

1 **Barton JG**, Barrett DA, Maricevich MA, Schnelldorfer T, Wood CM, Smyrk TC, Baron TH, Sarr MG, Donohue JH, Farnell MB, Kendrick ML, Nagorney DM, Reid Lombardo KM, Que FG. Intraductal papillary mucinous neoplasm of the biliary tract: a real disease? *HPB* (Oxford) 2009; **11**: 684-691 [PMID: 20495637 DOI: 10.1111/j.1477-2574.2009.00122.x]

2 **Sclabas GM**, Barton JG, Smyrk TC, Barrett DA, Khan S, Kendrick ML, Reid-Lombardo KM, Donohue JH, Nagorney DM, Que FG. Frequency of subtypes of biliary intraductal papillary mucinous neoplasm and their MUC1, MUC2, and DPC4 expression patterns differ from pancreatic intraductal papillary mucinous neoplasm. *J Am Coll Surg* 2012; **214**: 27-32 [PMID: 22112419 DOI: 10.1016/j.jamcollsurg.2011.09.025]

3 **Zen Y**, Fujii T, Itatsu K, Nakamura K, Minato H, Kasashima S, Kurumaya H, Katayanagi K, Kawashima A, Masuda S, Niwa H, Mitsui T, Asada Y, Miura S, Ohta T, Nakanuma Y. Biliary papillary tumors share pathological features with intraductal papillary mucinous neoplasm of the pancreas. *Hepatology* 2006; **44**: 1333-1343 [PMID: 17058219 DOI: 10.1002/hep.21387]

4 **Kim HJ**, Kim MH, Lee SK, Yoo KS, Park ET, Lim BC, Park HJ, Myung SJ, Seo DW, Min YI. Mucin-hypersecreting bile duct tumor characterized by a striking homology with an intraductal papillary mucinous tumor (IPMT) of the pancreas. *Endoscopy* 2000; **32**: 389-393 [PMID: 10817178 DOI: 10.1055/s-2000-8996]

5 **Oshikiri T**, Kashimura N, Katanuma A, Maguchi H, Shinohara T, Shimizu M, Kondo S, Katoh H. Mucin-secreting bile duct adenoma--clinicopathological resemblance to intraductal papillary mucinous tumor of the pancreas. *Dig Surg* 2002; **19**: 324-327 [PMID: 12207078]

6 **Yamashita Y**, Fukuzawa K, Taketomi A, Aishima S, Yoshizumi T, Uchiyama H, Tsujita E, Harimoto N, Harada N, Wakasugi K, Maehara Y. Mucin-hypersecreting bile duct neoplasm characterized by clinicopathological resemblance to intraductal papillary mucinous neoplasm (IPMN) of the pancreas. *World J Surg Oncol* 2007; **5**: 98 [PMID: 17725824 DOI: 10.1186/1477-7819-5-98]

7 **Minagawa N**, Sato N, Mori Y, Tamura T, Higure A, Yamaguchi K. A comparison between intraductal papillary neoplasms of the biliary tract (BT-IPMNs) and intraductal papillary mucinous neoplasms of the pancreas (P-IPMNs) reveals distinct clinical manifestations and outcomes. *Eur J Surg Oncol* 2013; **39**: 554-558 [PMID: 23506840 DOI: 10.1016/j.ejso.2013.02.016]

8 **Yeh TS**, Tseng JH, Chiu CT, Liu NJ, Chen TC, Jan YY, Chen MF. Cholangiographic spectrum of intraductal papillary mucinous neoplasm of the bile ducts. *Ann Surg* 2006; **244**: 248-253 [PMID: 16858187 DOI: 10.1097/01.sla.0000217636.40050.54]

9 **Shibahara H**, Tamada S, Goto M, Oda K, Nagino M, Nagasaka T, Batra SK, Hollingsworth MA, Imai K, Nimura Y, Yonezawa S. Pathologic features of mucin-producing bile duct tumors: two histopathologic categories as counterparts of pancreatic intraductal papillary-mucinous neoplasms. *Am J Surg Pathol* 2004; **28**: 327-338 [PMID: 15104295]

10 **Rocha FG**, Lee H, Katabi N, DeMatteo RP, Fong Y, D'Angelica MI, Allen PJ, Klimstra DS, Jarnagin WR. Intraductal papillary neoplasm of the bile duct: a biliary equivalent to intraductal papillary mucinous neoplasm of the pancreas? *Hepatology* 2012; **56**: 1352-1360 [PMID: 22504729 DOI: 10.1002/hep.25786]

11 **Jung G**, Park KM, Lee SS, Yu E, Hong SM, Kim J. Long-term clinical outcome of the surgically resected intraductal papillary neoplasm of the bile duct. *J Hepatol* 2012; **57**: 787-793 [PMID: 22634127 DOI: 10.1016/j.jhep.2012.05.008]

12 **Yeh TS**, Tseng JH, Chen TC, Liu NJ, Chiu CT, Jan YY, Chen MF. Characterization of intrahepatic cholangiocarcinoma of the intraductal growth-type and its precursor lesions. *Hepatology* 2005; **42**: 657-664 [PMID: 16116640 DOI: 10.1002/hep.20837]

13 **Jonas S**, Thelen A, Benckert C, Biskup W, Neumann U, Rudolph B, Lopez-Häänninen E, Neuhaus P. Extended liver resection for intrahepatic cholangiocarcinoma: A comparison of the prognostic accuracy of the fifth and sixth editions of the TNM classification. *Ann Surg* 2009; **249**: 303-309 [PMID: 19212186 DOI: 10.1097/SLA.0b013e318195e164]

14 **Nanashima A**, Sumida Y, Abo T, Nagasaki T, Takeshita H, Fukuoka H, Sawai T, Tanaka K, Yasutake T, Nagayasu T. Patient outcome and prognostic factors in intrahepatic cholangiocarcinoma after hepatectomy. *Hepatogastroenterology* 2007; **54**: 2337-2342 [PMID: 18265660]

15 **Zen Y**, Pedica F, Patcha VR, Capelli P, Zamboni G, Casaril A, Quaglia A, Nakanuma Y, Heaton N, Portmann B. Mucinous cystic neoplasms of the liver: a clinicopathological study and comparison with intraductal papillary neoplasms of the bile duct. *Mod Pathol* 2011; **24**: 1079-1089 [PMID: 21516077 DOI: 10.1038/modpathol.2011.71]

16 **Ohtsuka M**, Kimura F, Shimizu H, Yoshidome H, Kato A, Yoshitomi H, Furukawa K, Takeuchi D, Takayashiki T, Suda K, Takano S, Kondo Y, Miyazaki M. Similarities and differences between intraductal papillary tumors of the bile duct with and without macroscopically visible mucin secretion. *Am J Surg Pathol* 2011; **35**: 512-521 [PMID: 21412069 DOI: 10.1097/PAS.0b013e3182103f36]

17 **Tanaka M**, Fernández-del Castillo C, Adsay V, Chari S, Falconi M, Jang JY, Kimura W, Levy P, Pitman MB, Schmidt CM, Shimizu M, Wolfgang CL, Yamaguchi K, Yamao K. International consensus guidelines 2012 for the management of IPMN and MCN of the pancreas. *Pancreatology* 2012; **12**: 183-197 [PMID: 22687371 DOI: 10.1016/j.pan.2012.04.004]

18 **Schnelldorfer T**, Sarr MG, Nagorney DM, Zhang L, Smyrk TC, Qin R, Chari ST, Farnell MB. Experience with 208 resections for intraductal papillary mucinous neoplasm of the pancreas. *Arch Surg* 2008; **143**: 639-46; discussion 646 [PMID: 18645105 DOI: 10.1001/archsurg.143.7.639]

19 **Nakanuma Y**. A novel approach to biliary tract pathology based on similarities to pancreatic counterparts: is the biliary tract an incomplete pancreas? *Pathol Int* 2010; **60**: 419-429 [PMID: 20518896 DOI: 10.1111/j.1440-1827.2010.02543.x]

20 **Kim KM**, Lee JK, Shin JU, Lee KH, Lee KT, Sung JY, Jang KT, Heo JS, Choi SH, Choi DW, Lim JH. Clinicopathologic features of intraductal papillary neoplasm of the bile duct according to histologic subtype. *Am J Gastroenterol* 2012; **107**: 118-125 [PMID: 21946282 DOI: 10.1038/ajg.2011.316]

21 **Wan XS**, Xu YY, Qian JY, Yang XB, Wang AQ, He L, Zhao HT, Sang XT. Intraductal papillary neoplasm of the bile duct. *World J Gastroenterol* 2013; **19**: 8595-8604 [PMID: 24379576 DOI:

10.3748/wjg.v19.i46.8595]
22 **Kim JK**, Hwang HK, Park JS, Cho SI, Yoon DS, Chi HS. Left hemihepatectomy and caudate lobectomy and complete extrahepatic bile duct resection using transduodenal approach for hilar cholangiocarcinoma arsing from biliary papillomatosis. *J Surg Oncol* 2008; **98**: 139-142 [PMID: 18521837 DOI: 10.1002/jso.21089]
23 **Ohtsuka M**, Shimizu H, Kato A, Yoshitomi H, Furukawa K, Tsuyuguchi T, Sakai Y, Yokosuka O, Miyazaki M. Intraductal papillary neoplasms of the bile duct. *Int J Hepatol* 2014; **2014**: 459091 [PMID: 24949206 DOI: 10.1155/2014/459091]
24 **Jarnagin WR**, Bowne W, Klimstra DS, Ben-Porat L, Roggin K, Cymes K, Fong Y, DeMatteo RP, D'Angelica M, Koea J, Blumgart LH. Papillary phenotype confers improved survival after resection of hilar cholangiocarcinoma. *Ann Surg* 2005; **241**: 703-712; discussion 712-714 [PMID: 15849506]

P- Reviewer: Frider B, Ooi LL **S- Editor**: Ma YJ
L- Editor: AmEditor **E- Editor**: Zhang DN

World Journal of Gastroenterology

Submit a Manuscript: http://www.wjgnet.com/esps/
Help Desk: http://www.wjgnet.com/esps/helpdesk.aspx
DOI: 10.3748/wjg.v21.i14.4268

World J Gastroenterol 2015 April 14; 21(14): 4268-4274
ISSN 1007-9327 (print) ISSN 2219-2840 (online)

ORIGINAL ARTICLE

Prospective Study

Weekly docetaxel and gemcitabine in previously treated metastatic esophageal squamous cell carcinoma

Min-Young Lee, Ki Sun Jung, Hae Su Kim, Ji Yun Lee, Sung Hee Lim, Moonjin Kim, Hyun Ae Jung, Sung Min Kim, Jong Mu Sun, Myung-Ju Ahn, Jeeyun Lee, Se Hoon Park, Seong Yoon Yi, In Gyu Hwang, Sang-Cheol Lee, Hee Kyung Ahn, Do Hyoung Lim, Soon Il Lee, Keon Woo Park

Min-Young Lee, Ki Sun Jung, Hae Su Kim, Ji Yun Lee, Sung Hee Lim, Moonjin Kim, Hyun Ae Jung, Sung Min Kim, Jong Mu Sun, Myung-Ju Ahn, Jeeyun Lee, Se Hoon Park, Division of Hematology-Oncology, Department of Medicine, Samsung Medical Center, Sungkyunkwan University School of Medicine, Seoul 135-710, South Korea
Seong Yoon Yi, Division of Hematology-Oncology, Department of Internal Medicine, Inje University Ilsan-Paik Hospital, Goyang 411-706, South Korea
In Gyu Hwang, Division of Hematology-Oncology, Department of Internal Medicine, Chung-Ang University Hospital, Seoul 156-755, South Korea
Sang-Cheol Lee, Division of Hematology-Oncology, Department of Internal Medicine, Soonchunhyang University Hospital, Cheonan 330-721, South Korea
Hee Kyung Ahn, Division of Hematology-Oncology, Department of Internal Medicine, Gachon University Gil Hospital, Incheon 405-760, South Korea
Do Hyoung Lim, Soon Il Lee, Keon Woo Park, Division of Hematology-Oncology, Department of Internal Medicine, Dankook University College of Medicine, Cheonan 330-715, South Korea
Author contributions: Park SH, Park KW and Lee J designed the study and were also involved in editing the manuscript; Yi SY, Hwang IG, Lee SC, Ahn HK, Lim DH and Lee SI designed and performed the study; Sun JM and Ahn MJ consulted our study; Jung KS, Kim HS, Lee JY, Lim SH, Kim M, Jung HA and Kim SM organized patient data; Lee MY collected data and drafted the manuscript.
Supported by Dong-A ST (Seoul, Korea) for kindly provided the study drug (gemcitabine).
Ethics approval: This study was reviewed and approved by the Samsung Medical Center Institutional Review Board.
Clinical trial registration: This study is registered at http://clinicaltrials.gov/show/NCT01469598. The registration identification number is NCT01469598.
Informed consent: All study participants, or their legal guardian, provided informed written consent prior to study enrollment.
Conflict-of-interest: The authors made no disclosures.
Data sharing: No additional data are available.

Correspondence to: Keon Woo Park, MD, Division of Hematology-Oncology, Department of Internal Medicine, Dankook University College of Medicine, 16-5 Anseo-Dong, Dongnam-Gu, Cheonan 330-715, South Korea. pkw800041@naver.com
Telephone: +82-41-5509360
Fax: +82-41-5507058
Received: September 17, 2014
Peer-review started: September 19, 2014
First decision: October 29, 2014
Revised: January 2, 2015
Accepted: January 21, 2015
Article in press: January 21, 2015
Published online: April 14, 2015

Abstract

AIM: To assess the efficacy and safety of weekly docetaxel plus a fixed-dose rate (FDR) of gemcitabine in metastatic esophageal squamous cell carcinoma (SCC).

METHODS: A multi-center, open-label, prospective phase Ⅱ study was designed. Thirty-three esophageal SCC patients with documented progression after fluoropyrimidine/platinum-based first-line chemotherapy were enrolled and treated with docetaxel 35 mg/m^2 and gemcitabine 1000 mg/m^2 iv at a FDR (10 mg/m^2 per minute) on days 1 and 8. Treatment was repeated

every twenty-one days until disease progression, unacceptable toxicity, or consent withdrawal. The primary endpoint was response rate (RR), and secondary endpoints were safety, progression-free survival (PFS) and overall survival (OS).

RESULTS: Combination of weekly docetaxel and FDR gemcitabine was well tolerated: the most common treatment-related adverse events were anemia (97%), fatigue (64%) and neutropenia (55%). One patient with multiple lung and lymph node metastases died of respiratory failure after receiving four cycles of chemotherapy, and the possibility of drug-induced pneumonitis could not be completely excluded. Disease control (objective response plus stable disease) in the ITT population was achieved in 88% of patients, and the overall RR was 30% (95%CI: 15%-46%). The median PFS and OS were 4.0 (95%CI: 3.4-4.6) and 8.8 mo (95%CI: 7.8-9.8 mo), respectively.

CONCLUSION: A combination of weekly docetaxel and FDR gemcitabine showed promising antitumor activity and tolerability in previously treated, metastatic esophageal SCC.

Key words: Clinical trial; Phase Ⅱ; Chemotherapy; Carcinoma, Esophageal neoplasm; Squamous cell; Docetaxel; Gemcitabine

Core tip: Esophageal squamous cell carcinoma (SCC) is a lethal disease with a poor prognosis. Currently, there is no standard chemotherapy regimen for metastatic esophageal SCC patients who have failed platinum and fluoropyrimidine combination chemotherapy. In this multi-center, prospective phase Ⅱ study, we demonstrated that the combination of weekly docetaxel and a fixed-dose rate of gemcitabine is active and well tolerated as a salvage chemotherapy in patients with previously treated metastatic esophageal SCC.

Lee MY, Jung KS, Kim HS, Lee JY, Lim SH, Kim M, Jung HA, Kim SM, Sun JM, Ahn MJ, Lee J, Park SH, Yi SY, Hwang IG, Lee SC, Ahn HK, Lim DH, Lee SI, Park KW. Weekly docetaxel and gemcitabine in previously treated metastatic esophageal squamous cell carcinoma. *World J Gastroenterol* 2015; 21(14): 4268-4274 Available from: URL: http://www.wjgnet.com/1007-9327/full/v21/i14/4268.htm DOI: http://dx.doi.org/10.3748/wjg.v21.i14.4268

INTRODUCTION

Esophageal cancer is the eighth most common cause of cancer death worldwide. There are two main histological types; adenocarcinoma and squamous cell carcinoma (SCC). Although esophageal adenocarcinoma is more prevalent in Western countries, SCC is the most predominant histologic subtype globally[1]. Esophageal SCC is a highly lethal disease with a five-year survival rate of 15%-19%[2,3]. Treatments for metastatic esophageal SCC are limited; most patients are not eligible for surgery because more than two thirds of patients present with unresectable or metastatic disease at the time of initial diagnosis, and the majority of remaining patients with initially locoregional disease eventually develop distant metastases[4]. Therefore, palliative chemotherapy is the only treatment option for patients with metastatic esophageal SCC to prolong their survival and to improve their quality of life. A combination of cisplatin and infusional 5-fluorouracil (5-FU) is the most commonly used regimen for palliative first-line chemotherapy in metastatic esophageal SCC[4-6]. However, the number of effective cytotoxic agents for the treatment of patients with metastatic esophageal SCC is limited. When patients have failed platinum and fluoropyrimidine combination chemotherapy, it is commonly observed that patients experience a rapid clinical deterioration and decline in their performance status.

Docetaxel is one of the most widely used chemotherapeutic agents in metastatic esophageal SCC patients[7]. Although docetaxel is often combined with cisplatin, particularly in a salvage setting, the cisplatin-based chemotherapy had a clinically important toxicity profiles. To avoid cisplatin-related toxicity, there are several ways including omission or replacement of cisplatin with a cytotoxic agent with similar activity. Gemcitabine, among others, has a notable activity and tolerable toxicity profile in esophageal SCC[8], blocking cancer cells in a different cellular phase than docetaxel[9]. A randomized phase Ⅱ study in patients with pancreatic cancer suggested that gemcitabine given at a fixed-dose rate (FDR) infusion (*i.e.*, 10 mg/m^2 per minute) have did not have a greater activity than a bolus infusion[10]. Combinations of docetaxel and gemcitabine have been studied in treatment of various solid tumors including metastatic breast cancer[11], non-small cell lung cancer (NSCLC)[12], and other malignancies, because both drugs have good antitumor activity with non-overlapping toxicity[13]. For example, a clinical study by Hensley *et al*[14] demonstrated an impressive 53% response rate in patients with predominantly uterine leiomyosarcoma. In this study, patients received gemcitabine 900 mg/m^2 on days 1 and 8 plus docetaxel 100 mg/m^2 on day 8 with granulocyte-colony stimulation factor (G-CSF) support every 3 wk. Hematologic toxicity including neutropenia and thrombocytopenia was the most common dose-limiting toxicity and antitumor activity of the regimen was equivalent to cisplatin-based combinations.

Currently, optimal dose schedules for docetaxel plus gemcitabine combination chemotherapy have not been determined. A weekly docetaxel and

gemcitabine combination was attractive because of the low incidence of severe myelosuppression in weekly docetaxel compared to the standard 3-weekly docetaxel regimen[15-17], this altered toxicity profile suggested that, as a salvage treatment, there was the potential for better tolerance and increased dose intensity. We conducted a phase Ⅱ study in order to assess the efficacy and safety of weekly docetaxel plus a FDR of gemcitabine as a salvage chemotherapy in patients with metastatic esophageal SCC. The primary objective was to evaluate the anti-tumor activity in terms of response rate (RR), and secondary objectives were progression-free survival (PFS), overall survival (OS), and the safety profile of the regimen.

MATERIALS AND METHODS

This was an open-label, multi-center study of palliative chemotherapy with weekly docetaxel plus a FDR of gemcitabine. Patients with histologically confirmed metastatic or recurrent SCC of the esophagus were enrolled in this prospective phase Ⅱ study. All patients were required to have experienced progression after at least one cytotoxic chemotherapy regimen involving both fluoropyrimidine and platinum. Patients who experienced recurrence during or within 6 mo after the completion of adjuvant chemotherapy were allowed to enter the study. Only patients older than 18 years of age, with an Eastern Cooperative Oncology Group (ECOG) performance status of 0 to 2 were eligible for entry into this study. Other eligibility criteria included at least one bi-dimensionally measurable lesion by the RECIST 1.1 criteria[18], a life expectancy of at least 3 mo, and adequate bone marrow, renal, and liver functions. Patients with serious concomitant medical diseases prior to exposure to docetaxel or gemcitabine, who were pregnant or breast feeding, who had a history of significant neurologic or psychiatric disorders, or evidence of serious gastrointestinal bleeding were considered ineligible. A treatment-free interval of at least 4 wk was required to enter the study. Before the study was initiated, the protocol was approved by the Institutional Review Board of all the participating hospitals in accordance with the ethical principles of the Declaration of Helsinki and local guidelines, and all patients provided written informed consent prior to participation in any study-specific procedures.

The pre-treatment evaluation included medical history and a physical examination, complete blood count with differentials, chemistry, chest X-ray, computed tomography (CT) scans of the thorax and any other diagnostic procedures as clinically indicated. Gemcitabine 1000 mg/m^2 was administered intravenously at a FDR 10 mg/m^2 per minute on days 1 and 8. Docetaxel 35 mg/m^2 was also administered intravenously over 60 min on days 1 and 8. Premedications included adequate antiemetic therapy and dexamethasone 15 mg before each docetaxel infusion. All chemotherapy was administered on an outpatient basis unless hospitalization was required for other reasons, and the cycle was repeated every twenty-one days until there was documented progression of the disease, unacceptable toxicity, or the patients refusal. All patients received full supportive care, which included blood product transfusion, antiemetics, and analgesics as appropriate. Dose reductions were based on toxicities that were graded according to the National Cancer Institute Common Toxicity Criteria (NCI-CTC) scale version 4.0. Clinic visits and toxicity evaluation were performed on days 1 and 8 of each cycle. Each chemotherapy cycle was started only if neutrophil counts were $\geqslant$ 1500/mm^3, platelet counts were $\geqslant$ 75000/mm^3, and all non-hematologic toxicities had been reduced to grade 0 to 1. In the case of a delay of more than twenty-one days due to toxicity, the protocol treatment was discontinued. If the patient experienced febrile neutropenia, grade 4 neutropenia lasting > seven days, grade 4 thrombocytopenia, or grade 3 or 4 non-hematologic toxicities with the exception of nausea, vomiting and alopecia, subsequent doses of gemcitabine and docetaxel were lowered by 20% from the doses in the preceding cycles. Dose reduction on day 8 of each cycle was permitted in accordance with the protocols. In brief, the 8th day doses of gemcitabine and docetaxel were reduced if neutrophil counts were between 1000/mm^3 and 1500/mm^3, or if platelet counts were between 50000/mm^3 and 75000/mm^3. Gemcitabine and docetaxel doses were omitted on day 8 when neutrophil counts were < 1000/mm^3 or platelet counts were < 50000/mm^3.

Appropriate imaging studies including contrast-enhanced CT scans were conducted every two cycles to evaluate treatment response. As the primary endpoint of this study was objective RR, the clinical tumor response was assessed according to the RECIST criteria version 1.1[18]. Upon progression disease (PD), further salvage treatments were permitted at the investigators' discretion, and the nature of any treatments was recorded.

The secondary endpoints were PFS, OS and safety. PFS and OS were measured from day 1 on first study treatment cycle until the day of documented PD and death, respectively. OS and PFS were assessed using the Kaplan-Meier method, and the 95%CI for the median time to an event were calculated. Sample sizes were calculated to reject a 10% response rate in favor of a target response rate of 30%, with a significance level of 0.05 and a power of 90%. Considering a 10% drop-out rate, a total of 33 patients was planned. The statistical methods of this study were reviewed by Kyunga Kim (PhD in Statistics) from Biostatistics and Clinical Epidemiology Center at Samsung Medical Center.

RESULTS

The current phase Ⅱ study was opened in August 2011 among oncology departments in six tertiary Korean

Table 1 Patient characteristics *n* (%)

Characteristics	Patients
Total number of patients	33
Age (yr), median (range)	59 (44-76)
Gender	
Male	31 (94)
Female	2 (6)
ECOG PS	
1	32 (97)
2	1 (3)
Anatomic site	
Upper thoracic	1 (3)
Middle thoracic	26 (79)
Distal	6 (18)
Prior curative-aim treatment	
None	7 (21)
Surgery	23 (70)
Chemoradiotherapy	3 (9)
Number of prior chemotherapy regimens	
1	25 (76)
2	8 (24)
Tumor grade	
Well differentiated	3 (9)
Moderately differentiated	18 (55)
Poorly differentiated or unknown	12 (36)
Metastatic site (s)	
Lymph node	29 (88)
Lung	14 (42)
Liver	6 (18)
Bone	3 (9)

ECOG: Eastern Cooperative Oncology Group.

centers. The last patients entered the study in Mar 2014. The baseline characteristics of the 33 patients are listed in Table 1. All patients had histologically proven SCC arising from the esophagus. In a majority of patients the primary site was the middle (*n* = 26) or distal thoracic esophagus (*n* = 6). Twenty-three (70%) patients had undergone esophagectomy, and three patients (9%) had received curative-aim chemoradiotherapy. The median age was 59 years with a range of 44 to 76 years, and all patients had symptoms at baseline (ECOG performance status 1 in 32/33 patients and 2 in one patient). The most common first-line chemotherapy regimen was 5-FU plus cisplatin (76%) followed by capecitabine plus cisplatin or paclitaxel (24%). In eight patients who were treated with two prior chemotherapy regimens, second-line chemotherapy included 5-FU plus cisplatin (75%) and capecitabine plus cisplatin (25%). More than 75.8% of the patients received prior palliative chemotherapy and 54.5% of the patients received prior radiotherapy. All patients had metastatic disease at the time of treatment with the most common site of metastasis being the lymph node (88%) followed by the lung (42%), and liver (18%).

Safety

Patients received a total of 157 treatment cycles (median 5, range 1-16). Nine (6%) of the 8th day doses of docetaxel and gemcitabine were delayed or skipped because of toxic effects, as per the protocol criteria, and dose reduction was required in 24 patients. In the majority of treatment discontinuation was caused by PD (*n* = 22). Another minor reasons were consent withdrawal (*n* = 6) and toxicity (*n* = 5). The planned dose intensities for docetaxel were 23 mg/m^2 per week and gemcitabine were 667 mg/m^2 per week, thus, the relative dose intensity of both drugs was 82% (95%CI: 65%-97%).

Table 2 Toxicity profile per patient (*n* = 33): Worst grade reported during the treatment period *n* (%)

	NCI-CTC grade					
	1	2	3	4	1-4	3/4
Hematologic						
Anemia	13	16	3	0	32 (97)	3 (9)
Neutropenia	0	5	10	3	18 (55)	13 (39)
Thrombocytopenia	6	2	1	1	10 (30)	2 (6)
Febrile neutropenia	0	0	3	0	3 (9)	3 (9)
Non-hematologic						
Asthenia/Fatigue	13	4	4	0	21 (64)	4 (12)
Myalgia	5	1	0	0	6 (18)	0 (0)
Anorexia	10	2	1	0	13 (39)	1 (3)
Nausea	5	1	1	0	7 (21)	1 (3)
Vomiting	4	0	1	0	5 (15)	1 (3)
Mucositis/Stomatitis	6	2	0	0	8 (24)	0 (0)
Diarrhea	6	2	0	0	8 (24)	0 (0)
Hand-foot syndrome	2	2	0	0	4 (12)	0 (0)
Peripheral neuropathy	6	0	0	0	6 (18)	0 (0)
Alopecia	14	1	0	0	15 (46)	0 (0)
Headache	5	0	0	0	5 (15)	0 (0)
Dysphagia	7	1	0	0	8 (24)	0 (0)
Rash	4	2	0	0	6 (18)	0 (0)
Cough	4	1	1	0	6 (18)	1 (3)
Sputum	7	1	1	0	9 (27)	1 (3)
Chest discomfort	10	0	0	0	10 (30)	0 (0)

NCI-CTC: National Cancer Institute Common Toxicity Criteria.

All eligible patients were assessable for adverse events. The treatment-related adverse events are shown in Table 2. The most commonly observed all-grade toxicity was anemia (97%), followed by asthenia/fatigue (64%), neutropenia (55%), alopecia (46%), and anorexia (39%). The major grade 3 or 4 toxicities were hematologic ones including neutropenia (39%), followed by anemia (9%), febrile neutropenia (9%) and thrombocytopenia (6%). Although these adverse events were generally tolerated and easily manageable, one patient, a 64-year-old male, died of respiratory failure after receiving the fourth cycle. His chest CT revealed bilateral pneumonitis while the lung and lymph node metastases remained a partial response (PR). The patient was treated with corticosteroids and antibiotics but did not benefit.

Efficacy

Clinical response evaluations were assessable for 32 patients who received at least two cycles of study treatment. Disease control (objective response and

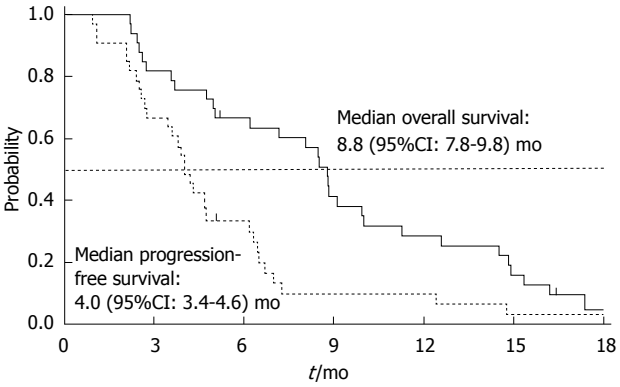

Figure 1 Progression-free and overall survival.

stable disease) in the ITT population was achieved in 88% of patients and the overall RR was 30% (95%CI: 15%-46%). Among the ten responders, one patient achieved a CR, which was maintained for 14 mo. The median duration of response in responders was 2 mo.

At the time of analysis, 30 patients were dead. With a median follow-up duration of 20 mo (95%CI: 18-21 mo), the median PFS and OS were 4.0 mo (95%CI: 3.4-4.6 mo) and 8.8 mo (95%CI: 7.8-9.8 mo), respectively. Kaplan-Meier curves for PFS and OS were depicted in Figure 1.

Salvage treatments

Although salvage treatment were not specified in the protocol, palliative radiotherapy was given to 4 patients with symptomatic progression in lung, bone, or lymph nodes. We performed salvage chemotherapy to 7 patients (21%) with irinotecan (n = 5) or pemetrexed (n = 2). Esophageal stenting to relieve obstructive symptoms was performed in 5 patients.

DISCUSSION

The objective of this phase Ⅱ study was to assess the efficacy and safety of a non-platinum-based combination of docetaxel and FDR gemcitabine administered weekly to patients previously treated for metastatic esophageal SCC. Because of their antitumor activity as single agents and different mechanisms of action, docetaxel and gemcitabine combinations have been tested previously, although myelosuppression has been a serious problem[13]. In a previous phase Ⅱ study involving weekly docetaxel and gemcitabine combination, a weekly regimen could be administered with acceptable toxicity to most patients[12]. The current study confirmed these results, the non-platinum combination of docetaxel 35 mg/m^2 and FDR gemcitabine 1000 mg/m^2 on days 1 and 8 every 3 wk had an acceptable toxicity profile.

In the second-line setting of esophageal SCC, docetaxel is one of the most frequently investigated, and the most widely used, regimens. Recently, a large retrospective study showed a moderated PFS advantage with docetaxel-based second-line chemotherapy in esophageal SCC[19,20]. Although 3-weekly docetaxel has proved to be active, it is associated with a significant incidence of severe neutropenia, often complicated by fever. Therefore, several clinical trials have examined docetaxel administered as weekly schedule, which demonstrated modest toxicity profiles with minimal myelosuppression[14]. In a randomized trial comparing weekly and 3-weekly schedules of docetaxel and cisplatin in patients with previously untreated NSCLC, the most frequent grade 3 or 4 toxicity was neutropenia in the 3-weekly regimen and fatigue in the weekly regimen[17]. Several phase Ⅰ and Ⅱ clinical trials have examined docetaxel administered in weekly doses of 30, 35, 40 mg/m^2. The weekly docetaxel 35 mg/m^2 chemotherapy group produced less myelosuppression, and better compliance and response rates than the 3-weekly docetaxel or other weekly dose groups[21,22]. Our clinical trial administered docetaxel at a weekly dose of 35 mg/m^2. Gemcitabine also had been tested in phase Ⅰ and Ⅱ clinical trials[8], and the combination of docetaxel and gemcitabine has been considered a rational approach for salvage setting esophageal SCC. An explanation for the high response rates observed may be that docetaxel and gemcitabine exhibit true *in vivo* synergy, and the combination has complementary mechanisms of action, docetaxel promoting cell death and gemcitabine inducing cell cycle arrest[23].

In addition to the weekly schedule of docetaxel, we employed a FDR schedule for gemcitabine infusion. To render gemcitabine more effective, longer exposures to the drug may be associated with greater antitumor effects by maximizing the amounts of gemcitabine that can accumulate intracellularly in a given time period. FDR infusion of gemcitabine is a term that refers to gemcitabine infusion at a rate that maintains gemcitabine concentration at levels that optimize the incorporation of the active gemcitabine metabolite, gemcitabine triphosphate, into DNA. Pre-clinical data have shown that the maintenance of gemcitabine triphosphate concentration at 20 μmol/L, optimizes *in vivo* cell killing[24,25]. The issue of whether prolonged-infusion gemcitabine (10 mg/m^2 per minute) results in higher clinical response rates compared to bolus infusions has been addressed in a randomized trial in pancreatic cancer[10]. Grade 3 and 4 myelosuppression occurred with both the FDR infusion and the bolus infusion group. This result seemed to be more toxic with the FDR infusion. However, a higher incidence of dose modification or discontinuation of gemcitabine was not observed[10]. The use of FDR infusion of gemcitabine as a combination treatment for esophageal cancer has been documented in a few phase Ⅰ and Ⅱ clinical trials[26].

Recently, several studies on combination chemotherapy for second-line treatment of previously treated metastatic esophageal cancer have been conducted. Among them, there are two reports of combination chemotherapy including docetaxel as a second-line

regimen in metastatic esophageal squamous cell carcinoma. Shim *et al*[27] did a phase Ⅱ study on docetaxel and cisplatin chemotherapy, which showed a response rate of 34.2%, a median PFS of 4.5 mo, and a median OS of 7.4 mo. However, this regimen showed toxicity with grade 3 or 4 neutropenia at 52.6%, asthenia at 31.6%, nausea at 18.4%, and neuropathy at 15.8%. In another phase Ⅱ study using docetaxel and nedaplatin for patients previously treated with cisplatin and fluorouracil by Jin *et al*[28], the reported response rates were 27.1%, the median PFS was 3.1 mo, and the median OS was 5.9 mo. This regimen showed toxicity of grade 3 or 4 of neutropenia at 19.6%, grade 1 to 4 anorexia at 47.8%, fatigue at 41.3%, and nausea/vomiting at 32.6%. The docetaxel-platinum based chemotherapy present similar response rates and survival data compared with the current study. However, it is important to recognize that docetaxel and gemcitabine combination chemotherapy is potentially associated with significant toxicity. There are several cumulative platinum induced toxicities observed after platinum-based chemotherapy is used as a first-line treatment in esophageal SCC, including emesis, decrease in glomerular filtration rate, and neurotoxicity.

In the current study, combination of weekly docetaxel plus FDR gemcitabine was well tolerated with only three episodes of febrile neutropenia. Unfortunately, one patient died of bilateral pneumonitis and respiratory failure after receiving the forth cycle. Some cases reported pulmonary toxicities associated with both docetaxel and gemcitabine, although not very common[29,30]. Because of the low incidence of severe myelosuppression, this combination of weekly docetaxel and FDR gemcitabine can be applied to a salvage setting, especially if the patient is not anticipated to tolerate a platinum-based chemotherapy.

In conclusion, a combination of weekly docetaxel with a FDR of gemcitabine showed promising antitumor activity in previously treated, metastatic esophageal SCC and a tolerable toxicity profile. A phase Ⅲ trial comparing this combination therapy to combination with other novel agents should be considered in esophageal cancer.

COMMENTS

Background

Esophageal squamous cell carcinoma (SCC) is a highly lethal disease with poor prognosis. Palliative chemotherapy is a treatment option in unresectable or metastatic esophageal SCC. In this paper, the authors conducted a phase II study on combination chemotherapy of weekly docetaxel and fixed-dose-rate (FDR) gemcitabine in previously treated metastatic esophageal SCC.

Research frontiers

There is limited data on effective cytotoxic agents for the treatment of patients with metastatic esophageal SCC, particularly when patients have failed first-line chemotherapy with fluoropyrimidine and platinum.

Innovations and breakthroughs

The results demonstrated that the combination of weekly docetaxel and FDR gemcitabine show promising antitumor activity and tolerable toxicity as a second-line therapy for patients with previously treated metastatic esophageal SCC.

Applications

The combination of weekly docetaxel and FDR gemcitabine is active and well tolerated as a second-line chemotherapy for patients previously treated with fluoropyrimidine and platinum for metastatic esophageal SCC.

Terminology

FDR infusion of gemcitabine is a term that refers to infusion of gemcitabine at a rate that maintains gemcitabine concentration levels that optimize incorporation of the active gemcitabine metabolite, gemcitabine triphosphate, into DNA.

Peer-review

This is a good descriptive study in which the authors assess the efficacy and safety of weekly docetaxel plus a FDR of gemcitabine in metastatic esophageal SCC. The results are interesting and suggest that the combination of the above two drugs is an active second-line therapy with tolerable toxicity for previously treated esophageal SCC.

REFERENCES

1 **Melhado RE**, Alderson D, Tucker O. The changing face of esophageal cancer. *Cancers* (Basel) 2010; **2**: 1379-1404 [PMID: 24281163 DOI: 10.3390/cancers2031379]

2 **Siegel R**, Naishadham D, Jemal A. Cancer statistics, 2013. *CA Cancer J Clin* 2013; **63**: 11-30 [PMID: 23335087 DOI: 10.3322/caac.21166]

3 **Enzinger PC**, Mayer RJ. Esophageal cancer. *N Engl J Med* 2003; **349**: 2241-2252 [PMID: 14657432 DOI: 10.1056/NEJMra035010]

4 **Scheithauer W**. Esophageal cancer: chemotherapy as palliative therapy. *Ann Oncol* 2004; **15** Suppl 4: iv97-i100 [PMID: 15477344 DOI: 10.1093/annonc/mdh911]

5 **Grünberger B**, Raderer M, Schmidinger M, Hejna M. Palliative chemotherapy for recurrent and metastatic esophageal cancer. *Anticancer Res* 2007; **27**: 2705-2714 [PMID: 17695436]

6 **Ajani JA**. Contributions of chemotherapy in the treatment of carcinoma of the esophagus: results and commentary. *Semin Oncol* 1994; **21**: 474-482 [PMID: 8042045]

7 **Muro K**, Hamaguchi T, Ohtsu A, Boku N, Chin K, Hyodo I, Fujita H, Takiyama W, Ohtsu T. A phase II study of single-agent docetaxel in patients with metastatic esophageal cancer. *Ann Oncol* 2004; **15**: 955-959 [PMID: 15151954]

8 **Sandler AB**, Kindler HL, Einhorn LH, Mitchell E, Masters G, Kraut M, Nicol S, Raghavan D. Phase II trial of gemcitabine in patients with previously untreated metastatic cancer of the esophagus or gastroesophageal junction. *Ann Oncol* 2000; **11**: 1161-1164 [PMID: 11061612]

9 **Pourquier P**, Gioffre C, Kohlhagen G, Urasaki Y, Goldwasser F, Hertel LW, Yu S, Pon RT, Gmeiner WH, Pommier Y. Gemcitabine (2',2'-difluoro-2'-deoxycytidine), an antimetabolite that poisons topoisomerase I. *Clin Cancer Res* 2002; **8**: 2499-2504 [PMID: 12171875]

10 **Tempero M**, Plunkett W, Ruiz Van Haperen V, Hainsworth J, Hochster H, Lenzi R, Abbruzzese J. Randomized phase II comparison of dose-intense gemcitabine: thirty-minute infusion and fixed dose rate infusion in patients with pancreatic adenocarcinoma. *J Clin Oncol* 2003; **21**: 3402-3408 [PMID: 12885837 DOI: 10.1200/JCO.2003.09.140]

11 **Laufman LR**, Spiridonidis CH, Pritchard J, Roach R, Zangmeister J, Larrimer N, Moore T, Segal M, Jones J, Patel T, Gutterman L, Carman L, Colborn D, Kuebler JP. Monthly docetaxel and weekly gemcitabine in metastatic breast cancer: a phase II trial. *Ann Oncol* 2001; **12**: 1259-1264 [PMID: 11697837]

12 **Park SH**, Hong J, Kim YS, Kim Y, Kyung SY, An CH, Lee SP, Park JW, Jeong SH, Park J, Cho EK, Shin DB, Lee JH. Phase II trial of weekly docetaxel and gemcitabine for previously untreated, advanced non-small cell lung cancer. *Lung Cancer* 2008; **62**: 72-77 [PMID: 18342982 DOI: 10.1016/j.lungcan.2008.02.001]

13 **Hainsworth JD**, Burris HA, Erland JB, Thomas M, Greco FA. Phase I trial of docetaxel administered by weekly infusion in patients with advanced refractory cancer. *J Clin Oncol* 1998; **16**:

2164-2168 [PMID: 9626217]
14 **Hensley ML**, Maki R, Venkatraman E, Geller G, Lovegren M, Aghajanian C, Sabbatini P, Tong W, Barakat R, Spriggs DR. Gemcitabine and docetaxel in patients with unresectable leiomyosarcoma: results of a phase II trial. *J Clin Oncol* 2002; **20**: 2824-2831 [PMID: 12065559]
15 **Baker SD**, Zhao M, Lee CK, Verweij J, Zabelina Y, Brahmer JR, Wolff AC, Sparreboom A, Carducci MA. Comparative pharmacokinetics of weekly and every-three-weeks docetaxel. *Clin Cancer Res* 2004; **10**: 1976-1983 [PMID: 15041715]
16 **Schuette W**, Nagel S, Blankenburg T, Lautenschlaeger C, Hans K, Schmidt EW, Dittrich I, Schweisfurth H, von Weikersthal LF, Raghavachar A, Reissig A, Serke M. Phase III study of second-line chemotherapy for advanced non-small-cell lung cancer with weekly compared with 3-weekly docetaxel. *J Clin Oncol* 2005; **23**: 8389-8395 [PMID: 16293869 DOI: 10.1200/JCO.2005.02.3739]
17 **Park SH**, Choi SJ, Kyung SY, An CH, Lee SP, Park JW, Jeong SH, Cho EK, Shin DB, Hoon Lee J. Randomized phase II trial of two different schedules of docetaxel plus cisplatin as first-line therapy in advanced nonsmall cell lung cancer. *Cancer* 2007; **109**: 732-740 [PMID: 17211861 DOI: 10.1002/cncr.22446]
18 **Eisenhauer EA**, Therasse P, Bogaerts J, Schwartz LH, Sargent D, Ford R, Dancey J, Arbuck S, Gwyther S, Mooney M, Rubinstein L, Shankar L, Dodd L, Kaplan R, Lacombe D, Verweij J. New response evaluation criteria in solid tumours: revised RECIST guideline (version 1.1). *Eur J Cancer* 2009; **45**: 228-247 [PMID: 19097774 DOI: 10.1016/j.ejca.2008.10.026]
19 **Song Z**, Zhang Y. Second-line docetaxel-based chemotherapy after failure of fluorouracil-based first-line treatment for advanced esophageal squamous cell carcinoma. *Onco Targets Ther* 2014; **7**: 1875-1881 [PMID: 25342911 DOI: 10.2147/OTT.S66525]
20 **Albertsson M**, Johansson B, Friesland S, Kadar L, Letocha H, Frykholm G, Wagenius G. Phase II studies on docetaxel alone every third week, or weekly in combination with gemcitabine in patients with primary locally advanced, metastatic, or recurrent esophageal cancer. *Med Oncol* 2007; **24**: 407-412 [PMID: 17917090]
21 **Chen YM**, Shih JF, Perng RP, Tsai CM, Whang-Peng J. A randomized trial of different docetaxel schedules in non-small cell lung cancer patients who failed previous platinum-based chemotherapy. *Chest* 2006; **129**: 1031-1038 [PMID: 16608954 DOI: 10.1378/chest.129.4.1031]
22 **Tanaka Y**, Yoshida K, Sanada Y, Osada S, Yamaguchi K, Takahashi T. Biweekly docetaxel, cisplatin, and 5-fluorouracil (DCF) chemotherapy for advanced esophageal squamous cell carcinoma: a phase I dose-escalation study. *Cancer Chemother Pharmacol* 2010; **66**: 1159-1165 [PMID: 20878160 DOI: 10.1007/s00280-010-1447-1]
23 **Smorenburg CH**, Sparreboom A, Bontenbal M, Verweij J. Combination chemotherapy of the taxanes and antimetabolites: its use and limitations. *Eur J Cancer* 2001; **37**: 2310-2323 [PMID: 11720823]
24 **Grunewald R**, Kantarjian H, Keating MJ, Abbruzzese J, Tarassoff P, Plunkett W. Pharmacologically directed design of the dose rate and schedule of 2',2'-difluorodeoxycytidine (Gemcitabine) administration in leukemia. *Cancer Res* 1990; **50**: 6823-6826 [PMID: 2208147]
25 **Houlihan WJ**, Munder PG, Handley DA, Nemecek GA. Preclinical pharmacology and possible mechanism of action of the novel antitumor agent 5-(4'-piperidinomethylphenyl)-2,3-dihydroimidazo [2,1-a]isoquinoline. *Arzneimittelforschung* 1995; **45**: 1133-1137 [PMID: 8595076]
26 **Attia S**, Morgan-Meadows S, Holen KD, Bailey HH, Eickhoff JC, Schelman WR, Traynor AM, Mulkerin DL, Campbell TC, McFarland TA, Huie MS, Cleary JF, Tevaarwerk AJ, Alberti DB, Wilding G, Liu G. Dose-escalation study of fixed-dose rate gemcitabine combined with capecitabine in advanced solid malignancies. *Cancer Chemother Pharmacol* 2009; **64**: 45-51 [PMID: 18841362 DOI: 10.1007/s00280-008-0844-1]
27 **Shim HJ**, Cho SH, Hwang JE, Bae WK, Song SY, Cho SB, Lee WS, Joo YE, Na KJ, Chung IJ. Phase II study of docetaxel and cisplatin chemotherapy in 5-fluorouracil/cisplatin pretreated esophageal cancer. *Am J Clin Oncol* 2010; **33**: 624-628 [PMID: 20142726 DOI: 10.1097/COC.0b013e3181bead92]
28 **Jin J**, Xu X, Wang F, Yan G, Liu J, Lu W, Li X, Tucker SJ, Zhong B, Cao Z, Wang D. Second-line combination chemotherapy with docetaxel and nedaplatin for Cisplatin-pretreated refractory metastatic/recurrent esophageal squamous cell carcinoma. *J Thorac Oncol* 2009; **4**: 1017-1021 [PMID: 19542899 DOI: 10.1097/JTO.0b013e3181add9c7]
29 **Merad M**, Le Cesne A, Baldeyrou P, Mesurolle B, Le Chevalier T. Docetaxel and interstitial pulmonary injury. *Ann Oncol* 1997; **8**: 191-194 [PMID: 9093730]
30 **Pavlakis N**, Bell DR, Millward MJ, Levi JA. Fatal pulmonary toxicity resulting from treatment with gemcitabine. *Cancer* 1997; **80**: 286-291 [PMID: 9217042]

P- Reviewer: Ameratunga M, Chen GS, Chen XL, Wu AB
S- Editor: Yu J **L- Editor**: A **E- Editor**: Ma S

World Journal of Gastroenterology

Submit a Manuscript: http://www.wjgnet.com/esps/
Help Desk: http://www.wjgnet.com/esps/helpdesk.aspx
DOI: 10.3748/wjg.v21.i14.4275

World J Gastroenterol 2015 April 14; 21(14): 4275-4283
ISSN 1007-9327 (print) ISSN 2219-2840 (online)

ORIGINAL ARTICLE

Prospective Study

Preparation of magnetic resonance probes using one-pot method for detection of hepatocellular carcinoma

You-Wei Li, Zheng-Guang Chen, Zhou-She Zhao, Hong-Li Li, Ji-Chen Wang, Zong-Ming Zhang

You-Wei Li, Department of Radiology, Beijing Chuiyangliu Hospital Affiliated to School of Medicine, Tsinghua University, Beijing 100022, China
Zheng-Guang Chen, Department of Radiology, Dongzhimen Hospital Affiliated to Beijing University of Chinese Medicine, Beijing 100700, China
Zhou-She Zhao, Hong-Li Li, GE Healthcare China, Beijing Economic and Technology Development Area, Beijing 100176, China
Ji-Chen Wang, Department of Radiology, Nanjing BenQ Hospital, Nanjing 210036, Jiangsu Province, China
Zong-Ming Zhang, Department of General Surgery, Beijing Electric Power Hospital, Capital Medical University, Beijing 100073, China
Author contributions: Zhang ZM and Zhao ZS designed the study; Li YW, Chen ZG and Li HL performed the study; Wang JC provided analytic tools and analyzed the data; Li YW and Chen ZG wrote the paper.
Supported by National Natural Science Foundation of China, No. 81071996.

Correspondence to: Zong-Ming Zhang, MD, PhD, Professor, Director, Department of General Surgery, Beijing Electric Power Hospital, Capital Medical University, No. 1 Taipingqiaoxili, Fengtai District, Beijing 100073, China. zhangzongming@mail.tsinghua.edu.cn
Telephone: +86-10-63503046
Fax: +86-10-63465865
Received: August 20, 2014
Peer-review started: August 20, 2014
First decision: November 4, 2014
Revised: November 17, 2014
Accepted: December 5, 2014
Article in press: December 8, 2014
Published online: April 14, 2015

Abstract

AIM: To prepare the specific magnetic resonance (MR) probes for detection of hepatocellular carcinoma (HCC) using one-pot method.

METHODS: The carboxylated dextran-coated nanoparticles were conjugated with anti-α-fetoprotein (anti-AFP) or anti-glypican 3 (anti-GPC3) antibodies through 1-(3-dimethylaminopropyl)-3-ethylcarbodiimide hydrochloride/N-hydroxysuccinimide (EDC/NHS)-mediated reaction to synthesize the probes. The physical and chemical properties of the probes were determined by transmission electron microscopy (TEM) and dynamic light scattering, and the relaxivity was compared to uncombined ultrasmall superparamagnetic iron oxide nanoparticles (USPIONs) using a 1.5T clinical MR scanner. The binding efficiency of the antibodies to nanoparticles was measured with an ultraviolet-visible spectrophotometer. In addition, the probes were incubated with targetable cells *in vitro*.

RESULTS: The superparamagnetic MR probes (anti-GPC3-USPION probe and anti-AFP-USPION probe) were synthesized using one-pot method. Their mean hydrodynamic diameter was 47 nm with a broader slight size distribution. The coupling efficiency of carboxylated dextran-coated ultrasmall superparamagnetic iron oxide (USPIO) with anti-GPC3 or anti-AFP antibody was 15.9% and 88.8%, respectively. Each of the USPIO nanoparticles may bind 3 GPC3 antibodies or 12 AFP antibodies. The statistical analysis showed no significance ($P > 0.05$) in shortening the T1 and T2 values when comparing the USPIO-AFP or USPIO-GPC3 to USPIO. Analysis of TEM images revealed that anti-GPC3-USPION probes and anti-AFP-USPION probes could specifically enter into the HepG2 cell by combining with the GPC3 receptors or AFP receptors, whereas the HepG2 cell sample incubated with USPIONs showed no or few nanoparticles in the cytoplasm.

CONCLUSION: The synthesized probes using one-pot method can be used for *in vitro* experimental study and have potential clinical application in MR imaging for detection of hepatocellular carcinomas.

Key words: Hepatocellular carcinoma; Ultrasmall superparamagnetic iron oxide nanoparticles; Specific probe; One-pot method; Magnetic resonance imaging

Core tip: The preparation process of magnetic resonance probes should be as simple as possible in order to have mass production. We developed a method named one-pot method by modifying the traditional methods to prepare an anti-glypican 3-ultrasmall superparamagnetic iron oxide nanoparticle (USPION) probe and an anti-α-fetoprotein-USPION probe and determined their physical and chemical properties and bioactivity. The results showed that this method is simple and convenient to synthesize the magnetic resonance molecular probes. The synthesized probes entered into the specific cells *in vitro*.

Li YW, Chen ZG, Zhao ZS, Li HL, Wang JC, Zhang ZM. Preparation of magnetic resonance probes using one-pot method for detection of hepatocellular carcinoma. *World J Gastroenterol* 2015; 21(14): 4275-4283 Available from: URL: http://www.wjgnet.com/1007-9327/full/v21/i14/4275.htm DOI: http://dx.doi.org/10.3748/wjg.v21.i14.4275

INTRODUCTION

Hepatocellular carcinoma is the fifth most common malignant tumor, more frequently seen in China. The results of treatment for hepatocellular carcinoma are poor, because it is most often diagnosed in late stages. Although there have been significant advances in various methods, early detection of hepatocellular carcinoma still needs further research.

With the advancement of the molecular imaging technology, the molecular magnetic resonance (MR) imaging is becoming immense interest because of its capability to yield highly detailed anatomic and molecular information *in vivo*. However, effective application of this technology relies greatly on the specific nanoprobes. Many specific probes have been reported in diagnosis of malignant tumors[1-3], such as breast cancer, pancreatic cancer, and ovarian tumors. However, little is known about the MR molecular probes specific for hepatic cell carcinoma, although there have been many studies using other ligands to synthesis nanoprobes for detection of HCC[4-6].

An MR molecular probe consists of two elements, magnetic nanoparticles and targetable markers such as antibodies or ligands. Ultrasmall superparamagnetic iron oxide (USPIO) was applied more commonly as a magnetic nanoparticle in life sciences, especially the nanoparticles with a diameter less than 100 nm and narrow distribution in size and high magnetism, which can significantly decrease T1 and T2/T2* values of a tissue. In addition, these nanoparticles have strongly magnetic susceptibility. The contrast between USPIO nanoparticles (USPIONs)-containing tissues and other USPIONs free tissues increased, especially in T2*-weighted imaging[7]. The USPIO nanoparticle has a magnetic core formed by Fe^{3+} and Fe^{2+} oxide crystal, which has ultrasuperparamagnetic behavior, and an external coat to produce biocompatibility *in vivo* and provide a place for conjugation with the antibodies or ligands. Because the specificity of MR nanoprobes was determined by the antibodies or ligands, we should make efforts in selecting antibodies for design of the probes. The antibodies should have high specificity, selectivity and stability.

Today many investigators[8-11] are prone to conjugate USPIONs with monoclonal antibodies or polypeptides to prepare the MR nanoprobes. These probes are only synthesized in laboratory through one-step or two-step method and cannot be produced largely. We developed a method named "one-pot method" by modifying the two-step method, to conjugate USPIONs with glypican 3 (GPC3) antibodies or anti-α-fetoprotein (AFP) antibodies because AFP is the most utilized surveillance biomarker for hepatocellular carcinoma and GPC3 is a more sensitive and specific biomarker for hepatocellular carcinoma which can be used to detect early-stage disease as recent studies have shown[12,13], and formed the MR probes specific for hepatic cell carcinoma. The average core size, size distribution, morphology and magnetic properties were measured by transmission electron microscopy (TEM), dynamic light scattering, and 1.5T MR scanning. The binding efficiency of the antibodies to nanoparticles was measured with an ultraviolet-visible spectrophotometer. In addition, the probes were incubated with targetable cells *in vitro*. The results showed that it is simple and convenient to synthesize the MR molecular probes using the one-spot method. Although the coupling difference with various antibodies (anti-AFP antibody or GPC3 antibody) was observed, the synthesized probes can be used as a contrast agent for clinical MR imaging.

MATERIALS AND METHODS

Materials

All reagents used for synthesis were purchased from commercial sources. These were sodium periodate and Dextran 10000 from Sinopharm Chemical Reagent Co., LTD. (China); ferric chloride hexahydrate from Shantou Xilong Chemical Co., LTD. (China); $FeNH_4SO_4 \cdot 6H_2O$ from Fuchen Chemical Reagent Company (Tianjin, China); NaOH from Beijing Chemical Works (China);

GPC3 monoclonal antibody from Htpharma Technology Development (Beijing) Co., Ltd; AFP monoclonal antibody from Baitai Biotechnology (Beijing) Co., Ltd.; and 1-(3-dimethylaminopropyl)-3-ethylcarbodiimide hydrochloride (EDC) and N-hydroxysuccinimide (NHS) from Thermo Company.

Synthesis of USPIONs with carboxylate groups

USPIONs coated by dextran with carboxylate groups were synthesized at Wangleyu lab, Department of Chemistry, Beijing University of Chemical Technology. Aqueous coprecipitation of magnetite was used. Briefly, 0.3 g of dextran 10000 was dissolved in 10 mL deionized water, and then 0.4 g of sodium periodate was added to a final concentration of 100 mmol. The hydroxyl groups on dextran were partially oxidized to carboxylate groups at 80 ℃ for 20 min. After purification by dialysis to remove excess sodium periodate, oxidized dextran resolution was mixed with 1 mmol ferric chloride hexahydrate and 2 mmol $FeNH_4SO_4 \cdot 6H_2O$ in an aqueous solution with an excess of concentrated sodium hydroxide (15 mmol). The mixture in a reaction boiler was heated to 160 ℃ for 10 h and then cooled down to room temperature. To make the products precipitate, 0.1 M/L HCl was added to the mixture. After centrifugation at 5000 rpm for 5 min, the supernatant was decanted. The process was repeated three times, and then the final black products were resuspended in deionized water for further use.

Carboxylated dextran-coated USPIONs coupled with antibodies

EDC (1 mg) and sulfo-NHS (2 mg) were dissolved in 0.5 mL phosphate-buffered saline (PBS, pH = 7.4), and the pH value was adjusted to 5.0 by titrating the mixture solution with 0.2 N HCl. Carboxylated dextran-coated USPIO (1 mL, 5 mg/mL) was added to the solution and allowed to react for 2 h. After adding 0.5 mL of 1 mg/mL anti-AFP or 200 μg/mL anti-GPC3 antibody (0.5 mL PBS was added to the control), the mixture was stirred and allowed to react for 3 h. The pH value of the mixture solution was then adjusted to 7.0 by titrating with 0.2 N NaOH. After reaction for further 30 min, the solution was centrifuged at 5000 rpm/min for 5 min and the supernatant was discarded to obtain the products. The formed USPIO-antibody probes were resuspended in PBS at 4 ℃ for further application.

The prepared MR molecular probes were divided into two parts, one for measurement of the coupling ability of carboxylated dextran-coated USPIO with antibody and the other for measurement of relaxivity.

Properties of the magnetic molecular probe

The average core size, size distribution, and morphology were examined using a transmission electron microscope (Hitach 7600, Japan) at a voltage of 100 kV in the magnification range from × 40000 to × 600000. Samples were drop-cast onto a 200-mesh copper grid and were air-dried at room temperature before being loaded into the microscope. To examine the hydrodynamic diameters of the magnetic molecular probes, dynamic light scattering measurements were performed using a Malvern laser granulometer (Zetasizer Nano ZS90, Malvern, United Kingdom) at 25 ℃. Their magnetic properties and the magnetic saturation were determined with a Superconducting Quantum Interference Device (SQUID).

Measurement of the coupling ability of carboxylated dextran-coated USPIO with antibody

Determination of iron content in antibody-USPIO: The flame atom absorbing law was used to measure the iron content in antibody-USPIO. Samples were prepared by acid digestion. Antibody-USPIO sample (40 μL) was aspirated exactly by means of micropipette aspiration. When the sample adsorbed on the tip of micropipette was wiped out, the micropipette was dipped 3-4 mm undersurface of the fluid in a centrifuge tube containing 1.2 mL dilute solution, and then the sample was discharged slowly. Forty microliters of dilute solution was absorbed and then discharged. This process was repeated two times. The prepared sample was measured by atomic absorption spectroscopy (BHS 100, Bohui Innovation Technology Co. Ltd, Beijing).

Determination of antibody content in antibody-USPIO: The free antibody content in supernatant fluid was determined after centrifugation, and then the content of antibody coupled with USPIO was calculated. The supernatant fluid (1.7 mL) was dialyzed with 0.2 M PBS (pH 7.0) to displace the solution disturbing the accuracy of measurement. During the dialyzing process using 2 L dialyzing fluid at 2-8 ℃ for 24 h, dialyzing fluid was changed 4 times per 2 h. After the last time the dialysis lasted overnight. The prepared samples were mixed with AB solution of the BCA Protein Assay Reagent, in which A solution was mixed with B solution at a rate of 50:1 and at a proportion of 20:1 for incubation at 37 ℃ in a water bath for 30 min. The incubated samples were taken out and then were measured with an ultraviolet-visible spectrophotometer (DU800, BECKMANCOULER Company).

Measurement of anti-AFP-USPIO, anti-GPC3-USPIO and USPIO relaxivity

Preparation of 1% agar solution: Agar (1 g) was added to 100 mL deionized water and was heated up to 80 ℃. After the agar was dissolved completely, the solution was cooled down to 50 ℃. The resulting 1% agar solution was used to carry the antibody-USPIO.

Preparation of samples for MR scanning: The concentration of 5 mg/mL iron of the anti-AFP-USPIO, anti-GPC3-USPIO or USPIO was diluted to 0.25, 0.125,

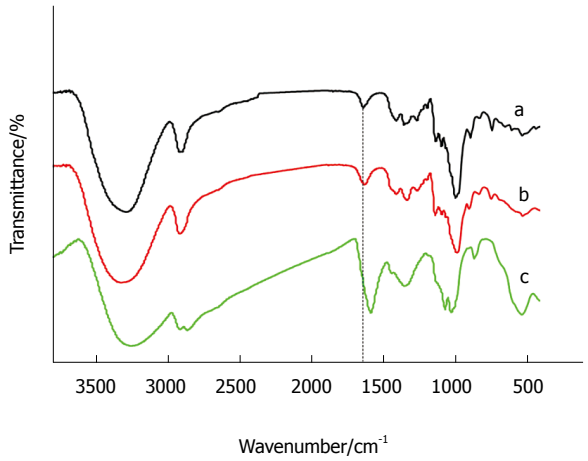

Figure 1 Fourier transform infrared spectrometer spectra of chemical groups of pure dextran (a), pure dextran coated ultrasmall superparamagnetic iron oxide nanoparticles (b), and oxidized dextran coated ultrasmall superparamagnetic iron oxide nanoparticles (c). The peak of 1615 indicates carboxylate groups (dot line).

0.0625, 0.031 or 0.016 mg/mL. These test samples were centrifuged and all the supernatant fluids were discarded. Each of the precipitated samples was added to a Pendoff test containing 2 mL of 1% agar solution. The mixture was shook well and then cooled down to room temperature.

MR scanning: The test tubes and control sample (2 mL of 1% agar solution) were imaged using a 1.5T MR scanner (Excite, GE Medical Systems, Milwaukee, WI, USA) with a standard circularly polarized quadrature knee coil. To avoid susceptibility artifacts from the surrounding air in the scans, all tubes were placed in a water-containing plastic container at room temperature.

To measure the T1 relaxation times, axial spin echo (SE) sequences were obtained with a fixed echo time (TE) of 9 ms and multiple repetition time (TR) values of 1200, 900, 600 and 300 ms, whereas axial SE images with a fixed TR of 2000 ms and increasing TEs of 12, 24, 36, and 48 ms were obtained for measurements of T2 relaxation times. All sequences were acquired with a field of view of 160 mm × 160 mm, a matrix of 192 × 160 pixels, a slice thickness of 5.0 mm, a gap of 1.0 mm and one acquisition.

Data analysis

The data acquired using the above mentioned methods were transferred into the Function tool on the workstation. T1 maps were calculated from four SE images with a fixed TE of 9 ms and variable TR values of 1200, 900, 600 and 300 ms using a nonlinear function least-square curve fitting on a pixel-by-pixel basis. T2 maps were calculated accordingly from four SE images with a fixed TR of 2000 and TE values of 12, 24, 36 and 48 ms. Then the T1 and T2 relaxation times of test tubes and control samples were derived by ROI measurements of the test samples on these T1 and T2 maps. T1 and T2 maps were calculated assuming monoexponential signal decay. Only data points with signal intensities significantly above the noise level were analyzed.

In vitro studies

HepG2 cells are human hepatocellular carcinoma cells expressing GPC3 receptors or AFP receptors, confirmed by flow cytometry using monoclonal anti-human glypican 3 antibody or anti-AFP antibody. Cells in 6-well plates, (each well containing 5 mL medium and 1 × 10^6 HepG2 cells) were incubated with anti-AFP-USPIO, anti-GPC3-USPIO or USPIO for 4 h in a humidified 5% CO_2 atmosphere at 37 ℃, respectively. The iron concentrations of the probes used were 500 or 125 μg/mL. Afterwards, the adherent cells were washed three times with PBS (0.1 mol/L, pH 7.4), trypsinized, and centrifuged for sedimentation (10 min, 250 g, 20 ℃) in order to remove unbounded particles. The cells were then fixed in electron microscopic specimen stationary liquid and analyzed using a transmission electron microscope (Hitachi 7600, Japan) at a voltage of 80 kV in the magnification range from × 40000 to × 600000.

Statistical analysis

Six regions of interest in each sample were measured. T1 and T2 values are presented as mean ± SE. To compare differences in quantitative data between different samples, a two-tailed paired *t*-test was used. $P < 0.05$ was considered statistically significant. All analyses were processed using SPSS 11.5 software (sequence license 30001359390).

RESULTS

Properties of the magnetic molecular probe

The hydroxyl groups on dextran were partially oxidized to carboxylate groups by using sodium periodate. From Figure 1 we can see the peak of carboxylate groups. The carboxylated dextran was then coated on the surface of USPIONs. Through covalent conjugation of carboxylate groups with antibodies the magnetic molecular probes were prepared.

As shown in Figure 2A, the magnetic molecular probe showed a core/shell spherical structure with a core diameter of 5-8 nm. The nanoparticles displayed homogeneous size and good dispersity in solution. Dynamic light scattering demonstrated a broader slightly size distribution and the mean hydrodynamic diameter of the magnetic molecular probes was 47 nm (Figure 2B).

The superparamagnetic behavior of the nanoparticles was checked by magnetization measurement SQUID). The hysteresis curve (Figure 3) indicated superparamagnetic characteristics at room temperature, meaning that the thermal energy can overcome the anisotropy energy barrier of a single particle, and the net magnetization of the particle assemblies in the

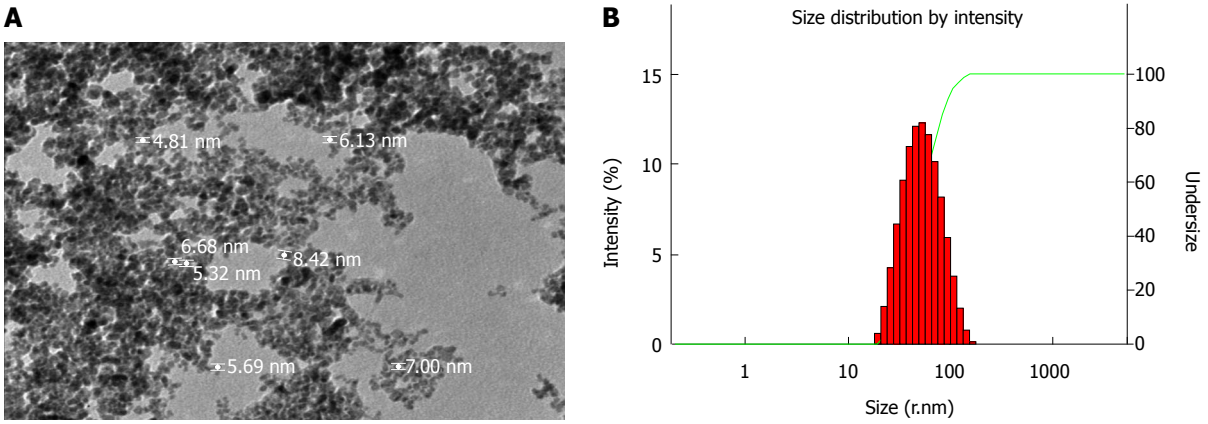

Figure 2 The properties of the magnetic molecular probes. A: Transmission electron microscopy demonstrates the size and morphology of the magnetic molecular probes under a magnification of × 40000; B: Malvern Zetasizer Nano ZS90 laser granulometer showed the mean hydrodynamic diameter of the magnetic molecular probes and their distribution.

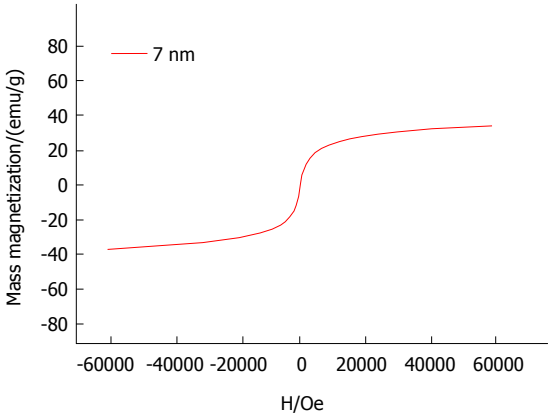

Figure 3 Hysteresis loops of the 7 nm (red line) magnetic probes at 0.6 T.

absence of an external field is zero. The nanoparticles showed a saturation magnetization of 35.5 emu/g at 0.6T with a coercivity of zero.

Measurement of the coupling ability of carboxylated dextran-coated USPIO with antibody

The iron content in antibody-USPIO was 1.20 mg measured by the flame atom absorbing law. The free antibody content in supernatant fluid (1.7 mL) was determined using an ultraviolet-visible spectrophotometer. The results showed the concentration of anti-GPC3 was 12 μg/mL and the anti-AFP 33 μg/mL. Therefore the contents of bound anti-GPC3 and bound anti-AFP were 79.6 μg/5 mg and 443.9 μg/5 mg, and the coupling efficiency was 15.9% and 88.8%, respectively. Each of the USPIO nanoparticles may bind three GPC3 antibodies or 12 AFP antibodies.

Measurement of anti-AFP-USPIO, anti-GPC3-USPIO and USPIO relaxivity

From Tables 1 and 2 we can see that all the USPIO-AFP, USPIO-GPC3 and USPIO could shorten T1 and T2 values of the agar solution, especially T2 value. The higher the concentration, the smaller the values. Although the statistical analysis showed no significance ($P > 0.05$) in shortening the T1 and T2 values among the USPIO-AFP, USPIO-GPC3 and USPIO, the degree of T1 and T2 value decrease was higher by pure USPIO than by USPIO-AFP or USPIO-GPC3. Moreover, the slight difference existed between USPIO-AFP and USPIO-GPC3 in shortening the T1 and T2 values, and USPIO-AFP with more antibodies affected magnetization more than USPIO-GPC3 with fewer antibodies (Figures 4 and 5).

In vitro studies

Figure 6A and 6B shows a TEM picture of a HepG2 cell sample incubated with anti-GPC3-USPION probes or anti-AFP-USPION probes for 4 h, respectively. Incorporation of the probes into intracellular organelles follows the endocytosis pathway. First, the probes interact with the GPC3 receptors or AFP receptors expressed on the surface of the HepG2 cell *via* antigen-antibody combinations. Then they accumulate into membrane invaginations and are enclosed into the cytoplasm. Analysis of TEM images revealed that densely packed nanoparticles were in the endosomes. But the content of the probes incorporated intracellularly was different between HepG2 cells incubated with anti-GPC3-USPION probes and HepG2 cells with anti-AFP-USPION probes, and a higher content of anti-GPC3-USPION probes was observed in our experiments.

In contrast, the TEM picture of a HepG2 cell sample incubated with USPIONs showed no or little nanoparticles in the cytoplasm (Figure 6C).

DISCUSSION

This study applied condensation coupling of carboxyl nanoparticles with amines on the antibodies to produce MRI biological probes. It is well known that there were two methods, single step method and two-step method, to couple carboxylate particles with amine-containing molecules such as antibody through an aqueous, carbodiimide-mediated process

Table 1 The T1 values of the samples

	1 (0.25 mg)	2 (0.125 mg)	3 (0.0625 mg)	4 (0.031 mg)	5 (0.016 mg)	Control
USPIO-AFP	427.72 ± 98.67	570.35 ± 110.75	994.36 ± 164.68	1535.9 ± 254.45	2658.2 ± 284.99	2783.4
USPIO-GPC3	392.50 ± 93.25	526.85 ± 109.83	923.55 ± 156.32	1341.8 ± 255.78	2718.1 ± 283.32	2916.1
USPIO	331.08 ± 86.73	523.08 ± 121.47	805.85 ± 145.60	1306.3 ± 202.93	2240.9 ± 268.20	2776.4

1-5 represent the sample of 2 mL 1% agar solution containing the iron concentrations of 0.25, 0.125, 0.0625, 0.031 and 0.016 mg/mL in the anti-AFP-USPIO, anti-GPC3-USPIO or USPIO solution, respectively. USPIO: Ultrasmall superparamagnetic iron oxide; USPIO-AFP: USPIO-α-fetoprotein; USPIO-GPC3: USPIO-glypican 3.

Table 2 The T2 values of the samples

	1 (0.25 mg)	2 (0.125 mg)	3 (0.0625 mg)	4 (0.031 mg)	5 (0.016 mg)	Control
USPIO-AFP		15.18 ± 0.67	15.92 ± 1.21	25.93 ± 1.13	43.48 ± 1.60	66.20
USPIO-GPC3		36.64 ± 0.42	14.98 ± 0.97	21.48 ± 1.20	42.18 ± 1.52	66.50
USPIO		14.83 ± 0.37	13.44 ± 0.85	22.17 ± 1.02	37.3 ± 1.37	67.67

1-5 represent the sample of 2 mL 1% agar solution containing the iron concentrations of 0.25, 0.125, 0.0625, 0.031 and 0.016 mg/mL in the anti-AFP-USPIO, anti-GPC3-USPIO or USPIO solution, respectively. The signal has gone in 1 test tube in given TEs because the concentration of USPIO-AFP, or USPIO-GPC3, or USPIO is higher. USPIO: Ultrasmall superparamagnetic iron oxide; USPIO-AFP: USPIO-α-fetoprotein; USPIO-GPC3: USPIO-glypican 3.

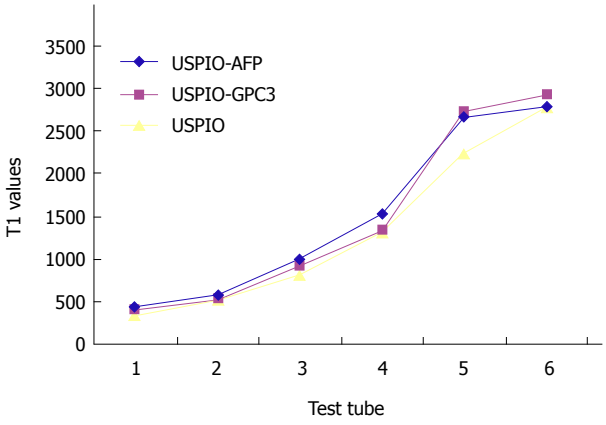

Figure 4 Relationship between T1 values and samples with different concentrations. The test tubes 1-5 contain the iron concentrations of 0.25, 0.125, 0.0625, 0.031 and 0.016 mg/mL in the anti-AFP-USPIO, anti-GPC3-USPIO or USPIO solution, respectively. The test tube 6 contains 1% agar solution as control. USPIO: Ultrasmall superparamagnetic iron oxide; USPIO-AFP: USPIO-α-fetoprotein; USPIO-GPC3: USPIO-glypican 3.

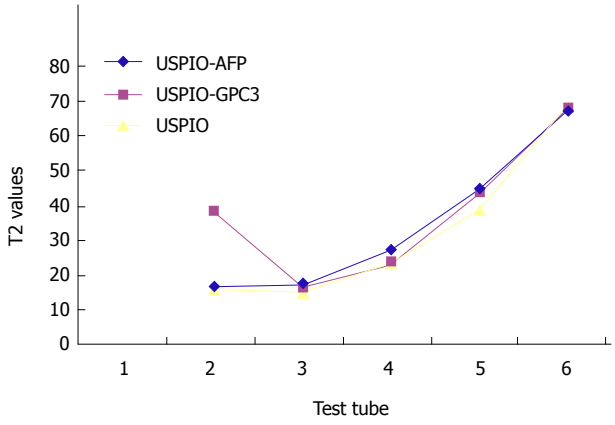

Figure 5 Relationship between T2 values and samples with different concentrations. The test tubes 1-5 contain the iron concentrations of 0.25, 0.125, 0.0625, 0.031 and 0.016 mg/mL in the anti-AFP-USPIO, anti-GPC3-USPIO or USPIO solution, respectively. The test tube 6 contains 1% agar solution as control. USPIO: Ultrasmall superparamagnetic iron oxide; USPIO-AFP: USPIO-α-fetoprotein; USPIO-GPC3: USPIO-glypican 3.

using EDC and/or sulfo-NHS[14]. The single-step method used EDC alone as coupling agent and is only for molecules having one or more amines without any carboxylates, whereas the two-step method is appropriate for molecules that have both amines and carboxylates, in which EDC and sulfo-NHS are all used. Firstly, the carboxylate particles are activated with the water-soluble EDC to create an intermediate ester under acidic conditions (pH 3.5-4.5), which is reactive directly with amines on molecules to form an unstable intermediate ester. With the addition of sulfo-NHS, another intermediate, the sulfo-NHS ester is produced. This intermediate is more stable and has high solubility, so that it reacts with the attacking amine groups quickly. After the formation of the intermediate ester the reaction medium was adjusted to mildly alkaline pH conditions (*e.g.*, pH 8.5), facilitating the covalent conjugation of carboxylate nanoparticles with antibodies. Because carbodiimide-mediated antibody polymerization will occur due to the presence of both amines and carboxylates on antibodies, the excess EDC in the solution must be removed before adding antibodies. This will prevent the decrease of the amount of antibodies coupled to carboxylate nanoparticles as well as the biologic function of the antibody[15]. This method has a good quality control, but the fussy operation and strict control per step limit mass production. In this study, we modified the two-step method to synthesize an MR nanoprobe based on the design conception, in which we focused on

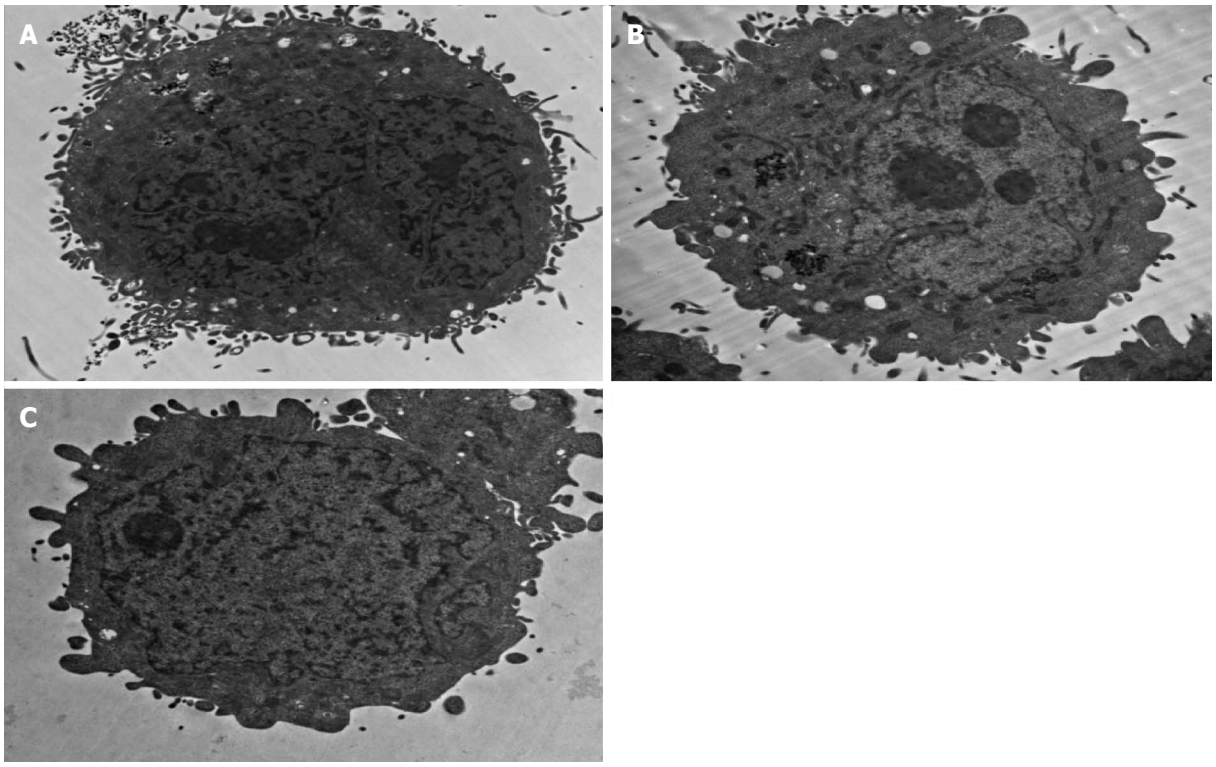

Figure 6 Transmission electron microscopy demonstrates the structure of the HepG2 cells under a magnification of × 10000. A: HepG2 cell with expression of GPC3 receptors incubated with anti-GPC3-USPIONs probes, and the probes were seen on the surface of the cell and in the cell (black aggregation); B: HepG2 cell with expression of AFP receptors incubated with anti-AFP-USPIONs probes, and the probes were seen in the cell (black aggregation); C: HepG2 cell with expression of GPC3 receptors incubated with USPIONs probes, and no USPION was seen. USPION: Ultrasmall superparamagnetic iron oxide nanoparticle; AFP: α-fetoprotein; GPC3: Glypican 3.

coupling effect and actual application effect, as well as the preparation process as simple as possible. It is known as "one-pot method", in which both activation and coupling processes were completed in entirely aqueous conditions without removing excess EDC and/or NHS before adding antibodies.

The synthesized probe must have some characteristics such as optimal size and the physical and chemical characteristics of the coating materials to escape the phagocytosis by the mononuclear phagocytic system and retain their biological activity of the targeted molecules in the bloodstream. The MR probes can cross the capillary into tissues and have a chance to combine the lesions specifically through the specific molecules such as monoclonal antibodies or a ligand on the surface of the probes. Many studies have shown that particle size has an important role in the blood clearance of stealth probes. The optimal size (hydrodynamic diameter) range is 8-50 nm[16-18]. The probe with a hydrodynamic diameter less than 5.5 nm can be removed quickly from the body *via* the renal system. When probes with a hydrodynamic diameter larger than 50 nm were injected into the body, they were also removed from the bloodstream rapidly, typically a matter of minutes, and usually accumulate in the liver and spleen.

A disadvantage of the molecular MR imaging is low sensitivity. If the magnetic strength of the USPIOs decreased greatly in the design and preparation of probes, the lesion will not be detected by MRI even though it was targeted with the probes. Leuschner *et al*[19] compared the probe combined 60 mg SPIONs to 3.7 mg LHRH and SPIONs. They demonstrated that the saturation magnetization and the Zeta potential of SPIONs were higher than those of LHRH-SPION. The Zeta potential of SPIONs was positively charged (28.5 ± 1.93 mV), whereas LHRH-SPION was almost neutral (-2.2 ± 0.85 mV). Although the magnetization values of LHRH-SPION decreased by 5%-6% compared to SPIONs due to binding LHRH in LHRH-SPION samples, they assumed that the decrease was acceptable. Chen *et al*[20] and Huang *et al*[21] came to the same conclusion. However, Zhang *et al*[22] reported that there was no difference between SPION and SPION-antibody. Our experimental results also showed no significance in shortening the T1 and T2 values among the USPIO-AFP, USPIO-GPC3 and USPIO.

From the above experiments, it was seen that the content of antibodies connected with nanoparticles was related to the kinds of antibodies used for conjugation, although their concentrations used for coupling were different. Our results were the same with others. Some laboratories[23] reported that 2-3 antibodies per nanoparticle was coupled, however, some investigators[19] reported up to 12 antibodies per nanoparticle, according to different tumor marker

requirement. The synthesized anti-GPC3 USPIO probes and anti-AFP USPIO probes were respectively transported into cells through combination of ligands or antibodies with specific receptors on the surface of cells, but the contents of the two probes were different. This phenomenon may be due to the different intensity of GPC3- or AFP- receptors expressed on the surface of HepG2 cells. However, HepG2 cells incubated with USPIONs showed few nanoparticles in cytoplasm. This may be due to nonspecific endocytosis, which will be further studied.

The present preparation method had several limitations. First, as described above, we used random covalent conjugation to couple the antibody with carboxylate nanoparticles. The antigen binding sites with antibody were inevitably connected to nanoparticles[24,25], which will decrease the function of the antibody. In addition, the immunogenicity of the synthesized probes was not determined.

In conclusion, it is simple and convenient to synthesize the MR molecular probes using one-pot method. The coupling efficiency of antibodies with nanoparticles was enough compared to results reported by other investigators. The amount of antibodies coupled with the probes can be controlled according to the needs and does not change the magnetization significantly. The synthesized probes can enter targetable cells in *in vitro* cell studies. Therefore, the probes synthesized using one-pot method can be used as an MR contrast agent for animal experimental study and have a potential clinical application in MR imaging for early detection of hepatic cell carcinoma.

COMMENTS

Background

Hepatocellular carcinoma is the fifth most common malignant tumor, more frequently seen in China. The results of treatment for hepatocellular carcinoma are poor because it is often diagnosed in late stages. Although there have been significant advances in various methods, early detection of hepatocellular carcinoma still needs further research.

Research frontiers

With the advancement of the molecular imaging technology, the molecular MR imaging is becoming immense interest because of its highly detailed anatomic and molecular resolution *in vivo*. Many specific probes have been reported in diagnosis of malignant tumors, such as breast cancer, pancreatic cancer, and ovarian tumors. However, little is known about the MR molecular probes specific for hepatic cell carcinoma.

Innovations and breakthroughs

This study synthesized the magnetic resonance (MR) molecular probes specific for hepatic cell carcinoma using one-pot method. The results suggest that the synthesized anti-glypican 3 (anti-GPC3)-USPION (ultrasmall superparamagnetic iron oxide nanoparticle) probes or anti-α-fetoprotein (anti-α-AFP)-USPION probes interact with the GPC3 receptors or AFP receptors expressed on the surface of the HepG2 cell and entered into the cytoplasm. This will be expected to make a breakthrough in the early diagnosis of liver cancer.

Applications

The synthesized probes can be used as an MR contrast agent for animal experimental study and have potential clinical application in MR imaging for early detection of hepatic cell carcinoma.

Peer-review

This is a good study in which the authors introduced a new method to prepare the MR probes for detection of hepatocellular carcinoma. The results showed that the method is simple and can be used to synthesize the MR molecular probes largely. The synthesized probes can specially enter targetable cells in *in vitro* cell studies.

REFERENCES

1 **Yan C**, Wu Y, Feng J, Chen W, Liu X, Hao P, Yang R, Zhang J, Lin B, Xu Y, Liu R. Anti-αvβ3 antibody guided three-step pretargeting approach using magnetoliposomes for molecular magnetic resonance imaging of breast cancer angiogenesis. *Int J Nanomedicine* 2013; **8**: 245-255 [PMID: 23345972 DOI: 10.2147/IJN.S38678]

2 **Zuo HD**, Yao WW, Chen TW, Zhu J, Zhang JJ, Pu Y, Liu G, Zhang XM. The effect of superparamagnetic iron oxide with iRGD peptide on the labeling of pancreatic cancer cells in vitro: a preliminary study. *Biomed Res Int* 2014; **2014**: 852352 [PMID: 24977163 DOI: 10.1155/2014/852352]

3 **Shahbazi-Gahrouei D**, Abdolahi M. Superparamagnetic iron oxide-C595: Potential MR imaging contrast agents for ovarian cancer detection. *J Med Phys* 2013; **38**: 198-204 [PMID: 24672155 DOI: 10.4103/0971-6203.121198]

4 **Jia FG**, Zhang XD, Xu YK, Meng Z. [Synthesis of Gal-BSA-SPIO and magnetic resonance imaging of ASG receptors in rabbits bearing liver VX2 tumor and human liver]. *Nanfang Yike Daxue Xuebao* 2009; **29**: 191-194 [PMID: 19246275]

5 **Lee CM**, Jeong HJ, Kim EM, Kim DW, Lim ST, Kim HT, Park IK, Jeong YY, Kim JW, Sohn MH. Superparamagnetic iron oxide nanoparticles as a dual imaging probe for targeting hepatocytes in vivo. *Magn Reson Med* 2009; **62**: 1440-1446 [PMID: 19859969 DOI: 10.1002/mrm.22123]

6 **Huo T**, Du X, Zhang S, Liu X, Li X. Gd-EDDA/HYNIC-RGD as an MR molecular probe imaging integrin alphanubeta3 receptor-expressed tumor-MR molecular imaging of angiogenesis. *Eur J Radiol* 2010; **73**: 420-427 [PMID: 19261416 DOI: 10.1016/j.ejrad.2008.11.025]

7 **Qiao R**, Yang C, Gao M. Superparamagnetic iron oxide nanoparticles: from preparations to in vivo MRI applications. *J. Mater Chem* 2009; **19**: 6274-6293 [DOI: 10.1039/b902394a]

8 **You XG**, Tu R, Peng ML, Bai YJ, Tan M, Li HJ, Guan J, Wen LJ. Molecular magnetic resonance probe targeting VEGF165: preparation and in vitro and in vivo evaluation. *Contrast Media Mol Imaging* 2014; **9**: 349-354 [PMID: 24729581 DOI: 10.1002/cmmi.1584]

9 **Guo Q**, Liu Y, Xu K, Ren K, Sun W. Mouse lymphatic endothelial cell targeted probes: anti-LYVE-1 antibody-based magnetic nanoparticles. *Int J Nanomedicine* 2013; **8**: 2273-2284 [PMID: 23818783 DOI: 10.2147/IJN.S45817]

10 **Shahbazi-Gahrouei D**, Abdolahi M. Detection of MUC1-expressing ovarian cancer by C595 monoclonal antibody-conjugated SPIONs using MR imaging. *ScientificWorldJournal* 2013; **2013**: 609151 [PMID: 24194685 DOI: 10.1155/2013/609151]

11 **Li Y**, Chen Z, Li F, Wang J, Zhang Z. Preparation and in vitro studies of MRI-specific superparamagnetic iron oxide antiGPC3 probe for hepatocellular carcinoma. *Int J Nanomedicine* 2012; **7**: 4593-4611 [PMID: 22956868 DOI: 10.2147/IJN.S32196]

12 **Kandil D**, Leiman G, Allegretta M, Trotman W, Pantanowitz L, Goulart R, Evans M. Glypican-3 immunocytochemistry in liver fine-needle aspirates : a novel stain to assist in the differentiation of benign and malignant liver lesions. *Cancer* 2007; **111**: 316-322 [PMID: 17763368]

13 **Ligato S**, Mandich D, Cartun RW. Utility of glypican-3 in differentiating hepatocellular carcinoma from other primary and metastatic lesions in FNA of the liver: an immunocytochemical study. *Mod Pathol* 2008; **21**: 626-631 [PMID: 18264086 DOI: 10.1038/modpathol.2008.26]

14 **Hermanson GT**. Polymeric microspheres and nanoparticles. In: Bioconjugate techniques (second edition). New York: Academic Press, 2008: vol.14, p. 588

15 **Bonfield TL**, John N, Barna BP, Kavuru MS, Thomassen MJ,

Yen-Lieberman B. Multiplexed particle-based anti-granulocyte macrophage colony stimulating factor assay used as pulmonary diagnostic test. *Clin Diagn Lab Immunol* 2005; **12**: 821-824 [PMID: 16002629]

16 **Nowak J**, Wiekhorst F, Trahms L, Odenbach S. The influence of hydrodynamic diameter and core composition on the magnetoviscous effect of biocompatible ferrofluids. *J Phys Condens Matter* 2014; **26**: 176004 [PMID: 24721897 DOI: 10.1088/0953-8984/26/17/176004]

17 **Antonelli A**, Sfara C, Battistelli S, Canonico B, Arcangeletti M, Manuali E, Salamida S, Papa S, Magnani M. New strategies to prolong the in vivo life span of iron-based contrast agents for MRI. *PLoS One* 2013; **8**: e78542 [PMID: 24223101 DOI: 10.1371/journal.pone.0078542]

18 **Dong C**, Irudayaraj J. Hydrodynamic size-dependent cellular uptake of aqueous QDs probed by fluorescence correlation spectroscopy. *J Phys Chem B* 2012; **116**: 12125-12132 [PMID: 22950363 DOI: 10.1021/jp305563p]

19 **Leuschner C**, Kumar CS, Hansel W, Soboyejo W, Zhou J, Hormes J. LHRH-conjugated magnetic iron oxide nanoparticles for detection of breast cancer metastases. *Breast Cancer Res Treat* 2006; **99**: 163-176 [PMID: 16752077]

20 **Chen DH**, Liao MH. Preparation and characterization of YADH-bound magnetic nanoparticles. *J Mol Cat B: Enzym* 2002; **16**: 283-291 [DOI: 10.1016/S1381-1177(01)00074-1]

21 **Huang SH**, Liao MH, Chen DH. Direct binding and characterization of lipase onto magnetic nanoparticles. *Biotechnol Prog* 2003; **19**: 1095-1100 [PMID: 12790688]

22 **Zhang K**, Li JD, Zhang RP, Xin L, Li J. The preliminary study of molecular imaging of colorectal cancer cells with superparamagnetic iron oxide-based MR targeting probe containing vascular endothelial growth factor in vitro. *J Chin Radiol* 2010; **44**: 84-89

23 **Funovics MA**, Kapeller B, Hoeller C, Su HS, Kunstfeld R, Puig S, Macfelda K. MR imaging of the her2/neu and 9.2.27 tumor antigens using immunospecific contrast agents. *Magn Reson Imaging* 2004; **22**: 843-850 [PMID: 15234453]

24 **Masuda T**, Miyoshi E. Cancer biomarkers for hepatocellular carcinomas: from traditional markers to recent topics. *Clin Chem Lab Med* 2011; **49**: 959-966 [PMID: 21428856 DOI: 10.1515/CCLM.2011.152]

25 **Lin PC**, Chen SH, Wang KY, Chen ML, Adak AK, Hwu JR, Chen YJ, Lin CC. Fabrication of oriented antibody-conjugated magnetic nanoprobes and their immunoaffinity application. *Anal Chem* 2009; **81**: 8774-8782 [PMID: 19874051 DOI: 10.1021/ac9012122]

P- Reviewer: Shen J **S- Editor**: Yu J
L- Editor: Wang TQ **E- Editor**: Liu XM

World Journal of Gastroenterology

Submit a Manuscript: http://www.wjgnet.com/esps/
Help Desk: http://www.wjgnet.com/esps/helpdesk.aspx
DOI: 10.3748/wjg.v21.i14.4284

World J Gastroenterol 2015 April 14; 21(14): 4284-4292
ISSN 1007-9327 (print) ISSN 2219-2840 (online)

ORIGINAL ARTICLE

Prospective Study

Prophylactic antiviral therapy in allogeneic hematopoietic stem cell transplantation in hepatitis B virus patients

Ya-Ping Liao, Jia-Lu Jiang, Wai-Yi Zou, Duo-Rong Xu, Juan Li

Ya-Ping Liao, Jia-Lu Jiang, Wai-Yi Zou, Duo-Rong Xu, Juan Li, Department of Hematology, the First Affiliated Hospital, Sun Yat-sen University, Guangzhou 510000, Guangdong Province, China

Author contributions: Zou WY and Li J designed the study and wrote the protocol; Zou WY and Liao YP designed the study and helped with all correspondence related to this paper; Zou WY and Liao YP instructed the whole study and manuscript writing; Liao YP, Jiang JL and Xu DR performed experimental studies; Liao YP and Jiang JL acquired the data; Liao YP managed the literature searches and analyses as well as the statistical analysis; Liao YP wrote the first draft of the manuscript; all the authors approved the final version of the manuscript.

Ethics approval: The study was reviewed and approved by Institutional Review Board of the First Affiliated Hospital, Sun Yat-sen University.

Informed consent: All study participants, or their legal guardian, provided informed written consent prior to study enrollment.

Conflict-of-interest: No potential conflicts of interest relevant to this article were reported.

Data sharing: No additional data are available.

Correspondence to: Wai-Yi Zou, Associate Professor, Department of Hematology, the First Affiliated Hospital, Sun Yat-sen University, No. 58 Zhongshan 2nd Road, Yuexiu District, Guangzhou 510000, Guangdong Province, China. waiyizou@medmail.com.cn
Telephone: +86-20-28823388

Received: August 25, 2014
Peer-review started: August 26, 2014
First decision: September 27, 2014
Revised: November 19, 2014
Accepted: January 8, 2015
Article in press: January 8, 2015
Published online: April 14, 2015

Abstract

AIM: To investigate the timing, safety and efficacy of prophylactic antiviral therapy in patients with hepatitis B virus (HBV) infection undergoing allogeneic hematopoietic stem cell transplantation (allo-HSCT).

METHODS: This prospective study recruited a total of 57 patients diagnosed with malignant hematological diseases and HBV infection at the First Affiliated Hospital of Sun Yat-sen University between 2006 and 2013. The patients were classified as hepatitis B surface antigen (HBsAg)-positive or HBsAg-negative/ antiHBc-positive. Patients were treated with chemotherapy followed by antiviral therapy with nucleoside analogues. Patients underwent allo-HSCT when serum HBV DNA was < 10^3 IU/mL. Following allo-HSCT, antiviral therapy was continued for 1 year after the discontinuation of immunosuppressive therapy. A total of 105 patients who underwent allo-HSCT and had no HBV infection were recruited as controls. The three groups were compared for incidence of graft-*vs*-host disease (GVHD), drug-induced liver injury, hepatic veno-occlusive disease, death and survival time.

RESULTS: A total of 29 of the 41 subjects with chronic GVHD exhibited extensive involvement and 12 exhibited focal involvement. Ten of the 13 subjects with chronic GVHD in the HBsAg(-)/hepatitis B core antibody(+) group exhibited extensive involvement and 3 exhibited focal involvement. Five of the 10 subjects with chronic GVHD in the HBsAg(+) group exhibited extensive involvement and 5 exhibited focal involvement. The non HBV-infected group did not differ significantly from the HBsAg-negative/antiHBc-positive and the HBsAg-positive groups which were treated with nucleoside analogues in the incidence of graft-*vs*-host disease (acute GVHD; 37.1%, 46.9% and 40%, respectively; P = 0.614; chronic GVHD; 39%, 40.6% and 40%, respectively; P = 0.98), drug-induced liver injury (25.7%, 18.7% and 28%, respectively; P = 0.7),

death (37.1%, 40.6% and 52%, respectively; P = 0.4) and survival times (P = 0.516). One patient developed HBV reactivation (HBsAg-positivity) due to early discontinuation of antiviral therapy.

CONCLUSION: Suppression of HBV DNA to < 10^3 IU/mL before transplantation, continued antiviral therapy and close monitoring of immune markers and HBV DNA after transplantation may assure the safety of allo-HSCT.

Key words: Hematopoietic stem cell transplantation; Hepatitis B virus; Antiviral therapy; Nucleotide analogues

Core tip: The threshold of pre-transplantation hepatitis B virus (HBV) DNA for allo-HSCT was defined as 10^3 IU/mL. Only 1 patient developed HBV reactivation due to early discontinuation of antiviral therapy. The hepatitis B surface antigen (HBsAg)(+), HBsAg(-)/hepatitis B core antibody(+) and non-HBV infected groups showed no statistically significant differences in the incidence of graft-*vs*-host disease, drug-induced liver injury, hepatic veno-occlusive disease death, survival times and post-transplantation cumulative survival rates. In summary, suppression of HBV DNA to < 10^3 IU/mL before transplantation, continued antiviral therapy and close monitoring of immune markers of hepatitis B and HBV DNA after transplantation may assure the safety of allogeneic hematopoietic stem cell transplantation.

Liao YP, Jiang JL, Zou WY, Xu DR, Li J. Prophylactic antiviral therapy in allogeneic hematopoietic stem cell transplantation in hepatitis B virus patients. *World J Gastroenterol* 2015; 21(14): 4284-4292 Available from: URL: http://www.wjgnet.com/1007-9327/full/v21/i14/4284.htm DOI: http://dx.doi.org/10.3748/wjg.v21.i14.4284

INTRODUCTION

Hepatitis B virus (HBV) infection is a major public health challenge worldwide, with almost 2 billion people showing serological evidence of infection[1]. China is a region of high endemicity and the percentage of hepatitis B surface antigen (HBsAg) carriers in the population aged 1-59 years old is estimated at 7.18%[2,3]. The major goals of antiviral therapy include: (1) loss of HBsAg; (2) seroconversion to anti-HBs; (3) seroconversion to anti-HBe in HBeAg-positive patients; and (4) loss of viral DNA[4].

Immune dysfunction arising from hematological diseases, intensive chemotherapy, immunosuppressive therapy, monoclonal antibody therapy or hematopoietic stem cell transplantation (HSCT) can result in exacerbation or reactivation of HBV infection after viral resolution[5-7]. Reactivation occurs when intracellular covalently closed circular HBV DNA is not completely eliminated after spontaneous resolution of acute or chronic HBV infection or after antiviral therapy[8].

HSCT is the current standard of care for patients with severe hematological disorders, where either a sibling donor or an unrelated matched donor can be used as a source of stem cells (allogeneic HSCT). In areas of high HBV endemicity where almost 15% of the patients receiving HSCT are HBsAg-positive prior to transplantation, HBV reactivation can significantly impact the post-transplant prognosis[9]. More than half of the HBV carriers who receive allo-HSCT develop HBV reactivation[10] and the incidence of impaired liver function, severity of liver injury and hepatitis-related mortality are significantly higher in HBV infected patients receiving allo-HSCT compared with non HBV-infected patients. In addition, HBV reactivation may cause the discontinuation of effective therapy of hematological diseases, which could then indirectly influence the prognosis of these patients[11]. Combined HBV infection was therefore once regarded a contraindication to allo-HSCT.

Nucleoside analogs such as lamivudine and entecavir have been used for the treatment of acute and chronic HBV infection[12,13], as well as for chemotherapy-induced HBV reactivation[14,15]. However, the timing of initiation and optimal duration of antiviral therapy with nucleoside analogues is still controversial. A recent report described late-onset HBV reactivation after long-term prophylactic treatment with lamivudine in an NHL patient who underwent HSCT[16]. It is also unclear if prophylactic use of nucleoside analogues for antiviral therapy is necessary for patients who are HBsAg-negative/antiHBc-positive. Additionally, there is not much information available about the HBV DNA levels in allo-HSCT donors and recipients at the time of transplantation which would predict viral reactivation.

In this study, we aimed to investigate the timing, safety and influence of antiviral therapy in HBsAg-positive and HBsAg-negative/antiHBc-positive HBV patients after allo-HSCT. The primary endpoint of the study was cumulative survival. Secondary endpoints included occurrence of complications, presence of acute or chronic graft-*vs*-host disease (GVHD), liver damage and veno-occlusive disease (VOD).

MATERIALS AND METHODS

Patients

This prospective cohort study recruited a total of 162 patients who received allo-HSCT at the First Affiliated Hospital of Sun Yat-sen University between September 2006 and December 2013. The study was reviewed and approved by the Institutional Review Board of the First Affiliated Hospital, Sun Yat-sen University. All study participants, or their legal guardian, provided informed written consent prior to study enrollment. There were 77 patients with acute myeloid leukemia (AML), 42 patients with acute lymphoblastic leukemia

(ALL), 21 patients with aplastic anemia, 3 patients with non-Hodgkin's lymphoma (NHL), 6 patients with myelodysplastic syndrome (MDS), 11 patients with chronic myeloid leukemia (CML), 1 patient with paroxysmal nocturnal hemoglobinuria (PNH) and 1 patient with myelofibrosis (MF). Based on the presence of immune markers for hepatitis B, patients were classified into: (1) non-HBV infection group (n = 105); (2) HBsAg-positive group (n = 25); and (3) Hepatitis B core antibody (HBcAb)-positive group (n = 32).

Inclusion criteria

(1) All patients were diagnosed based on the criteria for the diagnosis and the evaluation of therapeutic efficacy of hematological diseases[17]; (2) all transplantation procedures were performed according to the guidelines published in the Hematopoietic Stem Cell Transplantation Standard Practice Manual, Fred Hutchinson Cancer Research Center (Chinese Edition); Editors: BEN SHE and YI MING (ISBN:7117090782/97 87117090780); (3) study participation was voluntary and all patients agreed to receive allo-HSCT; and (4) all patients were aged < 60 years.

Exclusion criteria

(1) Presence of heart disease and/or kidney diseases or risk factors for these diseases; (2) presence of mental diseases; (3) patients who were pregnant or breast feeding; (4) presence of decompensated liver function prior to transplantation; (5) liver function indicating Child-Pugh grade B-C; (6) glutamate aminotransferase (ALT) levels which were higher than twice the upper limit of normal (> 2ULN); (7) increase in bilirubin levels prior to transplantation; (8) presence of concomitant hepatitis A, C, D or E; and (9) patients who were not compliant with the study protocol. Written informed consent was obtained from all patients and the study was approved by the Institutional Review Board of the First Affiliated Hospital of Sun Yat-sen University.

Treatment protocols

Patients infected with HBV were treated according to the EASL guidelines[4].

Pretreatment protocols: (1) Patients with acute leukemia, CML or MDS received the BuCy protocol prior to allo-HCST (busulfan total dose 16 mg/kg iv drip -8 d to -5 d；cyclophosphamide total dose 120 mg/kg iv drip -4 d to -3 d); (2) patients with aplastic anemia or PNH received the CTX + ATG protocol prior to allo-HCST (cyclophosphamide 50 mg/kg per day iv drip -5 d to -2 d; anti-thymocyte globulin total dose 12.5 mg/kg iv drip -5 d to -2 d); (3) patients with NHL received the BEAM protocol prior to HCST (BCNU total dose 300 mg/m^2 -6 d; etoposide total dose 800 mg/m^2 -5 d to -2 d; Ara-C total dose 800 mg/m^2 -5 d to -2 d; melphalan total dose 140 mg/m^2 -1 d）or CBV (BCNU total dose 300 mg/m^2 -6 d; etoposide total dose 800 mg/m^2 -5 d to -2 d; cyclophosphamide total dose 5 g/m^2 iv drip -5 d to -2 d); (4) prevention of GVHD was done with cyclosporine A (60 mg/d); mycophenolate mofetil (1 g/d); methotrexate 15 mg/m^2 (+ 1 d) or 10 mg/m^2 (+3, 6 and 11 d); and (5) patients receiving non-sibling allogeneic hematopoietic stem cell transplantation were treated with ATG (2.5 mg/kg per day × 3 to 4 d).

Allo-HSCT procedures

Patients with AML were initially treated with anthracyclines and Ara-C at a standard dose for induced chemotherapy. When complete remission was achieved, chemotherapy was consolidated with the original protocol or two courses of Ara-C at a large dose (3 g/m^2 q12h d1.3.5). Allo-HSCT was performed after this. Patients with ALL were initially treated with VDLP protocol for induced chemotherapy. When complete remission was achieved, chemotherapy was consolidated with the original protocol or anthracyclines in combination with Ara-C at a standard dose or two courses of the Hyper-CVAD protocol. Allo-HSCT was performed after this. Patients with aplastic anemia received sibling allo-HCST soon after diagnosis.

Laboratory investigations, therapeutic regimens and monitoring

Serum immune markers for hepatitis B were detected and quantitated using enzyme-linked immunosorbent assay (ELISA) kits (Shanghai Rongsheng Biotech Co., Ltd) according to the manufacturer's instructions. HBV DNA was quantitated using a PCR kit with a 100 IU/mL detection limit (Shenzhen Daji Biotech Co., Ltd).

Based on the presence of serum markers, patients in the HBsAg-positive group and those in the HBcAb-positive group were treated with nucleoside analogues (entecavir 0.5 mg qd). HSCT was performed when the HBV DNA was lower than 10^3 IU/mL. Antiviral therapy was continued after transplantation for a period of 1 year after discontinuation of immunosuppressive therapy. After transplantation, evaluation of liver function, quantitation of serum markers for hepatitis B and quantitation of HBV DNA was done monthly for 6 years, once every 3 mo after that for 2 years when abnormalities were absent and thereafter every 6 mo when there were no abnormalities.

HBV reactivation, presence of hepatic VOD, GVHD and liver failure were diagnosed as previously described[17-20].

Statistical analysis

Continuous variables were presented as mean and standard deviations (SDs). One-way ANOVA analysis was used for group comparisons in variables with normal distribution. Kruskal-Wallis tests were used for group comparisons in variables without normal distribution. The normal distributions were detected

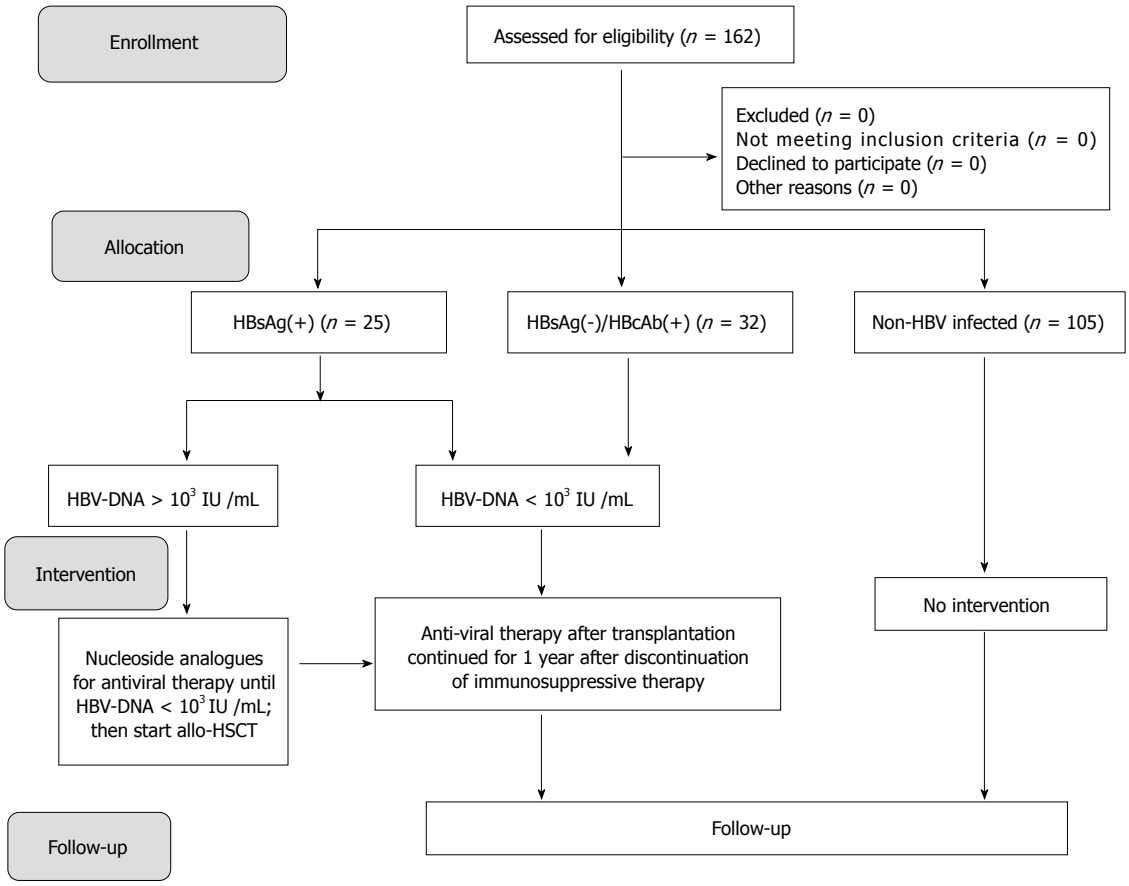

Figure 1 Flow diagram. HBV: Hepatitis B virus; allo-HSCT: Allogeneic hematopoietic stem cell transplantation; HBcAb: Hepatitis B core antibody; HBsAg: Hepatitis B surface antigen.

by Kolmogorov-Smirnov tests. Categorical variables were presented as counts and percentages. χ^2 tests or Fisher's exact tests were used for group comparison among categorical variables. Kaplan-Meier curves with log-rank test were used to evaluate the cumulative survival rates and the differences between the HBsAg(+) group, the HBsAg(-)/HBcAb(+) group and the non-HBV infected group. Statistical analyses were performed using SPSS software version 17 (SPSS Inc, Chicago, IL, United States). A two-tailed *P* of < 0.05 was considered significant. The statistical methods of this study were reviewed by a biostatistician from MedCom BioStat Inc (Taipei, Taiwan).

RESULTS

Baseline characteristics of subjects between groups

Of the 162 subjects included in this study, 105 were not infected with HBV, 32 subjects were HBsAg(-)/HBcAb(+) and 25 subjects were HBsAg(+) (Figure 1). The baseline characteristics of subjects are presented in Table 1. The included patients were aged 12-56 years (median: 32 years). There were no significant differences in gender, age, type of disease and methods of transplantation between the HBsAg(+), HBsAg(-)/HBcAb(+) and non-HBV infected groups.

Complications, death rate and HBV reactivation in subjects from the different groups

The complications observed in subjects from different groups are presented in Table 2. Of the 41 subjects with chronic GVHD in the non-HBV infected group, 29 subjects exhibited extensive involvement and 12 exhibited focal involvement. Of the 13 subjects with chronic GVHD in the HBsAg(-)/HBcAb(+) group, 10 subjects exhibited extensive involvement and 3 exhibited focal involvement. Of the 10 subjects with chronic GVHD in the HBsAg(+) group, 5 subjects exhibited extensive involvement and 5 exhibited focal involvement.

A total of 39 subjects in the non-HBV infected group (37.1%), 15 subjects in the HBsAg(-)/HBcAb(+) group (46.9%) and 10 subjects in the HBsAg(+) group (40%) had acute GVHD. Two subjects (5.1%) in the non-HBV infected group, 3 subjects (20%) in the HBsAg(-)/HBcAb(+) group and 2 subjects (20%) in the HBsAg(+) group had level Ⅰ GVHD. Nineteen subjects (48.7%) in the non-HBV infected group, 2 subjects (13.3%) in the HBsAg(-)/HBcAb(+) group and 2 subjects (20%) in the HBsAg(+) group had level Ⅱ GVHD. Sixteen subjects (41%) in the non-HBV infected group, 7 subjects (46.7%) in HBsAg(-)/HBcAb(+) group and 4 subjects (40%) in HBsAg(+) group had level Ⅲ GVHD. Two subjects (5.1%) in

Table 1 Baseline characteristics of subjects in the different groups *n* (%)

	Non-HBV infected (*n* = 105)	HBsAg(-)/HBcAb(+) (*n* = 32)	HBsAg(+) (*n* = 25)	*P* value
Gender				0.582
Male	69 (65.71)	22 (68.75)	14 (56)	
Female	36 (34.29)	10 (31.25)	11 (44)	
Age (yr)	31.35 ± 11.88	32 ± 10.31	32.48 ± 9.66	0.887
Type of disease[1]				0.576
Acute myeloid leukemia	44 (41.90)	18 (56.25)	15 (60)	
Acute lymphoblastic leukemia	30 (28.57)	6 (18.75)	6 (24)	
Aplastic anemia	16 (15.24)	4 (12.50)	1 (4)	
Others	15 (14.29)	4 (12.50)	3 (12)	
Methods of transplantation				0.548
Sibling	80 (76.19)	21(65.63)	20 (80)	
Unrelated	21 (20.00)	9 (28.13)	3 (12)	
Haploidy	4 (3.81)	2 (6.25)	2 (8)	

[1]Represented Fisher's exact tests used. Continuous variables were presented as mean ± SD or median (ranges). Categorical variables were presented as counts and percentages.

Table 2 Complications of subjects in the different groups *n* (%)

	Non-HBV infected (*n* = 105)	HBsAg(-)/HBcAb(+) (*n* = 32)	HBsAg(+) (*n* = 25)	*P* value
GVHD				
Acute	39 (37.14)	15 (46.88)	10 (40)	0.614
Chronic	41(39.05)	13 (40.63)	10 (40)	0.986
Involvement[1]				0.366
Extensive	29 (70.73)	10 (76.92)	5 (50)	
Limited	12 (29.27)	3 (23.08)	5 (50)	
Grade[1]				0.089
Ⅰ	2 (5.13)	3 (20)	2 (20)	
Ⅱ	19 (48.72)	2 (13.33)	2 (20)	
Ⅲ	16 (41.03)	7 (46.67)	4 (40)	
Ⅳ	2 (5.13)	3 (20)	2 (20)	
Drug-induced liver injury	27 (25.71)	6 (18.75)	7 (28)	0.717
Organ injury	34 (82.93)	11 (68.75)	9 (90)	0.372
Death	39 (37.14)	13 (40.63)	13 (52)	0.401
Time of granular cells engraftment (d), median (range)	12 (7-35)	12 (9-20)	10 (8-19)	0.091
Time of megakaryocytic cells engraftment (d), median (range)	15 (9-50)	15 (9-49)	15 (9-48)	0.880

[1]Represented Fisher's exact tests used. GVHD: Graft-*vs*-host disease.

the non-HBV infected group, 3 subjects (20%) in the HBsAg(-)/HBcAb(+) group and 2 subjects (20%) in the HBsAg(+) group had level Ⅳ GVHD. Twenty-seven subjects (25.7%) in the non-HBV infected group, 6 subjects (18.7%) in the HBsAg(-)/HBcAb(+) group and 7 (28%) subjects in the HBsAg(+) group had drug-induced liver injury. Thirty four subjects (82.9%) in the non-HBV infected group, 11 subjects (68.7%) in the HBsAg(-)/HBcAb(+) group and 9 (90%) subjects in the HBsAg(+) group had organ injury. There were 39 deaths (37.1%) in the non-HBV infected group, 13 deaths (40.6%) in the HBsAg(-)/HBcAb(+) group and 13 deaths (52%) in the HBsAg(+) group. Only 1 patient in the HBcAb-positive group died of GVHD (liver involvement). The cause of death in the remaining patients was unrelated to liver failure.

In the HBV-infected group, 1 patient who was HBsAg-positive received antiviral therapy with entecavir after the initial diagnosis and antiviral therapy was discontinued 2 mo after discontinuation of immunosuppressive therapy. Five months after discontinuation of immunosuppressive therapy, there was an increase in transaminase and bilirubin levels and HBV-DNA increased to 10^6 IU/mL. Antiviral therapy was resumed and there was a recovery of liver function. There was no HBV reactivation in any of the remaining patients. There were no significant differences in GVHD, drug-induced liver injury, organ injury, death, time of engraftment of granular cells and time of engraftment of megakaryocytic cells between the three groups (Table 2).

Cumulative survival rates among groups

The cumulative survival rates in the different groups are presented in Figure 2. There were no statistically significant differences in the post-transplantation cumulative survival rates between the HBsAg(+), HBsAg(-)/HBcAb(+) and non-HBV infected groups (*P* = 0.516) (Figure 2).

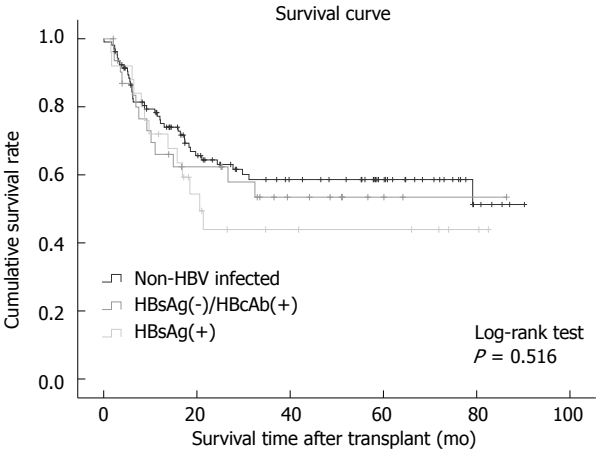

Figure 2 Cumulative survival rates in the non-hepatitis B virus infection group, HBsAg-positive group and HBsAg-negative/HBcAb positive group after allogeneic hematopoietic stem cell transplantation. HBcAb: Hepatitis B core antibody; HBsAg: Hepatitis B surface antigen.

DISCUSSION

In this study, we prospectively studied the timing, safety and efficacy of prolonged prophylactic antiviral therapy for HBsAg-positive and HBsAg-negative/antiHBc-positive patients with hematological malignancies who underwent allo-HSCT. Non HBV-infected patients with hematological malignancies were used as controls. Our data showed that HBV patients who received prophylactic antiviral therapy with nucleoside analogues showed no significant differences in the incidence of graft-*vs*-host disease (GVHD), drug-induced liver injury, organ injury, death or survival time compared to the non-HBV control group. We also showed that using prophylactic antiviral therapy to lower the HBV DNA load to < 10^3 IU/mL before transplantation improved the safety and efficacy of allo-HSCT by suppressing HBV reactivation.

In the present study, 16.4% of our study patients were HBsAg-positive. These data were consistent with other recent reports[21,22]. Serial evaluations of anti-HBs levels and HBV DNA are necessary to accurately determine the occurrence of reverse seroconversion and HBV reactivation[23]. The incidence of HBV reactivation in patients receiving HSCT has been shown to range from 21%-53%[17,24] and HBV reactivation-related mortality ranged from 5%-40%[25,26]. It was previously reported that HBV-exposed recipients who were HBsAg-negative pre-transplant did not show HBV reactivation after stopping prophylactic lamivudine treatment, while one HBV-carrier recipient had HBV reactivation and fulminant liver failure after stopping lamivudine prophylaxis as late as 31 mo post-transplant[27]. Prophylactic antiviral therapy remains controversial for this population of patients with prior HBV exposure who are considered cured[25].

The major challenges to treating patients who undergo HBV reactivation after HSCT are: (1) high viral loads; (2) immunosuppressed status of the recipient; (3) comorbidities; and (4) risk of generating drug-resistant variants. Although the Standard Practice Manual for HSCT (Seattle) recommends prophylactic antiviral therapy with lamivudine in HBsAg-positive patients receiving allo-HSCT[28], the duration of antiviral therapy is not defined. The Queen Mary Hospital in Hong Kong recommends continuation of prophylactic antiviral therapy after transplantation for at least 12 mo after discontinuation of immunosuppressive therapy in HBsAg-positive patients and the duration of antiviral therapy for patients with a high load of HBV DNA may be longer[29]. Prolonged prophylactic antiviral therapy is especially important in the light of recent reports of delayed immune recovery in HSCT recipients[30] and a case report of HBV reactivation 9 mo after discontinuation of lamivudine treatment in an NHL patient who underwent allo-HSCT[16]. A recent study reported that prolonged prophylactic treatment with entecavir in HBsAg-positive patients or prolonged preemptive treatment with entecavir in HBV-resolved patients prevented HBV reactivation associated with immunosuppression in patients with hematological malignancies[24]. Entecavir treatment was administered for 6 mo after the disappearance of HBsAg and HBV DNA from the serum.

Based on these data, we used antiviral therapy with nucleoside analogues for patients who were HBsAg-positive and those who were HBsAg-negative/HBcAb-positive in this study. HBV can remain in a stable form in the nucleus of affected hepatocytes as covalently closed circular DNA (cccDNA) and the first stage of HBV reactivation which occurs during therapy with potent cytotoxic drugs or with immunosuppressants is characterized by increased viral replication and elevated levels of serum HBeAg and HBV DNA. In HBsAg negative/HBcAb positive patients with normal immune function, HBV-specific CD8+T cells in the peripheral blood may attack infected hepatocytes *via* the Fas or perforin pathways and inhibit viral replication *via* release of IFN-γ and TNF-α[26]. However, after allo-HSCT, the incidence of recurrence of HBV infection and related mortality are very high since low levels of autogenous IgG levels may cause an increase in HBsAg levels and recurrence of HBV infection[7,31]. It is important to note that although the incidence of recurrence of HBV infection in these patients is lower than that seen in HBsAg-positive patients, recurrence can lead to fulminant hepatitis which has a high mortality. Rituximab therapy and HSCT are important risk factors of this condition. Previous studies have shown that the incidence of recurrence of HBV infection after HSCT was 10%-20%[22,32-36]. A retrospective long-term study reported that the incidence of recurrence of HBV infection after immunosuppression was 9.0%, 21.7% and 42.9% at 1, 2 and 4 years, respectively[23]. The Consensus on the Management of Lymphoma Patients with HBV Infection in China (2013)[37] recommends monitoring of hepatitis B immune markers and HBV DNA in patients with good

compliance and initiation of antiviral therapy when HBV DNA is detectable. Prophylactic antiviral therapy before chemotherapy is recommended for patients with poor compliance. Prophylactic antiviral therapy is also recommended for patients with a high risk for recurrence of HBV infection (including those receiving rituximab therapy or HSCT and those with concomitant hepatic cirrhosis).

In the present study, only 1 patient developed HBV reactivation (HBsAg-positivity) due to early discontinuation of antiviral therapy and HBV reactivation (HBV-DNA levels of 10^6 IU/mL at 5 mo after discontinuation of immunosuppressive therapy) occurred at the stage of immune reconstitution. However, HBV-DNA was < 500 IU/mL in the rest of the patients. Our data were consistent with a previous report showing that prophylactic lamivudine treatment administered for varying periods of time, ranging from 24 wk post-transplant until 18 mo after transplant, inhibited HBV reactivation[27]. These data suggested that antiviral therapy should be continued for 1 year after discontinuation of immunosuppressive therapy. However, it is important to note that prolonged lamivudine treatment for HBV reactivation has been shown to be associated with the generation of treatment-resistant variants, while tenofovir and adefovir are thought to negatively impact the renal function of patients[30,38-40]. Our choice of entecavir was based on data showing that entecavir was associated with significantly lower levels of resistance compared to lamivudine[40]. In this study, entecavir treatment was started at the time of chemotherapy initiation and was stopped at 1 year after discontinuation of immunosuppressive therapy. There was no significant difference in hematopoietic reconstitution, hematopoietic stem cell engraftment status or incidence of GVHD between the non-hepatitis B group (which received no entecavir therapy) and the hepatitis B group, suggesting that entecavir was safe for the transplantation of hematopoietic stem cells in HBV patients. There was also no significant difference in the incidence of drug-induced liver injury, hepatic vein obstruction syndrome and liver involvement of GVHD between the two groups, suggesting the efficacy of entecavir therapy for this group of patients. Our data agreed with an earlier report demonstrating the safety and tolerability of entecavir in HBV patients undergoing HSCT[41].

A high load of HBV DNA (> 10^5 copies/mL) prior to chemotherapy[6] or HSCT[5] is an important risk factor for HBV reactivation. In patients receiving chemotherapy, the incidence of recurrence of HBV infection was 37.8% in patients with detectable HBV DNA and 10.9% in patients with undetectable HBV DNA[7]. However, the exact threshold remains controversial. Three different studies proposed that the threshold of viral load dictating recurrence was 0.5 × 10^3 IU/mL, 1 × 10^3 IU/mL and 2 × 10^4 IU/mL, respectively[7,42,43]. These data suggested that it would be advantageous to use antiviral therapy with nucleos(t)ide analogues to reduce the viral load before transplantation. Quantification of viral DNA is a useful tool to identify patients who should receive antiviral therapy with nucleoside analogues prior to transplantation. In the present study, we defined the threshold of pre-transplantation HBV DNA as 10^3 IU/mL and HBV loads and medication compliance of patients with values above this threshold were closely monitored. Our data showed no hepatitis-related liver failure in patients with HBV DNA loads below the threshold value.

This study had several limitations. The factors initiating HBV reactivation were not identified or characterized and this is an important future goal. It is also essential to investigate the optimal course of antiviral therapy. Based on our study, we also could not conclude whether HBV reactivation in elderly patients (> 60 years old) can be also safely prevented with the threshold value of 10^3 IU/mL). Another limitation of this study was that we did not determine HBV genotypes. In our future studies, we would like to stratify HBV-infected patients based on the type of disease, HBV genotype, severity of GVHD and degree of HBV activity, and to explore individualized antiviral therapeutic strategies.

In summary, our data demonstrated that prolonged prophylactic antiviral therapy to lower the HBV DNA load to 10^3 IU/mL before transplantation and close monitoring of HBV DNA and immune markers of HBV after transplantation was beneficial in HBsAg-negative antiHBc-positive patients undergoing allo-HSCT. Antiviral therapy administered prior to transplantation was safe and had no influence on hematopoietic reconstitution. It is important to investigate whether the prolonged duration of antiviral therapy could cause resistant variants of HBV.

COMMENTS

Background

In areas of high hepatitis B virus (HBV) endemicity where almost 15% of the patients receiving hematopoietic stem cell transplantation are HBsAg-positive prior to transplantation, HBV reactivation can significantly impact the post-transplant prognosis. Nucleoside analogs such as lamivudine and entecavir have been used for the treatment of acute and chronic HBV infection, as well as for chemotherapy-induced HBV reactivation. However, the timing, safety and influence of prophylactic antiviral therapy in HBsAg-positive and in HBsAg-negative/antiHBc-positive HBV patients after allogeneic hematopoietic stem cell transplantation (allo-HSCT) remains unclear.

Research frontiers

Recent guidelines recommend continuation of prophylactic antiviral therapy after transplantation for at least 12 mo after discontinuation of immunosuppressive therapy in HBsAg-positive patients and the duration of antiviral therapy for patients with a high load of HBV DNA may be longer. Prolonged prophylactic treatment with entecavir in HBsAg-positive patients or prolonged preemptive treatment with entecavir in HBV-resolved patients prevented HBV reactivation associated with immunosuppression in patients with hematological malignancies. A high load of HBV DNA (> 10^5 copies/mL) prior to chemotherapy or HSCT is an important risk factor for HBV reactivation.

Innovations and breakthroughs

We used entecavir therapy for patients who were HBsAg-positive as well as those who were HBsAg-negative/HBcAb-positive. Entecavir treatment was

started at the time of chemotherapy initiation and was stopped at 1 year after discontinuation of immunosuppressive therapy. There was no significant difference in hematopoietic reconstitution, hematopoietic stem cell engraftment status or incidence of graft-*vs*-host disease (GVHD) between the non-hepatitis B group (which received no entecavir therapy) and the hepatitis B group, suggesting that entecavir was safe for the transplantation of hematopoietic stem cells in HBV patients. There was also no significant difference in the incidence of drug-induced liver injury, hepatic vein obstruction syndrome and liver involvement of GVHD between the two groups, suggesting the efficacy of entecavir therapy. We defined the threshold of pre-transplantation HBV DNA as 10^3 IU/mL and HBV loads and medication compliance of patients with values above this threshold were closely monitored. Our data showed no hepatitis-related liver failure in patients with HBV DNA loads below the threshold value.

Applications

Prolonged prophylactic antiviral therapy to lower the HBV DNA load to 10^3 IU/mL before transplantation and close monitoring of HBV DNA and immune markers of HBV after transplantation were beneficial in HBsAg-negative antiHBc-positive patients undergoing allo-HSCT.

Terminology

Allogeneic hematopoietic stem cell transplantation is a procedure where allogeneic stem cells are transfused in order to restore hematopoietic function in patients who are immunosuppressed, commonly during chemotherapy. HBV reactivation occurs when intracellular covalently closed circular HBV DNA is not completely eliminated after spontaneous resolution of acute or chronic HBV infection or after antiviral therapy.

Peer-review

The authors investigated the safety and efficacy of prophylactic antiviral treatment in HBV-infected patients who received allogeneic hematopoietic stem cell transplantation. Prevention of HBV reactivation is important in the management of HSCT and antiviral therapy with nucleoside analogues plays a key role in the clinical practice. In the present study, they defined the threshold of pre-transplantation HBV-DNA as 10^3 IU/mL and prospectively followed-up the clinical courses of the patients.

REFERENCES

1 Hepatitis B vaccines. *Wkly Epidemiol Rec* 2009; **84**: 405-419 [PMID: 19817017]

2 **He F**. Ministry of Health Official Reports: the results of the national serological survey of heptitis B. *Zhongguo Yiliaoqixie Xinxi* 2008; **23**: 1

3 **Shitani M**, Sasaki S, Akutsu N, Takagi H, Suzuki H, Nojima M, Yamamoto H, Tokino T, Hirata K, Imai K, Toyota M, Shinomura Y. Genome-wide analysis of DNA methylation identifies novel cancer-related genes in hepatocellular carcinoma. *Tumour Biol* 2012; **33**: 1307-1317 [PMID: 22457049 DOI: 10.1007/s13277-012-0378-3]

4 **European Association For The Study Of The Liver**. EASL clinical practice guidelines: Management of chronic hepatitis B virus infection. *J Hepatol* 2012; **57**: 167-185 [PMID: 22436845 DOI: 10.1016/j.jhep.2012.02.010]

5 **Lau GK**, Leung YH, Fong DY, Au WY, Kwong YL, Lie A, Hou JL, Wen YM, Nanj A, Liang R. High hepatitis B virus (HBV) DNA viral load as the most important risk factor for HBV reactivation in patients positive for HBV surface antigen undergoing autologous hematopoietic cell transplantation. *Blood* 2002; **99**: 2324-2330 [PMID: 11895763]

6 **Ling R**, Harrison TJ. Production of hepatitis B virus covalently closed circular DNA in transfected cells is independent of surface antigen synthesis. *J Gen Virol* 1997; **78** (Pt 6): 1463-1467 [PMID: 9191944]

7 **Yeo W**, Zee B, Zhong S, Chan PK, Wong WL, Ho WM, Lam KC, Johnson PJ. Comprehensive analysis of risk factors associating with Hepatitis B virus (HBV) reactivation in cancer patients undergoing cytotoxic chemotherapy. *Br J Cancer* 2004; **90**: 1306-1311 [PMID: 15054446 DOI: 10.1038/sj.bjc.6601699]

8 **Onozawa M**, Hashino S, Izumiyama K, Kahata K, Chuma M, Mori A, Kondo T, Toyoshima N, Ota S, Kobayashi S, Hige S, Toubai T, Tanaka J, Imamura M, Asaka M. Progressive disappearance of anti-hepatitis B surface antigen antibody and reverse seroconversion after allogeneic hematopoietic stem cell transplantation in patients with previous hepatitis B virus infection. *Transplantation* 2005; **79**: 616-619 [PMID: 15753855]

9 **Hsiao LT**, Chiou TJ, Gau JP, Liu JH, Tzeng CH, Chen PM. Hepatitis B infection in haematopoietic stem cell transplantation: still unresolved. *Hong Kong Med J* 2009; **15**: 42-44 [PMID: 19494397]

10 **Liang TJ**, Baruch Y, Ben-Porath E, Enat R, Bassan L, Brown NV, Rimon N, Blum HE, Wands JR. Hepatitis B virus infection in patients with idiopathic liver disease. *Hepatology* 1991; **13**: 1044-1051 [PMID: 2050320]

11 **Moses SE**, Lim Z, Zuckerman MA. Hepatitis B virus infection: pathogenesis, reactivation and management in hematopoietic stem cell transplant recipients. *Expert Rev Anti Infect Ther* 2011; **9**: 891-899 [PMID: 21973301 DOI: 10.1586/eri.11.105]

12 **Lai CL**, Chien RN, Leung NW, Chang TT, Guan R, Tai DI, Ng KY, Wu PC, Dent JC, Barber J, Stephenson SL, Gray DF. A one-year trial of lamivudine for chronic hepatitis B. Asia Hepatitis Lamivudine Study Group. *N Engl J Med* 1998; **339**: 61-68 [PMID: 9654535 DOI: 10.1056/NEJM199807093390201]

13 **Andreone P**, Caraceni P, Grazi GL, Belli L, Milandri GL, Ercolani G, Jovine E, D'Errico A, Dal Monte PR, Ideo G, Forti D, Mazziotti A, Cavallari A, Bernardi M. Lamivudine treatment for acute hepatitis B after liver transplantation. *J Hepatol* 1998; **29**: 985-989 [PMID: 9875646]

14 **Yeo W**, Chan PK, Ho WM, Zee B, Lam KC, Lei KI, Chan AT, Mok TS, Lee JJ, Leung TW, Zhong S, Johnson PJ. Lamivudine for the prevention of hepatitis B virus reactivation in hepatitis B s-antigen seropositive cancer patients undergoing cytotoxic chemotherapy. *J Clin Oncol* 2004; **22**: 927-934 [PMID: 14990649 DOI: 10.1200/JCO.2004.05.161]

15 **Huang YH**, Hsiao LT, Hong YC, Chiou TJ, Yu YB, Gau JP, Liu CY, Yang MH, Tzeng CH, Lee PC, Lin HC, Lee SD. Randomized controlled trial of entecavir prophylaxis for rituximab-associated hepatitis B virus reactivation in patients with lymphoma and resolved hepatitis B. *J Clin Oncol* 2013; **31**: 2765-2772 [PMID: 23775967 DOI: 10.1200/JCO.2012.48.5938]

16 **Milazzo L**, Corbellino M, Foschi A, Micheli V, Dodero A, Mazzocchi A, Montefusco V, Zehender G, Antinori S. Late onset of hepatitis B virus reactivation following hematopoietic stem cell transplantation: successful treatment with combined entecavir plus tenofovir therapy. *Transpl Infect Dis* 2012; **14**: 95-98 [PMID: 21749588 DOI: 10.1111/j.1399-3062.2011.00659.x]

17 **Smith LH**, Wyngaarden JB, Cooper JAD, Pappas PG. Cecil Review of General Internal Medicine. 6th ed. St. Louis: Saunders (W.B.) Co Ltd, 1988

18 **Yeo W**, Chan PK, Zhong S, Ho WM, Steinberg JL, Tam JS, Hui P, Leung NW, Zee B, Johnson PJ. Frequency of hepatitis B virus reactivation in cancer patients undergoing cytotoxic chemotherapy: a prospective study of 626 patients with identification of risk factors. *J Med Virol* 2000; **62**: 299-307 [PMID: 11055239]

19 **Jones RJ**, Lee KS, Beschorner WE, Vogel VG, Grochow LB, Braine HG, Vogelsang GB, Sensenbrenner LL, Santos GW, Saral R. Venoocclusive disease of the liver following bone marrow transplantation. *Transplantation* 1987; **44**: 778-783 [PMID: 3321587]

20 **Thomas E**, Storb R, Clift RA, Fefer A, Johnson FL, Neiman PE, Lerner KG, Glucksberg H, Buckner CD. Bone-marrow transplantation (first of two parts). *N Engl J Med* 1975; **292**: 832-843 [PMID: 234595 DOI: 10.1056/NEJM197504172921605]

21 **Li J**, Liu J, Huang B, Zheng D, Chen M, Zhou Z, Xu D, Zou W. Hepatitis B virus infection status is an independent risk factor for multiple myeloma patients after autologous hematopoietic stem cell transplantation. *Tumour Biol* 2013; **34**: 1723-1728 [PMID: 23436046 DOI: 10.1007/s13277-013-0709-z]

22 **Mikulska M**, Nicolini L, Signori A, Rivoli G, Del Bono V, Raiola AM, Di Grazia C, Dominietto A, Varaldo R, Ghiso A, Bacigalupo A, Viscoli C. Hepatitis B reactivation in HBsAg-negative/HBcAb-positive allogeneic haematopoietic stem cell transplant recipients: risk factors and outcome. *Clin Microbiol Infect* 2014; **20**:

O694-O701 [PMID: 24575948 DOI: 10.1111/1469-0691.12611]
23 **Papamichalis P**, Alexiou A, Boulbou M, Dalekos GN, Rigopoulou EI. Reactivation of resolved hepatitis B virus infection after immunosuppression: is it time to adopt pre-emptive therapy? *Clin Res Hepatol Gastroenterol* 2012; **36**: 84-93 [PMID: 21920838 DOI: 10.1016/j.clinre.2011.07.018]
24 **Tamori A**, Hino M, Kawamura E, Fujii H, Uchida-Kobayashi S, Morikawa H, Nakamae H, Enomoto M, Murakami Y, Kawada N. Prospective long-term study of hepatitis B virus reactivation in patients with hematologic malignancy. *J Gastroenterol Hepatol* 2014; **29**: 1715-1721 [PMID: 24730465 DOI: 10.1111/jgh.12604]
25 **Martyak LA**, Taqavi E, Saab S. Lamivudine prophylaxis is effective in reducing hepatitis B reactivation and reactivation-related mortality in chemotherapy patients: a meta-analysis. *Liver Int* 2008; **28**: 28-38 [PMID: 17976155 DOI: 10.1111/j.1478-3231.2007.01618.x]
26 **Loomba R**, Rowley A, Wesley R, Liang TJ, Hoofnagle JH, Pucino F, Csako G. Systematic review: the effect of preventive lamivudine on hepatitis B reactivation during chemotherapy. *Ann Intern Med* 2008; **148**: 519-528 [PMID: 18378948]
27 **Moses SE**, Lim ZY, Sudhanva M, Devereux S, Ho AY, Pagliuca A, Zuckerman M, Mufti GJ. Lamivudine prophylaxis and treatment of hepatitis B Virus-exposed recipients receiving reduced intensity conditioning hematopoietic stem cell transplants with alemtuzumab. *J Med Virol* 2006; **78**: 1560-1563 [PMID: 17063522 DOI: 10.1002/jmv.20705]
28 **Flowers ME**, McDonald G, Carpenter P, Boeckh M, Sanders J, Stern J, Holmberg L, Schubert M, Martin PJ. Long-term follow-up after hematopoietic stem cell transplant general guidelines for referring physicians. Seattle: Fred Hutchinson Cancer Research Center/ Seattle Cancer Care Alliance, 2014: 76-79. [Last accessed in April 2015]. Available from: http://www.fhcrc.org/content/dam/public/Treatment-Suport/Long-Term-Follow-Up/physician.pdf
29 **Liang R**. How I treat and monitor viral hepatitis B infection in patients receiving intensive immunosuppressive therapies or undergoing hematopoietic stem cell transplantation. *Blood* 2009; **113**: 3147-3153 [PMID: 19144986 DOI: 10.1182/blood-2008-10-163493]
30 **Allen MI**, Deslauriers M, Andrews CW, Tipples GA, Walters KA, Tyrrell DL, Brown N, Condreay LD. Identification and characterization of mutations in hepatitis B virus resistant to lamivudine. Lamivudine Clinical Investigation Group. *Hepatology* 1998; **27**: 1670-1677 [PMID: 9620341 DOI: 10.1002/hep.510270628]
31 **Dai MS**, Chao TY, Kao WY, Shyu RY, Liu TM. Delayed hepatitis B virus reactivation after cessation of preemptive lamivudine in lymphoma patients treated with rituximab plus CHOP. *Ann Hematol* 2004; **83**: 769-774 [PMID: 15338194 DOI: 10.1007/s00277-004-0899-y]
32 **Dhédin N**, Douvin C, Kuentz M, Saint Marc MF, Reman O, Rieux C, Bernaudin F, Norol F, Cordonnier C, Bobin D, Metreau JM, Vernant JP. Reverse seroconversion of hepatitis B after allogeneic bone marrow transplantation: a retrospective study of 37 patients with pretransplant anti-HBs and anti-HBc. *Transplantation* 1998; **66**: 616-619 [PMID: 9753342]
33 **Knöll A**, Boehm S, Hahn J, Holler E, Jilg W. Reactivation of resolved hepatitis B virus infection after allogeneic haematopoietic stem cell transplantation. *Bone Marrow Transplant* 2004; **33**: 925-929 [PMID: 15004543 DOI: 10.1038/sj.bmt.1704457]
34 **Hammond SP**, Borchelt AM, Ukomadu C, Ho VT, Baden LR, Marty FM. Hepatitis B virus reactivation following allogeneic hematopoietic stem cell transplantation. *Biol Blood Marrow Transplant* 2009; **15**: 1049-1059 [PMID: 19660717 DOI: 10.1016/j.bbmt.2009.05.001]
35 **Viganò M**, Vener C, Lampertico P, Annaloro C, Pichoud C, Zoulim F, Facchetti F, Poli F, Scalamogna M, Deliliers GL, Colombo M. Risk of hepatitis B surface antigen seroreversion after allogeneic hematopoietic SCT. *Bone Marrow Transplant* 2011; **46**: 125-131 [PMID: 20383209 DOI: 10.1038/bmt.2010.70]
36 **Seth P**, Alrajhi AA, Kagevi I, Chaudhary MA, Colcol E, Sahovic E, Aljurf M, Gyger M. Hepatitis B virus reactivation with clinical flare in allogeneic stem cell transplants with chronic graft-versus-host disease. *Bone Marrow Transplant* 2002; **30**: 189-194 [PMID: 12189538 DOI: 10.1038/sj.bmt.1703614]
37 **Experimental Diagnosis Group**, Hematology Society Chinese Medical Association. Consensus of Chinese experts on morphologic analysis of blood cells. *Zhongguo Xueyexue Zazhi* 2013; **34**: 558-560
38 **Chen FW**, Coyle L, Jones BE, Pattullo V. Entecavir versus lamivudine for hepatitis B prophylaxis in patients with haematological disease. *Liver Int* 2013; **33**: 1203-1210 [PMID: 23522150 DOI: 10.1111/liv.12154]
39 **Marinone C**, Mestriner M. HBV disease: HBsAg carrier and occult B infection reactivation in haematological setting. *Dig Liver Dis* 2011; **43** Suppl 1: S49-S56 [PMID: 21195372 DOI: 10.1016/S1590-8658(10)60692-5]
40 **Ghany MG**, Doo EC. Antiviral resistance and hepatitis B therapy. *Hepatology* 2009; **49**: S174-S184 [PMID: 19399794 DOI: 10.1002/hep.22900]
41 **Aoki J**, Kimura K, Kakihana K, Ohashi K, Sakamaki H. Efficacy and tolerability of Entecavir for hepatitis B virus infection after hematopoietic stem cell transplantation. *Springerplus* 2014; **3**: 450 [PMID: 25184113 DOI: 10.1186/2193-1801-3-450]
42 **Lau GK**, Suri D, Liang R, Rigopoulou EI, Thomas MG, Mullerova I, Nanji A, Yuen ST, Williams R, Naoumov NV. Resolution of chronic hepatitis B and anti-HBs seroconversion in humans by adoptive transfer of immunity to hepatitis B core antigen. *Gastroenterology* 2002; **122**: 614-624 [PMID: 11874993]
43 **Hui CK**, Cheung WW, Au WY, Lie AK, Zhang HY, Yueng YH, Wong BC, Leung N, Kwong YL, Liang R, Lau GK. Hepatitis B reactivation after withdrawal of pre-emptive lamivudine in patients with haematological malignancy on completion of cytotoxic chemotherapy. *Gut* 2005; **54**: 1597-1603 [PMID: 16000641 DOI: 10.1136/gut.2005.070763]

P- Reviewer: Doki N, Enomoto H, Makvandi M **S- Editor**: Qi Y
L- Editor: Roemmele A **E- Editor**: Zhang DN

World Journal of Gastroenterology

Submit a Manuscript: http://www.wjgnet.com/esps/
Help Desk: http://www.wjgnet.com/esps/helpdesk.aspx
DOI: 10.3748/wjg.v21.i14.4293

World J Gastroenterol 2015 April 14; 21(14): 4293-4301
ISSN 1007-9327 (print) ISSN 2219-2840 (online)

ORIGINAL ARTICLE

Prospective Study

Arpin contributes to bacterial translocation and development of severe acute pancreatitis

Wen-Sheng Deng, Jian Zhang, Hui Ju, Hong-Mei Zheng, Jiang Wang, Su Wang, Dian-Liang Zhang

Wen-Sheng Deng, Jiang Wang, Hong-Mei Zheng, Dian-Liang Zhang, Center of Colon and Rectum, Qingdao Municipal Hospital, Qingdao University, Qingdao 266011, Shandong Province, China
Jian Zhang, Su Wang, Department of General Surgery, The Affiliated Hospital of Qingdao University, Qingdao 266003, Shandong Province, China.
Hui Ju, Department of Gastroenterology, The Affiliated Hospital of Qingdao University, Qingdao 266003, Shandong Province, China
Author contributions: Zhang DL designed the study; Deng WS, Wang J and Wang S performed the research; Zhang J contributed new reagents and analytical tools; Deng WS analyzed the data; Deng WS wrote the paper; Ju H performed the endoscopy.
Supported by Natural Science Foundation of China, No. 81270448 and No. 81470890.

Correspondence to: Dian-Liang Zhang, MD, PhD, Center of Colon and Rectum, Qingdao Municipal Hospital, Qingdao University, No. 16 Jiangsu Road, Qingdao 266011, Shandong Province, China. phdzdl@yahoo.com
Telephone: +86-532-82852057
Fax: +86-532-82852058
Received: November 10, 2014
Peer-review started: November 12, 2014
First decision: December 11, 2014
Revised: January 11, 2015
Accepted: February 5, 2015
Article in press: February 5, 2015
Published online: April 14, 2015

Abstract

AIM: To assess the impact of Arpin protein and tight junction (TJ) proteins in the intestinal mucosa on bacterial translocation in patients with severe acute pancreatitis (SAP).

METHODS: Fifty SAP patients were identified as study objects and then classified into two groups according to the presence of bacterial translocation (BT) in the blood [*i.e.*, BT(+) and BT(-)]. Twenty healthy individuals were included in the control group. BT was analyzed by polymerase chain reaction, colonic mucosal tissue was obtained by endoscopy and the expression of TJ proteins and Arpin protein was determined using immunofluorescence and western blotting.

RESULTS: Bacterial DNA was detected in the peripheral blood of 62.0% of patients (31/50) with SAP. The expression of TJ proteins in SAP patients was lower than that in healthy controls. In contrast, Arpin protein expression in SAP patients was higher than in healthy controls (0.38 ± 0.19 *vs* 0.28 ± 0.16, $P < 0.05$). Among SAP patients, those positive for BT showed a higher level of claudin-2 expression (0.64 ± 0.27 *vs* 0.32 ± 0.21, $P < 0.05$) and a lower level of occludin (OC) (0.61 ± 0.28 *vs* 0.73 ± 0.32, $P < 0.05$) and zonula occludens-1 (0.42 ± 0.26 *vs* 0.58 ± 0.17, $P = 0.038$) expression in comparison with BT (-) patients. Moreover, the level of Arpin expression in BT (+) patients was higher than in BT (-) patients (0.61 ± 0.28 *vs* 0.31 ± 0.24, $P < 0.05$).

CONCLUSION: Arpin protein affects the expression of tight junction proteins and may have an impact on BT. These results contribute to a better understanding of the factors involved in bacterial translocation during acute pancreatitis.

Key words: Severe acute pancreatitis; Arpin; Tight junction proteins; Bacterial translocation; Epithelium; Intestinal epithelial barrier

Core tip: Tight junctions (TJs) are the structural basis for the intestinal epithelial barrier. Increased intestinal permeability caused by variations in TJ proteins may result in bacterial translocation (BT) and there is evidence that BT may contribute to infection and sepsis. However, the detailed mechanisms for BT remain unknown. Recent work has identified an Arp2/3 interacting protein called Arpin, which was shown to restrict the rate of actin polymerization and control cell migration. Our research shows that Arpin protein affects the expression of TJ proteins and may have an impact on BT.

Deng WS, Zhang J, Ju H, Zheng HM, Wang J, Wang S, Zhang DL. Arpin contributes to bacterial translocation and development of severe acute pancreatitis. *World J Gastroenterol* 2015; 21(14): 4293-4301 Available from: URL: http://www.wjgnet.com/1007-9327/full/v21/i14/4293.htm DOI: http://dx.doi.org/10.3748/wjg.v21.i14.4293

INTRODUCTION

Infection and sepsis are severe complications contributing to most late deaths in patients with severe acute pancreatitis (SAP)[1,2]. The organisms responsible for infection in cases of SAP are thought to be common enteric bacteria[3,4], which has generally been supported by animal experiments[5]. Bacterial translocation (BT) from the gut is the most widely accepted mechanism for the pathogenesis of infection and sepsis in SAP[4-6]. BT is defined as the passage of indigenous bacteria (or their products) colonizing the intestine through the intestinal mucosal barrier to the mesenteric lymph nodes and other distant sites[7]. The following three major factors have been proposed as promoters of BT: impairment of intestinal barrier function; alterations in gastrointestinal microflora; and deficiencies in host immunity[8]. During SAP, the structure and function of the intestinal mucosa are damaged, leading to gut barrier dysfunction[1,5]. The intestinal mucosal barrier is established by the intestinal epithelial barrier and distribution of microbial flora[9,10] and is composed of tight junctions (TJs) between intestinal epithelial cells. These TJ proteins form and regulate the paracellular pathway[11-13]; however, the detailed mechanism for this function remains unknown. Recent work has identified an Arp2/3 interacting protein called Arpin that restricts the rate of actin polymerization and is the latest component in the steadily expanding protein repertoire shown to control cell migration[14]. In the current study, we found that Arpin may contribute to BT occurrence and development through the regulation of TJs.

TJs, which are the structural basis of intestinal epithelial barrier, are comprised of the following 4 types of transmembrane proteins: occludin (OC), claudins (CLs), junctional adhesion molecules and tricellulin. CLs and OCs are the most prominent of these proteins[14]. Zonula occluden (ZO) proteins are linked with the main transmembrane proteins and form the CL-ZO protein interactions that are essential for TJ formation[15]. Extensive evidence has identified the Arp2/3 complex as an actin polymerizing complex localized to the tight junction[16]. Cell migration requires the generation of branched actin networks that power the protrusion of the plasma membrane in lamellipodia[17]. These structures are major sites of actin filament nucleation and typically display highly nonlinear kinetics, meaning that they are sharply defined in both space and time[18]. The Arp2/3 complex is the molecular machine that nucleates these branched actin networks by binding to the side of an existing filament and initiating branch formation[17,19]. The resulting two new filaments can then each be split again, creating a natural feed-forward mechanism, limited only by the supply of components, such as the Arp2/3 complex, actin monomers and activators, most of which diffuse from the cytoplasm[20]. Dang *et al*[14] reported that Arpin is a negative regulator of Arp2/3 activity and that cells utilize Arpin to fine-tune actin nucleation activity at the leading edge of the lamellipodium to steer the cell. These authors also performed a bioinformatics search for proteins containing a highly conserved carboxy-terminal Arp2/3 binding motif. The classical Arp2/3 binding domain consists of an amphipathic a-helix, sometimes referred to as the coil region, which binds to the barbed end groove of Arp2, followed by a short acidic motif with a highly conserved tryptophan residue at position-1 or -2 relative to the carboxyl terminus[21]. The acidic motif is thought to bind to Arp3[22]. The newly identified protein, Arpin, contains a prototypical acidic motif and through binding to the Arp2/3 complex, Arpin inhibits actin filament nucleation, thereby functioning as a competitive Arp2/3 inhibitor[14].

MATERIALS AND METHODS

Patients

This prospective observational study included 50 patients with SAP who were admitted to the Affiliated Hospital of Medical College, Qingdao University and Jinlin Hospital, Nanjing University between January 2012 and September 2013. Patients were recruited if the onset of upper abdominal pain was within 48 h of admission. The diagnosis of SAP was made during the first 12 h of admission, based on the presence of acute upper abdominal pain, serum amylase and/or lipase levels greater than three times the upper limit of normal, and the results of contrast-enhanced CT[23]. SAP was defined according to the Atlanta clinical criteria[23]. The severity of the disease was assessed using Acute Physiology and Chronic Health Evaluation (APACHE)-Ⅱ criteria[24]. Patients were treated on the basis of standardized protocols of interdisciplinary management, including

gastrointestinal decompression, intravenous (iv) fluids, nutritional support and/or organ system support. The patients received antibiotic prophylactic treatment within 48 h after SAP onset that continued until unequivocal clinical improvement. Patients with one of the following clinical findings were included in the study: (1) local complications (pancreatic necrosis, pancreatic pseudocyst, pancreatic abscess); (2) organ failure; (3) APACHE-Ⅱ score > 8; (4) Ranson criteria > 3; (5) Balthazar CT grading Ⅱ or above; and (6) clinical course in the first 3 d showing colonic involvement, severe abdominal distention and colonic irrigation treated by endoscopic decompression. Patients with any of the following were excluded from the study: (1) concurrent sepsis or pancreatic infection or peripancreatic infection caused by a second disease; (2) patients with acute or chronic gastrointestinal diseases; (3) patients sent directly to the intensive care unit for multiorgan failure; (4) post-endoscopic retrograde cholangiopancreatography or traumatic or operative pancreatitis; and (5) pregnancy, malignancy, immunodeficiency or moribund patients regardless of cause within 48 h prior to enrollment. Twenty healthy volunteers were recruited and acted as controls. The controls were in good health and had no history of either pancreatic or gastrointestinal disease. This study was approved by the Human Subjects Institutional Committee of Affiliated Hospital of Medical College, Qingdao University. Written informed consent was obtained from the participants.

Sample collection

During the first 3 d, the SAP clinical course with colonic involvement presenting with severe abdominal distention was treated with colonic irrigation and decompression with endoscopy, during which colonic mucosal tissue was obtained. Isolation of colonic mucosal cells was performed as described previously[11]. The specimens were separated into two small pieces, placed in RIPA buffer (Tris, NaCl, deoxycholic acid, Triton-X-100, sodium dodecyl sulfate, complete proteinase inhibitor mixture; Roche, Mannheim, Germany) and homogenized. Meanwhile, peripheral venous blood samples were obtained and 2 mL of blood was used to detect bacterial DNA. Samples of colonic mucosal tissue and peripheral venous blood were obtained at the same time for the control group.

DNA extraction and PCR amplification

Bacterial DNA was detected as described previously[25]. Briefly, 200 μL plasma was incubated in lysozyme-proteinase K buffer for 2 h and placed into QIAamp Spin Columns (Qiagen, Hilden, Germany). A broad range polymerase chain reaction (PCR) for the amplification of a conserved region of the 16S ribosomal RNA prokaryotic gene was carried out using the following universal primers: 5′-AGAGTTTGATCATGGCTCAG-3′ and 5′-ACCGCGACTGCTGCTGGCAC-3′. The primers were located at positions 7-27 and 531-514 [*Escherichia coli* (*E. coli*) numbering]. The total PCR volume was filtered with QIAquick Spin Columns (Qiagen) to remove the remaining primers and analyzed by 2% agarose gel electrophoresis and ultraviolet visualization. The final product was purified by precipitation with ethanol acetate and analyzed with an ABIPRISM 310 Automated Sequencer (Applied Biosystems, Foster City, CA, United States). Sequences obtained were compared with the database of the National Center for Biotechnology Information (http://www.ncbi.nih.gov). DNA extracted from *E. coli* was used as a positive control and sterile water and PCR mixtures (without template) were used as negative controls. The limit of detection of the method was evaluated. One colony from a culture of *E. coli* was diluted up to 100000-fold in sterile water and DNA isolation from 200 mL of each dilution was performed. The yield and purity of DNA were measured by reading the optical densities at 260/280 nm, respectively. From each sample, 2 μL was used for PCR.

Immunofluorescence

Immunofluorescent staining was carried out for Arpin, OC, CL-2 and ZO-1 in the obtained specimens. After blocking endogenous peroxidases activity to reduce nonspecific binding, slides were incubated in 1% bovine serum album for 30 min. After washing in phosphate-buffered saline, primary antibodies (rabbit anti-human Arpin antibody, rabbit anti-human CL-2 antibody: Zymed Laboratories, San Francisco; rabbit anti-OC antibody: Santa Cruz Biotechnology, Santa Cruz, CA, United States; mouse anti-ZO-2 antibody: BD, Heidelberg, Germany) were applied according to the dilutions advised by the manufacturers. Isotype staining assured specific staining results. Slides were then incubated with goat anti-rabbit Alexa546 or goat anti-mouse Alexa546 secondary antibody (Molecular Probes/Invitrogen, Karlsruhe, Germany). Nuclei were stained with 40, 6-diamidino-2-phenylindole in a mounting medium (Vectashield, Vector Laboratories). Immunofluorescent-stained sections (high-power fields) were visualized with a microscope at the indicated magnifications using fluorescent light (Axiovert, Zeiss, Goettingen, Germany).

Western blotting

Western blotting analyses were undertaken according to standard protocols using the following primary antibodies: rabbit anti-human Arpin antibody (1:250 dilution; Sinopharm Chemical Reagent Beijing Co.Ltd), rabbit anti-CL-2 (Zymed), mouse anti-OC (clone 19, 1:250 dilution; BD, San Diego, CA, United States) and mouse anti-ZO-2 (clone 1, 1:250 dilution; BD, San Diego, CA, United States). Membranes were blocked at room temperature for 1 h in Tris buffer saline containing 0.05% Tween 20 (TBS-T) and 5% non-fat dry milk. Nitrocellulose membranes were incubated

Table 1 Characteristics of subjects and healthy controls

	SAP	HC	*P* value
Gender (M/F)	31/19	13/7	0.082[1]
Age (yr)	55.0 ± 12.3	55.0 ± 5.2	0.753[2]
Ranson score	4.3 ± 1.8	2.0 ± 1.8	0.032[2]
APACHE-Ⅱ score	15.0 ± 5.8	4.5 ± 2.1	0.029[2]

[1]Pearson's two-test; [2]Two-sample *t*-test. HC: Healthy control; SAP: Severe acute pancreatitis; APACHE: Acute Physiology and Chronic Health Evaluation.

with primary antibodies for 1 h at room temperature under slight agitation. The specific of staining was confirmed using the corresponding isotype controls. Equal loading was ensured by staining with mouse anti-b-actin antibody (clone C4, 1:3000 dilution; Chemicon, Temecula, CA, United States). After washing, the horseradish peroxidase (HRP)-conjugated secondary antibody (goat anti-rabbit IgG-HRP, 1:8,000; goat anti-mouse IgG-HRP, 1:3000 dilution; BD, San Diego, CA, United States) was added accordingly and the membrane was incubated for an additional hour under gentle shaking. Proteins were detected using the ECL-Plus Western Blotting Detection System (Amersham Life Science, Braunschweig, Germany). Protein bands were quantified by densitometry using Image-Pro Plus 6.0 (Media Cybernetics, MD, United States).

Statistical analysis

Continuous variables are expressed as the mean ± SD. Categorical variables are expressed as frequencies or percentages. Significant differences in basal characteristics between groups were analyzed using the χ^2 test for categorical data and the 2-sample *t* test for quantitative data. The associations between Arpin and CL-2 expression in post-BT SAP, the BT ratio and APACHE-Ⅱ scores were determined by linear regression analysis using Pearson's test. One-way analysis of variance (ANOVA) was applied to compare parametric variables between the three aforementioned groups. $P < 0.05$ (two-sided) was considered significant. All analyses were performed using SPSS version 18.0 (SPSS, Chicago, IL, United States).

RESULTS

Patient characteristics

The clinical features of the SAP patients and healthy controls are shown in Table 1. No significant difference was noted in gender or age between groups ($P > 0.05$). However, statistically significant differences were found in the Ranson score and APACHE-Ⅱ score between SAP patients and healthy controls ($P < 0.05$).

BT ratio in different groups

Fragments of bacterial DNA were detected in 31 of the 50 patients with SAP (62.0%) and in 1 of 20 healthy (5.0%) controls, showing significant differences between patients and healthy controls ($P < 0.001$). A representative photograph of a DNA agarose electrophoresis gel is shown in Figure 1. In patients with an APACHE-Ⅱ score greater than 16 points, bacteria were detected in 15 patients (85.3%) (Figure 2A). For patients with an APACHE-Ⅱ score of 12-14 points, DNA was identified in 68.5%. Only five of the

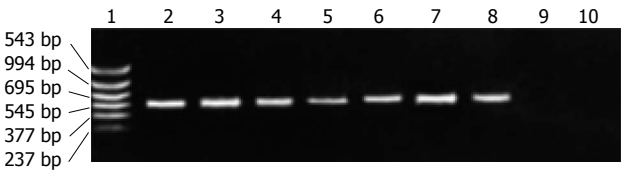

Figure 1 Agarose gel electrophoresis results from polymerase chain reaction. Lane 1, DNA marker; lane 2, positive control (*Escherichia coli*), lanes 3 to 8 and approximately 545 bp band corresponding to lane 3, *Escherichia coli*; lane 4, *Staphylococcus aureus*; lane 5, *Klebsiellapneumoniae*; lane 6, *Staphylococcus epidermidis*; lane 7, *Streptococcus pneumoniae*; lane 8, *Enterococcus faecalis*; lane 9 to 10, negative controls.

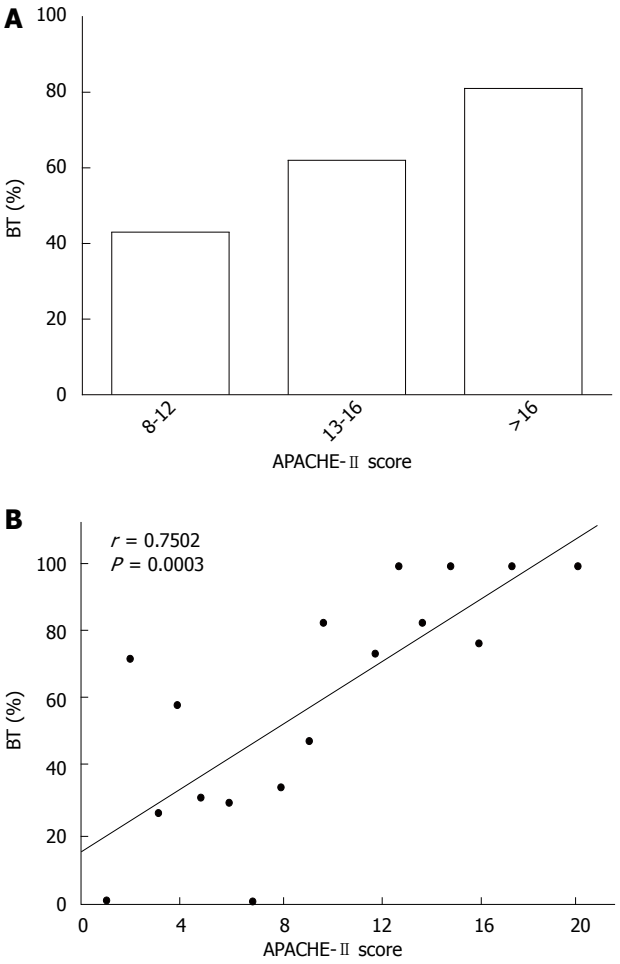

Figure 2 Percentage of bacterial translocation among patients with different severities of illness (A) and the prevalence of bacteremia was positively correlated with the APACHE-Ⅱ score in patients with severe acute pancreatitis. A: According to the APACHE-Ⅱ score; B: $r = 0.7502$, $P < 0.0001$ *vs* control. APACHE: Acute Physiology and Chronic Health Evaluation.

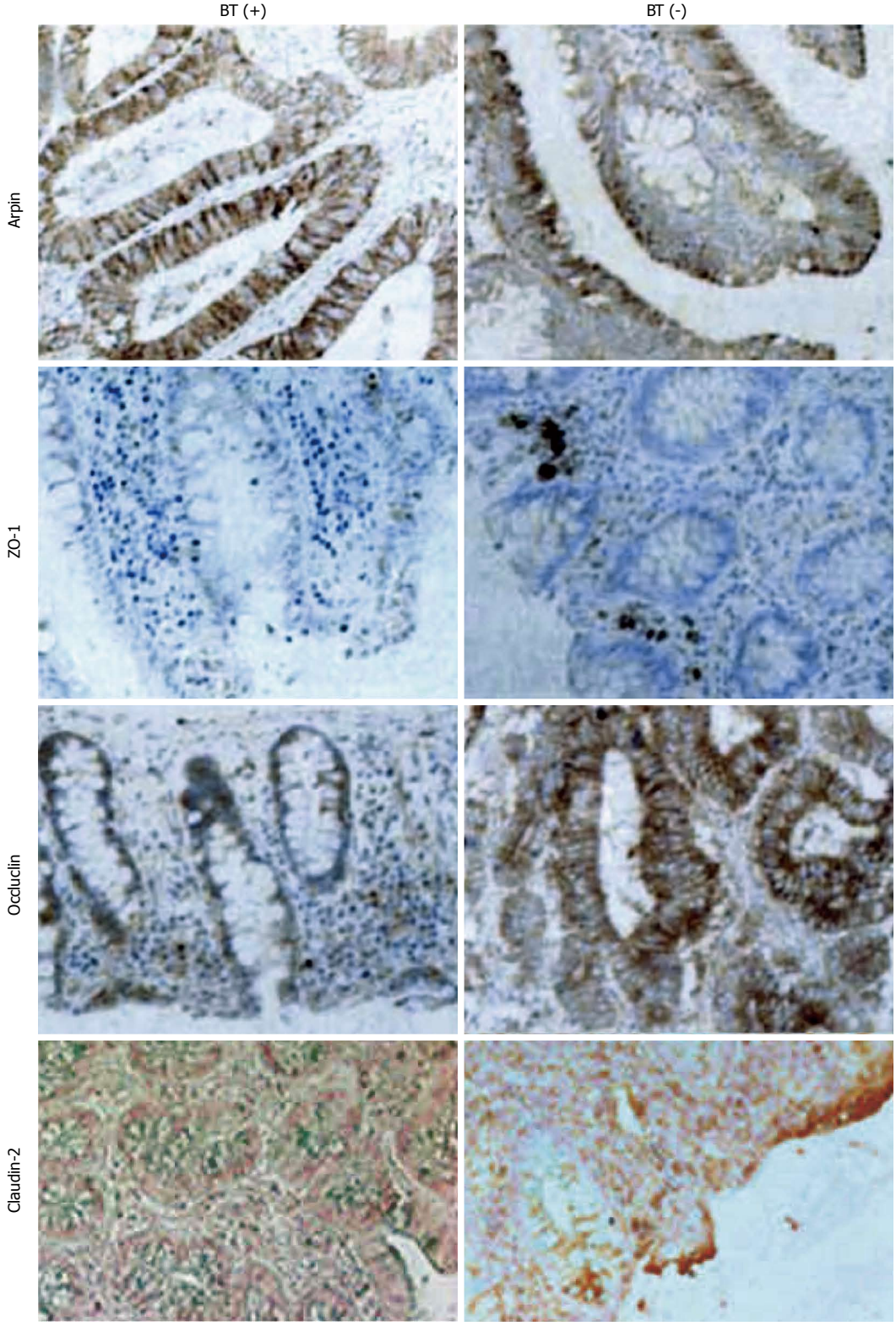

Figure 3 Expression of Arpin and tight junction proteins in the colonic mucosa of SAP-BT (-) patients and SAP-BT (+) patients (representative immunoblot). SAP: Severe acute pancreatitis; BT: Bacterial translocation.

patients (45.5%) with an APACHE-Ⅱ of score 12-14 points showed evidence of bacterial DNA, which was significantly decreased compared to those with a score greater than 12 points ($P < 0.01$). The prevalence of bacteremia was positively correlated with the APACHE-Ⅱ scores of patients with SAP ($r = 0.7502$; $P < 0.05$) (Figure 2B), suggesting a potential association between bacteremia and the severity of disease.

Table 2 Arpin and tight junction proteins expression

	HC (n = 20)	SAP			
		Total (n = 50)	BT(-) (n = 19)	BT(+) (n = 31)	P value[1]
Arpin	0.28 ± 0.16	0.38 ± 0.19	0.31 ± 0.24	0.61 ± 0.28	0.003
Zonula occludens-1	0.89 ± 0.46	0.48 ± 0.23	0.58 ± 0.17	0.42 ± 0.26	0.038
Claudin-2	0.73 ± 0.32	0.49 ± 0.19	0.32 ± 0.21	0.64 ± 0.27	0.021
Occludin	0.85 ± 0.36	0.68 ± 0.21	0.73 ± 0.32	0.61 ± 0.28	0.010

[1]SAP-BT (-) *vs* SAP-BT (+), one-way ANOVA. Data are expressed as mean ± SD. HC: Healthy control; SAP: Severe acute pancreatitis.

Arpin and TJ protein expression

As shown in Figure 3, compared to BT (-) SAP patients, increased levels of Arpin expression were detected in tissue samples obtained from BT (+) SAP patients detected by immunofluorescence staining. Arpin protein was primarily detected between epithelial cells in the epithelium of BT (+) SAP patients. The TJ proteins, which were detected throughout the mucosa, were clearly decreased in BT (+) SAP patients, whereas more granular staining was observed in whole epithelial cells in samples from BT (+) SAP patients. Western blot analysis confirmed these differences between the groups and the details are shown in Table 2 and Figure 4. The expression levels of Arpin were 0.31 ± 0.24 in the SAP-BT (-) group and 0.61 ± 0.28 in the SAP-BT (+) group and this difference was statistically significant (P = 0.003). SAP-BT (+) patients also showed a higher expression level of CL-2 (0.64 ± 0.27 *vs* 0.32 ± 0.21, P = 0.005) and a lower expression level of OC (0.73 ± 0.32 *vs* 0.61 ± 0.28, P = 0.023) and ZO-1 (0.58 ± 0.17 *vs* 0.42 ± 0.26, P = 0.012) compared to SAP-BT(-) patients. Moreover, we found that the higher expression of Arpin protein in the colonic mucosa was significantly (r = 0.421, P = 0.032) associated with a higher level of CL-2 expression in SAP-BT (+) patients (Figure 5).

DISCUSSION

In this study, SAP patients with colonic involvement were treated with endoscopy and an endoscopic biopsy was collected. In addition, peripheral blood was collected to detect bacterial DNA. Our results demonstrated a high prevalence of bacteremia in patients with SAP, indicating that the presence of circulating bacteria and their specific distribution are associated with the severity of pancreatitis. These conclusions are in accordance with the results of previous studies[26]. Bacterial translocation from the gut has been considered a central mechanism underlying the development of pancreatic infections and necrosis[27,28], although the detailed mechanism remains unknown. In this study, we also found that SAP-BT (+) patients showed higher levels of Arpin and Cl-2 expression than SAP-BT (-) patients, whereas ZO-1 and OC expression was lower in SAP-BT (+) patients. Moreover, we found that the expression of Arpin protein was also correlated with that of CL-2 protein in SAP-BT (+) patients. However, we could not determine the detailed mechanism of Arpin action and additional studies with improved methods are needed to explore this issue in the future.

Based on our results, we speculate that Arpin acts on cytoskeletal proteins of the TJ. TJs play a structural role in the regulation of intestinal permeability and may be important for BT. TJs are cell-cell adhesion structures in mucosal epithelial cell sheets and can migrate to maintain the function of the intestinal mucosal barrier[28,29]. In our research, we show that high expression of Arpin is correlated with low TJ expression in the mucosal epithelium, which suggests that Arpin acts as a competitive inhibitor of the Arp2/3 complex. To date, many proteins have been identified as components of the TJ and understanding their architectural organization and interactions is critical to understanding the biology of this barrier. CL-2, OC and ZO-1 are the most prominent proteins in TJs and their coupling to the TJ cytoskeleton is required for assembly of the junction and maintenance of the barrier[13]. In our study, the altered expression of these proteins provided important information about the function of Arpin protein. One common feature of physiological and pathological alterations of the barrier is changes to the junction-associated actin cytoskeleton. Unsurprisingly, the number of cytoskeletal proteins at the junction is large. Because Arpin was shown to act as an actin-polymerizing protein localized to TJs[14], this protein is a prime candidate for a local inhibitor, given that it functions as a competitive inhibitor of actin filament nucleation and has been shown experimentally to contribute to the collapse of lamellipodia. The absence or dysfunction of TJ protein is not sufficient to destroy the barrier and trigger pathogenesis, indicating a failure of the mechanism of the intestinal epithelial barrier and other processes. In cells subjected to ultraviolet irradiation, high temperature, osmotic pressure and a variety of stresses such as inflammation, the Rac signaling pathway is activated, which can activate downstream Arpin. Arpin then inhibits the Arp2/3 complex, leading to the formation of F-actin (produced by polymerization of inactive G-actin). When Arpin expression is elevated, inhibition of the Arp2/3 complex is enhanced, F-actin polymerization is reduced and the cytoskeleton rearranged. As our research shows, Arpin influences a variety of proteins such as CL-2, which may lead to TJ protein opening and barrier destruction. Thus, we can infer that Arpin is a negative regulator of Arp2/3 activity and that cells utilize Arpin to fine-tune actin nucleation activity at the leading edge of the lamellipodium to disrupt TJ proteins in intestinal permeability.

However, the present study had certain limitations. Due to a lack of technical assistance, we could not

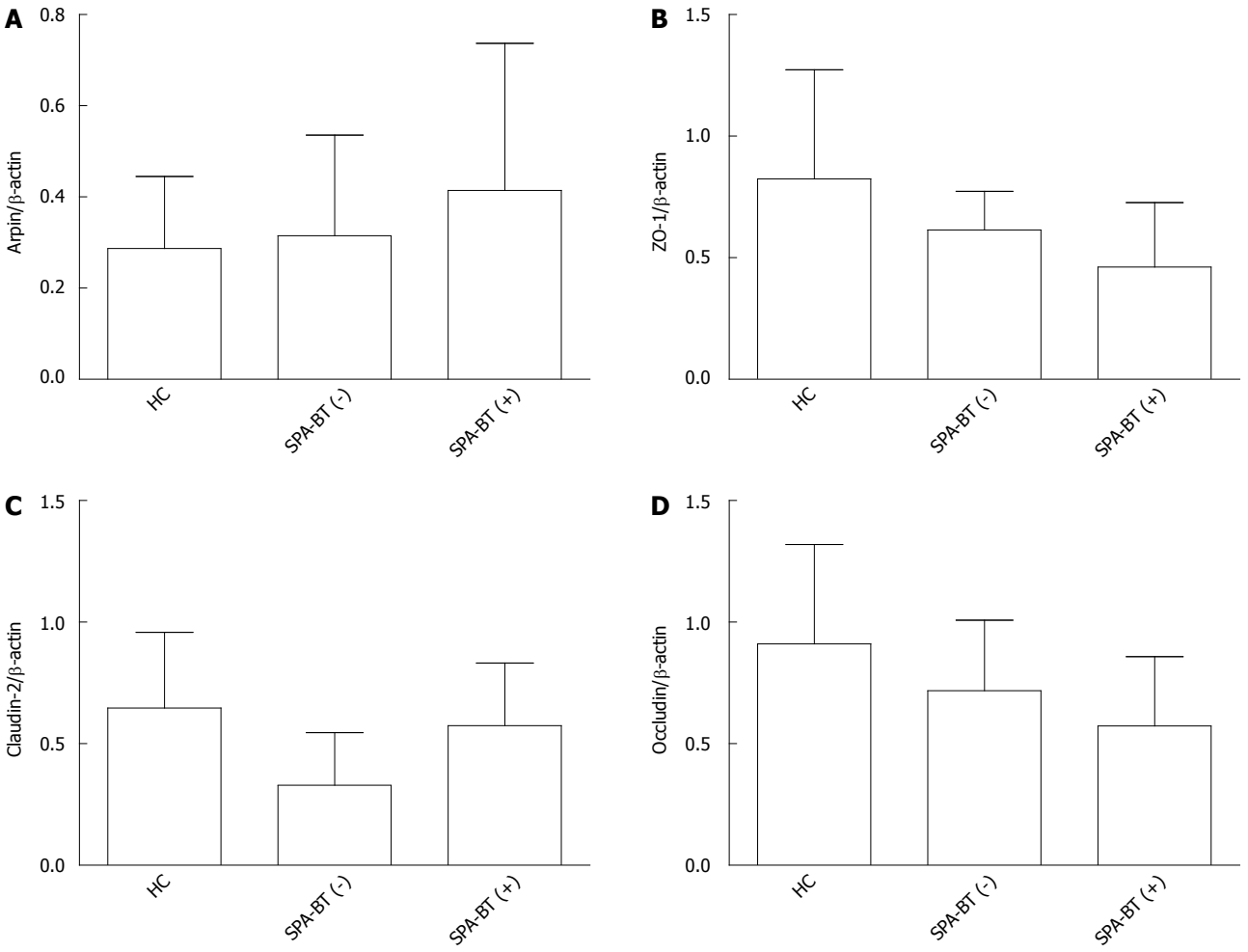

Figure 4 Arpin and tight junction proteins expression. A: Arpin expression; HC *vs* SAP-BT (-), $P = 0.325$; HC *vs* SAP-BT (+), $P = 0.015$; B: Zonula occludens-2 expression; HC *vs* SAP-BT (-), $P = 0.012$; HC *vs* SAP-BT(+), $P = 0.023$; C: Claudin-2 expression; HC *vs* SAP-BT (-), $P = 0.032$; HC *vs* SAP-BT (+), $P = 0.027$; D: Occludin expression; HC *vs* SAP-BT (-), $P = 0.038$; HC *vs* SAP-BT (+), $P = 0.019$. All performed one-way ANOVA. SAP: Severe acute pancreatitis; BT: Bacterial translocation; HC: Healthy control.

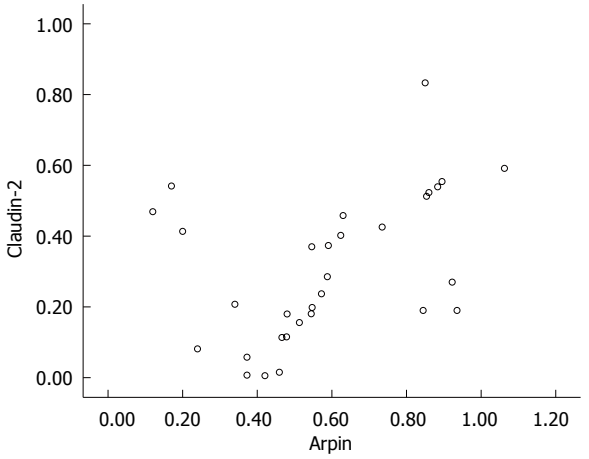

Figure 5 Relationship between Arpin and claudin-2 expression in severe acute pancreatitis-BT (+) patients. Pearson test, $r = 0.421$, $P = 0.003$. BT: Bacterial translocation.

visualize the relationship between Arpin and TJ protein. Thus, more effective methods are needed to explore this topic more thoroughly in the future.

In summary, Arpin contributes to BT occurrence and development by disrupting the cytoskeletal proteins of TJs in patients with SAP.

COMMENTS

Background

Infection and sepsis are severe complications contributing to most late deaths in severe acute pancreatitis (SAP). In most patients, infection is caused by gram-negative bacteria, suggesting failure in the gut barrier function, and the intestinal epithelial barrier is composed of tight junctions (TJs) between intestinal epithelial cells. However, the detailed mechanism remains unknown. Recent work has identified an Arp2/3 interacting protein called Arpin, which restricts the rate of actin polymerization and is the latest component in the steadily expanding protein repertoire that controls cell migration. Extensive evidence has shown that protein regulates the Arp2/3 complex and TJs, promoting epidermal barrier formation. However, there were few reports about the research on intestinal mucosa. Thus, the authors undertook further investigations about the roles of the Arpin protein in the gut barrier of SAP patients.

Research frontiers

TJs are considered among factors affecting the decision of the permeability of intestinal mucosa, with the intestinal epithelial barrier the first line of defense. Pure TJ protein expression is absent or dysfunctional but is not enough to destroy the barrier and disease, showing that there are other damage mechanisms of the intestinal epithelial barrier. In September 2013, the Duke

University Medical Center reported the Arp2/3 complex in the role of the epidermal barrier, living and cell culture, and found that a lack of Arp two-thirds complex causes TJ protein expression level to be decreased and that zonula occludens-1 TJ form is flawed. For the first time, it was confirmed that the Arp2/3 complex maintains skin TJ formation and its function has important significance. The effect of TJs and the potential significance of the Arp2/3 complex in the intestinal epithelial barrier has not been further discussed in the literature.

Innovations and breakthroughs

SAP intestinal epithelial barrier damage, actin cytoskeleton and intestinal epithelium appear to be researched rarely and how skeletal actin changes in intestinal epithelial permeability increase the role of the mechanism is unclear. This is the first report about detecting Arpin proteins in the intestinal mucosa and the authors found that Arpin proteins relate to the function of intestinal mucosa, speculating that Arpin open TJs in intestinal mucosa, leading to bacterial translocation.

Applications

Arpin affects the intestinal epithelial barrier in SAP and opens TJs and TJ protein changes in the SAP regulatory mechanism of intestinal epithelial barrier damage, in order to provide a new way for revealing the pathogenesis and prevention of SAP associated intestinal epithelial barrier dysfunction. Further studies are needed to clarify the detailed mechanisms involved.

Terminology

The newly discovered and reported proteins in 2013 are distributed in the intestine, pancreas and elsewhere. Arpin is implicated in cell movement and inflammation. The preliminary data suggest that the expressions of Arpin in SAP associated enterogenous infection changed but the mechanism needs to be further studied. Therefore, the authors put forward the hypothesis that the increase of Arpin opens the intestinal epithelial TJ, the reduced expression of TJ protein changes and Arpin affects the intestinal epithelial barrier function. To test this hypothesis, the roles of Arpin in SAP by means of SAP patients with the methods of Western blot and immunofluorescence were explored. The aim of the study was to clarify the mechanism of SAP associated intestinal epithelial barrier injury through open TJ and TJ protein changes caused by Arpin, in order to provide a new way for revealing the pathogenesis and prevention of SAP associated intestinal epithelial barrier dysfunction.

Peer-review

This report provides valuable insight into the pathophysiological mechanisms of bacterial translocation in the setting of acute pancreatitis. This is an area that remains in many ways a clinical and scientific unknown entity. The authors offer a comprehensive research method to answer the research question. Bacterial translocation is a main issue in the clinical management of severe acute pancreatitis. In this challenging scenario, molecular research could be an aid to clinicians and surgeons for a better management and in the staging of new severity predicting factors.

REFERENCES

1 **Schmid SW**, Uhl W, Friess H, Malfertheiner P, Büchler MW. The role of infection in acute pancreatitis. *Gut* 1999; **45**: 311-316 [PMID: 10403749 DOI: 10.1136/gut.45.2.311]

2 **Nathens AB**, Curtis JR, Beale RJ, Cook DJ, Moreno RP, Romand JA, Skerrett SJ, Stapleton RD, Ware LB, Waldmann CS. Management of the critically ill patient with severe acute pancreatitis. *Crit Care Med* 2004; **32**: 2524-2536 [PMID: 15599161 DOI: 10.1097/01.CCM.0000148222.09869.92]

3 **Beger HG**, Bittner R, Block S, Büchler M. Bacterial contamination of pancreatic necrosis. A prospective clinical study. *Gastroenterology* 1986; **91**: 433-438 [PMID: 3522342]

4 **Lumsden A**, Bradley EL. Secondary pancreatic infections. *Surg Gynecol Obstet* 1990; **170**: 459-467 [PMID: 2183376]

5 **Tarpila E**, Nyström PO, Franzén L, Ihse I. Bacterial translocation during acute pancreatitis in rats. *Eur J Surg* 1993; **159**: 109-113 [PMID: 8098624]

6 **MacFie J**, O'Boyle C, Mitchell CJ, Buckley PM, Johnstone D, Sudworth P. Gut origin of sepsis: a prospective study investigating associations between bacterial translocation, gastric microflora, and septic morbidity. *Gut* 1999; **45**: 223-228 [PMID: 10403734 DOI: 10.1136/gut.45.2.223]

7 **Gencay C**, Kilicoglu SS, Kismet K, Kilicoglu B, Erel S, Muratoglu S, Sunay AE, Erdemli E, Akkus MA. Effect of honey on bacterial translocation and intestinal morphology in obstructive jaundice. *World J Gastroenterol* 2008; **14**: 3410-3415 [PMID: 18528939 DOI: 10.3748/wjg.14.3410]

8 **Koh YY**, Jeon WK, Cho YK, Kim HJ, Chung WG, Chon CU, Oh TY, Shin JH. The effect of intestinal permeability and endotoxemia on the prognosis of acute pancreatitis. *Gut Liver* 2012; **6**: 505-511 [PMID: 23170158 DOI: 10.5009/gnl.2012.6.4.505]

9 **Ammori BJ**, Leeder PC, King RF, Barclay GR, Martin IG, Larvin M, McMahon MJ. Early increase in intestinal permeability in patients with severe acute pancreatitis: correlation with endotoxemia, organ failure, and mortality. *J Gastrointest Surg* 1999; **3**: 252-262 [PMID: 10481118 DOI: 10.1016/S1091-255X(99)80067-5]

10 **Juvonen PO**, Alhava EM, Takala JA. Gut permeability in patients with acute pancreatitis. *Scand J Gastroenterol* 2000; **35**: 1314-1318 [PMID: 11199373 DOI: 10.1080/003655200453683]

11 **Hofmann C**, Obermeier F, Artinger M, Hausmann M, Falk W, Schoelmerich J, Rogler G, Grossmann J. Cell-cell contacts prevent anoikis in primary human colonic epithelial cells. *Gastroenterology* 2007; **132**: 587-600 [PMID: 17258732 DOI: 10.1053/j.gastro.2006.11.017]

12 **Morales Ciancio RA**, Drain O, Rillardon L, Guigui P. Acute spontaneous spinal epidural hematoma: an important differential diagnosis in patients under clopidogrel therapy. *Spine J* 2008; **8**: 544-547 [PMID: 18455116 DOI: 10.1007/s00418-008-0424-9]

13 **Van Itallie CM**, Anderson JM. Architecture of tight junctions and principles of molecular composition. *Semin Cell Dev Biol* 2014; **36**: 157-165 [PMID: 25171873 DOI: 10.1016/j.semcdb.2014.08.011]

14 **Dang I**, Gorelik R, Sousa-Blin C, Derivery E, Guérin C, Linkner J, Nemethova M, Dumortier JG, Giger FA, Chipysheva TA, Ermilova VD, Vacher S, Campanacci V, Herrada I, Planson AG, Fetics S, Henriot V, David V, Oguievetskaia K, Lakisic G, Pierre F, Steffen A, Boyreau A, Peyriéras N, Rottner K, Zinn-Justin S, Cherfils J, Bièche I, Alexandrova AY, David NB, Small JV, Faix J, Blanchoin L, Gautreau A. Inhibitory signalling to the Arp2/3 complex steers cell migration. *Nature* 2013; **503**: 281-284 [PMID: 24132237]

15 **Findley MK**, Koval M. Regulation and roles for claudin-family tight junction proteins. *IUBMB Life* 2009; **61**: 431-437 [PMID: 19319969 DOI: 10.1002/iub.175]

16 **Zhou K**, Muroyama A, Underwood J, Leylek R, Ray S, Soderling SH, Lechler T. Actin-related protein2/3 complex regulates tight junctions and terminal differentiation to promote epidermal barrier formation. *Proc Natl Acad Sci USA* 2013; **110**: E3820-E3829 [PMID: 24043783 DOI: 10.1073/pnas.1308419110]

17 **Ardern H**, Sandilands E, Machesky LM, Timpson P, Frame MC, Brunton VG. Src-dependent phosphorylation of Scar1 promotes its association with the Arp2/3 complex. *Cell Motil Cytoskeleton* 2006; **63**: 6-13 [PMID: 16317717 DOI: 10.1002/cm.20101]

18 **Suraneni P**, Rubinstein B, Unruh JR, Durnin M, Hanein D, Li R. The Arp2/3 complex is required for lamellipodia extension and directional fibroblast cell migration. *J Cell Biol* 2012; **197**: 239-251 [PMID: 22492726 DOI: 10.1083/jcb.201112113]

19 **Kim DJ**, Kim SH, Lim CS, Choi KY, Park CS, Sung BH, Yeo MG, Chang S, Kim JK, Song WK. Interaction of SPIN90 with the Arp2/3 complex mediates lamellipodia and actin comet tail formation. *J Biol Chem* 2006; **281**: 617-625 [PMID: 16253999 DOI: 10.1074/jbc.M504450200]

20 **Deligianni DD**. MWCNTs enhance hBMSCs spreading but delay their proliferation in the direction of differentiation acceleration. *Cell Adh Migr* 2014; **8**: 487-492 [PMID: 25482637 DOI: 10.4161/19336918.2014.969993]

21 **Boczkowska M**, Rebowski G, Petoukhov MV, Hayes DB, Svergun DI, Dominguez R. X-ray scattering study of activated Arp2/3 complex with bound actin-WCA. *Structure* 2008; **16**: 695-704 [PMID: 18462674 DOI: 10.1016/j.str.2008.02.013]

22 **Ti SC**, Jurgenson CT, Nolen BJ, Pollard TD. Structural and biochemical characterization of two binding sites for nucleation-promoting factor WASp-VCA on Arp2/3 complex. *Proc Natl Acad Sci USA* 2011; **108**: E463-E471 [PMID: 21676862 DOI: 10.1073/

pnas.1100125108]
23 **Bradley EL**. A clinically based classification system for acute pancreatitis. *Ann Chir* 1993; **47**: 537-541 [PMID: 8105746]
24 **Larvin M**, McMahon MJ. APACHE-II score for assessment and monitoring of acute pancreatitis. *Lancet* 1989; **2**: 201-205 [PMID: 2568529 DOI: 10.1016/S0140-6736(89)90381-4]
25 **Such J**, Francés R, Muñoz C, Zapater P, Casellas JA, Cifuentes A, Rodríguez-Valera F, Pascual S, Sola-Vera J, Carnicer F, Uceda F, Palazón JM, Pérez-Mateo M. Detection and identification of bacterial DNA in patients with cirrhosis and culture-negative, nonneutrocytic ascites. *Hepatology* 2002; **36**: 135-141 [PMID: 12085357 DOI: 10.1053/jhep.2002.33715]
26 **Li Q**, Wang C, Tang C, He Q, Li N, Li J. Bacteremia in patients with acute pancreatitis as revealed by 16S ribosomal RNA gene-based techniques*. *Crit Care Med* 2013; **41**: 1938-1950 [PMID: 23863226 DOI: 10.1097/CCM.0b013e31828a3dba]
27 **Cicalese L**, Sahai A, Sileri P, Rastellini C, Subbotin V, Ford H, Lee K. Acute pancreatitis and bacterial translocation. *Dig Dis Sci* 2001; **46**: 1127-1132 [PMID: 11341659]
28 **Oláh A**, Pardavi G, Belágyi T, Romics L. Preventive strategies for septic complications of acute pancreatitis. *Chirurgia* (Bucur) 2007; **102**: 383-388 [PMID: 17966933]
29 **Kojima T**, Yamaguchi H, Ito T, Kyuno D, Kono T, Konno T, Sawada N. Tight junctions in human pancreatic duct epithelial cells. *Tissue Barriers* 2013; **1**: e24894 [PMID: 24665406 DOI: 10.4161/tisb.24894]

P- Reviewer: Boetto R, Haydock MD **S- Editor**: Yu J
L- Editor: Roemmele A **E- Editor**: Zhang DN

World Journal of Gastroenterology

Submit a Manuscript: http://www.wjgnet.com/esps/
Help Desk: http://www.wjgnet.com/esps/helpdesk.aspx
DOI: 10.3748/wjg.v21.i14.4302

World J Gastroenterol 2015 April 14; 21(14): 4302-4309
ISSN 1007-9327 (print) ISSN 2219-2840 (online)

ORIGINAL ARTICLE

Prospective Study

Anxiety and depression in patients with gastroesophageal reflux disease and their effect on quality of life

Xiao-Jun Yang, Hong-Mei Jiang, Xiao-Hua Hou, Jun Song

Xiao-Jun Yang, Hong-Mei Jiang, Xiao-Hua Hou, Jun Song, Division of Gastroenterology, Union Hospital, Tongji Medical College, Huazhong University of Science and Technology, Wuhan 430022, Hubei Province, China
Xiao-Jun Yang, Department of Gastroenterology, Chongqing Hospital of Traditional Chinese Medicine, Chongqing 400037, China
Author contributions: Yang XJ wrote the paper; Jiang HM performed the research and collected the data; Yang XJ and Hou XH analyzed the data; Song J designed the research.

Correspondence to: Jun Song, MD, Division of Gastroenterology, Union Hospital, Tongji Medical College, Huazhong University of Science and Technology, No. 1277 Jiefangdadao, Wuhan 430022, Hubei Province, China. song111jun@126.com
Telephone: 86-23-67953337
Fax: 86-27-85726930
Received: July 26, 2014
Peer-review started: July 31, 2014
First decision: August 15, 2014
Revised: October 26, 2014
Accepted: December 8, 2014
Article in press: December 8, 2014
Published online: April 14, 2015

Abstract

AIM: To explore the role of psychological factors in gastroesophageal reflux disease (GERD) and their effect on quality of life (QoL) of GERD patients.

METHODS: A total of 279 consecutive patients with typical symptoms and 100 healthy controls were enrolled in the study. All of the participants were evaluated with the Zung Self-Rating Anxiety Scale (ZSAS), the Zung Self-Rating Depression Scale (ZSDS) and the SF-36 questionnaire. The scores for anxiety, depression and QoL of the two groups were analyzed. The correlation between psychological factors and QoL was also analyzed.

RESULTS: Compared with healthy controls (34.70 ± 8.00), the scores of ZSAS in the non-erosive reflux disease (NERD) group (48.27 ± 10.34) and the reflux esophagitis (RE) group (45.38 ± 10.27) were significantly higher ($P < 0.001$). The mean ZSAS score of the NERD group was significantly higher than that of the RE group ($P = 0.01$). Compared with healthy controls (37.61 ± 8.44), the mean ZSDS scores were significantly higher in the NERD group (49.65 ± 11.09, $P < 0.001$) and the RE group (46.76 ± 11.83, $P < 0.001$). All dimensions of the SF-36 form were negatively correlated with the SAS and SDS scores in patients with NERD and RE ($P < 0.05$). According to the SF-36 form, vitality, mental health and social functioning were significantly correlated with symptoms of depression in patients with NERD and RE. General health was obviously affected by symptoms of depression in patients with NERD ($P < 0.05$).

CONCLUSION: Anxiety and depression may play an important role in the occurrence of GERD and especially that of NERD. The QoL of patients with GERD is reduced by anxiety and depression.

Key words: Anxiety; Depression; Gastroesophageal reflux disease; Zung Self-Rating Anxiety Scale; Zung Self-Rating Depression Scale; SF-36; Quality of life

Core tip: In our study, the degree of anxiety and depression in non-erosive reflux disease (NERD) and reflux esophagitis patients was significantly higher than

that of healthy controls, especially for the NERD group. The quality of life was negatively correlated with the degree of anxiety and depression.

Yang XJ, Jiang HM, Hou XH, Song J. Anxiety and depression in patients with gastroesophageal reflux disease and their effect on quality of life. *World J Gastroenterol* 2015; 21(14): 4302-4309 Available from: URL: http://www.wjgnet.com/1007-9327/full/v21/i14/4302.htm DOI: http://dx.doi.org/10.3748/wjg.v21.i14.4302

INTRODUCTION

Gastroesophageal reflux disease (GERD) is a condition characterized by the reflux of stomach contents into the esophagus, which causes several symptoms, such as heartburn and regurgitation. It is typically divided into three subtypes: reflux esophagitis (RE), non-erosive reflux disease (NERD) and Barrett's esophagus. GERD has been shown to have a significant negative impact on the quality of life (QoL) of affected patients and may even disrupt their daily activities. On a weekly basis, GERD affects up to 20% of the population in the United States and Europe[1], 12% to 15% in Australia, and 2% to 5% in Asia[2]. Therefore, a diagnosis of GERD is easily made based on the symptoms of the patients, which typically include heartburn and regurgitation and/or other atypical acid reflux-related symptoms. Meanwhile, a diagnosis can also be obtained from gastroendoscopic findings of visible esophageal mucosal injury. NERD has been defined as the presence of acid reflux-related symptoms with no esophageal mucosal injury.

The etiology of GERD is multifactorial. The disease results from an imbalance between the harmful properties of refluxed stomach contents, mechanisms of esophageal clearance, and esophageal mucosal resistance[3]. Common risk factors for GERD including the absence of a hiatus hernia, a low body mass index (BMI) and the presence of *Helicobacter pylori*, indicate that this condition is a milder form of disease within the GERD spectrum. The majority of patients with GERD use antacid drugs to control their symptoms. However, the symptoms of GERD are sometimes impossible to control, and these patients tend to have a lower response rate, even to the most potent proton-pump inhibitors (PPIs)[4,5]. Some studies have already demonstrated that up to 40% of patients with heartburn reported either a partial or complete lack of response to PPIs taken once daily[6-8]. According to clinical data, apart from the common risk factors listed above, psychological factors, including anxiety and depression, can also develop in patients with GERD. We supposed that the psychological factors associated with NERD may distinguish NERD from RE and Barrett's esophagus.

We hypothesized that psychological factors may comprise some of the essential influencing factors and that they might impair the QoL of individuals with GERD. However, it remains unknown how psychological factors induce GERD and affect the QoL in patients with GERD in China. To explore the link between psychological factors and the pathophysiology of GERD, this study evaluated the psychological status of patients with GERD and its effect on QoL.

MATERIALS AND METHODS

Subjects

A total of 279 consecutive patients with typical symptoms of heartburn or regurgitation from the Division of Gastroenterology (Union Hospital, Tongji Medical College) and 100 healthy controls selected among the staff of Union Hospital and medical students of Tongji Medical College were enrolled in this study.

Procedure

All subjects agreed to participate and signed an informed consent form. Subsequently, subjects underwent gastroendoscopy to evaluate for the presence of esophageal mucosal lesions. Based on the results of the gastroendoscopy, the patients were divided into two major groups: RE (including Barrett's esophagus; males = 71; females = 63) and NERD (males = 66; females = 79). GERD was diagnosed according to the previously proposed Rome Ⅲ criteria. Patients were excluded for the following reasons: use of prescribed non-steroidal anti-inflammatory drugs (NSAIDs) and aspirin; previous treatment with a proton pump inhibitor (patients who were treated with H2-blockers were allowed to participate if the treatment had been discontinued 14 d prior to the initial evaluation); incidence of a peptic stricture or duodenal and/or gastric ulcer visible on upper endoscopy; a history of upper gastrointestinal surgery; comorbidities, such as scleroderma, diabetes mellitus, autonomic or peripheral neuropathy, myopathy, functional bowel disorder or any underlying disease (or medication) that might affect the lower esophageal sphincter pressure or increase the acid clearance time; inability or unwillingness to fully complete all stages of the study; and inability or unwillingness to provide informed consent. This protocol was approved by the Ethics Committee of Tongji Medical College (No. 104).

Measures

The Zung Self-Rating Anxiety Scale (ZSAS) was designed by William WK Zung to evaluate the level of anxiety in patients who experience anxiety-related symptoms[9]. The ZSAS contains 20 questions. Each question is scored on a scale of 1-4 (never, some of the time, relatively often, most of the time). Fifteen questions involve the assessment of increasing anxiety levels, and five questions involve decreasing anxiety levels. The ZSAS scores were used to define four

Table 1 Patient demographics and clinical data (*n* = 379)

	Healthy controls	RE patients	NERD patients
n	100	134	145
Gender (M/F)[1]	49/51	71/63	66/79
mean age (yr)[2]	40.04 ± 12.22	41.07 ± 10.61	39.68 ± 10.80
Age range (yr)	19-67	23-68	16-71

[1]No significant differences were observed among the three groups with respect to age (F = 0.574; P = 0.564); [2]The constituent ratios of gender showed no significant differences among the three groups (χ^2 = 1.554; P = 0.460). RE: Reflux esophagitis; NERD: Non-erosive reflux disease.

Table 2 Characteristics of anxiety symptoms according to the Zung self-rating anxiety scale *n* (%)

Group	Normal	Mild to moderate	Severe	Extreme
Healthy control	86 (86)	13 (13)	1 (1)	0 (0)
RE	61 (45.52)	59 (44.03)	14 (10.44)	0 (0)
NERD	49 (33.79)	72 (49.66)	24 (16.55)	0 (0)

Compared with the healthy controls, the constituent ratios of the RE and the NERD groups were significantly different (χ^2 = 40.829, 66.222; P < 0.001, 0.001, respectively). The results of the RE group were similar to those of the NERD group (χ^2 = 4.805; P = 0.091). RE: Reflux esophagitis; NERD: Non-erosive reflux disease.

categories of anxiety severity: within normal range or no significant psychopathology (20-44 points); presence of mild to moderate anxiety levels (45-59 points); severe anxiety levels (60-74 points); and presence of extreme depression (75-80 points).

Similarly, the Zung Self-Rating Depression Scale (ZSDS) was used to assess the severity of depression in the patients[10]. The ZSDS includes 10 positively worded items and 10 negatively worded items that assess symptoms of depression. Item responses are ranked from 1 to 4, and higher scores correspond to more frequent symptoms. Therefore, for each item, patients give a score according to whether the item has occurred: 1 = never/very rarely/rarely; 2 = once in a while/some of the time/occasionally; 3 = relatively often/very often/often; 4 = most of the time/always/almost always. The ZSDS scores were used to define four categories of depression severity: within normal range or no significant psychopathology (below 40 points); presence of minimal to mild depression (40-47 points); presence of moderate to marked depression (48-55 points); and presence of severe to extreme depression (56 points and above). Total scores on the ZSDS do not correspond with a clinical diagnosis of depression but rather indicate the level of depressive symptoms that may be clinically relevant.

The 36-item Short-Form Health Survey (SF-36) is a commonly used generic questionnaire that includes 36 items clustered into eight dimensions (bodily pain, general health, mental health, physical functioning, role-emotional, role-physical, social functioning, and vitality)[11]. The item scores for each dimension are coded, summed and transformed to a scale from 0 (worst possible health status) to 100 (best possible health status). The SF-36 is well-documented in terms of reliability and validity in all available language versions. Each raw scale score is linearly transformed to *t* scores. The transformed scores range from 0 to 100; higher scores indicate a better health-related QoL. These physical and mental summary scores served as the dependent variables in our analysis. We performed a separate analysis for each score.

Statistical analysis

The statistical analyses were performed using SPSS software (SPSS, Version 18; Chicago, IL, United States). For all continuous variables, the mean and standard deviation are presented. One-way analysis of variance was used to compare the parametric quantitative variables, followed by LSD or Tamhane's T2 test for a post-hoc analysis to further examine the differences among the groups. A χ^2 test or Fisher's exact test was used to compare the proportions. All *P*-values were two-tailed, and the level of significance was defined at 0.05.

RESULTS

Demographic and clinical characteristics

A total of 279 patients and 100 healthy controls were included in this study. Patient demographics and clinical characteristics are shown in Table 1. No significant differences were observed with respect to sex or age among the three groups.

Prevalence of anxiety symptoms in patients with NERD

A total of 379 people completed the ZSAS questionnaire. The characteristics of the anxiety symptoms according to the ZSAS are detailed in Table 2. The results of the χ^2 test revealed a significant difference in the constituent ratio of the three groups (P < 0.001). Compared with healthy controls, the constituent ratios of both the NERD group and the RE group presented a significant difference (P < 0.001). The incidence of anxiety was significantly higher in the NERD group than in the RE group (Fisher's exact test, P = 0.050). As shown in Figure 1, the mean scores of the ZSAS in the NERD group (48.27 ± 10.34) and in the RE group (45.38 ± 10.27) were significantly higher than that of the healthy control group (34.70 ± 8.00) (P < 0.001). Moreover, the mean score of the NERD group was significantly higher than that of the RE group (P = 0.01), suggesting that patients with NERD experienced more severe anxiety than did patients with RE, despite the fact that patients with NERD lacked esophageal erosions.

Prevalence of depressive symptoms in patients with NERD

A significant difference was observed in the constituent ratios of the three groups (P < 0.001). The SDS scores were significantly higher in patients with NERD (49.65

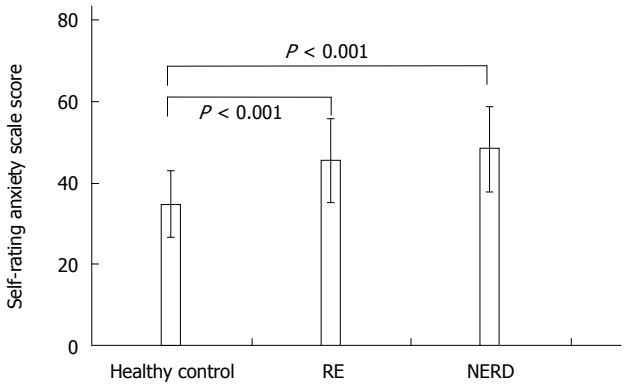

Figure 1 Comparison of the Zung self-rating anxiety scale scores in the three groups. RE: Reflux esophagitis; NERD: Non-erosive reflux disease.

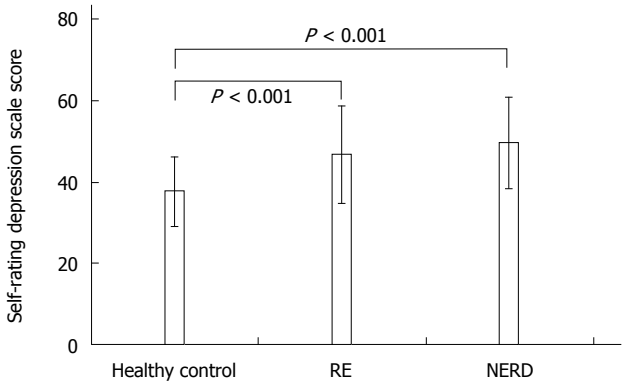

Figure 2 Comparison of Zung self-rating depression scale scores in the three groups. RE: Reflux esophagitis; NERD: Non-erosive reflux disease.

± 11.09, $P < 0.001$) and in patients with RE (46.76 ± 11.83, $P < 0.001$) compared with those of healthy controls (37.61 ± 8.44) (Figure 2). However, the constituent ratios between patients with NERD and patients with RE were not significantly different ($\chi^2 = 6.556$, $P = 0.085$) (Table 3). In addition, the incidence of depression in patients with NERD was higher than that in patients with RE (Fisher's exact test, $P = 0.020$).

QoL in the three groups

The standardized component scales of the SF36 are reported in this text as summary information on QoL shown in Figure 3. Compared with the healthy controls, all of the dimensions had statistically lower scores in the NERD and RE groups ($P < 0.05$), indicating that the QoL of patients with both NERD and RE was inferior to that of the healthy controls. In the NERD group, the scores of vitality and mental health were statistically lower than those of RE patients, which means that part dimensions of QoL in NERD patients were more decreased than those of RE patients ($P < 0.05$).

Negative correlation of the ZSAS scores with the SF-36 survey in NERD and RE patients

Correlations between the scores of SAS and SF-36 are shown in Figure 4. All of the dimensions of the SF-36 survey were significantly negatively correlated with the SAS anxiety scores in patients with NERD and RE, which means that QoL of patients with GERD was decreased by anxiety. At the same time, general health and mental health of patients with NERD seemed to decrease more readily due to anxiety symptoms compared with these same dimensions in patients with RE ($P < 0.05$). The correlation coefficients between the ZSAS scores and the other dimensions of the SF-36 survey, such as physical function, role-physical, role-emotional, and social functioning, were similar in both groups.

Table 3 Characteristics of anxiety symptoms according to the Zung self-rating depression scale *n* (%)

SDS	Normal	Mild to moderate	Severe	Extreme
Healthy, control	80 (86)	11 (13)	8 (1)	1 (0)
RE	42 (31.34)	43 (32.09)	26 (19.40)	23 (17.16)
NERD	32 (22.07)	38 (26.21)	35 (24.14)	40 (27.59)

Compared with the healthy controls, the constituent ratios of the RE and the NERD groups presented a significant difference ($\chi^2 = 35.14$, 64.582; $P < 0.001$, 0.001, respectively). The results of the RE group were similar to those of the NERD group ($\chi^2 = 6.556$; $P = 0.085$). RE: Reflux esophagitis; NERD: Non-erosive reflux disease.

Negative correlation of the SDS scores with the SF-36 survey in patients with NERD and RE

Correlations between the scores of SDS and SF-36 are shown in Figure 5. All of the dimensions of the SF-36 form were significantly negatively correlated with the SDS scores. As a result of the negative correlation between the ZSAS and the SF-36 form, vitality, mental health and social functioning were significantly correlated with depressive symptoms in both groups. Although bodily pain was significantly correlated with symptoms of depression in both groups, it appeared that patients with RE were more easily troubled by depression. However, the general health dimension was more likely to be lowered by symptoms of depression in patients with NERD ($P < 0.05$). The correlation coefficients between the ZSDS scores and the other dimensions of the SF-36 form, such as physical function, role-physical, and role-emotional, were similar in both groups.

DISCUSSION

According to previous epidemiological surveys, psychological factors play an important role in patients with GERD and have been shown to decrease QoL[12]. Although there have been some studies on the morbidity of GERD in China[13-16], no surveys have been reported on the role of psychological factors in GERD and their negative impact on QoL. In the current study,

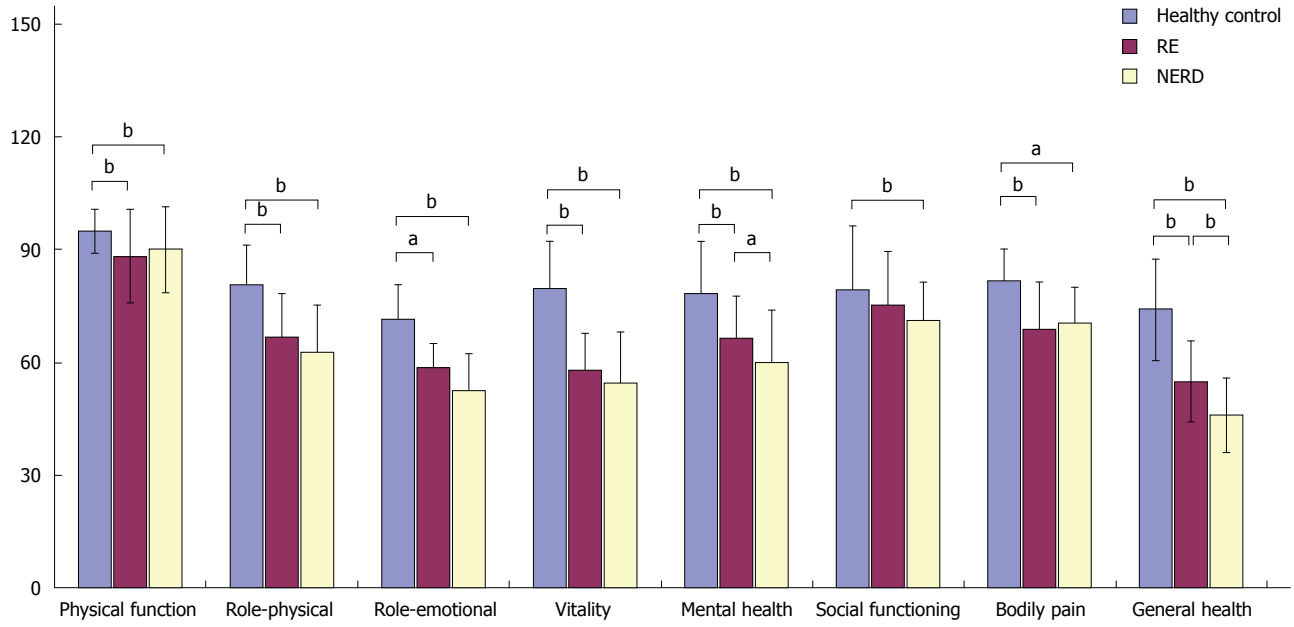

Figure 3 Comparison of the quality of life in the three groups. [a]$P < 0.05$, [b]$P < 0.01$. RE: Reflux esophagitis; NERD: Non-erosive reflux disease.

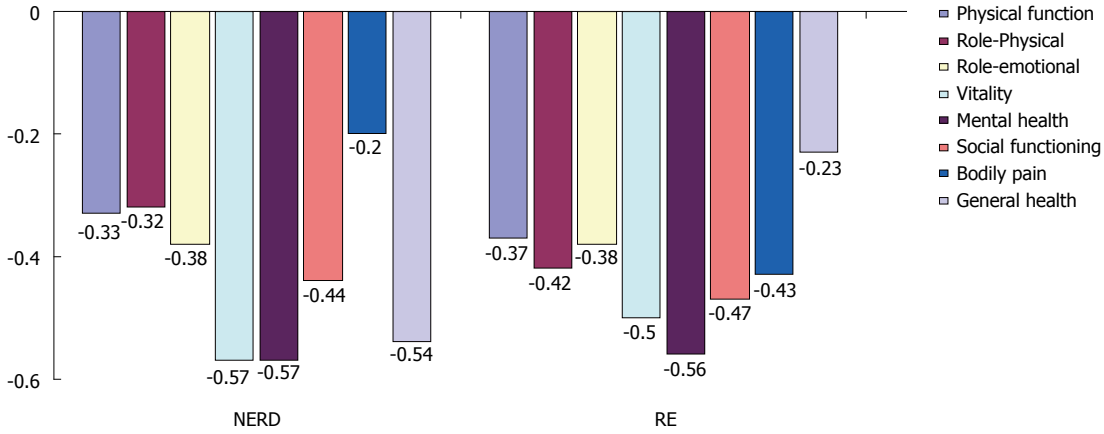

Figure 4 Negative correlations between the Zung self-rating anxiety scale scores and the SF-36 survey. All items of the SF-36 were significantly negatively correlated with the SAS anxiety scores in NERD and RE group ($P < 0.05$). RE: Reflux esophagitis; NERD: Non-erosive reflux disease.

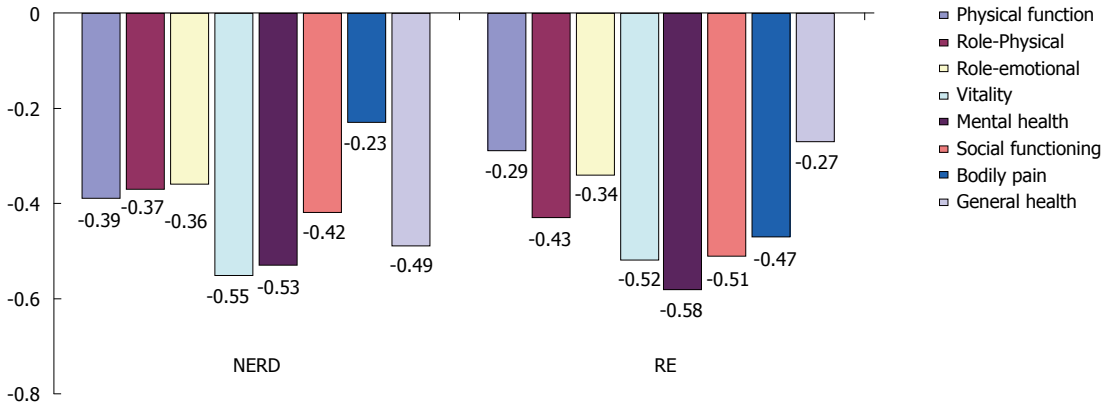

Figure 5 Negative correlations between the Zung self-rating depression scale scores and the SF-36 survey. All items of the SF-36 were significantly negatively correlated with the SDS depression scores in NERD and RE group ($P < 0.05$). RE: Reflux esophagitis; NERD: Non-erosive reflux disease.

we analyzed the roles of both anxiety and depression symptoms on the incidence of GERD, as well as their negative impact on QoL in patients with GERD. The results suggested that the incidence of GERD was correlated with anxiety and depression, and QoL of patients with GERD was reduced statistically.

GERD is associated with anxiety and depression. Another study showed that the psychological scores for neuroticism, anxiety and depression were higher in patients with GERD than in healthy controls[13,17]. Moreover, psychological disorders were found to be positively correlated with symptoms of heartburn[18]. In our study, anxiety and depression scores of patients with NERD and RE were obviously higher than those of healthy controls. The difference in the constituent ratios of the three groups also implied a moderate to severe degree of anxiety and depression in the patients with NERD and RE, suggesting an important role of anxiety and depression in the pathogenesis of GERD. Other studies have shown that patients with anxiety or depression are at an increased risk for the development of reflux symptoms[19-22]. Jansson *et al*[23] reported that patients with anxiety but no depression had a 3.2-fold (95%CI: 2.7-3.8) increased risk of reflux symptoms and that those with depression but no anxiety had a 1.7-fold (95%CI: 1.4-2.1) increased risk; subjects with both anxiety and depression presented a 2.8-fold (95%CI: 2.4-3.2) increased risk compared with subjects without anxiety/depression. Two explanations have been offered on the correlation between psychological factors and GERD. The first theory is that anxiety and depression develop secondary to the reflux and then cause increased sensitivity to the reflux symptoms. The second explanation is that the severity of reflux is greater in patients with psychiatric diseases[24].

Moreover, the scores of anxiety and depression in patients with NERD were significantly higher than those in patients with RE, which may indicate a different pathogenesis of NERD in our study. A large number of epidemiological investigations have also found that anxiety, depression, and chronic stress can lead to NERD[12]. NERD accounts for an estimated 50% to 70% of GERD cases[25,26]. NERD is considered a heterogeneous group because of the various characteristics and symptom patterns of acid reflux. Studies have also shown that RE and NERD respond differently to PPIs because of their distinct pathogenesis[27-29]. On one hand, NERD is significantly more refractory than RE to PPI treatment[30,31]. On the other hand, some studies have indicated that anxiety and depression can worsen the symptoms of reflux[23]. Patients with typical GERD symptoms were more likely to have atypical symptoms, dyspepsia and higher scores on psychological symptoms (*e.g.*, somatization, obsessive-compulsion and phobic anxiety) than those without GERD symptoms[32].

Apart from reflux symptoms, anxiety and depression can also decrease the QoL in patients with GERD. It has been reported that all dimensions of health-related QoL, as measured using the SF-36 questionnaire, were meaningfully impaired in subjects with symptomatic GERD compared with subjects without[33]. Those results are consistent with the results of our study, which indicate a lower QoL score in patients with GERD compared with healthy controls. In our study, the SF-36 questionnaire was employed to evaluate the QoL of the subjects. Generally, the scores for items of the SF-36 form were significantly decreased in patients with NERD and RE compared with the healthy controls. Interestingly, all of the scores for items in patients with NERD were more severely lowered than the scores in patients with RE, especially with respect to mental health and general health. Therefore, we suggest that psychological factors play important roles in the development of GERD, especially that of NERD. In addition, the study by Kovács *et al*[34] also reported that, along with anxiety, the symptoms of depression caused by persistent living pressure were elevated; the QoL of patients with GERD was also decreased. However, Lee reported that venlafaxine, an SNRI antidepressant, significantly improved symptoms in young adult patients with functional chest pain[35]. The results also indicated that GERD symptom was reversible by antidepressant. In our study, anxiety and depression were negatively correlated with all dimensions of the SF-36 questionnaire. However, Boltin *et al*[36] reported that lack of response to PPI was associated with lower life satisfaction but not anxiety or depression. Therefore, we posited that, except acid reflux symptoms, the increased anxiety and depression in patients with NERD and RE were other factors that lowered the QoL.

In summary, psychological factors, including anxiety and depression, play an essential role in the development of GERD and especially that of NERD. Meanwhile, they have obvious negative effects on QoL. Consequently, anti-anxiety and anti-depression medications may be alternative therapies for patients with NERD and RE if antacids cannot produce a satisfactory effect. This issue requires further study to identify the patients who might benefit from anti-anxiety and anti-depression therapy in the future. Moreover, this study was conducted in a university hospital. Therefore, the results may be different from those visiting a general physician. If this was a multicenter study, the results should be more reasonable.

COMMENTS

Background

Gastroesophageal reflux disease (GERD) has been shown to have a significant negative impact on the quality of life (QoL) of affected patients and may even disrupt their daily activities. The etiology of GERD is multifactorial. Common risk factors for GERD including the absence of a hiatus hernia, a low BMI and the presence of *Helicobacter pylori*, indicate that this condition is a milder form of disease within the GERD spectrum. The majority of patients with GERD use

antacid drugs to control their symptoms. However, the symptoms of GERD are sometimes impossible to control, and these patients tend to have a lower response rate, even to the most potent proton-pump inhibitors (PPIs). According to clinical data, apart from the common risk factors listed above, psychological factors, including anxiety and depression, can also develop in patients with GERD. So, this study investigated the role of anxiety and depression in GERD and their effect on quality of life.

Research frontiers

Functional gastrointestinal disease is always concerned with psychological factors. The quality of life of patients is often reduced. As for GERD, PPIs are not always effective. So, it is necessary to explore the course of GERD and its correlation with psychological factors.

Innovations and breakthroughs

Anxiety and depression were concerned with incidence of functional gastrointestinal disease. Our study results indicated the incidence and degree of anxiety in the NERD group were significantly higher than those in the reflux esophagitis (RE) group. As for depression in the NERD group, the results were the same. SF36 was employed to evaluate the quality of life, and the results indicated that QoL of patients with both NERD and RE was inferior to that of the healthy controls. The QoL of NERD and RE patients was significantly correlated with anxiety and depression.

Applications

This study may help gastroenterologist to understand the role of psychological factors in GERD. The results may help them to focus on other pathogenic factors for GERD, and try new therapy.

Peer-review

In this study, anxiety and depression scores of patients with NERD and RE were higher than those of healthy controls. The QoL of NERD and RE patients was significantly decreased, especially for NERD ones. The QoL was negatively correlated with anxiety and depression significantly.

REFERENCES

1 **Sonnenberg A**, El-Serag HB. Clinical epidemiology and natural history of gastroesophageal reflux disease. *Yale J Biol Med* 1999; **72**: 81-92 [PMID: 10780569]

2 **Locke GR**, Talley NJ, Fett SL, Zinsmeister AR, Melton LJ. Prevalence and clinical spectrum of gastroesophageal reflux: a population-based study in Olmsted County, Minnesota. *Gastroenterology* 1997; **112**: 1448-1456 [PMID: 9136821]

3 **Kongara K**, Varilek G, Soffer EE. Salivary growth factors and cytokines are not deficient in patients with gastroesophageal reflux disease or Barrett's esophagus. *Dig Dis Sci* 2001; **46**: 606-609 [PMID: 11318540]

4 **Dean BB**, Gano AD, Knight K, Ofman JJ, Fass R. Effectiveness of proton pump inhibitors in nonerosive reflux disease. *Clin Gastroenterol Hepatol* 2004; **2**: 656-664 [PMID: 15290657]

5 **Galmiche JP**. Non-erosive reflux disease and atypical gastro-oesophageal reflux disease manifestations: treatment results. *Drugs* 2006; **66** Suppl 1: 7-13; discussion 29-33 [PMID: 16869343]

6 **Hershcovici T**, Fass R. Management of gastroesophageal reflux disease that does not respond well to proton pump inhibitors. *Curr Opin Gastroenterol* 2010; **26**: 367-378 [PMID: 20571388 DOI: 10.1097/MOG.0b013e32833ae2be]

7 **Hershcovici T**, Fass R. An algorithm for diagnosis and treatment of refractory GERD. *Best Pract Res Clin Gastroenterol* 2010; **24**: 923-936 [PMID: 21126704 DOI: 10.1016/j.bpg.2010.10.004]

8 **Fass R**. Proton pump inhibitor failure--what are the therapeutic options? *Am J Gastroenterol* 2009; **104** Suppl 2: S33-S38 [PMID: 19262545 DOI: 10.1038/ajg.2009.50]

9 **Zung WW**. A rating instrument for anxiety disorders. *Psychosomatics* 1971; **12**: 371-379 [PMID: 5172928]

10 **Zung WW**. A self-rating depression scale. *Arch Gen Psychiatry* 1965; **12**: 63-70 [PMID: 14221692]

11 **Ware JE**, Sherbourne CD. The MOS 36-item short-form health survey (SF-36). I. Conceptual framework and item selection. *Med Care* 1992; **30**: 473-483 [PMID: 1593914]

12 **Hartono JL**, Mahadeva S, Goh KL. Anxiety and depression in various functional gastrointestinal disorders: do differences exist? *J Dig Dis* 2012; **13**: 252-257 [PMID: 22500787 DOI: 10.1111/j.1751-2980.2012.00581.x]

13 **Li YM**, Du J, Zhang H, Yu CH. Epidemiological investigation in outpatients with symptomatic gastroesophageal reflux from the Department of Medicine in Zhejiang Province, east China. *J Gastroenterol Hepatol* 2008; **23**: 283-289 [PMID: 17645475]

14 **Chen T**, Lu M, Wang X, Yang Y, Zhang J, Jin L, Ye W. Prevalence and risk factors of gastroesophageal reflux symptoms in a Chinese retiree cohort. *BMC Gastroenterol* 2012; **12**: 161 [PMID: 23153099 DOI: 10.1186/1471-230X-12-161]

15 **Lee SW**, Chang CM, Chang CS, Kao AW, Chou MC. Comparison of presentation and impact on quality of life of gastroesophageal reflux disease between young and old adults in a Chinese population. *World J Gastroenterol* 2011; **17**: 4614-4618 [PMID: 22147968 DOI: 10.3748/wjg.v17.i41.4614]

16 **He J**, Ma X, Zhao Y, Wang R, Yan X, Yan H, Yin P, Kang X, Fang J, Hao Y, Li Q, Dent J, Sung JJ, Zou D, Wallander MA, Johansson S, Liu W, Li Z. A population-based survey of the epidemiology of symptom-defined gastroesophageal reflux disease: the Systematic Investigation of Gastrointestinal Diseases in China. *BMC Gastroenterol* 2010; **10**: 94 [PMID: 20707933 DOI: 10.1186/1471-230X-10-94]

17 **Lee YC**, Wang HP, Chiu HM, Liao SC, Huang SP, Lai YP, Wu MS, Chen MF, Lin JT. Comparative analysis between psychological and endoscopic profiles in patients with gastroesophageal reflux disease: a prospective study based on screening endoscopy. *J Gastroenterol Hepatol* 2006; **21**: 798-804 [PMID: 16704526]

18 **Haug TT**, Mykletun A, Dahl AA. Are anxiety and depression related to gastrointestinal symptoms in the general population? *Scand J Gastroenterol* 2002; **37**: 294-298 [PMID: 11916191]

19 **Jansson C**, Wallander MA, Johansson S, Johnsen R, Hveem K. Stressful psychosocial factors and symptoms of gastroesophageal reflux disease: a population-based study in Norway. *Scand J Gastroenterol* 2010; **45**: 21-29 [PMID: 19961344 DOI: 10.3109/00365520903401967]

20 **Kim JY**, Kim N, Seo PJ, Lee JW, Kim MS, Kim SE, Jo SY, Lee DH, Jung HC. Association of sleep dysfunction and emotional status with gastroesophageal reflux disease in Korea. *J Neurogastroenterol Motil* 2013; **19**: 344-354 [PMID: 23875102 DOI: 10.5056/jnm.2013.19.3.344]

21 **Niu XP**, Yu BP, Wang YD, Han Z, Liu SF, He CY, Zhang GZ, Wu WC. Risk factors for proton pump inhibitor refractoriness in Chinese patients with non-erosive reflux disease. *World J Gastroenterol* 2013; **19**: 3124-3129 [PMID: 23716993 DOI: 10.3748/wjg.v19.i20.3124]

22 **Jiang C**, Shen YH, Qin XY, Li Y, Cai W, Li YL, Wu X, Hu YH. [A community-based epidemiologic study on gastroesophageal reflux disease in Haidian district of Beijing]. *Zhonghua Yufang Yixue Zazhi* 2010; **44**: 516-521 [PMID: 21055126]

23 **Jansson C**, Nordenstedt H, Wallander MA, Johansson S, Johnsen R, Hveem K, Lagergren J. Severe gastro-oesophageal reflux symptoms in relation to anxiety, depression and coping in a population-based study. *Aliment Pharmacol Ther* 2007; **26**: 683-691 [PMID: 17697202]

24 **Oh JH**, Kim TS, Choi MG, Lee H, Jeon EJ, Choi SW, Lee C, Chung IS. Relationship between Psychological Factors and Quality of Life in Subtypes of Gastroesophageal Reflux Disease. *Gut Liver* 2009; **3**: 259-265 [PMID: 20431758]

25 **Tack J**, Caenepeel P, Arts J, Lee KJ, Sifrim D, Janssens J. Prevalence of acid reflux in functional dyspepsia and its association with symptom profile. *Gut* 2005; **54**: 1370-1376 [PMID: 15972301]

26 **Wang K**, Duan LP, Chen H, Xia ZW, Lin SR. [Comparison of esophageal acid exposure characteristics between reflux oesophagitis and non-erosive reflux diseases]. *Zhonghua Neike Zazhi* 2005; **44**: 5-8 [PMID: 15769387]

27 **Fujiwara Y**, Higuchi K, Shiba M, Yamamori K, Watanabe Y, Sasaki E, Tominaga K, Watanabe T, Oshitani N, Arakawa T. Differences in clinical characteristics between patients with endoscopy-negative reflux disease and erosive esophagitis in Japan. *Am J Gastroenterol* 2005; **100**: 754-758 [PMID: 15784015 DOI: 10.1111/j.1572-0241.2005.40966.x]

28 **Wu JC**. Gastroesophageal reflux disease: an Asian perspective.

J Gastroenterol Hepatol 2008; **23**: 1785-1793 [PMID: 19120871 DOI: 10.1111/j.1440-1746.2008.05684.x]

29 **Fass R**. Erosive esophagitis and nonerosive reflux disease (NERD): comparison of epidemiologic, physiologic, and therapeutic characteristics. *J Clin Gastroenterol* 2007; **41**: 131-137 [PMID: 17245209 DOI: 10.1097/01.mcg.0000225631.07039.6d]

30 **Lee ES**, Kim N, Lee SH, Park YS, Kim JW, Jeong SH, Lee DH, Jung HC, Song IS. Comparison of risk factors and clinical responses to proton pump inhibitors in patients with erosive oesophagitis and non-erosive reflux disease. *Aliment Pharmacol Ther* 2009; **30**: 154-164 [PMID: 19392871]

31 **Hiyama T**, Yoshihara M, Tanaka S, Haruma K, Chayama K. Strategy for treatment of nonerosive reflux disease in Asia. *World J Gastroenterol* 2008; **14**: 3123-3128 [PMID: 18506915]

32 **Lee SP**, Lee KN, Lee OY, Lee HL, Choi HS, Yoon BC, Jun DW, Sohn W, Cho SC. The relationship between existence of typical symptoms and psychological factors in patients with erosive esophagitis. *J Neurogastroenterol Motil* 2012; **18**: 284-290 [PMID: 22837876]

33 **Masoumi SJ**, Khademolhosseini F, Mehrabani D, Moradi F, Mostaghni AA, Zare N, Montazeri A, Saberi-Firoozi M. Correlation of quality of life with gastroesophageal reflux disease amongst Qashqai nomads in Iran. *Arch Iran Med* 2012; **15**: 747-750 [PMID: 23199245]

34 **Kovács Z**, Seres G, Kerékgyártó O, Czobor P. Psychopathological symptom dimensions in patients with gastrointestinal disorders. *J Clin Psychol Med Settings* 2010; **17**: 378-386 [PMID: 21116695 DOI: 10.1007/s10880-010-9212-5]

35 **Lee H**, Kim JH, Min BH, Lee JH, Son HJ, Kim JJ, Rhee JC, Suh YJ, Kim S, Rhee PL. Efficacy of venlafaxine for symptomatic relief in young adult patients with functional chest pain: a randomized, double-blind, placebo-controlled, crossover trial. *Am J Gastroenterol* 2010; **105**: 1504-1512 [PMID: 20332772 DOI: 10.1038/ajg.2010.82]

36 **Boltin D**, Boaz M, Aizic S, Sperber A, Fass R, Niv Y, Dickman R. Psychological distress is not associated with treatment failure in patients with gastroesophageal reflux disease. *J Psychosom Res* 2013; **75**: 462-466 [PMID: 24182636]

P- Reviewer: Nishida T **S- Editor**: Yu J
L- Editor: Wang TQ **E- Editor**: Liu XM

World Journal of Gastroenterology

Submit a Manuscript: http://www.wjgnet.com/esps/
Help Desk: http://www.wjgnet.com/esps/helpdesk.aspx
DOI: 10.3748/wjg.v21.i14.4310

World J Gastroenterol 2015 April 14; 21(14): 4310-4322
ISSN 1007-9327 (print) ISSN 2219-2840 (online)

ORIGINAL ARTICLE

Prospective Study

Polymorphisms of glutathione S-transferase genes and survival of resected hepatocellular carcinoma patients

Kai Qu, Su-Shun Liu, Zhi-Xin Wang, Zi-Chao Huang, Si-Nan Liu, Hu-Lin Chang, Xin-Sen Xu, Ting Lin, Ya-Feng Dong, Chang Liu

Kai Qu, Su-Shun Liu, Zhi-Xin Wang, Zi-Chao Huang, Si-Nan Liu, Hu-Lin Chang, Xin-Sen Xu, Ting Lin, Chang Liu, Department of Hepatobiliary Surgery, The First Affiliated Hospital of Medical College, Xi'an Jiaotong University, Xi'an 710061, Shaanxi Province, China

Ya-Feng Dong, Department of Obstetrics and Gynecology, University of Kansas School of Medicine, Kansas City, KS 66160, United States

Author contributions: Qu K and Liu C designed the research and wrote this paper; Liu SS, Wang ZX and Huang ZC performed the statistical analysis; Liu SN, Chang HL and Xu XS were involved in collecting patient data; Qu K and Lin T took part in literature searches; Dong YF edited the manuscript.

Supported by Grants from National Natural Science Foundation of China, No. 81201549 and No. 81272644; and the Project of Innovative Research Team for Key Science and Technology in Xi'an Jiaotong University, No. 2003KCJ-23.

Correspondence to: Chang Liu, MD, PhD, Department of Hepatobiliary Surgery, the First Affiliated Hospital of Medical College, Xi'an Jiaotong University, No. 277 Yanta West Road, Xi'an 710061, Shaanxi Province, China. liuchangdoctor@163.com
Telephone: +86-29-82654746
Fax: +86-29-82654746

Received: July 24, 2014
Peer-review started: July 24, 2014
First decision: August 10, 2014
Revised: August 19, 2014
Accepted: October 21, 2014
Article in press: October 21, 2014
Published online: April 14, 2015

Abstract

AIM: To investigate the effects of single nucleotide polymorphisms (SNPs) in glutathione S-transferase (GST) genes on survival of hepatocellular carcinoma (HCC) patients.

METHODS: Twelve tagging SNPs in *GST* genes (including *GSTA1*, *GSTA4*, *GSTM2*, *GSTM3*, *GSTO1*, *GSTO2* and *GSTP1*) were genotyped using Sequenom MassARRAY iPLEX genotyping method in a cohort of 214 Chinese patients with resected HCC. The Cox proportional hazards model and log-rank test were performed to determine the SNPs related to outcome. Additionally, stratified analysis was performed at each level of the demographic and clinical variables. An SNP-gene expression association model was further established to investigate the correlation between SNP and gene expression.

RESULTS: Two SNPs (*GSTO2*: rs7085725 and *GSTP1*: rs4147581) were significantly associated with overall survival in HCC patients (P = 0.035 and 0.042, respectively). In stratified analysis, they were more significantly associated with overall survival in patients with younger age, male gender and cirrhosis. We further investigated cumulative effects of these two SNPs on overall survival in HCC patients. Compared with the patients carrying no unfavorable genotypes, those carrying 2 unfavorable genotypes had a 1.70-fold increased risk of death (P < 0.001). The cumulative effects were more significant in those patients with younger age, male gender and cirrhosis (HR = 2.00, 1.94 and 1.97, respectively; all P < 0.001). Additionally, we found that heavy smoking resulted in a significantly worse overall survival in those patients carrying variant

alleles of rs7085725 (HR = 2.07, 95%CI: 1.13-3.76, *P* = 0.018). The distributions of *GSTO2*: rs7085725 and *GSTP1*: rs4147581 genotypes were associated with altered gene expression and contributed to influences on overall survival.

CONCLUSION: Our study provides the first evidence that *GSTO2* and *GSTP1* gene polymorphisms may serve as independent prognostic markers for HCC patients.

Key words: Glutathione S-transferase; Polymorphism; Hepatocellular carcinoma; Clinical outcome; Surgery

Core tip: To determine the prognostic value of single nucleotide polymorphisms (SNPs) in *GST* genes in hepatocellular carcinoma (HCC) after liver resection, we analyzed the association between 12 tagging SNPs in *GST* genes and outcome of 214 HCC patients who underwent liver resection. Our data showed two SNPs (*GSTO2*: rs7085725 and *GSTP1*: rs4147581) to be significantly associated with overall survival in HCC patients. These two SNPs used in combination were more powerful prognostic markers for HCC patients. Our study provides the first evidence that *GSTO2* and *GSTP1* gene polymorphisms may serve as independent prognostic markers for HCC patients.

Qu K, Liu SS, Wang ZX, Huang ZC, Liu SN, Chang HL, Xu XS, Lin T, Dong YF, Liu C. Polymorphisms of glutathione S-transferase genes and survival of resected hepatocellular carcinoma patients. *World J Gastroenterol* 2015; 21(14): 4310-4322 Available from: URL: http://www.wjgnet.com/1007-9327/full/v21/i14/4310.htm DOI: http://dx.doi.org/10.3748/wjg.v21.i14.4310

INTRODUCTION

Glutathione S-transferases (GSTs) are a broadly expressed family of phase Ⅱ isoenzymes that protect normal cells against damage induced by hepatitis virus or aflatoxin-related hepatocarcinogen[1]. Recently, emerging evidence indicates that the detoxifying properties of the GSTs are genetically determined[2]. In human, several classes of *GST* genes exist: α (*GSTA*), μ (*GSTM*), π (*GSTP*), θ (*GSTT*), and ω (*GSTO*) with one or more genes in each class[3,4]. Altered expression of these *GST* genes has been suggested to increase the risk of cancer[4-6]. Polymorphisms in these genes have been shown to produce significant alterations in the metabolism of many substrates, including carcinogens and chemotherapeutic agents[7]. As a result, these polymorphisms also have been suggested to be associated with the risk of many malignances[2,8-16]. Some of them have also been suggested to affect the survival status of cancer patients[8-10,14].

Hepatocellular carcinoma (HCC) is the fifth most common cancer worldwide and the third most common cause of cancer mortality, resulting in about 500000 deaths per year. Half of HCC cases and deaths were estimated to occur in China[17]. Most of these cases in China arise due to the chronic infection with hepatitis virus, the common carcinogen to HCC[18]. Not only hepatitis virus infection, but also other environmental carcinogens, such as aflatoxin or chemical carcinogens, would contribute to hepatic carcinogenesis[19]. The metabolizing enzymes for detoxification or activation of these carcinogens to lower toxicity, potentially affect the individual cancer risk and progression of HCC. Evidence has shown that some SNPs of *GSTs* were associated with HCC risk[12]. However, none of these polymorphisms are investigated in relation to HCC survival.

In this study, we assessed the effects of 12 tagging SNPs in seven *GST* genes *GSTA1*, *GSTA4*, *GSTM2*, *GSTM3*, *GSTO1*, *GSTO2* and *GSTP1* on 5-year survival in a cohort of 214 Chinese HCC patients receiving surgical treatment. To the best of our knowledge, this is the first study to investigate the predictive value of SNPs in these *GST* genes for HCC prognosis in Chinese population.

MATERIALS AND METHODS

Study population

A total of 214 Han Chinese HCC patients were recruited at the Department of Hepatobiliary Surgery, the First Affiliated Hospital of Xi'an Jiaotong University in Xi'an, China. These patients were recruited between January 2009 and October 2013. HCC diagnosis was based on the National Comprehensive Cancer Network (NCCN) clinical practice guidelines in oncology. All subjects included in this study had histopathologically confirmed HCC. All cases received surgical treatment and had no previous history of other cancers or cancer-related treatments. There were no recruitment restrictions on age at diagnosis, gender and tumor stage. Participants received other treatments (such as chemotherapy, interventional therapy or biological target therapy) after surgical operation were excluded for further analysis. Ethics committee of the First Affiliated Hospital of Xi'an Jiaotong University approved this study. Written informed consent was obtained from each participant before enrollment.

Another 86 HCC patients derived from Queen Mary Hospital, the University of Hong Kong, were recruited as a validated cohort (Hong Kong Cohort). All genetic and SNP data were obtained from two microarray series (GSE28127 and GSE22058) in the National Center for Biotechnology Information (NCBI) Gene Expression Omnibus (GEO) database (http://www.

Table 1 Demographic and clinical characteristics of hepatocellular carcinoma patients

Variable	Our cohort		Hong Kong cohort	
	n	%	*n*	%
Total	214	100	401	100
Age (yr)				
≤ 55	108	50.5	NA	NA
> 55	106	49.5	NA	NA
Gender				
Male	176	82.2	322	80.3
Female	38	17.8	79	19.7
Smoking behavior				
Yes	70	32.7	223	55.6
No	144	67.3	178	44.4
Cirrhosis				
Present	126	58.9	229	57.1
Absent	88	41.1	172	42.9
Child-Pugh score				
A	172	80.4	390	97.3
B	42	19.6	11	2.7
AFP level (ng/mL)				
< 200	100	46.7	NA	NA
≥ 200	114	53.3	NA	NA
Tumor size				
< 5 cm	102	47.7	NA	NA
≥ 5 cm	112	52.3	NA	NA
TNM stage				
Ⅰ + Ⅱ	119	55.6	177	44.1
Ⅲ	95	44.4	224	55.9
Outcome				
Dead	111	51.9	272	67.8
Alive	103	48.1	129	32.2

ncbi.nlm.nih.gov/geo/).

Demographic and clinical data

Detailed demographic and clinical information was collected through in-person interview, medical chart review, or consultation with treating physicians. The demographic data included the date of diagnosis, smoking behavior, liver cirrhosis, Child-Pugh score, serum alpha-fetoprotein (AFP), and tumor-node-metastasis (TNM) stage. To calculate pack-years of smoking, the average of number of cigarettes smoked per day was divided by 20 to give packs per day and multiplied by the total number of years of smoking. At 3-mo intervals, follow-up information on death of patients was updated by a trained clinical specialist through on-site interview, direct calling or medical chart review. The latest follow-up data in this analysis were obtained in January 2014. Demographic and clinical characteristics of HCC patients are shown in Table 1.

Tagging SNP selection and genotyping

Tagging SNP selection was based on data from the NIEHS (National Institute of Environmental Health Sciences, http://snpinfo.niehs.nih.gov/snpinfo/snptag.htm). Together with SNPs within a gene, we also considered polymorphisms in the 5'- and 3'-flanking regions up to 5 kb. We chose common SNPs with a minor allele frequency (MAF) ≥ 0.05 in a population of Chinese Han in Beijing (CHB) and an SNP design score cutoff ≥ 0.6 (indicating a higher probability for a successful assay). To select tagging SNPs, we used a pairwise tagging approach with r^2 ≥ 0.8. Finally, a total of 12 potentially tagging SNPs in 7 genes were selected, including *GSTA1*: rs6917150; *GSTA4*: rs385636; *GSTM2*: rs638820; *GSTM3*: rs1109138, rs7483; *GSTO1*: rs2282326, rs17116779; *GSTO2*: rs156699, rs7085725, rs157077; *GSTP1*: rs4147581, rs2370141. Information of selected tagging SNPs is shown in Table 2 and Figure 1.

Table 2 Summarized information of selected tagging SNPs in *GST* genes

Gene	Tagging SNPs	bp position	Ref SNP alleles	MAF_CHB
GSTA1	rs6917150	Chr 6: 52760414	T/C	0.338
GSTA4	rs385636	Chr 6: 52948896	A/G	0.174
GSTM2	rs638820	Chr 1: 110011429	T/C	0.344
GSTM3	rs1109138	Chr 1: 110079472	G/A	0.167
	rs7483	Chr 1: 110081224	A/G	0.244
GSTO1	rs2282326	Chr 10: 106010388	A/C	0.244
	rs17116779	Chr 10: 106021185	G/A	0.078
GSTO2	rs156699	Chr 10: 106043631	T/C	0.222
	rs7085725	Chr 10: 106050199	T/C	0.122
	rs157077	Chr 10: 106027884	A/G	0.378
GSTP1	rs4147581	Chr 11: 67108161	G/C	0.273
	rs2370141	Chr 11: 67105105	A/G	0.181

MAF (minor allele frequency) was derived from CHB (Chinese Han people in Beijing) population in HapMap website (http://hapmap.ncbi.nlm.nih.gov/).

Genomic DNA extraction and genotyping

Genomic DNA was extracted from peripheral blood samples using E.Z.N.A. Blood DNA Midi Kit (Omega Bio-Tek, Norcross, GA, United States) according to the manufacture's instructions. Genotyping was performed using Sequenom MassARRAY iPLEX genotyping system (Sequenom Inc, San Diego, CA, United States). Laboratory personnel conducting genotyping were blinded to patients' information.

Statistical analysis

All statistical analyses were performed using the SPSS 21.0 statistical package for Microsoft Windows (SPSS, Chicago, IL, United States). The survival time was defined as the period from the date of first treatment to the date of death or last follow-up. Hazard ratios (HRs) and 95%CIs were estimated from a Cox proportional hazards model. Kaplan-Meier curve and log-rank test were also used to assess the differences of overall survival. All statistical tests were two-sided and $P < 0.05$ was considered statistically significant.

RESULTS

Characteristics of the study population

For the 214 patients included, the median age at the

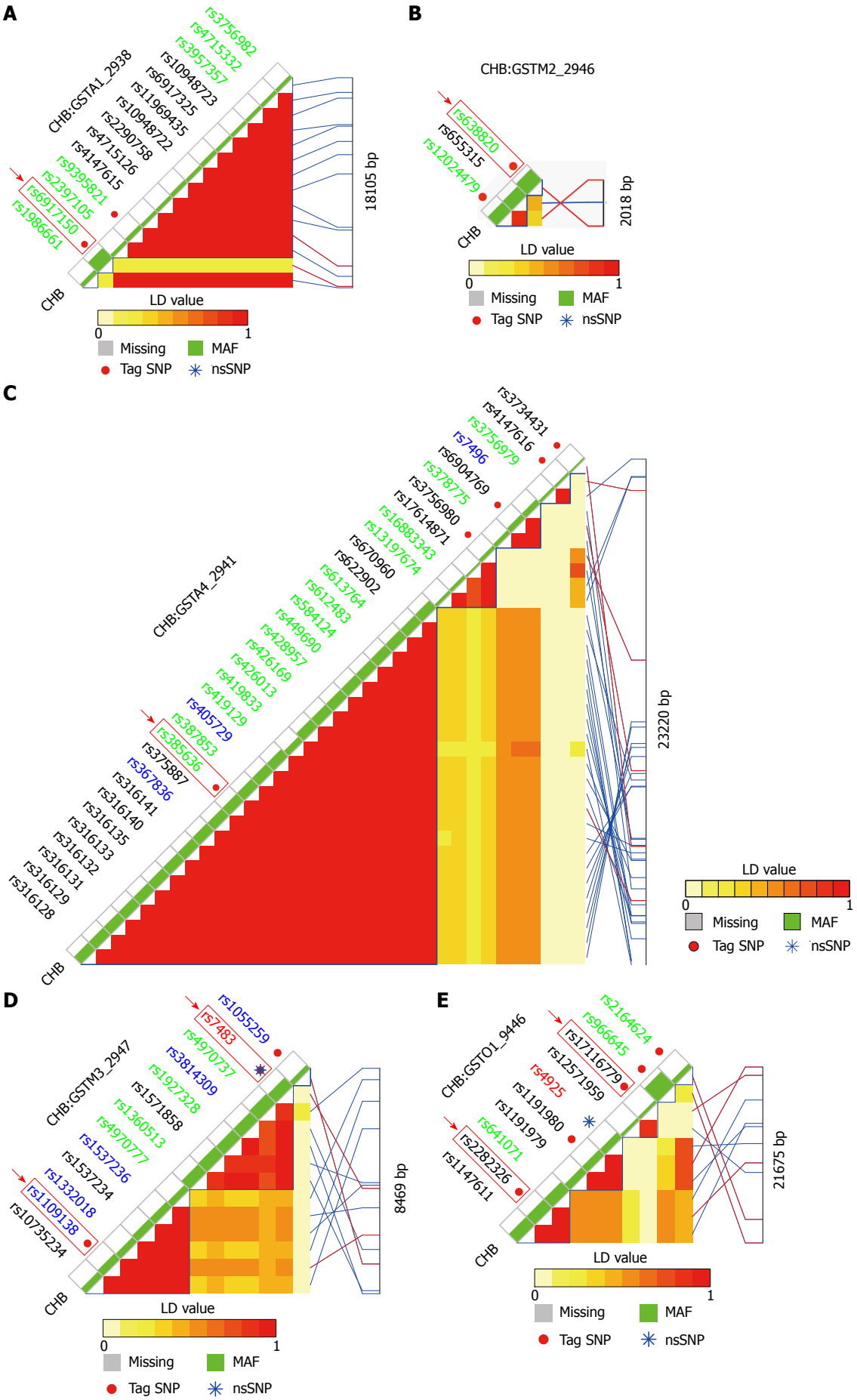
A
CHB:GSTA1_2938
rs3756982
rs4715332
rs3957357
rs10948723
rs6917325
rs11969435
rs10948722
rs2290758
rs4715126
rs4147615
rs9395821
rs2397105
rs6917150
rs1986661
18105 bp
CHB
LD value
0
1
Missing
MAF
Tag SNP
nsSNP
B
CHB:GSTM2_2946
rs638820
rs655315
rs12024479
2018 bp
CHB
LD value
0
1
Missing
MAF
Tag SNP
nsSNP
C
CHB:GSTA4_2941
rs3734431
rs4147616
rs3756979
rs7496
rs6904769
rs378775
rs3756980
rs17614871
rs16883343
rs13197674
rs670960
rs622902
rs613764
rs612483
rs584124
rs449690
rs428957
rs426169
rs426013
rs419833
rs419129
rs405729
rs387853
rs385636
rs375887
rs367836
rs316141
rs316140
rs316135
rs316133
rs316132
rs316131
rs316129
rs316128
23220 bp
CHB
LD value
0
1
Missing
MAF
Tag SNP
nsSNP
D
CHB:GSTM3_2947
rs1055259
rs7483
rs4970737
rs3814309
rs1927328
rs1571858
rs1360513
rs4970777
rs1537236
rs1537234
rs1332018
rs1109138
rs1073534
8469 bp
CHB
LD value
0
1
Missing
MAF
Tag SNP
nsSNP
E
CHB:GSTO1_9446
rs2164624
rs966645
rs17116779
rs12571959
rs4925
rs1191980
rs1191979
rs641071
rs2282326
rs1147611
21675 bp
CHB
LD value
0
1
Missing
MAF
Tag SNP
nsSNP

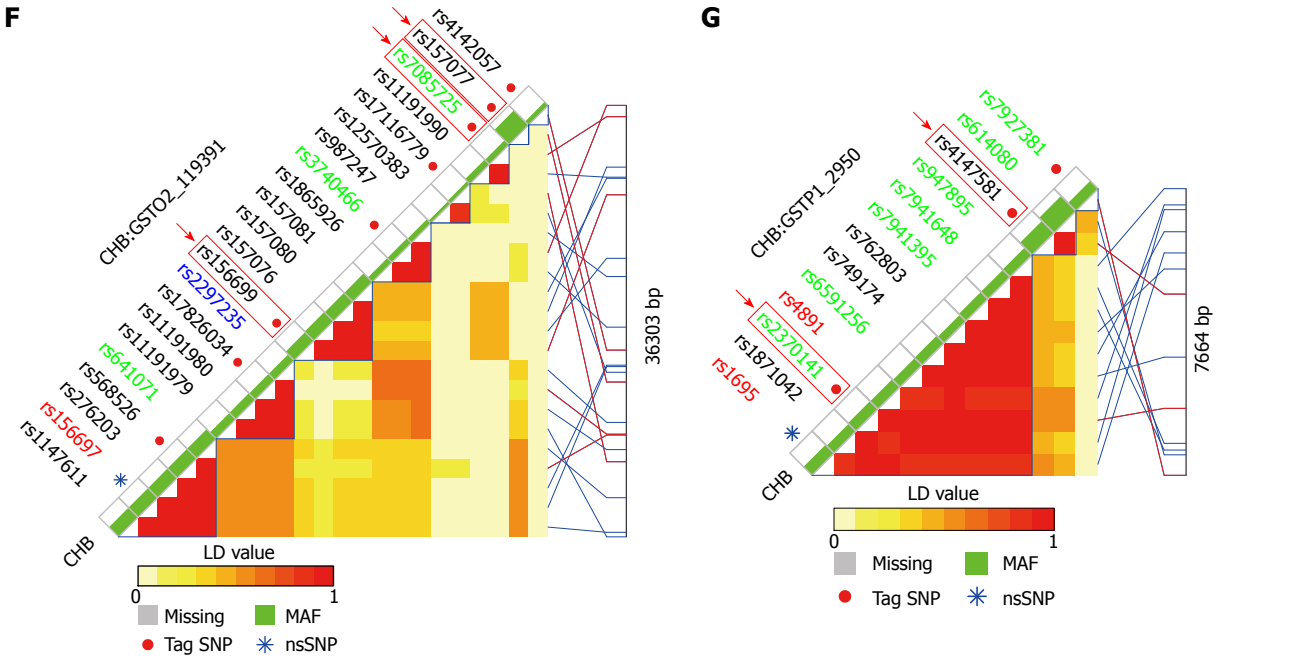

Figure 1 Relevant pictures of polymorphisms in seven *GST* genes. A: *GSTA1* (Gene ID: 2946); B: *GSTM2* (Gene ID: 2946); C: *GSTA4* (Gene ID: 2941); D: *GSTM3* (Gene ID: 2947); E: *GSTO1* (Gene ID: 9446); F: *GSTO2* (Gene ID: 119391); G: *GSTP1* (Gene ID: 2950). Genotype data were obtained from HapMap database (http://hapmap.ncbi.nlm.nih.gov) and SNPs were sorted by LD similarity using NIEHS tools (http://snpinfo.niehs.nih.gov). Twelve selected SNPs were labeled by red block.

time of HCC diagnosis was 55 years (range: 20-84 years). The majority of patients (82.2%, 176/214) were men and 32.7% (70/214) of all patients had smoking behavior. About 58.9% (126/214) of patients had cirrhosis and 80.4% (172/214) had Child-Pugh score A. There were 52.3% (112) of patients with tumor size ⩾ of 5 cm and 53.3% (114) with significantly increased serum AFP (200 ng/mL). The percentages of patients with TNM stage Ⅰ/Ⅱ or stage Ⅲ disease were 55.6% (119/214) and 44.4% (95/214), respectively. The median follow-up time was 24 mo (ranging from 3 to 60 mo). By the last follow-up, 51.9% (111/214) of patients were dead, and the median survival time for the entire cohort of patients was 33.6 mo.

Association between individual SNPs and overall survival in HCC patients

We assessed the effect of 14 tagging SNPs in seven *GST* genes on death of HCC patients using the Cox regression model. When the dominant genetic model was tested, our data showed that SNPs rs7085725 in *GSTO2* and rs4147581 in *GSTP1* gene were significantly associated with the overall survival of HCC patients (Table 3). Patients carrying at least one variant allele of rs7085725 (WV + VV genotypes) had a significantly increased risk of death (HR = 1.60; 95%CI: 1.03-2.47), meanwhile, those carrying WV + VV genotypes of rs4147581 had a decreased risk of death (HR = 0.68; 95%CI: 0.46-0.99), when compared with those carrying homozygous wild-type alleles (WW genotype) (P = 0.035 and 0.042, respectively). Kaplan-Meier analysis showed a significantly shorter median survival time in patients with WV + VV genotypes of SNP rs7085725 than those with WW genotype (19.8 mo *vs* 36.6 mo; log rank P = 0.03) (Figure 2A). In contrast, patients with WV + VV genotypes of SNP rs4147581 had a longer median survival time than those with WW genotype (33.9 mo *vs* 26.8 mo; log rank P = 0.04) (Figure 2B).

Significant association of rs7085725 and rs4147581 with overall survival in HCC patients

We further analyzed the effect of SNPs rs7085725 and rs4147581 on the overall survival in HCC patients stratified by demographic and clinicopathological characteristics. As shown in Table 4, the significantly increased death risk conferred by SNP rs7085725 was observed in younger patients [HR (95%CI) = 1.86 (1.02-3.38); P = 0.044], male patients [HR (95%CI) = 1.83 (1.14-2.94); P = 0.013], smoking patients [HR (95%CI) = 2.59 (1.27-5.27); P = 0.09], and those with cirrhosis [HR (95%CI) = 2.00 (1.11-3.59); P = 0.020], Child-Pugh score A [HR (95%CI:) = 2.28 (1.32-3.93); P = 0.003] and AFP ⩾ 200 ng/mL [HR (95%CI) = 2.40 (1.34-4.29); P = 0.003]. Meanwhile, the significantly decreased death risk conferred by SNP rs4147581 was observed in younger patients [HR (95%CI) = 0.52 (0.30-0.92), P = 0.024], male patients [HR (95%CI) = 0.64 (0.42-0.99), P = 0.042], non-smoking patients [HR (95%CI) = 0.58 (0.36-0.93); P = 0.024], and those with cirrhosis [HR (95%CI) = 0.50 (0.29-0.85); P = 0.011], Child-Pugh score B [HR (95%CI) = 0.45 (0.22-0.90); P = 0.024],

Table 3 Associations between polymorphisms of tagging SNPs in *GST* genes and overall survival in hepatocellular carcinoma patients

Gene	Tagging SNP	Genotype	Outcome, *n* (%)		HR (95%CI)	*P* value
			Dead	Alive		
GSTA1	rs6917150	WW	48 (51.6)	45 (48.4)	1 (ref)	
		WV + VV	63 (52.1)	58 (47.9)	1.01 (0.69-1.48)	0.961
GSTA4	rs385636	WW	82 (55.4)	66 (44.6)	1 (ref)	
		WV + VV	29 (43.9)	37 (56.1)	0.71 (0.46-1.09)	0.117
GSTM2	rs638820	WW	42 (51.9)	39 (48.1)	1 (ref)	
		WV + VV	69 (51.9)	64 (48.1)	1.13 (0.77-1.67)	0.526
GSTM3	rs1109138	WW	85 (54.1)	72 (45.9)	1 (ref)	
		WV + VV	26 (45.6)	31 (54.4)	0.81 (0.52-1.26)	0.353
	rs7483	WW	63 (56.2)	49 (43.8)	1 (ref)	
		WV + VV	48 (47.1)	54 (52.9)	0.94 (0.64-1.38)	0.760
GSTO1	rs2282326	WW	60 (56.1)	47 (43.9)	1 (ref)	
		WV + VV	51 (47.7)	56 (52.3)	0.92 (0.63-1.35)	0.675
	rs17116779	WW	99 (51.0)	95 (49.0)	1 (ref)	
		WV + VV	12 (60.0)	8 (40.0)	0.95 (0.52-1.75)	0.869
GSTO2	rs156699	WW	64 (50.0)	64 (50.0)	1 (ref)	
		WV + VV	47 (54.7)	39 (45.3)	1.10 (0.75-1.62)	0.612
	rs7085725	WW	81 (46.0)	95 (54.0)	1 (ref)	
		WV + VV	30 (78.9)	8 (21.1)	1.60 (1.03-2.47)[a]	0.035[a]
	rs157077	WW	50 (58.1)	36 (41.9)	1 (ref)	
		WV + VV	61 (47.7)	67 (52.3)	0.78 (0.54-1.14)	0.198
GSTP1	rs4147581	WW	57 (55.3)	46 (44.7)	1 (ref)	
		WV + VV	54 (48.6)	57 (51.4)	0.68 (0.46-0.99)[a]	0.042[a]
	rs2370141	WW	74 (52.1)	68 (47.9)	1 (ref)	
		WV + VV	37 (51.4)	35 (48.6)	0.90 (0.61-1.34)	0.597

[a]$P < 0.05$ was considered statistically significant. WW: Homozygous wild-type genotype; WV: Heterozygous genotype; VV: Homozygous variant genotype; SNP: Single nucleotide polymorphisms.

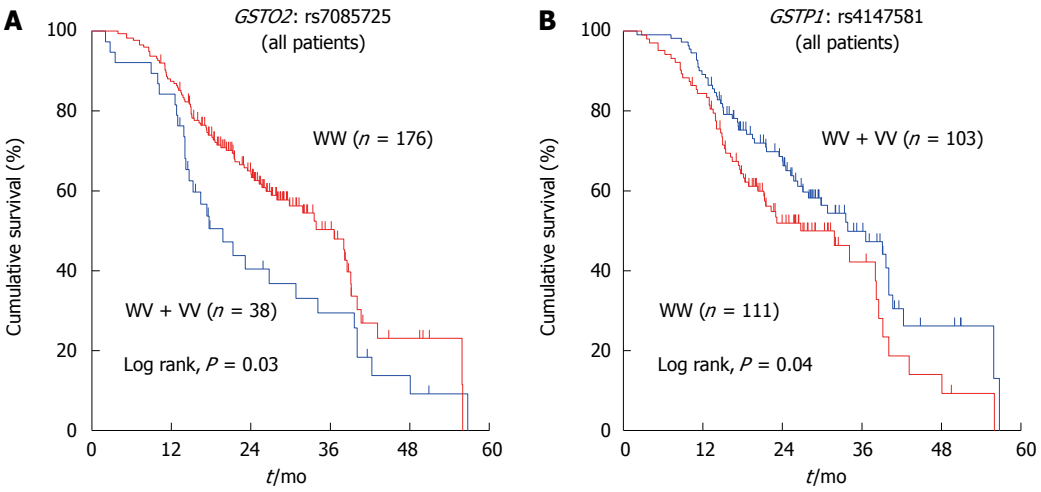

Figure 2 Kaplan-Meier curves for hepatocellular carcinoma patients carrying genetic variants of *GSTO2*: rs7085725 (A) and *GSTP1*: rs4147581 (B). WW: Homozygous wild-type genotype; WV: Heterozygous genotype; VV: Homozygous variant genotype.

AFP < 200 ng/mL [HR (95%CI) = 0.51 (0.29-0.89); $P = 0.018$] and tumor size ⩾ 5 cm [HR (95%CI) = 0.60 (0.37-1.00); $P = 0.048$]. Interestingly, both of the two SNPs were significantly associated with overall survival in patients with younger age, male gender and cirrhosis. Log-rank test further indicated significant differences in overall survival between WV + VV and WW genotypes of SNPs rs7085725 or rs4147581 in those patients with above-mentioned factors (Figure 3).

Cumulative effect of unfavorable genotypes on overall survival

To further assess the cumulative effects of genetic variants of SNPs rs7085725 and rs4147581 on overall survival in HCC, we did a joint analysis by including the two SNPs (Table 5). The unfavorable genotypes were defined as WV or VV for rs7085725 and WW for rs4147581. When using group 1 (with 0 unfavorable genotype) as reference, HCC patients in group 3

Table 4 Stratified analysis on the association between *GSTO2*: rs7085725 and *GSTP1*: rs4147581 genotype and overall survival of hepatocellular carcinoma patients

Variable	GSTO2: rs7085725				GSTP1: rs4147581			
	Dead/Alive		HR (95%CI)	*P* value	Dead/Alive		HR (95%CI)	*P* value
	WW	WV + VV			WW	WV + VV		
Age (yr)								
≤ 55	32/52	19/5	1.86[a] (1.02-3.38)	0.044[a]	28/25	23/32	0.52[a] (0.30-0.92)	0.024[a]
> 55	49/43	11/3	1.71 (0.89-3.31)	0.110	29/21	31/25	0.92 (0.55-1.54)	0.755
Gender								
Male	62/83	26/5	1.83[a] (1.14-2.94)	0.013[a]	44/38	44/50	0.64[a] (0.42-0.99)	0.042[a]
Female	19/12	4/3	0.76 (0.22-2.64)	0.663	13/8	10/7	1.06 (0.45-2.50)	0.902
Smoking behavior								
No	52/67	19/6	1.35 (0.78-2.37)	0.287	35/26	36/47	0.58[a] (0.36-0.93)	0.024[a]
Yes	29/28	11/2	2.59[a] (1.27-5.27)	0.009[a]	22/20	18/10	1.06 (0.56-1.99)	0.870
Cirrhosis								
Absent	41/30	12/5	1.21 (0.62-2.35)	0.579	23/17	30/18	0.91 (0.52-1.59)	0.746
Present	40/65	18/3	2.00[a] (1.11-3.59)	0.020[a]	34/29	24/39	0.50[a] (0.29-0.85)	0.011[a]
Child-Pugh score								
A	61/87	17/7	2.28[a] (1.32-3.93)	0.003[a]	39/44	39/50	0.83 (0.53-1.30)	0.422
B	20/8	13/1	0.97 (0.47-2.03)	0.940	18/2	15/7	0.45[a] (0.22-0.90)	0.024[a]
AFP level (ng/mL)								
< 200	39/40	14/7	1.09 (0.57-2.11)	0.793	26/17	27/30	0.51[a] (0.29-0.89)	0.018[a]
≥ 200	42/55	16/1	2.40[a] (1.34-4.29)	0.003[a]	31/29	27/27	0.85 (0.51-1.44)	0.552
Tumor size								
< 5 cm	37/50	10/5	1.51 (0.74-3.06)	0.254	23/26	24/29	0.77 (0.43-1.38)	0.379
≥ 5 cm	44/45	20/3	1.59 (0.90-2.80)	0.109	34/20	30/28	0.60[a] (0.37-1.00)	0.048
TNM stage								
Ⅰ + Ⅱ	44/60	11/4	1.24 (0.61-2.53)	0.555	27/26	28/38	0.64 (0.37-1.10)	0.104
Ⅲ	37/35	19/4	1.66 (0.94-2.93)	0.081	30/20	26/19	0.75 (0.43-1.30)	0.311

[a]*P* < 0.05 was considered statistically significant. WW: Homozygous wild-type genotype; WV: Heterozygous genotype; VV: Homozygous variant genotype.

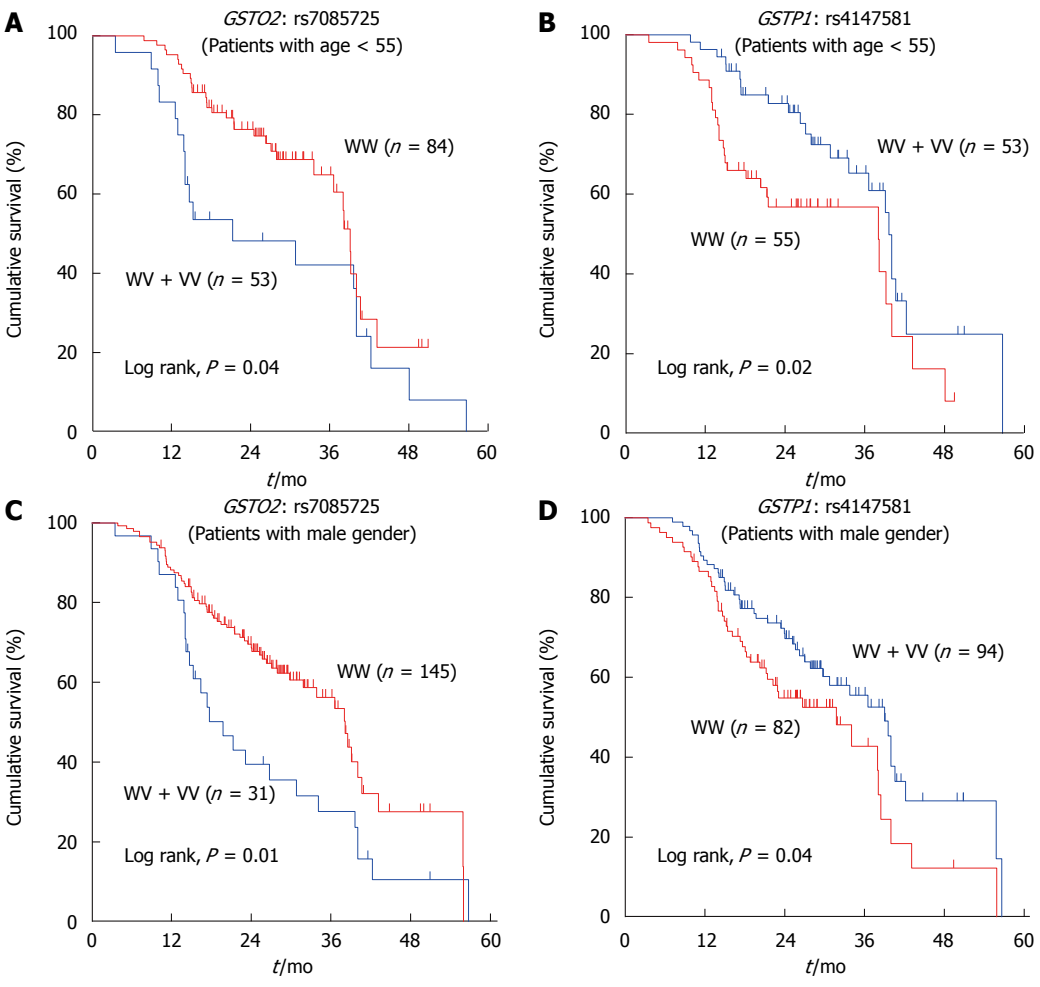

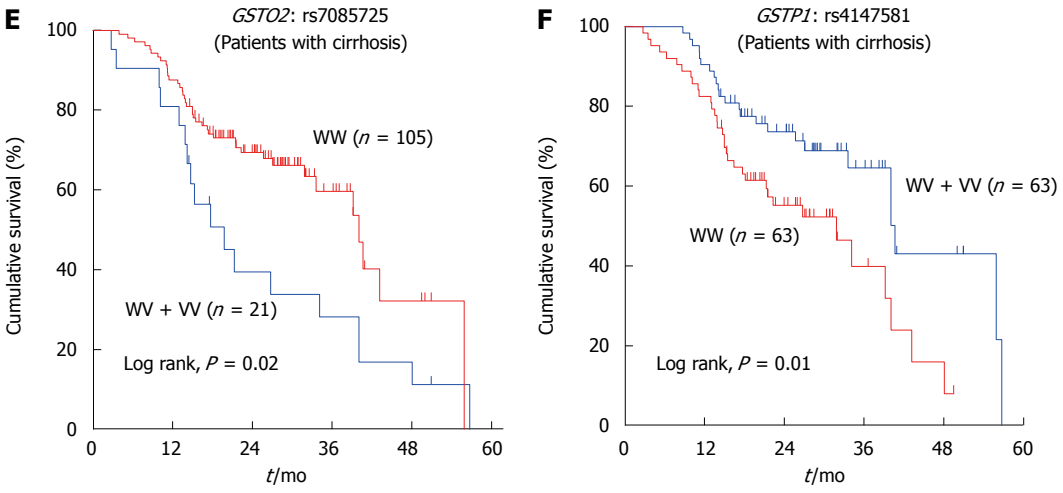

Figure 3 Kaplan-Meier curves for hepatocellular carcinoma patients carrying genetic variants of *GSTO2*: rs7085725 and *GSTP1*: rs4147581 in stratified subgroups. A and B: In patients with age < 55 years; C and D: In patients with male gender; E and F: In patients with cirrhosis. WW: Homozygous wild-type genotype, WV: Heterozygous genotype; VV: Homozygous variant genotype.

Table 5 Cumulative effects of unfavorable genotypes on overall survival of hepatocellular carcinoma patients

Group (number of unfavorable genotypes[1])	Death/Total	HR (95%CI)	*P* value
In all patients			
Group 1 (0)	44/95	1 (ref)	
Group 2 (1)	47/97	1.08 (0.71-1.63)	0.730
Group 3 (2)	20/22	1.70[a] (1.30-2.22)	< 0.001[a]
P for trend			0.004[a]
In patients with age ⩽ 55			
Group 1 (0)	18/47	1 (ref)	
Group 2 (1)	26/45	1.01 (0.52-1.95)	0.975
Group 3 (2)	14/16	2.00[a] (1.40-3.86)	< 0.001[a]
P for trend			0.003[a]
In patients with male gender			
Group 1 (0)	36/82	1 (ref)	
Group 2 (1)	34/75	0.97 (0.60-1.56)	0.898
Group 3 (2)	18/19	1.94[a] (1.45-2.59)	< 0.001[a]
P for trend			0.002[a]
In patients with cirrhosis			
Group 1 (0)	20/56	1 (ref)	
Group 2 (1)	24/56	1.29 (0.71-2.35)	0.410
Group 3 (2)	14/14	1.97[a] (1.39-2.79)	< 0.001[a]
P for trend			0.001[a]

[1]Unfavorable genotypes: *GSTO2*: rs7085725 (WV or VV) and *GSTP1*: rs4147581 (WW). [a]$P < 0.05$ was considered statistically significant. WW: Homozygous wild-type genotype; WV: heterozygous genotype; VV: Homozygous variant genotype.

(with two unfavorable genotypes) had a 1.70-fold increased risk of death (95%CI: 1.30-2.22; $P < 0.001$), when compared with those in the reference group. A significant dose-response trend was observed (P for trend = 0.004). Furthermore, the death risk of carriers of two unfavorable genotypes was significantly increased among HCC patients with younger age, male gender or cirrhosis, when compared with the reference group (HR = 2.00, 1.94 and 1.97, respectively; $P < 0.001$). Kaplan-Meier analysis showed that there was significantly decreased overall survival in patients carrying two unfavorable genotypes, when compared with others, either in all patients or in stratified subgroups (Figure 4).

Modulating effects of smoking on overall survival in HCC patients by rs7085725

Previous report from our center showed that cigarette smoking was associated with an increased risk of death in HCC[20]. As a metabolizing enzyme, *GSTP1* has been extensively investigated in the activation and detoxification of pro-carcinogens in tobacco smoke[11,21]. In line with this evidence, we further assessed the modulating effects on the association between smoking and overall patient survival, stratified by SNPs rs7085725 and rs4147581 (Table 6). We observed that the survival time of those patients carrying variant alleles of rs7085725 were adversely affected by smoking exposure [HR (95%CI) = 1.52 (1.02-2.26); $P = 0.042$]. This significant adverse effect on patient survival conferred by smoking was also observed in smoking quantity-stratified analysis [HR (95%CI) = 2.07 (1.13-3.76); $P = 0.018$]. Kaplan-Meier analysis further suggested that smoking exposure adversely affected overall survival of variant allele carriers of rs7085725, either in smoking behavior- or in smoking quantity-stratified analysis (Figure 5).

Genotype distributions of rs7085725 and rs4147581 in HCC patients with different gene expression

To further investigate the association between SNP and gene expression, we developed an SNP-gene expression model by integrating genotyping and gene expression data from Hong Kong Cohort. We selected two SNPs rs11191994 and rs614080 to predict genotypes of rs7085725 and rs4147581, respectively. Both of the two SNPs were completely linked with rs7085725 or rs4147581 [linkage disequilibrium (LD): $r^2 = 1.000$, D' = 1.000]. As shown in Figure 6, there

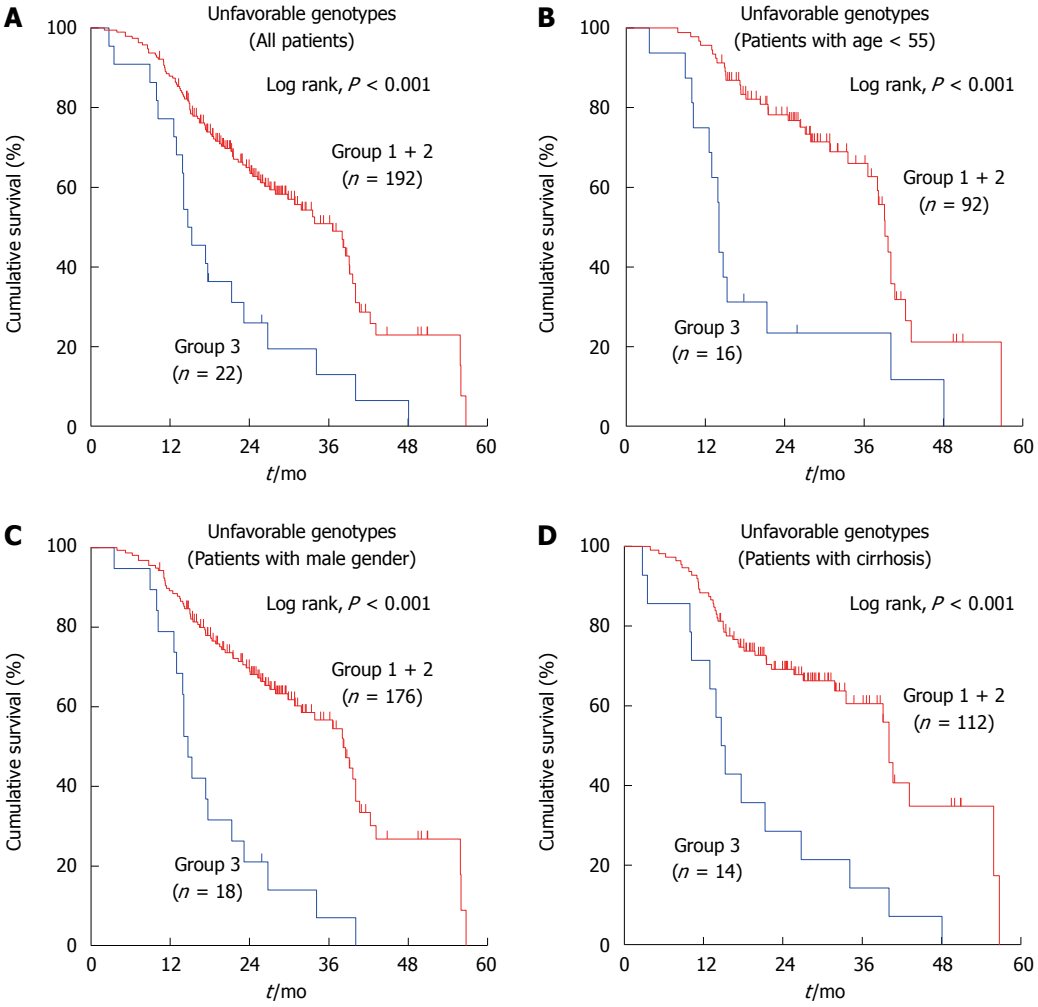

Figure 4 Kaplan-Meier curves for hepatocellular carcinoma patients carrying unfavorable genotypes. A: In all patients; B: In patients with age < 55 years; C: In patients with male gender; D: In patients with cirrhosis. Patients were classified into two groups, according to number of unfavorable genotypes carried. Group 1 + 2 carried 0 or 1 unfavorable genotype, while Group 3 carried 2 unfavorable genotypes. Unfavorable genotypes were *GSTO2*: rs7085725 (WV or VV) and *GSTP1*: rs4147581 (WW).

Table 6 Modulating effects of smoking on hepatocellular carcinoma overall survival by *GSTO2*: rs7085725 or *GSTP1*: rs4147581 genotypes

SNP and variables	Death/total	HR (95%CI)	*P* value
In patients with WW genotype of *GSTO2*: rs7085725			
Smoking behavior			
No smoking	52/119	1 (ref)	
Smoking	29/57	1.04 (0.82-1.31)	0.757
Smoking quantity (packs-year)[1]			
0	52/119	1 (ref)	
> 0 and < 20	20/45	1.06 (0.82-1.37)	0.667
⩾ 20	9/12	0.99 (0.76-1.30)	0.956
In patients with WV + VV genotypes of *GSTO2*: rs7085725			
Smoking behavior			
No smoking	19/25	1 (ref)	
Smoking	11/33	1.52 (1.02-2.26)[a]	0.042[a]
Smoking quantity (packs-year)[1]			
0	19/25	1 (ref)	
> 0 and < 20	9/11	1.42 (0.93-2.16)	0.106
⩾ 20	2/2	2.07 (1.13-3.76)	0.018[a]
In patients with WW genotype of *GSTP1*: rs4147581			
Smoking behavior			
No smoking	35/61	1 (ref)	
Smoking	22/42	0.95 (0.72-1.24)	0.697
Smoking quantity (packs-year)[1]			
0	35/61	1 (ref)	
> 0 and < 20	15/33	0.97 (0.71-1.31)	0.824
⩾ 20	7/9	0.95 (0.71-1.28)	0.754
In patients with WV + VV genotypes of *GSTP1*: rs4147581			
Smoking behavior			
No smoking	36/83	1 (ref)	
Smoking	18/28	1.27 (0.95-1.69)	0.101
Smoking quantity (packs-year)[1]			
0	36/83	1 (ref)	
> 0 and < 20	14/23	1.27 (0.93-1.74)	0.128
⩾ 20	4/5	1.16 (0.81-1.66)	0.426

[1]To calculate pack-years of smoking, the average of number of cigarettes smoked per day was divided by 20 to give packs per day and multiplied by the total number of years of smoking. [a]$P < 0.05$ was considered statistically significant. WW: Homozygous wild-type genotype; WV: Heterozygous genotype; VV: Homozygous variant genotype; SNP: Single nucleotide polymorphisms.

was a significant difference in the genotype distribution of rs7085725 between patients with high and median GSTO2 expression levels ($P = 0.042$). Additionally, the

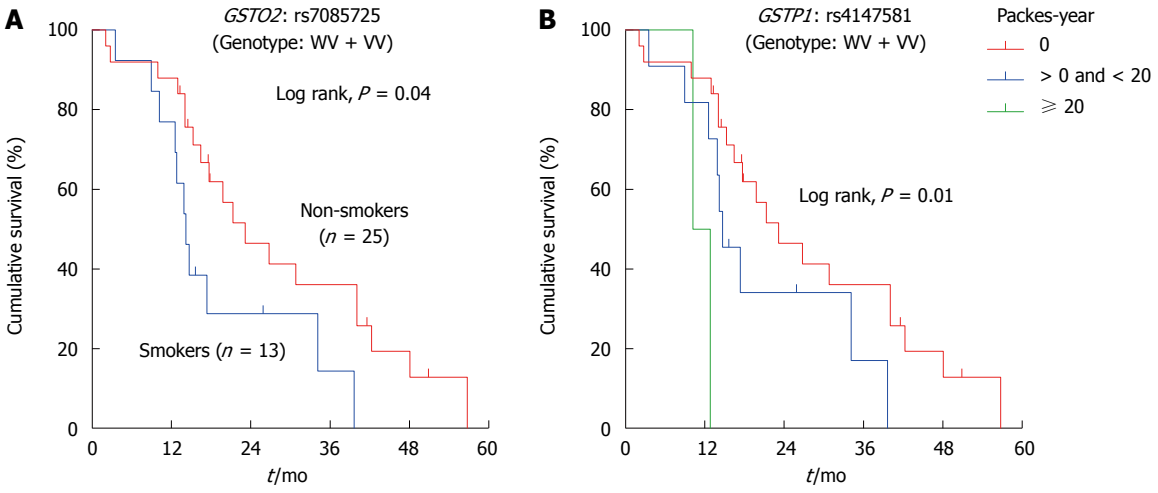

Figure 5 Kaplan-Meier curves for hepatocellular carcinoma patients carrying WV + VV genotypes in different smoking subgroups. A: HCC patients were classified by smoking behavior; B: HCC patients were classified by smoking quantity. WV: Heterozygous genotype; VV: Homozygous variant genotype.

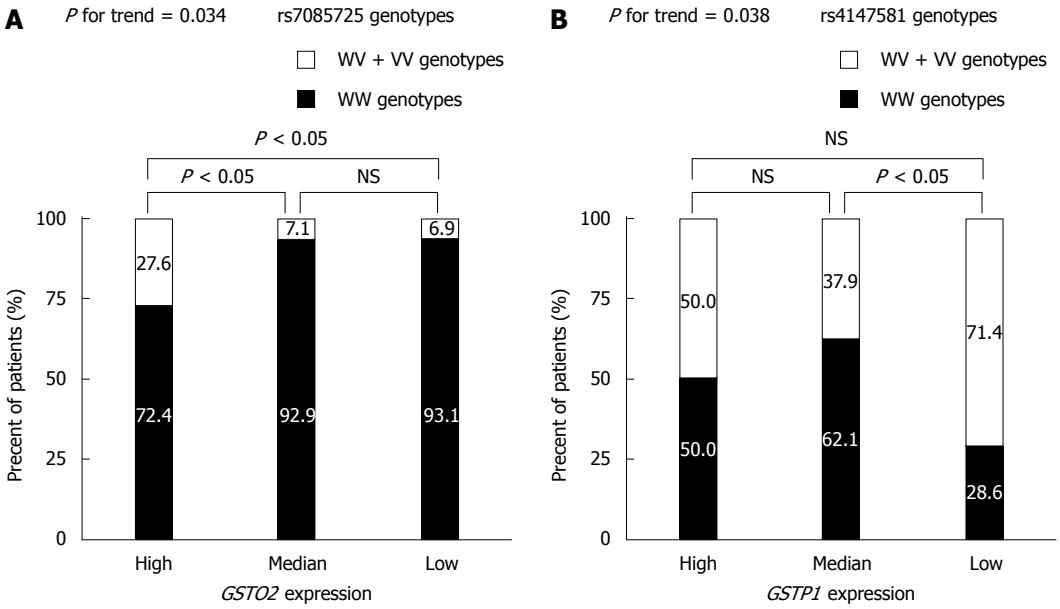

Figure 6 Comparison of genotype distribution in hepatocellular carcinoma patients with different *GSTO2* and *GSTP1* expression. A: rs7085725 genotype distribution in different *GSTO2* expression groups. rs7085725 genotype was predicted according to rs11191994 (LD r^2 = 1.000, D' = 1.000); B: rs4147581 genotype distribution in different *GSTP1* expression groups. rs4147581 genotype was predicted according to rs614080 (LD r^2 = 1.000, D' = 1.000). WV: Heterozygous genotype; VV: Homozygous variant genotype; NS: Not significant.

genotype distributions of rs4147581 in low and median *GSTP1* expression groups were also significantly different (P = 0.011). We found that patients carrying WV + VV genotypes of rs7085725 were more frequent in high *GSTO2* expression subgroup, while rs4147581 WW allele carriers were dominant in low *GSTP1* expression subgroup (Figure 6).

DISCUSSION

In this study, we evaluated the prognostic value of 12 tagging polymorphisms from seven *GST* genes in Chinese HCC patients. The most important finding was that SNPs *GSTO2:* rs7085725 and *GSTP1*: rs4147581 were significantly associated with the overall survival of HCC patients (P = 0.035 and P = 0.042, respectively). Our data indicated that SNPs *GSTO2:* rs7085725 and *GSTP1*: rs4147581 used alone or in combination were potential prognostic markers for HCC patients, especially in those patients with younger age, male gender and cirrhosis. If further validated, the two SNPs may potentially be developed as simple non-invasive predictive biomarkers for HCC patients.

GSTP1, an extensively studied member of GSTs, acts as a part of the protection system against a wide range of potentially harmful cytotoxic compounds. It was observed that altered expression of *GSTP1* existed in liver cancer cell lines[22], and in more than 77.8% of

HBV-associated HCC tissues[23]. Previous studied have extensively demonstrated that *GSTP1* polymorphisms would contribute to the increased risk and poor outcome of many cancers, including esophageal cancer[24], colorectal cancer[8], glioma[10], breast cancer[2,25], prostate cancer[26] and ovarian cancer[9,27]. However, little is known to date about their effect on HCC risk and prognosis. Chen *et al*[13] reported that *GSTP1* gene polymorphisms might be considered as factors increasing the susceptibility to HCC in Taiwanese aged ⩽ 57 years. In the present study, we similarly identified a tagging SNP of *GSTP1* (rs4147581) as a predictive biomarker in HCC patients aged ⩽ 55 years. Besides younger age, we additionally identified that *GSTP1*: rs4147581 polymorphism was associated with the overall survival in those patients with male gender, non-smoking behavior, liver cirrhosis, Child-Pugh score B, AFP < 200 ng/mL, or tumor size ⩾ 5 cm, all of which suggested this SNP as a more powerful predictor than previous SNP markers.

The function of *GSTP1*: rs4147581 to date remains to be unclear. In the present study, we first reported that genotype distribution of rs4147581 was associated with GSTP1 expression. It has been reported that *GSTP1*: rs4147581 was associated with DNA methylation[28], which has been clearly demonstrated to play a critical role in down-regulating *GSTP1* expression in HCC[6,22,23]. Considering that loss of *GSTP1* expression has been suggested to increase the risk of DNA damage[6], we put forward the hypothesis that rs4147581 may control *GSTP1* expression by influencing DNA methylation, and consequently induce high risk of carcinogenesis and cancer progression.

GSTO2 gene encodes omega class GST member GSTO2, which exhibits dehydroascorbate (DHA) reductase activity in addition to novel thioltransferase, and monomethylarsonate reductase activities[29,30]. GSTO2 has 70-100 times higher DHA reductase (DHAR) activity than GSTO1, another GST omega class GST member, and is considered to be the most active DHAR in mammalian cells[30]. Previous studies have extensively demonstrated that *GSTO2* polymorphisms might contribute to the increased risk of colorectal cancer[31], gastric cancer[32], ovarian cancer[33] and leukemia[34]. This finding suggested the hypothesis that *GSTO2* gene polymorphisms might contribute to the increased risk and outcome of HCC. Although Marahatta *et al*[35] did not find a difference in genotypic distribution for *GSTO2* polymorphism between HCC patients and controls, limited number of patients (only 28 cases of HCC and 98 controls) recruited in their study might contribute to this negative result. In our study, we identified that *GSTO2*: rs7085725 polymorphism was associated with overall survival of HCC patients. When combined with *GSTP1*: rs4147581, the predictive power of *GSTO2*: rs7085725 increased, especially in those younger, male and cirrhotic patients.

Recently, emerging evidence has shown that *GSTO2* gene polymorphism is associated with lung function modified by smoking exposure[36], and contributes to the development of lung cancer[37]. These reports suggest the critical role of *GSTO2:* rs7085725 in smoking related HCC risk. Our data indicated the significant association between *GSTO2*: rs7085725 and smoking behavior, which always predicts a relatively poor survival[21,38]. We further investigated the interaction between SNP *GSTO2:* rs7085725 and smoking exposure in modulating HCC patient survival. Interestingly, these variant allele carriers of *GSTO2:* rs7085725 were more susceptible to smoking exposure, when compared with wild type allele carriers. All the above results clearly demonstrated that the population carrying variant alleles of *GSTO2:* rs7085725 might obtain more benefit of smoking cessation, which may guide those patients to make better decision.

It has been reported that the polymorphisms in the *GSTO2* gene affect its expression levels in Alzheimer and Parkinson disease[39]; however, the influence of rs7085725 on *GSTO2* expression in HCC remains unclear. Our data showed that rs7085725 minor allele carriers were significantly increased in high *GSTO2* expression subgroup, when compared with median and low expression subgroups. Although the biological function of *GSTO2* has not been clearly demonstrated, it has been observed that the expression of *GSTO1*, which was an important paralog gene of *GSTO2* and exhibited very similar biological function to *GSTO2*, was over-expressed in chemo- and radio-resistant cancer cells[40,41]. Besides, elevation of GSTO1 protein in colorectal cancer cells was also involved in cell invasion and metastasis[42]. Above evidence suggested that high *GSTO2* expression might contribute to tumor progression. This hypothesis might partly explain why rs7085725 WV + VV allele carriers always had worse overall survival. To date there is no report of regulating mechanism of rs7085725 on *GSTO2* expression. The functional prediction indicates that rs7085725 is located in the 3'-UTR of the *GSTO2* gene. Previous evidence showed that SNP sequences in 3'-UTRs of many other genes are clearly involved in the regulation of mRNA expression either by providing mutated binding sites for proteins and microRNAs to alter mRNA stability, or by forming hairpin loop structures to stabilize and thus slow down mRNA degradation. This suggests a possibility of elevated expression regulation on the *GSTO2* gene by rs7085725. However, all given explanations are speculative and merit further research.

There are several strengths in this study. The patients analyzed in this study were enrolled from Xi' an and adjacent area, and these patients were all surgically treated to remove the primary tumors by the same medical center. The highly homogenous patient characteristics and treatments, as well as low rate of patient loss to follow-up, greatly reduced the confounding effects of the heterogeneous therapeutics

modalities in many other similar biomarker studies of HCC prognosis. The limitations of our study include the generalizability issue, because our study was restricted to Han Chinese. Further evaluation is necessary to determine whether these findings can be generalized to other ethnic groups. Moreover, the moderate sample size limited the validity of some stratified analyses. Following validation using larger independent populations is warranted.

In conclusion, our study presents the first epidemiological evidence supporting a role of *GSTO2:* rs7085725 and *GSTP1*: rs4147581 in the prognosis prediction in a Chinese population of HCC patients.

ACKNOWLEDGMENTS

We sincerely thank Dr. Ya-Min Liu and his colleague at Department of Cardiology and Peripheral Vascular Medicine, The First Affiliated Hospital of Medical College, Xi'an Jiaotong University for their support in sample collection. We also thank researchers at Queen Mary Hospital, the University of Hong Kong, who uploaded datasets to GEO database.

COMMENTS

Background

Previous studies have revealed that several *GST* genes are highly polymorphic, with particular genotypes shown to be associated with cancer risk and progression. Evidence has shown that some single nucleotide polymorphisms (SNPs) of *GST* were associated with HCC risk. However, none of these polymorphisms are investigated in relation to survival of patients with hepatocellular carcinoma (HCC).

Research frontiers

HCC is one of the most common malignancies worldwide, especially in China, and it largely remains an incurable disease. Traditional clinicopathological features such as tumor stage, histological grade and concentration of serum AFP seem to be insufficient to predict clinical outcomes in HCC patients after surgical treatment. Therefore, it is extremely urgent to explore novel biomarkers to discriminate patient with different clinical outcomes and direct future treatment for HCC patients.

Innovations and breakthroughs

In recent decades, widespread efforts have been made to investigate tumor tissue and serological markers that would predict survival of resected HCC patients. However, to date there have been very few studies to explore the prognostic value of genetic markers. This study presents the first epidemiological evidence supporting a role of genetic markers in the prognosis prediction in a Chinese population of HCC patients.

Applications

By establishing the novel prognostic predictive genetic markers, this study may represent a future strategy for cancer prediction in the follow-up of patients with HCC.

Terminology

The term "genetic polymorphism" refers to genetic variants within the population that allow evolution by natural selection. It is defined by the occurrence in the same population of multiple discrete allelic states of which at least two have a high frequency (conventionally of 1% or more). Genetic polymorphism as a predictive marker for clinical outcomes has been extensively investigated.

Peer-review

The manuscript investigates the effects of SNPs in *GST* genes on survival of HCC patients, and suggests that the *GSTO2* and *GSTP1* gene polymorphisms may serve as independent prognostic markers for HCC patients. This study may be very useful for a large number of hospitals worldwide.

REFERENCES

1 **Chasseaud LF**. The role of glutathione and glutathione S-transferases in the metabolism of chemical carcinogens and other electrophilic agents. *Adv Cancer Res* 1979; **29**: 175-274 [PMID: 474272 DOI: 10.1016/S0065-230X(08)60848-9]

2 **Curran JE**, Weinstein SR, Griffiths LR. Polymorphisms of glutathione S-transferase genes (GSTM1, GSTP1 and GSTT1) and breast cancer susceptibility. *Cancer Lett* 2000; **153**: 113-120 [PMID: 10779639 DOI: 10.1016/S0304-3835(00)00361-X]

3 **Daniel V**. Glutathione S-transferases: gene structure and regulation of expression. *Crit Rev Biochem Mol Biol* 1993; **28**: 173-207 [PMID: 8325038 DOI: 10.1146/annurev.biochem.58.1.743]

4 **Lee WH**, Morton RA, Epstein JI, Brooks JD, Campbell PA, Bova GS, Hsieh WS, Isaacs WB, Nelson WG. Cytidine methylation of regulatory sequences near the pi-class glutathione S-transferase gene accompanies human prostatic carcinogenesis. *Proc Natl Acad Sci USA* 1994; **91**: 11733-11737 [PMID: 7972132 DOI: 10.1073/pnas.91.24.11733]

5 **Niu D**, Zhang J, Ren Y, Feng H, Chen WN. HBx genotype D represses GSTP1 expression and increases the oxidative level and apoptosis in HepG2 cells. *Mol Oncol* 2009; **3**: 67-76 [PMID: 19383368 DOI: 10.1016/j.molonc.2008.10.002]

6 **Zhang YJ**, Chen Y, Ahsan H, Lunn RM, Chen SY, Lee PH, Chen CJ, Santella RM. Silencing of glutathione S-transferase P1 by promoter hypermethylation and its relationship to environmental chemical carcinogens in hepatocellular carcinoma. *Cancer Lett* 2005; **221**: 135-143 [PMID: 15808399 DOI: 10.1016/j.canlet.2004.08.028]

7 **Watson MA**, Stewart RK, Smith GB, Massey TE, Bell DA. Human glutathione S-transferase P1 polymorphisms: relationship to lung tissue enzyme activity and population frequency distribution. *Carcinogenesis* 1998; **19**: 275-280 [PMID: 9498276 DOI: 10.1093/carcin/19.2.275]

8 **Stoehlmacher J**, Park DJ, Zhang W, Groshen S, Tsao-Wei DD, Yu MC, Lenz HJ. Association between glutathione S-transferase P1, T1, and M1 genetic polymorphism and survival of patients with metastatic colorectal cancer. *J Natl Cancer Inst* 2002; **94**: 936-942 [PMID: 12072547 DOI: 10.1093/jnci/94.12.936]

9 **Howells RE**, Dhar KK, Hoban PR, Jones PW, Fryer AA, Redman CW, Strange RC. Association between glutathione-S-transferase GSTP1 genotypes, GSTP1 over-expression, and outcome in epithelial ovarian cancer. *Int J Gynecol Cancer* 2004; **14**: 242-250 [PMID: 15086723 DOI: 10.1111/j.1048-891X.2004.014207.x]

10 **Okcu MF**, Selvan M, Wang LE, Stout L, Erana R, Airewele G, Adatto P, Hess K, Ali-Osman F, Groves M, Yung AW, Levin VA, Wei Q, Bondy M. Glutathione S-transferase polymorphisms and survival in primary malignant glioma. *Clin Cancer Res* 2004; **10**: 2618-2625 [PMID: 15102663 DOI: 10.1158/1078-0432.ccr-03-0053]

11 **Wenzlaff AS**, Cote ML, Bock CH, Land SJ, Schwartz AG. GSTM1, GSTT1 and GSTP1 polymorphisms, environmental tobacco smoke exposure and risk of lung cancer among never smokers: a population-based study. *Carcinogenesis* 2005; **26**: 395-401 [PMID: 15528218 DOI: 10.1093/carcin/bgh326]

12 **White DL**, Li D, Nurgalieva Z, El-Serag HB. Genetic variants of glutathione S-transferase as possible risk factors for hepatocellular carcinoma: a HuGE systematic review and meta-analysis. *Am J Epidemiol* 2008; **167**: 377-389 [PMID: 18065725 DOI: 10.1093/aje/kwm315]

13 **Chen YL**, Tseng HS, Kuo WH, Yang SF, Chen DR, Tsai HT. Glutathione S-Transferase P1 (GSTP1) gene polymorphism increases age-related susceptibility to hepatocellular carcinoma. *BMC Med Genet* 2010; **11**: 46 [PMID: 20331903 DOI: 10.1186/1471-2350-11-46]

14 **Kilburn L**, Okcu MF, Wang T, Cao Y, Renfro-Spelman A, Aldape KD, Gilbert MR, Bondy M. Glutathione S-transferase polymorphisms are associated with survival in anaplastic glioma patients. *Cancer* 2010; **116**: 2242-2249 [PMID: 20187096 DOI: 10.1002/cncr.25006]

15 **Sergentanis TN**, Economopoulos KP. GSTT1 and GSTP1 polymorphisms and breast cancer risk: a meta-analysis. *Breast Cancer Res Treat* 2010; **121**: 195-202 [PMID: 19760040 DOI: 10.1007/s10549-009-0520-0]

16 **Xu Z**, Zhu H, Luk JM, Wu D, Gu D, Gong W, Tan Y, Zhou J, Tang J, Zhang Z, Wang M, Chen J. Clinical significance of SOD2 and GSTP1 gene polymorphisms in Chinese patients with gastric cancer. *Cancer* 2012; **118**: 5489-5496 [PMID: 22517484 DOI: 10.1002/cncr.27599]

17 **Jemal A**, Bray F, Center MM, Ferlay J, Ward E, Forman D. Global cancer statistics. *CA Cancer J Clin* 2011; **61**: 69-90 [PMID: 21296855 DOI: 10.3322/caac.20107]

18 **El-Serag HB**. Epidemiology of viral hepatitis and hepatocellular carcinoma. *Gastroenterology* 2012; **142**: 1264-1273.e1 [PMID: 22537432 DOI: 10.1053/j.gastro.2011.12.061]

19 **Gross-Steinmeyer K**, Eaton DL. Dietary modulation of the biotransformation and genotoxicity of aflatoxin B(1). *Toxicology* 2012; **299**: 69-79 [PMID: 22640941 DOI: 10.1016/j.tox.2012.05.016]

20 **Zhang XF**, Wei T, Liu XM, Liu C, Lv Y. Impact of cigarette smoking on outcome of hepatocellular carcinoma after surgery in patients with hepatitis B. *PLoS One* 2014; **9**: e85077 [PMID: 24454795 DOI: 10.1371/journal.pone.0085077]

21 **Munaka M**, Kohshi K, Kawamoto T, Takasawa S, Nagata N, Itoh H, Oda S, Katoh T. Genetic polymorphisms of tobacco- and alcohol-related metabolizing enzymes and the risk of hepatocellular carcinoma. *J Cancer Res Clin Oncol* 2003; **129**: 355-360 [PMID: 12759747 DOI: 10.1007/s00432-003-0439-5]

22 **Ding S**, Gong BD, Yu J, Gu J, Zhang HY, Shang ZB, Fei Q, Wang P, Zhu JD. Methylation profile of the promoter CpG islands of 14 "drug-resistance" genes in hepatocellular carcinoma. *World J Gastroenterol* 2004; **10**: 3433-3440 [PMID: 15526362]

23 **Zhong S**, Tang MW, Yeo W, Liu C, Lo YM, Johnson PJ. Silencing of GSTP1 gene by CpG island DNA hypermethylation in HBV-associated hepatocellular carcinomas. *Clin Cancer Res* 2002; **8**: 1087-1092 [PMID: 11948118]

24 **Zhao Y**, Wang F, Shan S, Zhao Y, Qiu X, Li X, Jiao F, Wang J, Du Y. Genetic polymorphism of p53, but not GSTP1, is association with susceptibility to esophageal cancer risk - a meta-analysis. *Int J Med Sci* 2010; **7**: 300-308 [PMID: 20827430 DOI: 10.7150/ijms.7.300]

25 **Yang G**, Shu XO, Ruan ZX, Cai QY, Jin F, Gao YT, Zheng W. Genetic polymorphisms in glutathione-S-transferase genes (GSTM1, GSTT1, GSTP1) and survival after chemotherapy for invasive breast carcinoma. *Cancer* 2005; **103**: 52-58 [PMID: 15565566 DOI: 10.1002/cncr.20729]

26 **Agalliu I**, Lin DW, Salinas CA, Feng Z, Stanford JL. Polymorphisms in the glutathione S-transferase M1, T1, and P1 genes and prostate cancer prognosis. *Prostate* 2006; **66**: 1535-1541 [PMID: 16921513 DOI: 10.1002/pros.20491]

27 **Nagle CM**, Chenevix-Trench G, Spurdle AB, Webb PM. The role of glutathione-S-transferase polymorphisms in ovarian cancer survival. *Eur J Cancer* 2007; **43**: 283-290 [PMID: 17084623 DOI: 10.1016/j.ejca.2006.09.011]

28 **Breton CV**, Byun HM, Wenten M, Pan F, Yang A, Gilliland FD. Prenatal tobacco smoke exposure affects global and gene-specific DNA methylation. *Am J Respir Crit Care Med* 2009; **180**: 462-467 [PMID: 19498054 DOI: 10.1164/rccm.200901-0135OC]

29 **Board PG**, Coggan M, Chelvanayagam G, Easteal S, Jermiin LS, Schulte GK, Danley DE, Hoth LR, Griffor MC, Kamath AV, Rosner MH, Chrunyk BA, Perregaux DE, Gabel CA, Geoghegan KF, Pandit J. Identification, characterization, and crystal structure of the Omega class glutathione transferases. *J Biol Chem* 2000; **275**: 24798-24806 [PMID: 10783391 DOI: 10.1074/jbc.M001706200]

30 **Whitbread AK**, Masoumi A, Tetlow N, Schmuck E, Coggan M, Board PG. Characterization of the omega class of glutathione transferases. *Methods Enzymol* 2005; **401**: 78-99 [PMID: 16399380 DOI: 10.1016/S0076-6879(05)01005-0]

31 **Masoudi M**, Saadat I, Omidvari S, Saadat M. Association between N142D genetic polymorphism of GSTO2 and susceptibility to colorectal cancer. *Mol Biol Rep* 2011; **38**: 4309-4313 [PMID: 21113667 DOI: 10.1007/s11033-010-0555-7]

32 **Masoudi M**, Saadat I, Omidvari S, Saadat M. Genetic polymorphisms of GSTO2, GSTM1, and GSTT1 and risk of gastric cancer. *Mol Biol Rep* 2009; **36**: 781-784 [PMID: 18398695 DOI: 10.1007/s11033-008-9245-0]

33 **Pongstaporn W**, Rochanawutanon M, Wilailak S, Linasamita V, Weerakiat S, Petmitr S. Genetic alterations in chromosome 10q24.3 and glutathione S-transferase omega 2 gene polymorphism in ovarian cancer. *J Exp Clin Cancer Res* 2006; **25**: 107-114 [PMID: 16761626]

34 **Pongstaporn W**, Pakakasama S, Sanguansin S, Hongeng S, Petmitr S. Polymorphism of glutathione S-transferase Omega gene: association with risk of childhood acute lymphoblastic leukemia. *J Cancer Res Clin Oncol* 2009; **135**: 673-678 [PMID: 18941778 DOI: 10.1007/s00432-008-0501-4]

35 **Marahatta SB**, Punyarit P, Bhudisawasdi V, Paupairoj A, Wongkham S, Petmitr S. Polymorphism of glutathione S-transferase omega gene and risk of cancer. *Cancer Lett* 2006; **236**: 276-281 [PMID: 15992993 DOI: 10.1016/j.canlet.2005.05.020]

36 **de Jong K**, Boezen HM, Hacken NH, Postma DS, Vonk JM. GST-omega genes interact with environmental tobacco smoke on adult level of lung function. *Respir Res* 2013; **14**: 83 [PMID: 23937118 DOI: 10.1186/1465-9921-14-83]

37 **de Andrade M**, Li Y, Marks RS, Deschamps C, Scanlon PD, Olswold CL, Jiang R, Swensen SJ, Sun Z, Cunningham JM, Wampfler JA, Limper AH, Midthun DE, Yang P. Genetic variants associated with the risk of chronic obstructive pulmonary disease with and without lung cancer. *Cancer Prev Res* (Phila) 2012; **5**: 365-373 [PMID: 22044695 DOI: 10.1158/1940-6207.CAPR-11-0243]

38 **Chen CJ**, Yu MW, Liaw YF. Epidemiological characteristics and risk factors of hepatocellular carcinoma. *J Gastroenterol Hepatol* 1997; **12**: S294-S308 [PMID: 9407350 DOI: 10.1111/j.1440-1746.1997.tb00513.x]

39 **Allen M**, Zou F, Chai HS, Younkin CS, Miles R, Nair AA, Crook JE, Pankratz VS, Carrasquillo MM, Rowley CN, Nguyen T, Ma L, Malphrus KG, Bisceglio G, Ortolaza AI, Palusak R, Middha S, Maharjan S, Georgescu C, Schultz D, Rakhshan F, Kolbert CP, Jen J, Sando SB, Aasly JO, Barcikowska M, Uitti RJ, Wszolek ZK, Ross OA, Petersen RC, Graff-Radford NR, Dickson DW, Younkin SG, Ertekin-Taner N. Glutathione S-transferase omega genes in Alzheimer and Parkinson disease risk, age-at-diagnosis and brain gene expression: an association study with mechanistic implications. *Mol Neurodegener* 2012; **7**: 13 [PMID: 22494505 DOI: 10.1186/1750-1326-7-13]

40 **Giri U**, Terry NH, Kala SV, Lieberman MW, Story MD. Elimination of the differential chemoresistance between the murine B-cell lymphoma LY-ar and LY-as cell lines after arsenic (As2O3) exposure via the overexpression of gsto1 (p28). *Cancer Chemother Pharmacol* 2005; **55**: 511-521 [PMID: 15761769 DOI: 10.1007/s00280-004-0920-0]

41 **Yan XD**, Pan LY, Yuan Y, Lang JH, Mao N. Identification of platinum-resistance associated proteins through proteomic analysis of human ovarian cancer cells and their platinum-resistant sublines. *J Proteome Res* 2007; **6**: 772-780 [PMID: 17269733 DOI: 10.1021/pr060402r]

42 **Liu L**, Zhao L, Zhang Y, Zhang Q, Ding Y. Proteomic analysis of Tiam1-mediated metastasis in colorectal cancer. *Cell Biol Int* 2007; **31**: 805-814 [PMID: 17376711 DOI: 10.1016/j.cellbi.2007.01.014]

P- Reviewer: Guo YM, Luo HS **S- Editor**: Yu J
L- Editor: Wang TQ **E- Editor**: Ma S

World Journal of Gastroenterology

Submit a Manuscript: http://www.wjgnet.com/esps/
Help Desk: http://www.wjgnet.com/esps/helpdesk.aspx
DOI: 10.3748/wjg.v21.i14.4323

World J Gastroenterol 2015 April 14; 21(14): 4323-4333
ISSN 1007-9327 (print) ISSN 2219-2840 (online)

SYSTEMATIC REVIEWS

Carbohydrate antigen 19-9 for differential diagnosis of pancreatic carcinoma and chronic pancreatitis

Si-Biao Su, Shan-Yu Qin, Wen Chen, Wei Luo, Hai-Xing Jiang

Si-Biao Su, Shan-Yu Qin, Wei Luo, Hai-Xing Jiang, Department of Gastroenterology, The First Affiliated Hospital of Guangxi Medical University, Nanning 530021, Guangxi Zhuang Autonomous Region, China
Wen Chen, Department of Educational Administration, The First Affiliated Hospital of Guangxi Medical University, Nanning 530021, Guangxi Zhuang Autonomous Region, China
Author contributions: Jiang HX designed the study, searched the databases, extracted the data, analyzed the results, and wrote the manuscript; Su SB helped design the study, search the databases, and write and revise the manuscript; Qin SY formulated the research question, and helped with database searches and analysis; Chen W and Luo W helped design the data abstraction form and served as second reviewers in extracting the data; all authors have read and approved the final manuscript.

Correspondence to: Dr. Hai-Xing Jiang, Department of Gastroenterology, The First Affiliated Hospital of Guangxi Medical University, No. 22 Shuangyong Road, Nanning 530021, Guangxi Zhuang Autonomous Region,
China. Jianghaixing2001@163.com
Telephone: +86-771-5312726
Fax: +86-771-5356758
Received: September 20, 2014
Peer-review started: September 21, 2014
First decision: October 14, 2014
Revised: October 30, 2014
Accepted: January 8, 2015
Article in press: January 8, 2015
Published online: April 14, 2015

Abstract

AIM: To evaluate the utility of carbohydrate antigen 19-9 (CA19-9) for differential diagnosis of pancreatic carcinoma and chronic pancreatitis.

METHODS: We searched the literature for studies reporting the sensitivity, specificity, and other accuracy measures of serum CA19-9 levels for differentiating pancreatic carcinoma and chronic pancreatitis. Pooled analysis was performed using random-effects models, and receiver operating characteristic (ROC) curves were generated. Study quality was assessed using Standards for Reporting Diagnostic Accuracy and Quality Assessment for Studies of Diagnostic Accuracy tools.

RESULTS: A total of 34 studies involving 3125 patients with pancreatic carcinoma and 2061 patients with chronic pancreatitis were included. Pooled analysis of the ability of CA19-9 level to differentiate pancreatic carcinoma and chronic pancreatitis showed the following effect estimates: sensitivity, 0.81 (95%CI: 0.80-0.83); specificity, 0.81 (95%CI: 0.79-0.82); positive likelihood ratio, 4.08 (95%CI: 3.39-4.91); negative likelihood ratio, 0.24 (95%CI: 0.21-0.28); and diagnostic odds ratio, 19.31 (95%CI: 14.40-25.90). The area under the ROC curve was 0.88. No significant publication bias was detected.

CONCLUSION: Elevated CA19-9 by itself is insufficient for differentiating pancreatic carcinoma and chronic pancreatitis, however, it increases suspicion of pancreatic carcinoma and may complement other clinical findings to improve diagnostic accuracy.

Key words: Pancreatic carcinoma; Chronic pancreatitis; Carbohydrate antigen; Diagnosis; Meta-analysis

Core tip: Pancreatic carcinoma and chronic pancreatitis show similar clinical manifestations. Differential diagnosis of pancreatic carcinoma and chronic pancreatitis remains

a challenge, particularly in patients with pancreatic masses that may be benign (inflammatory) or malignant. Carbohydrate antigen 19-9 (CA19-9) shows promise for differentiating the diseases. We evaluated the usefulness of CA19-9 in this systematic review.

Su SB, Qin SY, Chen W, Luo W, Jiang HX. Carbohydrate antigen 19-9 for differential diagnosis of pancreatic carcinoma and chronic pancreatitis. *World J Gastroenterol* 2015; 21(14): 4323-4333 Available from: URL: http://www.wjgnet.com/1007-9327/full/v21/i14/4323.htm DOI: http://dx.doi.org/10.3748/wjg.v21.i14.4323

INTRODUCTION

Pancreatic carcinoma is the fourth leading cause of cancer deaths in the United States[1]. Currently, the most effective treatment is surgical resection[2,3]. However, approximately 80% of tumors are unresectable at diagnosis, and these patients show a 5-year survival rate below 5%[1]. The clinical manifestations of pancreatic carcinoma resemble those of chronic pancreatitis. In fact, chronic pancreatitis is strongly associated with pancreatic malignancy and may help to cause it. For example, individuals in parts of Southern India with idiopathic chronic pancreatitis unassociated with alcohol abuse show a high incidence of pancreatic carcinoma[4].

Differential diagnosis of pancreatic carcinoma and chronic pancreatitis remains a challenge, particularly in patients with pancreatic masses that may be benign (inflammatory) or malignant. This differentiation is important in order to avoid unnecessary resection in patients with inflammatory masses: 5%-10% of patients subjected to pancreatic resection are ultimately diagnosed with pancreatitis rather than pancreatic carcinoma[5]. Differentiation is also important in order to identify correctly pancreatic masses as cancerous and avoid leaving behind malignant masses. Pancreatic carcinoma is incurable in many patients who also have chronic pancreatitis, because the cancer is multicentric or advanced.

Carbohydrate antigen 19-9 (CA19-9) is the most popular serum-based marker for diagnosis of pancreatic cancer, and it is useful for detecting disease recurrence after surgery[6,7]. However, this biomarker has limited diagnostic power. CA19-9 level can be normal in patients with localized disease, therefore, it is less effective for screening for early pancreatic cancer. High CA19-9 levels can also occur in benign diseases, including chronic pancreatitis and nonmalignant jaundice[6-8].

Diagnosis of pancreatic cancer at an early, resectable stage is especially difficult when the patient also presents with chronic pancreatitis[9,10], therefore, we wondered whether CA19-9 might be useful for differentiating the two diseases. We performed a systematic review and meta-analysis of the utility of CA19-9 as a serum tumor marker and its sensitivity and specificity for distinguishing pancreatic carcinoma and chronic pancreatitis.

MATERIALS AND METHODS

Search strategies

In June 2013 we searched MEDLINE (1980 to May 2013), EMBASE (1980 to May 2013), Web of Science (1990 to May 2013) and Cochrane databases. Although no language restrictions were imposed initially, for the full-text review and final analysis only English language articles were included. Additional articles were searched using the "Related articles" function in PubMed and by manually searching reference lists of identified articles and review articles. The following search terms were used: "pancreatic carcinoma" or "pancreatic cancer" and "chronic pancreatitis" and "carbohydrate antigen 19-9" and "diagnosis" or "sensitivity" or "specificity". We contacted experts in the field to ask about studies that we may have missed in the databases. Conference abstracts and letters to the editor were excluded because of the limited data they contained.

Study inclusion criteria

A study was included when it provided both the sensitivity (true-positive rate) and specificity (true-negative rate) of using serum CA19-9 levels to diagnose pancreatic carcinoma or chronic pancreatitis in patients of any age. Studies were also included if they reported CA19-9 values in a scatter plot format that allowed patient-level data to be extracted. Studies had to involve at least 10 patients with pancreatic carcinoma or chronic pancreatitis in order to reduce selection bias due to a small number of participants. Patients had to be diagnosed with pancreatic carcinoma based on cytology and/or histology of pancreatic tissue, or diagnosed with chronic pancreatitis based on clinical information alone or in combination with histopathological resection, radiology (endoscopic retrograde cholangiopancreatography and computed tomography) and/or endoscopic ultrasonography. Two reviewers (Su SB and Jiang HX) independently determined study eligibility, and disagreements were resolved by consensus.

Data extraction and quality assessment

These same two reviewers independently confirmed the eligibility of the final set of studies and extracted the following data: first author, publication year, participant characteristics, assay methods, sensitivity and specificity data, cut-off values, and methodological quality. Serum CA19-9 values provided in scatter plots were extracted by placing scalar grids over the plots. A receiver operating characteristic (ROC) curve was calculated for each study.

To enable us to assess the methodological quality

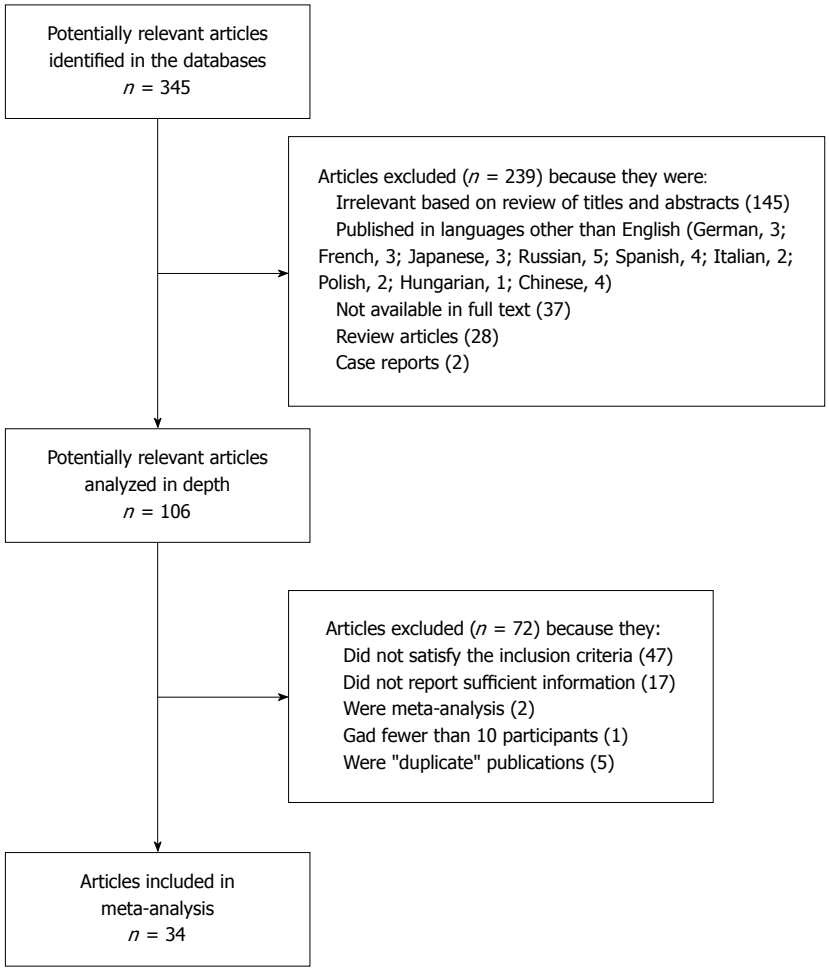

Figure 1 Flowchart of study selection.

of the included studies, we extracted data on the following study design characteristics: (1) cross-sectional or case-control design; (2) consecutive or random sampling of patients; (3) blinded (single or double) or non-blinded interpretation of experimental and reference measurements; and (4) prospective or retrospective data collection. Su SB and Jiang HX independently assessed the methodological quality of studies using the Standards for Reporting Diagnostic Accuracy (STARD) guidelines[11] (maximum score of 25) and the Quality Assessment for Studies of Diagnostic Accuracy (QUADAS) guidelines[12] (maximum score of 14). Average inter-rater agreement on the methodological quality checklists was 0.96. If primary studies did not report information needed to assess methodological quality, we contacted the authors in an effort to obtain the data. If the authors did not respond, we changed the response for the relevant items from "not reported" to "no" on the assessment instruments.

Statistical analysis

Standard methods recommended for meta-analyses of diagnostic test evaluations were used[13]. Analyses were performed using Meta-DiSc for Windows (XI Cochrane Colloquium; Barcelona, Spain) and Stata 12.0 (Stata Corporation, College Station, TX, United States). The following measures of test accuracy were analyzed for each study: sensitivity, specificity, positive likelihood ratio (PLR), negative likelihood ratio (NLR) and diagnostic odds ratio (DOR). A summary ROC (SROC) curve[14] was generated for each study based on a single test threshold for sensitivity and specificity[13,15]. A random-effects model was adopted to calculate the average sensitivity, specificity, and other measures across studies[16,17].

To assess the effects of STARD and QUADAS scores on the diagnostic power of CA19-9, we included them as covariates in univariate, inverse variance-weighted meta-regression. We also analyzed the effects of other covariates on DOR, such as cross-sectional design, consecutive or random sampling of patients, single- or double-blinded interpretation of experimental and reference measurements, and prospective or retrospective data collection. The relative DOR (RDOR) was calculated to analyze the change in diagnostic precision in each study per unit increase in the covariate[18,19]. $P < 0.05$ was considered to show statistical significance.

Table 1 Summary of carbohydrate antigen 19-9 assay methods, results, and overall methodological quality of included studies

Ref.	Number of patient	Assay method	Cut-off for elevated CA19-9 (U/mL)	Assay results				Quality score	
				TP	FP	FN	TN	STARD	QUADAS
Wang *et al*[21], 1986	58	RIA	37	20	0	4	34	15	10
Safi *et al*[22], 1987	191	RIA	37	80	28	7	76	16	10
Sakamoto *et al*[23], 1987	57	RIA	37	26	1	4	26	18	12
Friess *et al*[24], 1993	154	ELISA	37	53	14	6	81	17	11
Röthlin *et al*[25], 1993	97	RIA	37	54	8	14	21	17	12
Haglund *et al*[26], 1994	199	RIA	37	148	3	31	17	16	11
Kuno *et al*[27], 1994	117	RIA	37	41	10	6	60	19	13
Pasquali *et al*[28], 1994	103	RIA	37	47	2	11	43	12	9
Satake *et al*[29], 1994	941	RIA	37	454	56	118	244	19	13
Hámori *et al*[30], 1997	94	RIA	37	48	4	14	28	11	7
Safi *et al*[31], 1997	647	RIA	37	296	48	51	252	18	12
Hayakawa *et al*[32], 1999	76	RIA	37	21	14	6	35	16	11
Kim *et al*[33], 1999	160	ELISA	37	69	9	21	61	19	13
Manes *et al*[34], 1999	58	RIA	37	30	3	4	21	17	11
Slesak *et al*[35], 2000	122	LIA	37	32	14	14	60	18	12
Maire *et al*[36], 2002	78	ELISA	37	43	4	4	27	17	11
Akashi *et al*[37], 2003	46	RIA	37	15	7	5	19	12	9
Mu *et al*[38], 2003	24	RIA	37	4	3	5	12	15	10
Cwik *et al*[39], 2004	150	RIA	37	82	5	16	47	16	11
Jiang *et al*[40], 2004	148	ELISA	37	82	7	14	45	17	12
Ventrucci *et al*[41], 2004	81	EIA	60	45	2	15	19	18	12
Teich *et al*[42], 2005	59	ELISA	22	27	3	3	13	12	9
Chang *et al*[43], 2007	111	ELISA	37	63	11	9	28	18	12
		ELISA	100	57	7	15	32	18	12
Kuhlmann *et al*[44], 2007	62	EIA	37	17	4	11	30	16	11
Liao *et al*[45], 2007	150	ELISA	37	84	15	28	23	15	10
Bedi *et al*[46], 2009	84	ELISA	37	23	15	11	35	17	12
		ELISA	100	14	7	20	43	17	12
Firpo *et al*[47], 2009	107	ELISA	37	58	2	17	30	18	12
Liao *et al*[48], 2009	102	RIA	37	47	22	11	22	16	10
Morris-Stiff *et al*[49], 2009	188	ELISA	37	70	31	3	84	19	13
Talar-Wojnarowska *et al*[50], 2010	157	ELISA	37	71	18	14	54	17	12
Zapico-Muñiz *et al*[51], 2010	102	LIA	100	35	7	12	48	16	11
Chung *et al*[52], 2011	78	NR	30	40	2	15	21	12	9
Gold *et al*[53], 2013	284	EIA	37	180	16	54	34	18	11
Kaur *et al*[54], 2013	114	RIA	37	76	9	15	14	17	11

CA19-9: Carbohydrate antigen 19-9; EIA: Enzyme immunoassay; ELISA: Enzyme-linked immunosorbent assay; FN: False negative; FP: False positive; LIA: Luminescent immunoassay; NR: Not reported; RIA: Radioimmunoassay; TN: True negative; TP: True positive.

The heterogeneity, or variability, across studies was assessed for statistical significance using the χ^2 and Fisher exact tests. Publication bias can pose problems for meta-analyses of diagnostic studies, therefore, we tested for the potential presence of this bias using funnel plots and the Egger test[20].

RESULTS

Selection and summary of studies

We identified 345 citations *via* electronic searches, and 106 were retrieved for detailed analysis (Figure 1). Of these, 47 studies were excluded for failing to satisfy the inclusion criteria, and another 17 were excluded because they failed to provide sufficient information for meta-analysis. Five studies were duplicate publications. Two articles were meta-analyses, and one was excluded for involving fewer than 10 participants. In the end, 34 publications were included in the analysis[21-54], involving 3125 patients with pancreatic carcinoma and 2061 patients with chronic pancreatitis. The average sample size of the studies was 153 patients (range: 24-941). Table 1 summarizes the clinical characteristics of participants in each study; the numbers of true-positive, false-positive, false- negative and true-negative results; and STARD and QUADAS scores.

Methodological quality of the included studies

Of the 34 studies in the meta-analysis, 30 had STARD scores ⩾ 13, and 29 had QUADAS scores ⩾ 10. All studies collected data from consecutive patients using a prospective design. No study reported interpretation of CA19-9 measurements in which analysts were blinded to the corresponding reference measurements (Table 2).

Diagnostic accuracy

As shown in Figure 2, a Forest plot of serum CA19-9 levels in all 34 included studies showed that the

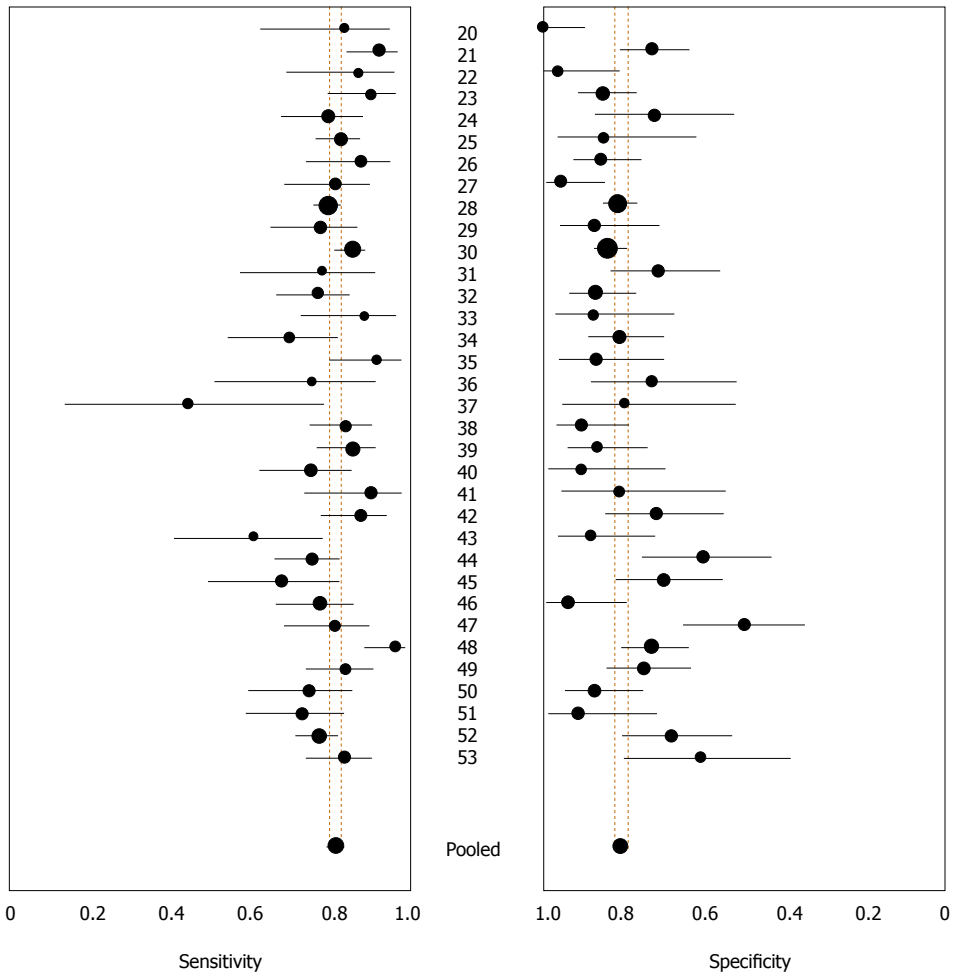

Figure 2 Forest plot showing sensitivity and specificity of carbohydrate antigen 19-9 in the diagnosis of pancreatic carcinoma. The point estimates of sensitivity and specificity from each study are shown as solid circles. Horizontal error bars indicate 95%CI. Numbers between the plots refer to references. Pooled estimates for the serum carbohydrate antigen 19-9 assay were 0.81 for sensitivity (95%CI: 0.80-0.83) and 0.81 for specificity (95%CI: 0.79-0.82).

sensitivity of this biomarker to differentiate between pancreatic carcinoma and chronic pancreatitis ranged from 0.44 to 0.96 [mean: 0.81, 95%CI: 0.80-0.83; χ^2 = 77.23, $P < 0.001$), while the specificity ranged from 0.50 to 1.0 (mean: 0.81, 95%CI: 0.79-0.82; χ^2 = 111.98, $P < 0.001$). The PLR was 4.08 (95%CI: 3.39-4.91; χ^2 = 113.62, $P < 0.001$), NLR was 0.24 (95%CI: 0.21-0.28; χ^2 = 86.13, $P < 0.001$) and DOR was 19.31 (95%CI: 14.4-25.9; χ^2 = 94.02, $P < 0.001$). These χ^2 values and associated *P*-values indicate significant heterogeneity among studies.

These measures of differential diagnostic power varied with different CA19-9 assays and cut-off values used to define CA19-9 levels as elevated or normal (Table 3). Data from the 11 studies that relied on the enzyme-linked immunosorbent assay (ELISA) method, involving 1396 patients, gave a sensitivity of 0.83 and specificity of 0.79. Data from the 17 studies using the radioimmunoassay method, involving 3074 patients, gave a sensitivity of 0.82 and specificity of 0.81. Data from the three studies that relied on an enzyme immunosorbent assay (EIA) gave a sensitivity of 0.75 and specificity of 0.79. Data from the 30 studies (4879 patients) using a cut-off value of 37 U/mL gave a sensitivity of 0.82 and specificity of 0.80. Data from the three studies using a cut-off value of 100 U/mL gave corresponding values of 0.69 and 0.85. These variations in sensitivity and specificity with CA19-9 assay and cut-off values did not achieve statistical significance ($P > 0.05$, Table 4), suggesting that high cut-off values such as 100 U/mL may better increase the specificity for differential diagnosis of pancreatic carcinoma.

Instead of assessing diagnostic power using the traditional ROC plot, we calculated an SROC plot to reveal the effect of varying thresholds on sensitivity and specificity within each study. In this plot, different studies appear as different data points, allowing SROC curves to provide a global summary of test performance and illustrate the trade-off between sensitivity and specificity. Figure 3 shows an SROC curve for rates of true- and false-positive results obtained with the CA19-9 assay in individual studies. From this plot we determined the *Q* value, which was

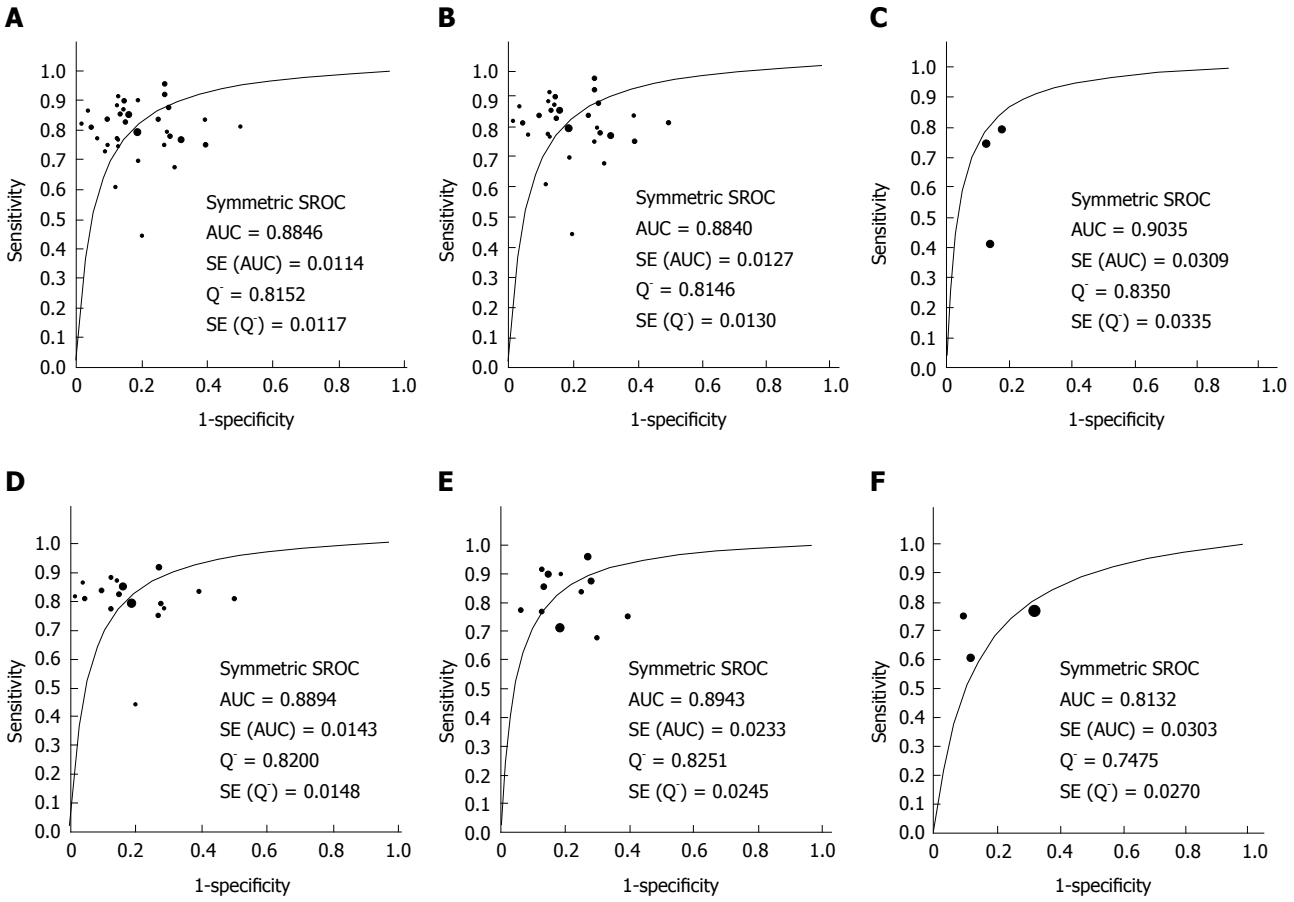

Figure 3 Summary receiver operating characteristic curves for carbohydrate antigen 19-9 assays for differential diagnosis of pancreatic carcinoma and chronic pancreatitis. Solid circles represent each study included in the meta-analysis, with circle size proportional to the number of participants in the study. SROC curves summarize the overall diagnostic accuracy for all included studies (A), studies using a cut-off of 37 U/mL carbohydrate antigen 19-9 (CA19-9) (B), studies using a cut-off of 100 U/mL CA19-9 (C), studies based on the radioimmunoassay method to assay CA19-9 (D), studies based on the ELISA method (E), and studies based on the enzyme immunoassay method (F). ELISA: Enzyme-linked immunosorbent assay; SROC: Summary receiver operating characteristic.

defined as the point of intersection of the SROC curve with a diagonal line extending from the left upper corner to the right lower corner of the plot. The *Q* value indicates the highest identical value of sensitivity and specificity, thereby serving as an overall measure of the discriminatory power of a test. Our SROC curve was desirably positioned near the upper left corner, and the maximum joint sensitivity and specificity was 0.81. The area under the curve (AUC) was 0.88 (Figure 3A), indicating high overall accuracy. SROC plots differed based on the CA19-9 assay method and cut-off values, but all plots were positioned near the upper left corner with AUCs near 0.88 (Figure 3B-F), again indicating high overall accuracy.

Multiple regression analysis and publication bias

Quality scores based on the STARD[11] and QUADAS[12] guidelines were generated for every study on the basis of the title and introduction, methods, results and discussion (Table 1). These scores were used in meta-regression to assess the effect of study quality on the RDOR of CA19-9 in the differential diagnosis of pancreatic carcinoma and chronic pancreatitis. Studies of higher quality (STARD score $\geqslant$ 13; QUADAS score $\geqslant$ 10) produced RDOR values similar to those of lower-quality studies. In addition, RDOR values did not differ significantly as a function of blinding, cross-sectional or case-control design, consecutive or random sampling, prospective or retrospective design, CA19-9 assay method, or cut-off values ($P > 0.05$). These results suggest that study design did not significantly affect diagnostic accuracy and that the risk of detection bias was low.

The Egger test showed no significant evidence of publication bias in reports about CA19-9 assays for differential diagnosis of pancreatic carcinoma ($P = 0.944$).

DISCUSSION

Timely and accurate diagnosis of pancreatic carcinoma is critical for patient prognosis, but it remains a challenge because the signs and symptoms of pancreatic cancer overlap considerably with those of chronic pancreatitis. Compounding this challenge is the fact that acute or chronic pancreatitis increases the risk of pancreatic carcinoma, as well as the fact that this cancer can

Table 2 Additional characteristics of patients and methodology in the included studies

Ref.	Country/area	PC/CP, *n*	PC reference	Cross-sectional design	Consecutive or Random sampling	Blinded design	Prospective design
Wang *et al*[21], 1986	Taiwan	24/34	His or Cyt	No	Yes	No	Yes
Safi *et al*[22], 1987	Germany	87/104	His	Yes	Yes	No	Yes
Sakamoto *et al*[23], 1987	Japan	30/27	His	No	Yes	No	Yes
Friess *et al*[24], 1993	Germany	59/95	His	Yes	Yes	No	Yes
Röthlin *et al*[25], 1993	Switzerland	68/29	His	No	Yes	No	Yes
Haglund *et al*[26], 1994	Finland	179/20	His	No	Yes	No	Yes
Kuno *et al*[27], 1994	Japan	47/70	His	Yes	Yes	No	Yes
Pasquali *et al*[28], 1994	Italy	58/45	His	No	No	NR	Yes
Satake *et al*[29], 1994	Japan	641/300	His	Yes	Yes	No	Yes
Hámori *et al*[30], 1997	Hungary	62/32	His	No	Yes	No	Yes
Safi *et al*[31], 1997	Germany	347/300	His or Bio	Yes	Yes	No	Yes
Hayakawa *et al*[32], 1999	Japan	27/49	His (Bio, Aut)	No	Yes	No	Yes
Kim *et al*[33], 1999	Korea	90/70	His	Yes	Yes	No	Yes
Manes *et al*[34], 1999	Italy	34/24	His or Cyt	Yes	Yes	No	Yes
Slesak *et al*[35], 2000	Poland	48/74	His	No	Yes	No	Yes
Maire *et al*[36], 2002	France	47/31	His or Cyt	No	Yes	No	Yes
Akashi *et al*[37], 2003	Japan	20/26	His or Aut	No	Yes	No	Yes
Mu *et al*[38], 2003	China	9/15	His or Cyt	No	Yes	No	Yes
Cwik *et al*[39], 2004	Lublin	98/52	His	NR	Yes	NR	Yes
Jiang *et al*[40], 2004	China	96/52	His	Yes	Yes	No	Yes
Ventrucci *et al*[41], 2004	Italy	60/21	His	Yes	Yes	No	Yes
Teich *et al*[42], 2005	Germany	30/16	His	No	No	No	Yes
Chang *et al*[43], 2007	Taiwan	72/39	His	Yes	Yes	No	Yes
	New York, United States	28/34	His	No	Yes	NR	Yes
Kuhlmann *et al*[44], 2007	China	112/38	His	No	Yes	No	Yes
Liao *et al*[45], 2007	India	34/50	His or Bio	Yes	Yes	No	Yes
Bedi *et al*[46], 2009	United States	75/32	His or Cyt	Yes	Yes	No	Yes
	Taiwan	58/44	His	Yes	Yes	No	Yes
Firpo *et al*[47], 2009	United Kingdom	73/115	His	Yes	Yes	No	Yes
Liao *et al*[48], 2009	Poland	85/72	His	Yes	Yes	No	Yes
Morris-Stiff *et al*[49], 2009	Spain	47/55	His	Yes	Yes	No	Yes
Talar-Wojnarowska *et al*[50], 2010	Korea	55/23	His	Yes	Yes	No	Yes
Zapico-Muñiz *et al*[51], 2010	New York, United States	234/50	His or Cyt	Yes	Yes	No	Yes
Chung *et al*[52], 2011	Germany	91/23	His	No	Yes	No	Yes

Aut: Autopsy; Bio: Biopsy; CP: Chronic pancreatitis; Cyt: Cytology; PC: Pancreatic carcinoma; His: Histology; NR: Not reported.

induce secondary inflammatory processes. In this systematic review, we find evidence that although CA19-9 levels on their own are inadequate for differentiating pancreatic carcinoma and chronic pancreatitis, elevated CA19-9 may complement other clinical tests to help confirm a diagnosis of pancreatic carcinoma.

CA19-9 is a sialylated Lewis (Le^a) blood-group antigen, which was first identified as a ligand bound by monoclonal antibody 1116 NS 19-9[55]. CA19-9 levels are elevated in > 80% of patients with advanced pancreatic cancer[56]. However, up to 40% of patients with chronic pancreatitis also have elevated CA19-9 levels, suggesting that these levels do not reliably differentiate between patients with pancreatic carcinoma and those with chronic pancreatitis[57]. In contrast to these earlier findings, our meta-analysis shows that the mean sensitivity of a CA19-9 assay was 0.81; mean specificity, 0.81; maximum joint sensitivity and specificity, 0.81; and AUC, 0.88. These values suggest high overall accuracy. These sensitivity and specificity values are similar to the corresponding values of 0.79-0.81 and 0.82-0.90 reported in two previous meta-analyses[6,58]. Interestingly, both previous meta-analyses examined the ability of serum CA19-9 to differentiate pancreatic carcinoma from benign pancreatic diseases in general, not specifically chronic pancreatitis.

DOR is an indicator of test accuracy that combines sensitivity and specificity data into a single number[59]. The DOR is the ratio of the odds of positive test results in the patient with disease relative to the odds of positive test results in the patient without disease. Thus, higher DOR values indicate better discriminatory test performance. The mean DOR in our study was 19.31, implying that CA19-9 levels may be useful in diagnosing pancreatic carcinoma.

Although SROC and DOR meta-analyses provide evidence that CA19-9 can help differentiate between pancreatic cancer and chronic pancreatitis, these diagnostic indicators are difficult to interpret and relate to clinical practice. Therefore, we examined the differential diagnostic power of CA19-9 using the more clinically meaningful likelihood ratio[60]. PLRs and NLRs of > 10 or < 0.1 indicate high accuracy. The overall PLR value in our meta-analysis was 4.08, indicating that patients with pancreatic carcinoma are ~ 4-fold

Table 3 Bivariate estimates of diagnostic precision based on different carbohydrate antigen 19-9 assay methods and cut-off values

Assay method or cut-off value	Number of studies	Number of participants	Sensitivity (95%CI)	Specificity (95%CI)	PLR (95%CI)	NLR (95%CI)	DOR (95%CI)
ELISA	11	1396	0.83 (0.80-0.86)	0.79 (0.75-0.82)	3.97 (2.96-5.33)	0.20 (0.15-0.28)	22.64 (12.44-41.22)
RIA	17	3074	0.82 (0.80-0.84)	0.81 (0.79-0.83)	4.16 (3.09-5.60)	0.23 (0.19-0.27)	20.14 (13.27-30.55)
EIA	3	427	0.75 (0.70-0.80)	0.79 (0.70-0.86)	3.84 (1.82-8.10)	0.34 (0.27-0.43)	10.29 (4.96-21.34)
LIA	2	224	ND	ND	ND	ND	ND
Cut-off of 37 U/mL	30	4879	0.82 (0.80-0.83)	0.80 (0.78-0.82)	3.94 (3.24-4.78)	0.24 (0.21-0.28)	18.79 (13.67-25.82)
Cut-off of 100 U/mL	3	297	0.69 (0.61-0.76)	0.85 (0.79-0.91)	4.35 (2.86-6.61)	0.38 (0.18-0.77)	11.53 (4.47-29.77)
All studies	34	5115	0.81 (0.80-0.83)	0.81 (0.79-0.82)	4.08 (3.39-4.91)	0.24 (0.21-0.28)	19.31 (14.40-25.90)

DOR: Diagnostic odds ratio; EIA: Enzyme immunoassay; ELISA: Enzyme-linked immunosorbent assay; LIA: Luminescent immunoassay; ND: Not done; NLR: Negative likelihood ratio; PLR: Positive likelihood ratio; RIA: Radioimmunoassay.

Table 4 Weighted meta-regression of the effects of study design, methodological quality and assay parameters on diagnostic accuracy of carbohydrate antigen 19-9

Covariate	Number of studies	Coefficient	RDOR (95%CI)	*P* value
Study design and quality				
STARD ⩾ 13	30	0.564	1.76 (0.14-22.68)	0.652
QUADAS ⩾ 10	29	-0.666	0.51 (0.06-4.11)	0.514
Consecutive or random design	32	0.924	2.52 (0.26-24.68)	0.411
Cross-sectional design	18	-0.512	0.60 (0.28-1.28)	0.178
Blinded design	0	ND	ND	ND
Prospective design	34	ND	ND	ND
Assay method or cut-off value				
RIA	17	-0.619	0.54 (0.12-2.51)	0.413
ELISA	11	-0.737	0.48 (0.10-2.26)	0.336
EIA	3	0.425	1.53 (0.29-8.14)	0.604
Cut-off of 37 U/mL	30	0.553	1.74 (0.36-8.36)	0.474
Cut-off of 100 U/mL	3	0.890	2.43 (0.72-8.26)	0.146

EIA: Enzyme immunoassay; ELISA: Enzyme-linked immunosorbent assay; ND: Not done; RIA: Radioimmunoassay; STARD: Standards for Reporting Diagnostic Accuracy; QUADAS: Quality Assessment for Studies of Diagnostic Accuracy.

more likely to have elevated CA19-9 than patients with chronic pancreatitis. On the other hand, NLR in our meta-analysis was 0.24, meaning that a patient without elevated CA19-9 would still have a 24% chance of having pancreatic carcinoma, or that 24% of patients with pancreatic carcinoma would not have elevated CA19-9. This proportion is too high to rule out pancreatic cancer in patients who do not have elevated CA19-9. These findings suggest that serum CA19-9 levels are insufficient on their own to differentiate between pancreatic carcinoma and chronic pancreatitis. A better approach may be a combined diagnostic strategy drawing on clinical information as well as findings from cytology and histology of pancreatic tissue, radiology and/or endoscopic ultrasonography.

The present meta-analysis had several limitations. First, the exclusion of conference abstracts, letters to the editor, and non-English-language studies may have led to publication bias, although our bias analysis suggests that this was not a significant problem. Second, nonrandom misclassification bias may have occurred given that different studies used different approaches to diagnose chronic pancreatitis, including histology of pancreatic tissue, radiology, endoscopic ultrasonography and/or clinical information alone. Third, CA19-9 is not routinely measured when patients present with chronic pancreatitis, so the individuals in our meta-analysis may not be completely representative of this patient population. Fourth, 5%-10% of patients lacked the Lewis enzyme, fucosyltransferase, and so cannot present elevated CA19-9 even when tumor burden is high. Finally, we did not identify any large, blinded randomized controlled trials that satisfied our inclusion criteria.

In conclusion, our meta-analysis suggests that although CA19-9 showed considerable sensitivity and specificity for differentiating pancreatic carcinoma and chronic pancreatitis, the relatively high NLR means that CA19-9 levels by themselves have insufficient diagnostic accuracy. At the same time, elevated CA19-9 should increase suspicion of pancreatic carcinoma and may complement other clinical and histological findings to help confirm a diagnosis of cancer.

COMMENTS

Background

Pancreatic carcinoma and chronic pancreatitis show similar clinical

manifestations. Carbohydrate antigen 19-9 (CA19-9) shows promise for differentiating the diseases.

Research frontiers

Differential diagnosis of pancreatic carcinoma and chronic pancreatitis remains a challenge, particularly in patients with pancreatic masses that may be benign (inflammatory) or malignant.

Innovations and breakthroughs

This is believed to be the first systematic review and meta-analysis of the utility of CA19-9 as a serum tumor marker and its sensitivity and specificity for distinguishing pancreatic carcinoma and chronic pancreatitis.

Applications

Available evidence suggests that elevated CA19-9 by itself is insufficient for differentiating pancreatic carcinoma and chronic pancreatitis. Nevertheless, elevated CA19-9 should increase suspicion of pancreatic carcinoma and therefore may complement other clinical findings to improve the accuracy of differential diagnosis.

Peer-review

This study evaluated the role of CA19-9 for differentiating pancreatic carcinoma and chronic pancreatitis and concluded that CA19-9 itself is insufficient, but elevated CA19-9 should increase suspicion of pancreatic carcinoma and therefore may complement other clinical findings to improve the accuracy of differential diagnosis. This result is reasonable and valuable for clinical practice.

REFERENCES

1 **Jemal A**, Siegel R, Ward E, Hao Y, Xu J, Murray T, Thun MJ. Cancer statistics, 2008. *CA Cancer J Clin* 2008; **58**: 71-96 [PMID: 18287387 DOI: 10.3322/CA.2007.0010]

2 **Sener SF**, Fremgen A, Menck HR, Winchester DP. Pancreatic cancer: a report of treatment and survival trends for 100,313 patients diagnosed from 1985-1995, using the National Cancer Database. *J Am Coll Surg* 1999; **189**: 1-7 [PMID: 10401733]

3 **Sohn TA**, Yeo CJ, Cameron JL, Koniaris L, Kaushal S, Abrams RA, Sauter PK, Coleman J, Hruban RH, Lillemoe KD. Resected adenocarcinoma of the pancreas-616 patients: results, outcomes, and prognostic indicators. *J Gastrointest Surg* 2000; **4**: 567-579 [PMID: 11307091 DOI: 10.1016/S1091-255X(00)80105-5]

4 **Ramesh H**, Augustine P. Surgery in tropical pancreatitis: analysis of risk factors. *Br J Surg* 1992; **79**: 544-549 [PMID: 1611449 DOI: 10.1002/bjs.1800790623]

5 **Taylor B**. Carcinoma of the head of the pancreas versus chronic pancreatitis: diagnostic dilemma with significant consequences. *World J Surg* 2003; **27**: 1249-1257 [PMID: 14502404 DOI: 10.1007/s00268-003-7245-8]

6 **Goonetilleke KS**, Siriwardena AK. Systematic review of carbohydrate antigen (CA 19-9) as a biochemical marker in the diagnosis of pancreatic cancer. *Eur J Surg Oncol* 2007; **33**: 266-270 [PMID: 17097848 DOI: 10.1016/j.ejso.2006.10.004]

7 **Zhang S**, Wang YM, Sun CD, Lu Y, Wu LQ. Clinical value of serum CA19-9 levels in evaluating resectability of pancreatic carcinoma. *World J Gastroenterol* 2008; **14**: 3750-3753 [PMID: 18595144 DOI: 10.3748/wjg.14.3750]

8 **Sawabu N**, Watanabe H, Yamaguchi Y, Ohtsubo K, Motoo Y. Serum tumor markers and molecular biological diagnosis in pancreatic cancer. *Pancreas* 2004; **28**: 263-267 [PMID: 15084968 DOI: 10.1097/00006676-200404000-00009]

9 **Li D**, Xie K, Wolff R, Abbruzzese JL. Pancreatic cancer. *Lancet* 2004; **363**: 1049-1057 [PMID: 15051286 DOI: 10.1016/S0140-6736(04)15841-8]

10 **Agarwal B**, Correa AM, Ho L. Survival in pancreatic carcinoma based on tumor size. *Pancreas* 2008; **36**: e15-e20 [PMID: 18192868 DOI: 10.1097/mpa.0b013e31814de421]

11 **Bossuyt PM**, Reitsma JB, Bruns DE, Gatsonis CA, Glasziou PP, Irwig LM, Lijmer JG, Moher D, Rennie D, de Vet HC. Towards complete and accurate reporting of studies of diagnostic accuracy: the STARD initiative. The Standards for Reporting of Diagnostic Accuracy Group. *Croat Med J* 2003; **44**: 635-638 [PMID: 14515428]

12 **Whiting P**, Rutjes AW, Reitsma JB, Bossuyt PM, Kleijnen J. The development of QUADAS: a tool for the quality assessment of studies of diagnostic accuracy included in systematic reviews. *BMC Med Res Methodol* 2003; **3**: 25 [PMID: 14606960 DOI: 10.1186/1471-2288-3-25]

13 **Devillé WL**, Buntinx F, Bouter LM, Montori VM, de Vet HC, van der Windt DA, Bezemer PD. Conducting systematic reviews of diagnostic studies: didactic guidelines. *BMC Med Res Methodol* 2002; **2**: 9 [PMID: 12097142 DOI: 10.1186/1471-2288-2-9]

14 **Lau J**, Ioannidis JP, Balk EM, Milch C, Terrin N, Chew PW, Salem D. Diagnosing acute cardiac ischemia in the emergency department: a systematic review of the accuracy and clinical effect of current technologies. *Ann Emerg Med* 2001; **37**: 453-460 [PMID: 11326181 DOI: 10.1067/mem.2001.114903]

15 **Moses LE**, Shapiro D, Littenberg B. Combining independent studies of a diagnostic test into a summary ROC curve: data-analytic approaches and some additional considerations. *Stat Med* 1993; **12**: 1293-1316 [PMID: 8210827 DOI: 10.1002/sim.4780121403]

16 **Irwig L**, Tosteson AN, Gatsonis C, Lau J, Colditz G, Chalmers TC, Mosteller F. Guidelines for meta-analyses evaluating diagnostic tests. *Ann Intern Med* 1994; **120**: 667-676 [PMID: 8135452 DOI: 10.7326/0003-4819-120-8-199404150-00008]

17 **Vamvakas EC**. Meta-analyses of studies of the diagnostic accuracy of laboratory tests: a review of the concepts and methods. *Arch Pathol Lab Med* 1998; **122**: 675-686 [PMID: 9701328]

18 **Suzuki S**, Moro-oka T, Choudhry NK. The conditional relative odds ratio provided less biased results for comparing diagnostic test accuracy in meta-analyses. *J Clin Epidemiol* 2004; **57**: 461-469 [PMID: 15196616 DOI: 10.1016/j.jclinepi.2003.09.017]

19 **Westwood ME**, Whiting PF, Kleijnen J. How does study quality affect the results of a diagnostic meta-analysis? *BMC Med Res Methodol* 2005; **5**: 20 [PMID: 15943861 DOI: 10.1186/1471-2288-5-20]

20 **Egger M**, Davey Smith G, Schneider M, Minder C. Bias in meta-analysis detected by a simple, graphical test. *BMJ* 1997; **315**: 629-634 [PMID: 9310563 DOI: 10.1136/bmj.315.7109.629]

21 **Wang TH**, Lin JT, Chen DS, Sheu JC, Sung JL. Noninvasive diagnosis of advanced pancreatic cancer by real-time ultrasonography, carcinoembryonic antigen, and carbohydrate antigen 19-9. *Pancreas* 1986; **1**: 219-223 [PMID: 3554223 DOI: 10.1097/00006676-198605000-00004]

22 **Safi F**, Roscher R, Bittner R, Schenkluhn B, Dopfer HP, Beger HG. High sensitivity and specificity of CA 19-9 for pancreatic carcinoma in comparison to chronic pancreatitis. Serological and immunohistochemical findings. *Pancreas* 1987; **2**: 398-403 [PMID: 3306667 DOI: 10.1097/00006676-198707000-00006]

23 **Sakamoto K**, Haga Y, Yoshimura R, Egami H, Yokoyama Y, Akagi M. Comparative effectiveness of the tumour diagnostics, CA 19-9, CA 125 and carcinoembryonic antigen in patients with diseases of the digestive system. *Gut* 1987; **28**: 323-329 [PMID: 3471687 DOI: 10.1136/gut.28.3.323]

24 **Friess H**, Büchler M, Auerbach B, Weber A, Malfertheiner P, Hammer K, Madry N, Greiner S, Bosslet K, Beger HG. CA 494--a new tumor marker for the diagnosis of pancreatic cancer. *Int J Cancer* 1993; **53**: 759-763 [PMID: 8449599 DOI: 10.1002/ijc.2910530509]

25 **Röthlin MA**, Joller H, Largiadèr F. CA 242 is a new tumor marker for pancreatic cancer. *Cancer* 1993; **71**: 701-707 [PMID: 8431849]

26 **Haglund C**, Lundin J, Kuusela P, Roberts PJ. CA 242, a new tumour marker for pancreatic cancer: a comparison with CA 19-9, CA 50 and CEA. *Br J Cancer* 1994; **70**: 487-492 [PMID: 8080735 DOI: 10.1038/bjc.1994.332]

27 **Kuno N**, Kurimoto K, Fukushima M, Hayakawa T, Shibata T, Suzuki T, Sakakibara A, Katada N, Nakano S, Takayama T. Effectiveness of multivariate analysis of tumor markers in diagnosis of pancreatic carcinoma: a prospective study in multiinstitutions. *Pancreas* 1994; **9**: 725-730 [PMID: 7531333 DOI: 10.1097/00006676-199411000-00009]

28 **Pasquali C**, Sperti C, D'Andrea AA, Costantino V, Filipponi C, Pedrazzoli S. Clinical value of serum TAG-72 as a tumor

marker for pancreatic carcinoma. Comparison with CA 19-9. *Int J Pancreatol* 1994; **15**: 171-177 [PMID: 7930777]
29 **Satake K**, Takeuchi T. Comparison of CA19-9 with other tumor markers in the diagnosis of cancer of the pancreas. *Pancreas* 1994; **9**: 720-724 [PMID: 7846015 DOI: 10.1097/00006676-199411000-00008]
30 **Hámori J**, Arkosy P, Lenkey A, Sápy P. The role of different tumor markers in the early diagnosis and prognosis of pancreatic carcinoma and chronic pancreatitis. *Acta Chir Hung* 1997; **36**: 125-127 [PMID: 9408313]
31 **Safi F**, Schlosser W, Kolb G, Beger HG. Diagnostic value of CA 19-9 in patients with pancreatic cancer and nonspecific gastrointestinal symptoms. *J Gastrointest Surg* 1997; **1**: 106-112 [PMID: 9834336]
32 **Hayakawa T**, Naruse S, Kitagawa M, Ishiguro H, Kondo T, Kurimoto K, Fukushima M, Takayama T, Horiguchi Y, Kuno N, Noda A, Furukawa T. A prospective multicenter trial evaluating diagnostic validity of multivariate analysis and individual serum marker in differential diagnosis of pancreatic cancer from benign pancreatic diseases. *Int J Pancreatol* 1999; **25**: 23-29 [PMID: 10211418]
33 **Kim HJ**, Kim MH, Myung SJ, Lim BC, Park ET, Yoo KS, Seo DW, Lee SK, Min YI. A new strategy for the application of CA19-9 in the differentiation of pancreaticobiliary cancer: analysis using a receiver operating characteristic curve. *Am J Gastroenterol* 1999; **94**: 1941-1946 [PMID: 10406263 DOI: 10.1111/j.1572-0241.1999.01234.x]
34 **Manes G**, Spada OA, Rabitti PG, Feola B, Misso S, Minerva A, Uomo G. Neopterin serum levels in pancreatic adenocarcinoma. *Int J Pancreatol* 1999; **25**: 31-37 [PMID: 10211419]
35 **Slesak B**, Harlozinska-Szmyrka A, Knast W, Sedlaczek P, van Dalen A, Einarsson R. Tissue polypeptide specific antigen (TPS), a marker for differentiation between pancreatic carcinoma and chronic pancreatitis. A comparative study with CA 19-9. *Cancer* 2000; **89**: 83-88 [PMID: 10897004]
36 **Maire F**, Micard S, Hammel P, Voitot H, Lévy P, Cugnenc PH, Ruszniewski P, Puig PL. Differential diagnosis between chronic pancreatitis and pancreatic cancer: value of the detection of KRAS2 mutations in circulating DNA. *Br J Cancer* 2002; **87**: 551-554 [PMID: 12189555 DOI: 10.1038/sj.bjc.6600475]
37 **Akashi T**, Oimomi H, Nishiyama K, Nakashima M, Arita Y, Sumii T, Kimura T, Ito T, Nawata H, Watanabe T. Expression and diagnostic evaluation of the human tumor-associated antigen RCAS1 in pancreatic cancer. *Pancreas* 2003; **26**: 49-55 [PMID: 12499917 DOI: 10.1097/00006676-200301000-00009]
38 **Mu DQ**, Wang GF, Peng SY. p53 protein expression and CA19.9 values in differential cytological diagnosis of pancreatic cancer complicated with chronic pancreatitis and chronic pancreatitis. *World J Gastroenterol* 2003; **9**: 1815-1818 [PMID: 12918127]
39 **Cwik G**, Wallner G, Skoczylas T, Krzyzanowski M, Ciechainski A, Madro P. Elevated tumor marker CA 19-9 in the differential diagnosis of pancreatic mass lesions. *Ann Univ Mariae Curie Sklodowska Med* 2004; **59**: 213-218 [PMID: 16146081]
40 **Jiang JT**, Wu CP, Deng HF, Lu MY, Wu J, Zhang HY, Sun WH, Ji M. Serum level of TSGF, CA242 and CA19-9 in pancreatic cancer. *World J Gastroenterol* 2004; **10**: 1675-1677 [PMID: 15162550]
41 **Ventrucci M**, Cipolla A, Racchini C, Casadei R, Simoni P, Gullo L. Tumor M2-pyruvate kinase, a new metabolic marker for pancreatic cancer. *Dig Dis Sci* 2004; **49**: 1149-1155 [PMID: 15387337]
42 **Teich N**, Kleeff J, Lochs H, Mössner J, Keim V, Friess H, Ockenga J. The presence of the proteolysis-inducing factor in urine does not predict the malignancy of a pancreatic tumour. *BMC Gastroenterol* 2005; **5**: 20 [PMID: 15969757 DOI: 10.1186/1471-230x-5-20]
43 **Chang MC**, Chang YT, Su TC, Yang WS, Chen CL, Tien YW, Liang PC, Wei SC, Wong JM. Adiponectin as a potential differential marker to distinguish pancreatic cancer and chronic pancreatitis. *Pancreas* 2007; **35**: 16-21 [PMID: 17575540 DOI: 10.1097/MPA.0b013e3180547709]
44 **Kuhlmann KF**, van Till JW, Boermeester MA, de Reuver PR, Tzvetanova ID, Offerhaus GJ, Ten Kate FJ, Busch OR, van Gulik TM, Gouma DJ, Crawford HC. Evaluation of matrix metalloproteinase 7 in plasma and pancreatic juice as a biomarker for pancreatic cancer. *Cancer Epidemiol Biomarkers Prev* 2007; **16**: 886-891 [PMID: 17507610 DOI: 10.1158/1055-9965.epi-06-0779]
45 **Liao Q**, Zhao YP, Yang YC, Li LJ, Long X, Han SM. Combined detection of serum tumor markers for differential diagnosis of solid lesions located at the pancreatic head. *Hepatobiliary Pancreat Dis Int* 2007; **6**: 641-645 [PMID: 18086633]
46 **Bedi MM**, Gandhi MD, Jacob G, Lekha V, Venugopal A, Ramesh H. CA 19-9 to differentiate benign and malignant masses in chronic pancreatitis: is there any benefit? *Indian J Gastroenterol* 2009; **28**: 24-27 [PMID: 19529898 DOI: 10.1007/s12664-009-0005-4]
47 **Firpo MA**, Gay DZ, Granger SR, Scaife CL, DiSario JA, Boucher KM, Mulvihill SJ. Improved diagnosis of pancreatic adenocarcinoma using haptoglobin and serum amyloid A in a panel screen. *World J Surg* 2009; **33**: 716-722 [PMID: 19082654 DOI: 10.1007/s00268-008-9853-9]
48 **Liao WC**, Wu MS, Wang HP, Tien YW, Lin JT. Serum heat shock protein 27 is increased in chronic pancreatitis and pancreatic carcinoma. *Pancreas* 2009; **38**: 422-426 [PMID: 19214136 DOI: 10.1097/MPA.0b013e318198281d]
49 **Morris-Stiff G**, Teli M, Jardine N, Puntis MC. CA19-9 antigen levels can distinguish between benign and malignant pancreaticobiliary disease. *Hepatobiliary Pancreat Dis Int* 2009; **8**: 620-626 [PMID: 20007080]
50 **Talar-Wojnarowska R**, Gasiorowska A, Olakowski M, Lekstan A, Lampe P, Malecka-Panas E. Clinical value of serum neopterin, tissue polypeptide-specific antigen and CA19-9 levels in differential diagnosis between pancreatic cancer and chronic pancreatitis. *Pancreatology* 2010; **10**: 689-694 [PMID: 21242708 DOI: 10.1159/000320693]
51 **Zapico-Muñiz E**, Farré-Viladrich A, Rico-Santana N, González-Sastre F, Mora-Brugués J. Standardized peptidome profiling of human serum for the detection of pancreatic cancer. *Pancreas* 2010; **39**: 1293-1298 [PMID: 20924310 DOI: 10.1097/MPA.0b013e3181dfcbe5]
52 **Chung HW**, Lim JB. Clinical significance of serum levels of immune-associated molecules, uric acid and soluble MHC class I chain-related molecules A and B, as diagnostic tumor markers for pancreatic ductal adenocarcinoma. *Cancer Sci* 2011; **102**: 1673-1679 [PMID: 21615621 DOI: 10.1111/j.1349-7006.2011.01989.x]
53 **Gold DV**, Gaedcke J, Ghadimi BM, Goggins M, Hruban RH, Liu M, Newsome G, Goldenberg DM. PAM4 enzyme immunoassay alone and in combination with CA 19-9 for the detection of pancreatic adenocarcinoma. *Cancer* 2013; **119**: 522-528 [PMID: 22898932 DOI: 10.1002/cncr.27762]
54 **Kaur S**, Chakraborty S, Baine MJ, Mallya K, Smith LM, Sasson A, Brand R, Guha S, Jain M, Wittel U, Singh SK, Batra SK. Potentials of plasma NGAL and MIC-1 as biomarker(s) in the diagnosis of lethal pancreatic cancer. *PLoS One* 2013; **8**: e55171 [PMID: 23383312 DOI: 10.1371/journal.pone.0055171]
55 **Koprowski H**, Herlyn M, Steplewski Z, Sears HF. Specific antigen in serum of patients with colon carcinoma. *Science* 1981; **212**: 53-55 [PMID: 6163212 DOI: 10.1126/science.6163212]
56 **Boeck S**, Stieber P, Holdenrieder S, Wilkowski R, Heinemann V. Prognostic and therapeutic significance of carbohydrate antigen 19-9 as tumor marker in patients with pancreatic cancer. *Oncology* 2006; **70**: 255-264 [PMID: 16899980 DOI: 10.1159/000094888]
57 **Rosty C**, Goggins M. Early detection of pancreatic carcinoma. *Hematol Oncol Clin North Am* 2002; **16**: 37-52 [PMID: 12063828 DOI: 10.1016/S0889-8588(01)00007-7]
58 **Ballehaninna UK**, Chamberlain RS. The clinical utility of serum CA 19-9 in the diagnosis, prognosis and management of pancreatic adenocarcinoma: An evidence based appraisal. *J Gastrointest Oncol* 2012; **3**: 105-119 [PMID: 22811878 DOI: 10.3978/j.issn.2078-6891.2011.021]
59 **Glas AS**, Lijmer JG, Prins MH, Bonsel GJ, Bossuyt PM. The diagnostic odds ratio: a single indicator of test performance. *J Clin Epidemiol* 2003; **56**: 1129-1135 [PMID: 14615004 DOI: 10.1016/

S0895-4356(03)00177-X]
60 **Deeks JJ**. Systematic reviews in health care: Systematic reviews of evaluations of diagnostic and screening tests. *BMJ* 2001; **323**: 157-162 [PMID: 11463691 DOI: 10.1136/bmj.323.7305.157]

P- Reviewer: Chen JQ, Kim TH **S- Editor**: Yu J
L- Editor: Wang TQ **E- Editor**: Liu XM

World Journal of Gastroenterology

Submit a Manuscript: http://www.wjgnet.com/esps/
Help Desk: http://www.wjgnet.com/esps/helpdesk.aspx
DOI: 10.3748/wjg.v21.i14.4334

World J Gastroenterol 2015 April 14; 21(14): 4334-4344
ISSN 1007-9327 (print) ISSN 2219-2840 (online)

META-ANALYSIS

Superparamagnetic iron oxide-enhanced magnetic resonance imaging for focal hepatic lesions: Systematic review and meta-analysis

You-Wei Li, Zheng-Guang Chen, Ji-Chen Wang, Zong-Ming Zhang

You-Wei Li, Department of Radiology, Beijing Chuiyangliu Hospital Affiliated to School of Medicine, Tsinghua University, Beijing 100022, China
Zheng-Guang Chen, Department of Radiology, Dongzhimen Hospital Affiliated to Beijing University of Chinese Medicine, Beijing 100700, China
Ji-Chen Wang, Department of Radiology, Nanjing BenQ Hospital, Nanjing 210036, Jiangsu Province, China
Zong-Ming Zhang, Department of General Surgery, Beijing Electric Power Hospital, Capital Medical University, Beijing 100073, China
Author contributions: Zhang ZM designed the study; Li YW, Chen ZG and Wang JC searched and reviewed the literature; Wang JC provided analytic tools and analyzed the data; Li YW and Chen ZG wrote the paper.

Correspondence to: Zong-Ming Zhang, MD, PhD, Professor, Director, Department of General Surgery, Beijing Electric Power Hospital, Capital Medical University, No. 1 Taipingqiaoxili, Fengtai District, Beijing 100073, China. zhangzongming@mail.tsinghua.edu.cn
Telephone: +86-10-63503046
Fax: +86-10-63465865
Received: September 9, 2014
Peer-review started: September 10, 2014
First decision: October 14, 2014
Revised: October 25, 2014
Accepted: November 19, 2014
Article in press: November 19, 2014
Published online: April 14, 2015

Abstract

AIM: To evaluate the performance of superparamagnetic iron oxide (SPIO)-enhanced magnetic resonance imaging (MRI) in the detection and characterization of focal hepatic lesions (FHLs).

METHODS: This meta-analysis compared relevant studies that were identified by searching PubMed, EMBASE, and the Cochrane Library databases for articles published between January 1988 and September 2014 and that met the following criteria: (1) SPIO-enhanced MRI was conducted to identify FHLs and data were sufficient for pooled analysis using Meta-DiSc 1.4; (2) hepatocellular carcinomas (HCCs) were differentiated from other FHLs; (3) well-differentiated HCCs (WD-HCCs) were contradistinguished from dysplastic nodules; and (4) WD-HCCs were compared with moderately and poorly differentiated HCCs (MD- and PD-HCCs, respectively).

RESULTS: The data obtained from 15 eligible studies yielded a sensitivity of 85% and a specificity of 78% for differentiating between HCCs and other FHLs. The sensitivity was unchanged and the specificity was increased to 87% when non-HCC malignancies were excluded. Comparative analyses between WD-HCCs and MD- and PD-HCCs from seven studies showed a sensitivity of 98% and a specificity of 50% for the diagnosis of MD- and PD-HCCs, and the area under the summary receiver operating characteristics (sROC) curve was 0.97. A comparison between WD-HCCs and dysplastic nodules revealed a sensitivity of 50% and a specificity of 92% for the diagnosis of WD-HCCs and the area under the sROC curve was 0.80.

CONCLUSION: SPIO-enhanced MRI is useful in differentiating between HCCs and other FHLs.

Key words: Hepatocellular carcinomas; Magnetic resonance imaging; Meta-analysis; Other lesions; USPIO

Core tip: Relevant studies on the performance of superparamagnetic iron oxide (SPIO)-enhanced magnetic resonance imaging (MRI) in the detection and characterization of focal hepatic lesions were identified by searching PubMed, EMBASE, and the Cochrane Library databases for articles published between January 1988 and September 2014 *via* a systematic review and meta-analysis. The results show that SPIO-enhanced MRI is useful in differentiating between hepatocellular carcinomas (HCCs) and other focal hepatic lesions. Using hyperintensity on SPIO-enhanced T2*-weighted images as the criterion, the sensitivity for diagnosing advanced HCC was 98%. SPIO-enhanced MRI is a valuable tool for the detection and characterization of focal lesions in cirrhotic liver.

Li YW, Chen ZG, Wang JC, Zhang ZM. Superparamagnetic iron oxide-enhanced magnetic resonance imaging for focal hepatic lesions: Systematic review and meta-analysis. *World J Gastroenterol* 2015; 21(14): 4334-4344 Available from: URL: http://www.wjgnet.com/1007-9327/full/v21/i14/4334.htm DOI: http://dx.doi.org/10.3748/wjg.v21.i14.4334

INTRODUCTION

Hepatocellular carcinoma (HCC) is one of the most common cancers, and the third leading cause of cancer-related death worldwide. During the last two decades, progress in multimodality therapy has increased the rate of survival and improved the quality of life for patients with HCC. However, the overall prognosis of HCC is still poor and early diagnosis remains the key to improving prognosis. HCC often arises from the liver with chronic hepatitis B or C virus infection or cirrhosis[1]. Based on the concept of stepwise hepatocarcinogenesis, HCC is considered to develop from a regenerative nodule to a dysplastic nodule (DN), and subsequently to a well-differentiated HCC (WD-HCC) and an advanced tumor [moderately differentiated (MD) and poorly differentiated (PD) HCCs]. WD-HCC has a relatively low malignant potential and rarely invades vessels or metastasizes to other sites. Patients with WD-HCC usually have a better survival rate than those with MD- or PD-HCC[1].

In clinical practice, it is critical to differentiate WD-HCC from advanced HCC and from other focal hepatic lesions (FHLs). Various imaging modalities have been used in the detection and characterization of HCCs, including ultrasonography (US), computed tomography (CT), magnetic resonance imaging (MRI), and positron emission tomography. MRI, especially dynamic contrast-enhanced MRI, provides better tissue contrast than US and CT, and is considered to be one of the most sensitive modalities for the diagnosis of HCC[2,3]. Currently, two types of MRI contrast agents have been used in liver MRI, extracellular fluid contrast agents such as gadolinium (Gd) chelates and liver-specific contrast agents such as superparamagnetic iron oxide (SPIO). Gd-enhanced MRI is based on the blood flow of lesions, while SPIO-enhanced MRI is largely dependent on the number and function of Kupffer cells in lesions. SPIO particles are taken up by Kupffer cells and predominantly shorten the T2 of hepatic parenchyma. Normal hepatic parenchyma and some FHLs contain Kupffer cells and therefore exhibit decreased signal intensity, whereas hepatic lesions without Kupffer cells show less or no change in signal intensity. In the case of lesions with Kupffer cells, the lesion-parenchyma contrast is enhanced, and thus the lesions are conspicuous on T2- and T2*-weighted MRI.

In recent years, the value of SPIO in the detection and characterization of FHLs has been emphasized and studies have demonstrated its usefulness[4-6]. In particular, SPIO-enhanced MRI is currently considered to be the only imaging modality that is capable of distinguishing HCC from DN, although it is limited when both HCC and DN contain a similar number of Kupffer cells[7-9]. The aim of this study was to determine the diagnostic performance of SPIO-enhanced MRI in differentiating between HCC and other FHLs *via* a systematic review and meta-analysis of the studies published on this topic.

MATERIALS AND METHODS

Study selection

PubMed, EMBASE, and the Cochrane Library databases were searched for articles published between January 1988 and September 2014. Eligible studies included those in which SPIO-enhanced MRI was conducted in patients with HCC or other hepatic lesions. The search strategy was: magnetic resonance imaging, MRI, or MR imaging and carcinoma, hepatocellular, liver neoplasms, liver lesion, HCC, or hepatic lesions and ferumoxtran-10, SPIO or USPIO. We identified additional articles by crosschecking related citations in the retrieved studies.

The inclusion criteria used in this meta-analysis were as follows: (1) MRI was conducted at a field strength of at least 0.5 T; (2) the diagnostic criteria for HCC and other malignant or benign lesions such as DN, focal nodular hyperplasia, and hemangioma, were clearly documented; (3) data were obtained with T2- or T2*-weighted MRI after intravenous injection of SPIO contrast agents; and (4) data were on a per-lesion basis and sufficient to construct a 2 × 2 contingency table so that the cells in the table could be labeled as true-positive (TP), false-positive (FP), true-negative (TN), or false-negative (FN). Studies were included when all criteria were met.

Four steps were used to select the articles for inclusion in this study. First, one reviewer screened the titles of all research articles identified from the database. Articles were selected when the studies met some of the inclusion criteria. Second, two reviewers screened the abstract of the selected articles

independently and the articles were further assessed if the information was sufficient. Third, the eligible full articles were obtained through online sources, library visits, and interlibrary loan requests. The full papers were then reviewed independently by two reviewers to decide whether the reported studies should be included. Disagreement between the two reviewers was resolved by consensus or by a third reviewer. The references listed in the selected articles were also searched to identify further relevant articles. Finally, the quality of all included articles was evaluated based on the quality assessment of diagnostic accuracy studies (QUADAS)[10].

Data extraction

To meta-analyze the diagnostic accuracy in different hepatic lesions and to calculate the number of TP, FP, FN, and TN results in each study, data were extracted using the following criteria: the lesions with iso- or hypointensity on SPIO-enhanced MR images were considered negative. The lesions with hyperintensity with a focal, high signal intensity were classified as positive. If there were two sets of data obtained by T2- and T2*-weighted imaging in the same study, the data obtained by T2*-weighted imaging were extracted as susceptibility is maximized on this sequence. Data extracted from studies also included some general information: publications (first author, country, language, and date of publication), patients and lesions (number and mean age of patients, and number, type and mean size of lesions), MRI (magnetic field strength, sequence, contrast agent, and dosage), and MR image evaluation (criteria used to confirm the lesions, and whether the interpreters of the MR images were blinded to clinical information and/or the reference-standard examination results).

To evaluate the diagnostic performance of SPIO-enhanced MRI in FHLs, the extracted data were subgrouped according to the lesion's characteristics and a comparison was made between: (1) HCC and all other lesions (benign and non-HCC malignant lesions); (2) HCC and benign lesions; (3) WD-HCC and DN; and (4) WD-HCC and advanced HCC (MD- and PD-HCC).

Pooled analysis

The software Meta-DiSc version 1.4 (http://www.hrc.es/investigation/metadisc-en.htm) was used for the meta-analysis. The sensitivity and specificity were calculated using the formulas of TP/(TP + FN) and TN/(TN + FP), respectively. The diagnostic odds ratio (DOR) was calculated using the formula of (TP*TN)/(FP*FN). If the DOR could not be calculated when one of the cells in the 2 × 2 table was zero, 0.5 was added to all cells in that study.

First, a forest plot was used to assess the accuracy of the sensitivity and specificity in each study and to evaluate the heterogeneity across studies. One of the primary reasons for the heterogeneity among studies is the threshold effect. This issue may arise when different cut-off values or thresholds are used to define a positive or a negative test result. Therefore, we considered that the threshold effect existed when the forest plots showed increasing sensitivities along with decreasing specificities, or *vice versa*. In this case, Spearman rank correlation was used as a further test for the threshold effect and an inverse correlation between sensitivity and specificity indicated the presence of the threshold effect. Considering that some other factors might also result in heterogeneity among studies, we also assessed the heterogeneity using the Cochran *Q*, χ^2 and I^2 tests. When the Cochran *Q* test was significant or the I^2 > 50%, heterogeneity was considered to exist.

Second, we calculated the pooled sensitivity and specificity. If heterogeneity due to the threshold effect was present, the accuracy data were pooled by fitting the summary receiver operating characteristics (sROC) curve, and the area under the curve and *Q** (defined by the point where sensitivity equaled specificity) were calculated. In cases where heterogeneity was due to sources other than the threshold effect, the random effects model (DerSimonian-Laird method) was used instead of the fixed effects model (Mantel-Haenszel method) for calculation of pooled sensitivity and specificity with a 95%CI. The asymmetric sROC curve was reconstructed with Moses' model regression.

Third, meta-regression analysis was performed by extending the Moses-Shapiro-Littenberg method to explore the sources of heterogeneity among studies. The covariates evaluated in this study included the number and mean size of lesions, the mean age of patients, the magnetic field strength and imaging sequence, the contrast agent and dosage, the criteria used to confirm the characteristics of lesions, and whether the interpreter of the MR images was blinded to clinical information and/or the reference-standard examination results. Because the number of studies was small, we tested one covariate at a time. A $P < 0.05$ was considered significant.

RESULTS

Study selection and data extraction

A total of 365 relevant articles were initially identified, of which 236 studies were excluded after reviewing the titles. Abstract review of the remaining 129 studies by two reviewers excluded an additional 105 studies. Twelve articles were added after checking the related citations and by screening the reference list of the included articles. On review of the full-texts of the 36 articles, 15 eligible studies were included and data were extracted (Table 1) for meta-analysis (Figure 1). Almost perfect agreement (κ = 0.95) was achieved between the two reviewers during selection of the articles.

The total number of hepatic lesions in the 15 studies was 958, ranging from 10 to 216. The majority of lesions were confirmed pathologically and a few

Table 1 Characteristics of 15 studies included in the meta-analysis

Ref.	Year	Country	Subject					MRI				Result	
			Patients (*n*)	Age (yr)	Lesions (*n*)	Lesion type	Size (cm)	Type	Sequence	Contrast agent	Dose	Iso-/hypo	Hyper-
Harisinghani *et al*[12]	1997	United States	35	46	15	Hemangioma	NC	1.5T	T2WI	Code-7227	1.1 mg Fe/kg	13	2
					17	Metastases	NC					0	17
					6	HCC	NC					2	4
Imai *et al*[19]	2000	Japan	27	62	6	DN	1.6	1.5T	T2*WI	Ferumoxide	10 μmol/kg	6	0
					13	WD-HCC	1.6					11	2
					10	MD-HCC	1.6					0	10
					8	PD-HCC	1.6					0	8
Lim *et al*[15]	2001	South Korea	68	51	10	WD-HCC	2.1	1.5T	T2*WI	Ferumoxide	15 μmol/kg	6	4
					69	MDPD-HCC	5.3					0	69
					19	DN	0.8					19	0
Zheng *et al*[11]	2002	China	43	51	22	HCC	< 3	1.5T	T2WI	Feridex	0.05 mL/kg	0	22
					7	Other malignancy	< 3					0	7
					4	Cirrhotic nodules	< 3					4	0
					5	Hemangioma						0	5
					5	FNH						0	5
					4	Others						0	4
Zhang *et al*[20]	2003	China	30	50	30	HCCs	NC	0.5T	T2WI	Feridex	0.56 mL/kg	0	30
					6	Regenerative nodules						6	0
Suzuki *et al*[21]	2004	Japan	45	66	41	HCCs	2.26	1.5T	T2*WI	Ferumoxide	0.05 mL/kg	7	34
					11	Benign						10	1
Kato *et al*[22]	2004	Japan	43	66	17	WD-HCC	3.00	1.5T	T2*WI	Ferumoxide	10 mmol/kg	4	13
					28	MD-HCC	3.00					1	27
					6	PD-HCC	3.20					0	6
Inoue *et al*[24]	2005	Japan	49	67	20	WD-HCC	2.70	1.5T	T2*WI	Ferumoxide	0.016 mL/kg	4	16
					20	MDPD-HCC						0	20
					9	DNs						8	1
Kobayashi *et al*[9]	2007	Japan	10	45	6	DNs	NC	1.5T	T2WI	Ferucarbotran	NC	6	0
					4	HCC						0	4
Park *et al*[18]	2009	South Korea	114	55	37	WD-HCC	2.38	3.0T	T2*WI	Ferucarbotran	8 mmol/kg	20	17
					156	MDPD-HCC	4.10					6	149
					23	DNs	1.28					22	1
Macarini *et al*[7]	2009	Italy	22	53	14	HCC	1.70	1.5T	T2*WI	Ferumoxide	NC	0	14
					3	WD-HCC							
					11	MDPD-HCC							
					4	DN with HCC	2.10					0	4
					39	DNs	0.80					39	0
					2	Cystadenoma	1.20					2	0
Yoon *et al*[16]	2009	South Korea	28	51	33	DNs	1.31	3.0T	T2*WI	Ferucarbotran	1.4 mL, ⩾ 60 kg	25	8
					32	WD-HCC	1.79				0.9 mL, < 60 kg	13	19
Yoo *et al*[8]	2009	South Korea	108	56	124	HCCs	3.00	3.0T	T2*WI	Ferucarbotran	1.4 mL, ⩾ 60 kg	16	108
					28	DNs					0.9 mL, < 60 kg	25	3
Okada *et al*[23]	2010	Japan	36	69	22	WD-HCC	1.40	1.5T	T2*WI	Ferucarbotran	0.45 mg Fe/kg	15	7
					15	MDPD-HCC	2.40					0	15
					4	DNs	1.60					4	0
Chou *et al*[25]	2011	Taiwan	12	56	11	HCC	2.30	1.5T	T2*WI	Ferucarbotran	1.4 mL, > 50 kg	3	8
					6	Benign	1.60					6	0

DN: Nodular dysplasia; FNH: Focal nodular hyperplasia; HCC: Hepatocellular carcinoma; hyper: Hyperintensity; iso-/hypo: Isointensity/hypointensity; MD: Moderately-differentiated, NC: Not clear; PD: Poorly-differentiated; WD: Well-differentiated; MRI: Magnetic resonance imaging.

were diagnosed on the basis of clinical findings, biochemical tests, and clinical follow-up (⩾ 6 mo). The pathologic specimens in all studies were obtained by needle biopsy, hepatic resection, or transplantation, except in two studies[11,12], in which the acquirement of specimens was not clearly stated. HCC was graded pathologically as WD-HCC, MD-HCC, and PD-HCC, according to the classification criteria of primary hepatic cancer by the Liver Cancer Study Group of Japan[13]. DN was defined using the criteria of the International Working Party on the Terminology of Nodular Hepatocellular Lesions[14].

We assessed the quality of the 15 studies using the 13-item QUADAS tool. All studies had an overall score of 10 or more, except one study that had a score of 6 (Table 2)[11]. Four of the 13 items were scored as "1" in all studies, including item 2 (clearly describing selection criteria), item 7 (execution of

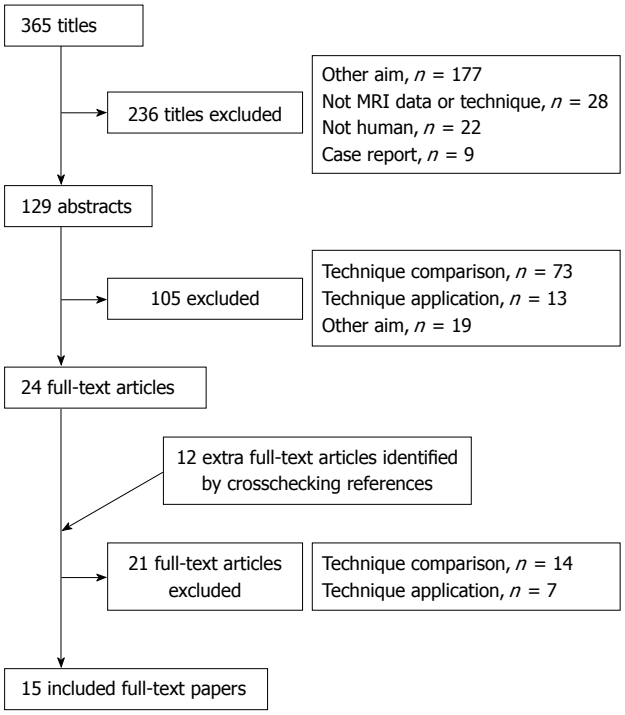

Figure 1 Flow chart of process used to select eligible articles.

the index test described in sufficient detail to permit its replication), item 12 (reporting of uninterpretable results), and item 13 (explanation of withdrawals from the study). Four of the 15 items were scored as "1" in 13/15 to 14/15 studies, including item 1 (the spectrum of tested patients representing the patients in whom the test will be used in practice), item 3 (the reference standard likely to correctly classify the target condition), item 5 (the whole sample receiving verification using a reference standard of diagnosis), and item 6 (patients receiving the same reference standard regardless of the index test result). Some items were poorly reported, which yielded various levels of bias. Item 9, related to information on clinical data during interpretation of test results, might affect the estimates of test performance as it was not reported clearly in any of the included studies. The period between the reference standard and index test, which might cause disease progression bias, was reported only in three studies. Nearly half of the studies insufficiently described the reference standard test, which may have had an impact on the test performance. Two other items that were reported in less than 50% of the included studies and might be related to review bias were the index test results interpreted without knowledge of the results of the reference standard (40%) and the reference standard results interpreted without knowledge of the results of the index test (33%).

Pooled analysis

The Spearman rank correlation coefficient used to test accuracy in all studies was -0.266 (P = 0.358) (Table 3), indicating no threshold effect. A comparison between HCC and all other liver lesions from 14 eligible studies showed that the sensitivity for diagnosing HCC was 85% (95%CI: 0.82-0.88) and the specificity was 78% (95%CI: 0.73-0.83). There was substantial heterogeneity across these studies for sensitivity (I^2 = 80.9) and specificity (I^2 = 89.0)

Table 2 Quality assessment of diagnostic accuracy studies scores[1] for each included study

Ref.	QUADAS items												
	1	2	3	4	5	6	7	8	9	10	11	12	13
Zheng *et al*[11]	0	1	0	0.5	0	0	1	0	0.5	0.5	0.5	1	1
Imai *et al*[19]	1	1	1	0.5	1	1	1	0	1	0.5	0.5	1	1
Lim *et al*[15]	1	1	1	0.5	1	1	1	1	0.5	1	0.5	1	1
Zhang *et al*[20]	1	1	1	0.5	1	1	1	0	0.5	1	0.5	1	1
Inoue *et al*[24]	1	1	1	0.5	1	1	1	1	0.5	1	0.5	1	1
Park *et al*[18]	1	1	1	0.5	1	1	1	1	0	0.5	0.5	1	1
Macarini *et al*[7]	1	1	1	1	1	1	1	0	1	0.5	0.5	1	1
Yoon *et al*[16]	1	1	1	0.5	1	1	1	1	1	1	0.5	1	1
Harisinghani *et al*[12]	1	1	1	0.5	0	1	1	1	1	0.5	0.5	1	1
Yoo *et al*[8]	1	1	1	0.5	1	1	1	1	0	0.5	0.5	1	1
Suzuki *et al*[21]	1	1	1	0.5	1	1	1	0	0.5	0.5	0.5	1	1
Kobayashi *et al*[9]	1	1	1	0.5	1	1	1	0	1	0.5	0.5	1	1
Kato *et al*[22]	1	1	1	1	1	1	1	1	1	0	0.5	1	1
Okada *et al*[23]	1	1	1	0.5	1	1	1	0.5	0.5	1	1	1	1
Chou *et al*[25]	1	1	1	1	1	1	1	0	0.5	0.5	0.5	1	1

[1]1 = yes; 0 = no; 0.5 = unclear. Quality assessment of diagnostic accuracy studies (QUADAS) items: (1) Was the spectrum of a patient representative of the patients who will receive the test in practice? (2) Were the selection criteria clearly described? (3) Is the reference standard likely to correctly classify the target condition? (4) Is the time period between the index test and reference standard short enough to ensure that the target condition did not change between the two tests? (5) Did the whole sample or a random selection of the sample receive verification using a reference standard of diagnosis? (6) Did patients receive the same reference standard regardless of the index test result? (7) Was the execution of the index test described in sufficient detail to permit replication of the test? (8) Was the execution of the reference standard test described in sufficient detail to permit its replication? (9) Were the index test results interpreted without knowledge of the results of the reference standard? (10) Were the reference standard results interpreted without knowledge of the results of the index test? (11) Were the same clinical data available when the test results were interpreted as would be available when the test is used in clinical practice? (12) Were uninterpretable or intermediate test results reported? (13) Were withdrawals from the study explained?

Table 3 Assessment of the threshold effect in all accuracy studies

Weighted regression (inverse variance)				
Variable	**Coefficient**	**SE**	***t***	***P* value**
a	3.643	0.548	6.652	0.0000
b(1)	-0.239	0.314	0.760	0.4617

τ^2 = 2.3703 (convergence is achieved after five iterations); Restricted Maximum Likelihood estimation (REML). n = 14; Filter OFF; Add 0.5 to all cells of the studies with zero. Spearman correlation coefficient: -0.266, P = 0.358; Logit (true positive rate) *vs* Logit (false positive rate); Moses' model (D = a + bS).

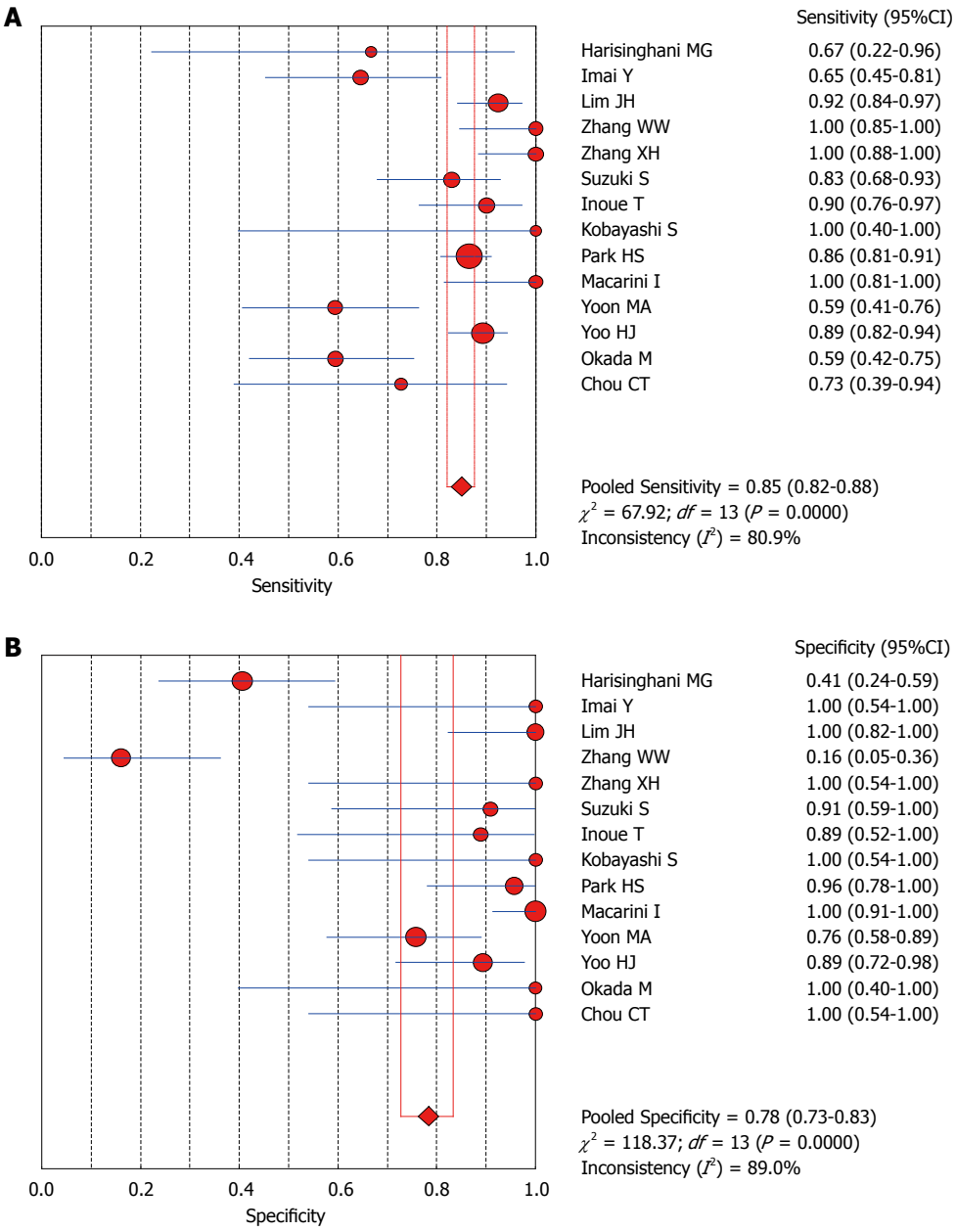

Figure 2 Forest plots for comparing hepatocellular carcinomas with all other liver lesions. A: Sensitivity; B: Specificity of 14 studies.

(Figure 2). The sensitivity was essentially unchanged when comparing HCC with benign liver lesions, but the specificity increased to 87% (95%CI: 0.82-0.91), with substantial heterogeneity across these studies for sensitivity (I^2 = 80.9) and specificity (I^2 = 81.2) (Figure 3). Seven eligible studies were used for a comparative analysis between advanced HCC (MD-/PD-HCC) and WD-HCC, and the sensitivity and specificity for diagnosing advanced HCCs were 0.98 (95%CI: 0.95-0.99) and 0.50 (95%CI: 0.41-0.60), respectively. The heterogeneity across these studies was less for sensitivity (I^2 = 30.9) and slightly larger for specificity (I^2 = 78.4) (Figure 4). The area under the sROC curve for the seven studies used for comparing advanced HCC with WD-HCC was 0.97, and the Q^* was 0.92 (Figure 5A). A comparison between WD-HCC and DN was performed with the data extracted from seven eligible studies, and the pooled sensitivity and specificity for diagnosing WD-HCC were 0.50 (95%CI: 0.41-0.58) and 0.92 (95%CI: 0.87-0.96), respectively, with substantial heterogeneity across these studies for sensitivity (I^2 = 74.4) and specificity (I^2 = 69.9) (Figure 6). The area under the sROC curve was 0.80, and the Q^* was 0.74 (Figure 5B). All calculations for the pooled sensitivity and specificity in the present analysis were based on the random effects model due to notable heterogeneity across the studies.

To explore the possible sources of heterogeneity, we performed meta-regression analysis using the extended Moses-Shapiro-Littenberg method. The results showed that none of the covariates described in Materials and Methods significantly contributed to the

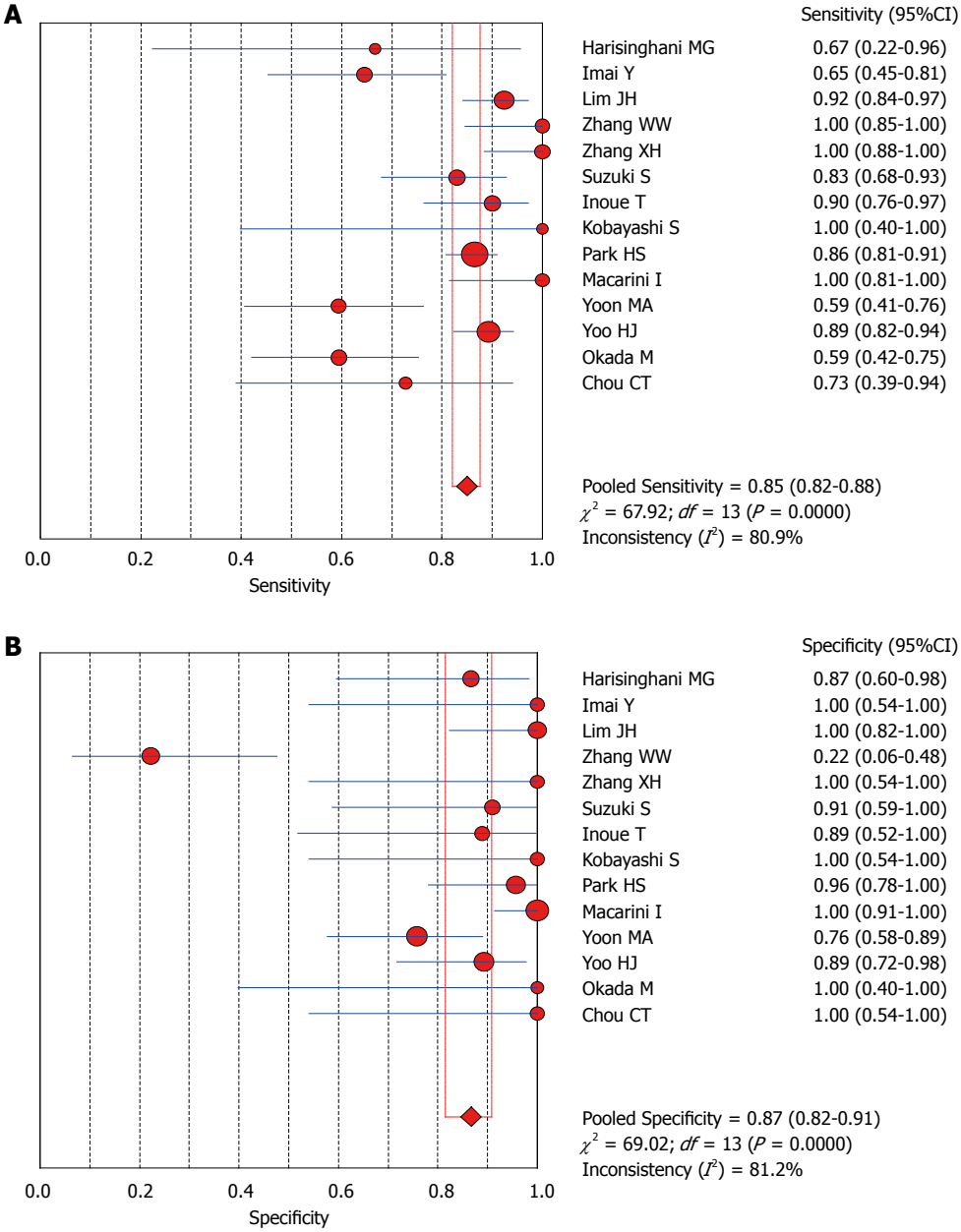

Figure 3 Forest plots for comparing hepatocellular carcinomas with benign liver lesions. A: Sensitivity; B: Specificity of 14 studies.

heterogeneity among the studies.

DISCUSSION

SPIO is a reticuloendothelial cell-specific contrast agent, which is used for the detection and characterization of focal liver lesions, largely based on the number and function of Kupffer cells. SPIO particles are taken up by Kupffer cells and predominantly shorten the T2 of the hepatic parenchyma. Healthy hepatic parenchyma and some focal liver lesions contain Kupffer cells and exhibit decreased signal intensity on SPIO-enhanced MRI, while lesions without Kupffer cells do not show this decrease. The signal intensity difference between lesions and liver parenchyma forms the basis of the detection and characterization of various lesions with SPIO-enhanced MRI. In clinical practice, the signal intensity of a lesion on SPIO-enhanced MR images can be lower (hypointensity) or higher (hyperintensity) than or similar to (isointensity) that of surrounding parenchyma. Because carcinoma lesions often show hyperintensity, we used hyperintensity as a criterion of malignancy to investigate the diagnostic accuracy of SPIO-enhanced MRI in the detection and characterization of focal liver lesions in this systematic review and meta-analysis.

Comparison between HCCs and other hepatic lesions

HCCs usually have different numbers of Kupffer cells, which are highly dependent on their degree of differentiation, whereas other malignant tumors such as metastases and cholangiocarcinoma generally do

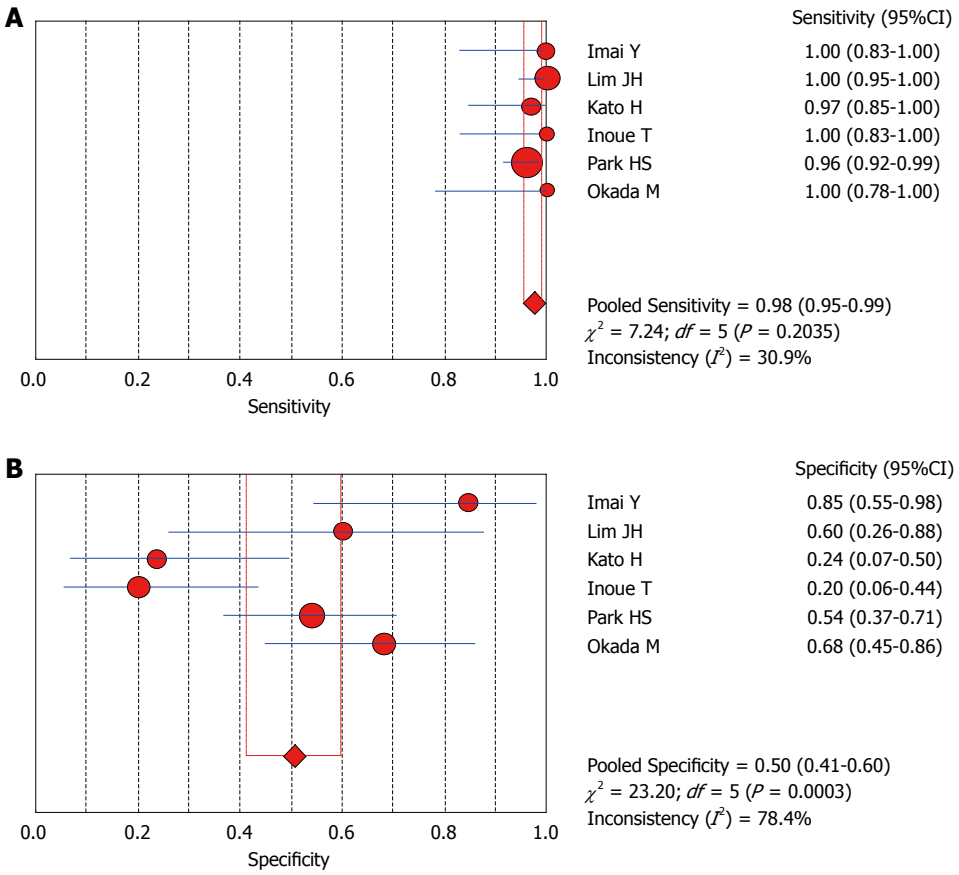

Figure 4 Forest plots for comparing advanced hepatocellular carcinomas with well-differentiated hepatocellular carcinomas. A: Sensitivity; B: Specificity of seven studies.

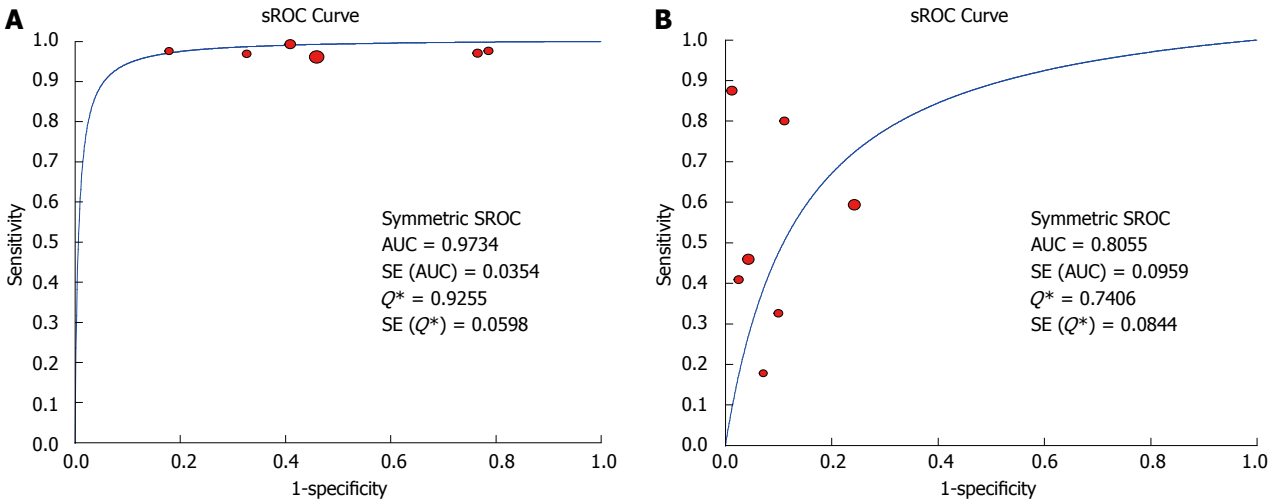

Figure 5 Summary receiver operating characteristics curves. Sensitivity and specificity are plotted for studies comparing advanced hepatocellular carcinomas (HCCs) with well-differentiated HCCs (A) and well-differentiated HCCs with dysplastic nodules (B). AUC: Area under the curve; sROC: Summary receiver operating characteristics.

not have Kupffer cells and exhibit hyperintensity on SPIO-enhanced images. In contrast, most benign lesions including hepatic adenoma, focal nodular hyperplasia, and cirrhotic regenerative nodules, often possess identical or more Kupffer cells than the surrounding parenchyma and thus demonstrate iso- or hypointensity on SPIO-enhanced images[7,15]. As a result, investigators have recently emphasized the value of SPIO-enhanced MRI in the detection and characterization of FHLs[7,8,16].

A comparison between HCCs and all other liver lesions revealed a diagnostic sensitivity of 86%

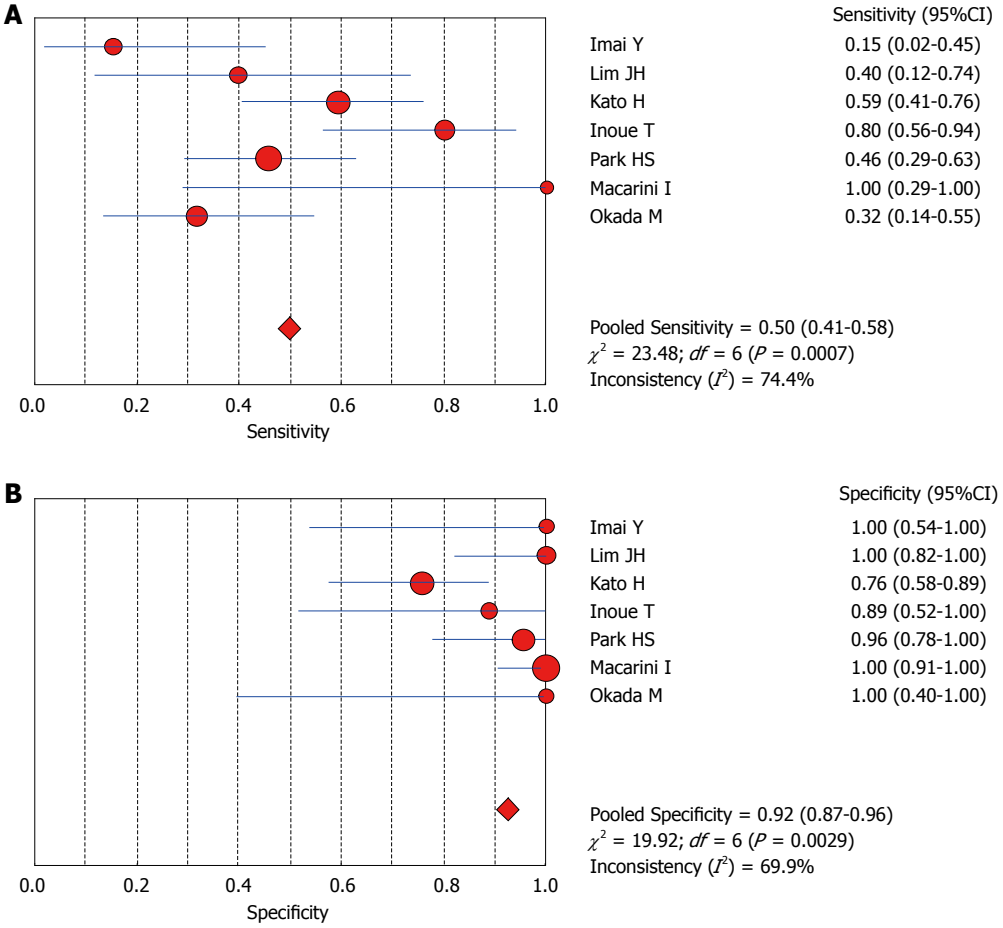

Figure 6 Forest plots for comparing well-differentiated hepatocellular carcinomas with dysplastic nodules. A: Sensitivity; B: Specificity of seven studies.

and a specificity of 76%. When non-HCC malignant lesions were excluded, the estimated sensitivity was essentially unchanged, but the specificity increased to 86%. Although notable heterogeneity existed among the studies, these results support the conclusion that SPIO-enhanced MRI is a valuable tool for the detection and characterization of focal lesions in cirrhotic liver.

Comparison between HCCs and DNs

HCCs develop in a multistep manner from regenerative nodules to DNs that are then transformed into WD-HCCs and advanced HCCs. The malignant transformation takes about 4-6 mo[17]. Precise differentiation of HCCs from DNs is critical for patient outcome. However, differentiation between DNs and HCCs in cirrhotic liver is often difficult because of marked architectural distortion of the parenchyma due to fibrosis, steatosis, necrosis, and regeneration[18].

Nodular hyperplasia and DNs possess identical or slightly more Kupffer cells than the surrounding normal parenchyma[7]. It has been reported that HCCs, especially WD-HCCs, also contain Kupffer cells. Some studies have shown that although there is no significant difference in Kupffer cell number between WD-HCCs and DNs, Kupffer cells are significantly reduced in MD- and PD-HCCs[18,19]. Thus, investigators concluded that SPIO-enhanced MRI can be used to differentiate WD-HCCs from advanced HCCs, but it is difficult to differentiate between WD-HCCs and DNs. Sometimes small WD-HCCs cannot be detected with SPIO-enhanced MRI due to their identical signal intensity to hepatic parenchyma[17].

Our analysis of seven eligible studies showed that the pooled sensitivity for differentiating advanced HCCs (MD/PD-HCCs) from WD-HCCs was 98% with low heterogeneity across these studies. Moreover, the frequency of hyperintensity on SPIO-enhanced MR images was very high in advanced HCCs, though the specificity was low (50%). A comparison between WD-HCCs and DN revealed that the pooled sensitivity and specificity for diagnosing WD-HCCs were 50% and 92%, respectively. These results indicate that both DNs and WD-HCCs may exhibit iso- or hypointensity on SPIO-enhanced MR images, but hyperintensity suggests a high probability of WD-HCCs.

Although the reasons for the heterogeneity among studies were not clear, we noticed an issue in all retrieved studies, *i.e.*, nearly half of the included studies did not report the causes and severity of cirrhosis[11,12,15,20-22]. The causes of liver cirrhosis, such as viral hepatitis B or C, alcoholic liver disease, or an unknown cause, were clearly documented in

other studies[7-9,16,18,19,23-25]. Only five studies reported the severity of cirrhosis based on the Child-Pugh classification[7,8,15,16,23]. Furthermore, none of the studies documented liver function. The functional status of Kupffer cells is more closely correlated with the signal intensity on MRI than the parenchymal pathology and degree of fibrosis[22]. Some investigators have denoted the mismatch between the signal-noise ratio and the number of Kupffer cells, and they consider that the mismatch is mainly due to decreased Kupffer cell function[15]. Therefore, decreased liver and Kupffer cell function may affect the SPIO-enhancement effect on liver parenchyma and lesions in MRI, and thus affect the detection and characterization of focal liver lesions. This may be partially responsible for the heterogeneity observed.

The present study has several limitations. First, potential publication bias may have arisen as some publications might not have been retrieved. In addition, there was notable heterogeneity between the studies. Neither the threshold effect nor the evaluated covariates were the sources and further studies are necessary to identify other parameters that may affect the detection and characterization of focal liver lesions with SPIO-enhanced MRI. Second, there was a considerable lack of reporting on the diagnostic study quality items, particularly QUADAS items 11, 9, 10, and 4. This may have resulted in review bias and disease progression bias. The third limitation in this study was the mandatory correction for zero entries by adding 0.5 to each cell of the study. This may have had an effect on the studies with small sample sizes.

In conclusion, the results of this meta-analysis suggest that SPIO-enhanced MRI is useful for differentiating between HCC and other FHLs as well as between DN and advanced HCC in cirrhotic livers. Using hyperintensity on SPIO-enhanced T2*-weighted images as the criterion, the sensitivity for diagnosing advanced HCC was 98%. SPIO-enhanced MRI is a valuable tool for the detection and characterization of focal lesions in cirrhotic liver.

COMMENTS

Background

Hepatocellular carcinoma (HCC) is the fifth most common malignant tumor worldwide, with 50% of cases occurring in China. The results of treatment are unsatisfactory, as HCC cannot be diagnosed early. Superparamagnetic iron oxide (SPIO) is a reticuloendothelial cell-specific contrast agent, which is widely used for the detection and characterization of focal liver lesions. Although the value of SPIO in the detection and characterization of focal hepatic lesions has been emphasized, some investigators have reported discordant results. Thus, the performance of SPIO-enhanced MRI in focal hepatic lesions still requires further research.

Research frontiers

Meta-analysis is a quantitative, formal, epidemiologic study design used to systematically assess previous research studies to derive conclusions regarding these studies. Outcomes of a meta-analysis may include a more precise estimate of the effect of treatment or risk factor for disease, or other outcomes, than any individual study contributing to the pooled analysis. It can be used to explain discordant findings regarding the value of SPIO in the detection and characterization of focal hepatic lesions, observed with different patient populations.

Innovations and breakthroughs

This meta-analysis included 15 eligible studies to evaluate the diagnostic performance of SPIO-enhanced MRI in focal hepatic lesions. Using hyperintensity on SPIO-enhanced T2*-weighted images as the criterion, the sensitivity for diagnosing advanced HCC was 98%. SPIO-enhanced MRI is a valuable tool for the detection and characterization of focal lesions in cirrhotic liver.

Applications

SPIO-enhanced MRI can be used for differentiating between HCC and other focal hepatic lesions as well as between DN and advanced HCC in cirrhotic livers.

Peer-review

This article evaluated the performance of SPIO-enhanced MRI in detection and characterization of focal hepatic lesions *via* systemic review and meta-analysis. The data showed that SPIO-enhanced MRI was useful for differential diagnosis between HCCs and other focal hepatic lesions. The study was well designed and the methods were accurately applied.

REFERENCES

1 **Lau WY**, Lai EC. Hepatocellular carcinoma: current management and recent advances. *Hepatobiliary Pancreat Dis Int* 2008; **7**: 237-257 [PMID: 18522878]

2 **Kim MJ**, Choi JY, Chung YE, Choi SY. Magnetic resonance imaging of hepatocellular carcinoma using contrast media. *Oncology* 2008; **75** Suppl 1: 72-82 [PMID: 19092275 DOI: 10.1159/000173427]

3 **Goshima S**, Kanematsu M, Kondo H, Shiratori Y, Onozuka M, Moriyama N, Bae KT. Optimal acquisition delay for dynamic contrast-enhanced MRI of hypervascular hepatocellular carcinoma. *AJR Am J Roentgenol* 2009; **192**: 686-692 [PMID: 19234264 DOI: 10.2214/AJR.08.1255]

4 **Teerasamit W**, Saiviroonporn P, Pongpaibul A, Korpraphong P. Benefit of double contrast MRI in diagnosis of hepatocellular carcinoma in patients with chronic liver diseases. *J Med Assoc Thai* 2014; **97**: 540-547 [PMID: 25065095]

5 **Maurea S**, Mainenti PP, Tambasco A, Imbriaco M, Mollica C, Laccetti E, Camera L, Liuzzi R, Salvatore M. Diagnostic accuracy of MR imaging to identify and characterize focal liver lesions: comparison between gadolinium and superparamagnetic iron oxide contrast media. *Quant Imaging Med Surg* 2014; **4**: 181-189 [PMID: 24914419 DOI: 10.3978/j.issn.2223-4292.2014.01.02]

6 **Muhi A**, Ichikawa T, Motosugi U, Sou H, Nakajima H, Sano K, Sano M, Kato S, Kitamura T, Fatima Z, Fukushima K, Iino H, Mori Y, Fujii H, Araki T. Diagnosis of colorectal hepatic metastases: comparison of contrast-enhanced CT, contrast-enhanced US, superparamagnetic iron oxide-enhanced MRI, and gadoxetic acid-enhanced MRI. *J Magn Reson Imaging* 2011; **34**: 326-335 [PMID: 21780227 DOI: 10.1002/jmri.22613]

7 **Macarini L**, Milillo P, Casavilla A, Scalzo G, Stoppino L, Vinci R, Moretti G, Ettorre G. MR characterization of dysplastic nodules and hepatocarcinoma in the cirrhotic liver with hepatospecific superparamagnetic contrast agents: pathological correlation in explanted livers. *Radiol Med* 2009; **114**: 1267-1282 [DOI: 10.1007/s11547-009-0464-9]

8 **Yoo HJ**, Lee JM, Lee JY, Kim SH, Kim SJ, Han JK, Choi BI. Additional value of SPIO-enhanced MR imaging for the noninvasive imaging diagnosis of hepatocellular carcinoma in cirrhotic liver. *Invest Radiol* 2009; **44**: 800-807 [PMID: 19838119 DOI: 10.1097/RLI.0b013e3181bc271d]

9 **Kobayashi S**, Matsui O, Kamura T, Yamamoto S, Yoneda N, Gabata T, Terayama N, Sanada J. Imaging of benign hypervascular hepatocellular nodules in alcoholic liver cirrhosis: differentiation from hypervascular hepatocellular carcinoma. *J Comput Assist Tomogr* 2007: 557-563 [PMID: 17882031 DOI: 10.1097/RCT.0b013e3180305bfb]

10 **Whiting P**, Rutjes AW, Reitsma JB, Bossuyt PM, Kleijnen J. The

development of QUADAS: a tool for the quality assessment of studies of diagnostic accuracy included in systematic reviews. *BMC Med Res Methodol* 2003; **3**: 25 [PMID: 14606960 DOI: 10.1186/1471-2288-3-25]

11 **Zheng WW**, Zhou KR, Chen ZW, Shen JZ, Chen CZ, Zhang SJ. Characterization of focal hepatic lesions with SPIO-enhanced MRI. *World J Gastroenterol* 2002; **8**: 82-86 [PMID: 11833077]

12 **Harisinghani MG**, Saini S, Weissleder R, Halpern EF, SchimaW, RubinDL, StillmanAE, SicaGT, SmallWC, HahnPF. Differentiation of liver hemangiomas from metastases and hepatocellular carcinoma at MR imaging enhanced with blood-pool contrast agent code-7227. *Radiology* 1997; **202**: 687-691 [DOI: 10.1148/radiology.202.3.9051017]

13 **Liver Cancer Study Group of Japan**. Classification of primary liver cancer. Tokyo, Japan: Kanehara & Co, 1997

14 **International Working Party**. Terminology of nodular hepatocellular lesions. *Hepatology* 1995; **22**: 983-993 [PMID: 7657307 DOI: 10.1002/hep.1840220341]

15 **Lim JH**, Choi D, Cho SK, Kim SH, Lee WJ, Lim HK, Park CK, Paik SW, Kim YI. Conspicuity of hepatocellular nodular lesions in cirrhotic livers at ferumoxides-enhanced MR imaging: importance of Kupffer cell number. *Radiology* 2001; **220**: 669-676 [PMID: 11526265 DOI: 10.1148/radiol.2203001777]

16 **Yoon MA**, Kim SH, Park HS, Lee DH, Lee JY, Han JK, Choi BI. Value of dual contrast liver MRI at 3.0T in differentiating well-differentiated hepatocellular carcinomas from dysplastic nodules: preliminary results of multivariate analysis. *Invest Radiol* 2009; **44**: 641-649 [DOI: 10.1097/RLI.0b013e3181ab6e57]

17 **Paley MR**, Mergo PJ, Torres GM, Ros PR. Characterization of focal hepatic lesions with ferumoxides-enhanced T2-weighted MR imaging. *AJR Am J Roentgenol* 2000; **175**: 159-163 [PMID: 10882267 DOI: 10.2214/ajr.175.1.1750159]

18 **Park HS**, Lee JM, Kim SH, Chang S, Kim SJ, Han JK, Choi BI. Differentiation of well-differentiated hepatocellular carcinomas from other hepatocellular nodules in cirrhotic liver: value of SPIO-enhanced MR imaging at 3.0 Tesla. *J Magn Reson Imaging* 2009; **29**: 328-335 [PMID: 19161184 DOI: 10.1002/jmri.21615]

19 **Imai Y**, Murakami T, Yoshida S, Nishikawa M, Ohsawa M, Tokunaga K, Murata M, Shibata K, Zushi S, Kurokawa M, Yonezawa T, Kawata S, Takamura M, Nagano H, Sakon M, Monden M, Wakasa K, Nakamura H. Superparamagnetic iron oxide-enhanced magnetic resonance images of hepatocellular carcinoma: correlation with histological grading. *Hepatology* 2000; **32**: 205-212 [PMID: 10915725 DOI: 10.1053/jhep.2000.9113]

20 **Zhang XH**, Liang BL, Huang SQ. [Correlation between SPIO-enhanced magnetic resonance imaging (MRI) and histological grading in hepatocellular carcinoma]. *Ai Zheng* 2003; **22**: 734-738 [PMID: 12866966]

21 **Suzuki S**, Iijima H, Moriyasu F, Sasaki S, Yanagisawa K, Miyahara T, Oguma K, Yoshida M, Horibe T, Ito N, Kakizaki D, Abe K, Tsuchiya K. Differential diagnosis of hepatic nodules using delayed parenchymal phase imaging of levovist contrast ultrasound: comparative study with SPIO-MRI. *Hepatol Res* 2004; **29**: 122-126 [PMID: 15163434 DOI: 10.1016/j.hepres.2004.02.010]

22 **Kato H**, Kanematsu M, Kondo H, Goshima S, Matsuo M, Hoshi H, Moriyama N. Ferumoxide-enhanced MR imaging of hepatocellular carcinoma: correlation with histologic tumor grade and tumor vascularity. *J Magn Reson Imaging* 2004; **19**: 76-81 [PMID: 14696223 DOI: 10.1002/jmri.10425]

23 **Okada M**, Imai Y, Kim T, Kogita S, Takamura M, Kumano S, Onishi H, Hori M, Fukuda K, Hayashi N, Wakasa K, Sakamoto M, Murakami T. Comparison of enhancement patterns of histologically confirmed hepatocellular carcinoma between gadoxetate- and ferucarbotran-enhanced magnetic resonance imaging. *J Magn Reson Imaging* 2010; **32**: 903-913 [PMID: 20882621 DOI: 10.1002/jmri.22333]

24 **Inoue T**, Kudo M, Watai R, Pei Z, Kawasaki T, Minami Y, Chung H, Fukunaga T, Awai K, Maenishi O. Differential diagnosis of nodular lesions in cirrhotic liver by post-vascular phase contrast-enhanced US with Levovist: comparison with superparamagnetic iron oxide magnetic resonance images. *J Gastroenterol* 2005; **40**: 1139-1147 [PMID: 16378178 DOI: 10.1007/s00535-005-1712-y]

25 **Chou CT**, Chen RC, Chen WT, Lii JM. Characterization of hyperintense nodules on T1-weighted liver magnetic resonance imaging: comparison of Ferucarbotran-enhanced MRI with accumulation-phase FS-T1WI and gadolinium-enhanced MRI. *J Chin Med Assoc* 2011; **74**: 62-68 [PMID: 21354082 DOI: 10.1016/j.jcma.2011.01.013]

P- Reviewer: Tang Y, Zhang BB **S- Editor**: Qi Y
L- Editor: AmEditor **E- Editor**: Ma S

World Journal of Gastroenterology

Submit a Manuscript: http://www.wjgnet.com/esps/
Help Desk: http://www.wjgnet.com/esps/helpdesk.aspx
DOI: 10.3748/wjg.v21.i14.4345

World J Gastroenterol 2015 April 14; 21(14): 4345-4357
ISSN 1007-9327 (print) ISSN 2219-2840 (online)

META-ANALYSIS

Probiotics in *Helicobacter pylori* eradication therapy: A systematic review and meta-analysis

Min-Min Zhang, Wei Qian, Ying-Yi Qin, Jia He, Yu-Hao Zhou

Min-Min Zhang, Department of Gastroenterology, Changhai Hospital, Second Military Medical University, Shanghai 200433, China
Wei Qian, Center for Clinical Epidemiology and Evidence-Based Medicine, Second Military Medical University, Shanghai 200433, China
Ying-Yi Qin, Jia He, Department of Health Statistics, Second Military Medical University, Shanghai 200433, China
Yu-Hao Zhou, Department of Rehabilitation Institute, Shanghai Seventh People's Hospital, Shanghai 200137, China
Author contributions: Zhang MM, Qian W, and Qin YY contributed equally to this work; Zhou YH and He J designed the research; Zhang MM, Qian W, and Qin YY performed the research; Zhou YH and He J contributed new reagents/analytic tools; Zhou YH analyzed the data; Qian W, Zhang MM and Zhou YH wrote the paper.
Supported by Grant from the Ministry of Science and Technology of China, No. 2008ZX10002-007, No. 2008ZX10002-018, and No. 2008ZX10002-025; the Leading Talents of Science in Shanghai 2010 (022); the Key Discipline Construction of Evidence-Based Public Health in Shanghai, No. 12GWZX0602; and the National Science Foundation of China, No. 81373105.
Correspondence to: Dr. Yu-Hao Zhou, Department of Rehabilitation Institute, Shanghai Seventh People's Hospital, No. 358 Datong Road, Pudong New Area, Shanghai 200137, China. zhou_ly@126.com
Telephone: +86-21-58611047
Fax: +86-21-58611047
Received: July 17, 2014
Peer-review started: July 17, 2014
First decision: August 15, 2014
Revised: September 4, 2014
Accepted: October 21, 2014
Article in press: October 21, 2014
Published online: April 14, 2015

Abstract

AIM: To summarize the evidence from randomized controlled trials (RCTs) regarding the effect of probiotics by using a meta-analytic approach.

METHODS: In July 2013, we searched PubMed, EMBASE, Ovid, the Cochrane Library, and three Chinese databases (Chinese Biomedical Literature Database, Chinese Medical Current Content, and Chinese Scientific Journals database) to identify relevant RCTs. We included RCTs investigating the effect of a combination of probiotics and standard therapy (probiotics group) with standard therapy alone (control group). Risk ratios (RRs) were used to measure the effect of probiotics plus standard therapy on *Helicobacter pylori* (*H. pylori*) eradication rates, adverse events, and patient compliance using a random-effect model.

RESULTS: We included data on 6997 participants from 45 RCTs, the overall eradication rates of the probiotic group and the control group were 82.31% and 72.08%, respectively. We noted that the use of probiotics plus standard therapy was associated with an increased eradication rate by per-protocol set analysis (RR = 1.11; 95%CI: 1.08-1.15; $P < 0.001$) or intention-to-treat analysis (RR = 1.13; 95%CI: 1.10-1.16; $P < 0.001$). Furthermore, the incidence of adverse events was 21.44% in the probiotics group and 36.27% in the control group, and it was found that the probiotics plus standard therapy significantly reduced the risk of adverse events (RR = 0.59; 95%CI: 0.48-0.71; $P < 0.001$), which demonstrated a favorable effect of probiotics in reducing adverse events associated with *H. pylori* eradication therapy. The specific reduction in adverse events ranged from 30% to 59%, and this reduction was statistically significant. Finally, probiotics plus standard therapy had little or no effect on patient compliance (RR = 0.98; 95%CI: 0.68-1.39; $P = 0.889$).

CONCLUSION: The use of probiotics plus standard therapy was associated with an increase in the *H. pylori* eradication rate, and a reduction in adverse events resulting from treatment in the general population. However, this therapy did not improve patient compliance.

Key words: Probiotics; *Helicobacter pylori*; Eradication;

Systematic review; Meta-analysis

Core tip: Probiotics have a positive effect on *Helicobacter pylori* (*H. pylori*) eradication since these compounds also induce anti-inflammatory and anti-oxidative mechanisms that regulate intestinal microbiota. The benefits of probiotics supplementation in the treatment of antibiotic resistant *H. pylori* are still unclear due to the lack of supporting evidence. In this meta-analysis of 45 randomized controlled trials involving nearly 6997 individuals, we found that the use of probiotics plus standard therapy was associated with an increase in the *H. pylori* eradication rate, and a reduction in adverse events resulting from treatment in the general population. However, this therapy did not improve patient compliance.

Zhang MM, Qian W, Qin YY, He J, Zhou YH. Probiotics in *Helicobacter pylori* eradication therapy: A systematic review and meta-analysis. *World J Gastroenterol* 2015; 21(14): 4345-4357 Available from: URL: http://www.wjgnet.com/1007-9327/full/v21/i14/4345.htm DOI: http://dx.doi.org/10.3748/wjg.v21.i14.4345

INTRODUCTION

Since its identification in 1982 by Barry Marshall and Robin Warren, *Helicobacter pylori* (*H. pylori*) has been studied for more than 30 years. The infection rate of this single dominant pathogen in the stomach varies between 1.2% and 95% according to age, geographic area, socioeconomic status, and other factors[1-5]. Infection with this organism results in a chronic effect by causing duodenal or gastric ulcers[6,7], gastric cancer[8,9], and gastric mucosa-associated lymphoid-tissue lymphoma[6,10]. The therapy used for the eradication of *H. pylori* also prevents the development of the diseases mentioned above in patients who are at high risk[8,11-13]. The success rate of standard therapy ranges from 60% to 90% using first-line treatment, and around 70% with second-line treatment[14-16]. Furthermore, the disruption of coevolved human and *H. pylori* genomes might play an important role in the high incidence of gastric disease[17,18]. Hence, the development of improved strategies is still under investigation to increase the efficiency of eradication or to increase patient compliance, which may contribute to a greater clinical value because of the prevalence of *H. pylori* infection in large populations[19]. Probiotics have a positive effect on *H. pylori* eradication since these compounds also induce anti-inflammatory and anti-oxidative mechanisms that regulate intestinal microbiota[20-23].

Although several meta-analyses[24-27] have assessed the efficacy and safety of probiotics plus standard therapy, most of these studies have investigated these effects with respect to specific strains or certain formulations of probiotics[24-26]. Tong *et al*[27] demonstrated that the administration of probiotics can both improve the eradication rate and reduce adverse events, but their study did not examine the effect of probiotics on patient compliance. The benefits of probiotics supplementation in the treatment of antibiotic resistant *H. pylori* are still unclear due to the lack of supporting evidence[28]. In this study, we performed a meta-analysis of available randomized controlled trials (RCTs) to evaluate the effect of probiotics on *H. pylori* eradication, adverse events, and patient compliance.

MATERIALS AND METHODS

Data sources, search strategy, and selection criteria

This review was conducted and reported according to the requirements outlined in Preferred Reporting Items for Systematic Reviews and Meta-Analysis Statement, 2009 (Checklist S1)[29]. RCTs of probiotics plus standard therapy compared with standard therapy were included in our study, regardless of the publication status, *i.e.*, published, in press, or in progress, and the effect of probiotic supplementation on *H. pylori* eradication, adverse events, and compliance were examined. Relevant trials were identified using the following procedure: (1) electronic searches: we searched PubMed, EMBASE, Ovid, The Cochrane Library, and three Chinese databases (Chinese Biomedical Literature Database, Chinese Medical Current Content, and Chinese Scientific Journals database) for articles published through July 2013. Both medical subject headings and free-language terms of *H. pylori* and probiotic, yeast, *Lactobacillus*, *Bifidobacterium*, *Streptococcus*, *Saccharomyces*, *Enterococcus*, and *Bacillus* were used as search terms; and (2) other sources: meeting abstracts, references of meta-analyses or reviews already published on related topics, and the clinicaltrials.gov website were also screened for completed or on-going studies. Authors were contacted for essential information regarding publications that were not available in full. Medical subject headings, methods, patient population, interventions, and outcome variables of these studies were used to identify relevant trials.

The literature search, data extraction, and quality assessment were independently undertaken by 2 investigators (Qian W and Qin YY) using a standardized approach. Any inconsistencies between these investigators were identified by the primary investigator (Zhou YH) and resolved by consensus. We restricted our study to RCTs that were less likely to be subject to confounding variables or bias than observational studies.

A study was eligible for inclusion in our meta-analysis if the following criteria were met: (1) the study was a RCT; (2) the probiotics were administrated as

adjuvant therapy in combination with the standard eradication therapy used for the treatment of *H. pylori*, including triple therapy, quadruple therapy and sequential therapy; (3) the probiotics group was treated with the standard eradication therapy plus probiotics and the control group received the same eradication regimens with or without a placebo; (4) the trial reported at least one of the following as an outcome: eradication rates, adverse events, or compliance; (5) if there were relevant studies with multiple arms, the data was combined to create a new study group and a new control group with reference to the criteria listed above; and (6) patient age or symptoms at the time of enrolment regardless of publication language were reported.

Finally, the exclusion criteria were as follows: (1) the study was not an RCT; (2) studies with only one group; and (3) studies in which patients were not treated with the standard therapy or in which the control group was treated differently from the group receiving the therapy.

Data collection and quality assessment

All data from included trials were extracted independently by 2 investigators (Qian W and Qin YY) using a standardized protocol. Each data set was reviewed by a third investigator (Zhou YH), and any discrepancies between the 2 investigators' data were resolved by discussion. The data collected from each study included characteristics of the enrolled patients, standard eradication therapy regimens, probiotic strains, dose and duration of probiotics, diagnostic methods of *H. pylori* infection, duration of the therapy and assessment, eradication rates, adverse events, and compliance. If the data of a study were published in more than one article, only the most recent publication was included. Both eradication rates by per-protocol set (PPS) analyses and intention-to-treat (ITT) analyses were collected.

The quality of the trials was assessed according to the recommendations of the Cochrane Collaboration[30], including random sequence generation (selection bias), allocation concealment (selection bias), blinding, intention-to-treat analysis, and completeness of follow-up. Judgments regarding the presence of methodological biases were determine by using the Cochrane criteria guidelines, Quality assessment was also performed independently by 2 researchers (Qian W and Qin YY), and was adjudicated by a third researcher (He J) when there were disagreements.

Statistical analysis

We computed the results of each RCT as dichotomous frequency data. Individual study risk ratios (RRs) and 95%CIs were calculated from event numbers extracted from each trial before data pooling. The overall RR and 95%CIs of eradication rates, adverse events, and compliance were also calculated. Both fixed-effect and random-effect models were used to assess the pooled RR for probiotics plus standard therapy compared with standard therapy. Results from the random-effects model were based on the assumption that the true underlying effect varied among the trials included in our meta-analysis presented here[31,32]. Heterogeneity of the treatment effects between studies was evaluated using the Q statistic, and we considered a P value < 0.10 to indicate significant heterogeneity[33,34].

Subgroup analyses were conducted for eradication rates by ITT analyses on the basis of the participant's age (0-17 years as children; ⩾ 18 years as adults; NM: the study was not mentioned or it contained both children and adults), single or multiple probiotic strains, high dose or low dose of probiotics (divided by the mean intake dosage per day of all included studies), duration of probiotics use longer than 15 d or not, duration of standard therapy longer than 7 d or not, duration between the end of the therapy and assessment longer than 4 wk or not, probiotic strains and types of standard therapy (first-line or second-line). Interaction tests[35] were performed to compare differences between the estimates of the 2 subsets, which were based on the Student t distribution rather than on a normal distribution because the number of inclusive studies was small. We also performed a sensitivity analysis by removing each individual trial from the meta-analysis[36]. Several methods were used to check for potential publication bias. Visual inspection of funnel plots for eradication rates, adverse events, and compliance were conducted. The Egger[37] and Begg test[38] were used to statistically assess publication bias for eradication rates, adverse events, and compliance. All reported P values were two-sided, and P values < 0.05 were considered statistically significant. Statistical analyses were performed using STATA software version 10.0 (Stata Corp., TX, United States).

RESULTS

Based on the literature search strategy, 4531 titles and abstracts were found from the 4 English databases; 102 of them were further searched based on abstracts or full articles, and 38 studies were enrolled. Another 7 studies from Chinese databases were enrolled later. Finally, 45 articles with 6997 participants were included[39-83] (PRISMA Flowchart). The characteristics of the 45 studies are listed in Table 1.

We acquired data relating to 6601 individuals to assess the effect of probiotics plus standard therapy on eradication rates. The pooled eradication rates for the probiotics group and the control group by PPS analysis were 86.23% and 76.60%, respectively. Overall, probiotics plus standard therapy significantly increased the eradication rates (RR = 1.11; 95%CI: 1.08-1.15; P < 0.001; Figure 1). Similarly, in ITT analysis, the pooled eradication rates for the probiotics group and the control group were 82.31% and 72.08%, respectively.

Table 1 Baseline characteristic of studies included in the systematic review and meta-analysis

Study	Patients (*n*)	Age (yr)	Methods of diagnosis	Methods of assessment	Probiotic regimens	Eradication therapy regimens and dosage (mg/d)[1]
Navarro-Rodriguez *et al*[39], 2013	107	Adults	UBT + HA + Giemsa + RUT	UBT + HA + Giemsa + RUT	Lacto + Bifido + Strep	400F + 60La/60M + 1000Te
Ahmad *et al*[40], 2013	66	Children	RUT/HA	HpSA	Lacto + Bifido + Strep	3000A + 360F + 60M
Shavakhi *et al*[41],2013	180	Adults	RUT/HA	UBT	Lacto + Bifido + Strep	2000A + 480B + 1000C + 40M
Kyriakos *et al*[42], 2013	70	Adults	RUT + HA	UBT	Saccha	2000A + 1000C + 40M
Jiang *et al*[43], 2013[2]	80	Adults	RUT + Giemsa	UBT	Bacillus	2000A + 60La + 3000Le
Dajani *et al*[44], 2013[2]	301	Both	UBT/RUT/HA/HpSA	UBT	Bifido	2000A + 1000C/800Me + PPI
Deguchi *et al*[45], 2012	229	Adults	Culture/(HA + RUT)	(UBT + HpSA) + Culture	Lacto	1500A + 400C + 20R
Tolone *et al*[46], 2012	68	Children	UBT + HA	UBT	Lacto + Bifido + Strep	6000A + 1800C + 60M
Mirzaee *et al*[47], 2012[2]	102	Adults	UBT	UBT	NM	2000A + 1000C + 40P
Manfredi *et al*[48], 2012[2]	227	Adults	RUT/HpSA	HpSA	Lacto + Bifido + Strep	2000A + 1000C + 40E + 1000Ti
Du *et al*[49], 2012[2]	234	Adults	UBT/RUT/Giemsa	UBT	Lacto + Bacillus + Strep	2000A + 1000C + 40M
Bekar *et al*[50], 2011	82	Adults	UBT	UBT	Lacto + Bifido	2000A + 1000C + 60La
Yoon *et al*[51], 2011	337	NM	UBT/RUT/HA	UBT	Lacto + Bifido + Strep	2000A + 1000C + 80E
He *et al*[52], 2011	84	Adults	UBT + RUT	UBT + RUT	Lacto + Bifido + Entero	2000A + 1000C + (40-60)R + 1000Ti
Xu *et al*[53], 2010	120	NM	(UBT/RUT) + HA	UBT	Lacto + Bifido + Entero	2000A + (20-40)E + 200F
Yaşar *et al*[54], 2010	76	Adults	HA	UBT	Bifido	2000A + 1000C + 80P
Wen *et al*[55], 2010	200	NM	UBT + RUT	UBT	Lacto + Bifido + Entero	2000A + 40P + 800Ti
Song *et al*[56], 2010[2]	991	Adults	RUT/HA	UBT	Saccha	2000A + 1000C + 40M
Szajewska *et al*[57], 2009	83	Children	2 of (UBT, RUT, HA)	UBT	Lacto	3000A + 1200C + 60M
Hurduc *et al*[58], 2009	90	Children	RUT + HA	RUT + HA	Saccha	3000A + 1800C + 60E/60M
Francavilla *et al*[59], 2008	40	NM	3 of (UBT, RUT, HA, HpSA)	UBT + HpSA	Lacto	2000A + 1000C + 40R + 1000Ti (sequential)
Kim *et al*[60], 2008	347	Adults	UBT/RUT/HA	UBT	Lacto + Bifido + Strep	2000A + 1000C + PPI
Huang *et al*[61], 2008	120	NM	UBT + RUT	UBT	Lacto + Bifido + Entero	1000C + (20-40)E/(20-40)R + 1000Rn
Imase *et al*[62], 20082	19	NM	NM	NM	Clost	1500A + 800C + 60La
Cindoruk *et al*[63], 2007	124	Adults	HA + Giemsa	UBT	Saccha	2000A + 1000C + 60La
Park *et al*[64], 2007	352	Adults	HA	UBT	Bacillus + Strep	2000A + 1000C + 40M
de Bortoli *et al*[65], 2007	206	NM	HA/(UBT + HpSA)	UBT	Lacto + Bifido + Strep	2000A + 1000C + 40E
Sahagún-Flores *et al*[66], 2007	71	Adults	HA	UBT	Lacto	2000A + 1000C + 40M
Lionetti *et al*[67], 2006	40	Children	2 of (UBT, RUT, HA)	UBT	Lacto	3000A + 900C + 60M + 1200Ti (sequential)
Goldman *et al*[68], 2006	65	Children	UBT	UBT	Lacto + Bifido	3000A + 900C + 60M
Sheu *et al*[69], 2006	138	NM	UBT + HA	UBT	Lacto + Bifido + Strep	2000A + 360B + 40M + 1000Me
Ziemniak *et al*[70], 20062	245	Adults	UBT	UBT	Lacto	2000A + 1000C + 80P
Sýkora *et al*[71], 2005	86	Children	2 of (RUT, HA, culture) + HpSA	UBT + HpSA	Lacto	3000A + 900C + (1200-2400)M
Myllyluoma *et al*[72], 2005	47	Adults	UBT + EIA	UBT	Lacto + Bifido + Propionibacterium	2000A + 1000C + 60La
Duman *et al*[73], 2005	389	NM	UBT + HA	NM	Saccha	2000A + 1000C + 40M
Shimbo *et al*[74], 2005	35	NM	RUT + Culture	UBT	Clost	3000A + 800C + 120La
Cao *et al*[75], 2005	128	NM	UBT + RUT	UBT + RUT	Lacto + Bifido + Entero	2000A + 300B + 40M + 800Me
Nista *et al*[76], 2004	106	Adults	UBT	UBT	Bacillus	2000A + 1000C + 40R
Tursi *et al*[77], 2004	70	NM	RUT + HA	UBT	Lacto	3000A + 800B + 40E/40P + 1000Ti
Guo *et al*[78], 2004	97	Adults	RUT + HA	UBT	Clost	1000A + 200F + 40M
Sheu *et al*[79], 2002	160	NM	(RUT/HA) + UBT	UBT/RUT/HA	Lacto + Bifido	2000A + 1000C + 60La
Cremonini *et al*[80], 2002[2]	85	Adults	UBT	UBT	Lacto	1000C + 40R + 1000Ti
Armuzzi *et al*[81], 2001[a]	60	Adults	UBT + EIA	UBT	Lacto	1000C + 40R + 1000Ti
Armuzzi *et al*[82], 2001[b]	120	Adults	UBT + EIA	UBT	Lacto	1000C + 80P + 1000Ti
Canducci *et al*[83], 2000	120	NM	UBT + HA	UBT + HA	Lacto	1500A + 750C + 40R

[1]"400F + 60L + 1000Te" means "Furazolidon 400 mg/d, lansoprazole 60 mg/d, and tetracycline 1000 mg/d". Patient's weight were assumed as 60 kg to calculate the exact dosage if only the dosage per kg were available in the article; [2]These articles were designed with multiple arms, but only relevant groups were combined and included in this meta-analysis. UBT: Urea breath test; RUT: Rapid urease test; HA: Histological assessment; Giemsa: Giemsa staining; HpSA: *H. pylori* stool antigen test; EIA: Enzyme-linked immunosorbent Assay; Culture: Culture test; Lacto: *Lactobacillus*; Bifido: *Bifidobacterium*; Strep: *Streptococcus*; Saccha: *Saccharomyces*; Entero: *Enterococcus*; Clost: *Clostridium*; A: Amoxicillin; B: Bismuth subcitrate; C: Clarithromycin; E: Esomeprazole; F: Furazolidon; La: Lansoprazole; Le: Levofloxacin; M: omeprazole; Me: Metronidazole; P: Pantoprazole; PPI: Proton pump inhibitor; R: Rabeprazole; Rn: Ornidazole; Ti: Tinidazole; Te: Tetracyline; NM: Not mentioned.

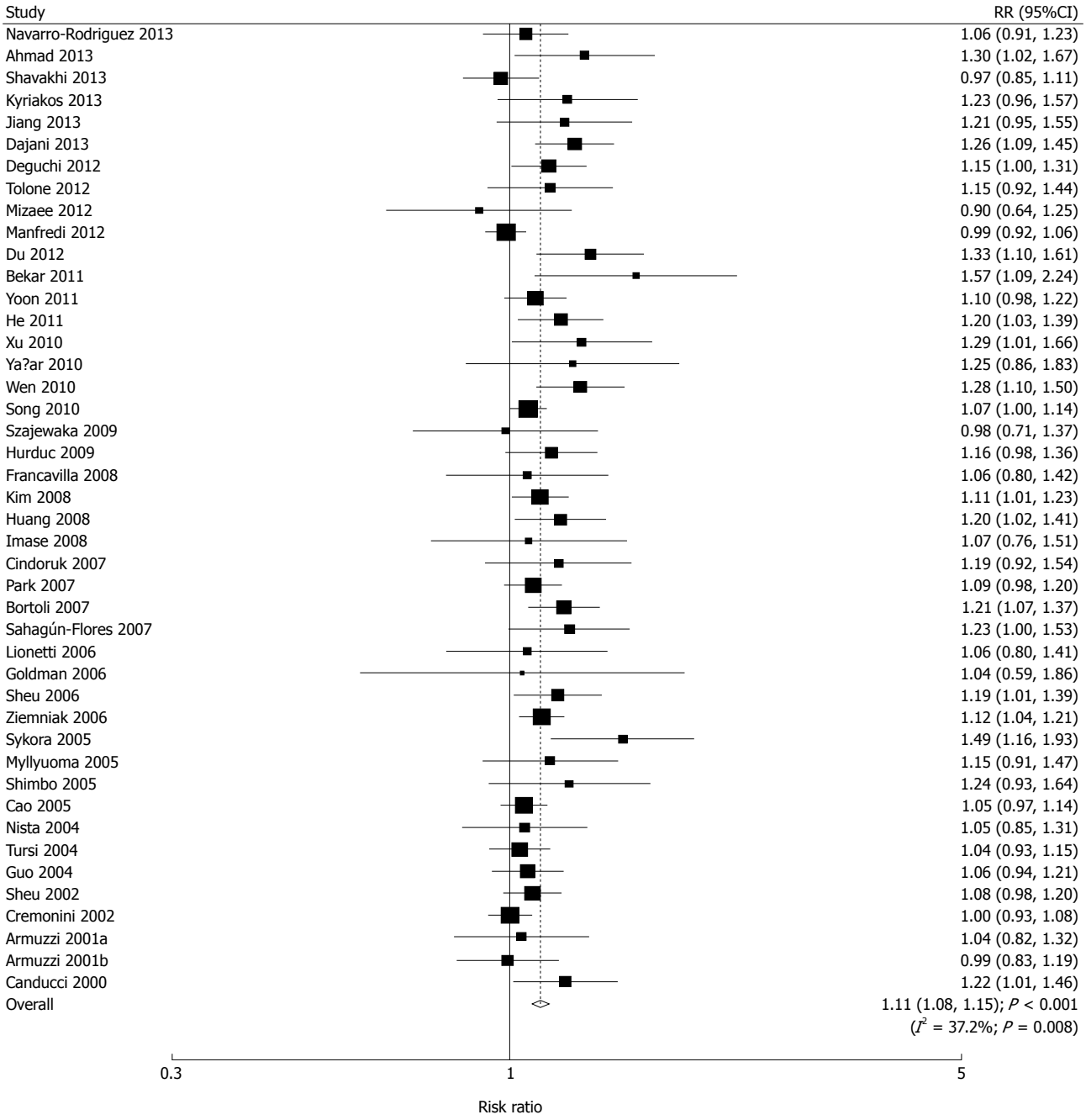

Figure 1 Effects of probiotics plus standard therapy on eradication rate by per-protocol set analysis compared with standard therapy alone. CI: Confidence interval.

Probiotics plus standard therapy significantly increased the eradication rates (RR = 1.13; 95%CI: 1.10-1.16; $P < 0.001$; Figure 2). Although there was significant heterogeneity across the trials by PPS analysis, a sensitivity analysis was conducted and the results suggested that the data were not affected by the sequential exclusion of any particular trial from the pooled analysis.

We acquired data on 5312 individuals to assess the effect of probiotics plus standard therapy on adverse events, and reported 1499 adverse events. We noted that probiotics plus standard therapy significantly reduced the risk of adverse events (RR = 0.59; 95%CI: 0.48-0.71; $P < 0.001$; Figure 3). Substantial heterogeneity was observed in the magnitude of the effect across the trials (I^2 = 81.6%; $P < 0.001$). However, following sequential exclusion of each trial from the pooled analysis, we found that the outcome was not affected by the exclusion of any specific trial. The incidence rates were 21.44% and 36.27% in the probiotics group and the control group, respectively, which demonstrated a favorable effect of probiotics on the reduction of adverse events during *H. pylori* eradication therapy. As presented in Table 2, the combined effects of probiotics were statistically significant for all the listed adverse events, which clarified the protective

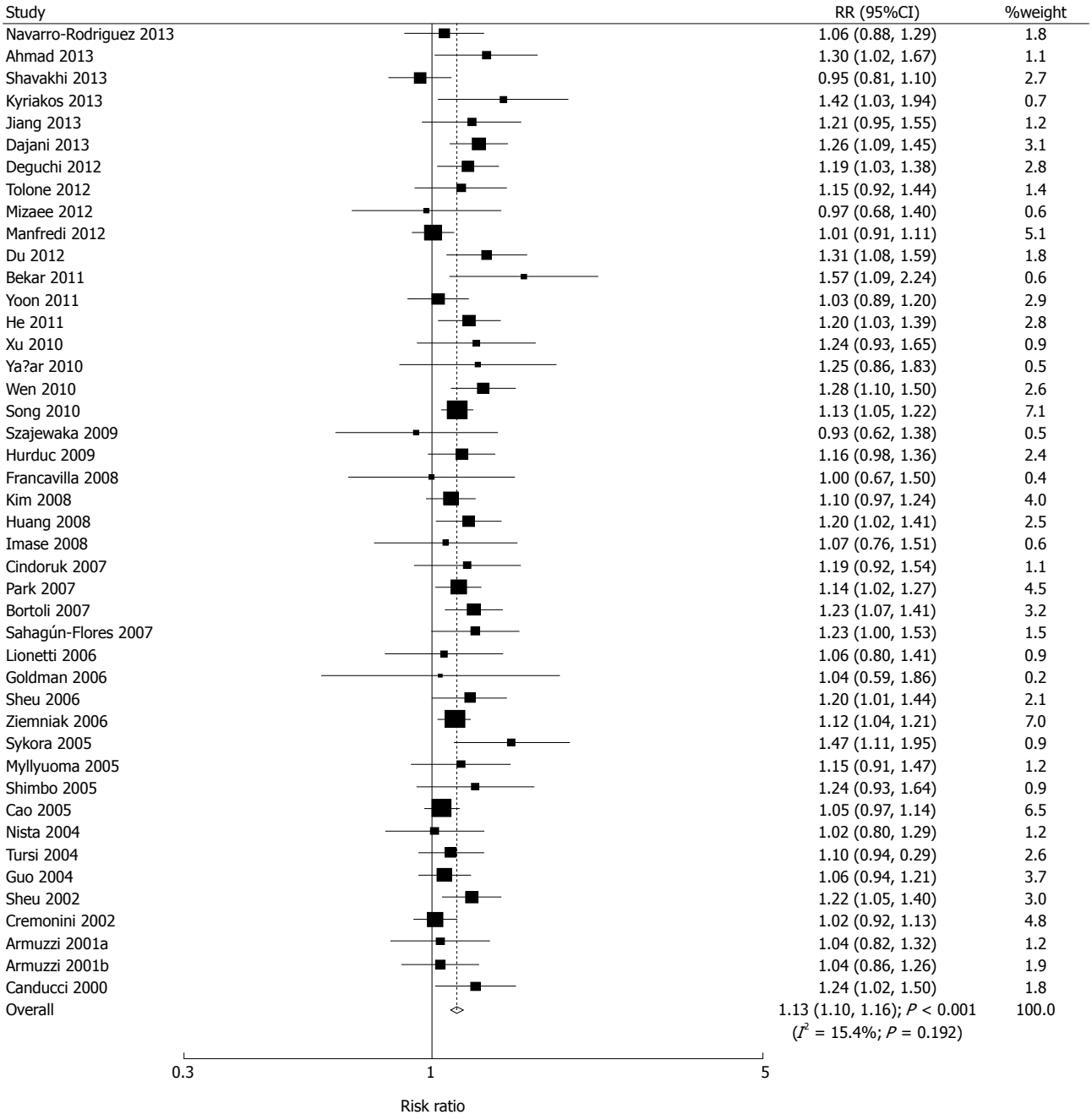

Figure 2 Effects of probiotics plus standard therapy on eradication rate by intention-to-treat analysis compared with standard therapy alone.

effects of probiotics against these adverse events.

We acquired data on 4033 individuals to assess the effect of probiotics plus standard therapy on compliance, and reported 132 events of non-compliance. The inclusion of probiotics in the *H. pylori* eradication treatment regimen did not improve patient compliance according to the results of the pooled analysis (RR = 0.98; 95%CI: 0.68-1.39; *P* = 0.889; without evidence of heterogeneity; Figure 4).

The studies were divided into subgroups based on the age of the patients, single or multiple probiotic strains, dosage of probiotics, duration of probiotics intake, duration of standard eradication therapy, duration between the end of the therapy and assessment, probiotic strains and types of eradication therapy (Table 3). Overall, we noted that *Clostridium* had no significant effect on the eradication rate, and furthermore, probiotics did not affect the eradication rate if patients received a second-line standard therapy. Subgroup analyses based on other factors were associated with a statistically significant increase in the eradication rate.

A review of funnel plots did not exclude the potential for publication bias for the eradication rate, adverse events, and patient compliance. The Egger test[37] results showed potential publication bias for the eradication rate, adverse events, and patient compliance. The Begg test[38] results showed potential

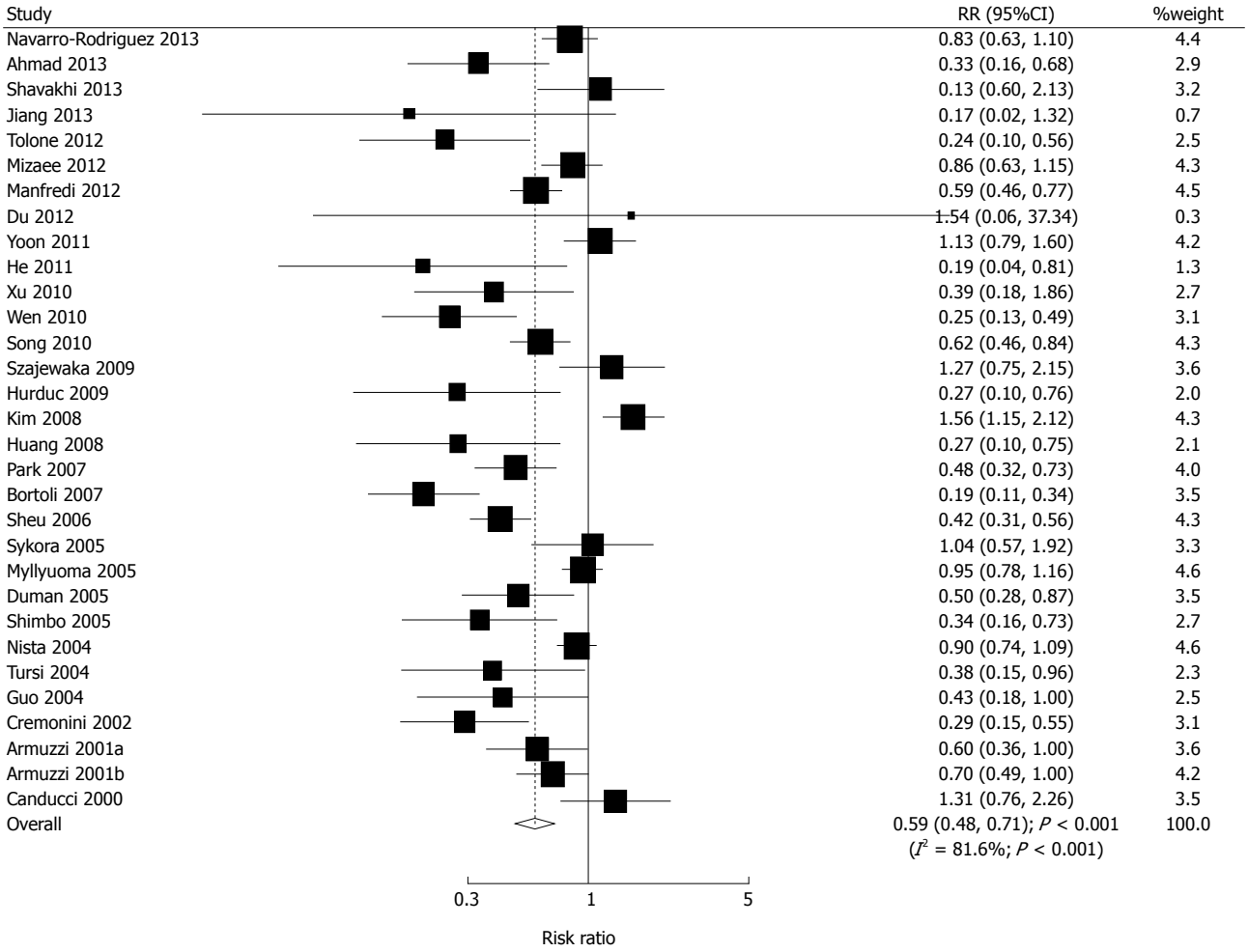

Figure 3 Effects of probiotics plus standard therapy on total adverse events compared with standard therapy alone.

publication bias for patient compliance. The conclusions did not change after adjustment for publication bias by using the trim and fill method[84].

DISCUSSION

Through systematic review and meta-analysis using the results from 45 studies as solid supporting evidence, the effectiveness of the use of probiotics in *H. pylori* eradication therapy is based on 3 criteria: eradication rate, adverse events, and patient compliance. Our results suggest that additional probiotic supplementation significantly increases the eradication rate, and reduces adverse events. However, there is no significant effect on patient compliance.

The eradication rate of *H. pylori* using standard therapy plus probiotics has been significantly improved by about 13% compared with standard therapy alone. The value of RR is small because both the probiotics group and the control group have a relatively large eradication rate. Therefore, an improved eradication rate is the best indicator of the effectiveness of probiotics supplementation. Hence, the addition of probiotics to standard *H. pylori* eradication therapy improves the *H. pylori* eradication success rate within a population.

The duration of antibiotic treatment, different regimens of standard therapy, patient age, dosage of probiotics, different strains of probiotics[4,40,85-87], and different types of standard therapy have been reported to potentially influence the eradication outcome. In our study, there was a statistically significant increase in eradication rates in nearly all the subgroups when these factors were also taken into consideration. These subgroups showed similar outcomes with strong statistical significance, which may be influenced by a large sample size. We consider that probiotics had a comparable effect on the *H. pylori* eradication rate in all these subgroups of more than 500 patients. More studies are needed to assess the outcome in groups with fewer patients, such as groups of children and patients who received second-line therapy.

In addition to the subgroups mentioned above, antibiotic resistance can create a significant problem in *H. pylori* eradication therapy because it can become a major cause of initial eradication failure[19,88-90]. The prevalence of clarithromycin resistance cases treated with clarithromycin-containing triple therapy was reported to be 10%-30%[19,91]. With an increasing number of patients infected with clarithromycin and/

Table 2 Effect of probiotics plus standard therapy *vs* standard therapy on adverse events

Adverse Event	Trials (*n*)	Participants (*n*)	Probiotics group, %	Control group	RR and 95%CI	*P* value	Heterogeneity (*P* value)
Diarrhea	26	4935	5.71%	13.72%	0.41 (0.30-0.57)	< 0.001	58% ($P < 0.001$)
Nausea/vomiting	23	4067	6.95%	12.83%	0.60 (0.48-0.76)	< 0.001	23% ($P = 0.16$)
Epigastric discomfort	8	1806	6.09%	14.13%	0.57 (0.44-0.74)	< 0.001	0% ($P = 0.60$)
Abdominal bloating	13	1516	10.82%	14.51%	0.70 (0.55-0.90)	0.005	0% ($P = 0.53$)
Abdominal pain	10	1373	8.40%	13.05%	0.54 (0.35-0.83)	0.005	31% ($P = 0.16$)
Constipation	13	2021	3.96%	6.73%	0.55 (0.37-0.81)	0.002	0% ($P = 0.77$)
Taste disturbance	19	3611	11.79%	18.76%	0.63 (0.48-0.83)	< 0.001	73% ($P < 0.001$)

RR: Risk ratio.

Table 3 Subgroup analyses comparing the effect of probiotics plus standard therapy *vs* standard therapy on eradication rate based on intention-to-treat

Subgroups	Studies (*n*)	Patients (*n*)	Probiotics group	Control group	RR and 95%CI	*P* value	*P* value for Q statistics
Age							
Adults	23	4116	81.86%	73.23%	1.12 (1.09-1.16)	< 0.001	0.224
Children	7	498	76.89%	64.78%	1.19 (1.07-1.32)	0.002	0.535
Probiotic strains							
Multiple	22	3598	83.29%	73.73%	1.12 (1.08-1.17)	< 0.001	0.046
Single	21	2908	81.60%	70.60%	1.16 (1.11-1.21)	< 0.001	0.724
Dosage of probiotics (CFU/d)							
$\geqslant 5 \times 10^9$	15	2470	82.84%	73.06%	1.13 (1.08-1.18)	< 0.001	0.571
$< 5 \times 10^9$	21	3283	81.49%	70.69%	1.14 (1.09-1.20)	< 0.001	0.046
Duration of probiotic intake							
⩾ 15 d	17	3411	81.15%	71.35%	1.14 (1.10-1.18)	< 0.001	0.976
< 15 d	24	2585	82.30%	71.28%	1.12 (1.06-1.18)	< 0.001	0.022
Duration of standard therapy							
> 7 d	17	2050	81.79%	74.32%	1.11 (1.06-1.17)	< 0.001	0.167
= 7 d	27	4558	82.39%	70.97%	1.16 (1.12-1.20)	< 0.001	0.502
Duration between therapy ending and assessment							
> 4 wk	20	2520	83.86%	73.36%	1.16 (1.11-1.21)	< 0.001	0.282
= 4 wk	22	3984	80.78%	70.91%	1.14 (1.10-1.18)	< 0.001	0.358
Probiotic (containing the following strains)							
Lactobacillus	31	4165	82.67%	73.05%	1.14 (1.10-1.18)	< 0.001	0.088
Bifidobacterium	20	3059	82.66%	71.69%	1.14 (1.10-1.19)	< 0.001	0.058
Streptococcus	11	2262	81.47%	72.65%	1.11 (1.06-1.17)	< 0.001	0.085
Saccharomyces	4	1275	81.14%	69.94%	1.15 (1.08-1.24)	< 0.001	0.594
Bacillus	4	772	80.71%	69.74%	1.17 (1.08-1.28)	< 0.001	0.408
Enterococcus	5	652	87.30%	73.29%	1.17 (1.06-1.30)	0.003	0.046
Clostridium	3	151	93.06%	86.08%	1.08 (0.97-1.21)	0.164	0.456
Therapy regimens							
First-line	16	3474	81.02%	71.00%	1.13 (1.08-1.17)	< 0.001	0.260
Second-line	3	435	88.63%	81.11%	1.08 (1.00-1.17)	0.058	0.185
Not specified	25	2699	82.67%	72.25%	1.18 (1.13-1.23)	< 0.001	0.268

or fluoroquinolone resistant *H. pylori*[92], quadruple therapy with bismuth colloid or sequential therapy has been suggested[92,93]. Probiotic supplementation in this population has rarely been studied before. In this meta-analysis, the studies focusing on antibiotic resistant *H. pylori* were far fewer than expected. Therefore, we have not included a thorough discussion on the topic of antibiotic-resistant strains here. The results from studies conducted so far seem promising and worth pursuing further through the initiation of studies using a larger population of patients.

In addition to improving the eradication rate of infectious organisms, the administration of probiotics can also reduce the incidence of adverse events by preventing or reducing pathogenic adherence, inducing the production of stomach acid, hydrogen peroxide, and bacteriocins to antagonize pathogen growth, and encourage the formation of normal balanced flora[68]. In our study, all the reported adverse events had RRs < 1, which indicated that the use of probiotics effectively protected the gut flora during *H. pylori* eradication. The overall incidence of adverse events was reduced by approximately 41% in the probiotics group. There are also studies confirming that the administration of probiotics can prevent diarrhea[94], abdominal bloating[95], and constipation[96-98].

Since probiotics are effective in the prevention of adverse events, they were also expected to promote patient compliance[22,28]. Non-compliance may drastically affect the *H. pylori* eradication success rate[2]; this

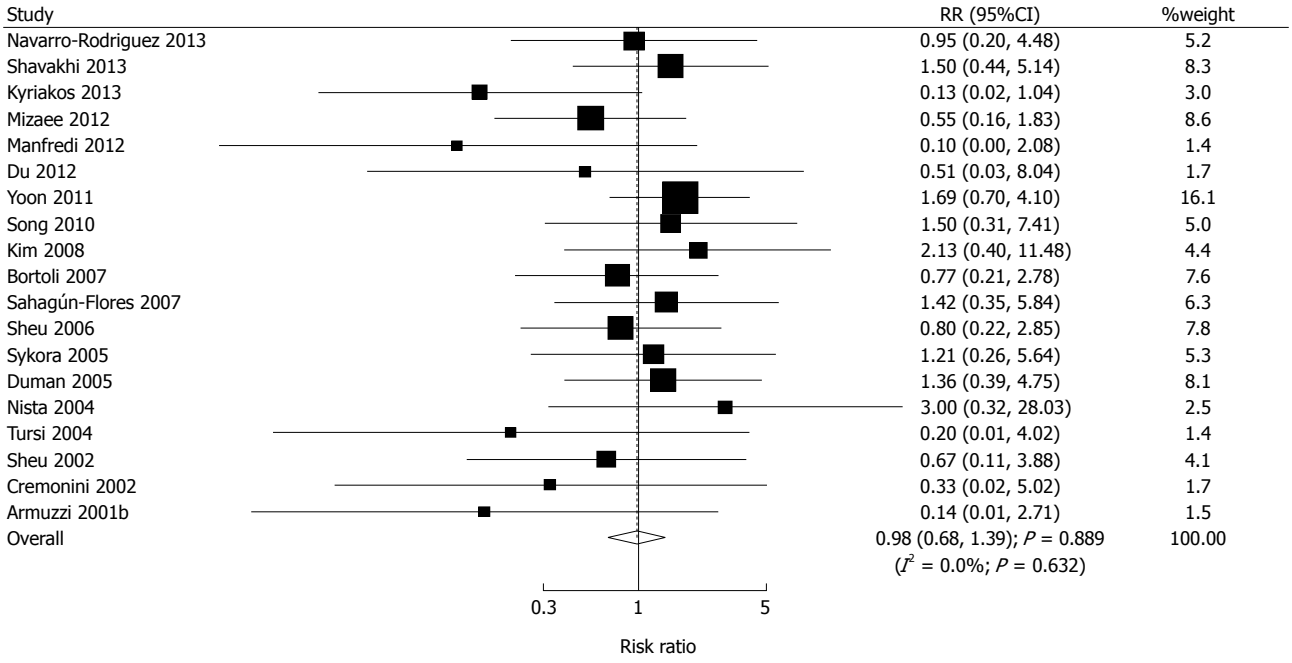

Figure 4 Effects of probiotics plus standard therapy on patients compliance compared with standard therapy alone.

aspect has seldom been studied. Manfredi *et al*[48] reported that the improvement in patient compliance in a study administering lactoferrin and probiotics to treat *H. pylori* infection was not statistically significant. Most studies had no dropouts or minimal losses to follow-up. The non-compliance rate was low and may relate to intrinsic personality traits, which can only be studied using a meta-analysis approach. Unexpectedly, there was no evidence showing a lower rate of non-compliance in the probiotics group. The RR showed a slight tendency for improved patient compliance, but this did not have any practical benefit on eradication success.

In clinical practice, the overall benefit of administering prophylactic probiotics to *H. pylori*-infected patients is not only related to the eradication success or reduced adverse events, but also to medical expenses; the influence of the latter factor in *H. pylori* eradication is still unclear. As *H. pylori* infection is more prevalent in developing countries or areas of lower socioeconomic status[4,99], the cost-effectiveness of taking probiotics may be subtle and difficult to evaluate. Tursi *et al*[77] reported that the extra cost of probiotics may be a limiting factor preventing widespread use. Some researchers report that probiotics were economical[100], but more evidence is required to support this statement.

This study may have the following limitations: (1) some publications may have been neglected to be added to the study because they were not included in any of the databases that were searched, leading to publication bias. Some publications that were unavailable were requested from the corresponding author in order to include their data in this study but only a few requests were answered; (2) there is a limited number of papers that include some subgroups, such as patients infected with antibiotic resistant *H. pylori* who were treated with probiotics. Analysis of these subgroups was not conducted; (3) there may be bias introduced by including studies with multiple arms, and routine means of measuring heterogeneity and publication bias; and (4) probiotics were analyzed by strains instead of by preparations that are available in clinical practice. Furthermore, the eradication therapies were divided into first-line or second-line therapies instead of into specific regimens to account for study number limitations. The correlation of probiotics and standard therapy was not included, and may contribute important information to this study.

In conclusion, the use of probiotics to supplement standard therapy in patients infected with *H. pylori* increased the eradication rate of the organism by about 13% and decreased the overall rate of adverse events by approximately 41%, independent of patient age, genera or dosage of probiotics, time of standard therapy or assessment, and therapy regimen. Unexpectedly, the patient compliance rate did not improve with the addition of probiotics to the therapeutic regimen. An economic evaluation is required to establish the cost-effectiveness of the addition of probiotics to *H. pylori* eradication therapy, and to determine whether the combination of probiotics with a standard therapy would be beneficial in clinical practice.

COMMENTS

Background

Certain studies have reported inconsistent results regarding the efficacy, safety and patient compliance of the use of probiotics in combination with a standard therapy when compared with standard therapy alone for the eradication of

Helicobacter pylori (*H. pylori*).

Research frontiers

The benefits of probiotics supplementation in the treatment of antibiotic resistant *H. pylori* are still unclear due to the lack of supporting evidence. We therefore conducted a meta-analysis to summarize the evidence from randomized controlled trials (RCTs) regarding the effect of probiotics by using a meta-analytic approach.

Innovations and breakthroughs

Several meta-analyses have assessed the efficacy and safety of probiotics plus standard therapy, and most of these studies have investigated these effects with respect to specific strains or certain formulations of probiotics. In this study, we performed a meta-analysis of available RCTs to evaluate the effect of probiotics on *H. pylori* eradication, adverse events, and patient compliance.

Applications

Probiotics supplementing standard therapy in patients infected with *H. pylori* increased the eradication rate and decreased the overall rate of adverse events, independent of patient age, genera or dosage of probiotics, time of standard therapy or assessment, and therapy regimen. This study may represent a future strategy in the treatment of patients with *H. pylori* infection.

Peer-review

In this meta-analysis the articles chosen are sufficient by number and the distribution is worldwide. Addition of probiotics may be an option for low eradication regions. Effect of these live but nonpathogenic bacteria on eradication therapy of *H. pylori* may be by reducing antibiotic related side effects and/or possible antibacterial properties. The studies relating yo cost-effectiveness of this supplementation should be assessed before clinical usage. Also some other measures increasing the compliance of the patient should be taken into account, as appropriate region-based regimens informing the patient.

REFERENCES

1 **Bik EM**, Eckburg PB, Gill SR, Nelson KE, Purdom EA, Francois F, Perez-Perez G, Blaser MJ, Relman DA. Molecular analysis of the bacterial microbiota in the human stomach. *Proc Natl Acad Sci USA* 2006; **103**: 732-737 [PMID: 16407106 DOI: 10.1073/pnas.0506655103]

2 **Hunt RH**, Xiao SD, Megraud F, Leon-Barua R, Bazzoli F, van der Merwe S, Vaz Coelho LG, Fock M, Fedail S, Cohen H, Malfertheiner P, Vakil N, Hamid S, Goh KL, Wong BC, Krabshuis J, Le Mair A. Helicobacter pylori in developing countries. World Gastroenterology Organisation Global Guideline. *J Gastrointestin Liver Dis* 2011; **20**: 299-304 [PMID: 21961099]

3 **Tonkic A**, Tonkic M, Lehours P, Mégraud F. Epidemiology and diagnosis of Helicobacter pylori infection. *Helicobacter* 2012; **17** Suppl 1: 1-8 [PMID: 22958148 DOI: 10.1111/j.1523-5378.2012.00975.x]

4 **Khalifa MM**, Sharaf RR, Aziz RK. Helicobacter pylori: a poor man's gut pathogen? *Gut Pathog* 2010; **2**: 2 [PMID: 20356368 DOI: 10.1186/1757-4749-2-2]

5 **Jafri W**, Yakoob J, Abid S, Siddiqui S, Awan S, Nizami SQ. Helicobacter pylori infection in children: population-based age-specific prevalence and risk factors in a developing country. *Acta Paediatr* 2010; **99**: 279-282 [PMID: 19839955]

6 **McColl KE**. Clinical practice. Helicobacter pylori infection. *N Engl J Med* 2010; **362**: 1597-1604 [PMID: 20427808 DOI: 10.1056/NEJMcp1001110]

7 **Yeomans ND**. The ulcer sleuths: The search for the cause of peptic ulcers. *J Gastroenterol Hepatol* 2011; **26** Suppl 1: 35-41 [PMID: 21199512 DOI: 10.1111/j.1440-1746.2010.06537.x]

8 **Fuccio L**, Zagari RM, Eusebi LH, Laterza L, Cennamo V, Ceroni L, Grilli D, Bazzoli F. Meta-analysis: can Helicobacter pylori eradication treatment reduce the risk for gastric cancer? *Ann Intern Med* 2009; **151**: 121-128 [PMID: 19620164 DOI: 10.7326/0003-4819-151-7-200910060-00015]

9 **Huang JQ**, Hunt RH. The evolving epidemiology of Helicobacter pylori infection and gastric cancer. *Can J Gastroenterol* 2003; **17** Suppl B: 18B-20B [PMID: 12845346]

10 **Parsonnet J**, Hansen S, Rodriguez L, Gelb AB, Warnke RA, Jellum E, Orentreich N, Vogelman JH, Friedman GD. Helicobacter pylori infection and gastric lymphoma. *N Engl J Med* 1994; **330**: 1267-1271 [PMID: 8145781 DOI: 10.1056/NEJM199405053301803]

11 **Malfertheiner P**, Megraud F, O'Morain CA, Atherton J, Axon AT, Bazzoli F, Gensini GF, Gisbert JP, Graham DY, Rokkas T, El-Omar EM, Kuipers EJ. Management of Helicobacter pylori infection--the Maastricht IV/ Florence Consensus Report. *Gut* 2012; **61**: 646-664 [PMID: 22491499 DOI: 10.1136/gutjnl-2012-302084]

12 **Hunt RH**, Sumanac K, Huang JQ. Review article: should we kill or should we save Helicobacter pylori? *Aliment Pharmacol Ther* 2001; **15** Suppl 1: 51-59 [PMID: 11488662 DOI: 10.1046/j.1365-2036.2001.00107.x]

13 **Lee YC**, Chen TH, Chiu HM, Shun CT, Chiang H, Liu TY, Wu MS, Lin JT. The benefit of mass eradication of Helicobacter pylori infection: a community-based study of gastric cancer prevention. *Gut* 2013; **62**: 676-682 [PMID: 22698649 DOI: 10.1136/gutjnl-2012-302240]

14 **Rokkas T**, Sechopoulos P, Robotis I, Margantinis G, Pistiolas D. Cumulative H. pylori eradication rates in clinical practice by adopting first and second-line regimens proposed by the Maastricht III consensus and a third-line empirical regimen. *Am J Gastroenterol* 2009; **104**: 21-25 [PMID: 19098844 DOI: 10.1038/ajg.2008.87]

15 **Liou JM**, Lin JT, Chang CY, Chen MJ, Cheng TY, Lee YC, Chen CC, Sheng WH, Wang HP, Wu MS. Levofloxacin-based and clarithromycin-based triple therapies as first-line and second-line treatments for Helicobacter pylori infection: a randomised comparative trial with crossover design. *Gut* 2010; **59**: 572-578 [PMID: 20427390 DOI: 10.1136/gut.2009.198309]

16 **Gisbert JP**, Calvet X, O'Connor A, Mégraud F, O'Morain CA. Sequential therapy for Helicobacter pylori eradication: a critical review. *J Clin Gastroenterol* 2010; **44**: 313-325 [PMID: 20054285]

17 **Kodaman N**, Pazos A, Schneider BG, Piazuelo MB, Mera R, Sobota RS, Sicinschi LA, Shaffer CL, Romero-Gallo J, de Sablet T, Harder RH, Bravo LE, Peek RM, Wilson KT, Cover TL, Williams SM, Correa P. Human and Helicobacter pylori coevolution shapes the risk of gastric disease. *Proc Natl Acad Sci USA* 2014; **111**: 1455-1460 [PMID: 24474772]

18 **Kanda T**, Yokosuka O. Paradoxical role of Helicobacter pylori in Gastric cancer. Editorial. Biohelikon: Cancer and Clinical Research 2, 2014: a12

19 **Olokoba AB**, Obateru OA, Bojuwoye MO. Helicobacter pylori eradication therapy: A review of current trends. *Niger Med J* 2013; **54**: 1-4 [PMID: 23661891 DOI: 10.4103/0300-1652.108884]

20 **Johnson-Henry KC**, Mitchell DJ, Avitzur Y, Galindo-Mata E, Jones NL, Sherman PM. Probiotics reduce bacterial colonization and gastric inflammation in H. pylori-infected mice. *Dig Dis Sci* 2004; **49**: 1095-1102 [PMID: 15387328]

21 **Lee JS**, Paek NS, Kwon OS, Hahm KB. Anti-inflammatory actions of probiotics through activating suppressor of cytokine signaling (SOCS) expression and signaling in Helicobacter pylori infection: a novel mechanism. *J Gastroenterol Hepatol* 2010; **25**: 194-202 [PMID: 20136974 DOI: 10.1111/j.1440-1746.2009.06127.x]

22 **Franceschi F**, Cazzato A, Nista EC, Scarpellini E, Roccarina D, Gigante G, Gasbarrini G, Gasbarrini A. Role of probiotics in patients with Helicobacter pylori infection. *Helicobacter* 2007; **12** Suppl 2: 59-63 [PMID: 17991178 DOI: 10.1111/j.1523-5378.2007.00565.x]

23 **Myllyluoma E**, Ahlroos T, Veijola L, Rautelin H, Tynkkynen S, Korpela R. Effects of anti-Helicobacter pylori treatment and probiotic supplementation on intestinal microbiota. *Int J Antimicrob Agents* 2007; **29**: 66-72 [PMID: 17141481 DOI: 10.1016/j.ijantimicag.2006.08.034]

24 **Szajewska H**, Horvath A, Piwowarczyk A. Meta-analysis: the effects of Saccharomyces boulardii supplementation on Helicobacter pylori eradication rates and side effects during treatment. *Aliment Pharmacol Ther* 2010; **32**: 1069-1079 [PMID: 21039671 DOI: 10.1111/j.1365-2036.2010.04457.x]

25 **Sachdeva A**, Nagpal J. Effect of fermented milk-based probiotic preparations on Helicobacter pylori eradication: a systematic review and meta-analysis of randomized-controlled trials. *Eur J Gastroenterol Hepatol* 2009; **21**: 45-53 [PMID: 19060631 DOI: 10.1097/MEG.0b013e32830d0eff]

26 **Wang ZH**, Gao QY, Fang JY. Meta-analysis of the efficacy and safety of Lactobacillus-containing and Bifidobacterium-containing probiotic compound preparation in Helicobacter pylori eradication therapy. *J Clin Gastroenterol* 2013; **47**: 25-32 [PMID: 23090045 DOI: 10.1097/MCG.0b013e318266f6cf]

27 **Tong JL**, Ran ZH, Shen J, Zhang CX, Xiao SD. Meta-analysis: the effect of supplementation with probiotics on eradication rates and adverse events during Helicobacter pylori eradication therapy. *Aliment Pharmacol Ther* 2007; **25**: 155-168 [PMID: 17229240 DOI: 10.1111/j.1365-2036.2006.03179.x]

28 **Gotteland M**, Brunser O, Cruchet S. Systematic review: are probiotics useful in controlling gastric colonization by Helicobacter pylori? *Aliment Pharmacol Ther* 2006; **23**: 1077-1086 [PMID: 16611267 DOI: 10.1111/j.1365-2036.2006.02868.x]

29 **Moher D**, Liberati A, Tetzlaff J, Altman DG. Preferred reporting items for systematic reviews and meta-analyses: the PRISMA statement. *PLoS Med* 2009; **6**: e1000097 [PMID: 19621072 DOI: 10.1371/journal.pmed.1000097]

30 **Higgins JP**, Altman DG, Gøtzsche PC, Jüni P, Moher D, Oxman AD, Savovic J, Schulz KF, Weeks L, Sterne JA. The Cochrane Collaboration's tool for assessing risk of bias in randomised trials. *BMJ* 2011; **343**: d5928 [PMID: 22008217 DOI: 10.1136/bmj.d5928]

31 **DerSimonian R**, Laird N. Meta-analysis in clinical trials. *Control Clin Trials* 1986; **7**: 177-188 [PMID: 3802833 DOI: 10.1016/0197-2456(86)90046-2]

32 **Ades AE**, Lu G, Higgins JP. The interpretation of random-effects meta-analysis in decision models. *Med Decis Making* 2005; **25**: 646-654 [PMID: 16282215 DOI: 10.1177/0272989X05282643]

33 **Deeks JJ**, Higgins JPT, Altman DG. Analyzing data and undertaking meta-analyses. In: Higgins J, Green S, eds. Cochrane Handbook for Systematic Reviews of Interventions 5.0.1. Oxford, UK: The Cochrane Collaboration, 2008: chap 9

34 **Higgins JP**, Thompson SG, Deeks JJ, Altman DG. Measuring inconsistency in meta-analyses. *BMJ* 2003; **327**: 557-560 [PMID: 12958120 DOI: 10.1136/bmj.327.7414.557]

35 **Altman DG**, Bland JM. Interaction revisited: the difference between two estimates. *BMJ* 2003; **326**: 219 [PMID: 12543843]

36 **Tobias A**. Assessing the influence of a single study in meta-analysis. *Stata Tech Bull* 1999; **47**: 15-17

37 **Egger M**, Davey Smith G, Schneider M, Minder C. Bias in meta-analysis detected by a simple, graphical test. *BMJ* 1997; **315**: 629-634 [PMID: 9310563 DOI: 10.1136/bmj.315.7109.629]

38 **Begg CB**, Mazumdar M. Operating characteristics of a rank correlation test for publication bias. *Biometrics* 1994; **50**: 1088-1101 [PMID: 7786990 DOI: 10.2307/2533446]

39 **Navarro-Rodriguez T**, Silva FM, Barbuti RC, Mattar R, Moraes-Filho JP, de Oliveira MN, Bogsan CS, Chinzon D, Eisig JN. Association of a probiotic to a Helicobacter pylori eradication regimen does not increase efficacy or decreases the adverse effects of the treatment: a prospective, randomized, double-blind, placebo-controlled study. *BMC Gastroenterol* 2013; **13**: 56 [PMID: 23530767 DOI: 10.1186/1471-230X-13-56]

40 **Ahmad K**, Fatemeh F, Mehri N, Maryam S. Probiotics for the treatment of pediatric helicobacter pylori infection: a randomized double blind clinical trial. *Iran J Pediatr* 2013; **23**: 79-84 [PMID: 23446685]

41 **Shavakhi A**, Tabesh E, Yaghoutkar A, Hashemi H, Tabesh F, Khodadoostan M, Minakari M, Shavakhi S, Gholamrezaei A. The effects of multistrain probiotic compound on bismuth-containing quadruple therapy for Helicobacter pylori infection: a randomized placebo-controlled triple-blind study. *Helicobacter* 2013; **18**: 280-284 [PMID: 23433200 DOI: 10.1111/hel.12047]

42 **Kyriakos N**, Papamichael K, Roussos A. A Lyophilized Form of Saccharomyces Boulardii Enhances the Helicobacter pylori Eradication Rates of Omeprazole-Triple Therapy in Patients With Peptic Ulcer Disease or Functional Dyspepsia. *Hospital Chronicles* 2013; **8**: 127-133

43 **Jiang YA**, Ou XL, Wang JN. Efficacy of Bacillus licheniformis combined with PPI triple therapy in eradication of Helicobacter pylori. *Shijie Huaren Xiaohua Zazhi* 2013; **21**: 840-844 [DOI: 10.11569/wcjd.v21.i9.840]

44 **Dajani AI**, Abu Hammour AM, Yang DH, Chung PC, Nounou MA, Yuan KY, Zakaria MA, Schi HS. Do probiotics improve eradication response to Helicobacter pylori on standard triple or sequential therapy? *Saudi J Gastroenterol* 2013; **19**: 113-120 [PMID: 23680708 DOI: 10.4103/1319-3767.111953]

45 **Deguchi R**, Nakaminami H, Rimbara E, Noguchi N, Sasatsu M, Suzuki T, Matsushima M, Koike J, Igarashi M, Ozawa H, Fukuda R, Takagi A. Effect of pretreatment with Lactobacillus gasseri OLL2716 on first-line Helicobacter pylori eradication therapy. *J Gastroenterol Hepatol* 2012; **27**: 888-892 [PMID: 22098133 DOI: 10.1111/j.1440-1746.2011.06985.x]

46 **Tolone S**, Pellino V, Vitaliti G, Lanzafame A, Tolone C. Evaluation of Helicobacter Pylori eradication in pediatric patients by triple therapy plus lactoferrin and probiotics compared to triple therapy alone. *Ital J Pediatr* 2012; **38**: 63 [PMID: 23114016 DOI: 10.1186/1824-7288-38-63]

47 **Mirzaee V**, Rezahosseini O. Randomized control trial: Comparison of Triple Therapy plus Probiotic Yogurt vs. Standard Triple Therapy on Helicobacter Pylori Eradication. *Iran Red Crescent Med J* 2012; **14**: 657-666 [PMID: 23285418]

48 **Manfredi M**, Bizzarri B, Sacchero RI, Maccari S, Calabrese L, Fabbian F, De'Angelis GL. Helicobacter pylori infection in clinical practice: probiotics and a combination of probiotics + lactoferrin improve compliance, but not eradication, in sequential therapy. *Helicobacter* 2012; **17**: 254-263 [PMID: 22759324 DOI: 10.1111/j.1523-5378.2012.00944.x]

49 **Du YQ**, Su T, Fan JG, Lu YX, Zheng P, Li XH, Guo CY, Xu P, Gong YF, Li ZS. Adjuvant probiotics improve the eradication effect of triple therapy for Helicobacter pylori infection. *World J Gastroenterol* 2012; **18**: 6302-6307 [PMID: 23180952 DOI: 10.3748/wjg.v18.i43.6302]

50 **Bekar O**, Yilmaz Y, Gulten M. Kefir improves the efficacy and tolerability of triple therapy in eradicating Helicobacter pylori. *J Med Food* 2011; **14**: 344-347 [PMID: 21186984 DOI: 10.1089/jmf.2010.0099]

51 **Yoon H**, Kim N, Kim JY, Park SY, Park JH, Jung HC, Song IS. Effects of multistrain probiotic-containing yogurt on second-line triple therapy for Helicobacter pylori infection. *J Gastroenterol Hepatol* 2011; **26**: 44-48 [PMID: 21175792]

52 **He QM**, Li BS, Li YJ. Bifid Triple Viable facilitates the sequential therapy for Helicobacter pylori eradication. *Xiandai Xiaohua Ji Jieru Zhenliao* 2011; **16**: 90-92

53 **Xu C**, Xiao L, Zou H. [Effect of birid triple viable on peptic ulcer patients with Helicobacter pylori infection]. *Zhongnan Daxue Xuebao Yixueban* 2010; **35**: 1000-1004 [PMID: 20871168]

54 **Yaşar B**, Abut E, Kayadıbı H, Toros B, Sezıklı M, Akkan Z, Keskın Ö, Övünç Kurdaş O. Efficacy of probiotics in Helicobacter pylori eradication therapy. *Turk J Gastroenterol* 2010; **21**: 212-217 [PMID: 20931422]

55 **Wen JJ**, Qiu RF. Effect of bifid triple viable on helicobacter pylori eradication. *Gannan Yixueyuan Xuebao* 2010; **30**: 902-903

56 **Song MJ**, Park DI, Park JH, Kim HJ, Cho YK, Sohn CI, Jeon WK, Kim BI. The effect of probiotics and mucoprotective agents on PPI-based triple therapy for eradication of Helicobacter pylori. *Helicobacter* 2010; **15**: 206-213 [PMID: 20557362 DOI: 10.1111/j.1523-5378.2010.00751.x]

57 **Szajewska H**, Albrecht P, Topczewska-Cabanek A. Randomized, double-blind, placebo-controlled trial: effect of lactobacillus GG supplementation on Helicobacter pylori eradication rates and side effects during treatment in children. *J Pediatr Gastroenterol Nutr* 2009; **48**: 431-436 [PMID: 19330931 DOI: 10.1097/MPG.0b013e318182e716]

58 **Hurduc V**, Plesca D, Dragomir D, Sajin M, Vandenplas Y. A randomized, open trial evaluating the effect of Saccharomyces boulardii on the eradication rate of Helicobacter pylori infection in children. *Acta Paediatr* 2009; **98**: 127-131 [PMID: 18681892 DOI: 10.1111/j.1651-2227.2008.00977.x]

59 **Francavilla R**, Lionetti E, Castellaneta SP, Magistà AM, Maurogiovanni G, Bucci N, De Canio A, Indrio F, Cavallo L,

Ierardi E, Miniello VL. Inhibition of Helicobacter pylori infection in humans by Lactobacillus reuteri ATCC 55730 and effect on eradication therapy: a pilot study. *Helicobacter* 2008; **13**: 127-134 [PMID: 18321302 DOI: 10.1111/j.1523-5378.2008.00593.x]

60 **Kim MN**, Kim N, Lee SH, Park YS, Hwang JH, Kim JW, Jeong SH, Lee DH, Kim JS, Jung HC, Song IS. The effects of probiotics on PPI-triple therapy for Helicobacter pylori eradication. *Helicobacter* 2008; **13**: 261-268 [PMID: 18665934]

61 **Huang JY**, Huang HP, Shi BY. Effect of bifid triple viable with standard triple therapy on helicobacter pylori eradication. *Shanghai Yiyao* 2008; **29**: 552-554

62 **Imase K**, Takahashi M, Tanaka A, Tokunaga K, Sugano H, Tanaka M, Ishida H, Kamiya S, Takahashi S. Efficacy of Clostridium butyricum preparation concomitantly with Helicobacter pylori eradication therapy in relation to changes in the intestinal microbiota. *Microbiol Immunol* 2008; **52**: 156-161 [PMID: 18402597 DOI: 10.1111/j.1348-0421.2008.00026.x]

63 **Cindoruk M**, Erkan G, Karakan T, Dursun A, Unal S. Efficacy and safety of Saccharomyces boulardii in the 14-day triple anti-Helicobacter pylori therapy: a prospective randomized placebo-controlled double-blind study. *Helicobacter* 2007; **12**: 309-316 [PMID: 17669103 DOI: 10.1111/j.1523-5378.2007.00516.x]

64 **Park SK**, Park DI, Choi JS, Kang MS, Park JH, Kim HJ, Cho YK, Sohn CI, Jeon WK, Kim BI. The effect of probiotics on Helicobacter pylori eradication. *Hepatogastroenterology* 2007; **54**: 2032-2036 [PMID: 18251154]

65 **de Bortoli N**, Leonardi G, Ciancia E, Merlo A, Bellini M, Costa F, Mumolo MG, Ricchiuti A, Cristiani F, Santi S, Rossi M, Marchi S. Helicobacter pylori eradication: a randomized prospective study of triple therapy versus triple therapy plus lactoferrin and probiotics. *Am J Gastroenterol* 2007; **102**: 951-956 [PMID: 17313499 DOI: 10.1111/j.1572-0241.2007.01085.x]

66 **Sahagún-Flores JE**, López-Peña LS, de la Cruz-Ramírez Jaimes J, García-Bravo MS, Peregrina-Gómez R, de Alba-García JE. [Eradication of Helicobacter pylori: triple treatment scheme plus Lactobacillus vs. triple treatment alone]. *Cir Cir* 2007; **75**: 333-336 [PMID: 18158878]

67 **Lionetti E**, Miniello VL, Castellaneta SP, Magistá AM, de Canio A, Maurogiovanni G, Ierardi E, Cavallo L, Francavilla R. Lactobacillus reuteri therapy to reduce side-effects during anti-Helicobacter pylori treatment in children: a randomized placebo controlled trial. *Aliment Pharmacol Ther* 2006; **24**: 1461-1468 [PMID: 17032283 DOI: 10.1111/j.1365-2036.2006.03145.x]

68 **Goldman CG**, Barrado DA, Balcarce N, Rua EC, Oshiro M, Calcagno ML, Janjetic M, Fuda J, Weill R, Salgueiro MJ, Valencia ME, Zubillaga MB, Boccio JR. Effect of a probiotic food as an adjuvant to triple therapy for eradication of Helicobacter pylori infection in children. *Nutrition* 2006; **22**: 984-988 [PMID: 16978844 DOI: 10.1016/j.nut.2006.06.008]

69 **Sheu BS**, Cheng HC, Kao AW, Wang ST, Yang YJ, Yang HB, Wu JJ. Pretreatment with Lactobacillus- and Bifidobacterium-containing yogurt can improve the efficacy of quadruple therapy in eradicating residual Helicobacter pylori infection after failed triple therapy. *Am J Clin Nutr* 2006; **83**: 864-869 [PMID: 16600940]

70 **Ziemniak W**. Efficacy of Helicobacter pylori eradication taking into account its resistance to antibiotics. *J Physiol Pharmacol* 2006; **57** Suppl 3: 123-141 [PMID: 17033111]

71 **Sýkora J**, Valecková K, Amlerová J, Siala K, Dedek P, Watkins S, Varvarovská J, Stozický F, Pazdiora P, Schwarz J. Effects of a specially designed fermented milk product containing probiotic Lactobacillus casei DN-114 001 and the eradication of H. pylori in children: a prospective randomized double-blind study. *J Clin Gastroenterol* 2005; **39**: 692-698 [PMID: 16082279 DOI: 10.1097/01.mcg.0000173855.77191.44]

72 **Myllyluoma E**, Veijola L, Ahlroos T, Tynkkynen S, Kankuri E, Vapaatalo H, Rautelin H, Korpela R. Probiotic supplementation improves tolerance to Helicobacter pylori eradication therapy--a placebo-controlled, double-blind randomized pilot study. *Aliment Pharmacol Ther* 2005; **21**: 1263-1272 [PMID: 15882248 DOI: 10.1111/j.1365-2036.2005.02448.x]

73 **Duman DG**, Bor S, Ozütemiz O, Sahin T, Oğuz D, Iştan F, Vural T, Sandkci M, Işksal F, Simşek I, Soytürk M, Arslan S, Sivri B, Soykan I, Temizkan A, Beşşk F, Kaymakoğlu S, Kalayc C. Efficacy and safety of Saccharomyces boulardii in prevention of antibiotic-associated diarrhoea due to Helicobacterpylori eradication. *Eur J Gastroenterol Hepatol* 2005; **17**: 1357-1361 [PMID: 16292090 DOI: 10.1097/00042737-200512000-00015]

74 **Shimbo I**, Yamaguchi T, Odaka T, Nakajima K, Koide A, Koyama H, Saisho H. Effect of Clostridium butyricum on fecal flora in Helicobacter pylori eradication therapy. *World J Gastroenterol* 2005; **11**: 7520-7524 [PMID: 16437727]

75 **Cao YJ**, Qu CM, Yuan Q. Control of intestinal flora alteration induced by eradication therapy of Helicobacter pylori infection in the elders. *Weichagnbingxue He Ganbingxue Zazhi* 2005; **14**: 195-199

76 **Nista EC**, Candelli M, Cremonini F, Cazzato IA, Zocco MA, Franceschi F, Cammarota G, Gasbarrini G, Gasbarrini A. Bacillus clausii therapy to reduce side-effects of anti-Helicobacter pylori treatment: randomized, double-blind, placebo controlled trial. *Aliment Pharmacol Ther* 2004; **20**: 1181-1188 [PMID: 15569121 DOI: 10.1111/j.1365-2036.2004.02274.x]

77 **Tursi A**, Brandimarte G, Giorgetti GM, Modeo ME. Effect of Lactobacillus casei supplementation on the effectiveness and tolerability of a new second-line 10-day quadruple therapy after failure of a first attempt to cure Helicobacter pylori infection. *Med Sci Monit* 2004; **10**: CR662-CR666 [PMID: 15567983]

78 **Guo JB**, Yang PF, Wang MT. The application of clostridium butyricum to the eradication of Helicobacter pylori. *Zhonghua Fubujibing Zazhi* 2004; **4**: 163-165

79 **Sheu BS**, Wu JJ, Lo CY, Wu HW, Chen JH, Lin YS, Lin MD. Impact of supplement with Lactobacillus- and Bifidobacterium-containing yogurt on triple therapy for Helicobacter pylori eradication. *Aliment Pharmacol Ther* 2002; **16**: 1669-1675 [PMID: 12197847 DOI: 10.1046/j.1365-2036.2002.01335.x]

80 **Cremonini F**, Di Caro S, Covino M, Armuzzi A, Gabrielli M, Santarelli L, Nista EC, Cammarota G, Gasbarrini G, Gasbarrini A. Effect of different probiotic preparations on anti-helicobacter pylori therapy-related side effects: a parallel group, triple blind, placebo-controlled study. *Am J Gastroenterol* 2002; **97**: 2744-2749 [PMID: 12425542 DOI: 10.1111/j.1572-0241.2002.07063.x]

81 **Armuzzi A**, Cremonini F, Bartolozzi F, Canducci F, Candelli M, Ojetti V, Cammarota G, Anti M, De Lorenzo A, Pola P, Gasbarrini G, Gasbarrini A. The effect of oral administration of Lactobacillus GG on antibiotic-associated gastrointestinal side-effects during Helicobacter pylori eradication therapy. *Aliment Pharmacol Ther* 2001; **15**: 163-169 [PMID: 11148433 DOI: 10.1046/j.1365-2036.2001.00923.x]

82 **Armuzzi A**, Cremonini F, Ojetti V, Bartolozzi F, Canducci F, Candelli M, Santarelli L, Cammarota G, De Lorenzo A, Pola P, Gasbarrini G, Gasbarrini A. Effect of Lactobacillus GG supplementation on antibiotic-associated gastrointestinal side effects during Helicobacter pylori eradication therapy: a pilot study. *Digestion* 2001; **63**: 1-7 [PMID: 11173893 DOI: 10.1159/000051865]

83 **Canducci F**, Armuzzi A, Cremonini F, Cammarota G, Bartolozzi F, Pola P, Gasbarrini G, Gasbarrini A. A lyophilized and inactivated culture of Lactobacillus acidophilus increases Helicobacter pylori eradication rates. *Aliment Pharmacol Ther* 2000; **14**: 1625-1629 [PMID: 11121911 DOI: 10.1046/j.1365-2036.2000.00885.x]

84 **Duvall S**, Tweedie R. A nonparametric ''trim and fill'' method for assessing publication bias in meta-analysis. *J Am Stat Assoc* 2000; **95**: 89-98 [DOI: 10.1080/01621459.2000.10473905]

85 **Zagari RM**, Bianchi-Porro G, Fiocca R, Gasbarrini G, Roda E, Bazzoli F. Comparison of 1 and 2 weeks of omeprazole, amoxicillin and clarithromycin treatment for Helicobacter pylori eradication: the HYPER Study. *Gut* 2007; **56**: 475-479 [PMID: 17028126 DOI: 10.1136/gut.2006.102269]

86 **Patel A**, Shah N, Prajapati JB. Clinical application of probiotics in the treatment of Helicobacter pylori infection--a brief review. *J Microbiol Immunol Infect* 2014; **47**: 429-437 [PMID: 23757373 DOI: 10.1016/j.jmii.2013.03.010]

87 **Gao XW**, Mubasher M, Fang CY, Reifer C, Miller LE. Dose-

response efficacy of a proprietary probiotic formula of Lactobacillus acidophilus CL1285 and Lactobacillus casei LBC80R for antibiotic-associated diarrhea and Clostridium difficile-associated diarrhea prophylaxis in adult patients. *Am J Gastroenterol* 2010; **105**: 1636-1641 [PMID: 20145608 DOI: 10.1038/ajg.2010.11]

88 **Giorgio F**, Principi M, De Francesco V, Zullo A, Losurdo G, Di Leo A, Ierardi E. Primary clarithromycin resistance to Helicobacter pylori: Is this the main reason for triple therapy failure? *World J Gastrointest Pathophysiol* 2013; **4**: 43-46 [PMID: 23946886 DOI: 10.4291/wjgp.v4.i3.43]

89 **Megraud F**. Helicobacter pylori and antibiotic resistance. *Gut* 2007; **56**: 1502 [PMID: 17938430 DOI: 10.1136/gut.2007.132514]

90 **Georgopoulos SD**, Papastergiou V, Karatapanis S. Helicobacter pylori Eradication Therapies in the Era of Increasing Antibiotic Resistance: A Paradigm Shift to Improved Efficacy. *Gastroenterol Res Pract* 2012; **2012**: 757926 [PMID: 22778723]

91 **Graham DY**, Shiotani A. New concepts of resistance in the treatment of Helicobacter pylori infections. *Nat Clin Pract Gastroenterol Hepatol* 2008; **5**: 321-331 [PMID: 18446147 DOI: 10.1038/ncpgasthep1138]

92 **De Francesco V**, Giorgio F, Hassan C, Manes G, Vannella L, Panella C, Ierardi E, Zullo A. Worldwide H. pylori antibiotic resistance: a systematic review. *J Gastrointestin Liver Dis* 2010; **19**: 409-414 [PMID: 21188333]

93 **Gisbert JP**, Pérez-Aisa A, Bermejo F, Castro-Fernández M, Almela P, Barrio J, Cosme A, Modolell I, Bory F, Fernández-Bermejo M, Rodrigo L, Ortuño J, Sánchez-Pobre P, Khorrami S, Franco A, Tomas A, Guerra I, Lamas E, Ponce J, Calvet X. Second-line therapy with levofloxacin after failure of treatment to eradicate helicobacter pylori infection: time trends in a Spanish Multicenter Study of 1000 patients. *J Clin Gastroenterol* 2013; **47**: 130-135 [PMID: 22647827 DOI: 10.1097/MCG.0b013e318254ebdd]

94 **Salari P**, Nikfar S, Abdollahi M. A meta-analysis and systematic review on the effect of probiotics in acute diarrhea. *Inflamm Allergy Drug Targets* 2012; **11**: 3-14 [PMID: 22309079 DOI: 10.2174/187152812798889394]

95 **Ringel-Kulka T**, Palsson OS, Maier D, Carroll I, Galanko JA, Leyer G, Ringel Y. Probiotic bacteria Lactobacillus acidophilus NCFM and Bifidobacterium lactis Bi-07 versus placebo for the symptoms of bloating in patients with functional bowel disorders: a double-blind study. *J Clin Gastroenterol* 2011; **45**: 518-525 [PMID: 21436726 DOI: 10.1097/MCG.0b013e31820ca4d6]

96 **Quigley EM**. The enteric microbiota in the pathogenesis and management of constipation. *Best Pract Res Clin Gastroenterol* 2011; **25**: 119-126 [PMID: 21382583 DOI: 10.1016/j.bpg.2011.01.003]

97 **Jayasimhan S**, Yap NY, Roest Y, Rajandram R, Chin KF. Efficacy of microbial cell preparation in improving chronic constipation: a randomized, double-blind, placebo-controlled trial. *Clin Nutr* 2013; **32**: 928-934 [PMID: 23561636 DOI: 10.1016/j.clnu.2013.03.004]

98 **Miller LE**, Ouwehand AC. Probiotic supplementation decreases intestinal transit time: meta-analysis of randomized controlled trials. *World J Gastroenterol* 2013; **19**: 4718-4725 [PMID: 23922468 DOI: 10.3748/wjg.v19.i29.4718]

99 **Bardhan PK**. Epidemiological features of Helicobacter pylori infection in developing countries. *Clin Infect Dis* 1997; **25**: 973-978 [PMID: 9402340 DOI: 10.1086/516067]

100 **Kamdeu Fansi AA**, Guertin JR, LeLorier J. Savings from the use of a probiotic formula in the prophylaxis of antibiotic-associated diarrhea. *J Med Econ* 2012; **15**: 53-60 [PMID: 22023067 DOI: 10.3111/13696998.2011.629015]

P- Reviewer: Ji JS, Kanda T, Ulasoglu C **S- Editor**: Yu J
L- Editor: Cant MR **E- Editor**: Liu XM

World Journal of Gastroenterology

Submit a Manuscript: http://www.wjgnet.com/esps/
Help Desk: http://www.wjgnet.com/esps/helpdesk.aspx
DOI: 10.3748/wjg.v21.i14.4358

World J Gastroenterol 2015 April 14; 21(14): 4358-4364
ISSN 1007-9327 (print) ISSN 2219-2840 (online)

META-ANALYSIS

Efficacy of S-1 *vs* capecitabine for the treatment of gastric cancer: A meta-analysis

An-Bing He, Xiu-Lan Peng, Jia Song, Ji-Xing Zhang, Wei-Guo Dong, Ren-Feng Luo, Yan Tang

An-Bing He, Xiu-Lan Peng, Yan Tang, Department of Oncology, the Fifth Hospital of Wuhan, Wuhan 430050, Hubei Province, China
Jia Song, Ji-Xing Zhang, Wei-Guo Dong, Department of Medical College, Jiang Han University, Wuhan 430056, Hubei Province, China
Wei-Guo Dong, Ren-Feng Luo, Department of Gastroenterology, Renmin Hospital of Wuhan University, Wuhan 430060, Hubei Province, China
Author contributions: Peng XL and He AB contributed equally to this work; Peng XL, He AB and Dong WG conceived and designed the paper; Song J, Zhang JX and Peng XL searched the data; Zhang JX, Song J, Peng XL and Tang Y analyzed the data; Peng XL, Zhang JX, He AB and Dong WG wrote the manuscript; all authors contributed to the manuscript.

Correspondence to: Wei-Guo Dong, MD, Department of Gastroenterology, Renmin Hospital of Wuhan University, No. 238 Jiefang Road, Wuhan 430060, Hubei Province, China. dongwg66@163.com
Telephone: +86-27-88041911
Fax: +86-27-88041911
Received: July 15, 2014
Peer-review started: July 16, 2014
First decision: August 15, 2014
Revised: September 12, 2014
Accepted: October 21, 2014
Article in press: October 21, 2014
Published online: April 14, 2015

Abstract

AIM: To rationally evaluate the effect of S-1 *vs* capecitabine for the treatment of gastric cancer.

METHODS: MEDLINE, EMBASE, Cochrane Controlled Trials Register, Google Scholar, and China Journal Full Text Database were accessed to collect clinical randomized controlled trials regarding the effect of S-1 *vs* capecitabine for the treatment of gastric cancer patients. Statistical analysis was performed by meta-analysis. Four randomized controlled trials met the inclusion criteria.

RESULTS: Compared with capecitabine regimens, the 1-year survival rate in gastric cancer patients was 0.80 (95%CI: 0.52-1.21, P = 0.29). The overall response rate of S-1 *vs* capecitabine was 0.94 (95%CI: 0.59-1.51, P = 0.93). Compared with capecitabine regimens, the most frequent hematologic toxicities were neutropenia (OR = 0.99, 95%CI: 0.65-1.49, P = 0.94) and thrombocytopenia (OR = 0.72, 95%CI: 0.31-1.67, P = 0.44). The most frequent non-hematologic toxicities included nausea (OR = 0.85, 95%CI: 0.56-1.28, P = 0.43) and hand-foot syndrome (OR = 0.16, 95%CI: 0.10-0.27, P < 0.00001).

CONCLUSION: The existing studies suggest that S-1 is not more effective than capecitabine in the treatment of gastric cancer patients, but does exhibit less toxicity with regard to hand-foot syndrome.

Key words: Gastric cancer; S-1; Capecitabine; Randomized controlled trials; Meta-analysis

Core tip: Systemic chemotherapy has proven to be an important treatment for advanced gastric cancer patients. A combination regimen containing 5-fluorouracil is most commonly used worldwide. S-1 and capecitabine are both oral fluoropyrimidine carbamates, and have proven to be effective for the treatment of gastric cancer patients. This is the first meta-analysis to systematically compare

the effects between S-1 and capecitabine against gastric cancer in order to better understand the efficacy, safety, and feasibility of these anticancer drugs. The results may contribute to better treatment and quality of life for patients with advanced gastric cancer.

He AB, Peng XL, Song J, Zhang JX, Dong WG, Luo RF, Tang Y. Efficacy of S-1 *vs* capecitabine for the treatment of gastric cancer: A meta-analysis. *World J Gastroenterol* 2015; 21(14): 4358-4364 Available from: URL: http://www.wjgnet.com/1007-9327/full/v21/i14/4358.htm DOI: http://dx.doi.org/10.3748/wjg.v21.i14.4358

INTRODUCTION

Gastric cancer is the second-leading cause of cancer-related deaths worldwide[1]. Although mortality rates of gastric cancer have declined over the past few decades, the disease still has a poor prognosis and remains a major health problem[2]. Surgical resection has been accepted as the gold standard and only possible curative treatment for patients with early stage gastric cancer[3,4]. However, most symptoms of gastric cancer are nonspecific, and screening strategies are unavailable in many areas; thus most patients with gastric cancer are diagnosed in an incurable stage.

Over the past two decades, multiple therapies, including systemic chemotherapy, have demonstrated efficacy in decreasing the risk of relapse and improving survival and quality of life for patients with advanced gastric cancer[5,6]. Although there is no single agent or globally-accepted standard chemotherapy treatment strategy for gastric cancer, combination regimens containing 5-fluorouracil (5-FU) are commonly used worldwide[7-11]. The efficacy of oral capecitabine in gastrointestinal cancers has been investigated in a series of studies[12-17], while adjuvant chemotherapy with S-1 is recommended in Japan[18,19].

In this study, we performed a meta-analysis to systematically compare the effects of S-1 and capecitabine in the treatment of gastric cancer in order to better understand the efficacy, safety, and feasibility of these anticancer drugs.

MATERIALS AND METHODS

Search strategy

Randomized trials comparing S-1 with capecitabine regimen (single agent, doublet, or triplet) for the treatment of gastric cancer were searched MEDLINE, EMBASE, Cochrane Controlled Trials Register, and China Journal Full Text Database up to 1 October 2013. The language was limited to English and Chinese. The following keywords were used: gastric cancer, capecitabine, and S-1. We also searched the reference lists of pertinent manuscripts in order to identify other potentially relevant articles.

Criteria for study selection

The inclusion criteria for selected articles were as follows: (1) all were random control tests; (2) adult studies were selected; (3) the experiments compared S-1 with capecitabine for the treatment of gastric cancer; and (4) full texts were selected. Preclinical studies, reviews, and case reports not covering the disease being studied were excluded.

Data extraction

Two reviewers selected papers, evaluated their quality, and then extracted the data independently. A third individual was consulted if there were any disagreements. Data on details pertaining to the patients, number of patients at the start of the study, and completed subjects, treatment type, outcomes, and adverse effects were extracted.

Statistical analysis

Statistical analyses were conducted *via* the Cochrane Collaboration's Review Manager version 5.1. Relative risks (RR) and 95%CI were calculated as summary statistics. The estimate of RR from individual studies was calculated. Statistical heterogeneity was assessed by using the I^2 test to quantify heterogeneity across studies. If the results of heterogeneity were significant, the random effects model was used to perform analysis, otherwise, the fix effects model was employed. Statistical significance was indicated by a P value less than 0.05.

RESULTS

Characteristics of eligible studies

A total of 371 papers were initially identified using the search strategy described above. After a thorough screening of the papers, 4 studies were ultimately selected based on the inclusion/exclusion criteria (Figure 1). All four papers assessed the one year survival rate, while three papers evaluated the overall response rate. The study duration ranged from 0.5 to 39.2 mo. The number of patients in each of the included studies ranged from 81 to 129. Two papers were published in English and two in Chinese. The characteristics of the selected studies are presented in Tables 1 and 2[20-23]. Two studies used SOX compared with XEOLX in gastric cancer[21,23]. One study compared S-1 alone with capecitabine[22]. One study compared TS with TC in patients with gastric cancer[20].

Analysis of efficacy

A total of 382 patients from 4 RCTs were included in the 1-year survival analysis; 190 patients were in the S-1 group and 192 were in the capecitabine group. The total recurrence rate of gastric cancer was 45.8% in the S-1 group and 50.5% in the capecitabine group. The pooled OR for the four studies was 0.80 (OR = 0.80, 95%CI: 0.52-1.21, P = 0.29) (Figure 2), suggesting no statistically significant difference between the

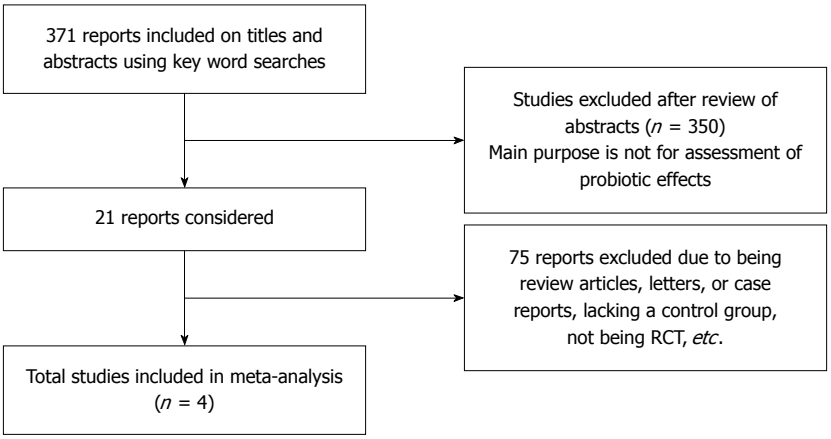

Figure 1 Flow diagram for studies evaluating S-1 *vs* capecitabine for gastric cancer included in this meta-analysis.

Table 1 Characteristics of trials included in meta-analysis

Study	Patients (S-1/capecitabine)	S-1 regimen	Capecitabine regimen
Kim *et al*[23]	65/64	S-1 80 mg/m^2 per day d1-14 + oxaliplatin 130 mg/m^2 d1 21-d cycle	Capecitabine 2000 mg/m^2 per day d1-14 + oxaliplatin 130 mg/m^2 d1 21-d cycle
Lee *et al*[22]	42/44	S-1: BSA < 1.25 m^2, 80 mg/d; BSA: 1.25-1.5 m^2, 100 mg/d; BSA > 1.5 m^2, 120 mg/d; d1-28 42-d cycle	Capecitabine 2500 mg/m^2 per day d1-14 21-d cycle
Zhang *et al*[21]	41/40	S-1 80 mg/m^2 per day d1-14 + oxaliplatin 130 mg/m^2 d1 21-d cycle	Capecitabine 2000 mg/m^2 per day d1-14 + oxaliplatin 130 mg/m^2 d1 21-d cycle
Xiong *et al*[20]	42/44	S-1 80 mg/m^2 per day d1-14 + docetaxel 25 mg/m^2 d1, 8, 15 28-d cycle	Capecitabine 1250 mg/m^2 per day d1-14 + docetaxel 25 mg/m^2 d1, 8, 15 28-d cycle

Table 2 Trial and patient characteristics

Study	Disease stage	Follow-up months	Trial randomization	Lost to follow-up	Survival analysis
Kim *et al*[23]	Advanced gastric cancer, chemotherapy-naive	0.5-39.2	Yes	Recorded	ITT
Lee *et al*[22]	Elderly patients (aged ≥ 65 yr) Advanced gastric cancer	Capecitabine: 21.9; S-1: 21.7	Yes	Recorded	ITT
Zhang *et al*[21]	Gastric cancer after surgery	24	Yes	Recorded	Evaluable
Xiong *et al*[20]	Advanced gastric cancer, chemotherapy-naive	2-28	Yes	Recorded	ITT

S-1 and capecitabine groups. No heterogeneity was observed between the selected studies for the treatment analysis (I^2 = 0%).

A total of 301 randomized patients from 3 RCTs were included in the overall response rate analysis; 149 patients were in the S-1 group and 152 were in the capecitabine group. A summary of the individual studies and pooled results from the primary analysis of overall response rate are presented in Figure 3. The total overall response rate was 37.6% in the S-1 group and 38.8% in the capecitabine group. The pooled OR for the three studies was 0.94 (OR = 0.94, 95%CI: 0.59-1.51, *P* = 0.93), suggesting no statistically significant difference between the S-1 and capecitabine groups. No heterogeneity was observed between the selected studies with regard to the treatment analysis (I^2 = 0%).

Analysis of toxicity

Overall, the toxicities observed in the 4 selected RCTs were tolerable. The most common grade 3-4 hematologic toxicities were neutropenia and thrombocytopenia. The most common grade 3-4 non-hematologic toxicities included nausea and vomiting. The pooled results suggested no significant difference between two treatment groups (Figures 4 and 5). In addition, hand-foot syndrome at any grade was more frequently noted in the capecitabine group than in the S-1 group (Figure 5).

Publication bias assessment

Publication bias was assessed by funnel plot. The funnel plots exhibited symmetry (Figure 6), thereby suggesting no publication bias among the selected studies.

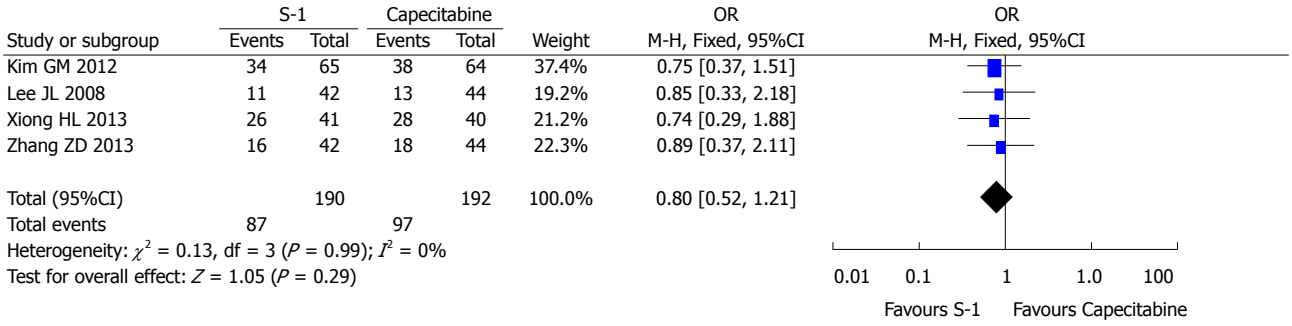

Figure 2 One year survival rate of S-1 regiment *vs* capecitabine regiment.

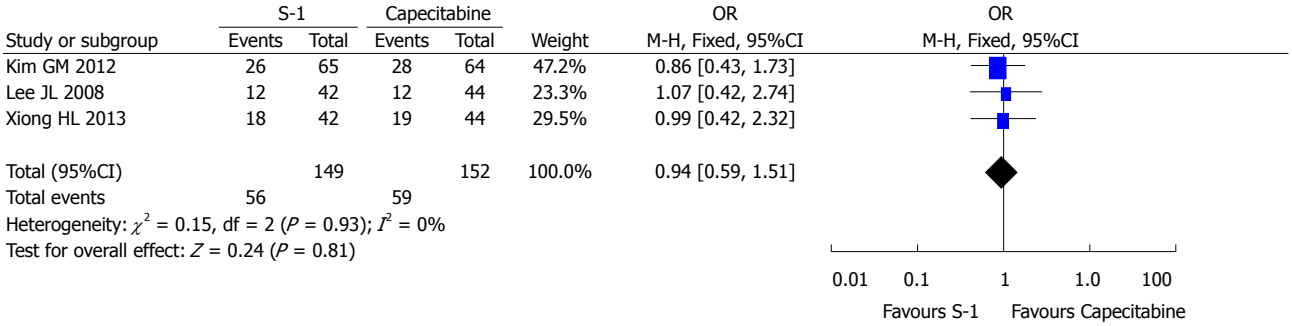

Figure 3 Overall response rate of S-1 regiment *vs* capecitabine regiment.

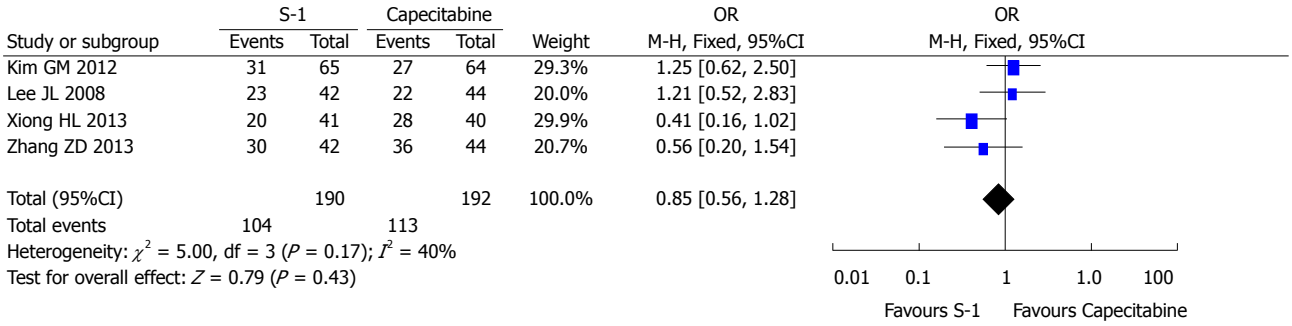

Figure 4 Nausea of S-1 regiment *vs* capecitabine regiment.

DISCUSSION

Treatment of gastric cancer has been a major challenge in the past decades given its high incidence. A large number of patients are diagnosed with advanced or metastatic disease. A wide range of studies determined that combination chemotherapy containing fluoropyrimidine prolongs survival in patients with advanced gastric cancer[24-28]. Combination regimes containing fluoropyrimidine have therefore made undeniable gains in improving survival rates for patients with advanced gastric cancer. Given the relatively short overall survival of advanced gastric cancer patients and the palliative nature of systemic chemotherapy, chemotherapeutic agents should be selected based on efficacy, low toxicity, and convenient administration.

S-1 is an oral combination anticancer drug consisting of: 5-fluorouracil prodrug tegafur; 5-chloro-2, 4-dihydroxypyridine; and potassium oxonate. In this combination 5-chloro-2, 4-dihydroxypyridine acts as a dihydropyrimidine dehydrogenase inhibitor, whereas potassium oxonate suppresses the gastrointestinal toxicity of tegafur[29]. In several studies of gastric cancer patients, S-1 has exhibited a similar efficacy and reduced toxicity compared with infusional 5-FU[9,30,31]. Capecitabine is also an oral fluoropyrimidine carbamate that is metabolized primarily in the liver and enzymatically converted to 5-fluorouracil by thymidine phosphorylase in tumor tissues. The levels of the enzyme thymidine phosphorylase are considerably higher in gastric cancers compared with normal tissue, which allows 5-fluorouracil to be concentrated in tumor tissues[32]. The efficacy and safety of capecitabine for advanced gastric cancer has been demonstrated[33], and a randomized phase Ⅲ trial indicated that capecitabine can replace 5-FU for the treatment of advanced esopha-

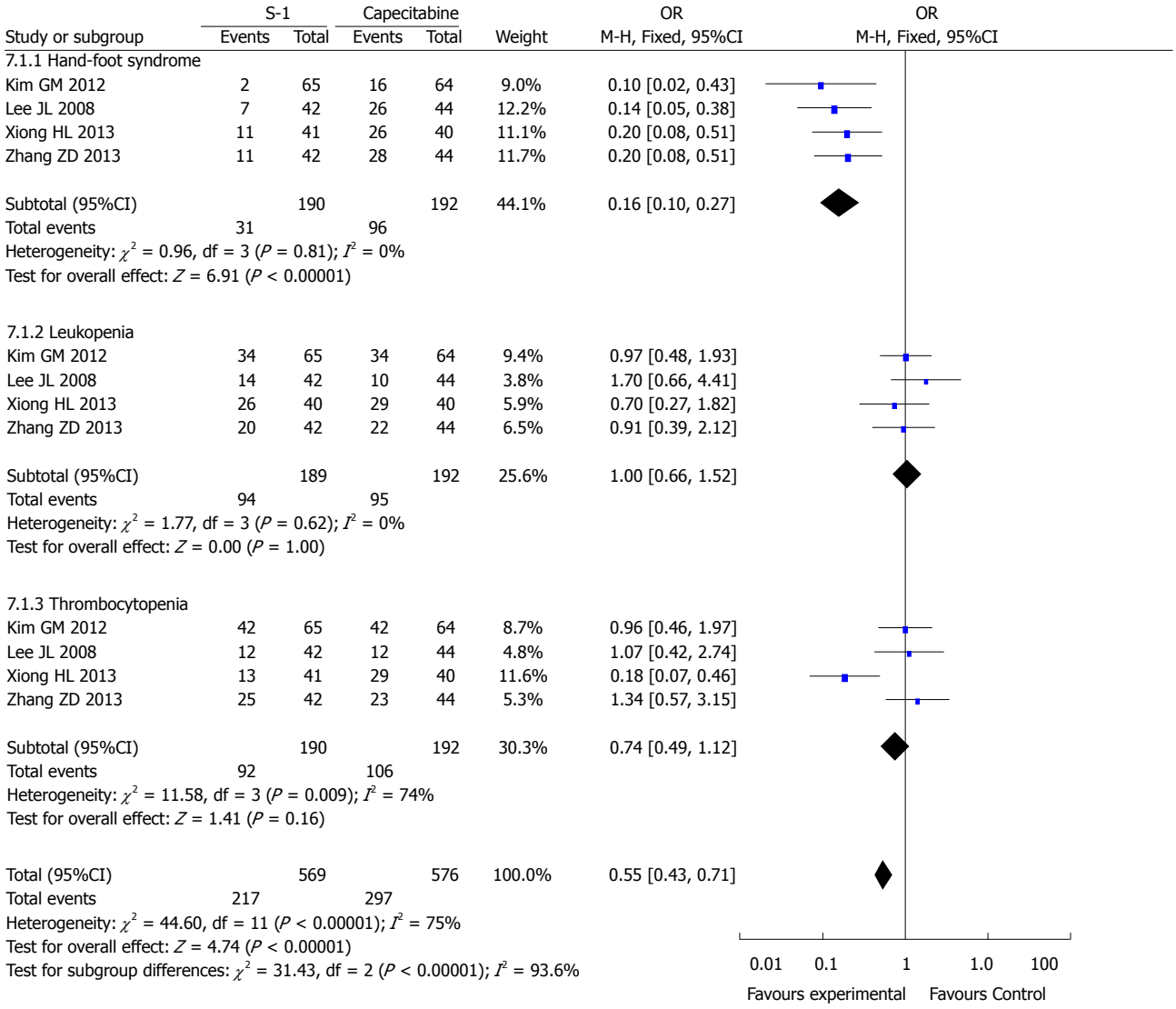

Figure 5 Toxicity of S-1 regiment *vs* capecitabine regiment.

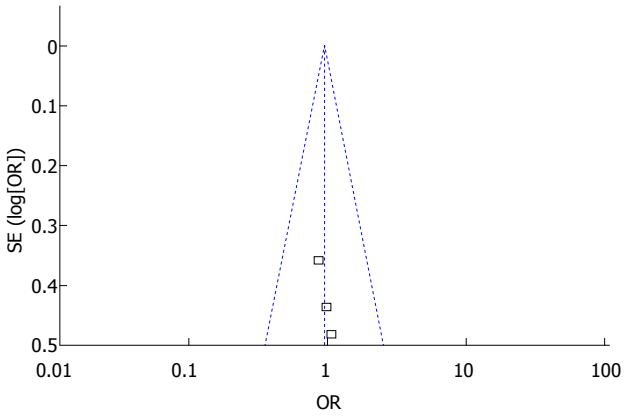

Figure 6 Publication bias assessed by funnel plot.

gogastric cancer[34].

This meta-analysis focused on the comparison of survival outcomes and toxicity between S-1-based regimens and capecitabine for the treatment of patients with gastric cancer. Only four randomized trials with 382 patients met our eligible criteria. Among the four studies, 1-year survival and overall response rate were selected as the primary study endpoints. Although overall survival is considered to be the most clinically meaningful measure of treatment effect in cancer patients, only two of the studies analyzed overall survival; these results did not exhibit sufficient robustness for the meta-analysis. The results indicate that treatment with regimens containing capecitabine were equally as effective as S-1-containing chemotherapies in patients with gastric cancer with regard to 1-year survival and overall response rate. This result was consistent with the results of the four included studies[20-23].

The most suitable treatment regimen for an individual patient is not only dependent on treatment efficacy, but also involves other factors, such as toxicity[35]. S-1 and capecitabine were both well-tolerated, and no treatment-related deaths were reported in the selected studies. The

most frequent hematological toxicities were neutropenia and thrombocytopenia, with no meaningful differences in hematologic toxicities being noted between the two treatment agents. The most frequently observed grade 3 or 4 non-hematologic toxicities included nausea and vomiting, and no meaningful differences were noted between the two treatment agents. The only notable non-hematologic difference in adverse events was the increased incidence of hand-foot syndrome in the capecitabine group compared with the S-1 group. Hand-foot syndrome is a characteristic non-hematologic toxicity of capecitabine that leads to treatment delays or dose reductions in many patients. Given these findings, we suggest that S-1 is superior to capecitabine for the treatment of gastric cancer.

Although this meta-analysis was based on RCTs and properly conducted, there were still some limitations to our study. One major limitation was that the number of selected studies was quite small, with this small sample size therefore likely not reflecting the actual situation. In addition, only two studies analyzed overall survival, with these results failing to exhibit sufficient robustness for the meta-analysis. However, 1-year survival and overall response rate, which are the most meaningful clinical measures of treatment efficacy in cancer patients, were analyzed.

In summary, although S-1 demonstrated no survival advantage over capecitabine, it resulted in a considerably lower incidence of hand-foot syndrome than capecitabine, thereby suggesting that S-1 is superior to capecitabine for the treatment of gastric cancer.

COMMENTS

Background

Gastric cancer is the second leading cause of cancer-related deaths globally, with most gastric cancer patients being diagnosed in an incurable stage. Systemic chemotherapy have been proved to decrease relapse risk and improve survival and quality of life for advanced gastric cancer patients, with a combination regimen containing 5-fluorouracil being most commonly used worldwide. S-1 and capecitabine are both oral fluoropyrimidine carbamates. The efficacy of oral capecitabine in gastrointestinal cancers has been investigated in a series of studies. Adjuvant chemotherapy with S-1 has been recommended in Japan. We aim to systematically compare the effects of S-1 and capecitabine in the treatment of gastric cancer for a better understanding of the efficacy, safety, and feasibility of these anticancer drugs.

Research frontiers

Systemic chemotherapy is an important treatment for advanced gastric cancer patients; S-1 and capecitabine were both proved to be effective in the treatment of gastric cancer, but the efficacy, safety, and feasibility of S-1 *vs* capecitabine remains unknown.

Innovations and breakthroughs

The authors performed a meta-analysis to systematically compare the effects of S-1 and capecitabine in the treatment of gastric cancer in order to better understanding the efficacy, safety, and feasibility of these anticancer drugs. This may contribute to better treatment and quality of life for gastric cancer patients.

Applications

The results showed that S-1 is not more effective than capecitabine in the treatment of gastric cancer patients, but does result in fewer instances of hand-foot syndrome.

Peer-review

In this manuscript, Peng *et al* determined that S-1 was not more effective than capecitabine in the treatment of gastric cancer patients, but does show fewer instances of hand-foot syndrome. The efficacy of oral capecitabine in gastrointestinal cancers has been investigated in a series of studies, with adjuvant chemotherapy with S-1 being recommended in Japan. The authors compared the effects of S-1 and capecitabine in the treatment of gastric cancer, resulting in a meaningful conclusion.

REFERENCES

1 **Jemal A**, Bray F, Center MM, Ferlay J, Ward E, Forman D. Global cancer statistics. *CA Cancer J Clin* 2011; **61**: 69-90 [PMID: 21296855 DOI: 10.3322/caac.20107]

2 **Siegel R**, Naishadham D, Jemal A. Cancer statistics, 2012. *CA Cancer J Clin* 2012; **62**: 10-29 [PMID: 22237781 DOI: 10.3322/caac.20138]

3 **Wu HL**, Tian Q, Peng CW, Liu SP, Li Y. Multivariate survival and outcome analysis of 154 patients with gastric cancer at a single Chinese institution. *Asian Pac J Cancer Prev* 2011; **12**: 3341-3345 [PMID: 22471477]

4 **O'Connor KG**. Gastric cancer. *Semin Oncol Nurs* 1999; **15**: 26-35 [PMID: 10074655 DOI: 10.1016/S0749-2081(99)80037-0]

5 **Kim YH**. Chemotherapy for advanced gastric cancer: slow but further progress. *Cancer Res Treat* 2005; **37**: 79-86 [PMID: 19956484 DOI: 10.4143/crt.2005.37.2.79]

6 **Wagner AD**, Grothe W, Haerting J, Kleber G, Grothey A, Fleig WE. Chemotherapy in advanced gastric cancer: a systematic review and meta-analysis based on aggregate data. *J Clin Oncol* 2006; **24**: 2903-2909 [PMID: 16782930 DOI: 10.1200/JCO.2005.05.0245]

7 **Hu JK**, Li CM, Chen XZ, Chen ZX, Zhou ZG, Zhang B, Chen JP. The effectiveness of intravenous 5-fluorouracil-containing chemotherapy after curative resection for gastric carcinoma: A systematic review of published randomized controlled trials. *J Chemother* 2007; **19**: 359-375 [PMID: 17855179 DOI: 10.1179/joc.2007.19.4.359]

8 **Van Cutsem E**, Moiseyenko VM, Tjulandin S, Majlis A, Constenla M, Boni C, Rodrigues A, Fodor M, Chao Y, Voznyi E, Risse ML, Ajani JA. Phase III study of docetaxel and cisplatin plus fluorouracil compared with cisplatin and fluorouracil as first-line therapy for advanced gastric cancer: a report of the V325 Study Group. *J Clin Oncol* 2006; **24**: 4991-4997 [PMID: 17075117 DOI: 10.1200/JCO.2006.06.8429]

9 **Koizumi W**, Kurihara M, Nakano S, Hasegawa K. Phase II study of S-1, a novel oral derivative of 5-fluorouracil, in advanced gastric cancer. For the S-1 Cooperative Gastric Cancer Study Group. *Oncology* 2000; **58**: 191-197 [PMID: 10765119 DOI: 10.1159/000012099]

10 **Bouché O**, Ychou M, Burtin P, Bedenne L, Ducreux M, Lebreton G, Baulieux J, Nordlinger B, Martin C, Seitz JF, Tigaud JM, Echinard E, Stremsdoerfer N, Milan C, Rougier P. Adjuvant chemotherapy with 5-fluorouracil and cisplatin compared with surgery alone for gastric cancer: 7-year results of the FFCD randomized phase III trial (8801). *Ann Oncol* 2005; **16**: 1488-1497 [PMID: 15939717 DOI: 10.1093/annonc/mdi270]

11 **Shitara K**, Sawaki A, Matsuo K, Kondo C, Takahari D, Ura T, Tajika M, Niwa Y, Muro K. A retrospective comparison of S-1 plus cisplatin and capecitabine plus cisplatin for patients with advanced or recurrent gastric cancer. *Int J Clin Oncol* 2013; **18**: 539-546 [PMID: 22552360 DOI: 10.1007/s10147-012-0416-6]

12 **Van Cutsem E**, Twelves C, Cassidy J, Allman D, Bajetta E, Boyer M, Bugat R, Findlay M, Frings S, Jahn M, McKendrick J, Osterwalder B, Perez-Manga G, Rosso R, Rougier P, Schmiegel WH, Seitz JF, Thompson P, Vieitez JM, Weitzel C, Harper P. Oral capecitabine compared with intravenous fluorouracil plus leucovorin in patients with metastatic colorectal cancer: results of a large phase III study. *J Clin Oncol* 2001; **19**: 4097-4106 [PMID: 11689577]

13 **Hoff PM**, Ansari R, Batist G, Cox J, Kocha W, Kuperminc M, Maroun J, Walde D, Weaver C, Harrison E, Burger HU, Osterwalder B, Wong AO, Wong R. Comparison of oral capecitabine versus intravenous fluorouracil plus leucovorin as first-line treatment in 605 patients with metastatic colorectal cancer: results of a randomized phase III study. *J Clin Oncol* 2001; **19**: 2282-2292 [PMID: 11304782]

14 **Twelves C**, Wong A, Nowacki MP, Abt M, Burris H, Carrato A, Cassidy J, Cervantes A, Fagerberg J, Georgoulias V, Husseini F, Jodrell D, Koralewski P, Kröning H, Maroun J, Marschner N, McKendrick J, Pawlicki M, Rosso R, Schüller J, Seitz JF, Stabuc B, Tujakowski J, Van Hazel G, Zaluski J, Scheithauer W. Capecitabine as adjuvant treatment for stage III colon cancer. *N Engl J Med* 2005; **352**: 2696-2704 [PMID: 15987918 DOI: 10.1056/NEJMoa043116]

15 **Cassidy J**, Clarke S, Díaz-Rubio E, Scheithauer W, Figer A, Wong R, Koski S, Lichinitser M, Yang TS, Rivera F, Couture F, Sirzén F, Saltz L. Randomized phase III study of capecitabine plus oxaliplatin compared with fluorouracil/folinic acid plus oxaliplatin as first-line therapy for metastatic colorectal cancer. *J Clin Oncol* 2008; **26**: 2006-2012 [PMID: 18421053 DOI: 10.1200/JCO.2007.14.9898]

16 **Rothenberg ML**, Cox JV, Butts C, Navarro M, Bang YJ, Goel R, Gollins S, Siu LL, Laguerre S, Cunningham D. Capecitabine plus oxaliplatin (XELOX) versus 5-fluorouracil/folinic acid plus oxaliplatin (FOLFOX-4) as second-line therapy in metastatic colorectal cancer: a randomized phase III noninferiority study. *Ann Oncol* 2008; **19**: 1720-1726 [PMID: 18550577 DOI: 10.1093/annonc/mdn370]

17 **Saltz LB**, Clarke S, Díaz-Rubio E, Scheithauer W, Figer A, Wong R, Koski S, Lichinitser M, Yang TS, Rivera F, Couture F, Sirzén F, Cassidy J. Bevacizumab in combination with oxaliplatin-based chemotherapy as first-line therapy in metastatic colorectal cancer: a randomized phase III study. *J Clin Oncol* 2008; **26**: 2013-2019 [PMID: 18421054 DOI: 10.1200/JCO.2007.14.9930]

18 **Sakuramoto S**, Sasako M, Yamaguchi T, Kinoshita T, Fujii M, Nashimoto A, Furukawa H, Nakajima T, Ohashi Y, Imamura H, Higashino M, Yamamura Y, Kurita A, Arai K. Adjuvant chemotherapy for gastric cancer with S-1, an oral fluoropyrimidine. *N Engl J Med* 2007; **357**: 1810-1820 [PMID: 17978289 DOI: 10.1056/NEJMoa072252]

19 **Japanese Gastric Cancer Association**. Japanese gastric cancer treatment guidelines 2010 (ver. 3). *Gastric Cancer* 2011; **14**: 113-123 [PMID: 21573742 DOI: 10.1007/s10120-011-0042-4]

20 **Xiong HL**, Liu XQ, Sun AH, He Y, Li J, Yuan X. Clinical comparison of Docetaxel combined with S-1 or Capecitabine in treating advanced gastric carcinoma. *Xiandai Zhongliu Yixue* 2013; **21**: 581-584

21 **Zhang ZD**, Kong Y, MA F, Liu HX, Zhang B, Huang JX, Ma EM, Hua YW. Adjuvant chemotherapy with Oxaliplatin plus S-1 versus XELOX regimen for postoperative gastric cancer. *Zhongguo Putong Waike Zazhi* 2013; **22**: 747-751

22 **Lee JL**, Kang YK, Kang HJ, Lee KH, Zang DY, Ryoo BY, Kim JG, Park SR, Kang WK, Shin DB, Ryu MH, Chang HM, Kim TW, Baek JH, Min YJ. A randomised multicentre phase II trial of capecitabine vs S-1 as first-line treatment in elderly patients with metastatic or recurrent unresectable gastric cancer. *Br J Cancer* 2008; **99**: 584-590 [PMID: 18665164 DOI: 10.1038/sj.bjc.6604536]

23 **Kim GM**, Jeung HC, Rha SY, Kim HS, Jung I, Nam BH, Lee KH, Chung HC. A randomized phase II trial of S-1-oxaliplatin versus capecitabine-oxaliplatin in advanced gastric cancer. *Eur J Cancer* 2012; **48**: 518-526 [PMID: 22243774 DOI: 10.1016/j.ejca.2011.12.017]

24 **Janunger KG**, Hafström L, Glimelius B. Chemotherapy in gastric cancer: a review and updated meta-analysis. *Eur J Surg* 2002; **168**: 597-608 [PMID: 12699095 DOI: 10.1080/11024150201680005]

25 **Oba K**, Morita S, Tsuburaya A, Kodera Y, Kobayashi M, Sakamoto J. Efficacy of adjuvant chemotherapy using oral fluorinated pyrimidines for curatively resected gastric cancer: a meta-analysis of centrally randomized controlled clinical trials in Japan. *J Chemother* 2006; **18**: 311-317 [PMID: 17129844]

26 **Koizumi W**, Narahara H, Hara T, Takagane A, Akiya T, Takagi M, Miyashita K, Nishizaki T, Kobayashi O, Takiyama W, Toh Y, Nagaie T, Takagi S, Yamamura Y, Yanaoka K, Orita H, Takeuchi M. S-1 plus cisplatin versus S-1 alone for first-line treatment of advanced gastric cancer (SPIRITS trial): a phase III trial. *Lancet Oncol* 2008; **9**: 215-221 [PMID: 18282805 DOI: 10.1016/S1470-2045(08)70035-4]

27 **Kang YK**, Kang WK, Shin DB, Chen J, Xiong J, Wang J, Lichinitser M, Guan Z, Khasanov R, Zheng L, Philco-Salas M, Suarez T, Santamaria J, Forster G, McCloud PI. Capecitabine/cisplatin versus 5-fluorouracil/cisplatin as first-line therapy in patients with advanced gastric cancer: a randomised phase III noninferiority trial. *Ann Oncol* 2009; **20**: 666-673 [PMID: 19153121 DOI: 10.1093/annonc/mdn717]

28 **Jeung HC**, Rha SY, Kim HK, Lim HY, Kim S, Kim SY, Gong SJ, Park CH, Ahn JB, Noh SH, Chung HC. Multi-institutional phase II study of S-1 monotherapy in advanced gastric cancer with pharmacokinetic and pharmacogenomic evaluations. *Oncologist* 2007; **12**: 543-554 [PMID: 17522242]

29 **Maehara Y**. S-1 in gastric cancer: a comprehensive review. *Gastric Cancer* 2003; **6** Suppl 1: 2-8 [PMID: 12775012]

30 **Sakata Y**, Ohtsu A, Horikoshi N, Sugimachi K, Mitachi Y, Taguchi T. Late phase II study of novel oral fluoropyrimidine anticancer drug S-1 (1 M tegafur-0.4 M gimestat-1 M otastat potassium) in advanced gastric cancer patients. *Eur J Cancer* 1998; **34**: 1715-1720 [PMID: 9893658]

31 **Ajani JA**, Rodriguez W, Bodoky G, Moiseyenko V, Lichinitser M, Gorbunova V, Vynnychenko I, Garin A, Lang I, Falcon S. Multicenter phase III comparison of cisplatin/S-1 with cisplatin/infusional fluorouracil in advanced gastric or gastroesophageal adenocarcinoma study: the FLAGS trial. *J Clin Oncol* 2010; **28**: 1547-1553 [PMID: 20159816 DOI: 10.1200/JCO.2009.25.4706]

32 **Hong YS**, Song SY, Lee SI, Chung HC, Choi SH, Noh SH, Park JN, Han JY, Kang JH, Lee KS, Cho JY. A phase II trial of capecitabine in previously untreated patients with advanced and/or metastatic gastric cancer. *Ann Oncol* 2004; **15**: 1344-1347 [PMID: 15319239]

33 **Cunningham D**, Starling N, Rao S, Iveson T, Nicolson M, Coxon F, Middleton G, Daniel F, Oates J, Norman AR. Capecitabine and oxaliplatin for advanced esophagogastric cancer. *N Engl J Med* 2008; **358**: 36-46 [PMID: 18172173 DOI: 10.1056/NEJMoa073149]

34 **Miwa M**, Ura M, Nishida M, Sawada N, Ishikawa T, Mori K, Shimma N, Umeda I, Ishitsuka H. Design of a novel oral fluoropyrimidine carbamate, capecitabine, which generates 5-fluorouracil selectively in tumours by enzymes concentrated in human liver and cancer tissue. *Eur J Cancer* 1998; **34**: 1274-1281 [PMID: 9849491]

35 **Schiller JH**, Harrington D, Belani CP, Langer C, Sandler A, Krook J, Zhu J, Johnson DH. Comparison of four chemotherapy regimens for advanced non-small-cell lung cancer. *N Engl J Med* 2002; **346**: 92-98 [PMID: 11784875]

P- Reviewer: Chen L **S- Editor**: Qi Y
L- Editor: Rutherford A **E- Editor**: Liu XM

World Journal of Gastroenterology

Submit a Manuscript: http://www.wjgnet.com/esps/
Help Desk: http://www.wjgnet.com/esps/helpdesk.aspx
DOI: 10.3748/wjg.v21.i14.4365

World J Gastroenterol 2015 April 14; 21(14): 4365-4372
ISSN 1007-9327 (print) ISSN 2219-2840 (online)

META-ANALYSIS

Anti-epidermal growth factor receptor monoclonal antibodies in metastatic colorectal cancer: A meta-analysis

Qi-Bin Song, Qi Wang, Wei-Guo Hu

Qi-Bin Song, Qi Wang, Wei-Guo Hu, Department of Oncology, Renmin Hospital of Wuhan University, Wuhan 430060, Hubei Province, China

Author contributions: Song QB, Wang Q and Hu WG contributed equally to this work; Song QB designed the research; Wang Q performed the research; Hu WG analyzed the data; Wang Q wrote the paper.

Correspondence to: Qi-Bin Song, Professor, Department of Oncology, Renmin Hospital of Wuhan University, Zhangzhidong District, Wuhan 430060, Hubei Province, China. qibinsong@163.com
Telephone: +86-27-88041911
Fax: +86-27-88041911

Received: July 20, 2014
Peer-review started: July 20, 2014
First decision: August 15, 2014
Revised: September 10, 2014
Accepted: October 15, 2014
Article in press: October 15, 2014
Published online: April 14, 2015

Abstract

AIM: To investigate the correlation between Kirsten rat sarcoma viral oncogene homolog (*KRAS*) status and the therapeutic effects of anti-epidermal growth factor receptor (EGFR) monoclonal antibodies (MoAbs) in metastatic colorectal cancer (mCRC).

METHODS: Randomized controlled trials (RCTs) were identified and the association between *KRAS* mutation and clinical outcome in mCRC patients treated with anti-EGFR MoAbs was investigated. Ten RCTs were included in this meta-analysis. Progression-free survival and overall survival were used to assess the strength of the relationship between *KRAS* mutation and clinical outcome.

RESULTS: In first-line treatment, survival benefit was confined to patients with wild-type *KRAS*. Chemotherapy regimens and angiogenesis inhibitor treatment influenced the results of the analysis. Wild-type *KRAS* mCRC patients did not seem to benefit from oxaliplatin-based chemotherapy (PFS: HR = 0.88, 95%CI: 0.70-1.10; OS: HR = 0.93, 95%CI: 0.82-1.04). Clinical benefit in mCRC patients was limited to therapeutic regimens which included anti-EGFR MoAbs and fluorouracil-based therapy (PFS: HR = 0.77, 95%CI: 0.69-0.86; OS: HR = 0.85, 95%CI: 0.75-0.95). When anti-EGFR MoAbs were used as second- or further-line treatment, clinical benefit was still confined to patients with wild-type *KRAS*.

CONCLUSION: *KRAS* status is a potential predictive marker of clinical benefit due to anti-EGFR MoAb therapy in mCRC patients.

Key words: Colorectal neoplasm; Kirsten rat sarcoma viral oncogene homolog; Cetuximab; Panitumumab; Meta-analysis

Core tip: In this study, we evaluated the correlation between Kirsten rat sarcoma viral oncogene homolog (*KRAS*) status and the therapeutic effects of anti-epidermal growth factor receptor (EGFR) monoclonal antibodies (MoAbs) in patients with metastatic colorectal cancer. We focused on the relationship between *KRAS* status and the curative effect of anti-EGFR MoAbs in patients with metastatic colorectal cancer, and conducted a systematic meta-analysis of chemotherapy regimens, line of treatment and

bevacizumab treatment. This analysis provides the first evidence that patients with wild-type *KRAS* metastatic colorectal cancer may not benefit from anti-EGFR MoAbs and oxaliplatin-based therapy as first-line treatment. Clinical benefit was confined to therapeutic regimens which included anti-EGFR MoAbs and fluorouracil-based therapy.

Song QB, Wang Q, Hu WG. Anti-epidermal growth factor receptor monoclonal antibodies in metastatic colorectal cancer: A meta-analysis. *World J Gastroenterol* 2015; 21(14): 4365-4372 Available from: URL: http://www.wjgnet.com/1007-9327/full/v21/i14/4365.htm DOI: http://dx.doi.org/10.3748/wjg.v21.i14.4365

INTRODUCTION

Colorectal cancer is one of the most common human malignant diseases and a leading cause of cancer-related death worldwide, accounting for approximately of all cancer incidence and mortality[1]. Over the last decade, the availability of combination chemotherapy and targeted agents has improved the median survival of patients with metastatic colorectal cancer (mCRC)[2,3]. Two biological agents, the monoclonal antibodies (MoAbs), cetuximab and panitumumab, which target the epidermal growth factor receptor (EGFR) have been approved by the food and drug administration (FDA) for mCRC. Kirsten rat sarcoma viral oncogene homolog (*KRAS*) mutations have emerged as major predictive markers of resistance to anti-EGFR MoAbs. These observations have been shown to be beneficial in small single-arm data and some retrospective analyses of large phase Ⅲ studies[4-7]. The results of previous reviews demonstrated that mCRC patients with mutant *KRAS* did not benefit from treatment with anti-EGFR MoAbs either alone or in combination with standard chemotherapy. However, these reviews included data from retrospective and non-randomized studies. Following the completion of several large phase Ⅲ clinical trials, the role of *KRAS* mutation in mCRC should be redefined. We aimed to provide a comprehensive evaluation of the relationship between *KRAS* status and the therapeutic effects of anti-EGFR MoAbs in mCRC patients. Analyses were conducted on chemotherapy regimens, line of treatment and bevacizumab treatment.

MATERIALS AND METHODS

Publication search

Systematic computerized searches of PubMed (up to December 14, 2013) were performed. The search was further augmented by checking the clinical trial registry (www.clinicaltrials.gov) for additional studies. The following search terms were used: "metastatic rectal cancer", "metastatic colon cancer", "metastatic colorectal cancer", "mCRC", "KRAS", "cetuximab", "panitumumab", "monoclonal antibodies", "MoAb". The search was limited to human studies. All eligible studies were retrieved, and their bibliographies were examined for other relevant publications. The results of a randomized controlled trial are often published in a series of articles, thus when the same data were used in several publications, the most recent, largest or complete study of these publications was included in this meta-analysis.

Inclusion criteria

The included studies met the following criteria: (1) Randomized controlled trials published as articles which compared anti-EGFR MoAbs plus chemotherapy or best supportive care (BSC) with chemotherapy or BSC alone in patients with mCRC; (2) Studies evaluating the relationship between *KRAS* mutation status and response to anti-EGFR MoAbs in mCRC patients; (3) Provide adequate data on progression-free survival (PFS) and overall survival (OS); and (4) Studies with full text articles.

Data extraction

Information was carefully extracted from all eligible studies. The following data were collected from each study: first author's name, year of publication, number of patients screened, study treatment protocols, response criteria, number of patients by *KRAS* mutation status, line of treatment, PFS and OS. The clinical endpoints were extracted separately according to *KRAS* status. Data extraction was performed independently by two of the authors. Disagreement was resolved by discussion between the two authors. If the two authors could not reach a consensus, another author was consulted and a final decision was made by voting.

Statistical analysis

The primary endpoints were PFS and OS. The association between *KRAS* status and PFS or OS was expressed as the hazard ratio (HR). Heterogeneity was assessed by the *Q*-test[8,9]. If significant heterogeneity was found ($P < 0.10$, $I^2 > 40\%$), the random-effects model instead of the fixed-effects model was used for further analysis. To investigate the possible sources of heterogeneity, we conducted subgroup analyses based on the following aspects: the use of bevacizumab, chemotherapy regimen, and the selection of fluorouracil or capecitabine. Egger's linear regression test[10] was used to assess publication bias, which was adjusted using the trim-and-fill method. All the statistical tests used in this meta-analysis were performed with RevMan 5.4 and STATA version 10.0 (Stata Corporation, College Station, TX, United States).

RESULTS

Characteristics of the included studies

After exclusion of duplicate and irrelevant studies (Figure 1), 10 studies[7,11-19] were identified according

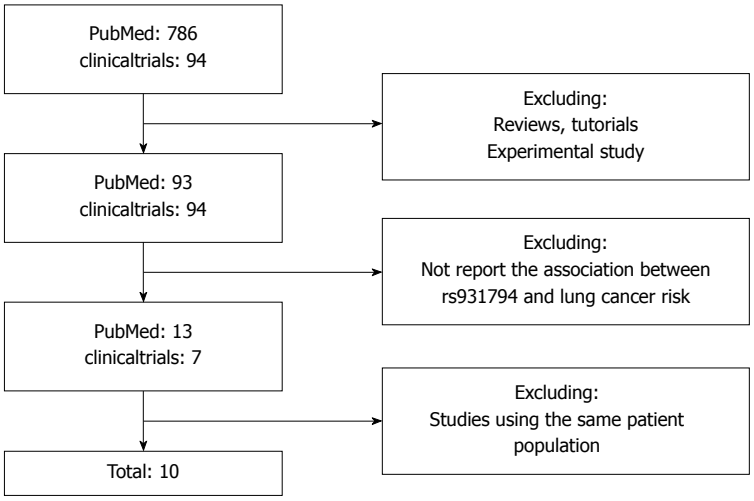

Figure 1 Flow chart of the literature search and study selection procedure.

Table 1 Characteristics of included studies

Ref.	Year	Patients assessed	*KRAS* wt	*KRAS* mut	Response criteria
1st line treatment					
Maughan *et al*[11]	2011	1630	729	565	RECIST
Van Cutsem *et al*[12]	2011	1198	666	397	WHO
Bokemeyer *et al*[7]	2011	337	179	136	WHO
Douillard *et al*[13]	2010	1183	656	440	RECIST
Hecht *et al*[14]	2009	823	404	260	RECIST
Hecht *et al*[14]	2009	230	115	86	RECIST
Tol *et al*[15]	2009	755	314	206	RECIST
Tveit *et al*[16]	2012	566	303	195	RECIST
2nd line treatment					
Peeters *et al*[17]	2010	1186	597	486	RECIST
Harbison *et al*[18]	2012	572	245	208	RECIST
Amado *et al*[19]	2008	463	243	184	RECIST

RECIST: Response Evaluation Criteria in Solid Tumor.

Table 2 Treatment protocols in included studies

Ref.	Study treatment protocol
1st line treatment	
Maughan *et al*[11]	Ox 85 mg/m^2 FA 350 mg/m^2 5FU 400 mg/m^2 bolus + 2400 mg/m^2 infusion ± cetuximab Ox 130 mg/m^2 Cap 2000 mg/m^2 ± cetuximab
Van Cutsem *et al*[12]	Iri 180 mg/m^2 FA 400 mg/m^2 5FU 400 mg/m^2 bolus + 2400 mg/m^2 infusion ± cetuximab
Bokemeyer *et al*[7]	Ox 85 mg/m^2 FA 400 mg/m^2 5FU 400 mg/m^2 bolus + 1200 mg/m^2 infusion ± cetuximab
Douillard *et al*[13]	Ox 85 mg/m^2 FA 400 mg/m^2 5FU 400 mg/m^2 bolus + 1200 mg/m^2 infusion ± panitumumab
Hecht *et al*[14]	Ox/FA/5FU/Bev
Hecht *et al*[14]	Iri/FA/5FU/Bev
Tol *et al*[15]	Ox/Cap/Bev
Tveit *et al*[16]	Ox 85 mg/m^2 FA 120 mg/m^2 5FU 1000 mg/m^2 bolus ± cetuximab
2nd line treatment	
Peeters *et al*[17]	Iri 180 mg/m^2 FA 400 mg/m^2 5FU 400 mg/m^2 bolus + 2400 mg/m^2 infusion ± panitumumab
Harbison *et al*[18]	BSC ± cetuximab
Amado *et al*[19]	BSC ± panitumumab

Ox: Oxaliplatin; FA: Folinic acid; 5FU: 5-fluourouracil; Cap: Capecitabine; Iri: Irinotecan; Bev: Bevacizumab; BSC: Best supportive care.

to the inclusion criteria of the meta-analysis. Tables 1 and 2 show the primary characteristics of the 10 studies which included patients treated with anti-EGFR MoAbs, all of which were randomized controlled trials. All 10 studies included a total of 8943 patients, and sample sizes ranged from 337 to 1630. *KRAS* status was available in 7614 patients, 4451 patients had wild-type *KRAS* and 3163 patients had mutant *KRAS*. Of the 10 studies, MoAbs were administered as first-line treatment with chemotherapy in 7 studies and MoAbs

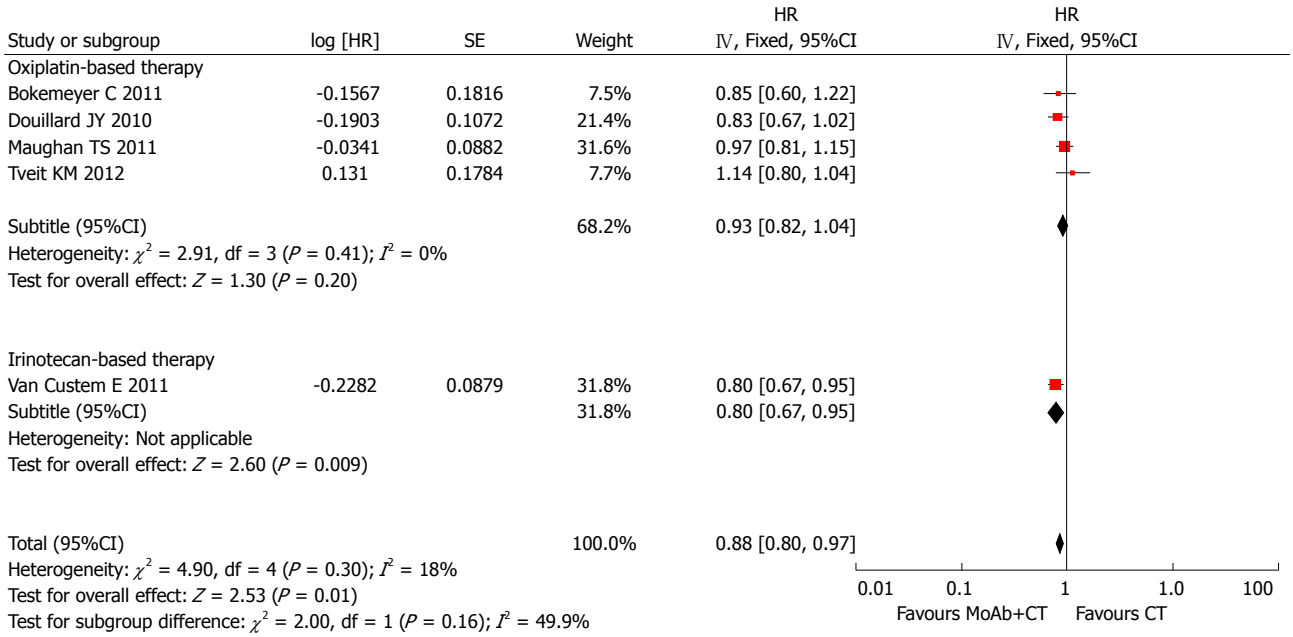

Figure 2 Subgroup analysis of overall survival based on chemotherapy regimen in KRAS wild-type patients following first-line treatment.

were administered as second-line or further-line treatment with or without chemotherapy in 3 studies. Hecht *et al*[14] used two different chemotherapy regimens (FOLFIRI or FOLFOX) combined with cetuximab, and we divided this study into two parts in order to conduct an analysis of chemotherapy regimen. Response Evaluation Criteria in Solid Tumor (RECIST) criteria or WHO criteria were used to classify tumor response in all studies.

Analysis of trials using MoAbs as first-line treatment

Patients with wild-type KRAS: In total, seven studies supplied adequate information on OS in patients with known *KRAS* status. The HR summarized survival in the arm treated with cetuximab combined with chemotherapy compared with the arm treated with chemotherapy alone. An HR of more than 1 indicated worse survival in patients treated with chemotherapy alone. There was no evidence of improved OS in patients with wild-type *KRAS* treated with MoAbs (HR = 1.00, 95%CI: 0.82-1.21), and significant intergroup heterogeneity was observed (I^2 = 73%, P = 0.002). In these seven studies, two studies used bevacizumab in both arms. Subgroup analysis was carried out, the pooled HR of trials using bevacizumab was 1.79 (95%CI: 1.26-2.54) and the pooled HR of trials using chemotherapy was 0.88 (95%CI: 0.80-0.97). We excluded trials using bevacizumab and conducted different subgroup analyses to determine heterogeneity. In the trials using oxaliplatin-based chemotherapy, the pooled HR was 0.93 (95%CI: 0.82-1.04), and the P value of Egger's test was 0.831. Only one study used irinotecan-based chemotherapy, and the HR was 0.80 (95%CI: 0.67-0.95; Figure 2). The relationship between chemotherapy regimen and clinical benefit in mCRC patients with wild-type *KRAS* treated with anti-EGFR MoAbs needs to be explored in further studies. However, patients with wild-type *KRAS* did not seem to benefit from anti-EGFR MoAbs and oxaliplatin-based chemotherapy as first-line treatment (HR = 0.93, 95%CI: 0.82-1.04, P = 0.20; Figure 2). Timothy S Maughan's study supplied sufficient information on the HR of patients treated with fluorouracil and those treated with capecitabine. Therefore, we divided this study into two different studies and conducted another subgroup analysis. The subgroup analysis indicated that fluorouracil and anti-EGFR MoAbs benefited patients in terms of longer OS (HR = 0.85, 95%CI: 0.75-0.95; I^2 = 10%, P = 0.34). However, only one trial used capecitabine with anti-EGFR MoAbs and no OS benefit was observed (HR = 0.97, 95%CI: 0.81-1.15).

Information on PFS in wild-type *KRAS* patients was available in 7 studies, and included 6722 patients. *KRAS* status was detected in 5651 patients and 3366 of these patients had wild-type *KRAS*. Anti-EGFR MoAbs had no benefit on PFS in trials of first-line treatment (HR = 0.96, 95%CI: 0.79-1.16), with significant intertrial heterogeneity (I^2 = 77%, P < 0.0001), and the P value of Egger's test was 0.824. In the trials using bevacizumab, the pooled HR was 1.27 (95%CI: 1.06-1.51). There was no significant heterogeneity or publication bias between these trials (I^2 = 0%, P = 0.59; P value of Egger's test was 0.571). The pooled HR of trials using conventional chemotherapy was 0.83 (95%CI: 0.68-1.03), and there was evidence of differences in the effect of MoAbs between trials (I^2 = 75%, P = 0.0003). No publication bias was found using Egger's test (P = 0.387). A subgroup analysis was performed to explore the sources of heterogeneity between studies using conventional chemotherapy. In the trials using oxaliplatin-based therapy, the pooled HR was 0.88 (95%CI: 0.70-1.10; I^2 = 73%, P = 0.002).

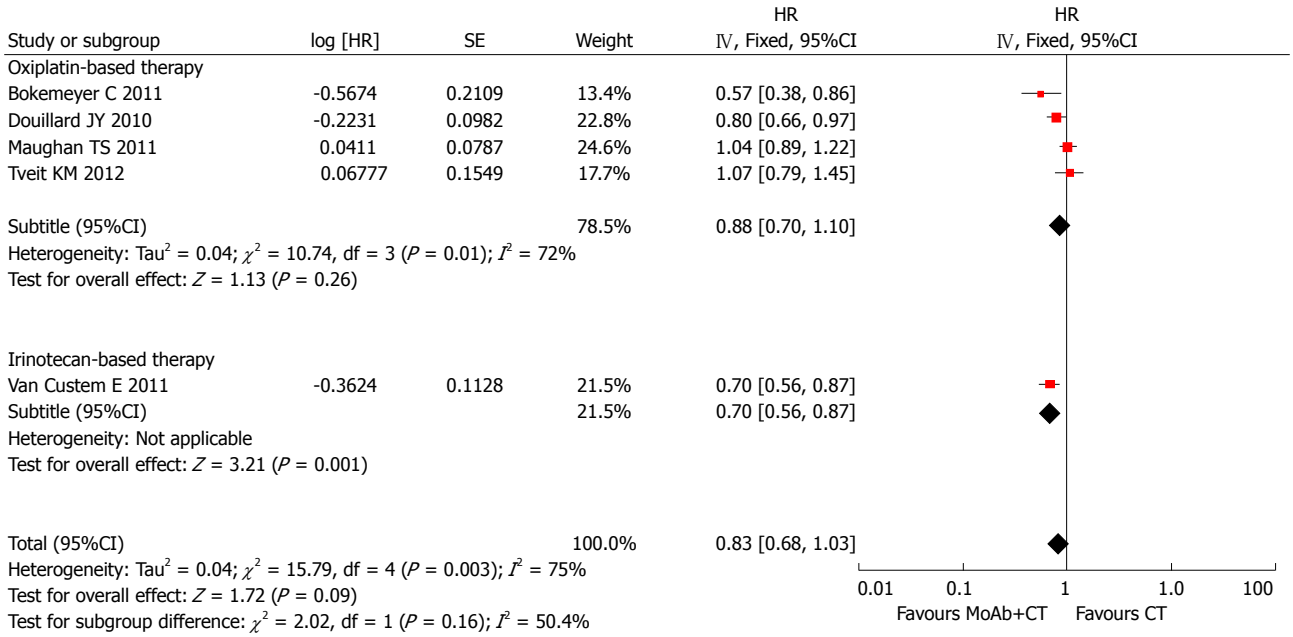

Figure 3 Subgroup analysis of progression-free survival based on chemotherapy regimen in KRAS wild-type patients following first-line treatment.

Only one trial used irinotecan-based chemotherapy, and the HR was 0.70 (95%CI: 0.56-0.87; Figure 3). In the subgroup analysis based on fluorouracil use, an improvement in PFS with MoAbs was observed, the pooled HR was 0.77 (95%CI: 0.69-0.86), with no publication bias (P = 0.786), however, significant heterogeneity was found (I^2 = 48%, P = 0.10). This heterogeneity may have been due to a different fluorouracil dosage form. In Tveit KM's trial, fluorouracil was given orally and was given intravenously in the other studies. Clinical benefit in mCRC patients with wild-type *KRAS* was confined to therapeutic regimens which included anti-EGFR MoAbs and fluorouracil based therapy.

Patients with mutant KRAS: For patients with mutant KRAS, there was no survival advantage when anti-EGFR MoAbs were administered as first-line treatment. The pooled HR of PFS was 1.18 (95%CI: 1.06-1.31), with no heterogeneity (I^2 = 37%, P = 0.15). The HR of OS was 1.10 (95%CI: 0.98-1.22). There was no significant heterogeneity between these trials. It is clear that the therapeutic effect of anti-EGFR MoAbs was dependent on KRAS status.

Analysis of trials using MoAbs as second- or further-line treatment

Patients with wild-type KRAS: Three studies supplied adequate information on OS in patients with *KRAS* mutation, two of these studies used BSC as the control group and BSC + anti-EGFR MoAbs as the experimental group. No significant benefit was observed when anti-EGFR MoAbs were used as second- or further-line treatment (HR = 0.81, 95%CI: 0.65-1.02), and heterogeneity was noted between the trials (I^2 = 61%, P = 0.08). No publication bias was observed using Egger's test (P = 0.773). There was a significant improvement in PFS following second-line or further treatment (HR = 0.52, 95%CI: 0.36-0.75), although heterogeneity was noted between these studies (I^2 = 84%, P = 0.002). Egger's test showed that no publication bias existed (P = 0.155). We excluded Marc Peeters's study as a different therapeutic regimen was used and conducted a new meta-analysis. The pooled HR was 0.43 (95%CI: 0.36-0.53), with no heterogeneity (I^2 = 0%, P = 0.73).

Patients with mutant KRAS: Data on survival and *KRAS* mutation in mCRC patients were reported in three studies involving 2221 patients. There was no evidence of survival benefit with anti-EGFR MoAbs in second-line or further-line treatment in OS (HR = 0.95, 95%CI: 0.82-1.11; I^2 = 0%, P = 0.87, Egger's test: P = 0.807) or PFS (HR = 0.95, 95%CI: 0.82-1.11; I^2 = 12%, P = 0.32, Egger's test: P = 0.358).

DISCUSSION

The main downstream signaling pathway of EGFR regulates crucial biological activities such as cell differentiation, cell survival, cell proliferation and cell migration[20]. Mutations of members of the downstream signaling pathways have been shown to result in resistance to anti-EGFR MoAbs. *KRAS* was the first molecular predictor shown to influence responsiveness to EGFR-targeted treatment with cetuximab and panitumumab. However, these data were mainly from retrospective and non-randomized studies. We focused on the relationship between *KRAS* status and the curative effect of anti-EGFR MoAbs in mCRC patients, and conducted a systematic meta-analysis of chemotherapy regimens, line of treatment and

bevacizumab treatment.

For patients with wild-type *KRAS* receiving MoAbs as first-line treatment no evidence of improved OS was observed. The subgroup analysis indicated a detrimental effect when anti-angiogenic agents were added to anti-EGFR MoAbs in the first-line treatment of mCRC. In theory, targeting both EGFR and VEGF pathways should increase curative effect[21]. A possible explanation for these findings may be that the combination of different antibodies increased toxicity and adverse effects. Another explanation may be that a negative pharmacokinetic interaction between these two biological agents occurred. After excluding trials using bevacizumab, another subgroup analysis was conducted to determine heterogeneity between trials using chemotherapy. We found that wild-type *KRAS* mCRC patients did not seem to benefit from anti-EGFR MoAbs and oxaliplatin-based chemotherapy as first-line treatment. Fluorouracil use influenced the OS of patients. Clinical benefit in mCRC patients with wild-type *KRAS* was confined to therapeutic regimens with anti-EGFR MoAbs and fluorouracil-based therapy. It was uncertain from our results whether combination of anti-EGFR MoAbs and capecitabine was effective in mCRC patients, since only one trial used capecitabine in this analysis. However, there were several studies have suggested that capecitabine might be less effective than 5-FU in first line treatment of mCRC patients[22-24]. The association between the chemotherapy regimen and clinical benefit in wild-type *KRAS* mCRC patients treated with anti-EGFR MoAbs needs to be explored in further studies due to limited available research.

Information on PFS in wild-type *KRAS* patients was available in 7 studies, and no benefit in PFS was observed in trials of first-line therapy. The subgroup analyses corresponded with the results from subgroup analyses of OS. After excluding trials using bevacizumab, the pooled HR of trials using chemotherapy was 0.83 (95%CI: 0.68-1.03), and significant heterogeneity was observed. Oxaliplatin-based chemotherapy with anti-EGFR MoAbs failed to prolong PFS in patients with wild-type *KRAS*. However, significant benefit in terms of PFS was observed in trials using MoAbs and fluorouracil. The subgroup analyses failed to explain the sources of heterogeneity. This may be due to different treatment protocols, such as different fluorouracil dosage forms. In Tveit KM's trial fluorouracil was given orally and was given intravenously in the other studies.

In trials using anti-EGFR MoAbs as second- or further-line treatment, no OS benefit was observed between the control group and experimental group in patients with wild-type *KRAS*. However, there was significant benefit in PFS. Heterogeneity disappeared after excluding Marc Peeters's study. The reason for the heterogeneity between these trials was due to different therapeutic regimens. Marc Peeters's study was the only study to use chemotherapy combined with anti-EGFR MoAbs as the therapeutic regimen, the other two studies used BSC combined with anti-EGFR MoAbs.

From this meta-analysis, it is clear that the clinical benefit of anti-EGFR MoAbs is dependent on *KRAS* status. For patients with mutant *KRAS*, there was no survival advantage when anti-EGFR MoAbs were used in any line of treatment.

Our results are in line with those of other studies. Zhang *et al*[25] evaluated the predictive value of *KRAS* mutation status and showed a clinical benefit in PFS with anti-EGFR MoAbs in patients with wild-type *KRAS*, and there was no significant difference in OS between cetuximab-based chemotherapy and chemotherapy alone. However, only 4 RCTs were included in their analysis. Most recently, Vale and colleagues[26] included 10 studies to examine anti-EGFR MoAbs treatment and found that there were clear benefits of anti-EGFR MoAbs in any line of treatment, when used with infusional 5FU-based regimens. In the present meta-analysis, 10 studies were included in the final analysis. We compiled years of research from several RCTs, and updated the conclusion regarding the relationship between *KRAS* status and the therapeutic effects of anti-EGFR MoAbs in mCRC patients. In this article, analyses of the therapeutic effects of anti-EGFR MoAbs in untreated patients and those who received prior chemotherapy were performed separately. This provided the first evidence that patients with wild-type *KRAS* did not benefit from anti-EGFR MoAbs with oxaliplatin-based therapy as first-line treatment. Clinical benefit in wild-type *KRAS* patients was confined to therapeutic regimens which included anti-EGFR MoAbs and fluorouracil-based therapy.

Several limitations of our meta-analysis need to be considered when interpreting these findings. Firstly, our results were based on unadjusted estimates, and a more precise analysis should be conducted with more detailed data based on adjusted estimates for other prognostic factors such as sex, age, tumor location and other biomarkers. Furthermore, although the initial trials were conducted prospectively, tissue specimens were only available for a small percentage of patients which may have resulted in selection bias. Secondly, chemotherapy regimens which were combined with anti-EGFR MoAbs may have influenced the therapeutic effect. The chemotherapy regimen that will provide most benefit to patients when combined with anti-EGFR MoAbs needs to be explored in large randomized trials. In this meta-analysis, oxaliplatin-based chemotherapy did not benefit patients with wild-type *KRAS* when combined with anti-EGFR MoAbs as first-line treatment. In addition, the number of trials of second- or further-line treatment was too small to drawn an accurate conclusion. This was due to poor recruitment and influenced the findings in our meta-analysis. Finally, although most mutations in *KRAS* were found at codons 12 and 13 of exon 2, more than 3000 point mutations have been detected in

KRAS and different point mutations have different effects on KRAS activity. The recognition of additional point mutations in *KRAS* and other key members of the EGFR downstream signal pathway may alter the conclusions drawn today.

In conclusion, this meta-analysis provided evidence that *KRAS* status is a predictive marker for the clinical benefit of anti-EGFR MoAbs in mCRC patients. Only patients with wild-type *KRAS* will benefit from first-line or further-line treatment with anti-EGFR MoAbs, and patients with mutant *KRAS* will not benefit. Line of treatment, chemotherapy regimen and combination with bevacizumab influence the clinical therapeutic effects of anti-EGFR MoAbs in these patients. This meta-analysis also provided the first evidence that wild-type *KRAS* mCRC patients do not benefit from anti-EGFR MoAbs with oxaliplatin-based therapy as first-line treatment. Clinical benefit was confined to therapeutic regimens which included anti-EGFR MoAbs and fluorouracil-based therapy.

COMMENTS

Background

Colorectal cancer is one of the most common human malignant diseases and the leading cause of cancer-related death worldwide. Over the last decade, the availability of combination chemotherapy and targeted agents has improved the median survival of patients with metastatic colorectal cancer. Monoclonal antibodies which target the epidermal growth factor receptor have been approved by the FDA for metastatic colorectal cancer. *KRAS* mutations have emerged as major predictive markers of resistance to anti-EGFR MoAbs. However, these results were obtained from retrospective and non-randomized studies.

Research frontiers

A meta-analysis was used to evaluate the relationship between *KRAS* status and the therapeutic effects of anti-EGFR MoAbs in mCRC patients.

Innovations and breakthroughs

In first-line treatment, survival benefit was confined to patients with wild-type *KRAS*. Chemotherapy regimens and angiogenesis inhibitor treatment influenced the results of the analysis. Wild-type *KRAS* mCRC patients did not seem to benefit from oxaliplatin-based chemotherapy (PFS: HR = 0.88, 95%CI: 0.70-1.10; OS: HR = 0.93, 95%CI: 0.82-1.04). Clinical benefit in mCRC patients was limited to therapeutic regimens wihich included anti-EGFR MoAbs and fluorouracil-based therapy (PFS: HR = 0.77, 95%CI: 0.69-0.86; OS: HR = 0.85, 95%CI: 0.75-0.95). When anti-EGFR monoclonal antibodies were used as second- or further-line treatment, clinical benefit was still confined to patients with wild-type *KRAS*. This meta-analysis provides the first evidence that wild-type *KRAS* mCRC patients did not benefit from anti-EGFR MoAbs with oxaliplatin-based therapy as first-line treatment. Clinical benefit was confined to therapeutic regimens which included anti-EGFR MoAbs and fluorouracil-based therapy.

Applications

Although the initial trials were conducted prospectively, tissue specimens were only available for a small percentage of patients which may have resulted in selection bias. Large prospective clinical trials are required to validate this conclusion. Furthermore, it is apparent that mCRC is a heterogeneous disease with numerous activation mutations in oncogenes and inactivation mutations in tumor suppressor genes. The identification of mutations in other members of the EGFR pathway and the synergetic effect of multiple genetic mutations in the oncogenic signaling cascades may increase the predictive ability of biomarkers.

Terminology

Anti-EGFR MoAbs: Cetuximab and panitumumab are examples of monoclonal antibodies aimed at the epidermal growth factor receptor. However, the former is of the IgG1 type, the latter of the IgG2 type; and the consequences on antibody-dependent cellular cytotoxicity can be quite different. Monoclonal antibodies block the extracellular ligand binding domain. With the binding site blocked, signal molecules can no longer attach there and activate the tyrosine kinase. *KRAS:* The *KRAS* gene provides instructions for making a protein called K-Ras which is involved primarily in regulating cell division. As part of a signaling pathway known as the RAS/MAPK pathway, the protein relays signals from outside the cell to the cell nucleus. These signals instruct the cell to grow and divide or to mature and determine cell differentiation, cell survival, cell proliferation and cell migration. Bevacizumab: Bevacizumab is an angiogenesis inhibitor, and slows the growth of new blood vessels. It is licensed to treat various cancers, including colorectal, lung, breast, glioblastoma, kidney and ovarian cancer. It is a recombinant humanized monoclonal antibody which inhibits angiogenesis by inhibiting vascular endothelial growth factor A.

Peer-review

This is an important analysis of KRAS status and the effects of anti-EGFR MoAbs in mCRC patients. The meta-analysis of randomized controlled trials may provide a comprehensive estimation of the relation between KRAS status and the effects of anti-EGFR MoAbs in mCRC patients.

REFERENCES

1 **Siegel R**, Naishadham D, Jemal A. Cancer statistics, 2013. *CA Cancer J Clin* 2013; **63**: 11-30 [PMID: 23335087 DOI: 10.3322/caac.21166]

2 **Kelly C**, Cassidy J. Chemotherapy in metastatic colorectal cancer. *Surg Oncol* 2007; **16**: 65-70 [PMID: 17521906 DOI: 10.1016/j.suronc.2007.04.006]

3 **Peeters M**, Price T, Van Laethem JL. Anti-epidermal growth factor receptor monotherapy in the treatment of metastatic colorectal cancer: where are we today? *Oncologist* 2009; **14**: 29-39 [PMID: 19144681 DOI: 10.1634/theoncologist.2008-0167]

4 **Lièvre A**, Bachet JB, Le Corre D, Boige V, Landi B, Emile JF, Côté JF, Tomasic G, Penna C, Ducreux M, Rougier P, Penault-Llorca F, Laurent-Puig P. KRAS mutation status is predictive of response to cetuximab therapy in colorectal cancer. *Cancer Res* 2006; **66**: 3992-3995 [PMID: 16618717]

5 **Barault L**, Veyrie N, Jooste V, Lecorre D, Chapusot C, Ferraz JM, Lièvre A, Cortet M, Bouvier AM, Rat P, Roignot P, Faivre J, Laurent-Puig P, Piard F. Mutations in the RAS-MAPK, PI(3)K (phosphatidylinositol-3-OH kinase) signaling network correlate with poor survival in a population-based series of colon cancers. *Int J Cancer* 2008; **122**: 2255-2259 [PMID: 18224685 DOI: 10.1002/ijc.23388]

6 **Sastre J**, Aranda E, Grávalos C, Massutí B, Varella-Garcia M, Rivera F, Soler G, Carrato A, Manzano JL, Díaz-Rubio E, Hidalgo M. First-line single-agent cetuximab in elderly patients with metastatic colorectal cancer. A phase II clinical and molecular study of the Spanish group for digestive tumor therapy (TTD). *Crit Rev Oncol Hematol* 2011; **77**: 78-84 [PMID: 20042346 DOI: 10.1016/j.critrevonc.2009.11.005]

7 **Bokemeyer C**, Bondarenko I, Hartmann JT, de Braud F, Schuch G, Zubel A, Celik I, Schlichting M, Koralewski P. Efficacy according to biomarker status of cetuximab plus FOLFOX-4 as first-line treatment for metastatic colorectal cancer: the OPUS study. *Ann Oncol* 2011; **22**: 1535-1546 [PMID: 21228335 DOI: 10.1093/annonc/mdq632]

8 **Higgins JP**, Thompson SG. Quantifying heterogeneity in a meta-analysis. *Stat Med* 2002; **21**: 1539-1558 [PMID: 12111919 DOI: 10.1002/sim.1186]

9 **Higgins JP**, Thompson SG, Deeks JJ, Altman DG. Measuring inconsistency in meta-analyses. *BMJ* 2003; **327**: 557-560 [PMID: 12958120 DOI: 10.1136/bmj.327.7414.557]

10 **Egger M**, Davey Smith G, Schneider M, Minder C. Bias in meta-analysis detected by a simple, graphical test. *BMJ* 1997; **315**: 629-634 [PMID: 9310563]

11 **Maughan TS**, Adams RA, Smith CG, Meade AM, Seymour MT, Wilson RH, Idziaszczyk S, Harris R, Fisher D, Kenny SL, Kay E, Mitchell JK, Madi A, Jasani B, James MD, Bridgewater J, Kennedy MJ, Claes B, Lambrechts D, Kaplan R, Cheadle JP. Addition of

cetuximab to oxaliplatin-based first-line combination chemotherapy for treatment of advanced colorectal cancer: results of the randomised phase 3 MRC COIN trial. *Lancet* 2011; **377**: 2103-2114 [PMID: 21641636 DOI: 10.1016/S0140-6736(11)60613-2]

12 **Van Cutsem E**, Köhne CH, Láng I, Folprecht G, Nowacki MP, Cascinu S, Shchepotin I, Maurel J, Cunningham D, Tejpar S, Schlichting M, Zubel A, Celik I, Rougier P, Ciardiello F. Cetuximab plus irinotecan, fluorouracil, and leucovorin as first-line treatment for metastatic colorectal cancer: updated analysis of overall survival according to tumor KRAS and BRAF mutation status. *J Clin Oncol* 2011; **29**: 2011-2019 [PMID: 21502544 DOI: 10.1200/JCO.2010.33.5091]

13 **Douillard JY**, Siena S, Cassidy J, Tabernero J, Burkes R, Barugel M, Humblet Y, Bodoky G, Cunningham D, Jassem J, Rivera F, Kocákova I, Ruff P, Błasińska-Morawiec M, Šmakal M, Canon JL, Rother M, Oliner KS, Wolf M, Gansert J. Randomized, phase III trial of panitumumab with infusional fluorouracil, leucovorin, and oxaliplatin (FOLFOX4) versus FOLFOX4 alone as first-line treatment in patients with previously untreated metastatic colorectal cancer: the PRIME study. *J Clin Oncol* 2010; **28**: 4697-4705 [PMID: 20921465 DOI: 10.1200/JCO.2009.27.4860]

14 **Hecht JR**, Mitchell E, Chidiac T, Scroggin C, Hagenstad C, Spigel D, Marshall J, Cohn A, McCollum D, Stella P, Deeter R, Shahin S, Amado RG. A randomized phase IIIB trial of chemotherapy, bevacizumab, and panitumumab compared with chemotherapy and bevacizumab alone for metastatic colorectal cancer. *J Clin Oncol* 2009; **27**: 672-680 [PMID: 19114685 DOI: 10.1200/JCO.2008.19.8135]

15 **Tol J**, Koopman M, Cats A, Rodenburg CJ, Creemers GJ, Schrama JG, Erdkamp FL, Vos AH, van Groeningen CJ, Sinnige HA, Richel DJ, Voest EE, Dijkstra JR, Vink-Börger ME, Antonini NF, Mol L, van Krieken JH, Dalesio O, Punt CJ. Chemotherapy, bevacizumab, and cetuximab in metastatic colorectal cancer. *N Engl J Med* 2009; **360**: 563-572 [PMID: 19196673 DOI: 10.1056/NEJMoa0808268]

16 **Tveit KM**, Guren T, Glimelius B, Pfeiffer P, Sorbye H, Pyrhonen S, Sigurdsson F, Kure E, Ikdahl T, Skovlund E, Fokstuen T, Hansen F, Hofsli E, Birkemeyer E, Johnsson A, Starkhammar H, Yilmaz MK, Keldsen N, Erdal AB, Dajani O, Dahl O, Christoffersen T. Phase III trial of cetuximab with continuous or intermittent fluorouracil, leucovorin, and oxaliplatin (Nordic FLOX) versus FLOX alone in first-line treatment of metastatic colorectal cancer: the NORDIC-VII study. *J Clin Oncol* 2012; **30**: 1755-1762 [PMID: 22473155 DOI: 10.1200/JCO.2011.38.0915]

17 **Peeters M**, Price TJ, Cervantes A, Sobrero AF, Ducreux M, Hotko Y, André T, Chan E, Lordick F, Punt CJ, Strickland AH, Wilson G, Ciuleanu TE, Roman L, Van Cutsem E, Tzekova V, Collins S, Oliner KS, Rong A, Gansert J. Randomized phase III study of panitumumab with fluorouracil, leucovorin, and irinotecan (FOLFIRI) compared with FOLFIRI alone as second-line treatment in patients with metastatic colorectal cancer. *J Clin Oncol* 2010; **28**: 4706-4713 [PMID: 20921462 DOI: 10.1200/JCO.2009.27.6055]

18 **Harbison CT**, Horak CE, Ledeine JM, Mukhopadhyay P, Malone DP, O'Callaghan C, Jonker DJ, Karapetis CS, Khambata-Ford S, Gustafson N, Trifan OC, Chang SC, Ravetto P, Iv GA. Validation of companion diagnostic for detection of mutations in codons 12 and 13 of the KRAS gene in patients with metastatic colorectal cancer: analysis of the NCIC CTG CO.17 trial. *Arch Pathol Lab Med* 2013; **137**: 820-827 [PMID: 23030695 DOI: 10.5858/arpa.2012-0367-OA]

19 **Amado RG**, Wolf M, Peeters M, Van Cutsem E, Siena S, Freeman DJ, Juan T, Sikorski R, Suggs S, Radinsky R, Patterson SD, Chang DD. Wild-type KRAS is required for panitumumab efficacy in patients with metastatic colorectal cancer. *J Clin Oncol* 2008; **26**: 1626-1634 [PMID: 18316791 DOI: 10.1200/JCO.2007.14.7116]

20 **Oda K**, Matsuoka Y, Funahashi A, Kitano H. A comprehensive pathway map of epidermal growth factor receptor signaling. *Mol Syst Biol* 2005; **1**: 2005.0010 [PMID: 16729045 DOI: 10.1038/msb4100014]

21 **Tabernero J**. The role of VEGF and EGFR inhibition: implications for combining anti-VEGF and anti-EGFR agents. *Mol Cancer Res* 2007; **5**: 203-220 [PMID: 17374728 DOI: 10.1158/1541-7786.MCR-06-0404]

22 **Díaz-Rubio E**, Tabernero J, Gómez-España A, Massutí B, Sastre J, Chaves M, Abad A, Carrato A, Queralt B, Reina JJ, Maurel J, González-Flores E, Aparicio J, Rivera F, Losa F, Aranda E. Phase III study of capecitabine plus oxaliplatin compared with continuous-infusion fluorouracil plus oxaliplatin as first-line therapy in metastatic colorectal cancer: final report of the Spanish Cooperative Group for the Treatment of Digestive Tumors Trial. *J Clin Oncol* 2007; **25**: 4224-4230 [PMID: 17548839 DOI: 10.1200/JCO.2006.09.8467]

23 **Porschen R**, Arkenau HT, Kubicka S, Greil R, Seufferlein T, Freier W, Kretzschmar A, Graeven U, Grothey A, Hinke A, Schmiegel W, Schmoll HJ. Phase III study of capecitabine plus oxaliplatin compared with fluorouracil and leucovorin plus oxaliplatin in metastatic colorectal cancer: a final report of the AIO Colorectal Study Group. *J Clin Oncol* 2007; **25**: 4217-4223 [PMID: 17548840 DOI: 10.1200/JCO.2006.09.2684]

24 **Fuchs CS**, Marshall J, Barrueco J. Randomized, controlled trial of irinotecan plus infusional, bolus, or oral fluoropyrimidines in first-line treatment of metastatic colorectal cancer: updated results from the BICC-C study. *J Clin Oncol* 2008; **26**: 689-690 [PMID: 18235136 DOI: 10.1200/JCO.2007.15.5390]

25 **Zhang L**, Ma L, Zhou Q. Overall and KRAS-specific results of combined cetuximab treatment and chemotherapy for metastatic colorectal cancer: a meta-analysis. *Int J Colorectal Dis* 2011; **26**: 1025-1033 [PMID: 21523374 DOI: 10.1007/s00384-011-1197-5]

26 **Vale CL**, Tierney JF, Fisher D, Adams RA, Kaplan R, Maughan TS, Parmar MK, Meade AM. Does anti-EGFR therapy improve outcome in advanced colorectal cancer? A systematic review and meta-analysis. *Cancer Treat Rev* 2012; **38**: 618-625 [PMID: 22118887 DOI: 10.1016/j.ctrv.2011.11.002]

P- Reviewer: Braet F **S- Editor**: Ma YJ
L- Editor: A **E- Editor**: Liu XM

World Journal of Gastroenterology

Submit a Manuscript: http://www.wjgnet.com/esps/
Help Desk: http://www.wjgnet.com/esps/helpdesk.aspx
DOI: 10.3748/wjg.v21.i14.4373

World J Gastroenterol 2015 April 14; 21(14): 4373-4378
ISSN 1007-9327 (print) ISSN 2219-2840 (online)

CASE REPORT

Ipilimumab associated colitis: An IpiColitis case series at MedStar Georgetown University Hospital

Pawan Rastogi, Mohamed Sultan, Aline J Charabaty, Michael B Atkins, Mark C Mattar

Pawan Rastogi, Department of Medicine, MedStar Georgetown University Hospital, Washington, DC 20007, United States
Mohamed Sultan, Aline J Charabaty, Mark C Mattar, Department of Gastroenterology, MedStar Georgetown University Hospital, Washington, DC 2007, United States
Michael B Atkins, Department of Oncology, Georgetown Lombardi Comprehensive Cancer Center, Washington, DC 20007, United States
Author contributions: Rastogi P reviewed cases, collected data, and wrote the manuscript and references; Sultan M formatted images and provided revisions to the manuscript; Mattar MC is the author guarantor, supervised the process, and made revisions to the manuscript; Charabaty AJ and Atkins MB provided invaluable support and revision to the manuscript; Procedures were conducted by physicians of the Department of Gastroenterology and Hepatology at MedStar Georgetown University Hospital.
Supported by MedStar Georgetown University Hospital, Washington, DC, United States.

Correspondence to: Mark C Mattar, MD, Department of Gastroenterology, MedStar Georgetown University Hospital, 3800 Reservoir Road NW, Main Building Second Floor, Washington, DC 20007,
United States. mark.c.mattar@gunet.georgetown.edu
Telephone: +1-202-4441031
Fax: +1-877-3031462
Received: August 19, 2014
Peer-review started: August 20, 2014
First decision: September 27, 2014
Revised: October 22, 2014
Accepted: December 16, 2014
Article in press: December 16, 2014
Published online: April 14, 2015

Abstract

Although ipilimumab has been shown to improve survival in patients with metastatic melanoma and cause regression of metastatic renal cell carcinoma, the associated immune-related toxicities are of concern. The resultant T cell activation by this monoclonal antibody causes an increased immune response, which has been associated with many immune-regulated adverse effects. One of the most concerning effects is the development of colitis. Upwards to 8% of patients have been reported to develop colitis, with 5% being severe (Grades 3-4). While initial treatment of such adverse effects is generally comprised of supportive and symptomatic treatment, more severe cases warrant the use of high dose steroids. Furthermore, use of anti-TNF agents is usually reserved for those cases that prove to be refractory to steroids. We describe a systematic case review of seven patients who developed gastrointestinal symptoms following initiation of ipilimumab immunotherapy, and present the steps in their evaluation, treatment and outcomes at our institution.

Key words: Colitis; Ipilimumab; Immunology; Infliximab; Immune-regulated adverse effects

Core tip: The development of colitis in the setting of ipilimumab use has become of great concern. Treatment regimens, predictive factors, and prognostic indicators have yet to become standardized and elucidated. Here we present one of the largest case series of ipilimumab associated colitis at a single tertiary care institution, as well as our approach to evaluating and treating suspected cases.

Rastogi P, Sultan M, Charabaty AJ, Atkins MB, Mattar MC. Ipilimumab associated colitis: An IpiColitis case series at MedStar Georgetown University Hospital. *World J Gastroenterol* 2015; 21(14): 4373-4378 Available from: URL: http://www.wjgnet.com/1007-9327/full/v21/i14/4373.htm DOI: http://dx.doi.org/10.3748/wjg.v21.i14.4373

INTRODUCTION

Although ipilimumab has been shown to improve survival in patients with metastatic melanoma and cause regression of metastatic renal cell carcinoma, the associated immune-related toxicities are of concern[1,2]. The resultant T cell activation by this monoclonal antibody causes an increased immune response, which has been associated with many immune-regulated adverse effects. One of the most concerning effects is the development of colitis. Upwards to 8% of patients have been reported to develop colitis, with 5% being severe (Grades 3-4). While initial treatment of such adverse effects is generally comprised of supportive and symptomatic treatment, more severe cases warrant the use of high dose steroids. Furthermore, use of anti-TNF agents is usually reserved for those cases that prove to be steroid resistant[3].

In March 2011, ipilimumab was approved for the treatment of patients with metastatic melanoma. This monoclonal antibody blocks inhibition of cytotoxic T lymphocyte antigen 4 (CTLA-4) causing T cell activation and proliferation, preventing tumor evasion. The resulting immune up-regulation has been associated with numerous immune-regulated adverse effects (irAEs) including colitis, dermatitis, hepatitis, and hypophysitis. Fatigue, weight loss, and electrolyte imbalances encompass the clinical manifestations of severe diarrhea, which can progress to colitis, and in the worst case, bowel perforation. Up to 46% of patients will experience such gastrointestinal toxicities after 7 wk of therapy[4]. Severity of diarrheal symptoms are graded based on the Common Terminology for Adverse Events (CTAE)[5], and further characterized as mild to moderate (Grades 1-2) or severe (Grades 3-4). Symptomatic management with loperamide is indicated for mild cases. If symptoms persist or become severe, initiation of steroid therapy is indicated along with endoscopy to assess for colitis. High dose steroids are used in severe cases, and infliximab being reserved for steroid resistant cases[6]. Here we report our experience in the diagnosis and treatment of gastrointestinal irAEs in our patients receiving ipilimumab.

A retrospective analysis was conducted to identify those patients who developed gastrointestinal symptoms in the setting of receiving ipilimumab treatment from December 2012 to December 2013. A total of 19 patients were identified as receiving ipilimumab as part of their infusion protocols. Seven cases were identified as having gastrointestinal symptoms warranting inpatient hospital evaluation. Of the 7 cases reviewed (four male, three female) a mean age of 58 years (range, 38-71 years) and diarrheal symptoms ranging from mild to severe (Grades 1-4) was noted. Below we present detailed descriptions of each of the seven cases and a summation presented in Table 1.

CASE REPORT

Case 1

A 63 years old female with history of melanoma of the nasal mucosa presented with non-bloody diarrhea six weeks after starting ipilimumab. She was empirically treated with oral prednisone, but had symptom recurrence with steroid tapering. Colonoscopy showed diffuse mucosal erythema and ulcers with pathology significant for cryptitis (Figure 1). The patient's course was further complicated by a perirectal abscess. The patient underwent drainage of the abscess and began treatment with budesonide (12 mg daily) with improvement of her symptoms within two days. She also received imatinib (400 mg twice daily) for her c-KIT mutant mucosal melanoma with significant anti-tumor response without reactivation of colitis symptoms.

Case 2

A 38 years old male with a history of melanoma of the back developed loose non-bloody bowel movements approximately four weeks after starting ipilimumab. Colonoscopy was unrevealing and the patient was treated symptomatically with loperamide (Figure 2). Upon further workup, the patient was found to have a Group G Beta-Hemolytic Streptococcus bacteremia. Treatment of the underlying bacteremia resulted in resolution of the patient's diarrhea.

Case 3

A 71 years old female diagnosed with facial melanoma began experiencing softer and more frequent stools five weeks after her first dose of ipilimumab. Colonoscopy revealed ulcers with no evidence of bleeding throughout the colon (Figure 3). She was started on budesonide (3 mg daily) and later switched to prednisone (60 mg twice daily). The patient's symptoms improved only temporarily; few weeks later she developed bloody diarrhea. She was transitioned to methylprednisolone (60 mg twice daily) and showed no improvement after four days. She received two infusions of infliximab at 5 mg/kg spaced two weeks apart. Within four weeks of the first infliximab infusion the patient's symptoms had resolved. C-reactive protein (CRP) levels were noted to decrease from 38.3 mg/L to < 2.9 mg/L ten days following the first infliximab infusion.

Table 1 Outlined summary of patient cases

No.	Age (yr)	Gender	Diagnosis	Symptom grade	Symptom onset	CRP levels (Normal 0-3 mg/L)
Case 1	63	Female	Nasal Mucosa Melanoma	3 → 4	6 wk	108
Case 2	38	Male	Back Skin Melanoma	1 → 2	4 wk	137
Case 3	71	Female	Facial Melanoma	2 → 4	5 wk	38.3 (< 2.9 ten days after first infliximab infusion)
Case 4	44	Female	Right Inguinal Melanoma	3	9 wk	55.7
Case 5	66	Male	Prostate Cancer, Melanoma	3	3 wk	34.7 (< 2.9 eight days following first dose methylprednisolone)
Case 6	67	Male	Right Forearm Melanoma	3	18 wk	NA
Case 7	55	Male	Back Skin Melanoma	4	4 wk	97.4

Symptom onset described as time from first dose of ipilimumab. NA: Not applicable; CRP: C-reactive protein.

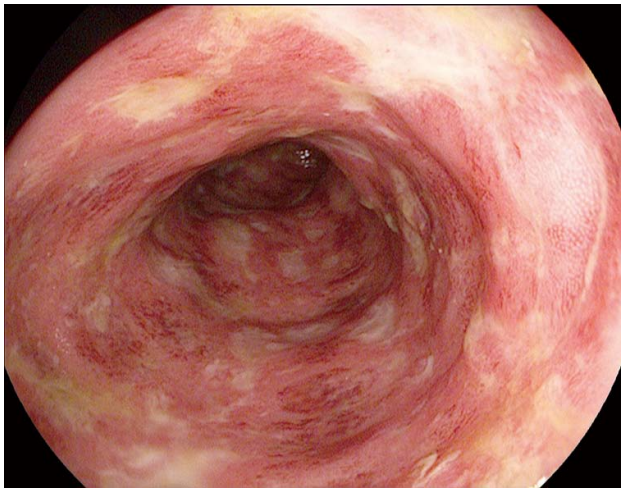

Figure 1 Erythematous mucosa, loss of normal vascular pattern, multiple ulcers most consistent with IpiColitis.

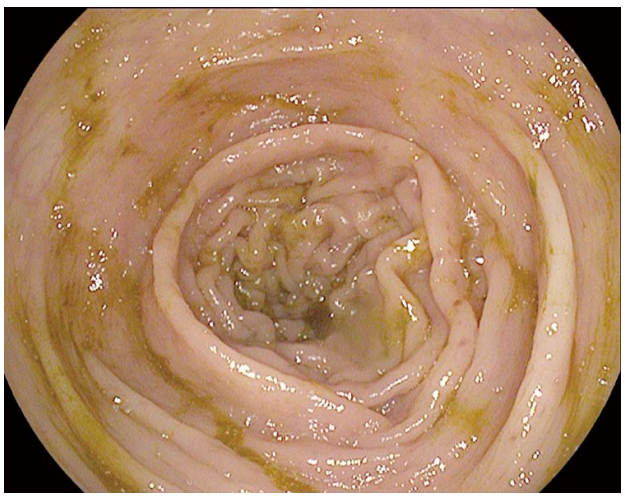

Figure 2 Normal colonoscopy.

Case 4

A 44 years old female with right inguinal melanoma developed nausea, fevers, and loose bowel movements nine weeks after her first dose of ipilimumab. A colonoscopy confirmed the diagnosis of colitis revealing loss of vascular pattern and mucosal friability.

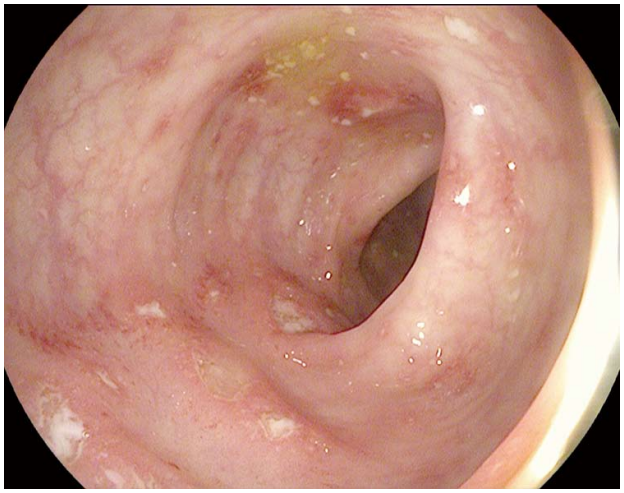

Figure 3 Erythema with ulceration and loss of vascular pattern.

Pathology revealed evidence of colitis with destructive cryptitis and crypt microabscesses. She was started on prednisone with a two week taper and experienced improvement of her symptoms.

Case 5

A 66 years old male with history of prostate cancer and melanoma began experiencing abdominal pain and diarrhea, which progressed to bright red blood per rectum, three weeks after his first dose of ipilimumab. Colonoscopy was significant for mucosal friability and multiple shallow punctate ulcerations, with pathology further confirming colitis. The patient experienced complete symptom resolution after only one day of treatment (methylprednisolone 85 mg daily). He was transitioned to oral steroids with a subsequent four week taper with no recurrence of symptoms. CRP levels were observed to decrease from 34.7 mg/L to < 2.9 mg/L eight days after his first dose of methylprednisolone.

Case 6

A 67 years old male diagnosed with melanoma of the right forearm started having loose non-bloody bowel movements eighteen weeks after his first dose of

ipilimumab. Colonoscopy showed evidence of colitis and pathological findings of increased inflammation and rare acute cryptitis. The patient was originally started on Budesonide 9 mg daily, but later switched to prednisone 100 mg daily after colonoscopy findings. The patient's symptoms gradually abated.

Case 7

A 55 years old male melanoma of the back presented with cramping abdominal pain associated with diarrhea four weeks following his first dose of ipilimumab. Multiple bland based ulcers were noted extending from the rectum to the ileum and pathology was consistent with acute colitis. The patient was originally started on prednisone 100 mg daily and later switched to methylprednisolone 100 mg twice daily when symptoms persisted. After three days of no improvement and progression of symptoms to bloody diarrhea, he was administered two doses of infliximab (5 mg/kg) two weeks apart. The patient noted near complete symptom resolution two weeks following the first infliximab infusion.

RESULTS

The majority of chief complaints were composed of diarrhea, fever, rash, abdominal pain, nausea and occurred three to eighteen weeks after initiation of ipilimumab (mean, 7 wk; following one to four doses of ipilimumab). Colonoscopy findings were consistent with those of colitis, including mucosal erythema, ulcerations, loss of vascular pattern, granulations, and friable mucosa. Common pathological observations on biopsy were granulomas, cryptitis, and crypt abscesses. Time to symptom resolution was noted to be variable (ranging from 1 d to 4 wk after initial treatment). CRP levels were elevated in all cases when measured, with normalization noted when measured serially post treatment in two of the cases. Two of the seven patients received infliximab infusions for treatment of their underlying colitis.

DISCUSSION

With the introduction of anti-CTLA-4 agent ipilimumab irAEs involving the digestive tract have become legitimate concern. Decision algorithms based on symptom grade have been developed to aid in the management of such toxicities, but much is to be elucidated. Although corticosteroids are recommended for moderate to severe symptoms, optimal dosing needs clarification. Management guidelines recommend starting prednisone or its equivalent (0.5 mg/kg/d for moderate and 1-2 mg/kg/d for severe enterocolitis), but case reports and trials have a myriad of steroid administration patterns. Furthermore, extended release formulations of the steroids have been developed, which have yet to be studied in such

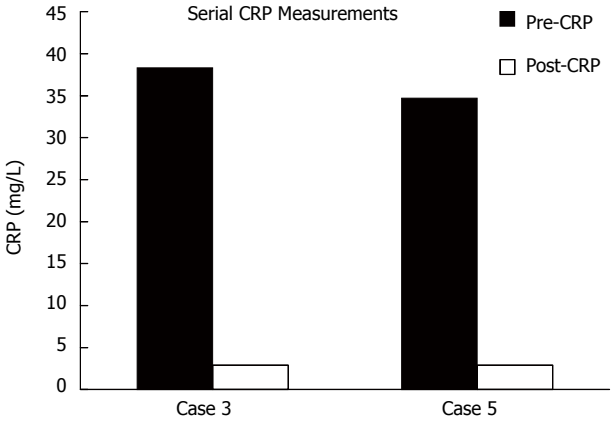

Figure 4 Graph demonstrating normalization of C-reactive protein levels after treatment in two of the seven cases. CRP: C-reactive protein.

patients.

At our institution, cases of suspected 'IpiColitis' undergo colonoscopy with biopsies. We feel that colonoscopy is warranted early to confirm diagnosis. While clinical course may support the diagnosis of ipilimumab associated colitis, it is not sufficient, thus requiring tissue biopsy for confirmation. Once confirmed and infectious etiologies are ruled out, patients are started on prednisone (1 mg/kg/d). Simultaneously, patients are checked for tuberculosis and hepatitis B infections in preparation for possible future anti-TNF therapy. Intravenous steroids (1 mg/kg/d) are reserved for more persistent cases. If symptoms continue three to five days following intravenous steroid treatment, two doses of infliximab (5 mg/kg/dose) are administered two weeks apart with coinciding steroid taper. Patients are followed clinically and treatment success is based on resolution of the patient's presenting symptoms and diarrhea. Repeat colonoscopy is not routinely conducted to confirm treatment response.

Phase 2 trials have shown no benefit of prophylactic budesonide use in the prevention of ipilimumab induced colitis[7]. To date we lack predictive and prognostic factors of severity of the immunological side effects prior to initiating ipilimumab therapy[8]. CRP, being a marker of acute inflammation, was noted to be elevated in all cases. The degree of elevation did not correlate to symptom severity, and did not serve as a surrogate indicator for the requirement of anti-TNF agents. In cases where CRP was checked after treatment, normal levels were noted, creating future interest in following this lab value as a measurement of treatment response (Figure 4). In Case 3, CRP levels were checked ten days following the first dose of infliximab and noted to have normalized. Similarly, in Case 5, CRP levels were noted to have normalized eight days following first dose of methylprednisolone.

With no definitive preventive strategy, and no predictive and prognostic factors, the physician has to assess disease severity and adjust medical treatment

based on patient's symptoms and the colonoscopy findings. Before attributing the diarrhea to ipilimumab, an infectious work-up should be done, including infectious enterocolitis and extra-intestinal infections, as illustrated by our patient diagnosed with Group G Beta Hemolytic Streptococcus bacteremia. The differential diagnosis of colitis remains broad and can arise from infectious pathogens, such as *Escherichia coli*, *Salmonella*, and *Clostridium difficile*. Immunocompromised individuals are more susceptible to colitis due to cytomegalovirus infections. Ischemic changes can also result in colonic inflammation representative of colitis. Furthermore, microscopic forms of colitis exist, including lymphocytic and collagenous forms[9].

Cases non-responsive to steroids will often proceed to a trial of anti-TNF agents such as infliximab. This monoclonal antibody has an established use in the treatment of inflammatory bowel disease, and builds much of the foundation of how we treat steroid resistant immune-mediated colitis. While endoscopic findings have been correlated with more clinically aggressive forms of Crohn's disease, further data and more rigorous studies are required to make such a correlation in ipilimumab-induced colitis[10]. Endoscopy is indicated in those patients whose symptoms are severe or refractory to oral steroids. The use of early endoscopy, its associated findings, and treatment implications are yet to be studied.

COMMENTS

Case characteristics

Case 1: 63 years old female with history of melanoma of the nasal mucosa presented with non-bloody diarrhea six weeks after starting ipilimumab.

Case 2: 38 years old male with a history of melanoma of the back developed loose non-bloody bowel movements four weeks after starting ipilimumab.

Case 3: 71 years old female diagnosed with facial melanoma began experiencing softer and more frequent stools five weeks after her first dose of ipilimumab.

Case 4: 44 years old female with right inguinal melanoma developed nausea, fevers, and loose bowel movements nine weeks after her first dose of ipilimumab.

Case 5: 66 years old male with history of prostate cancer and melanoma began experiencing abdominal pain and diarrhea, which progressed to bright red blood per rectum three weeks after his first dose of ipilimumab

Case 6: 67 years old male diagnosed with melanoma of the right forearm started having loose non-bloody bowel movements eighteen weeks after his first dose of ipilimumab.

Case 7: 55 years old male melanoma of the back presented with cramping abdominal pain associated with diarrhea four weeks following his first dose of ipilimumab.

Clinical diagnosis

Abdominal pain, nausea, fever, loose stools, diarrhea, bloody bowel movements.

Differential diagnosis

Infectious colitis (*E. coli, C. difficile, Salmonella,* CMV), Microscopic colitis, Viral Gastroenteritis, Ischemic colitis.

Laboratory diagnosis

Elevated CRP levels [range: 34.7 mg/L to 137 mg/L (Normal: < 2.9 mg/L)].

Imaging diagnosis

Colonoscopy revealing mucosal erythema, ulcerations, loss of vascular pattern, granulations, and friable mucosa

Pathological diagnosis

Pathological findings from colonic biopsies revealed granulomas, cryptitis, and crypt abscesses

Treatment

Case 1: Treated with budesonide 12 mg daily.

Case 2: Symptomatic treatment with loperamide.

Case 3: First treated with budesonide 3 mg daily, later switched to prednisone 60mg twice daily. Steroids later changed to intravenous methylprednisolone 60mg twice daily, and finally received two doses of infliximab (5 mg/kg) spaced two weeks apart.

Case 4: Treated with prednisone.

Case 5: Methylprednisolone 85 mg daily.

Case 6: Budesonide 9 mg daily, followed by prednisone 100 mg daily.

Case 7: Prednisone 100 mg daily, later switched to methylprednisolone 100 mg twice daily, and ultimately treated with two doses infliximab (5 mg/kg) two weeks apart.

Related reports

To date, we lack biomarkers that help predict the severity of irAEs or help determine patient's treatment response to steroid treatment.

Term explanation

Immune-regulated adverse effects (irAEs) are thought to be those effects due to the T cell activation and immune up-regulation caused by ipilimumab.

Experiences and lessons

This report not only represents the largest single institution case series of ipilimumab associated colitis, but also outlines our evaluation methods, treatment regimens, and outcomes of our patients. Furthermore, the authors suggest the use of serial CRP measurements as a possible surrogate biomarker to treatment response.

Peer-review

This article applies a retrospective case series review of those patients who developed gastrointestinal symptoms in the setting of receiving ipilimumab.

REFERENCES

1 **Hodi FS**, O'Day SJ, McDermott DF, Weber RW, Sosman JA, Haanen JB, Gonzalez R, Robert C, Schadendorf D, Hassel JC, Akerley W, van den Eertwegh AJ, Lutzky J, Lorigan P, Vaubel JM, Linette GP, Hogg D, Ottensmeier CH, Lebbé C, Peschel C, Quirt I, Clark JI, Wolchok JD, Weber JS, Tian J, Yellin MJ, Nichol GM, Hoos A, Urba WJ. Improved survival with ipilimumab in patients with metastatic melanoma. *N Engl J Med* 2010; **363**: 711-723 [PMID: 20525992 DOI: 10.1056/NEJMoa1003466]

2 **Yang JC**, Hughes M, Kammula U, Royal R, Sherry RM, Topalian SL, Suri KB, Levy C, Allen T, Mavroukakis S, Lowy I, White DE, Rosenberg SA. Ipilimumab (anti-CTLA4 antibody) causes regression of metastatic renal cell cancer associated with enteritis and hypophysitis. *J Immunother* 2007; **30**: 825-830 [PMID: 18049334 DOI: 10.1097/CJI.0b013e318156e47e]

3 **Hanaizi Z**, van Zwieten-Boot B, Calvo G, Lopez AS, van Dartel M, Camarero J, Abadie E, Pignatti F. The European Medicines Agency review of ipilimumab (Yervoy) for the treatment of advanced (unresectable or metastatic) melanoma in adults who have received prior therapy: summary of the scientific assessment of the Committee for Medicinal Products for Human Use. *Eur J Cancer* 2012; **48**: 237-242 [PMID: 22030452 DOI: 10.1016/j.ejca.2011.09.018]

4 **Graziani G**, Tentori L, Navarra P. Ipilimumab: a novel immunostimulatory monoclonal antibody for the treatment of cancer. *Pharmacol Res* 2012; **65**: 9-22 [PMID: 21930211 DOI: 10.1016/j.phrs.2011.09.002]

5 **U.S. Department of Health and Human Services**. Common Terminology Criteria for Adverse Events (CTCAE). 2009-05-28, cited 2015-01-12; 80 screens. Available from: URL: http://www.hrc.govt.nz/sites/default/files/CTCAE%20manual%20-%20DMCC.pdf

6 **Kähler KC**, Hauschild A. Treatment and side effect management of CTLA-4 antibody therapy in metastatic melanoma. *J Dtsch*

Dermatol Ges 2011; **9**: 277-286 [PMID: 21083648 DOI: 10.1111/j.1610-0387.2010.07568.x]

7 **Weber J**, Thompson JA, Hamid O, Minor D, Amin A, Ron I, Ridolfi R, Assi H, Maraveyas A, Berman D, Siegel J, O'Day SJ. A randomized, double-blind, placebo-controlled, phase II study comparing the tolerability and efficacy of ipilimumab administered with or without prophylactic budesonide in patients with unresectable stage III or IV melanoma. *Clin Cancer Res* 2009; **15**: 5591-5598 [PMID: 19671877 DOI: 10.1158/1078-0432.CCR-09-1024]

8 **Pagès C**, Gornet JM, Monsel G, Allez M, Bertheau P, Bagot M, Lebbé C, Viguier M. Ipilimumab-induced acute severe colitis treated by infliximab. *Melanoma Res* 2013; **23**: 227-230 [PMID: 23458760 DOI: 10.1097/CMR.0b013e32835fb524]

9 **Sherid M**, Ehrenpreis ED. Types of colitis based on histology. *Dis Mon* 2011; **57**: 457-489 [PMID: 21944389 DOI: 10.1016/j.disamonth.2011.05.004]

10 **Allez M**, Lemann M, Bonnet J, Cattan P, Jian R, Modigliani R. Long term outcome of patients with active Crohn's disease exhibiting extensive and deep ulcerations at colonoscopy. *Am J Gastroenterol* 2002; **97**: 947-953 [PMID: 12003431 DOI: 10.1111/j.1572-0241.2002.05614.x]

P- Reviewer: Forde PM **S- Editor**: Yu J **L- Editor**: A
E- Editor: Zhang DN

World Journal of Gastroenterology

Submit a Manuscript: http://www.wjgnet.com/esps/
Help Desk: http://www.wjgnet.com/esps/helpdesk.aspx
DOI: 10.3748/wjg.v21.i14.4379

World J Gastroenterol 2015 April 14; 21(14): 4379-4384
ISSN 1007-9327 (print) ISSN 2219-2840 (online)

CASE REPORT

Failure of interferon-γ pre-treated mesenchymal stem cell treatment in a patient with Crohn's disease

Andrea Taddio, Alberto Tommasini, Erica Valencic, Ettore Biagi, Giuliana Decorti, Sara De Iudicibus, Eva Cuzzoni, Giuseppe Gaipa, Raffaela Badolato, Alberto Prandini, Andrea Biondi, Alessandro Ventura

Andrea Taddio, Alessandro Ventura, Institute for Maternal and Child Health - IRCCS "Burlo Garofolo" - Trieste and University of Trieste, 34100 Trieste, Italy
Alberto Tommasini, Erica Valencic, Sara De Iudicibus, Institute for Maternal and Child Health - IRCCS "Burlo Garofolo" - Trieste, 34100 Trieste, Italy
Ettore Biagi, Giuseppe Gaipa, Andrea Biondi, "Matilde Tettamanti" Research Centre, Laboratory of Cell Therapy "Stefano Verri", Paediatric Clinic, University of Milano-Bicocca, San Gerardo Hospital, 20900 Monza, Italy
Giuliana Decorti, Sara De Iudicibus, Department of Life Sciences, University of Trieste, 34127 Trieste, Italy
Eva Cuzzoni, Clinical Department of Medical, Surgical and Health Sciences, University of Trieste, 34127 Trieste, Italy
Raffaela Badolato, Alberto Prandini, Department of Clinical and Experimental Sciences, Institute of Molecular Medicine "Angelo Nocivelli", University of Brescia, 26122 Brescia, Italy
Author contributions: All authors contributed equally to this work; Taddio A, Tommasini A, Badolato R, Ventura A and Biondi A contributed to study concept and design, and to interpretation of the data, drafting of the manuscript, critical revision of the manuscript for important intellectual content, obtaining the funding, administrative, technical, or material support, and study supervision; Biagi E, Valencic E, Decorti G, De Iudicibus S, Gaipa G, Cuzzoni E and Prandini A contributed to study concept and design, acquisition of the data, analysis of the data, drafting of the manuscript, critical revision of the manuscript for important intellectual content, administrative, technical, or material support, and contributions to new reagents; Taddio A and Tommasini A wrote the paper.

Correspondence to: Andrea Taddio, MD, Institute for Maternal and Child Health - IRCCS "Burlo Garofolo" - Trieste and University of Trieste, via dell'Istria 65/1, 34100 Trieste, Italy. andrea.taddio@burlo.trieste.it
Telephone: +39-40-3785312
Fax: +39-40-3785290
Received: August 6, 2014
Peer-review started: August 8, 2014
First decision: August 27, 2014
Revised: September 30, 2014
Accepted: November 19, 2014
Article in press: November 19, 2014
Published online: April 14, 2015

Abstract

Mesenchymal stem cells (MSC) are cells of stromal origin which exhibit unlimited self-renewal capacity and pluripotency *in vitro*. It has recently been observed that MSC may also exert a profound immunosuppressive and anti-inflammatory effect both *in vitro* and *in vivo* with consequent potential use in autoimmune disorders. We present the case of a patient suffering from childhood-onset, multidrug resistant and steroid-dependent Crohn's disease who underwent systemic infusions of MSC, which led to a temporary reduction in CCR4, CCR7 and CXCR4 expression by T-cells, and a temporary decrease in switched memory B-cells, In addition, following MSC infusion, lower doses of steroids were needed to inhibit proliferation of the patient's peripheral blood mononuclear cells. Despite these changes, no significant clinical benefit was observed, and the patient required rescue therapy with infliximab and subsequent autologous hematopoietic stem cell transplantation. The results of biological and *in vitro* observations after MSC use and the clinical effects of infusion are discussed, and a brief description is provided of previous data on MSC-based therapy in autoimmune disorders.

Key words: Autoimmune disease; Crohn's disease; Interferon-γ pretreatment; Mesenchymal stem cells;

Immune regulation

Core tip: This is the first report of a lack of clinical response using interferon-γ pre-treated mesenchymal stem cell infusion in a patient with intractable Crohn's disease. Data on the clinical effects of mesenchymal stem cell treatment in autoimmune disorders are sparse and usually report a good clinical response; however, since very few reports have been published, we think negative results are also worthy of attention. The use of mesenchymal stem cells pre-treated with interferon-γ is also of interest, and the lack of clinical benefit of bone marrow-derived interferon-γ pre-treated mesenchymal stem cell infusion has also been described, despite the lymphocyte immune regulation effect.

Taddio A, Tommasini A, Valencic E, Biagi E, Decorti G, De Iudicibus S, Cuzzoni E, Gaipa G, Badolato R, Prandini A, Biondi A, Ventura A. Failure of interferon-γ pre-treated mesenchymal stem cell treatment in a patient with Crohn's disease. *World J Gastroenterol* 2015; 21(14): 4379-4384 Available from: URL: http://www.wjgnet.com/1007-9327/full/v21/i14/4379.htm DOI: http://dx.doi.org/10.3748/wjg.v21.i14.4379

INTRODUCTION

Mesenchymal stem cells (MSC) are cells of stromal origin which exhibit unlimited self-renewal capacity and pluripotency *in vitro*; more specifically, several reports have described the capacity of MSC to differentiate *in vitro* into multiple cellular lineages, and their use in regenerative medicine has been extensively investigated in various clinical settings[1].

Much interest has been generated recently by the observation that MSC may also exert a pronounced immunosuppressive and anti-inflammatory effect, both *in vitro* and *in vivo*. The mechanisms behind this immunosuppressive effect are still unclear, but they seem to involve events mediated by both soluble factors and cell contact[2,3].

There are few studies describing treatment with systemic MSC in humans, and most of these are in patients treated for acute graft-*vs*-host disease (GvHD), indicating that infusions of MSC expanded *in vitro*, irrespective of the donor, might be an effective treatment for patients with steroid-resistant, acute GvHD[4]. MSC treatment has also been tried out in other autoimmune diseases such as systemic lupus erythematosus and Sjögren's disease[5,6], with encouraging results. Moreover, it has been demonstrated that systemic infusions of MSC lessen the clinical and histopathological severity of experimental colitis, reducing weight loss, diarrhea, and inflammation[7]. This potential role of MSC in modulating the immune response and tissue regeneration led to the idea of using MSC for a new cellular approach in the treatment of Crohn's disease (CD) in humans, with conflicting results[8]. Preclinical data obtained from cellular and animal models have suggested that the profile of immune activation in the host prior to administration of MSC can be a critical factor in the outcome of immune suppression. Indeed, treatment with interferon-γ (IFN-γ) can enhance the immunosuppressive action of MSC, especially when the MSC are used in a setting of ongoing immune activation[9], and several reports have suggested that exposure to activated lymphocytes, or to IFN-γ, is necessary to activate the immunosuppressive properties of MSC[10-12]. Based on these results, we hypothesized that MSC could be briefly incubated with IFN-γ in a clinical-grade setting in order to improve their capability for treating severe immune disorders. We present the case of a patient with intractable, childhood-onset, steroid-dependent CD, who underwent MSC infusion to no effect.

CASE REPORT

The patient was a 31-year-old woman suffering from CD. This diagnosis was made when she was 11 years old, and was characterized by diarrhea, weight loss, asthenia, and high levels of inflammatory markers. On that occasion, colonoscopy and esophagogastroduodenoscopy were performed and biopsy specimens confirmed the preliminary diagnosis of ileal and perianal CD.

The patient was initially treated with steroids and enteral nutrition, but frequent relapses occurred when steroids were tapered leading rapidly to ileocolic resection due to stenosis. As a consequence, thalidomide was started and there was some clinical improvement, but treatment was suspended when the patient showed evidence of thalidomide-related peripheral toxicity. Over the following years, several attempts were made to treat her with azathioprine, cyclosporine, and methotrexate, but the clinical response was poor. When she was 24 years old, she received treatment with infliximab, with some clinical improvement, but she then developed a new stenosis requiring surgical procedures and the drug was withdrawn. She was then started on adalimumab, but no clinical benefits were observed and she developed herpetic esophagitis. A second trial with thalidomide was suspended because of the re-appearance of neurological complications and dapsone was eventually started, on the basis of some anecdotal clinical reports, again with a poor clinical response.

Given the long clinical history, characterized by numerous complications and multiple surgical interventions, a disease that was steroid-dependent and still active, despite ample use of immunosuppressants, and the absence of opportunistic infections and small

intestine bacterial overgrowth, we decided to try MSC infusions.

At the time of the first infusion, the physical examination was unremarkable, but the patient had oral ulcers with a feeding inability requiring nocturnal enteral nutrition, abdominal pain, watery diarrhea (35 episodes per week), and perianal ulcers. Colonoscopy showed inflammation of the mucosa. Laboratory examinations were normal, including acute phase reactants (erythrocyte sedimentation rate: 18 mm/h; normal value 0-20; C-reactive protein: 0.34 mg/dL; normal value < 0.5) except for the presence of chronic normocytic anemia (hemoglobin: 9.2 g/dL; mean cell volume: 78 fl), hypergammaglobulinemia (IgG: 1780 mg/dL) and increased levels of fecal calprotectin (2200 mg/kg; normal value < 50). Magnetic resonance imaging of the gastrointestinal tract showed free fluid, peritoneal fat stranding with enhancement, diffuse thickening of the bowel wall, and stratified enhancement of sigmoid and ascending colon; ileal and ileo-colic strictures were also present. The CD activity index (AI) was 270. The patient was treated with dapsone (50 mg bid) and prednisone (25 mg/d).

The patient underwent the two scheduled MSC infusions (2×10^6 cells/kg per infusion) which were well tolerated. Ten days after the second infusion, despite CDAI improvement (215), there was exacerbation of abdominal pain and worsening of diarrhea, and the clinical picture deteriorated rapidly. Laboratory examinations remained normal, but calprotectin levels were still high, and the patient underwent rescue therapy with infliximab (10 mg/kg per infusion) with transient slight improvement; she was then directed to an autologous hematopoietic stem cell transplantation (HSTC) program.

The MSC were produced in the officially approved cell factory Laboratorio di Terapia Cellulare e Genica "Stefano Verri" in Monza (Italy), compliant with European good manufacturing practices, as determined by AIFA (Agenzia Italiana del Farmaco, Rome). The procedures were approved by the Istituto Superiore di Sanità (approval by ISS, Rome, 5.09.2007, n 45253(06)-PRE.21-882).

The medical ethical committee of the IRCCS "Burlo Garofolo" (Trieste, Italy) approved the use of IFN-γ pretreated MSC for compassionate use. The patient gave her written informed consent.

DISCUSSION

We present a case of refractory, drug-resistant, steroid-dependent childhood-onset CD which was then treated with two infusions of MSC, with rapid deterioration of the clinical picture and subsequent need for medical rescue therapy before autologous HSTC.

To our knowledge, this is the 15th patient affected by CD to be treated with systemic MSC infusion. The first report is by Duijvestein *et al*[8], in which 10 patients with chronic severe steroid-refractory CD were recruited for MSC treatment in a two-infusion protocol schedule. Two patients were withdrawn from the study and did not complete the protocol. Among the 8 patients who received both infusions, 5 showed improvement in the CDAI, but only 3 showed a clinical response (defined as a drop in CDAI by more than 70), while 3 patients required surgery over a 14-wk period following infusions. It should be pointed out that remission was not achieved in any of the patients. Liang *et al*[9] treated 7 patients, of whom 4 had CD and 3 ulcerative colitis. According to the authors, 5 patients had achieved remission at the 3-mo follow-up, and this remission lasted for over 24 mo in 2 patients. However, only one patient stopped steroid treatment completely, while 3 patients tapered partially and the other 3 could not reduce their total steroid dosage, an indirect indication of incompletely controlled disease.

In the current case, there was no observable clinical improvement after infusion, and indeed, soon after the second infusion, the patient required rescue therapy with infliximab before undergoing HSCT. We would also like to stress that in order to enhance the clinical response in our patient, the MSCs were pre-treated with IFN-γ, because it has been shown that IFN-γ activation of MSCs increases their immunosuppressive capabilities *in vitro* and (we therefore hoped), their therapeutic efficacy *in vivo*[13]. Unfortunately, we found no evidence of any positive clinical response.

It might be argued that the lack of clinical response to MSC infusion in our case could be due to weak biological properties of the cells. It should be pointed out that when the cells were thawed after cryopreservation before their infusion, a small sample was analyzed to check MSC vitality and immunosuppressive capacity: no difference was found before and after cryopreservation. In addition, a much higher percentage of natural killer (NK) cells was found in the patient's serum after the second infusion (4.52% before infusion, compared to 14.5% after, which could be interpreted as a "physiological" response to MSC infusion. In fact, it is known that MSC are susceptible to lysis by NK cells, and that there is a natural tendency for NK cells to proliferate in order to counteract the biological effect of MSC[14].

Another interesting finding which confirmed the biological effect of MSC infusion was that methylprednisolone IC_{50} levels (*i.e.*, the concentration required to reduce *in vitro* mononuclear proliferation to 50%) were similar before MSC treatment (T-7 and T0), while lower concentrations of the steroid were needed to inhibit proliferation of the patient's peripheral blood mononuclear cells after infusion (T+7 and T+14). After the last infusion, however (T+28), an increase in the IC50 was observed which coincided with the patient's worsening symptoms (Figure 1)[15].

Analysis of T-lymphocytes before the infusion and

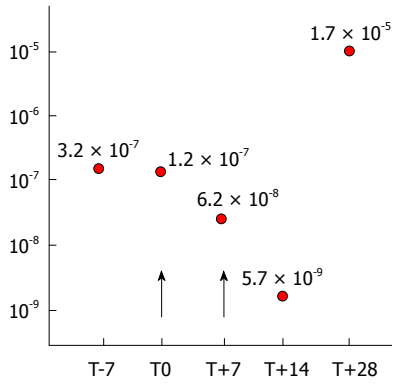

Figure 1 Increase in methylprednisolone IC50 coincided with worsening symptoms. Concentration of methylprednisolone that inhibited 50% of the proliferation (IC_{50}) of peripheral mononuclear blood cells obtained from the patient at various experimental times, before and after mesenchymal stem cells infusion (arrows). Inhibition of proliferation was determined by labelling metabolically active cells (stimulated with concanavalin-A) with [methyl-^{3}H]thymidine [12].

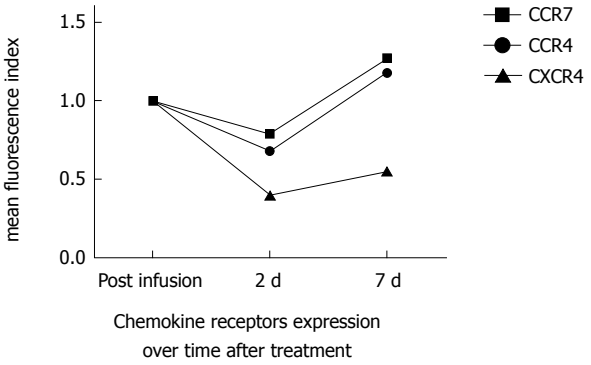

Figure 2 Time course of CCR7, CCR4 and CXCR4 expression by T-lymphocytes. Analysis of CCR7, CCR4 and CXCR4 expression by flow cytometry showed a transient reduction after 2 d. Expression levels were measured as mean fluorescence intensity index.

at days +2 and +7 respectively showed a transient reduction in CCR4, CCR7 and CXCR4 expression at day +2 compared with basal levels, while expression of CXCR4 was still reduced after 7 d (Figure 2). In addition, analysis of B-cells showed a transient decrease in switched B-cells, while the maturation of monocyte-derived dendritic cells, as measured by analysis of CD80, CD86, and CD83 expression, was not affected (data not shown). These results suggest that MSC infusion may have led to a mobilization of select T and B cell subsets to tissues within 2 d; these observations support previous reports suggesting a mechanism of B-cell suppression, with immunoglobulin impairment production induced by release of soluble factors[16].

In our case, despite the evidence of some *in vitro* properties and *in vivo* biological effects, no positive clinical response to MSC therapy was found. Of course, this is just a single case report and large multicenter trials, presently ongoing, need to be encouraged[17]. We should also stress the fact that MSCs were used in this case to treat a very severe form of CD, resistant to multiple attempts with standard treatments, and in a late phase of clinical progression. Studies of GvHD patients after allogeneic HSCT seem to support the hypothesis that MSC therapy should be promoted in the very early stage of disease immediately after steroid failure, while patients with more advanced or chronic GvHD failed to show any clinical benefit[18]. In line with this observation, we recently demonstrated that mediators derived from activated lymphocytes can suppress MSC which have not been previously activated[19]. In fact, the presence of soluble mediators in the environment can be a critical factor in the survival and action of MSC[20,21]. IFN-γ treatment has been proposed to enhance the action of MSC against already-activated lymphocytes, but this treatment may not to be sufficient to protect MSC from the effect of high concentrations of inflammatory mediators. Therapy with MSC has created great hope for advances in the treatment of autoimmune disorders, but at this moment in time, there is still only weak evidence of their clinical effectiveness. In fact, there is a great paucity of data available regarding clinical trials with MSC therapy in the field of autoimmune disorders. To confirm this, a PubMed search was carried out for the following terms "autoimmune disorders" and "mesenchymal stem cells". We found 485 articles, consisting mostly of reviews (177/485; 36.5%) and animal models and *in vitro* studies (285/485; 58.8%), while there were only 23 articles consisting of clinical trials and case reports (4.7%).

It is also important to bear in mind that negative findings tend not to be reported in the medical literature, which is why we think that describing this experience should be of interest to other physicians and researchers. Clearly, the data in our possession is still insufficient to be able to consider systemic infusion of MSC in the treatment of CD, at least in its very advanced, progressive and multiple drug-resistant forms. Our experience suggests that patients with intractable drug-resistant CD should still undergo HSCT, while MSC therapy may perhaps be considered in the earlier stages of the disease. The use of MSC therapy in CD fistulas, on the other hand, may be of some benefit[22].

COMMENTS

Case characteristics

After a long series of attempts at treatment with immunosuppressants and surgery, a 31-year-old woman with intractable Crohn's disease presented with oral ulcers, a feeding inability requiring nocturnal enteral nutrition, abdominal pain, watery diarrhea and perianal ulcers.

Clinical diagnosis

The diagnosis was Crohn's disease.

Differential diagnosis

Given the clinical history of the patient, characterized by numerous complications, a series of surgical interventions, a dependency on steroids, and long-term use of immunosuppressants, we ruled out the possible presence of opportunistic infections, malignancies and small intestine bacterial proliferation.

Laboratory diagnosis

The patient had chronic normocytic anemia (Hb: 9.2 g/dL; MCV: 78 fl), hypergammaglobulinemia (IgG: 1780 mg/dL) and increased levels of fecal calprotectin (2200 mg/kg; n.v. < 50).

Imaging diagnosis

The patient underwent magnetic resonance imaging of the gastrointestinal tract, which showed free fluid, peritoneal fat stranding with enhancement, diffuse thickening of the bowel wall, and stratified enhancement of the sigmoid and ascending colon; ileal and ileo-colic strictures were also found.

Pathological diagnosis

Biopsy specimens from both the colon and ileum were consistent with a diagnosis of ileal and perianal Crohn's disease.

Treatment

Interferon-γ pre-treated mesenchymal stem cells were infused at a dosage of 2 × 10^6 cells/kg. Two infusions were scheduled.

Term explanation

Mesenchymal stem cells are cells of a stromal origin which exhibit unlimited self-renewal capacity and pluripotency *in vitro* and have a pronounced anti-inflammatory and immunosuppressive effect.

Experiences and lessons

We describe a case of a patient with intractable Crohn's disease in which no clinical benefit was obtained from the use of interferon-γ pre-treated mesenchymal stem cells despite lymphocyte dysregulation. The usefulness of mesenchymal stem cell treatment in autoimmune disorders is still to be confirmed; the literature is scarce and results are uncertain.

Peer-review

The authors describe a case of intractable Crohn's disease which failed to respond to parenteral mesenchymal stem cell therapy. The article highlights the failure of interferon-γ pre-treated mesenchymal stem cell infusion, points to the effect on lymphocyte regulation and discusses the results obtained using mesenchymal stem cells to treat autoimmune diseases.

REFERENCES

1 **Bernardo ME**, Pagliara D, Locatelli F. Mesenchymal stromal cell therapy: a revolution in Regenerative Medicine? *Bone Marrow Transplant* 2012; **47**: 164-171 [PMID: 21478914 DOI: 10.1182/blood-2012-04-423822]

2 **Di Nicola M**, Carlo-Stella C, Magni M, Milanesi M, Longoni PD, Matteucci P, Grisanti S, Gianni AM. Human bone marrow stromal cells suppress T-lymphocyte proliferation induced by cellular or nonspecific mitogenic stimuli. *Blood* 2002; **99**: 3838-3843 [PMID: 11986244]

3 **Meisel R**, Zibert A, Laryea M, Göbel U, Däubener W, Dilloo D. Human bone marrow stromal cells inhibit allogeneic T-cell responses by indoleamine 2,3-dioxygenase-mediated tryptophan degradation. *Blood* 2004; **103**: 4619-4621 [PMID: 15001472]

4 **Le Blanc K**, Frassoni F, Ball L, Locatelli F, Roelofs H, Lewis I, Lanino E, Sundberg B, Bernardo ME, Remberger M, Dini G, Egeler RM, Bacigalupo A, Fibbe W, Ringdén O. Mesenchymal stem cells for treatment of steroid-resistant, severe, acute graft-versus-host disease: a phase II study. *Lancet* 2008; **371**: 1579-1586 [PMID: 18468541 DOI: 10.1016/S0140-6736(08)60690-X]

5 **Liang J**, Zhang H, Hua B, Wang H, Lu L, Shi S, Hou Y, Zeng X, Gilkeson GS, Sun L. Allogenic mesenchymal stem cells transplantation in refractory systemic lupus erythematosus: a pilot clinical study. *Ann Rheum Dis* 2010; **69**: 1423-1429 [PMID: 20650877 DOI: 10.1136/ard.2009.123463]

6 **Xu J**, Wang D, Liu D, Fan Z, Zhang H, Liu O, Ding G, Gao R, Zhang C, Ding Y, Bromberg JS, Chen W, Sun L, Wang S. Allogeneic mesenchymal stem cell treatment alleviates experimental and clinical Sjögren syndrome. *Blood* 2012; **120**: 3142-3151 [PMID: 22927248 DOI: 10.1182/blood-2011-11-391144]

7 **Gonzalez-Rey E**, Anderson P, González MA, Rico L, Büscher D, Delgado M. Human adult stem cells derived from adipose tissue protect against experimental colitis and sepsis. *Gut* 2009; **58**: 929-939 [PMID: 19136511 DOI: 10.1136/gut.2008.168534]

8 **Duijvestein M**, Vos AC, Roelofs H, Wildenberg ME, Wendrich BB, Verspaget HW, Kooy-Winkelaar EM, Koning F, Zwaginga JJ, Fidder HH, Verhaar AP, Fibbe WE, van den Brink GR, Hommes DW. Autologous bone marrow-derived mesenchymal stromal cell treatment for refractory luminal Crohn's disease: results of a phase I study. *Gut* 2010; **59**: 1662-1669 [PMID: 20921206 DOI: 10.1136/gut.2010.215152]

9 **Liang J**, Zhang H, Wang D, Feng X, Wang H, Hua B, Liu B, Sun L. Allogeneic mesenchymal stem cell transplantation in seven patients with refractory inflammatory bowel disease. *Gut* 2012; **61**: 468-469 [PMID: 21617158 DOI: 10.1136/gutjnl-2011-300083]

10 **Renner P**, Eggenhofer E, Rosenauer A, Popp FC, Steinmann JF, Slowik P, Geissler EK, Piso P, Schlitt HJ, Dahlke MH. Mesenchymal stem cells require a sufficient, ongoing immune response to exert their immunosuppressive function. *Transplant Proc* 2009; **41**: 2607-2611 [PMID: 19715984 DOI: 10.1016/j.transproceed.2009.06.119]

11 **Chang CJ**, Yen ML, Chen YC, Chien CC, Huang HI, Bai CH, Yen BL. Placenta-derived multipotent cells exhibit immunosuppressive properties that are enhanced in the presence of interferon-gamma. *Stem Cells* 2006; **24**: 2466-2477 [PMID: 17071860]

12 **Ryan JM**, Barry F, Murphy JM, Mahon BP. Interferon-gamma does not break, but promotes the immunosuppressive capacity of adult human mesenchymal stem cells. *Clin Exp Immunol* 2007; **149**: 353-363 [PMID: 17521318]

13 **Valencic E**, Piscianz E, Andolina M, Ventura A, Tommasini A. The immunosuppressive effect of Wharton's jelly stromal cells depends on the timing of their licensing and on lymphocyte activation. *Cytotherapy* 2010; **12**: 154-160 [PMID: 20078387 DOI: 10.3109/14653240903493417]

14 **Spaggiari GM**, Capobianco A, Becchetti S, Mingari MC, Moretta L. Mesenchymal stem cell-natural killer cell interactions: evidence that activated NK cells are capable of killing MSCs, whereas MSCs can inhibit IL-2-induced NK-cell proliferation. *Blood* 2006; **107**: 1484-1490 [PMID: 16239427]

15 **Cuzzoni E**, De Iudicibus S, Bartoli F, Ventura A, Decorti G. Association between BclI polymorphism in the NR3C1 gene and in vitro individual variations in lymphocyte responses to methylprednisolone. *Br J Clin Pharmacol* 2012; **73**: 651-655 [PMID: 22008062 DOI: 10.1111/j.1365-2125.2011.04130.x]

16 **Corcione A**, Benvenuto F, Ferretti E, Giunti D, Cappiello V, Cazzanti F, Risso M, Gualandi F, Mancardi GL, Pistoia V, Uccelli A. Human mesenchymal stem cells modulate B-cell functions. *Blood* 2006; **107**: 367-372 [PMID: 16141348]

17 ClinicalTrials.gov. Mesenchymal stem cells and crohn's disease. Available from: URL: http://www.clinicaltrials.gov/ct2/results?term=mesenchymal stem cells and crohn's disease&Search=Search

18 **Introna M**, Lucchini G, Dander E, Rovelli A, Balduzzi A, Longoni D, Pavan F, Masciochi F, Algarotti A, CMicò C, Grassi A, Cavattoni I, Deola S, Gaipa G, Belotti D, Perseghin P, Parma M, Pogliani EM, Golay J, Gotti E, Capelli C, Cortelazzo S, D'Amico G, Biondi A, Rambaldi A, Biagi E. Safe and Effective Treatment of Graft Vs Host Disease with Platelet Lysate-Expanded Human Mesenchymal Stromal Cells: A Phase 1 Study On 47 Adult and Pediatric Patients. *Blood* 2012; **120**: 743

19 **Valencic E**, Loganes C, Cesana S, Piscianz E, Gaipa G, Biagi E, Tommasini A. Inhibition of mesenchymal stromal cells by pre-activated lymphocytes and their culture media. *Stem Cell Res Ther* 2014; **5**: 3 [PMID: 24405828]

20 **Freytes DO**, Kang JW, Marcos-Campos I, Vunjak-Novakovic G. Macrophages modulate the viability and growth of human mesenchymal stem cells. *J Cell Biochem* 2013; **114**: 220-229 [PMID: 22903635 DOI: 10.1002/jcb.24357]

21 **Liu Y**, Wang L, Kikuiri T, Akiyama K, Chen C, Xu X, Yang R, Chen W, Wang S, Shi S. Mesenchymal stem cell-based tissue regeneration is governed by recipient T lymphocytes via IFN-γ and TNF-α. *Nat Med* 2011; **17**: 1594-1601 [PMID: 22101767 DOI: 10.1038/nm.2542]

22 **Ciccocioppo R**, Bernardo ME, Sgarella A, Maccario R, Avanzini MA, Ubezio C, Minelli A, Alvisi C, Vanoli A, Calliada F, Dionigi P, Perotti C, Locatelli F, Corazza GR. Autologous bone marrow-derived mesenchymal stromal cells in the treatment of fistulising Crohn's disease. *Gut* 2011; **60**: 788-798 [PMID: 21257987 DOI: 10.1136/gut.2010.214841]

P- Reviewer: Dimcevski G **S- Editor**: Ma YJ **L- Editor**: Cant MR
E- Editor: Liu XM

World Journal of Gastroenterology

Submit a Manuscript: http://www.wjgnet.com/esps/
Help Desk: http://www.wjgnet.com/esps/helpdesk.aspx
DOI: 10.3748/wjg.v21.i14.4385

World J Gastroenterol 2015 April 14; 21(14): 4385-4390
ISSN 1007-9327 (print) ISSN 2219-2840 (online)

CASE REPORT

Fatal submucosal invasive gastric adenosquamous carcinoma detected at surveillance after gastric endoscopic submucosal dissection

Akinori Shirahige, Haruhisa Suzuki, Ichiro Oda, Masau Sekiguchi, Genki Mori, Seiichiro Abe, Satoru Nonaka, Shigetaka Yoshinaga, Shigeki Sekine, Ryoji Kushima, Yutaka Saito, Takeo Fukagawa, Hitoshi Katai

Akinori Shirahige, Haruhisa Suzuki, Ichiro Oda, Masau Sekiguchi, Genki Mori, Seiichiro Abe, Satoru Nonaka, Shigetaka Yoshinaga, Yutaka Saito, Endoscopy Division, National Cancer Center Hospital, Tokyo 104-0045, Japan
Shigeki Sekine, Pathology Division, National Cancer Center Hospital, Tokyo 104-0045, Japan
Ryoji Kushima, Department of Clinical Laboratory Medicine and Diagnostic Pathology, Shiga University of Medical Science, Otsu 520-2192, Japan
Takeo Fukagawa, Hitoshi Katai, Gastric Surgery Division, National Cancer Center Hospital, Tokyo 104-0045, Japan
Author contributions: Shirahige A, Suzuki H and Oda I wrote the manuscript; Sekiguchi M, Mori G, Abe S, Nonaka S, Yoshinaga S, Sekine S, Kushima R, Saito Y, Fukagawa T and Katai H contributed to the manuscript discussion and reviewed the manuscript.
Informed consent: All study participants, or their legal guardian, provided informed written consent prior to study enrollment.
Conflict-of-interest: No conflict of interest was declared by the authors.

Correspondence to: Haruhisa Suzuki, MD, Endoscopy Division, National Cancer Center Hospital, 5-1-1 Tsukiji, Chuo-ku, Tokyo 104-0045, Japan. harusuzu@ncc.go.jp
Telephone: +81-3-35422511
Fax: +81-3-35423815
Received: October 14, 2014
Peer-review started: October 15, 2014
First decision: November 14, 2014
Revised: November 28, 2014
Accepted: January 30, 2015
Article in press: January 30, 2015
Published online: April 14, 2015

Abstract

An 80-year-old man was under annual surveillance esophagogastroduodenoscopy after endoscopic submucosal dissection (ESD) for early gastric cancer (EGC). Two years after the initial ESD, a 0-Ⅱc type metachronous EGC lesion, 8 mm in size, without an ulcer scar, was found in the gastric antrum. The estimated tumor depth was up to the mucosa, and biopsy revealed well and poorly differentiated adenocarcinoma. ESD was performed for this lesion and *en bloc* resection with negative margins was achieved. Histopathological examination revealed an adenosquamous carcinoma 8 mm in size invading the deep submucosal layer (1600 μm), with lymphovascular invasion, consistent with the diagnosis of non-curative resection. Additional gastrectomy was recommended for this patient; however, two months after the ESD, preoperative computed tomography revealed multiple liver metastases, and the patient was considered as an unsuitable candidate for surgical resection. Systemic chemotherapy was therefore started; however, the patient died of gastric cancer 27 mo after the second ESD. Early gastric adenosquamous carcinoma localized to the mucosa and submucosa is extremely rare and its clinical behavior is not well known. The present report is very significant in that it underscores the distinct possibility of gastric adenosquamous carcinoma being very aggressive and fatal even when detected at an early cancer.

Key words: Early gastric cancer; Endoscopic submucosal dissection; Gastric adenosquamous carcinoma; Gastric cancer-related death; Liver metastasis; Metachronous cancer; Surveillance

Core tip: Herein is described a rare case of gastric adenosquamous carcinoma which resulted in liver metastasis and gastric cancer-related death, even though the tumor was detected at an early cancer by periodic surveillance esophagogastroduodenoscopy after gastric endoscopic submucosal dissection. Early gastric adenosquamous carcinoma is extremely rare and its clinical behavior is not well known. The present study is very significant in that it underscores the distinct possibility of gastric adenosquamous carcinoma being very aggressive and fatal even when detected at an early cancer.

Shirahige A, Suzuki H, Oda I, Sekiguchi M, Mori G, Abe S, Nonaka S, Yoshinaga S, Sekine S, Kushima R, Saito Y, Fukagawa T, Katai H. Fatal submucosal invasive gastric adenosquamous carcinoma detected at surveillance after gastric endoscopic submucosal dissection. *World J Gastroenterol* 2015; 21(14): 4385-4390 Available from: URL: http://www.wjgnet.com/1007-9327/full/v21/i14/4385.htm DOI: http://dx.doi.org/10.3748/wjg.v21.i14.4385

INTRODUCTION

Adenosquamous carcinoma is an exceedingly rare tumor, accounting for only 0.14%-1.9% of all cases of gastric cancer[1-6]. It is a very aggressive cancer, and in the majority of cases, these tumors are already at an advanced stage at diagnosis, with lymph node metastasis and liver metastasis. This type of cancer is associated with a very poor prognosis, with the 5-year survival rate of 0-22%[1,3,6-8]. There are few reports on early gastric adenosquamous carcinoma localized to the mucosa and submucosa; therefore, the clinical behavior of this type of cancer is still not well known[6,9,10]. We document a rare case of gastric adenosquamous carcinoma which resulted in liver metastasis and gastric cancer-related death, even though the tumor was detected at an early cancer by periodic surveillance esophagogastroduodenoscopy (EGD) two years after curative endoscopic submucosal dissection (ESD) for early gastric cancer (EGC).

CASE REPORT

An 80-year-old man was admitted to our hospital in June 2005 for endoscopic treatment of EGC. We performed ESD for the initial EGC lesion, a 0-Ⅱa type well differentiated adenocarcinoma limited to the mucosa measuring 10 mm in diameter, with no ulcer scar, on the lesser curvature of the middle gastric body (Figure 1). Histopathological findings revealed a well differentiated mucosal adenocarcinoma measuring 10 mm in diameter without lymphovascular involvement or ulcer scar, and tumor-free margins. This lesion fulfilled the absolute pathological criteria and was diagnosed as a curative resection[11]. After the initial ESD, EGD was performed annually, and revealed no evidence of tumor recurrence; the serum levels of tumor markers such as carcinoembryonic antigen (CEA) also remained within normal range. However, in November 2007, 0-Ⅱc type metachronous gastric cancer (MGC), 8 mm in diameter, with no ulcer scar, was found on the greater curvature of the gastric antrum (Figure 2). The estimated tumor depth was up to the mucosa and biopsy revealed well and poorly differentiated adenocarcinoma. ESD was performed for this lesion and *en bloc* resection with negative margins was achieved. Histopathological examination revealed an adenosquamous carcinoma invading the deep submucosal layer (1600 μm), 8 mm in diameter, with lymphovascular invasion, consistent with the diagnosis of non-curative resection (Figure 3). Immunohistochemical staining was focally positive for CK5/6, CEA, CDX2, and a few cells were positive for CK14, P63, findings that were suggestive of adenosquamous differentiation of the tumor (Figure 4). Additional gastrectomy was recommended for the patient. However, two months after the ESD (in January 2008), preoperative computerized tomography (CT) revealed multiple liver metastases (Figure 5), and the patient was considered as an unsuitable candidate for surgical resection. Systemic chemotherapy was therefore started; however, the patient died of gastric cancer 27 mo after the second ESD.

DISCUSSION

Rolleston *et al*[12] first reported gastric adenosquamous carcinoma in 1905. Gastric adenosquamous carcinoma consists of both adenocarcinomatous and squamous cell carcinomatous components, more than a quarter of the tumor being composed of the squamous cell carcinoma component[13]. Gastric adenosquamous carcinoma is exceedingly rare, accounting for 0.14% to 1.9% of all cases of gastric cancer[1-6]. In the majority of cases of gastric adenosquamous carcinoma, the tumor is already at an advanced stage at diagnosis. The tumor carries a devastating prognosis, with 5-year survival rates ranging from 0 to 22%[1,3,6-8]. Early gastric adenosquamous carcinoma extending to the mucosa and submucosa is extremely rare. Samejima *et al*[9] first reported early gastric adenosquamous carcinoma in 1974 and there have been only 10 case reports of this type of carcinoma since, including the present case[6,9,10]. Among the 10 cases of early gastric adenosquamous carcinoma, five died of gastric cancer (50%) (four with liver metastases and one with distant lymph node metastasis). As compared to the excellent prognosis of the common type of early gastric adenocarcinoma, with 5-year survival rates of about 90%[14], the prognosis of early gastric adenosquamous carcinoma is much poorer. In addition, among the five fatal cases, including the present case, 3 were found to have liver metastasis or distant lymph node metastasis by the time of surgery; the present case had multiple

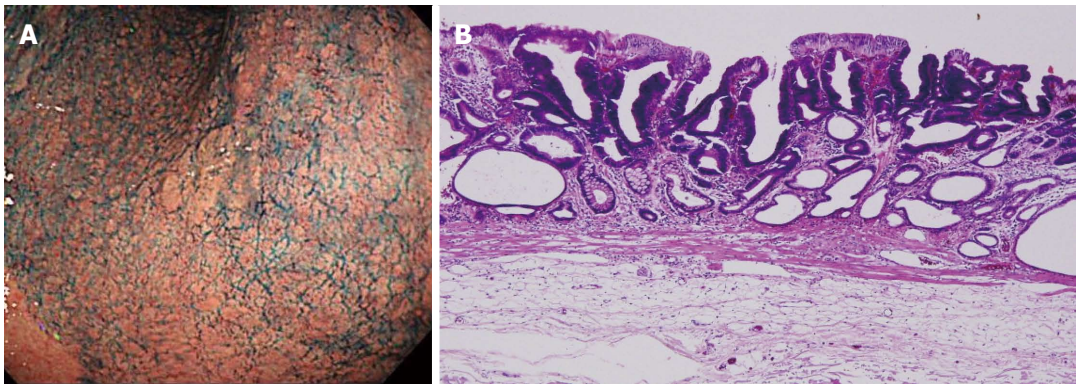

Figure 1 Initial early gastric cancer lesion in June 2005. A: 0-Ⅱa type well differentiated adenocarcinoma limited to the mucosa, 10 mm in size, without an ulcer scar, on the lesser curvature of the middle gastric body; B: Histopathological findings revealed a well differentiated mucosal adenocarcinoma, 10 mm in size, without lymphovascular involvement or ulcerative finding, as well as tumor-free margins.

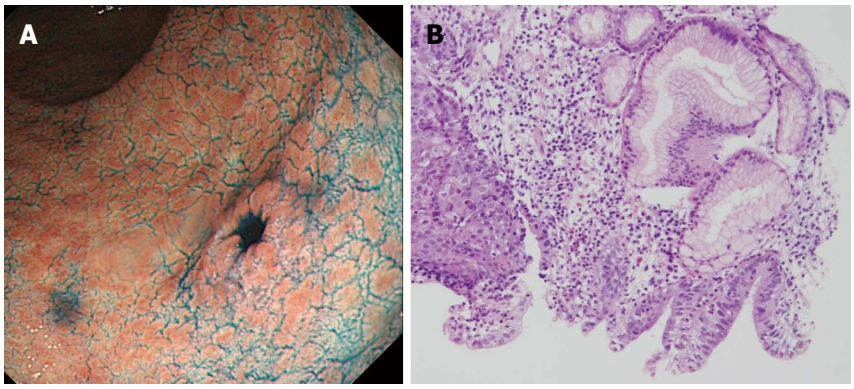

Figure 2 Metachronous early gastric cancer lesion in November 2007. A: 0-Ⅱc type metachronous early gastric cancer lesion, 8 mm in size, without an ulcer scar, on the greater curvature of gastric antrum. The estimated tumor depth was up to the mucosa; B: Biopsy revealed well and poorly differentiated adenocarcinoma (hematoxylin-eosin staining).

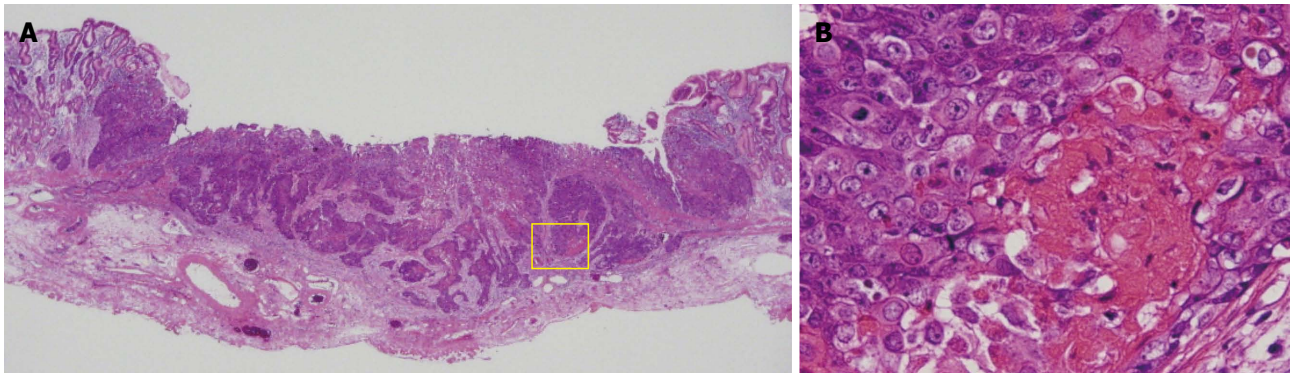

Figure 3 Histopathological findings of endoscopic submucosal dissection specimens. A: Low magnification view with hematoxylin and eosin staining. Endoscopic submucosal dissection specimen revealed adenosquamous carcinoma invading the deep submucosal layer (1600 μm); B: High magnification view of yellow box in A. The tumor shows a solid growth pattern and prominent keratinization suggesting squamous cell carcinomatous component.

liver metastases on a CT obtained two months after the ESD. Therefore, the present case report is very significant in that it underscores the distinct possibility of gastric adenosquamous carcinoma being very aggressive and fatal even when detected at an early cancer.

The histogenesis of adenosquamous carcinoma is not clear, although there are five hypotheses[1,4,6-8,10,15-17]: (1) squamous metaplasia of an adenocarcinoma; (2) cancerization of metaplastic non-neoplastic squamous cells; (3) cancerization of ectopic squamous epithelium; (4) differentiation of multipotential undifferentiated cancer cells toward both squamous and glandular cells; and (5) collision of concurrent adenocarcinoma and squamous cell carcinoma. Most of the squamous cell carcinomatous components

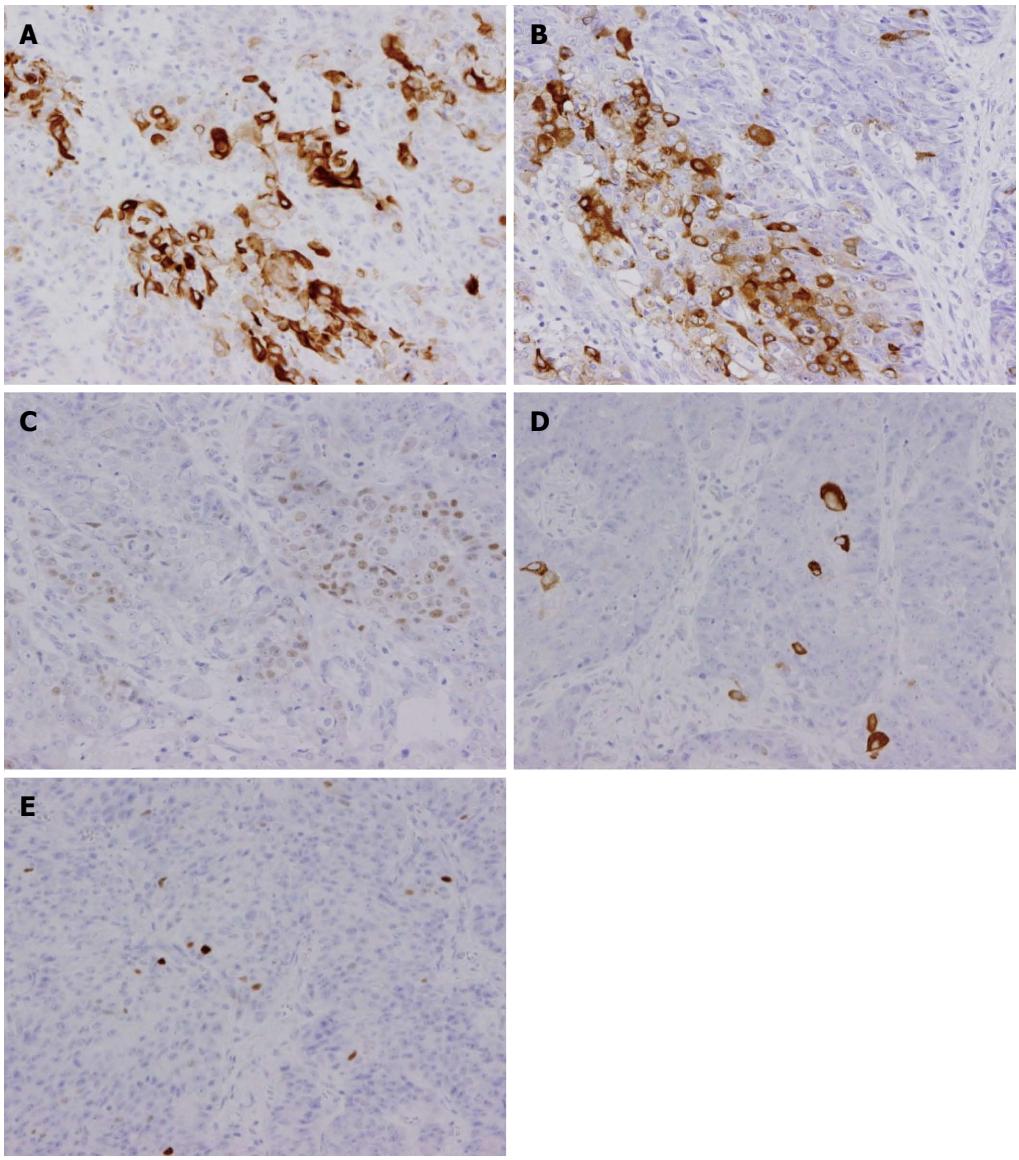

Figure 4 Immunochemical staining. Immunohistochemical staining was focally positive for CK5/6 (A), CEA (B), CDX2 (C), and a few cells were positive for CK14 (D), P63 (E).

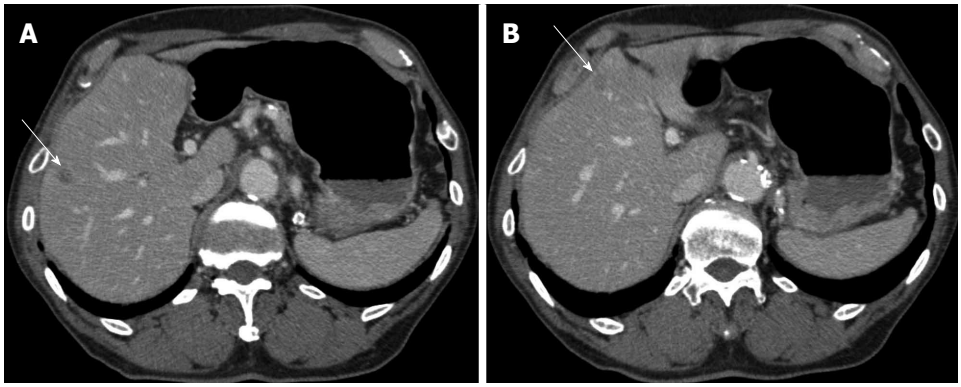

Figure 5 Computerized tomography in January 2008 (two months after the endoscopic submucosal dissection). A and B: Enhanced computerized tomography revealed multiple low density areas suggesting liver metastases (indicated by arrows).

were located at an invasive site, in contrast to the adenocarcinomatous components being located in the mucosal region adjacent to the squamous cell carcinoma component. Therefore, many authors now

believe that the squamous neoplastic component results from metaplastic change of the adenocarcinoma component. Our present case also showed pathological findings that were consistent with this hypothesis.

The tumor in the present patient was detected as an MGC during periodic EGD two years after curative ESD for an EGC lesion fulfilling the absolute indications for ESD[11]. Higher incidence of MGCs (in the range of 1.8% to 12.8%) after endoscopic treatment for EGC has been reported previously[18-22]. Among the 1537 EGC patients who underwent curative ESD for absolute indications or for expanded indications from 1999 to 2006 at our hospital, a total of 348 MGC lesions were detected in 244 patients (15.9%), consistent with previous reports. Unfortunately, we encountered seven cases of MGC with gastric cancer-related death, even though radical resection can be performed in most cases. Among these, in four cases, the advanced MGC was detected over 5 years after the initial ESD, because periodic surveillance examinations were not performed over 5 years. On the other hand, in the remaining three patients including the present case, the MGCs were of a higher malignancy grade at the time of their detection, despite the patient receiving periodic follow-up examinations. Thus, it is necessary to bear in mind the possibility of development of such fatal MGCs during periodic follow-up examinations after curative gastric ESD.

In conclusion, we have described a rare case of submucosal invasive gastric adenosquamous carcinoma that resulted in gastric cancer-related death, even though this tumor was detected at an early cancer during periodic surveillance examinations after curative gastric ESD.

COMMENTS

Case characteristics

An 80-year-old man was under annual surveillance esophagogastroduodenoscopy (EGD) after endoscopic submucosal dissection (ESD) for early gastric cancer (EGC).

Clinical diagnosis

0-Ⅱc type metachronous gastric cancer.

Differential diagnosis

Common type of early gastric cancer.

Laboratory diagnosis

The serum levels of tumor markers such as carcinoembryonic antigen were within normal range.

Imaging diagnosis

EGD revealed small gastric cancer clinically estimated as intramucosal lesion.

Pathological diagnosis

Histopathological examination of ESD resected specimen revealed an adenosquamous carcinoma invading the deep submucosal layer with lymphovascular invasion.

Treatment

The patient received systemic chemotherapy for multiple liver metastases detected after the ESD.

Related reports

Early gastric adenosquamous carcinoma localized to the mucosa and submucosa is extremely rare and its clinical behavior is not well known.

Term explanation

Gastric adenosquamous carcinoma consists of both adenocarcinomatous and squamous cell carcinomatous components, more than a quarter of the tumor being composed of the squamous cell carcinoma component.

Experiences and lessons

Herein is described a rare case of gastric adenosquamous carcinoma which resulted in liver metastasis and gastric cancer-related death, even though the tumor was detected at an early cancer by periodic surveillance EGD after gastric ESD.

Peer-review

This case report reveals the distinct possibility of gastric adenosquamous carcinoma being very aggressive and fatal even when detected at an early cancer.

REFERENCES

1 **Straus R**, Heschel S, Fortmann DJ. Primary adenosquamous carcinoma of the stomach. A case report and review. *Cancer* 1969; **24**: 985-995 [PMID: 5353950]

2 **Aoki Y**, Tabuse K, Wada M, Katsumi M, Uda H. Primary adenosquamous carcinoma of the stomach: experience of 11 cases and its clinical analysis. *Gastroenterol Jpn* 1978; **13**: 140-145 [PMID: 669198]

3 **Nakamura K**, Ueyama T, Yao T, Xuan ZX, Ambe K, Adachi Y, Yakeishi Y, Matsukuma A, Enjoji M. Pathology and prognosis of gastric carcinoma. Findings in 10,000 patients who underwent primary gastrectomy. *Cancer* 1992; **70**: 1030-1037 [PMID: 1515980]

4 **Toyota N**, Minagi S, Takeuchi T, Sadamitsu N. Adenosquamous carcinoma of the stomach associated with separate early gastric cancer (type IIc). *J Gastroenterol* 1996; **31**: 105-108 [PMID: 8808437]

5 **Kim YS**, Heo WS, Chae KH, Gang YS, Jung JH, Kim SH, Seong JK, Lee BS, Jeong HY, Song KS, Shin KS, Cho JS, Noh SM. [Clinicopathological features and differences of p53 and Ki-67 expression in adenosquamous and squamous cell carcinomas of the stomach]. *Korean J Gastroenterol* 2006; **47**: 425-431 [PMID: 16809949]

6 **Maeda M**, Taniguchi H, Sekiguchi S, Katai H, Kushima R. Adenosquamous cell carcinoma of the stomach - A clinicopathologic analysis of 23 cases. *Stomach and Intestine* (abstract in English) 2010; **45**: 1959-1966

7 **Altshuler JH**, Shaka JA. Squamous cell carcinoma of the stomach. Review of the literature and report of a case. *Cancer* 1966; **19**: 831-838 [PMID: 5939052]

8 **Mori M**, Iwashita A, Enjoji M. Adenosquamous carcinoma of the stomach. A clinicopathologic analysis of 28 cases. *Cancer* 1986; **57**: 333-339 [PMID: 3942965]

9 **Samejima Y**, Mizuno T, Sasakawa M, Takemura H, Watanabe A, Nagamatsu M. A case report of early gastric adenocarcinoma and brief review of its literature. *Stomach and Intestine* (abstract in English) 1974; **9**: 783-788

10 **Yoshida K**, Manabe T, Tsunoda T, Kimoto M, Tadaoka Y, Shimizu M. Early gastric cancer of adenosquamous carcinoma type: report of a case and review of literature. *Jpn J Clin Oncol* 1996; **26**: 252-257 [PMID: 8765185 DOI: 10.1093/oxfordjournals.jjco.a023224]

11 **Japanese Gastric Cancer Association**. Japanese gastric cancer treatment guidelines 2010 (ver. 3). *Gastric Cancer* 2011; **14**: 113-123 [PMID: 21573742 DOI: 10.1007/s10120-011-0042-4]

12 **Rolleston HD**, Trevor RS. A case of columnar-celled carcioma of stomach showing squamous celled metaplasia. *J Pathol Bacteriol* 1905; **10**: 418-422 [DOI: 10.1002/path.1700100412]

13 Japanese Research Society for Gastric Cancer: Japanese Classification of Gastric Carcinoma. 1st ed. Tokyo: Kanehara-Shuppan publisher, 1995: 42

14 **Nashimoto A**, Akazawa K, Isobe Y, Miyashiro I, Katai H, Kodera Y, Tsujitani S, Seto Y, Furukawa H, Oda I, Ono H, Tanabe S,

Kaminishi M. Gastric cancer treated in 2002 in Japan: 2009 annual report of the JGCA nationwide registry. *Gastric Cancer* 2013; **16**: 1-27 [PMID: 22729699 DOI: 10.1007/s10120-012-0163-4]

15 **Sailer S**. Diffuse metaplastic gastritis in a patient with prolonged cachexia and macrocystic anemia. *Arch Pathol* 1943; **35**: 730-743

16 **Wood DA**. Adenoacanthoma of the pyloric end of the stomach. *Arch Pathol* 1943; **36**: 177-189

17 **Boswell JT**, Helwig EB. Squamous cell carcinoma and adenoacanthoma of the stomach. a clinicopathologic study. *Cancer* 1965; **18**: 181-192 [PMID: 14254074]

18 **Takekoshi T**, Baba Y, Ota H, Kato Y, Yanagisawa A, Takagi K, Noguchi Y. Endoscopic resection of early gastric carcinoma: results of a retrospective analysis of 308 cases. *Endoscopy* 1994; **26**: 352-358 [PMID: 8076567 DOI: 10.1055/s-2007-1008990]

19 **Kojima T**, Parra-Blanco A, Takahashi H, Fujita R. Outcome of endoscopic mucosal resection for early gastric cancer: review of the Japanese literature. *Gastrointest Endosc* 1998; **48**: 550-54; discussion 550-54; [PMID: 9831855 DOI: 10.1016/S0016-5107(98)70108-7]

20 **Nakajima T**, Oda I, Gotoda T, Hamanaka H, Eguchi T, Yokoi C, Saito D. Metachronous gastric cancers after endoscopic resection: how effective is annual endoscopic surveillance? *Gastric Cancer* 2006; **9**: 93-98 [PMID: 16767364 DOI: 10.1007/s10120-006-0372-9]

21 **Kobayashi M**, Narisawa R, Sato Y, Takeuchi M, Aoyagi Y. Self-limiting risk of metachronous gastric cancers after endoscopic resection. *Dig Endosc* 2010; **22**: 169-173 [PMID: 20642604 DOI: 10.1111/j.1443-1661.2010.00987.x]

22 **Han JS**, Jang JS, Choi SR, Kwon HC, Kim MC, Jeong JS, Kim SJ, Sohn YJ, Lee EJ. A study of metachronous cancer after endoscopic resection of early gastric cancer. *Scand J Gastroenterol* 2011; **46**: 1099-1104 [PMID: 21668406 DOI: 10.3109/00365521.2011.591427]

P- Reviewer: Kiriyama S **S- Editor**: Yu J **L- Editor**: Logan S
E- Editor: Ma S

World Journal of Gastroenterology

Submit a Manuscript: http://www.wjgnet.com/esps/
Help Desk: http://www.wjgnet.com/esps/helpdesk.aspx
DOI: 10.3748/wjg.v21.i14.4391

World J Gastroenterol 2015 April 14; 21(14): 4391-4396
ISSN 1007-9327 (print) ISSN 2219-2840 (online)

CASE REPORT

Myoepithelial carcinoma of the stomach: A diagnostic pitfall

Chih-En Tseng, Yu-Hsi Hsieh, Chang-Kuo Wei, Hsuan-Ying Huang, Chen-Lin Chi

Chih-En Tseng, Chen-Lin Chi, Department of Pathology, Buddhist Dalin Tzu Chi Hospital, Chiayi 62247, Taiwan
Chih-En Tseng, Yu-Hsi Hsieh, School of Medicine, Tzu Chi University, Hualien 97004, Taiwan
Yu-Hsi Hsieh, Department of Gastroenterology, Buddhist Dalin Tzu Chi Hospital, Chiayi 62247, Taiwan
Chang-Kuo Wei, Department of General Surgery, Buddhist Dalin Tzu Chi Hospital, Chiayi 62247, Taiwan
Hsuan-Ying Huang, Department of Anatomical Pathology, Kaohsiung Chang Gung Memorial Hospital and Chang Gung University College of Medicine, Kaohsiung 83301, Taiwan
Author contributions: Hsieh YH and Wei CK provided the case and the clinical information; Tseng CE and Chi CL contributed to the artwork and pathological diagnosis; Huang HY, as the consultant, provided the molecular test for this case and confirmed the diagnosis.

Correspondence to: Dr. Chen-Lin Chi, Department of Pathology, Buddhist Dalin Tzuchi Hospital, No. 2 Minsheng Road, Dalin Township, Chiayi 62247, Taiwan. dm360385@tzuchi.com.tw
Telephone: +886-5-2648000-5728
Fax: +886-5-2648006
Received: August 19, 2014
Peer-review started: August 20, 2014
First decision: September 27, 2014
Revised: October 20, 2014
Accepted: December 16, 2014
Article in press: December 16, 2014
Published online: April 14, 2015

Abstract

Myoepithelioma/myoepithelial carcinomas are not commonly found in soft tissues and are especially rare at visceral sites. This report describes a case of a rare low-grade myoepithelial carcinoma of the stomach. A 61-year-old female patient presented with postprandial abdominal discomfort. Endoscopy revealed a 1.1 cm submucosal lesion. Local excision was performed after malignancy was confirmed by biopsy. The resection margin is free of tumor and she received no adjuvant therapy. The tumor was characterized by multinodular growth with biphasic epithelioid and spindle components. Infiltrative margin and nuclear pleomorphism are seen. Tumor cells were positive for both epithelial and myoepithelial markers. Evidence of epithelial differentiation was confirmed by electron microscopy. No *EWSR1* rearrangement was detected. The final diagnosis was low-grade myoepithelial gastric carcinoma. The patient is currently well, and no evidence of recurrence or metastasis was found after ten-month of follow-up. Myoepithelial carcinoma should be considered in the differential diagnosis of a biphasic gastric tumor.

Key words: Myoepithelioma; Myoepithelial carcinoma; Stomach

Core tip: Myoepithelial tumor can cause diagnostic pitfall due to its rarity and various morphology. This report reveals a rare low-grade myoepithelial carcinoma of stomach and its morphological, immunohistochemical and molecular characteristics.

Tseng CE, Hsieh YH, Wei CK, Huang HY, Chi CL. Myoepithelial carcinoma of the stomach: A diagnostic pitfall. *World J Gastroenterol* 2015; 21(14): 4391-4396 Available from: URL: http://www.wjgnet.com/1007-9327/full/v21/i14/4391.htm DOI: http://dx.doi.org/10.3748/wjg.v21.i14.4391

INTRODUCTION

Myoepithelioma, myoepithelial carcinoma, mixed tumor, and the synonym parachordoma are terms

placed into the same category in the recent edition of the World Health Organization classification of soft tissue tumors[1]. "Myoepithelial tumor" is an uncommon entity and refers to a tumor exhibiting immunohistochemical or ultrastructural evidence of myoepithelial differentiation. In addition to salivary glands, myoepithelial tumors have been reported to arise from cutaneous or soft tissues[2-5]. However, myoepithelial tumors of visceral organs are especially rare; very few case reports of such tumors have been published with most (8 of 11) describing tumors of pulmonary origin[6-10]. The present report describes a second case of a myoepithelial tumor of the stomach and the immunohistochemical, ultrastructural, and molecular findings for this tumor.

CASE REPORT

A 61-year-old female with a history of hypertension and grade A gastroesophageal reflux disease presented to our hospital with abdominal pain of one year duration. The abdominal pain was intermittent but gradually increased in intensity. The peak of her discomfort was usually observed 30-60 min after a meal. She denied nausea, vomiting, hematemesis, hematochezia, constipation, diarrhea, or weight loss. She also denied a family history of cancer or hereditary diseases. Panendoscopy revealed a 1.1 cm submucosal lesion at the posterior wall of the gastric high body (Figure 1A). Biopsy was performed, and the pathology report was positive for a malignant tumor. Computed tomography revealed a localized lesion without regional lymph node enlargement or distant metastasis (Figure 1B). Local excision was performed. Grossly, the mucosa overlying the lesion appeared ulcerated. Upon excision, the submucosal lesion appeared well-circumscribed, grayish-white, and elastic. The size of the tumor was 1.3 cm × 1.1 cm × 0.7 cm (Figure 1C and D).

Microscopically, the tumor was seen to be delineated by a fibrous capsule, and occasional lymphocytic cuffing was present (Figure 2A). Some satellite nodules were seen adjacent to the main tumor. A biphasic pattern of cells composed of epithelioid and oval to spindle cells embedded in myxoid to fibrous stroma was observed (Figure 2B). The tumor cells displayed pleomorphism, mitosis (1-2/10 HPFs), and visible nucleoli (Figure 2D). The epithelioid cells tended to form sheets, cords, or glandular structures whereas the spindle cells were aligned in a parallel fashion. The tumor cells penetrated the fibrous capsule focally (Figure 2C) and invaded the mucosa (Figure 2B). The deep margin was close (< 1 mm) but not involved with the tumor. No necrosis, neural invasion, or lymphovascular permeation was found. Immunohistochemically, the tumor cells were diffusely positive for vimentin (Dako, 1:200) and S-100 protein (Dako, 1:400) and were focally positive for cytokeratin (Genemed, 1:200), AE1/AE3 (Dako, 1:200), epithelial membrane antigen (Leica, 1:100), synaptophysin (Leica, 1:100), DOG1 (Leica, 1:100), CD10 (spotty; Novocastra, 1:50) and melan-A (weak; Leica, 1:50) but were negative for CD117 (Genemed, 1:300), HMB-45 (Leica, 1:100), calretinin (Leica, 1:100), CD34 (Leica, 1:100), glial fibrillary acidic protein (GFAP) (Dako, 1:100), CD56 (Leica, 1:50), desmin (Dako, 1:100), or actin-M851 (Leica, 1:100) (Figure 3). The tumor cells were positive for p53 (30%; Dako, 1:200) and Ki-67 (5%; Genemed, 1:300) (Figure 3A-C). Ultrastructurally, the tumor cells appeared epithelioid- to spindle-shaped, with irregular nuclei and abundant cytoplasm; the latter contained abundant rough endoplasmic reticulum, intermediate filaments, and small aggregates of dense bodies. Some cell junctions were also present (Figure 3D). For detection of *EWSR1* gene rearrangement, the break-apart FISH (fluorescence *in situ* hybridization) assay was performed on formalin-fixed, paraffin-embedded tissue sections of 4-μm thickness according to the instructions of the manufacturer. No break-apart signals were detected (Figure 3E). The final diagnosis was low-grade myoepithelial carcinoma based on the presence of mild pleomorphism, considerable mitotic activity, and the invasive nature of the borders.

No adjuvant chemotherapy was administered. The patient was alive without disease after 10 mo of follow-up.

DISCUSSION

This report describes a rare case of a low-grade myoepithelial carcinoma of the stomach. Only one other comparable case, describing a "parachordoma of the gastric serosa", has been reported in the literature (Table 1). The differential diagnosis of a myoepithelial tumor is challenging and dependent on the location of the tumor. Differential diagnoses of gastric biphasic tumors include carcinosarcoma, synovial sarcoma, gastrointestinal stromal tumor, mesothelioma, subtypes of neurogenic tumor (reticular schwannoma or epithelioid malignant peripheral nerve sheath tumor), and gastroblastoma. Rendering a diagnosis of carcinosarcoma requires identification of marked pleomorphism of both the carcinoma and the sarcoma components. Although synovial sarcomas are generally positive for cytokeratin and occasionally positive for S100 protein, the most sensitive marker for these sarcomas is TLE1[11,12]. Neither CD117 nor DOG-1 expression supports a diagnosis of gastrointestinal stromal tumor. The absence of calretinin expression by a tumor disfavors a mesothelial origin. Although lymphocytic cuffing was observed for the tumor described in the present report, the absence of Antoni structures and of cytokeratin expression disfavors a diagnosis of schwannoma. The cytological features of the tumor exclude a diagnosis of epithelioid malignant peripheral nerve sheath tumor. Gastroblastoma, a recently identified entity described in only five reports

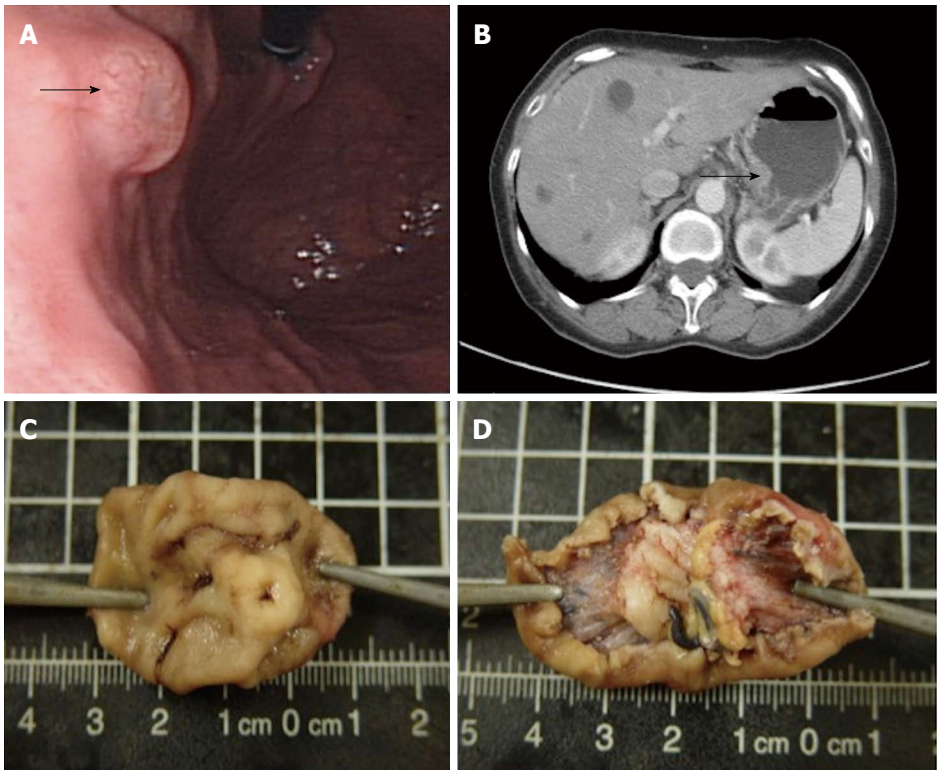

Figure 1 Endoscopy reveals a polypoid mass (arrow) (A); an isolated mural lesion was seen in computed tomography scan (arrow) (B); and grossly, a polypoid submucosal tumor is noted (C, D).

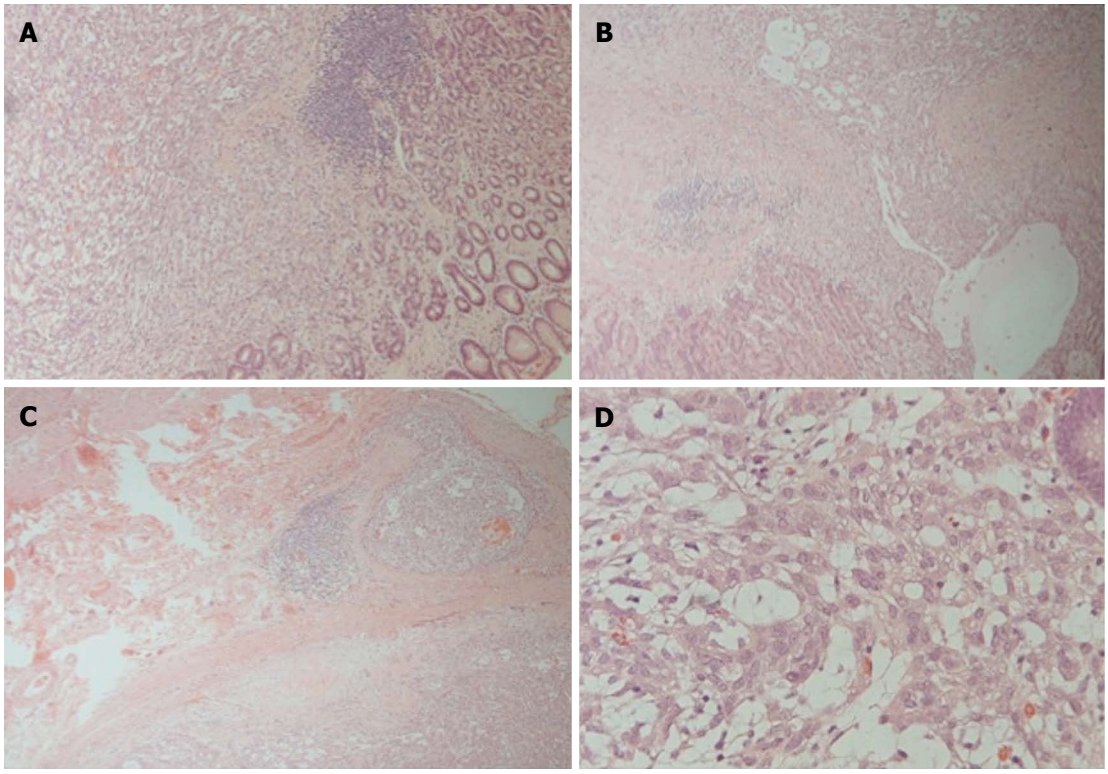

Figure 2 A submucosal biphasic tumor with lymphoid cuffing noted (Magnification × 40) (A); the tumor involves mucosa (Magnification × 100) (B); some infiltrative nests penetrate through the fibrous capsule (Magnification × 40) (C); and the epitheloid cells bearing low-grade pleomorphism and visible nucleoli are arranged in reticular pattern (Magnification × 400) (D).

to date, is also a biphasic tumor of the stomach[13-15]. Certain features of a gastroblastoma overlap with those of a myoepithelial neoplasm, such as a variable mixture of epithelial and mesenchymal components, a bland-

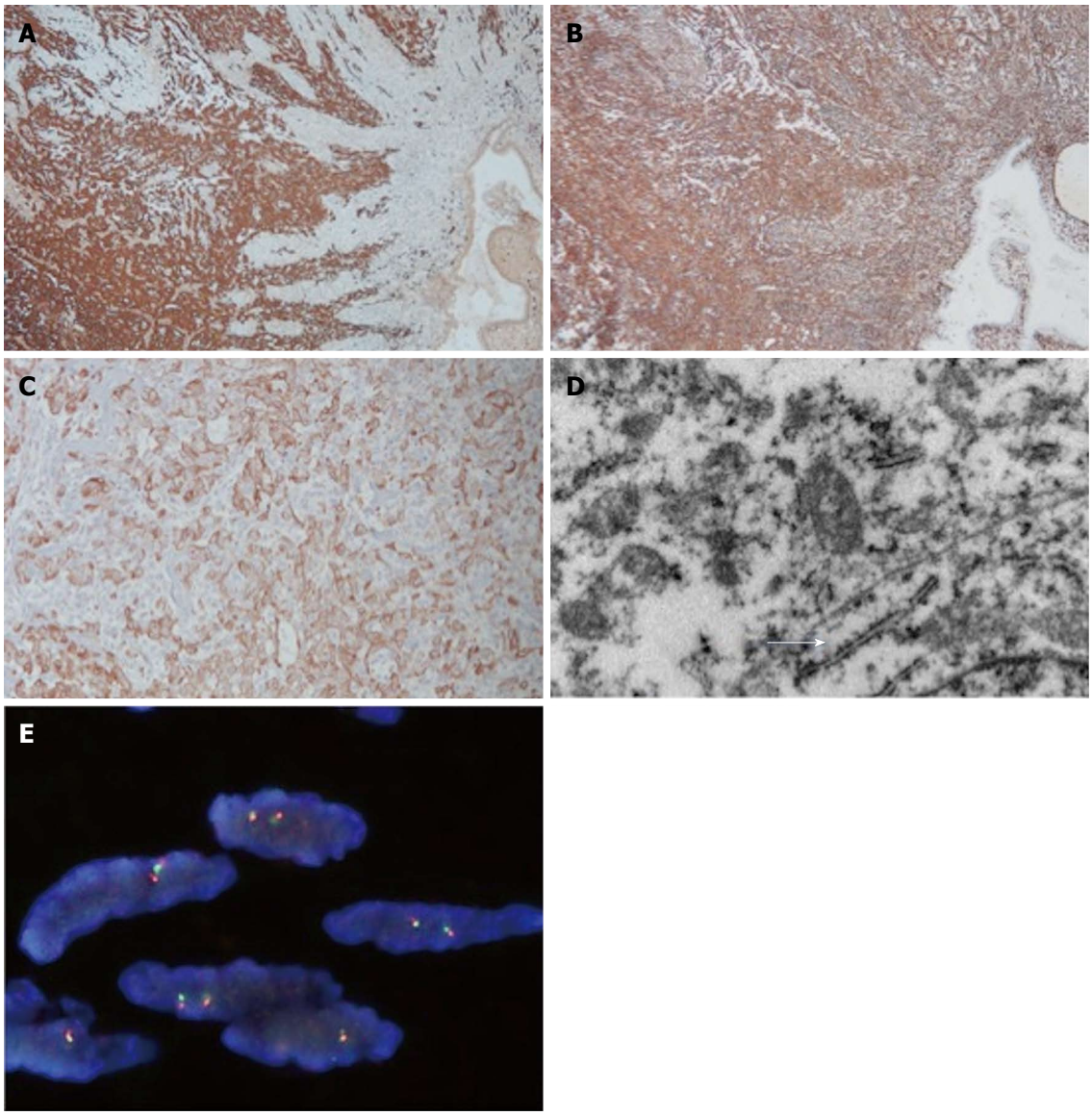

Figure 3 The tumor cells are diffusely positive for S-100 protein (Magnification × 40) (A); Vimentin is expressed by both components (Magnification × 40) (B); the tumor cells express AE1/AE3 (Magnification × 200) (C); and presence of cell junctions (arrow) indicates the epithelial differentiation (D); No break-apart signals observed by FISH (E).

appearing cytology, and a multinodular growth pattern with a potentially malignant behavior. Additionally, gastroblastomas and myoepithelial neoplasms share certain immunohistochemical and ultrastructural features including positivity for cytokeratins and vimentin and, indicative of epithelial differentiation, the presence of desmosomes and microvilli[14]. The epithelial components of gastroblastomas express cytokeratin and the mesenchymal components of these tumors express vimentin; however, the tumor described in the present case was diffusely positive for vimentin expression. Furthermore, the most striking difference between gastroblastomas and myoepithelial neoplasms is that gastroblastomas do not express myoepithelial markers including S100 protein, p63, calponin, GFAP, or smooth muscle actin. The only exception to the above is the expression of smooth muscle actin and desmin by an epitheliomesenchymal biphasic tumor/duodeno blastoma[16]. In the limited number of publications describing gastroblastomas, positivity for CD10 and CD56 of unknown significance was reported; in contrast, the tumor described in the present case was negative for CD56 expression and positivity for CD10 was spotty. Interestingly, the duodenoblastoma described by Poizat *et al*[16] was found to be negative for both markers. Forty-five percent of soft tissue myoepithelioma and myoepithelial carcinomas, including four pulmonary tumors, in a series were found to display *EWSR1* rearrangement[10]. Translocation of the gene with such known fusion partners as PBX1, ZNF444, and POU5F1 has been previously observed[10,17,18]. It was therefore considered important to examine the possibility that the tumor described in the present report exhibited *EWSR1* rearrangement; however, no "break-apart" signal was observed. Lack of *EWSR1* rearrangement was also reported for the gastric parachordoma described by

Table 1 Findings for currently described gastric myoepithelial tumors

Patient	Age (yr)	Gender	Tumor size (cm)	Diagnosis	Follow-up finding (mo)	Immunohistochemical findings
Spivach *et al*[8], 2007	65	Female	5.5	Parachordoma	NED1, 36	CK+2, EMA+, S100+, VIM+, BU-, CD117-, CD10-, GFAP-, calponin-, calretinin-, P63
The present case	61	Female	1.3	Low graders myoepithelial carcinoma	NED, 10	AE1/AE3+, CK+, EMA+, S100+, VIM+, synaptophysin+, DOG1-, desmin-, actin M851-, HMB-45-, melan-A(weak), CD117-, CD10(spotty), GFAP-, calretinin-, CD56

+: Positive finding; -: Negative finding. NED: No evidence of disease; CK: Cytokeratin; EMA: Epithelial membrane antigen; VIM: Vimentin; GFAP: Glial fibrillary acidic protein.

Spivach *et al*[8]. The recurrent cytogenetic changes present in gastric myoepithelial tumors remain to be characterized.

Discrimination between benign myoepithelioma and malignant myoepithelial carcinoma is essential. As compared with necrosis, mitotic index, and infiltrative pattern, the most reliable parameter for discrimination is cytological atypia[3]. The presence of non-negligible cytological pleomorphism and an infiltrative growth pattern, despite the small tumor size, prompted the diagnosis of low-grade myoepithelial carcinoma rather than myoepithelioma. Age of onset appears to influence prognosis for patients with myoepithelial carcinoma in that this cancer is more prevalent and aggressive in children[4]. Genetic events are proposed to account for the observation that *EWSR1* rearrangement, which is more common in children and young adults with these tumors, portends more aggressive tumor behavior[10]. These findings support the detection of *EWSR1* rearrangement in the diagnosis of these tumors and as an assessment of prognosis for patients with these tumors.

In conclusion, a case of a rare low-grade myoepithelial carcinoma is reported and the morphological, immunohistochemical, ultrastructural, and molecular features of this tumor are described. The rarity, diverse morphologies, and variable immunoprofiles of visceral myoepithelial tumors are potential causes for diagnostic pitfalls. Multidisciplinary approaches are therefore required for precise diagnosis of these tumors. Myoepithelial tumor should be considered in the differential diagnosis of gastric biphasic tumors.

COMMENTS

Case characteristics

A 61-year-old female with a history of hypertension and gastroesophageal reflux disease presented with abdominal pain.

Clinical diagnosis

A 1.1 cm submucosal lesion noted at gastric high body revealed by panendoscope.

Differential diagnosis

Gastrointestinal stromal tumor or other gastric neoplasms.

Laboratory diagnosis

Routine metabolic panel and complete blood counts were within normal limits.

Imaging diagnosis

Computed tomography revealed a localized lesion without regional lymph node enlargement or distant metastasis

Pathological diagnosis

A biphasic tumor composed of epithelioid and spindle cells is noted. Both CK and S100 protein are positive. No *EWSR1* rearrangement is seen. The diagnosis is a low-grade myoepithelial carcinoma.

Treatment

The patient received local excision without adjuvant therapy.

Related reports

A case of gastric parachordoma, which is classified in the spectrum of myoepithelial tumor, has been reported.

Term explanation

Dual-color florescence *in situ* hybridization is performed to detect *EWSR1* rearrangement. Positive cases were defined as those having split red and green signals separated by a distance at least twice the signal diameter in at least 20 of 100 counted tumor cells.

Experiences and lessons

As for gastric tumors, myoepithelial tumor is not listed in the differential diagnoses due to lack of reports in the literature. The authors exclude other possible mimickers cautiously and render the diagnosis of low grade myoepithelial carcinoma.

Peer-review

This case report illustrates a rare low-grade myoepithelial carcinoma of stomach and its morphological, immunohistochemical and molecular characteristics.

REFERENCES

1 **Fletcher C**, Bridge JA, Hogendoorn P, Mertens F. World Health Organization classification of tumours of soft tissue and bone. International Agency for Research on Cancer. 4th ed. Lyon: IARC Press, 2013

2 **Michal M**, Miettinen M. Myoepitheliomas of the skin and soft tissues. Report of 12 cases. *Virchows Arch* 1999; **434**: 393-400 [PMID: 10389622 DOI: 10.1007/s004280050358]

3 **Hornick JL**, Fletcher CD. Myoepithelial tumors of soft tissue: a clinicopathologic and immunohistochemical study of 101 cases with evaluation of prognostic parameters. *Am J Surg Pathol* 2003; **27**: 1183-1196 [PMID: 12960802 DOI: 10.1097/00000478-200309000-00001]

4 **Gleason BC**, Fletcher CD. Myoepithelial carcinoma of soft tissue in children: an aggressive neoplasm analyzed in a series of 29 cases. *Am J Surg Pathol* 2007; **31**: 1813-1824 [PMID: 18043035 DOI: 10.1097/PAS.0b013e31805f6775]

5 **Kilpatrick SE**, Hitchcock MG, Kraus MD, Calonje E, Fletcher CD. Mixed tumors and myoepitheliomas of soft tissue: a clinicopathologic study of 19 cases with a unifying concept. *Am J Surg Pathol* 1997; **21**: 13-22 [PMID: 8990137 DOI: 10.1097/00000478-199701000-00002]

6 **Higashiyama M**, Kodama K, Yokouchi H, Takami K, Kabuto T, Tsuji N, Mano M, Ishiguro S, Ueda T, Yoshikawa H, Tatsuta M. Myoepithelioma of the lung: report of two cases and review of the literature. *Lung Cancer* 1998; **20**: 47-56 [PMID: 9699187 DOI: 10.1016/S0169-5002(98)00006-3]

7 **Strickler JG**, Hegstrom J, Thomas MJ, Yousem SA. Myoepithelioma of the lung. *Arch Pathol Lab Med* 1987; **111**: 1082-1085 [PMID:

2821955]
8 **Spivach A**, Zanconati F, Tirabosco R, Falconieri G. Parachordoma of the gastric serosa: report of a myxoid mimicry in an unusual location. *Int J Surg Pathol* 2007; **15**: 307-310 [PMID: 17652546 DOI: 10.1177/1066896907302367]
9 **Gao HX**, Liu CX, Zou H, Chun CP, Cui X, Chen Y, Zhang W, Qi Y, Wang N, Liang W, Jiang J, Li F. Parachordoma/myoepithelioma of the kidney: first report of a myxoid mimicry in an unusual location. *Int J Clin Exp Pathol* 2014; **7**: 1258-1265 [PMID: 24696746]
10 **Antonescu CR**, Zhang L, Chang NE, Pawel BR, Travis W, Katabi N, Edelman M, Rosenberg AE, Nielsen GP, Dal Cin P, Fletcher CD. EWSR1-POU5F1 fusion in soft tissue myoepithelial tumors. A molecular analysis of sixty-six cases, including soft tissue, bone, and visceral lesions, showing common involvement of the EWSR1 gene. *Genes Chromosomes Cancer* 2010; **49**: 1114-1124 [PMID: 20815032 DOI: 10.1002/gcc.20819]
11 **Guillou L**, Wadden C, Kraus M, Deitos A, Fletcher C. S-100 protein reactivity in synovial sarcomas-A potentially frequent diagnostic pitfall-Immunohistochemical analysis of 100 cases. *Appl Immunohistochem* 1996; **4**: 167-175
12 **Terry J**, Saito T, Subramanian S, Ruttan C, Antonescu CR, Goldblum JR, Downs-Kelly E, Corless CL, Rubin BP, van de Rijn M, Ladanyi M, Nielsen TO. TLE1 as a diagnostic immunohistochemical marker for synovial sarcoma emerging from gene expression profiling studies. *Am J Surg Pathol* 2007; **31**: 240-246 [PMID: 17255769 DOI: 10.1097/01.pas.0000213330.71745.39]
13 **Miettinen M**, Dow N, Lasota J, Sobin LH. A distinctive novel epitheliomesenchymal biphasic tumor of the stomach in young adults ("gastroblastoma"): a series of 3 cases. *Am J Surg Pathol* 2009; **33**: 1370-1377 [PMID: 19718790 DOI: 10.1097/PAS.0b013e3181a6a792]
14 **Shin DH**, Lee JH, Kang HJ, Choi KU, Kim JY, Park do Y, Lee CH, Sol MY, Park JH, Kim HY, Montgomery E. Novel epitheliomesenchymal biphasic stomach tumour (gastroblastoma) in a 9-year-old: morphological, ultrastructural and immunohistochemical findings. *J Clin Pathol* 2010; **63**: 270-274 [PMID: 20203230 DOI: 10.1136/jcp.2009.074104]
15 **Wey EA**, Britton AJ, Sferra JJ, Kasunic T, Pepe LR, Appelman HD. Gastroblastoma in a 28-year-old man with nodal metastasis: proof of the malignant potential. *Arch Pathol Lab Med* 2012; **136**: 961-964 [PMID: 22849746 DOI: 10.5858/arpa.2011-0372-CR]
16 **Poizat F**, de Chaisemartin C, Bories E, Delpero JR, Xerri L, Flejou JF, Monges G. A distinctive epitheliomesenchymal biphasic tumor in the duodenum: the first case of duodenoblastoma? *Virchows Arch* 2012; **461**: 379-383 [PMID: 22961103 DOI: 10.1007/s00428-012-1307-y]
17 **Brandal P**, Panagopoulos I, Bjerkehagen B, Gorunova L, Skjeldal S, Micci F, Heim S. Detection of a t(1; 22)(q23; q12) translocation leading to an EWSR1-PBX1 fusion gene in a myoepithelioma. *Genes Chromosomes Cancer* 2008; **47**: 558-564 [PMID: 18383210 DOI: 10.1002/gcc.20559]
18 **Brandal P**, Panagopoulos I, Bjerkehagen B, Heim S. t(19; 22)(q13; q12) Translocation leading to the novel fusion gene EWSR1-ZNF444 in soft tissue myoepithelial carcinoma. *Genes Chromosomes Cancer* 2009; **48**: 1051-1056 [PMID: 19760602 DOI: 10.1002/gcc.20706]

P- Reviewer: Huerta-Franco MR **S- Editor**: Yu J **L- Editor**: A
E- Editor: Zhang DN

World Journal of Gastroenterology

Submit a Manuscript: http://www.wjgnet.com/esps/
Help Desk: http://www.wjgnet.com/esps/helpdesk.aspx
DOI: 10.3748/wjg.v21.i14.4397

World J Gastroenterol 2015 April 14; 21(14): 4397-4401
ISSN 1007-9327 (print) ISSN 2219-2840 (online)

CASE REPORT

Clostridium perfringens infection after transarterial chemoembolization for large hepatocellular carcinoma

Jing-Huan Li, Rong-Rong Yao, Hu-Jia Shen, Lan Zhang, Xiao-Ying Xie, Rong-Xin Chen, Yan-Hong Wang, Zheng-Gang Ren

Jing-Huan Li, Rong-Rong Yao, Hu-Jia Shen, Lan Zhang, Xiao-Ying Xie, Rong-Xin Chen, Yan-Hong Wang, Zheng-Gang Ren, Liver Cancer Institute, Zhongshan Hospital, Fudan University, Shanghai 200032, China

Author contributions: Li JH and Yao RR contributed equally to this work; Ren ZG designed the research; Li JH, Shen HJ, Yao RR, Zhang L, Xie XY, Chen RX and Wang YH collected the clinical data; Li JH and Yao RR wrote the paper.

Ethics approval: The study was reviewed and approved by the Ethnics Committee of Zhongshan Hospital, Fudan University.

Informed consent: All study participants, or their legal guardian, provided informed written consent prior to study enrollment.

Conflict-of-interest: Authors declares no conflicting interests.

Correspondence to: Zheng-Gang Ren, PhD, Professor of Medicine, Liver Cancer Institute, Zhongshan Hospital, Fudan University, No. 180 Fenglin Road, Shanghai 200032, China. renzhenggang@hotmail.com
Telephone: +86-13681971302

Received: September 17, 2014
Peer-review started: September 18, 2014
First decision: December 2, 2014
Revised: January 28, 2015
Accepted: March 19, 2015
Article in press: March 19, 2015
Published online: April 14, 2015

Abstract

We report an unusual case of *Clostridium perfringens* liver abscess formation after transcatheter arterial chemoembolization (TACE) for large hepatocellular carcinoma. Severe deterioration in liver and renal function accompanied with hemocytolysis was found on the 2nd day after TACE. Blood culture found *Clostridium perfringens* and abdominal computed tomography revealed a gas-containing abscess in the liver. Following antibiotics administration and support care, the infection was controlled and the liver and renal function turned normal. The 2nd TACE procedure was performed 1.5 mo later and no recurrent *Clostridium perfringens* infection was found.

Key words: Transcatheter arterial chemoembolization; Hepatocellular carcinoma; Major complication; *Clostridium perfringens*; Liver abscess

Core tip: Transcatheter arterial chemoembolization (TACE) is a major treatment for patients with hepatocellular carcinoma (HCC) that is not eligible for curative treatment. Though rare, *Clostridium perfringens* liver abscess after TACE is fatal. We successfully treated a 71-year-old man with large HCC who had liver and renal dysfunction and developed *Clostridium perfringens* liver abscess after TACE. After timely identification of the patient's deteriorating condition, aggressive treatments, including antibiotics administration, anticoagulation and intensive care, were provided.

Li JH, Yao RR, Shen HJ, Zhang L, Xie XY, Chen RX, Wang YH, Ren ZG. *Clostridium perfringens* infection after transarterial chemoembolization for large hepatocellular carcinoma. *World J Gastroenterol* 2015; 21(14): 4397-4401 Available from: URL: http://www.wjgnet.com/1007-9327/full/v21/i14/4397.htm DOI: http://dx.doi.org/10.3748/wjg.v21.i14.4397

INTRODUCTION

Hepatocellular carcinoma (HCC) is the fifth most common cancer worldwide and more than 50% of HCCs are treated with transcatheter arterial chemoembolization (TACE). Since the first case was reported in 1958, few cases of *Clostridium perfringens* liver abscess have been reported, among which only two cases were associated with TACE therapy[1]. Though rare, *Clostridium perfringens* liver abscess can be rapidly fatal. We report a case of a 71-year-old man with large HCC who had liver and renal dysfunction and developed *Clostridium perfringens* liver abscess after TACE.

CASE REPORT

A previously healthy 71-year-old man was admitted due to abdominal distension. He was diagnosed with HCC based on the HBV infection history, and magnetic resonance imaging (MRI) findings. Dynamic MRI revealed a lesion of 179 mm in diameter surrounded by multiple satellite nodes and presented typical arterial enhancement and venous phase washout (Figure 1A-C), and the patient had elevated level of serum α-fetoprotein (AFP) (38653 ng/mL)[2]. Neither ascites nor portal vein embolus was observed. According to the laboratory findings, the patient was clinically staged as BCLC B, Child-Pugh A and ECOG 1. He had no history of surgery or other diseases, such as diabetes mellitus. After evaluating the general condition of the patient, we performed TACE with hepatic infusion of 5-fluorouracil 1000 mg and Oxaliplatin 150 mg followed by a mixture of 5 mg mitomycin C and 10 mL lipoidol chemoembolization.

Laboratory results indicated liver and renal dysfunction on the 1st day after TACE, but symptoms were mild which were attributed to the post-embolization syndrome (Table 1). However, on the 2nd day, the patient presented with deterioration in liver and renal function, anemia and dysfunction of coagulation. Total bilirubin and direct bilirubin increased to 323 μmol/L and 209 μmol/L, respectively. He had high fever (39.4 ℃) accompanied with chill, and blood culture showed *Clostridium perfringens*. Then hematuria and hypotension occurred sequentially. Ultrasound and computed tomography (CT) both revealed a non-uniform abscess filled with gas but no liquid in the right lobe of the liver (Figure 1D-F).

Empirical piperacillin/tazobactam was used right after the blood sample was taken for culture, which was later combined with Levofloxacin when the bacterium was reported. Other treatments, including hydration, urinary alkalinisation and diuretics, were given at the same time. To tackle the dysfunction of coagulation and prevent disseminated intravascular coagulation, low molecular heparin and plasma transfusion were administrated.

Laboratory indexes turned normal in 2 or 3 d after intensive care, except D-dimer which peaked on the 11th day after TACE. The temperature was lowered to about 38 ℃ without chilling, while the blood culture yielded no more pathogenic bacterium 1 and 2 wk later, respectively. Mild ascites and pitting edema over both legs developed on the 6th day after TACE, which was relieved gradually in the following 10 d. Follow-up ultrasound demonstrated a significant reduction in both the size of the liver abscess and gas volume, although the gas-containing mass still existed. The patient was discharged on the 26th day after TACE in a generally good condition. CT scanning undertaken two weeks after the patient discharge showed that both the HCC lesion and gas-containing liver abscess became smaller (Figure 1G-I). However, serum AFP levels increased to 39868 ng/mL which was proximal to the initial level.

The patient received the 2nd TACE 1.5 mo after the 1st procedure. No infection was observed. Enhanced MRI on October 18, 2014 showed the gas-containing liver abscess was stable. However, tumor progress and lung metastasis were demonstrated (Figure 1J-L).

DISCUSSION

HCC is the fifth most common cancer and the second cause of cancer related deaths in men worldwide[3]. Though the surveillance of the disease is enhanced, only a small fraction of patients are eligible for curative treatment[4]. TACE, one of palliative treatments for HCC, has been shown to achieve partial responses in 15%-55% of patients, significantly delay tumor progression and vascular invasion, and prolong survival among HCC patients who are not candidates for curative treatment[5]. TACE is also the major treatment for unresectable HCC and is performed in 58% of patients with recurrence[4]. Even in elderly patients (≥ 75 years of age), this procedure was proved to be safe and effective, and was not associated with decreased survival or increased complication rate according to a recent prospective cohort study[6].

The reported rate of major complications associated with TACE procedure ranged from 2.68% to 12.5%[7,8]. Post-TACE liver abscess is one of these complications and sometimes life threatening. The incidence of liver abscess formation was low, ranging from 0.1% to 4.6%. However, high mortality rate from post-TACE liver abscess, ranging from 13.3% to 50%, has complicated the TACE management[9-11].

Generally, for patients receiving TACE treatment, abdominal surgery history may increase the risk of liver abscess formation. This patient had no history of abdominal surgery. Old age, large HCC, and the infusion of chemotherapeutic agents might lead to an immune suppression status which is vulnerable to infection. Under this condition, the pathogen *Clostridium perfringens*, an anaerobic bacillus which is naturally distributed in the alimentary tracts of humans, could superimpose upon the embolic and necrosis lesion after TACE.

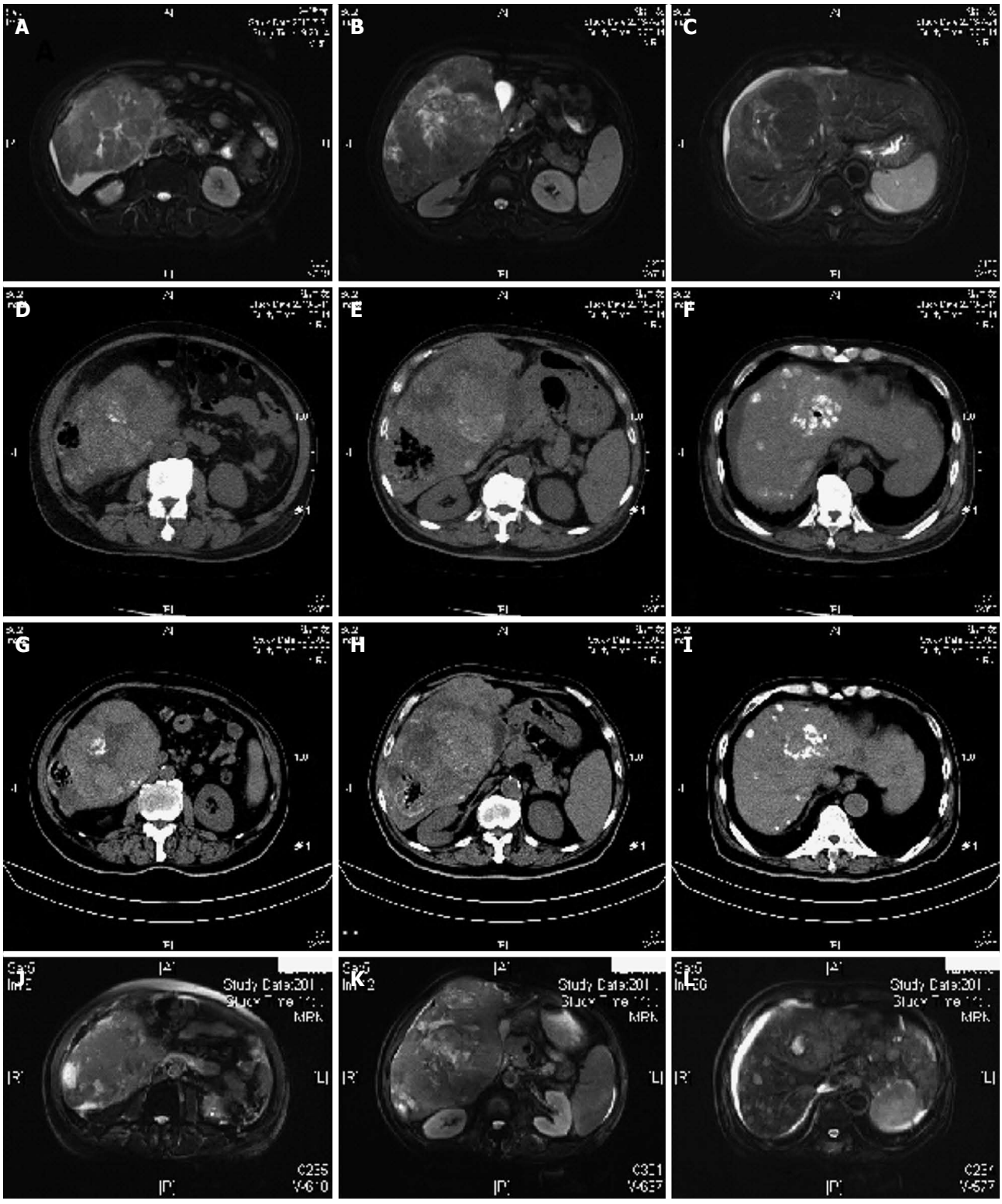

Figure 1 Magnetic resonance imaging and computed tomography findings. A-C: Magnetic resonance imaging (MRI) images before transcatheter arterial chemoembolization (TACE); D-F: Computed tomography (CT) images showing a gas-forming liver abscess when the first TACE was done; G-I: Five week after the first TACE procedure, CT image showed that the gas-forming liver abscess became smaller; J-L: Eleven week after the first TACE procedure, MRI showed no obvious liver abscess.

Though the incidence of *Clostridium perfringens* bacteremia is low (0.97/100000 in patients who were hospitalized[12] and 0.7/100000 in non-selected populations[13]), and the *Clostridium perfringens* liver abscess is even rare[14], and increasing age, poorly controlled diabetic mellitus, and presence of malignancies, especially gastrointestinal and genitourinary malignancies, could increase the risk for *Clostridium* septicemia development[14].

The patient presented typical clinical features

Table 1 Laboratory results in this patient

	Baseline	Days after TACE						Follow-up	
		1st	2nd	3rd	8th	13rd	21st	38th	
Date	27/7/2013	30/7/2013	1/8/2013	2/8/2013	6/8/2013	11/8/2013	19/8/2013	5/9/2013	11/10/2013
TB (μmol/L)	27.4	44.4		323	84.8	54.4	25	34.4	37.8
DB (μmol/L)	10.9	14.6		209	65.7	37.4	18.6	18.7	24.3
ALB (g/L)	31	35		27	27	29	30	32	31
ALT (U/L)	145	1652		2312	261	82	45	62	53
AST (U/L)	113	787		1953	120	73	68	75	87
UA	362	454		393	229	201	230		
BUN (mmol/L)	5.4	5.7		17.8	15	10.8	10.2	8.5	7.9
Cr (μmol/L)	81	75		152	153	123	119		109
Glucose(mmol/L)	4.7	9		9.6	9.9	8.7	5.2		
K+ (mmol/L)	4.7	4.1		3.8	3.4	3.4	3.9		
PT (s)	10.4	11.6		17	14.9	13.4	11.8		12.6
D-Dimer (mg/L)	2.39	2.13		4.46	8.72	8.68	4.58	3.56	
INR	0.91	1.02		1.48	1.31	1.17	1.03		1.1
RBC (10^{12}/L)	4.46	4.79	4.7	3.68	2.72	2.47	2.63	3.29	3.6
HEMO (g/L)	140	153	148	118	87	76	83	101	111
PLT (10^9/L)	201	154	120	128	81	158	192	264	294
WBC(10^9/L)	3.82	7.96	6.1	11.52	4.38	4.76	3.89	4.59	7.67
NEU%	64.2	90.1	84.4	92.7	85.6	82.4	68.1	69.9	84.5
CPR (mg/L)			65.9	128.9	89.6		56		
PCT (ng/mL)	0.35	0.39	1.72	51.61	13.39	2.52	0.95	0.697	
AFP (ng/mL)	36895	37104		24962	11129	10069	13310	38935	> 60500
Blood culture[1]			+			-			
Urine RBC[2]	-		+/-	+/-	-				
Urine-bilirubin			+	+	-				
Urinary-protein			+	+	+/-				

[1]Blood culture was positive on the 2nd day after TACE; [2]RBC detected in urine samples was non-uniform. TB: Total bilirubin; DB: Direct bilirubin; TACE: Transcatheter arterial chemoembolization; ALB: Albumin; ALT: Alanine transaminase; AST: Aspartate transaminase; UA: Uric acid; BUN: Usea nitrogen; Cr: Creatinine; K^+: Potassium ion; PT: Prothrombin time; INR: International normalized ratio; RBC: Red blood cell; HEMO: Hemoglobin; PLT: Platelet; WBC: White blood cell; NEU%: Neutrophils percentage; CPR: C reactive protein; PCT: Procalcitonin; AFP: Alpha-fetoprotein.

of *Clostridium perfringens* liver abscess with fever, abdominal pain, gas-containing lesion in imaging examinations, intravascular hemolysis (anemia, high Lactate dehydrogenase level, hyperbilirubinemia, and secondary renal injury) and positive blood culture. *Clostridium perfringens* with a short doubling time could produce a large amount of potent hemolysin, such as alpha-toxin, which could result in severe intravascular hemolysis[15]. A hospital-based study showed that intra-abdominal is the major source of *Clostridium perfringens* infection[12]. In the present case, the patient had chill and fever on the 2nd day after TACE. Thus, TACE was an important predisposing cause. Considering the operating room was routinely monitored with bacteria culture and re-checked after the patient was diagnosed with sepsis, and no other patient presented the same symptoms who received TACE simultaneously by the same physician group, it is likely an autogenous infection, although its specific origin was not clear.

The 30-d mortality of *Clostridium perfringens* infection is high, ranging from 26% to 100%[12,15]. Drainage combined with antibiotics is the basic treatment of liver abscess[16]. Law *et al*[13] reviewed 20 cases of *Clostridium perfringens* liver abscess between 1990 and 2011, and there were only 6 cases survived and 5 cases had the primary focus of infection removed.

But in the case we reported here, abscess excision or drainage is unavailable because of the risk of tumor rupture existing in the patient. We attribute our successful treatment to the timely identification of the patient's deteriorating condition, and aggressive treatments, including antibiotics administration, anticoagulation and intensive care. Given the presence of large tumor in this patient, hydration and urinary alkalinisation were administrated as soon as the TACE procedure was performed. Though his temperature was 39 ℃ on the 1st day after TACE, blood culture was sampled in the morning of the 2nd day when the patient had high fever along with chilling and obvious listlessness. At the same time, blood was tested; Piperacillin/tazobactam was used as prophylactic antibiotics. And Levofloxacin was added when the blood culture result was reported. Anticoagulation was administrated when the hematuria was first observed in the evening of the 2nd day (Table 1).

In conclusion, there are various risk factors in patients receiving TACE for *Clostridium perfringens* infection, such as old age, malignancy, and necrosis due to embolization. Timely identification of the liver and renal dysfunction and aggressive treatments

including both antibiotics administration and intensive care, are crucial in post-TACE management.

COMMENTS

Case characteristics

Mild symptoms were found on the first day after transcatheter arterial chemoembolization (TACE), whereas high fever, chill and abdominal pain were observed on the second day after TACE in a 71-year-old man with large hepatocellular carcinoma (HCC).

Clinical diagnosis

High fever, severe jaundice, hematuria, and hypotension were observed after TACE in the 71-year-old man with large HCC.

Differential diagnosis

Because of the non-specific symptoms, early diagnosis of *Clostridium perfringens* infection is difficulty, and its typical features included fever, abdominal pain, gas-containing lesion in imaging examinations, intravascular hemolysis and positive blood culture.

Laboratory diagnosis

Positive blood culture of *Clostridium perfringens* is confirmatory for diagnosis and other laboratory findings include anemia, dysfunction of liver and renal, disorder of coagulation and hematuria.

Imaging diagnosis

Ultrasound and computed tomography imaging both indicated a non-uniform abscess filled with gas but no liquid in the right lobe of the liver.

Pathological diagnosis

Blood culture revealed *Clostridium perfringens*.

Treatment

Upon identification of the patient's deteriorating condition, the patient was treated with antibiotics, anticoagulation and intensive care.

Related reports

"Two cases of liver abscess caused by *Clostridium perfringens* after transcatheter arterial chemoembolization" by Oshima *et al*.

Term explanation

TACE is an invasive procedure performed in interventional radiology to restrict a tumor's blood supply. Small embolic particles combined with chemotherapeutic agents are injected selectively into an artery directly supplying a tumor.

Experiences and lessons

The authors attribute their successful treatment in this patient to the timely identification of his deteriorating condition, and aggressive treatments, including antibiotics administration, anticoagulation and intensive care.

Peer-review

The authors reported an unusual case of *Clostridium perfringens* liver abscess formation after TACE for large HCC. They well reviewed the literature and discussed the results.

REFERENCES

1 **Oshima S**, Takaishi K, Tani N, Hirano M, Ikeda K, Makari Y, Hoshi M, Doi T, Kobori Y, Kurokawa E, Tamura S. [Two cases of liver abscess caused by Clostridium perfringens after transcatheter arterial chemoembolization]. *Gan To Kagaku Ryoho* 2013; **40**: 1795-1797 [PMID: 24393925]

2 **Maluccio M**, Covey A. Recent progress in understanding, diagnosing, and treating hepatocellular carcinoma. *CA Cancer J Clin* 2012; **62**: 394-399 [PMID: 23070690 DOI: 10.3322/caac.21161]

3 **Jemal A**, Bray F, Center MM, Ferlay J, Ward E, Forman D. Global cancer statistics. *CA Cancer J Clin* 2011; **61**: 69-90 [PMID: 21296855 DOI: 10.3322/caac.20107]

4 **Takayasu K**. Transcatheter arterial chemoembolization for unresectable hepatocellular carcinoma: recent progression and perspective. *Oncology* 2013; **84** Suppl 1: 28-33 [PMID: 23428855 DOI: 10.1159/000345886]

5 **Llovet JM**. Updated treatment approach to hepatocellular carcinoma. *J Gastroenterol* 2005; **40**: 225-235 [PMID: 15830281]

6 **Cohen MJ**, Bloom AI, Barak O, Klimov A, Nesher T, Shouval D, Levi I, Shibolet O. Trans-arterial chemo-embolization is safe and effective for very elderly patients with hepatocellular carcinoma. *World J Gastroenterol* 2013; **19**: 2521-2528 [PMID: 23674854 DOI: 10.3748/wjg.v19.i16.2521]

7 **Jang ES**, Yoon JH, Chung JW, Cho EJ, Yu SJ, Lee JH, Kim YJ, Lee HS, Kim CY. Survival of infiltrative hepatocellular carcinoma patients with preserved hepatic function after treatment with transarterial chemoembolization. *J Cancer Res Clin Oncol* 2013; **139**: 635-643 [PMID: 23283527 DOI: 10.1007/s00432-012-1364-2]

8 **Xia J**, Ren Z, Ye S, Sharma D, Lin Z, Gan Y, Chen Y, Ge N, Ma Z, Wu Z, Fan J, Qin L, Zhou X, Tang Z, Yang B. Study of severe and rare complications of transarterial chemoembolization (TACE) for liver cancer. *Eur J Radiol* 2006; **59**: 407-412 [PMID: 16621394]

9 **Woo S**, Chung JW, Hur S, Joo SM, Kim HC, Jae HJ, Park JH. Liver abscess after transarterial chemoembolization in patients with bilioenteric anastomosis: frequency and risk factors. *AJR Am J Roentgenol* 2013; **200**: 1370-1377 [PMID: 23701078 DOI: 10.2214/AJR.12.9630]

10 **Meyer T**, Kirkwood A, Roughton M, Beare S, Tsochatzis E, Yu D, Davies N, Williams E, Pereira SP, Hochhauser D, Mayer A, Gillmore R, O'Beirne J, Patch D, Burroughs AK. A randomised phase II/III trial of 3-weekly cisplatin-based sequential transarterial chemoembolisation vs embolisation alone for hepatocellular carcinoma. *Br J Cancer* 2013; **108**: 1252-1259 [PMID: 23449352 DOI: 10.1038/bjc.2013.85]

11 **Pua U**, Merkle EM. Case report. Spontaneous cholecystocolic fistula and locoregional liver tumour ablation: a cautionary tale. *Br J Radiol* 2011; **84**: e243-e245 [PMID: 22101592 DOI: 10.1259/bjr/13919678]

12 **Yang CC**, Hsu PC, Chang HJ, Cheng CW, Lee MH. Clinical significance and outcomes of Clostridium perfringens bacteremia--a 10-year experience at a tertiary care hospital. *Int J Infect Dis* 2013; **17**: e955-e960 [PMID: 23578849 DOI: 10.1016/j.ijid.2013.03.001]

13 **Ngo JT**, Parkins MD, Gregson DB, Pitout JD, Ross T, Church DL, Laupland KB. Population-based assessment of the incidence, risk factors, and outcomes of anaerobic bloodstream infections. *Infection* 2013; **41**: 41-48 [PMID: 23292663 DOI: 10.1007/s15010-012-0389-4]

14 **Law ST**, Lee MK. A middle-aged lady with a pyogenic liver abscess caused by Clostridium perfringens. *World J Hepatol* 2012; **4**: 252-255 [PMID: 22993668]

15 **Pita Zapata E**, Sarmiento Penide A, Bautista Guillén A, González Cabano M, Agulla Budiño JA, Camba Rodríguez MA. [Massive intravascular hemolysis secondary to sepsis due to Clostridium perfringens]. *Rev Esp Anestesiol Reanim* 2010; **57**: 314-316 [PMID: 20527348]

16 **Lai KC**, Cheng KS, Jeng LB, Huang CC, Lee YT, Chang HR, Chen CC, Chen SC, Lee MC. Factors associated with treatment failure of percutaneous catheter drainage for pyogenic liver abscess in patients with hepatobiliary-pancreatic cancer. *Am J Surg* 2013; **205**: 52-57 [PMID: 22794706 DOI: 10.1016/j.amjsurg.2012.03.006]

P- Reviewer: Zhu X **S- Editor**: Yu J
L- Editor: A **E- Editor**: Liu XM

World Journal of Gastroenterology

Submit a Manuscript: http://www.wjgnet.com/esps/
Help Desk: http://www.wjgnet.com/esps/helpdesk.aspx
DOI: 10.3748/wjg.v21.i14.4402

World J Gastroenterol 2015 April 14; 21(14): 4402-4407
ISSN 1007-9327 (print) ISSN 2219-2840 (online)

CASE REPORT

Secondary acute promyelocytic leukemia following chemotherapy for gastric cancer: A case report

Ying-Cheng Zhang, Yu-Qi Zhou, Bing Yan, Jun Shi, Li-Juan Xiu, Yu-Wei Sun, Xuan Liu, Zhi-Feng Qin, Pin-Kang Wei, Yong-Jin Li

Ying-Cheng Zhang, Yu-Qi Zhou, Bing Yan, Jun Shi, Li-Juan Xiu, Yu-Wei Sun, Xuan Liu, Zhi-Feng Qin, Pin-Kang Wei, Yong-Jin Li, Department of Traditional Chinese Medicine, Changzheng Hospital, Second Military Medical University, Shanghai 200003, China

Bing Yan, Department of Oncology, Hainan branch of PLA General Hospital, Sanya 572013, Hainan Province, China

Author contributions: Zhang YC, Zhou YQ and Yan B contributed equally to this work; Zhang YC, Zhou YQ, Yan B, Shi J, Sun YW, Qin ZF and Wei PK contributed to research design; Zhang YC, Yan B and Li YJ analyzed data; Zhou YQ, Xiu LJ and Liu X conducted paper revisions; and Zhang YC, Zhou YQ, Yan B and Li YJ wrote the paper.

Supported by National Natural Science Foundation of China, No. 81173403.

Ethics approval: The study was reviewed and approved by the Institutional Review Board of the Changzheng Hospital, Second Military Medical University.

Informed consent: Informed written consent was obtained from the study participant.

Conflict-of-interest: The authors have no conflicts of interest to declare.

Correspondence to: Yong-Jin Li, PhD, Department of Traditional Chinese Medicine, Changzheng Hospital of the Second Military Medical University, No. 415 Fengyang Road, Huangpu District, Shanghai 200003, China. yongjingli888@163.com
Telephone: +86-21-81885476
Fax: +86-21-63520020

Received: October 30, 2014
Peer-review started: October 31, 2014
First decision: November 14, 2014
Revised: November 29, 2014
Accepted: January 16, 2015
Article in press: January 16, 2015

Published online: April 14, 2015

Abstract

Therapy-related acute myeloid leukemia (t-AML) refers to a heterogeneous group of myeloid neoplasms that develop in patients following extensive exposure to either cytotoxic agents or radiation. The development of t-AML has been reported following treatment of cancers ranging from hematological malignancies to solid tumors; however, to our knowledge, t-AML has never been reported following treatment of gastric cancer. In this study, we report the development of t-acute promyelocytic leukemia in a cT4N1M0 gastric cancer patient after an approximate 44 mo latency period following treatment with 4 cycles of oxaliplatin (OXP) (85 mg/m^2 on day 1) plus capecitabine (1250 mg/m^2 orally twice daily on days 1-14) in combination with recombinant human granulocyte-colony stimulating factor treatment. Karyotype analysis of the patient revealed 46,XY,t(15;17)(q22;q21)[15]/46,idem,-9,+add(9)(p22)[2]/46,XY[3], which, according to previous studies, includes some "favorable" genetic abnormalities. The patient was then treated with all-trans retinoic acid (ATRA, 25 mg/m^2/d) plus arsenic trioxide (ATO, 10 mg/d) and attained complete remission. Our case illuminated the role of certain cytotoxic agents in the induction of t-AML following gastric cancer treatment. We recommend instituting a mandatory additional evaluation for patients undergoing these therapies in the future.

Key words: Gastric cancer; Acute promyelocytic leukemia; Oxaliplatin; Capecitabine; Chemotherapy

Core tip: In the current study, t-acute promyelocytic leukemia (t-APL) was likely induced by treatment with

oxaliplatin, capecitabine and recombinant human granulocyte-colony stimulating factor. The gastric cancer patient, classified as clinical stage cT4N1M0, had a rare karyotype: 46,XY,t(15;17)(q22;q21)[15]/46,idem,-9,+add(9)(p22)[2]/46,XY[3]. This case demonstrates that certain cytotoxic agents can induce t-APL in gastric cancer. We recommend mandatory additional evaluation for patients undergoing this treatment regimen.

Zhang YC, Zhou YQ, Yan B, Shi J, Xiu LJ, Sun YW, Liu X, Qin ZF, Wei PK, Li YJ. Secondary acute promyelocytic leukemia following chemotherapy for gastric cancer: A case report. *World J Gastroenterol* 2015; 21(14): 4402-4407 Available from: URL: http://www.wjgnet.com/1007-9327/full/v21/i14/4402.htm DOI: http://dx.doi.org/10.3748/wjg.v21.i14.4402

INTRODUCTION

Therapy-related acute myeloid leukemia (t-AML) refers to a heterogeneous group of myeloid neoplasms that develop in patients following extensive exposure to either cytotoxic agents or radiation[1]. In the past few decades, survival rates for cancer patients have improved, resulting in an increased risk of t-AML[2]. However, it is worth noting that while t-AML shares common phenotypic features with *de novo* AML, t-AML is relatively resistant to conventional therapies for leukemia. Additionally, t-AML has an overall poor prognosis with a median life expectancy of 8-10 mo following diagnosis[3].

While the underlying cause of t-AML remains to be elucidated, the development of t-AML has been confirmed to correlate with certain cytotoxic drugs. According to previous reports, alkylating agents (busulfan, carboplatin), topoisomerase-2 inhibitors (doxorubicin, mitoxantrone), antimetabolites (5-fluorouracil, fludarabine), antimicrotubule agents (docetaxel, paclitaxel) and growth factors (granulocyte-macrophage colony-stimulating factor; G-CSF) associate with the development of t-AML, although often with a varying latency period[4-6]. Interestingly, the chemical structure and dosage of these agents greatly affect the t-AML profile. For example, treatment with an alkylating agent usually results in a common subtype of t-AML, which is observed in approximately 75% of patients after 5-7 years of exposure. This subtype is often characterized by the loss of all or part of chromosomes 5 or 7[7]. Contrastingly, treatment with topoisomerase Ⅱ inhibitors often result in gene rearrangements involving 21q22 with a latency ranging from 1-3 years[7].

Recently, a relatively distinct subgroup of t-AML was reported as "good" leukemia. This "good" leukemia refers to acute promyelocytic leukemia (APL) characterized with inv(16)/t(15;17) or more rarely t(8;21)[8]. To our knowledge, t-acute promyelocytic leukemia (t-APL) has yet to be reported following treatment of gastric cancer.

CASE REPORT

A 68-year-old man, diagnosed with gastric cardia cancer, was referred to Shanghai Changzheng Hospital (Shanghai, China) in March 2007 (Figure 1A, B). Post-operative analysis confirmed a poorly differentiated adenocarcinoma with penetrating invasion of the gastric wall. One out of the 29 regional lymph nodes was positive for cancer cell infiltration (Figure 1C, D). According to the TNM/UICC staging system, the patient classified as cT4N1M0 (ⅢC). The patient then underwent 4 cycles of chemotherapy with oxaliplatin (OXP) (85 mg/m^2 on day 1) and capecitabine (1250 mg/m^2 orally twice daily on days 1-14) until August 2007. Treatment ended when the patient developed violent emesis. In the subsequent visit, the patient had recovered well, with no additional complications. On April 15, 2011, the patient suddenly presented fatigue and high fever (39.2 ℃). A blood examination indicated pancytopenia. The patient was treated with recombinant human granulocyte-colony stimulating factor (rHu-G-CSF), followed by a bone marrow biopsy. Peripheral smear analysis revealed an abnormal increase in the amount of myeloblasts and promyelocytes (91.5%), with leukemic hiatus (Figure 2A, B). Chromosome-based analysis revealed structural rearrangements involving chromosomes 9, 15 and 17. The patient's karyotype was 46,XY,t(15;17)(q22;q21)[15]/46, idem,-9,+add(9)(p22)[2]/46,XY[3]. Additionally, the Bcr1 subtype of the promyelocytic leukemia/retinoic acid receptor-alpha (PML/RARα) fusion gene was positive, whereas the Bcr2 and Bcr3 subtypes of the PML/RARα fusion were negative (Figure 3). According to WHO-based classification, these results verified the diagnosis as t-AML (M3a, which is also referred as t-APL). Routine blood examination indicated the following: red blood cells at 2.35 × 10^{12}/L, white blood cells at 1.8 × 10^9/L, absolute neutrophil count at 0.67 × 10^9/L, hemoglobin at 75 g/L, and platelets at 81 g/L. The patient then underwent induction therapy with all-trans retinoic acid (ATRA, 25 mg/m^2 per day) plus arsenic trioxide (ATO, 10 mg/d). Other supportive therapies were provided when necessary; these therapies included platelet and fresh frozen plasma transfusions as well as antibiotic administration. The patient presented complete remission (CR) in June 2011, and thus far, no other complications have been recorded.

DISCUSSION

As a relatively distinct subgroup of t-AML, t-APL is usually characterized with excellent prognosis. Regarding t-APL development, epirubicin and mitoxantron represent the most commonly implicated cytotoxic drugs[9]. In the current study, we investigate

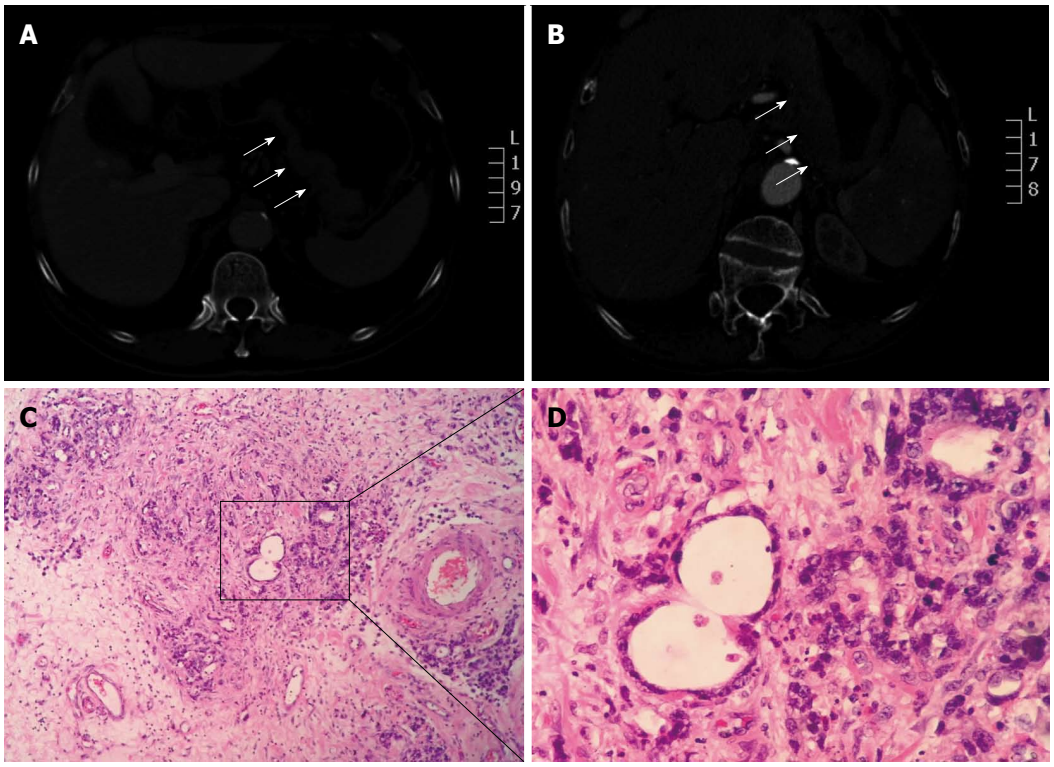

Figure 1 Upper abdomen computed tomography scan. A: Plain computed tomography (CT) indicated a localized, irregularly-shaped mass in the stomach; however, no obvious lymph node metastasis was observed; B: Contrast-enhanced CT scan revealed inhomogeneous enhancement of the gastric wall lesion; C, D. Biopsy results pathologically confirmed the diagnosis of a poorly differentiated adenocarcinoma. Microscopic examination revealed obvious atypical nuclei and large, bizarre, multinucleated cell mitosis. Generally, the normal structure of gastric gland was lost. (Hematoxylin and eosin staining, C: Magnification × 100; D: Magnification × 400).

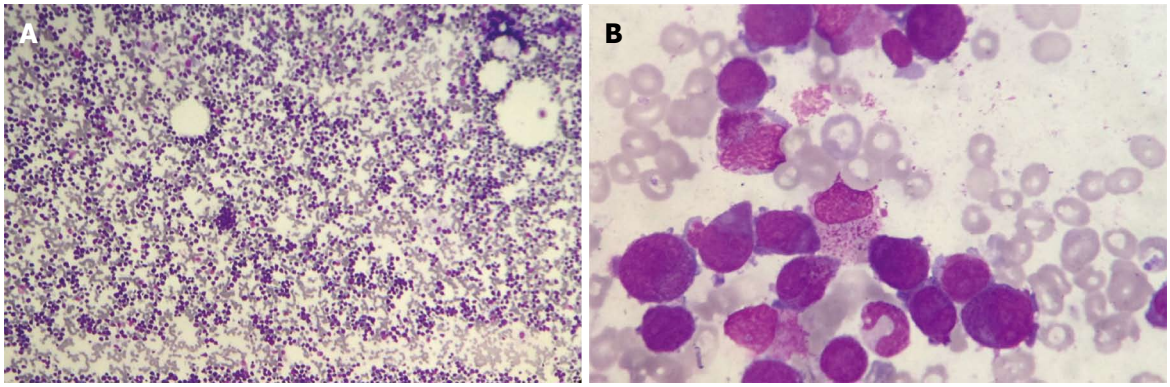

Figure 2 Peripheral blood smear, bone marrow biopsy and immunohistochemistry results revealed that the total number of primitive cells plus immature leukemia cells account up to 91.5% (2% + 89.5%) of the total cell population. Leukemic hiatus was detected, which supports the diagnosis of acute myeloid leukemia (M3a, APL). (Hematoxylin and eosin staining, A: Magnification × 10; B: Magnification × 400).

the occurrence of t-APL in gastric cancer, which was likely induced by OXP and capecitabine treatment. The patient was finally cured with a treatment regimen of ATRA plus ATO. To our knowledge, this study represents the first report of t-APL diagnosed following treatment of gastric cancer (Table 1).

While the underlying cause of t-AML remains to be fully elucidated, we have established the importance of DNA damage, which includes methylation and intra- and inter-strand DNA cross links[10]. Platinum-based agents kill cancer cells through the formation of DNA adducts; these adducts lead to the formation of intra- and inter-strand DNA cross links that ultimately disrupt the processes of DNA replication and transcription[11]. Previous studies have reported an association of cisplatin and carboplatin treatment with the onset of therapy-related leukemia (TRL); however, the role of OXP in TRL was overlooked. As shown in Table 1, t-AML was diagnosed in 3 of the 6 reports regarding OXP-related TRL. Furthermore, only 1 report of OXP-related TRL was confirmed as t-APL[12-17]. In Merrouche *et al*[12], a female patient was treated with LVFU2,

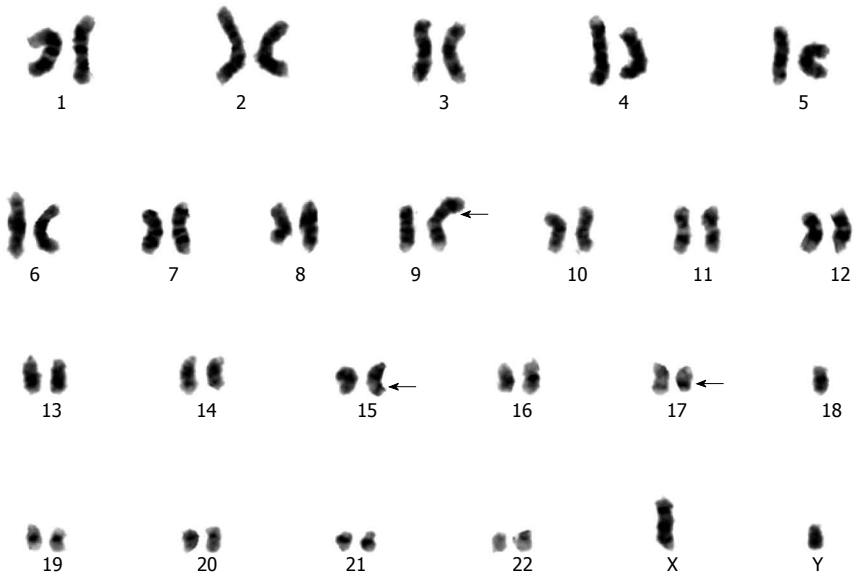

Figure 3 Chromosomal analysis *via* karyotype revealed 46 chromosomes with abnormities present in chromosomes 9, 15, and 17. Unbalanced translocation occurred in chromosomes 15 and 17. 46,XY,t (15;17)(q22;q21)[15]/46,idem,-9,+add(9)(p?22)[2]/46,XY[3].

Table 1 Reports of therapy-related leukemia development following oxaliplatin and/or capecitabine-containing chemotherapy

Ref.	Patient, age (yr)/gender	Primary cancer	Chemotherapy regimen	TRLs	Karyotype
Merrouche *et al*[12]	65/female	Colon	LVFU2, Irinotecan, OXP	APL	46,XX,add(6)(p23),-13,add(14)(p11),-16,add(17)(q?),-21,+3 mar
Carneiro *et al*[13]	56/female	Cecum	FOLFOX-4, FOLFOX-6	AML	Partial deletions of chromosomes 5, 7, 20, and 21, as well as trisomy 8 and loss of chromosomes 3 and 1
Merlin *et al*[14]	65/female	Colorectal	FOLFOX-4	ALL	Not available
Damodaran *et al*[15]	63/male	Esophagus	Capecitabine, OXP	AML	47,X,der(Y)t(Y;3)(q12;q21),+8(21)
Buxhofer-Ausch *et al*[16]	56/male	Colon	Capecitabine, 5-FU, Irinotecan, OXP	CML	Positive for Philadelphia chromosome
Kadikoylu *et al*[17]	66/male	Rectum	Cetuximab, OXP, Irinotecan, Capecitabine	CML	Positive for Philadelphia chromosome
Shapiro *et al*[18]	63/female	Cecum	Capecitabine	MLL	t(6;11) with breakpoint 11q23
Tansley *et al*[19]	66/male	Colon	Capecitabine	AML	Not available
Rashidi *et al*[20]	58/male	Rectum	Capecitabine, Radiation	APL	46,XY, t(15;17)(q24;q21)

APL: Acute promyelocytic leukemia; AML: Acute myeloid leukemia; ALL: Acute lymphoblastic leukemia; CML: Chronic myeloid leukemia; MLL: Chronic lymphoblastic leukemia; FOLFOX: Oxaliplatin plus 5-fluorouracil (5-FU); LVFU2: Leucovorin plus 5-FU; TRLs: Therapy-related leukemias.

irinotecan and OXP 12 mo prior to t-APL diagnosis. The karyotype examination indicated (46,XX,add(6)(p23),-13,add(14)(p11),-16,add(17)(q?),-21,+3mar), which differed from the commonly reported t(15;17)(q22;q21) translocation[12]. Furthermore, Carneiro *et al*[13] reported a study of a female patient, first treated by FOLFOX-4 (OXP plus 5-fluorouracil [5-FU]) followed by FOLFOX-6 plus bevacizumab. Importantly, 28 mo prior to t-AML development, her karyotype revealed trisomy 8, loss of chromosomes 3 and 11, as well as partial deletions in chromosomes 5, 7, 20 and 21[13]. In Damodaran *et al*[15], a male patient with esophageal cancer received OXP plus capecitabine, with additional radiation treatment 29 mo prior to the emergence of t-AML. His karyotype was 47,X,der(Y)t(Y;3)(q12;q21),+8(21). Merlin *et al*[14] reported t-ALL diagnosis in a female patient 12 mo after administration of FOLFOX-4. Unfortunately, the corresponding karyotype analysis was not performed in this study[14]. In colorectal cancer, 2 cases of therapy-related chronic myeloid leukemia (t-CML) following OXP treatment tested positive for Philadelphia chromosome[16,17]. In Buxhofer-Ausch *et al*[16], a male patient was treated by cetuximab, OXP, irinotecan and capecitabine 18 mo prior to t-CML diagnosis. Contrastingly, in Kadikoylu *et al*[17], a male patient was administered with capecitabine, 5-FU, irinotecan and OXP 12 mo prior to detection of t-CML.

However, the aforementioned case studies involved complex chemotherapy schedules, which complicate the process of defining the tumorigenic potential of a single drug. As shown in Table 1, capecitabine-induced t-AML was previously reported in 2 studies[18,19]. Furthermore, Rashidi *et al*[20] reported a case involving

capecitabine-induced t-APL with a karyotype of 46,XY,t(15;17)(q24;q21). Surprisingly, treatment with G-CSF was correlated with the development of TRL[21]. The results from these studies make it difficult to determine which agent is imperative in the development of TRL. Additionally, these studies highlight the considerable variation in the average time between treatment and onset of TRL. In our study, the patient was treated by OXP plus capecitabine and G-CSF, with a 44 mo latency period prior to onset of t-APL. The karyotype analysis of our patient presented 46,XY,t(15;17)(q22;q21)[15]/46,idem,-9,+add(9)(p22)[2]/46,XY[3], which was unlike previous studies. Balanced chromosome translocations were observed, although at low frequency, in t(15;17)(q22;q11). This genetic abnormality is often associated with treatments involving topoisomerase-2 inhibitors[22,23]; however, in an uncommon occurrence, balanced chromosome translocations were observed in our patient who was treated with OXP, capecitabine and G-CSF.

The prognosis of t-AML is thought to be worse than *de novo* AML, with a reported 5-year survival rate of less than 10%[24]. In Kayser *et al*[25], patients with t-AML were characterized with significantly inferior 4-year relapse-free survival (24.5% *vs* 39.5%) and 4-year overall survival (25.5% *vs* 37.9%) than *de novo* AML. Interestingly, karyotype variation provides key insight on the final outcome of t-AML patients[26]. As reported by Kern *et al*[27], patients with a favorable karyotype were characterized with a significantly higher median survival time (26.7 mo) compared to patients with an unfavorable karyotype (5.6 mo). However, in t-APL, these parameters are distinct from that of t-AML. t-APL patients with t(15;17)/PML-RARα have a complete remission rate of 63.6% compared to *de novo* APL (92.5%). Accordingly, the overall survival in t-APL is inferior to *de novo* APL (51% *vs* 84%)[28]. In our case, the patient partially displayed a favorable karyotype (t(15;17)/PML-RARα) and attained complete remission. However, further study is required to elucidate the function of other chromosomal abnormalities (for example, chromosome 9) in this outcome.

Our study presents the novel case of t-AML/t-APL following treatment of gastric cancer. We suggest establishing an additional evaluation process for patients undergoing treatment with certain cytotoxic therapies. For patients with t-APL, our case emphasized the importance of certain "favorable" genetic abnormalities. While standard treatment protocol is likely to yield a favorable outcome for patients, additional studies are required to elucidate the underlying process of t-APL development.

COMMENTS

Case characteristics

A 68-year-old man was diagnosed with gastric cardia cancer and was classified as cT4N1M0 (or ⅢC), according to the TNM/UICC staging system.

Clinical diagnosis

After surgery, post-operative examination of the patient confirmed a poorly differentiated adenocarcinoma with penetrating invasion of the gastric wall. Out of 29 regional lymph nodes, 1 tested positive for cancer cell infiltrate.

Differential diagnosis

Based on clinical symptoms, imageological examination and post-operative pathological analysis, the patient diagnosis was definitive.

Laboratory diagnosis

Routine hematological examination indicated the following: red blood cells (2.35 × 10^{12}/L), white blood cells (1.8 × 10^{9}/L), absolute neutrophil count (0.67 × 10^{9}/L), hemoglobin (75 g/L), and platelets (81 g/L).

Imaging analysis

Computed tomography scan indicated a localized, irregularly-shaped mass in the stomach. No obvious lymph node metastasis was observed.

Pathological diagnosis

Post-operative pathological examination confirmed gastric cancer. Bone marrow biopsy indicated acute myeloid leukemia. Leukemic hiatus was diagnosed as the total number of primitive cells plus immature leukemia cells accounted for 91.5% (2% + 89.5%) of the total cell population.

Treatment

Oxaliplatin, capecitabine and recombinant human granulocyte-colony stimulating factor was administered for the treatment of gastric cancer. All-trans retinoic acid and arsenic trioxide was delivered to treat t-acute promyelocytic leukemia (t-APL).

Related reports

In the literature, development of t-AML is rarely associated with treatment regimens involving oxaliplatin, capecitabine and recombinant human granulocyte-colony stimulating factor. The role of these cytotoxic agents in t-AML development remains unclear.

Term explanation

Therapy-related acute myeloid leukemia (t-AML) refers to a heterogeneous group of myeloid neoplasms that develops in patients who were extensively exposed to cytotoxic agents or radiation during prior treatment.

Experience and lessons

This case study elucidated that specific cytotoxic agents induce t-APL in gastric cancer patients. We recommend additional evaluation and follow-up for patients undergoing these therapies in the future.

Peer-review

This case report adds some information to the current literature. The case report and the discussion are well-written. They successfully managed a case of therapy-related acute myeloid leukemia. This case report provides an important update on therapy-related acute myeloid leukemias and presents an interesting patients who after diagnosis including karyotype analysis and treatment entered complete remission. The report is well illustrated and the authors well summarized current literature.

REFERENCES

1 **Kwong YL**. Azathioprine: association with therapy-related myelodysplastic syndrome and acute myeloid leukemia. *J Rheumatol* 2010; **37**: 485-490 [PMID: 20080917 DOI: 10.3899/jrheum.090834]

2 **Travis LB**. The epidemiology of second primary cancers. *Cancer Epidemiol Biomarkers Prev* 2006; **15**: 2020-2026 [PMID: 17057028 DOI: 10.1158/1055-9965.EPI-06-0414]

3 **Smith SM**, Le Beau MM, Huo D, Karrison T, Sobecks RM, Anastasi J, Vardiman JW, Rowley JD, Larson RA. Clinical-cytogenetic associations in 306 patients with therapy-related myelodysplasia and myeloid leukemia: the University of Chicago series. *Blood* 2003; **102**: 43-52 [PMID: 12623843 DOI: 10.1182/blood-2002-11-3343]

4 **Casorelli I**, Bossa C, Bignami M. DNA damage and repair in human cancer: molecular mechanisms and contribution to therapy-related leukemias. *Int J Environ Res Public Health* 2012; **9**: 2636-2657 [PMID: 23066388 DOI: 10.3390/ijerph9082636]

5 **Czader M**, Orazi A. Therapy-related myeloid neoplasms. *Am J Clin Pathol* 2009; **132**: 410-425 [PMID: 19687318 DOI: 10.1309/

AJCPD85MCOHHCOMQ]
6 **Godley LA**, Larson RA. Therapy-related myeloid leukemia. *Semin Oncol* 2008; **35**: 418-429 [PMID: 18692692 DOI: 10.1053/j.seminoncol.2008.04.012]
7 **Larson RA**, Le Beau MM. Prognosis and therapy when acute promyelocytic leukemia and other «good risk» acute myeloid leukemias occur as a therapy-related myeloid neoplasm. *Mediterr J Hematol Infect Dis* 2011; **3**: e2011032 [PMID: 21869918 DOI: 10.4084/mjhid.2011.032]
8 **Andersen MK**, Larson RA, Mauritzson N, Schnittger S, Jhanwar SC, Pedersen-Bjergaard J. Balanced chromosome abnormalities inv(16) and t(15; 17) in therapy-related myelodysplastic syndromes and acute leukemia: report from an international workshop. *Genes Chromosomes Cancer* 2002; **33**: 395-400 [PMID: 11921273 DOI: 10.1002/gcc.10043]
9 **Mistry AR**, Felix CA, Whitmarsh RJ, Mason A, Reiter A, Cassinat B, Parry A, Walz C, Wiemels JL, Segal MR, Adès L, Blair IA, Osheroff N, Peniket AJ, Lafage-Pochitaloff M, Cross NC, Chomienne C, Solomon E, Fenaux P, Grimwade D. DNA topoisomerase II in therapy-related acute promyelocytic leukemia. *N Engl J Med* 2005; **352**: 1529-1538 [PMID: 15829534 DOI: 10.1056/NEJMoa042715]
10 **Leone G**, Pagano L, Ben-Yehuda D, Voso MT. Therapy-related leukemia and myelodysplasia: susceptibility and incidence. *Haematologica* 2007; **92**: 1389-1398 [PMID: 17768113 DOI: 10.3324/haematol.11034]
11 **Raymond E**, Faivre S, Woynarowski JM, Chaney SG. Oxaliplatin: mechanism of action and antineoplastic activity. *Semin Oncol* 1998; **25**: 4-12 [PMID: 9609103]
12 **Merrouche Y**, Mugneret F, Cahn JY. Secondary acute promyelocytic leukemia following irinotecan and oxaliplatin for advanced colon cancer. *Ann Oncol* 2006; **17**: 1025-1026 [PMID: 16293675 DOI: 10.1093/annonc/mdj082]
13 **Carneiro BA**, Kaminer L, Eldibany M, Sreekantaiah C, Kaul K, Locker GY. Oxaliplatin-related acute myelogenous leukemia. *Oncologist* 2006; **11**: 261-262 [PMID: 16549810 DOI: 10.1634/theoncologist.11-3-261]
14 **Merlin F**, Prochilo T, Kildani B, Tucci A, Ferrari S, Rossi G, D' Adda P, Beretta GD. Secondary acute lymphoblastic leukaemia following oxaliplatin for adjuvant chemotherapy in colon cancer. *Acta Oncol* 2008; **47**: 464-466 [PMID: 17851873 DOI: 10.1080/02841860701558864]
15 **Damodaran S**, Bellavia T, Sait SN, Wang ES, Wetzler M, Khushalani NI. Acute myeloid leukemia secondary to oxaliplatin treatment for esophageal cancer. *Clin Colorectal Cancer* 2012; **11**: 151-154 [PMID: 22133502 DOI: 10.1016/j.clcc.2011.09.002]
16 **Buxhofer-Ausch V**, Hinterberger-Fischer M, Hinterberger W. Bcr-abl positive blast crisis of chronic myeloid leukemia emerging in a case of metastatic colorectal cancer 3 months after completion of an 8-month course of cetuximab and irinotecan. *Eur J Haematol* 2006; **76**: 447-448 [PMID: 16494624 DOI: 10.1111/j.1600-0609.2006.00630.x]
17 **Kadikoylu G**, Yavasoglu I, Barutca S, Meydan N, Bolaman Z. Chronic myeloid leukemia following the treatment of rectal adenocarcinoma. *Med Oncol* 2008; **25**: 467-470 [PMID: 18373227 DOI: 10.1007/s12032-008-9061-3]
18 **Shapiro S**, Hughes G, Al-Obaidi MJ, O'Reilly E, Ramesh S, Smith J, Ahmad R, Dawson C, Riddle P, Sekhar M. Acute myeloid leukaemia secondary to treatment with capecitabine for metastatic colorectal cancer. *Eur J Haematol* 2007; **78**: 543-544 [PMID: 17509107 DOI: 10.1111/j.1600-0609.2007.00864.x]
19 **Tansley S**, Gibbons S. Capecitabine-induced acute myeloid leukaemia. *N Z Med J* 2009; **122**: 118-119 [PMID: 19465957]
20 **Rashidi A**, Man L, Howard JR, Atienza D, Fisher SI. Therapy-related acute promyelocytic leukemia after chemoradiotherapy with capecitabine for rectal adenocarcinoma. *Leuk Lymphoma* 2014; **55**: 683-684 [PMID: 23837492 DOI: 10.3109/10428194.2013.797975]
21 **Beekman R**, Touw IP. G-CSF and its receptor in myeloid malignancy. *Blood* 2010; **115**: 5131-5136 [PMID: 20237318 DOI: 10.1182/blood-2010-01-234120]
22 **Andersen MK**, Johansson B, Larsen SO, Pedersen-Bjergaard J. Chromosomal abnormalities in secondary MDS and AML. Relationship to drugs and radiation with specific emphasis on the balanced rearrangements. *Haematologica* 1998; **83**: 483-488 [PMID: 9676019]
23 **Joannides M**, Grimwade D. Molecular biology of therapy-related leukaemias. *Clin Transl Oncol* 2010; **12**: 8-14 [PMID: 20080465 DOI: 10.1007/s12094-010-0460-5]
24 **Singh ZN**, Huo D, Anastasi J, Smith SM, Karrison T, Le Beau MM, Larson RA, Vardiman JW. Therapy-related myelodysplastic syndrome: morphologic subclassification may not be clinically relevant. *Am J Clin Pathol* 2007; **127**: 197-205 [PMID: 17210514 DOI: 10.1309/NQ3PMV4U8YV39JWJ]
25 **Kayser S**, Döhner K, Krauter J, Köhne CH, Horst HA, Held G, von Lilienfeld-Toal M, Wilhelm S, Kündgen A, Götze K, Rummel M, Nachbaur D, Schlegelberger B, Göhring G, Späth D, Morlok C, Zucknick M, Ganser A, Döhner H, Schlenk RF. The impact of therapy-related acute myeloid leukemia (AML) on outcome in 2853 adult patients with newly diagnosed AML. *Blood* 2011; **117**: 2137-2145 [PMID: 21127174 DOI: 10.1182/blood-2010-08-301713]
26 **Park SH**, Chi HS, Cho YU, Jang S, Park CJ. Evaluation of prognostic factors in patients with therapy-related acute myeloid leukemia. *Blood Res* 2013; **48**: 185-192 [PMID: 24086938 DOI: 10.5045/br.2013.48.3.185]
27 **Kern W**, Haferlach T, Schnittger S, Hiddemann W, Schoch C. Prognosis in therapy-related acute myeloid leukemia and impact of karyotype. *J Clin Oncol* 2004; **22**: 2510-2511 [PMID: 15197216 DOI: 10.1200/JCO.2004.99.301]
28 **Elliott MA**, Letendre L, Tefferi A, Hogan WJ, Hook C, Kaufmann SH, Pruthi RK, Pardanani A, Begna KH, Ashrani AA, Wolanskyj AP, Al-Kali A, Litzow MR. Therapy-related acute promyelocytic leukemia: observations relating to APL pathogenesis and therapy. *Eur J Haematol* 2012; **88**: 237-243 [PMID: 22023492 DOI: 10.1111/j.1600-0609.2011.01727.x]

P- Reviewer: Iizuka T, Ozkan OV, Tarnawski A
S- Editor: Ma YJ **L- Editor**: A **E- Editor**: Liu XM

World Journal of Gastroenterology

Submit a Manuscript: http://www.wjgnet.com/esps/
Help Desk: http://www.wjgnet.com/esps/helpdesk.aspx
DOI: 10.3748/wjg.v21.i14.4408

World J Gastroenterol 2015 April 14; 21(14): 4408-4412
ISSN 1007-9327 (print) ISSN 2219-2840 (online)

CASE REPORT

Mesorectum localization as a special kind of rectal metastasis from breast cancer

Fan Xue, Zhong-Lin Liu, Qing Zhang, Xiang-Nan Kong, Wen-Zhi Liu

Fan Xue, Zhong-Lin Liu, Wen-Zhi Liu, Department of Gastrointestinal Surgery, Affiliated Zhongshan Hospital of Dalian University, Dalian 116001, Liaoning Province, China
Qing Zhang, Department of Radiology, Affiliated Zhongshan Hospital of Dalian University, Dalian 116001, Liaoning Province, China
Xiang-Nan Kong, Department of Pathology, Affiliated Zhongshan Hospital of Dalian University, Dalian 116001, Liaoning Province, China
Author contributions: Xue F and Liu WZ designed the report; Liu ZL and Liu WZ performed the operation; Zhang Q and Kong XN collected imageology and pathology data; Xue F performed the literature search and wrote the paper.
Supported by Affiliated Zhongshan Hospital of Dalian University, Dalian, Liaoning, China.
Ethics approval: The study was reviewed and approved by the Affiliated Zhongshan Hospital of Dalian University's Institutional Review Board.
Informed consent: All study participants, or their legal guardian, provided informed written consent prior to study enrollment.
Conflict-of-interest: The authors report no conflicts of interest. The authors alone are responsible for the content and writing of this paper.

Correspondence to: Wen-Zhi Liu, PhD, Director, Department of Gastrointestinal Surgery, Affiliated Zhongshan Hospital of Dalian University, No. 6 Jiefang Street, Dalian 116001, Liaoning Province, China. liuwenzhi1965@163.com
Telephone: +86-411-62893015
Received: October 22, 2014
Peer-review started: October 27, 2014
First decision: November 26, 2014
Revised: December 10, 2014
Accepted: January 8, 2015
Article in press: January 8, 2015
Published online: April 14, 2015

Abstract

Breast cancer can metastasize to other organs following initial treatment. Bones, liver, and the lung are the most common sites of breast cancer metastases. The digestive tract, on the other hand, is rarely involved. The incidence of mesorectal metastasis (a special category of rectal metastases) from breast cancer has not been described before. The case reported herein concerns a 68-year-old woman who underwent mastectomy. A pelvic mass with no symptoms was subsequently identified by computed tomography in the patient. We ultimately confirmed that this mass was a metastasis from breast cancer located in the mesorectum using surgical exploration and pathology results.

Key words: Breast cancer; Mesorectum localization; Rectal metastasis; Gastrointestinal metastasis

Core tip: Breast cancer is the most frequent tumor in women and can metastasize to other organs following operation. The incidence of mesorectal metastasis, a special category of rectal metastases, from breast cancer has not been described before. In contrast to the rectal metastasis described in previous case reports, the lack of visible clinical symptoms makes mesorectal metastasis more difficult to be discovered and diagnosed. The radiographic and pathologic characteristics of mesorectal metastasis from breast cancer shown in this paper have not been described before.

Xue F, Liu ZL, Zhang Q, Kong XN, Liu WZ. Mesorectum localization as a special kind of rectal metastasis from breast cancer. *World J Gastroenterol* 2015; 21(14): 4408-4412 Available from: URL: http://www.wjgnet.com/1007-9327/full/v21/i14/4408.htm DOI: http://dx.doi.org/10.3748/wjg.v21.

i14.4408

INTRODUCTION

Breast cancer is the most frequently occurring tumor in women and can metastasize to other organs following the initial treatment[1]. A study analyzing 11676 pT1-4N0-2M0 breast cancer patients who underwent surgical resection between 1985 and 2009 showed that the total number of distant metastasis cases was 1349 (11.6%)[2]. Lymph node, bone, lung, and liver metastasis are considered to be the most frequent sites for breast cancer metastasis, but more rectal metastasis cases have also been recently reported. Metastatic involvement of the rectum is generally secondary to the lobular histological subtype of breast cancer[3], and usually some symptoms are observed, including obstruction, bleeding, and abdominal pain. Here we present the case of a 68-year-old woman with metastatic ductal breast cancer in the mesorectum with no clinical manifestation 7 years after diagnosis and surgery.

CASE REPORT

A 68-year-old, post-menopausal woman underwent modified radical mastectomy of the right breast in June 2006 due to breast carcinoma with a 10-year-history of type 2 diabetes. No abnormalities were discovered by chest imaging, liver function tests, and routine blood examination. A post-operative pathologic diagnosis confirmed the presence of invasive ductal carcinoma (pT2, N0/13, and M0), and immunohistochemical stains were positive (++) for the estrogen receptor and negative for the progesterone receptor and HER-2. The patient only received one cycle of chemotherapy, which was implemented as the CMF regimen. There were no abnormalities during follow-up until a 3.2 cm × 4.2 cm malignant lesion was found in the pelvic cavity with heterogeneous density by enhanced CT scan in December 2013 (Figure 1). The patient also had a highly elevated CA-125 level (519.5 U/mL). The patient had no complaints and the colonoscopy result was negative. Therefore, a laparoscopy was performed, and a mass was located in the mesorectum as a result. No other metastasis was identified. We therefore decided to perform a resection of the mass, the diseased mesorectum, and the portion of the rectum to which it belonged. Immunohistochemical analysis revealed metastatic cancer nodules from the breast (ER 30%$^+$, PR$^-$, c-erbB2$^+$, TOPO Ⅱ 35%$^+$, Ki-67 index 75%, CK7$^+$, CK20$^-$, Villin$^-$, CDX2$^-$, CEA$^-$, GCDFP-15$^{+/-}$, CA-125$^+$, WT-1$^+$) (Figure 2)

DISCUSSION

The gastrointestinal (GI) tract is an uncommon metastatic site for breast carcinoma. In a study of 12001 cases of breast carcinoma with metastatic disease, only 73 (approximately 0.6%) had metastasis to the GI tract, while 24 had colorectal metastasis[4]. To our knowledge, there have been at least 15 reports on rectal metastasis of breast carcinoma, but none of these cases mentioned mesorectal metastasis. Therefore, we presume that mesorectal metastasis is a special type of rectal metastasis. The metastatic pathway between these two types may be via the blood, and is presumed to start by the dislodgement and intravasation of tumor cells into the axillary vein (*e.g.*, by surgical manipulation)[5]. It has been suggested that the vertebral plexus of veins, also known as Batson's plexus, may also serve as a route for metastasis. Batson's plexus is a venous plexus stretching along the vertebrae from the skull base to the sacrum[6]. These vessels may allow for the transfer of cancer emboli to pelvic organs through the posterior intercostal arteries[7]. The pathological result of primary breast cancer in this case was the infiltration of the ductal BC. Rectal metastases are judged to occur more often in patients with invasive lobular BC[4]. Microscopically, we observed that the tumor consisted of single-file stands of infiltrating tumor cells with the presence of signet-ring cells, the same as has been described for rectal metastasis previously[8]. Moreover, we also found very similar immunohistochemical characteristics to rectal metastasis. Metastatic breast tumor cells in the rectum have been reported to be positive for ER, PR, CK7, and GCDFP-15 and negative for CK20, CEA, and CDX2[9]. In our case, the tumor cell was positive for ER, CK7, GCDFP-15, and CA-125 and negative for CK20, CEA, CDX2, and PR.

CA-125 is commonly known as a tumor marker for ovarian carcinoma, but there has been limited data and less emphasis on metastatic breast carcinoma. Interestingly, the patient in our case had an extremely high CA-125 level. It is now believed that CA-125 can be expressed not only by the mesothelial cells of coelomic-derived tissues, such as the pleura, peritoneum, and pericardium, but also by the breast ducts and bronchiolar epithelium. A retrospective study found that CA-125 had a relatively high rate of detection (65%) in patients with multiple metastases from breast cancer[10]. Furthermore, two analyses based on 26 and 33 patients, respectively, suggested that elevations of CA-125 in metastatic breast cancer implied pleural involvement[11,12]. The data from a retrospective review (51 patients) and a prospective study (40 patients) illustrated that the CA-125 level had parallel responses to the status of post-operative breast cancer[13,14]. Despite these studies, it is unclear whether CA-125 is useful for monitoring the course of disease. Further research and the analysis of larger patient cohorts are needed to determine the utility of CA-125.

Due to the rarity of cases, the management

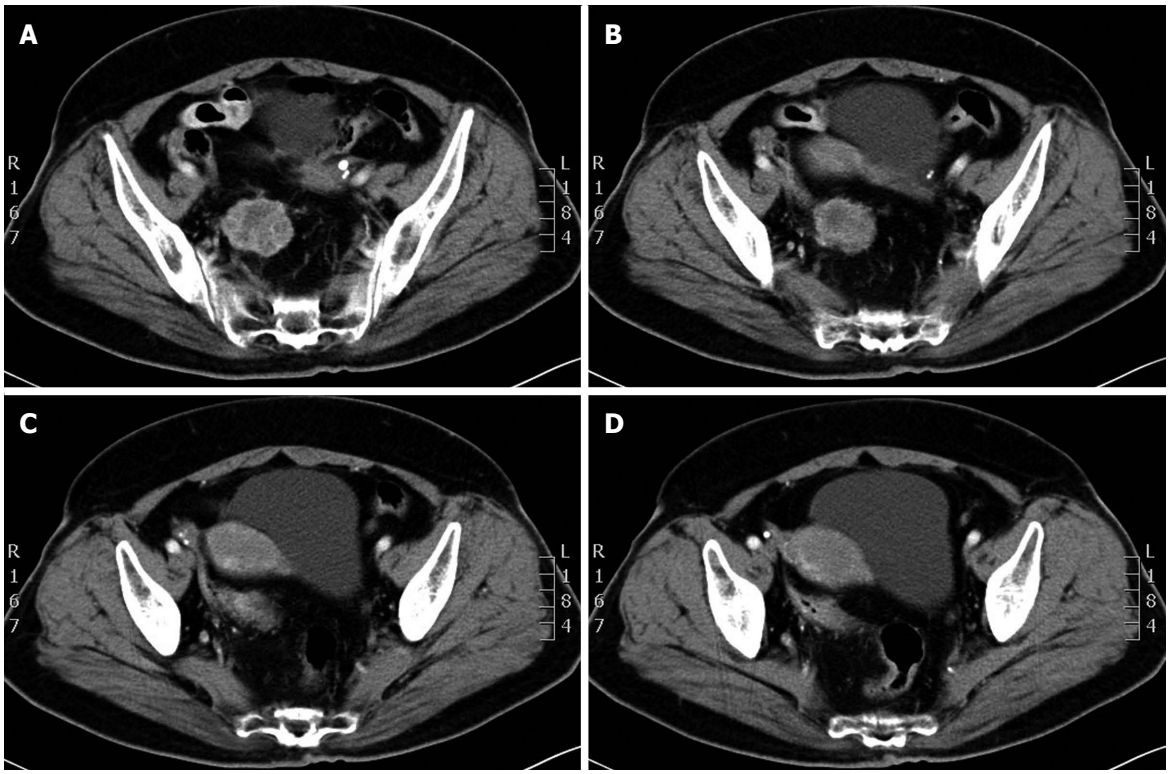

Figure 1 Contrast enhanced computed tomography showing a pelvic soft-tissue lesion which had heterogeneous density in the venous and delay phases, respectively.

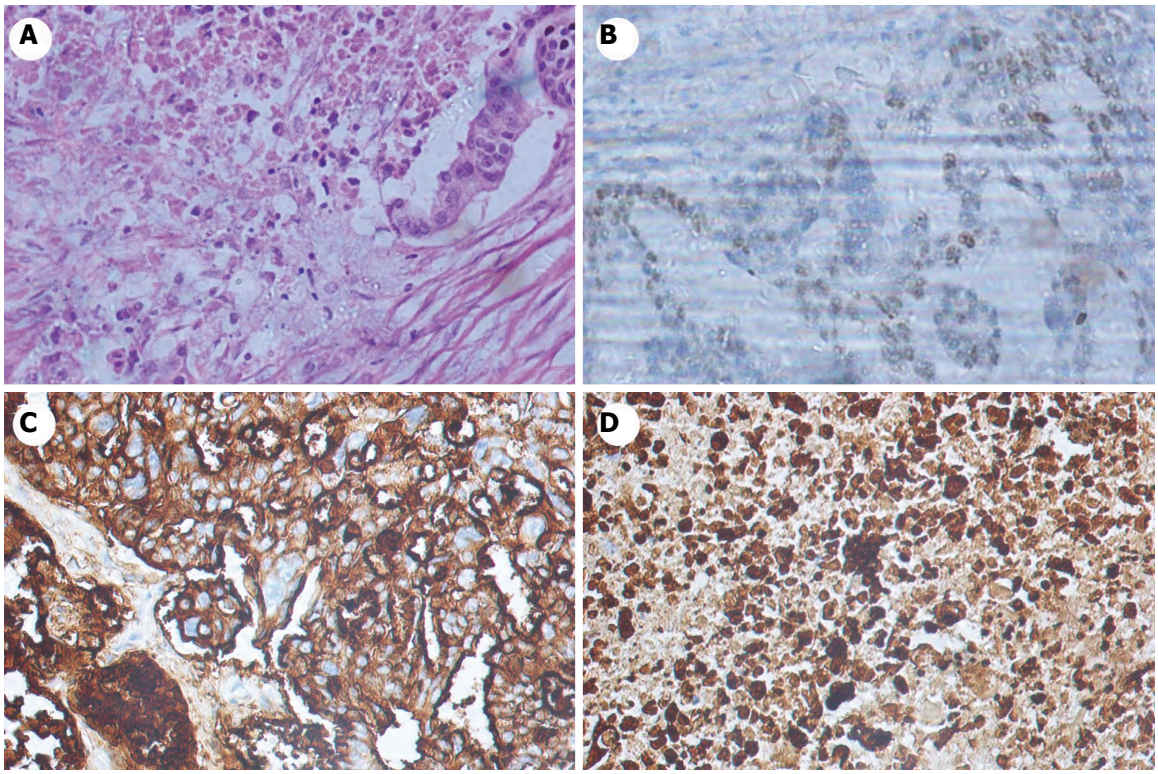

Figure 2 Mesorectum and portion of the rectum. A: Microscopically, the tumor consisted of single-file stands of infiltrating tumor cells with the presence of signet-ring cells (hematoxylin-eosin staining, magnification × 400). Immunohistochemical staining of tumor cells; B: Positive for estrogen receptor protein; C: Strongly positive for CA-125; D: Strongly positive for CK7.

of metastatic breast cancer in GI organs is still controversial. For a patient with serious complications such as obstruction, hematemesis, or perforation, surgery is certainly the first choice, although additional survival data for other treatments are still required. A retrospective review found that systemic chemotherapy or hormonal therapy has a positive effect on survival (P = 0.003)[4]. Moreover, Tang *et al*[15] reported that two cases with intestinal obstruction attributed to metastatic lobular BC were cured with hormonal therapy (fulvestrant). Additionally, combined treatment of surgery and chemotherapy on a patient with isolated GI involved caused remission[16]. For our patient, with consideration to the immunohistochemical analysis (ER 30%$^+$), we chose a strategy of surgery combined with hormonal therapy.

Mesorectal metastases from breast carcinoma are rare and there have been no prior reports on this disease. Therefore, it has been hard to differentiate between primary GI tumors and pelvic malignancies until the immunohistochemical profile has been determined. Awareness of this special kind of rectal metastasis is helpful for increasing diagnostic accuracy. Additional fundamental and clinical research concerning mesorectal metastases is needed to improve treatment.

COMMENTS

Case characteristics

A 68-year-old, post-menopausal woman underwent modified radical mastectomy of the right breast in June 2006 due to breast carcinoma with a 10-year-history of type 2 diabetes.

Clinical diagnosis

No physical sign was displayed other than that right breast had been excised.

Differential diagnosis

Primary tumors of pelvic organs, uterine, or ovarian metastasis from breast cancer, and other benign or malignant pelvic masses.

Laboratory diagnosis

CA-125: 519.5 U/mL, with other laboratory values being within normal limits.

Imaging diagnosis

A 3.2 cm × 4.2 cm malignant lesion was found in the pelvic cavity with a heterogeneous density by enhanced computed tomography scan.

Pathological diagnosis

Immunohistochemical analysis revealed metastatic cancer nodules from breast cancer (ER 30%$^+$, PR$^-$, c-erbB2$^+$, TOPO Ⅱ 35%$^+$, Ki-67 index 75%, CK7$^+$, CK20-, Villin$^-$, CDX2$^-$, CEA$^-$, GCDFP-15$^{+/-}$, CA-125$^+$, WT-1$^+$).

Treatment

The patient received a curative resection combined with hormonal therapy.

Related reports

The incidence of mesorectal metastasis from breast cancer has not been described before to our knowledge, while 15 reports on rectal breast cancer metastasis could be found in the literature.

Term explanation

CMF regimen is a conventional chemotherapy which is a cyclical application of cyclophosphamide, methotrexate, and fluorouracil. The medication dosages were adjusted based on individual patient characteristics.

Experiences and lessons

We know that mesorectal metastasis is a possibility once a pelvic mass has been found on a patient with a history of breast cancer.

Peer-review

The article highlights the clinical characteristics of mesorectal metastasis from breast cancer and provides insights into the etiology, diagnosis experiences, and therapy through the relevant literature.

REFERENCES

1 **Siegel R**, Ward E, Brawley O, Jemal A. Cancer statistics, 2011: the impact of eliminating socioeconomic and racial disparities on premature cancer deaths. *CA Cancer J Clin* 2011; **61**: 212-236 [PMID: 21685461 DOI: 10.3322/caac.20121]

2 **Makita M**, Sakai T, Ogiya A, Kitagawa D, Morizono H, Miyagi Y, Iijima K, Iwase T. Optimal surveillance for postoperative metastasis in breast cancer patients. *Breast Cancer* 2014; Epub ahead of print [PMID: 25294313 DOI: 10.1007/s12282-014-0571-x]

3 **Nazareno J**, Taves D, Preiksaitis HG. Metastatic breast cancer to the gastrointestinal tract: a case series and review of the literature. *World J Gastroenterol* 2006; **12**: 6219-6224 [PMID: 17036400 DOI: 10.3748/wjg.v12.i38.6219]

4 **McLemore EC**, Pockaj BA, Reynolds C, Gray RJ, Hernandez JL, Grant CS, Donohue JH. Breast cancer: presentation and intervention in women with gastrointestinal metastasis and carcinomatosis. *Ann Surg Oncol* 2005; **12**: 886-894 [PMID: 16177864 DOI: 10.1245/ASO.2005.03.030]

5 **Bockhorn M**, Jain RK, Munn LL. Active versus passive mechanisms in metastasis: do cancer cells crawl into vessels, or are they pushed? *Lancet Oncol* 2007; **8**: 444-448 [PMID: 17466902 DOI: 10.1016/S1470-2045(07)70140-7]

6 **Batson OV**. The function of the vertebral veins and their role in the spread of metastases. *Ann Surg* 1940; **112**: 138-149 [PMID: 17857618 DOI: 10.1097/00000658-194007000-00016]

7 **Efthimiadis C**, Kosmidis C, Fotiadis P, Anthimidis G, Vasiliadou K, Mekras A, Ioannidou G, Basdanis G. Breast cancer metastatic to the rectum: a case report. *Tech Coloproctol* 2011; **15** Suppl 1: S91-S93 [PMID: 21912949 DOI: 10.1007/s10151-011-0740-2]

8 **Saranovic D**, Kovac JD, Knezevic S, Susnjar S, Stefanovic AD, Saranovic DS, Artiko V, Obradovic V, Masulovic D, Micev M, Pesko P. Invasive lobular breast cancer presenting an unusual metastatic pattern in the form of peritoneal and rectal metastases: a case report. *J Breast Cancer* 2011; **14**: 247-250 [PMID: 22031809 DOI: 10.4048/jbc.2011.14.3.247]

9 **López Deogracias M**, Flores Jaime L, Arias-Camisón I, Zamacola I, Murillo Guibert J, Suescun García R, Querejeta Usabiaga J, Martínez García F. Rectal metastasis from lobular breast carcinoma 15 years after primary diagnosis. *Clin Transl Oncol* 2010; **12**: 150-153 [PMID: 20156785 DOI: 10.1007/S12094-010-0481-0]

10 **Yerushalmi R**, Tyldesley S, Kennecke H, Speers C, Woods R, Knight B, Gelmon KA. Tumor markers in metastatic breast cancer subtypes: frequency of elevation and correlation with outcome. *Ann Oncol* 2012; **23**: 338-345 [PMID: 21543625 DOI: 10.1093/annonc/mdr154]

11 **Jäger W**, Kissing A, Cilaci S, Melsheimer R, Lang N. Is an increase in CA 125 in breast cancer patients an indicator of pleural metastases? *Br J Cancer* 1994; **70**: 493-495 [PMID: 8080736 DOI: 10.1038/bjc.1994.333]

12 **Norum LF**, Erikstein B, Nustad K. Elevated CA125 in breast cancer--A sign of advanced disease. *Tumour Biol* 2001; **22**: 223-228 [PMID: 11399947 DOI: 10.1159/000050620]

13 **Jensen JL**, Maclean GD, Suresh MR, Almeida A, Jette D, Lloyd S, Bodnar D, Krantz M, Longenecker BM. Possible utility of serum determinations of CA 125 and CA 27.29 in breast cancer management. *Int J Biol Markers* 1991; **6**: 1-6 [PMID: 1856511]

14 **Perey L**, Hayes DF, Tondini C, van Melle G, Bauer J, Lemarchand T, Reymond M, Mach JP, Leyvraz S. Elevated CA125 levels in patients with metastatic breast carcinoma. *Br J Cancer* 1990; **62**: 668-670 [PMID: 2223588 DOI: 10.1038/bjc.1990.353]

15 **Tang JY**, Rampaul RS, Cheung KL. The use of fulvestrant, a parenteral endocrine agent, in intestinal obstruction due to

metastatic lobular breast carcinoma. *World J Surg Oncol* 2008; **6**: 128 [PMID: 19046426 DOI: 10.1186/1477-7819-6-128]
16 **Eljabu W**, Finch G, Nottingham J, Vaingankar N. Metastatic deposits of breast lobular carcinoma to small bowel and rectum. *Int J Breast Cancer* 2011; **2011**: 413949 [PMID: 22295221 DOI: 10.4061/2011/413949]

P- Reviewer: Gehmert S, Sidiropoulou Z **S- Editor**: Qi Y
L- Editor: Rutherford A **E- Editor**: Ma S

World Journal of Gastroenterology

Submit a Manuscript: http://www.wjgnet.com/esps/
Help Desk: http://www.wjgnet.com/esps/helpdesk.aspx
DOI: 10.3748/wjg.v21.i14.4413

World J Gastroenterol 2015 April 14; 21(14): 4413-4418
ISSN 1007-9327 (print) ISSN 2219-2840 (online)

CASE REPORT

Laparoscope resection of retroperitoneal ectopic insulinoma: A rare case

Jie Liu, Cheng-Wu Zhang, De-Fei Hong, Jia Wu, Hong-Guo Yang, Yuan Chen, Da-Jian Zhao, Yu-Hua Zhang

Jie Liu, Cheng-Wu Zhang, De-Fei Hong, Jia Wu, Da-Jian Zhao, Yu-Hua Zhang, Department of Hepatopancreatobiliary Surgery and Minimally Invasive Surgery, Zhejiang Provincial People's Hospital, Hangzhou 310014, Zhejiang Province, China
Hong-Guo Yang, Department of General Surgery, Haining Branch of Zhejiang Provincial People's Hospital, Jiaxing 314408, Zhejiang Province, China
Yuan Chen, Department of Pathology, Zhejiang Provincial People's Hospital, Hangzhou 310014, Zhejiang Province, China
Author contributions: Liu J and Zhang CW performed the surgery and perioperative treatment; Zhang YH provided figures and revised the manuscript; Yang HG and Wu J reviewed and analyzed the literature; Chen Y was responsible for pathology; Hong DF and Zhao DJ designed the surgical protocol.
Ethics approval: The study was reviewed and approved by the ZheJiang Provincial People's Hospital Institutional Review Board.
Informed consent: The study participant provided informed written consent for this study.
Conflict-of-interest: We declare that we have no financial and personal relationships with other people or organizations that can inappropriately influence our work, there is no professional or other personal interest of any nature or kind in any product, service and/or company that could be construed as influencing the position presented in, or the review of, the manuscript.

Correspondence to: Cheng-Wu Zhang, MD, Department of Hepatopancreatobiliary Surgery and Minimally Invasive Surgery, Zhejiang Provincial People's Hospital, Shangtang Road 158, Hangzhou 310014, Zhejiang Province, China. zcw1989@sina.com
Telephone: +86-571-85893419
Fax: +86-571-85131448
Received: November 4, 2014
Peer-review started: November 5, 2014
First decision: December 11, 2014
Revised: December 25, 2014
Accepted: January 21, 2015
Article in press: January 21, 2015
Published online: April 14, 2015

Abstract

Ectopic insulinoma is a very rare and dormant tumor. Here we report the case of a 79-year-old female who presented with repeated episodes of hypoglycemia and was diagnosed with insulinoma based on laboratory and imaging examinations. Computed tomography and positron emission tomography revealed a tumor in the retroperitoneum under and left of the hepatoduodenal ligament, which was resected successfully using a laparoscopic approach. Pathologic results revealed an ectopic insulinoma, which was confirmed immunohistochemically. Ectopic insulinomas are accompanied by hypoglycemia that can be misdiagnosed as drug- or disease-induced. These tumors are difficult to diagnose and locate, particularly in atypical cases or for very small tumors. Synthetic or targeted examinations, including low blood glucose, elevated insulin, proinsulin, and C-peptide levels, 48-h fasting tests, and relevant imaging methods should be considered for suspected cases of insulinoma. Surgery is the treatment of choice for patients with insulinoma, and laparoscopic resection is a feasible and effective method for select ectopic insulinoma cases.

Key words: Diagnosis; Ectopic insulinoma; Hypoglycemia; Laparoscopic resection; Localization

Core tip: Ectopic insulinoma is a very rare and dormant disease that is difficult to diagnose and locate. It should be considered in the differential diagnosis of cases of hypoglycemia thought to be caused by drugs and other diseases. Correlative laboratory and imaging examinations are necessary, and laparoscopic resection

is a feasible and effective treatment approach.

Liu J, Zhang CW, Hong DF, Wu J, Yang HG, Chen Y, Zhao DJ, Zhang YH. Laparoscope resection of retroperitoneal ectopic insulinoma: A rare case. *World J Gastroenterol* 2015; 21(14): 4413-4418 Available from: URL: http://www.wjgnet.com/1007-9327/full/v21/i14/4413.htm DOI: http://dx.doi.org/10.3748/wjg.v21.i14.4413

INTRODUCTION

Hypoglycemia is commonly encountered in daily clinical practice and often occurs during the treatment of diabetes mellitus. The condition is most often the result of insulin or other anti-diabetic agents and ethanol[1-3], though a small minority of hypoglycemia cases are spontaneous[4]. Hypoglycemia can also be caused by adrenal or hepatic diseases, gastrointestinal stromal and retroperitoneal tumors, endocrine deficiency, and even breast tumors[5-9], and rarely from hypocortisolism[10] and non-Hodgkin lymphoma[11]. Additionally, some fruits may lead to hypoglycemia[12].

Although rare, hypoglycemia can be caused by an insulinoma, the most common hormone-secreting islet cell tumor. In such instances, the diagnosis is made when hypoglycemia occurs in the presence of symptoms of neuroglycopenia and inappropriately high levels of insulin and C-peptide. Additional imaging is often required to detect the underlying insulinoma. In the present paper, we describe the clinical and pathologic features of a rare case of hypoglycemia involving a functioning retroperitoneal insulinoma, and review the literature related to this topic to provide a comprehensive overview of this very rare and challenging tumor type.

CASE REPORT

A 79-year-old woman was referred to our hospital because of recurrent vertigo, weakness, and loss of consciousness experienced over a period of 9 mo, which often occurred during fasting, hunger, or exercise. When an episode occurred, serum glucose fluctuated between 2.0 and 2.5 mmol/L (the lowest value was 1.5 mmol/L), and symptoms resolved after ingestion of glucose, dextrose, or dessert. The patient had never taken any sulfonylurea drugs.

Her physical examination was unremarkable; the thyroid was normal and no nodules were palpable. A brain computed tomography (CT) scan ruled out any focal or diffuse encephalic lesion. After admission, her serum glucose level was 2.4 mmol/L (normal value: 3.3-6.2 mmol/L), insulin was 35.4 μU/mL (normal value: 4.0-16.8 μU/mL), and C-peptide was 2.5 ng/mL (normal value: 1.0-4.5 ng/mL). Tumor markers were within normal limits. No symptoms related to upper gastrointestinal occlusion or bleeding were noted. The presence of the Whipple triad and results of the 48-h fasting test suggested a diagnosis of insulinoma.

Regular transabdominal ultrasound yielded negative findings in the pancreas. An abdominal CT/positron emission tomography (PET) scan also showed no evidence of a pancreatic tumor, but revealed a 2.5 × 1.0 cm solid polyp in the retroperitoneum under and left of the hepatoduodenal ligament (Figure 1). Thus, the presumptive diagnosis of ectopic insulinoma was made, and a laparoscopic tumor resection was performed. The gastrocolic ligament was detached with a harmonic scalpel to completely expose the neck, body, and tail of the pancreas, and no mass was detected. The lesser omentum was then opened to move the hepatoduodenal ligament to the right in order to expose the tumor. An isolated, pink, and slightly hard tumor (2.5 cm in diameter) was clearly identified in the retroperitoneum under the hepatoduodenal ligament with the assistance of intraoperative laparoscopic endoscopy. A laparoscopic resection of the tumor was successfully performed using a harmonic scalpel (Figure 2).

Pathologic evaluation of the resected tissue revealed a well-differentiated tumor with a distinct border surrounding the exocrine pancreatic tissue (Figure 3). Immunohistochemical evaluation showed that the cells were positive for tumor markers and insulin (Figure 4). Taken together, the findings confirmed the diagnosis of ectopic insulinoma, Heinrich's classification type Ⅰ.

Glucose blood levels were recorded every 15 min during surgery without dextrose infusion (Table 1). Normoglycemia was achieved promptly after tumor removal. The patient was discharged on postoperative day 7, and a routine follow-up showed no recurrence of hypoglycemic symptoms.

DISCUSSION

Insulinoma presents with various clinical manifestations, often with symptoms of hypoglycemia. These tumors are difficult to detect due to their small size. In a study of 114 articles encompassing 6222 cases of insulinoma, the vast majority (84%) were < 20 mm in diameter[13]. Almost all of these tumors were found in the pancreas parenchyma (43.3% head and uncinate, 25.3% body, and 30.9% tail), and < 1% were ectopic (extrapancreatic). Ectopic insulinomas with symptoms of hypoglycemia are extremely rare and can occur in the duodenal wall, ileum, jejunum, gastric wall, hilus of the spleen, gastrosplenic ligament, ligament of Treitz, lung, cervix, and ovary[14,15].

Symptoms of insulinomas include digestive bleeding, jaundice, and abdominal pain[16,17]. The Whipple triad, which includes documented hypoglycemia, neuroglycopenic symptoms, and rapid relief of symptoms with the administration of glucose, is the diagnostic hallmark of an insulinoma. Although the

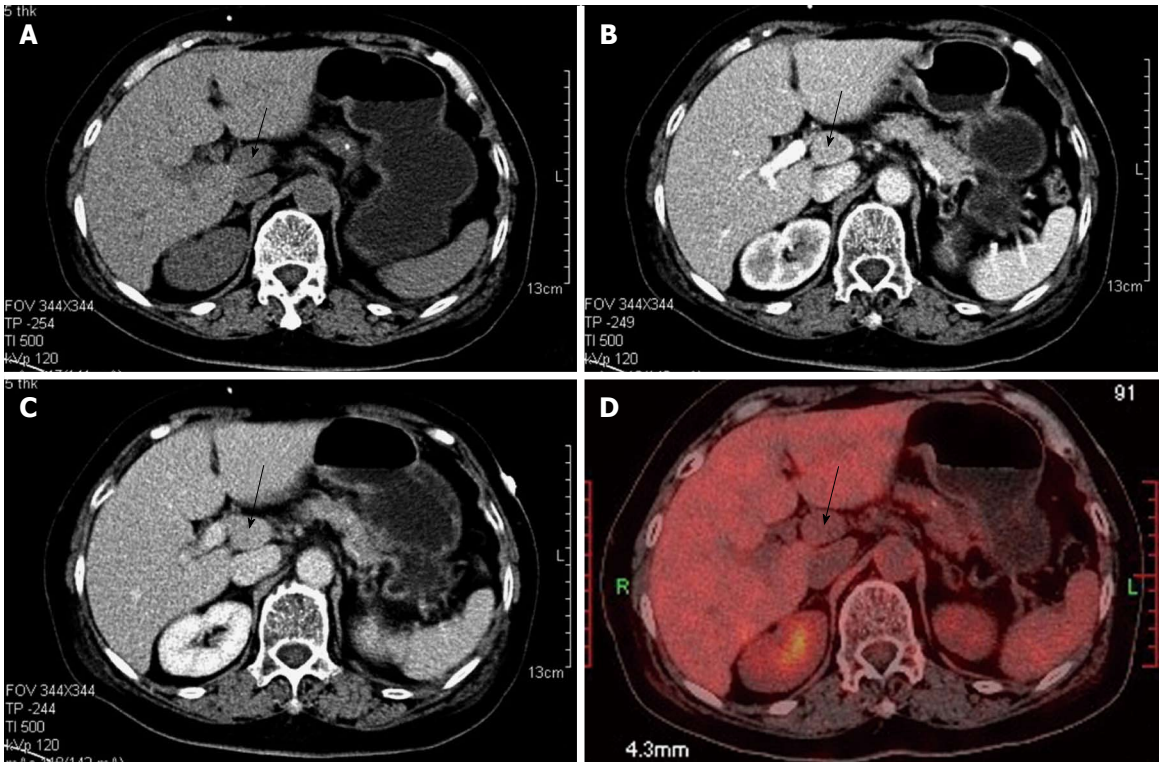

Figure 1 Radiologic findings. A: Plain scanning-phase computed tomography (CT); B: Arterial enhancement-phase CT; C: Equilibrium-phase CT showing the tumor (black arrow) in the retroperitoneum; D: Positron emission tomography showing the tumor in the retroperitoneum with no ^{18}fluorodeoxyglucose activity.

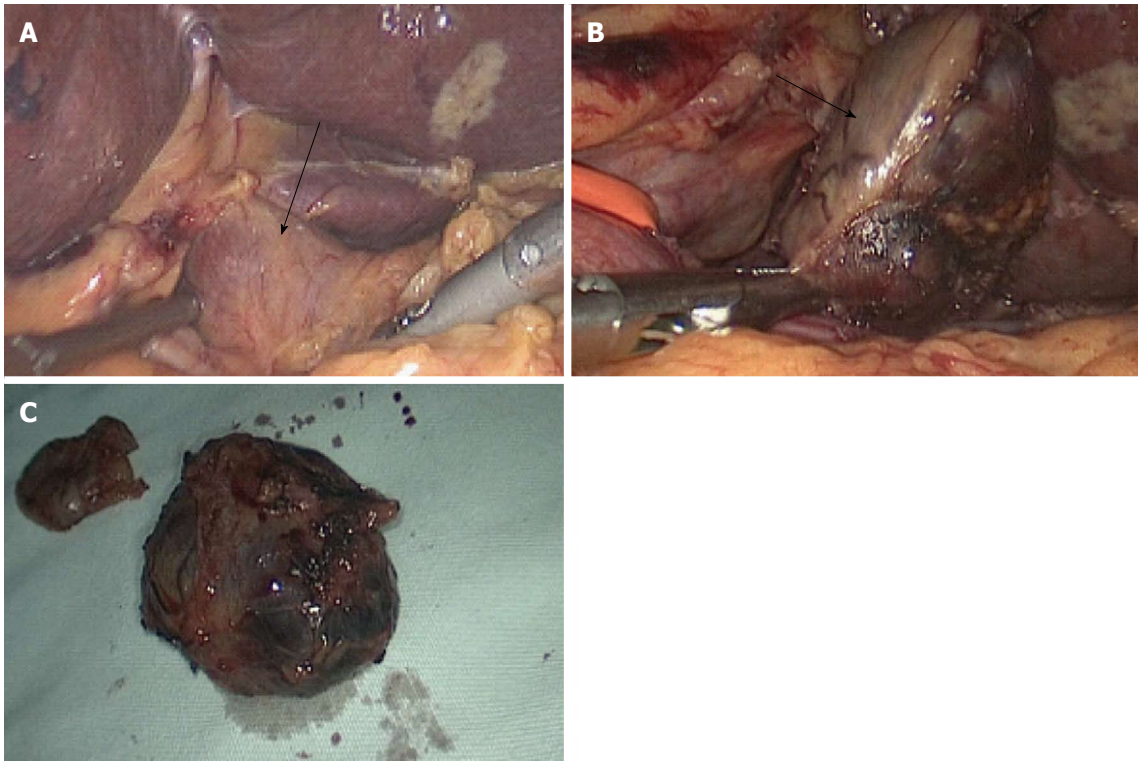

Figure 2 Tumor imaging during surgery. A: An isolated, pink, slightly hard tumor was clearly identified under and left of the hepatoduodenal ligament (black arrow); B: Resection of the tumor was successfully performed using a harmonic scalpel with a laparoscopic approach (black arrow); C: Tumor specimen.

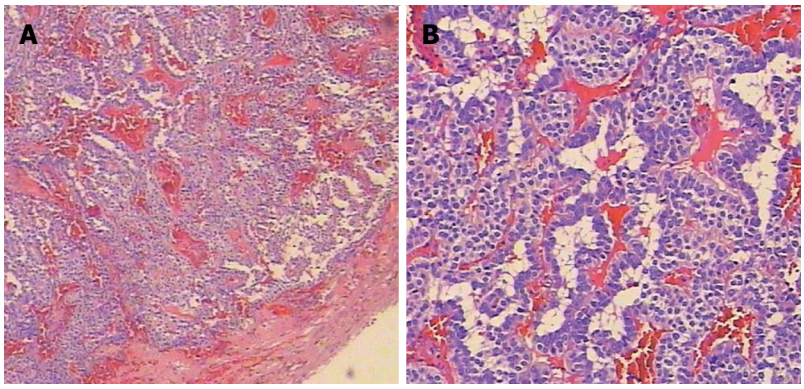

Figure 3 Pathologic results. Hematoxylin and eosin staining showing the tumor capsule and submucosal infiltration (A: Magnification × 40; B: Magnification × 100).

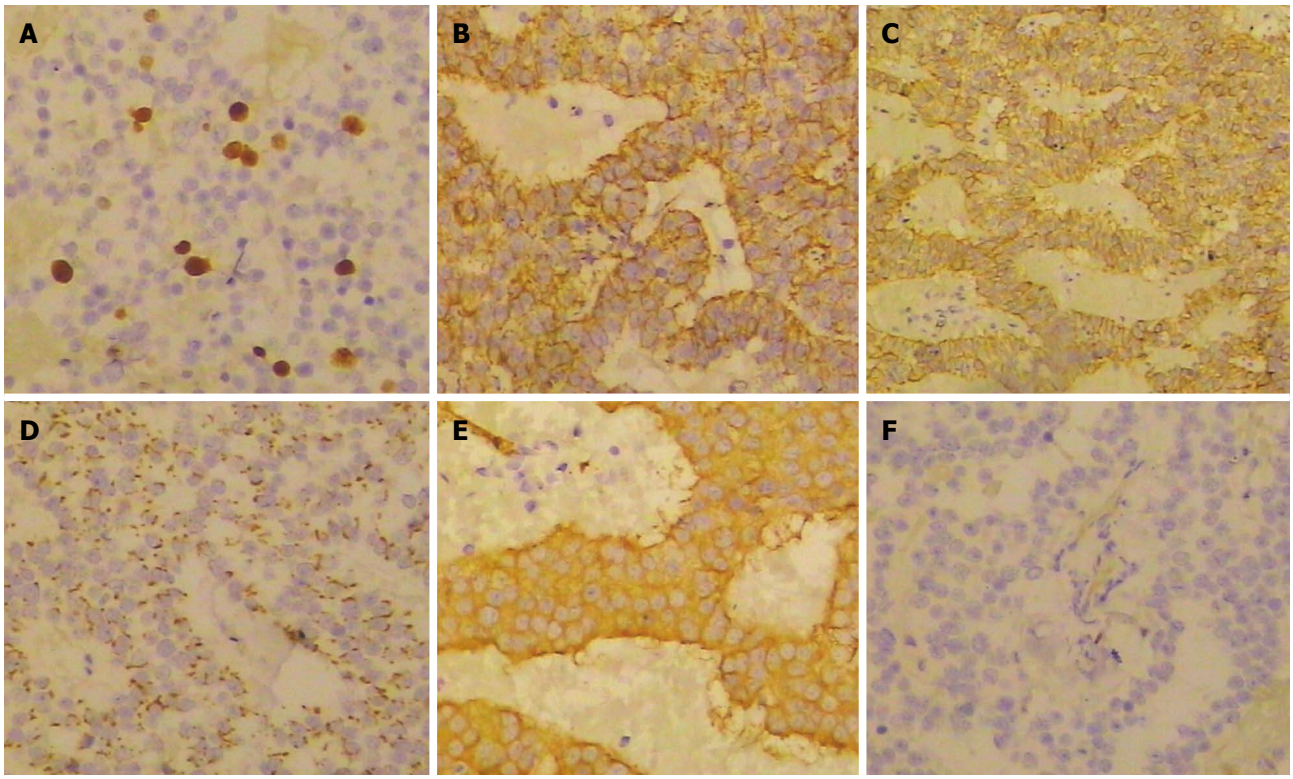

Figure 4 Immunohistochemical findings. Tumor cells were immunoreactive for Ki67 (A), Insulin (B), CD56 (C), Chromogranin A (D), Synaptophysin (E), but negative for Serotonin (F).

72-h fasting test has been the standard criterion for diagnosing insulinomas, recent data have verified that the diagnosis can be achieved in about 95.7% of cases undergoing a supervised fasting of 48 h[18].

Although insulinomas are generally observed by abdominal ultrasonography, CT, and magnetic resonance imaging, these methods cannot easily detect ectopic insulinomas, particularly those < 10 mm. Rather, more sensitive methods should be employed for more accurate detection, such as digital subtraction angiography, which uses the characteristic bloodstream distribution. Other methods, including endoscopic ultrasonography, transhepatic portal venous sampling, ^{18}fluorodopa PET/CT scanning, and arterial stimulation/venous sampling, have been widely used to localize insulinoma in clinical practice[19]. Fortunately for the patient in the present case,a combination of ultrasonography and contrast-enhanced CT detected the mass.

The treatment of choice for patients with insulinoma is surgery, including enucleation, segmental pancreatectomy, pancreatoduodenectomy, and distal pancreatectomy preserving the spleen[20]. Laparoscopic resection for insulinoma has now been widely accepted, which can be used for resection of small, benign, solitary, and superficial tumors[21,22], including ectopic insulinomas. This method reduces operation time, blood loss, and morbidity, and involves a shorter hospital stay and faster recovery period for the patient. In our case, ectopic insulinoma was diagnosed based on the

Table 1 Glucose blood levels

Time	Glucose blood level (mmol/L)
Perioperative	
Beginning of procedure	3.2
Tumor removal	5.6
15 min after removal	5.8
30 min after removal	6.6
45 min after removal	6.8
End of procedure	6.9
Postoperative	
Day 1	5.6
Day 2	5.6
Day 3	5.8
Day 4	6.2
Day 5	7.5

typical symptoms and imaging examinations, and was completely removed. However, for patients whose insulinomas have been missed during surgery and for those who refuse or are not candidates for surgery (including malignant insulinoma with metastasis), alternative medical treatment is needed[23].

Ectopic insulinoma is a very rare and dormant disease that is difficult to diagnose and locate, particularly very small tumors or atypical cases. This case report highlights that a diagnosis of ectopic insulinoma for hypoglycemia of unknown cause should be considered, even in cases with negative findings from the pancreas, and specific or targeted examinations for insulinoma need to be followed. In addition, laparoscopic resection is a feasible and effective method for treatment of ectopic insulinomas.

COMMENTS

Case characteristics

A 79-year-old woman with a 9-mo history of recurrent hypoglycemia that resolved after intake of glucose or dextrose.

Clinical diagnosis

Hypoglycemia.

Differential diagnosis

Drug-induced hypoglycemia; hypoglycemia caused by adrenal or hepatic diseases;insulinoma; hypocortisolism.

Laboratory diagnosis

Serum glucose level: 2.4 mmol/L; insulin: 35.37 μU/mL; C-peptide: 2.54 ng/mL; tumor markers were within normal limits.

Imagining diagnosis

Regular transabdominal ultrasonography showed negative findings in the pancreas. An abdominal computed tomography/positron emission tomography scan did not reveal a pancreatic tumor, but showed a 2.5 × 1.0 cm solid polyp localized in the retroperitoneum under and left of the hepatoduodenal ligament with no fluorodeoxyglucose activity.

Pathological diagnosis

Immunohistochemical results showed that tumor cells were immunopositive for Ki67, insulin, CD56, chromogranin, and synaptophysin, and negative for serotonin, which supported a diagnosis of insulinoma.

Treatment

Laparoscopic resection of the tumor was successfully performed by harmonic scalpel.

Related reports

Very few cases of ectopic insulinoma have been reported in the literature. The clinical characteristics of ectopic insulinomas are sometimes atypical and localization is difficult.

Experiences and lessons

This report showed a very rare and dormant disease that can be confused with non-insulinoma-induced hypoglycemia. Insulinomas are difficult to diagnose and locate, particularly for atypical or very small cases. The diagnosis of ectopic insulinoma for hypoglycemia of unknown cause should be considered even when there are negative findings of the pancreas, and specific or targeted examinations for insulinomas are needed.

Peer-review

The authors have described a case of ectopic insulinoma, which is a very rare, dormant disease that is difficult to diagnose and locate. The article highlights the importance of differential diagnosis with hypoglycemia caused by drugs and other diseases, and the need for correlative laboratory and imaging examinations. The report suggests that laparoscopic resection is a feasible and effective treatment approach.

REFERENCES

1 **Murad MH**, Coto-Yglesias F, Wang AT, Sheidaee N, Mullan RJ, Elamin MB, Erwin PJ, Montori VM. Clinical review: Drug-induced hypoglycemia: a systematic review. *J Clin Endocrinol Metab* 2009; **94**: 741-745 [PMID: 19088166 DOI: 10.1210/jc.2008-1416]

2 **Guettier JM**, Gorden P. Insulin secretion and insulin-producing tumors. *Expert Rev Endocrinol Metab* 2010; **5**: 217-227 [PMID: 20401170 DOI: 10.1586/eem.09.83]

3 **Breuer HW**, Ptak P. [Hypoglycemia - frequency, causes, induced costs]. *Dtsch Med Wochenschr* 2012; **137**: 988-992 [PMID: 22549254 DOI: 10.1055/s-0031-1299014]

4 **Martens P**, Tits J. Approach to the patient with spontaneous hypoglycemia. *Eur J Intern Med* 2014; **25**: 415-421 [PMID: 24641805 DOI: 10.1016/j.ejim.2014.02.011]

5 **Brown LM**, Corrado MM, van der Ende RM, Derks TG, Chen MA, Siegel S, Hoyt K, Correia CE, Lumpkin C, Flanagan TB, Carreras CT, Weinstein DA. Evaluation of glycogen storage disease as a cause of ketotic hypoglycemia in children. *J Inherit Metab Dis* 2014; Epub ahead of print [PMID: 25070466 DOI: 10.1007/s10545-014-9744-1]

6 **Soutelo J**, Saban M, Borghi Torzillo F, Lutfi R, Leal Reyna M. [Adrenal carcinoma induced hypoglycemia]. *Medicina* (B Aires) 2013; **73**: 339-342 [PMID: 23924534]

7 **Dutta P**, Aggarwal A, Gogate Y, Nahar U, Shah VN, Singla M, Khandelwal N, Bhansali A. Non-islet cell tumor-induced hypoglycemia: a report of five cases and brief review of the literature. *Endocrinol Diabetes Metab Case Rep* 2013; **2013**: 130046 [PMID: 24616774 DOI: 10.1530/EDM-13-0046]

8 **Dean K**, Hsieh J, Morosky C, Hoffman J. Gastrointestinal stromal tumor of the pelvic soft tissue presenting with symptomatic hypoglycemia: A case report and brief review of current literature of non-islet cell tumor-induced hypoglycemia. *Gynecol Oncol Case Rep* 2012; **2**: 87-88 [PMID: 24371628 DOI: 10.1016/j.gynor.2012.04.003]

9 **Mir A**, Raza S. Congenital ACTH deficiency as a cause of hypoglycemia in a newborn infant. *Clin Pediatr* (Phila) 2011; **50**: 1150-1152 [PMID: 22121139 DOI: 10.1177/0009922811388406]

10 **Savas-Erdeve S**, Yılmaz Agladioglu S, Onder A, Peltek Kendirci HN, Bas VN, Sagsak E, Cetinkaya S, Aycan Z. An uncommon cause of hypoglycemia: insulin autoimmune syndrome. *Horm Res Paediatr* 2014; **82**: 278-282 [PMID: 25060673 DOI: 10.1159/000362758]

11 **Elhomsy GC**, Eranki V, Albert SG, Fesler MJ, Parker SM, Michael AG, Griffing GT. „Hyper-warburgism," a cause of asymptomatic hypoglycemia with lactic acidosis in a patient with non-Hodgkin's lymphoma. *J Clin Endocrinol Metab* 2012; **97**: 4311-4316 [PMID: 23055548 DOI: 10.1210/jc.2012-2327]

12 **Aktan AH**, Ozcelik A, Cure E, Cure MC, Yuce S. Profound hypoglycemia-ınduced by vaccinium corymbosum juice and laurocerasus fruit. *Indian J Pharmacol* 2014; **46**: 446-447 [PMID:

25097289 DOI: 10.4103/0253-7613.135963]
13 **Mehrabi A**, Fischer L, Hafezi M, Dirlewanger A, Grenacher L, Diener MK, Fonouni H, Golriz M, Garoussi C, Fard N, Rahbari NN, Werner J, Büchler MW. A systematic review of localization, surgical treatment options, and outcome of insulinoma. *Pancreas* 2014; **43**: 675-686 [PMID: 24921202 DOI: 10.1097/MPA.0000000000000110]
14 **La Rosa S**, Pariani D, Calandra C, Marando A, Sessa F, Cortese F, Capella C. Ectopic duodenal insulinoma: a very rare and challenging tumor type. Description of a case and review of the literature. *Endocr Pathol* 2013; **24**: 213-219 [PMID: 24006218 DOI: 10.1007/s12022-013-9262-y]
15 **Stanciu IN**, Pitale S, Prinz RA, Jakate S, Webb G, Steiner D, Braithwaite S, Gordon D, Emanuele MA. Insulinoma presenting with hyperandrogenism: a case report and a literature review. *J Intern Med* 2003; **253**: 484-489 [PMID: 12653879]
16 **Watanabe W**, Kurumada T, Shirai T, Tsutsumi Y. Aberrant insulinoma of the duodenal bulb. *Pathol Int* 1995; **45**: 895-900 [PMID: 8581156]
17 **Tolentino LF**, Lee H, Maung T, Stabile BE, Li K, French SW. Islet cell tumor arising from a heterotopic pancreas in the duodenal wall with ulceration. *Exp Mol Pathol* 2004; **76**: 51-56 [PMID: 14738869]
18 **Quinkler M**, Strelow F, Pirlich M, Rohde W, Biering H, Lochs H, Gerl H, Strasburger CJ, Ventz M. Assessment of suspected insulinoma by 48-hour fasting test: a retrospective monocentric study of 23 cases. *Horm Metab Res* 2007; **39**: 507-510 [PMID: 17611903 DOI: 10.1055/s-2007-982516]
19 **Peranteau WH**, Palladino AA, Bhatti TR, Becker SA, States LJ, Stanley CA, Adzick NS. The surgical management of insulinomas in children. *J Pediatr Surg* 2013; **48**: 2517-2524 [PMID: 24314196 DOI: 10.1016/j.jpedsurg.2013.04.022]
20 **Guo Q**, Wu Y. Surgical treatment of pancreatic islet cell tumor: report of 44 cases. *Hepatogastroenterology* 2013; **60**: 2099-2102 [PMID: 24719954]
21 **Sciuto A**, Abete R, Reggio S, Pirozzi F, Settembre A, Corcione F. Laparoscopic spleen-preserving distal pancreatectomy for insulinoma: experience of a single center. *Int J Surg* 2014; **12** Suppl 1: S152-S155 [PMID: 24862672 DOI: 10.1016/j.ijsu.2014.05.023]
22 **Ueda J**, Nakamura Y, Aimoto T, Hiroi M, Cho K, Yamahatsu K, Kawamoto M, Uchida E. Laparoscopic distal pancreatectomy preserving spleen and splenic vessels for pancreatic insulinoma. *J Nippon Med Sch* 2010; **77**: 175-180 [PMID: 20610903]
23 **Usukura M**, Yoneda T, Oda N, Yamamoto Y, Takata H, Hasatani K, Takeda Y. Medical treatment of benign insulinoma using octreotide LAR: a case report. *Endocr J* 2007; **54**: 95-101 [PMID: 17124362]

P- Reviewer: Buanes TA, Gong JP, Pavlidis TE, Scheidbach H
S- Editor: Qi Y **L- Editor**: Cant MR **E- Editor**: Liu XM

World Journal of Gastroenterology

Submit a Manuscript: http://www.wjgnet.com/esps/
Help Desk: http://www.wjgnet.com/esps/helpdesk.aspx
DOI: 10.3748/wjg.v21.i14.4419

World J Gastroenterol 2015 April 14; 21(14): 4419-4422
ISSN 1007-9327 (print) ISSN 2219-2840 (online)

CASE REPORT

Collagenous nodule mixed simple cyst and hemangioma coexistence in the liver

Zhen-Jiang Zheng, Shu Zhang, Yang Cao, Guang-Chun Pu, Hong Liu

Zhen-Jiang Zheng, Shu Zhang, Yang Cao, Guang-Chun Pu, Department of General Surgery, The Third People's Hospital of Chengdu, The Second Affiliated Hospital of Chengdu, Chongqing Medical University, Chengdu 610031, Sichuan Province, China
Hong Liu, Department of Radiology, The Third People's Hospital of Chengdu, The Second Affiliated Hospital of Chengdu, Chongqing Medical University, Chengdu 610031, Sichuan Province, China
Author contributions: Zhang S, Cao Y and Pu GC performed the surgery; Liu H collected the radiographic images; Zheng ZJ prepared the figures and drafted the manuscript; Zhang S revised the manuscript; all authors read and approved the final manuscript.
Ethics approval: The study was reviewed and approved by the Third People's Hospital of Chengdu Institutional Review Board.
Informed consent: All study participants, or their legal guardian, provided informed written consent prior to study enrollment.
Conflict-of-interest: There is no conflict of interest related to the manuscript.

Correspondence to: Shu Zhang, PhD, Department of General Surgery, The Third People's Hospital of Chengdu, The Second Affiliated Hospital of Chengdu, Chongqing Medical University, 82 Qinglong Street, Chengdu 610031, Sichuan Province, China. zhangshu_1961@sina.com
Telephone: +86-28-61318737
Fax: +86-28-61318736
Received: October 27, 2014
Peer-review started: October 28, 2014
First decision: November 14, 2014
Revised: December 14, 2014
Accepted: January 30, 2015
Article in press: January 30, 2015
Published online: April 14, 2015

Abstract

A 20-year-old female patient presented with two masses located in the left liver. In this patient, a computed tomography (CT) scan revealed a hypodense mass and a second well-defined mass with a calcified nodule in the left hepatic lobe. No enhancements were apparent in or around the masses. A laparotomy was performed due to the patient's symptoms, namely, the atypical CT findings and a risk of rupture of the subcapsular lesion. The operation revealed two masses in the left hepatic lobe and a left liver resection was subsequently performed. One of the masses involved segment Ⅲ and the other mass was located in segment Ⅳ. The histopathologic findings supported a diagnosis of collagenous nodule mixed simple cyst and hemangioma. A diagnosis of collagenous nodule mixed simple hepatic cyst is extremely rare and radiologically mimics a teratoma, hepatolithiasis, parasitic cyst, or hemangioma. Although hepatic hemangiomas are the most common benign tumors found in the liver, the present case showed atypical radiographic features.

Key words: Collagenous nodule; Hepatic hemangioma; Liver; Mass; Simple cyst

Core tip: This case represents a rare presentation of a patient with multiple liver masses. A definitive diagnosis depends on the histopathologic findings. Collagenous nodules are a rare clinicopathologic finding in the liver. This paper discusses the pathogenesis of a collagenous nodule found in the liver. Although hepatic hemangiomas are the most common benign tumor in the liver, this case showed atypical radiographic features.

Zheng ZJ, Zhang S, Cao Y, Pu GC, Liu H. Collagenous nodule

mixed simple cyst and hemangioma coexistence in the liver. *World J Gastroenterol* 2015; 21(14): 4419-4422 Available from: URL: http://www.wjgnet.com/1007-9327/full/v21/i14/4419.htm DOI: http://dx.doi.org/10.3748/wjg.v21.i14.4419

INTRODUCTION

Collagenous nodule mixed simple hepatic cyst is an extremely rare mass that has not been reported previously in the publically available literature. Hyaline degeneration of the connective tissue is the predominant pathologic feature of a collagenous nodule. This form of degenerative alteration has been found in atrophic breast tissue, scar tissue, atheromatous plaques, and organized tissue. In contrast, hepatic hemangiomas are the most common benign tumor in the liver[1]. Diagnosis of a hepatic hemangioma is generally straightforward and accurately diagnosed by the various imaging modalities. The case described here, however, presented with atypical radiographic features. The diagnosis of hepatic hemangioma was considered due to the pathologic findings. Here, we present a case of hepatic hemangioma in conjunction with a collagenous nodule mixed simple hepatic cyst in a 20-year-old female patient.

CASE REPORT

A 20-year-old female patient presented with a two-month history of recurrent right epigastric pain. She had no history of exposure to parasites. Serum alpha-fetoprotein and eosinophil levels were normal. Serological testing for hydatid antibody was negative. A computed tomography (CT) scan revealed a hypodense mass and a second well-defined mass with a calcified nodule in the left hepatic lobe. Enhancements were not apparent in or around the masses (Figure 1). The chief radiographic differential diagnosis included teratoma, hepatolithiasis, parasitic cyst, or hemangioma. Both the patient and her relatives consented to a laparotomy. The operation revealed two masses in the left hepatic lobe and a left liver resection was performed. One of the masses involved segment Ⅲ and the other was localized to segment Ⅳ. The segment Ⅲ mass was a tender, rufous and subcapsular mass (diameter: 9 cm), while the mass in segment Ⅳ was described as a cystic mass (diameter: 5 cm). A hard, gray-white, translucent, and inelastic nodule (diameter: 2 cm) was observed in the inner wall of the cystic mass (Figure 2, arrow). Histologically, the segment Ⅲ mass had dilated vascular channels, fibrous stroma, and dark venous blood. The segment Ⅳ mass revealed thickened, banded and sheet-like collagenous fibers (Figure 3). No parasites were observed in the specimen obtained from the cystic mass. After a histopathologic analysis, the diagnosis of collagenous nodule mixed simple cyst and hemangioma was confirmed. The patient made an uneventful recovery.

DISCUSSION

Prior to surgery, high-density nodules were classified as hepatic calcifications. Bezerra *et al*[2] retrospectively analyzed 1362 consecutive CT scans of the abdomen and identified intrahepatic calcifications in 3.6% (49/1362) of the patients. Calcifications that develop within a hepatic mass are either produced by the tumor itself or, more commonly, represent dystrophic calcification secondary to necrosis and/or hemorrhage within the mass[3]. Calcifications may be found in inflammatory hepatic lesions and in benign and malignant liver masses[4]. The clinical appearance of a cystic mass with a high-density nodule is nonspecific and can mimic a teratoma, hepatolithiasis, parasitic cyst, or hemangioma. Although supporting evidence was lacking, a diagnosis of hepatic hydatidosis was primarily considered, as it is endemic in the Sichuan Province. The patient presented with no personal history of potential exposure to parasites, a normal level of eosinophils, and a negative hydatid antibody test. Thus, the patient underwent a left liver resection to avoid a misdiagnosis that may have potential deleterious consequences. A pathologic examination subsequently confirmed that the mass was a collagenous nodule mixed simple hepatic cyst, which has not been reported previously.

The predominant pathologic feature of a collagenous nodule is hyaline degeneration of connective tissue. This kind of degenerative alteration can be found in atrophic breast tissue, scar tissue, atheromatous plaques, and organized tissue. The cause of a collagenous nodule in a liver simple cyst is unclear. It is possible that the cyst was infected or bleeding, after which the pus or blood clot was replaced by granulation tissue, which is known as organization. This granulation tissue may then have been replaced by fibrous connective tissue. The process is analogous to wound healing and scar tissue formation. In this case, the collagenous nodule appeared as a high-density shadow on a CT scan. There are no specific radiologic features that differentiate a collagenous nodule from calcification. A definitive diagnosis is dependent on histopathologic findings. Had the diagnosis of a collagenous nodule mixed simple hepatic cyst been considered preoperatively, conservative observation may have been an option.

Cavernous hemangiomas are the most common benign tumor in the liver, with a reported incidence ranging from 1% to 20%[1]. This lesion occurs more frequently in women than in men. A hepatic hemangioma originates from the proliferation of vascular endothelial cells and enlarges by ectasia rather than hyperplasia[5]. Hemangiomas are usually detected incidentally while imaging for other purposes. The classic enhanced CT scan shows early peripheral enhancement of the mass, followed by centripetal fill-in of the contrast medium with persistent enhancement on delayed phase images[6].

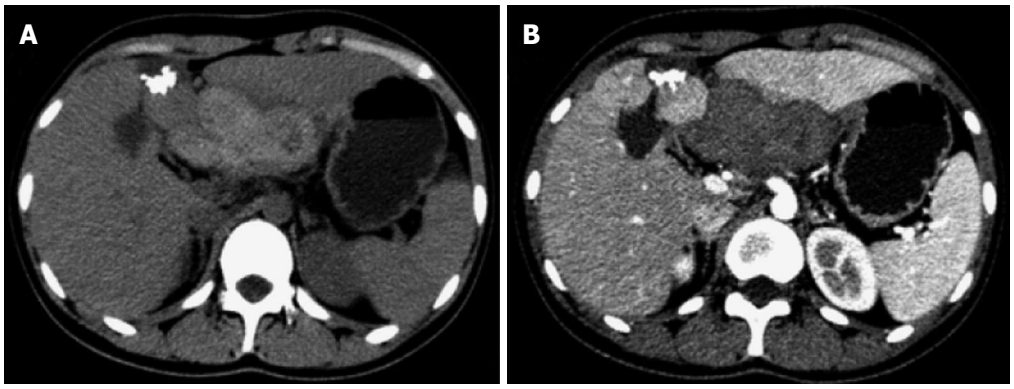

Figure 1 Radiographic findings. A: A non-enhanced computed tomography (CT) scan revealed two masses in the liver, one of which contained a high-density nodule; B: A contrast-enhanced CT scan obtained during the hepatic arterial phase showed no enhancement in or around the masses.

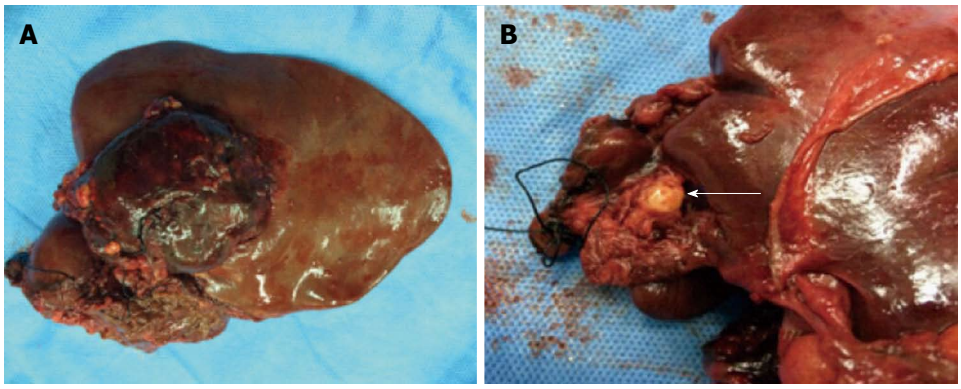

Figure 2 Intraoperative findings. A: A solid mass localized in segment Ⅲ; B: A cystic mass with a hard nodule (arrow) localized in segment Ⅳ.

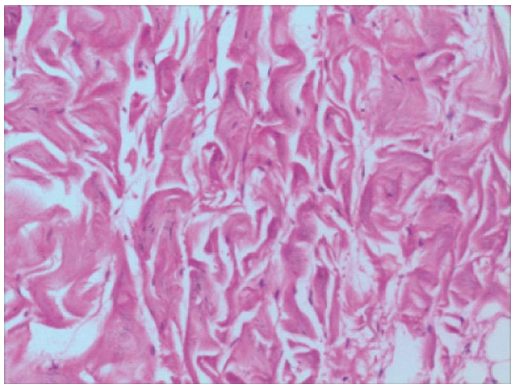

Figure 3 Histologic findings. A histologic section from the nodule revealed thickened, banded and sheet-like collagenous fibrous tissue (Hematoxylin and eosin stain, magnification × 200).

In this case, the radiographic finding was atypical, with a lesion that showed a hypodense mass without enhancement. Slow flow in the central sinusoids, central fibrosis, central thrombosis, and hemorrhage may have contributed to the nonenhancement of the hemangioma[7]. Knowledge of the broad spectrum of atypical hepatic hemangiomas is critical and can help avoid most diagnostic errors[8]. Atypical hemangioma findings include a non-enhancing central core and septa (usually seen in large hemangiomas), calcification, fluid-fluid level, and multicystic hemangiomas[9]. Hepatic hemangiomas that are larger than 4 cm in diameter are classified as giant hemangiomas[10]. The surgical indications for liver hemangiomas are Kasabach-Merritt syndrome, symptoms of organ compression that have been well established (excluding other diseases), and traumatic or spontaneous rupture[11]. Asymptomatic or minimally symptomatic patients can be safely observed[12]. Previous studies have demonstrated that nonoperative management of a giant liver hemangioma is safe in most patients, indicating that the size of the lesion is not a criterion for surgery[13].

In conclusion, this case represents a rare presentation of a patient with multiple liver masses. Surgical resection was performed due to the symptoms, uncertain diagnosis as a result of atypical CT findings, and a risk of rupture of the subcapsular lesion. Liver resection is a safe procedure. In our case, the preoperative diagnosis remained uncertain, and the surgical resection was justified. The management of liver masses should be based on a balance between the risks that might be prevented by surgical resection and the estimated risks of surgery.

COMMENTS

Case characteristics

A 20-year-old female patient presented with a two-month history of recurrent right epigastric pain.

Clinical diagnosis
Tenderness in the upper abdomen.

Differential diagnosis
Teratoma, hepatolithiasis, parasitic cyst, or hemangioma.

Laboratory diagnosis
Serum alpha-fetoprotein and eosinophil levels were normal and serologic testing for hydatid antibody was negative.

Imaging diagnosis
A computed tomography scan revealed a hypodense mass and a second well-defined mass with a calcified nodule in the left hepatic lobe, without enhancements in or around either mass.

Pathological diagnosis
Histological examination revealed a collagenous nodule mixed simple cyst and a hepatic hemangioma.

Treatment
A left liver resection was performed.

Related reports
A collagenous nodule is a rare clinicopathologic characteristic of the liver. This paper discusses the pathogenesis of a collagenous nodule occurring in the liver. Although a hepatic hemangioma is the most common benign tumor of the liver, our case presented with atypical radiographic features.

Term explanation
The primary pathologic feature of a collagenous nodule is hyaline degeneration of connective tissue. This form of degenerative alteration can be found in atrophic breast tissue, scar tissue, atheromatous plaques, and organized tissue. The cause of a collagenous nodule in a liver simple cyst is unclear. It is possible that the cyst was infected or bleeding after which the pus or blood clot was replaced by granulation tissue, which is known as organization. This granulation tissue may then be replaced by fibrous connective tissue.

Experiences and lessons
The diagnosis and treatment of atypical masses in the liver should depend on a histologic examination during surgery.

Peer-review
The article can be published due to the rarity of the three diseases at the same time. The surgical procedure has been performed well due to the difficulties of the diagnosis.

REFERENCES

1 **Gore RM**, Newmark GM, Thakrar KH, Mehta UK, Berlin JW. Hepatic incidentalomas. *Radiol Clin North Am* 2011; **49**: 291-322 [PMID: 21333779 DOI: 10.1016/j.rcl.2010.10.004]

2 **Bezerra ASA**, D'Ippolito G, Martelli P, Pinto GADH, Filho MMG, Szejnfeld J. Calcificações hepáticas: freqüência e significado. *Radiol Bras* 2003; **36**: 199-205[DOI: 10.1590/s0100-39842003000400004]

3 **Scatarige JC**, Fishman EK, Saksouk FA, Siegelman SS. Computed tomography of calcified liver masses. *J Comput Assist Tomogr* 1983; **7**: 83-89 [PMID: 6298290 DOI: 10.1097/00004728-198302000-00015]

4 **Stoupis C**, Taylor HM, Paley MR, Buetow PC, Marre S, Baer HU, Vock P, Ros PR. The Rocky liver: radiologic-pathologic correlation of calcified hepatic masses. *Radiographics* 1998; **18**: 675-685; quiz 726 [PMID: 9599391 DOI: 10.1148/radiographics.18.3.9599391]

5 **Trastek VF**, van Heerden JA, Sheedy PF, Adson MA. Cavernous hemangiomas of the liver: resect or observe? *Am J Surg* 1983; **145**: 49-53 [PMID: 6849494 DOI: 10.1016/0002-9610(83)90165-4]

6 **Moon HK**, Kim HS, Heo GM, Shin WG, Kim KH, Jang MK, Lee JH, Kim HY, Kim DJ, Cho SJ. A case of pedunculated hepatic hemangioma mimicking submucosal tumor of the stomach. *Korean J Hepatol* 2011; **17**: 66-70 [PMID: 21494080 DOI: 10.3350/kjhep.2011.17.1.66]

7 **Johnson CM**, Sheedy PF, Stanson AW, Stephens DH, Hattery RR, Adson MA. Computed tomography and angiography of cavernous hemangiomas of the liver. *Radiology* 1981; **138**: 115-121 [PMID: 7455071 DOI: 10.1148/radiology.138.1.7455071]

8 **Vilgrain V**, Boulos L, Vullierme MP, Denys A, Terris B, Menu Y. Imaging of atypical hemangiomas of the liver with pathologic correlation. *Radiographics* 2000; **20**: 379-397 [PMID: 10715338 DOI: 10.1148/radiographics.20.2.g00mc01379]

9 **Cha EY**, Kim KW, Choi YJ, Song JS, Cho KJ, Lee MG. Multicystic cavernous haemangioma of the liver: ultrasonography, CT, MR appearances and pathological correlation. *Br J Radiol* 2008; **81**: e37-e39 [PMID: 18238911 DOI: 10.1259/bjr/36041107]

10 **Adam YG**, Huvos AG, Fortner JG. Giant hemangiomas of the liver. *Ann Surg* 1970; **172**: 239-245 [PMID: 5433290 DOI: 10.1097/00000658-197008000-00010]

11 **Toro A**, Mahfouz AE, Ardiri A, Malaguarnera M, Malaguarnera G, Loria F, Bertino G, Di Carlo I. What is changing in indications and treatment of hepatic hemangiomas. A review. *Ann Hepatol* 2014; **13**: 327-339 [PMID: 24927603]

12 **Yoon SS**, Charny CK, Fong Y, Jarnagin WR, Schwartz LH, Blumgart LH, DeMatteo RP. Diagnosis, management, and outcomes of 115 patients with hepatic hemangioma. *J Am Coll Surg* 2003; **197**: 392-402 [PMID: 12946794 DOI: 10.1016/s1072-7515(03)00420-4]

13 **Schnelldorfer T**, Ware AL, Smoot R, Schleck CD, Harmsen WS, Nagorney DM. Management of giant hemangioma of the liver: resection versus observation. *J Am Coll Surg* 2010; **211**: 724-730 [PMID: 20980175 DOI: 10.1016/j.jamcollsurg.2010.08.006]

P- Reviewer: Di Carlo I **S- Editor**: Ma YJ
L- Editor: Wang TQ **E- Editor**: Liu XM

World Journal of Gastroenterology

Submit a Manuscript: http://www.wjgnet.com/esps/
Help Desk: http://www.wjgnet.com/esps/helpdesk.aspx
DOI: 10.3748/wjg.v21.i14.4423

World J Gastroenterol 2015 April 14; 21(14): 4423-4426
ISSN 1007-9327 (print) ISSN 2219-2840 (online)

Six month abstinence rule for liver transplantation in severe alcoholic liver disease patients

Aiman Obed, Steffen Stern, Anwar Jarrad, Thomas Lorf

Aiman Obed, Anwar Jarrad, Hepatobiliary and Liver Transplant Unit, Jordan Hospital, Amman 11152, Jordan
Steffen Stern, Fakultät für Rechtswissenschaft, Universität Bielefeld, 33615 Bielefeld, Germany
Thomas Lorf, Georg-August-University Goettingen, D-37073 Gottingen, Germany
Author contributions: All authors contributed to data analysis and the interpretation of papers mentioned in this manuscript, as well as drafting the manuscript, making critical revisions, and giving final approval of the version to be published.
Conflict-of-interest: The authors declare no conflict of interest.

Correspondence to: Aiman Obed, MD FACS, FEBBS, Hepatobiliary and Liver Transplant Unit, Jordan Hospital, PO Box 520248, Amman 11152, Jordan. aimanobed@hotmail.com
Telephone: +962-6-4608080
Fax: +962-6-4607575
Received: November 29, 2014
Peer-review started: December 1, 2014
First decision: December 26, 2014
Revised: January 1, 2015
Accepted: January 30, 2015
Article in press: January 30, 2015
Published online: April 14, 2015

Abstract

Alcoholic liver disease (ALD) is the second most common diagnosis among patients undergoing liver transplantation (LT). The recovery results of patients transplanted for ALD are often at least as good as those of patients transplanted for other diagnoses and better than those suffering from hepatitis C virus, cryptogenic cirrhosis, or hepatocellular carcinoma. In the case of medically non-responding patients with severe acute alcoholic hepatitis or acute-on chronic liver failure, the refusal of LT is often based on the lack of the required alcohol abstinence period of six months. The obligatory abidance of a period of abstinence as a transplant eligibility requirement for medically non-responding patients seems unfair and inhumane, since the majority of these patients will not survive the six-month abstinence period. Data from various studies have challenged the 6-mo rule, while excellent survival results of LT have been observed in selected patients with severe alcoholic hepatitis not responding to medical therapy. Patients with severe advanced ALD should have legal access to LT. The mere lack of pre-LT abstinence should not be an obstacle for being listed.

Key words: Alcohol; Alcoholic hepatitis; Cirrhosis; Six month abstinence rule; Abstinence; Liver transplantation

Core tip: Severe alcoholic liver diseases that do not respond to medical therapy, such as alcoholic hepatitis or acute-on chronic liver failure, show life threatening one-year mortality rates of up to 90%. The majority of transplant centers demand 6-mo of alcohol abstinence prior to transplantation, the so-called "6-mo rule". This rule is void of scientific evidence and frequently the subject of controversial discussions. Since most patients with severe alcoholic liver disease will die before meeting the criteria of the 6-mo period of abstinence, liver transplantation has to be taken into account irrespective of the 6-mo abstinence period.

Obed A, Stern S, Jarrad A, Lorf T. Six month abstinence rule for liver transplantation in severe alcoholic liver disease patients. *World J Gastroenterol* 2015; 21(14): 4423-4426 Available from: URL: http://www.wjgnet.com/1007-9327/full/v21/i14/4423.htm

DOI: http://dx.doi.org/10.3748/wjg.v21.i14.4423

TO THE EDITOR

We read the article "Acute alcoholic hepatitis, end stage alcoholic liver disease and liver transplantation: An Italian position statement" by Testino *et al*[1] with particularly great interest.

In general, alcohol avoidance in patients with liver disease (especially in alcoholic liver cirrhosis) is advisable and medically beneficial[2,3], however patients suffering from either severe acute alcoholic hepatitis (SAAH) or acute-on chronic liver failure (ACLF) and not responding to medical therapy have high 3-mo mortality rates ranging from 60%-70%, and even reaching as high as 90% within the first year[4-7].

SAAH and ACLF are life-threating situations demanding intensive care unit (ICU) therapy. Typically, patients in such clinical conditions are already too sick to drink, with the vast majority failing to recover by stopping their consumption of alcohol[8-11].

Stadlbauer *et al*[12] revealed that patients who do not respond to medical therapy will inevitably die without a potentially lifesaving liver transplantation.

A recent study by Kumar *et al*[13] found that a change in MELD score at 2 wk was effective in determining the outcome. However, the study showed that an interval of 2 wk was sufficient to demonstrate an increased mortality or need for liver transplant in patients with ACLF.

Mathurin *et al*[6] presented a comparable conclusion regarding mortality prognosis of SAAH with an interval from 7 to 14 d after ICU admission. A lack of clinical improvement in patients with SAAH and ACLF during the first 2 wk of ICU treatment indicates a poor outcome or vital need for liver transplant.

The cornerstone for practicing evidence-based medicine is applying the best current knowledge to medical decision-making for each individual patient.

Unfortunately, with regard to the advanced end-stage ALD, current prejudices, barroom clichés, and public half-truths seem to overshadow the available evidence-based information.

The debatable 6-mo abstinence rule has not only been controversial ever since its introduction, but has also been harshly criticized and labeled as an unfair and inhumane rule with fatal consequences for ALD patients[14,15].

The available data questions the 6-mo rule whilst confirming well-known uncertainties about its ability and usefulness in predicting (heavy) alcohol relapse after LT[16-18].

Death or graft loss occurs in only about 4% of all ALD patients who experience a relapse of their disease. The most common causes of death in patients who continued to consume alcohol were cardiovascular events and cancer, not liver failure directly caused by alcohol consumption[1].

Data presented by Schmeding *et al*[19] in 2011 clearly indicates that ALD patients have better 5 and 10-year survival rates compared with HCV-infected patients, even in the case of alcohol relapse after liver transplantation.

Recently, Deruytter *et al*[20] observed recidivism of alcohol after liver transplantation in 29% of ALD patients and heavy drinking after LTX in 16%. More importantly, no significant difference in survival was found between non-relapsers, occasional drinkers, and problem drinkers.

Simultaneously, medical law experts are repetitively reminded, albeit from a different point of view than those in practical medicine, that constitutional law prohibits discrimination against subgroups and life differentiations as being either worthy or unworthy of life. They stress that the exclusion of non-sober ALD patients from being listed discriminated them and violated said constitutional law[21].

Considering that patients who experience acute liver failure after ecstasy consumption[22] or are suffering from acute hepatitis B infections due to careless sexual practices[23] have full access to the waiting list raises the question as to why patients with SAAH or ACLF should be treated any differently.

The United Network for Organ Sharing (UNOS) has still adopted the 6-mo rule, although it does advise that "exceptional" cases be referred to regional review boards for consideration.

The American Association for the Study of Liver Disease contemporary guidelines also advise 6 mo of zero alcohol consumption before LT, but they highlighted that this rule as it stands is not a defining factor as to whether or not a patient is accepted as a candidate for a liver transplant[24].

In the end, alcoholism has to be accepted as a disease that, in some cases, has a genetic background[25,26]. The lack of pre-transplant abstinence should not be considered as a justification for denying the legal right to have access to the liver transplantation waiting list for patients with advanced ALD[27].

Transplantation for alcoholic liver disease is prejudged, with its worthiness often being questioned due to the common misconception of ALD being regarded as a type of self-inflicted harm[28-30].

The segregation of patients with severe alcoholic cirrhosis who are considered to be proper candidates for LT after complete evaluation must be avoided[31].

Furthermore, the necessity of LT for ALD patients is generally misperceived and not taken seriously by general physicians or the general public. However, there are no moral or ethical arguments that could justify the exclusion of very ill patients with ALD from potentially lifesaving LT[32,33]. On the contrary, it would be considered a death sentence for these patients. The number of patients who have already passed away before they were even presented to a transplant

center remains unclear.

Treatment with artificial liver support devices has value in correcting major pathophysiological disturbances, and might be of individual help as a bridging procedure in patients with ACLF and SAAH until transplant[34-37].

In the end, the 6-mo rule is insufficient in predicting relapse risk after liver transplantation. Liver transplantation may be lifesaving in cases of advanced ALD or alcoholic hepatitis, but inflexible sobriety rules eliminate patients with a low risk of relapse from transplant consideration[38].

Lastly, it must be noted that the United Nations' Universal Declaration of Human Rights acknowledges that all human beings are born free and equal in terms of dignity and rights. Everyone has the right to life, liberty, security, and a standard of living adequate for the health and well-being of themselves and their family[39].

National transplant policy boards, patient support groups, and legislation clearly need to act and collaborate transparently and closely in regards to national constitutional law in order to educate the public and clarify that liver transplantation for advanced ALD is not a matter of medical scientific discussion, but rather a societal dilemma that has the potential to improve the life expectancy of many desperate patients.

We agree with all suggestions made by Testino *et al*[1], particularly with regard to efforts made to improve the screening of *de novo* tumors after liver transplantation and the prevention of cardiovascular complications, which are indeed required within the follow-up care in order to achieve further improvement for long-term outcome.

In summary, we conclude that the selection and allocation criteria for advanced end-stage ALD, especially the abstinence rule, should be appropriately revised to avoid further preventable patient death. In cases of SAAH and ACLF that do not respond to medical therapy 2 wk after admission, liver transplantation should be compulsory, regardless of achieved abstinence time.

REFERENCES

1 **Testino G**, Burra P, Bonino F, Piani F, Sumberaz A, Peressutti R, Giannelli Castiglione A, Patussi V, Fanucchi T, Ancarani O, De Cerce G, Iannini AT, Greco G, Mosti A, Durante M, Babocci P, Quartini M, Mioni D, Aricò S, Baselice A, Leone S, Lozer F, Scafato E, Borro P. Acute alcoholic hepatitis, end stage alcoholic liver disease and liver transplantation: an Italian position statement. *World J Gastroenterol* 2014; **20**: 14642-14651 [PMID: 25356027 DOI: 10.3748/wjg.v20.i40.14642]

2 **Bendimerad P**, Blecha L. [Benefits in reducing alcohol consumption: how nalmefene can help]. *Encephale* 2014; **40**: 495-500 [PMID: 25454365 DOI: 10.1016/j.encep.2014.10.012]

3 **Shearn CT**, Petersen DR. Understanding the tumor suppressor PTEN in chronic alcoholism and hepatocellular carcinoma. *Adv Exp Med Biol* 2015; **815**: 173-184 [PMID: 25427907 DOI: 10.1007/978-3-319-09614-8_10]

4 **Addolorato G**, Mirijello A, Leggio L, Ferrulli A, D'Angelo C, Vassallo G, Cossari A, Gasbarrini G, Landolfi R, Agnes S, Gasbarrini A. Liver transplantation in alcoholic patients: impact of an alcohol addiction unit within a liver transplant center. *Alcohol Clin Exp Res* 2013; **37**: 1601-1608 [PMID: 23578009 DOI: 10.1111/acer.12117]

5 **Donckier V**, Lucidi V, Gustot T, Moreno C. Reply to: "liver transplantation and severe acute alcoholic hepatitis: an ethical consideration". *J Hepatol* 2014; **61**: 707 [PMID: 24882053 DOI: 10.1016/j.jhep.2014.05.029]

6 **Mathurin P**, Moreno C, Samuel D, Dumortier J, Salleron J, Durand F, Castel H, Duhamel A, Pageaux GP, Leroy V, Dharancy S, Louvet A, Boleslawski E, Lucidi V, Gustot T, Francoz C, Letoublon C, Castaing D, Belghiti J, Donckier V, Pruvot FR, Duclos-Vallée JC. Early liver transplantation for severe alcoholic hepatitis. *N Engl J Med* 2011; **365**: 1790-1800 [PMID: 22070476 DOI: 10.1056/NEJMoa1105703]

7 **Abenavoli L**, Milic N, Rouabhia S, Addolorato G. Pharmacotherapy of acute alcoholic hepatitis in clinical practice. *World J Gastroenterol* 2014; **20**: 2159-2167 [PMID: 24605014 DOI: 10.3748/wjg.v20.i9.2159]

8 **Shi Y**, Zheng MH, Yang Y, Wei W, Yang Q, Hu A, Hu Y, Wu Y, Yan H. Increased delayed mortality in patients with acute-on-chronic liver failure who have prior decompensation. *J Gastroenterol Hepatol* 2015; **30**: 712-718 [PMID: 25250673 DOI: 10.1111/jgh.12787]

9 **Moreau R**, Jalan R, Gines P, Pavesi M, Angeli P, Cordoba J, Durand F, Gustot T, Saliba F, Domenicali M, Gerbes A, Wendon J, Alessandria C, Laleman W, Zeuzem S, Trebicka J, Bernardi M, Arroyo V. Acute-on-chronic liver failure is a distinct syndrome that develops in patients with acute decompensation of cirrhosis. *Gastroenterology* 2013; **144**: 1426-1437, 1437.e1-e9 [PMID: 23474284 DOI: 10.1053/j.gastro.2013.02.042]

10 **Bajaj JS**, O'Leary JG, Reddy KR, Wong F, Biggins SW, Patton H, Fallon MB, Garcia-Tsao G, Maliakkal B, Malik R, Subramanian RM, Thacker LR, Kamath PS. Survival in infection-related acute-on-chronic liver failure is defined by extrahepatic organ failures. *Hepatology* 2014; **60**: 250-256 [PMID: 24677131 DOI: 10.1002/hep.27077]

11 **Bañares R**, Nevens F, Larsen FS, Jalan R, Albillos A, Dollinger M, Saliba F, Sauerbruch T, Klammt S, Ockenga J, Pares A, Wendon J, Brünnler T, Kramer L, Mathurin P, de la Mata M, Gasbarrini A, Müllhaupt B, Wilmer A, Laleman W, Eefsen M, Sen S, Zipprich A, Tenorio T, Pavesi M, Schmidt HH, Mitzner S, Williams R, Arroyo V. Extracorporeal albumin dialysis with the molecular adsorbent recirculating system in acute-on-chronic liver failure: the RELIEF trial. *Hepatology* 2013; **57**: 1153-1162 [PMID: 23213075 DOI: 10.1002/hep.26185]

12 **Stadlbauer V**, Davies NA, Sen S, Jalan R. Artificial liver support systems in the management of complications of cirrhosis. *Semin Liver Dis* 2008; **28**: 96-109 [PMID: 18293280 DOI: 10.1055/s-2008-1040324]

13 **Kumar R**, Krishnamoorthy TL, Tan HK, Lui HF, Chow WC. Change in model for end-stage liver disease score at two weeks, as an indicator of mortality or liver transplantation at 60 days in acute-on-chronic liver failure. *Gastroenterol Rep* (Oxf) 2014; Epub ahead of print [PMID: 25391261 DOI: 10.1093/gastro/gou075]

14 **Starzl TE**, Van Thiel D, Tzakis AG, Iwatsuki S, Todo S, Marsh JW, Koneru B, Staschak S, Stieber A, Gordon RD. Orthotopic liver transplantation for alcoholic cirrhosis. *JAMA* 1988; **260**: 2542-2544 [PMID: 3050180 DOI: 10.1001/jama.1988.03410170090040]

15 **Weinrieb RM**, Van Horn DH, McLellan AT, Lucey MR. Interpreting the significance of drinking by alcohol-dependent liver transplant patients: fostering candor is the key to recovery. *Liver Transpl* 2000; **6**: 769-776 [PMID: 11084066 DOI: 10.1053/jlts.2000.18497]

16 **Prince MI**, Hudson M. Liver transplantation for chronic liver disease: advances and controversies in an era of organ shortages. *Postgrad Med J* 2002; **78**: 135-141 [PMID: 11884694 DOI: 10.1136/pmj.78.917.135]

17 **Bird GL**, O'Grady JG, Harvey FA, Calne RY, Williams R .Liver transplantation in patients with alcoholic cirrhosis: selection

criteria and rates of survival and relapse. *BMJ* 1990; **301**: 15-17 [DOI: 10.1136/bmj.301.6742.15]
18 **Pereira SP**, Howard LM, Muiesan P, Rela M, Heaton N, Williams R. Quality of life after liver transplantation for alcoholic liver disease. *Liver Transpl* 2000; **6**: 762-768 [PMID: 11084065 DOI: 10.1053/jlts.2000.19030]
19 **Schmeding M**, Heidenhain C, Neuhaus R, Neuhaus P, Neumann UP. Liver transplantation for alcohol-related cirrhosis: a single centre long-term clinical and histological follow-up. *Dig Dis Sci* 2011; **56**: 236-243 [PMID: 20499174 DOI: 10.1007/s10620-010-1281-7]
20 **Deruytter E**, Van Steenkiste C, Trépo E, Geerts A, Van Vlierberghe H, Berrevoet F, de Hemptinne B, Rogiers X, Troisi R, Colle I. Liver transplantation for alcoholic liver disease: a retrospective analysis of recidivism, survival and risk factors predisposing to alcohol relapse. *Acta Gastroenterol Belg* 2013; **76**: 282-290 [PMID: 24261021]
21 **Gutmann T**, Fateh-Moghadam B. Grundlagen einer gerechten Organverteilung. 8th ed. Berlin: Springer, 2003: 59-78
22 **Colak Y**, Tuncer I, Enc FY, Ozturk O, Kiziltas S, Ulasoglu C. Ecstasy induced fatal hepatic failure. *J Gastrointestin Liver Dis* 2011; **20**: 215-216 [PMID: 21725523]
23 **Mendizabal M**, Marciano S, Videla MG, Anders M, Zerega A, Balderramo DC, Chan D, Barrabino M, Gil O, Mastai R, Yantorno S, Gadano A, Silva MO. Changing etiologies and outcomes of acute liver failure: perspectives from 6 transplant centers in Argentina. *Liver Transpl* 2014; **20**: 483-489 [PMID: 24425668 DOI: 10.1002/lt.23823]
24 **Leong J**, Im GY. Evaluation and selection of the patient with alcoholic liver disease for liver transplant. *Clin Liver Dis* 2012; **16**: 851-863 [PMID: 23101986 DOI: 10.1016/j.cld.2012.08.012]
25 **Kranzler HR**, Armeli S, Wetherill R, Feinn R, Tennen H, Gelernter J, Covault J, Pond T. Self-efficacy mediates the effects of topiramate and GRIK1 genotype on drinking. *Addict Biol* 2014; Epub ahead of print [PMID: 25496338 DOI: 10.1111/adb.12207]
26 **Ferraguti G**, Pascale E, Lucarelli M. Alcohol addiction: a molecular biology perspective. *Curr Med Chem* 2015; **22**: 670-684 [PMID: 25544474]
27 **Burroughs AK**. Liver transplantation for severe alcoholic hepatitis saves lives. *J Hepatol* 2012; **57**: 451-452 [PMID: 22285999 DOI: 10.1016/j.jhep.2012.01.003]
28 **Ahn CS**, Hwang S, Kim KH, Moon DB, Ha TY, Song GW, Jung DH, Park GC, Kang SH, Jung BH, Kim N, Lee SG. Long-term outcome of living donor liver transplantation for patients with alcoholic liver disease. *Transplant Proc* 2014; **46**: 761-766 [PMID: 24767343 DOI: 10.1016/j.transproceed.2013.12.032]
29 **Anand AC**, Ferraz-Neto BH, Nightingale P, Mirza DF, White AC, McMaster P, Neuberger JM. Liver transplantation for alcoholic liver disease: evaluation of a selection protocol. *Hepatology* 1997; **25**: 1478-1484 [PMID: 9185771]
30 **Anantharaju A**, Van Thiel DH. Liver transplantation for alcoholic liver disease. *Alcohol Res Health* 2003; **27**: 257-268 [PMID: 15535454]
31 **Duvoux C**. [Liver transplantation: which indications? which results?]. *Presse Med* 2001; **30**: 711-716 [PMID: 11360736]
32 **Neuberger J**. Public and professional attitudes to transplanting alcoholic patients. *Liver Transpl* 2007; **13**: S65-S68 [PMID: 17969090 DOI: 10.1002/lt.21337]
33 **Kotlyar DS**, Burke A, Campbell MS, Weinrieb RM. A critical review of candidacy for orthotopic liver transplantation in alcoholic liver disease. *Am J Gastroenterol* 2008; **103**: 734-743; quiz 744 [PMID: 18081918 DOI: 10.1111/j.1572-0241.2007.01691]
34 **Sen S**, Felldin M, Steiner C, Larsson B, Gillett GT, Olausson M, Williams R, Jalan R. Albumin dialysis and Molecular Adsorbents Recirculating System (MARS) for acute Wilson's disease. *Liver Transpl* 2002; **8**: 962-967 [PMID: 12360442 DOI: 10.1053/jlts.2002.35546]
35 **Xu X**, Liu X, Ling Q, Wei Q, Liu Z, Xu X, Zhou L, Zhang M, Wu J, Huang J, Sheng J, Zheng S, Li L. Artificial liver support system combined with liver transplantation in the treatment of patients with acute-on-chronic liver failure. *PLoS One* 2013; **8**: e58738 [PMID: 23516546 DOI: 10.1371/journal.pone.0058738]
36 **Ling Q**, Xu X, Wei Q, Liu X, Guo H, Zhuang L, Chen J, Xia Q, Xie H, Wu J, Zheng S, Li L. Downgrading MELD improves the outcomes after liver transplantation in patients with acute-on-chronic hepatitis B liver failure. *PLoS One* 2012; **7**: e30322 [PMID: 22291934 DOI: 10.1371/journal.pone.0030322]
37 **Olson JC**, Wendon JA, Kramer DJ, Arroyo V, Jalan R, Garcia-Tsao G, Kamath PS. Intensive care of the patient with cirrhosis. *Hepatology* 2011; **54**: 1864-1872 [PMID: 21898477 DOI: 10.1093/alcalc/agn013]
38 **Rice JP**, Lucey MR. Should length of sobriety be a major determinant in liver transplant selection? *Curr Opin Organ Transplant* 2013; **18**: 259-264 [PMID: 23492643 DOI: 10.1097/MOT.0b013e32835fb94b]
39 The Universal Declaration of Human rights. General Assembly resolution 217A. Available from: URL: http://www.un.org/en/documents/udhr/

P- Reviewer: Boin IFSF, Du C, Detry O, Dehghani SM, Fujino Y
S- Editor: Qi Y **L- Editor**: Rutherford A **E- Editor**: Liu XM

Published by **Baishideng Publishing Group Inc**
8226 Regency Drive, Pleasanton, CA 94588, USA
Telephone: +1-925-223-8242
Fax: +1-925-223-8243
E-mail: bpgoffice@wjgnet.com
Help Desk: http://www.wjgnet.com/esps/helpdesk.aspx
http://www.wjgnet.com

ISSN 1007-9327